7-1984

Glaciochemical Investigations as a Tool in the Historical Delineation of the Acid Precipitation Problem

William B. Lyons

Paul Andrew Mayewski
University of Maine, paul.mayewski@maine.edu

United States
Environmental Protection
Agency

Office of
Research and Development
Washington, DC 20460

EPA-600/8-83-016AF
July 1984

Research and Development

EPA

The Acidic Deposition Phenomenon and Its Effects

Critical Assessment Review Papers

Volume I Atmospheric Sciences

THE ACIDIC DEPOSITION PHENOMENON AND ITS EFFECTS: CRITICAL ASSESSMENT REVIEW PAPERS

VOLUME I

Aubrey P. Altshuller, Editor
Atmospheric Sciences

Rick A. Linthurst, Editor
Effects Sciences

Project Staff

Rick A. Linthurst-*Director*
Betsy A. Hood-*Coordinator*
Gary B. Blank-*Manuscript Editor*

Production

Clara B. Edwards
Wanda Frazier
Elizabeth McKoy
Benita Perry

Graphics

Mike Conley
David Urena
Steven F. Vozzo
C. Willis Williams

Advisory Committee

David A. Bennett-U.S. EPA
Project Officer

John Bachmann-U.S. EPA
Michael Berry-U.S. EPA
Ellis B. Cowling-NCSU
J. Michael Davis-U.S. EPA
Kenneth Demerjian-U.S. EPA
J. H. B. Garner-U.S. EPA
James L. Regens-U.S. EPA
Raymond Wilhour-U.S. EPA

This document has been prepared through the NCSU Acid Deposition Program, a cooperative agreement between the United States Environmental Protection Agency, Washington, D.C. and North Carolina State University, Raleigh, North Carolina. This work was conducted as part of the National Acid Precipitation Assessment Program and was funded by U.S. EPA.

DISCLAIMER

This document has been reviewed in accordance with U.S. Environmental Protection Agency policy and approved for publication. Mention of trade names or commercial products is not intended to constitute endorsement or recommendation for use.

U.S. Environmental Protection Agency

AUTHORS

Chapter A-1 Introduction

Altshuller, Aubrey Paul, Environmental Sciences Research Laboratory, U.S. Environmental Protection Agency, MD 59, Research Triangle Park, NC, 27711.

*Nader, John S., 2336 New Bern Ave., Raleigh, NC 27610.

*Niemeyer, Larry E., 4608 Huntington Ct., Raleigh, NC 27609.

Chapter A-2 Natural and Anthropogenic Emission Sources

Homolya, James B., Radian Corp., P. O. Box 13000, Research Triangle Park, NC 27709.

Robinson, Elmer, Civil and Environmental Engineering Dept., Washington State University, Pullman, WA, 99164.

Chapter A-3 Transport Processes

*Gillani, Noor V., Mechanical Engineering Dept., Washington University, Box 1185, St. Louis, MO 63130.

Patterson, David E., Mechanical Engineering Dept., Washington University, Box 1124, St. Louis, MO 63130.

Shannon, Jack D., Bldg. 181, Environmental Research Div., Bldg. 181, Argonne National Laboraory, Argonne, IL 60439.

Chapter A-4 Transformation Processes

Gillani, Noor V., Mechanical Engineering Dept., Washington University, Box 1185, St. Louis, MO 63130.

Hegg, Dean A., Atmospheric Sciences, AK-40, University of Washington, Seattle, WA 98195.

Hobbs, Peter V., Dept. of Atmospheric Sciences, AK-40, University of Washington, Seattle, WA 98195.

*Miller, David F., Desert Research Institute, University of Nevada, P. O. Box 60220, Reno, NV 89506.

*Served as co-editor.

Whitbeck, Michael, Desert Research Institute, University of Nevada, P. O. Box 60220, Reno, NV 89506.

Chapter A-5 Atmospheric Concentrations and Distributions of Chemical Substances

Altshuller, Aubrey Paul, Enviromental Sciences Research Laboratory, U.S. Environmental Protection Agency, MD 59, Research Triangle Park, NC 27711.

Chapter A-6 Precipitation Scavenging Processes

Hales, Jeremy M., Geosciences Research and Engineering, Battelle, Pacific Northwest Laboratories, P. O. Box 999, Richland, WA 99352.

Chapter A-7 Dry Deposition Processes

Hicks, Bruce B., NOAA/ERL, Atmospheric Turbulence and Diffusion Div., ARL, P. O. Box E, Oak Ridge, TN 37830.

Chapter A-8 Deposition Monitoring

Hicks, Bruce B., U.S. Dept. of Commerce, National Oceanic and Atmospheric Administration, Environmental Research Laboratories, P. O. Box E, Oak Ridge, TN 37830.

Lyons, William Berry, Dept. of Earth Sciences, James Hall, University of New Hampshire, Durham, NH 03824.

Mayewski, Paul A., Dept. of Earth Sciences, James Hall, University of New Hampshire, Durham, NH 03824.

Stensland, Gary J., Illinois State Water Survey, 605 E. Springfield Ave., P. O. Box 5050, Station A, Champaign, IL 61820.

Chapter A-9 Deposition Models

Bhumralkar, Chandrakant M., Atmospheric Science Center, SRI International, 333 Ravenswood Ave., Menlo Park, CA 94025.

Ruff, Ronald E., Atmospheric Science Center, SRI International, 333 Ravenswood Ave., Menlo Park, CA 94025.

Chapter E-1 Introduction

Linthurst, Rick A., Kilkelly Environmental Associates, Inc., P. O. Box 31265, Raleigh, NC 27622.

Chapter E-2 Effects on Soil Systems

Adams, Fred, Dept. of Agronomy and Soils, Auburn University, Auburn, AL 36849.

Cronan, Christopher S., Land and Water Resources Center, 11 Coburn Hall, University of Maine, Orono, ME 04469.

Firestone, Mary K., Dept. Plant and Soil Biology, 108 Hilgard Hall, University of California, Berkeley, CA 94720.

Foy, Charles D., U.S. Dept. of Agriculture, Agricultural Research Service, Plant Stress Lab-BARC West, Beltsville, MD 20705.

Harter, Robert D., College of Life Sciences and Agriculture, James Hall, University of New Hampshire, NH 03824.

Johnson, Dale W., Environmental Sciences Div., Oak Ridge National Laboratory, Oak Ridge, TN 37830.

*McFee, William W., Natural Resources and Environmental Sciences Program, Purdue University, West Lafayette, IN 47907.

Chapter E-3 Effects on Vegetation

Chevone, Boris I., Dept. of Plant Pathology, Virginia Polytechnic Institute and State University, Blacksburg, VA 24060.

Irving, Patricia M., Environmental Research Div., Bldg. 203, Argonne National Laboratory, Argonne, IL 60439.

Johnson, Arthur H., Dept. of Geology D4, University of Pennsylvania, Philadelphia, PA 19104.

*Johnson, Dale W., Environmental Sciences Div., Oak Ridge National Laboratory, Oak Ridge, TN 37830.

Lindberg, Steven E., Environmental Sciences Div., Bldg. 1505, Oak Ridge National Laboratory, Oak Ridge, TN 37830.

McLaughlin, Samuel B., Environmental Sciences Div., Bldg. 3107, Oak Ridge National Laboratory, Oak Ridge, TN 37830.

Raynal, Dudley J., Dept. of Environmental and Forest Biology, College of Environmental Science and Forestry, State University of New York (SUNY), Syracuse, NY 13210.

Shriner, David S., Environmental Sciences Div., Oak Ridge National Laboratory, Oak Ridge, TN 37830.

Sigal, Lorene L., Environmental Sciences Div., Oak Ridge National Laboratory, Oak Ridge, TN 37830.

Skelly, John M., Dept. of Plant Pathology, 211 Buckhout Laboratory, Pennsylvania State University, University Park, PA 16802.

Smith, William H., School of Forestry and Environmental Studies, Yale University, 370 Prospect Street, New Haven, CT 06511.

Weber, Jerome B., Dept. of Crop Science, North Carolina State University, Raleigh, NC 27650.

Chapter E-4 Effects on Aquatic Chemistry

Anderson, Dennis S., Dept. of Botany and Plant Pathology, University of Maine, Orono, ME 04469.

*Baker, Joan P., NCSU Acid Deposition Program, North Carolina State University, 1509 Varsity Dr., Raleigh, NC 27606.

Blank, G. B., School of Forest Resources, Biltmore Hall, North Carolina State University, NC 27650.

Church, M. Robbins, Corvallis Environmental Research Laboratory, U.S. Environmental Protection Agency, 200 SW 35th Street, Corvallis, OR 97333.

Cronan, Christopher S., Land and Water Resources Center, 11 Coburn Hall, University of Maine, Orono, ME 04469.

Davis, Ronald B., Dept. of Botany and Plant Pathology, Univeristy of Maine, Orono, ME 04469.

Dillon, Peter J., Ontario Ministry of the Environment, Limnology Unit, P. O. Box 39, Dorset, Ontario, Canada, POA 1EO.

Driscoll, Charles T., Dept. of Civil Engineering, 150 Hinds Hall, Syracuse University, NY 13210.

*Galloway, James N., Dept. of Environmental Sciences, University of Virginia, Charlottesville, VA 22903.

Gregory, J. D., School of Forest Resources, Biltmore Hall, North Carolina State University, NC 27650.

Norton, Stephen A., Dept. of Geological Sciences, 110 Boardman Hall, University of Maine, Orono, ME 04469.

Schafran, Gary C., Dept. of Civil Engineering, 150 Hinds Hall, Syracuse University, Syracuse, NY 13210.

Chapter E-5 Effects on Aquatic Biology

Baker, Joan P., NCSU Acid Deposition Program, North Carolina State University, 1509 Varsity Dr., Raleigh, NC 27606.

Driscoll, Charles T., Dept. of Civil Engineering, 150 Hinds Hall, Syracuse University, Syracuse, NY 13210.

Fischer, Kathleen L., Canadian Wildlife Service, National Wildlife Research Centre, Environment Canada, 100 Gamelin Blvd., Hull, Quebec, Canada, K1A 0E7.

Guthrie, Charles A., New York State Department of Environmental Conservation, Div. of Fish and Wildlife, Bldg. 40, SUNY-Stony Brook, Stony Brook, NY 11790.

*Magnuson, John J., Laboratory of Limnology, University of Wisconsin, Madison, WI 53706.

Peverly, John H., Dept. of Agronomy, University of Illinois, Urbana, IL 61801

*Rahel, Frank J., Dept. of Zoology, Ohio State University, 1735 Neil Ave., Columbus, OH 43210.

Schafran, Gary C., Dept. of Civil Engineering, 150 Hinds Hall, Syracuse University, Syracuse, NY 13210.

Singer, Robert, Dept. of Civil Engineering, 150 Hinds Hall, Syracuse University, Syracuse, NY 13210.

Chapter E-6 Indirect Effects on Health

Baker, Joan P., NCSU Acid Precipitation Program, North Carolina State University, 1509 Varsity Dr., Raleigh, NC 27606.

Clarkson, Thomas W., University of Rochester School of Medicine, P. O. Box RBB, Rochester, NY 14642.

Sharpe, William E., Land and Water Research Bldg., Pennsylvania State University, University Park, PA 16802.

Chapter E-7 Effects on Materials

Baer, Norbert S., Conservation Center of the Institute of Fine Arts, New York University, 14 East 78th Street, New York, NY 10021.

Kirmeyer, Gregory, Economic and Engineering Services, Inc., 611 N. Columbia, Olympia, WA 98507.

Yocom, John E., TRC Environmental Consultants, Inc., 800 Connecticut Blvd., East Hartford, CT 06108.

PREFACE

The Acidic Deposition Phenomenon and Its Effects: Critical Assessment Review Papers was written at the suggestion, in the summer of 1980, of the Chairman of the Clean Air Scientific Advisory Committee of EPA's Science Advisory Board. The document was prepared for EPA through the Acid Deposition Program at North Carolina State University. This document is the first of several documents of increasing sophistication that assess the acidic deposition phenomenon. It will be succeeded by assessment documents in 1985, 1987, and 1989, based largely on research of the National Acid Precipitation Assessment Program.

The document's original charge was to prepare "a comprehensive document which lays out the state of our knowledge with regard to precursor emissions, pollutant transformation to acidic compounds, pollutant transport, pollutant deposition and the effects (both measured and potential) of acidic deposition." The editors provided the following guidelines to the authors writing the Critical Assessment Review Papers to meet this overall charge:

1. Contributions are to be written for scientists and informed lay persons.

2. Statements are to be explained and supported by references; i.e., a textbook type of approach, in an objective style.

3. Literature referenced is to be of high quality and not every reference available is to be included.

4. Emphasis is to be placed on North American systems with concentrated effort on U.S. data.

5. Overlap between this document and the SOx Criteria Document is to be minimized.

6. Potential vs known processes/effects are to be clearly noted to avoid misinterpretation.

7. The certainty of our knowledge should be quantified, when possible.

8. Conclusions are to be drawn on fact only.

9. Extrapolation beyond the available data is to be avoided.

10. Scientific knowledge is to be included without regard to policy implications.

11. Policy-related options or recommendations are beyond the scope of this document and are not to be included.

The reader, to avoid possible misinterpretation of the information presented, is advised to consider and understand these directives before reading.

Again, the document has been designed to address our present status of knowledge of the acidic deposition phenomenon and its effects. It is not a Criteria Document; it is not designed to set standards and no connections to regulations should be inferred. The literature is reviewed and conclusions are drawn based on the best evidence available. It is an authored document, and as such, the conclusions are those of the authors after their review of the literature.

The success of the Critical Assessment Review Papers has depended on the coordinated efforts of many individuals. The document involved the participation of over 60 scientists contributing material on their special areas of expertise under the broad headings of either atmospheric processes or effects. Coordination within these two areas has been the responsibility of A. Paul Altshuller and Rick A. Linthurst, the atmospheric and effects section editors, respectively. Overall coordination of the project for EPA is under David A. Bennett's direction. Dr. Altshuller is an atmospheric chemist, past recipient of the American Chemical Society's Award in Pollution Control, and recently retired director of EPA's Environmental Sciences Research Laboratory; Dr. Linthurst is an ecologist and served as Program Coordinator for the Acid Precipitation Program at North Carolina State University. He is currently at Kilkelly Environmental Associates, Inc. Dr. Bennett is the Director of the Acid Deposition Assessment Staff in EPA's Office of Research and Development.

The written materials that follow are contributions from one to eight authors per chapter, integrated by the editors. Approximately 75 scientists, with expertise in the fields being addressed, reviewed early drafts of the chapters. In addition, 200 individuals participated in a public workshop held for the technical review of these materials in November 1982. Numerous changes resulted from these reviews, and this document reflects those comments. A public review draft of this document was distributed in June 1983 for a 45-day comment period. During that period, 130 sets of comments from 53 reviewers were received. These comments were summarized and evaluated by a technical and editorial panel, and then provided to the authors who addressed them by revision and rewriting to produce this final document. In response to the comments received, revisions were made to all chapters including a major revision of Chapter E-4, Effects on Aquatic Chemistry, and the addition of a section on corrosion in water piping systems in Chapter E-7, Effects on Materials.

ACKNOWLEDGMENTS FROM NORTH CAROLINA STATE UNIVERSITY

The editorial staff wishes to extend special thanks to all the authors of this document. They have been patient and tolerant of our changes, recommendations, and deadlines, leading to this fourth and final version of the document. These dedicated scientists are to be commended for their efforts.

We also wish to acknowledge our Steering Committee, who has been patient with our errors and deadline delays. These people have made major contributions to this product, and actively assisted us with their recommendations on producing this document. Their objectivity, concern for technical accuracy, and support is appreciated. Dr. J. Michael Davis of EPA deserves special thanks, as he directed the initial draft of the document in December of 1981. His concern for clarity of thought and writing in the interest of communicating our scientific knowledge was most helpful. Dr. David Bennett of EPA is specifically recognized for his role as a scientific reviewer, and an EPA staff member who buffered the editorial staff and the authors from the public and policy concerns associated with this document. Dr. Bennett's tolerance, patience, and understanding are also appreciated.

All the reviewers, too numerous to list, are gratefully acknowledged for helping us improve the quality and accuracy of this document. These people were from private, state, federal, and special-interest organizations in both the United States and Europe. Their concern for the truth, based on the available data, is a compliment to all the individuals and organizations who were willing to deal objectively with this most important topic. It has been a pleasure to see all groups, independent of their personal philosophies, work together in the interest of producing a technically accurate document.

Dr. Arthur Stern is acknowledged for his contribution as a technical editor of the atmospheric sciences early in the document's preparation. He has made an important contribution to the final product.

Finally, EPA is acknowledged for its willingness to give the scientists an opportunity to prepare this document. Its interest, as expressed through the staff and authors, in having this document be an authored document to assist in research planning, is most appreciated. Rarely does a group of scientists have such a free hand in contributing independently to such an important issue and in such a visible way. Although coordinating the efforts of so many scientists can be a difficult and lengthy process, we feel the authored scientific product makes a valuable contribution to the acidic deposition issue.

The entire staff of the NCSU Acid Deposition Program and several part-time workers have been involved in the production of this document since it began in 1981. In addition to the people listed on the title page, these include:

William R. Alsop - Program Assistant
Ann Bartuska - Program Coordinator

Jody D. Castleberry - Receptionist/Secretary
Connie S. Harp - Secretary
Jeanie Hartman - Librarian
Helen Koop - Library Assistant

THE ACIDIC DEPOSITION PHENOMENON AND ITS EFFECTS:
CRITICAL ASSESSMENT REVIEW PAPERS

Table of Contents

Volume I
Atmospheric Sciences

Page

AUTHORS iii

PREFACE ix

ABBREVIATION-ACRONYM LIST xxix

GLOSSARY xliii

A-1 INTRODUCTION

1.1 Objectives 1-1
1.2 Approach--Movement from Sources to Receptor 1-1
1.2.1 Chemical Substances of Interest 1-1
1.2.2 Natural and Anthropogenic Emissions Sources 1-1
1.2.3 Transport Processes 1-1
1.2.4 Transformation Processes 1-2
1.2.5 Atmospheric Concentrations and Distributions of Chemical Substances 1-2
1.2.6 Precipitation Scavenging Processes 1-2
1.2.7 Dry Deposition Processes 1-3
1.2.8 Deposition Monitoring 1-3
1.2.9 Deposition Models 1-4
1.3 Acidic Deposition 1-4

A-2 NATURAL AND ANTHROPOGENIC EMISSIONS SOURCES

2.1 Introduction 2-1
2.2 Natural Emission Sources 2-1
2.2.1 Sulfur Compounds 2-1
2.2.1.1 Introduction 2-1
2.2.1.2 Estimates of Natural Sources 2-2
2.2.1.3 Biogenic Emissions of Sulfur Compounds 2-3
2.2.1.4 Geophysical Sources of Natural Sulfur Compounds 2-15
2.2.1.4.1 Volcanism 2-17
2.2.1.4.2 Marine sources of aerosol particles and gases 2-19
2.2.1.5 Scavenging Processes and Sinks 2-21
2.2.1.6 Summary of Natural Sources of Sulfur Compounds 2-22
2.2.2 Nitrogen Compounds 2-23
2.2.2.1 Introduction 2-23
2.2.2.2 Estimates of Natural Global Sources and Sinks 2-24
2.2.2.3 Biogenic Sources of NO_x Compounds 2-28
2.2.2.4 Tropospheric and Stratospheric Reactions 2-30
2.2.2.5 Formation of NO_x by Lightning 2-30
2.2.2.6 Biogenic NO_x Emissions Estimate for the United States ... 2-32
2.2.2.7 Biogenic Sources of Ammonia 2-33
2.2.2.8 Oceanic Source for Ammonia 2-36
2.2.2.9 Biogenic Ammonia Emissions Estimates for the United States 2-37
2.2.2.10 Meteorological and Area Variations for NO_x and Ammonia Emissions 2-38
2.2.2.11 Scavenging Processes for NO_x and Ammonia 2-38
2.2.2.12 Organic Nitrogen Compounds 2-39
2.2.2.13 Summary of Natural NO_x and Ammonia Emissions 2-39

Table of Contents (continued)

		Page
2.2.3	Chlorine Compounds	2-39
2.2.3.1	Introduction	2-39
2.2.3.2	Oceanic Sources	2-40
2.2.3.3	Volcanism	2-44
2.2.3.4	Combustion	2-44
2.2.3.5	Total Natural Chlorine Sources	2-45
2.2.3.6	Seasonal Distributions	2-45
2.2.3.7	Environmental Impacts of Natural Chlorides	2-45
2.2.4	Natural Sources of Aerosol Particles	2-45
2.2.5	Precipitation pH in Background Conditions	2-48
2.2.6	Summary	2-52
2.3	Anthropogenic Emissions	2-53
2.3.1	Origins of Anthropogenically Emitted Compounds and Related Issues	2-53
2.3.2	Historical Trends and Current Emissions of Sulfur Compounds	2-57
2.3.2.1	Sulfur Oxides	2-57
2.3.2.2	Primary Sulfate Emissions	2-62
2.3.3	Historical Trends and Current Emissions of Nitrogen Oxides	2-68
2.3.4	Historical Trends and Current Emissions of Hydrochloric Acid (HCl)	2-72
2.3.5	Historical Trends and Current Emissions of Heavy Metals Emitted from Fuel Combustion	2-76
2.3.6	Historical Emissions Trends in Canada	2-84
2.3.7	Future Trends in Emissions	2-93
2.3.7.1	United States	2-93
2.3.7.2	Canada	2-93
2.3.8	Emissions Inventories	2-96
2.3.9	The Potential for Neutralization of Atmospheric Acidity by Suspended Fly Ash	2-97
2.4	Conclusions	2-102
2.5	References	2-106

A-3 TRANSPORT PROCESSES

3.1	Introduction	3-1
3.1.1	The Concept of Atmospheric Residence Times	3-2
3.2	Meteorological Scales and Atmospheric Motions	3-3
3.2.1	Meteorological Scales	3-3
3.2.2	Atmospheric Motions	3-4
3.3	Pollutant Transport Layer: Its Structure and Dynamics	3-10
3.3.1	The Planetary Boundary Layer (Mixing Layer)	3-10
3.3.2	Structure of the Transport Layer (TL)	3-12
3.3.3	Dynamics of the Transport Layer	3-16
3.3.4	Effects of Mesoscale Complex Systems on Transport Layer Structure and Dynamics	3-27
3.3.4.1	Effect of Mesoscale Convective Precipitation Systems (MCPS)	3-27
3.3.4.2	Complex Terrain Effects	3-31
3.3.4.2.1	Shoreline environment effects	3-31
3.3.4.2.2	Urban effects	3-34
3.3.4.2.3	Hilly terrain effects	3-35
3.4	Mesoscale Plume Transport and Dilution	3-38
3.4.1	Elevated Point-Source Emissions (Power Plant Plumes)	3-38
3.4.2	Broad Areal Emissions Near Ground (Urban Plumes)	3-60
3.5	Continental and Hemispheric Transport	3-65
3.6	Conclusions	3-88
3.7	References	3-92

Table of Contents (continued)

Page

A-4 TRANSFORMATION PROCESSES

4.1 Introduction 4-1
4.2 Homogeneous Gas-Phase Reactions 4-3
4.2.1 Fundamental Reactions 4-3
4.2.1.1 Reduced Sulfur Compounds 4-3
4.2.1.2 Sulfur Dioxide 4-4
4.2.1.3 Nitrogen Compounds 4-11
4.2.1.4 Halogens 4-17
4.2.1.5 Organic Acids 4-17
4.2.2 Laboratory Simulations of Sulfur Dioxide and Nitrogen Dioxide Oxidation 4-17
4.2.3 Field Studies of Gas-Phase Reactions 4-21
4.2.3.1 Urban Plumes 4-21
4.2.3.2 Power Plant Plumes 4-24
4.2.4 Summary 4-29
4.3 Solution Reactions 4-31
4.3.1 Introduction 4-31
4.3.2 Absorption of Acid 4-32
4.3.3 Production of HCl in Solution 4-38
4.3.4 Production of HNO_3 in Solution 4-38
4.3.5 Production of H_2SO_4 in Solution 4-42
4.3.5.1 Evidence from Field Studies 4-42
4.3.5.2 Homogeneous Aerobic Oxidation of $SO_2 \cdot H_2O$ to H_2SO_4 4-43
4.3.5.2.1 Uncatalyzed 4-43
4.3.5.2.2 Catalyzed 4-45
4.3.5.3 Homogeneous Non-aerobic Oxidation of $SO_2 \cdot H_2O$ to H_2SO_4 ... 4-47
4.3.5.4 Heterogeneous Production of H_2SO_4 in Solution 4-52
4.3.5.5 The Relative Importance of the Various H_2SO_4 Production Mechanisms 4-53
4.3.6 Neutralization Reactions 4-61
4.3.6.1 Neutralization by NH_3 4-61
4.3.6.2 Neutralization by Particle-Acid Reactions 4-62
4.3.7 Summary 4-63
4.4 Transformation Models 4-63
4.4.1 Introduction 4-63
4.4.2 Approaches to Transformation Modeling 4-66
4.4.2.1 The Fundamental Approach 4-66
4.4.2.2 The Empirical Approach 4-68
4.4.3 The Question of Linearity 4-71
4.4.4 Some Specific Models and Their Applications 4-74
4.4.4.1 Detailed Chemical Simulations 4-74
4.4.4.2 Parameterized Models 4-67
4.4.5 Summary 4-81
4.5 Conclusions 4-82
4.6 References 4-86

A-5 ATMOSPHERIC CONCENTRATIONS AND DISTRIBUTIONS OF CHEMICAL SUBSTANCES

5.1 Introduction 5-1
5.2 Sulfur Compounds 5-2
5.2.1 Historical Distribution Patterns 5-2
5.2.2 Sulfur Dioxide 5-3
5.2.2.1 Urban Measurements 5-3
5.2.2.2 Nonurban Measurements 5-4
5.2.2.3 Concentration Measurements at Remote Locations 5-12
5.2.2.4 Comparison of Sulfur Dioxide Emissions and Ambient Air Concentration 5-12

Table of Contents (continued)

		Page
5.2.3	Sulfate	5-13
5.2.3.1	Urban Concentration Measurements	5-13
5.2.3.2	Urban Composition Measurements	5-15
5.2.3.3	Nonurban Concentration Measurements	5-16
5.2.3.4	Nonurban Composition Measurements	5-19
5.2.3.5	Concentration and Composition Measurements at Remote Locations	5-22
5.2.3.6	Comparison of Sulfur Oxide Emissions and Ambient Air Concentrations of Sulfate	5-23
5.2.4	Particle Size Characteristics of Particulate Sulfur Compounds	5-24
5.2.4.1	Urban Measurements	5-24
5.2.4.2	Nonurban Size Measurements	5-27
5.2.4.3	Measurements at Remote Locations	5-27
5.3	Nitrogen Compounds	5-28
5.3.1	Introduction	5-28
5.3.2	Nitrogen Oxides	5-28
5.3.2.1	Historical Distribution Patterns and Current Concentrations of Nitrogen Oxides	5-28
5.3.2.2	Measurements Techniques-Nitrogen Oxides	5-29
5.3.2.3	Urban Concentration Measurements	5-29
5.3.2.4	Nonurban Concentration Measurements	5-30
5.3.2.5	Measurements of Concentrations at Remote Locations	5-34
5.3.3	Nitric Acid	5-38
5.3.3.1	Urban Concentration Measurements	5-38
5.3.3.2	Nonurban Concentration Measurements	5-40
5.3.3.3	Concentration Measurements at Remote Locations	5-44
5.3.4	Peroxyacetyl Nitrates	5-45
5.3.4.1	Urban Concentration Measurements	5-45
5.3.4.2	Nonurban Concentration Measurements	5-48
5.3.5	Ammonia	5-50
5.3.5.1	Urban Concentration Measurements	5-50
5.3.5.2	Nonurban Concentration Measurements	5-51
5.3.6	Particulate Nitrate	5-51
5.3.6.1	Urban Concentration Measurements	5-53
5.3.6.2	Nonurban Concentration Measurements	5-55
5.3.6.3	Concentration Measurements at Remote Locations	5-56
5.3.7	Particle Size Characteristics of Particulate Nitrogen Compounds	5-56
5.4	Ozone	5-58
5.4.1	Concentration Measurements Within the Planetary Boundary Layer (PBL)	5-60
5.4.2	Concentration Measurements at Higher Altitudes	5-63
5.5	Hydrogen Peroxide	5-63
5.5.1	Urban Concentration Measurements	5-64
5.5.2	Nonurban Concentration Measurements	5-64
5.5.3	Concentration Measurements in Rainwater	5-65
5.6	Chlorine Compounds	5-65
5.6.1	Introduction	5-65
5.6.2	Hydrogen Chloride	5-66
5.6.3	Particulate Chloride	5-66
5.6.4	Particle Size Characteristics of Particulate Chlorine Compounds	5-67
5.7	Metallic Elements	5-68
5.7.1	Concentration Measurements and Particle Sizes in Urban Areas	5-68
5.7.2	Concentration Measurements and Particle Sizes in Nonurban Areas	5-71
5.8	Relationship of Light Extinction and Visual Range Measurements to Aerosol Composition	5-73
5.8.1	Fine Particle Concentration and Light Scattering Coefficients	5-73
5.8.2	Light Extinction or Light Scattering Budgets at Urban Locations	5-74
5.8.3	Light Extinction or Light Scattering Budgets at Nonurban Locations	5-76
5.8.4	Trends in Visibility as Related to Sulfate Concentrations	5-78
5.9	Conclusions	5-78
5.10	References	5-84

Table of Contents (continued)

Page

A-6 PRECIPITATION SCAVENGING PROCESSES

6.1 Introduction 6-1
6.2 Steps in the Scavenging Sequence 6-2
6.2.1 Introduction 6-2
6.2.2 Intermixing of Pollutant and Condensed Water (Step 1-2) 6-5
6.2.3 Attachment of Pollutant to Condensed Water Elements (Step 2-3) ... 6-6
6.2.4 Aqueous-Phase Reactions (Step 3-4) 6-13
6.2.5 Deposition of Pollutant with Precipitation (Steps 3-5 and 4-5) ... 6-13
6.2.6 Combined Processes and the Problem of Scavenging Calculations 6-16
6.3 Storm Systems and Storm Climatology 6-16
6.3.1 Introduction 6-16
6.3.2 Frontal Storm Systems 6-17
6.3.2.1 Warm-Front Storms 6-19
6.3.2.2 Cold-Front Storms 6-23
6.3.2.3 Occluded-Front Storms 6-23
6.3.3 Convective Storm Systems 6-23
6.3.4 Additional Storm Types: Nonideal Frontal Storms, Orographic Storms and Lake-Effect Storms 6-27
6.3.5 Storm and Precipitation Climatology 6-28
6.3.5.1 Precipitation Climatology 6-28
6.3.5.2 Storm Tracks 6-28
6.3.5.3 Storm Duration Statistics 6-31
6.4 Summary of Precipitation-Scavenging Field Investigations 6-31
6.5 Predictive and Interpretive Models of Scavenging 6-41
6.5.1 Introduction 6-41
6.5.2 Elements of a Scavenging Model 6-50
6.5.2.1 Material Balances 6-50
6.5.2.2 Energy Balances 6-52
6.5.2.3 Momentum Balances 6-52
6.5.3 Definitions of Scavenging Parameters 6-53
6.5.4 Formulation of Scavenging Models: Simple Examples of Microscopic and Macroscopic Approaches 6-58
6.5.5 Systematic Selection of Scavenging Models: A Flow Chart Approach 6-61
6.6 Practical Aspects of Scavenging Models: Uncertainty Levels and Sources of Error 6-64
6.7 Conclusions 6-68
6.8 References 6-71

A-7 DRY DEPOSITION PROCESSES

7.1 Introduction 7-1
7.2 Factors Affecting Dry Deposition 7-1
7.2.1 Introduction 7-1
7.2.2 Aerodynamic Factors 7-6
7.2.3 The Quasi-Laminar Layer 7-9
7.2.4 Phoretic Effects and Stefan Flow 7-13
7.2.5 Surface Adhesion 7-14
7.2.6 Surface Biological Effects 7-15
7.2.7 Deposition to Liquid Water Surfaces 7-16
7.2.8 Deposition to Mineral and Metal Surfaces 7-17
7.2.9 Fog and Dewfall 7-19
7.2.10 Resuspension and Surface Emission 7-20
7.2.11 The Resistance Analog 7-21
7.3 Methods for Studying Dry Deposition 7-27
7.3.1 Direct Measurement 7-27
7.3.2 Wind-Tunnel and Chamber Studies 7-29
7.3.3 Micrometeorological Measurement Methods 7-33

Table of Contents (continued)

		Page
7.4	Field Investigations of Dry Deposition	7-37
	7.4.1 Gaseous Pollutants	7-37
	7.4.2 Particulate Pollutants	7-44
	7.4.3 Routine Handling in Networks	7-50
7.5	Micrometeorological Models of the Dry Deposition Process	7-51
	7.5.1 Gases	7-51
	7.5.2 Particles	7-53
7.6	Summary	7-54
7.7	Conclusions	7-58
7.8	References	7-60

A-8 DEPOSITION MONITORING

8.1	Introduction	8-1
8.2	Wet Deposition Networks	8-2
	8.2.1 Introduction and Historical Background	8-2
	8.2.2 Definitions	8-3
	8.2.3 Methods, Procedures and Equipment for Wet Deposition Networks	8-5
	8.2.4 Wet Deposition Network Data Bases	8-7
8.3	Monitoring Capabilities for Dry Deposition	8-12
	8.3.1 Introduction	8-12
	8.3.2 Methods for Monitoring Dry Deposition	8-18
	8.3.2.1 Direct Collection Procedures	8-19
	8.3.2.2 Alternative Methods	8-20
	8.3.3 Evaluations of Dry Deposition Rates	8-22
8.4	Wet Deposition Network Data With Applications to Selected Problems	8-31
	8.4.1 Spatial Patterns	8-31
	8.4.2 Remote Site pH Data	8-50
	8.4.3 Precipitation Chemistry Variations Over Time	8-60
	8.4.3.1 Nitrate Variation Since 1950's	8-60
	8.4.3.2 pH Variation Since 1950's	8-63
	8.4.3.3 Calcium Variation Since the 1950's	8-67
	8.4.4 Seasonal Variations	8-67
	8.4.5 Very Short Time Scale Variations	8-69
	8.4.6 Air Parcel Trajectory Analysis	8-69
8.5	Glaciochemical Investigations as a Tool in the Historical Delineation of the Acid Precipitation Problems	8-71
	8.5.1 Glaciochemical Data	8-72
	8.5.1.1 Sulfate - Polar Glaciers	8-73
	8.5.1.2 Nitrate - Polar Glaciers	8-73
	8.5.1.3 pH and Acidity - Polar Glaciers	8-74
	8.5.1.4 Sulfate - Alpine Glaciers	8-74
	8.5.1.5 Nitrate - Alpine Glaciers	8-74
	8.5.1.6 pH and Acidity - Alpine Glaciers	8-75
	8.5.2 Trace Metals - General Statement	8-75
	8.5.2.1 Trace Metals - Polar Glaciers	8-76
	8.5.2.2 Trace Metals - Alpine Glaciers	8-77
	8.5.3 Discussion and Future Work	8-78
8.6	Conclusions	8-80
8.7	References	8-85

A-9 LONG-RANGE TRANSPORT AND ACIDIC DEPOSITION MODELS

9.1	Introduction	9-1
	9.1.1 General Principles for Formulating Pollution Transport and Diffusion Models	9-1
	9.1.2 Model Characteristics	9-3
	9.1.2.1 Spatial and Temporal Scales	9-3
	9.1.2.2 Treatment of Turbulence	9-3

Table of Contents (continued)

		Page
	9.1.2.3 Reaction Mechanisms	9-5
	9.1.2.4 Removal Mechanisms	9-5
9.1.3	Selecting Models for Application	9-6
	9.1.3.1 General	9-6
	9.1.3.2 Spatial Range of Application	9-6
	9.1.3.3 Temporal Range of Application	9-6
9.2	Types of LRT Models	9-9
9.2.1	Eulerian Grid Models	9-9
9.2.2	Lagrangian Models	9-9
	9.2.2.1 Lagrangian Trajectory Models	9-9
	9.2.2.2 Statistical Trajectory Models	9-11
9.2.3	Hybrid Models	9-13
9.3	Modules Associated with Chemical (Transformation) Processes	9-13
9.3.1	Overview	9-13
9.3.2	Chemical Transformation Modeling	9-14
	9.3.2.1 Simplified Modules	9-14
	9.3.2.2 Multireaction Modules	9-15
9.3.3	Modules for NO_x Transformation	9-16
9.4	Modules Associated with Wet and Dry Deposition	9-17
9.4.1	Overview	9-17
9.4.2	Modules for Wet Deposition	9-20
	9.4.2.1 Formulation and Mechanism	9-20
	9.4.2.2 Modules Used in Existing Models	9-21
	9.4.2.3 Wet Deposition Modules for Snow	9-23
	9.4.2.4 Wet Deposition Modules for NO_x	9-23
9.4.3	Modules for Dry Deposition	9-24
	9.4.3.1 General Considerations	9-24
	9.4.3.2 Modules Used in Existing Models	9-25
	9.4.3.3 Dry Deposition Modules for NO_x	9-26
9.4.4	Dry Versus Wet Deposition	9-26
9.5	Status of LRT Models as Operational Tools	9-26
9.5.1	Overview	9-26
9.5.2	Model Application	9-27
	9.5.2.1 Limitations in Applicability	9-27
	9.5.2.2 Regional Concentration and Deposition Patterns	9-27
	9.5.2.3 Use of Matrix Methods to Quantify Source-Receptor Relationships	9-28
9.5.3	Data Requirements	9-33
	9.5.3.1 General	9-33
	9.5.3.2 Specific Characteristics of Data Used in Model Simulations	9-36
	9.5.3.2.1 Emissions	9-36
	9.5.3.2.2 Meteorological Data	9-37
9.5.4	Model Performance and Uncertainties	9-37
	9.5.4.1 General	9-37
	9.5.4.2 Data Bases Available for Evaluating Models	9-39
	9.5.4.3 Performance Measures	9-39
	9.5.4.4 Representativeness of Measurements	9-40
	9.5.4.5 Uncertainties	9-40
	9.5.4.6 Selected Results	9-40
9.6	Conclusions	9-46
9.7	References	9-48

THE ACIDIC DEPOSITION PHENOMENON AND ITS EFFECTS:
CRITICAL ASSESSMENT REVIEW PAPERS

Table of Contents

Volume II
Effects Sciences

Page

AUTHORS iii

PREFACE ix

ABBREVIATION-ACRONYM LIST xxix

GLOSSARY xliii

E-1 INTRODUCTION

1.1 Objectives 1-1
1.2 Approach 1-1
1.3 Chapter Organization and General Content 1-3
1.3.1 Effects on Soil Systems 1-3
1.3.2 Effects on Vegetation 1-4
1.3.3 Effects on Aquatic Chemistry 1-5
1.3.4 Effects on Aquatic Biology 1-5
1.3.5 Indirect Effects on Health 1-6
1.3.6 Effects on Materials 1-6
1.4 Acidic Deposition 1-6
1.5 Linkage to Atmospheric Sciences 1-7
1.6 Sensitivity 1-7
1.7 Presentation Limitations 1-7

E-2 EFFECTS ON SOIL SYSTEMS

2.1 Introduction 2-1
2.1.1 Importance of Soils to Aquatic Systems 2-1
2.1.1.1 Soils Buffer Precipitation Enroute to Aquatic Systems ... 2-2
2.1.1.2 Soil as a Source of Acidity for Aquatic Systems 2-2
2.1.2 Soil's Importance as a Medium for Plant Growth 2-2
2.1.3 Important Soil Properties 2-2
2.1.3.1 Soil Physical Properties 2-3
2.1.3.2 Soil Chemical Properties 2-3
2.1.3.3 Soil Microbiology 2-3
2.1.4 Flow of Deposited Materials Through Soil Systems 2-3
2.2 Chemistry of Acid Soils 2-5
2.2.1 Development of Acid Soils 2-5
2.2.1.1 Biological Sources of H^+ Ions 2-6
2.2.1.2 Acidity from Dissolved Carbon Dioxide 2-6
2.2.1.3 Leaching of Basic Cations 2-7
2.2.2 Soil Cation Exchange Capacity 2-8
2.2.2.1 Source of Cation Exchange Capacity in Soils 2-8
2.2.2.2 Exchangeable Bases and Base Saturation 2-8
2.2.3 Exchangeable and Solution Aluminum in Soils 2-9
2.2.4 Exchangeable and Solution Manganese in Soils 2-12
2.2.5 Practical Effects of Low pH 2-12
2.2.6 Neutralization of Soil Acidity 2-13
2.2.7 Measuring Soil pH 2-14
2.2.8 Sulfate Adsorption 2-15
2.2.9 Soil Chemistry Summary 2-18
2.3 Effects of Acidic Deposition on Soil Chemistry and Plant Nutrition 2-18
2.3.1 Effects on Soil pH 2-19
2.3.2 Effects on Nutrient Supply of Cultivated Crops 2-24
2.3.3 Effects on Nutrient Supply to Forests 2-28

Table of Contents (continued)

Page

2.3.3.1 Effects on Cation Nutrient Status 2-28
2.3.3.2 Effects on S and N Status 2-31
2.3.3.3 Acidification Effects on Plant Nutrition 2-33
2.3.3.3.1 Nutrient deficiencies 2-33
2.3.3.3.2 Metal ion toxicities 2-33
2.3.3.3.2.1 Aluminum toxicity 2-34
2.3.3.3.2.2 Manganese toxicity 2-35
2.3.4 Reversibility of Effects on Soil Chemistry 2-35
2.3.5 Predicting Which Soils will be Affected Most 2-36
2.3.5.1 Soils Under Cultivation 2-36
2.3.5.2 Uncultivated, Unamended Soils 2-36
2.3.5.2.1 Basic cation-pH changes in forested soils 2-37
2.3.5.2.2 Changes in aluminum concentration in soil solution in forested soils 2-40
2.4 Effects of Acidic Deposition on Soil Biology 2-40
2.4.1 Soil Biology Components and Functional Significance 2-40
2.4.1.1 Soil Animals 2-40
2.4.1.2 Algae 2-40
2.4.1.3 Fungi 2-41
2.4.1.4 Bacteria 2-41
2.4.2 Direct Effects of Acidic Deposition on Soil Biology 2-42
2.4.2.1 Soil Animals 2-42
2.4.2.2 Terrestrial Algae 2-42
2.4.2.3 Fungi 2-43
2.4.2.4 Bacteria 2-43
2.4.2.5 General Biological Processes 2-44
2.4.3 Metals--Mobilization Effects on Soil Biology 2-45
2.4.4 Effects of Changes in Microbial Activity on Aquatic Systems 2-46
2.4.5 Soil Biology Summary 2-46
2.5 Effects of Acidic Deposition on Organic Matter Decomposition 2-47
2.6 Effects of Soils on the Chemistry of Aquatic Ecosystems 2-52
2.7 Conclusions 2-54
2.8 References 2-57

E-3 EFFECTS ON VEGETATION

3.1 Introduction 3-1
3.1.1 Overview 3-1
3.1.2 Background 3-1
3.2 Plant Response to Acidic Deposition 3-3
3.2.1 Leaf Response to Acidic Deposition 3-3
3.2.1.1 Leaf Structure and Functional Modifications 3-5
3.2.1.2 Foliar Leaching - Throughfall Chemistry 3-8
3.2.2 Effects of Acidic Deposition on Lichens and Mosses 3-13
3.2.3 Summary 3-16
3.3 Interactive Effects of Acidic Deposition with Other Environmental Factors on Plants 3-17
3.3.1 Interactions with Other Pollutants 3-17
3.3.2 Interactions with Phytophagous Insects 3-20
3.3.3 Interactions with Pathogens 3-20
3.3.4 Influence on Vegetative Hosts That Would Alter Relationships with Insect or Microbial Associate 3-23
3.3.5 Effects of Acidic Deposition on Pesticides 3-23
3.3.6 Summary 3-25
3.4 Biomass Production 3-26
3.4.1 Forests 3-26
3.4.1.1 Possible Mechanisims of Response 3-27
3.4.1.2 Phenological Effects 3-29
3.4.1.2.1 Seed germination and seedling establishment .. 3-29
3.4.1.2.2 Mature and reproductive stages 3-32
3.4.1.3 Growth of Seedlings and Trees in Irrigation Experiments 3-32

Table of Contents (continued)

Page

3.4.1.4 Studies of Long-Term Growth of Forest Trees 3-33
3.4.1.5 Dieback and Decline in High Elevation Forests 3-36
3.4.1.6 Recent Observations on the German Forest Decline Phenomenon 3-39
3.4.1.7 Summary 3-41
3.4.2 Crops 3-41
3.4.2.1 Review and Analysis of Experimental Design 3-42
3.4.2.1.1 Dose-response determination 3-42
3.4.2.1.2 Sensitivity classification 3-44
3.4.2.1.3 Mechanisms 3-44
3.4.2.1.4 Characteristics of precipitation simulant exposures 3-45
3.4.2.1.5 Yield criteria 3-45
3.4.2.2 Experimental Results 3-46
3.4.2.2.1 Field studies 3-46
3.4.2.2.2 Controlled environment studies 3-50
3.4.2.3 Discussion 3-58
3.4.2.4 Summary 3-61
3.5 Conclusions 3-61
3.6 References 3-64

E-4 EFFECTS ON AQUATIC CHEMISTRY

4.1 Introduction 4-1
4.2 Basic Concepts Required to Understand the Effects of Acidic Deposition on Aquatic Systems 4-2
4.2.1 Receiving Systems 4-2
4.2.2 pH, Conductivity, and Alkalinity 4-3
4.2.2.1 pH 4-3
4.2.2.2 Conductivity 4-4
4.2.2.3 Alkalinity 4-5
4.2.3 Acidification 4-6
4.3 Sensitivity of Aquatic Systems to Acidic Deposition 4-7
4.3.1 Atmospheric Inputs 4-7
4.3.1.1 Components of Deposition 4-7
4.3.1.2 Loading vs Concentration 4-8
4.3.1.3 Location of the Deposition 4-8
4.3.1.4 Temporal Distribution of Deposition 4-9
4.3.1.5 Importance of Atmospheric Inputs to Aquatic Systems 4-9
4.3.1.5.1 Nitrogen (N), phosphorus (P), and carbon (C) 4-9
4.3.1.5.2 Sulfur 4-10
4.3.2 Characteristics of Receiving Systems Relative to Being Able to Assimilate Acidic Deposition 4-13
4.3.2.1 Canopy 4-13
4.3.2.2 Soil 4-14
4.3.2.3 Bedrock 4-16
4.3.2.4 Hydrology 4-17
4.3.2.4.1 Flow paths 4-17
4.3.2.4.2 Residence times 4-22
4.3.2.5 Wetlands 4-23
4.3.2.6 Aquatic 4-24
4.3.2.6.1 Alkalinity as an indicator of sensitivity 4-24
4.3.2.6.2 International production/consumption of ANC 4-28
4.3.2.6.3 Aquatic sediments 4-31
4.3.3 Location of Sensitive Systems 4-32
4.3.4 Summary--Sensitivity 4-35
4.4 Magnitude of Chemical Effects of Acidic Deposition on Aquatic Ecosystems 4-38

Table of Contents (continued)

		Page
4.4.1	Relative Importance of HNO_3 vs H_2SO_4	4-39
4.4.2	Short-Term Acidification	4-45
4.4.3	Long-Term Acidification	4-48
4.4.3.1	Analysis of Trends based on Historic Measurements of Surface Water Quality	4-53
4.4.3.1.1	Methodological problems with the evaluation of historical trends	4-53
4.4.3.1.1.1	pH	4-54
4.4.3.1.1.1.1	pH-early methodology	4-54
4.4.3.1.1.1.2	pH-current methodology	4-55
4.4.3.1.1.1.3	pH-comparability of early and current measurement methods	4-56
4.4.3.1.1.1.4	pH-general problems	4-57
4.4.3.1.1.2	Conductivity	4-60
4.4.3.1.1.2.1	Conductivity methodology	4-60
4.4.3.1.1.2.2	Conductivity-comparability of early and current measurement methods	4-60
4.4.3.1.1.2.3	Conductivity-general problems	4-61
4.4.3.1.1.3	Alkalinity	4-61
4.4.3.1.1.3.1	Alkalinity-early methodology	4-61
4.4.3.1.1.3.2	Alkalinity-current methodology	4-62
4.4.3.1.1.3.3	Alkalinity-comparability of early and current measurement methods	4-63
4.4.3.1.1.4	Sample storage	4-63
4.4.3.1.1.5	Summary of measurement techniques	4-63
4.4.3.1.2	Analysis of trends	4-64
4.4.3.1.2.1	Introduction	4-64
4.4.3.1.2.2	Canadian studies	4-66
4.4.3.1.2.3	United States studies	4-74
4.4.3.1.3	Summary--trends in historic data	4-98
4.4.3.2	Assessment of Trends Based on Paleolimnological Technique	4-99
4.4.3.2.1	Calibration and accuracy of paleolimnological reconstruction of pH history	4-100
4.4.3.2.2	Lake acidification determined by paleolimnological reconstruction	4-100
4.4.3.3	Alternate Explanations for Acidification-Land Use Changes	4-105
4.4.3.3.1	Variations in the groundwater table	4-105
4.4.3.3.2	Accelerated mechanical weathering or land scarification	4-105
4.4.3.3.3	Decomposition of organic matter	4-106
4.4.3.3.4	Changes in vegetation	4-106
4.4.3.3.5	Chemical amendments	4-107
4.4.3.3.6	Summary--alternate explanations for acidification	4-107

Table of Contents (continued)

		Page
4.4.4	Summary--Magnitude of Chemical Effects of Acidic Deposition	4-109
4.5	Predictive Modeling of the Effects of Acidic Deposition on Surface Waters	4-113
4.5.1	Almer/Dickson Relationship	4-114
4.5.2	Henriksen's Predictor Nomograph	4-119
4.5.3	Thompson's Cation Denudation Rate Model (CDR)	4-121
4.5.4	"Trickle-Down" Model	4-122
4.5.5	Summary of Predictive Modeling	4-125
4.6	Indirect Chemical Changes Associated with Acidification of Surface Waters	4-128
4.6.1	Metals	4-128
4.6.1.1	Increased Loading of Metals From Atmospheric Deposition	4-129
4.6.1.2	Mobilization of Metals by Acidic Deposition	4-130
4.6.1.3	Secondary Effects of Metal Mobilization	4-131
4.6.1.4	Effects of Acidification on Aqueous Metal Speciation	4-132
4.6.1.5	Indirect Effects on Metals in Surface Waters	4-132
4.6.2	Aluminum Chemistry in Dilute Acidic Waters	4-132
4.6.2.1	Occurrence, Distribution, and Sources of Aluminum	4-132
4.6.2.2	Aluminum Speciation	4-136
4.6.2.3	Aluminum as a pH Buffer	4-136
4.6.2.4	Temporal and Spatial Variations in Aqueous Levels of Aluminum	4-137
4.6.2.5	The Role of Aluminum in Altering Element Cycling Within Acidic Waters	4-140
4.6.3	Organics	4-141
4.6.3.1	Atmospheric Loading of Strong Acids and Associated Organic Micropollutants	4-141
4.6.3.2	Organic Buffering Systems	4-142
4.6.3.3	Organo-Metallic Interactions	4-142
4.6.3.4	Photochemistry	4-143
4.6.3.5	Carbon-Phosphorus-Aluminum Interactions	4-143
4.6.3.6	Effects of Acidification on Organic Decomposition in Aquatic Systems	4-144
4.7	Mitigative Strategies for Improvement of Surface Water Quality	4-144
4.7.1	Base Additions	4-144
4.7.1.1	Types of Basic Materials	4-144
4.7.1.2	Direct Water Addition of Base	4-148
4.7.1.2.1	Computing base dose requirements	4-148
4.7.1.2.2	Methods of base application	4-152
4.7.1.3	Watershed Addition of Base	4-154
4.7.1.3.1	The concept of watershed application of base	4-154
4.7.1.3.2	Experience in watershed liming	4-156
4.7.1.4	Water Quality Response to Base Treatment	4-158
4.7.1.5	Cost Analysis, Conclusions and Assessment of Base Addition	4-160
4.7.1.5.1	Cost analysis	4-160
4.7.1.5.2	Summary--base additions	4-162
4.7.2	Surface Water Fertilization	4-162
4.7.2.1	The Fertilization Concept	4-162
4.7.2.2	Phosphorous Cycling in Acidified Water	4-164
4.7.2.3	Fertilization Experience and Water Quality Response to Fertilization	4-164
4.7.2.4	Summary--Surface Water Fertilization	4-166
4.8	Conclusions	4-166
4.9	References	4-169

Table of Contents (continued)

Page

E-5 EFFECTS ON AQUATIC BIOLOGY

5.1 Introduction 5-1
5.2 Biota of Naturally Acidic Waters 5-3
5.2.1 Types of Naturally Acidic Waters 5-3
5.2.2 Biota of Inorganic Acidotrophic Waters 5-4
5.2.3 Biota in Acidic Brownwater Habitats 5-5
5.2.4 Biota in Ultra-Oligotrophic Waters 5-7
5.2.5 Summary 5-9
5.3 Benthic Organisms 5-14
5.3.1 Importance of the Benthic Community 5-14
5.3.2 Effects of Acidification on Components of the Benthos 5-16
5.3.2.1 Microbial Community 5-16
5.3.2.2 Periphyton 5-17
5.3.2.2.1 Field surveys 5-17
5.3.2.2.2 Temporal trends 5-18
5.3.2.2.3 Experimental studies 5-20
5.3.2.3 Microinvertebrates 5-21
5.3.2.4 Crustacea 5-22
5.3.2.5 Insecta 5-24
5.3.2.5.1 Sensitivity of different groups 5-24
5.3.2.5.2 Sensitivity of insects from different microhabitats 5-29
5.3.2.5.3 Acid sensitivity of insects based on food sources 5-29
5.3.2.5.4 Mechanisms of effects and trophic interactions 5-29
5.3.2.6 Mollusca 5-30
5.3.2.7 Annelida 5-31
5.3.2.8 Summary of Effects of Acidification on Benthos 5-32
5.4 Macrophytes and Wetland Plants 5-37
5.4.1 Introduction 5-37
5.4.2 Effects on Acidification on Aquatic Macrophytes 5-41
5.4.3 Summary 5-43
5.5 Plankton 5-44
5.5.1 Introduction 5-44
5.5.2 Effects of Acidification on Phytoplankton 5-45
5.5.2.1 Changes in Species Composition 5-45
5.5.2.2 Changes in Phytoplankton Biomass and Productivity 5-52
5.5.3 Effects of Acidification on Zooplankton 5-55
5.5.4 Explanations and Significance 5-67
5.5.4.1 Changes in Species Composition 5-67
5.5.4.2 Changes in Productivity 5-70
5.5.5 Summary 5-72
5.6 Fish 5-74
5.6.1 Introduction 5-74
5.6.2 Field Observations 5-75
5.6.2.1 Loss of Populations 5-75
5.6.2.1.1 United States 5-75
5.6.2.1.1.1 Adirondack Region of New York State 5-75
5.6.2.1.1.2 Other regions of the eastern United States 5-79
5.6.2.1.2 Canada 5-79
5.6.2.1.2.1 LaCloche Mountain Region of Ontario 5-79
5.6.2.1.2.2 Other areas of Ontario 5-83
5.6.2.1.2.3 Nova Scotia 5-83
5.6.2.1.3 Scandinavia and Great Britain 5-88
5.6.2.1.3.1 Norway 5-88
5.6.2.1.3.2 Sweden 5-93
5.6.2.1.3.3 Scotland 5-93

Table of Contents (continued)

	Page
5.6.2.2 Population Structure	5-93
5.6.2.3 Growth	5-98
5.6.2.4 Episodic Fish Kills	5-99
5.6.2.5 Accumulation of Metals in Fish	5-101
5.6.3 Field Experiments	5-101
5.6.3.1 Experimental Acidification of Lake 223 Ontario	5-102
5.6.3.2 Experimental Acidification of Norris Brook, New Hampshire	5-104
5.6.3.3 Exposure of Fish to Acidic Surface Waters	5-104
5.6.4 Laboratory Experiments	5-108
5.6.4.1 Effects of Low pH	5-109
5.6.4.1.1 Survival	5-109
5.6.4.1.2 Reproduction	5-112
5.6.4.1.3 Growth	5-119
5.6.4.1.4 Behavior	5-119
5.6.4.1.5 Physiological responses	5-120
5.6.4.2 Effects of Aluminum and Other Metals in Acidic Waters	5-122
5.6.5 Summary	5-125
5.6.5.1 Extent of Impact	5-125
5.6.5.2 Mechanism of Effect	5-127
5.6.5.3 Relationship Between Water Acidity and Fish Population Response	5-128
5.7 Other Related Biota	5-129
5.7.1 Amphibians	5-129
5.7.2 Birds	5-134
5.7.2.1 Food Chain Alterations	5-134
5.7.2.2 Heavy Metal Accumulation	5-134
5.7.3 Mammals	5-135
5.7.4 Summary	5-136
5.8 Observed and Anticipated Ecosystem Effects	5-139
5.8.1 Ecosystem Structure	5-139
5.8.2 Ecosystem Function	5-141
5.8.2.1 Nutrient Cycling	5-141
5.8.2.2 Energy Cycling	5-141
5.8.3 Summary	5-142
5.9 Mitigative Options Relative to Biological Populations at Risk	5-143
5.9.1 Biological Response to Neutralization	5-143
5.9.2 Improving Fish Survival in Acidified Waters	5-145
5.9.2.1 Genetic Screening	5-145
5.9.2.2 Selective Breeding	5-145
5.9.2.3 Acclimation	5-146
5.9.2.4 Limitations of Techniques to Improve Fish Survival	5-148
5.9.3 Summary	5-149
5.10 Conclusions	5-149
5.10.1 Effects of Acidification on Aquatic Organisms	5-149
5.10.2 Processes and Mechanisms by Which Acidification Alters Aquatic Ecosystems	5-155
5.10.2.1 Direct Effects of Hydrogen Ions	5-155
5.10.2.2 Elevated Metal Concentrations	5-156
5.10.2.3 Altered Trophic-Level Interactions	5-156
5.10.2.4 Altered Water Clarity	5-157
5.10.2.5 Altered Decomposition of Organic Matter	5-157
5.10.2.6 Presence of Algal Mats	5-157
5.10.2.7 Altered Nutrient Availability	5-157
5.10.2.8 Interaction of Stresses	5-157
5.10.3 Biological Mitigation	5-158
5.10.4 Summary	5-159
5.11 References	5-160

Table of Contents (continued)

Page

E-6 INDIRECT EFFECTS ON HEALTH

6.1 Introduction 6-1
6.2 Food Chain Dynamics 6-1
6.2.1 Introduction 6-1
6.2.2 Availability and Bioaccumulation of Toxic Metals 6-2
6.2.2.1 Speciation (Mercury) 6-2
6.2.2.2 Concentrations and Speciations in Water (Mercury) 6-4
6.2.2.3 Flow of Mercury in the Environment 6-4
6.2.2.3.1 Global cycles 6-4
6.2.2.3.2 Biogeochemical cycles of mercury 6-5
6.2.3 Accumulation in Fish 6-10
6.2.3.1 Factors Affecting Mercury Concentrations in Fish 6-10
6.2.3.2 Historical and Geographic Trends in Mercury Levels in Freshwater Fish 6-20
6.2.4 Dynamics and Toxicity in Humans (Mercury) 6-22
6.2.4.1 Dynamics in Man (Mercury) 6-22
6.2.4.2 Toxicity in Man 6-23
6.2.4.3 Human Exposure from Fish and Potential for Health Risks 6-27
6.3 Ground, Surface and Cistern Waters as Affected by Acidic Deposition 6-31
6.3.1 Water Supplies 6-32
6.3.1.1 Direct Use of Precipitation (Cisterns) 6-32
6.3.1.2 Surface Water Supplies 6-34
6.3.1.3 Groundwater Supplies 6-37
6.3.2 Lead 6-39
6.3.2.1 Concentrations in Noncontaminated Waters 6-39
6.3.2.2 Factors Affecting Lead Concentrations in Water, Including Effects of pH 6-39
6.3.2.3 Speciation of Lead in Natural Water 6-41
6.3.2.4 Dynamics and Toxicity of Lead in Humans 6-41
6.3.2.4.1 Dynamics of lead in humans 6-41
6.3.2.4.2 Toxic effects of lead on humans 6-42
6.3.2.4.3 Intake of lead in water and potential for human health effects 6-49
6.3.3 Aluminum 6-51
6.3.3.1 Concentrations in Uncontaminated Waters 6-53
6.3.3.2 Factors Affecting Aluminum Concentrations in Water 6-53
6.3.3.3 Speciation of Aluminum in Water 6-54
6.3.3.4 Dynamics and Toxicity in Humans 6-54
6.3.3.4.1 Dynamics of aluminum in humans 6-54
6.3.3.4.2 Toxic effects of aluminum in humans 6-55
6.3.3.5 Human Health Risks from Aluminum in Water 6-55
6.4 Other Metals 6-55
6.5 Conclusions 6-56
6.6 References 6-58

E-7 EFFECTS ON MATERIALS

7.1 Direct Effects on Materials 7-1
7.1.1 Introduction 7-1
7.1.1.1 Long Range and Local Effects 7-2
7.1.1.2 Inaccurate Claims of Acid Rain Damage to Materials 7-2
7.1.1.3 Complex Mechanisms of Exposure and Deposition 7-5
7.1.1.4 Deposition Velocities 7-6
7.1.1.5 Laboratory vs Field Studies 7-6
7.1.2 Damage to Materials by Acidic Deposition 7-8
7.1.2.1 Metals 7-9
7.1.2.1.1 Ferrous Metals 7-11
7.1.2.1.1.1 Laboratory Studies 7-13
7.1.2.1.1.2 Field Studies 7-14

Table of Contents (continued)

		Page
7.1.2.1.2	Nonferrous Metals	7-17
7.1.2.1.2.1	Aluminum	7-17
7.1.2.1.2.2	Copper	7-19
7.1.2.1.2.3	Zinc	7-19
7.1.2.2	Masonry	7-20
7.1.2.2.1	Stone	7-20
7.1.2.2.2	Concrete	7-26
7.1.2.2.3	Ceramics and Glass	7-27
7.1.2.3	Paint	7-27
7.1.2.4	Other Materials	7-31
7.1.2.4.1	Paper	7-32
7.1.2.4.2	Photographic Materials	7-32
7.1.2.4.3	Textiles and Textile Dyes	7-32
7.1.2.4.4	Leather	7-34
7.1.2.5	Cultural Property	7-34
7.1.2.5.1	Architectural Monuments	7-34
7.1.2.5.2	Museums, Libraries and Archives	7-34
7.1.2.5.3	Medieval Stained Glass	7-35
7.1.2.5.4	Conservation and Mitigation Costs	7-35
7.1.2.6	Economic Implications	7-37
7.1.2.6	Mitigative Measures	7-38
7.2	Potential Secondary Effects of Acidic Deposition on Potable Water Piping Systems	7-39
7.2.1	Introduction	7-39
7.2.2	Problems Caused by Corrosion	7-39
7.2.2.1	Health	7-39
7.2.2.2	Aesthetics	7-40
7.2.2.3	Economics	7-40
7.2.3	Principles of Corrosion	7-40
7.2.4	Factors Affecting Internal Piping Corrosion	7-42
7.2.5	Corrosion of Materials Used in Plumbing and Water Distribution Systems	7-48
7.2.5.1	Corrosion of Iron Pipe	7-48
7.2.5.2	Corrosion of Galvanized Pipe	7-49
7.2.5.3	Corrosion of Copper Pipe	7-49
7.2.5.4	Corrosion of Lead Pipe	7-49
7.2.5.5	Corrosion of Non-Metallic Pipe	7-50
7.2.6	Metal Leaching	7-50
7.2.6.1	Standing vs Running Samples	7-50
7.2.6.2	Metals Surveys	7-51
7.2.7	Corrosion Control Strategies	7-53
7.2.8	Economics	7-53
7.3	Conclusions	7-54
7.4	References	7-58

ABBREVIATION-ACRONYM LIST

δ-ALA	δ-aminolevulinic acid
ACHEX	Aerosol Characterization Experiment
ADI	Acceptable daily intake
Ag	Silver
AI	Aggresiveness index
Al	Aluminum
Al^{3+}	Aluminum ion
Al_2O_3	Aluminum oxide
$Al_2Si_2O_5(OH)_4$	Aluminosilicate
AL	Aeronomy Laboratory, NOAA
$Al(OH)_2H_2PO_4$	Varascite
$Al(OH)_3$	Aluminum hydroxide
ANC	Acid neutralizing capacity
APN	Air and Precipitation Monitoring Network
ARL	Air Resources Lab, NOAA
ARS	Agricultural Research Service, DOA
As	Arsenic
ASTRAP	Advanced Statistical Trajectory Regional Air Pollution Control Model
AWWA	American Water Works Association
B	Boron
BCF	Bioconcentration factor
BLM	Bureau of Land Management, DOI
BLMs	Boundary layer models

BM	Bureau of Mines, DOI
BNC	Base neutralizing capacity
BNC aq	Aqueous base neutralizing capacity
BOD	Biologic oxygen demand
Br	Bromine
BS	Base saturation
BSC	Base saturation capacity
BUREC	Bureau of Reclamation, DOI
BWCA	Boundary Water Canoe Area
C_B	Base cation level
Ca	Calcium
Ca^{2+}	Calcium ion
$CaCl_2$	Calcium chloride
$CaCO_3$	Calcium carbonate or crystalline calcite - limestone
$CaCO_3 \cdot MgCO_3$	Dolomite
$Ca(HCO_3)_2$	Calcium bicarbonate
CaO	Calcium oxide - lime
$Ca(OH)_2$	Calcium hydroxide - lime
$CaSO_4$	Calcium sulfate, sulfate salt
$CaSO_4 \cdot K_2SO_4 \cdot H_2O$	Syngenite
CAMP	Continuous Air Monitoring Program
CANSAP	Canadian Network for Sampling Acid Precipitation
CAPTEX	Cross-Appalachian Transport Experiment
CCN	Cloud condensation nuclei
Cd	Cadmium
CDR	Cation denudation rate

CEC	Cation exchange capacity
CEQ	Council on Environmental Quality
CH_3Br	Methyl bromide
CH_3Cl	Methyl chloride
CH_3COOH	Acetic acid
$(CH_3)_2Hg$	Dimethyl mercury
CH_3O	Methoxy radical
$(CH_3)_2S$	Dimethyl sulfide (also CH_3SCH_3)
$(CH_3)_2S_2$	Dimethyl disulfide
CH_3SH	Methyl sulfide (or methyl mercaptan)
CH_4	Methane
Cl^-	Chloride ion
Cl_2	Elemental chlorine
cm^3 molecule^{-1} s^{-1}	Cubic centimeters per molecule per second
cm	Centimeter
cm s^{-1}	Centimeters per second
cm yr^{-1}	Centimeters per year
CO	Carbon monoxide
CO_2	Carbon dioxide
-COOH	Carboxyl
COS	Carbonyl sulfide
Cr	Chromium
CS_2	Carbon disulfide
CSI	Calcite saturation index
CSRS	Cooperative States Research Service, DOA
Cu	Copper

DEC	Department of Environmental Conservation, NY
DFI	Driving force index
DO	Dissolved oxygen
DOA	Department of Agriculture
DOC	Dissolved organic carbon
DOD	Department of Defense
DOE	Department of Energy
DOI	Department of Interior
DOS	Department of State
ELA	Experimental Lakes Area
emf	Electromotive force
ENAMAP	Eastern North America Model of Air Pollutants
EPA	Environmental Protection Agency
EPRI	Electric Power Research Institute
eq	Equivalent
$eq\ ha^{-1}\ y^{-1}$	Equivalents per hectare per year
ERDA	Energy Research and Development Agency (defunct)
ESRL	Environmental Sciences Research Laboratory, EPA
F^-	Fluoride ion
FA	Fulvic acid
FDA	Flourescein diacetate
FDA	Food and Drug Administration
Fe	Iron
FeS_2	Pyrite
Fe_2SiO_4	Olivine (and Mg_2SiO_4)

$FeSO_4$	Ferrous sulfate
FEP	Free erythrocyte protoporphyrin
FGD	Flue gas desulfurization
FS	Forest Service, DOA
FWS	Fish and Wildlife Service, DOI
g	Gram
g ℓ^{-1}	Grams per liter
g dry wt m^{-2}	Grams dry weight per square meter
g m^{-2}	Grams per square meter
g m^{-2} s^{-1}	Grams per square meter per second
g m^{-2} yr^{-1}	Grams per square meter per year
g ha^{-1} hr^{-1}	Grams per hectare per hour
GAMETAG	Global Atmospheric Measurement Experiment of Tropospheric Aerosols and Gases
GTN	Global Trends Network
H	Hydrogen
H^+	Hydrogen ion
H_2CO_3	Carbonic acid
H_2O_2	Hydrogen peroxide
H_2O	Water
H_2S	Hydrogen sulfide
H_2SO_4	Sulfuric acid
H_3PO_4	Phosphoric acid
ha	Hectare
HAOS	Houston Area Oxidant Study
HC	Hydrocarbon

HCl	Hydrochloric acid
HCO_3^-	Bicarbonate ion
HCOH	Formaldehyde
HCOOH	Formic acid
HF	Hydrogen fluoride
Hg	Mercury
HIVOL	High-volume
Hg^{2+}	Mercuric ion
$HgCl_2$	Mercuric chloride
HgS	Mercuric sulfide
HHS	Department of Health and Human Services
HNO_2	Nitrous acid
HNO_3	Nitric acid
HO_2	Peroxy radical
HO_2NO_2	Pernitric acid
HO	Hydroxyl
HONO	Nitrous acid
$HOSO_2$	Bisulfite
hr	Hours
ILWAS	Integrated Lake Watershed Acidification Study
IRMA	Immission rate measuring apparatus
K	Potassium
K^+	Potassium ion
KCl	Potassium chloride
K_2SO_4	Potassium sulfate, sulfate salt
keq ha^{-1}	Kiloequivalents per hectare

keq ha^{-1} yr^{-1}	Kiloequivalents per hectare per year
kg	Kilogram
kg ha^{-1}	Kilograms per hectare
kg ha^{-1} wk^{-1}	Kilograms per hectare per week
kg km^{-2} yr^{-1}	Kilograms per square kilometer per year
kg ha^{-1} yr^{-1}	Kilograms per hectare per year
KHM	Kol-Halsa-Miljo Project
KJ mol^{-1}	Kilojoule per mole
km	Kilometer
km^2	Square kilometer
km hr^{-1}	Kilometers per hour
$KMnO_4$	Potassium permanganate
ℓ	Liter
(ℓ)	Liquid phase
ℓ m^{-3}	Liters per cubic meter
LAI	Leaf area index
LI	Langelier's index
LIMB	Limestone Injection/Multistage Burner
LR	Larson's ration
LRTAP	Long-Range Transport of Air Pollutants
LSI	Langelier Saturation Index
m^2	Square meter
m^3 yr^{-1}	Cubic meter per year
μeq	Microequivalent
μeq $ℓ^{-1}$	Microequivalents per liter

μg	Micrograms
μg ℓ^{-1}	Micrograms per liter
μg 100 ml^{-1}	Micrograms per 100 milliliters
μg dl^{-1}	Micrograms per decaliter
μg m^{-3}	Micrograms per cubic meter
μm	Micrometer
μm ℓ^{-1}	Micrometers per liter
μM	Micromolar
μm yr^{-1}	Micrometers per year
μmho cm^{-1}	micromhos per centimeter (conductivity)
m	Meter
M	Molar
m s-1	Meters per second
m yr^{-1}	Meters per year
MAP3S	Multi-State Atmospheric Power Production Pollution Study
mb	Millibars
MCC	Mesoscale convective complex
MCL	Maximum contaminant level
MCPS	Mesoscale convective precipitation systems
ME	Momentary excess
meq ℓ^{-1}	Milliequivalents per liter
meq 100 g-1	Milliequivalents per 100 grams
meq m^{-2} yr^{-1}	Milliequivalents per square meter per year
METROMEX	Metropolitan Meteorological Experiment
Mg	Magnesium

Mg^{2+}	Magnesium ion
mg	Milligram
mg ℓ^{-1}	Milligrams per liter
mg m^{-3} hr^{-1}	Milligrams per cubic meter per hour
$MgCO_3$	Magnesium carbonate
Mg_2SiO_4	Olivine and (Fe_2SiO_4)
$MgSO_4$	Magnesium sulfate, sulfate salt
mho cm^{-1}	mhos per centimeter (conductivity)
MISTT	Midwest Interstate Sulfur Transport and Transformations
mm	Millimeter
mm hr^{-1}	Millimeters per hour
mm s^{-1}	Millimeters per second
mm yr^{-1}	Millimeters per year
mM	Millimolar
Mn	Manganese
Mo	Molybdenum
MOI	Memorandum of Intent on Transboundary Air Pollution
mol	Mole
mol ℓ^{-1}	Moles per liter
mol ℓ^{-1} atm^{-1}	Moles per liter per atmosphere
mT	Metric ton
mT yr^{-1}	Metric tons per year
MW	Megawatt
N_2O_4	NO_2 dimer
N_2O_5	Nitrogen pentoxide

N_2O	Nitrous oxide
(-NH)	Imide
N	Nitrogen
N(III)	Liquid phase nitrogen
Na	Sodium
Na^+	Sodium ion
NaCl	Sodium chloride
Na_2CO_3	Sodium carbonate
$NaNO_2$	Sodium nitrite
Na_2SO_4	Sodium sulfate, sulfate salt
NADP	National Atmospheric Deposition Program
NAS	National Academy of Sciences
NASA	National Aeronautics and Space Administration
NASN	National Air Sampling Network
NATO	North Atlantic Treaty Organization
NBS	National Bureau of Standards, DOC
NCAC	National Conservation Advisory Council
NCAR	National Center for Atmospheric Research
NECRMP	Northeast Corridor Regional Modeling Program
NEDS	National Emissions Data System
ng ℓ^{-1}	Nanograms per liter
ng kg^{-1}	Nanograms per kilogram
ng m^{-3}	Nanograms per cubic meter
NH_3	Ammonia
NH_4^+	Ammonium ion

NH_4Cl	Ammonium chloride
NH_4OAc	Ammonium acetate
$(NH_4)_3H(SO_4)_2$	Letoricite
$(NH_4)_2HPO_4$	Ammonium phosphate
NH_4NO_3	Ammonium nitrate
$(NH_4)_2SO_4$	Ammonium sulfate
NH_4OH	Ammonium hydroxide
Ni	Nickel
nm	Nanometer
NMAB	National Materials Advisory Board
NO_2	Nitrogen dioxide
NO_3^-	Nitrate ion
NO	Nitric oxide
NO_x	Nitric oxides
NOAA	National Oceanic and Atmospheric Administration
NPS	National Park Service, DOI
NRCC	National Research Council Canada
NSF	National Science Foundation
NSPS	New Source Performance Standards
NTN	National Trends Network
NWS	National Weather Service, NOAA
O	Oxygen
O_2	Elemental oxygen
O_3	Ozone
(-OH)	Phenol

OECD	Organization for Economic Cooperation and Development
OH	Hydroxyl
OMB	Office of Management and Budget
ORNL	Oak Ridge National Laboratory
OSM	Office of Surface Mining, DOI
P	Phosphorus
PAH	Polycyclic aromatic hydrocarbons
PAN	Peroxyacetyl nitrate
Pb	Lead
Pb^{2+}	Lead ion
PBCF	Practical bioconcentration factor
PBL	Planetary boundary layer
$PbSO_4$	Lead sulfate
PCB	Polychlorinated biphenyl
PGF	Pressure gradient force
PHS	Public Health Service
PO_4^{3-}	Phosphate ion
ppb	Parts per billion
ppm	Parts per million
RAM	St. Louis Regional Air Modeling Study
RAPS	St. Louis Regional Air Pollution Study
RI	Ryznar index
RSN	Research Support Network
s	Second
S cm-1	Seconds per centimeter

S	Sulfur
S^{2-}	Sulfide
S(IV)	Gas-phase sulfur, an oxidation state
SAC	Sulfate adsorption capacity
SAES	State Agricultural Experiment Station, DOA
Sb	Antimony
SCS	Soil Conservation Service, DOA
Se	Selenium
Si	Silicon
SiO_2	Silicon dioxide
SMA	Swedish Ministry of Agriculture
SO_2	Sulfur dioxide
SO_3^{2-}	Sulfite
$SO4^{2-}$	Sulfate ion
STP	Standard temperature and pressure
SURE	Sulfate Regional Experiment, EPRI
TDS	Total dissolved solids
TFE	Total fixed endpoint alkalinity
Tg	Teragram (10^{12} gram)
Tg yr^{-1}	Teragrams per year
TIC	Total inorganic carbon
TIP	Total inflection point alkalinity
TPS	Tennessee Plume Study
TSP	Total suspended particulates

TVA	Tennessee Valley Authority
USGS	United States Geological Survey, DOI
V	Vanadium
V_2O_5	Vanadium pentoxide
V cm-1	Volts per centimeter
VDI	Verein Deutcher Ingenieure
VOC	Volatile organic compounds
WHO	World Health Organization
WMO	World Meteorological Organization
yr	Year
Zn	Zinc
ZnS	Zinc sulfide

GLOSSARY

Acceptable daily intake (ADI) - rate of safe consumption of a particular substance or element in human food or water, as determined by the U.S. Food and Drug Administration.

Acidic deposition - the deposition of acidic and acidifying substances from the atmosphere.

Acid neutralizing capacity (ANC) - equivalent sum of all bases that can be titrated with a strong acid; also known as alkalinity.

Adiabatic - occurring without gain or loss of heat by the substance concerned.

Adsorption - adhesion of a thin layer of molecules to a liquid or solid surface.

Advection - horizontal flow of air to the surface or aloft; one of the means by which heat is transferred from one region of the Earth to another.

Aerosols - suspensions of liquid or solid particles in gases.

Aliquoting - dividing into equal parts.

Alkalinity - measure of the ability of an aqueous solution to neutralize acid (also known as acid neutralizing capacity or ANC).

Allochthonous inputs - substances introduced from outside a system.

Ambient - the surrounding outdoor atmosphere to which the general population may be exposed.

Ammonium - cation (NH_4^+) or radical (NH_4) derived from ammonia by combination with hydrogen. Present in rainwater, soils, and many commercial fertilizers.

Anion - a negatively charged ion.

Aqueous phase - that part of a chemical transformation process when substances are mixed with water or water vapor in the atmosphere.

Antagonistic effects (less-than-additive) - results from joint actions of agents so that their combined effect is less than the algebraic sum of their individual effects.

Anthropogenic - manmade or related to to human activities.

Artifact - a spurious measurement produced by the sampling or analysis process.

Atmospheric residence time - the amount of time pollutant emissions are held in the atmosphere.

Autochthonous inputs - indigenous, formed or originating within the system.

Autotrophic - able to synthesize nutritive substances from inorganic compounds.

Background measurement - pollutants in ambient air due to natural sources; usually taken in remote areas.

Base neutralizing capacity - equivalent sum of all acids that can be titrated with a strong base.

Base saturation (BS) - the fraction of the cation exchange capacity satisfied by basic cations.

Benthic organisms - life forms living on the bottoms of bodies of water.

Bioaccumulation - the phenomenon wherein toxic elements are progressively amassed in greater quantities as individuals farther up the food chain ingest matter containing those elements.

Bioconcentration factor (BCF) - the ratio of the concentration of a substance in an organism to the concentration of the substance in the surrounding habitat.

Bioindicators - species of plants or animals particularly sensitive to specific pollutants or adverse conditions.

Biomass - that part of a given habitat consisting of living matter.

Biosphere - the part of the Earth's crust, waters, and atmosphere where living organisms can subsist.

Brownian diffusion - spread by random movement of particles suspended in liquid or gas, resulting from the impact of molecules of the fluid surrounding the particles.

Brownwater lakes and streams - acidic waters associated with peatlands, cypress swamps; acidity is caused by organic acids leached from decayed plant material and from hydrogen ions released by plants such as Sphagnum mosses.

Budget - a summation of the inputs and outputs of chemical substances relative to a given biological or physical system.

Buffer - a substance in solution capable of neutralizing both acids and bases and thereby maintaining the original pH of the solution.

Buffering capacity - ability of a body of water and its watershed to neutralize introduced acid.

Bulk sampling - method for collecting deposition that does not separate dry and wet deposition (see Chapter A-8).

Calcareous - resembling or consisting of calcium carbonate (lime), or growing on limestone or lime-containing soils.

Calcite saturation index (CSI) - measure of the degree of saturation of water with respect to $CaCO_3$, integrating alkalinity, pH, and Ca concentration.

Cation - a positively changed ion

Cation exchange capacity (CEC) - the sum of the exchangeable cations, expressed in chemical equivalents, in a given quantity of soil.

Chemoautotrophic - having the ability to synthesize nutritive substances using an inorganic compound as a source of available energy.

Colorimetric - a chemical analysis method relying on measurement of the degree of color produced in a solution by reaction of the compound of interest with an indicator.

Conductivity - the ability to conduct an electric current; this is a function of the individual mobilities of the dissolved ions in a solution, the concentrations of the ions, and the solution temperature; measured in mho cm^{-1}.

Continental scale - measurement of atmospheric conditions over an area the size of a continent.

Coriolis effect - an effect caused by the Earth's eastward rotation in which the speed of the movement falls off as the circumference of the Earth gets progressively smaller at higher latitudes; this results in the movement of winds, and subsequently ocean currents, to the right in the northern hemisphere and to the left in the southern hemisphere.

Cosmic ray - a stream of ionizing radiation of extraterrestrial origin, chiefly of protons, alpha particles, and other atomic nuclei but including some high energy electrons and protons, that enters the atmosphere and produces secondary radiation.

Coulomb - a meter/kilogram/second unit of electric charge equal to the quantity of charge transferred in one second by a steady current of one ampere.

Coarse particles - airborne particles larger than 2 to 3 micrometers in diameter.

Cultivar - cultivated species of crop plant produced from parents belonging to different species or different strains of the same species, originating and persisting under cultivation.

Cuticular resistance - the resistance to penetration of a leaf cuticle.

Cyclone track - the path of a low pressure system.

Denitrification - a bacterial process occurring in soils, or water, in which nitrate is used as the terminal electron acceptor and is reduced primarily to N_2. It is essentially an anaerobic process; it can occur in the presence of low levels of oxygen only if the microorganisms are metabolizing in an anoxic microzone (an oxygen-free microenvironment within an area of low oxygen levels).

Deposition velocity - rate at which particles from the atmosphere contact surfaces and adhere.

Detritus - loose material resulting directly from disintegration.

Diffusiophoresis - an effect created when particles approaching an evaporating surface are impacted by more molecules on the side nearer the surface.

Dissolved organic carbon (DOC) - the amount of organic carbon in an aqueous solution.

Dissolved inorganic carbon (DIC) - the amount of inorganic carbon in an aqueous solution.

Dose - the quantity of a substance to be taken all at one time or in fractional amounts within a given period; also the total amount of a pollutant delivered or concentration.

Dose-response curve - a curve on a graph based on responses occurring in a system as a result of a series of stimuli intensities or doses.

Edaphic differences - soil differences.

Eddies - currents of water or air running contrary to the main current.

Eddy diffusities - dispersive movements of particles, caused by circular motions in air currents.

Ekman layer - a layer of the atmosphere typically extending between 1 and 3 kilometers above the surface; see Section A-3.2.2 for detailed discussion.

Electromotive force (emf) - the amount of energy derived from an electrical source per unit quantity of electricity passing through the source (as a cell or generator).

Entrainment - the process of carrying along or over (as in distillation or evaporation).

Epifaunal - organism living on an animal.

Epilimnion - the upper layer of a lake in which the water temperature is essentially uniform.

Episodic precipitation event - a period during which rain, snow, etc., is occurring.

Ericaceous - heathlike or shrubby; a member of the Ericaceae family.

Eucaryotic algae - algae composed of one or more cells with visibly evident nuclei.

Eulerian models - models with reference frames fixed on the source or at the surface.

Eurytopic - having a wide range of tolerance to variation of one or more environmental factors.

Eutrophic - relating to or being in a well nourished condition; a lake rich in dissolved nutrients but frequently shallow and with seasonal oxygen deficiency in the hypolimnion.

Eutrophication - the process of becoming more eutrophic either as a natural phase in the maturation of a body of water or artificially, as by fertilization.

Exposure level - concentration of a contaminant with which an individual or population is in contact.

Extinction coefficient - a measure of the space rate of diminution, or extinction of any transmitted light; thus, it is the attenuation coefficient applied to visible radiation.

Fine particles - airborne particles smaller than 2 to 3 micrometers in diameter.

Fly ash - fine, solid particles of noncombustible ash carried out of a bed of solid fuel by a draft.

Foliar - referring to plant foliage (leaves).

Fumigate - to subject to smoke or fumes.

Gas-phase mechanism - a process occurring when pollutants are in a gaseous state, as opposed to being combined with moisture.

Geostrophic - of or pertaining to the force caused by the Earth's rotation.

Global scale - measurement of atmospheric conditions on a world-wide basis.

Ground loss - the effect of deposition of pollutant from atmposhere to Earth's surface.

Ground sink - the Earth's surface, where airborne substances may be deposited.

Haze - an aerosol that impedes vision and may consist of a combination of water droplets, pollutants, and dust.

Hemispheric scale - measurements of activity covering half of the Earth.

Heterotrophic - obtaining nourishment from outside sources, requiring complex organic compounds of nitrogen and carbon for metabolic synthesis.

Humic acid - any of various organic acids that are insoluble in alcohol and organic solvents and that are obtained from humus.

Hydrocarbons - a vast family of compounds containing carbon and hydrogen in various combinations; found especially in fossil fuels.

Hydrologic residence time - the amount of time water takes to pass from the surface through soil to a lake or stream.

Hydrometeor - a product of the condensation of atmospheric water vapor (e.g., raindrop).

Hydrophilic - of, relating to, or having a strong affinity for water; readily wet by water.

Hydrophobic particles - particles resistant to or avoiding wetting; of, relating to, or having a lack of affinity for water.

Hydroxyl radical - chemical prefix indicating the [OH] group.

Hygroscopic particles - absorbing moisture readily from the atmosphere.

Hypolimnion - the lowermost region of a lake, below the thermocline, in which the temperature from its upper limit to the bottom is nearly uniform.

Hysteresis - the failure of a property to return to its orginal condition after the removal of the causal external agent (i.e., irreversibility).

Infauna - population of organisms living in sediments.

Inorganic acidotrophic lakes - waters associated with geothermal areas or lignite burns; extremely acidic, often heated, and frequently containing elevated metal concentrations.

Interstitial water - water in the space between cells.

Isopleth - 1. a line of equal or constant value of a given quantity with respect to either space or time, also known as an isogram; 2. a line drawn through points on a graph at which a given quantity has the same numerical value as a function of the two coordinate variables.

Labile - readily or continually undergoing chemical or physical or biological change or breakdown.

Lacustrine sediments - deposits formed in lakes.

Lagrangian models - models with reference frames fixed on the puff of pollutants.

Langmuir equations - empirical derivations from kinetic treatment of the physical adsorption of gases or solids by soils; relating to the relative adsorption capacity of a soil for a specific anion.

Leaf area index (LAI) - ratio of the total foliar surface area to the ground surface area that supports it.

Lentic - of, relating to, or living in still waters.

Lidar - a laser-radar system operated from a mobile van.

Ligands - those molecules or anions attached to the central atom in a complex.

Limnological - of or relating to the scientific study of physical, chemical, meteorological, and biological conditions in freshwaters, especially ponds and lakes.

Lipophilicity - the strong affinity for fats or other lipids.

Liquid-phase mechanism - a process occurring when pollutants are combined with moisture, as opposed to being in a purely gaseous state.

Littoral - the shore zone between high and low watermarks.

Loading rate - the amount of a nutrient available to a unit area or body of water over a given period.

Long-range transport - conveyance of pollutants over extensive distances, commonly referring to transport over synoptic and hemispheric scales.

Macrophytes - higher plants.

Manometer - an instrument for measuring pressure of gases or work.

Mean (arithmetic) - the sum of observations divided by sample size.

Median - a value in a collection of data values which is exceeded in magnitude by one-half the entries in the collection.

Mesoscale - of or relating to meteorological phenomena from 1 to 100 kilometers in horizontal extent.

Metalimnion - the thermocline.

Microbial pathogens - microscopic organisms capable of producing disease, such as viruses, fungi, etc.

Microflora - a small or strictly localized plant.

Micrometeorological - referring to conditions specific to a very small area, such as a surface, a particular site, or locale.

Mist - suspension of liquid droplets formed by condensation of vapor or atomization; the droplet diameters exceed 10 micrometers and in general the concentration of particles is not high enough to obscure visibility.

Mixing layer - also called the planetary boundary layer (PBL); usually the domain of microscale turbulance.

Mobile sources - automobiles, trucks, and other pollution sources that are not fixed in one location.

Mole - The mass, in grams, numerically equal to the molecular weight of a substance.

Morphology - structure and form of an organism at any stage of its life history.

Mycorrhizal - relating to symbiotic association of a fungal mycelium with the roots of a seed plant.

Nitrification - the principal natural source of nitrate, in which ammonium (NH_4^+) ions are oxidized to nitrates by specialized microorganisms. Other organisms oxidize nitrites to nitrates.

Nocturnal jet - phenomenon in the atmosphere of a high-velocity air stream occuring at night above the nocturnal inversion layer.

Non-humic lakes - lakes without significant inputs of humic acid.

Ohm's law - a law in electricity: the strength or intensity of an unvarying electrical current is directly proportional to the electromotive force and inversely proportional to the resistance of the circuit.

Oligochaete worms - an annelid worm of the class Oligochaeta, i.e., having a segmented body.

Oligotrophic - a body of water deficient in plant nutrients; also generally having abundant dissolved oxygen and no marked stratification.

Ombrotrophic peat bog - a peat bog fed solely by rain water.

Oxic condition - the presence of oxygen.

Oxidant - a chemical compound that has the ability to remove electrons from another chemical species, thereby oxidizing it; also a substance containing oxygen which reacts in air to produce a new substance, or one formed by the action of sunlight on oxides of nitrogen and hydrocarbons.

Palearctic lake - a lake in the biogeographic region that includes Europe, Asia north of the Himalayas, northern Arabia, and Africa north of the Sahara.

Particle morphology - the structure and form of substances suspended in a medium.

Particulates - fine liquid or solid particles such as dust, smoke, mist, fumes, or smog found in air or in emissions.

Ped surfaces - surfaces of natural soil aggregates.

Pelagic - of, relating to, or living in the open sea.

Periphyton - organisms that live attached to underwater surfaces.

Photoautotrophic organisms - autotrophic organisms able to use light as an energy source.

Photochemical oxidants - primarily ozone, NO_2, PAN with lesser amounts of other compounds formed as products of atmospheric reactions involving organic pollutants, nitrogen oxides, oxygen, and sunlight.

Phytophagous insects - insects feeding on plants.

Phytoplankton - autotrophic, free-floating, mostly microscopic organisms.

Planetary boundary layer (PBL) - first layer of the atmosphere extending hundreds of meters from the Earth's surface to the geostrophic wind level, including, therefore, the surface boundary layer and the Ekman layer; above this level lies the free atmosphere.

Plume - emission from a flue or chimney, normally distributed streamlike downwind of the source, and which can be distinguished from surrounding air by appearance or chemical characteristics.

Plume touchdown - point of a plume's contact with the Earth's surface.

Podzol - any of a group of zonal soils that develop in a moist climate, especially under coniferous or mixed forests.

Point source - a single stationary location for pollutant discharge.

Precipitation scavenging - a complex process composed of four distinct but interactive steps: intermixing of pollutant and condensed water within the same airspace, attachment of pollutant to the condensed water, chemical reaction of pollutant within the aqueous phase, and delivery of pollutant-laden water to surfaces.

Precursor - a substance from which another substance is formed, specifically one of the anthropogenic or natural emissions or atmospheric constituents that reacts under sunlight to form secondary pollutants comprising photochemical smog.

Primary particles (or primary aerosols) - dispersion aerosols formed from particles emitted directly into the air that do not change form in the atmosphere.

Quasi-laminar layer - the internal viscous boundary layer above non-ideal or natural surfaces; it is frequently neither laminar nor constant with time.

Rayleigh scattering - spread of electromagnetic radiation by bodies much smaller than the wavelength of the radiation; for visible wavelengths, the molecules constituting the atmosphere cause Rayleigh scattering.

Secondary particles (or secondary aerosols) - dispersion aerosols that form in the atmosphere as a result of chemical reactions, often involving gases.

Sensitivity - the degree to which an ecosystem or organism may be affected by inputs or stimuli.

Sequential sampling - repeated, periodic collection of data concerning a phenomenon of interest.

Sinks - reactants with or absorbers of substances; collection surfaces or areas where substances are gathered.

Steady state exposure - exposure to air pollutants whose concentration remains constant for a period of time.

Stefan flow - results from injection into a gaseous medium of new gas molecules at an evaporating or subliming surface; Stefan flow is capable of modifying surface deposition rates by an amount that is larger than the deposition velocity appropriate for many small particles to aerodynamically smooth surfaces.

Stokes's law - a law in physics: the force required to move a sphere through a given viscous fluid at a low uniform velocity is directly proportional to the velocity and radius of the sphere.

Stoma - opening on a leaf surface through which water vapor and other gases diffuse; often term applies to the entire stomatal apparatus including surrounding specialized epidermal cells, guard cells.

Stream order - positions a stream in relation to tributaries, drainage area, total length, and age of water. First-order streams are the terminal twigs (headwaters or youngest segments of a stream system, having no tributaries). Second-order streams are formed by the junction of two first order streams, and so on. At least two streams of any given order are required to form the next highest order.

Sub-optical range - particles too small to be seen with the naked eye.

Surfactant - a substance capable of altering the physiochemical nature of surfaces, such as one used to reduce surface tension in a liquid.

Symbiotic - a close association between two organisms of different species, in which at least one of the two benefits.

Synergistic effects (more-than-additive) - result from joint actions of agents so that their combined effect is greater than the algebraic sum of their individual effects.

Synoptic scale - relating to or displaying atmospheric and weather conditions as they exist simultaneously over a broad area; the scale of weather maps.

Teragram (Tg) - one million metric tons, 10^{12} grams.

Thermocline - the stratum of a lake below the epilimnion in which there is a large drop in temperature per unit depth.

Thermophoresis - a force near a hot surface that drives small particles away from that surface.

Throughfall - precipitation falling through the canopy of a forest and reaching the forest floor.

Titration - the process or method of determining the concentration of a substance in solution by adding to it a standard reagent of a known concentration in carefully measured amounts until a reaction of definite and known proportion is completed, as shown by a color change or by electrical measurement, and then calculating the unknown concentration.

Total fixed endpoint alkalinity (TFE) - a measure of acid neutralizing capacity involving acidimetric titrations performed to an endpoint of pH 4.5 determined electrometrically or to an endpoint determined by either a colorimetric indicator or mixed indicators.

Total inflection point (TIP) - a measure of acid neutralizing capacity, involving acidimetric titration to the HCO_3-H^+ equivalence point of the titration curve.

Total suspended particulates (TSP) - solid and liquid particles present in the atmosphere.

Toxicity - the quality, state, or relative degree of being poisonous.

Trajectory - a path, progression, or line of development, as from a plume of pollutant carried through the atmosphere from a source to a receptor area.

Transport layer - the layer between the earth's surface and the peak mixing height of the day; for any given instant, it is made up of the current mixing layer below and the relatively quiescent layer above.

Troposphere - that portion of the atmosphere in which temperature decreases rapidly with altitude, clouds form, and mixing of air masses by convection takes place; generally extending to about 11 to 17 km above the Earth's surface.

Ultra oligotrophic lakes - lakes in areas where glaciation has removed calcareous deposits and exposed weather resistant granitic and siliceous bedrock; such lakes have little carbonate-bicarbonate buffering capacity and are very vulnerable to pH changes; they tend to be small and have low concentrations of dissolved ions.

Variance - a measure of dispersion or variation of a sample from its expected value.

Washout - the capture of gases and particles by falling raindrops.

Wet deposition - the combined processes by which atmospheric substances are returned to Earth in the form of rain or other precipitation.

Wind shear - a sudden shift in wind direction.

X-ray diffraction - technique by which patterns of diffraction can be used to identify a substance by its structure.

Zooplankton - minute animal life floating or swimming weakly in a body of water.

THE ACIDIC DEPOSITION PHENOMENON AND ITS EFFECTS

A-1. INTRODUCTION

(A. P. Altshuller, J. S. Nader, and L. E. Niemeyer)

1.1 OBJECTIVES

This portion of the Critical Assessment Review Papers addresses the various atmospheric processes starting with emissions to the atmosphere from natural and anthropogenic sources, leading up to the presence of acidic and acidifying substances in the atmosphere, and concluding with the deposition of these substances from the atmosphere to the surfaces of manmade and natural receptors. The objective is to provide an understanding of these phenomena and the latest technical data base supporting this understanding.

1.2 APPROACH--MOVEMENT FROM SOURCES TO RECEPTORS

1.2.1 Chemical Substances of Interest

The approach begins by identifying the acidic and acidifying substances emitted from natural and anthropogenic sources. The chemical species of principal concern are the hydrogen ion (H^+), ammonium ion (NH_4^+), sulfate ion (SO_4^{2-}), and the nitrate ion (NO_3^-). Chloride, in the form of hydrogen chloride, may be of concern, particularly downwind of some types of anthropogenic emission sources. A number of metal cations are of interest because they affect material balances or cause unique biologicial effects. Weaker acids such as nitrous acid, formic acid, and dibasic acid have been identified in the atmosphere but do not contribute significantly to the acidic deposition phenomenon.

1.2.2 Natural and Anthropogenic Emissions Sources

Natural sources are classified as geophysical and biological. The former includes volcanic and sea spray contributions, the latter, soil and vegetation contributions. The anthropogenic source categories include electric utilities, industrial combustion sources, commercial/residential combustion sources, highway (mobile) vehicles, and miscellaneous sources. Emission patterns are given for spatial, seasonal, and temporal variations. Although data are given for the United States and Canada, the main focus is on the area east of the Mississippi, where acidic deposition levels appear to be greatest.

1.2.3 Transport Processes

The movement of emissions from sources to receptors involves atmospheric transport and transformation processes. The transport process is discussed

with regard to the structure and dynamics of the planetary boundary layer. The impact of the source's physical configuration, elevated point source (power plant plume), and broad areal emissions near ground level (urban plumes) on the transport and dilution processes are reviewed. Transport is treated on the mesoscale, the continental scale, and the hemispherical scale and allows for the effects of complex terrain and shoreline environment.

1.2.4 Transformation Processes

Atmospheric transformation processes account for the chemical and physical changes in some of the emissions (precursors) into acidic and acidifying species that ultimately result in the presence and deposition of atmospheric acid matter. In relatively dry, cloudless atmospheres, these changes can be the result of homogeneous gas-phase reactions between radicals (such as hydroxyl) and sulfur dioxide and nitrogen dioxide to form sulfuric and nitric acids. Ammonia can subsequently partially or completely neutralize these acids. Solution reactions can occur also in water droplets on vegetation, in cloud droplets, in fog, and in dewdrops. The oxidation of sulfur dioxide can involve, to various extents, other chemical-reacting atmospheric constituents such as oxygen, ozone, hydrogen peroxide, and ammonia. In addition, catalytic metal constituents such as iron and manganese may participate in the oxidation process in low-lying clouds or fogs over highly polluted areas. The products of these transformation reactions add to the primary acid originally emitted from anthropogenic sources, and the net amalgam of substances continues downwind.

1.2.5 Atmospheric Concentrations and Distributions of Chemical Substances

Acidic and acidifying substances in the atmosphere prior to deposition on natural and manmade receptors include both those emitted directly into the atmosphere (primary pollutants) and those resulting from atmospheric transformations (secondary pollutants). Transport on various scales, as well as emissions that vary temporally with seasons and time of day and that vary spatially with meteorology and distribution of emission sources and geographic locations, provide a complex picture of concentrations of these substances of interest prior to deposition. Urban and nonurban concentration data on sulfur compounds, nitrogen compounds, chlorine compounds, basic substances, metals, and particle size characteristics of particulate constituents of these compounds are reviewed. Available information is given on geographic distribution, seasonal and diurnal variations, and variations with elevation above ground level.

1.2.6 Precipitation Scavenging Processes

The complex process of precipitation scavenging depends upon a host of interactive physical and chemical phenomena that occur prior to and during the precipitation process. Cloud droplets form and evaporate, airborne pollutants are incorporated into and released by condensed water, chemical reactions occur, ice crystals form and melt, energy is exchanged, and hydrometeors are created and evaporate. These and a multitude of additional processes create a continually changing environment for pollution elements within a storm system. The final stage of these complex scavenging processes

is the actual wet delivery of pollutants to the ground. A large number of models have been developed, but their very number is an indication of the work remaining before a satisfactory modeling capability is possible.

1.2.7 Dry Deposition Process

In addition to deposition of acidic and acidifying substances from the atmosphere by wet scavenging with rain, snow, and fog, dry deposition plays a similar role with respect to the same substances of interest in the gas phase and as solid particulate matter. The dry deposition processes take into account aerodynamic factors, the surface-boundary layer, phoretic effects, dewfall, surface effects, and deposition to water surfaces. The concept of resistance analog provides a model for identifying process parameters associated with the transfer of substances from the atmosphere to the vicinity of the final receptor surfaces.

Methods for measuring dry deposition consist of direct measurement with collection vessels and with surrogate surfaces specific to various receptor surfaces of interest. Laboratory studies have been conducted under controlled conditions to provide an understanding of the relative importance of various factors in the processes. These include chamber and wind-tunnel work, and they address resistances to deposition of selected trace gases onto various substrate surfaces and deposition velocities of different size particulate matter to a variety of surfaces. Micrometeorological techniques are also discussed and consist of eddy-correlation methods, gradient measurement techniques, and other new developments. Field investigations are providing data on the impact of the diurnal cycle on dry deposition rates of gaseous pollutants on different surfaces. Data are also available on deposition velocities of submicron particles. Results of many of these studies have led to the development of micrometeorological models of the dry deposition processes for gases and for particles.

1.2.8 Deposition Monitoring

Deposition monitoring networks have been established to collect wet deposition data during periods of precipitation and dry deposition data during periods of no precipitation. Networks have been designed to collect data on various spatial, temporal, and density scales. These data bases are essentially wet deposition monitoring networks. Dry deposition monitoring networks exist to a limited extent if any and are primarily of a research nature.

Wet deposition network data have been analyzed and interpreted to provide maps of the United States and Canada with sampling site locations and median concentration data for specified sampling periods for sulfates, nitrates, ammonium ion, calcium, chloride, and pH. Spatial patterns are generated by isopleths identifying regions of high and low values. Temporal variations are also analyzed and include seasonal variations and changes over both short and long time scales.

Glaciochemical investigations are being conducted and are shown to provide a tool in the historical delineation of acid precipitation problems. These

studies also provide a bench mark on the natural background void of anthropogenic pollution and contamination.

1.2.9 Deposition Models

Developing suitable models for acidic deposition is a difficult undertaking. The models have to have algorithms that take into account natural emissions, anthropogenic emissions, transport processes, transformation, precipitation scavenging processes, and dry deposition processes on scales from a few millimeters to thousands of kilometers. Moreover, the results must be compared to measurements made on a variety of scales for a variety of purposes. Therefore, in terms of the detail inherent in the models, there is a large variation from the simple to the complex. All need verification, and while progress has been made in the acquisition of data bases, more information is needed for a proper evaluation of long-range transport models.

1.3 ACIDIC DEPOSITION

Atmospheric pollutants consist of both acidic and basic substances and include both primary and secondary pollutants. The acidity in depositions from the atmosphere onto natural and manmade receptors such as soils, vegetation, bodies of water, pavements, and buildings is the net acidity after neutralization in the atmosphere of the acidic substances by the basic substances. Acidity measurements are usually expressed on a pH scale where pH is defined as the negative logarithm of the hydrogen ion concentration. The pH scale extends from 0 to 14. A neutral pH in water at 25 C is 7.0. Solutions with a pH below 7.0 are considered acid; those with a pH above 7.0 are considered alkaline or basic. The logarithmic pH scale means that a whole unit change in pH corresponds to a 10-fold change in acidity or hydrogen ion concentration. A pH of 6.0 is ten times more acidic than a pH of 7.0.

Atmospheric water droplets are in equilibrium with the geophysical concentrations of carbon dioxide in air. This equilibrium results in a pH of 5.6 for such droplets. However, even this pH value applies only to a perfectly "clean" atmosphere. Lower pH values have been measured at remote sites although these pH values are still well above those measured over eastern North America. If substantial amounts of basic particulate substances are present, the pH may be greater than 5.6.

The acidity measured in a manmade collector is not necessarily representative of the acidity in soil or water. Most deposition monitoring, being limited to collection of rain or snowfall, does not include monitoring of dry deposition. Acidic or basic substances can collect on vegetation or soil surfaces and subsequently be washed into the soil by rainfall. Once substances are within an ecosystem, additional changes in acidity can occur as a result of processes involving plants and organisms. Ammonia can be released from deposited particulate ammonium salts. Hydroxyl ions can be released as the result of metabolic processes. These processes may change the net acidity significantly.

THE ACIDIC DEPOSITION PHENOMENON AND ITS EFFECTS

A-2. NATURAL AND ANTHROPOGENIC EMISSIONS SOURCES

2.1 INTRODUCTION (Eds.)

Acidic and acidifying substances in the atmosphere may be produced by nature or by human (anthropogenic) activities. In either case, emissions become available for transport to other locations, for combination with other atmospheric substances, and for deposit to surfaces. Chapter A-2 discusses where acidic and acidifying substances originate, thus setting the stage for further examinations of transport, transformation, and deposition processes; concentrations and distributions; and modeling efforts. It considers natural and anthropogenic sources separately and subdivides the discussions among the various substances of concern.

Numerous questions arise relative to emissions sources. For instance, are natural sources of sulfur, nitrogen, and chlorine compounds significant, and, if so, where are they and how do emission rates vary seasonally? On the other hand, concerning anthropogenic sources, how have historical trends in fuel use changed emission rates and how are future trends likely to alter the rates? How are current emissions distributed between stationary and mobile sources, among geographic regions, between urban and rural areas, seasonally, and at various heights? Do non-combustion, anthropogenic sources of sulfur, nitrogen, and chlorine compounds exist, or do any additional materials emitted anthropogenically affect acidic deposition, either by catalysis or direct reaction with sulfur, nitrogen, and chlorine-containing compounds? In contrast to acidic or acidifying substances, what sources exist for neutralizing substances--including ammonia, soil-related or cement plant dusts, and alkaline particles from combustion--and how do these vary geographically and seasonally?

In addition to addressing these issues, Chapter A-2 also presents information concerning emissions of several heavy metals from combustion sources because information on these metals may be useful in assessing dispersion from specific sources.

2.2 NATURAL EMISSIONS SOURCES (E. Robinson)

2.2.1 Sulfur Compounds

2.2.1.1 Introduction--Sulfur compounds, including sulfates and sulfur dioxide, are ubiquitous trace constituents of the Earth's atmosphere even in very remote, natural areas. Thus, it is common to assume that these common, relatively reactive compounds result from natural sources in the unperturbed environment. Concentrations in most background situations are low, and sampling and analysis problems are major factors that limit the determination of

the gaseous sulfur compounds. Our present knowledge is strongly dependent on the analytical tools that have been available to the various investigators. It will be convenient to consider natural sulfur sources in terms of two general classifications: geophysical, including volcanic and sea spray contributions, and biological, including soil and vegetation contributions. This discussion will emphasize conditions appropriate for the area east of the Mississippi River, which seems to be the area of eastern North America most critically affected by acidic deposition. In this region of the United States natural sources may act in two ways to influence conditions. First, natural sources within the region may be contributors to the local concentration patterns. Second, natural sources in areas remote from this region may contribute to the global background concentration, and thus influence the total mass of the natural emissions that are advected across the region. Biogenic emissions from the soil, coastal wetlands, and vegetation are potential local sources that can contribute directly to the sulfur cycle in the local region. Volcanos and the open ocean are examples of natural sources that will impact on the local northeast United States primarily by influencing the general level of sulfur compounds in the global environment. The dilution and scavenging processes that regularly take place on a global scale limit the impact of remote volcanic and oceanic sources on the specific area of interest in the northeast United States. In the following discussion biogenic sources will be considered in some detail because of their possible local importance; the more distant sources that contribute primarily to the global background will be considered in a more general fashion.

2.2.1.2 Estimates of Natural Sources--Estimates of the magnitude of natural sulfur compound sources usually reference the initial estimate of the global sulfur flux published by Eriksson in 1960. Using the global balancing technique described below, Eriksson (1960) estimated natural sulfur sources, as sulfur, to be 77 x 10^6 mT (77 Tg S) from land areas and 190 x 10^6 mT (190 Tg S) from the oceans. (The unit Tg S yr^{-1} is 10^{12} grams per year). In the two decades since Eriksson's first estimate, a number of variations and "improved" global estimates have been made by a number of authors but the methods used have not undergone major changes. Some of the most frequently referenced global sulfur circulation models, which, of necessity, include estimates of natural sources, are those of Junge (1960, 1963), Robinson and Robbins (1970a), Kellogg et al. (1972), and Friend (1973). More recently, Granat et al. (1976) have assembled a more detailed sulfur budget and estimate of natural sources by drawing on the rapidly expanding research in this area.

The methods used by the above-mentioned authors employed the steady-state balancing of sources against sinks or removal mechanisms averaged over the Earth as a whole. On this scale, the sinks for sulfur compounds probably can be estimated with sufficient accuracy in terms of total mass to estimate a global cycle. The sulfur sinks are mostly accounted for by wet and dry deposition. On this basis, they typically exceed the estimated sources. Sources of sulfur compounds include anthropogenic and natural sources. The former can be estimated using emission factors and the magnitudes of production activities. Within the natural source area, volcanic and ocean spray sources have been estimated, but until recently, (Adams et al. 1980, 1981a), the much larger biological component had to be estimated from only fragmentary data.

Thus, in the various global sulfur cycles, it has been common practice to balance the steady-state sulfur cycle, after quantifying the sources and the dry and wet deposition sinks, by assuming that any difference was accounted for by biological emissions processes.

Estimates of the biogenic flux of sulfur components from land areas to the atmosphere made using this material balance approach have varied from 5 Tg S yr^{-1} (Granat et al. 1976) to 110 Tg S yr^{-1} (Eriksson 1963). To place the biogenic contribution in perspective, Granat et al. (1976) estimated anthropogenic sulfur emissions to be 65 Tg S yr^{-1} and the total land and oceanic biogenic sulfur emissions to be 32 Tg S yr^{-1}, so the global biogenic contribution was estimated to be roughly half the global anthropogenic emission. Earlier estimates had the biogenic fraction equal to or greater than the anthropogenic fraction (Eriksson 1960, 1963; Robinson and Robbins 1970a). Extrapolation of field data to a global cycle results in a value of 64 Tg S yr^{-1} (Adams et al. 1980), and, although this particular estimate is still only preliminary, since it is based on detailed field data it seems likely that better estimates will tend toward a value between previous extreme estimates rather than toward the high or low ends of the range.

Estimating natural emissions from a steady-state material balance can readily be seen as applicable to global considerations, but for continental and other smaller areas, the material balance procedure is less successful. This is because steady-state, homogeneous mixing across a limited area and a closed cycle of sources and sinks generally cannot be assumed. To treat smaller-than-global areas, such as the United States, one must deal with specific estimates for the natural sources.

Although, as mentioned above, there may be considerable doubts as to the total magnitude of natural sulfur compound sources on both local and global scales, the analytical techniques probably now have sufficient sensitivity to measure the major sulfur constituents of the global background. Sze and Ko (1980), as part of their photochemistry modeling studies of atmospheric sulfur compounds, tabulated tropospheric concentration data for these compounds. In Table 2-1, background concentration data are presented from the tabulations of Sze and Ko (1980) that are considered to be generally applicable to the northeastern U.S. conditions without anthropogenic influences; however, the SO_4^{2-} value appears to be significantly lower than has been ascribed frequently to remote background conditions. For the most part, these are not the same as measurements made at sites in the northeast that are currently designated as rural or nonurban because these latter sites can still be affected by pollutants through long-range transport. This was noted by Galloway et al. (1982) in as distant a location as Bermuda.

2.2.1.3 Biogenic Emissions of Sulfur Compounds--The initial estimates of biogenic emissions, such as those by Eriksson (1960), assigned the total biogenic estimate to hydrogen sulfide (H_2S) because this gas was easily identifiable by its odor as being evolved in swamps and certain other anaerobic situations and because there was little evidence that other compounds were also part of the natural background. It should be noted, however, that all of the authors dealing with the sulfur cycle recognized the probable complexity of the natural emission cycle, and the assumption that

TABLE 2-1. BACKGROUND CONCENTRATIONS OF SULFUR COMPOUNDS (ADAPTED FROM SZE AND KO 1980)

Compound	Concentration $\mu g\ m^{-3}$	Location
SO_2	0.52 ± 0.23	Western U.S. and Canada above boundary layer
	0.25 ± 0.12	Western U.S. and Canada within boundary layer
SO_4^{2-}	0.05	Remote ocean areas
COS	1.26 ± 0.15	$67^{\circ}N$-$57^{\circ}S$
H_2S	0.007 - 0.07	Southern Florida
$(CH_3)_2S$	0.15	Wallops Island, VA
CS_2	~ 0.31	England

the total emission was H_2S was recognized as a simplification of the probable real situation. These initial evaluations were not supported by measurements because there were no methods available for these measurements.

The obvious problem in measuring the biogenic component of the sulfur cycle, i.e., the emissions from natural sources, was one of having suitable analytical methodology. It was not until the 1970's that the measurement technology for H_2S and the organic sulfur compounds that might be expected to come from natural sources was developed. The nature of potential biogenic sulfur emissions had emphasized H_2S as the probable compound (e.g., see Eriksson 1960) although earlier Conway (1942) had concluded that non-sea-salt sulfur in precipitation away from anthropogenic sources may be due to volatile sulfur compounds such as H_2S or possibly mercaptans. Lovelock et al. (1972) showed that $(CH_3)_2S$ (dimethyl sulfide) was present in sea water and given off by enclosed soils, and they proposed $(CH_3)_2S$ as an important component of the natural atmospheric sulfur cycle. This proposal was supported by Hitchcock (1975, 1976) with calculations of the probable emissions from the turnover of biomass in the form of leaves, soil organic material, and marine algae (Hitchcock 1975) and by evaluations of seasonal atmospheric sulfate concentrations in several nonurban areas of the eastern United States (Hitchcock 1976). Reliable measurements were made subsequently of possible biogenic emissions present in the atmosphere above soil and water surfaces suspected of being strong sources of natural sulfur compounds. Jaeschke et al. (1978) describe one of the first such studies using a very sensitive sampling and analytical technique for H_2S. Maroulis and Bandy (1977) used gas chromatographic techniques for atmospheric studies of $(CH_3)_2S$. Delmas et al. (1980) carried out a number of measurements of the rate of evolution of H_2S from different soils in France and at a number of sites in the Ivory Coast. Atmospheric concentrations were also measured by Delmas et al. (1980) at many of these sites.

These research studies provided an initial test of the global mass balance estimates of biogenic sulfur emissions, but comprehensive studies of biogenic emissions were not carried out until gas chromatographic techniques covering a wide range of compounds were developed. Aneja et al. (1981) applied gas chromatography to soil emissions in the form of air samples collected from a small stirred chamber placed over selected soil and water surfaces. This gas chromatographic analytical technique was capable of detecting six potential biogenic sulfur emissions compounds: H_2S, $(CH_3)_2S$, $(CH_3)_2S_2$, COS, CS_2, and CH_3SH. In the sampling program used by Aneja et al. (1981) the detectable emission rate for H_2S, $(CH_3)_2S$, and COS was 0.01 g S m^{-2} yr^{-1} and for CS_2, CH_3SH, and $(CH_3)_2S_2$ it was 0.05 g S m^{-2} yr^{-1}. In their research they carried out a program of sampling on a variety of soils, marshland, and water surfaces in the North Carolina area in the summer and fall of 1978. The results of this study of seven types of surfaces showed that the emissions of most of the likely biogenic sulfur compounds from most of the test surfaces were below the analytical detection limits (Aneja et al. 1981, Table I). In particular, studies of "dry inland soils" showed none of the compounds to be above the detection limit while "saline marsh mud flat" showed detectable emissions only of H_2S and COS.

Further improvements in sulfur gas analysis by gas chromatography were made by Farwell et al. (1979) and used by Adams et al. (1980, 1981a,b,c) in an extensive examination of the emissions of sulfur compounds from soil surfaces in the eastern, midwestern, and southeastern United States. This program was part of the Electric Power Research Institute Sulfur Regional Experiment (SURE) program (Perhac 1978). Because this study produced the largest and most complete set of experimental data available at this time on biogenic emissions of sulfur gases and because it includes a considerable amount of measurement data from the area of the United States affected by acidic deposition, the results of this study by Adams et al. as reported in several available papers and reports will be used as a basis for the following evaluation of biogenic sulfur gas emissions in the United States. In general, the analytical techniques described by Farwell et al. (1979) were able to show an approximately one-order-of-magnitude improvement in detection limits over those reported in the earlier studies by Aneja et al. (1981). As a result, a variety of sulfur gases could be identified as being emitted even by dry, inland soils with low rates of evolution. The performance of the sampling and analytical system was evaluated by Adams et al. (1980) as being indicative of a minimum sulfur flux from the soil and water surfaces rather than an average or maximum flux value because of possible nonquantifiable losses of sulfur compounds within the system.

Table 2-2 shows the average sulfur flux by compound for the various soil orders and suborders (i.e., "types") sampled by Adams in the SURE region (Adams et al. 1981a). The results of 760 field samples gathered from 10 soil types over a period of 4 years were averaged for this table. As shown in this listing, six sulfur compounds were identified in a large fraction of the samples. H_2S typically ranked highest in the various samples with very high values in some of the samples taken in saltwater marsh areas. Among the other compounds, the emissions of carbonyl sulfide (COS) and carbon disulfide (CS_2) were typically higher than those of dimethylsulfide [$(CH_3)_2S$]. Dimethyldisulfide [$(CH_3)_2S_2$] was found in low concentrations in a large proportion of the samples, and methylmercaptan (CH_3SH) was found to be primarily an emission from saline marsh areas. Wide variations in emissions were encountered and statistical methods were used to establish average emission rates (Adams et al. 1980, 1981c).

In this research program on soil emissions, variations in sulfur emissions were found to be dependent not only on the soil order, but also on ambient temperature, time of day, and whether there was vegetative cover or bare soil. Temperature was a major variable through its control of biological activity in the soil, and relationships were developed between soil sulfur emissions and average temperature data (Adams et al. 1980). Detailed statistical analyses of the sampling data provided a basis for summarizing the experimental data into three general soil types--coastal wetlands, inland high organic, and inland mineral--and extending the emissions estimate over an annual temperature cycle. The results for the study area, essentially from 47°N to the Gulf Coast and east of the Mississippi River, are shown in Table 2-3 (Adams et al. 1981a). As shown at the bottom of the table, the average sulfur flux over the region is 0.03 g S m^{-2} yr^{-1}, and it is associated with a total SURE region biogenic emission of about 0.12 Tg S yr^{-1}.

TABLE 2-2. AVERAGE COMPOSITION OF SULFUR COMPOUND FLUXES AND TOTAL SULFUR FLUX BY SOIL ORDERS AND SUB-ORDERS (ADAPTED FROM ADAMS ET AL. 1981a)

Soil types/locales	Average sulfur flux, g S m^{-2} yr^{-1}							
	H_2S	COS	CH_3SH	$(CH_3)_2S$	CS_2	??a	$(CH_3)_2S_2$	S
Saline Marshes								
Cox's Landing, NC (11/77)	139.5	6.36	6.56					152.4
Cox's Landing, NC (7/78)	502.9	0.88	11.65	1.77	0.97		0.073	518.3
Cedar Island, NC (10/77)	0.02	0.002		0.007				0.029
Cedar Island, NC (5/78)	0.02	0.01		0.04	0.009		0.0004	0.079
Cedar Island, NC (7/78)	0.16	0.02	0.0003	1.57	0.060	0.003	0.0005	1.82
E. Wareham, MA		0.004		0.60	0.028	0.026	0.006	0.65
Lewes, DL	0.096	0.013		0.48	0.07	0.004	0.0005	0.66
Georgetown, SC	0.94	0.05	0.006	0.47	0.22	0.001	0.005	1.69
Wallops Island, VA		0.03	0.22	1.87	1.38	0.90	0.04	4.45
Everglades, N.P., FL	74.61	0.04	0.22	0.26	0.39	0.09	0.05	75.7
Sanibel Island W.R., FL	601.6	0.002	23.45	0.81	1.10	22.29	1.63	650.9
St. Marks W.R., FL	1.31	0.06	0.08	1.23	1.05	0.01	0.07	3.80
Rockefeller W.R., LA	0.09	0.001	0.001	0.008	0.02		0.003	0.12
Aransas W.R., TX	0.06		0.002	0.07	0.38		0.005	0.52
Non saline Swamp								
Liba, NY	0.16	0.006		0.004	0.006	0.003		0.19
Brunswick Co., NC	0.09	0.024		0.005	0.022			0.14
Okefenokee, GA	0.001	0.005		0.021	0.022		0.001	0.051
Jeanerette, LA		0.0002		0.029	0.001	0.002		0.032

TABLE 2-2. CONTINUED

Soil types/locales	Average sulfur flux, g S m^{-2} yr^{-1}							
	H_2S	COS	CH_3SH	$(CH_3)_2S$	CS_2	??a	$(CH_3)_2S_2$	S
Histosols (peat, muck)								
Dismal Swamp, NC (10/77)	0.018			0.0007	0.0001			0.019
Dismal Swamp, NC (5/78)	0.046	0.008		0.002	0.002		0.0003	0.058
Laingsburg, MI	0.044	0.011		0.001	0.004			0.056
One Stone Lake, WI	0.084	0.024		0.001	0.012			0.121
Fens, MN	0.042	0.01		0.001	0.003			0.056
Celeryville, OH	0.047	0.012		0.003	0.006	0.0004		0.068
Elba, NY	0.158	0.023		0.006	0.136	0.002	0.003	0.33
E. Wareham, MA				0.013	0.0004		0.0002	0.014
Brunswick Co., NC	0.09	0.007		0.006	0.017			0.12
Belle Glade, FL	0.005	0.002		0.001	0.004		0.0002	0.012
Lakeland, FL	0.069			0.003	0.008	0.0005		0.08
Jeanerette, LA	0.01	0.001		0.001	0.003			0.014
Fairhope, AL		0.001		0.002	0.014			0.017
Coastal Soils								
Georgetown, SC	0.008	0.008		0.002	0.005			0.023
Mollisols								
Ames, LA	0.147	0.017		0.003	0.016			0.18
Linneus, MO	0.104	0.009		0.003	0.005			0.12
Yankeetown, IN	0.073	0.023		0.002	0.021	0.0005		0.12
Stephenville, TX		0.002		0.001	0.004	0.0015		0.008

TABLE 2-2. CONTINUED

Soil types/locales	Average sulfur flux, g S m^{-2} yr^{-1}							
	H_2S	COS	CH_3SH	$(CH_3)_2S$	CS_2	??a	$(CH_3)_2S_2$	S
Alluvial Soils								0.002
Clarkedale, AR	0.0003	0.001		0.0001	0.003			
Alfisols								0.017
Wadesville, IN	0.01	0.002		0.001	0.002		0.002	0.13
Kearnysville, WV	0.082	0.029		0.002	0.022		0.0001	0.0
R.T.P., NC (Wooded)		0.004			0.001			0.013
R.T.P., NC (Cultivated)	0.008	0.003		0.0005	0.001			0.003
Jeanerette, LA	0.002	0.0003		0.0003	0.0004			0.013
Shreveport, LA		0.002		0.006	0.005			0.004
Stephenville, TX		0.0002		0.0003	0.003			
Inceptisols		0.002						0.008
Philo, OH	0.003	0.004		0.0002	0.001		0.0014	0.094
Belle Valley, OH	0.072		0.002	0.004	0.010	0.002		
Spodosols								
W. Wareham, MA				0.013			0.0002	0.013
Ultisols		0.003						
Calhoun, GA	0.009	0.001		0.002	0.011		0.0001	0.024
Fairhope, AL	0.0005	0.001		0.002	0.005	0.0001	0.0003	0.008
Hastings, FL	0.001			0.003	0.002	0.0003	0.0007	0.008
Freshwater Pond		0.02						
Belle Valley, OH	0.07			0.005	0.028		0.002	0.13

[a]Unidentified sulfur gases.

TABLE 2-3. SUMMARY OF ANNUAL SULFUR FLUX BY SOIL GROUPINGS WITHIN THE STUDY AREA (ADAMS ET AL. 1981a)

Soil grouping	Sulfur flux g S yr^{-1}	Land area m^2	Emission density g S m^{-2} yr^{-1}
Coastal wetlands	$48{,}822 \times 10^6$	2.56×10^{11}	0.191
Inland high organic	$13{,}451 \times 10^6$	6.85×10^{11}	0.020
Inland mineral	$56{,}843 \times 10^6$	27.26×10^{11}	0.021
Total	$119{,}116 \times 10^6$	36.7×10^{11}	0.032

In evaluating these results it must be remembered that the sample coverage of the test area was not complete. The program considered a total of 32 sites mostly in single visits of about 5 days each. Statistical techniques were used to select sites and to evaluate the data (Adams et al. 1980). Some surface soil types showed a high degree of variability, especially the wetlands and tide marsh areas, and these were assessed in detail by this research program. Adams et al. (1980) discusses in detail the problems of evaluating the biogenic sulfur flux from tide flat and wetland areas. The major conclusion was that the very high emissions were from 1 percent or less of the tide flat surface, and this was an even smaller fraction of the total coastal wetland soil type. Thus the average biogenic emission from this soil surface is weighted according to the relative emission areas within the soil type.

In this analysis, standard soil classifications were used as the basis for the soil identification. These soil classifications are shown as soil type subheadings in Table 2-2. In Table 2-3, coastal wetlands include the saline and nonsaline marshes or swamps and the coastal soils; inland high organic soils include the Histosols, Mollisols, and the Ultisol/Spodosol soil orders and suborders; and inland mineral soils comprise the remaining drier soils of the region (Adams et al. 1980). In terms of a percentage of the extended study area (essentially the area of the United States east of the Mississippi River), coastal wetlands are 7 percent of the area, inland high organic soils are 19 percent, and the inland mineral soils are the remainder, or 74 percent.

Table 2-3 and Figure 2-1 illustrate several features of the biogenic sulfur flux. First, and probably most important, the total biogenic or soil flux depends to a significant extent on the inland soils, even though their emissions density is an order of magnitude less than that of the wetland soils. The much larger area of inland soils, 93 percent of the study region, more than makes up for the low emissions density; and, as shown in the figure, the inland soils account for 59 percent of the sulfur emissions in the study area. It is of course recognized that there is considerable variability in the soil emission system and this must be allowed for in any application of these results.

Figure 2-2 (Adams et al. 1981a) shows the results of the estimates of biogenic sulfur flux measurements for the total SURE grid plotted in terms of the average sulfur emissions in metric tons per year per grid area (6,400 km^2) as a function of latitude from 47°N, about the latitude of Duluth, to 25°N, the latitude of the tip of the Florida peninsula. The relationship between annual sulfur flux per 6,400 km^2 grid as a function of latitude is:

$$\log Y = 4.70212 - 0.035588X$$

where Y is 10^6 g S per 6,400 km^2 and X is the north-south grid identification number (Adams et al. 1981c).

This relationship between sulfur flux and latitude shows an approximate exponential increase toward the south, especially south of about 33°N, the latitude of a line between Shreveport, LA, and Georgetown, SC. This rapid increase of sulfur flux southward is interpreted as being a result of an

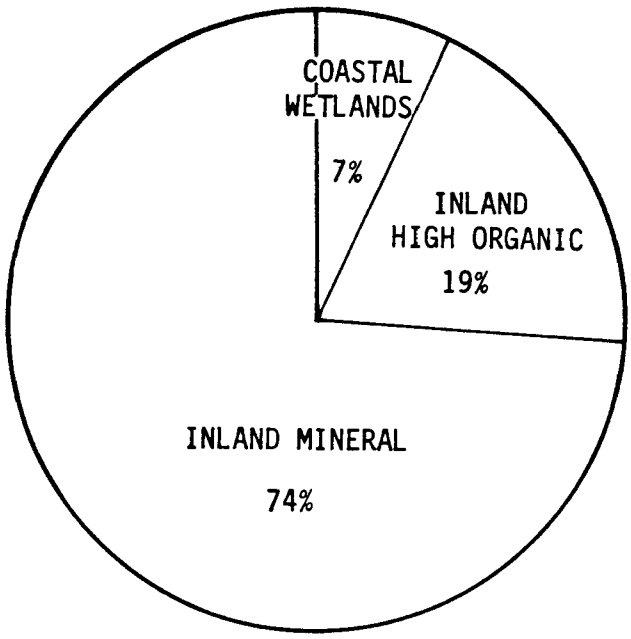

RELATIVE LAND AREA BY SOIL TYPE

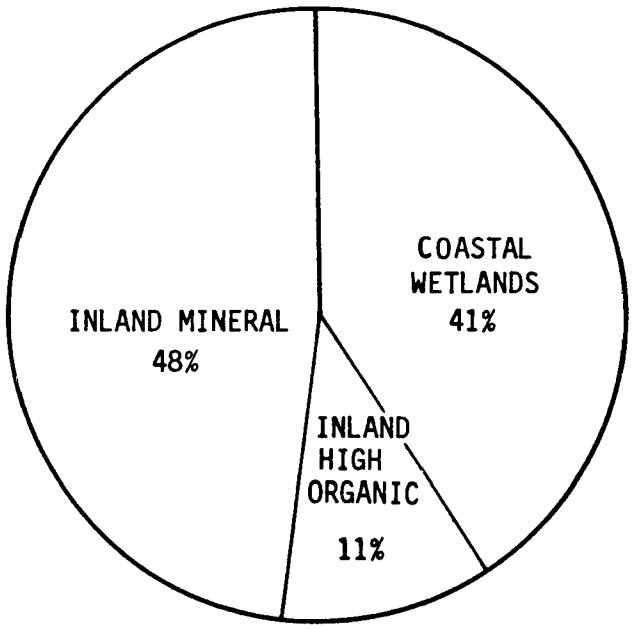

RELATIVE SULFUR FLUX BY SOIL TYPE

Figure 2-1. Comparison of relative land area and sulfur flux by soil type.

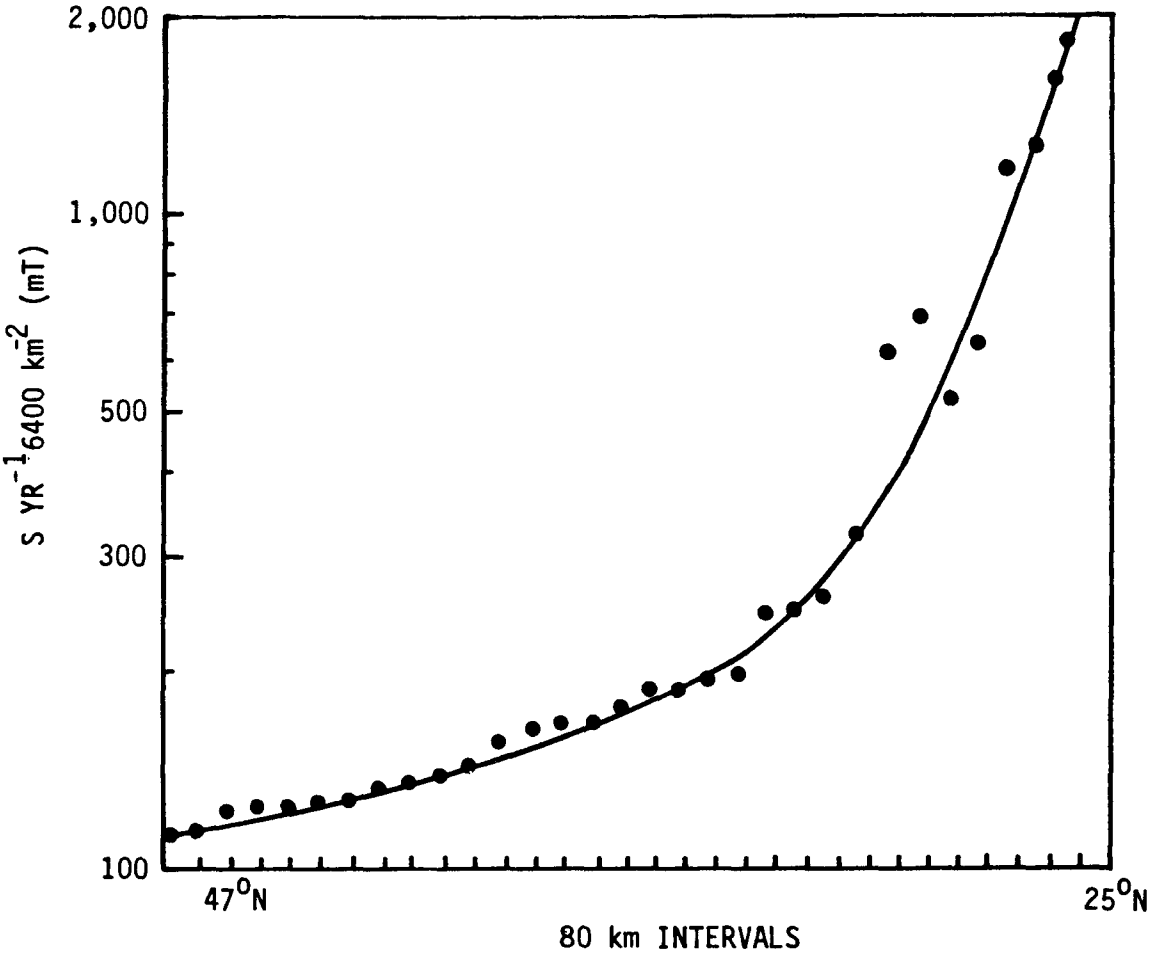

Figure 2-2. Total natural gaseous sulfur emissions averaged across latitude zones in the SURE study area, 47°N and 25°N, expressed as a function of latitude. Emission rate as metric tons of sulfur per year per SURE grid area (6400 km^2) (10^3 mT S yr^{-1} equals 0.16 g S m^{-2} yr^{-1}). Adapted from Adams et al. (1981b).

increase in temperatures, an increase in wetland areas, and a higher fraction and a higher fraction of high organic soils. To the north into Canada, biogenic emissions would be expected to decrease as shown by the downward trend toward higher latitudes in Figure 2-2.

Figure 2-2 has been used to estimate the potential biogenic sulfur flux from the State of Florida, as an example of a high biogenic emission area. For Florida, the area along the northern border near 30°N has an indicated annual flux density in units of metric tons (10^3 kg) of about 350 mT S per 6,400 km^2, or about 0.05 g S m^{-2} yr^{-1}; in southern Florida, at 25°N, the indicated annual emission density is about 2,000 mT S per SURE grid of 6,400 km^2, or about 0.3 g S m^{-2} yr^{-1}. The total statewide estimated sulfur flux for Florida is 16,980 mT S yr^{-1}. By comparison, the estimated statewide anthropogenic emissions of SO_2 for Florida in 1978 were about 606,000 mT SO_2 yr^{-1} or 303,000 mT S yr^{-1} (Section 2.3.2.1). Thus, the estimated biogenic emissions on a statewide basis in Florida are about 5 percent of the 1970 estimated anthropogenic emission.

Hawaii, with its generally warm and moist climate, would have a relatively high estimated biogenic sulfur emission density of about 3,000 mT S yr^{-1} per 6,400 km^2. For an area of 16,500 km^2, the biogenic sulfur emission estimate is about 7,600 mT S yr^{-1}. This compares with a 1970 statewide sulfur emission from anthropogenic sources of about 29,000 mT S yr^{-1} (U.S. EPA 1973). For large areas in the Northeast the ratio of biogenic to anthropogenic emissions would be much less than for either Florida or Hawaii where biogenic processes would be expected to be a maximum.

If areas smaller than a state are considered, it is, of course, possible to find areas where natural sources exceed anthropogenic estimates. The individual Hawaiian Islands other than Oahu, with its concentration of population and industry, probably have predominantly natural emission sources. Rice et al. (1981) assessed the ratio of natural and anthropogenic sources in a number of sectors of about 10^4 km^2 across the United States. They concluded that in rural and nonindustrial areas of the United States local natural sources may exceed local anthropogenic sources. However, they also concluded that in the eastern United States, where high SO_4^{2-} concentrations are found, the natural sources of sulfur probably make a minor contribution to the airborne sulfur compounds. Galloway and Whelpdale (1980) estimated that northeastern U.S. and southeastern Canadian anthropogenic emissions are about 16 Tg S yr^{-1}, which supports the conclusion that biogenic sources are unimportant on a regional basis.

It is not reasonable to evaluate the biogenic versus anthropogenic ratio over a small area relative to acidic precipitation problems because of the relatively long reaction times required for sulfate formation and incorporation in precipitating storm systems. These processes lead to longer travel times and thus considerable mixing of emanations from over a relatively large source area.

As a first approximation to a global system, Adams et al. (1981c) extended their model beyond the midlatitude zone of measurement shown in Figure 2-2 and concluded that, on a global basis, the biogenic sulfur emission flux from

land areas is about 64 Tg S yr^{-1}. This may be compared with Granat et al.'s (1976) estimate mentioned earlier, of 32 Tg S yr^{-1} for land and coastal areas. On a global basis, the emission of 64 Tg S yr^{-1} is an average emission density of about 0.43 g S m^{-2} yr^{-1} over the 149 x 10^{12} m^2 global land area. A similar figure for Granat's estimate is about 0.22 g S m^{-2} yr^{-1}. The model shown in Figure 2-2 when extended to equatorial latitudes predicts an emission value that is within the range of the measurements made by Delmas et al. (1980). Adams et al. (1981c) point out that the sulfur emission rates in tropical areas are probably at least an order of magnitude higher than those found at 25°N--along the U.S. Gulf Coast. Similarly, as illustrated by Figure 2-2, these latter rates are about 10 times higher than those found at about 35°N. The emissions rates decrease further by about another factor of two between 35°N and 47°N in the study area.

A summary of the natural or biological emissions rates for sulfur compounds in the United States east of the Mississippi River can be made by applying the average density from Table 2-3, 0.03 g S m^{-2} yr^{-1}, to an area of 2.23 x 10^{12} m^2 to yield an estimated natural emission flux of about 0.07 Tg S yr^{-1}. If this same emission density is extended to the contiguous United States, an area of 7.824 x 10^{12} m^2, the resulting natural source is 0.23 Tg S yr^{-1}. This latter figure assumes sulfur emission soil properties in the more arid areas of the west to be similar to those measured in the east. This is not likely to be the case. Also, in the west there is no counterpart to the moist Gulf Coast and its significant wetland areas.

Figure 2-3 illustrates the results of the measurements of biogenic emissions of gaseous sulfur compounds made over the EPRI SURE grid. Figure 2-3 was prepared from the individual grid estimates of annual soil sulfur flux (Adams et al. 1980, Figure 4-1). The highest emission areas are found along the coastal region from South Carolina north to southern New Jersey. This zone appears to be about 100 km wide, although the 80 x 80 km grid squares do not permit a detailed presentation. In this coastal zone the average annual emission is greater than 30 kg km^{-2} yr^{-1}. Another region with relatively high annual grid emissions is along the Mississippi River south from Illinois. Relatively low emissions are found along the coast north from central New Jersey and over most of the interior land areas. The New England states, except for the southern coastal zone, and southern Canada fall generally into the lowest soil emission category, an annual emission of less than 15 kg km^{-2} yr^{-1}. Open ocean areas are estimated by Adams et al. (1980) to have an emission of less than 10 kg km^{-2} yr^{-1}, although open ocean emissions were not measured. South of the SURE grid, soil emissions are expected to increase generally, as indicated by the latitudinal distribution of average emissions shown in Figure 2-2.

2.2.1.4 Geophysical Sources of Natural Sulfur Compounds--Natural emissions of sulfur from nonbiological sources include two classes of sources that are important to the northeastern United States mainly because they are part of the global sulfur cycle: sulfate aerosol particles produced by sea spray and sulfur compounds emitted by volcanic activity. In the global cycles estimated by material balances, both of these sources are determined to be relatively small contributors to background sulfur levels over land areas (Eriksson 1960, Robinson and Robbins 1970a, Granat et al. 1976); however,

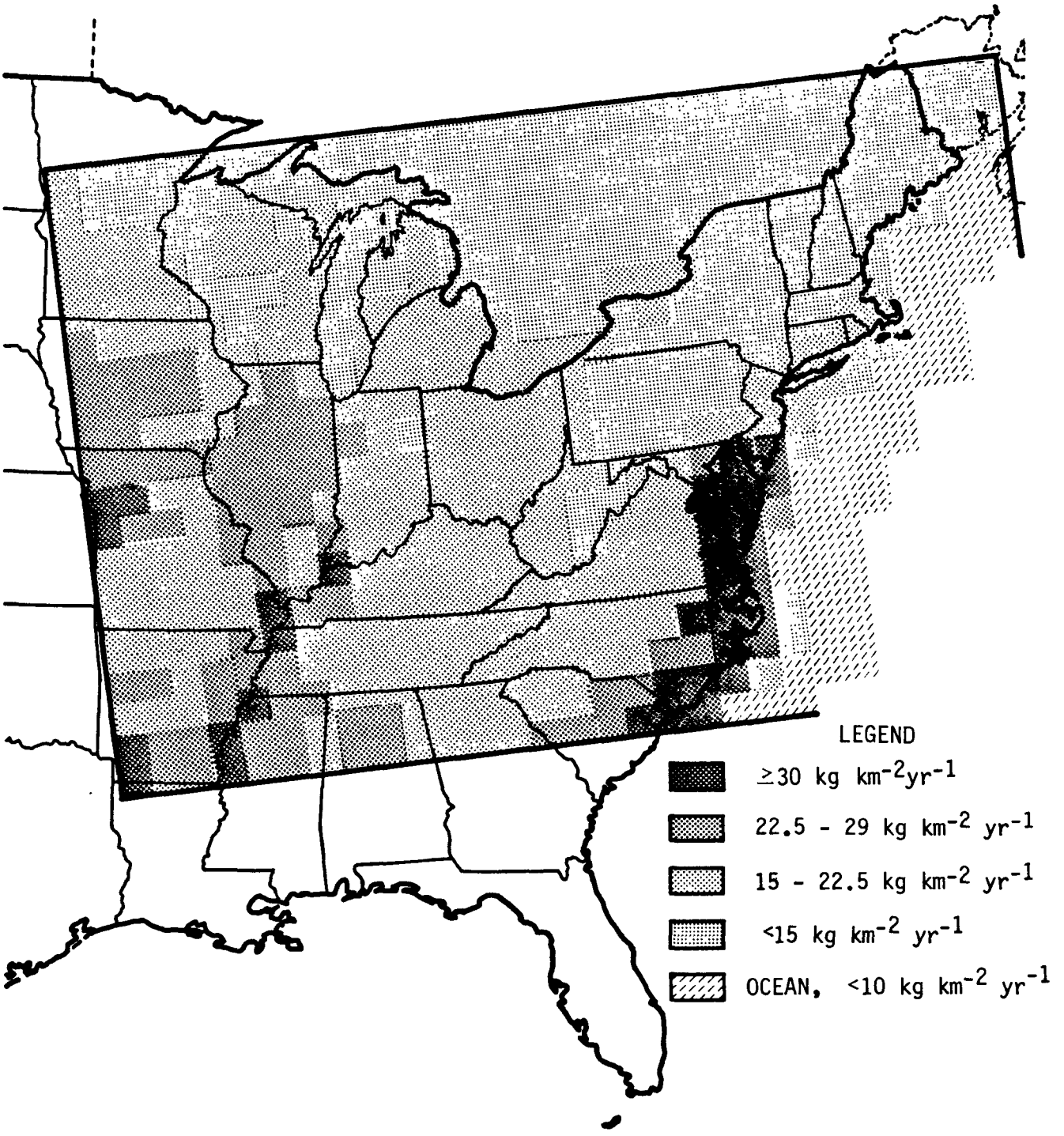

Figure 2-3. Annual biogenic sulfur emission pattern for the SURE grid over the northeastern United States. Adapted from Adams et al. (1980).

more recent estimates by Cadle (1980) may change the evaluation of the importance of volcanic emissions.

2.2.1.4.1 Volcanism. Volcanic eruptions are obvious sources of a wide variety of materials including sulfur compounds and, as such, volcanos can make important contributions to the global sulfur background. For example, the Mt. St. Helens eruption in Washington State on May 18, 1980, contained SO_2, H_2S, COS, SO_4^{2-}, and H_2SO_4 as well as chlorine- and nitrogen-containing compounds (Pollack 1981). Concentrations of CS_2 and COS in the Mt. St. Helens plumes were reported by Rasmussen et al. (1982). Although Mt. St. Helens was a major event locally, its total impact on the atmosphere was relatively short lived and its contributions to global back- ground concentrations in the troposphere are not likely to have caused major pertubations. The April 1982 eruption of El Chichon in southern Mexico was perhaps 20 times as large as that of Mt. St. Helens and injected a massive amount of sulfur gases into the middle atmosphere (Kerr 1982). However, the southern latitude of the El Chichon eruption, relative to the United States, prevented the early transport of most of the El Chichon plume across the United States. Significant northward spread of the stratospheric portion of the plume was not expected until the seasonal climatic shifts occurred in the fall of 1982 (Kerr 1982).

Estimates of volcanic sulfur compound contributions to the global atmosphere vary greatly because the emissions of volcanos differ in gas content, volume, and eruption frequency; each investigator must make a number of personal judgments of the relative importance of these factors. Granat et al. (1976), in reviewing emissions data up to about 1975, estimated the annual global volcanic emissions of sulfur compounds at about 3 Tg S yr^{-1}, or only a few percent of the total estimated global sulfur cycle.

Since Granat's evaluation of this emission classification, several important field programs have been carried out on the active volcanos of St. Augustine in Alaska and Mt. St. Helens in Washington. At St. Augustine, Stith et al. (1978) estimated SO_2 emissions at about 0.05 Tg S yr^{-1} and lesser amounts of H_2S. Emissions of sulfur gases from Mt. St. Helens in Washington over the year March 1980 to March 1981, which included the major eruptions in May and June 1980, were estimated by Hobbs et al. (1982) to be 0.15 Tg S yr^{-1} as SO_2 and 0.02 Tg S yr^{-1} as H_2S, for a total of about 0.17 Tg S yr^{-1}. This is three to four times the estimate made by Stith et al. (1978) for St. Augustine.

Cadle (1980) has summarized volcanic sulfur gas emissions and has commented on impacts of these emissions. There have been a number of estimates of average annual volcanic emissions, and Cadle describes the hazards of making the various assumptions that are necessary for a volcanic gaseous flux estimate. A number of estimates of volcanic sulfur gas emissions cited by Cadle (1980) are listed in Table 2-4. Cadle's (1980) conclusion relative to this published data was that volcanic emissions may contribute as much as a third of the global anthropogenic sulfur emission of about 65 Tg S yr^{-1}. This would be about 20 Tg S yr^{-1}. However, Cadle (1980) calculated volcanic sulfur gas emissions from lava flow data and the result was in the range of 2 to 8 Tg S yr^{-1}. The major sulfur compound from volcanic action,

TABLE 2-4 ESTIMATES OF VOLCANIC SULFUR GAS FLUX VALUES
(ADAPTED FROM DATA IN CADLE 1980)

Authors	Date	Estimated Flux (Tg S yr^{-1})
Bartels	1972	17
Kellogg et al.	1972	0.8
Friend	1973	2
Stoiber and Jepsen	1973	5
Naughton et al.	1975	24
Granat et al.	1976	3

as noted by Cadle, is SO_2. Cadle (1980) also considered the volcanic emissions of H_2S, COS, and CS_2 and concluded that they were unimportant on a global scale relative to SO_2.

Cadle (1980) has suggested that precipitation scavenging around volcanos is underestimated. Thus, as more data on volcanic activity become available, it might be more reasonable to assign any significant increase in volcanic emissions to the precipitation part of the global sulfur cycle, which would probably leave relatively unchanged the biogenic sulfur estimates made by difference. The discussion by Cadle (1980) relative to precipitation scavenging of volcanic emissions points up a fact that should be reemphasized; i.e., the long-term effects of volcanic emissions are due primarily to the part of the eruption cloud that reaches the stratosphere, where it will have a residence time long enough to cover a considerable distance from the source. Tropospheric emissions, while they can be devastating in the vicinity of the mountain, will decrease rapidly in importance with distance and will not be contributors to long-term, elevated background emissions over large areas.

Although it was stated earlier that the volcanic contribution should be considered primarily on a global basis, it also might be argued that the volcanic zones of North America could have an important impact on the United States. The volcanic activity in both Central America and Alaska can at times be significant to the United States, at least on a local basis. The volcanic emissions in Alaska are likely to be important because of the lower tropopause and the wind circulation toward the "lower 48" associated with the polar jet stream. A good example of pollutant transport over long distances from northern latitudes is the drift of Canadian forest fire smoke over the United States, which occurs from time to time. In Central America, the much higher tropopause exposes more of the volcanic emissions to rapid precipitation and cloud scavenging processes than might be typical in Alaska. Also, wind circulation systems near the equator are not generally favorable for transport north toward the United States (Ratner 1957, Kerr 1982). The Mt. St. Helens eruptions spread a plume over large portions of the United States; however, after several months of active emissions, the rate of activity has decreased to low levels. Unless Mt. St. Helens becomes more or less continuously active, it can probably be disregarded as an important background source both in the United States and on a global scale.

2.2.1.4.2 Marine sources of aerosol particles and gases. The oceans contain sulfur compounds in the form of sulfate salts, and, when sea water droplets evaporate in the atmosphere, some sulfate-containing particles are formed (Junge 1963). In the formation of marine aerosol particles, the larger particles from wind-blown waves and bursting bubbles rapidly fall back to the ocean surface and are of little consequence to the large-scale distribution of marine aerosols. Fine particles with some prospect of a prolonged atmospheric residence time are formed in the spray bubble process by the bursting of the bubble film or "skin." The numbers of particles, and whether they will remain airborne, will depend on wind and sea surface conditions. Quantitative estimates of these aerosol formation conditions are difficult to make. Most authors of atmospheric sulfur cycles reference Eriksson's (1960) estimate of 44 Tg S yr^{-1} as the sea spray contribution of more or less

persistent fine particles in the atmosphere. Of this total, he estimated that about 10 percent, or 4 Tg S yr^{-1} of sulfur, would be carried over land areas. Since 90 percent of sea spray remains in the oceanic regions rather than mixing into continental air masses, it may be considered as playing a secondary role in the overland phases of the global sulfur cycle (Eriksson 1959, 1960; Robinson and Robbins 1970a; Granat et al. 1976).

Another aspect of the oceanic contribution to the sulfur cycle is the release of gaseous sulfur compounds from the ocean surface. Because of the large area of the global oceans, even a relatively small emission rate may lead to a significant total emission. Sulfur or sulfate that cannot be balanced by considering the other common sea salt components such as sodium is called "excess" sulfur and has been noted by a number of authors. For example, Lodge et al. (1960) measured "excess sulfur" in the North Pacific Ocean atmosphere. Cadle et al. (1968) measured trace levels of SO_2 at coastal sites in Antarctica, and Lovelock et al. (1972) measured dimethylsulfide in the Atlantic.

In global sulfur balances, the "excess" marine sulfur source is sometimes identified as a separate biogenic source needed to balance the total sulfur cycle (Eriksson 1960, Robinson and Robbins 1970a); alternatively it is considered a coastal phenomenon and is combined with the biogenic land area sources (Granat et al. 1976).

In the United States, the transport of background gaseous or "excess" sulfur from oceanic areas should be considered along the Pacific and Gulf of Mexico coasts where onshore winds are predominant. The excess oceanic area sulfur is due to both sea surface emissions and volcanos. The magnitude of this onshore transport can be estimated using an average onshore or westerly wind of 8 m s^{-1} through a 3000-m mixing depth (Ratner 1957, U.S. DOC 1968). On an annual basis this gives an onshore transport of marine air of about 1.2 x 10^{18} m^3 yr^{-1} across the Gulf Coast (about 1600 km) and about 1.5 x 10^{18} m^3 yr^{-1} across the Pacific Coast (about 2000 km). Background sulfur compound concentrations applicable to marine air masses, from data summarized by Sze and Ko (1980), have been given in Table 2-1. In that list, SO_2, H_2S, $(CH_3)_2S$, and SO_4^{2-} have atmospheric residence times of up to a few days (Sze and Ko 1980) and thus could contribute to a background loading that might in turn participate in precipitation pH reactions and acidic dry deposition. The remaining compounds, COS and CS_2, have much longer atmospheric residence times, several years or longer (Sze and Ko 1980; Ravishankara et al. 1980) and, with this slow reaction rate, probably exert little influence on precipitation pH or acidic deposition. The four more-reactive compounds provide a total concentration of about 0.2 μg S m^{-3} in the marine air masses that could be expected to participate in acidic deposition processes. Considering the estimated total annual air mass volume transported across the Gulf and Pacific Coasts given above (1.2 x 10^{18} m^3 yr^{-1} across the Gulf Coast and 1.5 x 10^{18} m^3 yr^{-1} across the Pacific Coast) results in an estimated marine air input of about 0.36 Tg S yr^{-1} across the Pacific coast and about 0.24 Tg S yr^{-1} across the Gulf Coast for a total background marine air mass contribution of about 0.6 Tg S yr^{-1} to the total United States. We have not included an estimate of the possible transport across the Atlantic Coast because general wind climatology is

unfavorable for this transport (Ratner 1957). Local winds and individual short-lived circulation systems could bring some marine S across the Atlantic Coast, but it would not be a persistent situation such as occurs along the other coasts. We previously estimated the biogenic emissions for the contiguous United States at 0.23 Tg S yr^{-1}, and thus it would seem that incoming marine air masses may be more or less equivalent to biogenic sources in importance to background sulfur loading. The precision of these several estimates cannot be expected to be high, but, when they are compared to the estimated anthropogenic emissions of 12 to 15 Tg S yr^{-1}, these natural sources would still seem to be less than 10 percent of the total sulfur burden.

2.2.1.5 Scavenging Processes and Sinks--Ultimately, reactive materials such as the sulfur compounds return to the Earth's surface either through precipitation-related mechanisms or by direct attachment to the Earth's surface through processes known collectively as dry deposition. Both gases and aerosol particles participate in both deposition routes.

Sulfur compounds also participate in a variety of reactions in the atmosphere, generally tending toward oxidation to SO_4^{2-} and the formation of sulfuric acid or sulfate particles. Hydrogen sulfide, probably the most common natural sulfur emission to the atmosphere, is oxidized to SO_2 and then to sulfate. Graedel (1978), Sze and Ko (1980), and others describe this reaction. The initial reactant is probably the hydroxyl radical, OH, and the average lifetime of H_2S is given usually as only a few days at typical atmospheric concentrations. Reactions of SO_2 in the atmosphere due to both homogeneous and heterogeneous reaction processes have been estimated by a number of authors including Granat et al. (1976), Graedel (1978), Husar et al. (1978), Altshuller (1979), Sze and Ko (1980), and Rodhe and Isaksen (1980), to name only a few. Although some calculated SO_2 atmospheric lifetimes are quite long (e.g., Graedel [1978, pp. 29-30] estimates about 430 days), the general consensus seems to favor an atmospheric residence time of only a few days (e.g., Sze and Ko 1980). Altshuller (1979), in an extensive set of chemical model calculations of SO_2 reactions in nonurban situations, showed that the rate of reaction was more rapid in summer than winter, much more significant at low latitudes than at high latitudes, and more rapid at low altitudes than in the middle or upper troposphere. Altshuller (1979) concluded that the most significant reactant for SO_2 was OH. Rodhe and Isaksen (1980), on the basis of a global model, estimated the global average residence times for H_2S, SO_2, and SO_4^{2-} to be about 1, 1.5, and 5 days, respectively.

H_2S oxidation in liquid drops is also possible (Cox and Sandalls 1974). The product is sulfate, with an intermediary status as SO_2. The decay rate for H_2S via the liquid droplet route is given by Granat et al. (1976) as a day or more; and for $(CH_3)_2S$ the reaction rate is even slower. The reaction of $(CH_3)_2S$ apparently goes directly to sulfate without an SO_2 intermediate step (Cox and Sandalls 1974).

Gaseous reactions of the organic sulfur compounds commonly identified in natural emissions, CS_2, COS, $(CH_3)_2S$, $(CH_3)_2S_2$, and CH_3SH, are given by (1978), Sze and Ko (1980), and others. These reactions proceed to HSO_4

and/or sulfates, but not always through SO_2 as an intermediate compound. The common sulfate compound in the atmosphere is ammonium sulfate $[(NH_4)_2SO_4]$ as a result of the reaction, presumably in liquid droplets, between the two common gases ammonia (NH_3) and SO_2.

As mentioned above, pollutants are deposited on the Earth's surface by either wet or dry processes and these topics are discussed in detail in other chapters (Chapters A-6 and A-7) of this document. However, briefly with regard to acidic deposition, the precipitation scavenging mechanisms are directly involved in the precipitation pH or acidic deposition controversy, and it is useful to mention some aspects of deposition in this discussion. Various authors have pointed out that surface waters may be affected by deposited pollutants, whether they arrive as part of the precipitation chemistry or are deposited on the ground in a dry state and then are incorporated into the surface water. Resuspension of sulfur compounds is probably minor because of their general solubility and thus rapid incorporation into the soil. Desert areas and agricultural regions with exposed soils may create situations where strong winds may cause blowing dust. This would resuspend both the deposited material and natural soil constituents.

Granat et al. (1976) have attempted to estimate the relative importance of precipitation and dry deposition processes. They argue that dry deposition increases in relative importance for situations where the value of the dry deposition velocity, V_d, is large. This would occur where gaseous compounds are a relatively large fraction of the total atmospheric sulfur. Granat et al. (1976) also point out that wet deposition increases in importance when the SO_2 to SO_4^{2-} particle formation rate and the boundary layer mixing depth increase. This reduces the importance of dry deposition and increases the probability of water droplet interaction. For background sulfur emissions such as H_2S, V_d would probably be similar to that for SO_2. The mixing depth would be relatively great because atmospheric residence times of the trace compounds would be relatively long (e.g., one or more days). For this type of situation, the deposition process would be expected to be dominated by aerosol formation and wet, rather than dry, deposition processes. Thus, the natural sulfur emissions could be expected to affect the precipitation chemistry of an area more than the dry deposition accumulation onto the Earth's surface.

2.2.1.6 Summary of Natural Sources of Sulfur Compounds--There are many problems remaining in the natural sulfur cycle and many unknown factors; however, because of the importance of the acidic deposition problem it is useful to summarize the natural sulfur cycle and relate it to anthropogenic emissions. For land areas, probably the most important natural sources of sulfur compounds are the emissions from biological actions in the soil although on a global basis volcanos may also be significant. In midlatitudes, and specifically in the United States east of the Mississippi River, an average biogenic sulfur emission rate of about 0.03 g S m^{-2} yr^{-1} is indicated by extensive, although still incomplete, field experiments. The emission rate from soil sources increases with ambient temperature and in coastal wetlands. Thus, there is a rapid increase in the emission rate of sulfur compounds from the soil from north to south. Coastal wetlands, although they cover only about 7 percent of the land area, have an average emissions rate of about 10

times the rate of inland soils and account for about 40 percent of the biogenic sulfur emissions in the area east of the Mississippi. Figure 2-3 summarizes, on a grid basis, the results of a measurement program on gaseous sulfur emissions from soils in the midwestern and eastern United States. The more arid and alkaline soils in the west would be expected to have lower biogenic emissions than are found along the east coast, but actual measurements have not been made in these areas. Nevertheless, extending the east coast average emissions rate to the 48 contiguous states, an area of about 7.8 x 10^{12} m^2, results in an estimated total biogenic emission of about 0.23 Tg S yr^{-1}. U.S. anthropogenic sulfur oxide emissions are in the range of 12 to 15 Tg S yr^{-1}.

The compounds that are most important in the biogenic flux are H_2S, COS, and CS_2. Of secondary importance are $(CH_3)_2S$, $(CH_3)_2S_2$, and CH_3SH.

Ocean areas may also make a contribution to the natural sulfur burden over land areas through (1) the transport of particles from the evaporation of fine seawater aerosol particles formed in bubble-bursting processes, (2) sea-surface-generated gaseous sulfur compounds, and (3) the sulfate particles formed by atmospheric reactions of sea-surface-generated gaseous sulfur compounds. Estimates of oceanic transported sulfur were made using a 3-km mixing depth, an 8-m-sec^{-1} average onshore wind, and background sulfur concentrations of 0.18 x 10^{-6} g S m^{-3} for gaseous compounds and 0.02 x 10^{-6} g S m^{-3} for sulfate particles. The results of this calculation indicate that the annual sulfur input across the Pacific Coast is about 0.36 Tg S yr^{-1} and about 0.24 Tg S yr^{-1} across the Gulf Coast. Because large-scale onshore winds do not dominate the east coast, no attempt was made to extend this rough estimation procedure to that area. Thus, marine background input may introduce about 0.6 Tg S yr^{-1} across the United States coastal area; this is about three times the amount estimated to be generated by biological soil processes. As marine air masses travel inland, this sulfur compound content would be subject to a continuing process of scavenging reactions.

On a long-term basis, volcanic activity is not expected to be a major contributor to the levels of natural sulfur in the contiguous United States, although special situations like the 1980 eruption of Mt. St. Helens or the southern Mexico volcano El Chichon could perturb conditions for short time periods.

Thus, in total, the potential upper-limit background sulfur burden of the United States is about 1.0 Tg S yr^{-1}, which includes contributions from biospheric and oceanic generation processes. This figure does not include any correction for amounts "exported" by air masses moving across the coasts or borders. In terms of relative importance, it may be compared to anthropogenic sulfur oxide emissions that are in the range of 12 to 15 Tg S yr^{-1}.

2.2.2 Nitrogen Compounds

2.2.2.1 Introduction--Nitrogen compounds are emitted to the atmosphere from natural sources in several forms: as relatively inert nitrous oxide (N_2O), as potentially acidic nitric oxide (NO) and nitrogen dioxide (NO_2), and as potentially acid-neutralizing ammonia (NH_3). The sources for these

compounds, other than anthropogenic emissions, are, to a major extent, in the terrestrial biosphere with some injections into the troposphere from the oceans, from stratospheric photochemistry and from atmospheric fixation by lightning.

The estimation of natural sources of nitrogen oxides and ammonia has been severely restricted in the past by a lack of reliable data on concentrations of these compounds in the ambient atmosphere. Even at present, ambient atmospheric measurements in clean or background areas are research tasks rather than routine monitoring with continuous instruments, such as is carried out in urban area studies. Thus, the evaluation of likely impacts of natural sources of nitrogen compounds is subject to considerable variability, probably greater than is the case for estimates of natural sulfur compound emissions and their impacts.

Nitrous oxide is essentially inert in the troposphere and plays no role in problems of precipitation pH; thus, detailed consideration of its sources and sinks can be omitted without affecting the objective of this document.

Table 2-5 lists background concentrations of NO_X and NH_3, based on relatively recent research, which are probably applicable to nonanthropogenically-affected locations.

2.2.2.2 Estimates of Natural Global Sources and Sinks--A first approximation of the global magnitude of natural sources of nitrogen compounds can be obtained from a review of two previously published nitrogen compound cycles, one by Robinson and Robbins (1970b) and one by Soderlund and Svensson (1976). Major differences between these two environmental cycles exist, with the more recent one by Soderlund and Svensson (1976) proposing significantly smaller fluxes between reservoirs. This reduction in fluxes results from improved estimates of atmospheric concentrations, based on an increased number of better measurements of background concentrations. Table 2-6 lists, as a starting point for this discussion, emission and sink flux estimates adapted from Soderlund and Svensson (1976) for NO, NO_2, and NH_3 or NH_4^+. The nitrogen oxides, NO and NO_2, were combined as NO_X for this estimate, and the NH_3 values also include the ammonium ion $NH4^+$. The NO_X deposition values include nitrate (NO_3^-) compounds also. In the original reference by Soderlund and Svensson (1976), anthropogenic emissions of NO_X compounds totaling 19 Tg N yr^{-1} were included in the NO_X flux values, and the NH_3 emission estimates included the emissions from coal combustion, ranging from 4 to 12 Tg N yr^{-1}. These were estimated global emission values for 1970 (Soderlund and Svensson 1976). To emphasize the natural emission cycle in Table 2-6, we have subtracted these anthropogenic emissions from the original values to arrive at the tabulated values. Emissions and gaseous reactions are given in terms of NH_3 (N) while deposition terms are shown in reference to NH_4^+ (N).

In a detailed paper submitted for publication, Logan (1983) derived a nitrogen cycle with several important differences relative to that given in Table 2-6. Biogenic emission of NO_X is estimated by Logan at 8 Tg N yr^{-1} with a range of 4 to 16 Tg N yr^{-1} in comparison to a value of 21 to 89 Tg N yr^{-1} in Table 2-6. Logan (1983) also estimates lightning as a potential

TABLE 2-5. ATMOSPHERIC BACKGOUND CONCENTRATIONS OF NITROGEN OXIDES AND AMMONIA

Constituent	Concentration $\mu g\ m^{-3}$	Reference
NO_x (afternoon) as NO_2	0.4 - 0.5	Kelly et al. (1980)
NO (afternoon)	0.04 - 0.12	Kelly et al. (1980)
NH_3 (land)	1 - 8	Hoell et al. (1980)
NH_3 (ocean)	0.06	Ayers and Gras (1980)

TABLE 2-6. GLOBAL EMISSIONS OF NITROGEN COMPOUNDS[a]

	Total Tg N yr^{-1}	Global emission density g N m^{-2} yr^{-1}
Terrestrial[b]		
NO_x emissions[c]	21 - 89	0.14 - 0.59
NO_x wet deposition	13 - 30	0.09 - 0.20
NO_x dry deposition	19 - 53	0.13 - 0.36
NH_3 emissions[d]	109 - 232	0.73 - 1.56
NH_4 wet deposition	30 - 60	0.20 - 0.40
NH_4 dry deposition	61 - 126	0.41 - 0.85
Organic N wet deposition	10 - 100	0.07 - 0.67
Atmospheric Reactions (global)[e]		
NH_3 loss via OH	3 - 8	0.006 - 0.016
NO_x formation	3 - 8	0.006 - 0.016
NO_x lightning formation	?[g]	-
NO_x from N_2O + UV	0.3	0.0006
Oceanic[f]		
NO_x wet deposition	5 - 16	0.014 - 0.04
NO_x dry deposition	6 - 17	0.017 - 0.05
NH_4 wet deposition	8 - 25	0.022 - 0.07
NH_4 dry deposition	11 - 25	0.03 - 0.07
Organic N emissions	10 - 20	0.03 - 0.05
River flow to ocean		
NO_x	5 - 11	
NH_4	< 1	
Organic N	8 - 13	

[a]Adapted from Soderlund and Svensson (1976).

[b]Total land area: 1.49×10^{14} m^2.

[c]Original reference includes 19 Tg N yr^{-1} anthropogenic emissions. Deposition terms include anthropogenic contributions.

[d]Original reference includes 4 to 12 Tg N yr^{-1} from coal combustion. Deposition terms include anthropogenic contributions.

[e]Global area: 5.13×10^{14} m^2.

[f]Ocean area: 3.64×10^{14} m^2.

[g]Recent data indicate a possible value of 5-10 Tg N yr^{-1} (see Section 2.2.2.5).

source of 8 Tg N yr^{-1} (range 2 to 20 Tg N yr^{-1}). Logan estimated NO_x from fossil fuel sources at 21 Tg N yr^{-1} plus an additional 12 Tg N yr^{-1} from biomass burning (slash and burn agriculture, land clearing, forest fires). If these latter sources were considered man-caused sources then Logan's anthropogenic sources would total 33 Tg N yr^{-1} with a range of 18 to 52 Tg N yr^{-1}.

An estimate of the wet deposition of organic nitrogen compounds, e.g., amino acids, amines, and proteins, is included in the above-noted estimate. Soderlund and Svensson (1976) include some generation of organic nitrogen compounds at the ocean surface, but this process is not well known, as indicated by the order of magnitude range for the estimate of terrestrial deposition. Other sources or sinks (e.g., dry deposition) of organic nitrogen compounds are not identified in Table 2-6, nor is the organic nitrogen cycle balanced.

Table 2-6 also includes estimates of the global emission density in units of g N m^{-2} yr^{-1}. These figures were calculated from the values of the total fluxes shown in the table, using values from Butcher and Charlson (1972) for global land and ocean areas without attempting to correct for surface or climatic effects expected to change emissions in polar regions, deserts, etc.

Galbally (1975) has made separate estimates of NO_x and NH_3 sources and sinks, based on a boundary layer gradient method analogous to a calculation of dry deposition. For the Northern Hemisphere, he obtained an NO_x emission of 30 Tg N yr^{-1} and a value of 130 Tg N yr^{-1} for NH_4^+. Galbally (1975) also considered differences between tropical and temperate latitude conditions in background concentrations and between land and ocean conditions in making his estimates. His estimates may be converted to average emission densities of 0.32 g N m^{-2} yr^{-1} for NO_x and 0.55 g N m^{-2} yr^{-1} for NH_4^+. These values are comparable to those derived from Soderlund and Svensson (1976) and listed in Table 2-6. Galbally's estimating procedure would appear to be relatively insensitive to local high concentrations of anthropogenic emissions. In Table 2-6 natural NO_x emission densities of 0.14 to 0.60 g N m^{-2} yr^{-1} are indicated. More recent estimates (e.g., Logan 1983) arrive at lower values of natural emissions because they relate to newer and lower ambient background NO_x concentrations.

The nitrogen compounds NO_2 and NH_4^+ return to the Earth's surface by both dry and wet deposition mechanisms. Dry and wet deposition rates would be expected to vary between being of about equal importance in areas generally removed from industrial source areas (Granat et al. 1976) and situations where dry deposition was perhaps twice the magnitude of wet deposition near major source regions (Garland and Branson 1976). As pointed out by Galbally (1975), the natural sources of NO_x and NH_4^+ appear to be of sufficient magnitude to explain the observed global deposition of these compounds in precipitation; but this would not necessarily be true for individual regional areas because of the tendency for anthropogenic sources to be concentrated in relatively small areas (with reference to a global scale). It is generally assumed that natural sources are distributed more or less uniformly over relatively large areas of the globe, with their emission fluxes changing gradually in response to temperature, moisture, and soil conditions.

2.2.2.3 Biogenic Sources of NO_x Compounds--It seems to be generally concluded that the major natural sources of NO_x are found in the terrestrial biosphere (Junge 1963, Galbally 1975, Soderlund and Svensson 1976), although one set of observations indicating a tropical ocean source of NO will be described subsequently (Zafiriou et al. 1980). A wide variety of experiments have been carried out on nitrogen compound losses from soils of various types because of the impact such losses may have on the availability of fertilizer nitrogen to crops.

Altshuller (1958) pointed out that NO production can be quite large and rapid under certain conditions. He described how NO_2 concentrations of several hundred parts per million occurred in silos shortly after the storage of silage. These concentrations occurred under anaerobic conditions with high moisture content in an all-organic environment.

In this assessment of terrestrial sources it will not be possible to present a comprehensive review of all work in the soil sciences that relates to nitrogen compound releases from the soil, but work that can be related to an NO_x source for precipitation chemistry will be reviewed. In the past few years, interest has been renewed in nitrogen emissions from soil triggered by nitrogen fertilizer because N_2O is a significant fraction of this release (Nelson and Bremner 1970) and its impact on the stratospheric ozone layer is of great concern.

Nelson and Bremner (1970), as a result of laboratory experiments, concluded that soil or fertilizer nitrite can be a source of significant amounts of NO_2. Although the amounts of NO_2 released in these experiments were inversely related to soil pH, significant amounts of NO_2 were released from soils with pH greater than 7.0, i.e., from alkaline soils. Some of the experiments were consistent with the hypothesis that atmospheric NO_2 results from the breakdown of nitrous acid to NO and the atmospheric oxidation of the NO to NO_2. However, they did not have the capability of measuring NO in their experiments.

Nelson and Bremner (1970) found that in the laboratory, the organic content of the soil had an important effect on the amount of nitrite that was fixed to N_2; however, the proportion of the nitrite that was recovered as NO_2 was not dependent on the organic content. In many of their experiments, the evolution of NO_2 represented the largest fraction of the nitrite added to the soil; however, the total nitrogen recovered was divided among nitrate, nitrite, N_2, N_2O, and NO_2. In experiments on five soils in the pH range of 4.8 to 6.0, held for 2 days at 25 C, the evolved NO_2 accounted for 55 percent of the applied nitrite. At near neutral pH (6.6 to 7.0), 28 percent of the nitrite was evolved as NO_2. As indicated above, at least part of this NO_2 was released as NO and was subsequently oxidized to NO_2. Experiments with completely closed systems showed that NO_2 reacted further and was recovered as nitrate.

As mentioned, these experiments were done in the laboratory under a variety of conditions and cannot be translated to flux rate values under field conditions. However, they do indicate clearly the evolution of NO and NO_2 from

soils under a variety of conditions and the probable dominant role of NO_x in the spectrum of soil emissions.

The work of Nelson and Bremner (1970) cited above dealt with NO_2 evolved from nitrite applied to the soils as $NaNO_2$. Prior experiments by Makarov (1969) were related to applications of nitrate as NH_4NO_3 and the results showed a decrease in the evolution of NO_2 from these field soils when microbiological processes were reduced by the addition of inhibiting substances to the test soil field plots. Thus it was hypothesized that NO_2 soil emissions were related to microbiological activity. Perhaps the most interesting data for our considerations were produced by the conditions reported by Makarov (1969) for his unfertilized control plots. His control plot tests with a Sod-Podzolic soil in the U.S.S.R. showed that NO_2 evolution during one experimental period averaged 0.6 g ha^{-1} hr^{-1} from May 31 to September 26 (119 days). This NO_2 production is 0.17 g m^{-2}, which is equivalent to 0.05 g N m^{-2}, for the experimental period. A second experiment in the same soil over the 88-day period from 24 June to 20 September averaged 1.06 g NO_2 ha^{-1} hr^{-1}, which converts to a total of 0.07 g N m^{-2} for the period of the experiment. An experiment using a different soil, Chernozem, was shorter in duration and not reported in detail, but it appears that significant NO_2 emissions were produced similar to those shown in the other tests.

Because gaseous nitrogen evolution decreases with temperature (Keeney et al. 1979), it is likely that these summer NO_2 emissions can serve as at least a first approximation of an annual emissions rate for higher latitude areas. Thus we can compare Makarov's results, which approximate 0.06 g N m^{-2}, with the global cycle results shown in Table 2-6. In this tabulation, natural NO_x emissions were estimated to have an emission density of 0.14 to 0.6 g N m^{-2} yr^{-1}. The two sets of results seem compatible because the global estimate would be increased by the effect of warmer, low-latitude areas with longer warm seasons. This has been shown to be the case with biogenic sulfur emissions where field experiments have identified a strong temperature relationship (Adams et al. 1980).

Field experiments on NO evolution from grazed and ungrazed grassland areas were carried out by Galbally and Roy (1978). They were able to show, through the use of improved instrumentation, that NO is continuously evolved from natural grassland soils, and that NO_2 is a negligible fraction of the NO_x flux from the soil. In the atmosphere, the NO emission is rapidly oxidized to NO_2 by the ambient ozone (O_3) concentration. This emission of NO followed by an atmospheric reaction to form NO_2 was hypothesized earlier by Robinson and Robbins (1970b). In the Australian field measurements by Galbally and Roy, the observed NO emission density, if integrated over a year, amounted to a value of 0.1 g N m^{-2} yr^{-1}. If this rate is extended to a global land area value, it produces a total nitrogen emission of 10 Tg N yr^{-1}.

Bulla et al. (1970) also reported that the emission of NO from soil is not dependent on microbiological action. Their experiments were done on Oregon soils in the laboratory. In these experiments, as with those of Nelson and

Bremner (1970), NO as a fraction of added nitrite dominated the nitrogen emissions over both N_2 and N_2O.

The generation of NO_x in oceanic atmospheres has not been considered a significant feature of the global nitrogen cycle by most investigators (Galbally 1975, Soderlund and Svensson 1976). However, in an investigation in the central equatorial Pacific (7°N-10°S, 170°W), Zafiriou et al. (1980) found that nitrite photolysis in seawater produced concentrations of NO. They showed that in these tropical areas, the buildup of NO in the surface water layers occurred in daylight and disappeared quickly at night. From partial pressure comparisons of the water samples and atmospheric NO concentrations, Zafiriou et al. (1980) and Zafiriou and McFarland (1981) concluded that tropical ocean areas, especially areas rich in nitrite, may be sources of atmospheric NO, but on a global scale the source is less than 1 Tg N yr^{-1} and thus is insignificant in the global nitrogen oxide cycle.

2.2.2.4 Tropospheric and Stratospheric Reactions--A small transport of NO_2 into the troposphere from the stratosphere probably occurs. Soderlund and Svensson (1976) estimate this flow at 0.3 Tg N yr^{-1}, which on a global basis is 0.0006 g N m^{-2} yr^{-1}, a negligible part of the cycle. This stratospheric formation results from reactions of N_2O with $O(^1D)$, which occur at altitudes where wavelengths below 2500 nm are present to form $O(^1D)$ (Bates and Hays 1967). Robinson and Robbins (1970b) give some additional comments on this stratospheric NO_x source.

As a result of improved measurement techniques, Kley et al. (1981) have been able to develop observational data of vertical NO_x profiles through the troposphere. These profiles show that the concentrations of NO_x change from 0.19 μg m^{-3} as NO_2 in surface air to about 0.38 μg m^{-3} at the tropopause. They attribute this increase in concentration to the intrusion of NO_x into the troposphere from the stratosphere, which is consistent with a flux of about 1 Tg N yr^{-1} (Kley et al. 1981). This stratospheric NO_x flux is consistent with other transtropopause source estimates (Johnston et al. 1979). The NO_x source may be the stratospheric photochemical reactions of N_2O or the NO_x emissions of subsonic aircraft flying in the upper troposphere and lower stratosphere (Kley et al. 1981). There have been some questions raised relative to the importance of this stratospheric NO_x source to the tropospheric global nitrogen cycle (Fishman 1981).

Atmospheric reactions of NH_3 in the troposphere involving reactions with OH radicals have been proposed as another source of NO_x. Soderlund and Svensson (1976), using reaction systems suggested by Crutzen (1974) and McConnel (1973), estimated a formation rate of NO_x from NH_3 in the atmosphere of 3 to 8 Tg N yr^{-1}. As indicated in Table 2-6, this is equal to a global source emission density of 0.006 to 0.016 g N m^{-2} yr^{-1}. Thus, this is also an inconsequential source of NO_x.

2.2.2.5 Formation of NO_x by Lightning--The question of nitrogen fixation by lightning has been studied for more than 150 years, and no definitive answer is yet at hand. Soderlund and Svensson (1976) leave the possibility of lightning fixation as still a questionable atmospheric source

of NO_x, as indicated in Table 2-6. They note one reference on the question of lightning fixation of nitrogen, dated 1827 and authored by J. von Liebig.

Junge (1963) stated that the consensus of opinion at that time (1963) was that the evidence for lightning formation of NO_2 was marginal, and referenced Viemeister's studies of thunderstorms (Viemeister 1960) and the NO_2 concentration measurements done on the Zugspitz by Reiter and Reiter (1958). Georgii (1963), in reviewing the evidence to 1963 and including Visser's detailed analysis of rain chemistry in Uganda (Visser 1961), concluded that lightning was not a factor in nitrogen oxide concentrations.

Although Noxon (1976, 1978) was able to observe enhanced NO_2 patterns near thunderstorms, confirming the information of NO_x by lightning, it is still apparent that observational evidence linking atmospheric NO_x to electrical discharge is for the most part still lacking.[1] However, modeling and theoretical analyses done since the early 1960's indicate more strongly that lightning or electrical discharges in the atmosphere could be a source of NO_x.

One of the more recent assessments of lightning fixation of nitrogen is by Hill et al. (1980) who conclude that lightning may cause a maximum NO_2 production rate of 14.4 Tg yr^{-1} or 4.4 Tg N yr^{-1}. Dawson (1980), in an article published back-to-back with Hill et al. (1980), concluded that lightning may produce about 3 Tg N yr^{-1}. Dawson also used Noxon's (1976, 1978) data on solar spectral measurements of enhanced NO_2 around thunderstorms to deduce a global annual NO_2 production rate of 7 Tg N yr^{-1} but commented, "with considerable uncertainty" (Dawson 1980). Finally, the laboratory studies of nitrogen fixation by spark discharges (Levine et al. 1981) can be mentioned, which, when extended to a global NO_x budget, result in an estimated production of 1.8 Tg yr^{-1} of NO or about 0.8 Tg N yr^{-1}. Logan (1983) has reevaluated the lightning NO_x formation data and concludes that a reasonable annual global source is about 8 Tg N yr^{-1} with a range of between 2 and 20 Tg N yr^{-1}.

On the basis of the available assessments of nitrogen fixation by lightning, it is probably realistic at this time to assign a production rate of 5 to 10 Tg N yr^{-1} to this source in place of the question mark shown in Table 2-6. This production would translate to an emission density nitrogen flux of 0.01 g N m^{-2} yr^{-1} on a global basis, although lightning and thunderstorm distributions are geographically skewed toward warm, humid areas and seasons.

If further research can link lightning discharges more directly with significant NO_x formation, the frequent occurrence of thunderstorms and their accompanying lightning in the midwestern and eastern regions of the United

---

[1]Note added after external review: Drapcho et al. (1983) report increased NO_2 and NO at a ground station during and after passage of a midwestern thunderstorm. Their extrapolation of these measurements and other references indicate that global nitrogen fixation by lightning is in the range of 1 to 40 Tg N yr^{-1}.

States could be an important consideration with regard to acidic deposition in the northeastern states and southeastern Canada.

2.2.2.6 Biogenic NO_x Emissions Estimate for the United States--Quantitative measurements of NO_x emissions for a wide variety of biospheric situations, such as were made for biogenic sulfur emissions, have not been made for NO_x. Nevertheless there is little doubt that there are NO_x emissions from the biosphere, as described in the previous discussions. Thus, in order to arrive at some estimate of biogenic emission rates it will be necessary to use secondary methods of estimate. The material balance procedure has already been described, and, as noted in Table 2-6, the nonanthropogenic global emission of NO_x has been estimated to range between 21 and 89 Tg N yr^{-1}. If this NO_x emission is assumed to come only from land area processes in the nonpolar regions, an average calculated biogenic emission density is then in the range of 0.16 to 0.68 g N m^{-2} yr^{-1} for the 131 x 10^{12} m^2 of global nonpolar land area (70°N to 55°S). Applying these global emission rates derived from material balance considerations to the contiguous United states, 7.8 x 10^{12} m^2, and the area east of the Mississippi River, 2.23 x 10^{12} m^2, results in an annual biogenic NO_x emission estimate of 1.25 to 5.30 Tg N yr^{-1} for the United States and 0.36 to 1.52 Tg N yr^{-1} for the area east of the Mississippi River. The lack of precision and the large possibility for error in this very simple calculation is obvious, but it still can be used as a guide for further discussion.

Galbally (1975) has taken another approach in making an estimate of natural emissions by using the diffusivity and concentration gradient. With this calculation procedure and a surface layer average concentration of 4 ppb, Galbally (1975) estimates the Northern Hemisphere natural emission of NO_x to have an upper limit of 30 Tg N yr^{-1} or 0.31 g N m^{-2} yr^{-1} for the nonpolar regions of the Northern Hemisphere (equator to 70°N). Applying this emission density to the United States results in an estimated maximum biogenic NO_x emission of 2.4 Tg N yr^{-1} and 0.69 Tg N yr^{-1} for the contiguous United States and the area east of the Mississippi River, respectively. These values are about midway in the values derived from the range given by Soderlund and Svensson (1976) and given in Table 2-6.

More recently Logan (1983), using NO and NO_2 emission measurements from pasture plots of Galbally and Roy (1978), has estimated the global NO_x biogenic source to be 8 Tg N yr^{-1}. This is a value of about 0.06 g N m^{-2} yr^{-1} or about 20 percent of the emission density calculated above from Galbally (1975). Applying this value to the contiguous United States and the area east of the Mississippi River results in annual biogenic NO_x emission estimates of 0.47 and 0.13 Tg N yr^{-1}, respectively.

Measurement techniques for NO_x that are applicable to background situations have been available only in recent years and it appears that general NO_x background concentrations may be significantly lower than the values used by Galbally (1975) and Soderlund and Svensson (1976). This may be especially true for midlatitude areas such as the United States. For example, Kelly et al. (1980), after a program of background measurements in the Colorado Rockies, concluded that the NO_x concentration in the boundary layer was about 0.39 μg m^{-3}, as shown in Table 2-5. This is very much lower than

the 6 μg m^{-3} used by Galbally (1975) as the basis for his NO_x biogenic emission estimate. Thus, even the relatively low annual emissions derived for the United States from Logan's (1983) global emission estimate may be high by about a factor of 3 or so.

Table 2-7 summarizes these several estimates of the biogenic NO_x emission source as they may relate to the contiguous United States and to the region east of the Mississippi River. The 1978 estimates of anthropogenic NO_x emissions for these two areas is also shown (see this chapter, Sections 2.3.1 and 2.3.3, Figures 2-4 and 2-7). On the basis of Logan's estimate or the modified data based on the ambient air measurements of Kelly et al. (1980), the biogenic estimates are about 7 percent of the estimated anthropogenic emissions in the contiguous United States and 4 percent in the region east of the Mississippi River.

2.2.2.7 Biogenic Sources of Ammonia--The identification of a biogenic source for ammonia and ammonium compounds that are part of both atmospheric and precipitation trace chemistry is more or less circumstantial. Dawson (1977) summarizes the evidence by which a surface emission of ammonia can be inferred. First, ammonium is found in relatively high concentrations in rainwater, and, because it can be presumed that there are no major sources in the atmosphere (except of course the reactions to form NH_4^+ from NH_3), a surface NH_3 source can probably be inferred. Second, concentrations of NH_3 in the air are directly related to the pH of the underlying soil, increasing with soil temperature, and are higher over land than water areas. These factors favor an alkaline land source. Furthermore, atmospheric ammonia concentrations decrease rapidly with altitude above the ground surface but are trapped and tend to increase under an inversion layer.

Dawson (1977) provides a number of references that support these various features of the atmospheric NH_3/NH_4^+ distribution. He further states that "the evidence thus indicates that the soil is the primary source of the world's ammonia, though emission from uncultivated, unfertilized vegetated land has never been measured." This latter statement still seems to be correct, as of late 1982, although there have been a large number of investigations by soil scientists and agronomists examining NH_3 losses as a function of added fertilizer (Smith and Chalk 1980). Also, there is one set of measurements from Korean forest and grass soils by Kim (1973). In this study, Kim measured the evolution of NH_3 and NO_x by placing small plastic hoods over areas of topsoil in pine-, oak-, and grass-sod-covered areas. During his field test periods, 22 May to 27 July 1971, the average emission of NH_3 was 3.41 kg ha^{-1} wk^{-1} for topsoil in a pine stand, 2.62 kg ha^{-1} wk^{-1} for topsoil in the oak forest, and 1.84 kg ha^{-1} wk^{-1} for an adjacent grass sod area. If an average of 3 kg ha^{-1} wk^{-1} as NH_3 is taken for the forest soil emissions rate, it would translate into an annual nitrogen flux of about 13 g N m^{-2} yr^{-1}, a figure about an order of magnitude higher than that estimated for ammonia emissions by Soderlund and Svensson (1976) and listed in Table 2-6. Even if the NH_3 emissions estimate by Kim is considered as a peak seasonal value, which it probably was, it is still significantly greater than the NH_3 emissions factors listed in Table 2-6. However, because the emissions measured by Kim are from soil surfaces within vegetated canopies, they may indicate an emissions density

TABLE 2-7. SUMMARY OF BIOGENIC NO_x ESTIMATES FOR THE UNITED STATES

Author	Contiguous U.S. Tg N yr^{-1}	U.S. east of Mississippi River Tg N yr^{-1}
Soderlund and Svensson (1976)	1.25 - 5.30	0.36 - 1.52
Galbally (1975)	2.4	0.69
Logan (1983)	0.4	0.12
Boundary Layer Conc. = 0.25 ppb (see text)	0.15	0.04
1978 Anthropogenic (this chapter)	5.7[a]	3.2[b]

[a]Adapted from Table 2-32.

[b]Adapted from Table 2-21.

that needs to be corrected for some significant amount of canopy or vegetation reabsorption. This factor of canopy interaction has been discussed briefly by Dawson (1977) who cites the research of Denmead et al. (1976) and Porter et al. (1972).

To compensate for the fact that applicable, generalized flux measurements of NH_3 from soils or the land surface were not available, Dawson (1977) developed a "simplified" model for the production and emission of NH_3 from soil, based on "unsophisticated physical chemistry and microbiology." In this model, soil NH_4^+ concentrations were derived from comparisons of biomass decomposition and nitrification rates. After calculating equilibrium concentrations of NH_3 in the soil, Dawson incorporated a diffusion equation to generate the flux of NH_3 to the atmosphere. Model input parameters allowed for effects of soil moisture as determined by rainfall and evaporation, soil temperature as inferred from air temperature, and biomass or primary productivity. Soil pH was also a major model parameter. The necessary model parameters were estimated on a global basis for 10° latitude zones from 70°N to 60°S, and the zonal flux of NH_3 to the atmosphere was estimated and then totaled. The result was 32.5 Tg NH_3 yr^{-1} (27 Tg N yr^{-1}) from the Northern Hemisphere and 14 Tg NH_3 yr^{-1} from the Southern Hemisphere for a total of about 47 Tg NH_3 yr^{-1}, or 39 Tg N yr^{-1}.

The latitudinal pattern showed essentially zero emissions in the polar regions, a relative maximum in the midlatitudes, and a relative minimum in the tropics. The tropical minimum may be surprising at first, but it is explained by low pH values in the soil, which limit NH_3 release, accompanied by excessively high temperatures, which also are not conducive to high NH_3 emission. NH_3 emissions are modeled as having a maximum emis- sions rate in a temperature range from about 18 to 24 C. These model calculations agree well with the latitudinal emissions pattern for NH_4^+ that Dawson (1977) obtained from Eriksson's (1952) rain chemistry data and with Eriksson's total global estimate of 42.5 Tg NH_4^+ yr^{-1}. However, the value calculated by Dawson (1977) is only 16 to 35 percent of the ammonia emissions estimate of Table 2-6 from Soderlund and Svensson (1976), and, although it may closely approximate a precipitation deposition pattern, it does not account for any dry deposition of either gaseous or particulate components.

According to Soderlund and Svensson (1976), dry deposition processes are estimated to be about twice as effective an ammonia sink as precipitation. Dawson (1977) discounts dry deposition onto the soil because, as he states, "there is no reason for ammonia to be significantly absorbed by soils." This is a questionable assumption considering the solubility of ammonia and the wide distribution of moist vegetation and moist and acidic soil. A number of investigators have argued that ammonia will be readily absorbed in a dry deposition process similar to that for sulfur dioxide and other gases (Robinson and Robbins 1970a, McConnel 1973, Soderlund and Svensson 1976). Experiments on plants in growth chambers has shown significant uptake of ammonia through the leaves (Hutchinson et al. 1972).

The global nitrogen cycle proposed by Soderlund and Svensson (1976) mentions, in particular, the ammonia produced from animal urea and excreta.

The total amounts of NH_3 on a global basis from wild and domestic animals and humans is estimated to be between 22 and 41 Tg N yr^{-1} or 17 to 19 percent of the total emissions estimate for ammonia. The remainder, about 80 percent of the total (about 4 Tg N yr^{-1} is attributed to coal combustion), is assigned to ammonia emissions from the decomposition of dead organic matter, but presumably this could include the sort of microbiological emissions modeled by Dawson (1977). The estimate of ammonia losses from animal and human waste is based to a significant extent on the measurements by Denmead et al. (1974) of ammonia losses to the atmosphere from an actively grazed sheep pasture in Australia. Emission densities this pasture averaged 0.25 kg N ha^{-1} day^{-1} (9.5 g N m^{-2} yr^{-1}) for a 3-week, late summer period. If this very large emission rate is assumed, the ammonia losses from the global animal and human populations could play a role in the global nitrogen balance. It is still less than 75 percent of the forest soil emissions of Kim (1973) described above. Interestingly, however, the grazed pasture emission rate of Denmead et al. (1974) is larger than Kim's (1973) estimated rate from ungrazed grass sod of 8 g N m^{-2} yr^{-1}. Harriss and Michaels (1982) have shown that animal wastes and other man-caused NH3 sources are significant NH_3 emission sources in the United States.

The soil emission estimates by Galbally (1975) have already been mentioned in the discussion of NO_x sources. He has also applied his gradient transfer methods to make an ammonia soil source estimate. In his calculation, he assumes ammonia concentrations in the atmospheric boundary layer of 5 µg m^{-3} in temperate zones, 13 µg m^{-3} in tropical areas, and 3 µg m^{-3} over oceanic areas. His resulting ammonia emissions estimate is 130 Tg N yr^{-1} for the Northern Hemisphere. If this value were doubled to about 260 Tg N yr^{-1} to approximate a global ammonia emissions estimate, it would approximately equal the source estimate for ammonia given in Table 2-6.

Since Galbally (1975) made his global source estimates for ammonia, further improvements have been made in measurement techniques and indications are that actual boundary layer concentrations are probably significantly lower than those used by Galbally in his calculations. For temperate latitudes Galbally used an ammonia concentration of 5 µg m^{-3} whereas more recent data indicate a range from less than 0.7 µg m^{-3} to around 1.4 µg m^{-3} (e.g., Braman and Shelly 1981). For ocean areas Galbally used a value of 3.5 µg m^{-3}; more recent data indicate that about 0.07 µg m^{-3} is a more realistic concentration (Ayers and Gras 1980). Although recent data are apparently not available for tropical areas, it seems likely that Galbally's value of 13 µg m^{-3} is also high. Thus, global concentration patterns may be only 10 percent or less of those that Galbally used in his emission estimate and as a result it may be appropriate to reduce his global NH_3 emission estimates by this factor or to about 13 Tg N yr^{-1} for the Northern Hemisphere.

2.2.2.8 Oceanic Source for Ammonia--For the most part, investigators of the ammonia cycle tend to consider the ocean surface as being an improbable source of ammonia because of the latter's solubility. However, these conclusions fail to recognize that a steady ammonia background concentration of about 0.9 µg m^{-3} has been observed over the Atlantic Ocean by Georgii and Gravenhorst (1977) and that in the area of the Sargasso Sea and the

Caribbean, ammonia concentrations of 3.5 to 7 $\mu g\ m^{-3}$ were observed over relatively large areas. Also, in Panama, where air trajectories have some ocean fetch, Lodge and Pate (1966) measured ammonia concentrations of 14 $\mu g\ m^{-3}$, and Junge (1963) reported marine air concentrations of ammonia in Florida and Hawaii of 5 $\mu g\ m^{-3}$ and 2 $\mu g\ m^{-3}$, respectively. In the Southern Hemisphere (Tasmania), Ayers and Gras (1980) found that NH_3 averaged about 0.06 $\mu g\ m^{-3}$ in air that had not had a recent overland trajectory. In discussing ammonia emissions from the ocean, Junge (1963) pointed out that nitrate reduction by plankton in the surface layers may provide a marine source of ammonia.

Using their low measured concentrations of ammonia over marine areas, Georgii and Gravenhorst (1977) calculated an average ammonia emission density from the sea to the atmosphere of only 0.05 $\mu g\ m^{-2}\ hr^{-1}$ as ammonia. This converts to an annual emission density of about 0.0004 $g\ m^{-2}\ yr^{-1}$ or a total global ammonia emission of 0.15 Tg N yr^{-1}.

Graedel (1979) approached the problem of the trace chemistry of ammonia on the basis of a photochemical reaction system. He considered organic, inorganic, and halogenated compounds in the marine atmosphere and in particular a set of precursor compounds. His selection was based on limiting consideration to those compounds that were potential natural emissions; thus, obvious anthropogenic compounds such as the Freons or CCL_4 were not included in the study. Tabulated data on the trace constituents in the atmosphere were used along with an extended set of reactions and rate constants to estimate a steady-state trace chemical composition of the marine atmosphere. For this consideration, a set of 13 precursor compounds (e.g., ozone and hydrochloric acid) were introduced into the computation system. The photochemical modeling system, including scavenging processes, was run along with typical diurnal changes in meteorological conditions such as solar flux and mixing depth. Emission fluxes into the atmosphere must be added to the system to establish a steady-state situation; these calculated emission rates for a steady-state situation are one product of the model. For NH_3, Graedel (1979) starts with an average marine atmosphere concentration of about 0.7 $\mu g\ m^{-3}$, probably significantly higher than is now considered realistic on the basis of the newest measurement techniques. Thus, his estimated global ammonia emission from the ocean of 3.2 Tg (NH_3) yr^{-1} or about 2.6 Tg N yr^{-1} is probably high. It is also significantly larger than the estimate of Georgii and Gravenhorst (1977). However, even this value is only a small percentage of the estimated global ammonia emissions given in Table 2-6. Thus, although the ocean probably is a net source of ammonia to the atmosphere, it would not be expected to play a significant role in the global ammonia cycle.

2.2.2.9 Biogenic Ammonia Emission Estimates for the United States--In the previous discussion of biogenic NO_x emissions, procedures based on atmospheric concentration estimates were used to estimate biogenic emissions for the United States. Similar procedures can be used for estimates of ammonia or biogenic emissions. Applying Galbally's (1975) estimate of the natural or biogenic NH_3 emission density of 0.55 g N $m^{-2}\ yr^{-1}$ to the contiguous United States ($7.82 \times 10^{12}\ m^2$) and to the area east of the Mississippi River ($2.23 \times 10^{12}\ m^2$) results in estimated biogenic ammonia emissions of

4.3 Tg N yr^{-1} and 1.2 Tg N yr^{-1}, respectively. However, as noted above, NH_3 concentrations in the atmosphere are now believed to be only about 10 percent of the concentrations used by Galbally (1975). These changes, of course, are the result of major improvements in measurement techniques in recent years and not of any errors on the part of Galbally or other authors of previous studies. A proportionate change in Galbally's estimate would result in an indicated global emission rate of 13 Tg N yr^{-1} for the Northern Hemisphere, and if this is assumed to be essentially a nonpolar land area (0° to 70°N) source, the average emission density is about 0.14 g N m^{-2} yr^{-1}. Applying this emission value to the contiguous United States (7.8×10^{12} m^2) and the region east of the Mississippi River (2.23×10^{12} m^2) results in estimated annual NH_3 emissions of 1.1 Tg N yr^{-1} and 0.3 Tg N yr^{-1}, respectively.

This biogenic emission source can be compared to manmade sources in the United States, which are a summation of the emissions from livestock waste products, fossil fuel combustion, and agricultural fertilizer usage (Harriss and Michaels 1982). The total emission for the United States from these three sources is estimated by Harriss and Michaels (1982) to be 3.4 Tg yr^{-1} as NH_3 or 3.0 Tg N yr^{-1}. Of this total, 62 percent is from domestic livestock, 21 percent from fossil fuel combustion, 12 percent from fertilizer usage, and the remainder from various industrial sources. From a state-by-state tabulation by Harriss and Michaels (1982) of the ammonia emission through the upper Mississippi Valley and the Ohio Valley, the states of Iowa, Illinois, Indiana, and Ohio are shown to be a region of maximum ammonia emissions density of about 1 g N m^{-2} yr^{-1}. This is about seven times the biogenic emission density of 0.14 g N m^{-2} yr^{-1} estimated above. Harriss and Michaels (1982) concluded that emissions from natural or undisturbed soil surfaces were insignificant compared to their summation of anthropogenic ammonia sources.

2.2.2.10 Meteorological and Area Variations for NO_x and Ammonia Emissions --The natural emissions of NO_x and ammonia are both related primarily to microbiological and physical processes in the soil. These processes are enhanced by warm weather and rainfall. Thus, warm, moist summer weather, such as that found in the eastern and southern parts of the United States, would be expected to maximize natural emissions of both NO_x and ammonia.

On an area basis, soil pH tends to affect emissions for both compounds, with NO_x emanations being higher with more acidic soils. On the other hand, ammonia emissions probably tend to increase in alkaline soils. However, soil moisture plays a role in both situations; thus, a simple area distribution approximation should not be made in which ammonia emissions are assigned to alkaline western areas and NO_x to the more acidic midwest and east. For one thing, the desert soils of the west may be too dry and too hot for high ammonia production, as would be inferred from Dawson (1977).

2.2.2.11 Scavenging Processes for NO_x and Ammonia--The previous discussions have indicated that both dry and wet deposition processes are important sinks for NO_x and ammonia gases and their reaction products. In their global model, Soderlund and Svensson (1976) estimate the dry deposition processes as being about twice as important as precipitation scavenging

mechanisms. This seems to be a reasonable estimate, although significant variation in this ratio could be expected on the basis of local rainfall frequencies and characteristics. In desert areas, dry deposition may be even more important than usual, while in periods or regions of persistent rain or showers, the balance could shift toward precipitation scavenging.

2.2.2.12 Organic Nitrogen Compounds--For a complete nitrogen cycle through the atmosphere, the generation, transfer, and deposition of organic nitrogen compounds should be considered. These compounds may be either gaseous or particulate materials and include amines, amino acids, and proteins. Some investigators have found strong evidence that the organic nitrogen compounds are gaseous. Denmead et al. (1974), for example, found in samples over grazed pasture that, at times, as much as 50 percent of the total collected nitrogen compounds was not ammonia; the excess has been attributed to volatile amines.

On the basis of organic nitrogen concentrations in precipitation, Soderlund and Svensson (1976) postulated an annual deposition over land of 10 to 100 Tg N yr^{-1}. This wide range is indicative of the fact that little is known about these compounds. Because at least some are not particulate compounds when emitted to the atmosphere, a gaseous cycle involving reactions and further scavenging mechanisms may be present in addition to the fine particle/precipitation scavenging mechanisms.

2.2.2.13 Summary of Natural NO_x and Ammonia Emissions--The environmental effect of natural emissions of the nitrogen compounds, NO_x and ammonia, will be seen primarily as a part of the pattern of precipitation chemistry. The NO_x component, if it occurs as HNO_3 after atmospheric reactions, may lower precipitation pH, while ammonia, when absorbed into liquid drops as NH_4^+, will act as a weak neutralizing compound for absorbed acidic factors. Because the natural sources are spread over wide areas in patterns that change only slowly with distance, impacts from natural sources would not change markedly from place to place in a given regional area.

Although our data on natural sources of both NO_x and ammonia within the United States are inadequate, estimates of natural emissions have been made. These comparisons indicate that natural NO_x emissions in the contiguous United States likely range between 0.1 and 2.4 Tg N yr^{-1}. For NH_3, the natural emissions for the contiguous United States is of the order of 1.0 Tg N yr^{-1}. For the area east of the Mississippi River, the range of natural NO_x emissions is between 0.04 and 0.7 Tg N yr^{-1}. In this same region, the estimated natural ammonia emission is of the order of 0.3 Tg N yr^{-1}.

2.2.3 Chlorine Compounds

2.2.3.1 Introduction--Part of the acidity of precipitation is contributed by chlorides. It is hypothesized by many investigators that hydrochloric acid important sinks for NO_x and ammonia gases and their reaction products. In their global model, Soderlund and Svensson (1976) estimate the dry (HCl) and elemental chlorine (Cl_2) are the precursor compounds. In terms of its contribution to precipitation chemistry, chloride is generally much less significant than sulfate. Richardson and Merva (1976) list precipitation

chloride at about half that of sulfate on an annual basis in rural Michigan. Long-term (1964-74) records of precipitation at Hubbard Brook Experimental Forest in New Hampshire indicate that, on the average, chloride accounts for about 13 percent of the total anion content (Likens et al. 1976). Although there are some pollutant emissions of Cl^- or Cl_2, especially as a result of fossil fuel combustion (see Section 2.3.4), a significant part of the total atmospheric burden of chlorine compounds is due to natural sources. Cicerone (1981) has described the atmospheric chlorine compound cycle in detail.

There are three major natural sources of chlorine compounds to consider: the ocean with emissions of sea salt (primarily NaCl) and organic chloride as CH_3Cl, volcanic emissions, and forest fires. The sea salt processes will be shown to be dominant. This was also Cadle's (1980) conclusion. Table 2-8 shows the atmospheric background concentrations of several chlorine compounds as summarized mainly by Cicerone (1981).

This discussion mentions both Cl_2 and HCl as gaseous atmospheric chlorine compounds to be considered because they were considered in the original references; however, as pointed out by Eriksson (1959), the only stable gaseous chlorine compounds likely to be formed in the atmosphere are hydrochloric acid and ammonium chloride, NH_4Cl. Gaseous chlorine, Cl_2, would not be expected because of the relatively large concentration of atmospheric hydrogen.

2.2.3.2 Oceanic Sources--The production of sea salt spray is the largest source of atmospheric chloride. Eriksson (1959) has estimated the production of fine salt particles resulting from the evaporation of sea spray particles to be on the order of 10^3 Tg yr^{-1}. The chloride fraction of 10^3 Tg of sea salt would be 550 Tg. Eriksson (1959) made a further estimate, based on river chemistry, that about 10 percent of the ocean-generated spray particles are carried over land areas. Thus, on a global basis, the ocean is a potential source of about 55 Tg Cl yr^{-1} over land areas. This aerosol will be deposited on land areas by both precipitation and dry deposition processes. It was Eriksson's estimate that dry deposition processes would be about twice as important as precipitation over land areas; a one-third to two-thirds division of 55 Tg Cl yr^{-1} allots about 18 Tg Cl yr^{-1} to precipitation deposition processes and 36 Tg Cl yr^{-1} to dry deposition on a global basis.

The deposition of chloride over land areas is biased toward the coastal zones. Eriksson (1960) gives examples of patterns in Australia, South Africa, Europe, and the United States. In each of these areas the gradient inland from the coast is marked, with chloride concentrations decreasing by an order of magnitude or more at inland sites as compared to coastal stations. U.S. data cited by Eriksson (1960) were gathered by Junge and Werby (1958) from an extensive, nationwide rain chemistry network. The data show a range of annual deposition rates from a high of 32 kg ha^{-1} yr^{-1} (3.2 g Cl m^{-2} yr^{-1}) in the Pacific Northwest to low values of less than 0.5 kg ha^{-1} yr^{-1} on the west and east slopes of the Rocky Mountains in the area from about Utah and New Mexico to Nebraska and eastern Colorado. Along the Gulf Coast, precipitation chloride is about 16 kg ha^{-1} yr^{-1}. Eastward from the Pacific Coast, chloride concentrations decrease rapidly

TABLE 2-8. ATMOSPHERIC BACKGROUND CONCENTRATIONS OF NATURAL CHLORINE COMPOUNDS

Compound	Concentration $\mu g\ m^{-3}$	Reference
Inorganic gaseous Cl^-	1.4 - 2.8	Cicerone (1981)
Aerosol Cl^-	1-10	Cicerone (1981)
CH_3Cl	~ 1.2	Rasmussen et al. (1980)

into the Great Basin. Along the Gulf and East Coasts, most of the chloride in precipitation falls south and east of the Appalachian Mountains. In the northeastern states, except for immediate coastal locations, precipitation chloride deposition is less than 3 kg ha^{-1} yr^{-1} (0.3 g Cl m^{-2} yr^{-1}). At Hubbard Brook, Likens et al. (1976) report an annual chloride deposition rate of 0.47 x 10^{-3} g ℓ^{-1}, which is about one-third of what would have been inferred from Junge and Werby's (1958) data.

As a first approximation, it would appear that the chloride content of precipitation over the northeastern United States can be explained by the rainout and washout of transported sea salt aerosol particles that had their origin in sea spray generated at the ocean surface.

All of the airborne chlorine is not in the form of chloride particles. Gaseous chlorine compounds, either as Cl_2 or HCl, are also reported (Junge 1963, Cicerone 1981). Ryan and Mukherjee (1975) summarize the admittedly scanty gaseous chlorine compound data as indicating a global average concentration of about 1 ppb Cl in the form of HCl and/or Cl_2. Eriksson (1959) considered Cl_2 as an unlikely atmospheric constituent because of its reactivity.

The natural source of atmospheric gaseous chlorine is frequently given as being a product of atmospheric reactions of sea salt particles with other species. Eriksson (1960) proposed a reaction process involving the absorption of SO_3 or H_2SO_4, produced originally in the atmosphere from SO_2, and the release of chlorine from the particle. Eriksson (1960) also suggested that NO could act in a similar manner to produce gaseous chlorine from a sea salt aerosol. Robbins et al. (1959) carried out laboratory experiments on sea salt (NaCl) reactions with NO_2. As a result of these experiments, these authors proposed a reaction system involving the hydrolysis of NO_2 to HNO_3 vapor, followed by HNO_3 absorption by dry NaCl or into NaCl solution droplets, followed by the reaction between HNO_3 and NaCl leading to the release of HCl.

A more complex chemical reaction model for HCl production in clouds has been proposed by Yue et al. (1976). This model includes the initial oxidation of SO_2 to H_2SO_4 and competing reactions with NH_3 for H_2SO_4 in a mechanism that produces HCl from the NaCl-H_2SO_4 reaction. The model proposed by Yue et al. (1976) includes cloud parameters such as temperature and liquid water content. In many respects it is a more complete development of the basic system proposed by Eriksson (1960). Yue et al. (1976) used their model to estimate the annual global HCl production with more or less typical background concentrations and cloud parameters. The result was an HCl production of about 2 x 10^2 Tg yr^{-1}. Duce (1969) has estimated the production of HCl in the marine atmosphere to be about 6 x 10^2 Tg yr^{-1}.

In assessing the possibility of a sea salt source for chloride, Ryan and Mukherjee (1975) suggest that about 3 percent of the sea salt aerosol may be converted to gaseous chlorine compounds. Using Eriksson's (1959) sea spray production estimate of 10^3 Tg yr^{-1} or 550 Tg Cl yr^{-1}, this 3 percent estimate gives an estimated gaseous Cl production rate of 17 Tg yr^{-1}. This lower value compared to the 200 to 600 Tg yr^{-1}, quoted above for gaseous

chlorine from the work of Yue et al. (1976) and Duce (1969) would seem to be more reasonable. Junge (1963) found particulate and gaseous chloride to be in about equal proportions in marine air in Florida. Chlorine production in the range of 200 to 600 Tg yr^{-1} would consume essentially all of the sea salt spray produced, as estimated by Eriksson (1959). Although each of these estimates of chlorine production may be in error, they can be used as a basis for a consistent estimate of the atmospheric transport of chlorine.

Eriksson's (1959) estimate of sea salt aerosol of 1000 Tg yr^{-1} translates to 550 Tg Cl yr^{-1} as aerosol particles and 17 Tg Cl yr^{-1}, converted to gaseous chloride. For land area impact, 10 percent of the aerosol, or 55 Tg Cl yr^{-1} is estimated to be carried over the coast (Eriksson 1959) while the gaseous chlorine appears over the land in proportion to the fraction of land over the Earth, 29 percent, or 5 Tg Cl yr^{-1}, assuming that gaseous chloride will have a significantly longer residence time in the atmosphere than the sea salt spray aerosol particles. The total ocean contribution to land area deposition is thus about 60 Tg Cl yr^{-1} or 0.6 g m^{-2} yr^{-1}, averaged over the global land area.

An additional natural source of atmospheric gaseous Cl_2 or HCl involves atmospheric reactions of CH_3Cl, which is biogenically produced in the ocean and released to the atmosphere. Measurements from aircraft over the United States, the north and south Pacific, and in Antarctica (Cronn et al. 1977, Rasmussen et al. 1980) indicate generally uniform concentrations through the troposphere. A concentration of about 1.2 μg m^{-3} is indicated by these measurements as an appropriate average concentration. Although CH_3Cl is not highly reactive in the troposphere, it does undergo a reaction process involving oxidation by OH with the potential production of gaseous chlorine. Graedel (1978) lists an atmospheric lifetime of about 1.5 years for CH_3Cl. Using this lifetime estimate with an average concentration of 1.2 μg m^{-3} gives a CH_3Cl emissions rate of 2.6 Tg yr^{-1} or 1.8 Tg Cl yr^{-1}. This is much less than any of the estimates of chlorine production from sea salt particles.

Graedel has carried out an extensive chemical and photochemical modeling study of the marine atmosphere (Graedel 1979) during which he was able to estimate the flux of various trace atmospheric constituents from the ocean into the atmosphere. From this study, he estimated a CH_3Cl flux to the atmosphere of 1.8 Tg yr^{-1} and an HCl flux of 2.0 Tg yr^{-1}. His combined flux of gaseous chlorine is 3.2 Tg Cl yr^{-1}. The generation of CH_3Cl is presumed to be a biogenic process (Rasmussen et al. 1980) while the formation of HCl can result from reactions involving CH_3Cl or sea salt, as previously mentioned.

Although the chemical release of chlorine from sea salt particles can be supported experimentally (Robbins et al. 1959), theoretically (Yue et al. 1976), and by the decrease in Cl/Na ratios in precipitation with distance from the ocean (Eriksson 1960), this oceanic HCl generation mechanism is not consistently supported by field measurements. Valach (1967), using a detailed analysis of the gaseous and aerosol chlorine data gathered by Junge (1956, 1963) in Florida, and the analysis of the atmospheric chlorine cycle by Eriksson (1959, 1960), argued for a volcanic source for gaseous chlorine

compounds in the atmosphere. Lazrus et al. (1970), after carrying out a program of cloud water analyses, concluded that excess chloride in the atmosphere does not originate from sea salt. They also concluded that volcanic emissions could be the source of gaseous chlorine compounds in marine atmospheres since, in their cloud water experiments, they found neither depletion nor enhancement of the cloud water chloride ratios compared to seawater mixtures.

2.2.3.3 Volcanism--The chlorine compound emissions to the atmosphere from volcanic activity have been estimated by several authors. Ryan and Mukherjee (1975), using estimates of particle and lava production coupled with probable gas and chlorine ratios, estimated the volcanic source of atmospheric gaseous chlorine at 0.25 Tg Cl yr^{-1}. Lazrus et al. (1979) have reported on the changes in stratospheric chlorine compound concentrations caused by a number of Western Hemisphere volcanos that were active in the 1976-78 time period. Johnston (1980), after an examination of data from Alaskan volcanos, proposed ash degassing as a significant source of atmospheric chlorine in addition to the magma outgassing processes considered by other investigators. For St. Augustine in Alaska, Johnston (1980) estimated a Cl emission of about 0.5 Tg during the January to April 1976 eruptions. About 16 percent of this Cl entered the stratosphere (Johnston 1980). Cadle (1980), in a summary of information from a variety of sources, has estimated the annual global emission of HCl from volcanos at 7.8 Tg yr^{-1} with the comment that this value may still be "somewhat low." It represents a tenfold increase in his earlier estimate (Cadle 1975). Measurements of Cl^- particles and acidic vapor in the Mt. St. Helens plume by Gandrud and Lazrus (1981) indicate that Cl^- concentrations were significantly less than for SO_4^{2-}. Although flux values were not calculated, one may infer from this and the SO_2 and SO_4^{2-} data of Hobbs et al. (1982) that Mt. St. Helens's Cl contributions to the atmosphere would be less than 0.15 Tg yr^{-1}. The usual expected change in atmospheric chemistry would be an increase as more sources and longer periods of eruptive activity are assessed. Anticipating this and recognizing Cadle's evaluation of his 7.8 Tg yr^{-1} figure, it is probably realistic to estimate volcanic chlorine emissions to the atmosphere at about 10 Tg yr^{-1}, with a range of at least plus or minus a factor of 2, perhaps more. Volcanic emissions are estimated to be deposited uniformly in oceanic and land areas, in proportion to total area.

2.2.3.4 Combustion--Other possible sources of atmospheric chlorine are combustion processes because of the production of CH_3Cl in these operations. Although combustion is usually considered an anthropogenic source, it is also reasonable to consider some fraction as a natural source because a significant fraction of combustion is nonindustrial. Falling more or less logically into this natural source category is fuel wood combustion, agricultural waste burning, forest residue combustion, and wildfires. Palmer (1976) estimated that in the United States, combustion in the "natural" categories accounted for a total emission of 0.13 Tg yr^{-1} of CH_3Cl, the typically observed chlorine combustion effluent. Wildfires are about one-third of this total. If it is estimated that these natural combustion sources of CH_3Cl in the United States are perhaps 5 percent of the world's total in these categories (probably an overestimate), a potential emission of about 2 Tg Cl yr^{-1} is indicated for combustion sources. This is a minor global source of Cl and

does not seem to justify further detailed treatment. It is assumed that this source will be mainly a contributor to land area deposition.

2.2.3.5 Total Natural Chlorine Sources--In Table 2-9 these estimates of the several proposed natural chlorine sources are listed in terms of global totals and in terms of the estimated deposition on land areas. As indicated, sea salt aerosols are the source for all but a small percentage of the atmospheric chlorine, either directly through salt deposition or following reactions in the atmosphere to form gaseous chlorine compounds. The land area deposition of chlorine, 65 Tg Cl yr^{-1}, averages to about 0.4 g Cl m^{-2} yr^{-1} if it were to be deposited evenly on the total land area. This is not an unreasonable value for combined wet and dry depositions considering Eriksson's (1960) findings that, away from coastal areas, chloride in precipitation is generally 0.5 g m^{-2} yr^{-1} or less.

In summary, it seems that the recognized sources of atmospheric chlorine are generally comparable to the identified sinks.

2.2.3.6 Seasonal Distributions--As shown in Table 2-9, chlorides in the atmosphere are due primarily to sea salt aerosols or chloride compounds derived from sea salt. The airborne sea salt has its origin in aerosols lifted away from the ocean surface after their formation, either as windblown spray or in the bubble-bursting process. Rain and clouds over the ocean might be expected to increase the local scavenging rate and decrease the air mass transport of sea salt aerosols, although there does not seem to be any data on this subject. In the absence of storms and strong winds, the aerosol generation processes may be reduced but the particle residence time might be expected to increase. From arguments such as these, it is apparent that a significant seasonal cycle in chloride transport and deposition would not be expected. Rainfall chemistry data gathered by Johannes et al. (1981) in the Adirondack region of New York do not show any clearly identifiable seasonal cycle for chloride. In this area of the United States, a trend toward a winter minimum for marine aerosols could be expected because of the increasing exposure to polar continental air masses during this season rather than the maritime tropical air masses typical of much of the summer.

2.2.3.7 Environmental Impacts of Natural Chlorides--Chloride compounds transported from oceanic areas to land areas occur primarily in very low concentrations, probably in the range of fractions of a microgram per cubic meter for both gases and aerosol particles at areas away from the coast. The chloride ions may contribute 10 to 15 percent or so of the total anion content in precipitation at stations in the northeastern United States. As such they would be relatively unimportant in altering precipitation pH by themselves.

2.2.4 Natural Sources of Aerosol Particles

The atmosphere near the surface over land areas probably has a concentration of particulate materials at all times except under some very unique circumstances. Natural sources produce materials that are blown up from exposed soil surfaces by wind and remain suspended in the atmosphere for a period of time. These solid particles may be removed from the atmosphere by

TABLE 2-9. ESTIMATED ANNUAL CHLORINE COMPOUND (AS_1Cl) EMISSIONS AND LAND DEPOSITION - Tg Cl yr^{-1}

Source	Global emission	Land Deposition[a]
Sea salt aerosol	550	55
Gaseous Cl from NaCl particles	17	5
Biogenic CH_3Cl	2	0.5
Volcanos	10.0	3.0
Combustion CH_3Cl	2.0	2.0
Total	581	65.5
or approximately	580	65

[a]See text for details.

gravitational settling, impaction onto exposed surfaces, or they may become incorporated in cloud and precipitation particles and fall out with the precipitation. These materials form the natural atmospheric dust loading and result from a variety of soil surfaces being exposed to wind and other impacts that cause the particles to become airborne. These dust particles are caused by breaking and other natural comminution processes. As described by Whitby and Cantrell (1976), dust particles of this type are classed as "coarse particles" and would normally be in the 2 to 10 μm diameter size range. Although dust storms and periods of strong winds over dry, exposed soil surfaces may produce periods of spectacular soil movement and exceptional atmospheric transport, in the normal situation dust sources and atmospheric dust concentrations are local source problems.

In the eastern part of the United States, the National Air Sampling Network has had a number of HIVOL sampling stations in rural or nonurban locations (Spirtas and Levin 1970). During the 10-year period from 1957 to 1966 in the area east of the Mississippi, 12 nonurban sampling stations were in operation. The average total suspended particle concentration for these stations for this period was 36 $\mu g\ m^{-3}$. The range was from a high of 57 $\mu g\ m^{-3}$ in Kent Co., DE, to a low of 18 $\mu g\ m^{-3}$ in Coos Co., NH. This average, nonurban particle concentration can be used to estimate the regional emission rate of this material if we make several assumptions. First, we can assume that these larger dust particles are uniformly mixed to a depth of 500 m, or through about the lower half of the mixing layer. Since these particles are relatively large and we are considering an average concentration over both day and night, this seems to be a reasonable assumption. Next, we will assume that these dust particles have an average atmospheric residence time of 1 day. This seems reasonable considering the size of the particles and the effectiveness of scavenging processes for larger-sized particles. Using these values, an annual emission density results from the following calculation:

$$36\ \mu g\ m^{-3} \times 500\ m \times 365 = 6.6\ g\ m^{-2}\ yr^{-1}.$$

Applying this annual emission density rate of 6.6 $g\ m^{-2}\ yr^{-1}$ to the United States east of the Mississippi River, about $2 \times 10^{12}\ m^2$, gives an estimated emission of dust into the nonurban atmosphere of about 13 $Tg\ yr^{-1}$ or $13 \times 10^6\ mT\ yr^{-1}$.

Of the total natural dust loading in the atmosphere, probably the most important constituent for precipitation chemistry is its calcium and magnesium content (Stensland and Semonin 1982). These elements make up about 3.6 percent and 2.1 percent, respectively, of the Earth's crust (Weast 1973). If the composition of the dust aerosol is representative of the crustal composition as studies have indicated (Lawson and Winchester 1979), then the background concentration and annual emissions can be estimated for Ca and Mg. The results for Ca are: 1.3 $\mu g\ m^{-3}$ for an estimated average concentration and 0.5 $Tg\ yr^{-1}$ for an estimated annual emission. For Mg the estimated values are: 0.8 $\mu g\ m^{-3}$ for the average concentration and 0.3 $Tg\ yr^{-1}$ for the annual emission.

The extension of these estimates of dust particle emissions and chemistry to an estimate of the concentrations of these constituents in rainfall in the region is not within the framework of this section. However, it can be noted that Hidy (1982) has tabulated some summer particle concentration and chemistry data along with concurrent precipitation chemistry data at three western Pennsylvania rural stations from Pierson et al. (1980). It appears from the analysis by Hidy (1982) that both Ca^{2+} and Mg^{2+} appear at greater ratios relative to sulfate in rainwater than in dry atmospheric particles. These are only limited data from a short summer period and should not be considered definitive. The topic of precipitation scavenging is considered in detail in Chapter A-6.

2.2.5 Precipitation pH in Background Conditions

The pH of precipitation under conditions not affected by air pollutant emissions is an important consideration for acidic deposition situations. We will examine briefly some of the aspects of natural pH variations in this section. Because these pH variations can most reasonably be linked to the effects of natural emissions on precipitation, it is reasonable to consider them as part of the discussion of natural emissions.

A completely neutral precipitation pH would be a value of 7.0. However it has long been realized that natural precipitation would likely be slightly acidic because the precipitation would tend to come into equilibrium with atmospheric trace constituents, which when absorbed into the precipitation would lower the pH value. Probably the most common assumption has been that an equilibrium would be set up with the CO_2 concentration in the atmosphere and that this would produce a controlling natural pH value of 5.6. Likens and Butler (1981) and a great many other investigators have used this CO_2-equilibrium pH value of 5.6 as a criterion to separate natural precipitation pH, any value equal to or higher than 5.6, and acidic precipitation, any value lower than 5.6. Since there had not been a considerable amount of precipitation pH data from locations that could not have been influenced by anthropogenic pollutant sources, this assumption of a CO_2-equilibrated limiting value seemed reasonable.

Two types of research investigations have now been undertaken that raise considerable doubt about whether a limiting pH value of 5.6 is in fact realistic and, as will be described below, there is considerable evidence that, at least in some natural situations, the pH of precipitation can be significantly lower than 5.6. First, atmospheric chemists have begun to look more carefully at the factors in addition to CO_2 that affect the pH of precipitation (Charlson and Rodhe 1982). These assessments show that there are a number of factors in the natural or background atmosphere that can cause precipitation pH to be lower than 5.6. Second, under the auspices of the Global Precipitation Chemistry Project, a program of measurements has been started at five remote sites in the Northern and Southern Hemispheres (Galloway et al. 1982). The findings of Charlson and Rodhe (1982) and Galloway et al. (1982) will be described briefly below.

Charlson and Rodhe (1982) have taken the chemist's view of the precipitation pH situation and have considered the impact of natural compounds of the

atmospheric sulfur cycle on pH. In the absence of common basic compounds such as NH_3 and $CaCO_3$ in the atmosphere, it is shown that pH values due to natural sulfur compounds could be expected to be about 5.0. Because the atmospheric concentrations resulting from natural emissions are highly variable, these authors conclude that even in background situations the pH may range from pH 4.5 to 5.6. Sulfur compound data for a variety of background situations have been summarized by Sze and Ko (1980), and they conclude that SO_4^{2-} concentrations in very remote, clean areas can be about 0.05 $\mu g\ m^{-3}$. This very low SO_4^{2-} concentration with a background SO_2 value of 0.26 $\mu g\ m^{-3}$ and 0.66 $g\ m^{-3}$ for CO_2 will result in a cloud water pH value of 5.4 in a cloud of 0.5 $g\ m^{-3}$ liquid water according to Charlson and Rodhe (1982). This is a moderate density for cloud liquid water content. Higher concentrations of SO_4^{2-} would lead to lower pH values, as would lower cloud water content. Situations where HNO_3 was present in the atmosphere would also reduce the pH. Concentrations of NH_3 or $CaCO_3$ in the atmosphere would raise the precipitation pH. Thus, over land areas where biogenic NH_3 and dust containing $CaCO_3$ could be expected, a higher pH than 5.4 might be expected if the SO_4^{2-} were as low as 0.05 $\mu g\ m^{-3}$ and no other acids were present.

Remote area precipitation chemistry data have been reported by Galloway et al. (1982) as the initial results from the Global Precipitation Chemistry Project have become available. The stations in this program are: St. Georges, Bermuda; Poker Flat, Alaska (Fairbanks area); Amsterdam Island (South Indian Ocean), Katherine, Australia (northern part); and San Carlos, Venezuela (Amazon jungle). Although the results of the first year or so of measurements cannot be considered conclusive the results are certainly important factors in the total acidic deposition picture.

In summarizing the data from these stations for the available rainfall events, the number of which ranged from 14 for San Carlos to 67 for St. Georges, Galloway et al. (1982) concluded that all stations experienced acidic precipitation, on the average, as a result of varying combinations of strong H_2SO_4 and HNO_3, and weak, probably organic, acids. The higher acidities were primarily due to H_2SO_4. Especially in the case of St. Georges, Bermuda, the higher acidic events were shown to be due to air mass transport from the United States. These transports caused the average precipitation pH at Bermuda to be 4.8. When trajectories were considered that apparently had not been influenced by North America, the average pH was 5.0. At Poker Flat, Alaska, the average pH for 16 precipitation events was 5.0, but since these events included periods when pollutants from Fairbanks or arctic haze pollutants were present, the "background" pH at this site is believed to be greater than 5.0.

The precipitation events at San Carlos, Venezuela; Amsterdam Island; and Katherine, Australia, were much less likely to be influenced by pollutant emissions, although Katherine may have been influenced by agricultural burning at the beginning of the rainy season. At San Carlos, the 14 available precipitation events averaged a pH of 4.8, with a relatively high contribution from organic acids compared to the other stations. At Amsterdam Island (37°47'S-77°31'E) in the remote Southern Indian Ocean, the average pH for 26 rainfall events was 4.9. Galloway et al. (1982) speculated that some

pollutant transport from the heavy industrial areas of South Africa might have influenced this remote station also and so they concluded that the natural pH was likely to be greater than 5.0.

As a result of the detailed chemical analyses of the precipitation event samples, Galloway et al. (1982) were able to estimate the relative contribution of the three acids, H_2SO_4, HNO_3, and "others" (probably organic), to the free acidity. The results for the three stations with the least probable influences of pollutants, Amsterdam Island, San Carlos, and Katherine, are shown in Table 2-10.

Although each of the sites in this Global Precipitation Chemistry Project was remote in location, each had a different combination of compounds that determined the precipitation chemistry. Furthermore, none was located in an area that was apparently similar to eastern North America in vegetation, soil and climate. Thus, care should be taken in applying these results to United States locations.

In the United States there are no long-term measurements of background pH that are directly applicable to the northeastern area that is presently of concern because of frequent low pH values. Likens and Butler (1981), however, have approximated the pH patterns over much of the eastern United States in 1955-56 on the basis of detailed precipitation chemistry data obtained by C. E. Junge and his colleagues (Junge and Gustafson 1956, Junge 1958, Junge and Werby 1958). These calculations of pH indicate that most of the Mississippi Valley and the Gulf Coast states had average pH values of 5.6 or perhaps higher in the time period 1955-56 (Likens and Butler 1981). These results are more alkaline than the background station data reported by Galloway et al. (1982); the influence of NH_3 from soil areas and $CaCO_3$ content in soil dust could be an explanation.

A different interpretation of the Junge (1958) precipitation chemistry data with regard to indications of background pH was developed by Stensland and Semonin (1982). They concluded that the Junge samples in general indicated greater than normal pH because the sampling period was during a general low rainfall or drought period and, as a result of this drought, excessive amounts of soil dust containing alkaline salts were present in the precipitation samples. By comparisons with more recent precipitation analyses, Stensland and Semonin (1982) developed dust correction factors for the 1955-56 Junge data and estimated pH values after removing the effect due to anomalously high values of calcium and magnesium. The result, as might be expected, was a set of significantly lower pH values in nonindustrial areas of the Midwest and Gulf Coast. In most of the areas where Likens and Butler (1981) had estimated the pH to be 5.6 or higher, Stensland and Semonin (1982) estimated pH values to range between 4.4 and 5.2. From these results and considering the fact that some pollutant emission impacts were probably a factor in the 1955-56 Junge data, the conclusions of Galloway et al. (1982) indicating naturally acidic precipitation with a pH somewhat greater than 5.0 may also be applicable to the eastern parts of the United States.

TABLE 2-10. CONTRIBUTIONS OF ACIDS TO FREE ACIDITY (%)
(ADAPTED FROM GALLOWAY ET AL. 1982)

	Amsterdam Island	Katherine, Australia	San Carlos, Venezuela
H_2SO_4	< 73	< 33	< 18
HNO_3	< 14	< 26	< 17
HX[a]	> 13	> 41	> 65

[a]HX could be HCl, organic acids, or H_3PO_4; Galloway et al. (1982) believe it was an organic acid.

2.2.6 Summary

This discussion of natural emission sources has examined a number of factors related to precipitation pH with reference to the situation in northeastern United States and southeastern Canada. In most cases it was necessary to draw analogies between global conditions and the situation in the northeast region, so considerable discussion was centered on global background air chemistry. With specific regard to precipitation pH, it was shown by theoretical chemistry and measurements in remote locations of the world that a pH value of near 5.0 may occur as a result of the acidic compounds that occur naturally in the atmosphere.

In the eastern part of the United States, it was shown that natural sulfur compounds emissions are relatively minor contributors to the total mass of sulfur emissions in the area. This is shown by a comparison of emissions from the United States east of the Mississippi River, where the natural sources were estimated to total about 0.07 Tg S yr^{-1} and 1978 anthropogenic sources totaled about 11 Tg S yr^{-1} (see Figure 2-6). For the contiguous United States, a total natural source emissions rate of about 0.5 Tg S yr^{-1} can be compared with a total 1978 anthropogenic emissions rate of about 13 Tg S yr^{-1} (see Figure 2-4). Thus, even considering the numerous probable errors that can be associated with natural emissions estimates, natural sulfur emissions do not appear to be as significant as pollutant emissions in establishing the regional atmospheric sulfur cycle.

For nitrogen compounds, both acidic NO_x emissions and basic NH_3 emission sources must be considered. In precipitation pH, acidic NO_x compounds may play an important role. In this discussion the emissions of NO_x compounds from natural sources in the area east of the Mississippi were estimated to range between 0.04 and 0.13 Tg N yr^{-1}. This value is significantly less than the estimated 1978 anthropogenic emissions of 8.9 Tg N yr^{-1} for this same area. Natural biogenic emissions of NH_3, which lead to NH_4^+ ions in precipitation, have been estimated to be about 1.1 Tg N yr^{-1} for the whole United States. Anthropogenic sources of NH_3 include significant contributions from domestic animal waste and other sources and have been estimated to be about 3 Tg N yr^{-1} over the contiguous United Sates.

Chlorides may contribute to precipitation pH, although present evidence from areas such as Hubbard Brook, New Hampshire, indicates that their contribution is perhaps only 10 to 15 percent of the total anion content. The source for naturally generated Cl^- is almost exclusively sea salt swept from the ocean by marine air masses. Deposition of Cl^- on land areas east of the Mississippi is estimated at about 0.4 g Cl m^{-2} yr^{-1}. Air pollutant sources of Cl^- are believed to be relatively small and are primarily from the combustion of fossil fuel containing trace amounts of chlorine.

Fugitive dust may contribute to precipitation pH by contributing soluble ions. For the most part these are expected to be calcium and magnesium and they would be expected to raise pH values. Estimates of background dust loading in the northeastern region of the United States show relatively low mass loadings and thus atmospheric contributions of calcium and magnesium would be relatively low.

2.3 ANTHROPOGENIC EMISSIONS (J. B. Homolya)

2.3.1 Origins of Anthropogenically Emitted Compounds and Related Issues

Large quantities of sulfur and nitrogen oxides are discharged annually into the atmosphere from the combustion of fossil fuels such as coal, oil, and gas. Through chemical reaction in the atmosphere, these pollutants can be transformed into acids, which may return to ground level as components of either rain or snow. The deposition of these acids by precipitation has been associated with terrestrial, aquatic, and materials effects (see Chapters E-3, E-5, and E-7).

In addition to SO_2 and NO, other fossil fuel combustion products are emitted that may influence acid precipitation formation. These include H_2SO_4, HCl, and particulate matter. Sulfuric acid represents a variable fraction (0.01 to about 0.05) of the SO_2 emissions and exists as a vapor in combustion emissions. Upon mixing and cooling in the atmosphere, the acid condenses as fine particles. Field measurements have shown that a larger fraction of SO_2 is emitted as H_2SO_4 from oil combustion than from coal burning. Hydrochloric acid emissions have been identified with coal combustion. Little information is available on the rate of fossil fuel HCl emissions to the atmosphere. Figure 2-4 illustrates trends in total anthropogenic emissions of particulate matter, SO_2, and NO_x for the United States from 1940 to 1978. Sulfur dioxide emissions were about 29 percent higher in 1978 than in 1940. Although the generation of electricity has increased many-fold, a switch in fuel from coal to oil in the northeastern United States during the late 1960's and early 1970's has lowered both total SO_2 and particulate matter emissions. As noted by the marked reduction in particulates to about 31 percent of the 1940 total emissions, both fuel switching and incorporating electrostatic precipitators onto coal-fired units have dramatically changed the pollutant atmospheric composition. The NO_x component has increased mainly because of increases in electric power generation and vehicular traffic.

Reporting emissions on a nationwide basis, although useful as a general indicator of pollutant levels, has definite limitations. National totals or averages are not the best guide for estimating trends for particular localities. They are only an indication of the extent of total installed control technologies and economic growth or decline. They are not useful as an indicator of air quality. With the concern for the increasing acidity of precipitation over the eastern United States, it is important to evaluate the effects of changing emissions characteristics on the historical trends noted for the geographical distribution of acidity. Issues of prime importance that must be addressed in such an assessment include:

(1) Historical changes of emissions with variations in fuel use patterns. What changes are projected in future years?

(2) Current emissions for SO_x and NO_x from stationary and mobile source categories as a function of geographical region, urban compared to rural, and height of emissions.

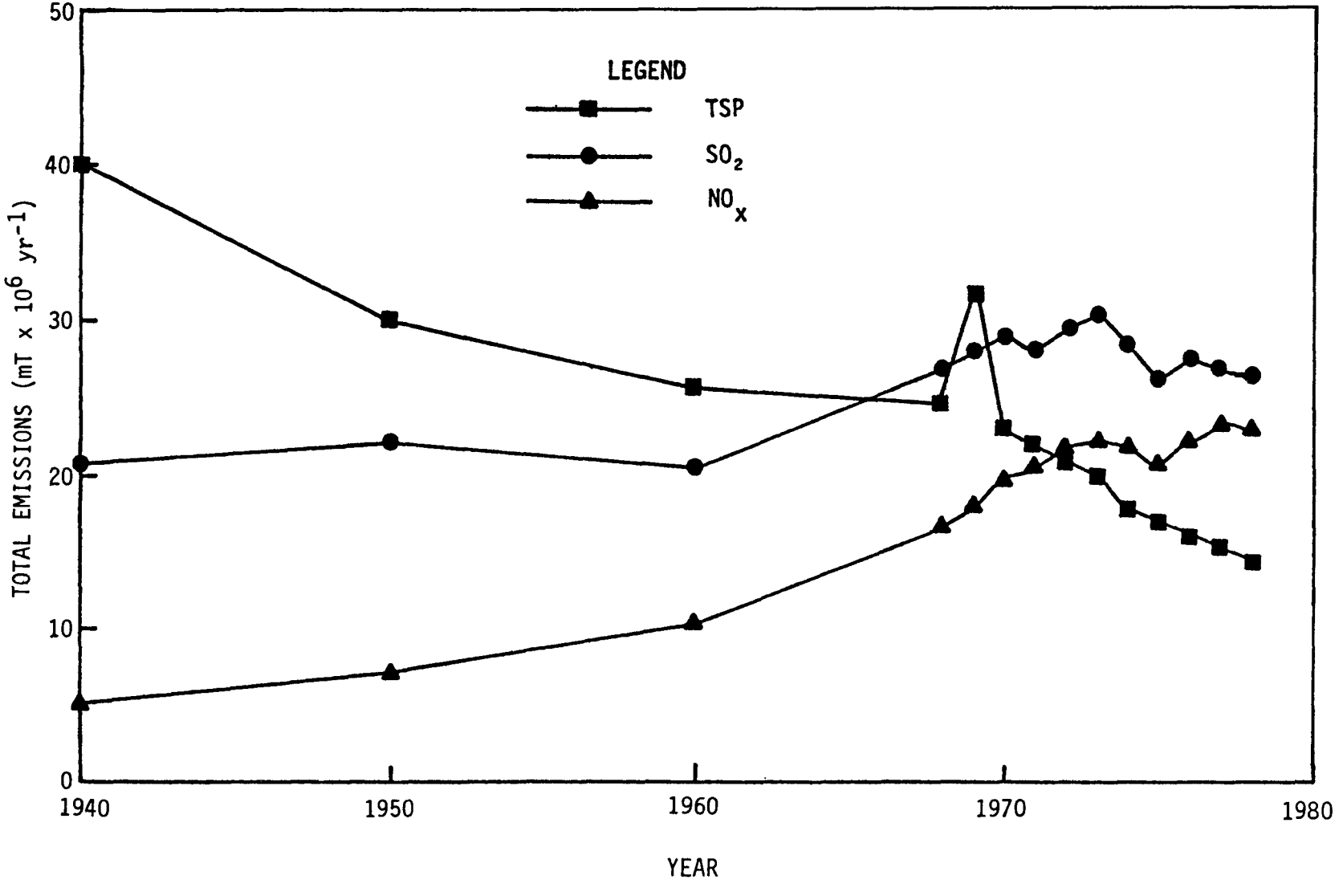

Figure 2-4. Total emissions of particulate matter, SO_2, and NO_x for the United States from 1940 to 1978. Adapted from U.S. EPA (1978).

(3) Current emissions of primary sulfate and HCl. How significant are these primary emissions by geographical region and season of the year?

(4) Primary acid emissions in terms of short-range impact downwind of individual large emission sources or clusters of sources.

(5) Emission sources of neutralizing substances including NH_3 and alkaline particles from combustion sources. How do such sources vary geographically and by season of the year? How significant is atmospheric neutralization by fly ash materials?

Examining these issues requires a degree of geographic resolution in emissions trends beyond that given in Figure 2-4. It is difficult to perceive the possibilities of the roles of primary acidic emissions and regional changes in emission levels on measured changes in precipitation acidity without further subclassifying historical emissions estimates. However, subclassification to the single-source level, if not impossible, would seem inappropriate relative to the degree of spatial resolution to which changes in acidity are noted and discussed. Therefore, an attempt has been made to examine estimates of anthropogenic emissions specifically from the eastern United States over the past 30 years and to present a discussion of the trends of both emission quantities and characteristics in degrees of spatial and temporal resolution that translate to correlation with observed acidity patterns over the same period.

The work of Gschwandtner et al. (1981) was used as the basis for examining historical trends in the emissions of acids, acid precursors, and certain heavy metals between 1950 and 1978. Gschwandtner was able to compile a data file of estimates of historical emissions of oxides of sulfur and nitrogen for the eastern United States. The estimates were calculated from fuel consumption data available for each state, emissions factors, and in the case of sulfur oxides, sulfur content of the fuel. So that these data could be used for a detailed analysis of emissions trends, the files were assembled in a microcomputer and operated with additional emissions factors for sulfur dioxide, nitrogen oxides, primary sulfate (H_2SO_4), chloride (HCl), volatile metals (As, Hg), and certain key metals indigenous to residual oil combustion (V, Ni). There have been no estimates of the uncertainty of this data set. However, it is reasonable to assume that the earlier records prior to development of the National Emissions Data System within the EPA are less accurate than those compiled from about 1970.

The calculated annual emissions were then normalized with respect to land area of each state and reported as annual emissions densities (kg km^{-2}). This procedure was chosen to provide a perspective of the regional-scale flux in emissions to the atmosphere. Obviously, one cannot compare fluxes between states whose land areas are quite different (e.g., Texas and Delaware). However, emissions density calculations are useful to the study of relative contributions of a state within a region (e.g., Indiana in the Midwest and Massachusetts in New England). Calculations were performed on all data between 1950 and 1975 in 5-year increments and for 1978. The source categories for sulfur and nitrogen oxides emissions are listed in Table 2-11.

TABLE 2-11. MAJOR SOURCE CATEGORIES AND SUBCATEGORIES FOR EMISSIONS INVENTORY (GSCHWANTDNER ET AL. 1981)

Electric Utilities
Industrial Sources of Fuel Combustion
Commercial/Residential Sources of Fuel Combustion
Pipelines
Highway Vehicles:
Gasoline Powered
Diesel Powered
Miscellaneous Sources:
Railroads
Vessels
Miscellaneous Off-Highway Mobile Sources
Chemical Manufacturers
Primary Metal Fabricators
Mineral Products Manufacturers
Petroleum Refineries
Other Sources

A map of the study area for emissions estimates is shown in Figure 2-5. Since emissions estimates are based upon fuel composition and consumption data, their validity depends on the detail with which fuel usage records have been maintained over the past 30 years.

In each state, Gschwandtner et al. (1981) compiled information on fuel consumption by stationary sources over the years from 1950 to 1978 in 5-year intervals. However, data on statewide consumption of bituminous coal by industries and commercial/residential sources were not available for 1950.

2.3.2 Historical Trends and Current Emissions of Sulfur Compounds

2.3.2.1 Sulfur Oxides--Historical trends of total sulfur oxide emissions by source category are shown in Figure 2-6. In recent years, electric utilities appear to have contributed to more than half of the total sulfur oxide emissions. Sulfur oxide contributions from industrial sources increased up to 1965 and then significantly decreased. The marked increase in sulfur oxide emissions from the commercial/residential and industrial sectors between 1950 and 1955 may be somewhat misleading because bituminous coal combustion data were not available for the 1950 input. During the 1950's, there was a marked shift in residential fuel from coal to oil and natural gas. After 1965, industrial sources switched from coal and high-sulfur oils to natural gas and low-sulfur oils. Fuel switches within these source categories have resulted in their decreasing contribution to the total sulfur oxides emissions.

Since electric utilities are estimated to contribute an increasingly greater proportion of sulfur oxides to the atmosphere, then regions of rapid utility power generation growth should have experienced a proportionate increase in sulfur oxide emissions. Table 2-12 presents a ranking of the 10 states that exhibited the largest increases in sulfur oxides emissions densities between 1950 and 1978. Also given are the contributions (percent) of utility and industrial fuel combustion sources to the total sulfur oxides emitted within each state. The numerical ranking indicates that both Tennessee and Kentucky have exhibited order of magnitude increases in sulfur oxides emissions densities over the past 28 years. In general, the largest increases in emissions density have been estimated for the area bound by 80°W 30°N, 80°W 42°N and 90°W 30°N, 90°W 42°N. Wisconsin is the only state that does not lie within these bounds. Within the region in 1978, sulfur oxides emitted by electric utilities and industrial fuel combustion sources dominated the anthropogenic burden to the atmosphere.

Along with the increases in sulfur oxides emissions densities, the areas of the eastern United States exhibiting the highest emissions densities would be expected to influence strongly the sulfuric acid component of precipitation, whether through long-range transport and/or transformation or by primary emissions. Table 2-13 lists annual sulfur oxides emissions densities by state for each decade from 1950 through 1970 along with 1978 and, in parentheses, the numerical rankings of the 10 highest emissions densities excluding the District of Columbia. The areas of highest emissions densities have shifted from the North Atlantic Coastal region in the 1950's to the Midwest in the 1970's. Connecticut, New York, and Rhode Island have been

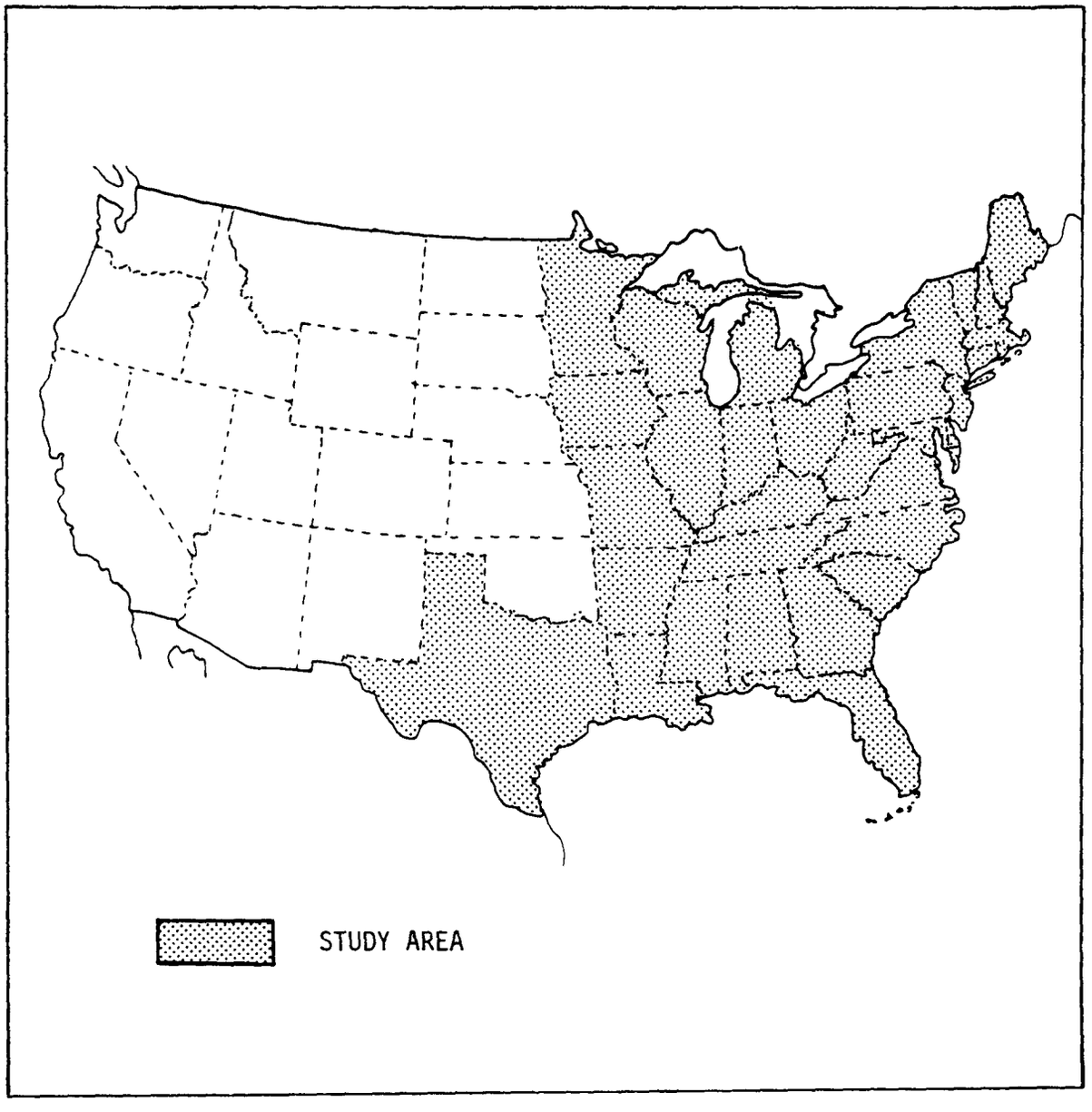

Figure 2-5. Map showing the study area included for emissions density calculations. Adapted from Gschwandtner et al. (1981).

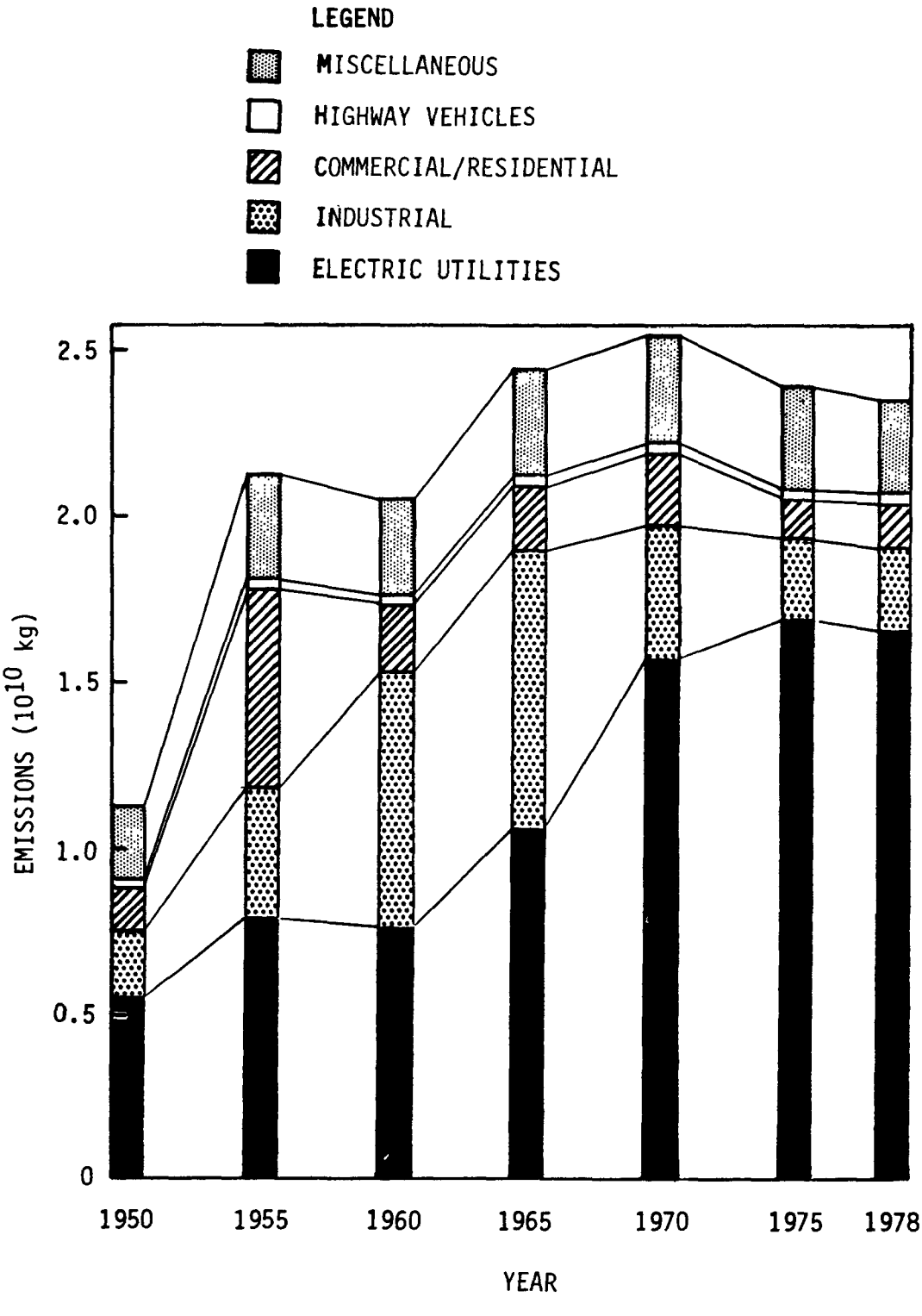

Figure 2-6. Historical trends of sulfur oxide emissions by source category for the study area. Adapted from Gschwandtner et al. (1981).

TABLE 2-12. TEN LARGEST INCREASES IN SULFUR OXIDES EMISSION DENSITIES BETWEEN 1950 and 1978

State	Increase (%)	SO_x Percentage of total sulfur oxides attributable to electric utilities and industrial fuel combustion sources	
		1950	1978
Tennessee	1096	90	93
Kentucky	1076	76	96
South Carolina	558	61	88
Georgia	489	48	89
Mississippi	483	21	83
Alabama	477	34	84
West Virginia	331	80	96
Ohio	248	80	93
Indiana	247	83	93
Wisconsin	206	67	87

TABLE 2-13. ANNUAL EMISSIONS DENSITIES OF SULFUR OXIDES
(kg km^{-2} yr^{-1})

	1950	1960	1970	1978
Alabama	944	4168	6646	5446
Arkansas	276	173	262	829
Connecticut	9834 (6)	16907 (7)	22201 (5)	7836
Delaware	17960 (4)	33414 (1)	38063 (1)	32061 (1)
District of Columbia	169070	200904	407038	91344
Florida	1344	2043	5757	4104
Georgia	714	1180	2443	4204
Illinois	5403 (10)	15245 (9)	15672 (9)	10860 (10)
Indiana	5148	17797 (6)	18750 (6)	17851 (3)
Iowa	1081	2270	2306	2397
Kentucky	981	5475	11114	11541 (9)
Louisiana	1680	1589	2297	2597
Maine	398	577	865	696
Maryland	13220 (5)	13502 (10)	15500 (10)	11840 (8)
Massachusetts	38436 (2)	15935 (8)	24425 (4)	17070 (4)
Michigan	3114	6538	9153	6728
Minnesota	1689	1634	1880	1580
Mississippi	344	301	586	2007
Missouri	3596	2934	5566	6574
New Hampshire	2615	1099	3614	2551
New Jersey	58539 (1)	22273 (4)	26396 (3)	14483 (7)
New York	6011 (9)	10088	10288	7427
North Carolina	2043	1553	3550	3750
Ohio	7609 (7)	24943 (3)	26568 (2)	26486 (2)
Pennsylvania	7500 (8)	18269 (5)	17906 (7)	14691 (6)
Rhode Island	19486 (3)	25288 (2)	17352 (8)	6174
South Carolina	502	1308	2088	3305
Tennessee	807	6065	8199	9652
Texas	1199	1180	1516	1671
Vermont	149	313	470	317
Virginia	1353	1471	4076	3087
West Virginia	3532	7682	14192	15209 (5)
Wisconsin	1353	3768	2016	4140

Note: Numbers in parentheses indicate numerical ranking of 10 highest emissions densities (D.C. excluded).

displaced from the ranking by Indiana, Kentucky, and West Virginia. During 1950, the 10 ranked states emitted a total of 5.9×10^9 kg of sulfur oxides compared with 1.11×10^{10} kg of sulfur oxides for the ranked states in 1978, an increase of 88 percent. Although Delaware remains a region of dense SO_x emissions because of its large chemical complexes, notable reductions have occurred in Connecticut, Rhode Island, Maryland, and New Jersey as a result of changes in fuel type and fuel sulfur content. If the transformation of SO_2 in the atmosphere results in the deposition of acidic sulfur compounds, then the increase in midwestern SO_2 emissions should result in an enlarged geographical domain in which acidity is measured.

Table 2-14 presents the estimates of the annual emissions of sulfur oxides for each of the 31 states for the period from 1950 through 1980. Total emissions from this region declined slightly after 1970. The largest quantities of emissions can be attributed to the midwestern United States. Significant increases in emissions have occurred in the southern part of the country, notably in Kentucky, Tennessee, Mississippi, Alabama, Georgia, and Florida. Emissions of sulfur dioxide in the Northeast show a substantial reduction after 1970.

With establishment of sulfur dioxide and particulate matter emissions standards, most sources in the northeastern United States found it advantageous to switch to fuels of lower sulfur content rather than install SO_2 scrubbers, which were relatively unproven at the time. Also, many coal-fired sources were design-limited with respect to the potential installations of high efficiency particulate removal devices such as electrostatic precipitators. Cost considerations also precluded upgrading sources that were approaching their design operating lifetime. Therefore, as a means of complying with both sulfur dioxide and particulate matter emissions standards, many source operators switched from burning coal to burning residual oils, which were lower in sulfur content, produced little ash, eliminated the need for electrostatic precipitators, and were economical and readily available along the East Coast.

2.3.2.2 Primary Sulfate Emissions--Results over the past 7 years have shown that primary sulfate emissions from oil combustion are 5 to 10 times higher than those from coal of a similar sulfur content (Homolya and Cheney 1978). Primary sulfate is that emitted as sulfate. Secondary sulfate is that produced by atmospheric reactions involving other chemical substances. Sulfuric acid has been identified as the major constituent of the total water-soluble sulfate emissions from both oil and coal firing (Cheney and Homolya 1978). Ambient air measurements taken in the vicinity of an isolated oil-fired power plant have demonstrated a correlation between primary sulfate emissions and an increase of up to twofold in ambient sulfate levels ~ 6 km downwind from the source (Boldt et al. 1980).

Shannon (1979) and Shannon et al. (1980), using the Advanced Statistical Trajectory Regional Air Pollution model (ASTRAP), have studied the relationship between primary and secondary sulfate at the regional scale. Using the emissions inventory compiled as part of the SURE study (Klemm and Brennan 1979), the model simulations showed that primary sulfate has a less uniform distribution than does secondary sulfate, but that in the

TABLE 2-14. ESTIMATES OF ANNUAL EMISSIONS OF SULFUR OXIDES (10^6 kg yr^{-1})

	1950	1960	1970	1978	1980
Alabama	126.2	557.3	888.6	728.2	821.2
Arkansas	38.0	23.8	36.0	114.1	92.1
Connecticut	127.6	219.4	288.1	101.7	65.2
Delaware	95.7	178.1	202.8	170.9	99.2
District of Columbia	29.4	35.0	70.9	15.9	13.4
Florida	203.9	309.9	873.4	622.6	993.3
Georgia	108.9	180.0	372.6	641.2	761.7
Illinois	789.5	2227.5	2290.0	1586.8	1334.1
Indiana	484.0	1673.2	1762.8	1678.3	1821.5
Iowa	157.6	331.0	336.3	349.6	298.2
Kentucky	102.7	573.0	1163.1	1207.8	1016.7
Louisiana	211.2	199.8	288.8	326.5	276.0
Maine	34.3	49.7	74.4	59.9	86.0
Maryland	362.3	370.0	424.7	324.4	306.6
Massachusetts	822.2	340.9	522.5	365.1	312.5
Michigan	469.7	986.1	1380.5	1014.7	822.7
Minnesota	367.9	355.9	409.5	344.1	236.2
Mississippi	42.5	37.2	72.4	248.1	250.5
Missouri	649.2	529.7	1004.9	1186.8	1180.4
New Hampshire	63.0	26.5	87.1	61.5	84.3
New Jersey	1188.3	452.1	535.8	294.0	253.3
New York	772.0	1295.7	1021.3	953.9	856.7
North Carolina	278.3	211.6	483.6	510.9	546.4
Ohio	812.6	2663.7	2837.3	2828.5	2401.1
Pennsylvania	880.8	2145.4	2102.8	1725.2	1834.5
Rhode Island	61.3	79.5	54.6	19.4	13.8
South Carolina	40.4	105.3	168.0	265.3	295.8
Tennessee	88.3	663.8	897.4	1056.4	976.6
Texas	830.4	817.3	1050.0	1157.3	1158.2
Vermont	3.7	7.8	11.7	7.9	6.2
Virginia	143.1	155.6	431.0	326.4	327.5
West Virginia	321.3	481.2	889.1	952.8	986.8
Wisconsin	196.8	548.2	293.3	602.3	566.7
	10784.1	18852.6	23492.1	21741.6	20960.4

acid-sensitive areas of the northeastern United States and eastern Canada, primary sulfate concentrations are 25 to 50 percent of secondary sulfate during the winter.

To estimate long-term trends in primary sulfate emissions characteristics, historical sulfur oxides emissions estimates summarized in Figure 2-6 were adjusted by appropriate primary sulfate emissions factors for each source category and fuel type, to yield a mass emission of sulfate for each category. The aggregate mass emissions for each state were then normalized with respect to state area and reported as a primary sulfate emissions density. Table 2-15 lists the sulfate emissions factors used as multipliers of the sulfur oxide emissions. The factors are comparable with those used by Shannon et al. (1980) in ASTRAP simulations with the exception of the mobile and miscellaneous source categories. A conservative emissions factor of 3 percent was assumed for the mobile source category and a factor of 5 percent was assumed to represent an average of the miscellaneous source categories, which consist of fossil fuel combustion, petroleum refining, and chemical and mineral products manufacturing.

The annual sulfate emissions densities for each state are presented in Table 2-16 along with the ranking of the 10 highest emissions densities for each period. The data indicate that the Northeast has been historically the area of highest primary sulfate emissions density within the eastern United States. The estimates demonstrate that primary sulfate emissions have decreased in the northeastern United States, except for Delaware, over the past 28 years, along with the corresponding decrease in sulfur oxides emissions densities given in Table 2-13. However, the Northeast continues to exhibit the highest primary sulfate emissions density.

Table 2-17 presents estimates of annual emissions of primary sulfate for the 31-state region between 1950 and 1980. Total emissions in this region have declined since 1970 in a trend similar to the decline in SO_2 emissions given in Table 2-14. However, the states estimated to emit the highest amounts of primary sulfates are not the same states estimated to be the major sources of SO_2 emissions. For example, Pennsylvania, New York, and Florida are estimated to be the top three states with highest primary sulfate emissions in 1980. By comparison, Ohio, Pennsylvania, and Indiana are estimated to be the top three states with highest sulfur oxide emissions for the same period. These differences in rankings can be attributed to the differences in the types of fuels being burned. Midwestern states burn coal predominantly whereas northeastern states consume significant quantities of residual fuel oils. The higher primary sulfate emission factor for oil compared to coal accounts for the disproportionate quantities of sulfates estimated to be emitted from those states that burn the largest volumes of residual fuel oils for utility, industrial, commercial, and residential use.

The influence of primary sulfate emissions on acidic precipitation is unclear. During the winter season when photochemical activity is minimal, primary acid emissions should exert the greatest contribution through long-range transport to the northeastern United States and/or local low-level

TABLE 2-15. SULFATE EMISSIONS FACTORS FOR SOURCE CATEGORIES AND FUELS (SHANNON ET AL. 1980)

Source category	Sulfate emissions factor (%)
Coal point sources	1.5
Residual oil--utility and industrial	7.0
Residual oil--commercial and residential	13.4
Distillate oil	3.0
Mobile sources	3.0
Miscellaneous	5.0

TABLE 2-16. ANNUAL EMISSIONS DENSITIES OF PRIMARY SULFATE
(kg km^{-2} yr^{-1})

	1950	1960	1970	1978
Alabama	39	89	130	116
Arkansas	15	8	14	45
Connecticut	595 (6)	649 (5)	1307 (5)	590 (4)
Delaware	952 (5)	1371 (1)	1544 (2)	1584 (1)
District of Columbia	6419	10079	32608	6366
Florida	80	111	230	214
Georgia	32	39	73	104
Illinois	164 (9)	332 (10)	354 (10)	255
Indiana	154	333 (9)	344	367 (10)
Iowa	28	41	47	50
Kentucky	28	91	179	193
Louisiana	94	79	118	151
Maine	25	35	62	50
Maryland	982 (4)	428 (8)	551 (7)	494 (5)
Massachusetts	2924 (2)	962 (4)	1952 (1)	1298 (2)
Michigan	115	158	193	168
Minnesota	45	67	82	76
Mississippi	17	15	24	106
Missouri	158	69	133	133
New Hampshire	163 (10)	56	141	110
New Jersey	3260 (1)	1008 (3)	1507 (4)	878 (3)
New York	292 (8)	380	555 (6)	459 (8)
North Carolina	50	44	84	98
Ohio	210	451 (6)	470 (9)	485 (7)
Pennsylvania	302 (7)	431 (7)	482 (8)	387 (9)
Rhode Island	1589 (3)	1090 (2)	1535 (3)	494 (6)
South Carolina	28	44	62	111
Tennessee	35	118	156	182
Texas	65	57	75	72
Vermont	8	14	23	23
Virginia	77	53	190	151
West Virginia	83	143	319	261
Wisconsin	38	82	51	83

Note: Numbers in parentheses indicate numerical ranking of 10 highest emissions densities (D.C. excluded).

TABLE 2-17. ESTIMATES OF ANNUAL EMISSIONS OF PRIMARY SULFATE (10^6 kg yr^{-1})

	1950	1960	1970	1978	1980
Alabama	5.2	11.9	17.4	15.5	21.1
Arkansas	2.1	1.1	1.9	6.2	4.1
Connecticut	7.7	8.4	17.0	7.7	4.7
Delaware	5.1	7.3	8.2	8.4	3.4
District of Columbia	1.1	1.8	5.7	1.1	1.0
Florida	12.1	16.8	34.9	32.5	38.0
Georgia	4.9	4.0	11.1	15.9	15.0
Illinois	24.0	48.5	51.7	37.3	23.4
Indiana	14.5	31.3	32.3	34.6	31.8
Iowa	4.1	6.0	6.9	7.3	4.8
Kentucky	2.9	9.5	18.8	20.2	13.6
Louisiana	11.8	9.9	14.8	19.0	18.3
Maine	2.2	3.0	5.3	4.3	9.0
Maryland	26.9	11.7	15.1	13.5	9.2
Massachusetts	62.6	20.6	41.8	27.8	18.6
Michigan	17.3	23.8	29.1	25.3	17.3
Minnesota	9.8	14.6	17.9	16.6	5.7
Mississippi	2.1	1.9	3.0	13.1	9.9
Missouri	28.5	12.5	24.0	24.0	15.8
New Hampshire	4.0	1.4	3.5	2.7	4.1
New Jersey	66.2	20.5	30.6	17.8	10.7
New York	37.5	48.8	71.3	59.0	39.9
North Carolina	6.8	6.0	11.4	13.4	13.7
Ohio	22.4	48.2	50.2	51.8	36.5
Pennsylvania	35.5	50.6	56.6	45.5	41.5
Rhode Island	5.0	3.4	4.8	1.6	1.0
South Carolina	2.3	3.5	5.0	8.9	7.9
Tennessee	3.8	12.9	17.1	19.9	14.5
Texas	45.0	39.5	51.9	49.9	31.3
Vermont	0.2	0.4	0.6	0.6	0.5
Virginia	8.1	5.6	20.1	16.0	8.3
West Virginia	5.2	9.0	20.0	16.4	14.5
Wisconsin	5.5	11.9	7.4	12.1	10.6
	491.5	506.4	704.6	643.0	496.1

emissions sources. Similarly, the low-level emissions source influence may be exacerbated by space-heating needs during winter months.

The differences in the release height of point source emissions will affect the relative local deposition of emissions compared to those which may be carried aloft to undergo a variety of transport and transformation processes for extended periods in the atmosphere. As a comparison, Table 2-18 was constructed to illustrate the regional differences in the quantities of sulfur oxides emitted as a function of stack height. Emissions and stack data were taken from the EPA 1980 National Emissions Data System (NEDS) files for Ohio, Pennsylvania, Florida, and New Jersey. The number of point sources and their cumulative emissions of sulfur oxides were aggregated according to four increments of stack heights. The aggregated data indicate that for Ohio and Pennsylvania, the bulk of the sulfur oxides emissions in each state are emitted at stack heights of from 152 to 305 m. Emissions in this release height increment represent in excess of 60 percent of the total sulfur oxides emitted and serve as the basis of the hypothesis involving long-range transport/transformation of sulfur oxides with deposition in the northeastern United States.

Of the four states compared in Table 2-18, neither Florida nor New Jersey emitted sulfur oxides at release heights above 152 m during 1980. In fact, 60 percent of the point source emissions of sulfur oxides in New Jersey are estimated to be emitted at heights between 31 and 76 m. In Florida, 55 percent of the sulfur oxide emissions from point sources are emitted at heights between 77 and 151 m. Therefore, the deposition of both primary and secondary sulfates and/or acidic materials from point source emissions in these states may occur at shorter downwind distances than from midwestern sources. In fact the amount of sulfur oxides emitted from stack heights less than 30 meters in Florida is nearly eight times that emitted from a similar height in either Ohio or Pennsylvania.

Table 2-19 compares the estimated utility-generated sulfur oxide and primary sulfate emissions for 1980 from two states that differ in the predominate release height of emissions. For both Ohio and Florida, utility emissions account for all of the sulfur oxides and primary sulfate estimated to be emitted from the highest stack height intervals. Although the sulfur oxide emissions in Ohio are about 3.5 times those emissions from the sources in Florida, the primary sulfate emissions in Florida are about 5 percent higher than those from the sources in Ohio. These differences can be attributed to the use of residual fuel oils by the utility industry in Florida. The total emission of primary sulfates by industry in Florida is greater than those emissions generated by the coal-fired utilities in Ohio. Therefore, one might expect a greater deposition of primary sulfates from local sources in Florida compared with Ohio.

2.3.3 Historical Trends and Current Emissions of Nitrogen Oxides

Table 2-20 summarizes the annual emissions densities of nitrogen oxides for each state over the interval from 1950 to 1978. The table also indicates the numerical ranking of the 10 highest emission densities for the period of calculation. Ohio, Pennsylvania and the northeastern Atlantic coastal

TABLE 2-18. ESTIMATED POINT SOURCE SO_2 EMISSIONS AS A FUNCTION OF STACK HEIGHT FOR SELECTED STATES IN 1980
(10^6 kg yr)

State	Stack Height									
	0 - 30 meters		31 - 70 m		71 - 152 m		153 - 305 m		Total	
	No. Sources	Emissions	No. Sources	Emissions	No. Sources	Emissions	No. Sources	Emissions	No. Sources	Emissions
Ohio	14	24.0	70	183.1	47	580.0	48	1,722.9	185	2,510.0
Pennsylvania	9	24.0	102	412.9	50	238.8	33	1,084.4	194	1,760.1
Florida	61	184.2	74	205.6	30	469.6	0	0	165	859.4
New Jersey	16	60.3	18	111.0	4	14.0	0	0	38	185.3

TABLE 2-19. ESTIMATED SO_2 AND PRIMARY SULFATE EMISSIONS FOR 1980 FROM UTILITY SOURCES IN FLORIDA AND OHIO (10^6 kg yr^{-1})

	Stack Height m	No. of point sources	SO_2 emissions	Sulfate emissions
Florida	0-30	12	99.9	3.7
	31-76	23	107.9	4.0
	77-152	30	469.6	17.5
	153-305	0	0	0
Ohio	0-30	3	4.5	0.1
	31-76	17	48.5	0.5
	77-152	35	441.4	4.8
	153-305	48	1722.8	18.6

TABLE 2-20. ANNUAL EMISSIONS DENSITIES OF NITROGEN OXIDES
(kg km^{-2} yr^{-1})

	1950	1960	1970	1978
Alabama	1171	2088	2824	3214
Arkansas	756	763	1271	1435
Connecticut	6311 (4)	9851 (4)	14137 (3)	12803 (3)
Delaware	3378 (10)	8726 (5)	12249 (5)	12031 (5)
District of Columbia	165891	182598	304180	174790
Florida	1235	1925	3305	4649
Georgia	1017	1353	2370	3269
Illinois	3723 (6)	5566 (10)	7019	7019 (10)
Indiana	2860	5648 (9)	5566	5802
Iowa	1044	1344	1925	1998
Kentucky	1262	2424	4313	4885
Louisiana	2324	3868	7346 (9)	11513 (6)
Maine	449	518	799	808
Maryland	3604 (8)	7382 (8)	9897 (7)	10397 (8)
Massachusetts	6973 (3)	10823 (3)	15272 (2)	15490 (2)
Michigan	1916	3532	5094	5076
Minnesota	690	999	1389	1662
Mississippi	672	1108	1334	1998
Missouri	999	1480	2134	2833
New Hampshire	690	1171	1397	2515
New Jersey	12639 (1)	16226 (1)	24080 (1)	22110 (1)
New York	3487 (9)	5430	7073 (10)	6429
North Carolina	1280	1934	3641	3941
Ohio	4240 (5)	8163 (6)	9906 (6)	10860 (7)
Pennsylvania	3705 (7)	7890 (7)	8426 (8)	8662 (9)
Rhode Island	9670 (2)	13048 (2)	13910 (4)	12240 (4)
South Carolina	990	1698	2679	3387
Tennessee	1371	2788	3877	4921
Texas	1135	2170	3341	4349
Vermont	409	499	1162	944
Virginia	1580	2542	3723	3741
West Virginia	1725	3260	5030	6701
Wisconsin	1226	1852	2842	2951

Note: Numbers in parentheses indicate numerical ranking of 10 highest emissions densities (D.C. excluded).

states consistently have been the areas of highest emissions density. The emissions densities have increased by a factor of two or three over the 28-year interval of record. In New England, there is a contrast between changes in sulfur oxides and nitrogen oxides emissions. Comparing Table 2-13 with Table 2-20 shows that, although sulfur oxides emissions have been decreasing substantially in the northeastern United States, nitrogen oxides emissions have not decreased comparably.

Table 2-21 provides estimates of the annual emissions of nitrogen oxides for the 31-state region during the period from 1950 through 1980. Total emissions have increased from 1950 and show little change over the last ten years. During 1980, highest emissions occurred in Texas, Ohio, Pennsylvania, and Illinois. With few exceptions, emissions appear to have increased in all states from 1960 to 1980. This contrasts the apparent regional differences in SO_2 and primary sulfate emissions discussed earlier.

The high emissions densities of nitrogen oxides in the Northeast appear to be strongly influenced by mobile sources. Table 2-22 gives the percentage of nitrogen oxides emitted by mobile sources for six northeastern states chosen from the 10 highest nitrogen oxides emissions density areas in 1978. With the exception of Delaware, this region exhibits a mobile source contribution in excess of 40 percent of the total NO_x emitted. By comparison, areas such as Ohio and Illinois exhibit a 25 percent contribution by mobile sources to nitrogen oxides emissions. Figure 2-7 summarizes the composite of source category contributions to total nitrogen oxide emitted between 1950 and 1978. Within the last decade, mobile sources and electric utilities have been the predominant contributors. Comparison with Figure 2-6, a similar representation of sulfur oxide emissions, indicates a marked and consistent increase in nitrogen oxide emissions during a period (1955-78) when sulfur oxide emissions have shown little variation. Chemical analyses (Likens 1976) of precipitation samples suggest that nitric acid is comprising a larger fraction of total acidity relative to sulfuric acid in the Northeast. Because of the importance of the low-level mobile source contribution, the argument could be made that correlation with the changes in emissions could indicate a substantial influence of local and subregional sources on rainwater acidity through both primary emissions and atmospheric transformations.

2.3.4 Historical Trends and Current Emissions of Hydrochloric Acid (HCl)

Hydrochloric acid is an emission component that has received little attention with respect to its potential for acidic precipitation formation. Burning coal is one of the major sources of HCl emissions to the atmosphere (Stahl 1969). Chlorine is present in coals in the form of inorganic chloride salts which are soluble in water. During combustion, most of the chlorine salts are converted to hydrogen chloride and emitted into the atmosphere.

Chlorine is found in relatively high concentration in coals from the Illinois Basin and the eastern United States (Gluskoter et al. 1977), but only in low concentrations in coals from the western United States. The chlorine content ranges from 0.01 to 0.50 percent. Coals from western Pennsylvania through

TABLE 2-21. ESTIMATES OF ANNUAL EMISSIONS OF NITROGEN OXIDES (10^6 kg yr^{-1})

	1950	1960	1970	1978	1980
Alabama	156.6	279.2	377.6	429.7	480.5
Arkansas	104.0	105.0	174.9	197.4	197.2
Connecticut	91.9	127.8	183.4	166.1	121.6
Delaware	18.0	46.5	65.3	64.1	47.1
District of Columbia	28.9	31.8	52.9	30.4	19.9
Florida	187.4	292.0	501.4	705.3	588.0
Georgia	155.1	206.4	361.5	498.6	448.3
Illinois	544.0	813.3	1025.6	1036.1	912.0
Indiana	268.9	531.0	523.3	545.5	701.3
Iowa	132.3	196.0	280.7	291.4	290.9
Kentucky	132.1	253.7	451.4	511.2	482.0
Louisiana	292.1	486.2	923.4	1447.3	842.2
Maine	38.6	44.6	68.8	69.5	53.9
Maryland	98.8	202.3	271.2	284.9	225.1
Massachusetts	149.2	231.5	326.7	331.4	230.0
Michigan	289.0	532.7	768.3	765.6	625.9
Minnesota	150.3	217.6	302.5	362.0	338.8
Mississippi	83.1	137.0	164.9	247.0	258.8
Missouri	180.4	267.2	385.3	311.4	314.9
New Hampshire	16.6	28.2	57.8	60.6	75.5
New Jersey	256.6	329.4	488.8	448.8	368.3
New York	447.9	697.4	908.4	825.7	616.5
North Carolina	174.4	263.5	496.0	536.9	586.5
Ohio	452.8	871.8	1057.9	1159.8	1038.4
Pennsylvania	435.1	926.6	989.5	1017.2	941.2
Rhode Island	30.4	41.0	43.8	39.5	33.1
South Carolina	79.7	136.6	215.6	272.5	236.1
Tennessee	150.1	305.1	424.3	533.6	469.2
Texas	786.1	1302.9	2313.9	3012.1	2307.7
Vermont	10.2	12.4	29.9	23.5	22.4
Virginia	167.1	268.8	398.7	395.6	367.1
West Virginia	108.1	204.2	315.1	419.8	410.3
Wisconsin	178.4	269.4	413.5	429.3	381.4
	6386.0	10817.2	15299.6	17609.4	15059.7

TABLE 2-22. MOBILE SOURCE CONTRIBUTION TO NITROGEN OXIDES EMISSIONS DENSITIES IN NORTHEAST UNITED STATES

State	Percentage of total NO_x emissions density attributable to mobile sources		
	1950	1960	1975
New Jersey	27	34	47
Massachusetts	36	35	43
Connecticut	23	34	46
Rhode Island	30	34	64
Delaware	29	21	28
Maryland	29	25	41

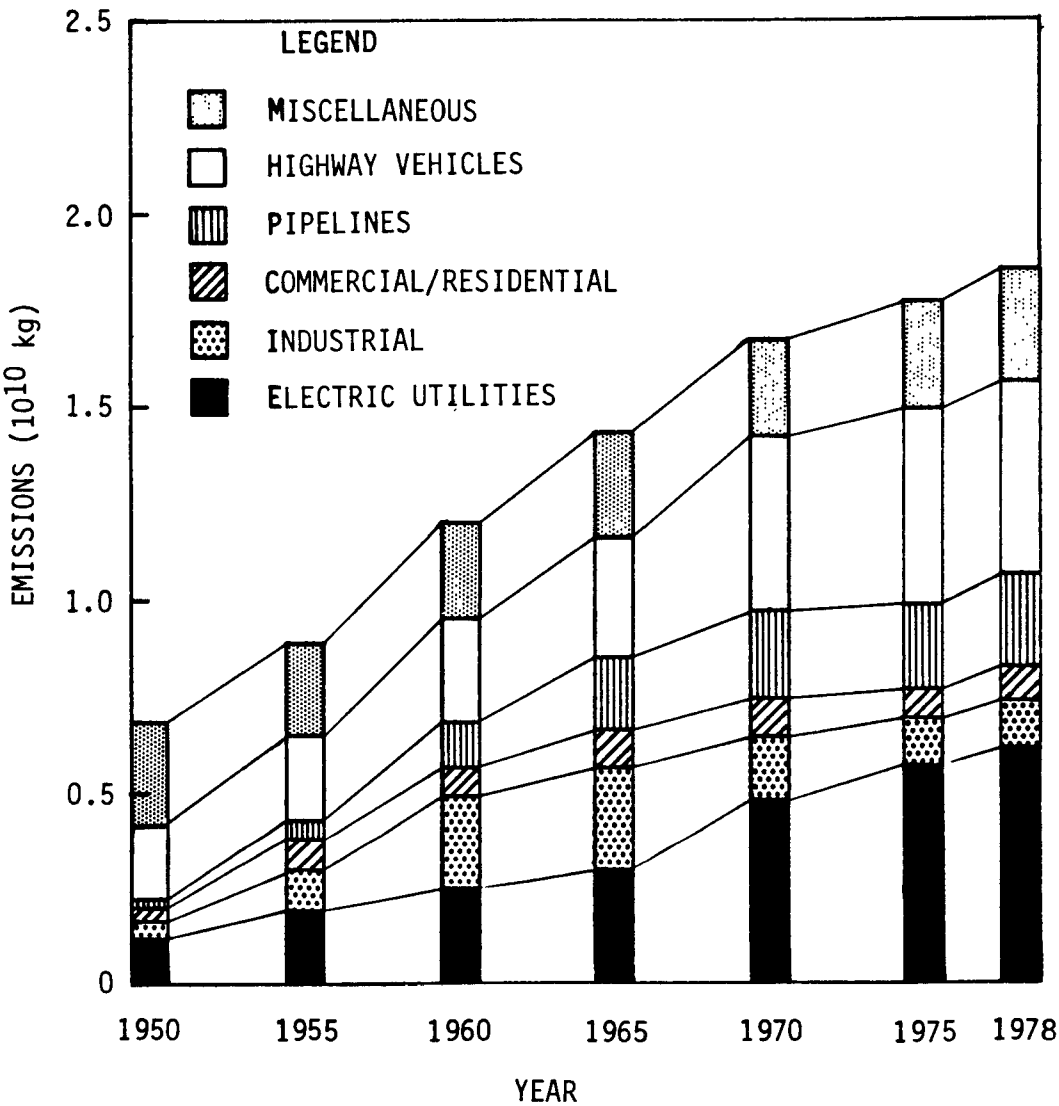

Figure 2-7. Historical trends of nitrogen oxide emissions by source category for the study area. Adapted from Gschwandtner et al. (1981).

southern Illinois (a high SO_2 emission density region) contain about 0.2 percent chlorine. Estimated emissions of hydrochloric acid from this region in 1974 amount to over 450,000 tons. Furthermore, the amount of hydrochloric acid pollution by coal burning may be increased when calcium chloride is added to the coal as an antifreeze or dust-proofing agent (Stahl 1969).

Cogbill and Likens (1974) have estimated that the acidity of precipitation has a 5 percent contribution from HCl. However, the data set used to apportion the stoichiometric balance of hydrogen ion and anions was taken from measurements in New York and New England. Pack (1980) noted in his analysis of EPRI and MAP3S precipitation data that, excluding sea salt contributions, the two networks were within 6 percent agreement on molar concentrations of all anions except chloride, which differed by 47 percent. Although no reason could be given for this discrepancy, the differences may be due to either sampling hardware and analytical errors or a poor distribution of monitoring sites with respect to major anthropogenic HCl emission sources. The latter possibility could be studied by examining individual precipitation event data. The high solubility of HCl in water suggests that emissions would be assimilated rapidly into cloud processes involved in precipitation formation. Also, during a precipitation event, washout of HCl and NH_4Cl should occur in the lower atmosphere.

An estimate of HCl emissions densities as chloride is given in Table 2-23. These values do not include additional chloride emissions due to chemical de-icers added to fuel prior to combustion. The 10 highest emissions densities are also ranked for each calculation period. Consistently, West Virginia, Ohio, Pennsylvania, and Illinois have remained the greatest chloride emissions areas. Significant increases have been noted for Kentucky and Tennessee because of their increased coal consumption.

2.3.5 Historical Trends and Current Emissions of Heavy Metals Emitted from Fuel Combustion[1]

As with calculated emissions densities for sulfur and nitrogen oxides, fuel composition data can be used to estimate emissions densities for certain metals that might be of use as tracers to evaluate the transport, transformation, and deposition of acidic components. Arsenic and mercury are emitted as volatiles from coal combustion but are present only in minute quantities in fuel oils. In contrast, vanadium is the major metal associated with residual fuel burning but is only a minor component of coal.

Table 2-24 is a compilation of arsenic, mercury, and vanadium levels found in coals burned in each state in the eastern United States. Gluskoter et al. (1977) presented the ranges of concentrations and mean values of concentrations for these metals. The range of arsenic concentrations in

---

[1]Editor's Note: Although several public reviewers questioned the relevancy of this section, it has been included based on the importance of some metals to tracer studies and effects studies. The decision that this section remain in the chapter was also made at the November 1982 Technical Review Meeting.

TABLE 2-23. ANNUAL EMISSIONS DENSITIES OF CHLORIDE
(kg km^{-2} yr^{-1})

	1950	1960	1970	1978
Alabama	2.1	30.0	37.2	34.5
Arkansas	0.0	0.0	0.0	4.1
Connecticut	71.7 (7)	254.2 (9)	128.9	4.7
Delaware	1.5 (4)	315.1 (7)	298.0 (6)	153.5 (9)
District of Columbia	4106.0	5374.4	5843.9	437.7
Florida	0.0	2.7	9.4	12.5
Georgia	8.6	34.1	80.1	173.9
Illinois	232.4 (2)	816.3 (2)	769.9 (2)	728.2 (3)
Indiana	54.6 (10)	264.2	258.8 (7)	285.1 (6)
Iowa	2.1	6.2	7.7	13.3
Kentucky	8.3	63.7	114.9	134.4 (10)
Louisiana	0.0	0.1	0.0	0.4
Maine	0.0	2.7	0.5	0.2
Maryland	45.2	252.0 (10)	240.6 (9)	172.5 (8)
Massachusetts	0.4	178.9	32.4	3.2
Michigan	35.0	139.8	171.6	133.9
Minnesota	0.5	2.6	3.4	5.3
Mississippi	0.0	0.1	6.1	22.5
Missouri	3.3	22.0	39.5	66.7
New Hampshire	1.1	11.7	47.0	29.8
New Jersey	91.7 (6)	306.0 (8)	226.0 (10)	91.7
New York	64.1 (9)	190.8	126.8	65.1
North Carolina	12.9	34.8	86.7	85.5
Ohio	175.9 (3)	697.1 (3)	746.2 (3)	770.9 (2)
Pennsylvania	99.0 (5)	444.9 (5)	316.7 (5)	305.1 (5)
Rhode Island	71.3 (8)	374.1 (6)	2.0	3.2
South Carolina	1.0	69.4	117.1	146.9
Tennessee	6.5	210.3	255.1 (8)	331.2 (4)
Texas	0.0	0.3	0.0	7.4
Vermont	0.0	2.6	2.8	0.2
Virginia	113.5 (4)	459.0 (4)	436.4 (4)	261.5 (7)
West Virginia	262.9 (1)	829.9 (1)	1287.5 (1)	1905.9 (1)
Wisconsin	0.4	15.4	21.2	17.7

Note: Numbers in parentheses indicate numerical ranking of 10 highest emissions densities (D.C. excluded).

TABLE 2-24. ARSENIC, MERCURY, AND VANADIUM CONTENT OF BITUMINOUS COAL

State	Arsenic (ppm)	Mercury (ppm)	Vanadium (ppm)
Alabama	53	0.30	52
Arkansas	53	0.30	52
Connecticut	17	0.18	40
Delaware	17	0.18	40
District of Columbia	17	0.18	40
Florida	53	0.30	52
Georgia	26	0.13	33
Illinois	15	0.19	32
Indiana	10	0.30	26
Iowa	22	0.22	27
Kentucky	11	0.17	34
Louisiana	53	0.30	52
Maine	17	0.18	40
Maryland	17	0.18	40
Massachusetts	17	0.18	40
Michigan	10	0.30	26
Minnesota	2	0.10	10
Mississippi	26	0.13	33
Missouri	9	0.18	40
New Hampshire	17	0.18	40
New Jersey	17	0.18	40
New York	17	0.18	40
North Carolina	11	0.17	34
Ohio	19	0.23	38
Pennsylvania	17	0.18	40
Rhode Island	17	0.18	40
South Carolina	26	0.13	33
Tennessee	26	0.13	33
Texas	5	0.09	7
Vermont	17	0.18	40
Virginia	6	0.12	23
West Virginia	6	0.12	23
Wisconsin	22	0.22	27

Source: Values assigned from Gloshoter et al. 1977.

eastern U.S. coals is 1.8 to 100 ppm, for mercury, 0.05 to 0.47 ppm, and for vanadium, 14 to 73 ppm. The metal concentrations presented in Table 2-24 for each state were obtained by assuming that the fuel consumed in each state forcombustion was obtained from coal producing areas located near the state. For example, an average arsenic concentration of 53 ppm in coal was assigned to Alabama, Arkansas, Florida, and Louisiana with the assumption that these states would be receiving coal from about the same producing region. Of course there would be a range of concentrations expected for each state but such data are not readily available.

The fuel consumption data computed by Gschwandnter et al. (1981) can be multiplied by the concentration of arsenic and mercury in coal to arrive at the normalized annual emissions densities given in Tables 2-25 and 2-26. For 1978, Ohio exhibited the highest emissions density for both arsenic and mercury. These data can be used with the corresponding estimates for SO_2, NO_x, and primary sulfate to evaluate the transport and deposition of emissions. As tracers, the SO_x/metals or NO_x/metals ratios could be useful in identifying origins of specific precipitation event samples.

The ratios of atmospheric sulfate to vanadium, arsenic, and mercury might be used to apportion that quantity of sulfate that is formed by progressive oxidation of atmospheric SO_2. The presence of vanadium in atmospheric aerosols could be used in conjunction with meteorological measurements to estimate the regional origins of the air mass containing such aerosols. For example, air masses of midwestern U.S. origin would be expected to contain less vanadium than an air mass being transported along the eastern United States because of the predominant use of fuel oil along the East Coast. Estimates of vanadium in atmospheric aerosols as opposed to arsenic or mercury could be used.

Vanadium is not emitted as a volatile element from fuel combustion. It is present as porphyrin compounds in the fuels and is converted to the oxide form in the combustion zone. The oxides, mainly V_2O_5, are incorporated into the fly ash. Residual oil-fired sources for utility, industrial, and commercial categories usually do not employ particulate removal devices. Therefore, one can calculate vanadium emissions from oil burning, given the fuel consumption, the particulate emission factors (U.S. EPA 1981), and the vanadium content of oil ash.

The vanadium content of oil fly ash will vary with the vanadium content of the oil and with certain combustion operating parameters such as excess boiler oxygen and emissions controls. Vanadium in fuel oil will vary according to the regional production source of the crude and the degree of hydrodesulfurization. It is assumed that most of the residual fuels burned in the eastern United States are derived from Venezuelen crudes. These fuels are noted for their elevated vanadium levels. However, only approximate fuel vanadium values can be applied to the fuel consumption inventories.

For these calculations, it is assumed that the average vanadium content of residual oil consumed by electric utilities and industrial sources is 200 ppm. Commercial/residential sources are assumed to burn hydrodesulfurized oils containing 15 ppm vanadium. Experimental measurements of particulate

TABLE 2-25. ANNUAL EMISSIONS DENSITIES OF ARSENIC
(kg km^{-2} yr^{-1})

	1950	1960	1970	1978
Alabama	0.18	2.62	1.96	0.61
Arkansas	0.01	0.01	0.00	0.07
Connecticut	0.60	2.13	0.65	0.01
Delaware	0.01	2.66	1.51	0.26
District of Columbia	34.70	45.40	29.63	0.74
Florida	0.00	0.24	0.50	0.17
Georgia	0.07	0.26	0.36	0.26
Illinois	0.56	1.95	1.10	0.35
Indiana	0.29	1.42	0.84	0.35
Iowa	0.12	0.34	0.26	0.15
Kentucky	0.08	0.59	0.63	0.25
Louisiana	0.00	0.01	0.00	0.01
Maine	0.00	0.02	0.00	0.00
Maryland	0.38	2.12	1.22	0.29
Massachusetts	0.33	1.51	0.14	0.01
Michigan	0.19	0.76	0.56	0.14
Minnesota	0.06	0.25	0.20	0.10
Mississippi	0.00	0.00	0.03	0.03
Missouri	0 .03	0.17	0.18	0.10
New Hampshire	0.01	0.10	0.24	0.05
New Jersey	0.78	2.59	1.15	0.16
New York	0.54	1.62	0.64	0.13
North Carolina	0.12	0.32	0.48	0.16
Ohio	1.03	4.07	2.62	0.90
Pennsylvania	0.84	3.72	1.61	0.51
Rhode Island	0.60	3.49	0.01	0.01
South Carolina	0.08	0.52	0.53	0.22
Tennessee	0.05	1.59	1.15	0.50
Texas	0.00	0.00	0.00	0.02
Vermont	0.00	0.02	0.01	0.00
Virginia	0.08	0.32	0.18	0.04
West Virginia	0.18	0.58	0.54	0.27
Wisconsin	0.22	0.86	0.70	0.19

TABLE 2-26. ANNUAL EMISSIONS DENSITIES OF MERCURY
(kg km^{-2} yr^{-1})

	1950	1960	1970	1978
Alabama	0.002	0.030	0.037	0.035
Arkansas	0.000	0.000	0.000	0.004
Connecticut	0.013	0.045	0.023	0.001
Delaware	0.000	0.057	0.054	0.028
District of Columbia	0.739	0.968	1.052	0.079
Florida	0.000	0.003	0.010	0.009
Georgia	0.001	0.003	0.006	0.012
Illinois	0.014	0.049	0.046	0.043
Indiana	0.018	0.088	0.086	0.091
Iowa	0.002	0.007	0.008	0.015
Kentucky	0.002	0.018	0.033	0.038
Louisiana	0.000	0.000	0.000	0.000
Maine	0.000	0.001	0.000	0.000
Maryland	0.008	0.045	0.043	0.031
Massachusetts	0.007	0.032	0.005	0.001
Michigan	0.012	0.047	0.057	0.045
Minnesota	0.001	0.003	0.003	0.005
Mississippi	0.000	0.000	0.001	0.002
Missouri	0 .001	0.007	0.012	0.020
New Hampshire	0.000	0.002	0.009	0.005
New Jersey	0.017	0.055	0.041	0.017
New York	0.012	0.034	0.023	0.012
North Carolina	0.004	0.010	0.025	0.024
Ohio	0.025	0.100	0.165	0.111
Pennsylvania	0.018	0.080	0.057	0.055
Rhode Island	0.013	0.067	0.000	0.001
South Carolina	0.001	0.005	0.009	0.011
Tennessee	0.001	0.016	0.020	0.020
Texas	0.000	0.001	0.001	0.000
Vermont	0.003	0.012	0.011	0.007
Virginia	0.003	0.012	0.011	0.007
West Virginia	0.007	0.022	0.034	0.050
Wisconsin	0.004	0.017	0.009	0.020

emissions from such sources under these conditions have shown fuel oil ash vanadium concentrations of 5.3 percent for utility and industrial sources (Boldt et al. 1980) and 3.4 percent for residential and commercial sources (Homolya and Lambert 1981). Therefore, simply multiplying total particulate emissions factors by vanadium fly ash contents will result in a vanadium emissions factor for residual oils.

Estimates of vanadium emissions from coal combustion pose an additional problem in that various levels of particulate emissions controls were enacted in each state between 1950 and 1978. For calculation purposes, an emissions control scenario has been assumed to have been uniformly implemented in the eastern United States over this period. Between 1950 and 1965, we have assumed that 50 percent of the particulate matter generated by coal combustion is emitted to the atmosphere. This emission level is reduced to 15 percent in 1970 and finally to 10 percent in 1978. Therefore, vanadium emissions were estimated by multiplying the particulate emissions factor for uncontrolled bituminous coal-fired sources by the fuel vanadium content (given in Table 2-24) and the appropriate particulate control factor for 1950, 1960, 1970, and 1978.

Vanadium emissions from both coal and oil were summed, and the totals reported as emissions densities for each state. The calculations, shown in Table 2-27, indicate highest vanadium emissions densities in the northeast due to residual oil burning. However, the values have decreased somewhat since 1970, reflecting a switch to hydrodesulfurized residuals containing less vanadium. The greatest change in vanadium emissions has occurred in the Gulf Coast, where utilities switched from gas to oil along with increased coal combustion.

A major application of atmospheric trace metal measurements is identifying specific sources of air pollution at particular times and places. If a particular emitted quantity can be identified with some single source (or group of sources), then measurements of its concentrations can be used to identify occasions when air quality is affected by that specific source. The philosophy is like that of atmospheric tracer studies, except that tracers "of opportunity" are employed. In practice, however, it is usually impossible to find a single tracer that is unique to some particular source or set of sources. Instead, groups of trace metals can be chosen to provide statistically identifiable "fingerprints" or "signatures" of different kinds of emission sources. Cooper and Watson (1980) identify five distinct kinds of statistical analysis that can be used, and they illustrate the utility of the methods by assessing the contribution to air pollution in Portland, Oregon, of emissions from categories of sources such as automotive exhaust, kraft mills, home heating, asphalt production, coal burning, and road dust. Kowalczyk et al. (1982) used trace metal concentration data obtained in Washington, DC, to search for effects associated with refuse incineration, automotive exhaust, and coal- and oil-fired power plants.

These statistical techniques (also known as receptor models) are designed to relate observed characteristics of air pollution to corresponding features of emissions. The statistical treatments assume that the trace metals (or similar materials) used in the analysis are transported in the same way

TABLE 2-27. ANNUAL EMISSIONS DENSITIES OF VANADIUM
(kg km^{-2} yr^{-1})

	1950	1960	1970	1978
Alabama	0.66	2.95	2.25	2.35
Arkansas	0.48	0.10	0.32	3.54
Connecticut	35.20	33.65	77.65	75.57
Delaware	12.09	27.39	32.77	56.02
District of Columbia	212.69	365.91	1,422.65	280.44
Florida	3.20	4.82	10.31	16.60
Georgia	0.98	1.22	2.25	2.38
Illinois	4.31	8.04	6.76	6.17
Indiana	5.39	7.48	4.89	5.82
Iowa	0.68	0.55	0.35	0.26
Kentucky	0.57	1.86	2.16	1.39
Louisiana	2.54	0.17	0.49	7.85
Maine	1.09	1.56	3.12	3.36
Maryland	13.91	16.71	20.44	25.81
Massachusetts	35.88	46.70	98.60	88.07
Michigan	2.71	3.86	3.27	4.85
Minnesota	0.33	0.91	0.73	0.52
Mississippi	0.08	0.08	0.24	4.94
Missouri	0 .08	1.11	1.25	0.92
New Hampshire	2.20	2.88	7.89	6.16
New Jersey	63.18	56.98	100.39	71.21
New York	14.24	14.19	27.01	28.89
North Carolina	0.56	1.73	2.69	3.04
Ohio	6.85	11.17	6.78	4.94
Pennsylvania	11.26	17.29	16.31	14.31
Rhode Island	85.69	51.93	71.30	31.23
South Carolina	1.33	1.74	2.11	4.89
Tennessee	0.41	2.08	1.64	1.21
Texas	1.97	0.18	0.11	1.00
Vermont	0.40	0.57	0.91	1.55
Virginia	3.14	2.41	7.66	9.48
West Virginia	1.36	2.68	5.21	2.18
Wisconsin	0.54	1.68	1.36	0.58

between sources and sampling sites, and that they are sampled with precisely the same efficiency. Although this is undoubtedly true in many circumstances, the accuracy of the assumption becomes less obvious as distances and time scales increase or whenever meteorological factors such as rainfall intervene.

The statistical methods of receptor modeling have recently been extended to address visibility (Friedlander 1981, Barone et al. 1981). Some attempts to apply receptor modeling methods to investigate long-range transport have been conducted, but the results obtained are contentious. Applying methods involved in receptor modeling to questions of precipitation chemistry is difficult because of the complexity of the processes involved in precipitation scavenging and the need to assume identical pollutant pathways and scavenging rates for source apportionment methods to work properly.

2.3.6 Historical Emissions Trends in Canada

Historical emissions data have been developed for SO_2 and NO_x for the years 1955, 1965, and 1976 as a contribution to the effort undertaken by the U.S./Canada Work Group 3B (Engineering, Costs, and Emissions) in accordance with the Memorandum of Intent on Transboundary Air Pollution concluded between Canada and the United States on August 5, 1980. Information regarding production and fuel consumption was obtained from internal files and, for other source categories, U.S. or Canadian emissions factors were applied to the basic data. Actual emissions data were available for copper-nickel smelters and some power plants. For 1976, emissions data were taken from a nationwide inventory prepared by SNC/GECO Canada, Inc., and the Ontario Research Foundation (1975).

Total Canadian emissions of SO_2 and NO_x for each of the years 1955, 1965, and 1976 are given in Table 2-28. Total SO_2 emissions in Canada were approximately 5.3 million metric tons for 1976, 6.6 million metric tons in 1965, and 4.5 million metric tons in 1955. The fluctuations in emissions levels were due to changes in production by the copper-nickel smelting industry, which is centered in eastern Canada. Sulfur dioxide emissions from power plants were 0.05 million metric tons in 1955 and rose to 0.55 million metric tons in 1976, with over 90 percent of the total emitted in eastern Canada. Sulfur dioxide emissions from nonutility fuel combustion decreased slightly between 1955 and 1965 as a result of fuel switching from coal to oil. Industrial fuel combustion represents the major contributor to nonutility combustion emissions.

Iron ore processing emissions of SO_2 increased by about 75 percent between 1955 and 1976, along with increases in natural gas processing and petroleum refining. The increases in these categories account for 78 percent of the "other" SO_2 emissions for the country.

Tables 2-29 and 2-30 contain estimates of emission densities for SO_2 and primary sulfate (Vena 1982). Sulfur dioxide emission densities have been calculated for the years 1955, 1965, and 1976. Primary sulfate emission densities are available for 1978. The highest emissions densities occur in the Maritime Provinces as compared to western Canada and can be explained by

TABLE 2-28. HISTORICAL EMISSIONS OF SO_2 AND NO_x - CANADA
(U.S./CANADA WORK GROUP 3B DRAFT REPORT 1982)
(10^3 kg yr^{-1})

	1955		1965		1976	
Sector	SO_2	NO_x[a]	SO_2	NO_x[a]	SO_2	NO_x[a]
Cu-Ni smelters[b]	2,887,420	-	3,901,950	-	2,604,637	-
Power plants	56,246	10,335	261,837	57,402	614,323	206,454
Other combustion[c]	1,210,108	227,837	1,129,548	247,323	884,867	445,315
Transportation	83,474	323,785	48,669	511,868	77,793	1,017,936
Iron ore processing	109,732	-	155,832	-	175,829	-
Others	189,876	68,065	1,095,341	33,778	954,215	190,327
TOTAL	4,536,856	630,022	6,593,177	850,371	5,311,664	1,860,032

[a]NO_x expressed as NO_2.

[b]Includes emissions from pyrrhotite roasting operations.

[c]Includes residential, commercial, industrial, and fuelwood combustion. Industrial fuel combustion also includes fuel combustion emissions from petroleum refining and natural gas processing.

TABLE 2-29. ESTIMATES OF ANNUAL EMISSIONS DENSITIES OF SULFUR OXIDES (VENA 1982) ($kg\ km^{-2}\ yr^{-1}$)

Province	Year 1955	1965	1976
Newfoundland	52	71	158
Prince Edward Island	675	690	1,557
Nova Scotia	1,943	1,761	3,180
New Brunswick	1,894	2,230	2,181
Quebec	697	949	822
Ontario	3,136	3,829	2,532
Manitoba	4 57	1,047	1,112
Saskatchewan	108	339	74
Alberta	98	506	811
British Columbia	125	565	417
Yukon-N.W.T.	< 1	< 1	< 1

TABLE 2-30. ESTIMATED OF ANNUAL EMISSIONS DENSITIES OF PRIMARY SULFATES FOR 1978 (VENA 1982)
(kg km^{-2} yr-1)

Province	Total SO_4 (10^3 kg)	Density
Newfoundland	4,081	11
Prince Edward Island	435	77
Nova Scotia	12,320	233
New Brunswick	12,582	176
Quebec	53,452	39
Ontario	45,714	50
Manitoba	13,217	24
Saskatchewan	3,742	7
Alberta	7,321	12
British Columbia	33,380	37
Yukon & N.W.T	213	< 1

the significant difference in the size of the provinces. With few exceptions, emissions in Ontario are concentrated near the southern part of the province.

Total NO_x emissions for Canada have increased significantly due to changes in the transportation sector and power plants. Automobile and diesel-powered engine emissions of NO_x have increased by factors of three and five, respectively, from 1955 to 1976. Eastern Canadian provinces still contribute the major portion of NO_x emissions, although a shift in industrial activity and population to the west has changed the contribution from 71 percent in 1955 to 61 percent in 1976.

Table 2-31 contains estimates of NO_x emissions densities for Canadian provinces for 1955, 1965, and 1976. The highest emission densities occur in the maritime provinces of Prince Edward Island and Nova Scotia. Over this period, NO_x emission densities in Canada were increasing similarly to those estimated for the eastern United States as shown in Table 2-20.

Qualitative assessments of the geographical distribution of emissions in the United States and Canada can be made by graphically displaying emissions aggregated on a state or province level. Figures 2-8, 2-9, and 2-10 are displays of annual emissions of SO_2, primary sulfate, and NO_x for the United States and Canada. Emissions data for the United States was obtained from the EPA 1980 National Emissions Data System (NEDS) files. Canadian SO_2 and NO_x data are from Environment Canada 1980 files and the Canadian primary sulfate data represents 1978 emissions calculated by Vena (1982). The area of highest SO_2 emissions in the United States is bound by Pennsylvania on the east and Missouri on the west. Highest Canadian provincial SO_2 emissions summaries are comparable to state-level emissions tn the southeastern United States.

The U.S. region of highest primary sulfate emissions extends beyond the highest SO_2 emission region shown in Figure 2-8. Much of New England is estimated to have total primary sulfate emissions comparable to the Midwest because of the extensive use of residual fuel oils in the Northeast. As mentioned earlier, the combustion emissions from residual oils contain more primary sulfate than combustion emissions from coal of similar sulfur content. The use of such fuels in the eastern provinces of Canada results in the estimation shown in Figure 2-9 that primary sulfate emissions in eastern Canada are comparable to total emission levels for the midwestern and northeastern United States.

The summary of NO_x emissions shown in Figure 2-10 illustrates the regional differences in the cumulative effect of both stationary and mobile combustion sources. The regions of highest NO_x emissions are in the Midwest, Gulf Coast, and California. Total Canadian NO_x emissions are much lower than in the United States with the highest Canadian NO_x emission area occurring along the Great Lakes region.

TABLE 2-31. ESTIMATES OF ANNUAL EMISSION DENSITIES OF NITROGEN OXIDES (VENA 1982)
(kg km^{-2} yr^{-1})

Province	Year 1955	1965	1976
Newfoundland	25	37	123
Prince Edward Island	451	767	1,461
Nova Scotia	529	581	1,483
New Brunswick	251	364	820
Quebec	94	130	242
Ontario	246	294	600
Manitoba	82	82	156
Saskatchewan	87	102	231
Alberta	104	204	515
British Columbia	86	113	221
Yukon-N.W.T.	2	1	18

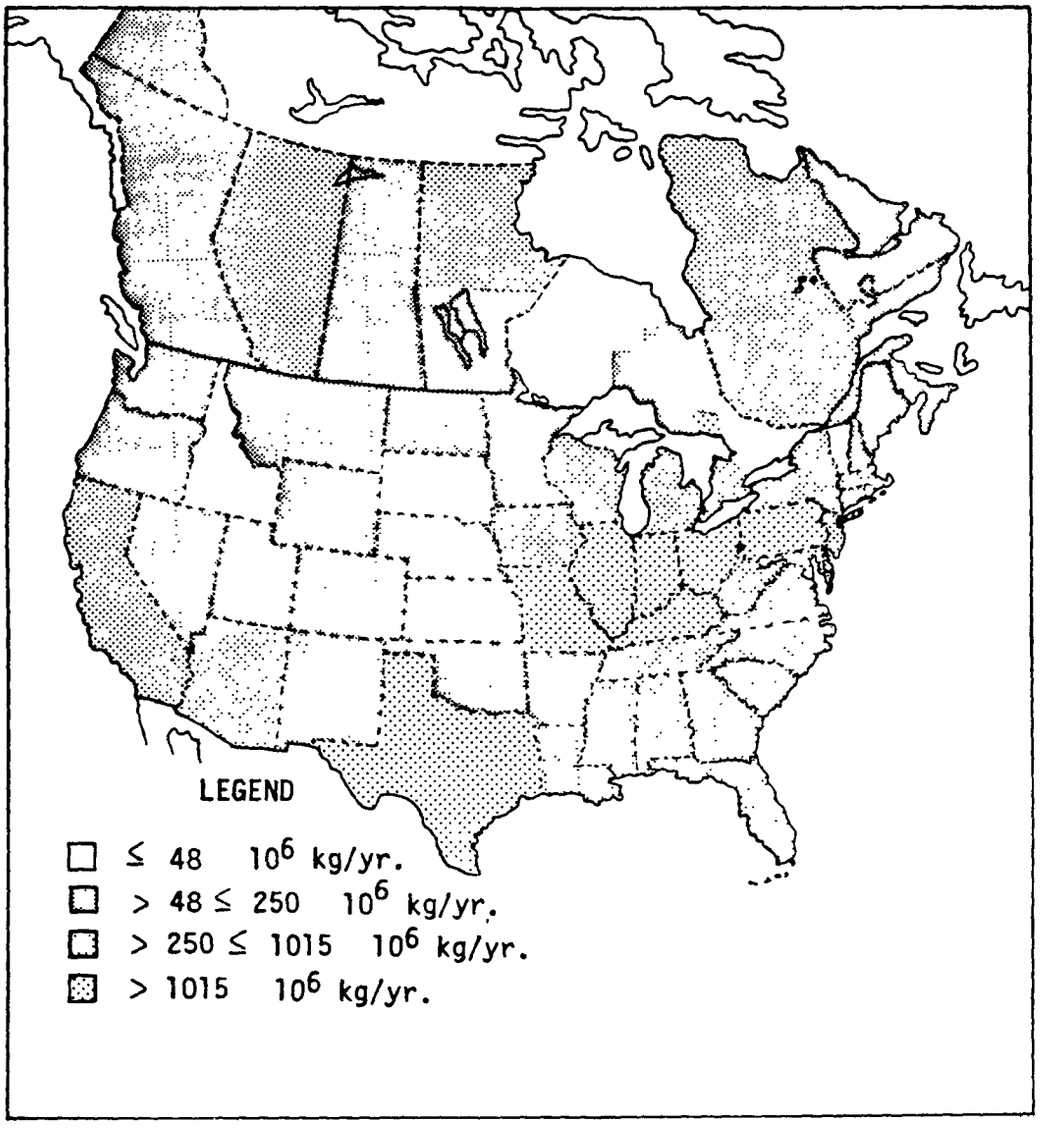

Figure 2-8. Annual emissions of SO_2 by state. Data are from National Emissions Data System 1980.

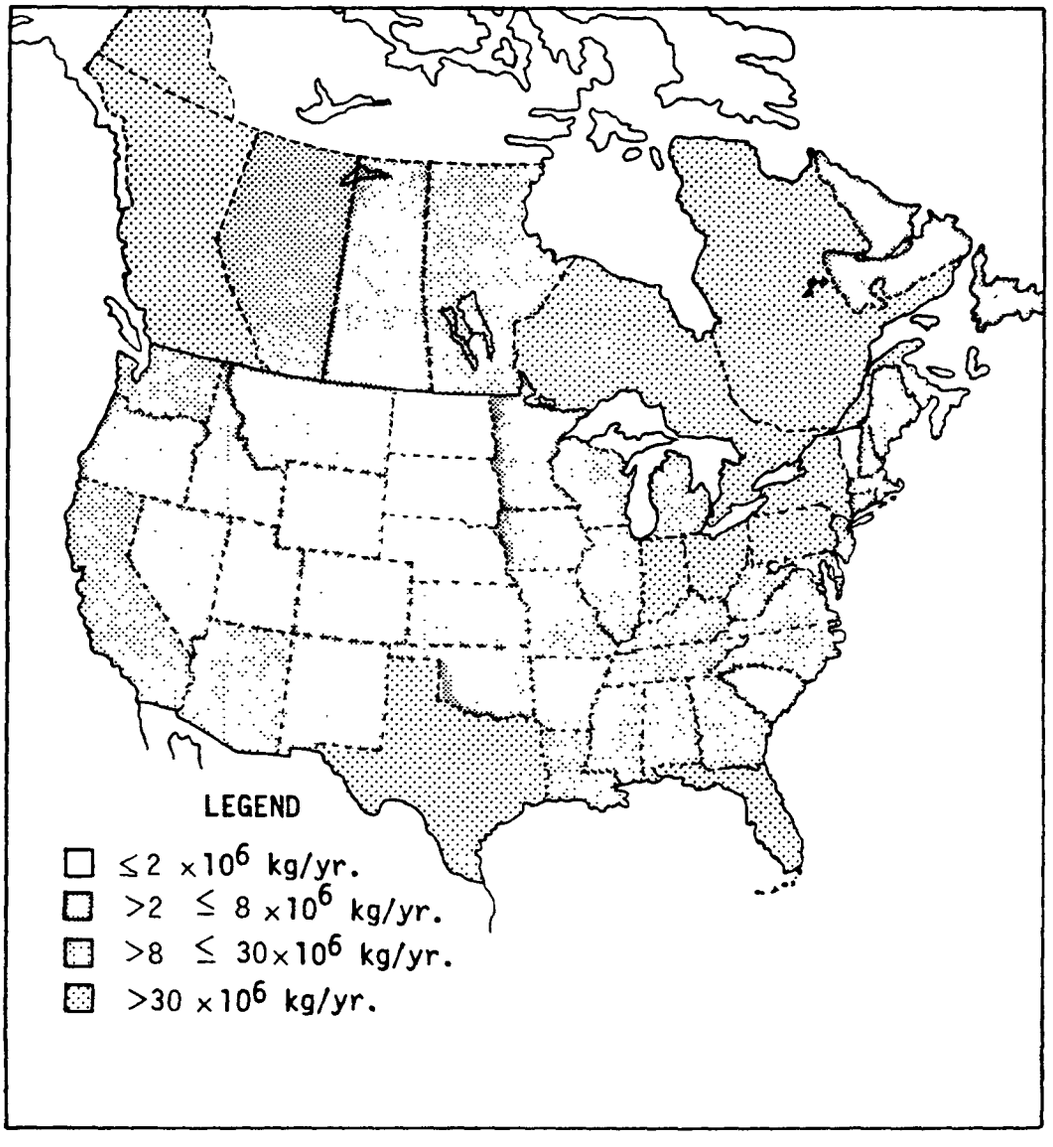

Figure 2-9. Annual emissions of SO_4 by state. Data are from National Emissions Data System 1980.

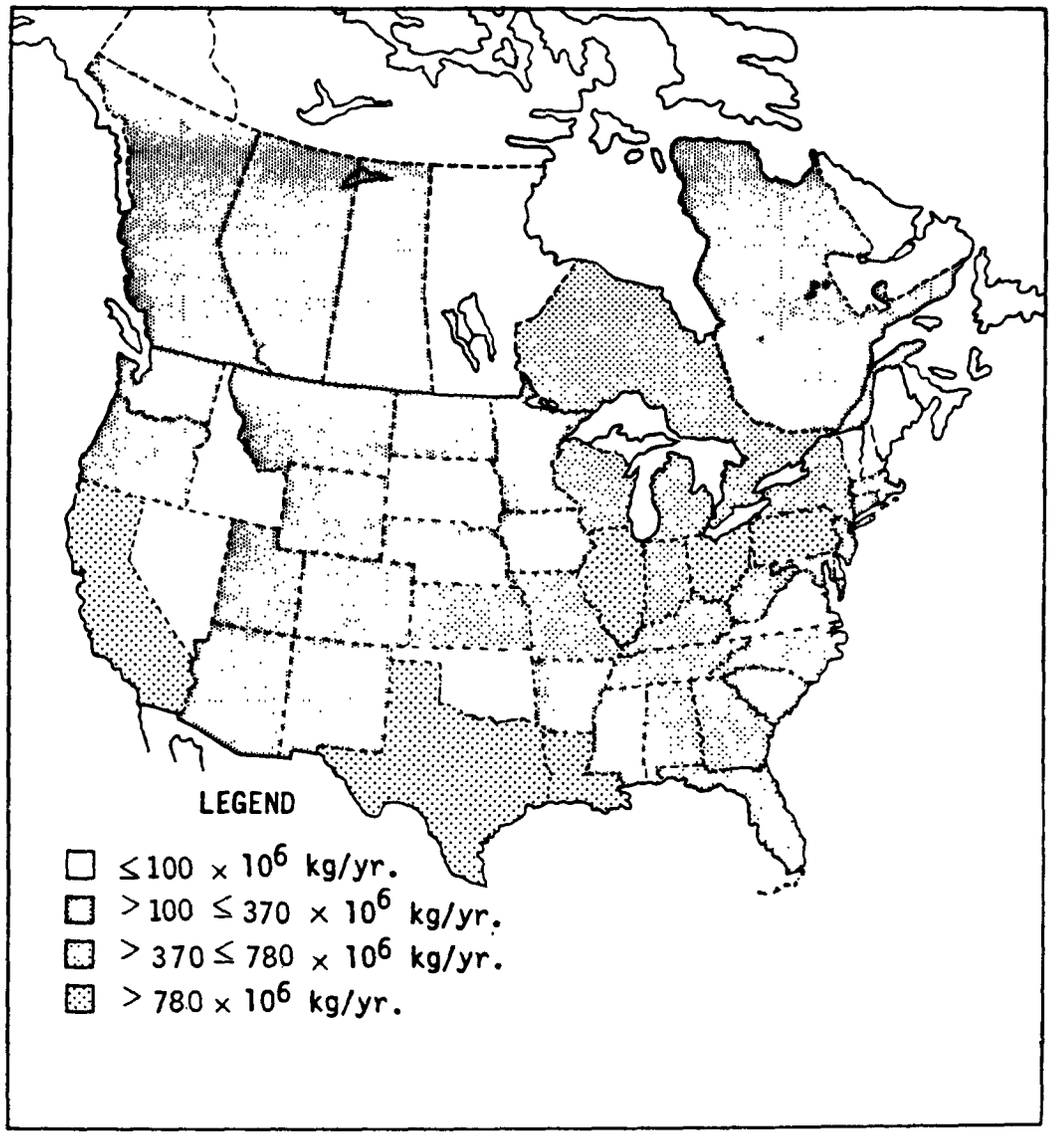

Figure 2-10. Annual emissions of NO_x by state. Data are from National Emissions Data System 1980.

2.3.7 Future Trends in Emissions

2.3.7.1 United States--Electric utility plants fired by fossil fuels are projected to continue to contribute the greatest amount of SO_2 emissions as well as significant amounts of NO_x. One estimate of the electricity demand growth rate is 1.5 percent per year from 1981 to 1985 and about 2.7 percent per year from 1985 to 2000 (U.S./Canada 1982). These growth rates are assumed to vary slightly by region, with higher growth rates in the West, West South Central, and Mountain areas, and lower than average rates in the East.

Within the nonutility sectors, industrial combustors contribute the greatest amount of SO_2, followed by nonferrous smelters and residential/commercial furnaces and boilers. Table 2-32 summarizes current SO_x and NO_x emissions for 1980 and projected emissions to 2000 as estimated by the U.S./Canada Work Group 3B (1982). The estimates are based on numerous assumptions incorporated into simulation growth models. The forecasting ability and sensitivity of such models are based on the assumptions made upon critical input parameters such as:

- Fuel price, boiler capital cost, operating and maintenance costs;
- Regulatory assumptions involving New Source Performance Standards and State Implementation Plans, including nonattainment policy; and
- The technological and physical constraints regarding the use of coal or natural gas.

These economic and regulatory factors influence other source emissions categories of sulfur and nitrogen oxides such as nonferrous smelting, where emissions are proportional to the production estimates of copper, lead, and zinc.

2.3.7.2 Canada--Canada's electrical generating capacity is expected to increase substantially by 1980, exceeding 1977 capacity by over 60 percent. This expansion will be noticeable in all three major types of generation: hydroelectric, nuclear, and conventional fossil fuels. Hydroelectric power will maintain its leading role in the utility sector, nuclear power will grow by a factor of three, and thermal generation will increase by about 50 percent from 1977 to 1990. All projected fossil-fired steam unit additions will use coal, which will result in a 12 percent increase in annual coal consumption over this period.

Natural gas processing may be a significant source of SO_2 emissions over the coming 15 years because approximately half of the gas found to date in Canada contains significant quantities of hydrogen sulfide, which is converted to sulfur during processing. Residuals, approximately 3 percent of the hydrogen sulfide, are incinerated and emitted to the atmosphere as SO_2. Alberta and British Columbia are the major gas-processing provinces. Table 2-33 summarizes Canadian SO_2 and NO_x emissions projected to 2000. These estimates were compiled from the U.S./Canada Work Group 3B forecasts (1982),

TABLE 2-32. NATIONAL U.S. CURRENT AND PROJECTED SO_2 AND NO_x EMISSIONS (Tg yr^{-1})

Source category	Current 1980		Projected 1990		Projected 2000	
	SO_2	NO_x	SO_2	NO_x	SO_2	NO_x
1. Electric utilities	15.0	5.6	15.9	7.2	16.2	8.7
2. Industrial boilers and process heaters	2.4	3.5	3.4	3.0	6.5	4.0
3. Nonferrous smelters	1.4		0.5		0.5	
4. Residential/commercial	0.8	0.7	1.0	0.7	0.9	0.6
5. Other industrial processes	2.9	0.7	1.2	0.8	1.5	1.1
6. Transportation	0.8	8.5	0.8	7.8	1.0	9.7
TOTALS	24.1	19.0	22.8	19.5	26.6	24.1

Summarized from: U.S./Canada Work Group 3B Draft Report (1982).

TABLE 2-33. NATIONAL CANADIAN CURRENT AND PROJECTED SO_2 AND NOx EMISSIONS (Tg yr^{-1})

Source category	Current 1980		Projected 1990		Projected 2000	
	SO_2	NO_x	SO_2	NO_x	SO_2	NO_x
1. Electric utilities	0.7	0.2	0.7	0.2	0.7	0.3
2. Industrial boilers and process heaters	0.6	0.3	0.3	0.3	0.2	0.3
3. Nonferrous smelters	2.1		2.3		2.3	
4. Residential/commercial	0.2	0.1	0.08	0.07	0.03	0.07
5. Transportation		1.1		1.3		1.7
6. Petroleum refining	0.1		0.1		0.0	
7. Natural gas processing	0.4		0.5		0.4	
8. Tar sands	0.1		0.3		0.3	
TOTALS	4.2	1.7	4.3	1.9	4.0	2.4

Summarized from: U.S./Canada Work Group 3B Draft Report (1982).

which again are based on assumptions concerning costs and regulatory controls similar to those used to prepare the U.S. estimates.

2.3.8 Emissions Inventories

Numerous source emission inventories have been used by EPA and the Department of Energy. Historically, most of these inventories start with the National Emissions Data System (NEDS) data base to modify, correct, or update specific source categories such as electric power plants. With different assumptions, time frames, and emissions factors, these various inventories have yielded differing results in terms of emissions totals and geographical distributions. Inventories have been developed that range from national trends summaries to annual and seasonal point and area source-specific data at the county and metropolitan level. The diversity of inventories reflects the differences in the objectives for which they were produced. These include:

1. Historical Trends Analysis. An example is the Emissions History Information System by the Office of Air Quality Programs and Standards. The inventory contains national emissions levels of particulate matter, sulfur oxides, hydrocarbons, and carbon monoxide for 1940, 1950, 1960, and all years from 1970 to 1980. The Historical Trends inventory (which was used extensively for the emission density calculations in this contribution) is a set of SO_2 and NO_x state-level emissions for 33 states in the eastern United States for 1950 to 1978.

2. Air Quality Simulation Models. The SURE inventory was sponsored by the Electric Power Research Institute as a point and area source SO_x inventory for the eastern United States for 1977-78. The data were compiled to reflect spatial, seasonal, and temporal source variabilities. Similarly, Brookhaven National Laboratory compiled a national inventory of criteria pollutants from 1978 to include selected Canadian emittors.

The EPA and Environment Canada sponsored a collaborative effort through the Emissions, Costs, and Engineering Assessment Subgroup (Work Group 3B) in response to the needs identified in the Memorandum of Intent between the United States and Canada on acidic deposition. The inventory for 1980 presents state-level and provincial summaries of SO_2 and NO_x for all area and point source categories. The inventory will be used in comparative Lagrangian transport and transformation model studies by the United States and Canada.

The Northeast Corridor Regional Modeling Program (NECRMP) inventory is perhaps the most sophisticated inventory to have been developed for modeling purposes. NECRMP contains 1980 area and point source emissions of NO_x and hydrocarbons for a 13-state area in the northeastern United States. Area sources have been gridded to 20 x 20 km resolution, and a complex data handling system applies seasonal and temporal distribution factors to

emissions. The inventory is to be used as input to an oxidant simulation model for control strategy assessment.

Because the research community is using many of these inventories to study acidic deposition from various perspectives, it is essential that the inventories be consistent and accurate. The National Acid Precipitation Assessment Program (NAPAP) has established a Task Group on Man-made Emissions (Task Group B). The primary function of Task Group B is to provide quantitative information on the emissions of pollutants from significant manmade sources in relevant areas of the United States for selected time periods. Task Group B is responsible for four major objectives:

1. Quantify emissions of pollutants of interest from various sources and regions at various times.

2. Provide economic, energy, and emissions information to support NAPAP research areas.

3. Provide data and tools to assist policy analysts in other task groups to identify and assess cost-effective strategies to control acidic precipitation.

4. Ensure that the information and analytic tools used to evaluate possible control strategies are accurate and available.

In response to the latter objective, Task Group B has undertaken development of a coordinated emissions inventory plan, which embodies an assessment of the current emissions data needs for transport/transformation modeling, source-receptor modeling, historical studies relating to materials damage effects, and the disaggregation of manmade sources from natural sources. Through this activity, the 1980 U.S./Canada inventory and the NECRMP 1980 inventory will be cross-checked and augmented to provide a common basis for acidic deposition modeling efforts. A uniform historical emissions data base will also be established for use in supporting retrospective studies of materials damage.

2.3.9 The Potential for Neutralization of Atmospheric Acidity by Suspended Fly Ash

Likens and Bormann (1974) have suggested that increases in the acidity of precipitation in the northeastern United States have been associated with augmented use of natural gas and with installation of particle-removal devices in tall smoke stacks. They have maintained that where the major source of anthropogenic sulfur to the atmosphere was coal combustion, much of the sulfur was precipitated to the land near the combustion source in particulate form as neutralized salts.

The speculative conclusion by Likens and Bormann is based on their assumption that fly ash is a highly reactive alkaline material. Table 2-34 summarizes approximate limits of ash composition for various coals in the United States, England, and Germany. Examining Table 2-34 reveals that the potential for alkalinity of eastern U.S. bituminous coals is associated with their calcium,

TABLE 2-34. APPROXIMATE LIMITS OF FLY ASH COMPOSITION FOR VARIOUS COALS (GLOSKOTER ET AL. 1977)

	Chemical analysis, weight-percent of ash									
	SiO_2	Al_2O_3	Fe_2O_3	TiO_2	P_2O_5	CaO	MgO	Na_2O	K_2O	SO_3
American coals										
Anthracite	48-68	25-44	2-10	1.0-2	0.1-4	0.2-4	0.2-1	-	-	0.1-1
Bituminous	7-68	4-39	2-44	0.5-4	0.0-3	0.7-36	0.1-4	0.2-3.0	0.2-4	0.1-32
Subbituminous	17-58	4-35	3-19	0.6-2	0.0-3	2.2-52	0.5-8	-	-	3.0-16
Lignite	6-40	4-26	1-34	0.0-0.8	0.0-1	12.4-52	2.8-14	0.2-28	0.1-1.3	8.3-32
British coal										
Brituminous	25-50	20-40	0-30	0.0-3.0	-	1.0-10	0.5-5	1.0-6	-	1.0-12
German coals										
Bituminous	25-45	15-21	20-45	-	-	2.0-4	0.5-1	-	-	4.0-10
Brown	7-46	6-29	17.26	-	-	4.0-43	0.9-4	-	-	2.0-22

magnesium, sodium, and potassium content. However, it is also reported that these elements are found in ash samples in the sulfate form. Aqueous solutions of these salts are neutral and, therefore, should exhibit no appreciable scavenging of SO_2. Newman (1975) has also pointed out the inability of coal fly ash to neutralize SO_2 further in the atmosphere.

Therefore, from available data, we could conclude that the roles of SO_2, NO_x, and mineral acid emissions from eastern and midwestern coal-fired sources in producing acidic precipitation are not changed significantly by incorporating particulate emissions controls such as electrostatic precipitators. Even if one could demonstrate a minimal effect of further reaction of combustion particles with SO_2 at atmospheric concentrations, asserting that eliminating all particulate controls would enhance neutralization of the atmosphere is misleading. The absence of controls would result in a continual massive fallout of large particles from each combustion source. The short residence time of these particles in the atmosphere would exert no positive benefit on air quality because their deposition velocity would not permit appreciable reaction with ambient SO_2.

The composition of oil ashes differs significantly from that of coal. Table 2-35 is a summary of the analysis of a typical residual oil-fired power plant fly ash. Water-soluble sulfate, carbon, and vanadium are the principal components. Vanadium is a characteristic element present as a porphyrin in Venezuelan crude oil. This particular type of crude serves as the main source of heavy residual and base-hydrode sulfurized residual oils for fuel-firing in the Northeast and Gulf Coast areas. Recent studies (Homolya and Fortune 1978) have shown that ash emitted from the combustion of these oils is highly acidic due to the absorption of sulfuric acid on the carbonaceous oil ash particles. Table 2-36 compares total water-soluble sulfate and free sulfuric acid content of particulate matter collected from coal- and oil-fired boilers. Oil ash samples are found to contain about 20 times more water-soluble sulfate and about 10 times more free sulfuric acid than does ash from coal combustion.

The implication of sulfate and sulfuric acid aerosols as direct emissions to the acidification of precipitation is complex. Coal typically contains 10 percent ash, but major combustion sources employ particulate controls such as electrostatic precipitators with collection efficiencies exceeding 95 percent. Residual oils contain 0.05 percent ash; therefore, sources burning residuals generally have no particulate controls other than perhaps mechanical collectors if the power plant was of the type converted from coal to oil in the mid-1960's. The mean aerodynamic particle diameter of oil ash has been measured as 3 μm, with 30 percent weight of the ash sized less than 0.5 μm (Boldt et al. 1980). This suggests that mechanical cyclones remove little material and that material emitted to the atmosphere is transportable in the same air parcels wherein atmospheric transformations of SO_2 and NO_x occur. Therefore, it is conceivable that the sulfuric acid fraction of acidic precipitation consists of a mixture of primary (particles and condensed H_2SO_4 aerosols) and secondary (atmospheric oxidation of SO_2) components of varying properties, depending upon the origin, season, and transport time of an air parcel and the magnitude of a precipitation event.

TABLE 2-35. ANALYSIS OF A TYPICAL RESIDUAL OIL ASH (BOLDT ET AL. 1980)

Oil Ash Constituents	Mean deviation (wt. %)	Standard (%)
Water-soluble components		
SO_4^{2-}	47.5	9.1
Cl-	1.1	1.5
NH_4^+	0.7	0.5
NO_3-	0.1	0.03
Metals		
V	5.4	1.2
Na	3.7	1.5
Mg	3.2	1.1
Ni	1.3	0.3
Fe	0.3	0.2
K	0.1	0.1
Mn	0.02	0.01
Carbon		
C	38.1	6.3
	101.5	

TABLE 2-36. SULFURIC ACID AND SULFATE CONTENT IN PARTICULATE MATTER COLLECTED FROM COAL- AND OIL-FIRED BOILERS (HOMOLYA AND FORTUNE 1978)

Source of ash	Collection site	Sulfur content Wt %	Ash composition (dry basis)	
			Wt % H_2SO_4	Wt % total SO_4
A. Coal-fired boilers:				
1. Wilmington, N.C.	ESP	1.7	0.06	0.41
2. Chapel Hill, N.C.	Stack	1.7	0.08	0.97
3. Moncure, N.C.	ESP	2.0	0.02	0.20
4. Kentucky, CR No. 4	ESP	3.9	0.04	1.06
5. Kentucky, CR No. 6	ESP	3.9	0.07	4.96
6. Kentucky, MC No. 1	ESP	3.9	0.03	1.31
7. Kentucky, MC No. 2	ESP	3.9	0.01	1.44
8. Ohio, PC	ESP	3.9	0.02	0.79
9. Kansas City, Mo.	ESP	1.7	0.02	0.90
10. Arizona, NFL	ESP	0.5	0.01	0.42
B. Oil-fired boilers:				
11. Raleigh, N.C.--2nd week	Stack	1.5	0.45	15.31
12. Raleigh, N.C.--4th week	Stack	1.5	1.25	23.35
13. Raleigh, N.C.--6th week	Stack	1.5	1.46	30.33
14. Raleigh, N.C.--8th week	Stack	1.5	5.66	43.89
15. Anclote, Fla.	Stack	2.6	0.20	22.24
16. Nassau Co., N.Y.	Cyclone	0.3	0.03	21.62
17. Albany, N.Y., No. 1, 4/77	Cyclone	1.8	0.34	30.62
18. Albany, N.Y., No. 2, 4/77	Cyclone	1.8	0.26	34.35
19. Albany, N.Y., No. 1, 7/77	Cyclone	1.8	0.35	35.56
20. Albany, N.Y., No. 2, 7/77	Cyclone	1.8	0.34	33.40
21. Long Island, N.Y., No. 2	Air heater	2.4	0.03	29.01
22. Long Island, N.Y., No. 3	Air heater	2.4	0.02	25.75
23. Long Island, N.Y., No. 3	ESP	2.4	0.26	32.45

ESP = Electrostatic precipitator.

Other types of alkaline particulate emissions may have an effect on the deposition of acids. For example, particulate emissions from cement manufacturing processes could act as a neutralizing sink in the atmosphere. However, no assessments have been performed to examine the distribution of such sources and their emissions relative to historical deposition patterns.

2.4 CONCLUSIONS (E. Robinson and J. B. Homolya)

The review of natural sources of sulfur, nitrogen oxides, ammonia, and chlorine compounds has been directed toward natural emissions and background concentrations of those compounds that may have direct impacts on precipitation pH, more popularly known as acid rain. The emphasis has been on conditions that relate to the northeastern region of the United States. Within the definition of "natural" sources are the emissions from the biosphere, which include biological processes on land and in the water, volcanos, oceanic or marine sources, atmospheric processes including lightning, and, in some cases, combustion of a nonindustrial nature.

The most important conclusions for this assessment appear to be the following:

- Present evidence does not show that natural sources of sulfur compounds are significant contributors to excessively low precipitation pH when compared to anthropogenic sources (Sections 2.2.1 and 2.3.1).

- On a quantitative basis and for the area of the United States east of the Mississippi River, soil-generated natural sources of sulfur compounds are estimated to total about 0.07 Tg S yr^{-1}. Thus, less than 1 percent of the sulfur compound emissions in this regional area seem to be due to natural sources, even though this natural source estimate might vary by a factor of 2 or 3 (Section 2.2.1.3).

- Natural emissions of nitrogen oxides (NO_x) are primarily due to processes in the biosphere, although these emissions are much less well known than the natural sulfur compounds (Section 2.2.2.1).

- NO_x from natural sources in the area east of the Mississippi River have been estimated to be in the range of 0.04 to 1.5 Tg N yr^{-1} with values from the lower part of the range being the more recent and more likely correct ones. These estimates should be compared with estimated anthropogenic NO_x emissions in 1978 of about 8.9 Tg N yr^{-1} from this same area. Thus, perhaps only a few percent of the NO_x contribution to acid precipitation may be due to natural NO_x sources (Sections 2.2.2.6, 2.2.2.13, and 2.2.6).

- Ammonia, when incorporated into precipitation, tends to counterbalance the effects of acidic compounds such as sulfates, nitrates, and chlorides. Most of the ammonium compounds in the atmosphere and thus in precipitation are due to nonindustrial sources (Section 2.2.2.7).

- Biogenic sources of ammonium compounds in the area east of the Mississippi River are estimated to be about 0.3 Tg N yr^{-1}, but certainly a factor of 2 or more must be induced in this estimate (Sections 2.2.2.9 and 2.2.2.13).

- Chloride compounds may also contribute to acidic values of precipitation pH. Anthropogenic sources of chlorine or chloride compounds are believed to be small relative to natural sources (Section 2.2.3.1).

- Natural chlorine sources affecting the eastern United States are almost totally--99 percent or more--due to oceanic area processes. These mainly involve the generation of sea salt aerosol particles (Section 2.2.3.2).

- The total natural chlorine compound deposition affecting the United States east of the Mississippi River is about 0.9 ($0.4 \times 2.34 \times 10^{12}$) Tg Cl yr^{-1}, mostly sea salt (Sections 2.2.3.5 and 2.2.6).

- Fugitive dust concentrations in rural and more remote locations in the northeastern region are relatively low (Section 2.2.6).

Thus, in areas where the acidity of precipitation occurs outside the normal range of variations and where ecological impacts are suspected to be occurring, it seems very unlikely that the products of natural sources of acidic material are significant factors (Section 2.2.5).

A review of the historical anthropogenic emissions in the United States and Canada from 1950 to about 1980 identified the following trends:

(1) Sulfur Dioxide (Section 2.3.2.1)

- Total emissions in the eastern United States doubled from 1950 to 1980 with a peak in 1970. Emissions in 1980 were about 9 percent less than those in 1970.

- Electric utility contributions tripled over this period.

- Highest SO_2 emissions occur in the Midwest. Within the 31-state region, the five highest levels of estimated SO_2 emissions for 1980 occurred in Ohio, Indiana, Pennsylvania, Illinois, and Missouri (Table 2-14).

- The largest increases in SO_2 emissions over this period occurred in the Southeast, where nearly 90 percent of the total sulfur oxides emitted are attributed to electric utilities and industrial fuel combustion sources.

- Changes in fuels from coal to oil reduced emissions in New England by 20 percent. These reductions in SO_2 emissions ocurred during the mid- to late-1960s.

- Estimates of Canadian SO_2 emissions indicate a 20 percent increase from 1955 to 1976 (Section 2.3.6). There was a marked increase in SO_2 emissions in Canada between 1955 and 1965 of about 44 percent.

- Copper and nickel smelters represent the major Canadian SO_2 source category, with most point sources located in eastern Canada.

(2) Primary Sulfate (Section 2.3.2.2)

- Sulfate emission factors were significantly larger for oil combustion than for coal. Primary sulfate emission factors for industrial and residential oil combustion were larger than for utility oil combustion.

- The highest primary sulfate emission densities occur in New England and the Atlantic seaboard. Emissions from nonutility sources concentrated in metropolitan areas may be significant during winter months because of space-heating.

- Primary sulfate emissions increased in the Midwest in proportion to increases in coal consumption.

(3) Nitrogen Oxides (Section 2.3.3)

- Total emissions in the eastern United States increased by a factor of 2.4 from 1950 to 1980 with a peak in 1978.

- Electric utilities and highway vehicles are the largest contributors to NO_x.

- Highest NO_x emissions densities occur in the northeastern United States and are influenced by highway vehicles.

- Coal-fired utilities significantly affect the NO_x emissions in the Midwest.

- Canadian NO_x emissions tripled between 1955 and 1976 (Section 2.3.6).

(4) Hydrochloric Acid (Section 2.3.4)

- Coal combustion represents the major HCl emitter.

- Midwestern coals contain the highest chloride levels.

- Mass emissions of HCl from major coal-consuming states are equal to or greater than corresponding primary sulfate emissions. Because chloride is emitted as free HCl and primary sulfate may consist of free H_2SO_4 and sulfated ash, their relative contribution to acidity patterns is unclear. A detailed analysis of precipitation

chemistry data is needed to discern local deposition of HCl in precipitation samples.

(5) Arsenic, Mercury, and Vanadium (Section 2.3.5)

- Arsenic and mercury are emitted from coal combustion. Mercury is emitted in the vapor phase and is not collected efficiently by particulate emissions controls.
- Implementing particulate controls reduced arsenic emissions in the eastern United States, but mercury emissions increased in proportion to coal consumption.
- Vanadium is emitted from residual oil combustion in varying amounts.
- Highest vanadium emissions occur in the northeastern United States.

(6) Acid Neutralization in the Atmosphere by Fly Ash or Alkaline Particles (Section 2.3.9)

- Available data on the chemical analysis of fly ash from coal or oil combustion indicate these materials are either neutral or slightly acidic. The capacity of fly ash for neutralizing acidic aerosols in the atmosphere is not apparent.
- Data is lacking on neutralization capacity of other particles (e.g., cement dust) which should be alkaline.

2.5 REFERENCES

Adams, D. F., S. O. Farwell, E. Robinson, and M. R. Pack. 1980. Biogenic sulfur emissions in the SURE region. Final Report by Washington State University for Electric Power Research Institute, EPRI Report No. EA-1516.

Adams, D. F., S. O. Farwell, E. Robinson, M. R. Pack, and W. L. Bamesberger. 1981a. Biogenic sulfur source strengths. Presented at 74th Annual Meeting Air Pollution Control Assoc., Philadelphia, PA, June 21-26, 1981. Paper No. 81-153.

Adams, D. F., S. O. Farwell, M. R. Pack, and E. Robinson. 1981b. Biogenic sulfur gas emissions from soils in eastern and southeastern United States. J. Air Pollut. Contr. Assoc. 31:1083-1089.

Adams, D. F., S. O. Farwell, E. Robinson, M. R. Pack, and W. L. Bamesberger. 1981c. Biogenic sulfur source strengths. Environ. Sci. Technol. 15:1493-1498.

Altshuller, A. P. 1958. Natural sources of gaseous pollutants in the atmosphere. Tellus 10:479-492.

Altshuller, A. P. 1979. Model predictions of the rates of homogeneous oxidation of sulfur dioxide to sulfate in the troposphere. Atmos. Environ. 13:1653-1661.

Aneja, V. P., J. H. Overton, and A. P. Aneja. 1981. Emission survey of biogenic sulfur flux from terrestrial surfaces. J. Air Pollut. Contr. Assoc. 31:256-258.

Ayers, G. P. and J. L. Gras. 1980. Ammonia gas concentrations over the Southern Ocean. Nature 284:539-540.

Bartels, O. G. 1972. An estimate of volcanic contributions to the atmosphere and volcanic gases and sublimates as the source of radioisotopes ^{10}Be, ^{35}S, ^{32}P, and ^{22}Na. Health Phys. 22:387-392.

Barone, J. B., L. L. Ashbaugh, B. H. Kusko, and T. A. Cahill. 1981. The effect of Owens Dry Lake on air quality in the Owens Valley with implications for the Mono Lake area, pp. 327-346. In Atmospheric Aerosol, Source/Air Quality Relationships. E. S. Macias and P. K. Hopke, eds. ACS Symposium Series Number 167. American Chemical Society, Washington, D.C. 359 pp.

Bates, D. R. and P. B. Hays. 1967. Atmospheric nitrous oxide. Planet. Space Sci. 15:189-197.

Boldt, K. R., C. P. Chany, E. J. Kaplin, J. M. Stansfield, and B. Webber. 1980. Impact of a primary emission source on air quality. EPA-600/2-80-109, U.S. Environmental Protection Agency, Research Triangle Park, NC.

Braman, R. S. and T. J. Shelley. 1981. Gaseous and particulate ammonia and nitric acid concentrations: Columbus, Ohio area - Summer 1980. Report No. EPA-600/57-80-179, Environmental Protection Agency, Research Triangle Park, NC, February 1981. (Available as PB 81-125007 from NTIS).

Bulla, L. A., Jr., C. M. Gilmour, and W. B. Bollen. 1970. Non-biological reduction of nitrite in soil. Nature 225:664.

Butcher, S. S. and R. J. Charlson. 1972. An Introduction to Atmospheric Chemistry. Academic Press, New York.

Cadle, R. D. 1975. Volcanic emissions of chlorides and sulfur compounds to the troposphere and stratosphere. J. Geophys. Res. 80:1650-1652.

Cadle R. D. 1980. A comparison of volcanic with other fluxes of atmospheric trace gas constituents. Rev. Geophys. Space Phys. 18:746-752.

Cadle, R. D., W. H. Fisher, E. R. Frank, and J. P. Lodge, Jr. 1968. Particles in the Antarctic atmosphere. J. Atmos. Sci. 25:100-103.

Charlson, R. J., and H. Rodhe. 1982. Factors controlling the acidity of natural rainwater. Nature 295:683-685.

Cheney, J. L. and J. B. Homolya. 1978. Workshop proceeding on primary sulfate emissions from the combustion of fossil fuels. EPA-600/9-78-020a. U. S. Environmental Protection Agency, Research Triangle Park, NC. pp. 53-63.

Cicerone, R. J. 1981. Halogens in the atmosphere. Rev. Geophys. Space Phys. 19:123-139.

Cogbill, C. V. and G. E. Likens. 1974. Acid precipitation in the northeastern United States. Water Resources Res. 10:1133-1137.

Conway, E. J. 1942. Mean geochemical data in relation to oceanic evolution. Royal Irish Acad. Proc. A48:119-159.

Cooper, J. A. and J. G. Watson, Jr. 1980. Receptor oriented methods of air particulate source apportionment. J. Air Pollut. Contr. Assoc. 30:1116-1125.

Cox, R. A. and F. J. Sandalls. 1974. The photooxidation of hydrogen sulfide and dimethyl sulfide in air. Atmos. Environ. 8:1269-1281.

Cronn, D. R., R. A. Rasmussen, E. Robinson, and D. E. Harsch. 1977. Halogenated compound identification and measurement in the trosposphere and lower stratosphere. J. Geophys. Res. 82:5935-5944.

Crutzen, P. J. 1974. Photochemical reactions initiated by and influencing ozone in unpolluted tropospheric air. Tellus 26:47-57.

Dawson, G. A. 1977. Atmospheric ammonia from undisturbed land. J. Geophys. Res. 82:3125-3133.

Dawson, G. A. 1980. Nitrogen fixation by lightning. J. Atmos. Sci. 37:174-178.

Delmas, R., J. Baudet, J. Servant, and Y. Baziard. 1980. Emissions and concentrations of hydrogen sulfide in the air of the tropical forest of the Ivory Coast and of temperate regions in France. J. Geophys. Res. 85:4468-4474.

Denmead, O. T., J. R. Simpson, and J. R. Freney. 1974. Ammonia flux into the atmosphere from a grazed sheep pasture. Science 185:609-610.

Denmead, O. T., J. R. Freney, and J. R. Simpson. 1976. A closed ammonia cycle within a plant canopy. Soil Biol. Biochem. 8:161-164.

Drapcho, D. L., D. Sisterson, and R. Kumar. 1983. Nitrogen fixation by lightning activity in a thunderstorm. Atmos. Environ. 17:729-734.

Duce, R. A. 1969. The source of gaseous chlorine in the marine atmosphere. J. Geophys. Res. 74:4597-4599.

Eriksson, E. 1952. Composition of atmospheric precipitation I. Nitrogen compounds. Tellus 6:261-267.

Eriksson, E. 1959. The yearly circulation of chloride and sulfur in nature; meteorological, geochemical, and pedological implications. Part I. Tellus 11:375-403.

Eriksson, E. 1960. The yearly circulation of chloride and sulfur in nature; meteorological, geochemical, and pedological implications. Part II. Tellus 12:63-109.

Eriksson, E. 1963. The yearly circulation of sulfur in nature. J. Geophys. Res. 68:4001-4008.

Farwell, S. O., S. J. Gluck, W. L. Bamesberger, T. M. Schutte, and D. F. Adams. 1979. Determination of sulfur-containing gases by a deactivated cryogenic enrichment and capillary gas chromatographic system. Anal. Chem. 51:609-615.

Fishman, J. 1981. The distribution of NO_x and the production of ozone: comments on "origin of tropospheric ozone" by S. C. Liu et al. J. Geophys. Res. 86:12161-12164.

Friedlander, S. K. 1981. New developments in receptor modeling theory, pp. 1-20. In atmospheric Aerosol, Source/Air Quality Relationships. E. S. Macias and P. K. Hopke, eds. ACS Symposium Series No. 167, American Chemical Society, Washington, D.C. 359 p.

Friend, J. F. 1973. The global sulfur cycle, pp. 177-201. In Chemistry of the Lower Atmosphere. S. I. Rasool, ed. Plenum Press, New York.

Galbally, I. E. 1975. Emission of oxides of nitrogen (NO_x) and ammonia from the earth's surface. Tellus 27:67-70.

Galbally, I. E. and C. R. Roy. 1978. Loss of fixed nitrogen from soils by nitric oxide exhalation. Nature 275:734-735.

Galloway, J. N. and D. M. Whelpdale. 1980. An atmospheric sulfur budget for eastern North America. Atmos. Environ. 14:409-417.

Galloway, J. N., G. E. Likens, W. C. Keene, and J. M. Miller. 1982. The composition of precipitation in remote areas of the world. J. Geophys. Res. 87:8771-8786.

Gandrud, B. W. and A. L. Lazrus. 1981. Filter measurements of stratospheric sulfate and chloride in the eruption plume of Mt. St. Helens. Science 211:826-827.

Garland, J. A. and J. R. Branson. 1976. The mixing height and mass balance of SO_2 in the atmosphere above Great Britain. Atmos. Environ. 10:353-362.

Georgii, H. W. 1963. Oxides of nitrogen and ammonia in the atmosphere. J. Geophys. Res. 68:3963-3970.

Georgii, H. W. and G. Gravenhorst. 1977. The ocean as source or sink of reactive trace-gases. Pur. and Appl. Geophys. (PAGEOPH) 115:503-511.

Gluskoter, H. J., R. R. Ruch, W. G. Miller, R. A. Chahill, G. B. Dreher, and J. K. Kuhn. 1977. Trace elements in coal, occurrence and distribution. EPA-600/7-77-064. U. S. Environmental Protection Agency, Research Triangle Park, NC.

Graedel, T. E. 1977. The homogeneous chemistry of atmospheric sulfur. Rev. Geophys. Space Phys. 15:421-428.

Graedel, T. E. 1978. Chemical Compounds in the Atmosphere. Academic Press, New York. 440 pp.

Graedel, T. E. 1979. The kinetic photochemistry of the marine atmosphere. J. Geophys. Res. 84:273-286.

Granat, L., R. O. Hallberg, and H. Rodhe. 1976. The global sulfur cycle, pp. 89-134. In Nitrogen, Phosphorus and Sulfur - Global Cycles. B. H. Svensson and R. Soderlund, eds. Ecological Bulletins No. 22, SCOPE Report 7, Royal Swedish Academy of Sciences, Stockholm.

Gschwandtner, G., C. O. Mann, B. C. Jordan, and J. C. Bosch. 1981. Historical emissions of sulfur and nitrogen oxides in the Eastern United States by state and county. Presented at the 74th Annual Meeting, Air Pollution Control Association, Philadelphia, Pennsylvania, June 21-26, 1981. Paper 81-30.1.

Harriss, R. C. and J. T. Michaels. 1982. Sources of atmospheric ammonia. Proceedings Second Symposium, Composition of the Nonurban Troposphere, pp. 33-35, American Meteorological Society, Boston, Mass.

Hidy, G. M. 1982. Bridging the gap between air quality and precipitation chemistry. Water, Air, Soil Pollut. 18:191-198.

Hill, R. D., R. G. Rinker, and H. D. Wilson. 1980. Atmospheric nitrogen fixation by lightning. J. Atmos. Sci. 37:179-192.

Hitchcock, D. R. 1975. Dimethyl sulfide emissions to the global atmosphere. Chemosphere 4:137-138.

Hitchcock, D. R. 1976. Atmospheric sulfates from biological sources. J. Air Pollut. Contr. Assoc. 26:210-215.

Hobbs, P. V., J. P. Tuell, L. F. Radke, D. A. Hegg, and M. W. Eltgroth. 1982. Particles and gases in the emissions from the 1980-81 volcanic eruptions of Mt. St. Helens. J. Geophys. Res. 87:11062-11086.

Hoell, J. M., C. N. Harward, and B. S. Williams. 1980. Remote infrared heterodyne radiometer measurements of atmospheric ammonia profiles. Geophys. Res. Lett. 7:313-316.

Homolya, J. B. and C. R. Fortune. 1978. The measurement of the sulfuric acid and sulfate content of particulate matter resulting from the combustion of coal and oil. Atmos. Environ. 12:2511-2514.

Homolya, J. B. and J. L. Cheney. 1978. Workshop proceedings on primary sulfate emissions from the combustion of fossil fuels. EPA-600/9- 78-020b, U.S. Environmental Protection Agency, Research Triangle Park, NC. pp. 3-13.

Homolya, J. B. and S. Lambert. 1981. Characterization of sulfate emissions from nonutility boilers firing low-S residual oils in New York City. J. Air Pollut. Contr. Assoc. 31:139-143.

Husar, R. B., D. E. Patterson, J. D. Husar, N. V. Gillani, and W. E. Wilson, Jr. 1978. Sulfur budget of a power plant. Atmos. Environ. 12:549-568.

Hutchinson, G. L., R. J. Millington, and D. B. Peters. 1972. Atmospheric ammonia: Absorption by plant leaves. Science 175:771-772.

Jaeschke, W., H-W. Georgii, H. Claude, and H. Malewski. 1978. Contributions of H_2S to the atmospheric sulfur cycle. Pure and Appl. Geophys. 116:465-475.

Johannes, A. H., E. R. Altwicker, and N. L. Clesceri. 1981. Characterization of acidic precipitation in the Adirondack region. Final EPRI Research Project 1155-1, EPRI Report EA-1826, Electric Power Research Institute, Palo Alto, California.

Johnston, D. A. 1980. Volcanic contribution of chlorine to the stratosphere: More significant to ozone than previously estimated? Science 209:491-493.

Johnston, H. S., O. Serang, and J. Podolski. 1979. Instantaneous global nitrous oxide photochemical rates. J. Geophys. Res. 84:5077-5082.

Junge, C. E. 1956. Recent investigations of air chemistry. Tellus 8:127-130.

Junge, C. E. 1958. The distribution of ammonia and nitrate in rain water over the United States. Trans Am. Geophys. Union 39:241-248.

Junge, C. E. 1960. Sulfur in the atmosphere. J. Geophys. Res. 65:227-237.

Junge, C. E. 1963. Atmospheric Chemistry and Radioactivity. Academic Press, New York, 382 pp.

Junge, C. E., and P. E. Gustafson. 1956. Precipitation sampling for chemical analysis. Bull. Am. Meteorol. Soc., 37:244-245.

Junge, C. E. and R. T. Werby. 1958. The concentration of chloride, sodium, potassium, calcium and sulfate in rain water over the United States. J. Meteorol. 15:417-425.

Junge, C. E., C. W. Chagnon, and J. W. Manson. 1961. Stratospheric aerosols. J. Meteorol. 18:81-108.

Keeney, D. R., I. R. Filbery, and G. P. Marx. 1979. Effect of temperature on the gaseous nitrogen products of dentrification in a silt loam soil. Soil Sci. Soc. Am. J. 43:1124-1128.

Kellogg, W. W., R. D. Cadle, E. R. Allen, A. L. Lazrus, E. A. Martel. 1972. The sulfur cycle. Science 175:587-596.

Kelly, T. J., D. H. Stedman, J. A. Ritter, and R. B. Harvey. 1980. Measurements of oxides of nitrogen and nitric acid in clean air. J. Geophys. Res. 85:7417-7425.

Kerr, R. A. 1982. El Chichon forebodes climate change. Science 217:1023.

Kim, C. M. 1973. Influence of vegetation types on the intensity of ammonia and nitrogen dioxide liberation from soil. Soil Biol. Biochem. 5:163-166.

Klemm, H. A. and R. J. Brennan. 1979. Emissions inventory for the SURE region. EPRI Report EA-1913, Electric Power Research Institute, Palo Alto, California.

Kley, D., J. W. Drummond, M. McFarland, and S. C. Liu. 1981. Tropospheric profiles of NO_X. J. Geophys. Res. 86:3153-3161.

Kowalczyk, G. S., G. E. Gordon, and S. W. Rheingrover. 1982. Identification of atmospheric particulate sources in Washington, D.C., using chemical element balances. Environ. Sci. Technol. 16:79-90.

Lawson, D. R. and J. W. Winchester. 1979. A standard crustal aerosol as a reference for elemental enrichment factors. Atmos. Environ. 13:925-930.

Lazrus, A. L., H. W. Boynton, and J. P. Lodge, Jr. 1970. Trace constituents in oceanic cloud water and their origin. Tellus 22:106-114.

Lazrus, A. L., R. D. Cadle, B. W. Gandrud, J. P. Greenberg, B. J. Heubert, and W. I. Rose, Jr. 1979. Sulfur and halogen chemistry of the stratosphere and of volcanic eruption plumes. J. Geophys. Res. 84:7869-7875.

Levine, J. S., R. S. Rogoruski, G. L. Gregory, W. E. Howell and J. Fishman. 1981. Simultaneous measurements of NO_X, NO, and O_3 production in a laboratory discharge: Atmospheric implications. Geophys. Res. Lett. 8:357-360.

Likens, G. E. 1976. Acid precipitation. Chem. Eng. News 54:29-44.

Likens, G. E. and F. H. Bormann. 1974. Acid rain: A serious regional environmental problem. Science 184:1176-1179.

Likens, G. E. and T. J. Butler. 1981. Recent acidification of precipitation in North America. Atmos. Environ. 15:1103-1109.

Likens, G. E., F. H. Bormann, J. S. Eaton, R. S. Pierce, and N. M. Johnson. 1976. Hydrogen ion input to the Hubbard Brook Experimental Forest, New Hampshire during the last decade. Water, Air, Soil Pollut. 6:435-445.

Lodge, J. P. Jr. and J. B. Pate. 1966. Atmospheric gases and particulates in Panama. Science 153:408-410.

Lodge, J. P., Jr., A. J. MacDonald, Jr., and E. Vihman. 1960. A study of the composition of marine atmosphere. Tellus 12:184-187.

Logan, J. A. 1983. Nitrogen oxides in the troposphere: Global and regional budgets. J. Geophys. Res.: In press.

Lovelock, J. E., R. J. Maggs, and R. A. Rasmussen. 1972. Atmospheric dimethyl sulfide and the natural sulfur cycle. Nature 237:452-453.

Makarov, B. N. 1969. Liberation of nitrogen dioxide from soil (in Russian). Pochvovedeniye, 49-53. (Translation from Russian available in: Soil Chemistry).

Maroulis, P. J., and A. R. Bandy. 1977. Estimate of the contribution of biologically produced dimethyl sulfide to the global sulfur cycle. Science 196:647-648.

McConnel, J. C. 1973. Atmospheric ammonia. J. Geophys. Res. 78:7812-7821.

Naughton, J. J., V. Lewis, D. Thomas, and J. B. Finlayson. 1975. Fume compositions found at various stages of activity at Kilavea volcano, Hawaii. J. Geophys. Res. 80:2963-2966.

Nelson, D. W. and J. M. Bremner. 1970. Gaseous products of nitrite decomposition in soils. Soil Biol. Biochem. 2:203-215.

Newman, L. 1975. Correspondence: Alkalinity of fly ash. Science 185:957-959.

Noxon, J. F. 1976. Atmospheric nitrogen fixation by lightning. Geophys. Res. Lett. 3:463-465.

Noxon, J.F. 1978. Tropospheric NO_2. J. Geophys. Res. 83:3051-3057.

Ontario Research Foundation. 1975. A nationwide inventory of anthropogenic sources and emissions of primary fine particulate matter. Unpublished Document.

Pack, D. H. 1980. Precipitation chemistry patterns: A two-network data set. Science 108:1143-1145.

Palmer, T. Y. 1976. Combustion sources of atmospheric chlorine. Nature 263:44-46.

Perhac, R. M. 1978. Sulfate regional experiment in northeastern United States: The "SURE" program. Atmos. Environ. 12:641-647.

Pierson, W., W. Brachaczek, T. Truex, J. Butler, and T. Korniski. 1980. Ambient sulfate measurements on Allegheny mountain and the question of atmospheric sulfate in Northeastern United States. In Aerosols: Anthropogenic and Natural, Sources and Transport. T. J. Kneip and P. J. Lioy, eds. Ann. N.Y. Acad. Sci. 338-145-173.

Pollack, J. B. 1981. Measurements of the volcanic plumes of Mount St. Helens in the stratosphere and troposphere: Introduction. Science 211:815-816.

Porter, L. K., F. G. Viets, Jr., and G. L. Hutchinson. 1972. Air containing nitrogen-15 ammonia: Foliar absorption by corn seedlings. Science 175:759-761.

Rasmussen, R. A., L. E. Rasmussen, M. A. Khalil, and R. W. Dalluge. 1980. Concentration distribution of methyl chloride in the atmosphere. J. Geophys. Res. 85:7350-7356.

Rasmussen, R. A., M. A. K. Khalil, R. W. Dalluge, S. A. Penkett, and B. Jones. 1982. Carbonyl sulfide and carbon disulfice from the eruptions of Mount St. Helens. Science 215:665-667.

Ratner, B. 1957. Upper-air climatology of the United States. Tech. Paper No. 32, U.S. Weather Bureau, U.S. Dept. of Commerce, Washington, D.C.

Ravishankara, R. A., N. M. Kreutter, R. C. Shah, and P. H. Wine. 1980. Rate of reaction of OH with COS. Geophys. Res. Lett. 7:861-864.

Reiter, R. and M. Reiter. 1958. Relations between the contents of nitrate and nitrite ions in precipitation and simultaneous atmospheric electric processes, pp. 175. In Recent Advances in Atmospheric Electricity. L. G. Smith, ed. Pergamon Press, London.

Rice, H., D. H. Nochumson, and G. M. Hidy. 1981. Contribution of anthropogenic and natural sources to atmospheric sulfur in parts of the United States. Atmos. Environ. 15:1-9.

Richardson, C. J. and G. E. Merva. 1976. The chemical composition of atmospheric precipitation from selected stations in Michigan. Water, Air, Soil Pollut. 6:385-393.

Robbins, R. C., R. D. Cadle, and D. L. Eckhardt. 1959. The conversion of sodium chloride to hydrogen chloride in the atmosphere. J. Meteorol. 16:53-56.

Robinson, E. and R. C. Robbins. 1970a. Gaseous sulfur pollutants from urban and natural sources. J. Air Pollut. Contr. Assoc. 20:233-235.

Robinson, E. and R. C. Robbins. 1970b. Gaseous nitrogen compound pollutants from urban and natural sources. J. Air Pollut. Contr. Assoc. 20:303-306.

Rodhe, H. and I. Isaksen. 1980. Global distribution of sulfur compounds in the troposphere estimated in a height/latitude transport model. J. Geophys. Res. 85:7401-7409.

Ryan, J. A. and N. R. Mukherjee. 1975. Sources of stratospheric gaseous chlorine. Rev. Geophys. Space Phys. 13:650-658.

Shannon, J. D. 1979. The advanced statistical trajectory regional air pollution model. Argonne National Laboratory Radiological and Environmental Research Division Topical Report ANL/RER-79-1. pp. 1-34.

Shannon, J. D., J. B. Homolya, and J. L. Cheney. 1980. The relative importance of primary vs. secondary sulfate. EPA Project Report IAG-AD-89-F-1-116-0.

Smith, C. J. and P. M. Chalk. 1980. Gaseous nitrogen evolution during nitrification of ammonia fertilizer and nitrite transformation in soils. Soil Sci. Soc. Am. J. 44:277-282.

Soderlund, R. and B. H. Svensson. 1976. The global nitrogen cycle, pp. 22-73. In Nitrogen, Phosphorous and Sulfur-Global Cycles. SCOPE Report 7, Ecological Bulletins No. 22. Swedish Natural Science Research Council, Stockholm.

Spirtas, R., and H. J. Levin. 1970. Characteristics of particulate patterns. National Air Pollution Control Admin. Publ AP-61, Raleigh, NC.

Stahl, Q. R. 1969. Preliminary air pollution survey of hydrochloric acid APTD-69-36. U. S. Department of Health, Education and Welfare, National Air Pollution Control Administration, Cincinnati, Ohio.

Stensland, G. J., and R. G. Semonin. 1982. Another interpretation of the pH trend in the United States. Bull. Am. Meteorol. Soc. 63:1277-1284.

Stith, J. L., P. V. Hobbs, and L. F. Radke. 1978. Airborne particles and gas measurements in the emissions from six volcanoes. J. Geophys. Res. 83:4009-4017.

Stoiber, R. E. and A. Jepsen. 1973. Sulfur dioxide contributions to the atmosphere by volcanoes. Science 182:577-578.

Sze, N. D. and M. K. W. Ko. 1980. Photochemistry of COS, CS_2, CH_3, SCH_3, and H_2S: Implications for the atmospheric sulfur cycle. Atmos. Environ. 14:1223-1239.

U.S. Department of Commerce. 1968. Climatic Atlas of the United States. Environmental Data Service, Washington, D.C.

U.S. Environmental Protection Agency. 1973. The National Air Monitoring Program: Air Quality and Emissions Trends, Annual Report, Volume II, EPA-450/1-73-001-b, Office of Air and Water Programs, USEPA, Research Triangle Park, NC.

U.S. Environmental Protection Agency. 1978. National air pollution emission estimates, 1940-1976. EPA-450/1-78-003.

U.S. Environmental Protection Agency. 1981. Compilation of air pollution emission factors. 2nd Edition. Publication No. AP-42.

U.S./Canada Memorandum of Intent on Transboundary Air Pollution. 1982. Emissions, costs, and engineering assessment. Work Group 3B. Final Report. June 15, 1982.

Valach, R. 1967. The origin of the gaseous form of natural atmospheric chlorine. Tellus 19:509-516.

Vena, F. 1982. Environment Canada, Personal Communication. August 19, 1982.

Viemeister, P. E. 1960. Lightning and the origin of nitrates found in precipitation. J. Meterol. 17:681-683.

Visser, S. 1961. Chemical composition of rainwater in Kampala, Uganda, in its relation to meteorological and topographical conditions. J. Geophys. Res. 66:3759-37.

von Liebig, J. 1827. Une note sur la nitrification. Annales de Chemie et de Physique 35:329-333.

Weast, R. C. (ed). 1973. Handbook of Chemistry and Physics, 54th Ed., pg. F-188. CRC Press, Cleveland, Ohio.

Whitby, K. T., and B. Cantrell. 1976. Atmospheric aerosols-measurement and characteristics, Paper 29-1. In International Conference on Environmental Sensing and Assessment, Inst. of Electrical and Electronics Engineers, Inc., New York. (IEEE Catalog #75-CH 1004-1 ICESA).

Yue, G. K., V. A. Mohnen, and C. S. Kiang. 1976. A mechanism for hydrochloric acid production in cloud. Water, Air, Soil Pollut. 6:277-294.

Zafiriou, O. C. and M. McFarland. 1981. Nitric oxide from nitrate photolysis in the central equatorial Pacific. J. Geophys. Res. 86:3173-3182.

Zafiriou, O.C., M. McFarland, and R. H. Bromund. 1980. Nitric oxide in seawater. Science 207:637-639.

THE ACIDIC DEPOSITION PHENOMENON AND ITS EFFECTS

A-3. TRANSPORT PROCESSES

3.1 INTRODUCTION (N. V. Gillani)

Atmospheric contributions to the acidification of a sensitive receptor site can best be assessed if the contributing sources can be identified unambiguously, and if the atmospheric transport of their emissions can be determined quantitatively. For a number of reasons, it is not possible to make such a assessment precisely. Atmospheric depositions include not only primary emissions, but also chemically-transformed secondary products. Some pollutants such as sulfate are both primary and secondary in origin. The transport age of the deposited materials cannot generally be determined accurately from their physical-chemical form. Furthermore, the complexity and considerable variability of the transport winds and the practical limitations on the detail and resolution with which we do, or even can, measure them in a routine manner, make the tasks of source recognition and uncertainty assessment extremely difficult.

For several years now researchers in North America as well as in Europe have recognized that the regional distribution of secondary pollutants such as sulfates is a consequence of long-range transport and chemical transformations of pollutant emissions into the atmosphere (Altshuller 1977, OECD 1977). Transboundary exchanges of acidic pollutants no doubt occur among the nations of Europe as well as between the United States and Canada. The extent to which pollutants are dispersed and deposited far beyond their sources is highly variable and depends significantly on the processes of atmospheric transport and dispersion. Atmospheric transport processes also play an important, sometimes critical role in the chemical transformations and deposition of pollutants during plume transport. For example, the gas-to-particle conversion of sulfur in power plant plumes depends upon atmospheric mixing, which facilitates interaction between primary species in the plume and reactive species from the polluted background air (Gillani and Wilson 1980). Also, turbulent vertical dispersion is the principal mechanism for delivering elevated emissions to the ground for dry deposition. Thus, indirectly, transport processes play an important role in determining the overall atmospheric residence time of pollutants in the atmosphere.

Deposition of a pollutant marks the end of its atmospheric residence. The concept of atmospheric residence time (τ) is of critical concern in any assessment of relative locations of source areas of acid precursors and impacted areas of acidic depositions. The other critical factor influencing such an assessment is the spread of material trajectories during the atmospheric residence time. Transport processes exert a major, or possibly even a controlling, influence on τ and the trajectories.

The main objective of this chapter is to identify and describe the principal mechanisms of pollutant transport, specifically in terms of their influence on the atmospheric residence time of the pollutant. To depict the role of transport, an attempt has been made to estimate τ of sulfur emissions from different types of major sources and during different seasons. Atmospheric processes influencing pollutant trajectories and spread over regional areas are described, but methods of trajectory calculations and a quantitative assessment of uncertainties associated with them are not covered here. Chapter A-9 discusses transport models and their status as operational tools.

3.1.1 The Concept of Atmospheric Residence Time

The atmospheric residence time of a given pollutant emission is defined here as the characteristic time during which the emission mass is depleted by removal processes (transformation and deposition) to 1/e or about 37 percent of its initial value. If the depletion were due to first-order processes only, such a definition of τ would make it the effective time constant of exponential decay of the pollutant from the atmosphere. In general, the value of τ depends on the kinetics and mechanisms of the processes of transport, transformation, and deposition. Because transformation and deposition rates are specific to chemical species, τ is different for different species (for example, SO_x versus NO_x, or even SO_2 versus aerosol sulfates).

Transport processes are, however, essentially independent of chemical speciation. In this chapter, the nature and significance of the role of transport processes are explored specifically for SO_2 emissions, partly because SO_2 is an important precursor of acidification and partly because we have a better quantitative understanding of the rates of transformation and deposition of SO_2 than for other precursor species. This role of transport processes may also vary depending on the type of emission source. Consequently, we explore the difference for the two most important types of acid precursor sources: large, tall-stack power plants and urban-industrial complexes.

Acidification of an ecological system is a long-term process. Seasonal averages of τ and of the influencing transport parameters are, therefore, more pertinent in the present context than short-term variations and effects. Accordingly, this chapter reflects such a bias in favor of monthly- or seasonally-averaged data and interpretations. Seasonal averages, however, are merely integrations of shorter-term events. In particular, atmospheric transmission processes (transport, transformations, and deposition) are characterized by strong diurnal variations, and proper resolution of these is necessary. Therefore, we have also tried to describe the diurnal cycle of transport layer structure and dynamics in some detail.

Four meteorological variables are of particular significance in the transport and dispersion of air pollution: the height of the pollutant transport layer, and the wind, temperature, and moisture fields within this layer. The Earth's atmosphere is about 100 km deep. Anthropogenic pollutants are typically confined and transported within the lowest 2 km of the atmosphere. The flow field within this boundary layer is driven by the planetary flow

above and at the same time is subject to influences of interaction with the Earth's surface below. This flow field governs the mean transport of the pollutants. The spread of the pollutants during transport is largely governed by spatial and temporal inhomogeneities in the flow field. The dispersive capacity of the transport layer is also influenced strongly by the temperature distribution within it, which is determined principally by insolation and the nature of the ground surface. The moisture field governs cloudiness and precipitation and also influences atmospheric chemistry. The local moisture field depends on transport from upwind, as well as on local evaporation of surface water.

General features of the planetary and the boundary layer flows are described in Section 3.2. The structure and dynamics of the transport layer, as well as more detailed features of the boundary layer flow and dispersive capacity, are presented in Section 3.3. The remainder of the chapter describes how the transport of pollutant emissions takes place by atmospheric motions of various scales.

3.2 METEOROLOGICAL SCALES AND ATMOSPHERIC MOTIONS (N. V. Gillani)

3.2.1 Meteorological Scales

Atmospheric motions and transport phenomena vary over a wide range of spatial scales. In general, as a pollutant plume spreads during transport, atmospheric motions of progressively larger scales influence its further dispersion. The relationship between plume dynamics and atmospheric motions must therefore be considered in the context of their relative spatial-temporal scales.

Meteorological scales are typically classified into micro, meso, synoptic, and global regimes. The meteorological microscale is defined by the vertical dimension of the planetary boundary layer (PBL), within which anthropogenic pollutants are typically emitted and distributed. This dimension is about a kilometer, and its associated time scale is measured in tens of minutes (approximately the time required for a plume to spread over the vertical extent of the mixing layer under daytime convective conditions). The microoscale phenomena include atmospheric turbulence.[1] The meteorological mesoscale extends up to about 500 km, and its associated time scale is about a day, approximately the time needed for a mean horizontal transport of 500 km. Mesoscale effects include plume dynamics and the diurnal variability of the PBL. They are strongly influenced by surface inhomogeneities of terrain as well as heat and moisture fluxes. Within the range of the mesoscale, a specific plume from a power plant or urban complex will commonly lose its identity by mixing with other plumes or by diluting indistinguishably into

[1] Atmospheric turbulence is sometimes interpreted broadly to include vortex motions over all meteorological scales. Our use of the term is more specific, and refers only to random microscale eddy motions ranging in size from a few millimeters to a few hundred meters. Thus, we use the terms turbulence and microscale turbulence synonymously.

the background. Transport over the microscale and mesoscale is sometimes also referred to as short- and intermediate-range transport, respectively. Beyond the mesoscale is the synoptic scale, the scale of the weather maps, with characteristic horizontal dimensions of about 1000 km and a transport time of about 1 to 5 days (the approximate range of residence times of sulfur in the air in eastern North America). Finally, the hemispherical or global scale is about a week and includes intercontinental transport. The discussion of pollutant transport processes is divided into mesoscale transport (Section 3.4) and continental (synoptic) and hemispheric transport (Section 3.5). The term "long-range transport" commonly refers to transport over the synoptic and hemispherical scales.

3.2.2 Atmospheric Motions

The energy that drives the atmosphere comes from the sun in the form of radiation. However, solar radiation is not uniformly distributed over the surface of the Earth. Because the Earth's pole is tilted, a given horizontal area in high latitudes receives far less solar radiation than an equal area closer to the equator. If there were no transfer of heat poleward, the equatorial regions would heat up. In a fluid as mobile as air, temperature differences will immediately give rise to currents that tend to reduce the thermal gradient. Unequal heating of the Earth's surface thus leads to horizontal pressure gradients that provide the driving force of the winds.

Wind, of course, is air in motion and although it is a motion in three directions, usually only the horizontal component is reported in terms of direction and speed. In the free atmosphere (above the effects of the Earth's friction) two forces are important in describing fluid motion in the moving reference frame of an observer on the Earth's surface. One is the pressure gradient force, which tends to move the air in a direction from high to low pressure. The second force is called the Coriolis force. The Coriolis force is a consequence of the rotation of the Earth, and is directly proportional to the speed of this rotation. It increases at higher latitudes. The Coriolis force also increases with wind speed, and its effect is to deflect the wind to the right (in the northern hemisphere) relative to the pressure gradient force. In the free atmosphere where the Earth's friction is not felt significantly, the horizontal flow becomes established nearly normal to the pressure gradient force (hence, parallel to the iso- bars). The pressure gradient force and the Coriolis force act equally and opposite to each other. This condition is called geostrophic balance, and the corresponding flow is the geostrophic flow.

Friction between the flow and the surface is felt significantly in the so-called Ekman layer which typically extends one to three kilometers above the surface. Ordinarily the wind speed and wind deflection (veer) are maximum at the top of the Ekman layer. Within the Ekman layer, wind speed decreases as the surface is approached. Correspondingly, the Coriolis force decreases and so also does the amount of wind deflection. Wind deflection under the idealized Ekman layer conditions decreases from 90° at geostrophic level to 0° at the surface. Thus, the surface flow is nearly perpendicular to the pressure isobars while geostrophic flow is nearly parallel to the isobars. The condition of wind speed shear and wind directional veer with

height in the idealized Ekman layer is called the Ekman spiral (see, for example, Brown 1974 and Figure 3-1). In actuality, the surface is never completely homogeneous, and the Ekman layer is characterized by varying degrees of vertical stratification (i.e., lack of homogeneity of turbulence structure), and the idealized Ekman spiral is only approximately realized.

On the global scale, the general circulation outside the boundary layer is driven by the global pressure gradients due to the unequal heating of the Earth's surface between the equator and the poles, and it is modified by the Coriolis force. This planetary flow is approximately geostrophic horizontally. Vertically, a weak pressure gradient force (pressure decreases with height) is nearly balanced by the gravitational force (hydrostatic balance). Hence, on the global scale, vertical motions are relatively weak, except over the high and low pressure zones of the Earth. Hot air rises over the equatorial low pressure belt and sinks at the tropics (25° to 30° latitude). Aloft, the wind blows horizontally from the equator to the tropics (southwesterlies in the northern hemisphere); near the surface, the flow is towards the equator (northeasterlies). Poleward of the tropics, the Coriolis force is stronger, and the flow pattern is more complicated, being characterized by synoptic-scale cyclones and anticyclones, which are rotating horizontal flows, rather than simple straight flows (see, for example, Chapter 4 in Anthes et al. 1975).

Cyclones are low pressure cells with rising motion near the center and a counterclockwise flow spiraling towards the eye near the ground. Anticyclones are large high pressure cells with slowly sinking air at the center and weaker outward and clockwise spiraling surface flow in the northern hemisphere. Cyclones and anticyclones rotate about their own centers but also move downstream, generally eastward, in the broad-scale westerly general circulation in which they are embedded. Anticyclones are characterized not only by weak rotating flow within the cell, particularly in the core, but frequently they are also characterized by weak or stagnant motion. When an anticyclone stagnates for multiday periods over pollutant source regions such as the Ohio River Valley, considerable pollutant accumulation and aging can occur over a synoptic scale, and episodes of regional haziness occur. Such hazy air masses become richly loaded with acidic material. A summary of the climatology of synoptic-scale "air stagnations" (covering area greater than 200,000 km^2 for more than 36 hours) in the eastern United States is presented in Figure 3-2. The greatest likelihood of such stagnations is over the dense source regions of the TVA and the Ohio River Valley. For a discussion of the relationship between haziness and concentrations of acidic substances see Chapter A-5.

Another important large-scale flow feature is the jet stream. Temperatures do not vary gradually from the tropics toward the poles. Sometimes, regions of relatively weak thermal gradients are interrupted by regions of strong gradients, called "frontal zones." These frontal zones are associated with localized regions of strong winds located above these zones. Such frontal zones exist at interfaces of air masses of different origins and physical properties. In the interior of the North American continent, there are no significant geophysical obstructions to air movements, particularly between the north and the south. Southward intrusions of the dry, cold Canadian

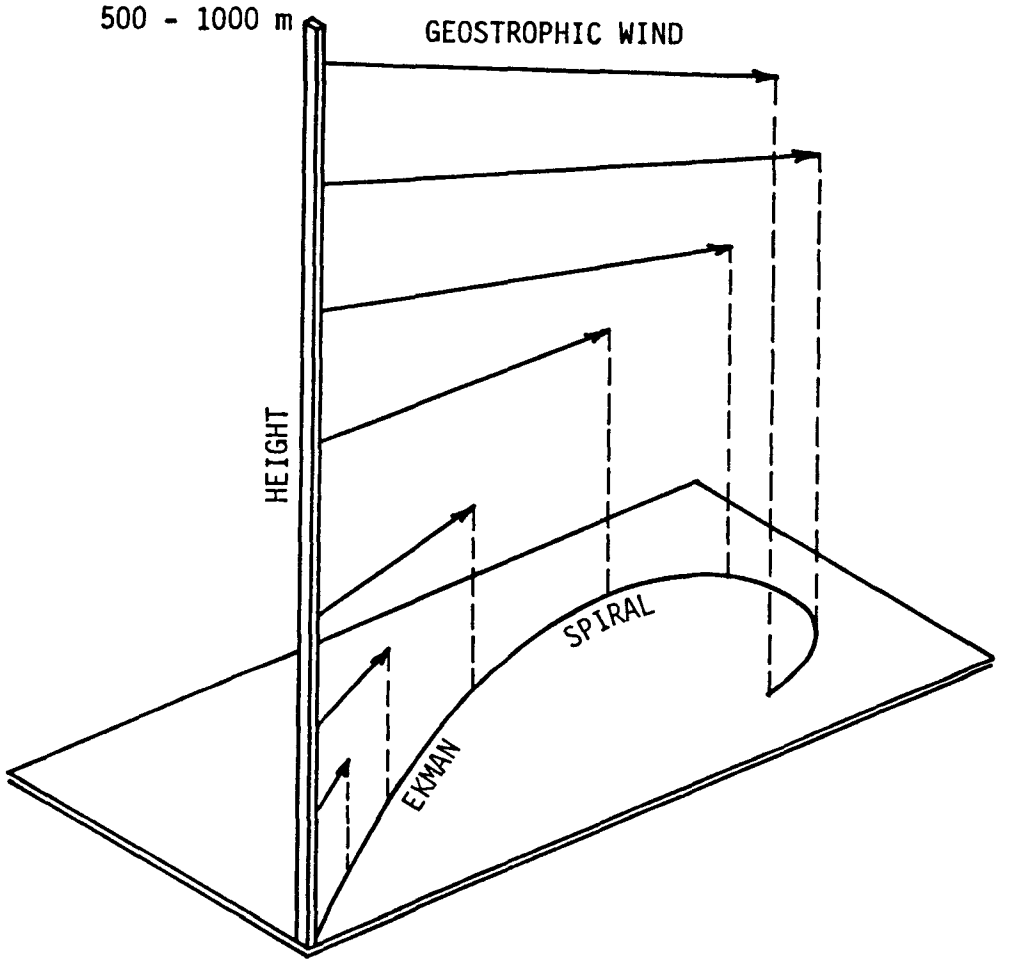

Figure 3-1. The Ekman spiral of wind with height in the northern hemisphere. Adapted from Barry and Chorley (1977).

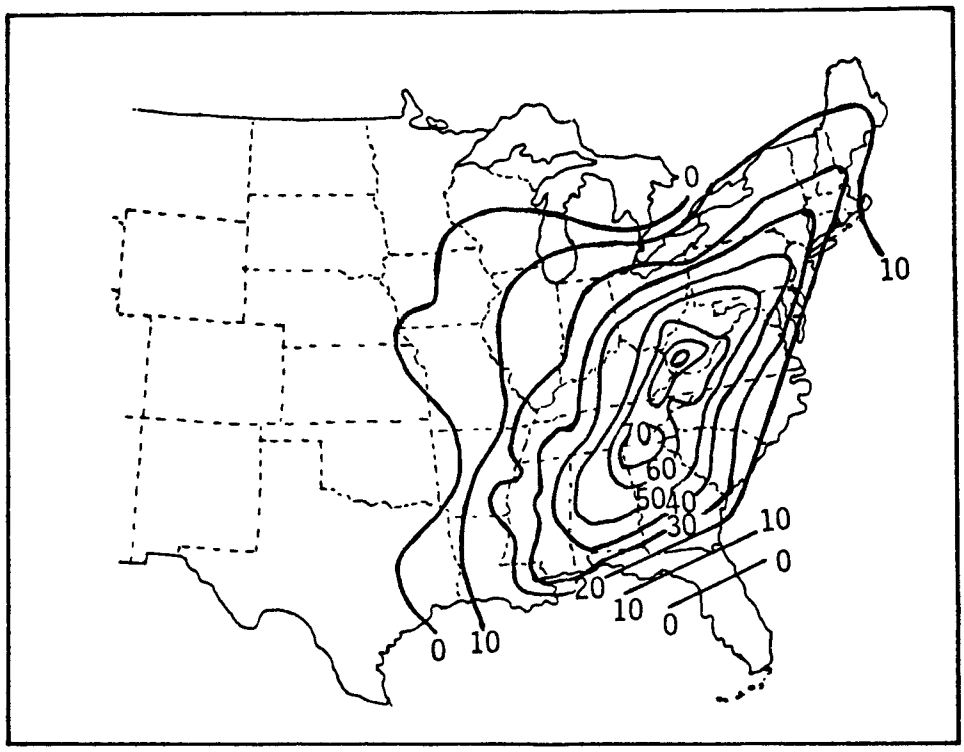

Figure 3-2. Climatology of air stagnation advisories issued over a ten-year period. Adapted from Lyons (1975).

continental polar air mass and northward intrusions of the moisture-laden maritime air mass from the Gulf of Mexico often give rise to frontal zones, with the associated jet stream and its strong, generally westerly flow. Associated with such frontal zones is also strong horizontal convergence of flow at lower levels, and upward motion aloft; clouds and precipitation are concentrated at frontal zones. (For detailed descriptions of North American air masses, frontal zones, and the jet stream, see Chapters 4 and 5 of Barry and Chorley 1977.)

Mesoscale systems are perturbations of the synoptic flow on scales that are too small to be resolved on weather maps but are larger than the microscale. They are particularly important in producing local weather, which can be quite variable spatially within the same synoptic system. Except in frontal zones and near cyclone centers, synoptic and global flows are largely dominated by horizontal winds, with very weak vertical components. Mesoscale systems, in contrast, are characterized by significant vertical flows, hence are often termed complex flows. Whereas average vertical velocities in large-scale systems are typically on the order of 1 cm s^{-1}, vertical speeds in local mesoscale systems are typically on the order of 1 m s^{-1}, and may even exceed 10 m s^{-1} in strong updrafts, especially in thunderstorms (Panofsky 1982).

Mesoscale complex flows may be terrain-induced or synoptically-induced (see, for example, Pielke 1981). Terrain-induced effects include land and sea breezes and other effects related to shoreline environments, as well as forced air flow over rough terrain, mountain valley winds resulting from natural convection phenomena, and urban and other circulations related to specific land use patterns. Synoptically-induced vertical motions, such as at frontal zones, may be complicated by interactions with local mesoscale disturbances such as squall lines, which are narrow lines of thunderstorm cells that may extend for several hundred kilometers. Later sections will show that substantial depositions of sulfur emissions occur within the mesoscale range, particularly in summer, in the eastern United States. Mesoscale flow systems are therefore of considerable importance in source-receptor relationships. A more detailed discussion of mesoscale complex flows is given in Section 3.3.4.

Turbulence is the most important microscale motion. Unlike large-scale motions (synoptic and global), it is essentially random and three-dimensional motion. The vertical component of the motion is comparable to the horizontal component. Microscale turbulent eddies may be generated in two ways, by thermal convection or by mechanical shear. Water boiling in a pan is full of thermal turbulence. In the atmosphere, heating from the ground below in the daytime sets up convection currents with turbulent eddies often as large as 100 m or more in size. On the other hand, the interaction of wind with surface roughness also generates turbulent eddies that are characteristically smaller than thermal eddies. Friction between the ground and the air gives rise to strong wind shear in the surface layer of air (lowest few meters) and gives rise to intense small-scale mechanical turbulence. Patches of mechanical turbulence may sometimes also occur high in the upper atmosphere in locally strong wind shear zones associated with frontal zones (see, for

example, Panofsky 1982). This type of clear-air turbulence (CAT) sometimes causes discomfort to aircraft passengers even at cruising altitudes.

Turbulence is an important mechanism for mixing or spreading a pollutant emission horizontally but, more importantly, it is often the only mechanism for vertical mixing. It is principally responsible for delivering elevated emissions to the ground. It is also an important agent for dilution of concentrated pollutant releases from point sources. Turbulence is also the mechanism for vertical spreading of moisture evaporating from the ground. This, of course, is the stuff of which clouds and precipitation are made. The significance of turbulence as a dispersion mechanism, particularly in the vertical, is not restricted to mass only (i.e., pollutants and moisture). It disperses momentum and energy just as effectively. Turbulent eddies distribute surface drag (friction) over the Ekman layer. Vertical turbulence, in fact, is the principal means for communication of mass, momentum, and energy between the Earth's surface and the large scale upper air flow, thereby gradually changing large-scale conditions. This is an example of interaction between the extreme scales of atmospheric motions.

Interactions occur between all scales of atmospheric motions. Such interactions play an important role in pollutant transport and dispersion. In fact, such interactions pose a major difficulty in the modeling of long-range transport, in which a rather coarse spatial-temporal resolution of the mean flow field is commonly used. Mesoscale and microscale effects are not resolved adequately in an explicit manner in such a coarse "grid" structure. The net effects of such "sub-grid" phenomena are often most important and must be included by means of parameterizations or bulk representations.

As an important example, consider the question of long-range trajectory calculations. It is still common practice to calculate an "average" long-range trajectory of a polluted air parcel, based on the average wind speed and direction in the entire vertical domain of the transport layer (see, for example, Heffter 1980). Such an average trajectory hides the fact that, as a result of the spatial-temporal variation of wind speed, wind direction, and turbulence characteristics within the transport layer, the ensemble of pollutant particles in the air parcel of interest actually follows an ensemble of noncoincident trajectories. The spread of this ensemble of trajectories is, in fact, the measure of pollutant spread during transport. In long-range transport, such spread can amount to hundreds of kilometers. For proper modeling of pollutant transport and spread, the average calculated trajectory must be accompanied by a measure of pollutant spread based on an appropriate parameterization of the wind variations within the transport layer.

A considerable amount of micrometeorological field data and research have yielded more or less acceptable approximate parameterizations of dispersion due to microscale wind fluctuations. Dispersion due to shear and veer in the mean wind field is only now beginning to be modeled realistically and explicitly, and has not progressed to the point of formulating reliable parameterizations. Field data pertinent to mesoscale motions are very limited. Routine monitoring of upper air winds is confined to a sparse

spatial network (stations being separated, on the average, by well over 300 km), and the temporal resolution of the measurements is also coarse (typically at 12-hourly intervals). Such monitoring is adequate for the reconstruction of the synoptic flow field (as seen on the weather maps) but inadequate to resolve mesoscale effects. Possibly the major uncertainty in the assessment of regional impacts of emissions is due to this lack of resolution of mesoscale and diurnal variations of the flow field, particularly under short-term episodic conditions.

The extremely important role of microscale turbulence in vertical mixing is characterized by strong spatial-temporal variabilities in vertical turbulence structure. Turbulent eddies range over a wide spectrum of size as well as turbulent kinetic energy distribution. The large thermally-generated eddies contain the most turbulent energy, and thus are capable of the most vigorous mixing up to a scale of several hundred meters. They exist in the central part of the PBL, which is generally quite well-mixed. Because the source of their energy is surface heat flux which, in turn, depends directly on insolation, their existence exhibits a strong diurnal cycle. Close to the surface, small-scale mechanically-generated eddies predominate. They contain much less energy and have more limited mixing capacity. Consequently, the near-surface layer presents the most resistance to the downward transport of momentum and elevated emissions, or to upward transport of heat and moisture fluxes. Small-scale turbulence exists also in the well-mixed bulk of the PBL because individual large eddies are very transient in nature (as indeed are all eddies), and are continuously being generated on the one hand by surface heating, and degenerated on the other hand to small eddies by a rapid and continuous transfer of energy from larger to smaller eddies. At the lower end of this "spectral energy cascade" (Tennekes 1974), viscous dissipation of the smaller eddies ultimately removes turbulent kinetic energy by converting it to heat. This process of kinetic energy dissipation is responsible for dissipation of as much as half of the kinetic energy of the large-scale atmospheric flow patterns (Tennekes 1974).

The role of these spatially-temporally varying microscale motions must be included in transport models by appropriate parameterizations. Because vertical stratification of the transport layer occurs in terms of wind speed, wind direction, and wind shear as well as turbulence, it is increasingly evident that realistic transport models must adopt a degree of vertical layering. In the next section, we explore the characteristics of the transport layer in somewhat greater detail.

3.3 POLLUTANT TRANSPORT LAYER: ITS STRUCTURE AND DYNAMICS (N. V. Gillani)

3.3.1 The Planetary Boundary Layer (Mixing Layer)

The troposphere is the lowest portion of the Earth's atmosphere in which temperature, on the average, decreases with height. In the tropics, its depth is about 10 km. The bulk of anthropogenic pollutant emissions, including precursors of acidic depositions, is released and transported in the lowest 2 km or so of the troposphere. This is also the layer where the primary meteorological variables [i.e., the thermal field (temperature), the

momentum field (winds), and the moisture field] are perturbed significantly as a direct consequence of the Earth's surface. In air pollution meteorology, pollutant concentrations in the air represent a fourth type of primary variable. For each variable, the layer perturbed by surface effects is its boundary layer. The surface sources of disturbances of the primary variables may be different for the different variables, and for each variable, the distribution of such sources may be spatially inhomogeneous and temporally variable also. However, all types of disturbances are communicated vertically by the same physical mechanism, turbulence. Consequently, the boundary layer of most practical significance is the so-called mixing layer (also called the planetary boundary layer, PBL). The principal characteristic of this layer is the continuous presence of significant microscale turbulence within it.

The definition of the mixing layer as the vertical domain of microscale turbulence must be qualified. In certain complex flow situations, this definition may be inappropriate. For example, in the presence of strong convective instability associated with towering cumulus clouds and thunderstorms, vigorous turbulent mixing within clouds may extend into the upper troposphere. In such cases, the base of the clouds may be considered as the PBL height. When strong orographic, shoreline, or other topographical effects are present, the PBL needs special consideration. Perhaps a more appropriate definition of the top of the mixing layer is "the lowest level in the atmosphere at which the ground surface no longer directly influences the dependent variables through turbulent mixing" (Pielke 1981).

The mixing layer is so called because, within it, atmospheric turbulence effectively and quickly manages to mix up, spread out, or dilute any concentrated release of mass, momentum, or heat. In all other parts of the atmosphere, the dilution of pollutants is very slow. The mixing layer grows during the daytime, typically to heights of 1 to 2 km, due to increased thermal convection, and subsides at night to heights typically ranging up to about 200 m.

While the deep daytime mixing layer is dominated by large-scale thermal turbulence, the shallow nighttime mixing layer contains only small-scale mechanical turbulence. The daytime mixing layer is extremely efficient in quickly delivering any elevated pollutant releases within it to its entire vertical extent, including the ground. On the other hand, elevated nighttime releases from tall stacks are typically outside the shallow mixing layer and, in the absence of any mechanism to bring them down to the ground, are transported over long distances while remaining decoupled from the ground. Nighttime urban releases within the shallow mixing layer, on the other hand, often remain trapped at relatively high concentration and, being in constant contact with the ground sink, may become substantially depleted of pollutants during relatively short-range transport. Pollutants that become well-mixed in the deep daytime mixing layer are transported at night in this deep transport layer, decoupled from the ground except for the lowest portion in the shallow nocturnal mixing layer.

The depth of the mixing layer is a critical parameter with respect to pollutant transport. The top of the mixing layer usually distinctly

delineates the turbulent, polluted air below from the calmer, cleaner air above. This is particularly the case during midday, convective periods. The height of the mixing layer can be measured most accurately by turbulence monitors in instrumented research aircraft flying a vertical spiral, or by remote soundings of the turbulent fluctuations of temperature and atmospheric refractive index using sodars and lidars. In daytime, the mixing height commonly coincides with the lowest temperature inversion. Accordingly, it is most commonly estimated from vertical temperature and humidity soundings by standard radiosonde releases. The daytime mixing height may even be estimated from the height of the cloud base in fair-weather cumulus conditions, or often from the height of the visible polluted layer.

A number of excellent review articles describe the structure and dynamics of the PBL. Tennekes (1974) presents a useful qualitative description of the PBL. Arya (1982) presents a more detailed review of the PBL over homogeneous smooth terrain, including a section summarizing techniques of parameterization of the PBL. PBL parameterization and attempts at simulation of observed PBL structure and dynamics are thoroughly reviewed also by Pielke (1981). The features of the PBL over non-homogeneous terrain, and simulation of these, are described in detail by Hunt and Simpson (1982). Also, a WMO Technical Note devoted to the PBL (McBean et al. 1979) contains a number of excellent chapters summarizing PBL features, observed and modeled, for simple and complex terrain.

The sections that follow are substantially based on the above references. In addition, however, the author has chosen to present illustrative examples from previously unpublished data of very recent, very sophisticated, major EPA-sponsored mesoscale field programs, particularly Projects MISTT (Midwest Interstate Sulfur Transport and Transformations), RAPS (the St. Louis Regional Air Pollution Study), and TPS (Tennessee Plume Study). Collectively, these data bases reflect state-of-the art technology, seasonal coverage, and some of the most detailed measurements of mesoscale plume transport. The results of earlier well-known PBL field studies such as the Great Plains Experiment at O'Neill, Nebraska (Lettau and Davidson 1957), the Wangara Experiment in Australia (Clarke et al. 1971, Deardorff 1980), the 1968 Kansas Field Program (Izumi 1971, Haugen et al. 1971, Businger et al. 1971), the 1973 Minnesota study (Kaimal et al. 1976, Caughey et al. 1979), and the 1975, 1976 Sangamon Field Program (Hicks et al. 1981) are well covered in the original references and are also included in the PBL review articles identified earlier. These earlier studies were focused more on micrometeorological measurements and analyses.

3.3.2 Structure of the Transport Layer (TL)

For a given day, the transport layer may be defined as the layer between the surface and the peak mixing height of the day. For any given instant, it is therefore made up of the current mixing layer below and a relatively quiescent layer above. This minimum stratification of the TL into two layers is essential in any transport model. The daytime mixing layer itself may be further subdivided into a surface layer (extending typically to 50 m or so) and a "mixed" layer above.

The surface layer is principally characterized by strong gradients in all the primary variables, the influence of surface effects being most concentrated there. The wind speed increases from zero at the surface to near-geostrophic in the mixed layer. The land surface has a relatively smaller heat capacity than the air above, and therefore undergoes more rapid and greater temperature changes than the air during the diurnal cycle. The transition between the surface temperature and the mixed layer temperature distribution is also most concentrated in the surface layer. Owing to the dry deposition of pollutants at the surface, a significant increase in pollutant concentration occurs as height in the surface layer increases. Also pronounced in the surface layer is the frictional force. Thus, the average wind speed is low here, and consequently the Coriolis effect is relatively unimportant. In turn, the wind direction remains relatively constant and more nearly aligned with the pressure gradient.

The large wind speed shear in the surface layer leads to the generation of intense small-scale mechanical turbulence. While thermal buoyancy effects are also intense here in the daytime, the proximity of the surface limits the size of turbulent eddies. As a result, surface layer turbulence is characterized chiefly by small eddies. Consequently, the dispersion within the surface layer is relatively much slower than in the mixed layer, and dissipation of turbulent kinetic energy is locally high relative to the total amount of turbulent energy present. Also, the relatively slow vertical transfer of the pollutants in this layer is at a nearly constant rate. Hence, it is often also called the "constant flux layer." Shear effects generally predominate over buoyancy effects in the lower part of the surface layer (forced convection layer), but under midday convective conditions, buoyancy effects may predominate in the upper part of the surface layer (free convection layer).

The surface layer is by far the most studied part of the PBL. The parameterization of the mean flow as well as its turbulent components are well-established and, at least over smooth terrain under relatively stationary conditions, fairly reliable. Turbulent dispersion is parameterized in terms of an "eddy diffusivity," by analogy with the concepts of molecular diffusion. Eddy "diffusion" is on a relatively larger scale, however, because the scale of the transporting medium, the eddies, is considerably larger than the mean free path (mean distance between collisions) of the molecules. In the surface layer, the vertical eddy diffusivity, K_z, increases linearly with height as larger eddies can exist farther from the surface. Higher up, in the mixed layer, the distribution of eddy scales and turbulent energy is more nonlinearly distributed with height, and the concept of eddy diffusion becomes less reliable.

In the mixed layer, as the name suggests, the variables (wind speed, "potential" temperature, moisture, and pollutant concentrations) are more or less homogeneously distributed vertically, owing to the more thorough and rapid mixing by the large-scale, thermally-generated eddies or convection currents. Buoyant effects predominate, and the turbulent dispersive capacity of the atmosphere is more commonly expressed in terms of atmospheric stability. The potential temperature (θ) is a closely related concept. Both concepts are defined below.

A hot (buoyant) puff of gas released into the atmosphere will rise, expand, and cool nearly adiabatically (i.e., without exchanging heat with its surroundings) at the rate of about 1 C per 100 m in dry air (a dry adiabatic lapse rate, Γ_{dry}), and more slowly in moist air (a wet adiabatic lapse rate, Γ). The puff will continue to rise and expand as long as it remains buoyant, i.e., warmer than the ambient air. Whether its buoyancy will increase, decrease, or remain unaltered as it rises depends on whether the ambient atmospheric lapse rate (dT/dz) is superadiabatic ($dT/dz < \Gamma$), subadiabatic ($dT/dz > \Gamma$), or adiabatic ($dT/dz = \Gamma$, which is negative). The potential temperature is defined by $d\theta/dz = dT/dz - \Gamma$. The potential temperature decreases with height in a superadiabatic atmosphere, increases with height in a subadiabatic atmosphere, and remains constant with height in an adiabatic atmosphere. A superadiabatic layer is unstable because the puff will become continuously more buoyant in it and will rise and dilute faster. A subadiabatic layer is stable because it tends to slow down and terminate puff rise. An adiabatic layer is neutral because it does not alter the initial puff buoyancy. The puff will thus continue to rise in neutral and unstable surroundings until it reaches a stable thermal environment. In the daytime, the surface layer is typically very unstable, and the mixed layer is in near-neutral condition. Any surface perturbations of mass, momentum, or energy in the daytime mixing layer will thus be convected upwards by the turbulent eddies. Surface heating will continually release "thermal plumes" or convective updrafts, some of which may rise to the top of the mixing layer, carrying along with them any evaporated moisture. Some of these updrafts will also rise into the quiescent layers aloft, thus causing an upward growth of the mixing layer by penetrative convection.

The rise of buoyant updrafts in the unstable daytime convective mixing layer is frequently obstructed by a thin temperature "inversion" layer (stable) capping the mixing layer. The climatology of daytime mixing layers over the continental United States has been documented (Holzworth 1972). Figure 3-3 illustrates the vertical structure of temperature, small-scale turbulence, and SO_2 in a rather well-mixed power plant plume within the bulk of the peak daytime mixing layer on a cloudless summer day in the midwestern United States. The turbulence clearly decays rapidly at the elevated inversion base. Unlike the rather uniform distribution of small-scale turbulence in the mixing layer, the vertical distribution of large-scale turbulence in the mixing layer (that most responsible for rapid mixing) is quite inhomogeneous, peaking in the middle of the mixing layer (where tall-stack plumes are released) and decaying rapidly at the top and bottom boundaries (much like the SO_2 profile). Typically, no physical or stable boundaries exist horizontally, and the turbulence structure is more homogeneous. Turbulent eddies are horizontally larger, and turbulent plume dispersion is generally faster horizontally than it is vertically.

A number of major factors influence the structure of the PBL. The mean flow field is principally driven by the planetary flow, and modified by surface friction and the local thermal wind due to horizontal temperature gradients. The modifications can be locally dominant as over extremely complex terrain, in shoreline environments, over urban heat islands, and in the vicinity of mesoscale convective precipitation systems. The turbulence structure is principally governed by surface heating and cooling and by wind shear, either

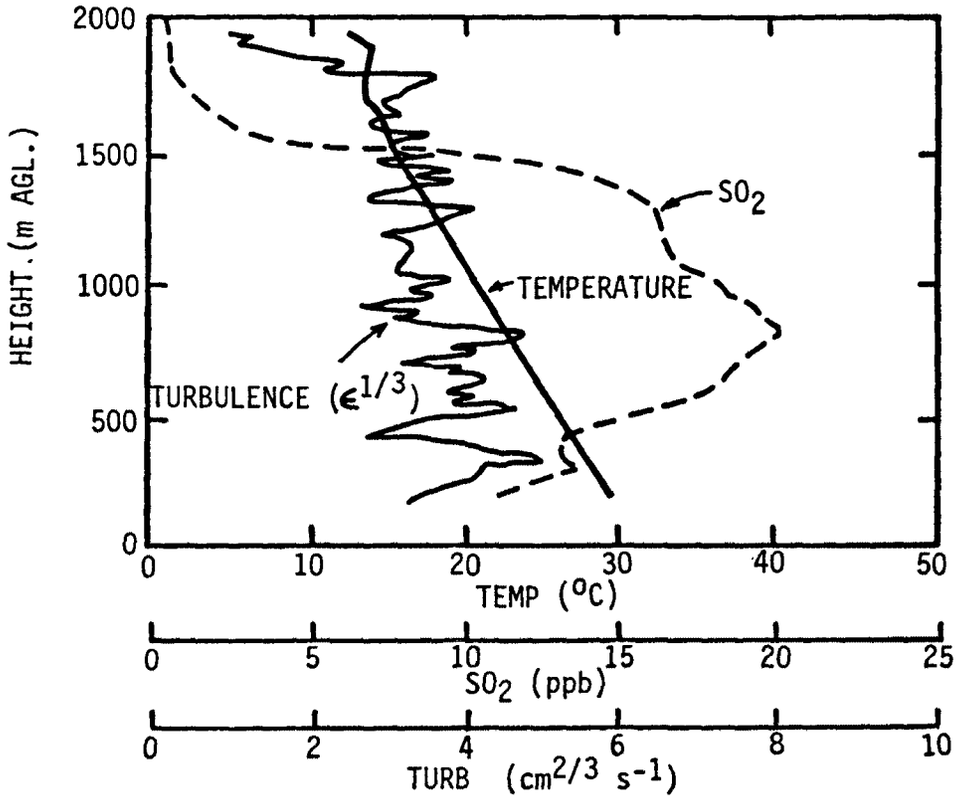

Figure 3-3. Vertical profiles of temperature, small scale turbulence, and SO_2 concentration in a diluted power plant plume within the daytime mixed layer near St. Louis, MO. Observe the temperature inversion and sharp turbulence decay between 1700 and 1900 m (Gillani 1978).

due to surface roughness or other causes. Wind shears and turbulence intensities also depend strongly on mixing layer height, which essentially fixes the dimensions of the largest eddies. This height depends principally on the sensible heat flux from the ground, which in turn depends strongly on insolation, local land use, and surface condition. The heat flux not only has strong diurnal variability, but also substantial spatial variability in urban as well as rural areas on the scale of a few kilometers (Ching et al. 1983). The mixing height can also be influenced significantly by synoptic influences on mixed layer growth, such as cold air subsidence and large-scale lifting as in frontal zones (Ching et al. 1983).

3.3.3 Dynamics of the Transport Layer

Strong diurnal and seasonal variations occur in the mean thermal and flow fields, as well as in the turbulent fields, within the PBL. Good qualitative descriptions of the diurnal effects have been given by Plate (1971) and by Smith and Hunt (1978).

Diurnal and seasonal variations of the thermal stratification of the transport layer are shown in Figure 3-4, and the average diurnal profiles of the mixing height during the different seasons are shown in Figure 3-5. The temperature data are based on RAPS radiosonde measurements at a rural site near St. Louis, and each profile is based on 31 daily soundings in 1976. The mixing height data are deduced from a composite of 6-hourly temperature and wind soundings as well as turbulence measurements during a large number of aircraft spirals.

At night, the ground is cooler than the air layers above. Hence, a surface based inversion (very stable) extends upward to about 300 m in the summer and to nearly 600 m in the winter near St. Louis. A shallow mechanical mixing layer exists within the inversion layer. As the sun comes up in the morning and heats up the ground, surface temperature rises above that of the air layers immediately above. Consequently, an upward sensible heat flux by conduction and convection is established, and a continuous warming trend of the surface layer air occurs. With increasing insolation and warming of the air, the nocturnal inversion layer is eroded from the surface up. As the heating continues into the mid- and late-morning hours, an unstable layer develops near the ground, while convective eddies aid in the growth of the mixing layer by penetrative convection into the quiescent layers aloft. On a clear day, this growth proceeds quite rapidly in the morning and more slowly in the early afternoon, until the transport layer is fully established, with the mixing height at its peak value typically by midafternoon. This daytime mixing layer is typically capped by an elevated inversion layer, which is very stable and quite thick in the winter (700 to 1200 m, on the average, in January in St. Louis; Figure 3-4) and quite high and narrow in summer (1800 to 2000 m, on the average, in July in St. Louis). The peak mixing height, or the full transport layer height, is thus much deeper in the summer than in the winter. This fact, above all else, is likely to lead to a substantial difference in the atmospheric residence times of emissions from tall stacks during summer and winter. Within this daytime mixing layer are embedded the surface layer with high gradients of the primary variables, and the mixed layer with nearly uniform vertical distribution of the variables.

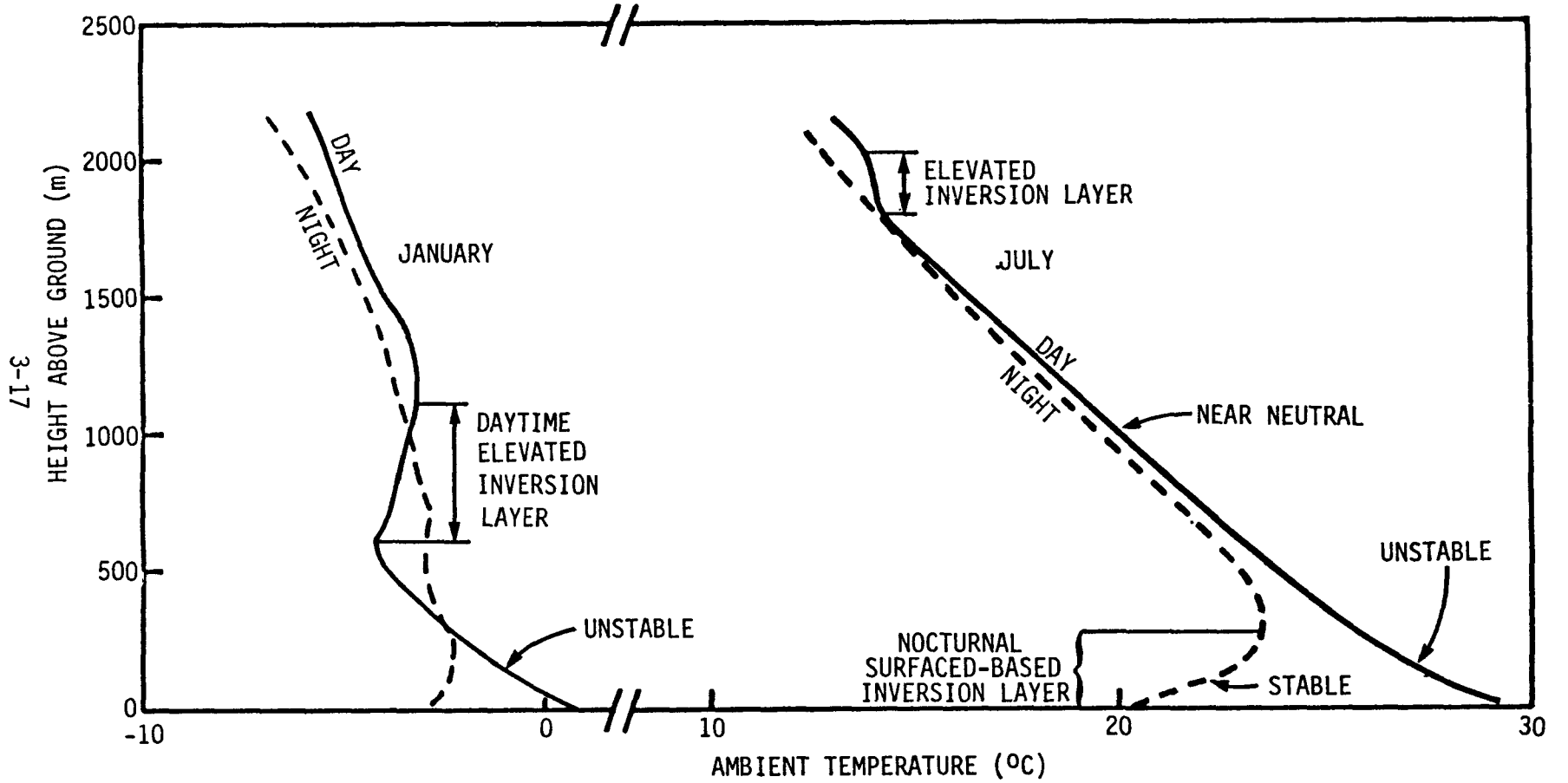

Figure 3-4. Monthly-average diurnal and seasonal variations of the vertical thermal structure of the PBL for a rural site near St. Louis, MO based on 1976 data.

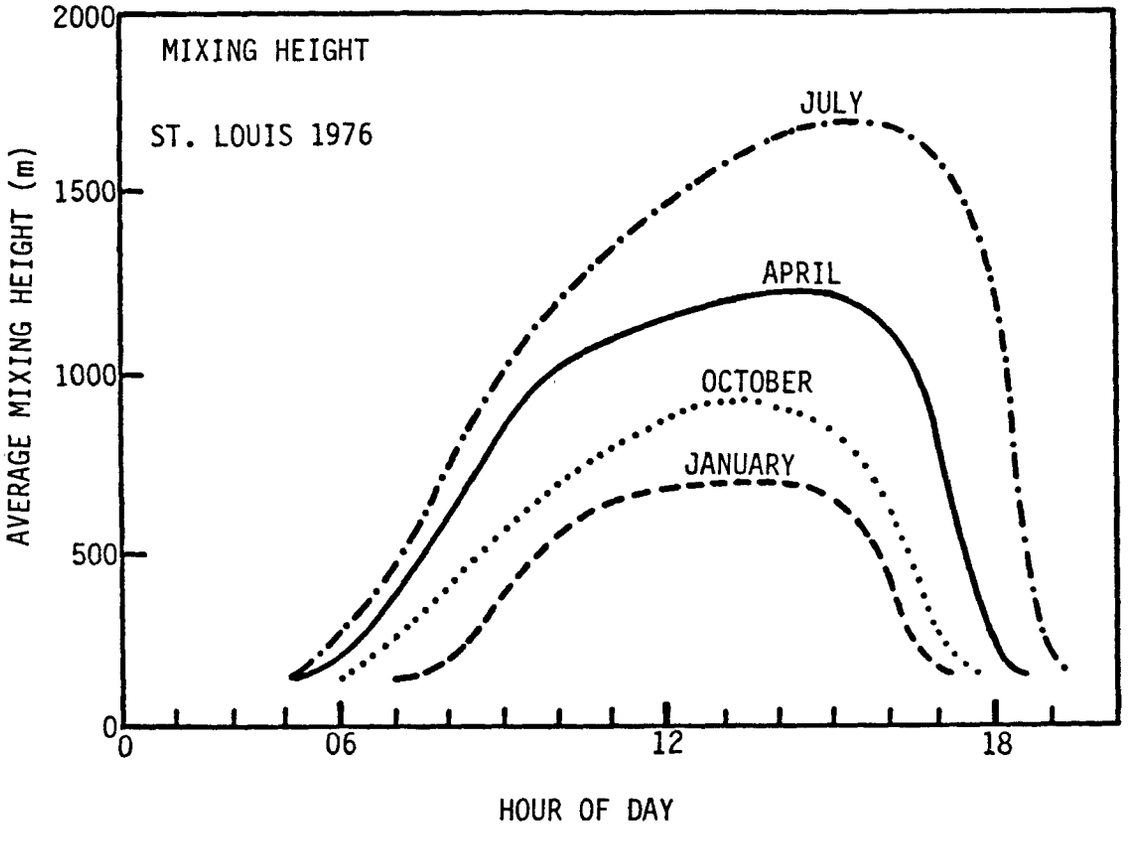

Figure 3-5. Monthly-average diurnal and seasonal variations of mixing height near St. Louis, MO, based on 1976 data (Gillani et al. 1981).

Late in the afternoon, when ground level insolation has diminished siderably, the ground begins to cool gradually. For a brief period, it attains nearly the same temperature as the air immediately above, there is negligible heat flux at the interface, and the potential temperature is nearly constant throughout the PBL (neutral). Thereafter, no upward heat flux occurs, and no energy supply sustains the convective eddies. Consequently, the intensity of the turbulence diminishes quite rapidly from the top of the PBL downwards (Caughey and Kaimal 1977, Ching et al. 1983) and the mixed layer collapses. After sunset, the ground cools off rapidly by release of its stored thermal energy in the form of long-wave radiation. Thermal relaxation of the air above is much slower. Hence, the ground becomes increasingly colder than the air above, and a deepening surface-based inversion slowly develops.

The change in the lowest portion of the transport layer from very unstable in the day to very stable at night is especially dramatic in summer. Particularly on evenings with clear skies and light-to-moderate winds, the surface inversion layer becomes extremely stable and strongly suppresses vertical transport of mass, momentum, or energy. The heat flux is now downward owing to the inverted temperature profile. Turbulence is inhibited except for the small-scale turbulence in the shallow surface layer (also the only mixing layer, since there is no nocturnal mixed layer). The height of this surface mixing layer is typically 100 to 200 m (Garrett 1982). Above the inversion layer, remnant small-scale turbulence from the daytime gradually dissipates. In the absence of any effective vertical transfer mechanism, the layers above the stable layer become decoupled from the mixing layer and the ground.

Because turbulent interaction is limited, the nocturnal boundary layer reacts slowly to change. The surface inversion continues to grow very slowly long after surface cooling has ceased. This growth may be by a process of gradual entrainment of air from above, made possible by local generation of weak turbulence by wind shear (Blackadar 1957). The existence of very strong wind shear in the inversion layer will be discussed in the next paragraphs. Because the nocturnal inversion layer continues to grow for a long time, steady-state assumptions concerning nocturnal dynamics may not be warranted in some problems (Businger and Arya 1974). For a fine review of the nocturnal boundary layer dynamics, the reader is referred to Shipman (1979).

The stable inversion layer not only decouples trapped as well as new release of pollutants in the elevated daytime mixed layer from the ground sink, but also prevents communication of surface friction to these layers above the nocturnal inversion layer. The winds in these upper layers are thus released from the retarding effect of friction, and thus begin to accelerate. In contrast, layers further aloft where friction is weak at all times, are relatively unaffected. The surface layer winds, however, now are subjected to a more concentrated effect of friction in the absence of momentum transfer from above, and are decelerated. There is thus an opposite diurnal oscillation of winds in the middle layers as compared to that in the surface layer (Goualt 1938, Wagner 1939, Farquaharson 1939).

The behavior of the flow above the nocturnal inversion layer was described by Blackadar (1957). The inertial oscillation there is quite pronounced, and

wind speeds frequently become supergeostrophic in these layers. The phenomenon has become widely known as the "nocturnal jet." Perhaps a more appropriate description of it is "low-level nocturnal wind maxima" (Frenzen 1980), because these accelerated layers are not restricted horizontally as jets are, in the usual sense. Rather, they are broad sheets of faster moving air.

The nocturnal jet is a very frequent occurrence in St. Louis, particularly in summer, as shown in the upper air St. Louis wind data of January and July 1976 (Figure 3-6). The figure shows monthly-average vertical profiles of wind speed near midday and midnight for January and July near St. Louis, based on RAPS data. The following major observations may be made about diurnal and seasonal variations in transport layer wind speeds, based on the average St. Louis wind data:

- There is a nearly three-fold increase in the free stream wind speed (at 2 km, say) from summer (~ 6 m s^{-1}) to winter (~ 18 m s^{-1}). Wind speeds are correspondingly greater in winter in the boundary layer below.

- In summer as well as in winter, the wind speeds are greater at night than during the day in the layers between 100 and 1000 m. In particular, the wind speed is supergeostrophic in much of these layers in the middle of summer nights and, on the average, peaks at about 500 m. The peak value is about 10 m s^{-1}, on the average. However, values as high as 20 m s^{-1} (72 km hr^{-1}) have been observed on occasions.

- Based on the average mixing height data of St. Louis (Figure 3-5), the maximum transport layer depth (peak mixing height of the day) is about 700 m in January and about 1700 m in July. During the daytime in both seasons, relatively little wind shear with height occurs in the transport layers above the surface layer (~ 100 m). In contrast, considerable wind shear occurs at night on the lower side of the nocturnal jet (below 500 m) in both seasons.

- In the mean pollutant transport layers, the average 24-hr transport range based on St. Louis winds and mixing heights is estimated at 500 to 600 km in the summer, and about 800 to 900 km in winter. These, however, are transport distances along wind trajectories and not along straight lines. They thus represent upper bounds on the average seasonal transport ranges. The actual straightline displacement of point emissions during 24 hr of transport may, on the average, be closer to half of these upper bounds. It is quite possible, however, for an individual elevated pollutant release to start its journey lodged in a strong nocturnal jet and be transported 500 km or more within a single night. On the other hand, it is also quite possible for pollutant trajectories to be quite stagnant or highly meandering, thus resulting in very short net displacement from the source in several hours.

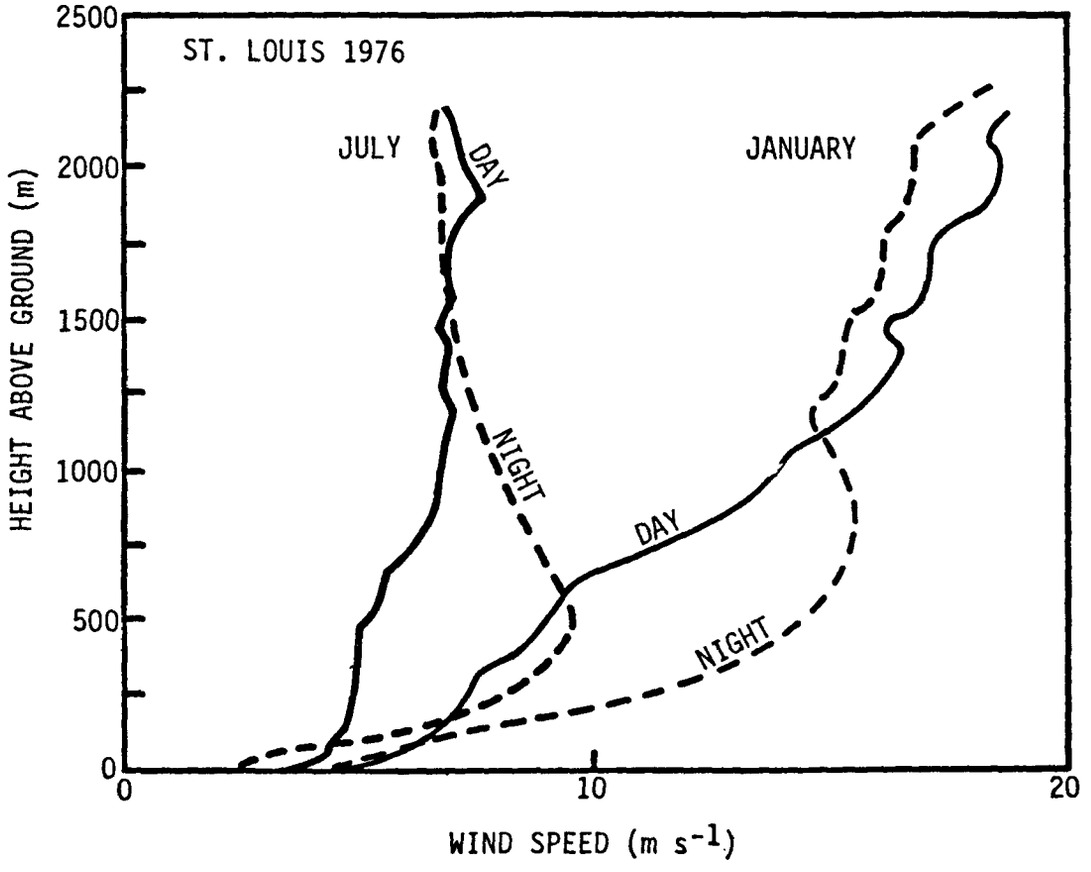

Figure 3-6. Monthly-average diurnal and seasonal variations of the vertical profiles of wind speed near St. Louis, MO, based on 1976 data.

The inertial oscillation is not restricted to wind speed only. As the wind speed increases from the surface wind to the peak jet wind, a corresponding increase occurs in the strength of the Coriolis force, and hence in wind veer with height. Thus, a strong wind speed shear on the underside of the jet is also associated with a strong wind directional shear. This is evident in the St. Louis data (Figure 3-7), which show average vertical profiles of the absolute difference in local wind direction at any height relative to the direction of the surface wind. On summer nights, on the average, the 500 m winds (at peak jet level) blow at a 60° angle compared to surface winds, and this difference is about 100° for layers near the top of the transport layer (about 1700 m). In other words, a daytime summer pollutant release that has become well-mixed over the entire afternoon transport layer, may be subjected at night to a layered transport in which the uppermost layers may move nearly perpendicular to the surface layers. Clearly, this phenomenon will cause highly distorted and extensive lateral dispersion of the pollutant plume at night. The combined effect of nocturnal amplification of wind speed and directional shear, followed next day by vertical homogenization of all the separated layers into a deep mixing layer, will result in vastly greater lateral dispersion over the time scale of a day than that due to horizontal turbulence. The role of vertical turbulence in mixing all individual layers throughout the next daytime mixing layer, however, is of critical importance in such large-scale pollutant dilution and dispersion. Only such a large-scale dispersive mechanism can explain the rather rapid incorporation of strong pollutant plumes indistinguishably into the regional background. In special plume studies based on aircraft sampling designed to track large power plant or urban plumes over long distances, our success in identifying daytime well-mixed plumes during subsequent night-time transport has been rather limited. Only on rare occasions has it been possible to track such plumes for over 300 km (Gillani et al. 1978).

Blackadar (1957) attributed the cause of the nocturnal jet to be the shift of the lower-level thermal structure from unstable and convective in the day to stable and inhibitive of turbulence at night. This is consistent with the St. Louis observation that the jet is most pronounced in summer, when the lower-level thermal oscillation is also most pronounced. This explanation, however, may not be complete, particularly since the occurrence of the jet shows some geographical preference also, as well as some extreme behavior not fully consistent with Blackadar's explanation (Paegel 1969). Other possible influencing factors that have been implicated are horizontal variations of surface heat flux (Holton 1967) and variations of surface elevation (Lettau 1967, Mahrt and Schwerdtfeger 1969).

While nocturnal low-level wind maxima have been observed in many parts of the world (for a comparison of Wangara, Australia and O'Neill, Nebraska data see Mahrt 1980), they are especially remarkable in the Great Plains region of the United States. It is there also that the phenomenon has been most fully documented.

Strong, southerly jets over the Great Plains have been observed in all seasons, but especially in summer (Bonner et al. 1968, Bonner 1968). They are most frequent and generally better developed at night. The jet becomes most pronounced sometime between midnight and sunrise. The observed wind

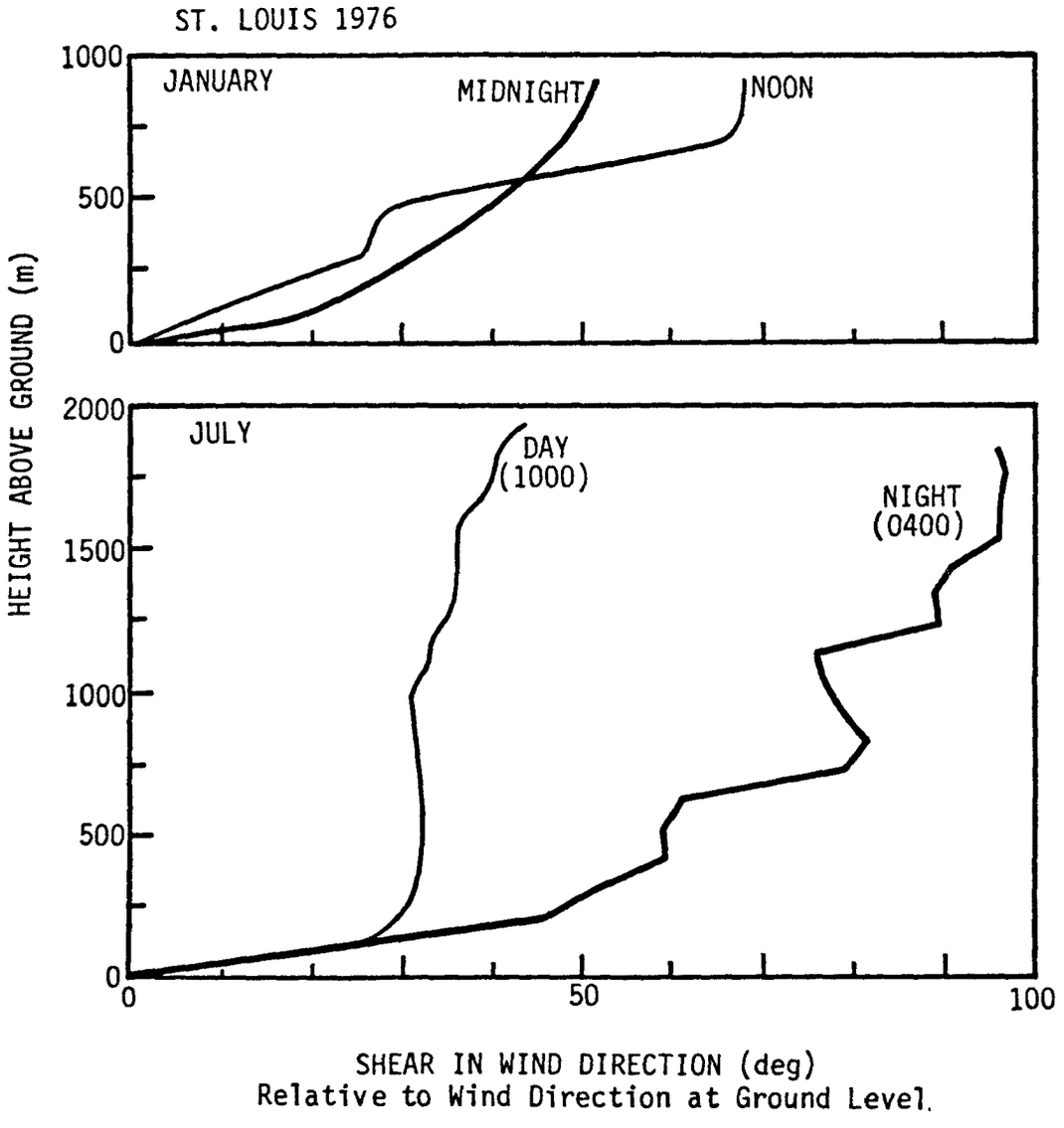

Figure 3-7. Monthly-average absolute change in wind direction with height relative to wind direction at ground level. Data are for July 1976 near St. Louis, MO.

speeds in the jets are frequently supergeostrophic. In their analysis of 10 selected cases over the Great Plains, Bonner et al. (1968) observed the peak speed to be, on the average, 1.7 times the apparent geostrophic speed, which ranged from 10 to 26 m s^{-1}, and the ratio was as high as 2.8 on one occasion. Measurements in Australia showed speeds at 300 m reaching 1.5 times the magnitude of geostrophic wind (Clarke 1970). Perhaps the most remarkable documented jet (on the night of March 18, 1918 at Drexel, NB) was characterized by speeds of up to 36 m s^{-1} (130 km h^{-1}) at a height of 238 m, while surface winds were at 3 m s^{-1}, and the geostrophic wind at about 10 m s^{-1} (Blackadar 1957).

Spatially, the diurnal inertial oscillation is believed to be a function of latitude (Thompson et al. 1976), being stronger at lower latitudes. The amplitude of the oscillation about the mean speed was just detectable in Minnesota, significant in Kansas (amplitude = 2 m s^{-1}), and more pronounced in Texas (2 to 3 m s^{-1}). Hering and Borden (1962) observed the average amplitude based on 6-hourly data of July 1958 in Fort Worth, TX and Shreveport, LA to be about 3.5 m s^{-1}. The average St. Louis data of July 1976 show the amplitude to be about 2 to 3 m s^{-1}.

Wind field measurements are routinely made in the United States at hourly intervals at several hundred ground stations. Rawinsonde measurements of upper air winds are made over a much sparser network, typically at 12-hr intervals, at noon and midnight GMT, or approximately early morning and early evening in the eastern United States. At some stations, 6-hourly soundings are made. Bonner (1968) studied the climatology of the lower-level jet based on the 6-hourly (if available) or 12-hourly data of 47 rawinsonde stations in the United States over a period of 2 years. The most relaxed criterion he used for the definition of a low-level jet was the occurrence of wind speed of at least 12 m s^{-1} in the boundary layer, and decreasing above by at least 6 m s^{-1} below a height of 3 km. His plots of the frequency distributions of low-level nocturnal jet occurrence in the United States east of the Rockies for the periods October through March (winter) and April through September (summer) are reproduced in Figure 3-8. Bonner's findings confirm the prominence of the Great Plains as the most likely region of these jets and that, in this region at least, nocturnal jets are more common and stronger in summer than in winter. He also found that the early morning period was preferred over daytime. From Kansas southwards the jets tend to be more southerly and in the northern plains more northerly. Between the Mississippi River and the Appalachian Mountains, the frequency of low-level jet observations drops off sharply. There is a second but much weaker maximum in frequency along the East Coast.

Presumably, St. Louis represents a borderline location as far as frequency and strength of nocturnal jets are concerned. Nocturnal jets are apparently much stronger west of St. Louis, and somewhat weaker to the east.

Bonner's plots also show a generally westerly flow in the states between Missouri and the Appalachians. The St. Louis wind direction data are shown in Figure 3-9 in the form of wind roses (wind direction frequency distributions) in 22 1/2° sectors for the winds at 500 m MSL (about 1000 ft above ground). By and large, the transport winds are southwesterly in summer

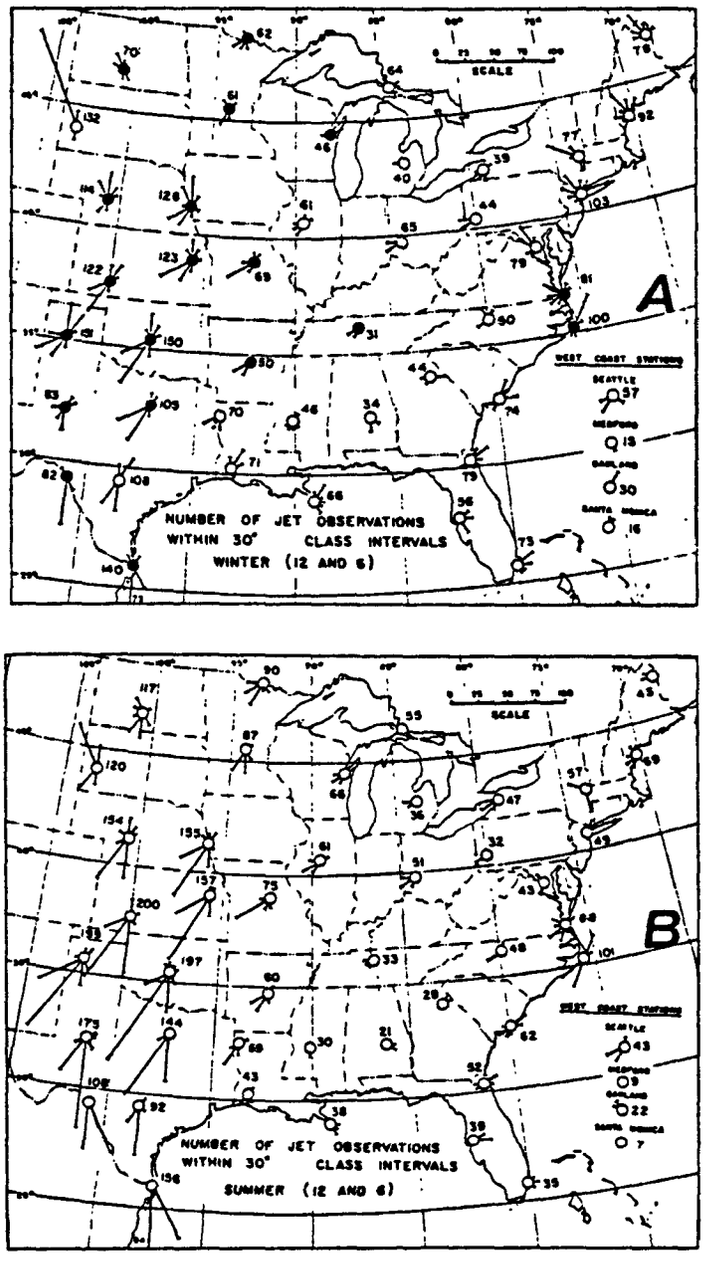

Figure 3-8. Frequency distribution of low-level jet observations within 30° class intervals of wind direction at the level of maximum wind. Distributions are for (A) winter months; October through March, and (B) summer months; April through September. Total number of jets observed during each season (over the two years) are given for each site. Black circles in (A) indicate stations with greater frequency of jets in summer than in winter. Adapted from Bonner (1968).

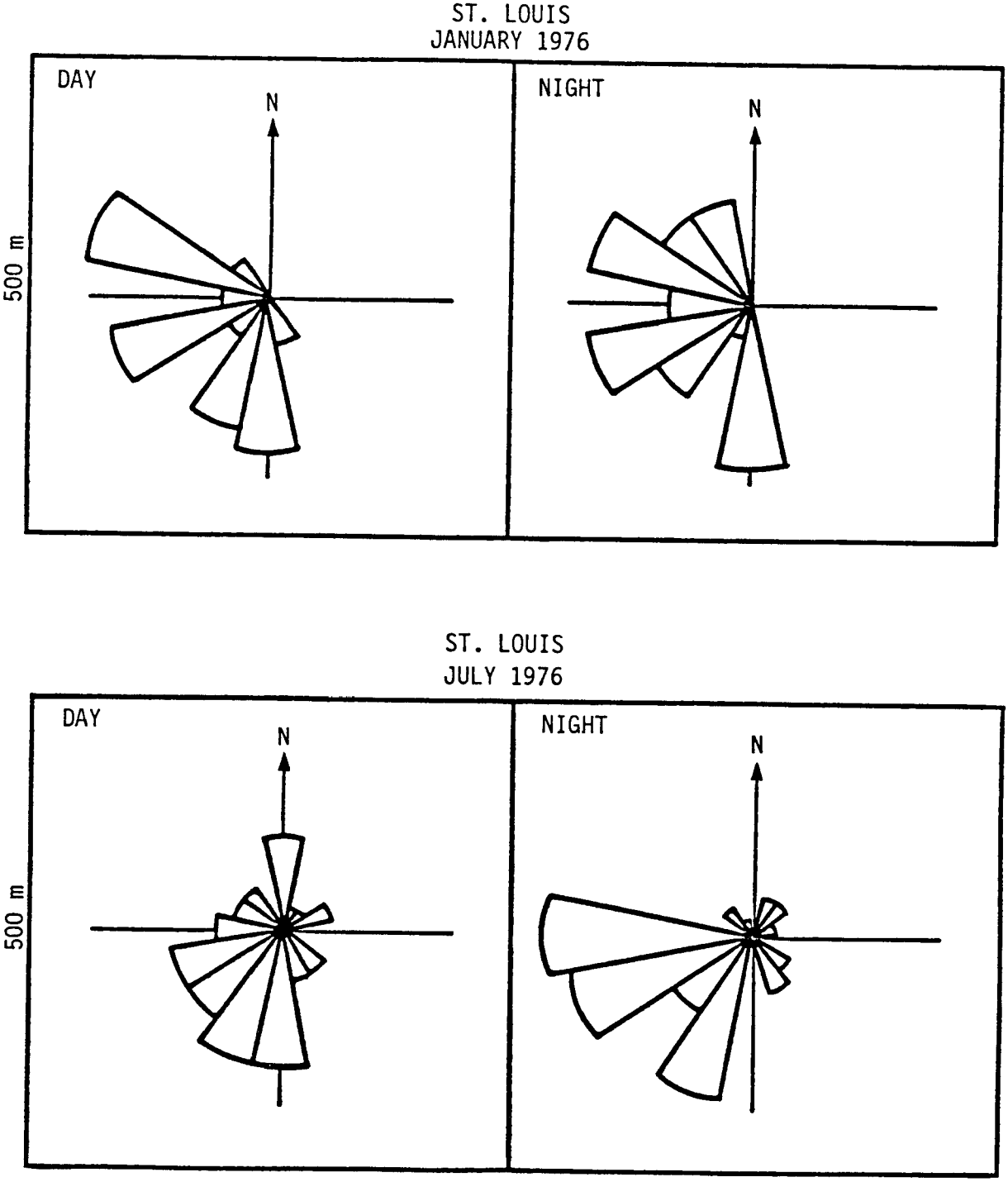

Figure 3-9. Monthly-average diurnal and seasonal variations of the frequency distribution of wind direction (wind rose) based on 500 m (MSL) wind data near St. Louis, MO, for 1976.

and westerly in winter, with northwesterly as well as southwesterly components.

The emphasis on St. Louis data in this chapter is not intended to claim its representativeness for eastern U.S. conditions. Primarily the choice was based on data availability and their broad diurnal and seasonal coverage. For a comparison of average seasonal St. Louis winds with those in other parts of the continent, the reader is referred to Figure 3-28 (Section 3.5) which shows a regional distribution of wind vectors at four levels over many U.S. rawinsonde sites. The seasonal averages in the regional wind plot include twice daily soundings at each site. For a comparison of average winds in Missouri and Ohio, the annual average (1960-64) wind roses at 1000 m MSL for the Columbia, MO and the Dayton, OH rawinsonde sites were also examined. Those wind roses (not presented here) indicate little difference in the evening soundings, and about 10 percent higher wind speeds at Columbia in the morning soundings. On the average, the wind direction over Columbia had a somewhat greater northwesterly component and somewhat smaller westerly component than over Dayton. The regional and seasonal distribution of the peak afternoon mixing heights are shown in Figure 3-29 and may be compared with the St. Louis data presented in Figure 3-5.

3.3.4 Effect of Mesoscale Complex Systems on Transport Layer Structure and Dynamics (N. V. Gillani)

Mesoscale complex systems are subdivided here into mesoscale convective precipitation systems and complex terrain-induced systems.

3.3.4.1 Effect of Mesoscale Convective Precipitation Systems (MCPS)--Among the mesoscale storm systems are air mass thundershower cells, frontal storms, squall lines, and mesoscale convective complexes. Such systems are characterized by significant vertical as well as horizontal motions. Lyons and Calby (1983) have recently summarized the effects of MCPS on polluted boundary layers.

In frontal zones where cold and warm air masses meet, warm air rises over cold air, and if sufficient moisture is present in the rising air, the formation of clouds and precipitation may occur. An advancing cold front may cause cold air to move under warmer air (Figure 3-10a), while in an advancing warm front, warm air will ride over colder air (Figure 3-10b). In each case, a frontal inversion forms atop the cold air layer. Horizontal convergence of surface flow into the frontal zone is also associated with such vertical motions. A pollutant plume reaching a frontal zone may be subjected to complex vertical motions, encounters with the liquid phase, and sharp changes of transport direction if it traverses into the other air mass. The situation is further complicated by the dynamic nature of fronts and by local interactions with terrain inhomogeneities. For example, squall lines form in frontal zones and are undoubtedly influenced by geographic features. They are also highly variable in space and time (Pielke 1981). Fritsch and Maddox (1980) have shown that the occurrence of these squall lines causes major alteration in the synoptic flow field. These areas of intensive cumulus convection can be tracked for days across the United States. Squall lines

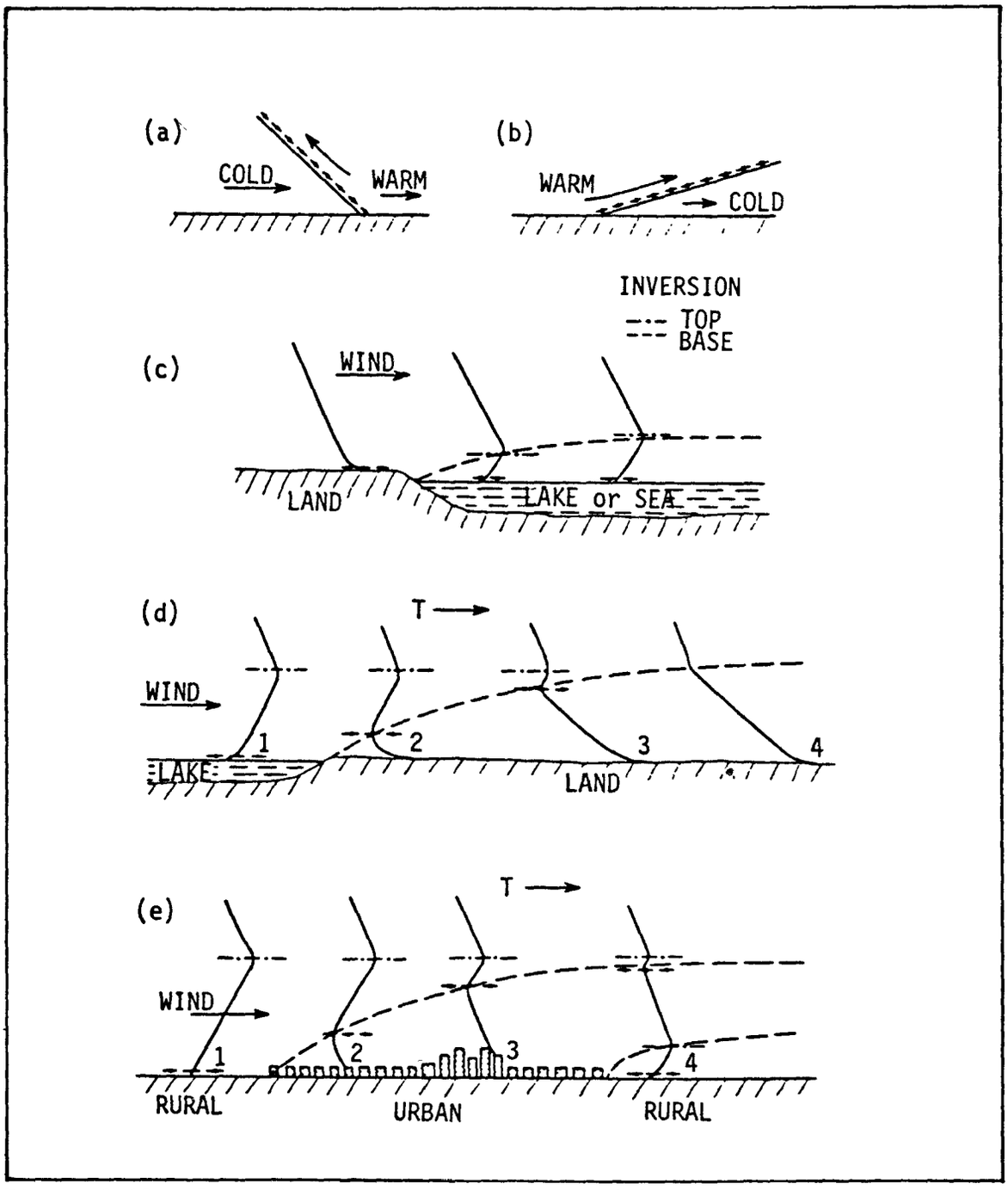

Figure 3-10. Inversions due to advection and internal boundary layer growth. (a) Frontal inversion caused by cold air wedging under warmer air (advancing cold front); (b) Frontal inversion caused by warm air overriding colder air (advancing warm front); (c) Modification of an unstable overland mixing layer within a growing stable internal boundary layer (dashed) over water during offshore daytime advection on a warm day (temperature profiles are shown); (d) Modification of a stable over-water inversion layer within a growing unstable internal boundary layer (dashed) over land during onshore daytime advection on a warm day; (e) The growth of an internal mixed layer (between dashed lines) due to urban heat flux into an otherwise stable nocturnal boundary layer. Adapted from Oke (1978).

that become stagnant over one area can produce devastating floods such as the one in Johnstown, PA in July 1977 (Hoxit et al. 1978).

Cloud processes in MCPS have a strong influence on PBL height, mean and turbulent flow and thermal structure, and pollutant distribution. The formation of cumulus clouds, like PBL growth, is related to vertical convection (e.g., see Manton 1982). The top of the mixing layer is an uneven and undulating interface, characterized by patches of mixed layer air extending into the quiescent layers above. The mixing layer is deepened by penetrative convection; i.e., individual thermals or updrafts that rise to the tops of these patches penetrate further into the upper layer (e.g., Mahrt and Lenschow 1976). Cumulus clouds form when rising moisture-laden air in updrafts finds its condensation level at or below the elevated inversion base. The latent heat released by the condensation of moisture generates strong convective currents within the clouds and causes them to expand upwards. Large storm clouds can grow to heights of several kilometers and can thus provide an avenue for boundary layer material to ascend to such heights.

Convective mesosystems ranging in size from large isolated cumulonimbus clouds to massive mesoscale convective complexes (MCCs) (Fritsch and Maddox 1981) profoundly alter the structure of the PBL out of which they evolve (Lyons and Calby 1983). The upward transport of PBL material in relatively compact supercell thunderstorm systems has been estimated to be on the order of 10 million metric tons per second (Mack and Wylie 1982). MCC storms are larger, with greater associated upward transport. Associated with such updrafts are compensating downdrafts around the clouds, large infusions of mid- and upper-tropospheric cold and clear air into the PBL, and surface mesoscale high-pressure regions. Such mesoscale vertical circulations were detailed by Byers and Braham (1949), and the production of the surface mesohighs were reported by Fujita (1959). The divergent surface mesohighs associated with the larger MCC storms occupy multi-state areas (Maddox 1980). Such mesoscale systems are also common over much of the eastern United States during the warm seasons.

Cloud venting of PBL pollutants has been discussed by Lamb (1981), Ching et al. (1983), and Lyons and Calby (1983). With satellite imagery, Lyons and Calby observed the development of a mesoscale "hole" of clean air in the PBL, embedded within a polluted air mass. They performed a case study of this event, and attributed its cause to several types of MCPS. The "hole" covered Virginia, Maryland, Delaware, northern North Carolina and extended more than 500 km out to sea. Within the "hole", daytime surface ozone levels were considerably depressed and visibility considerably enhanced. The "hole" existed for at least 36 hours. The authors used visibility data and assumed typical sulfate/visibility relations to estimate the total removal of sulfate in the development of the hole. This estimate ranged from 16 to 32 thousand metric tons of total sulfate removal in the MCPS area. Based on precipitation amount and "typical" precipitation sulfate concentrations reported in the literature for the area, the authors established an estimate for the likely fraction of sulfate removal attributable to wet deposition. The remainder was assumed to have been transported vertically by the clouds. The conclusion was that massive quantities of sulfate, perhaps two-thirds of

the total removal, may have been transported in thunderstorm updrafts to heights of 10 km or more.

Cloud venting of pollutants out of the PBL subsequently results in floating elevated debris when moisture supply to the cloud system terminates in the evening and the clouds finally dissipate. Such floating debris manifests itself as elevated haze layers, which have been observed frequently (over large areas of eastern United States, according to lidar measurements made during EPA's Project PEPE field study in summer 1980). Such floating debris is likely to have a long residence time in the atmosphere and may be brought down by downdrafts of future mesoscale systems. Cloud venting processes, and many other vertical motions, are largely ignored in current long-range transport process models. A highly sophisticated regional model, currently under development by EPA (Lamb 1981), aims to incorporate many such processes in the formulation. However, considerable further quantitative research is needed before adequate information is available to parameterize such processes.

Even nonprecipitating fair-weather cumuli play an important role in pollutant budgets. Cloud droplets provide the medium for rapid liquid-phase chemistry resulting in the transformation of precursor emissions to acidic products. Once formed, the aerosol products may have longer atmospheric residence time, hence farther range of impact. Gillani and Wilson (1983) have observed that when an elevated power plant plume is entrained into a growing late morning mixing layer capped by clouds, it passes en masse through the clouds, giving a rapid burst of aerosol formation. In the afternoon, such a plume becomes well-mixed in the mixing layer, and if scattered clouds still prevail at the elevated inversion base, the plume material is cycled into and out of such clouds, giving rise to additional aerosol formation. The period of such cycling may typically be about 30 to 50 minutes, with perhaps one-tenth of the time being spent in the cloud stage (Lamb 1981).

Cloud processes also influence PBL growth. By reducing ground level insolation and heating, clouds cause a decrease in surface heat flux and hence in PBL growth by penetrative convection. The downdraft of colder upper level air around clouds, injected into the sub-cloud layer, leads to the stabilization of the cloud base level layer in the region between cloud patches, thus tending to inhibit further cloud formation as well as further mixing layer growth in the cloud free areas (Garstang and Betts 1974). Reduction of insolation by clouds also inhibits photochemical reactions involved in the processes of chemical transformation of precursor emissions to acidic products.

Mesoscale convective systems cannot be adequately resolved spatially or temporally by the existing upper air weather monitoring network. Nor can the denser monitoring network of surface winds adequately fill the gap, particularly with respect to vertical motions. Errors once introduced in long-range trajectory calculations as a result of inadequate treatment of the mesoscale flow will, of course, be simply amplified during subsequent simulation. Uncertainties in such trajectory calculations must be recognized and assessed through special field measurements aimed at characterizing and parameterizing mesoscale flow systems. A number of mesoscale observational programs have

probed into such mesoscale phenomena (e.g., Project SESAME, Lilly 1975, Alberty et al. 1979; Project GATE, Zipser and Gautier 1978, Frank 1978; and Project VIMHEX, Betts et al. 1976), while a Prototype Regional Observing and Forecast Service (PROFS, Beran 1978) has proposed development of a mesoscale forecast service, initially for the Denver area.

3.3.4.2 Complex Terrain Effects--Surface inhomogeneities in terrain roughness, height, and heat and moisture fluxes can perturb the downwind condition of the existing atmospheric boundary layer. The perturbed layer, originating at the surface source of the disturbance, grows upward with increasing downwind distance and constitutes an internal growing boundary layer within the outer existing boundary layer. Such mesoscale perturbations are most commonly encountered in shoreline environments, downwind of urban complexes or other heterogeneous land use sites, and in hilly or mountainous regions. The internal boundary layer may be characterized by altered mean flow field, mechanical turbulence, stability, or a combination of any of these changes. Examples of inner boundary layer growth are shown in Figure 3-10 (c,d,e) for offshore and onshore flows at land/sea interfaces, and for flow past an urban complex. These examples are for relatively strong upwind flow (i.e., the undisturbed synoptic flow). In such cases, the effects of the disturbances are transported along in a growing internal boundary layer until they weaken and become indistinguishable within the outer boundary layer. Under weak synoptic flow conditions, the effects of the disturbances are not thus stretched out far downwind, but are trapped in localized recirculating flow patterns dominated by the nature of the disturbance. In such cases, pollutant accumulation is likely.

3.3.4.2.1 Shoreline environment effects. The continental United States (excluding Alaska) has about 16,000 miles of coastline (including the Great Lakes). The Great Lakes cover 95,000 square miles and have a shoreline of nearly 3600 miles. About 15 percent of the United States population, over 60 percent of the Canadian population, and even larger fractions of U.S. and Canadian national industrial activities are concentrated in the Great Lakes Basin (Lyons 1975). A large number of power plants and several major urban complexes dot the shoreline of the Great Lakes. Large bodies of water undergo far fewer diurnal and seasonal variations in temperature than do the surrounding lands. Also, the water surface is relatively smooth. Turbulence and mixing depths over water are thus considerably different from those over land. Because of these sharp differences in thermal and mechanical features, the potential exists for extreme mesoscale air mass modifications in shoreline environments. Only a brief outline of some of the major effects of coastal flows on pollutant transport is given here. For a more detailed review of this subject, see Lyons (1975), Hunt and Simpson (1982), and Pielke (1981).

During the "warm" season, as warm and well-mixed air flows offshore over the cooler water surface, intense stabilization occurs, giving rise to a low-level inversion that decouples the warmer air aloft from the water surface (Figure 3-10c). Pollutants from elevated sources in such cases may be transported over water for long distances without any deposition. In contrast, during periods of cold air advection over warmer water in the "cold" season, a stable air mass can be rapidly transformed to a growing

boundary layer of neutral or slightly superadiabatic lapse rate. As a result, the mixing depth and diffusion may increase, and also snow squalls frequently develop. Shoreline plume releases may be fumigated to the water surface more quickly than inland plumes are fumigated to the land surface.

Of greater interest is the behavior of shoreline plume releases during onshore flow conditions (Figure 3-10d). During the warm season, the land is warmer than the water during the day. Even in July, it is common to find pools of cold water (4 C) at the center of the Great Lakes. Sharp temperature gradients exist in a narrow band of warmer near-shore water. An airstream blowing toward land and already stabilized by long passage over water is subjected to internal boundary-layer growth as it passes over the warmer surfaces during the daytime. Within this boundary layer, the air becomes unstable and conducive to rapid mixing. Above, the air is relatively stable. Emissions released from short-stack sources at the shoreline will become trapped within this internal boundary layer and rapidly brought to ground. Emissions from tall stacks, however, may be transported inland in the stable layer aloft for many kilometers until the boundary-layer growth reaches the plume height. Subsequently, the elevated plume will be fumigated to the ground. Because the internal boundary layer may be present for many hours in the daytime, continuous elevated source emissions may continue to be fumigated for several hours, thus creating potentially high doses of local pollutants. Similar elevated emissions farther inland would be released in the convective daytime mixing layer and would be rapidly mixed vertically within a short distance from the source.

Analyzing onshore flows under weak synoptic flow conditions is far more complex in the presence of recirculating land, sea, or lake breezes, which are caused by the thermal gradients between land and water. An excellent qualitative description of the diurnal variations of coastal circulations during weak synoptic flows is given by Defant (1951). In the daytime, the land surface is warmer and causes the air above to rise. Colder air from the sea flows onshore to fill the void. The risen air over the land then flows offshore and sinks over water. A vertical circulation with a sea breeze near the surface is thus established if the prevailing synoptic winds are weak. At night, the air over the sea is warmer, and the situation is reversed, with an offshore land breeze. An example of the lake breeze recirculation observed by means of the trajectory of a balloon launched at the Chicago shoreline is shown in Figure 3-11. In the case of a coastal urban area with a high emission density, pollution levels can become quite elevated during a lake breeze due to the recirculation effect. During the lake breeze, an elevated emission can be released in the upper offshore air flow and be blown back in the lower level onshore flow of the circulation. Land and sea breezes play a particularly important role in local air pollution climatology in locations such as the Los Angeles basin, where significant blocking effects of complex terrain are also present.

Numerous observational studies of coastal circulations and precipitation have been made. A sampling of these includes Day (1953), Gentry and Moore (1954), Plank (1966), and Burpee (1979) for the Florida coast; Lyons (1975) and Keen and Lyons (1978) for the Lake Michigan coast; Hsu (1969) for the Texas coasts; Neumann (1951) and Skibin and Hod (1979) for Israel; and Johnson and

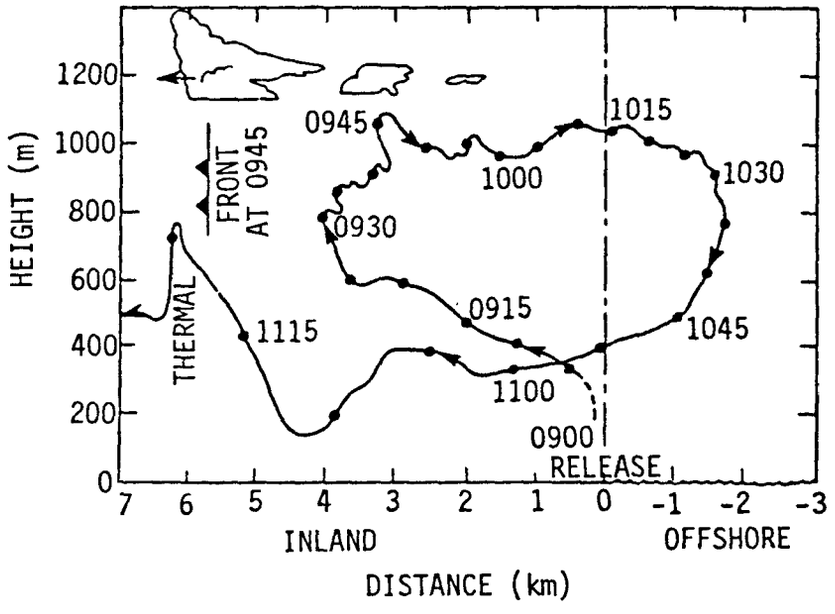

Figure 3-11. Side view of the trajectory of a balloon launched at 0900 hr on 12 August 1967 at the Chicago shoreline of Lake Michigan. Positions of the balloon are plotted every 5 min. Also shown are the positions of the lake breeze front at 0945 hr and of prevailing clouds. Adapted from Lyons and Olsson (1973).

O'Brien (1973) for the Oregon coast. These studies have demonstrated that transport, and diffusion and precipitation patterns are significantly altered in the coastal zone, and that such mesoscale circulations are poorly resolved in conventional weather-observing network systems, thus creating a serious problem in developing routine operational forecasts of mesoscale phenomena. Analytical and numerical models of mesoscale systems, based on field data of special studies, are thus particularly important. Early model studies were based on linearized analytical simulations (e.g., Defant 1950, Kimura and Eguchi 1978). Nonlinear numerical models were at first two-dimensional (e.g., Estoque 1961, 1962; Pielke 1974a; Estoque et al. 1976). With extended computer capabilities in the last decade or so, three-dimensional numerical models are now possible and provide valuable new insight (e.g., Pielke 1974b, Warner et al. 1978, Carpenter 1979). For a complete review of mesoscale numerical modeling, the reader is referred to Pielke (1981).

3.3.4.2.2 Urban effects. As in the case of coastal circulations, urban-induced circulations are primarily due to the differential heating and cooling between urban and rural areas. Indeed, this phenomenon is commonly referred to as the urban heat island effect. The urban area also represents rougher terrain and a source of enhanced mechanical turbulence (automobile traffic also contributes to this effect). Moisture fluxes may also be greater in the urban area.

The most direct evidence of the heat island concept is the observed higher air temperatures in the urban areas, on the average, than in rural areas (Chandler 1970, Clarke and McElroy 1970, Landsberg 1956, Oke 1974). Matson et al. (1978) used satellite imagery to illustrate maximum urban-rural differences ranging up to 6.5 C in the midwestern and northeastern United States on a particular summer day. Price (1979), using high resolution statellite imagery, estimated this difference to be as high as 17 C for New York City--a value considerably higher than those estimated from surface-based air temperature measurements. His explanation for the apparent discrepancy is that the satellite sensing includes industrial areas, rooftops, as well as the trapping of energy within urban canyons (Nunez and Oke 1977), which are not sensed by surface observations. Numerous other studies of the urban heat island have been based on satellite and surface-based observations, as well as on numerical calculations. Many of these are reviewed by Pielke (1981) and by McBean et al. (1979, Chapter 6). In particular, the St. Louis area has been studied extensively as part of the RAPS and METROMEX programs (a series of articles in the May 1978 issue of the Journal of Applied Meteorology was devoted to results of Project METROMEX).

The urban heat island effect is most pronounced at night under weak synoptic flow conditions. The rise of heated air over the city is compensated by a radial and horizontal convergence of flow into the urban area near the surface. A vertical circulation is completed when the risen air flows outwards, then subsides over the rural areas, and recirculates to the urban source near the surface. Such a recirculation traps urban pollution emissions when the larger-scale flow is weak. When the outer flow is strong, the urban boundary layer is stretched out downwind (Figure 3-10e) rather than closed and recirculating. The inflow velocity in the recirculating heat

island flow is typically about 1.0 m s^{-1} in New York City (Bornstein and Johnson 1977) and about 0.4 m s^{-1} in St. Louis (Schreffler 1978). There is also apparently a tendency for anticyclonic turning in this convergent inflow (Bornstein and Johnson 1977, Lee 1977). The heating within the nocturnal urban heat island also produces a local unstable mixing layer deeper than the rural mechanical mixing layer. Oke (1973) concluded that the heat island effect of a city on the surroundings under cloudless skies is inversely proportional to the large-scale wind speeds, and directly related to the logarithm of the urban populations.

Quite apart from the local stability and circulation changes due to the urban area, the emission of primary fine aerosols and the secondary generation of aerosols during downwind transport of urban plumes can produce significant haziness and reduction of incoming solar radiation (White et al. 1976, Viskanta et al. 1977). There is also evidence of the effect of large urban areas on climate and weather. Project METROMEX (1976) results indicate preferred regions of thunderstorm development downwind of urban areas.

3.3.4.2.3 Hilly terrain effects. Hills and mountains alter local atmospheric flows in two ways--by physically blocking or channeling the flow, and by adding a secondary thermally-induced flow resulting from differential heating of the surface and the free atmosphere at the same elevation (above mean sea level). Complex terrain effects are particularly important for urban and industrial complexes in river valleys and in coastal and inland plains backed by mountains. Denver and Los Angeles are good examples. Emissions from tall stacks in mountainous terrain may impinge upon the elevated ground after only short-range transport. Stagnation in blocked flows (e.g., Los Angeles) can lead to high levels of secondary pollution. Also, mesoscale modifications of pollutant flow trajectories past mountainous terrain (e.g., the Appalachians) cannot be ignored in an assessment of long-range transport when the source and the impacted regions are separated by a mountain chain.

In the discussion below, certain important features of complex terrain flows are highlighted. More detailed reviews are given by Egan (1975), Pielke (1981), and Hunt and Simpson (1982).

The principal features of the primary flow in and immediately upwind and downwind of the complex terrain will be determined largely by the shape and size of the obstruction, the strength and direction (relative to the orientation of the obstruction) of the oncoming flow, and by the stratification (stability) of the undisturbed upwind boundary layer. There will naturally be preferential and accelerated flow through mountain gaps and passes. When the flow can neither go over or around the obstruction because it is too slow or stable, blocking will occur, with propagation of effects upwind. Such damming effect of the Southern Appalachians is discussed by Richwien (1978).

The flow of a neutrally stratified atmosphere with an elevated inversion atop (the typical daytime mixing layer) past a two-dimensional obstruction (i.e., perpendicular to the flow) of height H less than the mixing height h is illustrated in Figure 3-12 for low (a) and high (b) wind speeds. In each

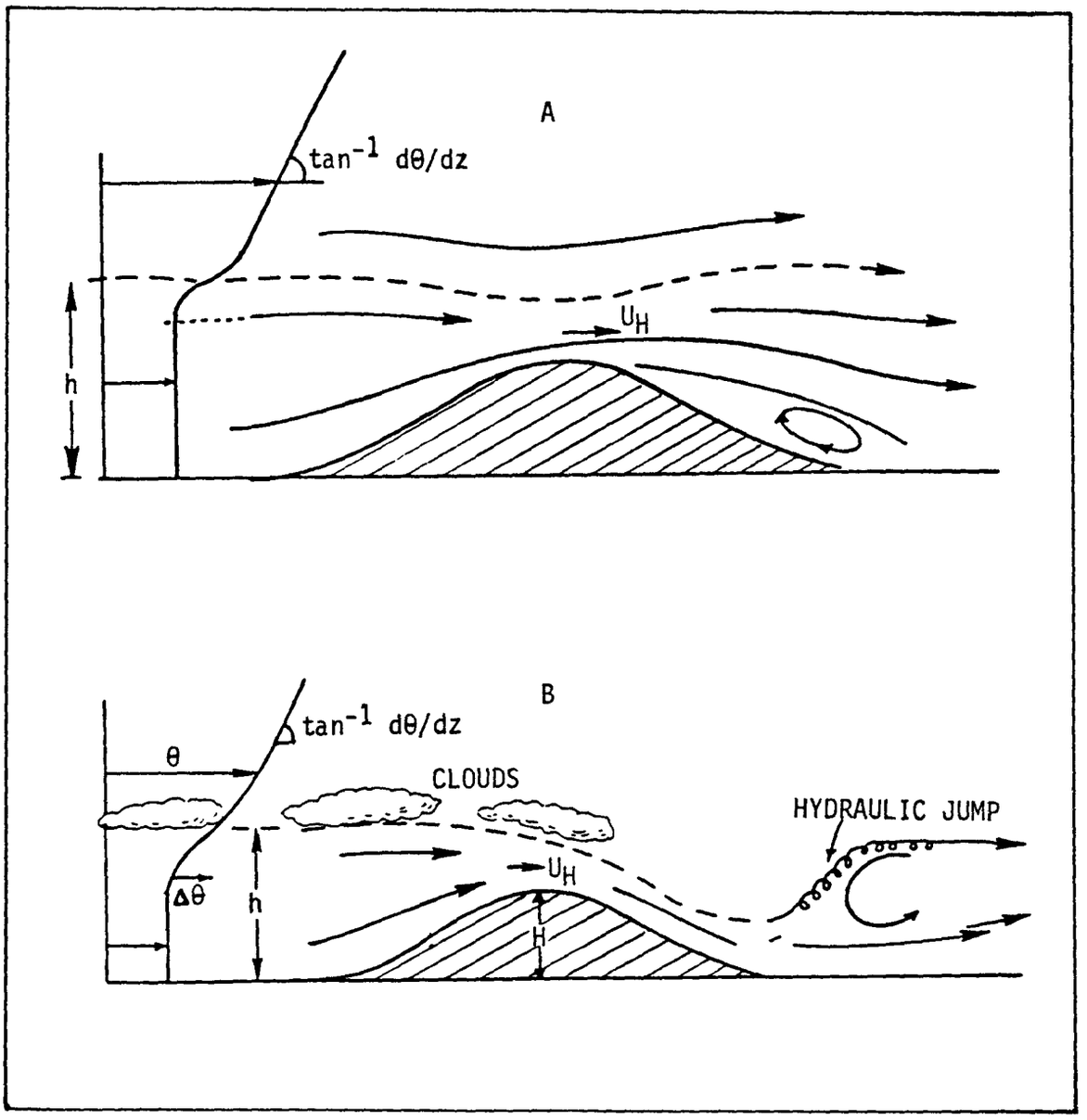

Figure 3-12. Air flow over a two-dimensional ridge with an elevated inversion upwind.
(A) Case of low wind speed; separation can occur downwind.
(B) Case of high wind speed; mixed layer flows down lee side; no separation; hydraulic jump downwind. Adapted from Hunt and Simpson (1982).

case, as the flow ascends the windward slope, it accelerates, and the elevated inversion drops somewhat. If the upwind slope is steep, a captive recirculating eddy may form at the base of the slope. The leeward flow pattern is generally more complicated. Depending on the speed of the flow and the leeward slope of the hill, flow separation may occur downwind, and separate the main flow above from a captive recirculating eddy below (a). The wavy nature of the main flow field can persist for a significant distance downwind and can even generate additional secondary eddy motions downwind. For increasing oncoming wind speeds, the downward displacement of the elevated inversion base increases until, under an appropriate combination of the flow speed, atmospheric stability, and obstruction height, the whole mixed layer may flow down the lee side of the hill, producing a highly turbulent and sometimes recirculating flow (b). Such a wind is known as the chinook or foehn. Lilly and Zipser (1972) observed wind gusts of about 50 m s^{-1} associated with a chinook immediately downwind of the Rockies. With the downwind displacement of the warmer inversion layer air, such a flow is often also associated with some warming of the lower elevation air on the leeward side. At some point downwind, the mixing layer will return to its prevailing larger-scale condition by rapid dissipation of the mean kinetic energy through a phenomenon known as the hydraulic jump. Considerable mixing and dilution is associated with the hydraulic jump, while captive recirculating eddies represent localized stagnant flow. The atmospheric residence time, dilution, and overall trajectory of pollutants in such flows is significantly influenced by these mesoscale features. Also, the forced lifting of moist air on the upwind slopes causes condensation and precipitation, while comparatively dry air flows on the lee side. Such orographic rainfall can be responsible for significant localized acidification (OECD 1977).

When the flow is three-dimensional around isolated or clustered hills, the flow may also go around the obstructions. The flow field on the lee side is generally even more complex in such cases. The relative split between the flow around and over the obstruction will depend not only on the height of the obstruction and the free flow speed, but also significantly on free flow stability. The greater the stability, the less will be the likelihood of flow going over the hill.

Thermal or mountain-valley winds result from the unequal heating and cooling of the terrain surface at different heights. Consequently, such secondary flows exhibit a strong diurnal variation. During the day, the higher terrain becomes an elevated heat source, while at night it is an elevated heat sink. In the day, heated air rises from the higher terrain drawing compensating upslope flow. A vertical circulation may be completed by sinking air motion to the valley floor. At night, the reverse situation prevails, with nocturnal drainage down the slope. These daytime upslope and nocturnal drainage flows are also called anabatic and katabatic winds, respectively. In a closed valley, a recirculating flow pattern may be established by such mountain-valley winds, and if a pollutant source emits into this flow, considerable accumulation can occur. A number of observational and modeling studies of complex terrain flows have been reviewed by Pielke (1981).

3.4 MESOSCALE PLUME TRANSPORT AND DILUTION (N. V. Gillani)

Mesoscale plume transport and dilution are influenced by the height of plume release and the configuration of the source, as well as by transport layer structure and dynamics. Two principal types of source releases are of special concern: stationary elevated point-source releases, and near-ground releases from an aggregate of sources in a broad area such as an urban-industrial complex. In the eastern United States, about 92 percent of the anthropogenic SO_2 emissions are due to fossil fuel combustion, with about 70 percent from power plants, many with tall stacks. Automobiles emit little sulfur. In contrast, NO_x emissions in the United States are almost equally due to automobiles, electric utility sources, and industrial fuel combustion (Husar and Patterson 1980; see also Chapter A-2). Thus, while most SO_2 is emitted from elevated sources, NO_x emissions are more evenly distributed between elevated and low sources. On the average, elevated releases spend a substantial fraction of their mesoscale transport time decoupled from the ground sink, while near-ground releases maintain continuous ground contact. Important diurnal and seasonal patterns of dry deposition, attributable directly to variations in the transport phenomena, exist for both types of sources.

3.4.1 Elevated Point-Source Emissions (Power Plant Plumes)

The proliferation of tall stacks in the eastern United States in the past two decades was motivated primarily by the regulatory requirement for abatement of ground-level concentrations of SO_2 from large emission sources such as central power-generating stations (Thomas et al. 1963). That tall stacks were largely successful in this objective is quite evident (Pooler and Niemeyer 1970). At the same time, however, taller stacks and greater thermal effluxes from them may have resulted in increased atmospheric residence times for pollutant emissions. In turn, farther distribution of the emissions and increased formation of secondary products may be occurring. Tall stacks no doubt result in substantial reductions in ground losses during short-range transport. But source height is unimportant once the plume becomes well mixed vertically in the mixed layer. The extent to which tall stacks increase pollutant residence time during long-range transport and result in increased secondary formation and deposition has not yet been fully resolved. Results of some new and previously unpublished analyses pertaining to this question are presented in this chapter.

The Ohio River Valley (ORV) region is well known to have a large concentration of central electrical power-generating stations burning fossil fuels, particularly coal. In a recent study of trends related to power plant stack heights and SO_2 emissions in this region, Koerber (1982) focused attention on power plants with a generating capacity greater than 50 MW, and located in a two county row on both sides of the Ohio River in Illinois, Indiana, Ohio, Kentucky, West Virginia, and Pennsylvania. A total of 62 such power plants were operational there between 1950 and 1980. Figure 3-13 (top) shows the trend of total SO_2 emissions from the study plants during the 30 year study period. Nearly a ten-fold increase in generating capacity was realized during this period. Figure 3-13 (bottom) shows the corresponding trend of SO_2 emissions broken down by stack heights. In 1950, more than 75 percent

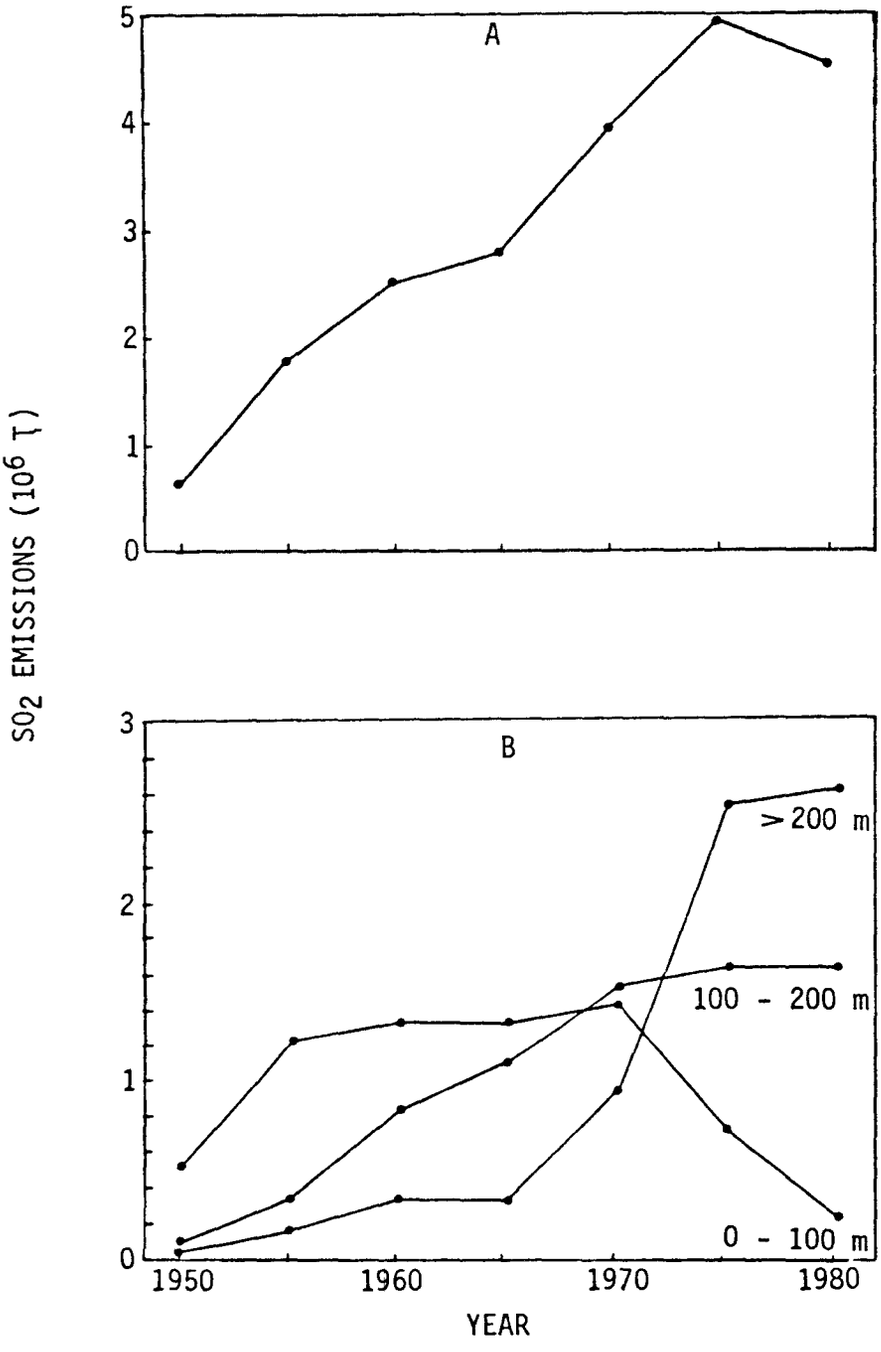

Figure 3-13. Trend in emissions of SO_2 from 62 study power plants in the Ohio River Valley:
(A) Total tonnage;
(B) Tonnage breakdown according to specified physical stack height intervals.
Adapted from Koerber (1982).

of the SO_2 emissions were from stacks lower than 100 m, most of the remainder being from stacks between 100 and 200 m tall. By 1980, less than 5 percent of the SO_2 emissions were from stacks lower than 100 m, while nearly 60 percent of the emissions were from stacks taller than 200 m. Of the 62 stacks in 1980, 32 were taller than 244 m (800 ft.), and 11 were superstacks of 305 m (1000 ft.) height or taller. The average stack height, based on weighting with respect to SO_2 emissions, increased from under 100 m in 1950 to about 225 m in 1980. The ORV study area is quite representative of the corresponding picture for the United States and Canada, as a whole. In the latter case, more than 90 percent of the SO_x emissions from major point sources during 1977-78 were from stacks higher than 100 m, about 63 percent from stacks taller than 200 m, and about 38 percent from superstacks taller than 300 m (Benkovitz 1982). It is interesting to note, however, that relatively little of this national increase in stack heights occurred in the northeast coastal states, where the average height of major point source stacks remained close to 100 m (Benkovitz 1982).

The range over which an elevated emission maintains its identity is highly variable. Tall-stack emissions may be brought down to ground and mixed rather uniformly throughout a deep daytime mixing layer within just a few kilometers of the source (Figure 3-14, top), or they may remain elevated, coherent, and decoupled from the ground for hundreds of kilometers at night and in winter (Figure 3-14, bottom). Such diverse plume dispersion is due to the pronounced vertical stratification in the transport layer structure (unstable mixing layer versus stable layers aloft), and the enormous diurnal and seasonal variations in PBL dynamics. Vertical plume spread is caused predominantly by atmospheric turbulence; turbulence continues to play a vital role in plume dilution long after the plume fills up the peak daytime mixing layer, and loses its source identity. Horizontal plume spread by turbulent diffusion, on the other hand, is mostly significant only during initial transport, i.e., until the plume is a few kilometers wide. Increasingly, wind shear and veer effects, and wind shifts, become the principal mechanisms of horizontal spread. As a well-mixed daytime plume journeys into night, it may become sheared into multiple layers moving off in different directions. The next day, as the mixing layer grows, each higher layer is entrained in turn and diluted over the entire height of the mixing layer by turbulent vertical diffusion. This process of nocturnal horizontal shearing followed by daytime vertical dilution may be repeated through successive diurnal cycles and is most probably the mechanism whereby individual large plumes are homogenized rather quickly into the regional background.

The vertical and temporal features of the transport and dispersion of a tall-stack plume during a typical hot and humid midwestern U.S. summer day are illustrated in Figure 3-15. The emissions represent the 0700 hr release on 23 August 1978 from the two identical 305-m stacks of the Tennessee Valley Authority's (TVA) Cumberland Steam Plant (2600 MW generating capacity) in rural northwestern Tennessee. Such multiple stack emissions typically become mixed and indistinguishable rather quickly. The buoyancy of the efflux led to a plume rise that resulted in an effective stack height (physical stack height plus plume rise) of about 500 m and an initial plume spread in excess of 100 m vertically. The bent-over plume was then transported in a stable environment at this height in relatively coherent form until the rapid

Figure 3-14. (TOP) Rapid vertical dispersion of a tall-stack plume within a midday unstable mixing layer in the summer. Such a plume is typically brought down to ground within a short distance from the source.

(BOTTOM) Transport of a coherent tall-stack plume in an elevated stable layer during winter. Such a plume has a significant likelihood of remaining aloft over long-range transport.

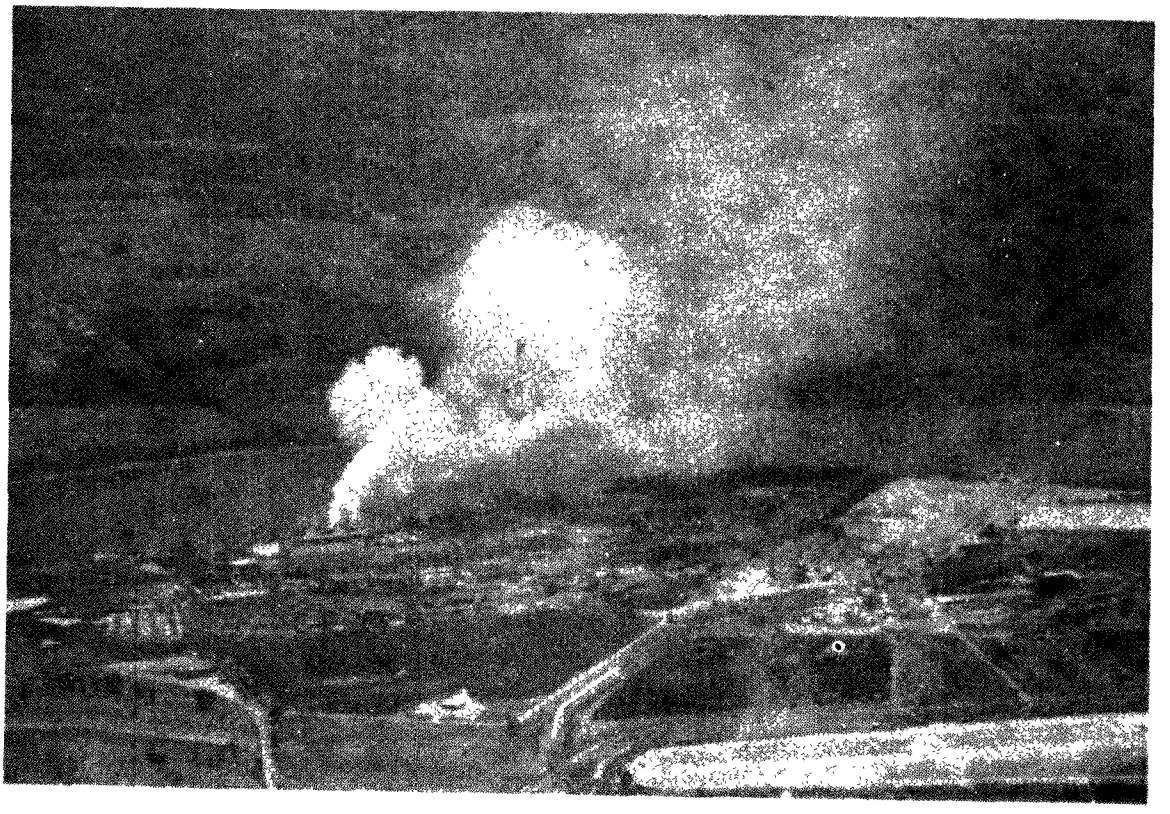

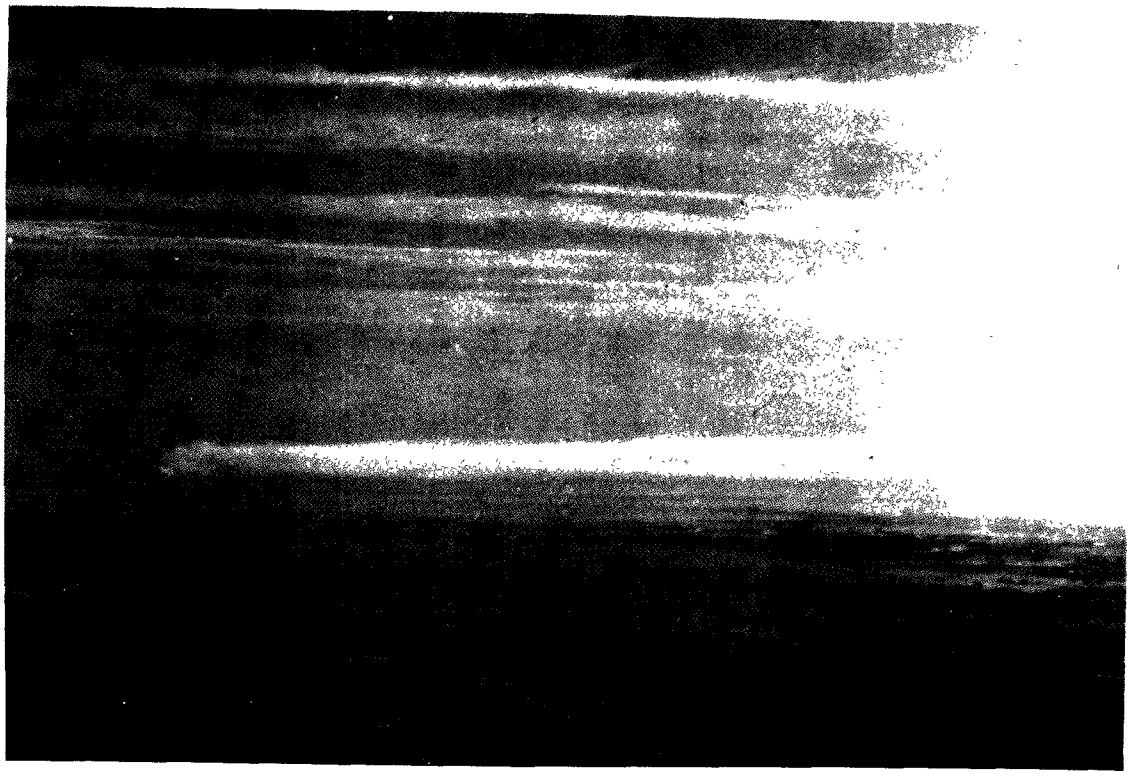

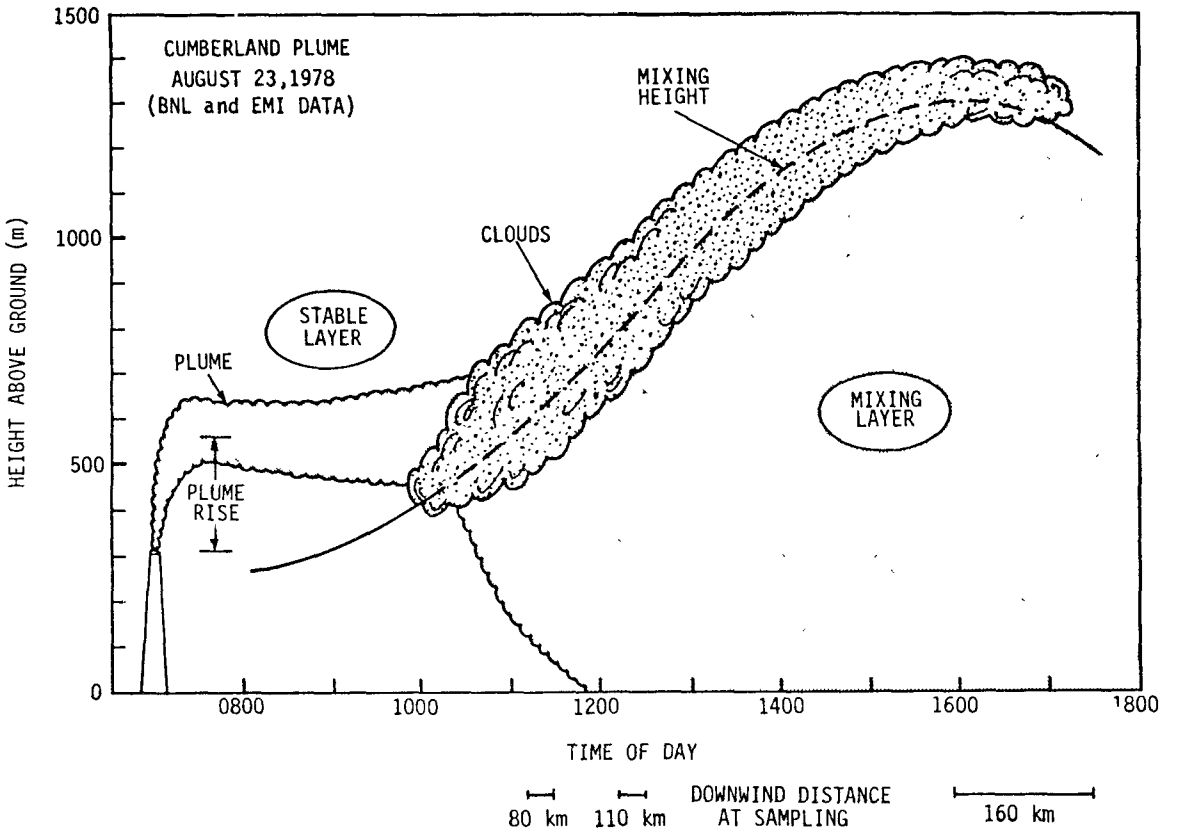

Figure 3-15. The physical behavior of a tall-stack plume on a rather typical summer day. The plume shown is the reconstruction of the Lagrangian transport of the 0700 release on 23 August 1978 from the 305 m tall stacks of the 2600 MWe Cumberland Stream Plant in northwestern Tennessee. The reconstruction is based on aircraft sampling, ground-based lidar returns, and tetroon transport data (Gillani and Wilson 1983).

midmorning rise of the unstable mixing layer reached and exceeded the plume height. Entrainment into the mixing layer followed, subjecting the plume to vigorous mixing and rapid spread. Within about 1 hour, plume touchdown occurred on the ground, and ground removal of the pollutants by dry deposition began. The plume quickly filled the entire mixing layer following entrainment, becoming rather uniformly spread out in the vertical domain. Thereafter, pollutant concentration, and hence the rate of ground loss, varied inversely with the mixing height. The plume continued to dilute until the mixing height reached its peak value in the midafternoon. Subsequently, as the mixing intensity diminished and the mixed layer collapsed, the plume remained diluted, with its top at the height of the peak daytime mixing height. If any further upward dilution occurred, it must have been small. In the evening, with the formation of the nocturnal, surface-based inversion layer, the bulk of this daytime plume (except the bottom part in the shallow nocturnal, mechanical mixing layer) presumably became decoupled from the ground sink (no data was taken after 1800 hr). During the night, if the nocturnal jet developed (as it frequently does), this bulk probably experienced relatively rapid transport, as well as considerable shearing spread and distortion.

In the example described above, convective clouds also developed at the elevated inversion base during midday. Direct evidence of substantial plume-cloud interaction, particularly during plume entrainment into the mixing layer, was observed; this interaction was accompanied by significant in-cloud chemistry (Gillani and Wilson 1983, Gillani et al. 1983). Such fair weather cumulus formation is fairly common in the eastern United States on summer days, being more common in the southern half of the eastern United States than it is in the north. Elevated nocturnal plume releases that do not rise sufficiently high and become entrained before such cloud formation begins may experience no interaction with clouds during entrainment.

The reconstruction of the physical evolution of the example plume was based on aircraft data and on ground-based lidar data. It illustrated the "Lagrangian" transport of a particular plume release (the 0700 hr Cumberland plume release of 23 August 1978) in terms of variations in the time-height plane. The lidar data (Figure 3-16) were collected by the Stanford Research Institute (SRI) lidar (Uthe et al. 1980)--a laser-radar system operated from a mobile van. In this system, a laser beam is fired at equal intervals of travel distance (horizontally under the plume section in the crosswind direction, in the samples shown), and the lidar returns (backscatter of the beam by atmospheric aerosols) are processed into these visual images. Dense aerosol layers (e.g., the plume and clouds) appear whiter than the background, as does the more polluted mixing layer, in contrast to the cleaner stable air farther aloft. As the laser beam penetrates a cloud, it becomes attenuated; black bands thus appear above the point of total beam extraction. In the pictures the letter C identifies a cloud, P refers to a plume, and T denotes the top of the mixing layer. The time frame of the measurements is marked atop each picture. In the example shown, the lidar was in operation about 30 km downwind of the power plant.

In Figure 3-17, "Eulerian" views of the plume vertical cross sections at a fixed downwind distance (35 km) from the Cumberland stacks are illustrated at

Figure 3-16. SRI lidar photographs showing the structure and dynamics of the boundary layer and the Cumberland power plant plume, 30 km downwind of the source, on 23 August 1978. (P=plume, C= cloud, T=top of mixing layer.) Adapted from Gillani and Wilson (1983).

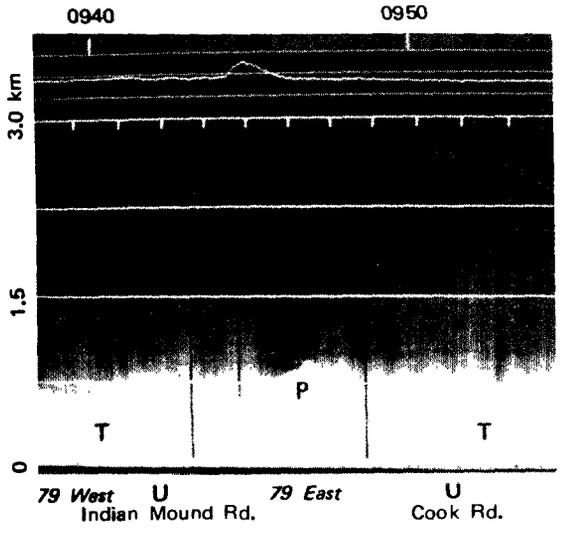
0940
0950
3.0 km
1.5
0
P
T
T
79 West
U
79 East
U
Indian Mound Rd.
Cook Rd.

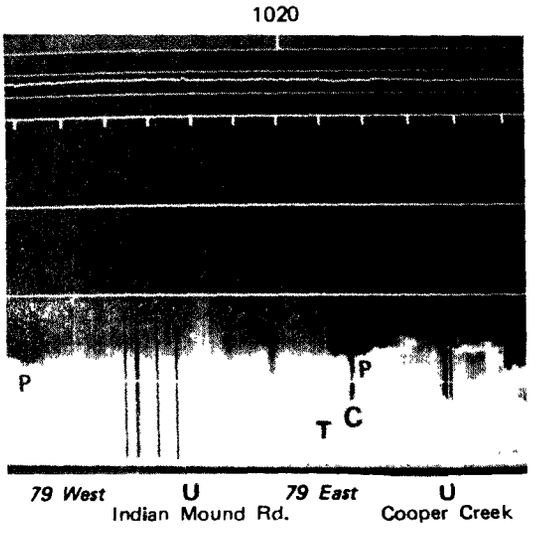
1020
P
P
T
C
79 West
U
79 East
U
Indian Mound Rd.
Cooper Creek

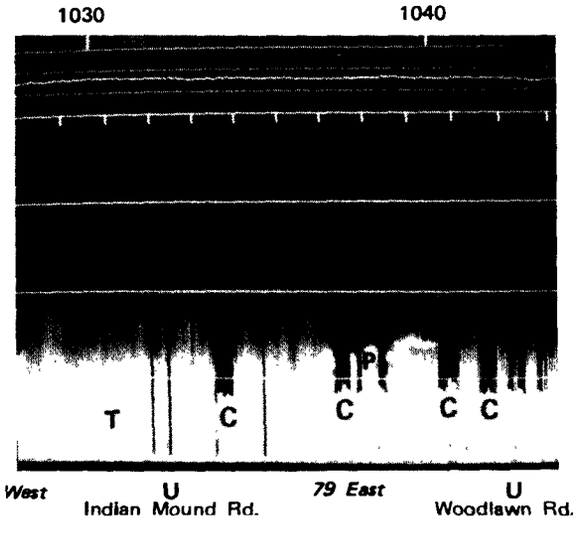
1030
1040
T
C
C
C
C
West
U
79 East
U
Indian Mound Rd.
Woodlawn Rd.

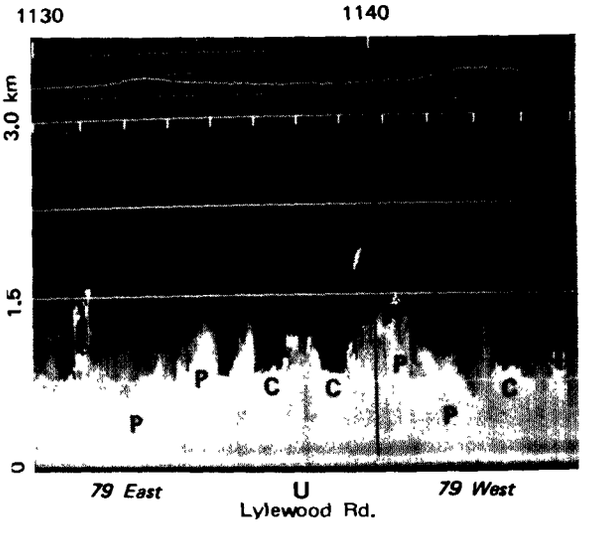
1130
1140
3.0 km
1.5
0
P
P
C
C
P
C
P
79 East
U
79 West
Lylewood Rd.

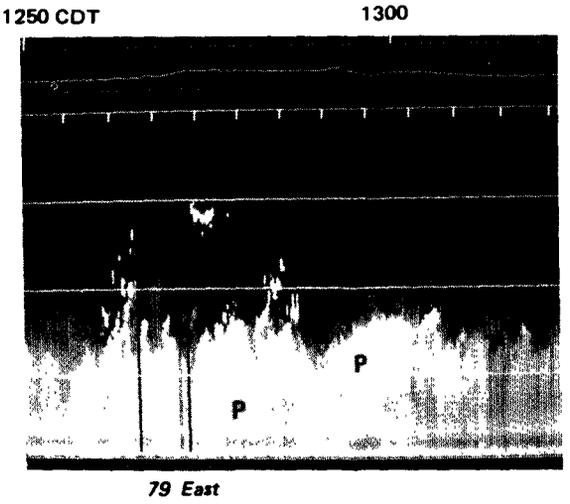
1250 CDT
1300
P
P
79 East

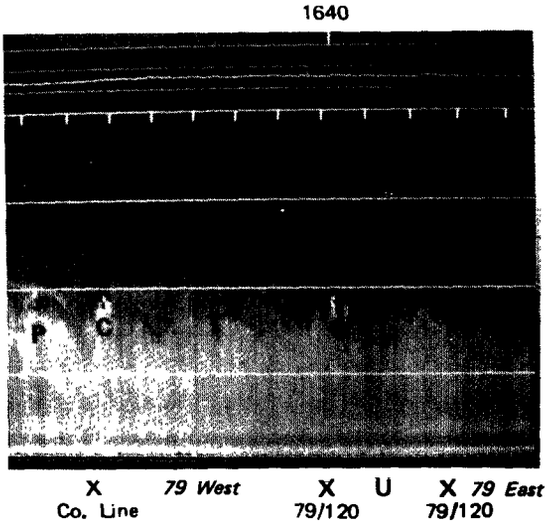
1640
P
C
X
79 West
X
U
X
79 East
Co. Line
79/120
79/120

Figure 3-17. Lidar photographs depicting the diurnal variation of the vertical cross-sectional structure of the Cumberland plume on 18 August 1978. All data were collected at the same distance (about 35 km) downwind of the source (Uthe et al. 1980).

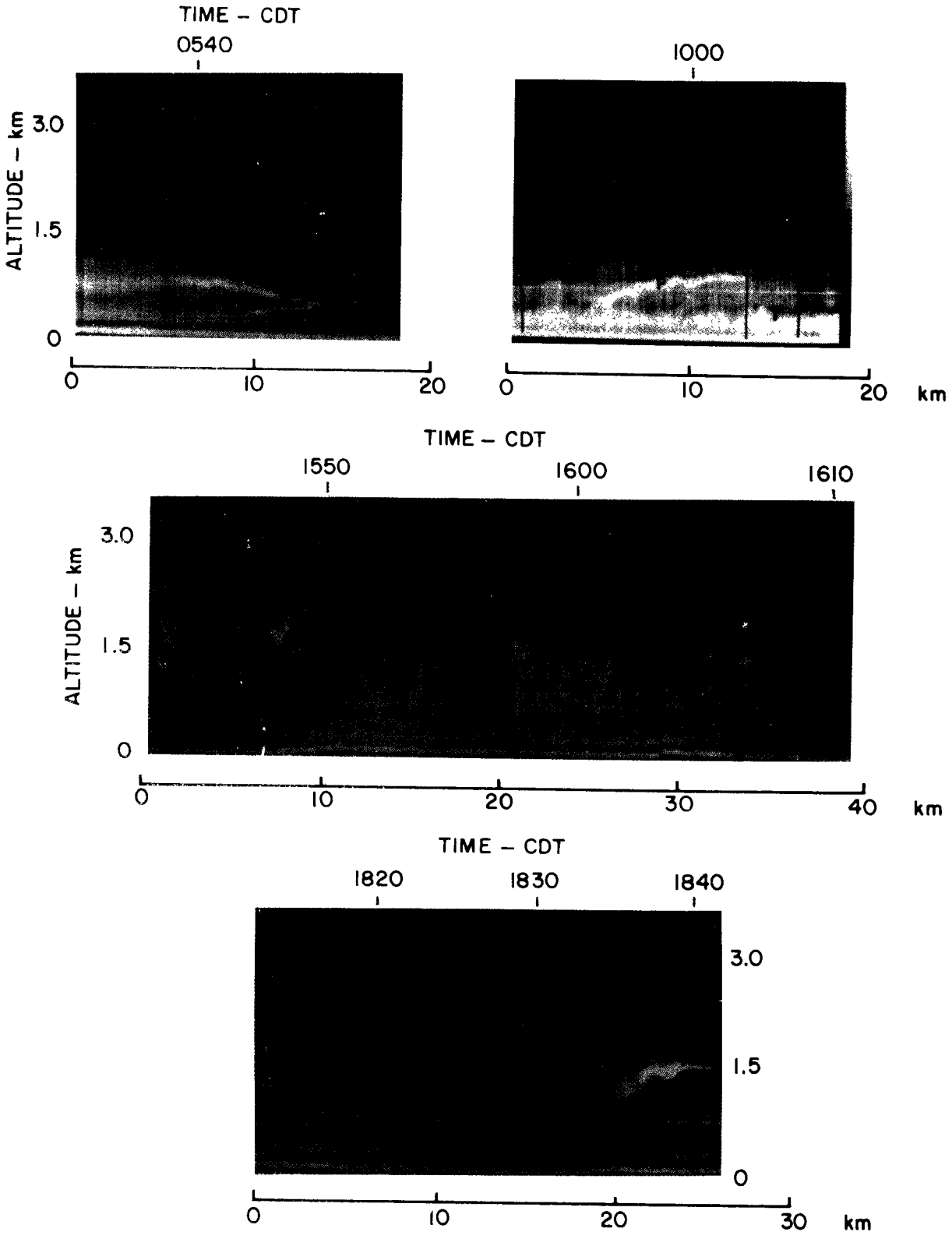
TIME – CDT
0540
1000
ALTITUDE – km
3.0
1.5
0
0
10
20
km
TIME – CDT
1550
1600
1610
3.0
1.5
0
0
10
20
30
40
km
TIME – CDT
1820
1830
1840
3.0
1.5
0
0
10
20
30
km

different times of another day (18 August 1978) under different stability conditions. At 0540 hr, the elevated Cumberland plume is in stable air and has a curious >-shaped vertical cross section, which is anything but the horizontal, elliptical, Gaussian shape commonly assumed in many plume diffusion models. The distorted shape is a consequence of wind shear both of speed and direction with height. At 1000 hr, the plume section is vertically very thin (100 to 200 m) but is fanned out (about 10 km or more wide) in the crosswind direction, and is tilted. Such plume fanning is typical in stable air. The plume is still elevated and decoupled from the ground sink, but an unstable daytime mixed layer has formed and risen to a height of about 400 m (P = plume, T = top of mixed layer). Upon further rise of the mixing-layer top, this elevated plume would become entrained and mixed down to the ground. Subsequent plume releases within this layer might fail to penetrate out of the inversion lid at the top of the mixing layers.

By 1600 hr, the mixed layer has grown to 1500 m, and the plume is entirely within it, well mixed throughout, and subject to ground removal. Also, the plume has a large cross section, with lateral spread exceeding 25 km (at a distance of 35 km downwind from the source). The plume is diluted by the background air, and the conditions within it are conducive to photochemically-driven formation of sulfates and nitrates (assuming the presence of reactive radical and organic species in the background). By 1830 hr, the mixing layer has collapsed (the daytime mixed layer of aerosols, of course, cannot reconcentrate). The boundary layer has a neutral-to-stable stratification. Two plumes are evident: (1) a fresher (about 1.5 hr old) elevated plume (middle right), released at about 1700 hr, which has risen quite high (1500 m or five times the physical stack height) and is coherent, and (2) an older well-mixed plume (lower left), within the daytime mixed layer. During the night, the lower plume has a greater likelihood of getting a ride in the nocturnal jet, with expected wind maxima in the 300 to 900 m layers. The upper plume would be expected to remain concentrated and transported at about 1500 m throughout the night and much of the next day until (and if) the mixing layer on the next day rises high enough to entrain it. If the next day's mixing layer does not rise to 1500 m, the plume will travel on, decoupled from the ground, until it is brought down in the future, either by a deep enough mixing layer, by sinking air, or by rain. That particular plume release is likely to have a longer atmospheric residence time than does the average summer plume and, accordingly, its impact range is likely to be farther afield. Rise of coherent plumes to heights of 1500 m is probably not very common except possibly in the case of emissions from superstacks (> 300 m).

An important feature of tall-stack emissions is that they can remain decoupled from the ground for a long time. An example of such elevated plume transport in the stable layers appears in Figure 3-18, which shows the nocturnal transport of the Labadie power plant plume near St. Louis, MO, on 14-15 July 1976. The Labadie stacks are 214 m high. Lidar data (Uthe and Wilson 1979) show a side view (time-height plane) of longitudinal plume transport over 85 km and a vertical cross-sectional view of the plume at nearly 100 km downwind distance. During much of the night, the plume was transported in a thin layer at a height of 400 to 500 m and had the fanning spread characteristic of stable plumes (see the cross section at 100 km

Figure 3-18. The longitudinal and cross-sectional structure of the Labadie power plant (2400 MW) plume during nocturnal transport on 14-15 July 1976 (Uthe and Wilson 1979).

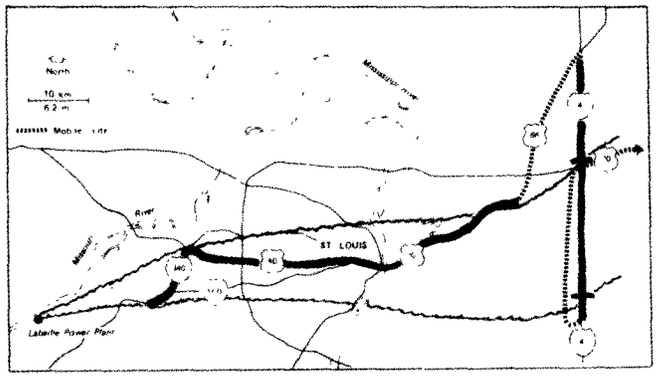

Top View

Route of mobile lidar observations of the Labadie plume on 14-15 July 1976

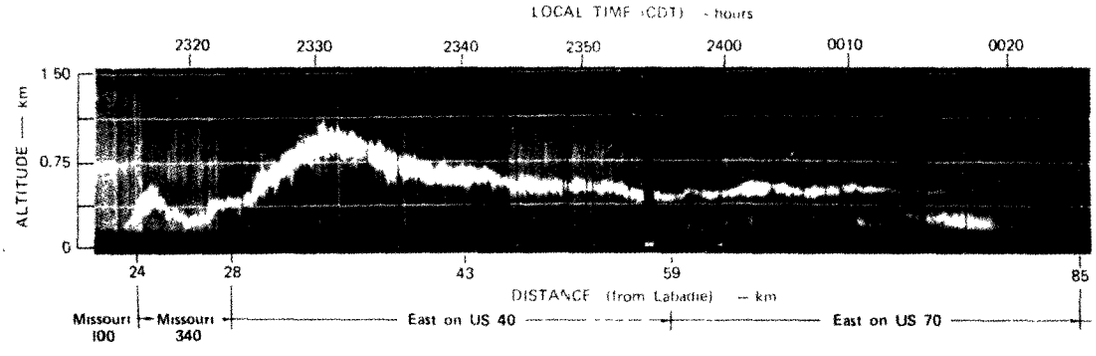

Side View

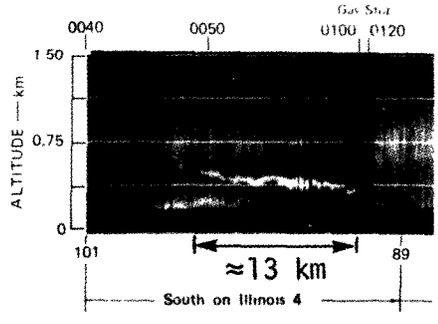

Cross-sectional View at 90-100 km Downwind

Downwind Labadie plume structure observed on 14-15 July 1976 using the SRI mobile Mark IX lidar system

downwind, with a lateral width of 13 km and a vertical thickness < 100 m). The plume was also horizontally tilted at this cross section. The apparent looping of the plume during early transport (over rather flat terrain) is most probably not what it seems to be; rather, in its zig-zag course under the plume, the lidar may simply have been sequentially looking up at parts of a tilted or a >-shaped plume that had highly variable local heights. The nocturnal plume transport shown had a speed of about 10 m s^{-1} (35 km hr^{-1}). Trapped in such a high-speed layer, the plume can be transported well over 500 km from 1800 hr to 1000 hr the next day without any deposition.

Because tall-stack emissions of acid precursors represent a large fraction of the total, the following question is of considerable importance to the subject of chemical transformations, atmospheric residence time, range of transport, and deposition: How much time does a given tall-stack emission spend aloft and decoupled from the ground sink? This question pertains to interactions of the plume and the mixing layer. Because mixing-layer dynamics are out of our control, the height of the plume is the controllable variable of interest. This height depends on the physical stack height and the plume rise (Figure 3-15), which at times can be several times the physical stack height.

The emissions from a tall stack are accompanied by an efflux of heat and momentum. Consequently, the plume initially is a rising buoyant jet. Its interaction with the prevailing wind and the ambient atmospheric turbulence results in plume bending and plume spread by the entrainment of ambient air (Briggs 1969, 1975). In a stable atmosphere, the plume rapidly loses buoyancy and attains its final plume rise. It remains vertically quite thin while fanning out horizontally by shearing effects. In a neutral or unstable atmosphere, the plume maintains buoyancy for longer times as it loops up and down in the convective up-and-down drafts. Plume dilution counters its net buoyant rise, and the prevailing wind causes it to bend over. In general, plume rise increases with increasing stack heat flux and decreases with increasing wind speed and atmospheric stability. For the same stability, wind speed, and exit conditions, plume rise is also greater with lower ambient temperature. At night and in winter, the effects of increased stability and wind speed are partially countered by lower ambient temperature.

Local wind speed, stability, and ambient temperature in the vertically stratified atmosphere are in turn related to physical stack height. An example of the effect of physical stack height on plume rise is shown in Figure 3-19. The Johnsonville stacks (all shorter than 125 m) and the Cumberland stacks (305 m tall) are only 60 km apart (in northwestern Tennessee). The plume releases shown are rather close in time and are both in a nocturnal-type regime. The lower Johnsonville release, however, is within the very stable nocturnal inversion layer, while the Cumberland release is in near-neutral layers aloft. Even with somewhat higher wind speeds acting on the Cumberland plume, this plume rose up to 1000 m in the example shown and remained decoupled from the ground throughout the morning. In stark contrast, the Johnsonville plume remained trapped in the surface inversion layer and was "fumigated" to ground before 0800 hr, when the sun caused the erosion of the surface inversion. At least during short-range

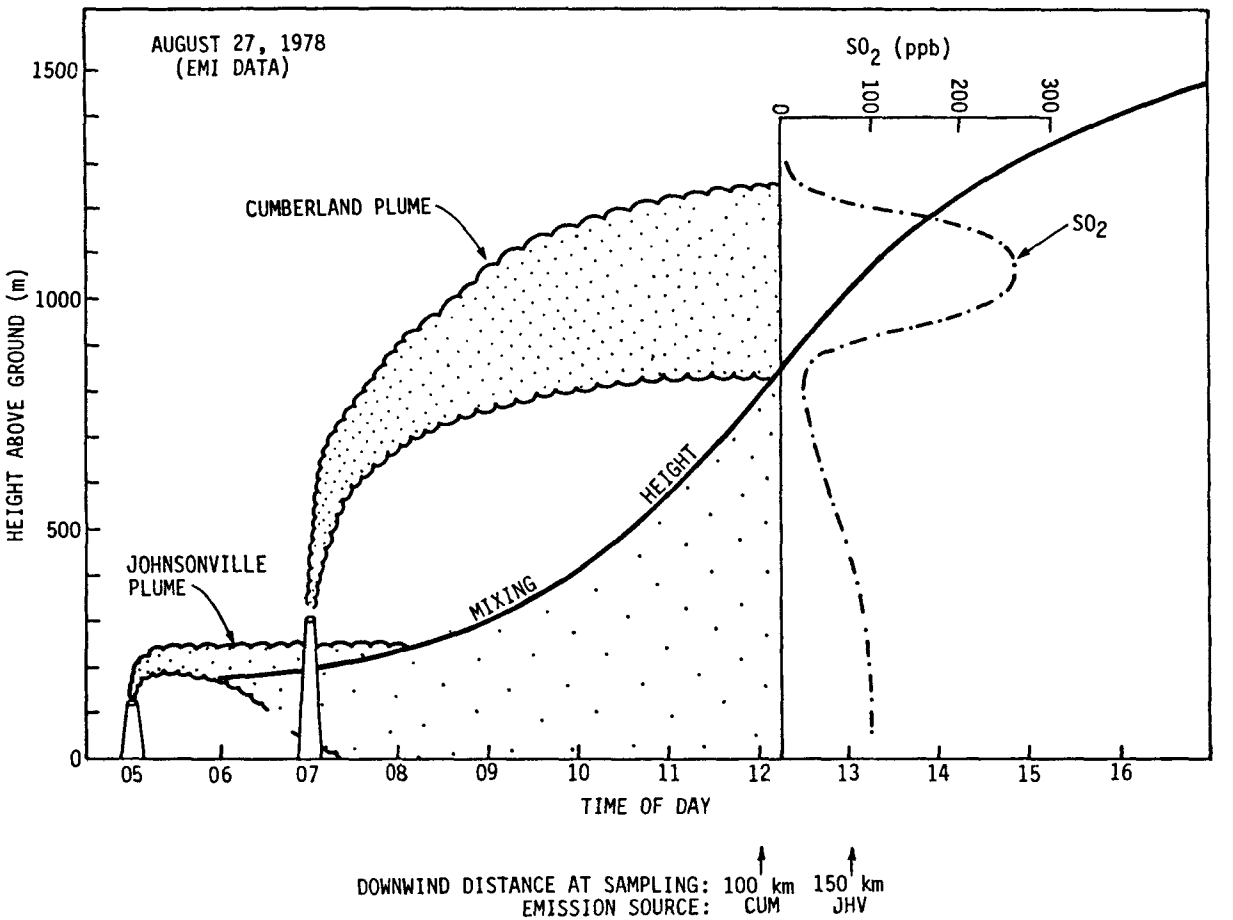

Figure 3-19. The physical behavior of the emissions from the Johnsonville (ten stacks, all less than 125 m tall) and Cumberland (two stacks, both 305 m tall) power plants. Reconstruction is based on aircraft and tetroon data. Adapted from Gillani and Wilson (1983).

transport (< 100 km), the Johnsonville plume probably experienced considerable ground removal, while the Cumberland plume was spared such losses. The Johnsonville plume was also exposed to morning fog and its chemistry, while the Cumberland plume was not. On this day (27 August 1978), no cumulus formation occurred before 1400 hr at the top of the mixing layer. If such clouds had formed, the Cumberland plume would have experienced substantial interaction with them during entrainment into the mixing layer, while the Johnsonville plume would not have. Evidently, plume rise can have important influence on plume sulfur and nitrogen budgets, but the relationship is complex.

To investigate the diurnal and seasonal dynamics of plume mixing-layer interactions, one must resort to a time-varying, plume-transport and diffusion model that explicitly considers the distinction between diffusion characteristics in the mixing layer and aloft. Such a two-layer (mixing layer below and a decoupled "reservoir" layer aloft) model was used by Husar et al. (1978) to study the sulfur budget of a power plant plume. That model did not include temporally variable plume rise or atmospheric stability in the two layers. We have refined that earlier model to include plume rise and spread more explicitly in terms of local meteorological parameters. (Detailed description of the model will be included in another paper now under preparation by Gillani.) The meteorological data used in the model calculations are from ground-level and upper-air measurements made as part of the St. Louis Regional Air Pollution Study (RAPS). All plume calculations refer to the case of emissions from the largest of the three stacks (height = 214 m) of the Labadie power plant near St. Louis. A steady thermal output from this stack corresponding to electrical power generation of 1000 MW is assumed. (This assumption is quite realistic.) In the model, plume rise is calculated based on the well-known Briggs empirical formulas (Briggs 1969). The model results for such an emission are believed to be quite representative also for the average current tall-stack emissions in the Ohio River Valley source region.

The model results are presented in Figures 3-20 through 3-22. The upper graphs of Figure 3-20 show the diurnal patterns of monthly median values of mixing-layer height and effective stack height for January and July. The reader is reminded of the substantial difference in daytime mixing heights in summer and winter--peak mixing heights averaging about 1800 m in July and only about 700 m in January. The greater stability and wind speeds typical in January tend to keep plume rise lower, but the lower ambient temperatures tend to offset this tendency significantly. The result is that the 24-hr average values of median plume rise are about 525 m in January and about 625 in July, but a somewhat greater day-to-day variability exists about this average in July. On the median basis, the July plume generally remains confined within the mixing layer for releases between 0900 and 1700 hr, while the January plume release even during midday has nearly a 50-50 chance of rising out of the mixing layer.

The lower graphs of Figure 3-20 show plots of the probability, for two plume releases at 12-hr intervals in the diurnal cycle, that the plume will remain decoupled from the ground during and up to 24 hr of transport. The two releases chosen for each month represent nearly the extreme conditions of

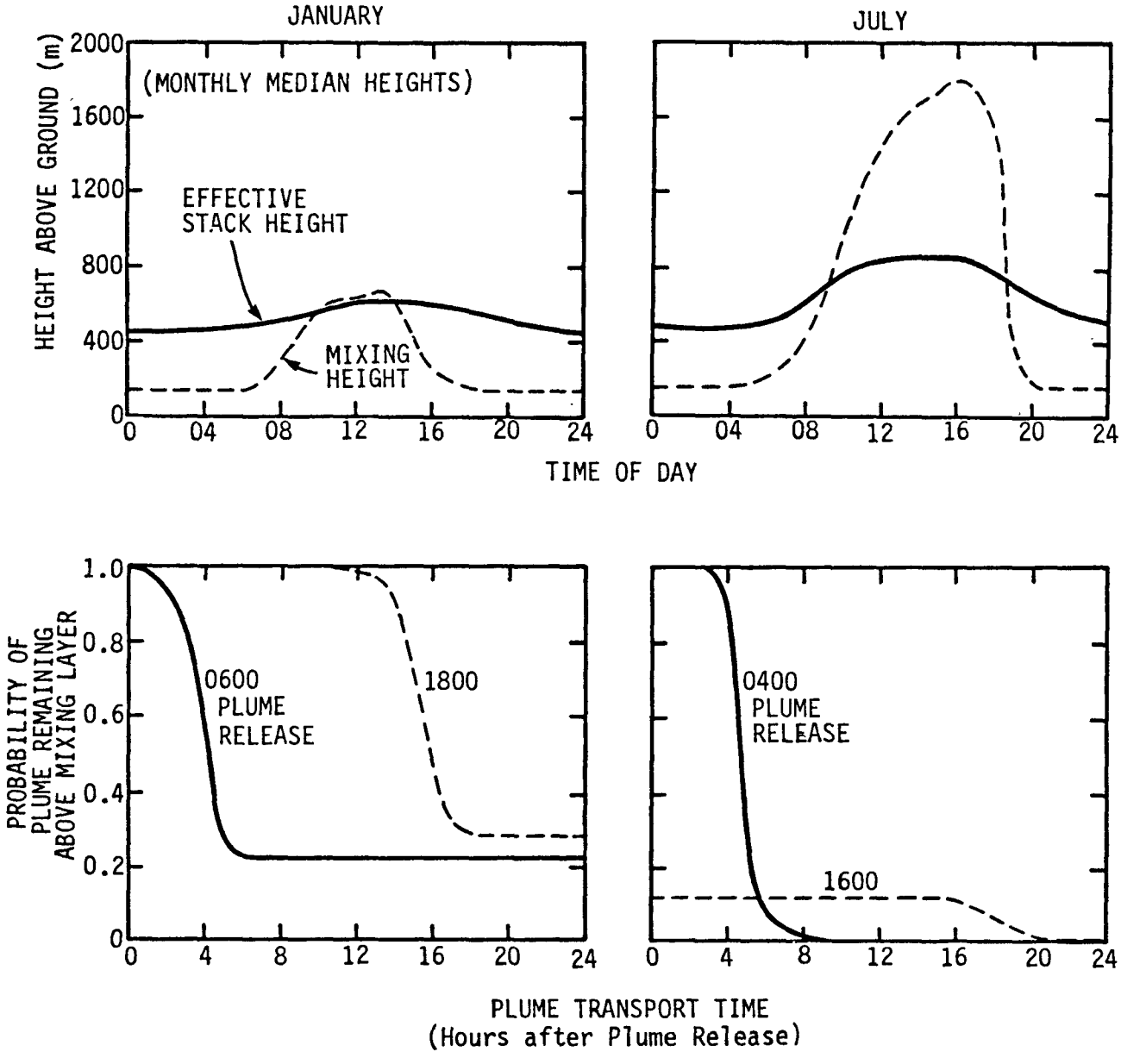

Figure 3-20. A summary of the expected diurnal and seasonal variation of the interaction of the Labadie power plant plume with the mixing layer. The upper graphs show comparisons of the monthly-median diurnal profiles of the measured mixing heights and calculated effective stack heights (based on Briggs formula for plume rise and 1976 upper air meteorological data from a site near the source). The lower graphs show the distributions, for two extreme plume release conditions, of the probability that the plume will remain aloft and decoupled from the ground up to 24 hr after release.

plume rise. The probability distribution functions for all other releases fall more or less within these two extremes. The July data show that the 0400 hr release will always start out decoupled but that within 12 hr of transport it will almost certainly experience entrainment into the mixing layer. The late afternoon release (1600 hr) has a low probability (12 percent) of penetrating out of the mixing layer and, except for some outlier cases, this release is also almost certain to have experienced ground contact within 24 hr of transport. Thus, the probability is almost zero for any release from such a large emission at about 200 m to remain continuously decoupled from the ground for a full 24 hr during summer. The situation is significantly different in January. For almost all January releases, a 20 to 30 percent chance exists that, even after 24 hr of plume transport, the plume is likely not to have experienced any interaction with the mixing layer or the ground. Plume measurements in summer are plentiful and fully support the above summer results. Winter plume measurements are indeed rare. The limited observations of the recent Cold Weather Plume Study jointly conducted by the U.S. Environmental Protection Agency (EPA) and the Electric Power Research Institute (EPRI) in February 1981 at the Kincaid power plant (183 m high stacks) near Springfield, IL, do indeed bear out the above winter results. In that field study, measurements were made on 5 different days. Of these 5 days, 3 were typified by very cold winter conditions (T_{max} < -5 C), while the other 2 days were not typical of winter (T_{max} > 15 C). On 2 out of the 3 cold days, the plume releases, even those at midday, rose above the mixing layer and remained decoupled from the ground. In winter, then, a significant fraction of the plume releases may remain decoupled from the ground for well over 24 hr, and even over 36 hr. In the meantime, this fraction may be transported to well beyond 500 km without any ground removal at all.

To investigate the implications of this important seasonal difference in plume-mixing-layer interaction on seasonal plume sulfur budgets, transformation and ground removal modules are added to the above plume model. Transformations of SO_2 to sulfates by the gas-phase and liquid-phase mechanisms are included in accordance with their empirical parameterizations by Gillani et al. (1981, 1983). All transformation and removal rates are based on St. Louis, MO, data for 1976, are assumed to be pseudo-first-order rates, and include diurnal and seasonal variabilities. The transformation rates are assumed to have seasonal and diurnal variations such that the 24-hr average rates are about 1.3 percent hr^{-1} in July (about 0.8 percent hr^{-1} average by gas-phase mechanism and about 0.5 percent hr^{-1} by liquid-phase mechanism) and about 0.4 percent hr^{-1} in January (mostly by liquid-phase mechanism). Ground removal of SO_2 by dry deposition is based on a diurnally varying deposition velocity, being 0.3 cm s^{-1} at night and peaking at 1.9 cm s^{-1} at noon in July, with corresponding values of 0.15 cm s^{-1} and 0.95 cm s^{-1} in January. Deposition velocity of sulfate is assumed to be constant (0.1 cm s^{-1}) at all times. These values are consistent with those most commonly used in current regional models. The model calculations assume that no precipitation scavenging occurs during the simulated 48 hr of transport.

The results of the model calculations are shown in Figures 3-21 (January) and 3-22 (July). The figures illustrate plume dynamics (top) and the sulfur

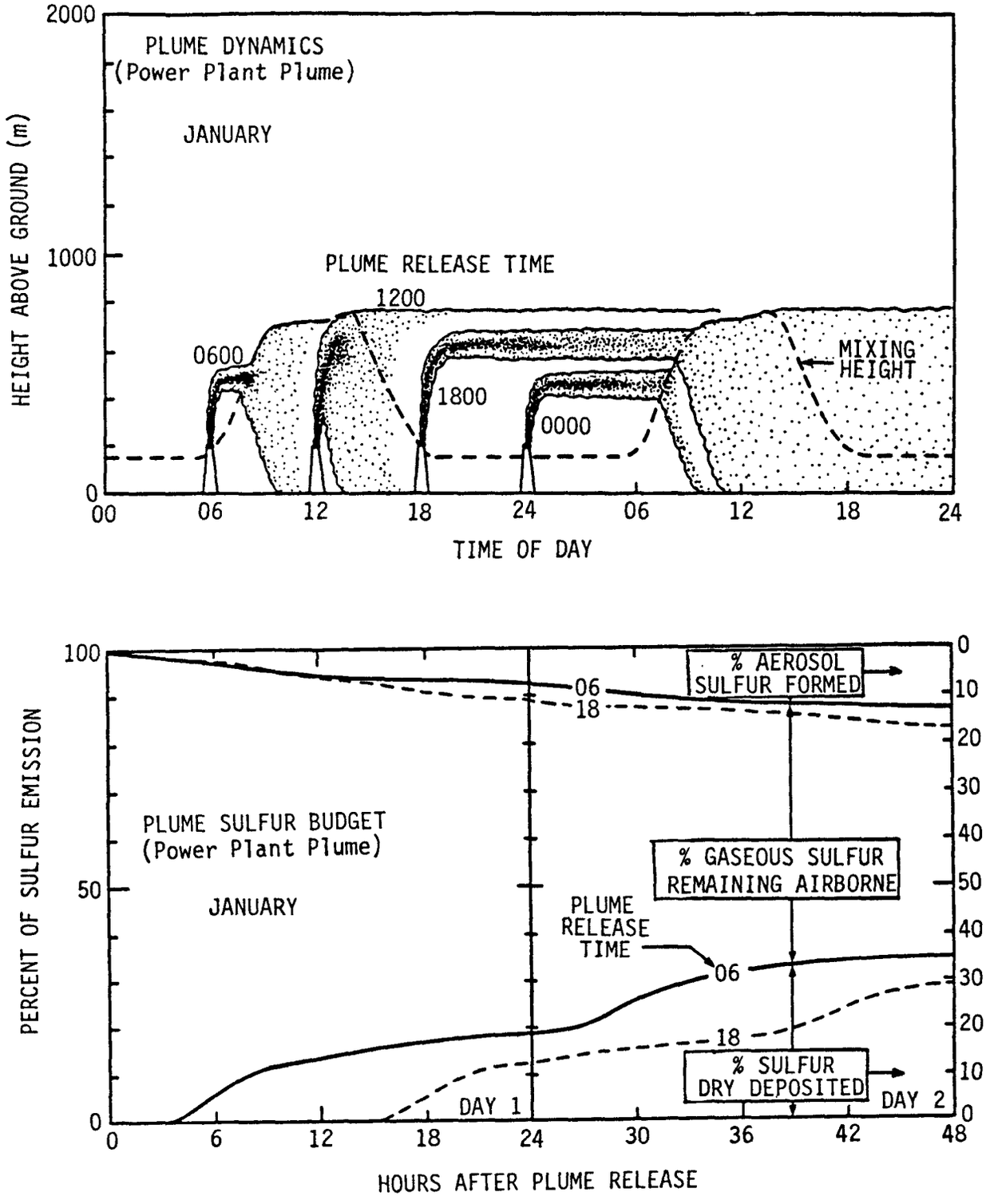

Figure 3-21. (TOP) Calculated Labadie plume dynamics, on a monthly-average basis, for plume releases at 000, 0600, 1200, and 1800 hr in January 1976.
(BOTTOM) Calculated monthly-average sulfur budget of the Labadie plume in January during 48 hr of transport, in the absence of wet deposition. Results are shown for the 0600 1800 hr plume releases.

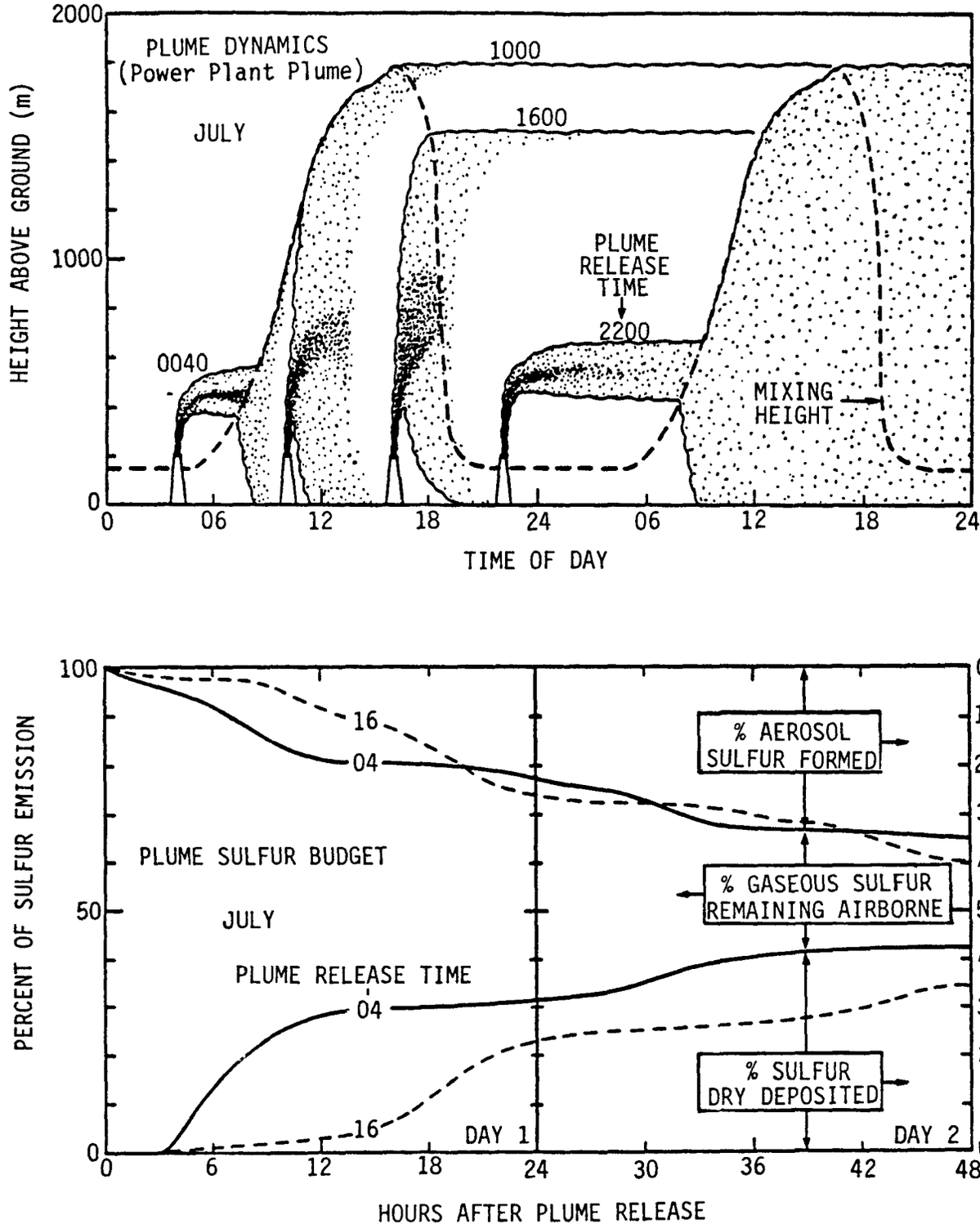

Figure 3-22. (TOP) Calculated Labadie plume dynamics, on a monthly-average basis, for plume releases at 2200, 0400, 1000, and 1600 hr in July 1976.
(BOTTOM) Calculated monthly-average sulfur budget of the Labadie plume in July during 48 hr of transport, in the absence of wet deposition. Results are shown for the 0400 and 1600 hr plume releases.

budget (bottom) for different plume release times during 48 hr of transport. The median plume-rise (at the time of release) and mixing-height (diurnal profile) values are used in these model calculations. Ground removal is about 16 percent on each day in January. In July, the ground loss is about 25 to 30 percent on the first day and an additional 10 to 12 percent on the second day. In the absence of wet deposition, the 1/e atmospheric residence time of SO_2 in such a plume is about 30 hours in summer and about double that in winter. With wet deposition, this time will be shorter. Of greater importance, however, is the residence time of total sulfur. In July, about 40 percent of the sulfur emission is dry deposited in 48 hours. While the wet deposition is highly variable and discrete in nature, it is reasonable to assume that, on the average, another 20 to 40 percent of the sulfur may be wet deposited during this period. It would appear reasonable then to assume that about two-thirds of the sulfur emission from a typical tall stack in the Midwest may be deposited (wet and dry) within two days during summer, i.e., the 1/e residence time of total sulfur emission from tall stacks is probably about 2 days during summer in the Midwest. During this time, the plume is likely to have been transported about 1000 km along the particle trajectories, and probably half that distance along the straight line joining the source and the plume center of mass, on the average. After two days, the plume is likely to be so spread out that it is probably not even meaningful to speculate about the transport of the plume center of mass. Parts of the plume may even be moving closer to the source as other parts move farther away. In any case, it would appear that perhaps more than half of the sulfur released in St. Louis from a 200 m stack may become deposited within a 500 km radius of St. Louis. In the Ohio River Valley, with less frequent and weaker nocturnal jets and generally somewhat lighter winds than in St. Louis, the effective transport range of the emissions is likely to be shorter. The presence of the mountainous terrain of the Appalachian, and vertical motions due to other mesoscale influences, may further slow down net horizontal transport and reduce the sphere of influence of the source region. Cloud venting of pollutants, however, could increase the atmospheric residence of pollutants considerably. Emissions from shorter stacks (less than 215 m) may be expected to have shorter atmospheric residence, while those from superstacks may remain airborne for longer periods. Emissions in the coastal areas of the northeast, may experience significant local shoreline recirculations, thereby reducing their impact range over the land mass.

In winter, the atmospheric residence of sulfur is expected to be significantly longer, and the potential for long-range transport significantly greater. Cloud venting is expected to be of less significance than in summer. The tall-stack effect, that is a significant increase in long-range transport as a direct result of increasing the average stack height from less than 100 m in 1950 to more than 200 m by 1975, for example, is also likely to be much more important in winter than in summer.

The sulfur budgets described above depend on the particular choices of conversion and removal parameters. While the reliability of the absolute values of the results may be questioned, important and consistent information lies in the relative values corresponding to different release times. In both seasons, ground loss is highest for the early morning releases (0400 or 0600 hr) because plume rise is lowest at these times due to maximum stability

and wind speeds. Consequently, these releases are entrained early in the day and fumigated to ground at relatively high concentrations, leading to substantial ground removal within the first 12 hr. The higher ground loss of SO_2 from these early morning releases leads to lower net sulfate formation. At the other extreme, ground loss is minimum for the late afternoon releases (1600 or 1800 hr), which have the highest plume rise and, consequently, a late entrainment the next day. In the case of the 1800 hr releases in January, a significant portion do not get at all entrained into the average peak mixing layer and are transported over long distances without any depletion. In winter, the plume spends more time decoupled from the ground than it does in summer, mainly because of the substantially lower daytime mixing height. When the winter plume is entrained, however, ground-level concentrations will be higher for the same reason. In terms of ground removal, these two effects have partially offsetting results.

3.4.2 Broad Areal Emissions Near Ground (Urban Plumes)

Urban plumes result from urban emissions from low sources such as automobiles and short stacks. Emissions from such multiple point sources in urban-industrial complexes are generally treated as broad areal emissions. The effective plume release height of such an urban plume is typically close to the ground.

From the point of view of secondary product formation and deposition, two principal differences exist between the power plant plume and the urban plume. The first difference is in plume release height (elevated vs low); the second is in the chemical composition of emissions from precursors of acidic products. Compared to urban emissions, power plant emissions are relatively richer in SO_x than they are in NO_x. Urban emissions are substantially richer in reactive hydrocarbon species, which play an important role in the chemistry not only of urban plumes but also of power plant plumes. The role of transport and turbulent mixing in the physical interaction of power plant plumes with polluted air originating from urban-industrial complexes is thus important in determining the contribution of power plant emissions to secondary product formation during long-range transport.

The difference in the characteristic release heights of the two plume types is important only during mesoscale transport. Once the two plumes become vertically well mixed throughout the mixing layer, they are physically indistinguishable. The principal difference during mesoscale transport is that elevated releases spend their early transport period decoupled from the ground and in a relatively stable environment, while near-ground releases continuously experience ground removal, and at least in the daytime, are subjected immediately to rapid dilution.

The principal difference between elevated and low-level plume transport concerns nocturnal transport. While an elevated nocturnal plume release is decoupled from the ground, a plume released near the ground will be trapped within the ground-based shallow, stable, mechanical mixing layer unless it has sufficient buoyancy to escape this mixing layer. If trapped, plume concentrations of the primary emissions in contact with the ground will be

high, and, accordingly, even with the reduced nocturnal ground absorption capacity, substantial ground losses can occur. Husar et al. (1978) presented convincing evidence (Figure 3-23) that the central-city plume of St. Louis is at least partially trapped in the nocturnal mixing layer in summer. The figure shows S_g (gaseous sulfur) and NO_x concentration data averaged for five ground-level monitoring stations of the St. Louis Regional Air Monitoring network for the month of July 1976. The S_g data are segregated by sectors pointing to three major local sources: the central-city area; the Alton-Wood River petroleum refinery complex, which includes a power plant; and the tall-stack Portage des Sioux Power Plant. The diurnal patterns for the S_g data show that while the Alton-Wood River and Sioux contributions to ground-level sulfur concentration peak in the daytime (when their elevated source plumes are entrained into the mixing layer and brought to ground), the central-city concentration peaks at night (presumably due to trapping in the shallow nocturnal mixing layer) and is minimal during the day, when the emissions are effectively diluted in the deeper, daytime mixing layer. The drop in contribution of the elevated source plumes at night indicates their nocturnal decoupling from the ground.

The NO_x data shown are averaged not only for all five stations but also for all sectors. The sector-segregated NO_x data (not shown here) support the conclusions drawn below. The diurnal NO_x pattern is indicative of the predominance of local, low-level sources of NO_x, particularly automobile emissions. During the day, NO_x is dilute, both at gound-level and aloft (except in a fresh plume). During the evening traffic rush hour, ground-level NO_x increases sharply and remains high throughout the night, indicating that it is trapped in the shallow mixing layer. This observation is consistent with the fact that automobile exhaust is rich in NO_x but not SO_x.

The diurnal and seasonal variations of urban plume dynamics in the time-height plane and of plume sulfur budget (not including precipitation scavenging) based on model calculations using St. Louis meteorological data for 1976 are shown in Figures 3-24 and 3-25 (January and July, respectively). In the urban plume model, the gas-phase oxidation rate of SO_2 is assumed to depend only on sunlight (linearly), such that its peak daytime values are typically 5.5 percent hr^{-1} in July and 3.5 percent hr^{-1} in January. Liquid-phase oxidation of SO_2 is calculated in the same way as it is for power plant plumes. The resulting estimates of sulfate formation in the urban plume may be considered as reasonable but unsubstantiated (particularly for winter). However, sulfate formation only weakly influences the sulfur ground-loss estimates. The model calculations of the ground losses may be considered valid at least for comparing diurnal and seasonal variations for the urban plume and differences between urban and power plant plumes. For the daytime urban releases (for example, the 1200 hr releases in January and the 1000 hr releases in July) during both seasons, the plume is brought to ground close to the source area at high concentration and is subsequently rapidly diluted throughout the mixing layer. Consequently, ground removal is more rapid initially and much slower as the plume dilutes and the ground-level concentration of the pollutants diminishes. As a result of the rapid daytime plume-spread throughout the mixing layer, the transport range over which source characteristics are still physically distinguishable is

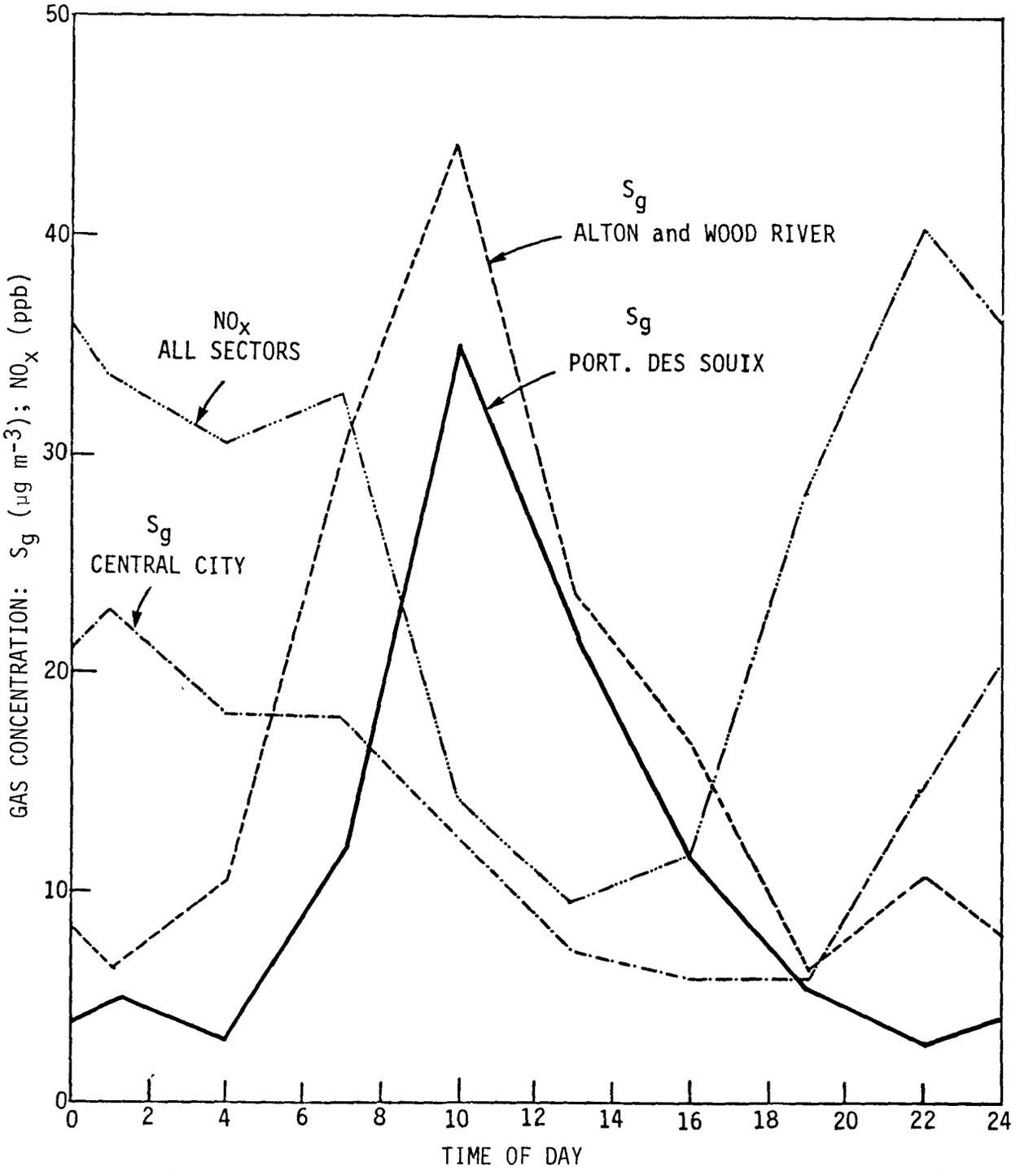

Figure 3-23. The diurnal behavior of sulfur and nitrogen concentrations in St. Louis, MO, based on monthly average data of the RAPS ground network for July 1976. The data are averaged for five stations. For gaseous sulfur, Sg, they are segregated by wind-direction sectors which pointed to three major sources: the central city area; the Wood River refinery complex (including a 650 MW power plant); and the tall-stack Portage des Sioux power plant (1000 MW) (Husar et al. 1978).

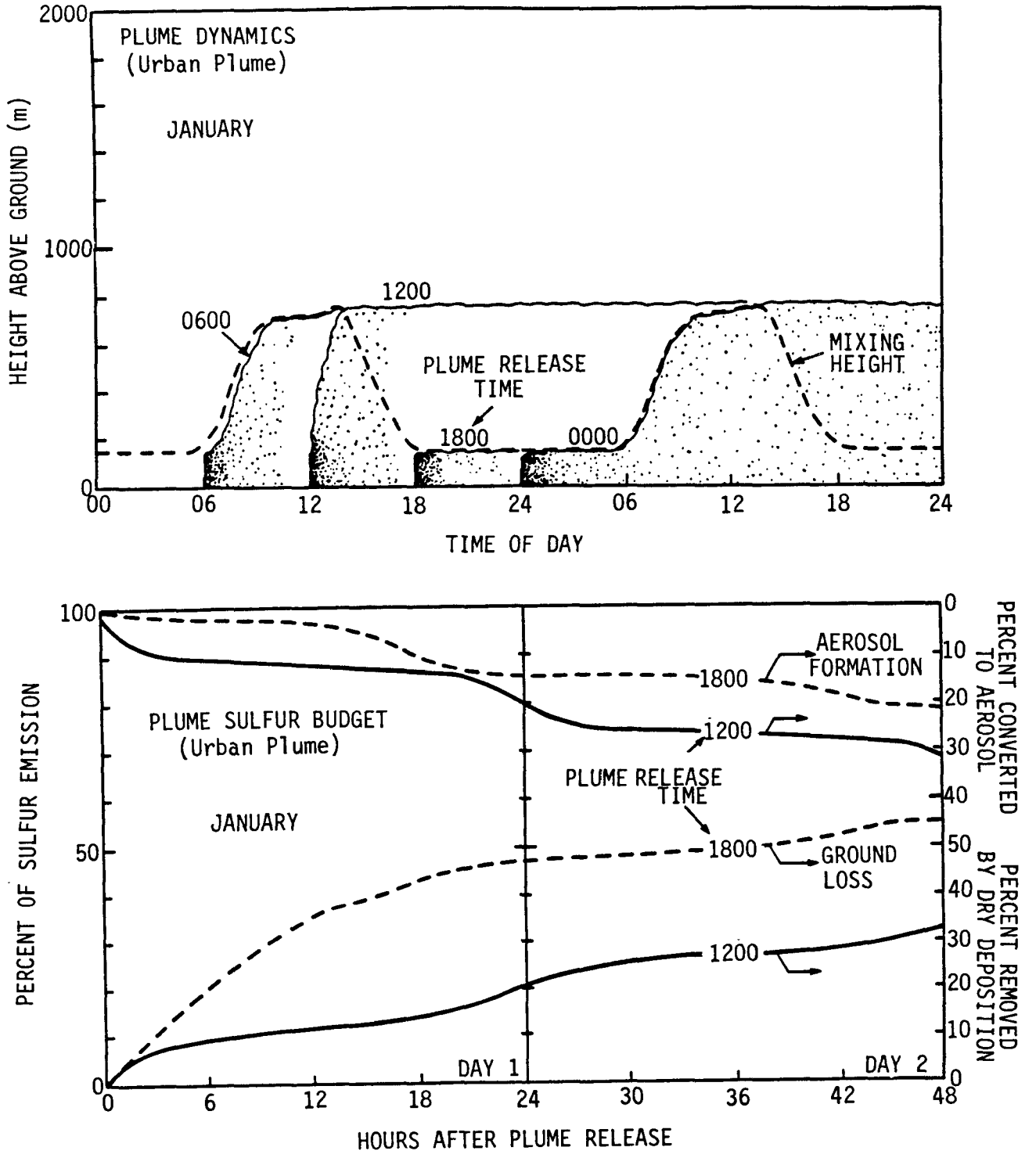

Figure 3-24. (TOP) Calculated dynamics of the St. Louis plume (low-level emissions only), on a monthly-average basis, for plume releases at 000, 0600, 1200, and 1800 hr in January 1976.
(BOTTOM) Calculated monthly-average sulfur budget of the St. Louis plume in January during 48 hr of transport, in the absence of wet deposition. Results are shown for the 1200 and 1800 hr.

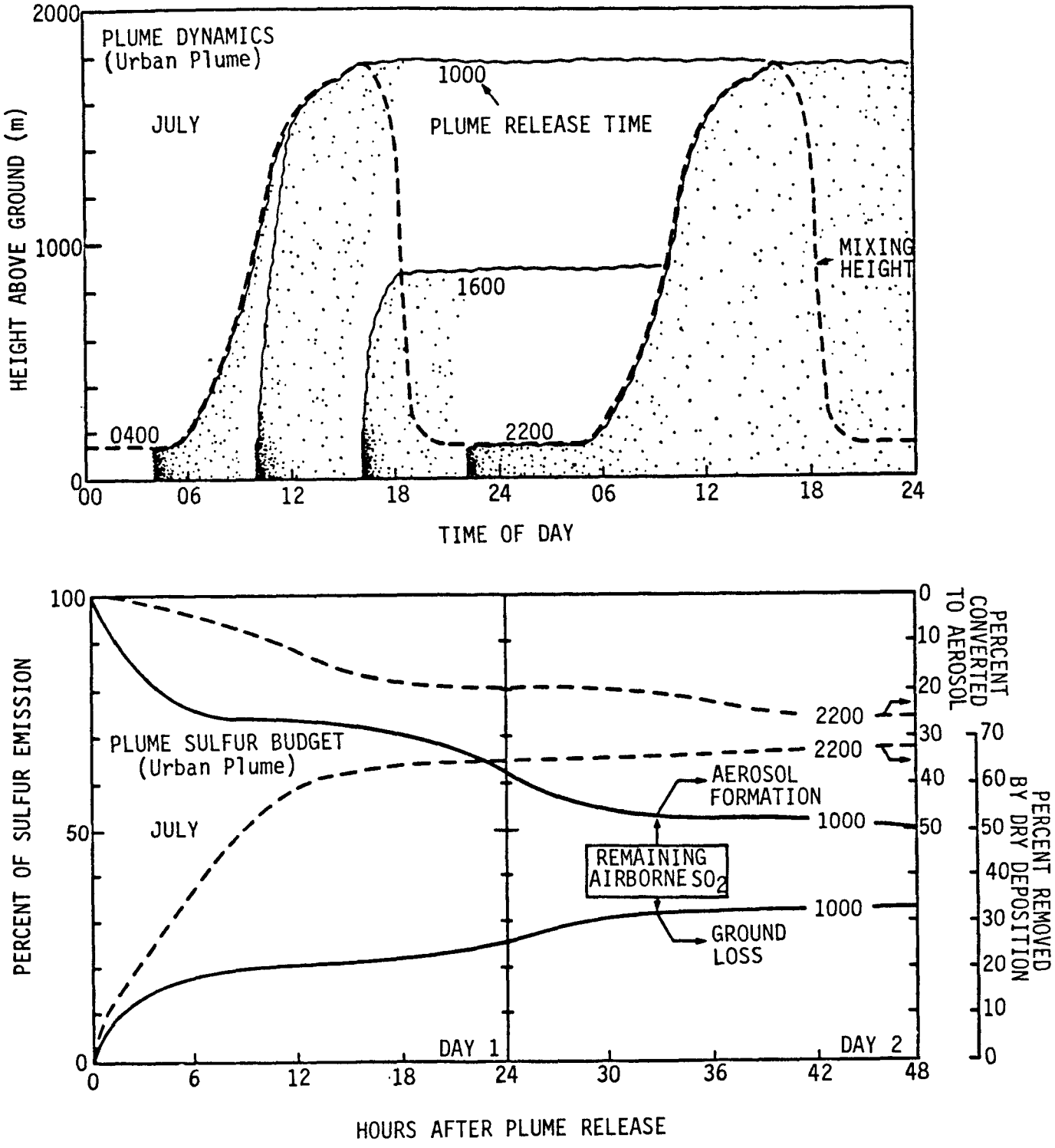

Figure 3-25. (TOP) Calculated dynamics of the St. Louis city plume (low-level emissions only), on a monthly-average basis, for plume releases at 0400, 1000, 1600, and 2200 hr January to July 1976.
(BOTTOM) Calculated monthly-average sulfur budget of the St. Louis city plume in January to July during 48 hr of transport, in the absence of wet deposition.
Results are shown for the 1200 and 2200 hr plume releases.

short. Hence, the difference between ground losses from urban and power plant plumes is smallest for the daytime releases. An exception is apparent in the daytime power plant releases in winter, which penetrate out of the mixing layer and remain detached from the ground for long distances.

In stark contrast to the daytime urban plume releases, the nocturnal releases (1800 hr in January and 2200 hr in July) remain trapped in the shallow mechanical mixing layer throughout the night. Being concentrated and in continuous ground contact, nocturnal releases experience heavy ground losses. After 12 hr of such nighttime transport, the urban plume ground losses range between about 40 and 60 percent of the emissions, compared to almost no ground loss in 12 hr for the elevated nocturnal releases from power plants. Thus, for the nocturnal releases, the effect of source height difference, though short-lived in terms of multiday, long-range transport, can be quite substantial. The loss of about half of the precursor emissions during the nighttime transport of the urban plume in July before the chemistry even begins (assuming the absence of the liquid phase at night) substantially limits the amount of secondary formation during further transport. Actual nighttime measurements of ground loss from trapped urban plumes are not available in the published literature. Nor does any documentation exist for the fraction of all urban releases (from either low or intermediate and tall stacks) that remains trapped within the shallow nocturnal mixing layer. Analyses of field data of pollutant transformation and removal during urban plume transport have lagged behind such analyses for power plant plumes.

In summary, dry deposition during the first 12 hr of transport appears to play a dominant role in urban plume sulfur budget. This is particularly true for nocturnal releases. After the first 12 hr, most further loss of sulfur and nitrogen compounds may be significant only for daytime releases under convective conditions. While long-range transport of urban plumes is more likely in winter, seasonal differences in sulfur budget are not as pronounced as they are in the case of power plant plumes. The bulk of the urban emissions of acid precursors, particularly NO_x, are likely to be deposited within 500 km of the source.

3.5 CONTINENTAL AND HEMISPHERIC TRANSPORT (J. D. Shannon and D. E. Patterson)

Pollutants transported over continental and larger scales may be subject to repeated "breathing" of the planetary boundary layer (PBL) over land, i.e., the diurnal cycle of daytime growth of the mixing layer and vertical coupling between upper layers and the surface, followed by the nocturnal decoupling of flow and pollutants aloft from surface removal processes (Sisterson and Frenzen 1978). In addition, transport over long ranges may be sufficient in duration that vertical motions associated with large-scale weather systems, such as subsidence in a region of high pressure or ascent over a frontal surface (Davis and Wendell 1976), become significant and result in a greater depth of the troposphere affecting long-range transport than is typical for mesoscale transport. This leads to more uncertainty in defining the transport layer, particularly in simulation models that use a single horizontal transport layer. Decoupled layers of haze and sulfate on the regional scale above the mixing layer have been noted in the literature

(Sisterson et al. 1979, McNaughton and Orgill 1980) and during the recent EPA Project PEPE/NEROS.

In addition, transport over continental and larger scales may involve flow over oceanic areas, such as anticyclonic flow from the Midwest or Northeast around an offshore high pressure center into the South (Lyons et al. 1978). The structure and dynamics of the PBL over water differ considerably from that over land. Oceanic (or Great Lake) surface temperatures show little diurnal variation because of mixing processes. As a result, the marine PBL is relatively constant. In addition, the ocean is a homogeneous surface over large areas, while the continent varies from forest to field to city, etc. Broad stretches of strong atmospheric inversions overlie cold water, while well-mixed regions overlie relatively warm water. While pollutants within the PBL are subject to dry deposition processes and will eventually be removed, pollutants above the PBL, perhaps transported there by convective processes over land, will remain above the PBL until transported down by precipitation processes or by large-scale subsidence.

Any single trajectory is a stochastic process from an ensemble of possible trajectories for a given set of meteorological conditions. There are some occasions, such as a stationary pattern of well-defined flow, in which there is considerable accuracy (i.e., little ensemble spread) for an individual trajectory calculated for daytime well-mixed flow. However, if the meteorological systems are moving, a small initial error produced in temporal interpolation can lead to a large eventual error, and if the flow is ill-defined or rapidly changing, a small initial error in calculations can lead to a large change in downstream position. Currently, the network of routine upper air wind measurements is sparser than the network for measurements of precipitation chemistry over eastern North America. Considering the normal 12-hr spacing of the upper air measurements, it is optimistic to hope for knowledge of the prevailing wind at an arbitrary location in space and time to better than 5 degrees about the "actual" advecting wind; this alone leads to an uncertainty in the crosswind direction of 15 to 20 percent of the trajectory length for every timestep in the simulation. The statistics of multiple trajectories contain much less uncertainty than individual trajectories, because the sample size is much larger, and can be extended further downstream in time. In addition, the problem of estimating horizontal diffusion becomes easier because over long-term regional scales, horizontal dispersion is due primarily to the spread of plume or trajectory centerlines, rather than to the spread about some individual plume centerline (Durst et al. 1959, Sheih 1980).

Calculation of transport distances for pollutants subject to chemical transformation and deposition requires simulation modeling (as is done earlier in this chapter when wet removal processes are not considered), but the results are a function of the modeling parameterizations, such as the dry deposition velocities or the transport layer height, and the source location and meteorological conditions. Therefore, the transport distance associated with sulfur oxides will differ from the corresponding scale of influence for nitrogen oxides, even when both are emitted in one plume. The regional-scale transport field experiments currently planned, such as the Cross-Appalachian Transport Experiment (CAPTEX) sponsored by the Department of Energy, use

inert, non-depositing tracers. The CAPTEX experiment is intended to be a diagnostic study of the transport and diffusion processes associated with flow over large-scale mountainous terrain and, as such, could be said to examine, for the situations studied, the upper limit of transport distance scales associated with depositing pollutants. More definitive experiments must await development of suitable reactive and depositing tracers.

Another transport issue requiring simulation models is the importance of tall stacks. Qualitatively, use of tall stacks must increase transport distance scales because upper-level emissions are often decoupled from surface removal processes, thus decreasing near-source dry deposition, and because wind speeds generally increase with height. A model comparison of hypothetical surface-layer and upper-level emissions from a source in southern Ohio by Shannon (1981) indicates that net transport past the Atlantic coast could be one third higher for the elevated source. The difference between mid-level and upper-level sources, somewhat more realistic for examination of the effect of the introduction of tall stacks, would be less.

It may prove instructive to examine a few examples of key "forcing functions" which determine the transmission of pollutant emissions over the North American continent. For elucidation of the meteorological nature of long-range transport, two excellent reviews are those of Munn and Bolin (1971) and Pack et al. (1978). For a more thorough exposition of climatological factors influencing long-range deposition, the reader is referred to a series of studies by Niemann et al. (e.g., Niemann 1982).

That long-range transport of acidifying pollutants actually occurs can be inferred or modeled in a number of ways. The simplest demonstration may be seen in observations of the motion of polluted air masses from satellite images or from surface reports of aerosol sulfate or reduced visibility (Tong et al. 1976, Chung 1978, Wolff et al. 1981). The episode during 23 June to 7 July 1975 shown in Figure 3-26 indicates the apparent motion of a large hazy air mass over a two-week period; this particular episode of long-range transport in a stagnating anticyclonic system was documented through visibility, sulfate, and ozone measurements (Husar et al. 1976), as well as by satellite imagery (Lyons and Husar 1976).

It is evident that the day-to-day transport of air pollutants on the regional scale is controlled by the synoptic passages of fronts, cyclonic, and anticyclonic systems. Smith and Hunt (1978) have pointed out that receptor regions remote from major sources may receive a disproportionately large fraction of deposition during a few events, and thus the average transport conditions may be irrelevant because the episodes have their own distinctive meteorology. In particular, precipitation along a frontal zone on the edge of an anticyclone can contribute a large deposition of acidifying species which are built up over the prolonged continental residence. Vukovich et al. (1977) illustrated that the air with the longest residence time (and highest mass loading of pollutants) within an anticyclonic system is found on the periphery, where frontal activity is most likely.

On the regional scale, the spreading of emissions is dominated by the action of vertical wind shear and wind direction changes acting in combination with

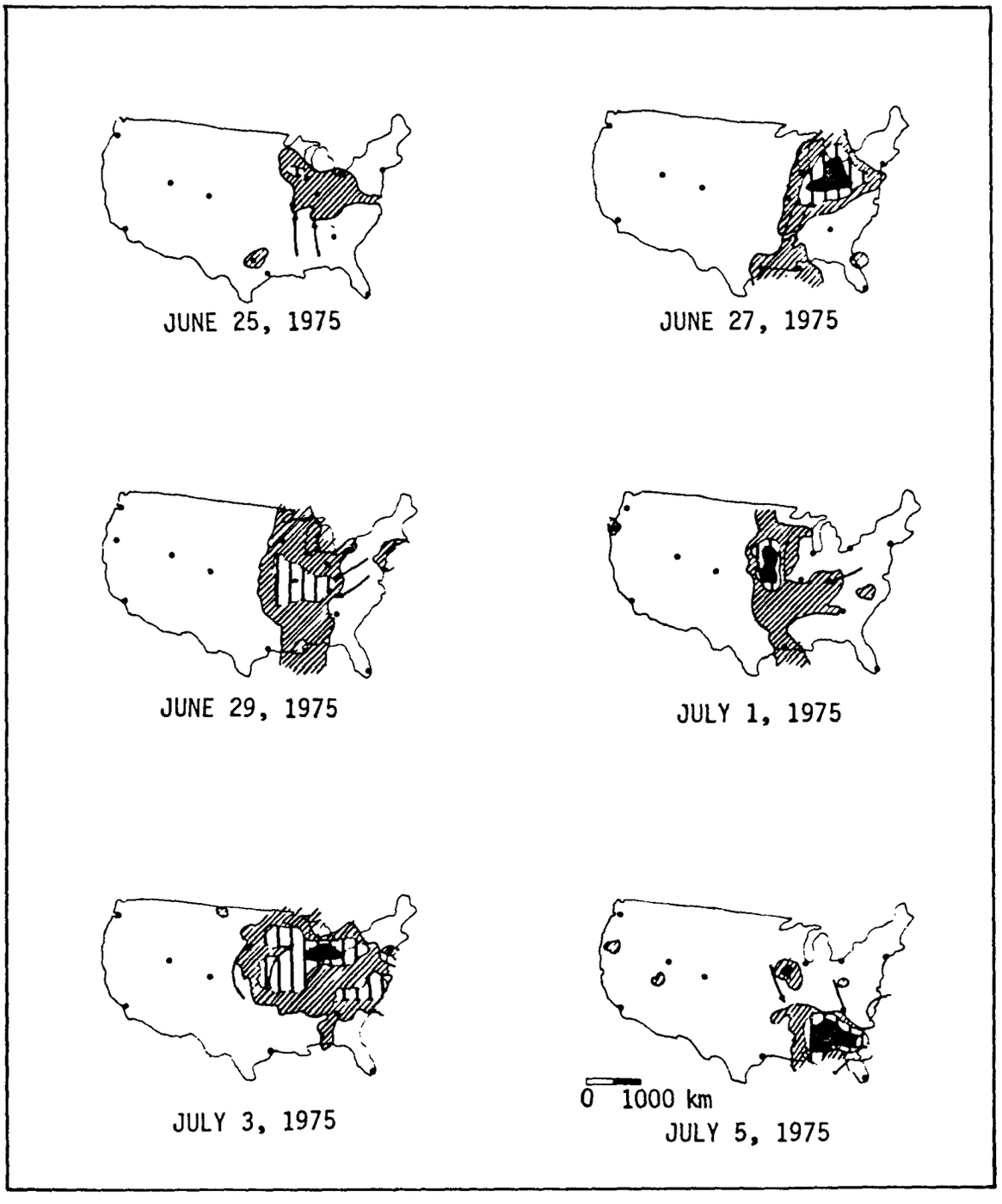

Figure 3-26. Sequential contour maps of noon visibility for June 25-July 5, 1975 illustrate the evolution and transport of a large-scale hazy air mass. Contours correspond to visual range 6.5-10 km (light shade), 5-65 km (medium shade) and <5 km (black). (Husar et al. 1976).

the diurnal cycle of daytime mixing and nighttime layering of the atmosphere (e.g., Draxler and Taylor 1982). A graphical example of the dispersal of a puff released in St. Louis, during four days of transport, by interactions of vertical wind shear and synoptic motion is given in Figure 3-27. Here an ensemble of 100 trajectories begun at midday are represented by the lines shown; the mean trajectory is indicated by the heavier line with dotted nodes, and ellipses at 12-hr intervals indicate the spread of end points of the ensemble relative to the mean position. During daylight hours, lateral puff spread is minimal due to lack of wind shear. By early evening, as mixing greatly diminishes, vertical layers (here simulated by four 300-m layers) begin to diverge, and continue independent paths until midmorning of the next day. At that time, the clusters in each layer act as a new puff beginning a well-mixed day until the next evening, when each puff again divides into layers, and so on. Within one day of such dispersion, shear spreads the puff out over a scale of the width of Michigan. After four days (trajectory endpoints), the puff is smeared across all of the eastern Canadian border. Edinger and Press (1982) expressed the effect of such spreading and mixing in terms of a regional dilution volume over 1 to 3 days. They show that episodes of haze occur when the dilution volumes from sites in the northeastern U.S. overlap; the overlap produces sufficient homogeneity to explain large regions of haze emanating from just four representative source cities. The mixing and spreading are due more to shear in the vertical than to horizontal nonuniformity in the flows field.

Rodhe (1974) illustrated that the assumptions made about the intensity of turbulent mixing in the vertical may dramatically alter the output of model transport computations. Other vertical motions are important in long-range transport in the troposphere, although difficult to simulate properly. Transmission of pollutants across major topographical obstacles (e.g., the Rocky Mountains), along warm and cold fronts, and near convective cells involves vertical transport that is problematic for the modeler. Unfortunately, these are also the situations which are crucial in simulating events of wet deposition. The motion of low pressure systems and, more importantly, the significant accumulation of pollutants during the passage of slow-moving anticyclonic systems are also major factors in determining the extent and severity of source impacts. Korshover (1967) has shown that the Smoky Mountain area is particularly subject to stagnating anticyclones, leading to a lower overall ventilation of its emissions on a regional scale.

Although the shorter temporal and spatial scales of transport are known to be important, the characterization of episodes has been limited for the most part either to case studies or to simple term tabulations of occurrence. The understanding of such events in the detail required for policy decisions, including the development of models, is incomplete at present (see Bass 1979, for review). The estimation of long-term transmission coefficients from sources to receptors is inextricably tied to transformation chemistry and deposition mechanisms, and is beyond the scope of this section (see Chapters A-4 and A-7). Similarly, consideration of "pure transport" without kinetics involves model simulations which are not described here. It may be mentioned that very recent computations at Washington University indicate that the seasonal and annual mean trajectories within eastern North America give mean displacement rate on the order of 3 m s^{-1} over the first few days, with

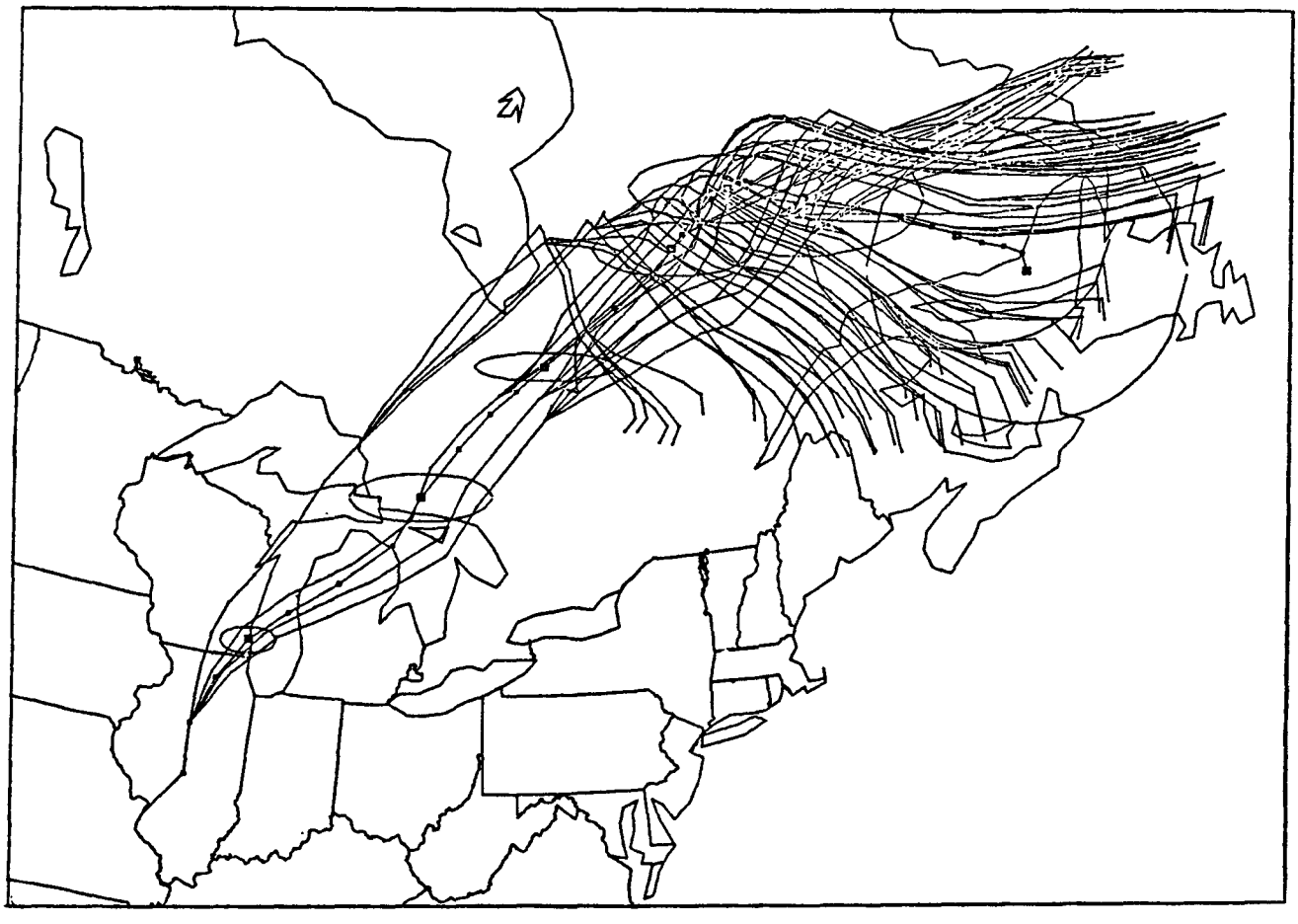

Figure 3-27. Dispersion of a plume emitted at St. Louis, on August 26, 1977, assuming 1-layer daytime transport and 4-layer nighttime transport. The spread occurs as a result of the interactions of vertical wind shear with synoptic wind fields over a 4-day period.

root mean square deviation from the mean path being large enough to include the source. Comparable computations by several models in the MOI studies yielded roughly comparable results. It is perhaps more direct, however, to examine climatological examples of key meteorological parameters: wind fields, mixing height, and precipitation.

The most obvious determinant of transport is, of course, the wind field. For the years 1975-77, the available rawinsonde upper air data (Figure 3-28) yield some clear patterns: (1) the general flow is west to east, with also a significant flow upward from the Gulf of Mexico to the Great Lakes; (2) winter and fall exhibit the highest speeds; (3) the southeastern United States lies within a region of low mean velocity during late spring and summer; (4) the midwestern United States exhibits very strong shear during summer and spring, with southerly surface flow and westerlies at the top of the PBL. Mean winds include artifacts of averaging and should be interpreted with caution; for example, alternating NW and SW flows will produce a mean W flow. It is also important to note that these are local mean winds; not only are the existence and interactions of synoptic-scale circulations not shown, but as mentioned earlier, the flow associated with wet deposition may be quite different from the mean. Wendland and Bryson (1981) have used climatological near-surface wind fields to identify airstream source regions and mean frontal locations; the Ohio Valley is identified as an airstream source region during summer and fall.

An important notion in both mesoscale and continental-scale transport is the existence of a top to the layer in which pollutants are found. The height of such a layer will vary during the day as well as geographically and from day to day. There is also an unknown but likely important loss of material from the mixed layer to upper layers by convective motion (Ching et al. 1983). Well-mixed aged pollutants in nocturnal stable layers aloft may sometimes not be reentrained into the mixing layer the next morning. As noted earlier the maximum afternoon mixing depths at several locations in the United States have been determined by Holzworth (1972). Similar studies were conducted for Canadian sites by Portelli (1977). Contours of these literature values of representative mixed depths (Figure 3-29) provide some insight into the gross interactions of advecting winds and the depth of the mixing layer, although synoptic temporal and spatial scales of interaction may be at least as important as the seasonal averages in determining the net transport of emissions. It is seen that the northern regions generally have lower inversion heights, with the deepest layers occurring in the desert regions of the United States. Most important is the considerable uniformity, separately, in the eastern United States and in the western United States. On the average, some of the well-mixed, aged pollutants will ride over the daytime mixed layer when moving either from south to north or from west to east, due to decreasing mixed depths along the trajectory. Thus, an appropriate parameterization of the spatial-temporal variation of the mixing layer height is required for simulation of continental-scale transport over several days and thousands of kilometers.

Another "forcing function," precipitation, is critical in long-range transport, not only in determining the local impact of wet deposition of pollutants, but also as a mechanism for removal of pollutants from the

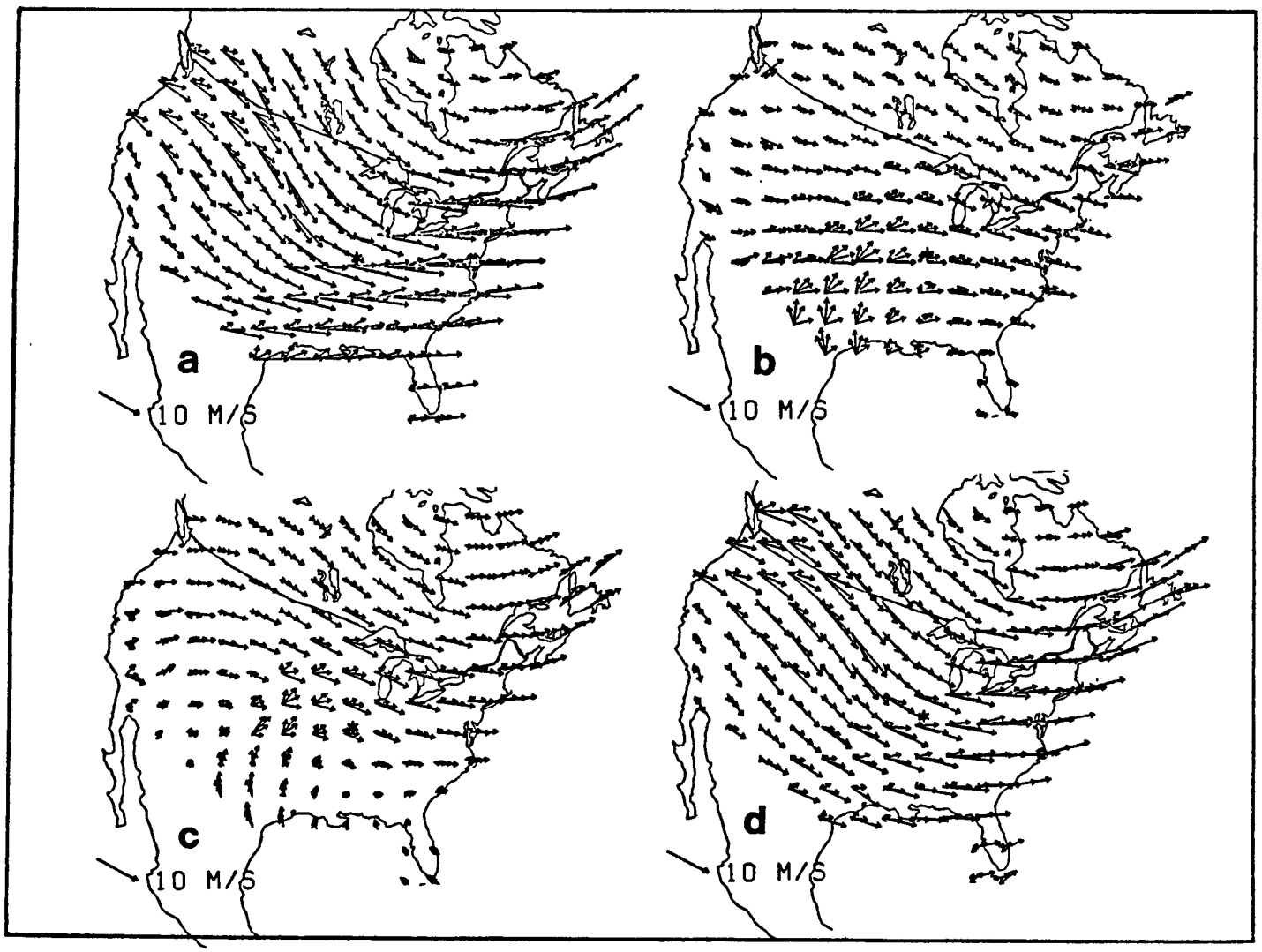

Figure 3-28. Averages for 1975-77 of winds in the layers 0-500, 50-1000, 1000-2000, and 2000-3000 m ag l for the 0000 and 1200 GMT soundings. Lower-level winds generally lie to the left and are of lower speed. (a) January through March; (b) April through June; (c) July through September; and (d) October through December.

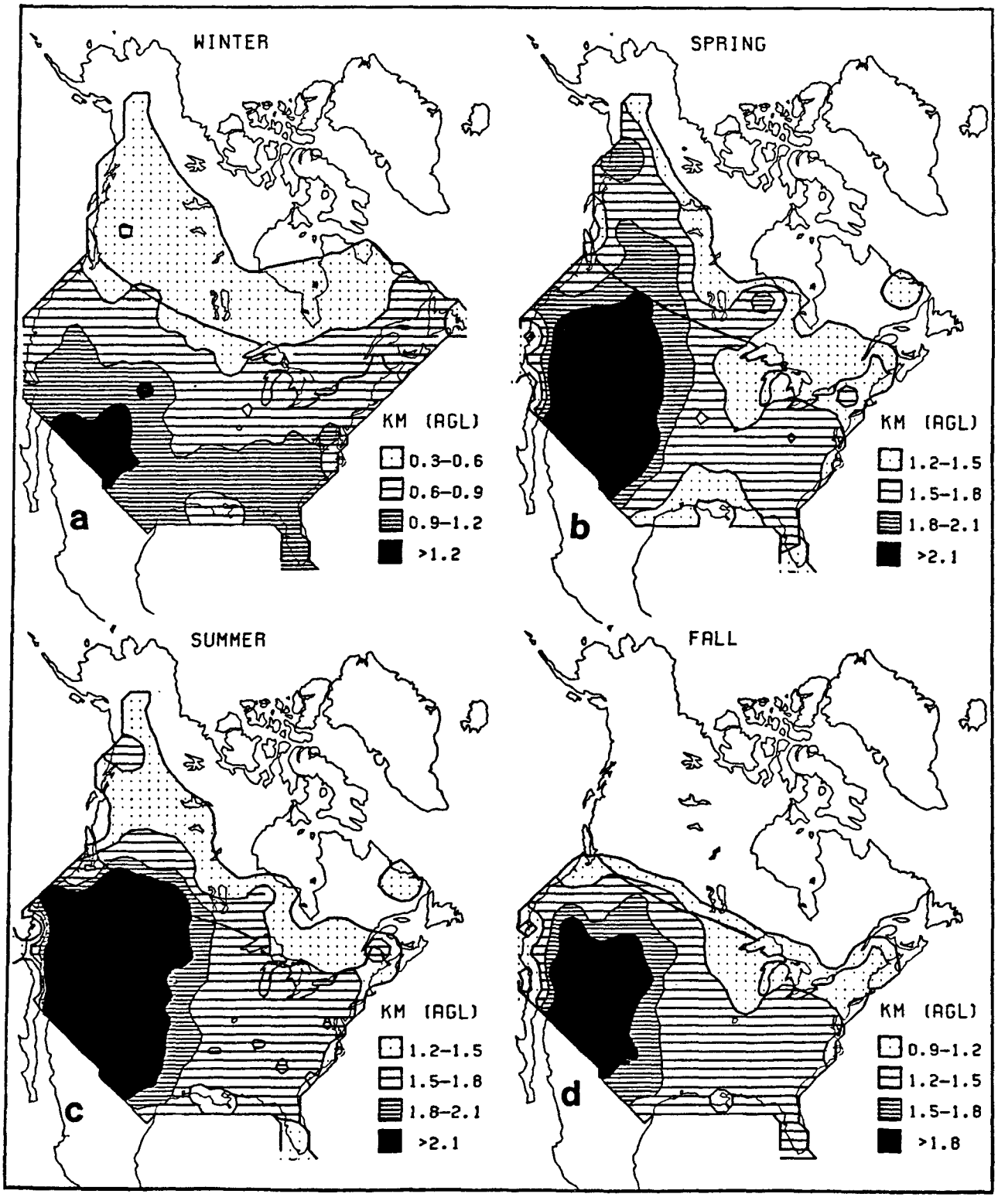

Figure 3-29. Contour plots of maximum afternoon mixing depths by season, indicating qualitative patterns only. Note change of contour scales. (a) January through March; (b) April through June; (c) July through September; and (d) October through December.

atmosphere, thus preventing further transport. Prevalent trajectories from a source to a receptor region will not indicate actual impact if the air mass is very likely to experience precipitation along the way. The exact nature of wet removal is still a matter of debate; presumably some combination of the amount of precipitation, the type and intensity of precipitation events, and the frequency of precipitation may be an appropriate measure of this "forcing function" on a regional scale. As illustrated in Figure 3-30, these three alternative measures can lead to very different conclusions. A pollutant emitted in northeast Canada is more likely, less likely, or equally likely than a pollutant in the southeastern United States to be locally wet deposited, depending on whether frequency, intensity, or total amount of rainfall is the determining wet deposition factor during the summer months.

To examine the average sulfur deposition pattern produced by a single source as a function of time after emission, the ASTRAP model (Shannon 1981) has been exercised with summer meteorological data for a single hypothetical elevated source located near Kansas City. The wet and dry deposition patterns for the first, second, and third days after emission, respectively, are shown (Figures 3-31 through 3-33). Note that these are season average patterns, and not the patterns produced by emissions on a particular day; the latter patterns likely would be much more plume-shaped. If flow during both wet and dry patterns were random, with no prevailing direction, the deposition patterns would be centered on the source location. Here, the deposition maxima progress to the northeast with time, but since flow is not always in the prevailing direction, some deposition occurs in all quandrants, particularly during the first 24 hr of transport. In the Midwest, a region where rainfall is typically 75 to 100 cm yr^{-1}, with frequent summer showers, wet deposition dominates dry deposition after the first day. This is because dry deposition is a function of the steadily decreasing surface concentration, while wet removal occurs through the depth of the mixed layer. The wet deposition maxima can also be seen to progress faster with time; in the Midwest, the Gulf of Mexico is the usual source of precipitation moisture and thus the flow during precipitation has a somewhat higher degree of prevalence than during dry periods.

A similar exercise has been carried out for ten hypothetical sources distributed across the United States and southern Canada (Figures 3-34 through 3-36). Even though the sources (indicated by the symbols) are widely separated, the maxima become difficult to associate with a single source (other than the western sources) after the first 24 hours. The greater relative importance of dry deposition for the southern California source is due both to lighter winds and to less precipitation. The wet deposition contours over the ocean have little meaning because no precipitation observations beyond coastal regions were available for model use; thus, the wet deposition maxima cannot progress beyond the coast, although there is no significant bias caused in simulations over the land.

An example of both current modeling capabilities in long-range transport and deposition and current source/receptor spatial relationships (at least as treated by a particular model) is given in the series Figures 3-37 through 3-40. The ASTRAP model (Shannon 1981) was exercised with a current sulfur

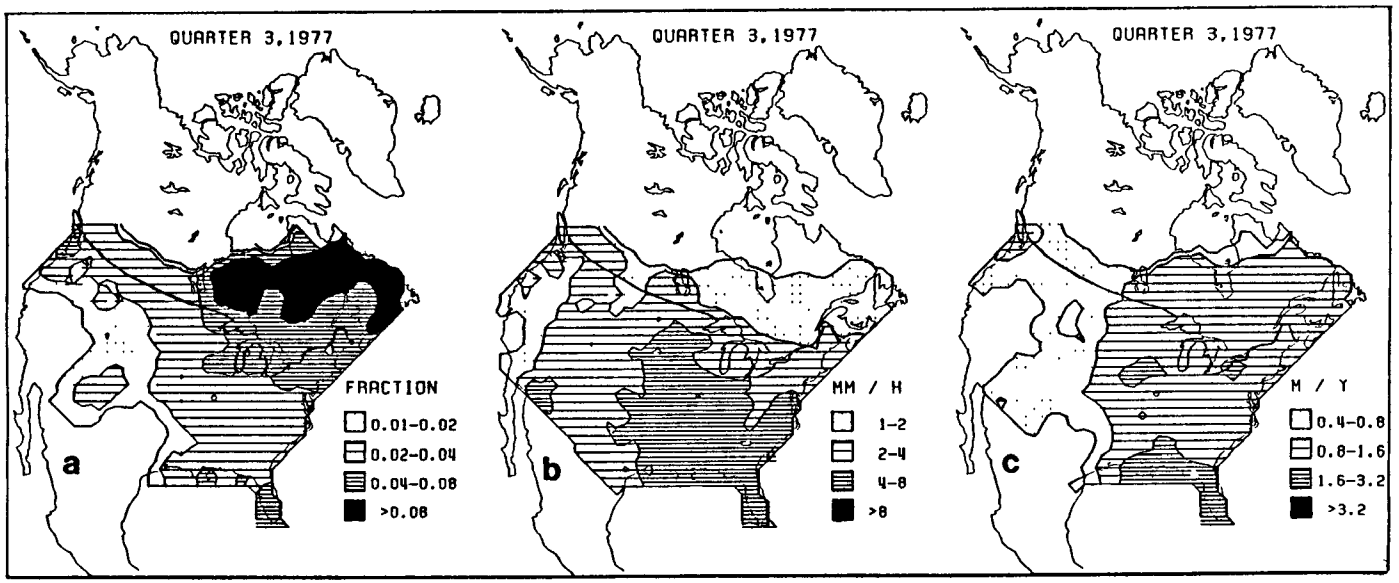

Figure 3-30. Statistics of hourly precipitation data during July-September of 1977. (a) Fraction of hours with precipitation; (b) intensity of rate of rainfall during precipitation events; and (c) total rainfall during the quarter, which is the product of (a) and (b).

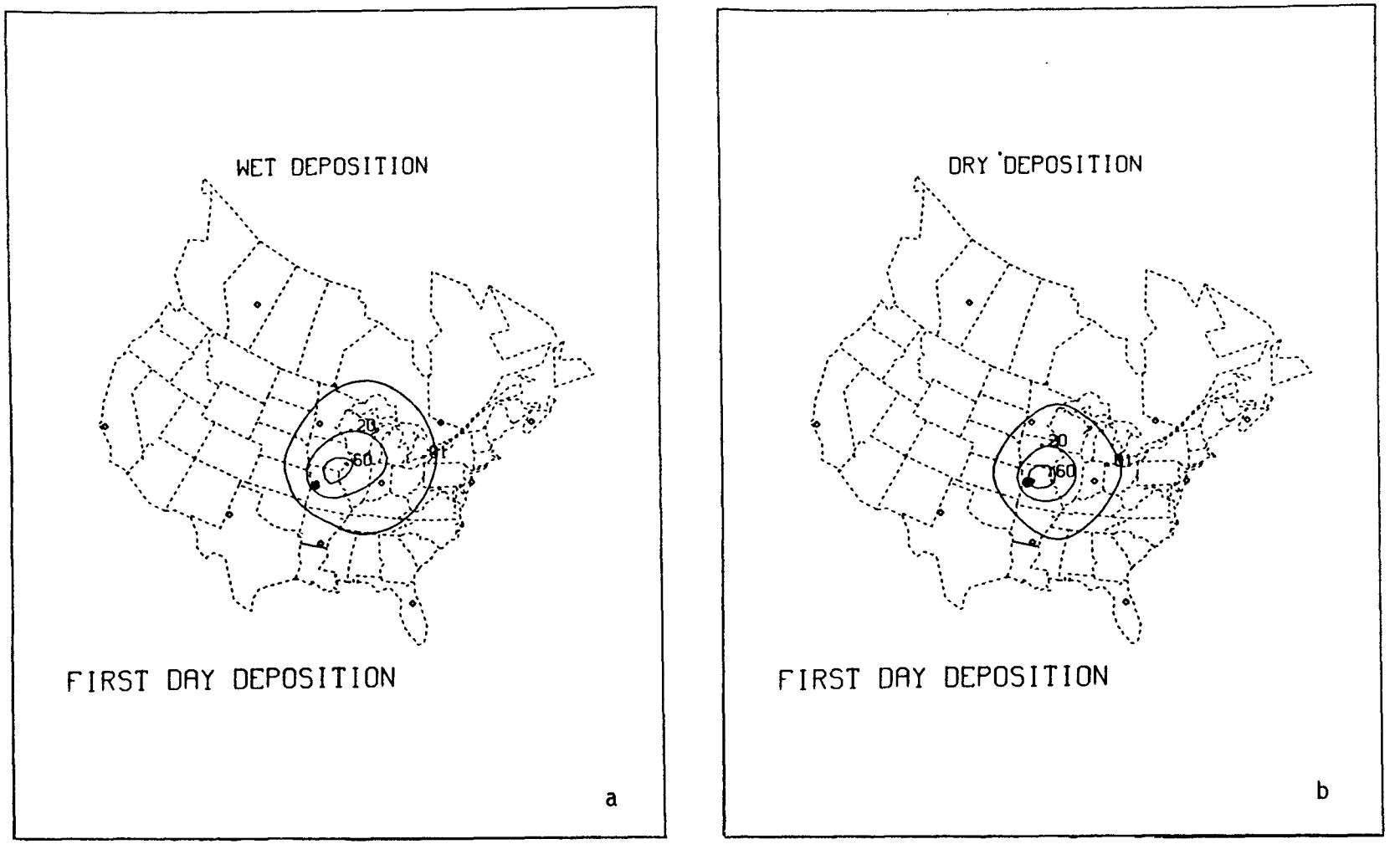

Figure 3-31. Cumulative wet and dry total sulfur deposition patterns during the first day of transport, for a hypothetical source near Kansas City in summer.

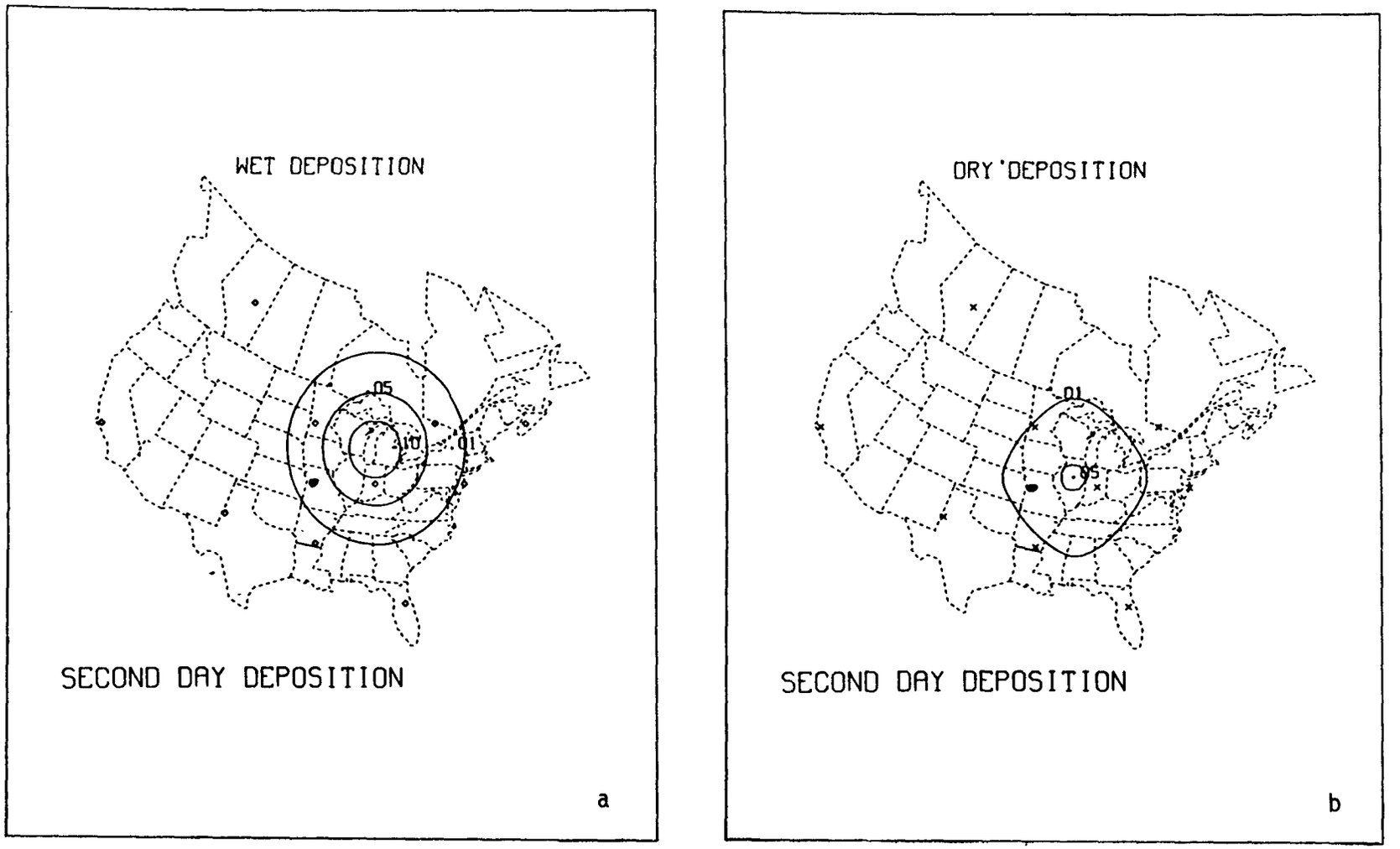

Figure 3-32. Cumulative wet and dry total sulfur deposition patterns during the second day of transport.

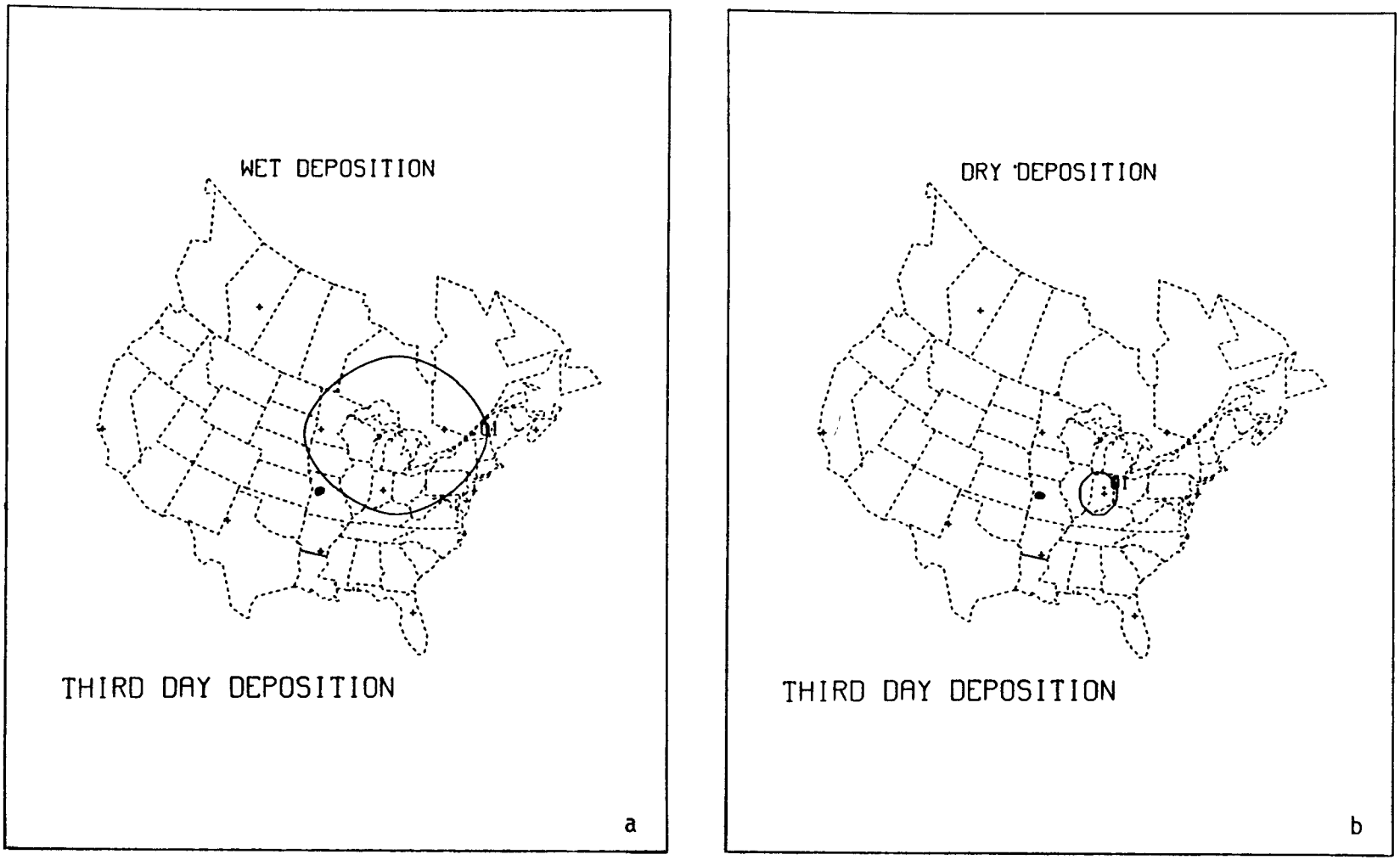

Figure 3-33. Cumulative wet and dry total sulfur deposition patterns during the third day of transport.

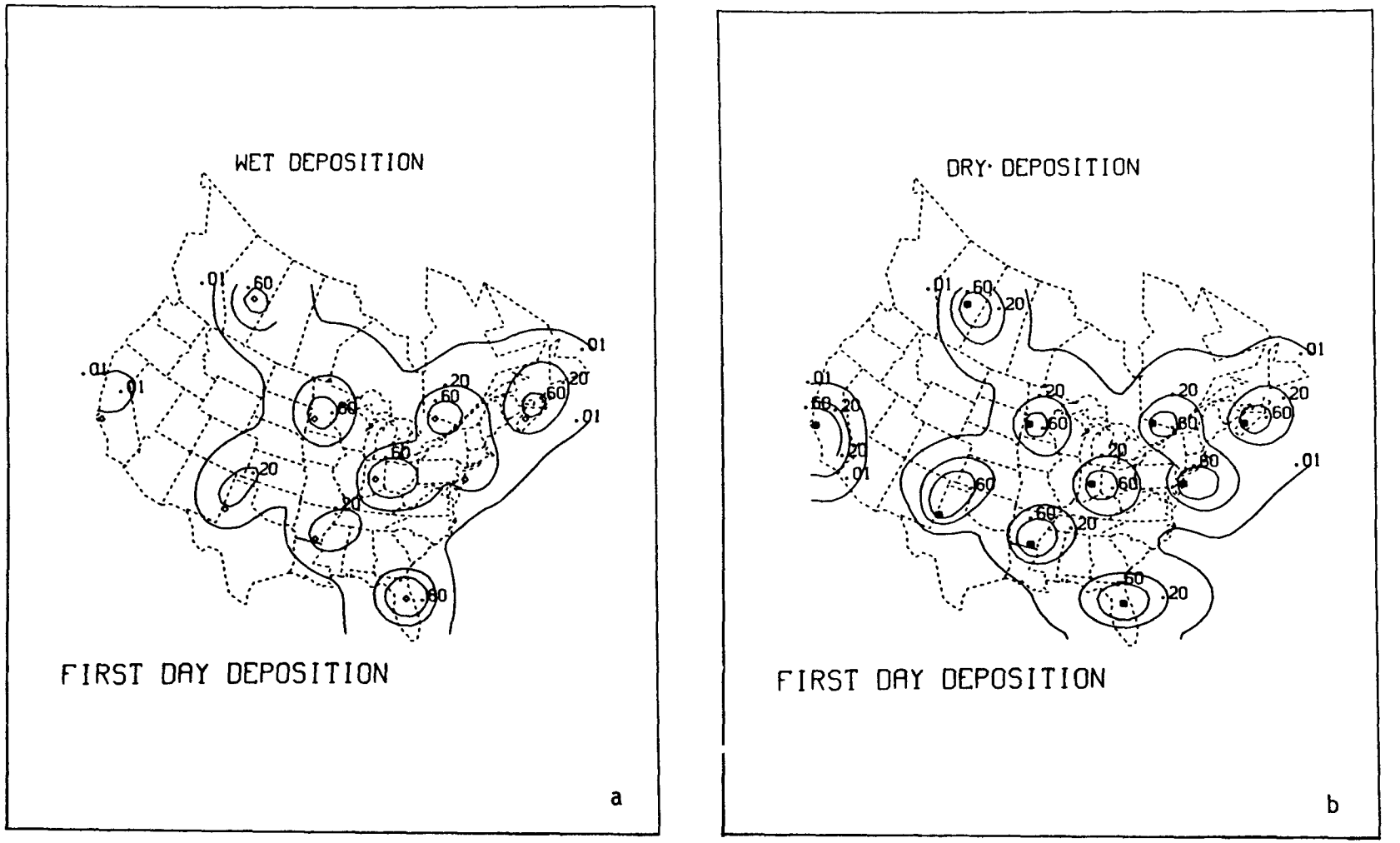

Figure 3-34. Cumulative wet and dry total sulfur deposition patterns during the first day of transport, for ten hypothetical sources.

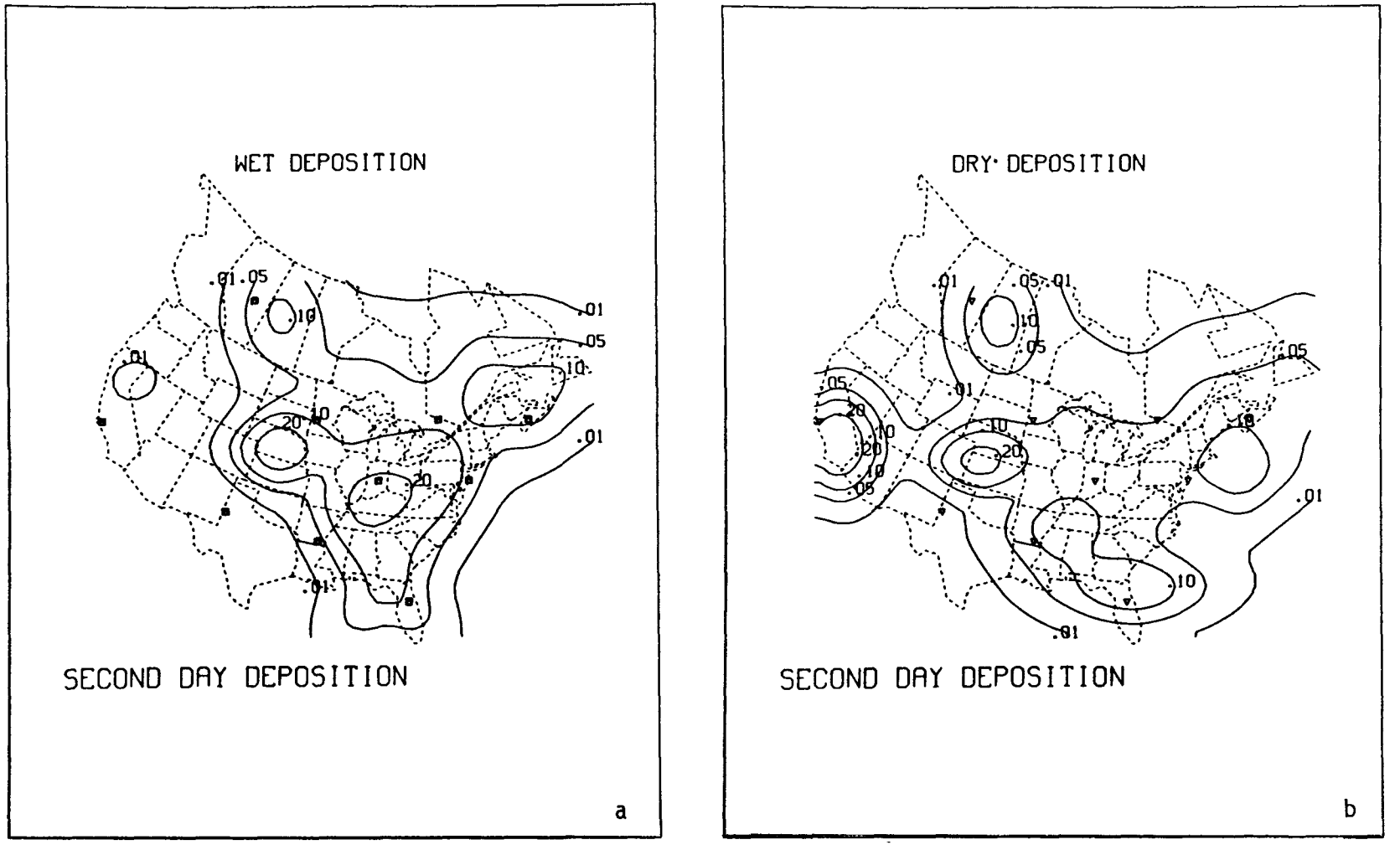

Figure 3-35. Cumulative wet and dry total sulfur deposition patterns during the second day of transport, simulated for ten hypothetical sources.

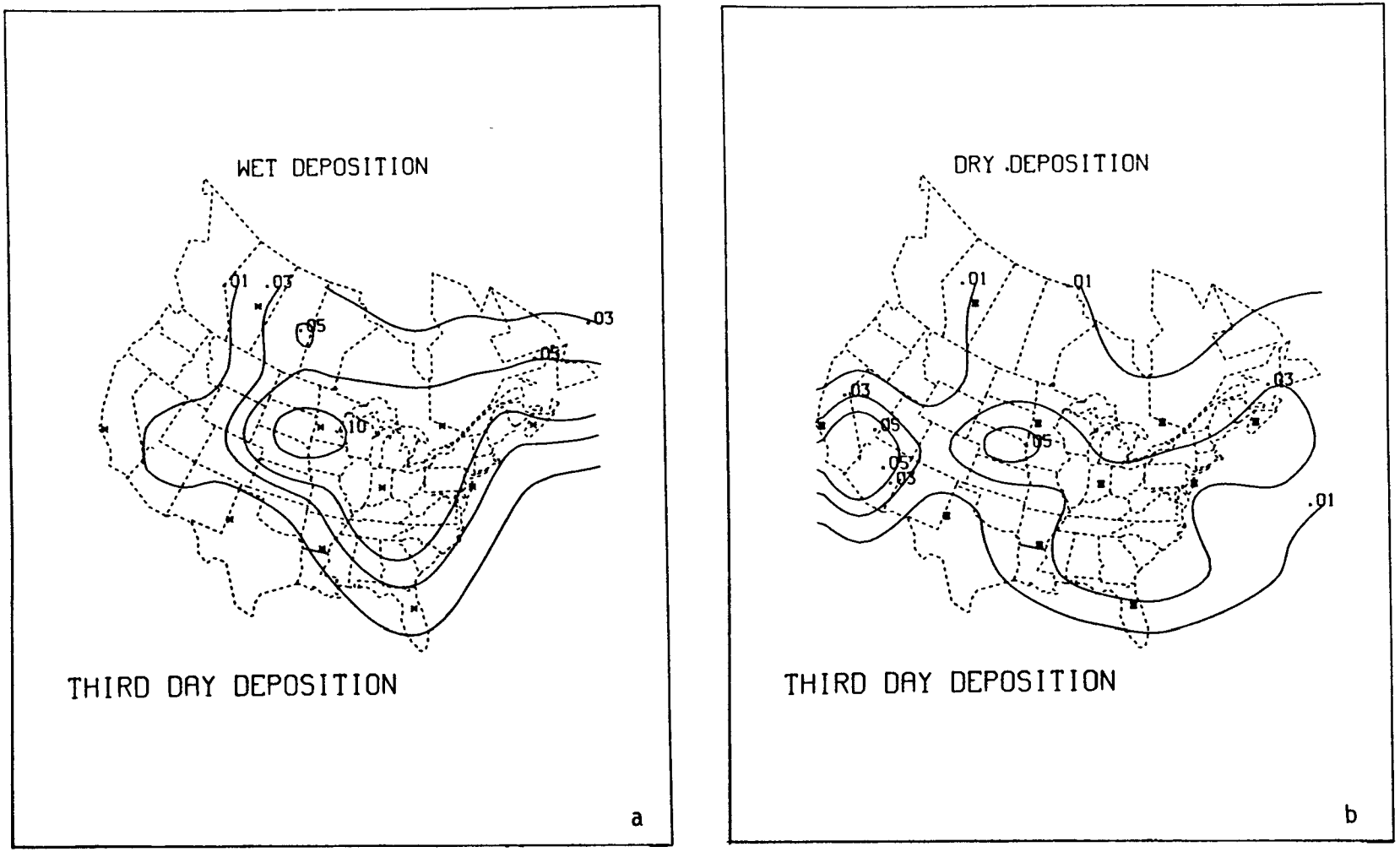

Figure 3-36. Cumulative wet and dry total sulfur deposition patterns during the third day of transport, simulated for ten hypothetical sources.

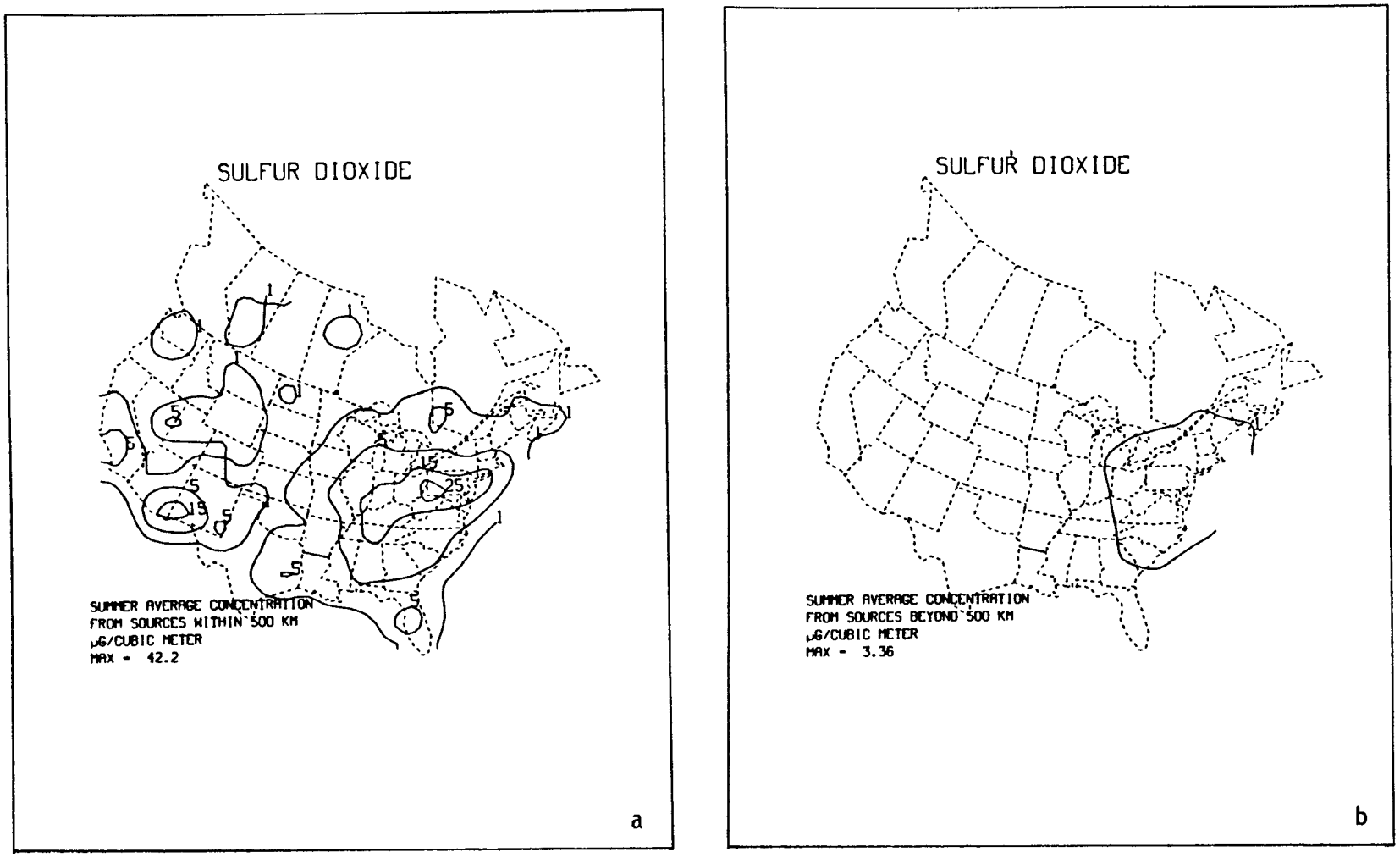

Figure 3-37. Contribution to average summer SO_2 concentrations resulting from U.S. and Canadian anthropogenic sulfur sources within 500 km and from sources beyond 500 km.

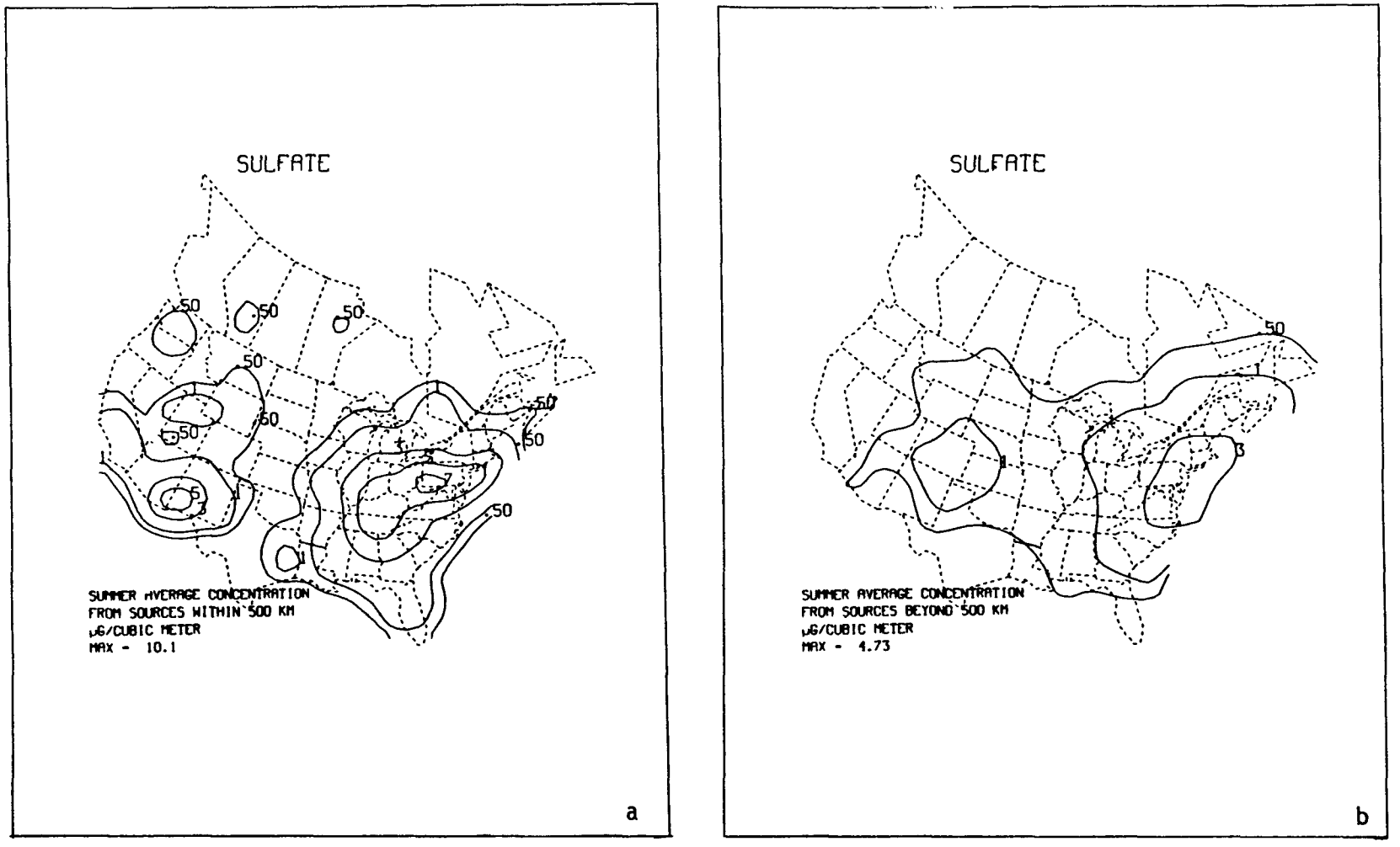

Figure 3-38. Contribution to average sulfate concentration resulting from U.S. and Canadian anthropogenic sulfur sources within 500 km and from sources beyond 500 km.

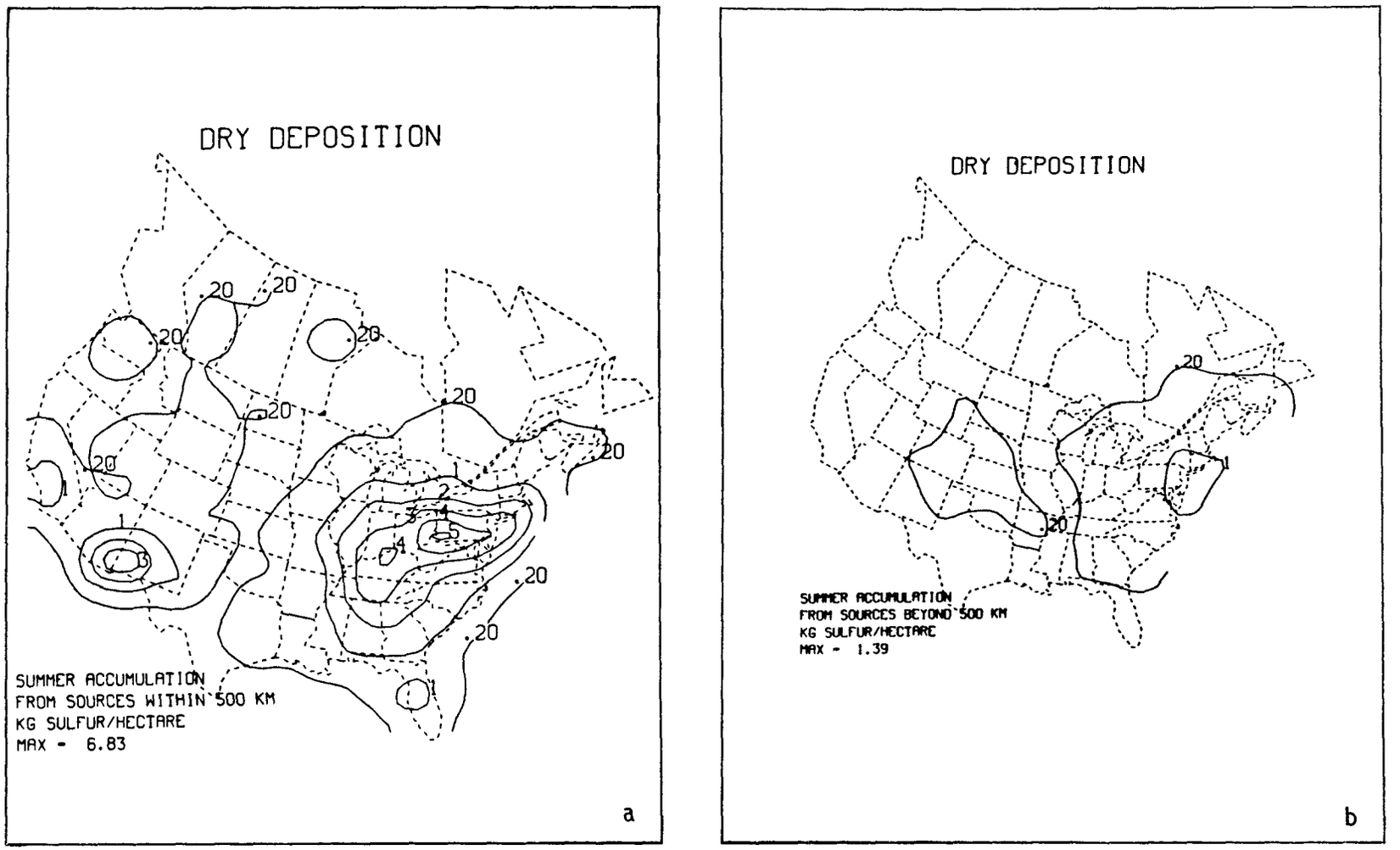

Figure 3-39. Contribution to cumulative dry deposition of total sulfur resulting from U.S. and Canadian anthropogenic sources within 500 km and from sources beyond 500 km.

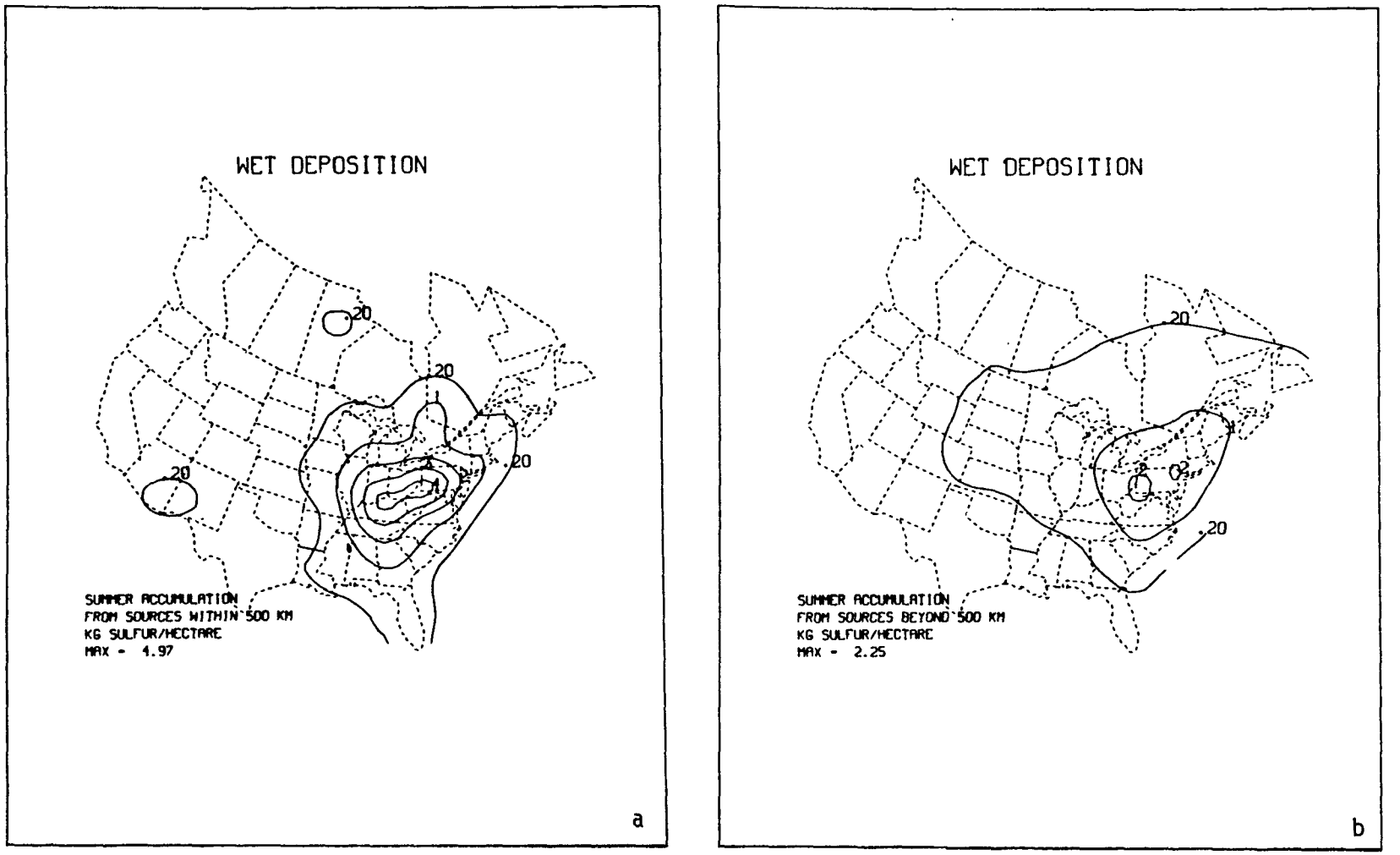

Figure 3-40. Contribution to cumulative wet deposition of total sulfur resulting from U.S. and Canadian anthropogenic sulfur sources within 500 km and from sources beyond 500 km.

oxide emission inventory for the United States and Canada and with meteorological data for June-August 1980. The concentration and deposition patterns were separately calculated for sources within 500 km of each of the (51 x 37) points in a grid across North America, and for sources beyond 500 km from each point. If the two source/receptor separation categories are termed local and long-range, respectively, it can be seen that average SO_2 concentrations from sources beyond 500 km are almost nil, while the long-range contribution to sulfate is more than half of the average concentration in New England and much of eastern Canada. The fraction of dry deposition in those regions from long-range transport is also significant, although the total amounts are low. Wet deposition of sulfur has the most significant long-range component of the four fields examined for this single season. If one considers the low emission density of most of New England, upper New York State, and the Maritimes, the relatively greater influence of sources beyond 500 km is not surprising. In particular, there are few emissions within 200 km of most of the area. While other models might give somewhat different results, there is general agreement that sulfate and wet deposition of total sulfur have a larger long-range component than do sulfur dioxide and dry deposition of total sulfur. Since the input data have a minimum resolution of about 100 km, local deposition maxima on smaller scales are not simulated. It should be emphasized that the results shown are from a particular model, and that no model of long-range transport and deposition is as yet fully verifiable.

Seasonal ASTRAP simulations for all anthropogenic sulfur emissions from the United States and Canada during 1980 gave a budget of 28 to 32 percent dry deposition on the continent and 13 to 31 percent wet, with annual totals of 29 percent dry and 24 percent wet. The budget remainder, 47 percent for annual totals, is an upper estimate of coastal net mass sulfur flux, as deposition, particularly dry deposition, is likely underestimated within 100 km of sources, the minimum resolution of the ASTRAP simulations. Wet deposition is more variable than dry deposition because of regional droughts and wet periods. Rigorously determined confidence limits cannot be placed on the simulation results, because only wet deposition is monitored.

Hemispheric transport of acidic deposition precursors from sources in North America to receptor regions in the Northern Hemisphere has been examined primarily in regard to two particular issues: the contribution of North American sources to acidic deposition in Europe, particularly Scandinavia; and the contribution of North American sources to Arctic haze. The latter issue has been raised more in reference to visibility or modification of radiation balance. For long periods, the Arctic is a polar "desert" with essentially no wet deposition and very little dry deposition due to strong low-level stability.

According to Rahn (1981), the two pathways to the Arctic of greatest significance are northward transport from Europe via Scandinavia and a cyclonic pathway from Europe and the central U.S.S.R. into the Norwegian Arctic. These air masses may be transported over the pole into the North American Arctic. The cyclonic track is less effective as a transport mechanism because of much greater wet removal. North American pollutant sources, which lie mostly in the eastern or downwind portion of the

continent, occassionally contribute haze precursors to the Canadian Arctic islands via a track around Greenland. Concentrations of pollutant aerosols in the Arctic show a definite winter peak when the removal mechanisms are almost inactive. Rahn and McCaffrey (1980) indicate winter residence times of 2 to 3 weeks for Arctic aerosol particles.

The contribution of North American sources to acidic deposition in Europe, particularly Scandinavia, is not firmly established but is thought to be relatively small. Studies of "clean" Atlantic aerosol (i.e., not downwind of European sources) indicate concentrations of 0.2 $\mu g\ m^{-3}$ of SO_2 and 0.8 $\mu g\ m^{-3}$ of sulfate (Prahm et al. 1976), but in part the concentrations result from production/destruction activities in the sea, greatly complicating the analysis of box-budget studies. While the North American contribution is not the major share in acidic deposition in Scandinavia, the multiplicity of sovereign source regions in Europe and the resulting fragmentation of contributions to the deposition burden make quantification of the North American input desirable.

An issue receiving increasing attention is the occurrence in presumably pristine areas of precipitation pH as low as 4.3 (Miller and Yoshinaga 1981). While most pristine areas receive precipitation hydrogen ion concentrations an order of magnitude less than in industrialized regions, the pH of elevated sites, in particular, can be considerably lower. The relative importance of natural biogenic sources and hemispheric transport of manmade pollutants has yet to be determined. Transport above the PBL over oceanic areas might not encounter either wet or dry removal processes for great distances until mountainous islands, which can extend above the marine PBL, are reached. Calculations of back trajectories from Hawaii (Miller 1981) show a strong east-west flow dichotomy.

There are many uncertainties in diagnostic analysis and modeling of transport of acidic or acidifying pollutants. These uncertainties involve both understanding and quantifying individual processes, and development of tractable parameterizations for use in computer simulation models of transport and deposition. An illustrative, although not necessarily complete, list includes the following:

1) The transport layer or layers must be defined. Should calculations be for constant-level flow, or for isentropic flow (common above the mixed layer)?

2) Synoptic-scale and mesoscale vertical motions redistribute the pollutants and thus complicate the definition of the transport layer.

3) Transport and diffusion over complex terrain, such as mountain ranges or shorelines, is more complicated and less understood than over homogeneous terrain. Current experimental plans such as CAPTEX will help here.

4) Three-dimensional flows through precipitation systems over all scales are not well understood.

5) The effect of wet and dry removal cannot be separated from transport distance calculations. For continental transport, the air mass must pass over surfaces of very different roughness, vegetation, and stability characteristics. Dry deposition rates are still contentious matters, and the "best estimate" can vary widely. Wet deposition has been investigated in detail mostly on the local scale, although the OSCAR experiment of the EPA/DOE MAP3S program in 1981 was aimed at the regional scale (Easter 1981). Wet removal parameterizations, developed for the local scale but then modified for continental scales, have yet to be thoroughly verified.

6) Most atmospheric processes have a strong diurnal variation, such as the pronounced shear effects associated with nocturnal decoupling and the nocturnal "jet." While in simulation modeling of long-range transport and deposition one may elect not to apply diurnally varying parameters explicitly, the diurnal variations in the real atmosphere must be considered in the choice of any average parameterization values.

7) Evaluation of recurvature of trajectories back to the North American land mass has been far more qualitative than quantitative.

3.6 CONCLUSIONS (N. V. Gillani, J. D. Shannon, and D. E. Patterson).

The flow field in the PBL, which is responsible for pollutant transport between a source and the receptor sites, is characterized by a broad spectrum of atmospheric motions ranging from microscale turbulent eddies to global-scale circulation. As a pollutant cloud is transported and dispersed, it is influenced by a progressively larger range of atmospheric motions. The horizontal winds are primarily responsible for pollutant advection, while turbulent eddies, wind shear, and direction changes with height, as well as sudden wind shifts, cause vertical and lateral pollutant dispersion (Section 3.3).

There is no universal agreement as to proper scale divisions in the transport of acidic or acidifying pollution. In general, the dominant time scales are diurnal, synoptic (2 to 5 days), and annual. The diurnal scale is critical because so many transport and removal processes (including air mass convection showers) are strongly affected by the solar heating cycle. The synoptic scale is significant both because flow patterns may "box the compass" during passage of a circulation center and because the precipitation frequency is largely controlled on this scale. The annual scale is important because so many important atmospheric variables show a marked seasonal pattern (e.g., synoptic flow pattern, PBL height, pollutant transformation rates, etc.) (Section 3.2).

We wish to highlight the following aspects of transport processes which appear to be of particular significance at this stage in our assessment of acidic deposition.

- Mixing height is an important transport parameter. It governs not only vertical dilution of the pollutant, but also horizontal

dilution by wind shear effects in the vertical domain of transport. Mixing height has a very pronounced diurnal and seasonal variability but is spatially relatively uniform in the eastern United States. It peaks daily in the afternoon and seasonally in summer. In particular, as a result of substantially lower mixing heights in winter than in summer, a significant portion (perhaps greater than 20 percent) of the elevated emissions from tall power plant stacks in northeastern United States may remain elevated and relatively coherent for more than 24 hr and 500 km of transport (Section 3.3.1).

- Atmospheric dispersive processes also play critical roles in chemical transformations of emissions (by facilitating their dilution with chemically different background air) and in pollutant removal by dry deposition (by governing the vertical delivery to or away from the ground sink). Elevated emissions remain mostly decoupled from the ground at night and reach it substantially diluted during the day. In contrast, ground-level emissions (for example, from automobiles) may remain trapped within a shallow mixing layer at night, experiencing substantial dry deposition within short-range transport. Tall-stack emissions of sulfur and nitrogen oxides thus have longer atmospheric residence times than do the general urban emissions of these compounds (Sections 3.4 and 3.5).

- The PBL flow field is characterized by strong diurnal and seasonal variations. In the dense source region in the northeastern United States, prevailing winds are, on the average, from the southwestern quadrant in summer and more westerly in winter. The vertical pollutant transport layer for long-range transport varies typically from the ground up to 1 or 2 km in summer and about half that in winter. Diurnal variability of the flow field is particularly pronounced in summer, especially in the midwestern states, where a "nocturnal jet" with strong associated wind shear is a frequent occurrence, following relatively slower and vertically more homogeneous wind during the daytime. The pollutant plumes undergo a sequence of sheared stratification and distortion during the night followed by vertical homogenization by day. This results in a rapid dispersion of emissions over a regional scale (Sections 3.2, 3.3.2, and 3.4.1).

- Prevailing winds are strongly influenced locally by mesoscale effects such as complex terrain and storm fronts. Alterations of air parcel trajectories by local vertical flows remain inadequately understood, at least partly due to the lack of routine vertical wind data. Conventional methods of air trajectory analyses in frontal zones, near squall lines and other storm systems, may be quite inadequate (Section 3.3.4).

- A major source of uncertainty in long range trajectory calculations is related to the inadequacy of currently available routine upper air wind data, which represent relatively sparse, two-dimensional, Eulerian measurements. Their spatial-temporal coverage cannot provide important information concerning mesoscale flows. Field

experiments to characterize long-range transport under a variety of flow conditions are needed (Sections 3.2.2 and 3.5).

- Individual trajectory calculations can be highly uncertain, and the use of the statistics of multiple trajectories is to be preferred. In general, the uncertainties associated with transport processes are known only in a qualitative sense; rigorous estimation of uncertainties is limited to particular models, at best (Sections 3.1 and 3.5).

- Deposition from a pollutant source is greatest near the source and decreases more or less exponentially away from the source. In the summer, on the average, well over half of the eastern U.S. sulfur emissions may be deposited within two days and 500 km from the source. The transport range is likely to be considerably greater in winter. Average or cumulative deposition, particularly dry deposition, extends in all directions from the source, but the deposition pattern is not homogeneous. The prevailing flow is reflected in a shift of the deposition maxima downstream in time; in the ecologically sensitive regions of eastern North America, downstream generally means toward the east or northeast. This conclusion is based primarily on observations and modeling of SO_x. The conclusion probably applies to NO_x, but in general, information related to atmospheric residence times of nitrogen compounds is less complete and more tentative than for sulfur compounds (Sections 3.4 and 3.5).

- Based on modeling simulations for summer conditions, one may identify three approximate regions in northeastern United States and eastern Canada in which the relative contributions to acidic depositions due to emissions from near (< 500 km) versus distant (> 500 km) sources may be significantly different. In the upper Ohio River Valley (a dense source region), sources within 500 km appear to dominate the maxima of ambient SO_2 and aerosol sulfate concentrations, as well as the total wet and dry depositions of sulfur. At the other extreme, in upper New England and parts of eastern Canada which are remote from major sources of sulfur, long-range transport may be responsible for most of the aerosol sulfate and total wet deposition of sulfur. In the intermediate regions, including the Adirondacks, contributions to total acidic depositions from near and far sources may be more comparable, considered on a regional and summer average basis. These simulations have a minimum resolution of about 100 km and thus do not reflect local source "hot spots." The relative contributions of long-range transport and local circulations to the deposition patterns in the eastern coastal region of the United States are not well understood. In general, modeling uncertainties make the boundary between local and long-range domination somewhat tentative. Also, estimates of regional dry depositions must be viewed as tentative since they are based on indirect, very local, and rather sparse measurements of dry deposition parameters rather than on direct regional monitoring of dry deposition fluxes (Section 3.5).

Acknowledgment: A significant amount of the material presented in this chapter was developed under cooperative agreement between Washington University and the U.S. Environmental Protection Agency (CR-80-9713, CR-81-0325, and CR-81-0351).

3.7 REFERENCES

Alberty, R. L., D. W. Burgess, C. E. Hand, and J. F. Weaver. 1979. SESAME 1979 Operations Summary, Technical Report, NOAA-ERL, Boulder, CO.

Altshuller, A. P. 1977. Formation and removal of SO_2 and oxidants from the atmosphere. Adv. Environ. Sci. Technol. 8:9.

Anthes, R. A., H. A. Panofsky, J. J. Cahir and A. Rango. 1975. The Atmosphere. Chas. E. Merrill Publ., Columbus, OH.

Arya, S. P. 1982. Atmospheric boundary layers over homogeneous terrain, Ch. 6. In Engineering Meteorology. E. J. Plate, ed. Elsevier, Amsterdam.

Barry, R. G. and R. J. Chorley. 1977. Atmosphere, Weather, and Climate. Third Ed., Methuen & Co., Ltd., London.

Bass, A. 1979. Modeling long range transport and diffusion. Proceedings, Second Joint Conference on Applications of Air Pollution Meteorology. American Meteorol. Society, Boston MA.

Benkovitz, C. M. 1982. Compilation of an inventory of anthropogenic emissions in the United States and Canada. Atmos. Environ. 16:1551-1564.

Beran, D. W. 1978. Prototype Regional Observing and Forecasting Service. NOAA Executive Summary of a Program Development Plan. NOAA-ERL, Boulder, CO.

Betts, A. K., R. W. Grover and M. W. Monerieff. 1976. Structure and motion of tropical squall lines over Venezuela. Quart. J. Roy. Met. Soc. 102:395-404.

Blackadar, A. K. 1957. Boundary layer wind maxima and their significance for the growth of nocturnal inversions. Bull. Amer. Meteorol. Soc. 38: 283-290.

Bonner, W. D. 1968. Climatology of the low level jet. Monthly Weather Rev. 96:833-850.

Bonner, W. D., S. Esbensen, and R. Greenberg. 1968. Kinematics of the low-level jet. J. Appl. Meteorol. 7:339-347.

Bornstein, R. D. and D. S. Johnson. 1977. Urban-rural wind differences. Atmos. Environ. 11:597.

Briggs, G. A. 1969. Plume Rise. USAEC Critical Review Series, TID-25075, Clearinghouse for Federal Scientific and Technical Information.

Briggs, G. A. 1975. Plume rise predictions. In Lectures on Air Pollution and Environmental Impact Analyses. Amer. Meteorol. Soc., Boston, MA.

Brown, R. A. 1974. Analytical Methods in PBL Modelling. Halsted Press (John Wiley), New York.

Burpee, R. W. 1979. Peninsula-scale convergence in the south Florida sea breeze. Mon. Weather Rev. 107:852-860.

Businger, J. A. and S. P. Arya. 1974. Height of the mixed layer in stably stratified boundary layer. Advances in Geophysics, Vol. 18A:73-92.

Businger, J. A., J. C. Wyngaard, Y. Izumi, and E. F. Bradley. 1971. Flux-profile relationships in the atmospheric surface layer. J. Atmos. Sci. 28:181-189.

Byers, H. R. and R. R. Braham, Jr. 1949. The Thunderstorm. U.S. Printing Office, Washington, DC.

Carpenter, K. 1979. An experimental forecast using non-hydrostatic meso-scale model. Quart. J. Roy. Met. Soc. 105:629-655.

Caughey, S. J. and J. C. Kaimal. 1977. Vertical heat flux in the convective boundary layer. Quart. J. Roy. Met. Soc. 103:811-815.

Caughey, S. J., J. C. Wyngaard, and J. C. Kaimal. 1979. Turbulence in the evolving stable boundary layer. J. Atmos. Sci. 36:1041-1052.

Chandler, T. J. 1970. Urban Climatology-Inventory and Prospect. WMO TN No. 108:2-14.

Ching, J. K. S., J. F. Clark, J. S. Irwin, and J. M. Godowitch. 1983. Relevance of mixed layer sealing for daytime dispersion based on RAPS and other field programs. Atmos. Environ.:In press.

Chung, Y. S. 1978. The distribution of atmospheric sulfates in Canada and its relationship to long-range transport of pollutants. Atmos. Environ. 12:1471-1480.

Clarke, R. H. 1970. Observational studies in the atmospheric boundary layer. Quart. J. Roy. Met. Soc. 96:91-114.

Clarke, T. F. and F. G. McElroy. 1970. Experimental studies of Nocturnal Urban Boundary Layer. WMO TN No. 108:108-112.

Clarke, R. H., A. J. Dyer, R. R. Brook, D. G. Reid, and A. J. Troup. 1971. The Wangara Experiment: Boundary Layer Data, Tech. Paper No. 19, CSIRO. Div. Meteor. Phys.

Davis, W. E. and L. L. Wendell. 1976. Some effects of isentropic vertical motion simulation in a regional-scale quasi-Lagrangian air quality model. In Proc., Third Symposium on Atmospheric Turbulence, Diffusion, and Air Quality, Oct. 19-22, Raleigh, NC. American Meteorological Society, 403-406.

Day, S. 1953. Horizontal convergence and the occurrence of summer precipitation at Miami, Florida. Mon. Weather Rev. 81:155-161.

Deardorff, J. W. 1980. Progress in understanding entrainment at the top of the mixed layer. Proc. AMS Workshop on the Planetary Boundary Layer. J. C. Wyngaard, ed. American Meteorological Society, Boston, MA.

Defant, F. 1950. Theorie der land-und seewind. Arch. Meteorol., Geophys. Bioklimatol., Ser. A 2:404-425.

Defant, F. 1951. Local winds. In Compendium of Meteorology, pp. 655-672. American Meteorological Society, Boston, MA.

Draxler, R. R. and A. D. Taylor. 1982. Horizontal dispersion parameters for long-range transport modeling. J. Appl. Meteorol. 21:367-372.

Durst, C. S., A. F. Crossley and N. E. Davis. 1959. Horizontal diffusion in the atmosphere as determined by geostrophic trajectories. J. Fluid Mech. 6:401-422.

Easter, R. C. 1981. The OSCAR experiment. In Proc., ACS Symposium on Acid Rain. Las Vegas, NV.

Edinger, J. G. and T. F. Press. 1982. Meteorological factors in the formation of regional haze. Final report, EPA ORD ESRL. October 1982.

Egan, B. A. 1975. Turbulent diffusion in complex terrain. In Lectures on Air Pollution and Environmental Impact Analyses. Amer. Meteorol. Soc., Boston, MA.

Estoque, M. A. 1961. A theoretical investigation of sea breeze. Quart. J. Roy. Met. Soc. 87:136-146.

Estoque, M. A. 1962. The sea breeze as a function of prevailing synoptic situation. J. Atmos. Sci. 19:244-250.

Estoque, M. A., J. Gross and H. W. Lai. 1976. A lake breeze over southern L. Ontario. Mon. Weather Rev. 104:386-396.

Farquaharson, S. J. 1939. The diurnal variations of wind over tropical Africa. Quart. J. Roy. Met. Soc. 65:165-183.

Frank, W. M. 1978. The life cycles of GATE convective systems. J. Atmos. Sci. 35:1256-1264.

Frenzen, P. 1980. Discussion following paper by L. Mahrt in Proceedings of the Workshop on the Planetary Boundary Layer, Boulder, CO, 14-18 August. Amer. Meteorol. Soc., Boston, MA.

Fritsch, J. M. and R. A. Maddox. 1980. Analysis of upper tropospheric wind perturbations associated with mid-altitude mesoscale convective complexes. Preprint volume, AMS Conf. on Weather Forecasting Anal., 339-345.

Fritsch, J. M. and R. A. Maddox. 1981. Convectively driven mesoscale weather systems aloft. Part I: Observations. J. App. Meterol. 20:1, 9-19.

Fujita, T. T. 1959. Precipitation and cold air production in mesoscale thunderstorm systems. J. Meteorol. 16:459-466.

Garrett, J. R. 1982. Observations in the nocturnal boundary layer. Boundary Layer Met. 22:21-48.

Garstang, M., and A. K. Betts. 1974. A review of the tropical boundary layer and cumulus convection: Structure parameterization and modeling. Bull. Am. Meteorol. Soc. 55:1195-1205.

Gentry, R. C. and P. L. Moore. 1954. Relation of local and general wind interaction near the sea coast to time and location of air-mass showers. J. Meteorol. 11:507-511.

Gillani, N. V. 1978. Project MISTT: Mesoscale plume modeling of the dispersion, transformation and ground removal of SO_2. Atmos. Environ. 12:569-588.

Gillani, N. V. and W. E. Wilson. 1980. Formation and transport of ozone and aerosols in power plant plumes. Annals N.Y. Acad. Sci. 338:276-296.

Gillani, N. V. and W. E. Wilson. 1983. Gas-to-particle conversion of sulfur in power plant plumes: II. Observation of liquid-phase conversions. Atmos. Environ. 17(9):1739-1752.

Gillani, N. V., J. A. Colby, and W. E. Wilson. 1983. Gas-to-particle conversion of sulfur in power plant plumes: III. Parameterization of plume-cloud interactions. Atmos. Environ. 17(9):1753-1764.

Gillani, N. V., S. Kohli, and W. E. Wilson. 1981. Gas-to-particle conversion of sulfur in power plant plumes - I. Parameterization of the conversion rate for dry, moderately polluted ambient conditions. Atmos. Environ. 15:2293-2313.

Gillani, N. V., B. R. Husar, J. D. Husar, D. E. Patterson, and W. E. Wilson. 1978 . Project MISTT: Kinetics of particulate sulfur formation in a power plant plume out to 300 km. Atmos. Environ. 12:589-598.

Goualt, J. 1938. Vents en altitude a fort Lamy (Tchad). Ann. Phys. du Globe de la France d'Outre-Mer 5:70-91.

Haugen, D. A., J. C. Kaimal, and E. F. Bradley. 1971. An experimental study of Reynolds stress and heat flux in the atmospheric surface layer. Quart J. Roy. Met. Soc. 97:168-180.

Heffter, J. L. 1980. Air Resources Laboratories Atmospheric Transport and Disperion Model (ARL-ATAD), NOAA Tech. Memo., ERL ARL-81, Air Resources Laboratories, Silver Spring, MD.

Hering, W. S. and T. R. Borden. 1962. Diurnal variations in the summer wind field over the central U.S. J. Atmos. Sci. 19:81-86.

Hicks, B. B., G. D. Hess, M. L. Wesely, T. Yamada, P. Freugen, R. L. Hart, D. L. Sisterson, P. E. Hess, F. C. Kulhanek, R. C. Lipschutz, and G. A. Zerbe. 1981. The Sangamon Field Experiments: Observations of the diurnal variations of the PBL over land. Atmospheric Physics Section, Argonne National Laboratory, Report ANL-RER-81-1, Argonne, IL.

Holton, J. R. 1967. The diurnal boundary layer wind oscillation over sloping terrain. Tellus 19:199-205.

Holzworth, G. C. 1972. Mixing heights, wind speeds, and potential for urban air pollution throughout the contiguous United States. U.S. EPA AP-101.

Hoxit, L. R., R. A. Maddox, C. F. Chappell, F. L. Zurkerberg, H. M. Mogil, I. Jones, D. R. Greene, R. E. Saffle, and R. E. Scofield. 1978. Meteorological aspects of the Johnstown, PA flash flood, 19-20 July 1977. NOAA TR ERL 401-APCL-43:1-71.

Hunt, J. C. R. and Simpson, J. E. 1982. Atmospheric boundary layers over non-homogeneous terrain. Ch. 7. In Engineering Meteorology. E. J. Plate, ed. Elsevier, Amsterdam.

Hsu, S. 1969. Mesoscale structure of the Texas Coast Sea Breeze. Rep. No. 16, Atmospheric Science Group, Univ. of Texas, College of Engineering, Austin, TX.

Husar, R. B. and D. E. Patterson. 1980. Regional scale air pollution: Sources and effects. Annals N.Y. Acad. Sci. 338:399-417.

Husar, R. B., D. E. Patterson, J. D. Husar, N. V. Gillani, and W. E. Wilson. 1978. Sulfur budget of a power plant plume. Atmos. Environ. 12:549-568.

Husar, R. B., D. E. Patterson, C. C. Paley, and N. V. Gillani. 1976. Ozone in hazy air masses. Proceedings of International Conference on Photochemical Oxidant and its Control, Sept. 12-17, Raleigh NC.

Izumi, Y. 1971. Kansas 1968 Field Program Data Report. Air Force Cambridge Research Laboratories, Environmental Research Papers. No. 379.

Johnson, A. Jr. and O'Brien, J. J. 1973. A study of an Oregon sea breeze event. J. Appl. Meteorol. 12:1267-1283.

Kaimal, J. C., J. C. Wyngaard, D. A. Haugen, O. R. Cote, Y. Izumi, J. S. Caughey, and C. J. Readings. 1976. Turbulence structure in the convective boundary layer. J. Atmos. Sci. 33:2152-2169.

Keen, C. S. and W. A. Lyons. 1978. Lake/land breeze circulations on the western shore of L. Michigan. J. Appl. Meteorol. 17:1843-1855.

Kimura R. and T. Eguchi. 1978. On dynamical processes of sea and land breeze circulations. J. Meteorol. Soc. Japan 56:67-85.

Koerber, W. M. 1982. Trends in SO_2 emissions and associated release height for Ohio River Valley power plants. Paper No. 82-105, 75th Annual Meeting of the Air Pollution Control Association, New Orleans, LA.

Korshover, J. 1967. Climatology of stagnating anticyclones east of the Rocky Mountains, 1936-65. U.S. Public Health Service Publication No. 999-AP-34.

Lamb, R. G. 1981. A regional scale (1000 km) model of photochemical air pollution. Part I: Theoretical formulation. USEPA Technical Report.

Landsberg, H. E. 1956. The climate of towns. Proc. Int. Symp. on Man's Role in Changing the Face of the Earth. Univ. of Chicago Press, 584-606.

Lee, D. O. 1977. Urban influence on wind direction over London. Weather. 32:162.

Lettau, H. H. 1967. Small to large scale features of boundary layer structure over mountain slopes. In Proc., Symposium on Mountain Meteorology. Atmospheric Sciences Paper No. 122. Colorado State Univ., Fort Collins, CO, pp. 1-74.

Lettau, H. H. and B. Davidson. 1957. Exploring the Atmosphere's First Mile, Vol. 1 and 2. Pergamon Press, New York, NY.

Lilly, D. K. 1975. "Open SESAME," Proceedings of SESAME Open Meeting at Boulder, CO, Sept. 4-6, 1974. NOAA-ERL, Boulder, CO.

Lilly, D. K. and E. J. Zipser. 1972. The front range windstorm of 11 January 1972. Weatherwise. 25:56-63.

Lyons, W. A. 1975. Turbulent diffusion and pollutant transport in shoreline environments. In Lectures on Air Pollution and Environmental Impact Analyses. Amer. Meteorol. Soc., Boston, MA.

Lyons, W. A. and R. H. Calby. 1983. Impact of Mesoscale Convective Precipitation Systems on Regional Visibility and Ozone Distributions. MESOMET, Inc. Final Report of Contract No. 68-02-3740 to EPA.

Lyons, W. A. and R. B. Husar. 1976. SMS/GOES visible images detect a synoptic-scale air pollution episode. Mon. Weather Rev. 104:1623-1626.

Lyons, W. A. and L. E. Olsson. 1973. Detailed mesometeorological studies of air pollution dispersion in the Chicago lake breeze. Mon. Wea. Rev. 101: 387-403.

Lyons, W. A., J. C. Dooley, Jr., and K. T. Whitby. 1978. Satellite detection of long-range pollution transport and sulfate aerosol hazes. Atmos. Environ. 12:621-531.

Mack, R. A. and D. P. Wylie. 1982. An estimation of the condensation rates in three severe storm systems from satellite observation of the convective mass flux. Mon. Wea. Rev. 110:725-744.

Maddox, R. A. 1980. Mesoscale convective complexes. Bull. Amer. Meteorol. Soc. 61:1374-1387.

Mahrt, L. 1980. Boundary layer mean flow dynamics. Proc. AMS Workshop on Planetary Boundary Layer, J. C. Wyngaard, ed. American Meteorological Society, Boston, MA.

Mahrt, L. and W. Schwerdtfeger. 1969. Ekman spiral for exponential thermal wind. Boundary Layer Met. 1:137-145.

Mahrt, L. and D. H. Lenschow. 1976. Growth dynamics of the convectively mixed layer. J. Atmos. Sci. 33:41-51.

Manton, M. J. 1982. A model of fair-weather cumulus convection. Boundary Layer Met. 22:91-107.

Matson, M., E. P. McClain, D. F. McGinnis, Jr., and J. A. Pritchard. 1978. Satellite detection of urban heat islands. Mon. Wea. Rev. 106: 1725-1734.

McBean, G. A., K. Bernhardt, S. Bodin, Z. Lytyuska, A. P. Van Ulden, and J. C. Wyngaard. 1979. The Planetary Boundary Layer, WMO Technical Note No. 165, G. A. McBean, ed. WMO, Geneva, Switzerland.

McNaughton, D J. and M. M. Orgill. 1980. Synoptic case study of elevated layers of high airborne sulfate concentration. Mon. Weather Rev. 108:655-662.

Miller, J. M. 1981. A five-year climatology of back trajectories from the Mauna Loa Observatory, Hawaii. Atmos. Environ. 15:1553-1558.

Miller, J. M. and A. M. Yoshinaga. 1981. The pH of Hawaiian precipitation - a preliminary report. Geophysical Research Letters 8:779-782.

Munn, R. E. and B. Bolin. 1971. Global air pollution - meteorological aspects. Atmos. Environ. 5:363-402.

Neumann, J. 1951. Land breezes and nocturnal thunderstorms. J. Meteorol. 8:60-67.

Niemann, B. L. 1982. Analysis of wind and precipitation data for assessments of transboundary transport and acid deposition between Canada and the United States. Proceedings, American Chemical Society Symposium on Acid Precipitation March 29, Las Vegas, NV.

Nunez, M. and T. R. Oke. 1977. The energy balance of an urban canyon. J. Appl. Meteorol. 16:11-19.

Oke, T. R. 1973. City size and the urban heat island. Atmos. Environ. 7:769-779.

Oke, T. R. 1974. Review of Urban Climatology, 1968-1973. WMO TN No. 134.

Oke, T. R. 1978. Air pollution on the boundary layer, Ch. 9. In Boundary Layer Climates. Methuen & Co. Ltd., pp. 268-301.

Organization for Economic Cooperation and Development. 1977. Final Report of the OECD Programme on long range transport of air pollutants. Measurements and Findings.

Pack, D. H., G. J. Ferber, J. L. Heffter, K. Telegadas, J. K. Angell, W. H. Hoecker and L. Machta. 1978. Meteorology of long range transport. Atmos. Environ. 12:425-444.

Paegel, J. 1969. Studies of diurnally periodic boundary layer winds. Ph.D. Thesis, Dept. of Meterology, UCLA.

Panofsky, H. A. 1982. The Atmosphere, Ch. 1. In Engineering Meteorology. E. J. Plate (ed.), Elsevier, Amsterdam.

Pielke, R. A. 1974a. A three-dimensional numerical model of the sea breezes over south Florida. Mon. Wea. Rev. 102:115-139.

Pielke, R. A. 1974b. A comparison of three-dimensional and two-dimensional numerical predictions of sea breeze. J. Atmos. Sci. 31:1577-1585.

Pielke, R. A. 1981. Mesoscale numerical modeling. In Adv. in Geophys. 23:185-344.

Plank, V. G. 1966. Wind conditions in situations of patternform and non-patternform cumulus convection. Tellus 18:1-12.

Plate, E. J. 1971. Aerodynamic Characteristics of Atmospheric Boundary Layers, U.S. AEC Critical Review Series.

Pooler, F. and L. E. Niemeyer. 1970. Dispersion from tall stacks: An evaluation. Paper No. ME-14D presented at the Second International Clean Air Congress, Washington, D.C., December 6-11, 1970.

Portelli, R. V. 1977. Mixing heights, wind speeds and ventilation coefficients for Canada. Environment Canada, Atmospheric Environment Service, Climatological Studies Number 31, UDC:551.554.

Prahm, L. P., U. Torp, and R. M. Stern. 1976. Deposition and transformation rates of sulfur oxides during atmospheric transport over the Atlantic. Tellus 28:335-372.

Price, J. C. 1979. Assessment of the urban heat island effect through the use of satellite data. Mon. Weather Rev. 107:1554-1557.

Project METROMEX. 1976. METROMEX update. Bull. Am. Meteorol. Soc. 57, 304-308.

Rahn, K. A. 1981. Relative importances of North America and Eurasia as sources of Arctic aerosol. Atmos. Environ. 15:1447-1455.

Rahn, K. A. and R. J. McCaffrey. 1980. On the origin and transport of the winter Arctic aerosol. Ann. N. Y. Acad. Sci. 388:486-503.

Richwien, B. A. 1978. The damming effect of the southern Appalachians. Am. Meteorol. Soc. Conf. Proc. Weather Forecast. Anal.; Aviat. Meteorol., 1978. pp. 94-101.

Rodhe, H. 1974. Some aspects of the use of air trajectories for the computation of large-scale dispersion and fallout patterns. In Advances in Geophysics, Vol. 18B, Academic Press, New York.

Schreffler, J. W. 1978. Detection of centripetal, heat island circulations from tower data in St. Louis. Boundary Layer Meteorology. 15:229.

Shannon, J. D. 1981. A model of regional long-term average sulfur atmospheric pollution, surface removal, and net horizontal flux. Atmos. Environ. 15:689-701.

Sheih, C. M. 1980. On lateral dispersion coefficients as functions of averaging time. J. Appl. Meteorol. 19:557-561.

Shipman, M. S. 1979. Dynamics of the nocturnal boundary layer. M.S. Thesis, Dept. of Meteorology, NC State University, Raleigh.

Sisterson, D. L. and P. Frenzen. 1978. Nocturnal boundary-layer wind maxima and the problem of wind power assessment. Environ. Sci. Technol. 12:218-221.

Sisterson, D. L., J. D. Shannon and J. M. Hales. 1979. An examination of regional pollutant structure in the lower troposphere--some results of the diagnostic atmospheric cross-section experiment (DASCE-I). J. Appl. Meteorol. 18:1421-1428.

Skibin, D. and A. Hod. 1979. Subjective analysis of mesoscale flow patterns in northern Israel. J. Appl. Meteorol. 18:329-337.

Smith, F. B. and R. D. Hunt. 1978. Meteorological aspects of the transport of pollution over long distances. Atmos. Environ. 12:461-477.

Tennekes, H. 1974. The atmospheric boundary layer. Phys. Today 52-63.

Thomas, F. W., S. B. Carpenter, and F. E. Gartrell. 1963. Stacks - how high? JAPCA 13(5):198-204.

Thompson, D. E., P. A. Arkin, and W. D. Bonner. 1976. Diurnal variations of the summertime winds and force field at three mideastern locations. Mon. Weather Rev. 104:1012-1022.

Tong, E. Y., G. M. Hidy, T. F. Lavery, and F. Berlandi. 1976. Regional and local aspects of atmospheric sulfates in the northeastern quadrant of the U.S. Proceedings, Third Symposium on Turbulence, Diffusion and Air Quality, American Meteor. Society, Boston, MA.

Uthe, E. E. and W. E. Wilson. 1979. Lidar observations of the density and behavior of the Labadie power plant plume. Atmos. Environ. 13:1395-1412.

Uthe, E. E., F. L. Ludwig, and F. Pooler. 1980. Lidar observations of the diurnal behavior of the Cumberland power plant plume. JAPCA 30(8):889-893.

Viskanta, R., R. W. Bergstrom, and R. O. Johnson. 1977. Effects of air pollution on thermal structure and dispersion in an urban planetary boundary layer. Contrib. Atmos. Phys. 50:419-440.

Vukovich, F. M., W. D. Bach, Jr., B. W. Cressman, and W. J. King. 1977. On the relationships between high ozone in the rural boundary layer and high pressure systems. Atmos. Environ. 11:967-983.

Wagner, A. 1939. Uber die Tageswinde in der freien Atmosphere. Beitr. Phys. Atmos. 25:145-170.

Warner, T. J., R. A. Anthes, and A. L. McNab. 1978. Numerical simulations with a three-dimensional mesoscale model. Mon. Wea. Rev. 106:1079-1099.

Wendland, W. M. and R. A. Bryson. 1981. Northern hemisphere airstream regions. Mon. Weather Rev. 109:255-270.

White, W. H., J. A. Andersen, D. L. Blumenthal, R. B. Husar, N. V. Gillani, J. D. Husar, and W. E. Wilson. 1976. Formation and transport of secondary air pollutants: Ozone and aerosols in the St. Louis urban plume. Science 194:187-189.

Wolff, G. T., N. A. Kelly, M. A. Furman. 1981. On the sources of summertime haze in the eastern United States. Science 211:703-705.

Zipser, E. J. and C. Gautier. 1978. Mesoscale events within a GATE tropical depression. Mon. Wea. Rev. 106:789-805.

THE ACIDIC DEPOSITION PHENOMENON AND ITS EFFECTS

A-4. TRANSFORMATION PROCESSES

4.1 INTRODUCTION (D. F. Miller)

This chapter addresses the atmospheric processes by which pollutants are transformed chemically into species that ultimately may result in deposition of acidic matter. When chemical transformations are considered, a fundamental concern is for the kinetics of reactions that limit the production and consumption of acidic species and their precursors. In this chapter, many individual equations pertaining to gas-phase and aqueous-phase reactions have been written and assigned best estimates for their kinetics. However, to assess the relative importance of these reactions with respect to acid deposition under various atmospheric conditions, one must evaluate this information along with the other facets of this document; i.e., the pollutant emissions and distributions (Chapters A-2 and A-5); transport (Chapter A-3); and other meteorological processes (Chapters A-6 and A-7), including precipitation-deposition processes.

To integrate the detailed aspects of atmospheric chemistry with models of atmospheric physics requires an operational scheme referred to in this chapter as transformation modeling. The basic approaches to transformation modeling, the problems encountered and some exemplary results are discussed at the end of this chapter.

Figure 4-1, taken from Schwartz (1982), depicts in simplified form the types of transformation processes by which common pollutants become more acidic in the atmosphere.

The diagram shows areas for interactions between gas-phase and aqueous-phase processes. While gas-phase oxidation is conceptualized as a direct route for producing acidic products, the aqueous-phase route is somewhat more complex. There is partitioning of the gaseous reactants between the two phases followed by oxidation and possibly neutralization. Since most of this occurs in cloud droplets which evaporate rather than precipitate, the acidic products are vented into the atmosphere, primarily in the form of aerosol particles. In general, these particles will have longer atmospheric lifetimes (and transport times) than their gaseous precursors. In many respects, cloud droplets have the property of forcing pollutants to undergo reactions at much faster rates than experienced in the gas phase. Oxidation of SO_2 by O_3 and H_2O_2 are the two familiar examples.

In Sections 4.2 and 4.3 of this chapter, gas-phase and aqueous-phase transformations are discussed separately. The section on homogeneous gas-phase reactions suggests that the fundamental chemistry is fairly well

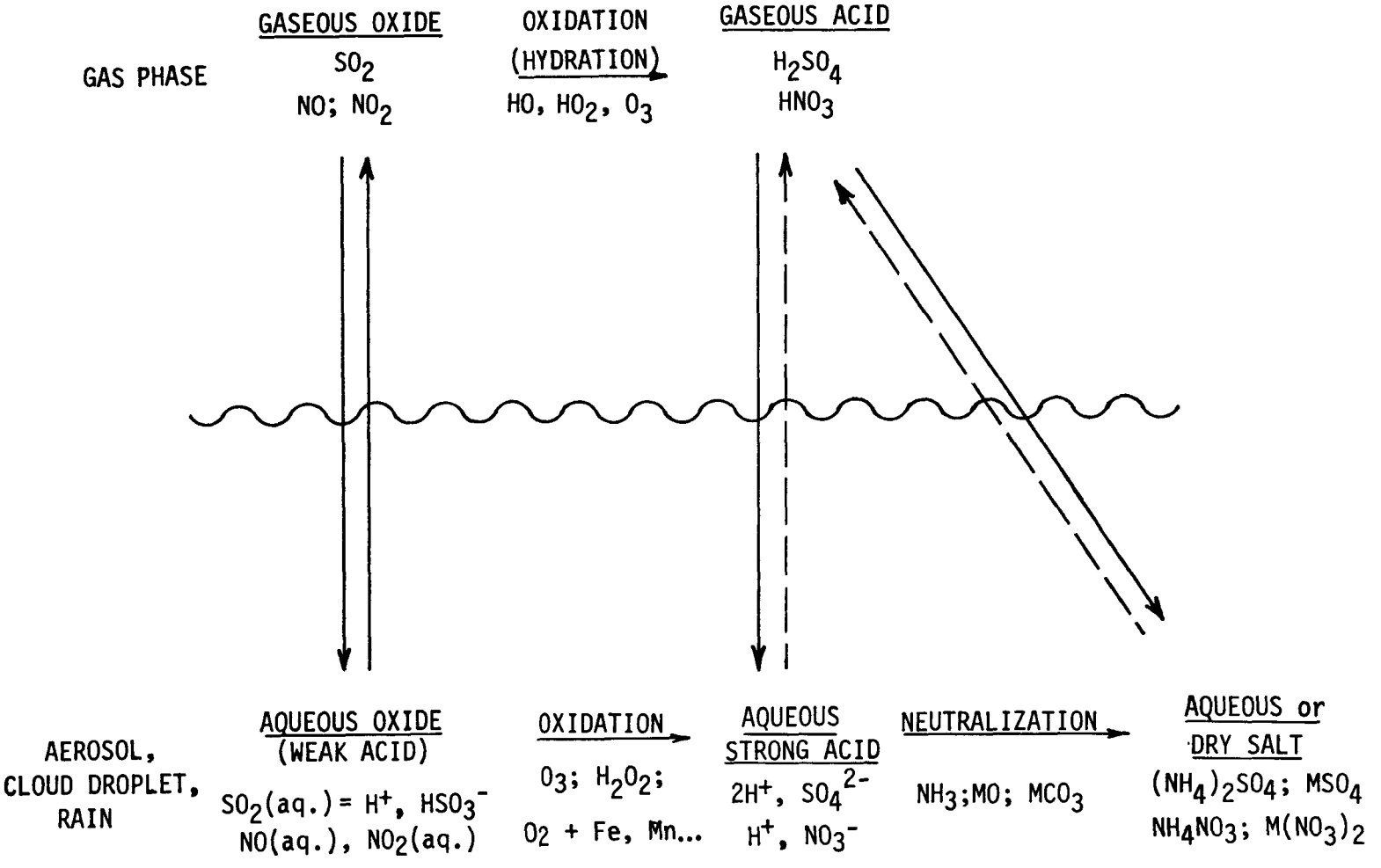

Figure 4-1. Schematic representation of pathways for atmospheric formation of sulfate and nitrate. Adapted from Schwartz (1982).

established, although there are specific areas of uncertainty pertaining to the formation of acidic species. A major problem is that field measurements have not been adequate to definitely test the chemical models based on laboratory studies.

An appreciation of the time scales that characterize gas-phase transformation paths can be had by direct measurements, theoretical calculations, or budget calculations based on time and space averages (Rodhe 1978). When a gas-phase transformation process can be described by a first-order reaction, the lifetime of the reacting species with respect to the particular reaction is equal to the reciprocal of the rate coefficient (k^{-1}). For a bimolecular gas-phase reaction (A + B $\rightarrow$ C + D), a pseudo first-order rate for the removal of A may be approximated by K [B] when the concentration of B can be estimated.

In contrast to the situation for gas-phase chemistry, the fundamental chemistry of aqueous-phase reactions leading to acid products in the atmosphere is not well known. Thus, in this chapter there is very little discussion of the myriad chemical mechanisms likely to be occurring in cloud, fog and even dew droplets. Aqueous-phase chemistry is discussed primarily on the basis of generalized rate expressions, and assessments of the atmospheric significance of various chemical processes in clouds are made using best available information and necessary assumptions.

The rate of a gas-liquid reaction (as in aqueous cloud droplets) depends upon the physical solubility of the reactant gas, the rate of mass transport of the reactant and the aqueous phase reaction rate. To estimate the lifetime of a given reactant, one must further consider the liquid water content of the cloud; other solutes which may affect ionic strength, pH or act as oxidizers; and the residence time of air within clouds. Since the liquid water content may vary from 1×10^{-5} g m^{-3} for embryonic cloud nuclei to > 1 g m^{-3} for dense clouds, there are problems in evaluating the lifetimes of species that react under such conditions.

References specifically to heterogenous (gas-solid) reactions in the atmosphere are not included in this chapter. Although there has been valuble research on this topic, it is not yet possible to assess the importance of these reactions to the acidic deposition problem. The consensus at this time seems to be that heterogeneous reactions make significant contributions to acidic deposition but only under rather special circumstances which have not been well defined.

4.2 HOMOGENEOUS GAS-PHASE REACTIONS (D. F. Miller and M. R. Whitbeck)

4.2.1 Fundamental Reactions

4.2.1.1 Reduced Sulfur Compounds--Sulfur (S) occurs in the troposphere in diverse forms involving oxidation states from -2 (H_2S) to +6 (H_2SO_4). The chemical mechanisms and kinetics of reduced S compounds such as hydrogen sulfide (H_2S) and carbonyl sulfide (COS) have not been studied as extensively as sulfur dioxide (SO_2) and sulfuric acid (H_2SO_4) have.

The oxidation of reduced S compounds in the troposphere presumably leads to SO_2 formation. Some possible reactions are listed in Table 4-1. Except for the first reaction, OH + H_2S, considerable uncertainty surrounds the products and rate constants (Baulch et al. 1980).

The atmospheric lifetimes of these reduced S compounds with respect to gas-phase reactions are expected to be determined by their reactions with hydroxyl (OH) radicals. Table 4-2 lists some typical background concentrations for the compounds (Sze and Ko 1980) and estimated lifetimes for removal by a background OH level of 4×10^{-5} ppb.

Data are insufficient to assess quantitatively the importance of reduced S compounds on acidic precipitation; but, relative to the strong local SO_2 emissions from anthropogenic sources, their contribution may be insignificant. They do, however, significantly contribute to the global S budget, but further work in this area is needed to clarify reaction pathways. In particular, rate constants and products for the reactions of OH with COS, carbon disulfide (CS_2), dimethyl sulfide (CH_3SCH_3), and other biogenic, reduced S compounds need to be identified.

4.2.1.2 Sulfur Dioxide--The atmospheric chemistry of SO_2 has been studied extensively, yet some aspects are still not well delineated. Removal mechanisms for SO_2 are complex and involve aqueous droplet, gas-phase, and possibly particulate reactions. The gas-phase reactions for SO_2 represent a major oxidative path in the troposphere, although it has been argued that the aqueous-phase route is dominant (Moller 1980).

Direct photo-oxidation reactions for SO_2 play a minor role in its oxidation. Reactions 4-7a and 4-7b (Table 4-3) dominate the fate of $SO_2(^3B_1)$, while reactions 4-8, 4-9 or 4-10, and 4-11 may account for photo-oxidation of SO_2 at a rate of ~ 0.02 percent hr^{-1} (Calvert et al. 1978).

Oxidation of SO_2 by excited oxygen ($^1\Delta_g$, $^1\Sigma_g^+$), nitrogen dioxide (NO_2), nitrogen trioxide (NO_3), nitrogen pentoxide (N_2O_5), or ozone (O_3), is unimportant in the troposphere (Calvert et al. 1978). The reaction of SO_2 with $O(^3P)$ is not a significant route for oxidation in the troposphere but should be included in models for plume chemistry, where it may play a significant role in early stages of plume dilution (Calvert et al. 1978).

The reaction of SO_2 with hydroperoxy (HO_2) radicals is not well defined. At one time, it was felt that the reaction with HO_2 was a significant path for oxidation in a highly polluted troposphere with $[HO_2]$ ~ 0.24 ppb (Calvert et al. 1978). More recent evidence, e.g., Graham et al. (1979), suggests that the reaction of SO_2 with HO_2 is much too slow to be significant in the troposphere. An analogous reaction is that of SO_2 with methylperoxy radicals (CH_3O_2). Although this system has received attention in recent years, the tropospheric role of the CH_3O_2 + SO_2 reaction has not been interpreted concretely. Table 4-4 lists some recent rate constant determinations for this reaction.

TABLE 4-1. REACTIONS OF REDUCED SULFUR

Reaction	Rate constant at 298 K (cm^3 $molecule^{-1}$ s^{-1})	Reference	Reaction number
$OH + H_2S \rightarrow HS + H_2O$	5.3×10^{-12}	Baulch et al. (1980)	[4-1]
$OH + OCS \rightarrow CO_2 + HS(?)$	$\leq 6 \times 10^{-14}$	Baulch et al. (1980)	[4-2]
	1×10^{-14}	Demore et al. (1981)	
	5.8×10^{-16}	Leu and Smith (1981)	
$OH + CS_2 \rightarrow ?$	$\leq 2 \times 10^{-13}$	Baulch et al. (1980)	[4-3]
	4.3×10^{-13}	Cox and Sheppard (1980)	
	1.5×10^{-15}	Wine et al. (1980)	
$HS + O_2 \rightarrow SO + OH$	$< 10^{-13}$	Baulch et al. (1980)	[4-4a]
$HS + O_2 \rightarrow SO_2 + H$			[4-4b]
$SO + O_2 \rightarrow SO_2 + O$	9×10^{-18}	Baulch et al. (1980)	[4-5]

TABLE 4-2. OCCURRENCE OF REDUCED SULFUR

Molecule	Typical Concentration[a] (ppb)	Lifetime for removal by OH ($s \times 10^{-5}$)
H_2S	0.004 - 0.40	1.9
COS	0.49	1,000
CS_2	0.069 - 0.370	6,750

[a]Sze and Ko (1980).

TABLE 4-3. PHOTOOXIDATION REACTIONS OF SO_2

Reaction	Reaction number
$SO_2(\tilde{X}\ ^1A_1) + h\nu\ (340\text{-}400\ nm) \rightarrow SO_2(^3B_1)$	[4-6]
$SO_2(^3B_1) + O_2(^3\Sigma_g^-) \rightarrow SO\ (\tilde{X}\ ^1A_1) + O_2(^1\Sigma_g^+)$	[4-7a]
$SO_2(^3B_1) + O_2(^3\Sigma_g^-) \rightarrow SO_2(\tilde{X}\ ^1A_1) + O_2(^1\Delta_g)$	[4-7b]
$SO_2\ (^3B_1) + O_2\ (^3\Sigma_g^-) \rightarrow SO_4$ (cyclic)	[4-8]
SO_4(cyclic) $+ O_2 \rightarrow SO_3 + O_3$	[4-9]
$SO_2(^3B_1) + O_2(^3\Sigma_g^-) \rightarrow SO_3 + O(^3P)$	[4-10]
$O + O_2 + M \rightarrow O_3 + M$	[4-11]

TABLE 4-4. RATE CONSTANTS FOR CH_3O_2 + SO_2 → PRODUCTS

k (cm^3 $molecule^{-1}$ s^{-1})	Reference
< 5 x 10^{-17}	Sander and Watson (1981)
8.2 x 10^{-15}	Sanhueza et al. (1979)
5.3 x 10^{-15}	Kan et al. (1979)
1.4 x 10^{-14}	Kan et al. (1981)

The rate constant for the SO_2 and methoxy radical (CH_3O) reaction should be measured to assess its significance accurately; a rough estimate of 6 x 10^{-15} cm^3 $molecule^{-1}$ s^{-1} for this reaction (Calvert et al, 1978) has been reported. Kan et al. (1981) used a larger rate (5.5 x 10^{-13}) in their assessment of this mechanism.

An important competitive fate for methoxy radicals is the reaction with O_2 which has a rate constant of 5.7 x 10^{-16} cm^3 $molecule^{-1}$ s^{-1} (Demore et al. 1981). That rate, combined with the ambient level of O_2, keeps the level of CH_3O very low; probably lower than that for OH. Thus, if $[CH_3O] << [OH]$ and $k(CH_3O + SO_2) < k(OH + SO_2)$, then oxidation of SO_2 by CH_3O is not important.

The combined oxidation of SO_2 will depend on the concentration of other reactive species (e.g., HO_2, CH_3O_2, CH_3O, NO, NO_2), as suggested in a recent study by Kan et al. (1981). Their mechanism and suggested rate constants are given in Table 4-5. Further study is needed to evaluate the significance of this reaction sequence. If the Kan et al. (1981) mechanism is correct, the influence of atmospheric levels of NO on the rate of SO_2 oxidation by CH_3O_2 will need to be assessed.

Ozone-alkene reactions are complex and give rise to diverse reactive radicals that may oxidize SO_2. Some possible reactions are listed in Table 4-6. Cox and Penkett (1972) observed that water markedly inhibits SO_2 oxidation in these systems. Calvert et al. (1978) have evaluated the data of Cox and Penkett (1972) for the cis-2-butene, O_3, SO_2, H_2O system in terms of:

$$O_3 + C_4H_8 \rightarrow \text{molozonide} \rightarrow CH_3\dot{C}HOO + CH_3CHO \quad [4\text{-}23]$$

$$O_3 + C_4H_8 \rightarrow RCHO, RCOOH, \text{etc.} \quad [4\text{-}24]$$

$$CH_3\dot{C}HOO + SO_2 \rightarrow CH_3CHO + SO_3 \quad [4\text{-}25]$$

$$CH_3\dot{C}HOO + C_4H_8 \rightarrow CH_3CHO + C_4H_8O + \text{other products} \quad [4\text{-}26]$$

$$CH_3\dot{C}HOO + O_3 \rightarrow CH_3CHO + 2O_2 \quad [4\text{-}27]$$

$$CH_3\dot{C}HOO + H_2O \rightarrow CH_3COOH + H_2O \quad [4\text{-}28]$$

$$CH_3\dot{C}HOO \rightarrow (CH_3COOH)^{\dagger} \rightarrow CH_4 + CO_2 \ (+ CH_3OH, CO, \text{etc.}) \quad [4\text{-}29]$$

and have concluded that reactions with the Criegee intermediate (Criegee 1957) cannot be neglected as a loss mechanism for SO_2. The lack of direct observation of these elementary reactions and subsequent determinations of their rate constants hampers a quantitative assessment but SO_2 conversion rates by this mechanism are not expected to be large.

The predominant gas-phase mechanism for SO_2 oxidation is the reaction with OH.

$$OH + SO_2 \rightarrow HOSO_2 \quad [4\text{-}30]$$

TABLE 4-5. CH_3O_2 + SO_2 MECHANISM OF KAN ET AL. (1981)

Reaction	Suggested rate constant	Reaction number
$CH_3O_2 + SO_2 \rightarrow CH_3O_2SO_2$	1.4×10^{-14} cm^3 molecules^{-1} s^{-1}	[4-12]
$CH_3O_2SO_2 \rightarrow CH_3O_2 + SO_2$	< 24 s^{-1}	[4-13]
$CH_3O_2SO_2 + O_2 \rightarrow CH_3O_2SO_2O_2$	$K_{14}/k_{15} = 1.7 \times 10^{20}$	[4-14]
$CH_3O_2SO_2O_2 \rightarrow CH_3O_2SO_2 + O_2$	cm^3 molecule^{-1}	[4-15]
$CH_3O_2SO_2O_2 + NO \rightarrow NO_2 + CH_3O_2SO_2O$	6.2×10^{-12} cm^3 molecule^{-1} s^{-1}	[4-16]
$CH_3O_2SO_2O_2 + CH_3O_2 \rightarrow CH_3O_2SO_2O + CH_3O + O_2$	3.3×10^{13} cm^3 molecule^{-1} s^{-1}	[4-17]
$CH_3O_2SO_2O \rightarrow CH_3O_2 + SO_3$	-----	[4-18]

TABLE 4-6. POSSIBLE SO_2-O_3-ALKENE REACTIONS

Reaction	Reaction number
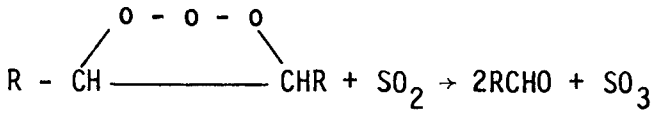	[4-19]
	[4-20]
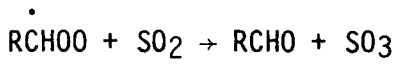	[4-21]
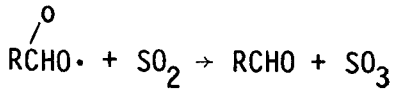	[4-22]

The recommended rate constant for this reaction is 2 x 10^{-12} cm^3 $molecule^{-1}$ s^{-1} (Baulch et al. 1980). Further improvement on this rate constant and studies on the subsequent fate of the $HOSO_2$ radical have been recommended (Seinfeld et al. 1981). Calvert et al. (1978), Davis and Klauber (1975), and Davis et al. (1979) have speculated on the fate of the $HOSO_2$ radical in the troposphere (Table 4-7). The determination of rate constants and fate of the $HOSO_2$ radical constitute a pressing need for further research. At this writing, however, all evidence suggests that a final product of the HO + SO_2 reaction is sulfuric acid and that this initial step is rate limiting.

The fate of sulfur trioxide (SO_3) in the atmosphere is expected to be dominated by its reaction with water (Calvert et al. 1978), although Baulch et al. (1980) make no recommendation for this reaction because only one investigation of the process (Castleman et al. 1975) was conducted and the reaction products were not identified. The presumed reaction is:

$$SO_3 + H_2O \rightarrow (SO_3 \cdot H_2O) \rightarrow H_2SO_4 \qquad [4\text{-}58]$$

4.2.1.3 Nitrogen Compounds--The chemistry of N in the troposphere rivals that of S, both in the diversity of compounds present and in their impacts on acidity of precipitation. N is found with oxidation states ranging from -3 (ammonia [NH_3]) to +5 (pernitric [HO_2NO_2] acid), including both bases (ammonia [NH_3] and amines) and acids (nitrous [HONO], nitric [HNO_3], and pernitric [HO_2NO_2] acids).

NH_3 is the most abundant form of reduced N (after molecular nitrogen and nitrous oxide) in the troposphere, but, it is one of the most poorly understood of the trace atmospheric gases. It is the only common gaseous base and plays a key role in neutralizing acidic gases, particles, and droplets.

The principal loss mechanism for NH_3 is probably heterogeneous (Seinfeld et al. 1981). Recent model calculations were made to fit a set of ambient measurements when the heterogeneous lifetime of NH_3 was set at 10 days and its homogeneous lifetime was set at 40 days (Levine et al. 1980). The homogeneous loss mechanism should be dominated by reaction with OH, but the fate of the product of this reaction, NH_2, is unknown. The NH_3 reaction rate with gaseous acids (HNO_3, H_2SO_4) is not well established but should be rapid (Seinfeld et al. 1981).

The most abundant nitrogen oxides (NO_x) in the troposphere (excluding the relatively unreactive nitrous oxide [N_2O]) are nitric oxide (NO) and nitrogen dioxide (NO_2). Chemistry that is rather complex and not completely understood interconverts these compounds (which are also primary emissions) to NO_3, N_2O_5, HONO, HNO_3, and HO_2NO_2 (Table 4-8). NO is converted to NO_2 and HONO through reactions with O_2, O_3, HO, and H_2O. Nitric oxide, as such, does not contribute to the acidity of precipitation.

Nitrous acid (HONO) has been measured in urban areas at concentrations as high as 1 ppb (Perner and Platt 1979). Concentrations this high are not

TABLE 4-7. PROPOSED MECHANISMS FOR THE FATE OF $HOSO_2$

Reaction	~ ΔH, kcal $mole^{-1}$	Reaction number
Mechanism of Calvert et al. (1978)		
$HO + SO_2 + (+M) \rightarrow HOSO_2 (+M)$	-37	[4-31]
$HOSO_2 + O_2 \rightarrow HOSO_2OO$	-16	[4-32]
$HOSO_2OO + NO \rightleftarrows HOSO_2O + NO_2$	-25	[4-33]
$HOSO_2OO + NO_2 \rightleftarrows HOSO_2OONO_2$	?	[4-34]
$HOSO_2OONO_2 \rightarrow HOSO_2O + NO_3$	?	[4-35]
$HOSO_2OO + NO_2 \rightarrow HOSO_2O + NO_3$	- 2	[4-36]
$HOSO_2OO + HO_2 \rightarrow HOSO_2O_2H + O_2$	-43	[4-37]
$2HOSO_2OO \rightarrow 2HOSO_2O + O_2$	-22	[4-38]
$HOSO_2O + NO \rightarrow HOSO_2ONO$	-26	[4-39]
$HOSO_2ONO + h\nu \rightarrow HOSO_2O + NO$		[4-40]
$HOSO_2O + NO_2 \rightarrow HOSO_2ONO_2$	-22	[4-41]
$HOSO_2O + HO_2 \rightarrow HOSO_2OH + O_2$	-57	[4-42]
$HOSO_2O + C_3H_8 \rightarrow HOSO_2OH + iso\text{-}C_3H_7$	-10	[4-43]
$HOSO_2O + C_3H_6 \rightarrow HOSO_2OCH_2CHCH_3$	?	[4-44]
H_2SO_4 + aerosol (H_2O, NH_3, CH_2O, C_nH_{2n} ..) $\rightarrow$ (growing aerosol)		[4-45]
$HOSO_2ONO$ + aerosol (H_2O) $\rightarrow$ aerosol (H_2SO_4, $HONO_2$...)		[4-46]
$HOSO_2ONO$ + aerosol (H_2O) $\rightarrow$ aerosol (H_2SO_4, HONO ...)		[4-47]

TABLE 4-7. CONTINUED

Reaction	~ Δ H, kcal mole^{-1}	Reaction number
Alternative mechanisms of Davis and Klauber (1975)		
$HOSO_2O + O_2(+M) \rightarrow HOSO_2O_3(+M)$		[4-48]
$HOSO_2O_3 + NO \rightarrow HOSO_2O_2 + NO_2$		[4-49]
$HOSO_2O_2 + NO \rightarrow HOSO_2O + NO_2$		[4-50]
Mechanisms of Davis et al. (1979) for $HOSO_2$		
$HOSO_2 + O_2 + M \rightarrow HOSO_4 + M$		[4-51]
$HOSO_4 + H_2O \rightarrow HSO_5 \cdot H_2O$		[4-52]
$HSO_5 \cdot H_2O \rightleftarrows HSO_5 \cdot (H_2O)_2$		[4-53]
$HSO_5 \cdot (H_2O)_x \rightleftarrows HSO_5 \cdot (H_2O)_{x+1}$		[4-54]
$HSO_5(H_2O)_x + NO \rightarrow HSO_4(H_2O)_xNO_2$		[4-55]
$HSO_5(H_2O)_x + SO_2 \rightarrow HSO_4(H_2O)_xSO_3$		[4-56]
$HSO_5(H_2O)_x + HO_2 \rightarrow H_2SO_5(H_2O)_x + O_2$		[4-57]

TABLE 4-8. REACTIONS OF NITROGEN COMPOUNDS

Reaction	Rate constant k (cm^3 $molecule^{-1}$ s^{-1})	Reference	Reaction number
$NH_3 + HO \rightarrow NH_2 + H_2O$	$2.3 \times 10^{-12} \exp(-800/T)$	Hampson and Garvin (1977)	[4-59]
$NO + NO_2 + H_2O \rightleftarrows 2HONO$	$k = 1.56$ atm^{-1}	Hampson and Garvin (1977)	[4-60]
$2NO + O_2 \rightarrow 2NO_2$	$3.3 \times 10^{39} \exp(530/T)$[a]	Hampson and Garvin (1977)	[4-61]
$HO + NO + M \rightarrow M + HONO$	1×10^{-11} 3×10^{-11}	Baulch et al. (1980) Demore et al. (1981)	[4-62]
$NO + O_3 \rightarrow NO_2 + O_2$	1.8×10^{-14}	Baulch et al. (1980)	[4-63]
$NO_2 + O_3 \rightarrow NO_3 + O_2$	3.2×10^{-17}	Baulch et al. (1980)	[4-64]
$HONO + h\nu \rightarrow HO + NO$	--	Baulch et al. (1980)	[4-65]
$HO + HNO_3 \rightarrow H_2O + NO_3$	8.5×10^{-14} 1.3×10^{-13} 8.2×10^{-14}	Baulch et al. (1980) Demore et al. (1981)	[4-66]
$NO_2 + NO_3 \rightarrow N_2O_5$	5×10^{-12}	Baulch et al. (1980)	[4-67]
$NO_3 + NO \quad 2NO_2$	2×10^{-11}	Baulch et al. (1980)	[4-68]
$N_2O_5 \rightarrow NO_2 + NO_3$	0.2 s^{-1}	Baulch et al. (1980)	[4-69]
$NO_2 + h\nu \rightarrow NO + O$	--	Baulch et al. (1980)	[4-70]

TABLE 4-8. CONTINUED

Reaction	Rate constant k (cm^3 $molecule^{-1}$ s^{-1})	Reference	Reaction number
$NO_3 + h\nu \rightarrow NO_2 + O$	--	Baulch et al. (1980)	[4-71]
$NO_3 + h\nu \rightarrow NO + O_2$	--	Baulch et al. (1980)	[4-72]
$HO + NO_2 + M \rightarrow HNO_3 + M$	1.6×10^{-11} 2.4×10^{-11}	Baulch et al. (1980) Demore et al. (1981)	[4-73]
$HO_2 + NO_2 \rightarrow HO_2NO_2$	5.0×10^{-12}	Baulch et al. (1980)	[4-74]
$HO_2NO_2 \rightarrow HO_2 + NO_2$	0.09 s^{-1} at 298 K	Baulch et al. (1980)	[4-75]
$CH_3COO_2 + NO_2 \rightarrow CH_3COO_2NO_2$	1.4×10^{-12}	Cox and Roffey (1977)	[4-76]
$CH_3COO_2NO_2 \rightarrow CH_3COO_2 + NO_2$	7.94×10^{-14} exp (-25000/RT)	Cox and Roffey (1977)	[4-77]
N_2O_5 $H_2O \rightarrow 2HNO_3$	$< 1 \times 10^{-20}$	Hampson and Garvin (1977)	[4-78]

[a] cm^6 $molecule^{-2}$ s^{-1}.

readily explained from the known homogeneous reactions that produce HONO and the photolysis rates that destroy it. Additional homogeneous sources might exist, and the heterogeneous promotions of the reaction of NO + NO_2 + H_2O $\rightleftarrows$ 2HONO are possibilities. HONO is a relatively weak acid (pK_a 5.22) and has its greatest tropospheric significance as a photolytic source of OH radicals.

NO_2 has a gas-phase removal mechanism dominated by reaction with OH to form HNO_3. With an OH concentration of 4 x 10^{-5} ppb, NO_2 would have a lifetime of ~ 17 hr. NO_2 also reacts with ozone to form NO_3, which can photolyze to give back NO_2.

HNO_3 like H_2SO_4, is a major acidic compound in the troposphere. It is likely removed from the atmosphere by both heterogeneous and homogeneous routes. The gas-phase removal mechanism is relatively slow, because it is dominated by reaction with OH to form NO_3. The lifetime of HNO_3 with respect to the OH reaction, HO ~ 4 x 10^{-5} ppb, is 2 to 3 x 10^3 hr.

NO_3 is a strong oxidizer in the atmosphere and may be removed by oxidation of NO to NO_2, reactions with organic compounds (Bandow et al. 1980) such as terpenes (Noxon et al. 1980, Platt et al. 1980), and by photolysis (Graham and Johnston 1978). The oxidation of SO_2 by NO_3 is not considered an important reaction (Calvert et al. 1978). NO_3 also exists in equilibrium with N_2O_5 which may be removed by heterogeneous or homogeneous hydrolysis to HNO_3. Because NO_3 readily photolyzes in daylight, peak concentrations are expected in the evening hours, and levels as high as 0.35 ppb have been reported in the Los Angeles area, with calculated equilibrium values of N_2O_5 as high as 11 ppb (Platt et al. 1980). Similar values have been reported for a more remote Colorado mountain site (Noxon et al. 1980).

The chemistry of NO, NO_2, NO_3, N_2O_5, OH, and O_3 involves a close interrelationship that should have a profound significance to the acidity of precipitation, especially in remote areas where HNO_3 may dominate the pH of acidic precipitation (Seinfeld et al. 1981). Further studies are warranted involving field measurements of NO_3 and N_2O_5 and kinetic studies of their reactions.

The organic nitrate esters should not hydrolyze under ordinary conditions and thus should not contribute to the acidity of precipitation. Peroxyacetyl nitrate (PAN), found in urban smog, hydrolyzes to give nitrate in basic solutions (as would the other organic nitrates), but its behavior in neutral or slightly acidic solution is unknown.

The dominant gas-phase loss mechanism for PAN is thermal decomposition, k ~ 7.94 x 10^{14} exp (-25000/RT) (Cox and Roffey 1977). Its thermal decomposition rate is considerably slower than that for pernitric acid, HO_2NO_2, k ~ 1.4 x 10^{14} exp (-20700/RT) (Graham et al. 1977). Pernitric acid has a thermal decomposition lifetime of only 12 s at 298 K (Graham et al. 1977). Both PAN and HO_2NO_2 are essentially in equilibrium with their decomposition products, and although an assessment to acidic deposition cannot be made at this time, any of these species is potentially important.

4.2.1.4 Halogens--Table 4-9 lists some halogenated compounds found in the troposphere. The compounds characterized as predominantly natural emissions are thought to be oceanic in origin (Seinfeld et al. 1981).

Methylchloride (CH_3Cl) and methylbromide (CH_3Br) have tropospheric lifetimes probably dominated by aqueous-phase processes that produce and consume hydrochloric acid (HCl). HCl is also produced by gas-phase reactions following the reaction of OH with a halocarbon as the rate-limiting step. It has been suggested that rainwater acidity in remote areas is controlled principally by the presence of HCl and HNO_3 (Seinfeld et al. 1981). More data are needed to determine the relative importance of these reactions in the production of HCl and their effect on acidic deposition.

4.2.1.5 Organic Acids--Organic acids are expected to occur as photooxidation products of both natural and anthropogenic hydrocarbons. In general, organic acids are only weakly dissociated in solution (their ionization constants tend to decrease with increasing chain length), but the two simplest acids--(HCOOH) and acetic (CH_3COOH)--have appreciable ionization constants (pK_a ~ 3.75 and 4.75, respectively).

The sources and sinks for these acids are not known at this time. HCOOH is expected as a product of formaldehyde (HCOH) oxidation. Su et al. (1979) have suggested a mechanism based on reaction of HCOH with HO_2 radicals and HCOOH formation in the ozone-ethene reaction (Su et al. 1980). Similarly, CH_3COOH is formed in the cis-2-butene-ozone-H_2O reaction from the Criegee intermediate (Calvert et al. 1978),

$$CH_3CHOO + H_2O \rightarrow CH_3COOH + H_2O. \qquad [4\text{-}79]$$

The loss mechanisms for these acids are not known but should be a combination of reaction with OH, wet and dry deposition, and rainout. Recent measurements (Dawson et al. 1980) indicate that both acids are present in the troposphere at significant levels (Table 4-10).

These acids can be assessed through further tropospheric measurements (remote and urban) and rate data for their reactions with OH. Thus far, it appears they should not be neglected as compounds affecting acidity of rain in remote areas. These and other organic acids will contribute to titratable H^+.

4.2.2 Laboratory Simulations of Sulfur Dioxide and Nitrogen Dioxide Oxidation

In addition to the aforementioned work on the fundamental gas-phase reactions germain to atmospheric acidity, a number of laboratory studies have attempted to simulate atmospheric conditions in controlled experiments and thereby obtain insight into the combined effects of simultaneous reactions. These experiments were usually conducted in "smog chambers" with artificial or natural solar radiation.

Numerous smog chamber studies have described the evolution of sulfate aerosol from SO_2 oxidation, in terms of growth and size distribution trends (e.g.,

TABLE 4-9. ATMOSPHERIC HALOGEN COMPOUNDS[a]

Compound	Concentration (ppb)	Lifetime[a] (s x 10^7)
(Natural)		
CH_3Cl	0.81	3.8
CH_3Br	0.01	4.1
CH_3I	0.01	---
HCl	0.20	---
(Anthropogenic)		
$CHCl_3$	0.02	1.9
C_2Cl_4	0.03	10.1
$CHCl_2F$	0.01	6.6
CH_3CCl_3[b]	0.1	13.9

[a]From Seinfeld et al. (1981), assuming an HO concentration of 3.7×10^{-5} ppb.

[b]Source not clear.

TABLE 4-10. TROPOSPHERIC HCOOH AND CH_3COOH (DAWSON ET AL. 1980)

Acid	pKa	Remote site (ppb)	Urban site	Lifetime[a] (hr)
HCOOH	3.75	2	3.5	8
CH_3COOH	4.75	1	6.0	48

[a]Assuming removal by HO ~ 2 x 10^{-4} ppb and assuming k(HO + HCOOH) ~ 6 x 10^{-12} cm^3 $molecule^{-1}$ s^{-1} and k(HO + CH_3COOH) ~ 10^{-12} cm^3 $molecule^{-1}$ s^{-1}.

Kocmond and Yang 1976, Friedlander 1978, Whitby 1978, McMurry and Wilson 1982). In general, sulfate condenses to form particles with a relatively sharp peak in mass distribution at particle diameters between 0.1 and 0.2 μm. Because other SO_2 conversion processes (aqueous and heterogeneous) result in particles of larger mean diameters, sulfate particles < 0.2 μm in diameter are thought to be characteristic of gas-phase SO_2 oxidation.

Gas-phase oxidation of SO_2 to sulfate particles has been detected in the absence of sunlight when olefins and O_3 reacted (Groblicki and Nebel 1971, Cox and Penkett 1972, McNelis 1974). As indicated earlier, the significance of this oxidation path has been assessed by computer simulations of the SO_2 reaction with the Criegee intermediate (Calvert et al. 1978). This mechanism should be significant only in highly polluted air.

Smog chamber studies also have been conducted to investigate the relative importance of SO_2 oxidation via the free radicals OH, HO_2, and CH_3O_2 (Kuhlman et al. 1978, Graham et al. 1979, Miller 1980). The experimental results, aided by computer simulations of the experiments, indicated that SO_2 is oxidized predominantly by OH under urban-air conditions.

Chemical kinetics and smog chamber results indicate that the OH radical is responsible for the majority of the H_2SO_4 and HNO_3 formed via gas-phase reactions in the atmosphere. OH concentrations in the troposphere are related to a complex and tightly coupled series of reactions involving NO_x, hydrocarbons (HC), and O_3. Smog chamber experiments have been used to investigate, on a macroscopic level, how the HC-NO_x-O_3 cycle affects the OH population and the formation of H_2SO_4 and HNO_3.

A series of smog experiments focused on SO_2 oxidation indicated that the maximum rate of SO_2 conversion to H_2SO_4 depends strongly on the HC/NO_x ratio, increasing with higher ratios (Miller 1978). Parallel reductions in HC and NO concentrations in these experiments did not reduce the average SO_2 conversion rate. Computer modeling of these experimental conditions indicated that OH was primarily responsible for SO_2 oxidation, and the effects of HC and NO_x concentrations on the relative levels of OH were qualitatively consistent with the observed trends in SO_2 oxidation rates. This study indicated that during a diurnal period the gas-phase conversion of SO_2 to sulfate would likely be 10 to 20 percent of the initial SO_2 concentration for most urban HC-NO_x precursor conditions.

Outdoor chamber experiments using ambient air in St. Louis, MO, supported the contention that variations in OH concentrations, and thus SO_2 oxidation rates, are more strongly affected by HC/NO_x ratios than by absolute HC-NO_x concentrations (Miller 1978). Unfortunately, neither of these studies indicated a critical concentration region for HC-NO_x below which SO_2 oxidation might drop to rates typical of the background troposphere.

Laboratory simulations aimed at unraveling the terminating reactions of NO_x in the atmosphere are limited. An early breakthrough was the identification of PAN as an important product of NO_x reactions in irradiated atmospheres (Stephens et al. 1956). The development of new but imperfect methods for monitoring HNO_3 (Miller and Spicer 1975, Joseph and Spicer 1978, Huebert

and Lazrus 1979) and particulate nitrate (Appel et al. 1980) has finally enabled some assessments of the fate of NO_x in the atmosphere.

Smog chamber experiments with HC mixtures representing rural and urban conditions revealed that the conversion rate of NO_2 to products depended strongly on the HC/NO_x ratio, increasing with increasing ratio (Spicer et al. 1981b). Here, too, the HC/NO_x ratio effect is most likely the result of governing the concentration of hydroxyl radicals. The product ratio of PAN to HNO_3 was nearly proportional to the HC/NO_x ratio and the more reactive "urban" HC's yielded higher PAN/HNO_3 ratios than did "rural" HC mixture. Negligible amounts of particulate nitrate were observed in these experiments, and, if certain assumptions regarding wall losses are accepted, reasonably good material balances for NO_x were obtained.

Regarding absolute values for conversion rates for SO_2 and NO_2 to acidic products it should be noted that indoor smog chamber experiments generally are conducted with a constant radiation flux, whereas true solar radiation has temporal and spatial variations in spectral distribution and intensity. Winer et al. (1979) demonstrated radiation effects during smog chamber simulations. With this caveat in mind, one can discuss the pseudo-first-order rates for SO_2 and NO_x conversion to acids, as presented in the two smog chamber studies with similar HC components (Miller 1978, Spicer et al. 1981b). For HC/NO_x ratios near 5/1, the average pseudo-first-order rate for SO_2 oxidation was ~ 0.012 hr^{-1}, so an average SO_2 lifetime toward H_2SO_4 formation would be 83 hours. For similar conditions, the pseudo-first-order rate for NO_2 oxidation to HNO_3 (given PAN/HNO_3 ~ 1/3) was ~ 0.09 hr^{-1}. Thus, a lifetime for NO_2 is estimated to be 11 hours with respect to HNO_3 formation.

There are important transport implications associated with these results. SO_2, having an average lifetime for oxidation of 3 to 4 days, will be transported over greater distances than NO_2 and would be expected to be removed from the atmosphere by dry deposition processes to a greater extent than NO_2. Likewise, the sulfate produced from SO_2 oxidation, being in the aerosol phase, would be expected to have a longer atmospheric lifetime and transport time than the acidic vapors produced from NO_2 oxidation. Therefore, both the precursors and acid products of gas-phase sulfur transformations will have substantially greater potential for long-range transport than the precursors and products of nitrogen transformation.

4.2.3 Field Studies Of Gas-Phase Reactions

4.2.3.1 Urban Plumes--Studies of acid formation from gas-phase reactions under actual atmospheric conditions are confounded by many difficulties. Proper assessments of expanding mixing volumes, deposition losses, entrainment of fresh pollutants, and long averaging periods for analytical purposes are only some of the problems. In addition, few ambient studies have attempted to measure in detail the attendant pollutants and conditions (e.g., hydrocarbons, aldehydes, NO_x, O_3, and ultraviolet radiation) generally needed to interpret the data.

Many observations of SO_2 oxidation within urban plumes and under long-range transport conditions are listed in Table 4-11. The cited oxidation rates for SO_2 range from 0 to 32 percent hr^{-1}.

When such reports are examined, it is not always clear whether the data pertained exclusively to the gas-phase reactions or included aqueous-phase chemistry. Another reason that may account, in part, for the apparently divergent rates of SO_2 oxidation found in these citations is the tendency to compare rates derived by different methods; e.g., in one case the oxidation rates may represent 1-hour maxima, while in another case, the rates may represent averages taken over periods of a day or more.

As might be expected, the highest SO_2 oxidation rates have been reported for the more highly polluted atmospheres associated with urban areas. For example (Table 4-11), gas-phase SO_2 oxidation rates as large as 32 percent hr^{-1} have been inferred for St. Louis, MO, 13 percent hr^{-1} for Los Angeles, CA, and 9 percent hr^{-1} for Milwaukee, WI. In contrast, the "average" oxidation rates reported for distant transport situations are generally in the range of 0.5 to 2 percent hr^{-1}.

The several studies conducted in and around St. Louis, MO, offer interesting comparisons. The largest SO_2 oxidation rates reported by Breeding et al. (1976) were measured near noon and on a day having the largest nonmethane hydrocarbon concentration for their study period. Two Lagrangian-type studies conducted by Alkezweeny and Powell (1977) and Alkezweeny (1978) yielded fairly consistent oxidation rates in the range of 10 to 12 percent hr^{-1}. Measurements taken aboard a manned balloon (Forrest et al. 1979) resulted in upper-limit estimates of 4 percent hr^{-1} for SO_2 conversion under stagnant urban conditions. The experiments of White et al. (1976) led to similar estimates of SO_2 oxidation rates for the St. Louis plume. Numerical simulations of White's data by Isaksen et al. (1978) indicated SO_2 oxidation rates of about 5 percent hr^{-1} and a diurnally integrated conversion of about 25 percent.

Perhaps the most puzzling aspect of the data regarding urban plumes is the widely divergent SO_2 oxidation rates observed within single studies; e.g., a range of 1.2 to 13 percent hr^{-1} for Los Angeles, CA (Roberts and Friedlander 1975), and 1 to 9 percent for Milwaukee, WI (Miller and Alkezweeny 1980). In the latter study, such extreme rates were observed on two consecutive days of nearly identical relative humidity and temperature. The higher rate occurred when polluted air moved through Milwaukee from the southwest. On the following day, when the SO_2 oxidation rate was < 1 percent hr^{-1}, relatively clean "background" air passed through Milwaukee. In both cases, comparable levels of fresh pollutants emitted from the Milwaukee complex were entrained in the downwind plume, yet the previous history of the air masses seemed to govern the SO_2 oxidation rates. Detailed kinetic modeling of the two cases was conducted, taking into account differences in reactive hydrocarbons, NO_x, and O_3. The associated free-radical chemistry could not account for the observed differences in SO_2 oxidation rates. Thus, the agreement often claimed between kinetic modeling results and data observed for polluted atmospheres may sometimes be fortuitous, and a comprehensive body of data should be scrutinized before

TABLE 4-11. SO_2 OXIDATION RATES (% hr^{-1}) FROM STUDIES OF URBAN PLUMES AND LONG RANGE TRANSPORT

Range	Average	Location/period[a]	References
6-25	16.6	Rouen, France/W/D	Benarie et al. (1972)[b]
1.2-13	7.1	Los Angeles, CA/S & F/D	Roberts and Friedlander (1975)[b]
1.1	1.1	British Isles/W/L	Prahm et al. (1976)[c]
0.3-1.7	0.7	Western Europe/S & W/L	Eliassen and Saltbones (1975)
5.3-32	16	St. Louis, MO/F/D	Breeding et al. (1976)[d]
5	5	St. Louis, MO/S/D	White et al. (1976)[e]
31	31	Budapest, Hungary/S/D	Meszaros et al. (1977)[c]
10-14	12	St. Louis, MO/S/D	Alkezweeny and Powell (1977)
8-11.5	9.8	St. Louis, MO/S/D	Alkezweeny (1978)
0.6-4	1.7	Arnhem-Amsterdam, Netherlands/S & W/D & N	Elshout et al. (1978)
0-4	2	St. Louis, MO/S/D	Forrest et al. (1979)
1-9	4	Milwaukee, WI/S/D	Miller and Alkezweeny (1980)

[a]Season: W = winter; S = summer; F = spring or fall. Time of day: D = daytime; N = nighttime; L = long term (> 24 hr) averaging periods.

[b]Higher rates possibly related to aqueous-phase reactions.

[c]Calculated from their half-life data.

[d]Calculated from their data by Alkezweeny and Powell (1977).

[e]Based on kinetic analysis of data by Isaksen et al. (1978).

existing knowledge of gas-phase chemistry is applied to predict SO_2 oxidation in urban areas.

Information on the gas-phase transformations of NO_x to acid products in urban plumes is scarce. Spicer (1980) estimated NO_x transformation/removal rates for the Phoenix, AZ, urban plume to be less than 5 percent hr^{-1}. The low rates were attributed at least in part to the thermal deposition of PAN-type compounds at the high ambient temperatures of the desert area. Spicer (1977a) reported rates of NO_x conversion to products of about 10 percent hr^{-1} for Los Angeles, CA, if certain assumptions for material balances were granted. In more recent measurements, downwind of Los Angeles (Spicer et al. 1979), typical conversion rates of 5 to 10 percent hr^{-1} were observed. Measurements by Spicer et al. (1981a) resulted in pseudo-first-order rates for NO_x removal ranging from 14 to 24 percent hr^{-1} for the Boston, MA, plume. The average lifetime for NO_x was estimated to be 5.9 hr. In the Boston study, the ratio of PAN to HNO_3 was 1.8 and the conversion of NO_x to particulate NO_3^- was < 1 percent of the total product. Given an average PAN/HNO_3 ratio of 1.8, the pseudo-first-order rate for NO_2 conversion to acid would have been 6.3 percent hr^{-1}, and the NO_x lifetime with respect to HNO_3 production would be about 16 hrs. These values are similar to estimates given earlier with respect to global OH concentrations.

Somewhat different findings were recently reported by Hanst et al. (1982) in an investigation of Los Angeles smog by long-path infra-red absorption spectroscopy. Hanst et al. concluded that most of the NO_2 was removed by reaction with O_3 and subsequent reactions of N_2O_5 and NO_3 into condensed products (particulate nitrates) not amenable to detection in their cell.

This interpretation conflicts with the conclusion reached by the Battelle researchers (Spicer et al. 1981a) which asserts that 95 percent of the NO_x losses in urban plumes can be accounted for as gaseous HNO_3 and PAN, and that the amounts of particulate nitrate produced in urban plumes are very small.

As indicated earlier, it is apparent that more research is needed concerning the fate of PAN, N_2O_5 and NO_3 in the atmosphere and their potential contributions as acidic species.

4.2.3.2 Power Plant Plumes--The majority of studies of SO_2 oxidation in the atmosphere have been conducted in association with power plant plumes. Compared to studies of urban air chemistry, power plant plumes offer the advantages of higher pollutant concentrations, definitive plume boundaries, the presence of inert tracers, and less severe deposition losses.

In general, the gas-phase chemistry pertaining to reactions within power plant plumes is the same as for ambient air. However, an important concern when plume data are interpreted and kinetics of the gas-phase reactions in plumes are modeled is adequate treatment of the turbulent exchange processes (Donaldson and Hilst 1972, Lamb and Shu 1978, Shu et al. 1978).

Interpretations of power-plant plume data show that, under most conditions where plumes can be discerned against background, the rates of formation of sulfate and nitrate are slower in power plant plumes compared to urban plumes. The main reasons for this are imperfect mixing and an abundance of NO which effectively competes with SO_2 and NO_2 for hydroxyl radicals. Under some conditions, SO_2 and NO_2 transformation rates in power plant plumes can exceed those in ambient air (Miller and Alkezweeny 1980), and under such conditions an excess of O_3 in the plume can be expected.

Selected studies of power plant plumes are listed in Table 4-12. The selection is restricted to studies where gas-phase SO_2 oxidation was emphasized and/or NO_x reactions were investigated.

Studies concentrating on heterogeneous aspects of plume reactions have been reviewed by Newman (1981) and are not discussed here. As is the case in studying urban plumes, one cannot always distinguish gas-phase reactions from other conversion mechanisms.

The experiments cited in Table 4-12 were conducted with widely varied analytical procedures, transport times, ambient pollutants, meteorological conditions, and emission rates, all of which greatly influence the results. Considering all these factors in an interpretation of the data is beyond the scope of this document. In general, SO_2 transformation rates were estimated by measuring either the increase in submicron particle concentrations (inferred as H_2SO_4 mass) or the actual increase in filtered sulfate mass relative to total S concentration, or to an inert tracer, such as sulfur hexafluoride (SF_6). In the few cases where NO_x transformations were measured, rates of NO_x loss or NO_3^- formation were based on total S as the conservative tracer of plume dilution.

Pueschel and Van Valin (1978) measured the formation of new particles downwind of the Four Corners, NM, plant and estimated a flux of 10^{16} particles s^{-1} of H_2SO_4 that could act as cloud condensation nuclei (CCN) in the atmosphere. Comparison of the source strengths of CCN from the power plant relative to those for natural CCN in the area led to the assertion that the photochemically derived CCN from power plants could have major effects on cloud structure and precipitation processes in the West.

At about the same time, experiments in Canada (Lusis et al. 1978) indicated that, under relatively dry conditions, SO_2 oxidation was related primarily to photochemical reactions. In accord with photochemical mechanisms, oxidation rates were low in February (< 0.5 percent hr^{-1}) and relatively high in June (1 to 3 percent hr^{-1}). Increased rates of oxidation were apparent at the leading edges of plumes.

Similar "edge effects" were observed in early studies of the Labadie, MO, plume (Cantrell and Whitby 1978, Wilson 1978). Another important feature of the Labadie experiments (Gillani et al. 1978, Husar et al. 1978) was the apparent diurnal variation in the SO_2 oxidation rate and the inference that solar radiation and extensive mixing of the plume with ambient air were required for substantial SO_2 oxidation rates. During noon hours, the SO_2 conversion rate was found to be 1 to 4 percent hr^{-1} compared to nighttime

TABLE 4-12. SUMMARY OF POWER PLANT PLUME STUDIES WITH EMPHASIS ON GAS-PHASE TRANSFORMATION RATES

Plant/location	Season	Range of SO_2 conversion rates (% hr^{-1})	Range of NO_x conversion rates (% hr^{-1})	Reference
Four Corners, NM	October	2 - 8	-	Pueschel and Van Valin (1978)
GCOS/Alberta	Feb. & June	0 - 3	-	Lusis et al. (1978)
Labadie/MO	July	0.41 - 4.9	-	Cantrell and Whitby (1978)
Labadie/MO	July	0 - 4	-	Wilson (1978), Husar et al. (1978), Gillani (1978), Gillani et al. (1978)
Four Corners, NM	June	0.9 - 5.4	-	Hobbs et al. (1978), Hegg and Hobbs (1979a), Hegg and Hobbs (1980)
Centralia/WA	Spring & fall	0.03 - 1.4	-	
Leland-Olds/ND	June	0 - 0.7	0.2 as particulate NO_3^-	
Sherco/MN	June	0 - 3	0.2 as particulate NO_3^-	
Big Brown/TX	June	0.4 - 14.9	0.2 as particulate NO_3^-	

TABLE 4-12. CONTINUED

Plant/location	Season	Range of SO_2 conversion rates (% hr^{-1})	Range of NO_x conversion rates (% hr^{-1})	Reference
Colorado River Basin/CO	Summer	1.5	-	Eatough et al. (1981)
TVA Cumberland/TN	August	0.1 - 4	3 - 12	Forrest et al. (1981)
Navajo/AZ	Summer & winter	0 - 0.8	3 - 10 times R_{SO_2}	Richards et al. (1981)
Labadie/MO	July	0.08 - 5.4	-	
Sherco/MN	-	2.3 - 14.2	-	Whitby et al. (1980)
Cumberland/TN	August	1.1 - 7.1	-	
Navajo/AZ	Summer	0.3 - 2.9	-	
Cobb/MI	May & Nov	0.1 - 11	23 - 31 as NO_x loss	
Andrus/MS	May & Oct	0.1 - 5.9	5 - 21 as NO_x loss	Easter et al. (1980)
Breed/IN	Jun & Nov	0 - 1.5	-	

rates < 0.5 percent hr^{-1}. Mesoscale modeling of the Labadie experiments (Gillani 1978, Gillani et al. 1978) was an important attempt to budget the S in a dispersing plume. It was concluded that, for the Labadie conditions, some 20 to 40 percent of the emitted SO_2 may be converted to SO_4^{2-} while the remainder is lost by deposition mechanisms.

Power plant experiments conducted by the University of Washington (Hobbs et al. 1978, Hegg and Hobbs 1979b) employed a variety of particle-measuring techniques. SO_2 oxidation rates derived by the various methods showed considerable scatter. Higher SO_2 oxidation rates generally were found in the southwest United States, and rates tended to increase with travel time and ultraviolet (UV) intensity. Measurements of particulate NO_3^- at three of the plants (Hegg and Hobbs 1980) showed minimal NO_3^- in the condensed phase (generally < 2 $\mu g\ m^{-3}$) and a maximum NO_x conversion rate to particulate nitrate of 0.2 percent hr^{-1}.

The employment of different analytical methods by Eatough et al. (1981) has led to interesting differences between the chemical composition of secondary SO_4^{2-} particles, depending on regions of the United States. In the East, where SO_2 conversion rates are generally high, secondary SO_4^{2-} is predominantly H_2SO_4 and ammonium sulfate, $(NH_4)_2SO_4$, with nominally 10 percent as an organic-S(IV) compound. In the West, 25 to 75 percent of secondary S may be organic-S(IV). Furthermore, in arid western states the principal SO_4^{2-} salts formed in plumes were metal salts such as gypsum.

Reports from the measurements of the Cumberland, TN, plume (Forrest et al. 1981) are similar to findings from the Labadie plume. Nighttime SO_2 conversion rates ranged from 0.1 to 0.8 percent hr^{-1}, while daytime rates ranged from 1 to 4 percent hr^{-1}. Important new information was obtained on NO_x transformations. Total NO_3^- formation (gaseous and particulate NO_3^-) rates were 0.1 to 3 percent hr^{-1} at night and 3 to 12 percent hr^{-1} during the day. The authors point out that the rate of plume mixing with ambient air might have been a limiting factor for NO_2 conversion to NO_3^-.

SO_2 and NO_x rates of conversion reported for the Navajo Generating Station in Arizona (Richards et al. 1981) were much lower than those reported from the Cumberland plant. The maximum rate for SO_2 conversion in the summer was 0.8 percent hr^{-1} and 0.2 percent hr^{-1} in the winter. Rates of gaseous nitrate formation (HNO_3) were generally 3 to 10 times larger than for SO_4^{2-} formation.

Experiments conducted in Michigan, Indiana, and Mississippi, where SF_6 was used to trace plume dispersion, resulted in generally moderate SO_2 conversion rates, 0 to 3 percent hr^{-1}, with occasional exceptions (Easter et al. 1980). SO_2 transformation rates exhibited correlation with ambient HC reactivities and concentrations, although for many cases this could also be interpreted as seasonal variation related to solar intensity, plume dispersion, or temperature. For example, SO_2 oxidation rates at Cobb, MI, were 2 to 11 percent hr^{-1} in May and 0.1 to 0.3 percent hr^{-1} in November. Rates at Breed, IN, were 0 to 1.5 percent hr^{-1} in June and 0 to 0.1 percent

hr^{-1} in November. At Andrus, MI, the rates were 0.5 to 4.9 percent hr^{-1} in May and 0.1 to 3.7 percent in October.

Measurements of NO_x transformation rates in the above study were inconclusive. Chemical analyses indicated that transformations to HNO_3 and particulate NO_3^- were minimal, yet large NO_x losses were often calculated when NO_x was compared to SF_6 or total S. The wide scatter in the data suggests analytical problems.

4.2.4 Summary

Organic acids generally are not regarded as significant contributors to the acidic deposition problem, mainly because their ionization constants are weak relative to those for most inorganic acids. However, the scarcity of information on the abundance and fate of organic acids in the atmosphere makes it impossible to estimate their importance with assurance.

Halogenated compounds (RX) are potentially important to precipitation chemistry, but little information is available on the gas-phase reactions that might yield HX. Halocarbons of both natural and anthropogenic origin exist at low concentrations and react slowly or not at all in the troposphere. Thus, their contribution to the production of acid compounds is potentially significant only on a global scale.

Most of the concern regarding acidic deposition has focused on S and N chemistry. Measurements of the rates of SO_2 and NO_2 oxidation in the atmosphere have been crude and imprecise. This relates to analytical difficulties, extensive spatial and temporal averaging and, particularly in the case of SO_2, a lack of distinction between gas-phase and aqueous-phase reaction paths.

Rates of SO_2 oxidation measured in urban areas and plumes range from near zero to 30 percent hr^{-1}. The preponderance of data, however, indicates upper-level rates of 12 percent hr^{-1} for midday, summer conditions. Average daytime conversion rates are in a range of 3 to 5 percent hr^{-1} for summertime conditions. Systematic measurements of seasonal and diurnal variations have not been made; peripheral data indicate that nighttime and wintertime conversion rates are < 1 percent hr^{-1}.

Like the case of sulfuric acid formation, the rate of nitric acid formation under various atmospheric conditions is not well documented. Most of the available data are consistent with the conclusion that the reaction of NO_2 with hydroxyl radicals is the principal gas-phase route for HNO_3 formation, although other reactions are also important. In general, NO_2 conversion rates under daylight, summertime conditions range from < 5 percent hr^{-1} to 24 percent hr^{-1}, with at least half of the product yield being nitric acid vapor.

There is conflicting evidence about the role of N_2O_5 in nitrate formation; its gas-phase reaction with water is slow, but it hydrolyzes rapidly on moist surfaces. There is also considerable uncertainty regarding the fate of peroxyacetyl nitrate (PAN) in the atmosphere and its potential to

contribute to acidic deposition. Adequate assessments of the impact of these species to atmospheric acidity cannot be made, and further studies are warranted involving field measurements of NO_3, N_2O_5, and PAN and kinetic measurements of their hydrolysis reactions.

Despite some conflicting data regarding sulfur and nitrogen oxides transformations in power plant plumes, a few tentative conclusions emerge. Under most conditions, rates of transformations to acidic products are generally slower in power plant plumes than in ambient air. SO_2 oxidation rates under daylight conditions fall in the range of 1 to 6 percent hr^{-1}, although some exceptions exist. SO_2 conversion rates in plumes from some plants in southwestern states are lower than in other parts of the country; the basis for this trend is not apparent.

A paucity of data exists regarding nitric acid formation in power plant plumes. A few studies in which this measurement was attempted indicated HNO_3 formation rate in a range 3 to 10 times greater than that for H_2SO_4 formation. This result would seem likely if the hydroxyl radical was the principal oxidant.

Overall, field studies of SO_2 and NO_2 transformations in air have not provided conclusive evidence to support predominant reaction pathways or to identify the most important atmospheric variables affecting transformation rates. Most of the information on these processes comes from chemical kinetic studies, model simulations and smog chamber experimentation.

A survey of fundamental reactions confirms that the rate of gas-phase oxidation of SO_2 is governed by free-radical concentrations in the atmosphere, primarily by the OH radical and to a much lesser, but uncertain, extent by CH_3O_2 and HO_2. Of the reduced forms of sulfur gases, H_2S is by far the most reactive in the atmosphere. Its reaction with OH radicals is faster than is the rate between SO_2 and OH and the product of the reaction is SO_2. Other reduced sulfur compounds such as COS oxidize much more slowly in the atmosphere, and their reaction products have not been well characterized.

A survey of the fundamental reactions of nitrogen oxides in the atmosphere indicates that gaseous HNO_3 formation will be dominated by the reaction of NO_2 with OH radicals. The rate for this reaction is approximately ten times faster than the rate for SO_2 oxidation by OH. As mentioned above, other products of nitrogen oxides reactions in air are potentially important to acidic deposition, particularly N_2O_5 and PAN and to a lesser extent NO_3 and HNO_2, and the fate of these species in the atmosphere must be better characterized before assessments can be made.

Smog chamber studies of gas-phase transformations revealed that the rates of SO_2 and NO_2 oxidation, under simulated urban conditions, were strongly dependent on the ratio of hydrocarbons (HC) to nitrogen oxides (NO_x). The findings were qualitatively consistent with kinetic models that predicted OH concentrations to rise with increasing HC/NO_x ratios but remain relatively constant with proportional variations in HC and NO_x. The product ratio of PAN to HNO_3 was also found to be nearly proportional to the HC/NO_x

ratios. Such relationships, however, have not been investigated under actual atmospheric conditions and other atmospheric variables will undoubtedly muddy the water.

The number of free radicals and competitive reaction paths that comprise atmospheric chemistry is quite large and many of the reactions are highly coupled. Calculations indicate that the free-radical concentrations have pronounced diurnal and seasonal variations. Unfortunately, real-time measurements of free radicals have not been very successful, and knowledge of the factors influencing the concentrations of free radicals is largely theoretical. In polluted air, the concentration of OH is considered to be strongly related to the concentrations of hydrocarbons, aldehydes, carbon monoxide and nitrogen oxides, whereas, in relatively clean "background" air, the OH concentration is dominated by levels of carbon monoxide, ozone and water vapor. In both cases, the characteristics of incident sunlight play an important role. The effect of trace amounts of anthropogenic pollutants on "background" OH concentrations is unknown and unlikely to be resolved by computer modeling.

If, as in the case of SO_2 and NO_2, oxidation is largely limited by the availability of free radicals such as OH, an assessment of the relationship between precursor concentrations and acid formation rates requires full knowledge of the factors governing the oxidizing species. While there is ample reason to expect the relationships to be nonlinear, kinetic models of the processes should somehow be tested. Such applications, when considered in the context of atmospheric transport and other atmospheric phenomena present many difficulties, as discussed in a later section of this chapter.

4.3 SOLUTION REACTIONS (D. A. Hegg and P. V. Hobbs)

4.3.1 Introduction

The importance of chemical reactions within cloud drops and rain (hereafter called hydrometeors) to the formation of strong acids has been suggested on both theoretical (Scott and Hobbs 1967, Barrie et al. 1974, Larson and Harrison 1977) and experimental (Junge and Ryan 1958, Van den Heuval and Mason 1963, Penkett et al. 1979) grounds. Postulating such reactions has been necessary to explain the observed acidity of precipitation (Petrenchuk and Selezneva 1970, Hobbs 1979, Newman 1979, McNaughton and Scott 1980). Recent studies have even suggested that solution reactions may play a rate-limiting role in SO_2 absorption by raindrops (Baboolal et al. 1981, Walcek et al. 1981). Most of these studies have dealt exclusively with S species. Even in this case, considerable uncertainty exists concerning reactions that convert the precursor species, aqueous SO_2, into H_2SO_4. Moreover, a considerable body of data suggests that N and Cl compounds also contribute significantly to precipitation acidity (Gorham 1958, Petrenchuk and Drozdova 1966, Marsh 1978, Hendry and Brezonik 1980, Galloway and Likens 1981).

Contributions to the acidity of rain by various aqueous reactions that can produce HCl, HNO_3, and H_2SO_4 in hydrometeors are evaluated in this section. During this evaluation, the relative importance of direct acid

vapor absorption reactions and acid-precursor oxidation reactions is considered. In addition, the importance of neutralization in acidic hydrometeors is assessed. Whenever possible, detailed discussion of kinetic mechanisms is avoided and experimental rate expressions are employed.

The various steps in the production of acidic precipitation, especially those discussed in this chapter, are indicated schematically in Figure 4-2.

4.3.2 Absorption of Acid

The most direct means of producing acidity in hydrometeors is through direct absorption of acid vapors and the collection of acidic aerosol, either through nucleation capture in clouds or scavenging by hydrometeors. While both of these mechanisms are discussed in detail in Chapter A-6, the former mechanism, involving gas scavenging, lies on the borderline between reactions in solution and scavenging processes. Because it sometimes involves solution reactions and will be useful in assessing the relative importance of various reactions producing acids in solution compared with direct absorption of the corresponding reaction products, acid vapor absorption will also be considered here.

With regard to particle scavenging, Chapter A-6 shows that scavenging of particulate sulfuric acid by cloud droplets occurs with essentially the same efficiency as scavenging of sulfuric acid vapor. Therefore, despite the fact that most of the sulfuric acid in the atmosphere is in particulate form (due to the very low vapor pressure of sulfuric acid), we can treat the scavenging of sulfuric acid by considering the scavenging of sulfuric acid vapor having a pressure equivalent to a typical mass concentration of atmospheric, particulate sulfuric acid. This procedure allows us to treat the incorporation of H_2SO_4 into hydrometeors with the same methodology required to treat HNO_3 and HCl (both of which are primarily gases in the atmosphere).

Two steps are necessary to evaluate the importance of absorption of acid vapors: (1) determining the solubilities of the chemical species of interest, and (2) determining their concentrations in air. Regarding solubility, the Henry's law constants for the three acids identified as significant contributors to the acidity of precipitation (HCl, HNO_3, and H_2SO_4) and for the various trace gases (Cl_2, NO_2, N_2O_4, HNO_2, and SO_2) assumed to be the precursors of these acids in the atmosphere are listed in Table 4-13.

For these constants to be suitable measures of solubility, equilibrium must exist between the gases and the liquid phase. While such equilibria no doubt exist for cloud droplets, they may not for raindrops falling through a strong concentration gradient of gases. Furthermore, the Henry's law constants shown in Table 4-13 are based on measurements at vapor pressures far above atmospheric values. Thus, gross extrapolations must be used when they are applied to atmospheric conditions. Indeed, the very large values for some of the Henry's law constants ($\geq 10^5$ mol ℓ^{-1} atm^{-1}) shown in Table 4-13 cannot possibly be applied to conditions in the atmosphere; they simply

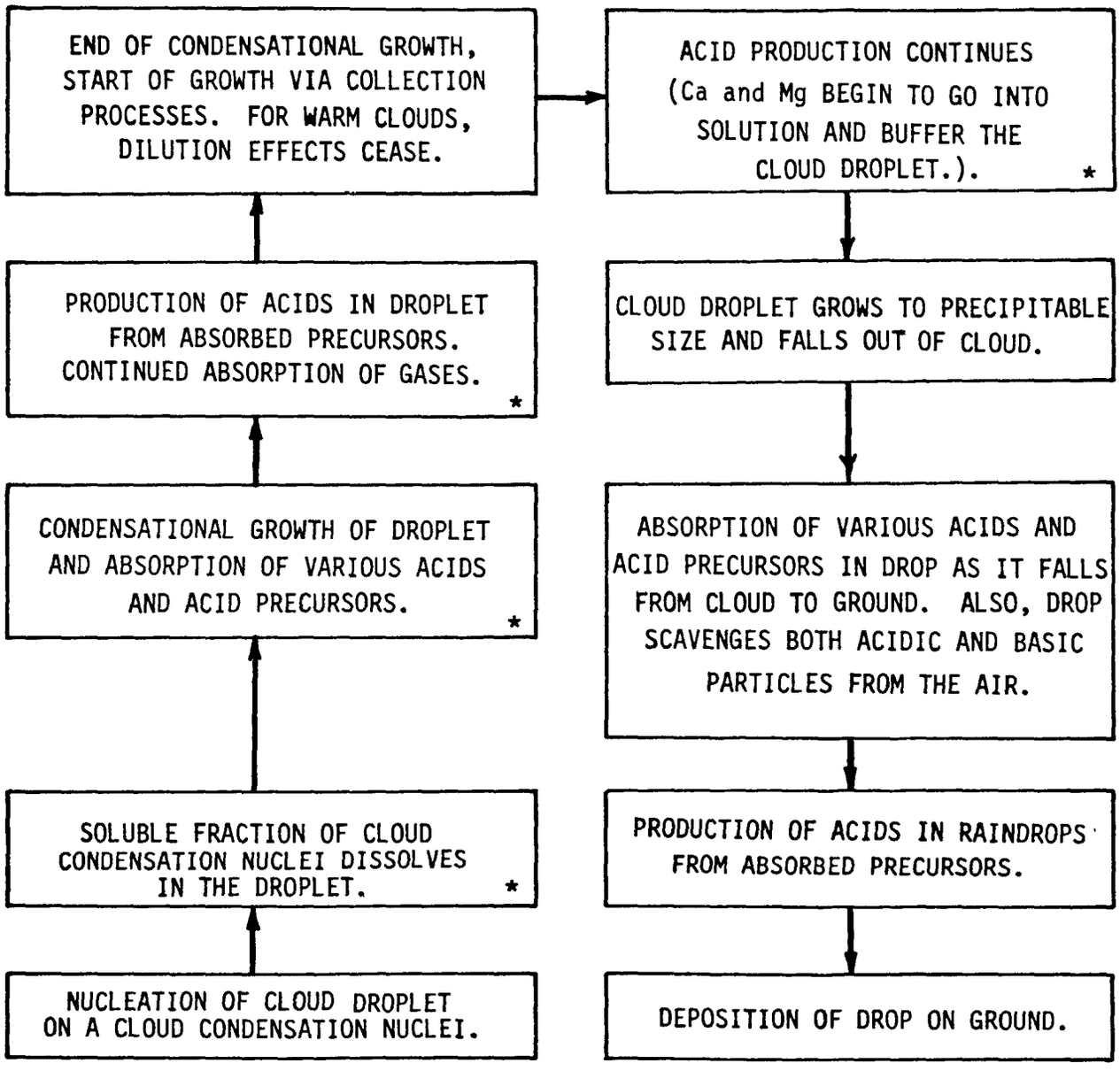

Figure 4-2. Schematic diagram of the steps in the production of acidic precipitation. Steps discussed in this section are indicated by asterisks in the lower right corner of the box.

TABLE 4-13. HENRY'S LAW CONSTANTS (H) FOR GASES OF INTEREST IN ACIDIC PRECIPITATION FORMATION

Gas[a]	H (mol ℓ^{-1} atm^{-1})	Temperature (C)	Source
Cl_2	6.2×10^{-2}	25	Whitney and Vivian (1941)
(HCl)	2.5×10^{3}	25	Calculated from vapor pressure data in International Critical Tables (1928)
NO_2	2.48×10^{-2}	15	Komiyama and Inoue (1980)
N_2O_4	2.15	15	Komiyama and Inoue (1980)
HNO_2	4.76×10^{1}	25	Martin et al. (1981)
(HNO_3)	1.98×10^{5}	25	Davis and de Bruin (1964)
SO_2	1.24	25	Johnstone and Leppla (1934)
(H_2SO_4)	10^{8}	25	Calculated from vapor pressure data in International Critical Tables (1928)

[a]The strong acids are in parentheses and their precursors precede them.

indicate large deviation from Raoults's law suggested by the exothermicity of acid solution reactions. The large magnitudes of the Henry's law constants also suggest that the associated vapors are essentially completely absorbed by hydrometeors and that liquid-phase concentrations must be calculated from considerations of mass conservation; we will return to this subject later. Despite these problems, the values of the Henry's law constants listed in Table 4-13 are useful as measures of relative solubility and will be so employed.

The values shown in Table 4-13 illustrate the very high solubility of HCl, HNO_3, and H_2SO_4 relative to their gaseous precursors. This high solubility suggests that the direct absorption of acid vapors might play an important role in acidic formation in hydrometeors. The range of the species listed in Table 4-13 is shown in Table 4-14 to explore this possibility further.

The information in Tables 4-13 and 4-14 permits estimates of the liquid-phase concentrations of both directly absorbed acids and their absorbed precursors in the atmosphere. The ratio of these concentrations indicates the potential importance of aqueous-phase acid production reactions. For example, if the ratio of an acidic concentration in the liquid phase to the concentration of its absorbed precursor is high, very high reaction rates will be necessary to increase acidity significantly during the lifetime of a hydrometeor. For HCl, this ratio is infinite under most atmospheric conditions. Indeed, only Cl_2 is listed as a precursor of HCl in Table 4-14. The implication is not that other precursors do not exist, for it is well known that in urban areas, large quantities of chlorine and chlorinated organics are emitted into the atmosphere (NAS 1976). However, the lifetime of free chlorine in the atmosphere is very brief, and the reduced product is HCl. Any chlorine that might survive long enough to be scavenged would undergo absorption via the very fast reaction (Whitney and Vivian 1941):

$$Cl_2 + H_2O\ (\ell) \rightarrow H^+ + Cl^- + HOCl, \qquad [4\text{-}80]$$

and could therefore be considered the anhydride of HCl. Chlorinated organics, on the other hand, should be stable in solution and produce little acid. For a more detailed discussion of the possible inclusion of free chlorine and chlorinated organics in precipitation, see Mills et al. (1979).

Of more interest are the N and S species, which contribute substantially to the acidity of precipitation. The concentration of H_2SO_4 in cloud water can be taken as the mole (mol) concentration of H_2SO_4 per cubic meter in the gas phase divided by the cloud water concentration in liters per cubic meter of air. When a concentration of 1 ppb for H_2SO_4 (Table 4-14) and a cloud water concentration of $\sim 5 \times 10^{-4}\ \ell\ m^{-3}$ are taken, a value of 8×10^{-5} mol ℓ^{-1} is reached for the maximum concentration of directly absorbed H_2SO_4 in cloud water. The concentration in background air is almost certainly at least an order of magnitude less than this value. For comparison, the concentration of S(IV) (the immediate precursor of H_2SO_4) in solution is given by:

TABLE 4-14. GAS-PHASE CONCENTRATIONS OF ACIDS AND THEIR PRECURSORS IN THE ATMOSPHERE

Gas[a]	Concentration in "background" air (ppb)	Concentration in urban air (ppb)	Source
Cl_2	-	-	-
(HCl)	1	8	Kritz and Rancher (1980), Okita et al. (1974)
NO_2	0.1-4	10-100	Robinson and Robbins (1969), Noxon (1975), Spicer (1977b)
N_2O_4	Negligible	Negligible	No measurements available.
HNO_2	0.003	2-4	Crutzen (1974), Winer (1979).
(HNO_3)	0.02-5	10	Huebert and Lazrus (1978), Kelly et al. (1979), Spicer (1977b).
SO_2	1-14	10-50	Georgii (1978), Hidy et al. (1978)
(H_2SO_4)	$\leq$ 1[b] (0.5)	$\leq$ 1[b](0.5,4)	Commins (1963), Tanner et al. (1977), Elshout et al. (1978), Yue and Hamill (1979)

[a]The strong acids are in parentheses and their precursors precede them.

[b]The extremely low vapor pressure of H_2SO_4 results in extensive nucleation of H_2SO_4-H_2O droplets under atmospheric conditions when the vapor pressure of H_2SO_4 exceeds ~ 1 ppb (Yue and Hamill 1979). The bracketed concentration of 4, listed under urban concentrations, which appears to contradict this view, is derived from Commins (1963) and probably includes substantial particulate H_2SO_4. The bracketed concentrations of 0.5, for background and urban air, are from Elshout et al. (1978); these also include particulate H_2SO_4. Furthermore, rapid condensation of H_2SO_4 vapor onto ambient particles may be assumed to reduce the equilibrium concentration of the vapor far below 1 ppb. The value of 1 ppb is used as an analog for approximately 4 $\mu g\ m^{-3}$ of both particulate and gaseous H_2SO_4.

$$[S(IV)] = H_{SO_2} \cdot P_{SO_2} \left[1 + \frac{K_{1s}}{[H^+]} + \frac{K_{1s} K_{2s}}{[H^+]^2} \right] \qquad [4\text{-}81]$$

where H_{SO_2} is the Henry's law constant for SO_2, and K_{1s} and K_{2s} are the first and second dissociation constants for $SO_2 \cdot H_2O$. When appropriate values are used for those constants and a cloud water pH of ~ 5 (Petrenchuk and Drozdova 1966, Hegg and Hobbs 1981a) is assumed, a maximum concentration of S(IV) in urban air is found to be 7.9 x 10^{-5} mol ℓ^{-1}. If we assume a cloud droplet life of ~ 1 hr, S(IV) oxidation rates on the order of 100 percent hr^{-1} would be required for significant acid production.[1] "Significant" refers to acid production at concentrations at least equal to those produced by direct absorption of acid vapor.

Furthermore, assuming a background concentration of H_2SO_4 of ~ 0.1 ppb and a background concentration of SO_2 of ~ 10 ppb in the northeast United States (Hidy et al. 1978), an S(IV) oxidation rate of only ~ 50 percent hr^{-1} would be required for significant acid production in background air.

The situation with respect to HNO_2 formation in solution is quite different. Again, acid concentration must be estimated from considerations of mass conservation. Assuming gas-phase concentrations of 5 and 0.5 ppb in urban and background atmospheres, respectively, the same procedure used above for S yields liquid-phase HNO_3 concentrations of 4.1 x 10^{-4} mol ℓ^{-1} and 4.1 x 10^{-5} mol ℓ^{-1} for urban and background atmospheres, respectively. The corresponding liquid-phase N(III) (the N species generally assumed to be the precursor of HNO_3 in solution) concentrations would be ~ 8 x 10^{-5} mol ℓ^{-1} in an urban atmosphere and 3 x 10^{-8} mol ℓ^{-1} in the background atmosphere (based on a pH of 5.0, concentrations for NO_2 of 50 ppb and 1 ppb in urban and background atmospheres, and concentrations of HNO_2 of 4 ppb and 0.003 ppb in urban and background atmospheres). These concentrations suggest that oxidation rates of ~ 5 x 10^2 percent hr^{-1} and ~ 1 x 10^5 percent hr^{-1} in urban and background atmospheres, respectively, are necessary for significant acid production to occur via precursors. As shown later in the chapter, these rates are far higher than are those of any known reactions for N(III).

A possible alternative to the production of HNO_3 in solution from absorbed N(III) is its production from absorbed N_2O_5 at night (Platt et al. 1981).

---

[1] By comparison, raindrops have lifetimes from 1 to 5 min, assuming cloud bases from 1 to 3 km and a mean fallspeed of ~ 10 m s^{-1}. Solution reactions in raindrops will therefore make a relatively small contribution to hydrometeor activity (although direct absorption of acids may be substantial). Attention is therefore focused on solution reactions in cloud droplets.

However, since N_2O_5 is an hydride of HNO_3, this mechanism is really only an interesting variant on the direct absorption of HNO_3; therefore, we will not treat it here as a solution reaction.

It may be tentatively concluded that liquid-phase oxidation reactions do not play a role in HNO_3 formation in cloud droplets. A recent modeling study by Durham et al. (1981) suggests that such oxidation also plays no role in the acidity production in raindrops. The principal reason for the lack of any contribution to the formation of HNO_3 from liquid-phase oxidation in hydrometeors is the low rate of N(III) formation from absorbed NO_2. The complex nature of NO_2 absorption by water has led to considerable misunderstanding and is discussed more thoroughly in Section 4.3.4.

4.3.3 Production of HCl in Solution

While little evidence currently supports the formation of HCl in solution from gaseous precursors, HCl has long been thought to be produced by particles of sea salt dissolving in hydrometeors, either by absorption or by production in solutions of HNO_3 and/or H_2SO_4 (Robbins et al. 1959, Eriksson 1960). For both HNO_3 and H_2SO_4, the reaction is simply a cation exchange between chloride and the less volatile nitrate and sulfate anions. The HNO_3 reaction has been shown to convert as much as 16 percent of initial NaCl to HCl within a 5-minute reaction time; presumably, the H_2SO_4 reaction is equally fast. However, while HCl produced in this fashion will contribute to the acidity of hydrometeors and possibly contributes a major fraction of the background gaseous Cl in the atmosphere (Duce 1969), it obviously cannot increase the acidity of hydrometeors above what would be produced by the HNO_3 and/or H_2SO_4 from which it is derived.

4.3.4 Production of HNO_3 in Solution

The production of HNO_3 in solution by means of nitrite NO_2^- (or HNO_2) oxidation has been proposed as a significant atmospheric reaction. The oxidants currently considered significant are O_3 (Penkett 1972) and H_2O_2 (Durham et al. 1981). While the oxidation rates produced by these oxidants have been studied (Halfpenny and Robinson 1952, Penkett 1972), the results of the previous section suggest that these reactions are not likely to be important in the atmosphere, due to the low levels of N(III) in hydrometeors. The low levels of N(III) result from the low solubility of NO_2 in hydrometeors and the relatively slow rate of N(III) formation from the absorbed NO_2. This has led to some confusion. For example, Flack and Matteson (1979) derive a value of 100 mol ℓ^{-1} atm^{-1} for the Henry's law constant of NO_2, compared to the value of 2.48×10^{-2} mol ℓ^{-1} given in Table 4-13. The higher value is obviously wrong because it exceeds the constant for the NO_2 dimer (N_2O_4), which is well known to be considerably more soluble than is NO_2 (Andrew and Hanson 1961, Kameoka and Pigford 1977, Komiyama and Inoue 1980).

Much of the confusion over this matter is due to the complexity of the NO_x - H_2O system at the high NO_2 concentrations that commonly have been employed in laboratory experiments (> 5 ppm and commonly > 200 ppm). At these concentrations the gas-phase reaction,

$$3NO_2 + H_2O = NO + 2HNO_3, \quad [4\text{-}82]$$

occurs and spontaneously forms a two-phase system consisting of HNO_3 vapor and droplets of dilute HNO_3 over the absorption surface (England and Corcoran 1974). Also, at high NO_2 concentrations the gas-phase equilibrium,

$$2NO_2 = N_2O_4, \quad [4\text{-}83]$$

results in appreciable N_2O_4, which can then absorb into solution via the fast disproportionation reaction:

$$N_2O_4(g) + H_2O(\ell) = HNO_2(\ell) + HNO_3(\ell) \quad [4\text{-}84]$$

NO_2 absorbs in a straightforward manner but then forms N_2O_4 (ℓ), which undergoes the disproportionation reaction given by Equation 4-84 (Komiyama and Inoue 1980). This reaction's rate is slow enough ($k \sim 4 \times 10^5$ s^{-1}; Kameoka and Pigford 1977, Komiyama and Inoue 1980) to render it a rate-limiting step in formation of N(III) from absorbed NO_2 over the time scale of a cloud (~ 1 hr). Recent studies by Lee and Schwartz (1981) support this viewpoint.

Finally, because of the low surface-to-volume ratios of solutions used in laboratory experiments compared to those existing in the atmosphere, even absorption rates measured in laboratory experiments at relatively low NO_2 concentrations can be limited by mass transport. For NO_2 concentrations that exist in the atmosphere (~ 1 to 100 ppb), and for the surface-to-volume ratios of drops characteristic of clouds (~ 3×10^5 m^{-1}), only direct NO_2 adsorption is of any consequence. Thus, the total amount of N(III) in solution derived from NO_2 is governed by the Henry's law constant for NO_2, given in Table 4-13, the equilibrium constant for the liquid-phase analog Equation 4-83 (7.5×10^4 ℓ mol^{-1}; Komiyama and Inoue 1980), and the rate constant for Equation 4-84 (liquid phase). For estimates of N(III) used in Section 4.3.2, we assume a time scale of one-half the total cloud lifetime in determining the amount of N(III) formed from absorbed NO_2. Because of the disproportionation reaction upon solution of NO_2, each mole of NO_2 absorbed produces 1 mole of HNO_3 for each mole of N(III) produced. Therefore, the reaction rates for N(III) oxidation necessary to produce HNO_3 levels rivaling those due to direct absorption, either of NO_2 or HNO_3, are increased to roughly 10^3 hr^{-1} and 2×10^5 hr^{-1} for urban and background atmospheres, respectively.

Of the two oxidation reactions mentioned early in this section, the oxidation of N(III) by O_3 (Penkett 1972) has been studied with direct consideration of atmospheric applicability. The reaction was studied in a stopped-flow reactor, the rate being determined when the O_3 aqueous concentration was

monitored with a UV spectrophotometer at a wavelength of 255 nm. Such devices require reactant concentrations far exceeding atmospheric levels.

For example, the O_3 concentrations Penkett employed were equivalent to gas-phase concentrations of several hundred ppm, 10^3 to 10^4 times atmospheric levels. However, the agreement between the oxidation rate for S(IV) by O_3 measured in this study and that measured by wet-chemical techniques at much lower O_3 levels (Larson et al. 1978) suggests that extrapolation of the N(III) rate to atmospheric levels may be valid. The reaction was found to be first-order in both O_3 and N(III). The second-order rate expression at 283 K and a pH of 5.9 was:

$$-\frac{d[N(III)]}{dt} = -\frac{d[O_3]}{dt} = k_2\,[O_3]\,[N(III)] \qquad [4\text{-}85]$$

with $k_2 = (1.60 \pm 0.13) \times 10^5$ ℓ mol^{-1} s^{-1}. Assuming that the ambient O_3 concentration at cloud level is generally at or below 50 ppb (at STP), the characteristic time[2] for N(III) oxidation at 283 K and a pH of 5.9 would be ~ 2 hr, and the conversion rate (R) 50 percent hr^{-1}.[3] Clearly, this reaction will be of little importance in HNO_3 production.

The oxidation of N(III) in solution by H_2O_2 received attention in several investigations (Halfpenny and Robinson 1952, Anbar and Taube 1954). The rate expression determined by Halfpenny and Robinson over the pH range of ~ 4.3 to 4.7 at a temperature of 292 K was:

$$-\frac{d[H_2O_2]}{dt} = k\,[H_2O_2]\,[HNO_2]\,[H^+] \qquad [4\text{-}86]$$

with $k = 1.4 \times 10^2$ ℓ^2 mol^{-2} s^{-1}. These investigators considered HNO_2 to be the reducing species in solution, although they point out that NO_2^- might still be the reducing agent because of the equilibrium between HNO_2 and NO_2^-. Anbar and Taube, on the other hand, determined the reaction rate by monitoring the concentration of NO_2^- spectrophotometrically at a wavelength of 357 nm and imply that NO_2^- is the reducing agent in the reaction. Their rate expression for pH's from 4.6 to 5.1 at 298 K was:

$$-\frac{d[H_2O_2]}{dt} = \frac{k_3\,k_2\,[H^+]^2\,[NO_2^-]\,[H_2O_2]}{k_{-2} + k_3\,[H_2O_2]} \qquad [4\text{-}87]$$

---

[2]The e^{-1} decay time.

[3]R_i (% of hr^{-1}) = $100 \times \frac{d(\ell \ln C_i)}{dt}$, where C_i is the concentration of the the reactant under consideration. Consequently, R_i (% hr^{-1}) = 100 x k', where k' is the pseudo-first-order rate coefficient.

where the k's are rate constants as defined by Anbar and Taube, $k_3 = 5.8 \times 10^6$ ℓ^3 mol^{-3} s^{-1}, and $k_3/k_{-2} = 2.4$. For atmospheric levels of H_2O_2, this reduces to

$$-\frac{d[H_2O_2]}{dt} = k' [H^+]^2 [NO_2^-] [H_2O_2] \qquad [4\text{-}88]$$

with $k' = 1.4 \times 10^7$ ℓ^3 mol^{-3} s^{-1}.

The rate expression of Anbar and Taube must be converted to one with explicit HNO_2 dependence by means of the NO_2^- - HNO_2 equilibrium to compare this value directly with that of Halfpenny and Robinson. This results in a rate coefficient of 6.3×10^2 ℓ^2 mol^{-2} s^{-1}, roughly 4.5 times that of Halfpenny and Robinson. Given the different experimental temperatures, methodologies, and concentrations of reactants, this may be considered good agreement. However, both experiments were conducted at H_2O_2 concentrations (> 0.05 mol ℓ^{-1}) and N(III) concentrations (> 0.017 mol ℓ^{-1}) far higher than those encountered in the atmosphere. This should be considered when the rates are applied to atmospheric conditions, particularly because no activation energy was determined for the reaction, and the temperatures at which these rates were made were appreciably higher than those typical of clouds over the United States. Nevertheless, the rate determined by Anbar and Taube can be employed as a rough indication of this reaction's importance.

For typical cloud water pH's of 4.0 to 6.0, most of the N(III) in solution will be NO_2^-, and the values of N(III) calculated in Section 4.3.2 will be so interpreted and inserted into the rate expression. Once again, a pH of 5.0 will be selected for the mean cloud water pH. For the H_2O_2 concentration in hydrometeors, a value of 1.5×10^{-5} mol ℓ^{-1} will be employed (based on measurements in precipitation [Kok 1980] and a few, as yet unpublished, measurements in clouds over the eastern United States [Kok, pers. comm.]). Inserting these values into Anbar and Taube's rate expression yields a characteristic time for N(III) oxidation of 1.3×10^4 hr, surprisingly slow. Clearly, this reaction can be of no importance to HNO_3 production in hydrometeors.

The above results support the tentative conclusion reached in Section 4.3.2, i.e., that HNO_3 production in solution by oxidation of N(III) is unimportant compared to direct absorption of this species from the gas phase. Of course, future research may suggest other oxidation reactions appreciably faster than the two that have been suggested to date, or future rate studies may suggest higher rates for these two reactions. Our conclusion concerning the importance of N(III) oxidation to HNO_3 formation in solution is highly dependent on relatively few rate studies, compared to the case for H_2SO_4 production. This dependence should be considered when the influence of HNO_3 on acidic deposition is assessed.

At this juncture, we conclude that HNO_3 concentration in solution generally is determined by HNO_3 production in the gas phase (or possibly on aerosol particles) and its subsequent rate of absorption into hydrometeors.

4.3.5 Production of H_2SO_4 in Solution

4.3.5.1 Evidence from Field Studies--From analyses presented in Section 4.3.2, it appears that H_2SO_4 is the acid most likely to be produced in cloud droplets in significant quantities. Furthermore, field studies show that sulfate (SO_4^{2-}) is produced in clouds. Such evidence has been accumulating for some time, although early data were somewhat indirect. For example, Radke and Hobbs (1969), Saxena et al. (1970), Dinger et al. (1970), and Radke (1970) observed higher concentrations of cloud condensation nuclei (assumed to be mainly sulfates) in evaporating clouds than in ambient air. Georgii (1970) found that while sulfate concentrations decrease with altitude in dry air, they peak at cloud levels in air subject to cloud formation. Similarly, Jost (1974) found anomalously high SO_4^{2-} concentrations in clear, subsiding air near the bases of cumulus clouds--the sample air being considered to have passed through the clouds. McNaughton and Scott (1980) concluded, on the basis of mass balance calculations, that SO_4^{2-} production in clouds is necessary to account for the acidity and SO_4^{2-} levels found in precipitation. Also, recent field results (Lazrus et al. 1983) suggest appreciable sulfate formation in warm frontal clouds. Finally, Gillani and Wilson (1983), in a study of power plant plumes interacting with clouds, present particulate and gaseous S measurements that strongly suggest that SO_4^{2-} production is occurring in clouds. The in-cloud SO_2 to SO_4^{2-} conversion rates observed were on the order of 10 percent hr^{-1}, a significant rate even in light of the analysis in Section 4.3.2, because SO_2 concentrations in power plant plumes were far higher than were values used in Section 4.3.2 and thus could produce considerable acid even if only a relatively small fraction of the SO_2 were converted to H_2SO_4.

The most direct and quantitative evidence for SO_4^{2-} production in clouds has come from recent measurements of SO_4^{2-} concentrations in the air entering and leaving wave clouds (Hegg and Hobbs 1981a,b). These measurements have yielded SO_2-to-SO_4^{2-} conversion rates typically on the order of 10^2 percent hr^{-1}, a significant value according to the analysis of Section 4.3.2. This in situ data set is sufficiently large (18 cases) to allow determination of an empirical rate expression. It is of the form:

$$\frac{d\,[SO_4^{2-}]}{dt} = k_1\,[H^+]^{\alpha}\,[SO_3^{2-}]\,\exp\,(E_A/RT) \qquad [4\text{-}89]$$

where $k_1 = (3.3 \times 10^5 \pm 6.2 \times 10^5)\ \ell^{1.1}\ mol^{-1.1}\ s^{-1}$,
$\alpha = 1.1 \pm 0.1$, and $E_A = (2.9 \pm 2.7)\ kJ\ mol^{-1}$.

Section 4.3.3 shows that the value of α is similar to that expected if the SO_4^{2-} is produced in solution via O_3 oxidation. However, the SO_4^{2-} production rates measured in these field studies showed no significant correlations with O_3 concentrations.

These field measurements dictate examination of H_2SO_4 production in hydrometeors in greater detail than for HCl and HNO_3.

4.3.5.2 Homogeneous Aerobic Oxidation of $SO_2 \cdot H_2O$ to H_2SO_4--

4.3.5.2.1 Uncatalyzed. This reaction is the most extensively studied of any of those to be dealt with. It has been proposed for some time as a reaction of considerable importance in the atmosphere (Scott and Hobbs 1967, McKay, 1971, Miller and de Pena 1972). However, some controversy exists concerning its atmospheric importance. For example, Beilke and Gravenhorst (1978) dismissed this reaction as being of no importance in the atmosphere. However, Hegg and Hobbs (1978) considered it currently impossible to arrive at a firm conclusion as to its importance, due to the wide range of conversion rates and rate expressions measured in the laboratory by different workers (Figure 4-3).

While little has been done to resolve the discrepancies shown in Figure 4.3 and debate continues as to its atmospheric significance (see, for example, Penkett et al. 1979; Dasgupta 1980a,b), Hegg and Hobbs (1979a) employed an updated version of the Easter-Hobbs interactive cloud-chemistry model (Easter and Hobbs 1974) to demonstrate that most of the rates shown in Figure 4-3 would yield significant sulfate concentrations in the atmosphere. These rates will therefore be included in the evaluation of the potential importance of H_2SO_4 production reactions in clouds, although, as pointed out by Hegg and Hobbs (1978), these rate expressions could reflect a low level catalysis of the aerobic reaction rather than a strictly uncatalyzed reaction.

Larson et al.'s (1978) rate expression was chosen to evaluate the significance of this reaction in the atmosphere. This study has been selected because it was conducted with great care. For example, oxidation rates relative to sulfite (SO_3^{2-}) were measured by monitoring SO_3^{2-} (and sometimes sulfate) concentrations, and SO_2 degassing from solution was evaluated quantitatively. Such procedures obviate criticisms made of other laboratory studies of SO_3^{2-} oxidation rates with respect to mass-transport limitation of the oxidation (Kaplan et al. 1981, Schwartz and Freiberg 1981). Similar procedures were employed by Fuller and Crist (1941) and by Brimblecombe and Spedding (1974). Hence, the disparities shown in Figure 4-3 are not entirely due to mass-transport problems.

Because it is unlikely that the reaction is much faster than that measured by Larson et al. (1978) (and it may be appreciably lower due to inhibitors; Hegg and Hobbs 1978), the Larson et al. rate may be considered an upper limit to the atmospheric oxidation rate. The rate expression for this reaction at pH $\leq$ 7.0 is:

$$\frac{d[SO_4^{2-}]}{dt} = (k_1 + k_2 [H^+]^{1/2}) [SO_3^{2-}] \qquad [4\text{-}90]$$

with $k_1 = (4.8 \pm 0.6) \times 10^{-3}$ s^{-1} and

$k_2 = (8.9 \pm 1.0)$ $\ell^{1/2}$ $mol^{-1/2}$ s^{-1}.

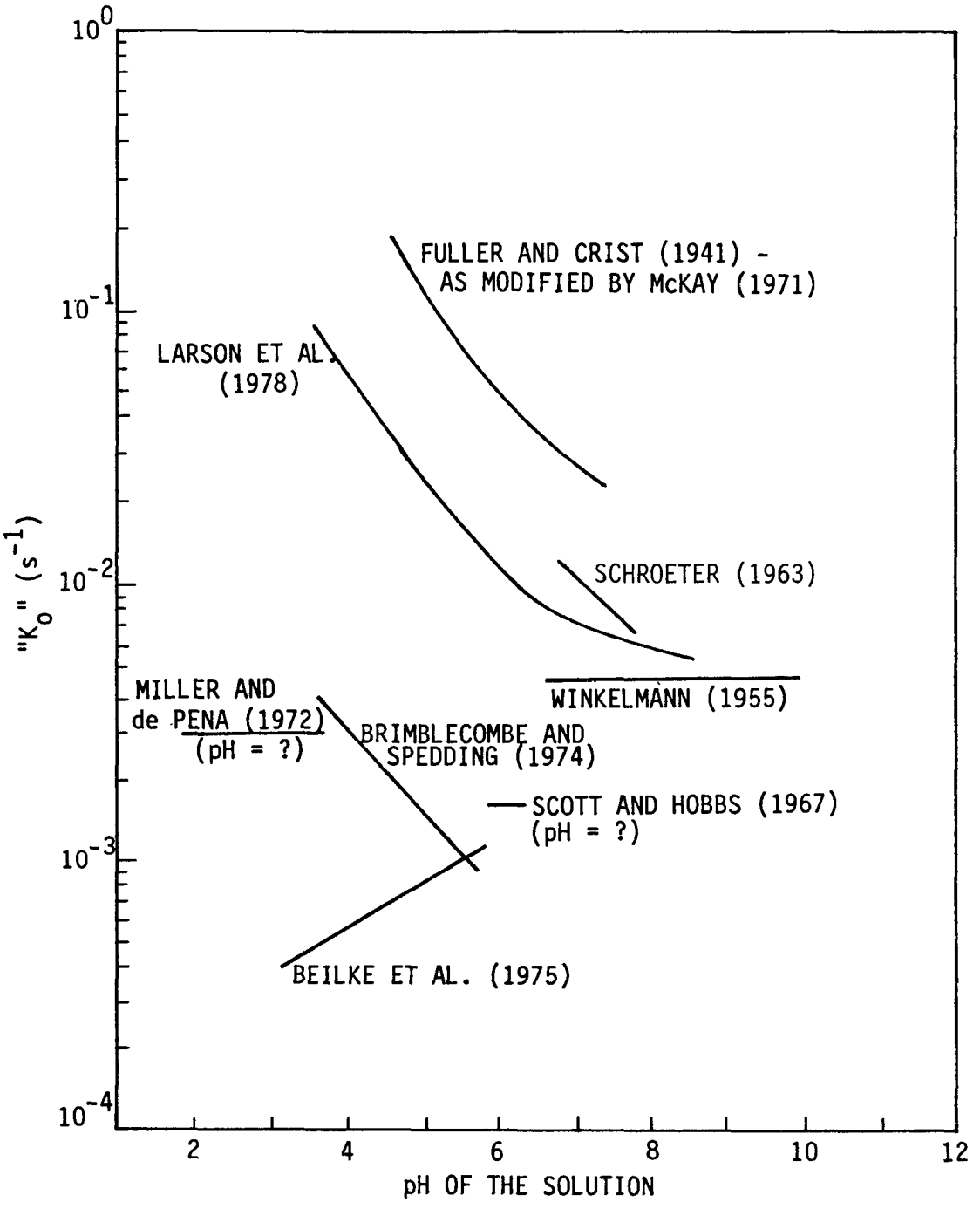

Figure 4-3. Pseudo first-order rate coefficients ("K_o") for the non-catalyzed aerobic oxidation of SO_3^{2-} in solution (Hegg and Hobbs 1978).

Activation energies for these two coefficients are 40 ± 10 kJ mol^{-1} and 7 ± 6 kJ mol^{-1}, respectively. Assuming a hydrometeor pH of 5.0 and a temperature of 278 K (henceforth all rates will be evaluated at this temperature, because it is representative of those encountered in warm clouds), this expression yields a characteristic time for sulfate oxidation of ~ 44 s, implying a conversion rate of ~ 8 x 10^3 percent hr^{-1}.

Before Equation 4-90 and the criterion rate[4] calculated in Section 4.3.2 can be compared, Equation 4-90 must be changed from a SO_3^{2-} to a S(IV) dependence. This change can be done by multiplying the righthand side of Equation 4-90 by the ratio of SO_3^{2-} to S(IV) in solution at the given pH. For a pH of 5.0 at 278 K, this is essentially the ratio of SO_3^{2-} to bisulfite (HSO_3^-) and equals 1 x 10^{-2}. This ratio implies an S(IV) oxidation rate and thus an H_2SO_4 production rate, of 80 percent hr^{-1}. Comparing this to the rates calculated in Section 4.3.2 for significant H_2SO_4 production (50 to 100 percent hr^{-1}), shows that Equation 4-90 can produce significant H_2SO_4 under background atmospheric conditions.

4.3.5.2.2 Catalyzed. The catalyzed aerobic oxidation of S(IV) to H_2SO_4 has received nearly as much laboratory study as has the uncatalyzed reaction. Reviews by Beilke and Gravenhorst (1978) and Hegg and Hobbs (1978) indicate the range of rates measured for such a reaction. However, most of the studies conducted have involved catalyst and reactant concentrations far exceeding those encountered in the atmosphere. Furthermore, Kaplan et al. (1981) and Freiberg and Schwartz (1981) have suggested that in most, if not all, laboratory studies the oxidation rates have been limited by mass transport and are therefore not applicable to the atmosphere. Freiberg and Schwartz specifically cite the study of Barrie and Georgii (1976) as one where mass transport may have compromised measured rates because of the large size of the droplets employed as the reaction medium. However, Freiberg and Schwartz observe that the droplets used by Barrie and Georgii were ventilated at an unspecified rate and that if this rate were high enough, the reaction rate would not have been limited by mass transport. Because Barrie and Georgii's study was conducted with both reactant and catalyst concentrations approaching atmospheric levels, it is worthwhile to attempt to establish whether rates these workers measured accurately reflect the chemical kinetics. This can be done by comparing the rates of Barrie and Georgii with chemical rate data derived from experiments where mass transport definitely did not limit reaction rates.

If one extrapolates the results of Kaplan et al. (1981) for Mn catalysis to the low catalyst levels Barrie and Georgii employed, assuming the reaction rate is first-order in catalyst concentration (Hegg and Hobbs 1978), the rate derived is much slower than what Barrie and Georgii observed. Because Kaplan et al. performed their study under conditions free from mass-transport limitations (according to the theory of Freiberg and Schwartz), the relatively fast rate of Barrie and Georgii must also be considered free of

---

[4]The rate necessary to produce a sulfate concentration similar to that obtainable by direct adsorption of H_2SO_4.

this constraint. Comparison of the Barrie and Georgii rate for Fe catalysis with that of Brimblecombe and Spedding (1974), from which mass-transport effects were eliminated by direct measurement of both S(IV) and S(IV) in solution, again reveals that the Barrie and Georgii rate is the faster of the two.

It may be concluded that the rates measured by Barrie and Georgii were not significantly limited by mass transport and should therefore be applicable to cloud droplets. Reactions in large raindrops, on the other hand, will most likely be limited by mass transport.

Barrie and Georgii (1976) studied three catalysts: Fe, Mn (the two most widely accepted catalysts of atmospheric significance), and an equimolar combination of these two elements. From Table 1 and Figure 2 of their paper, the following rate expressions for these three catalysts have been derived:

$$\text{For Mn:} \quad \frac{d[SO_4^{2-}]}{dt} = k_{Mn}\,[Mn^{+2}]\,[H^+]^{0.46}[SO_3^{2-}] \qquad [4\text{-}91]$$

$$\text{For Fe:} \quad \frac{d[SO_4^{2-}]}{dt} = k_{FE}\,[Fe^{+2}]\,[SO_3^{2-}] \qquad [4\text{-}92]$$

$$\text{For Mn and Fe:} \quad \frac{d[SO_4^{2-}]}{dt} = k_{mix}[Mn^{+2} + Fe^{+2}][H^+]^{0.64}\,[SO_3^{2-}] \qquad [4\text{-}93]$$

with $k_{Mn} = 1.6 \times 10^8\ \ell^{1.46}\ mol^{1.46}\ s^{-1}$, $k_{Fe} = 5.8 \times 10^6\ \ell\ mol^{-1}\ s^{-1}$, and $k_{mix} = 1.8 \times 10^9\ \ell^{1.64}\ mol^{1.64}\ s^{-1}$, all at 298 K.

The activation energies were not determined explicitly in this study, but the data shown are in accord with previous determinations of the activation energies of the Mn- and Fe-catalyzed reactions (~ 113 and ~ 126 kJ mol^{-1}, respectively; Hegg and Hobbs 1978). The Mn plus Fe catalyst not only showed a synergistic effect relative to individual catalysts, but also displayed negligible temperature dependence. The catalyst therefore could be of considerable importance, at least in an urban atmosphere. The relatively large temperature dependence of the two single metal catalysts, on the other hand, somewhat decreases their potential atmospheric importance.[5]

---

[5]The cited activation energy for the Mn reactions for example, lowers the given rate coefficient for this reaction to $6 \times 10^6\ \ell^{1.46}\ mol^{-1.46}\ s^{-1}$ at a temperature of 278 K, a reasonable temperature for clouds. In general, the relationship between activation energy and rate coefficient, which determines the temperature sensitivity of a rate expression, is given by the Arrhenius equation: $k_j = A_j \exp\{-E_j/RT\}$, where k_j is the rate the rate coefficient with activation energy E_j, and A_j is a constant determinable from measurements at several temperatures.

The major problem in evaluating the significance of catalyzed reactions in the atmosphere is in estimating concentrations of possible catalysts in the atmospheric hydrometeors. Assume the maximum concentrations of Mn and Fe in urban air to be ~ 0.2 and ~ 6 $\mu g\ m^{-3}$, respectively (Miller et al. 1972, Lee and von Lehmden 1973, McDonald and Duncan 1979, Lewis and Macias 1980). The soluble fractions for the Mn and Fe species found in the atmosphere are ~ 0.25 and 0.15 percent, respectively (Gordon et al. 1975). For a liquid water content of ~ 0.5 g m^{-3}, these figures yield cloud water concentrations of ~ 2 x 10^{-8} mol ℓ^{-1} of Mn and ~ 3 x 10^{-7} mol ℓ^{-1} of Fe, with perhaps an order of magnitude of uncertainty in these values. These values compare reasonably well with the maximum levels of Mn and Fe found in Florida rainwater, which are reported to be 6 x 10^{-8} mol ℓ^{-1} of Mn and 4 x 10^{-7} mol ℓ^{-1} of Fe (Tanaka et al. 1980). However, these values are somewhat lower than rainwater concentrations reported by Liljestrand and Morgan (1981) for southern California (Mn: ~ 2 x 10^{-7} mol ℓ^{-1}; Fe: ~ 10^{-6} mol ℓ^{-1} and by Drozdova and Makhon'ko (1970) for the Soviet Union (Mn: ~ 5 x 10^{-7} mol ℓ^{-1}; Fe: ~ 10^{-6} mol ℓ^{-1}). On this basis, and assuming some variability in liquid water content, upper limits for Mn and Fe of ~ 10^{-6} mol ℓ^{-1} will be assumed. The dependence of these rates on cloud liquid water content are examined later. Employing these concentrations at a temperature of 278 K and pH of 5.0, yields characteristic oxidation times for S(IV) of: 0.93 hr (Mn), 0.19 hr (Fe), and 0.01 hr (Mn + Fe). The corresponding conversion rates are ~ 100 percent hr^{-1} (Mn), 500 percent hr^{-1} (Fe), and ~ 5 x 10^3 percent hr^{-1} (Mn + Fe). These values certainly suggest that the catalyzed reaction will be considerably important, at least in urban air. However, a word of caution is required.

It is not clear that the Mn rate or the mixed catalyst rate Barrie and Georgii (1976) measured can be extrapolated to the atmospheric case. Barrie and Georgii observed negligible oxidation with 10^{-6} mol ℓ^{-1} of Mn as a catalyst. No clear evidence shows that the mixed catalyst effect occurs at concentrations below 10^{-5} mol ℓ^{-1}. Furthermore, these estimates have yielded rates that produce substantial H_2SO_4 in solution relative to initial concentrations of H_2SO_4. One would therefore expect the solution pH to drop substantially. Given the inverse square dependence on H^+ concentration of the SO_3^{2-} concentration in solution, the rate expressions for the catalyzed (and the uncatalyzed as well) reactions suggest they may be self limiting in hydrometeors. Hence, the rates calculated above from the characteristic times, based on initial pH's, will be upper limits to the time-average rates. Finally, the mixed catalyst rate is so fast that it will be almost certainly limited by mass transport, even in raindrops of modest size, as suggested by Freiberg and Schwartz (1981).

4.3.5.3 Homogeneous Non-aerobic Oxidation of $SO_2 \cdot H_2O$ to H_2SO_4--SO_2 absorbed into atmospheric hydrometeors can be oxidized by oxidants other than O_2. Indeed, recent work on H_2SO_4 production in clouds and rain has tended to emphasize the oxidation rates by O_3 and H_2O_2 (Penkett et al. 1979, Durham et al. 1981). Recently, interest has also revived in the classic reaction involving SO_3^{2-} oxidation by N(III) in solution

(Martin et al. 1981, Chang et al. 1981). Of these three oxidants, O_3 has been the most widely studied and will therefore be examined first.

The relevance of O_3 to SO_4^{2-} formation in hydrometeors was first examined by Penkett (1972), who studied SO_3^{2-} oxidation by O_3 in a stopped-flow reactor at a solution pH of 4.65 and a temperature of 283 K, values representative of the atmosphere. However, the reactant concentrations employed were far higher than those encountered in the atmosphere. More recently, several other studies have been conducted on the O_3 reaction with reactant concentrations closer to those in the atmosphere. These studies are summarized in Table 4-15. The study by Penkett et al. (1979) contains a number of errors in the derived rate expression. It is therefore preferable to show the rate expression derived by Dasgupta (1980a) from the data of Penkett et al. However, the rate for atmospheric conditions (last column in Table 4-15) is that directly measured by Penkett et al.

Examination of rates shown in Table 4-15 suggests nearly as much uncertainty about the O_3 oxidation rate as for uncatalyzed aerobic oxidation. Rates tend to increase as the ratio of O_3 to S(IV) in solution increases, suggesting that oxidation rates measured in the laboratory were limited by mass transport of O_3. However, O_3 concentrations in solution were measured directly in experiments of Penkett et al., thus precluding any limitations due to mass transport. In any case, the mole ratios of O_3 to S(IV) used in the studies with the higher derived rates are far above atmospheric values ($\sim 10^{-4}$). Because the rates derived for atmospheric conditions from measurements of Penkett (1972) and Larson et al. (1978) differ only by a factor of 3, despite extrapolations over several orders of magnitude in reactant concentrations, the higher of the two rates (Penkett 1972) has been selected to estimate the importance of this reaction in H_2SO_4 production in hydrometeors. While the relatively conservative nature (compared to the upper end of the range in rates given in Table 4-15) of this estimate should be considered, Hegg and Hobbs's (1981b) observations discussed in Section 4.3.5.1 cast doubt on the applicability to the atmosphere of the higher rates shown in Table 4-15.

Table 4-15 shows that the characteristic time for S(IV) oxidation is ~ 1 hr for the Penkett rate, and the conversion rate is ~100 percent hr^{-1}, which should be significant in the atmosphere.[6]

It has been proposed (Penkett et al. 1979) that the O_3 reaction mechanism is a free-radical chain, similar to that of the O_2 oxidation reaction. If so, like the aerobic oxidation, it should be both catalyzed and inhibited by certain trace metals and organics in solution (Hegg and Hobbs 1978). Interestingly, Barrie and Georgii (1976) reported a substantial enhancement

---

[6]The characteristic or e^{-1} folding time is given by $\frac{1}{(S(IV)}\frac{d\,S(IV)^{-1}}{dt}$; in the atmospheric pH range of ~ 3 to 6, $HSO_4^- \simeq$ S(IV) and this becomes: $\frac{1}{[HSO_3^-]}\frac{d\,S(IV)^{-1}}{dt} = \{K_1[O_3]^{-1}\}$.

TABLE 4-15. LABORATORY STUDIES OF S(IV) OXIDATION BY O_3 IN AQUEOUS SOLUTION

	Rate expression	Experimental pH	Molar ratio of reactants $[O_3]/[S(IV)]$	Reaction rate[a] (in mol ℓ^{-1} s^{-1}) at 278 K, 1 ppb SO_2 40 ppb O_3, and a pH of 5.0
Penkett (1972)	$k_1[O_3][HSO_3^-]$ $k_1 = 3.3 \times 10^5$ ℓ mol^{-1} s^{-1} at 283 K	4.65	0.03 - 0.5	1.5×10^{-9}
Barrie (1975)	--	4.0	10^{-6}-5×10^{-5}	5×10^{-11}[b]
Erickson et al. (1977)	$k_2[O_3][HSO_3^-] + k_3$ $[O_3][SO_3^{2-}]$ $k_2 = 3.1 \times 10^5$ ℓ mol^{-1} s^{-1} $k_3 = 2.2 \times 10^9$ ℓ mol^{-1} s^{-1} at 298 K	-1.3 - 4.02	5 - 50	2×10^{-7}
Larson et al. (1978)	$k_4[O_3][HSO_3^-]$ $[H^+]^{-0.1}$ $k_4 = 4.4 \times 10^4$ $\ell^{0.9}$ $mol^{-0.9}$ s^{-1} at 298 K	4.0 - 6.2	6×10^{-4} -2×10^{-3}	5×10^{-10}
Penkett et al. (1979) as modified by Dasgupta (1980a)	$k_2[O_3][HSO_3^-] + K_3$ $[O_3][SO_3^{2-}]$ $k_2 = 3.73 \times 10^5$ ℓ mol^{-1} s^{-1} $k_3 = 3.12 \times 10^8$ ℓ mol^{-1} s^{-1} at 298 K	1 - 5	0.1 - 0.4	6.6×10^{-9}

[a]Shows derived rates for atmospheric conditions.

[b]The measured rate at pH = 4 and 283 K was converted to that at pH = 5 and 278 K by assuming that the rate is proportional to $[HSO_3^-]$, and changes negligibly with temperatures over 5 K.

in sulfite oxidation rate by O_3 when Mn ions were present at roughly 10^{-5} mol ℓ^{-1}. However, no data or discussion of this result was given, and only recently has a study of the catalyzed O_3 reaction appeared in the literature. This study, by Harrison et al. (1982), found that Mn and Fe on the order of 10^{-5} mol ℓ^{-1} enhance the oxidation rate, though over a relatively narrow pH range centered at ~ 4.4. The maximum enhancement is roughly a factor of 2 for Fe and about 5 for Mn. Given the large uncertainty in the uncatalyzed O_3 rate, and that at a pH of 5.0 the Mn and Fe enhancements were negligible for Fe and about a factor of 3 for Mn at the high concentration of 10^{-5} mol ℓ^{-1}, this rate will be considered indistinguishable from the uncatalyzed rate already discussed.

Oxidation by H_2O_2 has only recently been considered important for acid production in hydrometeors. While early laboratory work on this reaction was done by Mader (1958), the first study relevant to the atmosphere was reported by Hoffmann and Edwards (1975). Penkett et al.'s (1979) study essentially repeated the study of Hoffmann and Edwards, with explicit extrapolation to atmospheric conditions. Martin and Damschen (1981) have attempted to integrate all extant measurements on the reaction within the framework of the nucleophilic displacement mechanism, first advocated by Hoffmann and Edwards. While this approach has the advantage of producing both a simple and widely applicable rate expression, it is not yet clear whether all the objections Dasgupta (1980a,b) raised to the Hoffmann and Edwards mechanism have been met. However, from the point of view of this document, details of the mechanism are unimportant as long as a rate expression is available that can plausibly be applied to the atmosphere. In this regard, the relatively simple rate expression derived by Martin and Damschen (1981) is adequate and appealing. It is

$$\frac{d[SO_4]}{dt} = k\,[H_2O_2]\,[SO_2 \cdot H_2O] \qquad [4\text{-}94]$$

with $k = 8.3 \times 10^5$ ℓ mol^{-1} s^{-1} at 298 K and an activation energy of ~ 28 kJ mol^{-1}.

This expression is independent of pH for a constant SO_2 partial pressure. However, as the pH of the solution increases, less and less S(IV) in solution will be in the form of $SO_2 \cdot H_2O$. Thus, the effective S(IV) oxidation rate decreases rapidly with increasing pH.

Before the above rate expression is employed, the H_2O_2 concentration to be used must be determined. Many recent calculations of the importance of the H_2O_2 oxidation reaction have employed gas-phase H_2O_2 concentrations of 1 ppb or greater (based on actual measurements) and a value of the H_2O_2 Henry's law constant, based on H_2O_2 vapor pressure data (Scatchard et al. 1952) taken under conditions far removed from atmospheric. While the rather careful extrapolations on such data appear plausible, they cannot be applied directly to atmospheric conditions. For example, Martin and Damschen calculate a value for the Henry's law constant of 6.07×10^5 mol ℓ^{-1} at 273 K. At 273 K, 1×10^{-9} atm H_2O_2 is equivalent to

4.46×10^{-8} mol m^{-3} of H_2O_2. For a cloud water content of 0.5 g m^{-3}, and assuming all of the H_2O_2 goes into solution, the resultant concentration would be only 8.9×10^{-5} mol ℓ^{-1}, close to an order of magnitude less than the concentration predicted by the Henry's law constant. Hence, as was the case for several of the strong acids, the H_2O_2 concentration in solution cannot be based on Henry's law equilibrium. Furthermore, H_2O_2 is reactive in solution with a variety of organic and inorganic species (Ardon 1965) that could rapidly deplete it without producing acid. Kok (1980) found concentrations of H_2O_2 in precipitation considerably lower than those predicted for Henry's law equilibrium. Because of this uncertainty in the value of the H_2O_2 concentration in hydrometeors derived from gas-phase measurements, values derived from direct measurements of this species in rain and cloud water (Kok 1980, pers. comm.) will be employed. The value selected is 0.5 ppm or $\sim 1.5 \times 10^{-5}$ mol ℓ^{-1}. Employing this value in the Martin and Damschen rate expression for atmospheric conditions results in a characteristic time with respect to S(IV) oxidation of 0.14 hr at a pH of 5.0, which yields a highly significant conversion rate of 700 percent hr^{-1}. Indeed, this rate is high enough that limitations due to mass transport are likely to be important for larger hydrometeors.

The last oxidant considered in this section is N(III) (i.e., either NO_2^- or HNO_2 in solution). The reaction(s) between N(III) and S(IV) species in solution has been known for many years because it was integral to the old lead-chamber process for producing H_2SO_4 (Duecker and West 1959, Schroeter 1966) and remains considerably important in flue-gas scrubbing technology (Takeuchi et al. 1977). Because NO_x's and SO_2 commonly coexist in polluted air, several recent studies have attempted to evaluate the possibility of a significant aqueous reaction between these two species (Nash 1979, Chang et al. 1981). Oblath et al. (1981) and Martin et al. (1981) have presented explicit rate expressions they use to evaluate the reaction's significance in the atmosphere. The Oblath et al. study contains considerably more information on the conversion mechanism. Furthermore, it was conducted in the pH range of 4.5 to 7.0, whereas Martin et al.'s was conducted at pH's less than 3.0. On the other hand, the sulfite and nitrite concentrations employed by Martin et al. were closer to atmospheric levels than were those used by Oblath et al. Also, Martin et al.'s rate expression is relatively simple and easily applied to atmospheric conditions. In any case, the two rates agree within a factor of 3 at pH's near atmospheric. Therefore, Martin et al.'s expression will be employed as a significance test. This expression is:

$$\frac{d[SO_4^{2-}]}{dt} = k_1[H^+]^{1/2}\{[HNO_2] + [NO_2]\}\{[SO_2 \cdot H_2O] + [HSO_3]\} \qquad [4\text{-}95]$$

with $k_1 = 142\ \ell^{3/2}\ mol^{-3/2}\ s^{-1}$ at 298 K. No activation energy was determined by Martin et al. (nor by Oblath et al. for atmospheric conditions); it will be assumed to be negligible. Employing this rate expression with the appropriate values of N(III) from Section 4.3.2 yields a characteristic time with respect to oxidation of S(IV) of 70 hr for urban

conditions. This reaction's importance to the H_2SO_4 production in hydrometeors is therefore negligible.

Finally, we note that, based on their interpretation of the data of Takeuchi et al. (1977), Schwartz and White (1982) have suggested that aqueous NO_2 may oxidize S(IV) at a significant rate under somewhat polluted conditions. However, more work must be carried out on this reaction before its atmospheric significance can be assessed.

In closing this section, it should be noted that aerobic oxidation of sulfite is subject to inhibition by numerous atmospheric constituents (Hegg and Hobbs 1978). Presumably, the same will be true of the O_3 reaction, if it is in fact produced by a free-radical chain mechanism. Furthermore, both O_3 and H_2O_2 are highly reactive in water and can suffer either catalytically or photochemically induced decay. The rates discussed do not account for such inhibition or decay. Therefore, in some cases these rates may overestimate those in the atmosphere.

4.3.5.4 Heterogeneous Production of H_2SO_4 in Solution--Few heterogeneous reactions in solution have been proposed for H_2SO_4 production. The only such reaction that has been studied extensively is the oxidation of S(IV) on graphitic carbon suspended in solution (Brodzinsky et al. 1980, Chang et al. 1981). Before this reaction is discussed in detail, heterogeneous reactions involving metal oxides are discussed briefly, prompted by the fact that many trace metal catalysts commonly invoked for homogeneous oxidation of SO_3^{2-} occur in relatively insoluble form in the atmosphere. Heterogeneous oxidation processes involving trace metals could therefore be of some importance. Certainly, gas-solid heterogeneous reactions involving trace metals are treated extensively in the literature on atmospheric SO_4^{2-} production (Urone et al. 1968). However, in solution, only one such reaction appears to have been examined: the study by Bassett and Parker (1951) of the oxidation of SO_3^{2-} to H_2SO_4 by various oxides of Mn. While not a quantitative rate study, this work suggests that substantial H_2SO_4 can be produced by this reaction relative to aerobic oxidation, at least for high concentrations of metal oxides.

Recent modeling studies of the heterogeneous carbon-sulfite reaction have concluded that this reaction may play an important role in sulfate production in water films on atmospheric particles (Middleton et al. 1980, Chang et al. 1981). Both studies emphasize that the reaction would require quite low pH solutions and a long reaction time to be competitive with other sulfate production mechanisms. The rate expression of Brodzinsky et al. (1980) is employed to evaluate the significance of this reaction for H_2SO_4 production in atmospheric hydrometeors:

$$\frac{dS(IV)}{dt} = k\,[C_x]\,[O_2]^{0.69}\,\frac{\alpha\,[S(IV)^2]}{(1 + \beta\,[S(IV)] + \alpha\,[S(IV)]^2)} \qquad [4\text{-}96]$$

where $k = 1.69 \times 10^{-5}$ mol$^{.03}$ $\ell^{0.69}$ g^{-1} s^{-1}, $\alpha = 1.50 \times 10^{12}$ ℓ^2 mol^{-2}, $\beta = 3.06 \times 10^6$ ℓ ml^{-1}, $[C_x]$ = grams of carbon per

liter, and $[O_2]$ and [S(IV)] are in molar concentrations. The activation energy of the reaction is given as 48 kJ mol^{-1}.

It should be noted that the graphitic carbon used to derive Equation 4-96 was Nuchar C-190, a commercial product with a well-characterized elemental composition and BET surface area (550 m^2 g^{-1}). However, soot generated in various combustion processes (i.e., combustion of acetylene, natural gas, and oil) was also employed. Chang et al. (1981) report an average Arrhenius factor five times larger for these soots than for Nuchar-90. This higher value will be employed in these calculations. Another novelty concerning Equation 4-96 is that it is nonlinear in [S(IV)] and therefore has characteristic times that are functions of the concentration of S(IV). Finally, use of Equation 4-96 requires an estimate of the graphitic carbon concentration in hydrometeors. A recent direct measurement of elemental carbon in rainwater collected in Seattle that was 2.4×10^{-4} g ℓ^{-1} (Ogren 1980) has been employed. All of the elemental carbon is assumed to act as an efficient catalyst.

Assuming a temperature of 278 K, a cloud water pH of 5.0, and an urban S(IV) concentration in solution of 7.9×10^{-5} mol ℓ^{-1}, the rate expression of Brodzinsky et al. yields a characteristic time for S(IV) oxidation of $\sim 10^3$ hr. Therefore, this reaction should be of little importance in H_2SO_4 production in precipitation, although it might be important in fogs of low liquid water content in urban areas.

4.3.5.5 The Relative Importance of the Various H_2SO_4 Production Mechanisms--In sharp contrast to HCl and HNO_3 production in hydrometeors, numerous reactions are capable of producing significant levels of H_2SO_4 in solution. It is therefore important to assess the relative magnitudes of these reactions under differing atmospheric conditions. To do this, two relatively extreme cases that can produce precipitation are considered.

Much has been made of production of acid in mists and fogs, which is of some importance from the standpoint of SO_4^{2-} production in the atmosphere. However, it is of little consequence to acidic deposition because even a modestly precipitating cloud will deposit far more acid on the ground than will a fog. As an example of a "polluted" case, a low-lying stratus cloud in urban air with a liquid water content of ~ 0.1 g m^{-3} (about the lowest liquid water content that can produce precipitation in a warm cloud) is considered. H_2SO_4 production by O_2 (catalyzed and uncatalyzed), by O_3, and by H_2O_2 oxidation of S(IV) in solution is considered. Values of the various parameters to be employed are given in Table 4-16. The value for the partial pressure of O_3 is based on numerous measurements in urban air, the concentration of H_2O_2 is derived from Kok's (1980) measurements, and the cloud water pH range is based on measurements reviewed by Falconer and Falconer (1979). The mechanisms considered have different pH dependencies, so the production rates over the pH range of polluted clouds must be considered.

Figure 4-4 plots the production rates for the various oxidants. The H_2O_2 reaction dominates H_2SO_4 production in polluted clouds, with the possible

TABLE 4-16. VALUES OF PARAMETERS USED TO ESTIMATE H_2SO_4 PRODUCTION IN A POLLUTED CLOUD

Parameter	Value
Partial pressure of H_2SO_4	1 ppb
Partial pressure of SO_2	50 ppb
Temperature	288 K
Cloud liquid water content	0.1 g m^{-3}
pH of cloud water	3.5 - 4.5
Partial pressure of O_3	100 ppb
Concentration of H_2O_2	4.7×10^{-5} mol ℓ^{-1}
Concentration of Mn	10^{-6} mol ℓ^{-1}
Concentration of Fe	10^{-6} mol ℓ^{-1}

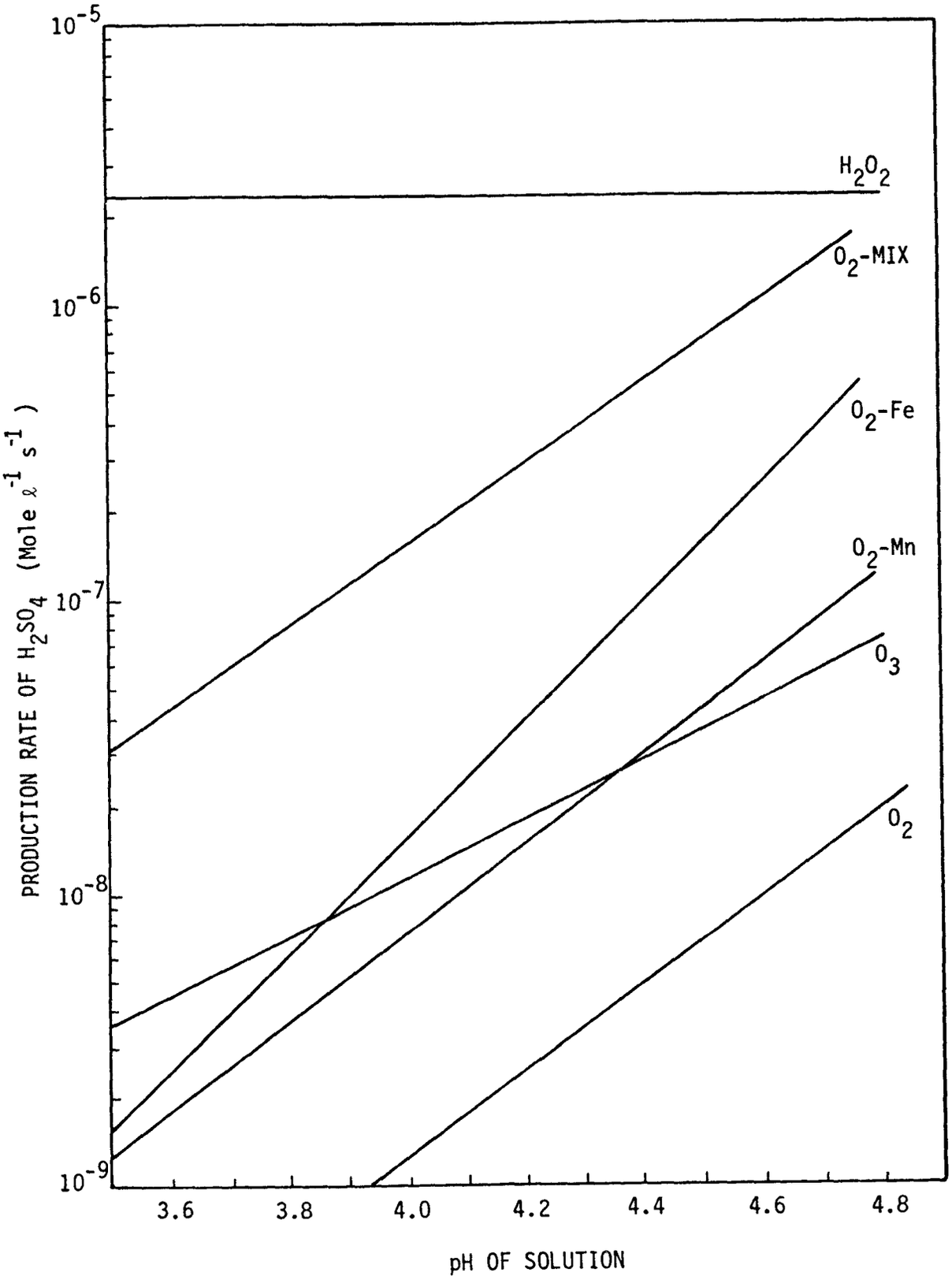

Figure 4-4. H_2SO_4 production rates for various oxidants over the pH range of polluted clouds.

exception of the upper end of the pH range (where the rather speculative mixed-catalyst rate becomes comparable to that of H_2O_2).

We next consider a more typical mid-level cloud (at the ~ 800-mb pressure level) with a more substantial liquid water content of ~ 1 g m^{-3}, situated in a moderately industrial region. The parameter values used in this case are listed in Table 4-17. The pH range is again derived from Falconer and Falconer (1979) and the H_2O_2 concentrations from rainwater measurements by Kok (1980). The metal concentrations were estimated by employing typical (rather than peak) metal concentrations in clear air, divided by the cloud liquid water content given in Table 4-17, using the same percent solubilities as previously employed. The resultant low metal concentrations preclude consideration of catalytic oxidation by Mn or Mn plus Fe. Because some experimental support exists for Fe-catalyzed oxidation at these levels (Brimblecombe and Spedding 1974), it is considered here.

Figure 4-5 plots the rates for the oxidants considered. While the H_2O_2 reaction again appears to be the single most important reaction over much of the pH range, the most striking result revealed by Figure 4-5 is that all of the oxidants can contribute significantly to H_2SO_4 production above a pH of ~ 5.2. Of course, this result is quite sensitive to the concentration of H_2O_2 employed; further data on this important parameter would be highly desirable. Nevertheless, it is important to note that, on the basis of available field data and rate studies, no one oxidant dominates H_2SO_4 production in all atmospheric situations.

Another important point that can be addressed with the aid of Figures 4-4 and 4-5 is the time scale for acid produced in solution to reach the concentrations produced by direct absorption of gases into cloud drops. This question was approached in the derivation of the S(IV) conversion rates necessary to produce significant acid in solution. However, Figures 4-4 and 4-5 allow a more precise estimate.

The maximum concentration of directly absorbed H_2SO_4 in an urban polluted cloud should be ~ 4.2×10^{-4} mol ℓ^{-1} (based on the H_2SO_4 and cloud water concentrations in Table 4-16, 1 ppb and 0.1 g m^{-3}, respectively). For a mid-level cloud, the maximum H_2SO_4 concentration should be 4.4×10^{-6} mol ℓ^{-1} (based on the values for H_2SO_4 and cloudwater in Table 4-17: 0.1 ppb and 1 g m^{-3}, respectively). These concentrations would be reached by the H_2O_2 reaction alone in ~ 3 min for both urban and mid-level clouds if the H_2O_2 were undepleted. With depletion, the time dependence of H_2SO_4 production is more complex, which is shown in Figures 4-6 and 4-7 for the urban and mid-level clouds. For an urban cloud (Figure 4-6), H_2SO_4 production is dominated by H_2O_2 oxidation until the H_2O_2 is completely depleted after about 2 min. Thereafter, H_2SO_4 production is maintained by catalyzed aerobic oxidation at a much slower rate (solution pH is assumed to be 4.0). Indeed, it would take roughly 41 min for the H_2SO_4 produced in solution to reach the concentration of the H_2SO_4 directly absorbed. In a mid-level cloud (Figure 4-7), the H_2O_2 concentration, even with depletion, is sufficient to produce concentrations of H_2SO_4 equal to those produced by direct absorption in about 4.5 min. However, if the solution pH is assumed to be in the upper half of the

TABLE 4-17. VALUES OF PARAMETERS USED TO ESTIMATE H_2SO_4 PRODUCTION IN A MID-LEVEL CLOUD

Parameter	Value
Partial pressure of H_2SO_4	0.1 ppb
Partial pressure of SO_2	5 ppb
Temperature	278 K
Cloud liquid water content	1 g m^{-3}
pH of cloud water	4.5 - 6.0
Partial pressure of O_3	40 ppb
Concentration of H_2O_2	5.9×10^{-6} mol ℓ^{-1}
Concentration of Mn	2×10^{-9} mol ℓ^{-1}
Concentration of Fe	3.3×10^{-8} mol ℓ^{-1}

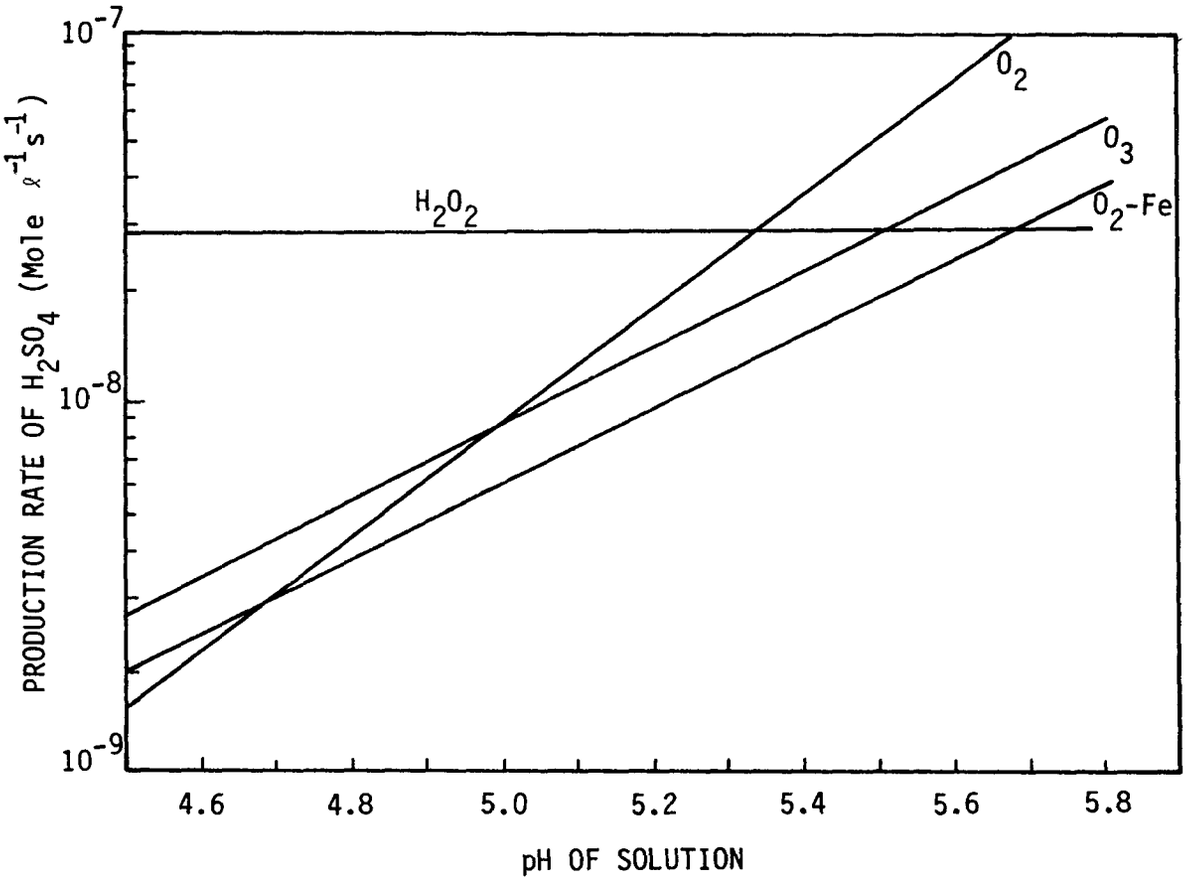

Figure 4-5. H_2SO_4 production rates for various oxidants over the pH range of mid-level clouds.

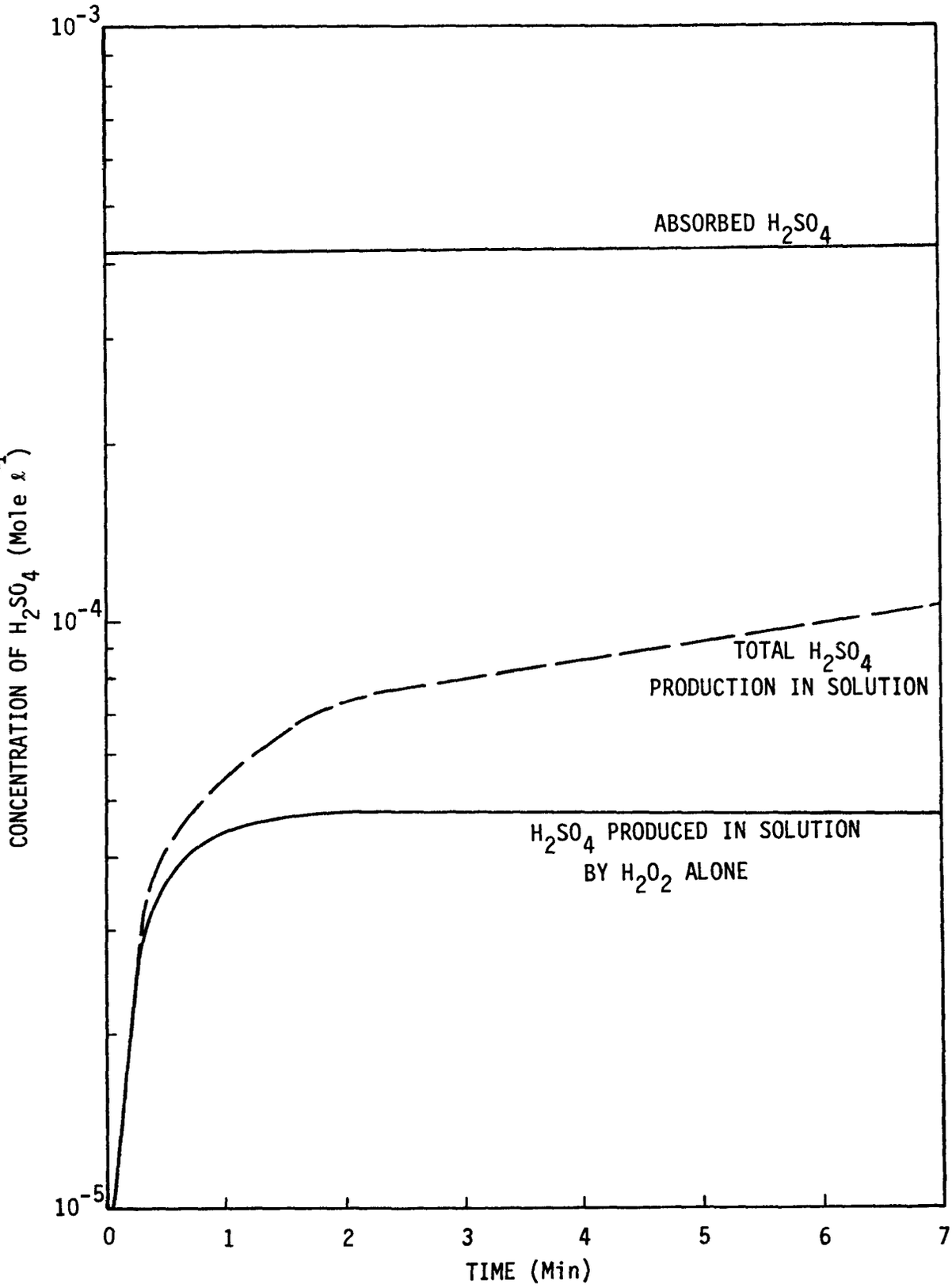

Figure 4-6. Time dependence of H_2SO_4 production in an urban polluted cloud (cloud water pH = 4.0).

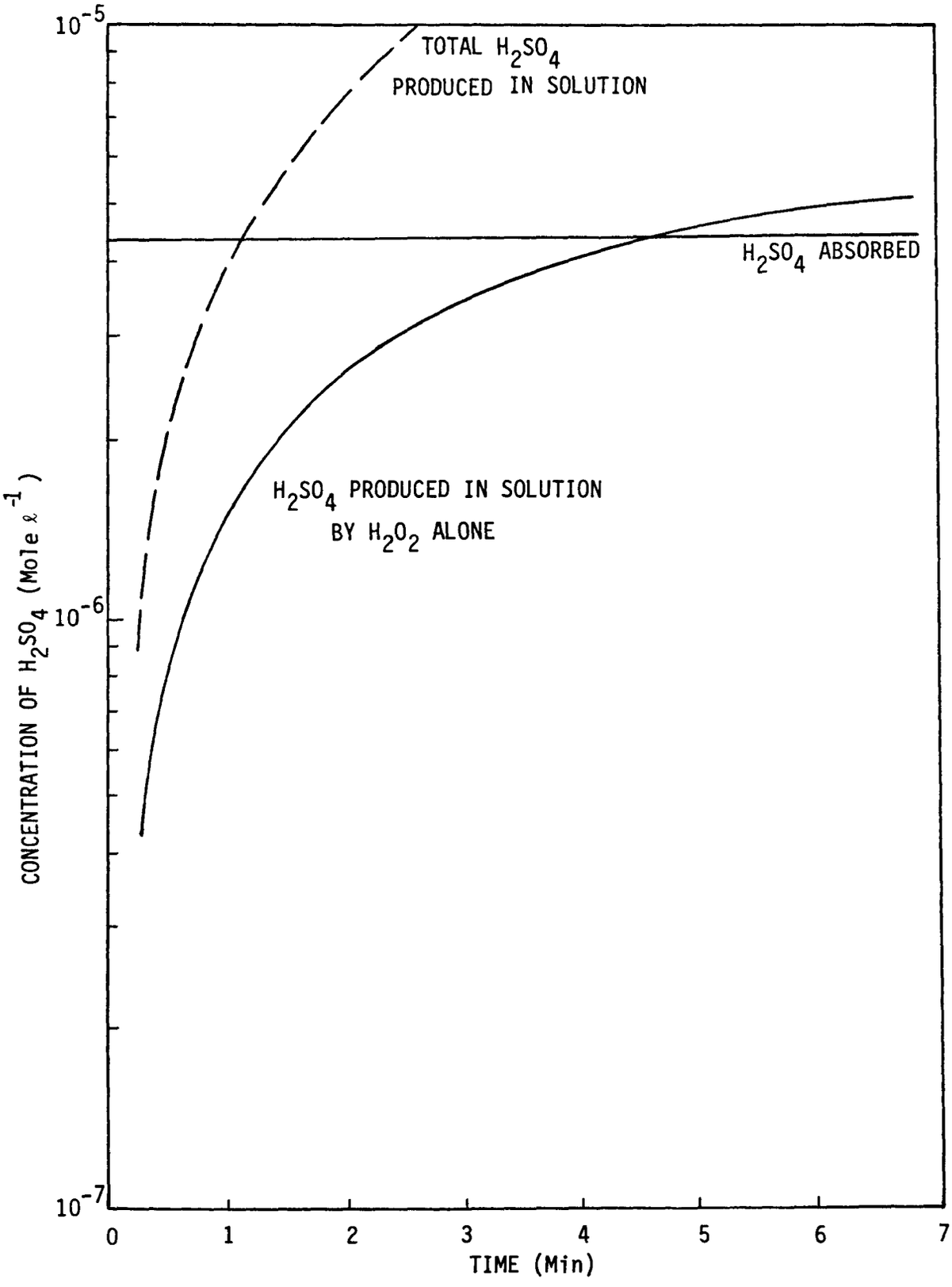

Figure 4-7. Time dependence of H_2SO_4 production in a mid-level cloud (cloud water pH = 5.3).

range listed in Table 4-17, oxidation by O_2 and O_3 produces sufficient additional H_2SO_4 to reduce this time to ~ 1 min. These results suggest that not only the rate, but also the pH dependence of the H_2SO_4 production in solution, will depend on the H_2O_2 concentration and the pH, because these two parameters determine how much of the H_2SO_4 produced in solution is due to the non-pH-dependent H_2O_2 reaction and how much to the other highly pH-dependent reactions.

One final point is suggested by Figures 4-6 and 4-7. The rates shown in these figures produce substantial quantities of acid in a relatively short time. Furthermore, a major component of this production is a pH-independent reaction (H_2O_2 oxidation) that will not be self-limiting in the usual sense of the term. If absorbed concentrations of H_2SO_4, HNO_3, and HCl are considered as well, within a few minutes of cloud formation, cloud water pH's in urban air might be expected to reach a value of 2.0 or even lower. Because such low pH's are not observed and because the anion levels predicted by direct absorption and the rates shown in Figures 4-5 and 4-6 are similar to those observed in urban precipitation (Larson et al. 1975, Liljestrand and Morgan 1981), acid neutralization must play a role.

4.3.6 Neutralization Reactions

4.3.6.1 Neutralization by NH_3--Probably the most important single neutralization process in the atmosphere is the absorption-hydration of NH_3 by acid aerosols and hydrometeors and, in the case of hydrometeors, the subsequent dissociation reaction

$$[NH_3]_{gas} + [H_2O]_{liq} = [NH_4OH]$$

$$[NH_4OH] = [NH_4^+] + [OH^-]. \qquad [4\text{-}97]$$

The preeminence of this neutralization process arises because NH_3 is the only basic gas of widespread, substantial occurrence in the atmosphere. The hydration and dissociation reactions are generally assumed to be fast compared to acid production reactions in solution (Scott and Hobbs 1967, Beilke and Gravenhorst 1978). Therefore, the concentration of NH_3 (and OH^-) consequently is given by the equilibrium expressions for NH_3 absorption and dissociation in solution.

This appears to be the case even for the fastest of the reactions shown in Figures 4-3 and 4-4. For example, the H_2O_2 reaction in urban air produces ~ 2.3×10^{-6} mol ℓ^{-1} s^{-1} of H_2SO_4, or 9.6×10^{-18} mol s^{-1} in a 10 μm radius droplet. If a background concentration of NH_3 of 1 ppb (Levine et al. 1980) is assumed, the rate of NH_3 scavenging due to collisions with a 10 μm droplet will be 8.25×10^{-15} mol s^{-1}.

Recent work by Huntzicker et al. (1980) suggests that the reaction coefficient for the collisions will be close to unity for acidic droplets 10 μm in radius. In this case, the collision frequency becomes the rate of NH_3 delivery to the droplet. The NH_3 is hydrated virtually instantly in solution, and the product ammonium hydroxide (NH_4OH) dissociates with a

rate constant of $k_d = 6 \times 10^5$ s^{-1} (Eigen 1967). Thus, after ~ 10-6 s, the rate of OH^- production equals the collision frequency and NH3 neutralization will not be transport limited. It is therefore possible to estimate the NH_4^+ concentration (and the associated OH^- concentration) in solution from equilibrium considerations, even for these fast reactions.

When the equilibria are employed for an NH_3 solution, NH_4OH dissociation and water dissociation, the concentration of NH_4^+ in solution is given by

$$[NH_4^+] = \frac{H_a P_a K_a [H^+]}{K_w} \qquad [4\text{-}98]$$

where P_a is the partial pressure of NH_3, H_a the Henry's Law constant for NH_3, and K_a and K_w the equilibrium constants for NH_4OH and H_2O dissociation, respectively.

Recent measurements of ambient NH_3 concentrations range from 0.5 to 25 ppb (McClenny and Bennett 1980, Levine et al. 1980). While the values for K_a and K_w are well known, recent work by Hales and Drewes (1979) has suggested that the commonly accepted value for H_a of 55 mol ℓ^{-1} atm^{-1} at 298 K is too high by about a factor of ~ 5 for atmospheric hydrometeors (due to interaction between dissolved NH_3 and CO_2 at atmospheric concentrations). When this is taken into account, the NH_4^+ concentration at 278 K is given by

$$[NH_4^+] \simeq 3.3 \times 10^{11} P_a [H^+]. \qquad [4\text{-}99]$$

This yields a range of NH_4^+ concentrations from 1.65×10^{-4} to 0.8 mol ℓ^{-1}. Thus, 1.65×10^{-4} to 0.8 equivalent of acid could be neutralized by NH_3 alone. However, a word of caution is in order. While concentrations of NH_4^+ found in cloud water lie toward the lower end of this range (Petrenchuk and Drozdova 1966, Sadasivan 1980, Hegg and Hobbs 1981a), most rainwater samples have substantially lower NH_4^+ concentrations than are predicted by the above calculations (Lau and Charlson 1977). While this discrepancy is well known, it remains unresolved.

4.3.6.2 Neutralization by Particle-Acid Reactions--Reactions between strong acids produced in hydrometeors and particles incorporated into these hydrometeors by scavenging (either nucleation or below cloud scavenging) are well known. But these generally have been considered from the standpoint of initially alkaline droplets produced from, say, sea salt nucleation acidified by absorption or production of strong acids (Robbins et al. 1959, Eriksson 1960, Hitchcock et al. 1980). The initial "alkaline" salt for such a reaction is predominantly NaCl.

However, the widespread occurrence of CA^{2+} in rainwater and the fact that calcite ($CaCO_3$) and dolomite ($CaCO_3 \cdot MgCO_3$) are often substantial components of the atmospheric aerosol have led to the assertion (Winkler

1976) that these minerals will act to neutralize H_2SO_4 in hydrometeors via the substitution reaction:

$$CaCO_3 + H_2SO_4 = CaSO_4 + H_2CO_3. \quad [4\text{-}100]$$

The relative weakness of carbonic acid ensures that this reaction produces a net decrease in acidity. Certainly, $CaSO_4$ has been measured in significant quantities in urban atmospheres (Sumi et al. 1959, Kasina 1980), and Ca^{2+} and Mg^{2+} are known to be important components of the ionic precipitation in the United States (Chapter A-8). Therefore, observational support exists for this idea. Indeed, Sequeira (1981) recently found that excess Ca in precipitation (in excess of that attributable to sea salt and thus of soil origin) correlates much better with excess sulfate than does NH_3, and that Ca and Mg concentrations in precipitation are often more than sufficient to offset observed SO_4^{2-} loadings. Sequeira also suggests a role for calcium oxide (CaO) derived from fly ash as well as for $CaCO_3$ and $MgCO_3$. The interesting point about these three minerals is their low solubility in water (e.g., compared to sea salt) and their increasing solubility with increased acidity. They may, therefore, act as hydrometeor buffers in the atmosphere, much like NH_3. The absolute amount of Ca and Mg available for such buffering is highly variable, with Ca ranging from 10^{-7} to 10^{-4} mol ℓ^{-1} and Mg fairly uniformly a factor of 5 to 10 lower in both rainwater and cloud water (Petrenchuk and Drozdova 1966, Hendry and Brezonik 1980, Sadasivan 1980, Liljestrand and Morgan 1981). Clearly, Ca, at least, can substantially contribute to acid neutralization in hydrometeors.

4.3.7 Summary

The three acids that dominate the acidity of precipitation are H_2SO_4, HNO_3, and HCl, in decreasing order of importance. The methodology employed to assess the importance of their formation within clouds and rain has been to compare the solution concentrations of these acids produced by direct absorption of their respective acidic vapors from the gas phase with those generated by plausible solution reactions over the lifetime of the cloud and raindrops. If an aqueous-phase reaction produced solution concentrations comparable to those resulting from absorption, the reaction was considered significant. In cases where several reactions were found capable of producing significant concentrations of a particular acid, their relative importance has been evaluated. Finally, because the potential acidity of precipitation far exceeds that commonly observed, plausible aqueous-phase neutralization reactions have been examined.

4.4 TRANSFORMATION MODELS (N. V. Gillani)

4.4.1 Introduction

Secondary products of chemical transformations of SO_x and NO_x emissions are generally more acidic than their precursors. In the context of acidification of lakes, vegetation, and soil, however, the chemical form in which the deposition arrives at the surface is of relatively little significance (because precursor depositions are rapidly converted to the secondary forms following deposition) compared to the fact that the rate of the deposition

process itself depends strongly on its chemical form. Thus, for example, sulfate particles are believed to have a considerably longer average atmospheric residence than SO_2, and hence a larger range of impact. Nitric acid, on the other hand, is likely to be removed from the atmosphere more efficiently and rapidly than its precursors. Consequently, it is necessary for transport-deposition models to distinguish between primary and secondary pollutants, and to facilitate atmospheric chemical transformations through appropriate modules.

The chemical transformation module is an integral part of the overall transport-transformation-removal model. The framework within which the larger model is formulated and solved may be Lagrangian (trajectory), or Eulerian (grid), or some hybrid scheme (details in Chapter A-9). Lagrangian or trajectory models simulate the changing concentration field within a given polluted air parcel (e.g., a puff or plume release) as a result of the combined effects of dilution, chemistry, and depositions. Typically, the concentration field as well as meteorological variables are assumed to be homogeneous within the air parcel. Recent attempts have also been made to obtain simulations with finer spatial resolutions within the air parcel. Lagrangian models are tailored for simulations of pollutant kinetics at the plume scale. Regional Lagrangrian simulations are commonly based on simple linear superpositions of individually-calculated concentrations of multiple plumes. Individual plumes may be referred to as point sources or area sources. For the modeling of nonlinear processes in multiple interacting plumes over regional scales, Eulerian grid models are more appropriate. They are based on the solution of coupled transport-transformation-removal mass balance equations of individual species over specified two- or three-dimensional spatial grids. Typical grid sizes in regional models vary from 50 to 100 km to a side. Within each grid cell, pollutant concentrations, as well as meteorological variables, are assumed to be uniformly distributed. In a pure grid model, emissions within a grid cell are considered in an aggregate sense, and are instantaneously homogenized over the entire cell volume. The error of this approximation is particularly severe in two-dimensional grid models which lack vertical resolution. The effects of sub-grid scale processes are sometimes included in terms of bulk parameterizations. Alternately, a hybrid scheme may be used in which individual plumes may be modeled in a Lagrangian sense and detail until they acquire the spatial dimensions of the Eulerian grid size, and subsequent simulation is within the Eulerian framework. The output from a grid model is an evolving series of snapshots of the deposition field over the entire modeled region. This is clearly very desirable in regional modeling. Grid models, however, require far more extensive input information, computations, and computational resources than trajectory models, and are generally quite expensive to implement. The chemical transformation module does not depend, per se, on the framework of the larger model formulation. However, its validity does depend on the spatial-temporal resolution of the simulation, and on the facility for accommodating nonlinear processes and plume interactions with its chemically different environment. The remainder of this section is focused on the transformation module.

An objective of this section is to review and assess briefly our present ability to predict the rates of chemical transformations of primary emissions

of SO_x and NO_x to secondary acidic products (sulfates and nitrates) during atmospheric transport. Such predictions are based on transformation models, which are mathematical formulations relating secondary pollutant formation rates to concentrations of the precursor gases (e.g., SO_2, NO), and to any other chemical and meteorological factors considered to contribute to the transformation processes. The principal approaches in formulating such models are discussed for S and N compounds, for power plant and urban plumes, and for each of the major conversion mechanisms believed to be important. Specific formulations of practical interest are reviewed briefly along with their applications, and major outstanding problem areas are identified. An overall assessment is presented of our present standing in terms of the desired goals of transformation modeling. Emphasis is placed on formulations believed to be suitable for inclusion as transformation modules in current long-range transport-transformation models aimed at simulating regional-scale acidic depositions.

The atmospheric transformation processes are very complex, involving multiple parallel pathways (mechanisms) of physical diffusion and homogeneous and heterogeneous chemical reactions of a wide variety of reactants and catalysts. The reactants may be of primary or background origin or intermediate or secondary products of concurrent reactions. A variety of meteorological factors--UV radiation, temperature, relative humidity, clouds, fogs, atmospheric turbulence, and others--also have important influence on atmospheric transformation processes. Many of these factors are interdependent; e.g., UV radiation, temperature, clouds, and turbulent mixing are closely related to insolation. Furthermore, a given factor may simultaneously have opposite effects on different chemical reactions; e.g., the effect of plume dispersion should be to "quench" reactions between co-emitted species (Schwartz and Newman 1978), but also to promote reactions of primary emissions with background species (Wilson 1978, Gillani and Wilson 1980). Given the complex array of reactants and their reactions influenced in a complicated manner by interdependent environmental factors, one must recognize that no single and simple mathematical expression can describe adequately the transformation processes of a given pollutant. Realistic transformation models should be capable of distinguishing among the different conversion mechanisms and, for each mechanism, should reasonably reflect the dependence of the conversion rate on current plume, background, and environmental conditions.

Historically, the science of transformation modeling is young. As recently as 1977, the state of the art was such that in a widely acclaimed regional monitoring and modeling program, the conversion rate of SO_2 to SO_4^{2-} was represented by a single constant number over a regional scale, regardless of time of day, season, or prevailing meteorological conditions (OECD 1977). Even today, such practice is not uncommon in regional models, perhaps with some justification. Since 1977, however, significant progress has been made in developing transformation modules appropriate for regional models, particularly for the gas-phase mechanism of S conversions. Applicable models for the liquid-phase mechanism are still rare and primitive. Current transformation models for N compounds are generally complex, requiring extensive computational resources even for mesoscale applications. Their validations are limited.

4.4.2 Approaches to Transformation Modeling

Basically two approaches to transformation modeling exist--a fundamental approach and an empirical approach.

4.4.2.1 The Fundamental Approach--The fundamental approach consists of the so-called "explicit mechanisms method" and its simplified counterparts. In theory, the explicit mechanisms method involves consideration of all significant reactants and their elementary reactions involved in each mechanism of sulfate or nitrate formation. Concentration changes by all chemical reactions are calculated simultaneously for all species at short-term intervals (typically a few seconds). Reactants include not only the precursors (e.g., SO_2, and NO), their principal oxidizing agents (e.g., OH, HO_2, and RO_2 in the gas-phase mechanism, and O_2, O_3 and H_2O_2 in the liquid-phase mechanism), and the secondary products of concern (e.g., H_2SO_4 and HNO_3) but also catalysts and significant intermediate species involved in the mechanisms. Of particular significance are the multitude of reactive HC species and their derivatives involved in gas-phase chain reactions that contribute to photochemical smog formation, as well as to sulfate and nitrate formation. In a spatially homogeneous system (well-mixed plume) consisting of n species, a total of 2n first-order, nonlinear, ordinary differential equations must be solved simultaneously at each time step to evaluate the changing species concentrations in the plume and in the background with which the plume interacts. Plume-background interactions must be facilitated in the model. If spatial inhomogeneities are important and need to be resolved, the system of equations becomes substantially larger. Also, because a wide range of reaction-time scales are generally involved, computations for the equations' solutions at each time step are quite involved, time-consuming, and expensive.

Implementation of the explicit mechanisms method has many associated problems. The list of possible reactants is long, and sometimes there is even disagreement about what the products are in given individual reactions. Values of many elementary reaction rate constants have either not been measured or are not quite reliable. Model input requirements also include specification of initial concentrations of all species in the plume and in the background. While primary emissions from major point sources are reasonably well characterized, area source emissions are not. This is particularly true for the hydrocarbons. Also, the spatial-temporal resolution of the current area source emissions inventories is generally inadequate to verify model performance based on the available mesoscale field data of power plant and urban plume transport and transformations. Atmospheric measurements are either rare or nonexistent for many short-lived species, some of crucial importance (e.g., OH, HO_2, RO_2, and H_2O_2). Detailed HC and aldehyde measurements in the atmosphere are not common. Input specifications and model validations are thus only partial and very approximate.

Perhaps the best example of an attempt to simulate smog chemistry by explicit mechanisms is the work of Demerjian et al. (1974), which incorporated more than 200 species, the great majority of them arising from the explicit use of specific reactive HC and corresponding organic intermediates and sinks.

Despite this model's comprehensiveness, the authors warn that its representation of the real atmosphere, which undoubtedly contains hundreds of organic compounds, may be an oversimplification. Such complex chemical modeling is currently impractical for application in regional models. Simplifications and further approximations are necessary. The key is to achieve a reasonable condensation of the vast number of HC and aldehydes, and their reactions, while adequate representation is maintained. Such condensation is attempted either by "lumping" groups of species by some common criterion and then treating each group as a single species in the model, or by substituting a single surrogate species either for all HC (e.g., propylene by Graedel et al. 1976, "nonmethane HC" by Miller et al. 1978) or for a particular lumped group of HC (e.g., xylene for aromatics, by Hov et al. 1977). Two principal methods of "lumping" have been developed: the HSD method (Hecht et al. 1974), and the carbon bond mechanism (CBM) method (Whitten et al. 1980). In the HSD method, organic species of like reactivities are grouped into four main classes: paraffins, aromatics, olefins, and aldehydes. Many models use a modification of this in which the following six lumped classes are used after Falls and Seinfeld (1978) and Falls et al. (1979): ethylene, higher molecular weight olefins, paraffins, aromatics, formaldehyde, and higher molecular weight aldehydes. In the CBM method, similarly bonded C atoms are lumped into four or more classes. In principle, the CBM is closer to the explicit mechanism and is also easier to use in conjunction with measured data than is the HSD mechanism. Such formulations have been further condensed in specific simulations by reducing the number of species modeled through the use of surrogate reactions and rate coefficients which effectively include the role of the omitted species (Levine and Schwartz 1982).

Validation of simulations performed by detailed chemical models has, to date, been generally based on matching calculated concentrations of certain key aspects of photochemical smog formation (e.g., HC loss, and OH or O_3 formation) with those measured in controlled smog chamber studies in the laboratory. The roles of such meteorological variables as sunlight, temperature, and relative humidity are simulated directly in the experiments and included in the calculations through the dependence of elementary reaction rates on them. The role of other meteorological variables such as turbulence and inhomogeneous mixing generally is not simulated in laboratory experiments. This is probably a serious limitation.

In the real polluted atmosphere, the deficiency of certain key reactive ingredients in a primary emission may well be overcome through entrainment of such ingredients from the background air. The formation of ozone and sulfates in HC-poor power plant emissions in the eastern United States during summer afternoons is thus almost as rapid as in HC-rich urban emissions (Figure 4-8 on p. 4-73; also see Gillani and Wilson 1980). Appropriate background characterization and treatment of plume-background interaction can be of critical importance in realistic modeling of transformation processes.

An important positive feature of detailed chemical models is that nonlinear chemical couplings between species, including the coupling between sulfur and nitrogen chemistry, is explicitly retained. In this sense, the same model can, in principle, perform simulations of SO_x and NO_x transformations, as

well as of urban or power plant plume chemical evolution. With appropriate spatial-temporal resolution, the effect of plume-plume and plume-background interactions can also be performed.

One of the major undesirable features of the detailed chemical approach is the necessity of performing extensive computations. However, considerable differences exist in amounts of computation necessary, depending on choice of numerical method and degree of chemical approximations involved. The number of species in the chemical schemes commonly used varies between 10 and 100. The amount of computations increases nonlinearly and rapidly with increasing number of species. For any given chemical scheme of smog simulation, the main numerical problem arises from the fact that the various chemical reactions occur at speeds which vary by several orders of magnitude. This wide range of time scales involved in this problem makes the corresponding set of differential equations quite "stiff." Standard techniques for integrating sets of differential equations (e.g., the Runge-Kutta Method) cannot provide stable solutions of such stiff systems at realistic cost. Special techniques such as those developed by Gear (1971) provide much more efficient numerical integrations by performing automatic time and error control, and are capable of providing accurate numerical solutions, albeit at considerable cost and requiring the use of large high-speed computers. The Gear technique has been used widely in simulations of photochemical smog. Other attempts to reduce computations have resorted to the use of quasi-steady-state assumptions for certain very reactive species. Such assumptions are not always justified and have been shown to lead to large inaccuracies not only under polluted conditions but also in relatively clean background conditions (Farrow and Edelson 1974, Dimitriades et al. 1976, Jeffries and Saeger 1976, Hesstvedt et al. 1978). Judiciously invoked steady-state approximations (QSSA), based on continuous monitoring of pollutant time scales during on-going simulations, can permit locally analytical solutions (Hesstvedt et al. 1978) and even locally linearized analytical solutions (Hov 1983a). Such numerical techiques can provide solutions comparable in accuracy to the Gear solutions at a fraction of the cost, and can be implemented on smaller computers.

Examples of specific detailed chemical model calculations for atmospheric applications are considered in Section 4.4.4.1. A recent review paper by Hov (1983c) is also recommended for those interested in further details pertaining to the fundamental approach of transformation modeling.

4.4.2.2 The Empirical Approach--Given the substantial uncertainties and gaps in the input information needed for detailed chemical models, and given the discrepancies in reported transformation rates of SO_x and NO_x, the use of detailed kinetic models continues to be questioned, and simpler empirical rate expressions are often favored. A great deal of experimental research on chemical transformations has been directed at obtaining estimates of the conversion rates of SO_2 to sulfates, and of NO to NO_2 to nitrates in the laboratory and in the field. In recent years, some success has been achieved in relating field estimates of the conversion rates to specific conversion mechanisms and to specific, measured influencing factors. A large number of source-related and environmental factors have been implicated as influencing transformations. They include the time and height of source release, the

nature and amounts of the acid precursors, other co-emitted species, the reactivity of the air mass in which emissions are transported, as well as such meteorological factors as sunlight, temperature, absolute humidity, clouds and fogs, and atmospheric stability.

In the empirical approach, an attempt is made to identify the rate-controlling factors for each mechanism and to formulate and validate an overall rate expression for measured sulfate or nitrate formation by each mechanism directly in terms of these factors, which are also measured. In other words, the effect of the multiple elementary reactions is parameterized in terms of pertinent, measurable chemical and meteorological factors. Such parameterizations of the conversion rate are simple rate expressions, which can be inserted directly into regional models as the transformation module. They entail very few computations and require inputs that are, for the most part, relatively readily available even on a regional scale. In spite of their simplicity, they often yield quite reliable estimates of actual atmospheric formations of such final products as sulfates. This is particularly true when their formulation is based directly on field data and their application is based on measured input data. Their principal disadvantage is that they lack generality, being applicable mainly under environmental conditions reasonably close to those for which they have been successfully validated. In specific applications for which relevant parameterizations are available, their simplicity and reliability make them immensely valuable.

The existing empirical parameterizations of sulfur chemistry are largely based on mesoscale plume data. At least three important practical implications of this limitation may be identified. First of all, given the dominance of source-specific characteristics in mesoscale plume transport, empirical parameterizations which are mesoscale in origin must be considered to be specific to the source type (e.g., power plant plumes versus urban-industrial plumes) for which they were developed. Secondly, because the characteristic time scales of the atmospheric residence of secondary pollutants such as sulfates and ozone are significantly longer than mesoscale, it must be presumed that the parameterizations for plumes would be sensitive to boundary conditions. In fact, empirical observations have shown that sulfate and ozone formation rates in power plant as well as urban plumes are strongly sensitive to the chemical condition of the background air, and to the rate of plume dilution by entrainment of this background air (Gillani and Wilson 1980, Miller and Alkezweeny 1980). Plume-background interactions can sometimes even obscure the initial chemical distinctions between a power plant plume and a petroleum refinery plume (see Figure 4-8). Finally, one must question the validity of empirical parameterizations of mesoscale origin in synoptic scale applications. On the positive side, however, it has been demonstrated empirically that pollutant plumes evolve to the chemical maturity characteristic of regional air masses within only a few hours of transport during sunny convective conditions typical of summer days in the eastern United States (Gillani and Wilson 1980). At least under such conditions, chemical parameterizations derived from data of chemically-aged plumes may have validity even during long range.

The reactions governing SO_2 oxidation have the general form

$$SO_2 + O_X + (M) \rightarrow \text{products} \rightarrow SO_4^{2-}, \qquad [4\text{-}101]$$

where O_X represents the principal oxidizing agents; i.e., OH and possibly HO_2 and RO_2 for gas-phase oxidation (Calvert et al. 1978), and H_2O_2, O_3, and O_2 for liquid-phase oxidation (Penkett et al. 1979); (M) represents the catalysts, if and when any are involved. With the possible exception of catalyzed reactions (Freiberg 1974), the rate of sulfate formation, r_S, may be expressed as:

$$r_S = \frac{\partial}{\partial t}(SO_4^{2-}) = k_S \cdot (SO_2), \qquad [4\text{-}102]$$

where the fractional conversion rate, k_S, depends on O_X, the oxidizing species. Such a relationship is valid as long as SO_2 is not in stoichiometric excess. The validity and linearity of this equation are further discussed in a separate section (Section 4.4.3). Parameterization of k_S, which is the goal of empirical transformation models, is thus a representation of the weighted contributions of factors which effectively determine the O_X concentrations. It may be broken down by mechanisms into:

$$k_S = k_{S_G} + k_{S_L} + k_{S_{HET}}, \qquad [4\text{-}103]$$

where components on the right hand side represent, respectively, the fractional conversion rates by gas-phase, liquid-phase, and heterogeneous aerosol surface reaction mechanisms. No parameterizations have been attempted for the heterogeneous mechanism, partly because reliable and particular atmospheric data are lacking and partly because the mechanism generally is not considered important on the regional scale. Specific parameterizations of S conversions are most developed for k_{S_G}, and efforts to parameterize k_{S_L} have just begun. These are discussed in the next section.

Similarly, the formation of the two principal secondary nitrates (HNO_3 and PAN) are largely governed by the reactions

$$NO_2 + OH \rightarrow HNO_3 \qquad [4\text{-}104a]$$

and $$NO_2 + RCOO_2 \rightarrow PAN. \qquad [4\text{-}104b]$$

Hence, their formation rates may be expressed as:

$$r_{HNO_3} = k_{HNO_3} \cdot (NO_2) \qquad [4\text{-}105a]$$

$$r_{PAN} = k_{PAN} \cdot (NO_2), \qquad [4\text{-}105b]$$

where the fractional conversion rates, k_N (N = HNO_3, PAN), depend on the concentrations of OH and $RCOO_2$, respectively. The parameterizations of k_N would represent the weighted contributions of the factors which

effectively determine these free radical concentrations. Empirical parameterizations of k_N based on field data have not been formulated or tested. Sensitivity of k_N to the HC-NO_x mix has been studied in smog chamber experiments. Some of the most recent specific results and their implications will be discussed in a later section.

4.4.3 The Question of Linearity

A much debated matter, and one of considerable practical importance in terms of regional modeling and control strategy, is the question of linearity (or lack of it) in the source/receptor relationships between emissions of SO_x and NO_x and their depositions. An important subset of this larger question pertains to the linearity of relationships between r_S and SO_2, and r_N and NO_x. In this section, the discussion is limited to the question of linearity of the chemical transformation processes. If the transformation chemistry is nonlinear, certain common modeling practices based on the assumption of linearity must be viewed with caution. For example, regional models typically have a spatial resolution over grids of 50 to 100 km to a side. The assumption of uniform species concentrations within a grid cell that includes concentrated emissions sources may give erroneous transformation estimates unless some appropriate parameterization of sub-grid scale processes is included. Distinctions in the chemical mix of different source emissions are also presumably important in the case of nonlinear chemistry. Linear superpositions of species concentrations, calculated for individual plumes assumed to be isolated, will also give erroneous estimates of nonlinear secondary formations in regions with multiple plume interactions. The validity of the linearity assumption is also crucial to the success of attempts to control secondary pollutants by a strategy of linear rollback of precursor emissions.

The lack of consensus on the question of linearity, particularly with respect to sulfur chemistry, is probably due to different interpretations of the definition of the term linear relationship. By definition, the relationship between r_S and SO_2 is linear if it can be stated in the form of Equation 4-102, and if k_S is independent of SO_2. Clearly, k_S is variable through its dependence on species, such as the OH free radical, that are responsible ultimately for the oxidation of SO_2. Therefore, the critical question is whether these oxidizing agents are themselves dependent on SO_2. There is no doubt that in a fresh plume with high concentration of SO_2, OH level is significantly controlled by SO_2 itself, and the oxidation of SO_2 is a nonlinear process. Such conditions, however, are short-lived. Subsequently, if there are no further fresh injections of SO_2 into this plume, the formation of OH will be governed by the HC-NO_x chemistry in the plume and by entrainment from the background of OH itself and of other reactive species contributing to OH formation. The direct dependence of plume HC-NO_x chemistry on local SO_2 concentration is very weak in this stage of plume transport. Consequently, one commonly finds in the published literature explicit or implicit statements about linear sulfur chemistry under such conditions. If the mathematical definition of linearity is to be interpreted strictly, such statements are correct within the context of the transport of a particular plume release. In the broader context of modeling of longer-term averages or continuous emissions, possibly varying with time, and

with inevitable plume-plume and plume-background interactions, an indirect form of nonlinearity does exist because of the correlation between SO_2 emissions and the co-emissions of NO_x and HC. A broader definition of linearity which requires k_s to be independent not only of SO_2 but also of co-emitted species is implicit in the works of Cahir et al. 1982 and Hidy 1982.

The significance of the role of the co-emitted species is illustrated in the following practical example. Suppose we wish to answer the following question: "Will a 50 percent reduction of SO_2 emission from source A (or region A) result in a corresponding 50 percent decrease in downwind sulfate formation?" There is no unique answer to this question. First, the manner in which the emission reduction is achieved is important. If source A is a coal-fired power plant, and the reduction in SO_2 emission is achieved by a 50 percent reduction in the amount of fuel burned, there may also be an accompanying reduction in NO_x emissions which, in turn, will cause k_s to be different. The answer to the question, therefore, is "no". The cause of this apparent or effective nonlinearity is the indirect dependence of k_s on SO_2 through the correlation between co-emitted SO_2 and NO_x. The 50 percent reduction in SO_2 emission could also have been achieved by the use of fuel of 50 percent lower sulfur content or by scrubbing SO_2 from the combustion products prior to stack emission. To the extent that these latter procedures may not have changed NO_x emissions, k_s will remain unchanged except during initial transport, and the downwind sulfate formation would be expected to decrease by about 50 percent, all other conditions being the same. The answer to the question is therefore "yes".

A second factor that will profoundly influence downwind sulfate formation is the composition of the air that the plume encounters during mesoscale and long-range transport. Field evidence suggests that the role of co-emitted species may be substantially enhanced, or overwhelmed, by the role of the background air which the plume entrains by mixing processes. Like the co-emitted species, a polluted background can also serve as the source of the oxidizing agents. Figure 4-8 shows an example of the side-by-side transport of two St. Louis plumes of very different emission composition, yet comparable secondary formations. The Labadie power plant emission is characterized by a very low HC/NO_x ratio. The urban plume of St. Louis, including the emissions from a large petroleum refinery complex, by contrast is much richer in reactive HC emissions. The secondary formation of ozone in large plumes on summer days is closely related to the formation of sulfates (White et al. 1976, Gillani and Wilson 1980). The formation of ozone and sulfates in power plant plumes at rates comparable to those in urban plumes is due to the entrainment of polluted background air. During long-range transport, the role of the background air may well predominate as a source of reactive species which oxidize SO_2. In laboratory measurements with no role of a variable background, a first-order dependence of sulfate formation on SO_2 concentrations has been observed for gas-phase reactions (Miller 1978) as well as for liquid-phase reactions (Penkett et al. 1979). Mesoscale field measurements are also generally consistent with pseudo-first-order dependence between r_s and SO_2, except during early transport.

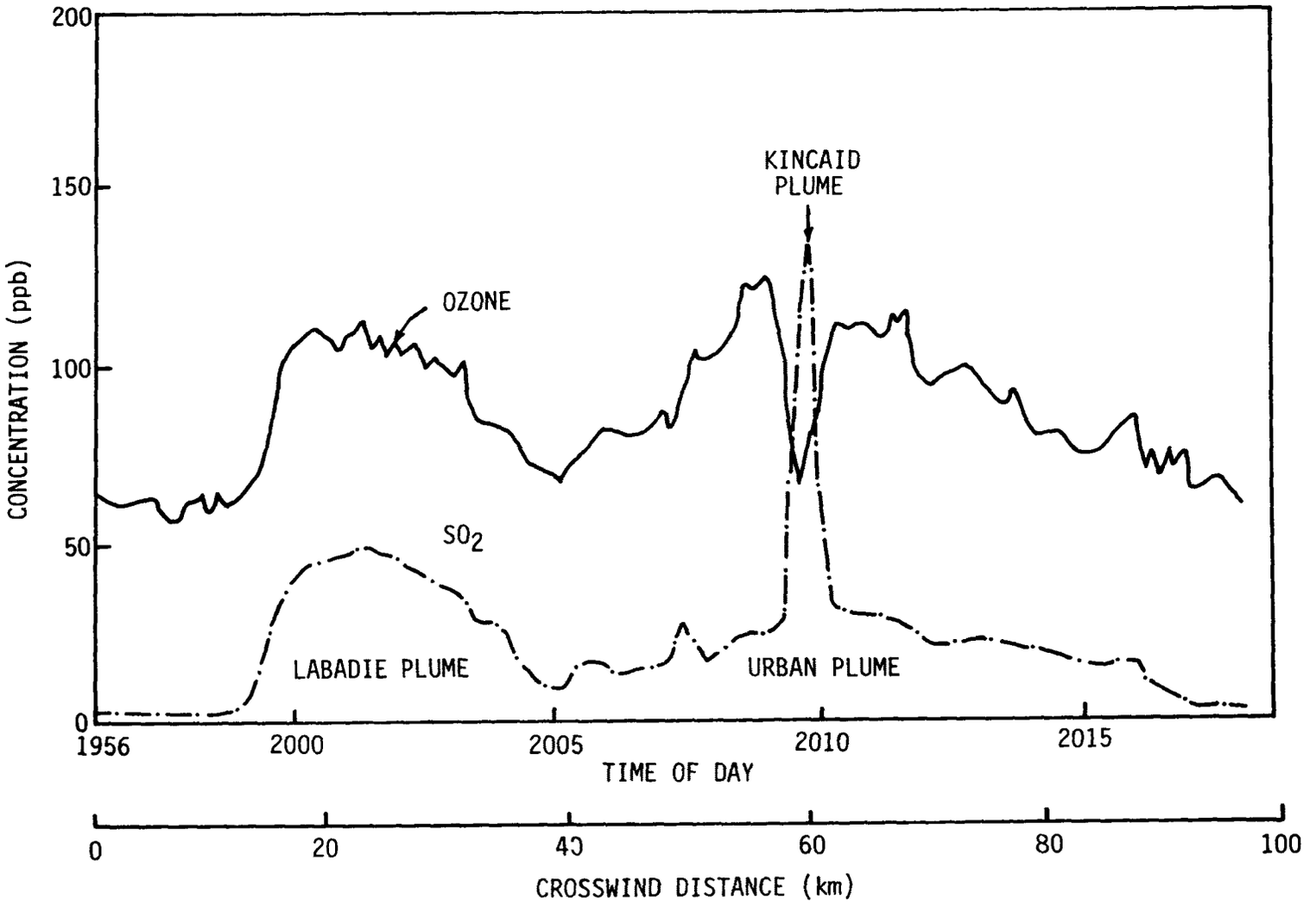

Figure 4-8. Crosswind profiles of primary (SO_2) and secondary (O_3) pollutants in the Labadie power plant plume and in the urban plume of St. Louis. The data were collected during an aircraft traverse through the plumes at about 450 m AGL. The plumes were released around midday; the traverse was made around 2000. Observe the comparable levels of excess ozone in both plumes. The Kincaid power plant plume represents a relatively fresh emission into the aged urban plume. Adapted from Gillani et al. (1978).

A common practice in detailed models of sulfur chemistry in the atmosphere is to represent the SO_2 + OH reaction as a terminal reaction, effectively leading to the formation of H_2SO_4 and depletion of the OH radical concentration. This dependence of OH on SO_2 therefore contributes to nonlinearity of the sulfur transformation process. It has been pointed out recently (Stockwell and Calvert 1983) that the SO_2-OH reaction may initiate a chain of reactions which may lead not only to formation of H_2SO_4, but also to regeneration of OH in the presence of NO_x and hydrocarbons. Such recycling of OH would have the effect of weakening the nonlinearity of sulfur chemistry. An important conclusion of the recent NAS report on acid deposition (NAS 1983) was indeed that nonlinearity of sulfur chemistry is probably quite weak, and that even the broader coupling between sulfur emissions and depositions may be substantially linear on a long-term average basis over the spatial scale of eastern North America.

Based on theoretical considerations, the relationship between r_N and NO_x is expected to be nonlinear, because k_N depends on OH, for example, which depends directly on the NO_x chemistry. Results of recent smog chamber experiments suggest, however, that the nonlinearity of r_N may also be short-lived relative to the time scale of long-range transport (Spicer 1983). Pseudo-first-order parameterizations of r_N may be justifiable, but k_N may also need to reflect the make-up of the air an emission encounters during transport.

4.4.4 Some Specific Models and Their Applications

4.4.4.1 Detailed Chemical Simulations--Detailed chemical modules based on the explicit mechanisms approach have been used within Eulerian as well as Lagrangian formulations, and in model applications at the plume scale as well as the regional scale. Such transformation modules differ principally in terms of their representations of the hydrocarbons, and in the methods used for the numerical solution of the set of nonlinear differential equations describing the species concentration changes by chemical reactions. The following discussion outlines some specific representative models and is not intended as an extensive review of chemical models.

The LIRAQ model (McCracken et al. 1978, Duewer et al. 1978) is an example of a two-dimensional grid model (single well-mixed vertical layer). The transformation module attempts to simulate photochemical smog formation based on the HSD scheme (Hecht et al. 1974), and the numerical solution is based on the Gear technique. The SAI Airshed Model (Reynolds et al. 1979) is a three-dimensional grid model which permits initial isolation of elevated point sources from surface sources. It uses the carbon-bond mechanism of photochemical smog simulation (Whitten and Hogo 1977), and numerical solution is by a finite difference technique (SHASTA) developed by Boris and Book (1973). An ambitious three-dimensional regional grid model currently under development at EPA (Lamb 1981) presently uses the chemical scheme of Demerjian and Schere (1979) which uses four hydrocarbon classes of different reactivities. In some regional models (e.g., McRae et al. 1979), point source plumes are simulated in a Lagrangian sense within the framework of an Eulerian grid network until they attain the dimensions of the grid cell. Thereafter, the simulation is continued in the Eulerian frame.

On a global basis, the troposphere is presumed to be clean and the organic species most relevant to smog formation are carbon monoxide (CO) and methane (CH_4). Recently, a two-dimensional global model was employed by Fishman and Crutzen (1978) to predict the global distribution of OH, HO_2, and CH_3O_2 radical concentrations. Predicted OH concentrations were reasonably comparable with recent, measured atmospheric concentrations (Sheppard et al. 1978). Altshuller (1979) used this model for OH to investigate the variability of the sulfate formation rate by the homogeneous gas-phase mechanism with respect to latitude and altitude. His results showed that in the clean enviroment, OH is the principal oxidizing agent, and that, at higher latitudes, e.g., in the northeastern United States, Canada, and northern Europe, large seasonal differences in sulfate formation by this mechanism are to be expected. Very little sulfate formation is likely in winter by gas-phase mechanisms.

The regional model of Carmichael and Peters (1979) is based on the chemistry of a clean background in which the only organic species are CO and CO_2. They invoke the pseudo-steady-state assumption for the oxidizing species OH, HO_2, H_2O_2, and O_3, and use their iterative solution for these species in first-order expressions for the oxidation of SO_2 to estimate the sulfate formation rate.

Most plume simulations are based on trajectory-type models. Calculations made for polluted industrial regions and urban areas have simulated certain observed phenomena related particularly to O_3 behavior (Graedel et al. 1978) but at the same time have yielded conflicting results concerning important control strategies. Results by Graedel et al. (1978) suggest OH levels to be directly proportional to NO_2 levels, implying that reduction of NO_x emissions would help control nitrate and sulfate production. Miller (1978) showed rather that NO_x emissions tend to delay SO_2 oxidation and that the ratio ($NMHC/NO_x$) of initial concentrations of nonmethane HC's and NO_x's dominates the SO_2 oxidation rate. Miller's conclusions were verified experimentally. Actually, as suggested by Miller (1978), precursor effects may significantly differ in the first several hours of daytime plume transport from their effects during subsequent regional transport.

Detailed chemical calculations also have been applied to simulate sulfate and nitrate formation in urban plumes (Isaksen et al. 1978, Miller and Alkezweeny 1980, Bazzell and Peters 1981) and in power plant plumes (Miller et al. 1978, Bottenheim and Strausz 1979, Levine 1981, Hov and Isaksen 1981, Stewart and Liu 1981). In these calculations, proper simulations of the changing background air and of plume-background interactions were necessary for at least qualitative agreement with field observations. Levine (1981) neglected plume-background interactions and, as a result, his conclusion that power plant plume dilution inhibits sulfate formation is contrary to field observations in moderately polluted regions (Gillani and Wilson 1980). Hov and Isaksen (1981), on the other hand, treated crosswind spatial inhomogeneities in sulfate formation resulting from plume-background interaction and succeeded in simulating, at least qualitatively, many features of the crosswind plume data of Gillani and Wilson. Stewart and Liu (1981) similarly provided cross-wind resolution and plume-background interactions with their reactive plume model which was based on the carbon-bond mechanism for the

simulation of chemical kinetics. Recently, Hov (1983b) performed a plume simulation in which vertical stratification of the concentration field was considered. In general, plume simulations have indicated that O_3 and aerosol formation are greater when the background is polluted, that OH is the dominant oxidizing species for SO_2 and NO_2, and that OH and peroxy radical (HO_2, RO_2) concentrations, which play an important role in O_3 formation, peak at midafternoon in polluted regions.

In all of the above simulations, only the homogeneous gas-phase chemistry was included. Rodhe et al. (1979) added reactions of SO_2 and NO_2 with H_2O_2 in the presence of "clouds" to a highly lumped gas-phase chemistry model. H_2O_2 generation was calculated based on the gas-phase reactions. The authors recognized qualitatively that the effective rate constants for cloud reactions must include not only the effect of the liquid-phase transformations occurring in cloud droplets and in precipitating clouds, but also exchange rates of the reacting species between the droplets and the surrounding air, and the frequency and occurrence of clouds and precipitation. They then proceeded to choose rate constant values such that overall gas- and liquid-phase oxidation rates of SO_2 became comparable and the liquid-phase oxidation of NO_2 became relatively insignificant compared to its gas-phase counterpart. This procedure for the liquid-phase mechanism represents a highly parameterized approach, with parameter values assumed rather subjectively. Their calculations were applied regionally to the European industrial environment under summertime conditions. The relative contributions of gas-phase and liquid-phase mechanisms to sulfate and nitrate formation, of course, reflected their assumptions.

4.4.4.2 Parameterized Models--For many years, no consensus could be reached concerning the relative importance of the many chemical and meteorological factors implicated as influencing gas-to-particle S conversion. Most transport-transformation models used constant pseudo-first-order rates for the oxidation of SO_2. Documentation of sunlight as a dominant environmental factor governing sulfate formation in power plant plumes (Gillani et al. 1978) has since been verified and widely accepted and used. In particular, in a recent review of field data on sulfate formation in power plant plumes during all seasons in the United States, Canada, and Australia, Wilson (1981) observed that the outstanding common pattern in this broad data base was the diurnality of the sulfate formation directly related to solar radiation. Such a role of sunlight is also consistent with the observed distinct summer peak in regional SO_4^{2-} distribution in the eastern United States (Husar and Patterson 1980), even though corresponding SO_2 emissions are distributed fairly uniformly over all seasons (U.S. DOE 1979).

A sunlight-dependent model of the form $k_S \propto R_T$, the total incoming solar radiation flux at ground level, was used by Gillani (1978) in a diagnostic mesoscale plume model and by Husar et al. (1978) in a multiday plume S budget study. A similar parameterization has been used by Shannon (1981) and by others. Gillani found that such a model based only on sunlight could not simulate the observed day-to-day variation in sulfate formation. Evidently, factors other than sunlight must be included. Also, the manner in which sunlight influences the conversion process must be more carefully considered. As Wilson (1981) noted, observed correlations of the conversion

rate with sunlight, or with air temperature (Eatough et al. 1981), do not imply the direct role of these factors in the underlying mechanisms. These two factors are highly correlated, as are both to turbulent mixing, convective cloud formation, and a number of other factors, which alone can exert rate-controlling influences on specific conversion mechanisms. Accordingly, formulation of meaningful parameterizations must be based on mechanistic considerations.

Gillani et al. (1981) recently advanced a parameterization of the gas-to-particle S conversion by the gas-phase mechanism based on plume data collected during the summer in the Midwest (Missouri and Tennessee). The motivation for their gas-phase parameterization was derived from their earlier identification of a recurrent pattern of O_3 and aerosol generation in power plant plumes, which evidently involved participation of reactive species entrained from the background (Gillani and Wilson 1980). Gillani et al. argued that accelerated photochemical generation of the radical species OH, HO_2, and RO_2 that oxidize gas-phase SO_2 would be facilitated by reactions involving NO_x emissions, entrained reactive HC, and free radical species. Consequently, the quality of the background air and the extent of plume dilution by its entrainment were judged to be important contributing factors, in addition to sunlight which powers the photochemical reactions. Given the lack of detailed data of the oxidizing species, the authors resorted to using O_3 as a surrogate for, or an indicator of, air mass reactivity. Vertical plume spread, Δz_p, was chosen as a measure of the extent of plume dilution. The resulting gas-phase parameterization is:

$$k_{SG} \simeq (.03 \pm .01) R_T \cdot (\Delta z)_p \cdot (O_3)_o, \qquad [4\text{-}106]$$

where k_{SG} is in percent hr^{-1}, R_T is in kW m^{-2}, $(\Delta z)_p$ is in meters, and background ozone, $(O_3)_o$, is in ppm. The coefficient 0.03 $\pm$ 0.01 was chosen on the basis of the best fit between the calculated (Equation 4-106) and measured values of k_{SG}. The measured values were for dry (relative humidity < 75 percent), cloudless conditions when gas-phase reactions may safely be assumed to predominate. The parameterization was validated successfully by data collected in the plumes of three large central power generating stations in Missouri and Tennessee during two different summers. The empirical coefficient (0.03) thus pertains to such large power plant plumes in which the initial NO_x/SO_2 ratio is about 1:3.

The above parameterization is believed to provide good estimates of the gas-phase sulfate formation rate under the moderately polluted conditions characteristic of the eastern United States in summer and appears to be valid even under more polluted conditions during stagnation episodes. Its validity in winter, even in this region, remains to be tested. Its performance in clean regions such as the Southwest, and in extremely polluted areas such as Los Angeles, CA, on a smoggy day is also unproven. Furthermore, the parameterization has no validity for urban plumes and possibly also plumes from small power plants owing to substantially different composition of the emissions. In spite of these restrictions, the parameterization is of practical significance. Its input requirements are minimal and can be satisfied presently over a regional scale in the eastern United States. Its explicit inclusion of plume-background interactions and air mass conditions

probably gives it some validity even during long-range transport when the role of the background is expected to be dominant. Application of the parameterization based on 1976 St. Louis, MO, data of the input variables yields the diurnal and seasonal pattern of k_{SG} as shown in Figure 4-9. The magnitudes and temporal variations shown are plausible and consistent with available field data, as well as with expectations based on detailed chemical calculations (Calvert et al. 1978, Altshuller 1979). The results predict that in the Midwest, gas-phase mechanisms may be expected to convert about 10 to 20 percent of the SO_2 in a power plant plume to SO_4^{2-} during an average summer day, while corresponding conversion in winter may be about an order of magnitude smaller. By comparison, measured values of SO_2 to SO_4^{2-} conversion by all mechanisms range between 15 and 35 percent for summer conditions in the same region (Gillani and Wilson 1983). It may be inferred, therefore, that liquid-phase mechanisms may convert about 5 to 15 percent of the SO_2 to SO_4^{2-} per day during summer in the Midwest.

Gillani et al. (1983) have recently also made a first attempt to formulate a parameterization of liquid-phase SO_4^{2-} formation resulting from plume-cloud interactions. The formulation explicitly recognizes that the overall conversion rate, k_{S_L}, depends not only on the chemical reaction rate within cloud droplets, K_{S_L}, but also on the physical extent of plume-cloud interactions. Because clouds are discrete entities in space and time, and plume-cloud interactions are somewhat random events, the authors choose to describe plume-cloud interactions in probabilistic terms. The overall formulation has the general form

$$k_{S_L} = P \cdot K_{S_L} \qquad [4\text{-}107]$$

where P represents a measure of the probability and extent of plume-cloud interactions. All three quantities in the equation are time dependent. The dependence of P on local plume and cloud dimensions has been derived explicitly (details given in original reference), and its values are determined during an actual power plant plume model run based on current, calculated plume dimensions and local cloud data from surface weather observations of the National Weather Service network of stations, as well as on local lidar and aircraft measurements. P represents a measure of the fraction of a given plume volume which is in contact with the liquid phase.

The authors did not attempt to parameterize K_{S_L}. It depends on such variables as liquid water concentration, droplet pH, and concentrations of dissolved S, oxidizing agents (H_2O_2, O_3, and O_2), and catalysts (Fe and Mn). No data were available for such cloud chemical composition. The authors did, however, obtain an average daytime estimate for K_{S_L} under typical summertime fair-weather convective cloud conditions in the Kentucky-Tennessee area. The inferred value of K_{S_L} (summer daytime average conversion rate within clouds) was 12 ± 6 percent hr^{-1}. This value compares with values of 0 to 104 percent hr^{-1} estimated by Hegg et al. (1980), based on ambient SO_2 and SO_4^{2-} measurements in wave cloud situations and with predicted values ranging from 10 to 20 percent hr^{-1} in large storm cloud systems in the summer based on an indirect mass balance technique (Scott 1982). Also, the value of P averaged over 24 hr is expected to be significantly less than 0.1 during summer as well as winter. In other

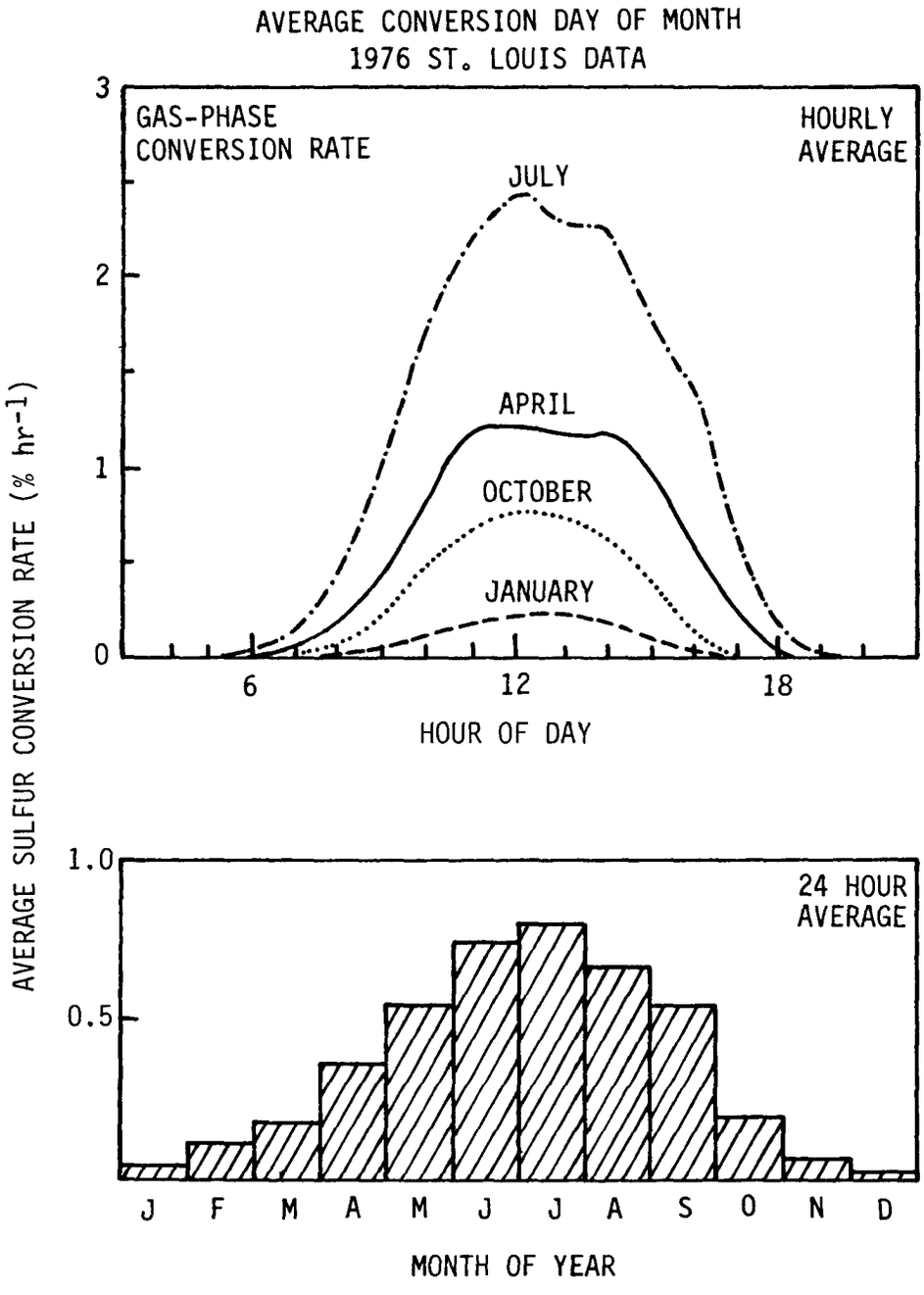

Figure 4-9. Diurnal and seasonal patterns of the gas-to particle conversion of sulfur by gas-phase mechanisms, according to calculations based on the parameterizations by Gillani et al. (1981).

words, the average bulk plume conversion rate by liquid-phase mechanisms is likely to be less than the local droplet-phase conversion rate by more than an order of magnitude. All of these estimates involve several assumptions and approximations and must be used with caution. Values of K_{SL} at night and in winter are believed to be substantially smaller as a result of lower concentrations of the photochemically-generated oxidizing species, O_3 and H_2O_2.

Based on the above parameterizations and St. Louis, MO, data, it is estimated that the 24-hr average, overall sulfate formation rates in July are likely to be 0.8 $\pm$ 0.3 percent hr^{-1} by gas-phase reactions and at least 0.4 + 0.2 percent hr^{-1} by liquid-phase reactions. Winter rates by gas-phase reactions are estimated to be an order of magnitude smaller than in summer and by liquid-phase reactions are estimated to be comparable during the two seasons.

A variety of empirical data suggest that liquid-phase conversions in wetted aerosols may be significant at relative humidity between 75 and 100 percent (Dittenhoefer and de Pena 1980, McMurry et al. 1981). Winchester (1983) has formulated the following empirical parameterization of k_S which highlights the role of absolute humidity and temperature:

$$k_S \propto (P_{H_2O})^{3.08} (P_{H_2O,sat})^{1.213},$$

where P_{H_2O} denotes the partial pressure of water vapor, and $P_{H_2O,sat}$ denotes the saturation vapor pressure of water vapor (a measure of temperature).

No comparable parameterizations of NO_x transformations have been formulated. Summertime plume measurements suggest that NO_3^- formation is primarily in the form of nitrate vapor (Forrest et al. 1979, 1981; Hegg and Hobbs 1979b; Richards et al. 1981) and that oxidation of NO_2 to HNO_3 may proceed about three times faster than does oxidation of SO_2 to H_2SO_4 (Forrest et al. 1981, Richards et al. 1981). Gas-phase mechanisms of HNO_3 formation are believed to predominate in the summer.

Whitby recently used a simple model assuming the total accumulation mode aerosol formation rate to be directly proportional to UV radiation intensity, to simulate observations of aerosol formation in the St. Louis, MO, urban plume of 18 July 1975. He estimated that about 1000 tons of secondary fine aerosol may be produced in the St. Louis plume in one summer irradiation day (Whitby 1980). For the same plume transport, Isaksen et al. (1978) used a detailed chemical model to simulate the measured data of O_3 and SO_4^{2-} formation presented by White et al. (1976) and estimated peak H_2SO_4 and HNO_3 formation rates of 5 and 20 percent hr^{-1}, respectively, to occur in the early afternoon. Alkezweeny and Powell (1977) also measured the St. Louis plume and estimated afternoon SO_4^{2-} formation rates to be 10 to 14 percent hr^{-1}. Miller and Alhezweeny (1980) measured SO_4^{2-} formation rates in the Milwaukee urban plume, particularly related to the quality of the background air mass, to range from 1 to 11 percent hr^{-1}.

Spicer (1977a) estimated the NO_2-to-products transformation rate in the Los Angeles urban plume as 10 $\pm$ 5 percent hr^{-1}. In more recent measurements downwind of Los Angeles (Spicer et al. 1979), the observed lower limit of NO_x conversion rates ranged from 1 to 16 percent hr^{-1}, with typical rates in the 5 to 10 percent hr^{-1} range. Spicer (1980) estimated NO_x transformation/removal rate for the Phoenix urban plume to be less than 5 percent hr^{-1}, while data for Boston showed rates in the 14 to 24 percent hr^{-1} range. Transformation products of NO_x transformations include not only inorganic nitrate (e.g., HNO_3), but also organic species (e.g., PAN). Spicer attributes the low conversion rate in Phoenix at least partly to thermal decomposition of PAN and its analogs at the high ambient temperatures of the desert area.

Recently, Middleton et al. (1980) performed a model study of relative amounts of sulfate production in wetted aerosols in a polluted environment by two different mechanisms: condensation of SO_2 gas-phase oxidation products, and catalytic and noncatalytic SO_2 oxidation in the liquid phase. The microphysical vapor transfer to the aerosols and the chemical conversion within the aerosols were treated as coupled kinetic processes. Concentrations of the oxidizing species (e.g., OH, and H_2O_2) and of the catalysts (e.g., Fe, Mn, and soot) were assumed known, and representative values for day and night and summer and winter were used. The study concluded that in the daytime, photochemical reactions and liquid-phase oxidation by H_2O_2 are likely to predominate, with particle acidity playing a minor role. At night, sulfate production rates are low, being principally by catalytic and noncatalytic liquid-phase mechanisms involving O_3 and O_2. The daytime H_2O_2 reaction rate was enhanced by the lower winter temperatures.

4.4.5 Summary

Transformation models can, at best, be only as good as our understanding of the transformation processes. Significant gaps in this understanding remain, particularly with respect to the physical and chemical kinetics of the liquid-phase processes. The validity and extrapolation of laboratory results to real atmospheric conditions are often questionable. Field measurements, in general, are insufficient, particularly for wet conditions. For example, simultaneous physical and chemical measurements pertaining to plume-cloud interactions are almost nonexistent.

Detailed chemical models are not yet practical for application in regional models to predict acidic product formation and deposition. Many individual pieces of information--microphysical pathways and chemical reactions--must be put together correctly and we are still struggling to assemble an adequate information base about the individual pieces. To complicate matters, important couplings exist between the different major mechanisms of sulfate and nitrate formation (e.g., H_2O_2 formed by gas-phase photochemistry is of paramount importance in liquid-phase chemistry), and significant interdependences exist among the major influencing environmental factors. Detailed chemical models already can simulate qualitatively many field observations, but the validity of quantitative predictions based on these

models is questionable. Furthermore, their application requires substantial computational resources.

It appears that, for the foreseeable future, empirical parameterizations will serve as transformation modules in regional models. Preliminary parameterizations have been developed only for sulfate formation in power plant plumes, and will undoubtedly continue to be improved. No practical parameterizations exist yet for nitrate formation or for urban plumes. Adherence to mechanistic considerations is recommended in formulating the parameterizations. More, and more reliable, measurements of such important variables as the atmospheric concentrations of OH, H_2O_2, NH_3, HC, sulfate, and nitrate and of cloud dimensions and cloud chemical composition are needed direly.

H_2SO_4 and HNO_3 formation apparently peaks during daytime and in summer. Gas-phase mechanisms are believed to contribute a larger share, on the average, to these secondary formations under warm, sunny conditions. Typically, on a summer day (24 hr) in the eastern United States, about 25 $\pm$ 10 percent of the airborne SO_2 in power plant plumes is likely to be converted to sulfates. Nighttime conversion is a small part (about 5 percent or less). S transformations may be somewhat higher than these in the southeastern United States. HNO_3 formation rate in power plant plumes is about three times as fast as the sulfate formation rate by gas-phase mechanisms. Aerosol NO_3^- formation rate is apparently very small, at least in the summer. Both sulfate and nitrate formation are faster in urban plumes.

4.5 CONCLUSIONS

The discussion of homogeneous gas-phase reactions has led to the following conclusions:

- Organic acids produced during gas-phase oxidation of hydrocarbons are expected to make only minor or insignificant contributions to precipitation acidity because of their relatively small dissociation constants. More information is needed for assessment (Section 4.2.1).

- Acids (HX) produced from gas-phase reactions of halocarbons are also expected to make insignificant contributions to regional disposition problems; their effects on global precipitation chemistry are more plausible but uncertain. Direct anthropogenic emissions of HX are potentially important (Section 4.2.1; Chapter A-2).

- Oxidation of reduced forms of sulfur in the atmosphere generally leads to sulfur dioxide (SO_2) formation (Section 4.2.1).

- SO_2 oxidation in air is dominated by reaction with hydroxyl (OH) radicals, and although the reactions of the $HOSO_2$ adduct and other possible intermediates are unknown, the final product is sulfuric acid aerosol (Section 4.2.1).

- The average lifetime of SO_2 with respect to this reaction is approximately 3 to 4 days (Section 4.2.2).

- Of the remaining free-radical processes for SO_2 oxidation, only the reaction by peroxyalkyl radicals appears to have possible atmospheric significance; additional information is needed for assessment (Section 4.2.1).

- Gas-phase oxidation of nitrogen dioxide (NO_2) leads to a variety of products; nitric acid, dinitrogen pentoxide (N_2O_5) and peroxyacetyl nitrate (PAN) are in greatest abundance. Nitrogen trioxide and nitrous acid play active roles in photochemical cycles but make smaller direct contributions to acid deposition. Further research on the fate of PAN and N_2O_5 is direly needed (Section 4.2.1).

- The average lifetime of NO_2 with respect to reaction with hydroxyl radicals is approximately one-half day and the product is nitric acid vapor (Section 4.2.2).

- Field data tend to confirm overall transformation rates for nitrogen and sulfur oxides, as established in laboratory experiments, but fail to give conclusive evidence about dominant reaction pathways and meteorological effects. Gas-phase transformation rates in power plant plumes are usually smaller than in urban plumes because of imperfect mixing and an abundance of nitric oxide which suppresses the concentration of hydroxyl radicals (Section 4.2.3).

- The concentrations of hydroxyl radicals in the atmosphere are governed by a tightly coupled reaction cycle involving HC-CO-NO_x-O_3, but not SO_2, and the OH concentrations are not satisfactorily defined except, perhaps, on a global scale. In polluted air, the ratio of hydrocarbons (HC) to nitrogen oxides (NO_x) is expected to be a dominant variable for the OH radical concentration. The cause-effect relationships governing the free radical composition of the atmosphere need further clarification (Section 4.2.1).

- Overall, the kinetics and mechanistic details of gas-phase chemistry affecting acidic species are understood, albeit some important gaps remain. Adequate models of gas-phase chemistry can be formulated but their application to real atmospheric situations remains a problem (Sections 4.2.1, 4.2.2, and 4.2.3).

The review of the current understanding of the production of acidity within hydrometeors has led to the following conclusions:

- The production of both HNO_3 and HCl within hydrometeors is negligible compared with direct absorption of these species from the gas phase. Here, the concentration of these species in precipitation will be influenced strongly by homogeneous gas-phase chemistry (Sections 4.3.3 and 4.3.4).

- Production of H_2SO_4 in solution within hydrometeors, by any of several different mechanisms, can rival or even surpass direct absorption of H_2SO_4 by hydrometeors (Section 4.3.5).

- Of the various production mechanisms for H_2SO_4 in solution, catalyzed and uncatalyzed aerobic oxidation and oxidation by H_2O_2 appear to be most important (Section 4.3.5).

- While oxidation by H_2O_2 appears to be the single most important reaction producing H_2SO_4, the extent of its contribution to the acidity of hydrometeors will depend directly on the H_2O_2 available in solution, a parameter not well characterized at this time (Section 4.3.5).

- The amount of acid absorbed and produced in hydrometeors is such that the pH's of precipitation particles should be much lower than observed (Section 4.3.5).

- Neutralization of hydrometeor acidity by NH_3 absorption and by reaction with scavenged particulate $CaCO_3$, $MgCO_3$, and CaO may be of considerable importance (Section 4.3.6).

Considerable progress has been made in transformation modeling in recent years. Significant gaps remain, however, in our ability to predict transformation rates of SO_x and NO_x under atmospheric conditions. The following observations summarize the current status of the principal aspects of transformation modeling:

- It is now possible to simulate the principal features of the smog chamber chemistry of the SO_x-NO_x-HC system rather accurately by detailed modeling of the chemical kinetics based on lumped representations of the hydrocarbons, even though details of the chemical mechanisms are not fully understood (Section 4.4.4).

- Detailed chemical models of plume transformations under atmospheric conditions have successfully simulated many qualitative features of field observations, including some details of crosswind profiles influenced by plume-background interactions. These simulations are mainly restricted to gas-phase chemistry (Section 4.4.4).

- The principal current limitations in detailed chemical modeling are probably related to inadequate characterization of the emission field and of the ambient polluted regional background. Improved and more detailed inventories of the emissions of SO_x, NO_x, and HC from major sources, including the urban area sources, and reliable measurements of reactive species (e.g., OH, RO_2, H_2O_2) in the ambient atmosphere are needed before reliable conclusions concerning regional-scale transformation processes can be made. The relative importance of co-emissions vs background entrainment as sources of oxidizing agents (OH, RO_2, H_2O_2, etc.) is not understood at the present time (Section 4.4.4).

- Current detailed chemical models generally do not include liquid-phase chemistry. Quantitative descriptions of the liquid-phase environment (e.g., cloud dynamics, plume-cloud interaction, etc.) are not adequately incorporated into transformation models. Cloud and fog

chemistry measurements are sparse and much needed. Coupled modeling of gas- and liquid-phase chemistry is necessary, particularly under summer conditions. First steps in this direction have been taken (Sections 4.4.2 and 4.4.4).

- For the near future, it appears that transformation modules based on empirical parameterizations will continue to predominate in operational regional models. All models, to varying degrees, use parameterizations based on laboratory and field data. Currently, regional models mostly employ pseudo-first-order or constant first-order bulk conversion rates. The basis for refining these estimates to reflect at least the gross diurnal and seasonal variations, and even the role of a changing background, exists. Increasingly, new models are incorporating such empirical expressions, which are constantly being improved. The state-of-the-art of such parameterizations will be further advanced as more data are obtained and analyzed, particularly for NO_x precursors and products, for urban plumes, and for other than summer conditions. Detailed chemical models also serve to improve our understanding and basis for the formulation of empirical parameterizations which reflect the underlying physical-chemical processes rather than merely expressing statistical correlations. At this time, the major sources of uncertainty in determining atmospheric transport ranges of pollutants are probably associated with transport and deposition processes rather than with transformation processes (Sections 4.4.2 through 4.4.4).

4.6 REFERENCES

Alkezweeny, A. J. 1978. Measurements of aerosol particles and trace gases in METROMEX. J. Appl. Meteorol. 17:609-614.

Alkezweeny, A. J. and D. C. Powell. 1977. Estimation of transformation rate of SO_2 to SO_4 from atmospheric concentration data. Atmos. Environ. 11:179-182.

Altshuller, A. P. 1979. Model predictions of the roles of homogeneous oxidation of sulfur dioxide to sulfate in the troposphere. Atmos. Environ. 13:1653-1661.

Anbar, M. and H. Taube. 1954. Interaction of nitrous acid with hydrogen peroxide and with water. J. Am. Chem. Soc. 76:6243-6247.

Andrew, S. P. S. and D. Hanson. 1961. The dynamics of nitrous gas adsorption. Chem. Eng. Sci. 47:105-113.

Appel, B. R., S. M. Wall, Y. Tokiwa, and M. Haik. 1980. Simultaneous nitric acid, particulate nitrate and acidity measurements in ambient air. Atmos. Environ. 14:549-554.

Ardon, M. 1965. Oxygen, Elementary Forms and Hydrogen Peroxide. W. A. Benjamin Pub. Co., New York.

Baboolal, L. B., H. R. Pruppacher, and J. Topalian. 1981. A sensitivity study of a theoretical model of SO_2 scavenging by water drops in air. J. Atmos. Sci. 38:856-870.

Bandow, H., M. Okuda, and H. Akimoto. 1980. Mechanisms of gas-phase reactions of C_3H_6 and NO_3 radicals. J. Phys. Chem. 84:3604-3608.

Barrie, L. A. 1975. An experimental investigation of the adsorption of sulphur dioxide by cloud and raindrops containing heavy metals. Ph.D. Thesis, University of Frankfurt.

Barrie, L. and H. W. Georgii. 1976. An experimental investigation of the adsorption of sulphur dioxide by water drops containing heavy metal ions. Atmos. Environ. 10:743-749.

Barrie, L., S. Beilke, and H. W. Georgii. 1974. SO_2 removal by cloud and fog drops as affected by ammonia and heavy metals. In Precipitation Scavenging, Proceedings of a Symposium held at Champaign, Ill., Oct. 14-18. R. G. Semonin and R. W. Beadle, eds. Technical Information Center, ERDA (NTIS No. CONF - 741003).

Bassett, H. and W. G. Parker. 1951. The oxidation of sulphurous acid. J. Chem. Soc. 47:1540-1560.

Baulch, D. L., R. A. Cox, R. F. Hampson, J. A. Kerr, J. Troe, and R. T. Watson. 1980. Evaluated kinetic and photochemical data for atmospheric chemistry. J. Phys. and Chem. Ref. Data 9:295-471.

Bazzell, C. C. and L. K. Peters. 1981. The transport of photo-chemical pollutants to the background troposphere. Atmos. Environ. 15:957-968.

Beilke, S. and G. Gravenhorst. 1978. Heterogeneous SO_2-oxidation in the droplet phase. Atmos. Environ. 12:231-239.

Beilke, S., D. Lamb, and J. Muller. 1975. On the uncatalyzed oxidation of atmospheric SO_2 by oxygen in aqueous systems. Atmos. Environ. 9:1083-1090.

Benarie, M., A. Nonat, and T. Menard. 1972. The transformation of sulfur dioxide into sulfuric acid in relation to the climatology of an urban/ industrial area (Rouen, France). Intern. Clean Air Conf. May 15-18, Melbourne, Australia. pp. 176-186.

Boris, J. P. and D. L. Book. 1973. Flux corrected transport. I. SHASTA, an algorithm that works. J. Comp. Phys. 11:38-69.

Bottenheim, J. W. and O. P. Strausz. 1979. The effect of a polluting source on the air quality downwind of pristine northern areas. Atmos. Environ. 13:1085-1089.

Breeding, R. J., H. B. Klonis, J. P. Lodge, J. B. Pate, D. C. Sheesley, T. R. Englert, and D. R. Sears. 1976. Measurements of atmospheric pollutants in the St. Louis area. Atmos. Environ. 10:181-194.

Brimblecome, P. and D. J. Spedding. 1974. The catalytic oxidation of micromolar aqueous sulphur dioxide-I. (Oxidation of dilute solutions by iron (III)). Atmos. Environ. 8:937-945.

Brodzinsky, R., S. G. Chang, S. S. Markowitz, and T. Novakov. 1980. Kinetics and mechanisms for the catalytic oxidation of sulfur dioxide on carbon in aqueous suspensions. J. Phys. Chem. 84:3354-3358.

Cahir, J. J., J. N. Pitts, J. Ross, S. A. Twomey, and J. R. Wiesenfeld. 1982. The source-receptor relationship in acid precipitation: Implications for generation of electric power from coal. Physical Dynamics, Inc. Report No. PD-LJ-82-268R on Workshop of January 18-22.

Calvert, J. C., S. Fu, J. W. Bottenheim, and O. P. Strausz. 1978. Mechanism of the homogeneous oxidation of sulfur dioxide in the troposphere. Atmos. Environ. 12:197-226.

Cantrell, B. K. and K. T. Whitby. 1978. Aerosol size distributions and aerosol volume formation for a coal fired power plant plume. Atmos. Environ. 12:323-333.

Carmichael, G. R. and L. K. Peters. 1979. Numerical simulation of the regional transport of SO_2 and sulfate in the eastern United States. Preprint, 4th. AMS Symp. Turbulence, Diffusion, and Air Pollution. Reno, NV. January 15-18.

Castleman, A. W., R. E. Davis, H. R. Munkelwitz, I. N. Tang, and W. P. Wood. 1975. Kinetics of association reactions pertaining to sulfuric acid aerosol formation. Int. J. Chem. Kinet. Symp. 1:629.

Chang, S. G., R. Toorsi, and T. Novakov. 1981. The importance of soot particles and nitrous acid in oxidizing SO_2 in atmospheric aqueous droplets. Atmos. Environ. 15:1287-1292.

Clark, W. W., D. A. Landis, and A. B. Harker. 1976. Measurements of the photochemical production of aerosols in ambient air near a freeway for a range of SO_2 concentrations. Atmos. Environ. 10:637-644.

Commins, B. T. 1963. Determination of particulate acid in town air. Analyst 88:364-367.

Cox, R. A. and S. A. Penkett. 1972. Aerosol formation from sulfur dioxide in the presence of ozone and olefinic hydrocarbons. J. Chem. Soc. Faraday Trans. I. 68:1735-1753.

Cox, R. A., and M. J. Roffey. 1977. Thermal decomposition of peroxyacetyl nitrate in the presence of nitric oxide. Environ. Sci. Technol. 11:900-906.

Cox, R. A. and D. Sheppard. 1980. Reactions of OH radicals with gaseous sulfur compounds. Nature 284:330-331.

Criegee, R. 1957. The course of ozonation of unsaturated compounds. Record Chem. Progr. 18:111-120.

Crutzen, P. J. 1974. Photochemical reactions initiated by and influencing ozone in unpolluted tropospheric air. Tellus 26:47-56.

Dasgupta, P. K. 1980a. Discussion of the importance of atmospheric ozone and hydrogen peroxide in oxidizing sulphur dioxide in cloud and rainwater. Atmos. Environ. 14:272-274.

Dasgupta, P. K. 1980b. Further discussion of the importance of atmospheric ozone and hydrogen peroxide in oxidizing sulphur dioxide in cloud and rainwater. Atmos. Environ. 14:620-621.

Davis, D. D. and G. Klauber. 1975. Atmospheric gas phase oxidation mechanisms for the molecule SO_2. Int. J. Chem. Kinet. Symp. 1:543-556.

Davis, D. D., A. R. Ravishankara, and S. Fischer. 1979. SO_2 oxidation via the hydroxyl radical: Atmospheric fate of HSO_x radicals. Geophys. Res. Lett. 6:113-116.

Davis, W. Jr. and H. J. de Bruin. 1964. New activity coefficients of 0-100 percent aqueous nitric acid. J. Inorg. Nucl. Chem. 26:1069-1088.

Dawson, G. A., J. C. Farmer, and J. L. Moyers. 1980. Formic and acetic acids in the atmosphere of the southwest USA. Geophys. Res. Lett. 9:725-728.

Demerjian, K. L. and K. L. Schere. 1979. Applications of a photochemical box model for ozone air quality in Houston, Texas. Proc. APCA Conference on Ozone/Oxidants: Interactions with the Total Environment II, Houston, TX. October 14-17.

Demerjian, K. L., J. A. Kerr, and J. G. Calvert. 1974. The mechanism of photochemical smog formation. In Advances in Environmental Science and Technology, Vol. 4, John Wiley, N.Y. 262p.

Demore, W. B., L. J. Stief, F. Kaufman, D. M. Golden, R. F. Hampson, M. H. Kurylo, J. J. Margitan, M. J. Molina, and R. T. Watson. 1981. Chemical kinetic and photochemical data for use in stratospheric modeling. JPL Publication 81-3, California Inst. of Tech., Pasadena, CA.

Dimitriades, B., M. C. Dodge, J. J. Bufalini, K. L. Demerjian, and A. P. Altshuller. 1976. Letter to the Editor. Environ. Sci. Technol. 10:934-936.

Dinger, J. E., H. B. Howell, and T. A. Wojciechowski. 1970. On the source and composition of cloud nuclei in a subsident air mass over the North Atlantic. J. Atmos. Sci. 17:791-797.

Dittenhoefer, A. C. and R. G. de Pena. 1980. Sulfate aerosol production and growth in coal-fired power plant plumes. J. Geophys. Res. 85, No. C-8, 4499-4506.

Donaldson, C. D. and G. R. Hilst. 1972. Effects of inhomogeneous mixing on atmospheric photochemical reactions. Environ. Sci. Technol. 6:812-816.

Drozdova, V. M. and E. P. Makhon'ko. 1970. Content of trace elements in precipitation. J. Geophys. Res. 18:3610-3612.

Duce, R. A. 1969. On the source of gaseous chlorine in the marine atmosphere. J. Geophys. Res. 74:4597-4599.

Duecker, W. and J. West (eds.). 1959. The Manufacture of Sulfuric Acid. American Chemical Society Monograph Series No. 144.

Duewer, W. H., M. C. McCracken, and J. J. Walton. 1978. The Livermore Regional Air Quality Model: II. Verification and sample application in the San Francisco Bay area. J. Appl. Meteorol. 17:273-311.

Durham, J. L., J. H. Overton, Jr., and V. P. Aneja. 1981. Influence of gaseous nitric acid on sulfate production and acidity in rain. Atmos. Environ. 15:1059-1068.

Easter, R. C. and P. V. Hobbs. 1974. The formation of sulfates and the enhancement of cloud condensation nuclei in clouds. J. Atmos. Sci. 31:1586-1594.

Easter, R. C., K. M. Busness, J. M. Hales, R. N. Lee, D. A. Arbuthnot, D. F. Miller, G. M. Sverdrup, C. W. Spicer, and J. E. Howes. 1980. Plume conversion rates in the SURE region. EPRI EA-1498, 1-2. Electric Power Research Institute, Palo Alto, CA.

Eatough, D. J., B. E. Richter, N. L. Eatough, and L. D. Hansen. 1981. Sulfur chemistry in smelter and power plant plumes in the western U.S. Atmos. Environ. 15(10):2241-2253.

Eigen, M. 1967. Proton transfer and general acid base catalysis. In Fast Reactions and Primary Processes in Chemical Kinetics. Interscience Publishers, New York, NY.

Eliassen, A. and J. Saltbones. 1975. Decay and transformation rates of SO_2 as estimated from emission data, trajectories and measured air concentrations. Atmos. Environ. 9:425-429.

Elshout, A. J., J. W. Viljeer, and H. Van Duren. 1978. Sulfates and sulfuric acid in the years 1971-1976 in the Netherlands. Atmos. Environ. 12:785-790.

England, C. and W. H. Corcoran. 1974. Kinetics and mechanisms of the gas-phase reaction of water vapor and nitrogen dioxide. Ind. Eng. Chem. Fundam. 13:373-384.

Erickson, R. E., L. M. Yates, R. L. Clark, and D. McEwen. 1977. The reaction of sulfur dioxide with ozone in water and its possible atmospheric significance. Atmos. Environ. 11:813-817.

Eriksson, E. 1960. The yearly circulation of chloride and sulfur in nature; meteorological, geochemical and pedological implications. Part II. Tellus 12:63-109.

Falconer, R. E. and P. D. Falconer. 1979. Determination of cloud water acidity at a mountain observatory in the Adirondack Mountains of New York state. Publication 741, Atmospheric Sciences Research Center, SUNY, Albany, NY.

Falls, A. H. and J. H. Seinfeld. 1978. Continued development of a kinetic mechanism for photochemical smog. Environ. Sci. Technol. 12:1398-1406.

Falls, A. H., G. J. McRae, and J. H. Seinfeld. 1979. Sensitivity and uncertainty of reaction mechanisms for photochemical air pollution. Int. J. Chem. Kinetics 11:1137-1162.

Farrow, L. A. and D. Edelson. 1974. The steady-state approximation: Fact or fiction? Int. J. Chem. Kinetics 6:787-800.

Fishman, J. and P. J. Crutzen. 1978. The distribution of the hydroxyl radical in the troposphere. Atmospheric Science Paper No. 284, Colorado State University, Boulder.

Flack, W. W. and M. J. Matteson. 1979. Mass transfer of gases to growing water droplets. In Polluted Rain, T. Y. Toribara, M. W. Miller, and P. E. Morrow, eds. Plenum Press, New York, NY.

Forrest, J., R. Garber, and L. Newman. 1979. Formation of sulfate, ammonium and nitrate in an oil-fired power plant plume. Atmos. Environ. 13:1287-1297.

Forrest, J., R. Garber, and L. Newman. 1981. Conversion rates in power plant plumes based on filter pack data - Part I: The coal-fired Cumberland plume. Atmos. Environ. 15:2273-2282.

Forrest J. F., S. E. Schwarts, and L. Newman. 1979. Conversion of sulfur dioxide to sulfate during the Da Vinci flights. Atmos. Environ. 13:157-167.

Freiberg, J. 1974. Effects of relative humidity and temperature on iron-catalyzed oxidation of SO_2 in atmospheric aerosols. Environ. Sci. Technol. 8:731-734.

Freiberg, J. E. and S. E. Schwartz. 1981. Oxidation of SO_2 in aqueous droplets: Mass-transport limitation in laboratory studies and the ambient atmosphere. Atmos. Environ. 15:1145-1154.

Friedlander, S. K. 1978. A review of the dynamics of sulfate containing aerosols. Atmos. Environ. 12:187-195.

Fuller, E. C. and R. H. Crist. 1941. The rate of oxidation of sulfite ions by oxygen. Am. Chem. Soc. 63:1644-1650.

Galloway, J. N. and G. E. Likens. 1981. Acid precipitation: The importance of nitric acid. Atmos. Environ. 15:1081-1086.

Gear, C. W. 1971. Chapter 11 in Numerical Initial Value Problems in Ordinary Differential Equations. Prentice-Hall, Englewood Cliffs, NJ.

Georgii, H. W. 1970. Contributions to the atmospheric sulfur budget. J. Geophys. Res. 75:2365-2371.

Georgii, H. W. 1978. Large scale spatial and temporal distribution of sulfur compounds. Atmos. Environ. 12:681-690.

Gillani, N. V. 1978. Project MISTT: Mesoscale plume modeling of the dispersion, transformation and ground removal of SO_2. Atmos. Environ. 12:569-588.

Gillani, N. V. and W. E. Wilson. 1980. Formation and transport of ozone and aerosols in power plant plumes. Annals N.Y. Acad. Sci. 338:276-296.

Gillani, N. V. and W. E. Wilson. 1983. Gas-to-particle conversion of sulfur in power plant plumes: II. Observations of liquid phase conversions. Atmos. Environ. 17(9): 1739-1752.

Gillani, N. V., J. A. Colby, and W. E. Wilson. 1983. Gas-to-particle conversion of sulfur in power plant plumes: III. Parameterization of plume-cloud interactions. Atmos. Environ. 17(9): 1753-1764.

Gilliani, N. V., R. B. Husar, D. E. Patterson, and W. E. Wilson. 1978. Project MISTT: Kinetics of particulate sulfur formation in a power plant plume out to 300 km. Atmos. Environ. 12:589-598.

Gillani, N. V., S. Kohli, and W. E. Wilson. 1981. Gas to particle conversion of sulfur in power plant plumes: I. Parameterization of the conversion rate for dry, moderately polluted ambient conditions. Atmos. Environ. 15:2293-2313.

Gordon, G. E., D. D. Davis, G. W. Israel, H. E. Landsberg, T. C. O'Haver, S. W. Staley, and W. H. Zoller. 1975. Atmospheric impact of major sources and consumers of energy. Progress Report-75, EPA Grant No. ESR75-02667.

Gorham, E. 1958. Atmospheric pollution by hydrochloric acid. Quart. J. R. Met. Soc. 84:274-276.

Graedel, T. E., L. A. Farrow, and T. A. Weber. 1976. Kinetic studies of the photochemistry of the urban troposphere. Atmos. Environ. 10:1095-1116.

Graedel, T. E., L. A. Farrow, and T. A. Weber. 1978. Urban kinetic calculations with altered source conditions. Atmos. Environ. 12:1403-1412.

Graham, R. A. and H. S. Johnston. 1978. The photochemistry of NO_3 and the kinetics of the N_2O_5 - system. J. Phys. Chem. 82:254-268.

Graham, R. A., A. M. Winer, R. Atkinson, and J. N. Pitts. 1979. Rate constants for the reaction of HO_2, SO_2, CO, N_2O, trans-2-butene and 2, 3-dimethyl-2-butene at 300 K. J. Phys. Chem. 18:1563-1567.

Graham, R. A., A. M. Winer, and J. N. Pitts, Jr. 1977. Temperature dependence of the unimolecular decomposition of pernitric acid and its atmospheric implications. Chem. Phys. Letters 51:215-220.

Groblicki, P. J. and G. J. Nebel. 1971. The photochemical formation of aerosols in urban atmospheres, pp. 241-267. In Chemical Reactions in Urban Atmospheres. C. S. Tuesday, ed. American Elsevier, New York.

Hales, J. M. and D. R. Drewes. 1979. Solubility of ammonia in water at low concentrations. Atmos. Environ. 13:1133-1147.

Halfpenny, E. and P. L. Robinson. 1952. Pernitrous acid. The reaction between hydrogen peroxide and nitrous acid, and the properties of an intermediate product. J. Chem. Soc. 48:928-938.

Hampson, R. F., Jr. and D. Garvin. 1977. Reaction rate and photochemical data for atmospheric chemistry. NBS Special Publication, U.S. Dept. of Commerce.

Hanst, P. L., N. W. Wong, and J. Bragin. 1982. A long path infra-red study of Los Angeles smog. Atmos. Environ. 16:969-981.

Harrison, H., T. V. Larson, and C. S. Monkton. 1982. Aqueous phase oxidation of sulfites by ozone in the presence of iron and manganese. Atmos. Environ. 16(5):1039-1042.

Hecht, T. A., J. H. Seinfeld, and M. C. Dodge. 1974. Further development of generalized kinetic mechanism for photoche ical smog. Environ. Sci. Technol. 8:327-339.

Hegg, D. A. and P. V. Hobbs. 1978. Oxidation of sulfur dioxide in aqueous systems with particular reference to the atmosphere. Atmos. Environ. 12:241-253.

Hegg, D. A. and P. V. Hobbs. 1979a. The homogeneous oxidation of sulfur dioxide in cloud droplets. Atmos. Environ. 13:981-987.

Hegg, D. A. and P. V. Hobbs. 1979b. Some observations of particulate nitrate concentration in coal-fired power plant plumes. Atmos. Environ. 13:1715-1716.

Hegg, D. A. and P. V. Hobbs. 1980. Measurements of gas-to-particle conversion in the plumes from five coal-fired electric power plants. Atmos. Environ. 14:99-116.

Hegg, D. A. and P. V. Hobbs. 1981a. Cloud water chemistry and the production of sulfates in clouds. Atmos. Environ. 15:1597-1604.

Hegg, D. A. and P. V. Hobbs. 1981b. Field Studies of the oxidation of SO^2 in clouds. Quarterly Progress Report for April 1-June 30. EPA Grant R805263010, Dept. of Atmospheric Sciences, University of Washington, Seattle, WA.

Hegg, D. A. and P. V. Hobbs, and L. F. Radke. 1980. A preliminary study of cloud chemistry, pp. 7-10. In Preprint Volume, E hth Intern. Conf. on the Physics of Clouds, Clermont-Ferrand, France.

Hendry, C. D. and P. L. Brezonik. 1980. Chemistry of precipitation at Gainesville, Florida. Environ. Sci. Technol. 14:843-849.

Hesstvedt, E., O. Hov, and I. Isaksen. 1978. Quasi-steady-state approximations in air pollution modeling: Comparisons of two numerical schemes for oxidant prediction. Int. J. Chem. Kinetics 10:971-994.

Hidy, G. M. 1982. Potential fallacy in assuming linear proportionality between SO_2 emissions and acid deposition. Paper presented at Second National Symposium on Acid Rain, Pittsburgh, PA, October 6-7.

Hidy, G. M., P. K. Mueller, and E. Y. Tong. 1978. Spatial and temporal distributions of airborne sulfate in parts of the United States. Atmos. Environ. 12:735-752.

Hitchcock, D. R., L. L. Spriller, and W. E. Wilson. 1980. Sulfuric acid aerosols and HCl release in coastal atmospheres: Evidence of rapid formation of sulfuric acid particulates. Atmos. Environ. 14:165-182.

Hobbs, P. V. 1979. A reassessment of the mechanisms responsible for the sulfur content of acid rain. In Proceedings: Advisory Workshop to Identify Research Needs on the Formation of Acid Precipitation. Electric Power Research Institute Rpt. EA-1074.

Hobbs, P. V., D. A. Hegg, M. W. Eltgroth, and L. F. Radke. 1978. Evolution of particles in the plumes of coal-fired electric power plants. Atmos. Environ. 12:935-951.

Hoffman, M. R. and J. O. Edwards. 1975. Kinetics of the oxidation of sulfite by hydrogen peroxide in acidic solution. J. Phys. Chem. 79:2096-2098.

Hov, O. 1983a. Numerical solution of a simplified form of the diffusion equation for chemically reactive atmospheric species. Atmos. Environ. 17:551-562.

Hov, O. 1983b. One-dimensional vertical model for ozone and other gases in the atmospheric boundray layer. Atmos. Environ. 17:535-550.

Hov, O. 1983c. Aspects of the parameterization of transformation and removal processes in air quality modeling. Paper presented at the 14th NATO International Technical Meeting on Air Pollution Modeling and Its Applications, Copehagen, September 27-30.

Hov, O., I. S. A. Isaksen. 1981. Generation of secondary pollutants in a power plant plume: A model study. Atmos. Environ. 15:2367-2376.

Hov, O., I. S. A. Isaksen, and E. Hesstvedt. 1977. Diurnal variations of ozone and other pollutants in an urban area. Report No. 24, Institute for Geophysics, Univ. of Oslo.

Huebert B. J. and A. L. Lazrus. 1978. Global tropospheric measurements of nitric acid vapor and particulate nitrate. Geophys. Res. Lett. 5:577-580.

Huebert, B. J. and A. L. Lazrus. 1979. Tropospheric measurements of nitric acid vapor and particulate nitrate. In Nitrogeneous Air Pollutants. D. Grosjean, ed. Ann Arbor Science, Ann Arbor, MI.

Huntzicker, J. J., R. A. Cary, and C. Ling. 1980. Neutralization of sulfuric acid aerosol by ammonia. Environ. Sci. Technol. 14:819-824.

Husar, R. B. and D. E. Patterson. 1980. Regional scale air pollution: Sources and effects. Annals N.Y. Acad. Sci. 338:399-417.

Husar, R. B. and Patterson. 1980. Regional scale air pollution: Sources and effects. Annals N.Y. Acad. Sci. 338:399-417.

Husar, R. B. and D. E. Patterson, J. D. Husar, N. V. Gillani, and W. E. Wilson. 1978. Sulfur budget of a power plant plume. Atmos. Environ. 12:549-568.

International Critical Tables 3. 1928. Washburn, E. W., ed. McGraw-Hill, New York, NY.

Isaksen, I. S. A., E. Hesstvedt, and O. Hov. 1978. A chemical model for urban plumes: Test for ozone and particulate sulfur formation in the St. Louis urban plume. Atmos. Environ. 12:599-604.

Jeffries, H. E. and M. Saeger. 1976. Letter to the Editor. Environ. Sci. and Technol. 10:936-937.

Johnstone, H. J. and P. W. Leppla. 1934. The solubility of sulfur dioxide at low partial pressures. J. Amer. Chem. Soc. 56:2233-2238.

Joseph, D. W. and C. W. Spicer. 1978. Chemiluminescence method for atmospheric monitoring of nitric acid and nitrogen oxides. Anal. Chem. 50:1400-1403.

Jost, D. 1974. Aerological studies on the atmospheric sulfur budget. Tellus 26:206-212.

Junge, C. and T. G. Ryan. 1958. Study of SO_2 in oxidation in solution and its role in atmospheric chemistry. Quart. J. R. Met. Soc. 84:46-55.

Kameoka, Y. and R. L. Pigford. 1977. Adsorption of nitrogen dioxide into water, sulfuric acid, sodium hydroxide, and alkaline sodium sulfite aqueous solutions. Ind. Eng. Chem. Fundam. 16:163-169

Kan, C. S., J. G. Calvert, and J. H. Shaw. 1981. Oxidation of sulfur dioxide by methylperoxy radicals. J. Phys. Chem. 85:1126-1132.

Kan, C. S., R. D. McQuigg, M. R. Whitbeck, and J. Calvert. 1979. Kinetic flash spectroscopic study of the CH_3O_2 and CH_3O_2 - SO_2 reactions. Int. J. Chem. Kinetics 11:921-933.

Kaplan, D., D. Himmelblau, and C. Kanoaka. 1981. Oxidation of sulfur dioxide in aqueous ammonium sulfate aerosols containing manganese as a catalyst. Atmos. Environ. 15:763-773.

Kasina, S. 1980. On precipitation acidity in southeastern Poland. Atmos. Environ. 14:1217-1221.

Kelly, T. J., D. H. Stedman, and G. L. Kok. 1979. Measurements of H_2O_2 and HNO_3 in rural air. Geophys. Res. Lett. 6:375-378.

Kocmond, W. C. and J. Y. Yang. 1976. Sulfur dioxide photoxidation rates, and aerosol formation mechanisms, a smog chamber study. EPA 600/3-76-0900, U.S. Environmental Protection Agency, Research Triangle Park, NC.

Kok, G. L. 1980. Measurements of hydrogen peroxide in rainwater. Atmos. Environ. 14:653-656.

Komiyama, H. and H. Inoue. 1980. Adsorption of nitrogen oxides into water. Chem. Eng. Sci. 35:154-161.

Kritz, M. A. and J. Rancher. 1980. Circulation of Na, Cl, and Br in the tropical marine atmosphere. J. Geophys. Res. 85:1633-1639.

Kuhlman, M. R., D. L. Fox, and H. E. Jeffries. 1978. The effect of CO on sulfate aerosol formation. Atmos. Environ. 12:2415-2423.

Lamb, R. G. 1981. A regional scale (1000 km) model of photochemical air pollution: I. Theoretical formulation. U.S. EPA. Technical Report. In press.

Lamb, R. G. and W. R. Shu. 1978. A model of second-order chemical reaction in turbulent fluid - part I. Atmos. Environ. 12:1685-1694.

Larson, T. and H. Harrison. 1977. Acidic sulfate aerosols: Formation from heterogeneous oxidation by O_3 clouds. Atmos. Environ. 11:1133-1141.

Larson, T., R. Charlson, E. Knudson, G. Christian, and H. Harrison. 1975. The influence of a sulfur dioxide point source on the rain chemistry of a single storm in the Puget Sound region. Water, Air, Soil Pollut. 4:319-328.

Larson, T., N. Horiko, and H. Harrison. 1978. Oxidation of sulfur dioxide by oxygen and ozone in aqueous solution: a kinetic study with significance to atmospheric rate processes. Atmos. Environ. 12:1597-1611.

Lau, N. C. and R. J. Charlson. 1977. On the discrepancy between background atmospheric ammonia gas measurements and the existence of acid sulfates as a dominant atmospheric aerosol. Atmos. Environ. 11:475-478.

Lazrus, A. L., P. L. Haggenson, G. L. Kok, B. J. Huebert, C. W. Kreitzberg, G. E. Likens, V. A. Mohnen, W. E. Wilson, J. W. Winchester. 1983. Acidity in air and water in a case of warm frontal precipitation. Atmos. Environ. 17:581-592.

Lee, R. E. and D. J. von Lehmden. 1973. Trace metal pollution in the environment. J. Air. Pollu. Control Assoc. 23:853-857.

Lee, Y. N. and S. E. Schwartz. 1981. Evaluation of the rate of uptake of nitrogen dioxide by atmospheric and sulfate liquid water. J. Geophys. Res. 86:11971-11983.

Leu, M. T. and R. H. Smith. 1981. Kinetics of the gas phase reactions between hydroxyl and carbonyl sulphide over the temperature range 300-517 K. J. Phys. Chem. 85:2570.

Levine, J. S., T. R. Augustsson, and J. M. Hoell. 1980. The vertical distribution of tropospheric ammonia. Geophys. Res. Lett. 17:317-320.

Levine, S. Z. 1981. A model for stack plumes reactions with atmospheric dilution (SPREAD). Atmos. Environ. 15:2573-2581.

Levine, S. Z. and S. E. Schwartz. 1982. Construction and testing of a Surrogate CHEmical MEchanism (SCHEME) for tropospheric photochemical reactions. Chap. 11. In Trace Atmospheric Constituents, S. E. Schwartz, ed. Vol. 12 in Advance's in Environmental Science and Technology. John Wiley & Sons, Inc., New York.

Lewis, C. W. and E. S. Macias. 1980. Composition of size-fractionated aerosol in Charleston, West Virginia. Atmos. Environ. 14:185-194.

Liljestrand, H. M. and J. J. Morgan. 1981. Spatial variations of acid precipitation in southern California. Environ. Sci. Technol. 15:333-338.

Lusis, M. A., K. G. Anlauf, L. A. Barrie, and H. A. Wiebe. 1978. Plume chemistry studies at a northern Alberta power plant. Atmos. Environ. 12:2429-2437.

Mader, R. M. 1958. Kinetics of the hydrogen peroxide-sulfite reaction in alkaline solution. J. Amer. Chem. Soc. 80:2634-2639.

Marsh, A. R. W. 1978. Sulphur and nitrogen contributions to the acidity of rain. Atmos. Environ. 12:401-406.

Martin, L. R., and D. E. Damschen. 1981. Aqueous oxidation of sulfur dioxide by hydrogen peroxide at low pH. Atmos. Environ. 9:1615-1621.

Martin, L. R., D. E. Damschen, and H. L. Judeiker. 1981. The reactions of nitrogen oxides with SO_2 in aqueous aerosols. Atmos. Environ. 15:191-195.

McClenny, W. A. and C. A. Bennett, Jr. 1980. Integrative technique for detection of atmospheric ammonia. Atmos. Environ. 14:641-645.

McCracken, M. C., D. J. Wuebbles, J. J. Walton, W. H. Duewer, and K. E. Grant. 1978. The Livermore Regional Air Quality (LIRAQ) model: I. Concept and development. J. Appl. Meteorol. 17:254-272.

McDonald, C. and H. J. Duncan. 1979. Particle size distribution of metals in the atmosphere of Glasgow. Atmos. Environ. 13:977-980.

McKay, H. A. C. 1971. The atmospheric oxidation of sulfur dioxide in water droplets in the presence of ammonia. Atmos. Environ. 5:7-14.

McMurry, P. H., and J. C. Wilson. 1982. Growth laws for formation of secondary ambient aerosols: Implications for chemical conversion mechanisms. Atmos. Environ. 16:121-134.

McMurry, P. H., D. J. Rader, and J. Stith. 1981. Growth laws for secondary aerosols in power plant plumes: Implications for chemical conversion mechanisms. Atmos. Environ. 15:2315-2327.

McNaughton, D. J. and B. C. Scott. 1980. Modeling evidence of in cloud transformation of sulfur dioxide to sulfate. J. Air. Pollut. Control Assoc. 30:272-273.

McNelis, D. N. 1974. Aerosol formation from gas-phase reactions of ozone and olefin in the presence of sulfur dioxide. EPA 650/4-74-034, U.S. Environmental Protection Agency, Research Triangle Park, NC.

McRae, G. J., W. R. Goodin, and J. H. Seinfeld. 1979. Development of a second-generation airshed model for photochemical air pollution. Proc. 4th AMS Symp. on Turbulence, Diffusion and Air Pollution, Reno, Nevada, January 15-19.

Meszaros, E., D. J. Moore, and J. P. Lodge. 1977. Sulfur dioxide-sulfate relationships in Budapest. Atmos. Environ. 11:345.

Middleton, P., C. S. Kiang, and V. A. Mohnen. 1980. Theoretical estimates of the relative importance of various urban sulfate aerosol production mechanisms. Atmos. Environ. 14:463-472.

Miller, D. F. 1978. Precurser effects on SO_2 oxidation. Atmos. Environ. 12:273-280.

Miller, D. F. 1980. A model of SO_2 oxidation in smog. EPA, U.S. Environmental Protection Agency, Research Triangle Park, NC.

Miller, D. F. and A. J. Alkezweeny. 1980. Aerosol formation in urban plumes over Lake Michigan. Annals. N.Y. Acad. Sci. 338:219-232.

Miller, D. F. and C. W. Spicer. 1975. Measurements of nitric acid in smog. J. Air. Poll. Control Assoc. 25:940-942.

Miller, D. F., A. J. Alkezweeny, J. M. Hales, and R. N. Lee. 1978. Ozone formation related to power plant emissions. Science 202:1186-1188.

Miller, J. M. and R. de Pena. 1972. Contribution of scavenged sulfur dioxide to the sulfate of rainwater. J. Geophys. Res. 30:5905-5916.

Miller, M. S., S. K. Friedlander, and G. M. Hidy. 1972. A chemical element balance for the Pasadena aerosol. In Aerosols and Atmospheric Chemistry, G. M. Hidy, ed. Academic Press, New York, NY.

Mills, E. L., C. B. Murphy Jr., and J. A. Bloomfield. 1979. Oxidants in precipitation. In Polluted Rain. T. Y. Toribara, M. W. Miller and P. E. Morrow, eds. Plenum Press, New York, NY.

Moller, D. 1980. Kinetic model of atmospheric SO_2 oxidation based on published data. Atmos. Environ. 14:1067-1076.

Nash, T. 1979. The effect of nitrogen dioxide and of some transition metals on the oxidation of dilute bisulphite solutions. Atmos. Environ. 13:1149-1154.

National Academy of Sciences. 1976. Chlorine and hydrogen chloride. In Medical and Biologic Effects of Environmental Pollutants. National Academy Press, Washington, DC.

National Academy of Sciences. 1983. Acid deposition - Atmospheric Processes in Eastern North American, National Academy of Sciences Report, National Academy Press, Washington, D.C.

Newman, L. 1979. General considerations on how rainwater must obtain sulfate nitrate and acid. In Proceedings of the International Symposium on Sulphur Emission to the Environment, London, UK.

Newman, L. 1981. Atmospheric oxidation of sulfur dioxide as viewed from power plant and smelter plume studies. Atmos. Environ. 15(11):2231-2239.

Noxon, J. F. 1975. NO_2 in the stratosphere and troposphere by ground based absorption spectroscopy. Science 189:547-549.

Noxon, J. F., R. B. Norton, and E. Marovich. 1980. NO_3 in the troposphere. Geophys. Res. Lett. 7:125-128.

Oblath, S. B., S. S. Markowitz, T. Novakov, and S. G. Chang. 1981. Kinetics of the formation of hydroxylamine disulfonate by reactions of nitrites with sulfites. J. Phys. Chem. 85:1017-1021.

Organization for Economic Cooperation and Development. 1977. The OECD programme on long range transport of air pollutants: Measurements and findings. Final Report. Organization for Economic Cooperation and Development, Paris.

Ogren, J. A. 1980. Deposition of particulate elemental carbon from the atmosphere. Presented at General Motors International Symposium on Particulate Carbon: Atmospheric Life Cycle, Warren, MI, October 13-14.

Okita, T., K. Kaneda, T. Yanaka, and R. Sugai. 1974. Determination of gaseous and particulate chloride and fluoride in the atmosphere. Atmos. Environ. 8:927-936.

Penkett, S. A. 1972. Oxidation of SO_2 and other atmospheric gases by ozone in aqueous solution. Nature Physical Science 240:105-106.

Penkett, S. A., B. M. R. Jones, K. A. Brice, and A. E. J. Eggleton. 1979. The importance of atmospheric ozone and hydrogen peroxide in oxidizing sulfur dioxide in cloud and rainwater. Atmos. Environ. 13:123-137.

Perner, D. and U. Platt. 1979. Detection of nitric acid in the atmosphere by differential optical adsorption. Geophys. Res. Lett. 6:917-920.

Petrenchuk, O. P. and V. M. Drozdova. 1966. On the chemical composition of cloud water. Tellus 18:280-286.

Petrenchuk, O. P. and E. S. Selezneva. 1970. Chemical composition of precipitation in regions of the Soviet Union. J. Geophys. Res. 75:3629-3634.

Platt, U., D. Perner, J. Schroder, C. Kessler, and A. Toennissen. 1981. The diurnal variation of NO_3. J. Geophys. Res. 86:11965-11970.

Platt, U., D. Perner, A. M. Winer, G. W. Harris, and J. Pitts Jr. 1980. Detection of NO_3 in the polluted troposphere by differential optical adsorption. Geophys. Res. Lett. 7:89-92.

Prahm, L. P., U. Torp, and R. M. Stern. 1976. Deposition and transformation rates of sulfur oxides during atmospheric transport over the Atlantic. Tellus 28:355-372.

Pueschel, R. V. and C. C. Van Valin. 1978. Cloud nucleus formation in a power plant plume. Atmos. Environ. 12:307-312.

Radke, L. F. 1970. Field and laboratory measurements with an improved automatic cloud condensation nucleus counter. Preprints of Papers Presented at the American Meteorological Society, Conference on Cloud Physics, Fort Collins, CO, August 24-27, 1970:7-8.

Radke, L. R. and P. V. Hobbs. 1969. Measurements of cloud condensation nuclei, light scattering coefficient, sodium-containing particles, and Aitken nuclei in the Olympic Mountains of Washington. J. Atmos. Sci. 26:281-288.

Reynolds, S. D., T. W. Tesche, and L. E. Reid. 1979. An introduction to the SAI airshed model and its usage. SAI Technical Report EF 79-31. Systems Applications, Inc., San Rafael, CA.

Richards, L. W., J. A. Anderson, D. L. Blumenthal, A. A. Brandt, J. A. McDonald, N. Watus, E. S. Macias, and P. S. Bhardwaja. 1981. The chemistry aerosol physics, and optical properties of a western coal-fired power plant. Atmos. Environ. 15:2111-2134.

Robbins, R. C., R. D. Cadle, and D. L. Eckhardt. 1959. The conversion of sodium chloride to hydrogen chloride in the atmosphere. J. Meteorol., 16:53-56.

Roberts, P. T. and S. K. Friedlander. 1975. Conversion of SO_2 to sulfur particulate in the Los Angeles atmosphere. Environ. Health Prospective 10:103-108.

Robinson, E. and R. E. Robbins. 1969. Sources, abundance and fate of gaseous atmospheric pollutants. Report 6755, Stanford Res. Inst., Menlo Park, CA.

Rodhe, H. 1978. Budgets and turnover times of atmospheric sulfur compounds. Atmos. Environ. 12:671-680.

Rodhe, H., P. Crutzen, and A. Vanderpol. 1979. Formation of sulfuric and nitric acid in the atmosphere during long range transport. Proc. WMO Symposium on Long Range Transport of Pollutants, Sofia, Bulgaria, October 1-5.

Sadasivan, S. 1980. Trace constituents in cloud water, rainwater and aerosol samples collected near the west coast of India during the southwest monsoon. Atmos. Environ. 14:33-38.

Sander, S. P. and R. T. Watson. 1981. A kinetics study of the reactions of SO_2 with CH_3O_2. Chem. Phys. Lett. 77:473-475.

Sanhueza, E., R. Simonintis, and J. Heicklen. 1979. The reaction of CH_3O_2 with SO_2. Int. J. Chem. Kinetics 11:907-914.

Saxena, V. K., J. N. Burford, and J. L. Kassner. 1970. Operation of a thermal diffusion chamber for measurements on cloud condensation nuclei. J. Atmos. Sci. 27:73-80.

Scatchard, G., G. M. Havanagh, and L. B. Ticknor. 1952. Vapor-liquid equilibrium. VIII. Hydrogen peroxide-water mixtures. J. Amer. Chem. Soc. 74:3715-3720.

Schroeter, L. C. 1963. Kinetics of air oxidation of sulfurous acid salts. J. Pharm. Sci. 52:559-563.

Schroeter, L. C. 1966. Sulfur Dioxide: Application in Foods, Beverages, and Pharmaceuticals. Pergamon Press, Oxford, UK.

Schwartz, S. E. 1982. Gas-aqueous reactions of sulfur and nitrogen oxides in liquid water clouds. Presented at Acid Rain Symposium, American Chemical Society, Las Vegas, NY, March-April, 1982.

Schwartz, S. E. and L. Newman. 1978. Processes limiting oxidation of sulfur dioxide in stack plumes. Environ. Sci. Technol. 12:67-73.

Schwartz, S. E. and J. E. Freiberg. 1981. Mass-transport limitation to the rate of reaction in liquid droplets: Application to oxidation of SO_2 in aqueous solutions. Atmos. Environ. 15:1129-1145.

Schwartz, S. E. and W. H. White. 1982. Kinetics of reactive dissolution of nitrogen oxides into aqueous solution. In Advanc. Enviro. Sci. Technol., 12, S. E. Schwartz, ed. Wiley and Sons, Inc., New York.

Scott, B. C. 1982. Predictions of in-cloud conversion rates of $-SO_2$ to SO_4 based upon a simple chemical and dynamical model. Atmos. Environ. 16:1735-1752.

Scott, W. D. and P. V. Hobbs. 1967. The formation of sulfate in water droplets. J. Atmos. Sci. 24:54-57.

Seinfeld, J. H., F. Allario, W. R. Bandeen, W. L. Chaimeides, D. D. Davis, E. D. Hinkley, and R. W. Stewart. 1981. Report of the NASA working group on tropospheric program planning. NASA Reference Publication 1062. National Aeronautics and Space Administration, Washington, D.C.

Sequeira, R. 1981. Acid rain: Some preliminary results from global data analysis. Geophys. Res. Lett. 8:147-150.

Shannon, J. D. 1981. A model of regional long-term average sulfur atmospheric pollution, surface removal, and net horizontal flux. Atmos. Environ. 15:689-701.

Sheppard, J. C., M. J. Campbell, and B. Au. 1978. Boundary layer hydroxyl measurements by a ^{14}C tracer technique. Presented before the Div. Environmental Chemistry, American Chemical Society, Miami, FL. September 11-14.

Shu, W. R., R. G. Lamb, and J. H. Seinfeld. 1978. A model of second-order chemical reactions in turbulent fluid - part II. Atmos. Environ. 12:1695-1704.

Spicer, C. W. 1977a. The fate of nitrogen oxides in the atmosphere. Adv. Environ. Sci. Technol. 1:163-261.

Spicer, C. W. 1977b. Photochemical atmospheric pollutants derived from nitrogen oxides. Atmos. Environ. 11:1089-1095.

Spicer, C. W. 1980. The rate of NO_x reaction in transported urban air. In Atmospheric Pollution 1980, Proc. 14th Int. Colloq., Paris, May 5-8. M. M. Benarie, ed. Elsevier Scientific Publishing Company, Amsterdam.

Spicer, C. W. 1983. Smog chamber studies of NO_x transformation rate and nitrate-precursor relationship. Environ. Sci. Technol. 17:112-120.

Spicer, C. W., D. W. Joseph, P. R. Sticksel, G. M. Sverdrup, and G. F. Ward. 1979. Reactions and transport of nitrogen oxides and ozone in the atmosphere. Battelle-Columbus Report to EPA.

Spicer, C. W., J. R. Koetz, G. W. Keigley, G. M. Sverdrup, and G. F. Ward. 1981a. A study of nitrogen oxides reactions within urban plumes transported over the ocean. EPA, U.S. Environmental Protection Agency, Research Triangle Park, NC.

Spicer, C. W., G. M. Sverdrup, and M. R. Kuhlman. 1981b. Smog chamber studies of NO_x chemistry in power plant plumes. Atmos. Environ. 15:2353-2366.

Stephens, E. R., W. E. Scott, P. L. Hanst, and R. C. Doerr. 1956. Recent developments in the study of the organic chemistry of the atmosphere. J. Air. Pollut. Contr. Assoc. 6:159-165.

Stewart, D. A. and M. K. Liu. 1981. Development and application of a reactive plume model. Atmos. Environ. 15:2377-2393.

Stockwell, W. R. and J. G. Calvert. 1983. The mechanism of the HO-SO_2 reaction. Atmos. Environ. 17:2231-2236.

Su, F., J. G. Calvert, J. H. Shaw, H. Niki, C. M. Savage, and L. D. Breitenbach. 1979. Spectroscopic and kinetic studies of a new metastable species in the photooxidation of gaseous formaldehyde. Chem. Phys. Lett. 65:221-225.

Su, F., J. G. Calvert, and J. H. Shaw. 1980. A FTIR spectroscopic study of the ozone-ethane reaction mechanism in O_2-rich mixtures. J. Phys. Chem. 84:239-246.

Sumi, L., A. Corkery, and J. L. Monkman. 1959. Calcium and sulfate content of urban air. Amer. Geophys. Union, Geophys. Mon. 3:69-80.

Sze, N. D. and M. K. W. Ko. 1980. Photochemistry of COS, CS_2, CH_3SCH_3 and H_2S: Implications for the atmospheric sulfur cycle. Atmos. Environ. 14:1223-1239.

Takeuchi, H., K. Takahashi, and N. Kizawa. 1977. Absorption of nitrogen dioxide in sodium sulfite solution from air as a diluent. Ind. Eng. Chem. Process Des. Dev. 16:486-490.

Tanaka, S. M. Dargi, and J. W. Winchester. 1980. Short term effect of rainfall on elemental composition and size distribution of aerosols in north Florida. Atmos. Environ. 14:1421-1426.

Tanner, R. L., R. Cederwall, R. Garber, D. Leahy, W. Marlow, R. Meyers, M. Phillips, and L. Newman. 1977. Separation and analysis of aerosol sulfate species at ambient concentrations. Atmos. Environ. 11:955-966.

U.S. Department of Energy. 1979. Monthly Energy Review, DOE/E1A0035/10(79), October.

Urone, P., H. Instep, C. Noyes, and J. T. Parcher. 1968. Static studies of sulfur dioxide reactions in air. Environ. Sci. Technol. 2:611-618.

Van den Heuval, A. P. and B. J. Mason. 1963. The formation of ammonium sulphate in water droplets exposed to gaseous sulphur dioxide and ammonia. Quart. J. R. Met. Soc. 89:271-275.

Walcek, C., P. K. Wang, J. H. Topalian, S. K. Mitra, and H. R. Pruppacher. 1981. An experimental test of a theoretical model to determine the rate at which freely falling water drops scavenge SO_2 in air. J. Atmos. Sci. 38:871-876.

Whitby, K. T. 1978. The physical characteristics of sulfur aerosols. Atmos. Environ. 12:135-159.

Whitby, K. T. 1980. Aerosol formation in urban plumes. Annals N.Y. Acad. Sci. 338:258-275.

Whitby, K. T., R. Vijayakumar, and G. R. Anderson. 1980. New particle and volume formation rates in five coal-fired power plant plumes. Presented at the Symposium on Plumes: Measurements and Model Components, Grand Canyon, AZ.

White, W. H., J. A. Anderson, D. L. Blumenthal, R. B. Husar, N. V. Gillani, J. D. Husar, and W. E. Wilson. 1976. Formation and transport of secondary air pollutants: Ozone and aerosols in the St. Louis urban plume. Science 194:187-189.

Whitney, R. P. and J. E. Vivian. 1941. Solubility of chlorine in water. Ind. Eng. Chem. 33:741-744.

Whitten, G. Z. and H. Hogo. 1977. Mathematical modeling of simulated photochemical smog. U.S. EPA Technical Report, EPA-6003-77-011.

Whitten, G. Z., H. Hogo, and J. P. Killus. 1980. The carbon bond mechanism: A condensed kinetic mechanism for photochemical smog. Environ. Sci. Technol. 14:690-700.

Wilson, W. E. 1978. Sulfates in the atmosphere: A progress report on Project MISTT. Atmos. Environ. 12:537-547.

Wilson, W. E. 1981. Sulfate formation in point-source plumes: A review of recent field studies. Atmos. Environ. 15:2573-2582.

Winchester, J. W. 1983. Sulfur, acidic aerosols, and acid rain in the eastern United States. Ch. 6 in Adv. Environ. Sci. Technol. Vol. 12. John Wiley and Sons, New York.

Wine, P. H., R. C. Shah, and A. R. Ravishankara. 1980. Rate of reaction of OH with CS_2. J. Phys. Chem. 84:2499-2503.

Winer, A. M. 1979. Detection of nitrous acid and nitrate radical in the polluted atmosphere by differential optical absorption spectroscopy. In Proceedings of the Workshop on the Formation and Fate of Atmospheric Nitrates. EPA, Research Triangle Park, NC.

Winer, A. M., G. M. Brewer, W. P. L. Carter, K. R. Darnell, and J. N. Pitts. 1979. Effects of ultraviolet spectral distribution on the photochemistry of simulated polluted atmosphere. Atmos. Environ. 13:989-998.

Winkelmann, D. 1955. Die electrochemishe messung von oxidations geschwindigkeit von NO_2SO_3 durch gelosten sauerstoff. Z. Electrochemie 59:891-895.

Winkler, E. M. 1976. Natural dust and acid rain. Water, Air, and Soil Pollut. 6:295-302.

Yue, G. K. and P. Hamill. 1979. The homogeneous nucleation rates of H_2SO_4-H_2O aerosol particles in air. J. Atmos. Sci. 10:609-614.

THE ACIDIC DEPOSITION PHENOMENON AND ITS EFFECTS

A-5. ATMOSPHERIC CONCENTRATIONS AND DISTRIBUTIONS OF CHEMICAL SUBSTANCES

(A. P. Altshuller)

5.1 INTRODUCTION

Air quality measurements of those substances that may contribute directly or indirectly to acidic deposition processes are discussed in this chapter. Substances such as sulfur dioxide and nitrogen dioxide may contribute to acidic deposition in two ways: (1) They can undergo dry and wet deposition to soil and subsequently undergo reactions to acidic species in soils; (2) They can undergo atmospheric chemical transformations to particle sulfate and gaseous and particle forms of nitrate which, in turn, can undergo deposition to soils, lakes, and streams. These substances may be acidic in their original forms as are NH_4HSO_4, H_2SO_4, and HNO_3, or they may undergo reactions in soil that result in release of hydrogen ions. Ammonia is an important nitrogen species that can neutralize airborne acidic substances, but in soils in the form of ammonium ion it can react to form hydrogen ions.

A number of other elements are of interest as airborne substances. Alkaline earth metals such as calcium can react as calcium ions to neutralize acidic substances. Iron and manganese ions are of significance to the extent that they can be demonstrated to participate in catalytic reactions in aqueous droplets to enhance the conversion of sulfur dioxide to sulfate (Chapter A-4, Section 4.3.5). Other airborne metallic elements may, upon deposition, have possible adverse biological effects in soils, lakes, and streams. Aluminum and manganese ions have been identified as possible causes of toxic effects in soils (Chapter E-2, Section 2.3.3.3.2). Aluminum ions are of particular concern in causing adverse effects in lakes and streams (Chapter E-4, Section 4.6.2). Zinc, manganese, cadmium, lead, and nickel at sufficiently high concentrations also can have toxic effects in lakes and streams (Chapter E-5, Section 5.6.4.2), and indirect health effects have been associated with lead, aluminum, and mercury (Chapter E-6).

Ozone and hydrogen peroxide participate in oxidation of sulfur dioxide to sulfate in aqueous droplets (Chapter A-4, Section 4.3.5.3). The ambient air concentrations of both of these oxidants will be considered, although substantial difficulties have been encountered in the measurement of hydrogen peroxide.

The effect of light scattering by submicron aerosols such as sulfates and nitrates is significant in the areas of eastern North America impacted by acidic deposition. Particle sulfate appears to be particularly important in

its adverse effects on visibility when suspended in air and a significant contributor to acidic deposition to soils, lakes, and streams. Therefore, a discussion of visibility degradation effects of these aerosol species is included in this chapter.

Measurements of airborne substances that may contribute to acidic deposition are of particular interest in rural areas. However, in the past, most measurements of airborne substances were made in urban areas. Cities were the major sources of pollutants of concern until after World War II. They still contribute substantially to the total burden of airborne sulfur and nitrogen compounds. Urban plumes also are significant because, through dry and wet deposition processes, they contribute directly to the loading into soils, lake, and streams substantially downwind of cities (Chapter A-3, Section 3.4.2).

5.2 SULFUR COMPOUNDS

5.2.1 Historical Distribution Patterns

Substantial changes in the geographical and seasonal distributions of sulfur oxides and in the stack heights of emission sources of sulfur oxides have occurred over time. Many of these changes occurred before air quality monitoring networks were established.

Wood was the predominant fuel used in the United States until the late 19th century (Schurr et al. 1960) when coal use began to increase. The coals burned, unlike wood, contained substantial amounts of sulfur, emitted to the atmosphere as sulfur oxides. Before and during World War II, the major uses of coal included residential/commercial heating, production of coke, and the operation of railroad locomotives (Schurr et al. 1960). Most of these sources of sulfur oxide emissions, except for locomotives, were in the cities. In addition, small coal-fired power plants were often located in cities. Thus, most sulfur oxides were emitted from sources near the ground surface. These near-surface emissions plumes impacted on the adjacent countryside resulting in high sulfur oxide concentrations in and near urban centers.

Coal usage declined in the United States immediately after World War II. By the late 1940's and 1950's, coal use in residential/commercial heating and railroad locomotives dropped off rapidly as coal was replaced by oil and gas. In cities, coal for residential/commercial heating was replaced by gas, which reduced sulfur oxide emissions substantially, and by fuel oil containing high sulfur contents, which did not reduce sulfur oxide emissions appreciably. Sulfur oxide emissions increased in the 1960's from industrial sources and the rapid growth of electric utility sources. However, emissions from industrial sources decreased in the 1970's (Chapter A-2, Figure 2-6). In the late 1960's and early 1970's, regulations were enacted to limit the sulfur content of fuels, thus reducing emissions from fuel oils. These regulations were applicable in particular to cities in the northeastern United States.

The spread of cities into suburban areas after World War II resulted in more diffuse sources of urban plumes, although emission sources in suburban

areas usually used low-sulfur fuels. Coal-fired electrical utility capacity in the midwestern and southeastern United States increased rapidly. These power plants were constructed outside of cities and with increasingly tall stacks. By the 1970's, numerous large power plants with stacks of varying heights were distributed throughout nonurban areas of the United States. These complex and varied emissions sources contributed to the loadings of sulfur oxides in rural areas on a seasonal and annual basis.

Where local contributions are negligible, the impact of urban plumes on remote areas is unclear, although long-range transport is more likely in winter (Chapter A-3, Section 3.4.2) because of atmospheric conditions. The plumes from sulfur oxide emission sources with tall stacks can be isolated from the surface for varying diurnal periods depending on the hour of release and season of the year (Chapter A-3, Figures 3-19, 3-20, 3-21, and 3-22). During these diurnal periods, these sources contribute to the total sulfur loading of the lower troposphere, but not to the sulfur oxides measured at ground level. Therefore, ground-level monitoring alone is inadequate to evaluate the total sulfur loading of the atmosphere available to participate in subsequent wet and dry deposition. Chapter A-8 presents further discussion of deposition monitoring.

5.2.2 Sulfur Dioxide

5.2.2.1 Urban Measurements--Most of the sulfur content of fuels is emitted to the atmosphere in the form of sulfur dioxide (SO_2). Sulfur dioxide was monitored in various large cities in earlier years, but no nationwide monitoring network existed until the 1960's.

Jacobs (1959a) reported ambient air concentrations of SO_2 in Manhattan and several other sites in the New York, NY, area for 1954-56, with higher concentrations in winter than in summer. The diurnal profiles showed midmorning and late afternoon peaks or early morning peaks in SO_2 concentrations. Jacobs reported hourly SO_2 concentrations as high as 2500 to 3000 $\mu g\ m^{-3}$ during some winter and fall air stagnation episodes. On an annual average basis, SO_2 concentrations at the Manhattan monitoring site averaged 420, 520, and 500 $\mu g\ m^{-3}$ in 1954, 1955, and 1956, respectively. Methods of sampling and chemical analysis were reported also (Jacobs 1959b).

A National Air Sampling Network (NASN) was initiated in the United States in the 1950's, but sulfur dioxide was not measured until the early 1960's. In comparison with the SO_2 concentrations reported by Jacobs (1959a), the NASN measurements in Manhattan in 1964 and 1965 averaged 450 and 370 $\mu g\ m^{-3}$, respectively (Dept. of Health, Education and Welfare 1966). These results appear to indicate relatively little change in concentration from the 1950's to the mid-1960's. This is not unexpected because fuel sulfur content was not restricted during this time.

In the 1963-72 period the decreasing order of annual average SO_2 concentrations was (1) East Coast, (2) Midwest (east of Mississippi), (3) Southeast, (4) West Coast, and (5) Midwest (west of the Mississippi River), and (6) western states. Many urban sites west of the Mississippi River had

SO_2 concentrations averaging only 10 to 20 percent of the concentrations at sites on the East Coast (Altshuller 1973).

Trends in the annual average, seasonal, and episodic concentration levels of SO_2 with time have been evaluated by geographical region and in specific urban areas (Altshuller 1980). Between 1963-65 and 1971-73, SO_2 concentrations (3-year quarterly averages) at urban sites decreased by about 80 percent in the northeastern United States (Figures 5-1 to 5-4) and by 30 to 50 percent in the midwestern United States (Altshuller 1980). The declining SO_2 concentration levels in cities appear to relate better to reductions in local sources of sulfur oxide emissions than to regional-scale utility emissions.

SO_2 concentrations in the northeastern United States, in the earliest period (1963-65) for which measurements are available, by quarter of the year, were in the order: fourth quarter > second quarter > third quarter (Figures 5-1 to 5-3). In 1971-73, the same order prevailed (Altshuller 1980).

Trends in SO_2 concentrations in urban areas in the 1970's are available on an annual average basis for the United States and geographical regions within the United States (U.S. EPA 1977a, 1978b). Based on 1,233 U.S. sampling sites, the composite average of urban SO_2 concentrations decreased by 15 percent between 1972 and 1977 from the 1972 level of 23 $\mu g\ m^{-3}$ (U.S. EPA 1978b). The 90th percentile concentrations of SO_2 decreased by 23 percent between 1972 and 1977 from a 1972 level of 52 $\mu g\ m^{-3}$. There were no significant changes in either the 90th percentile concentrations or in the composite average concentrations during the last few years of the 1970's.

By the latter part of the 1970's, ambient air concentrations of SO_2 had been reduced to relatively low levels. In 1976 the composite annual average (and 90th percentile) concentrations were: United States--20 $\mu g\ m^{-3}$ (40 $\mu g\ m^{-3}$), New England--25 $\mu g\ m^{-3}$ (40 $\mu g\ m^{-3}$); Great Lakes--28 $\mu g\ m^{-3}$ (50 $\mu g\ m^{-3}$) (U.S. EPA 1977a, 1978b). These concentrations were well below the SO_2 concentrations experienced in the 1960's or the early 1970's. During the last few years, SO_2 concentration levels appear to have stabilized.

5.2.2.2 Nonurban Measurements--Measurements for SO_2 concentrations at nonurban sites in the United States are more limited than those at urban sites. In addition, the concentrations measured often are near the limits of detectability. Measurements of six nonurban sites in the United States over a period of years for which results are available in the NASN data bank are listed in Table 5-1.

The annual average concentrations range near 10 $\mu g\ m^{-3}$. First- and fourth-quarter concentrations often exceeded second-quarter concentrations, and concentrations during the third quarter of the year were almost always the lowest values at each site. No clear trends in nonurban SO_2 concentrations with time are evident on an annual average or quarterly basis (Figures 5-1 to 5-3). Although average SO_2 concentrations at nonurban sites were much lower than at urban sites during the 1960's, the difference

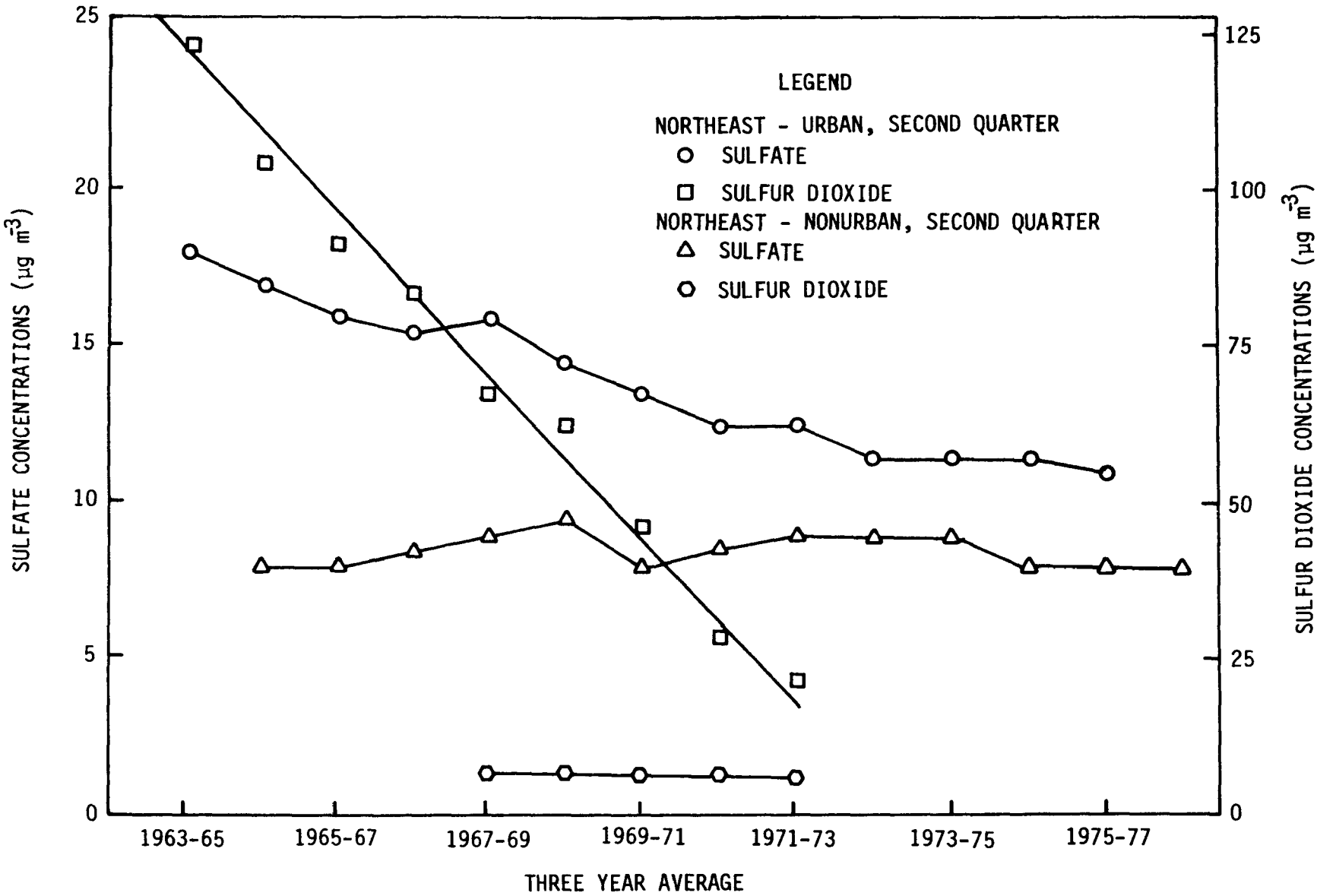

Figure 5-1. Three year running average sulfur dioxide and sulfate concentrations during second quarter of year for urban and nonurban sites in the northeastern United States. Adapted from Altshuller (1980).

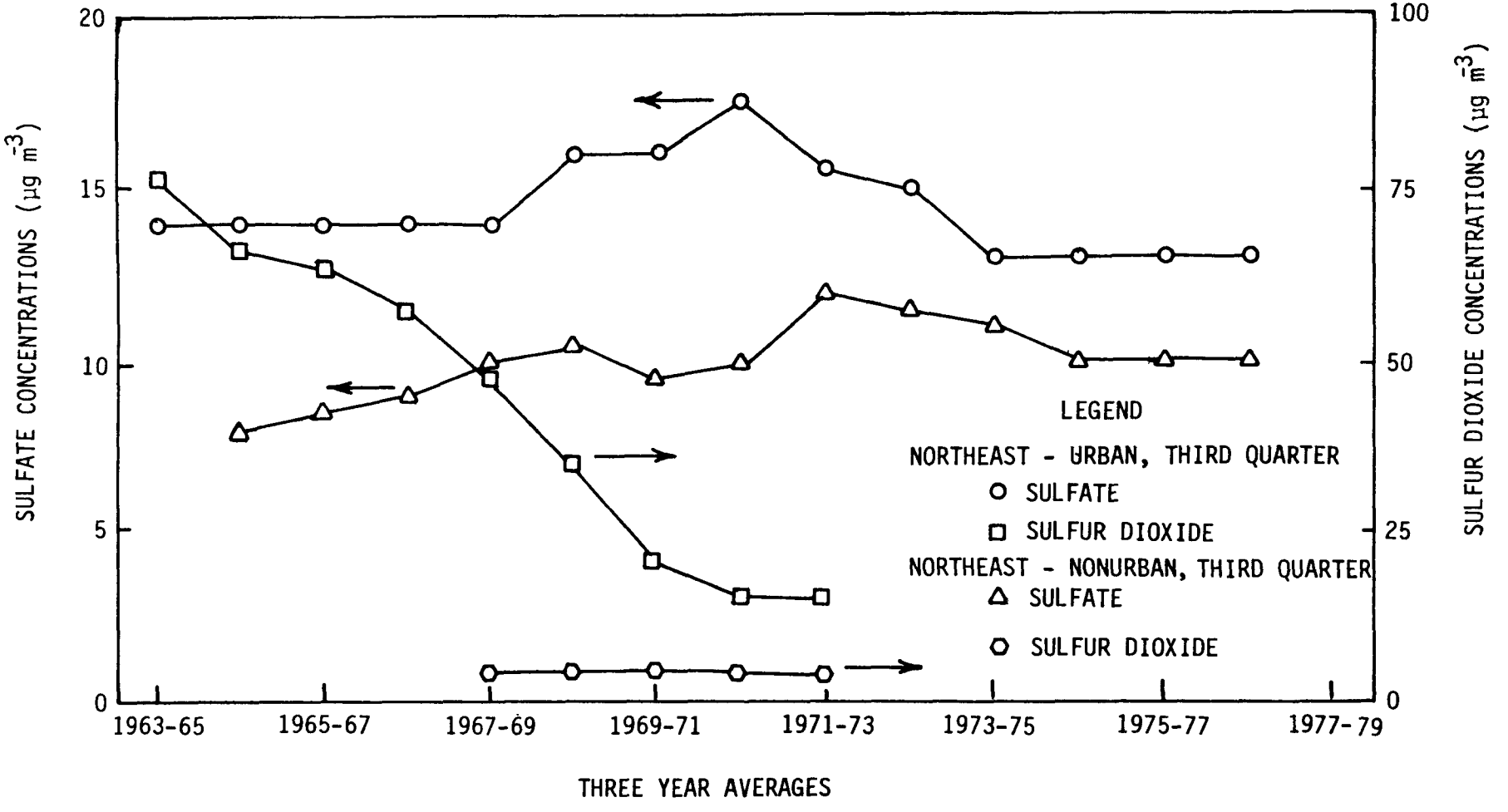

Figure 5-2. Three year running average sulfur dioxide and sulfate concentrations during third quarter of year for urban and nonurban sites in the northeastern United States. Adapted from Altshuller (1980).

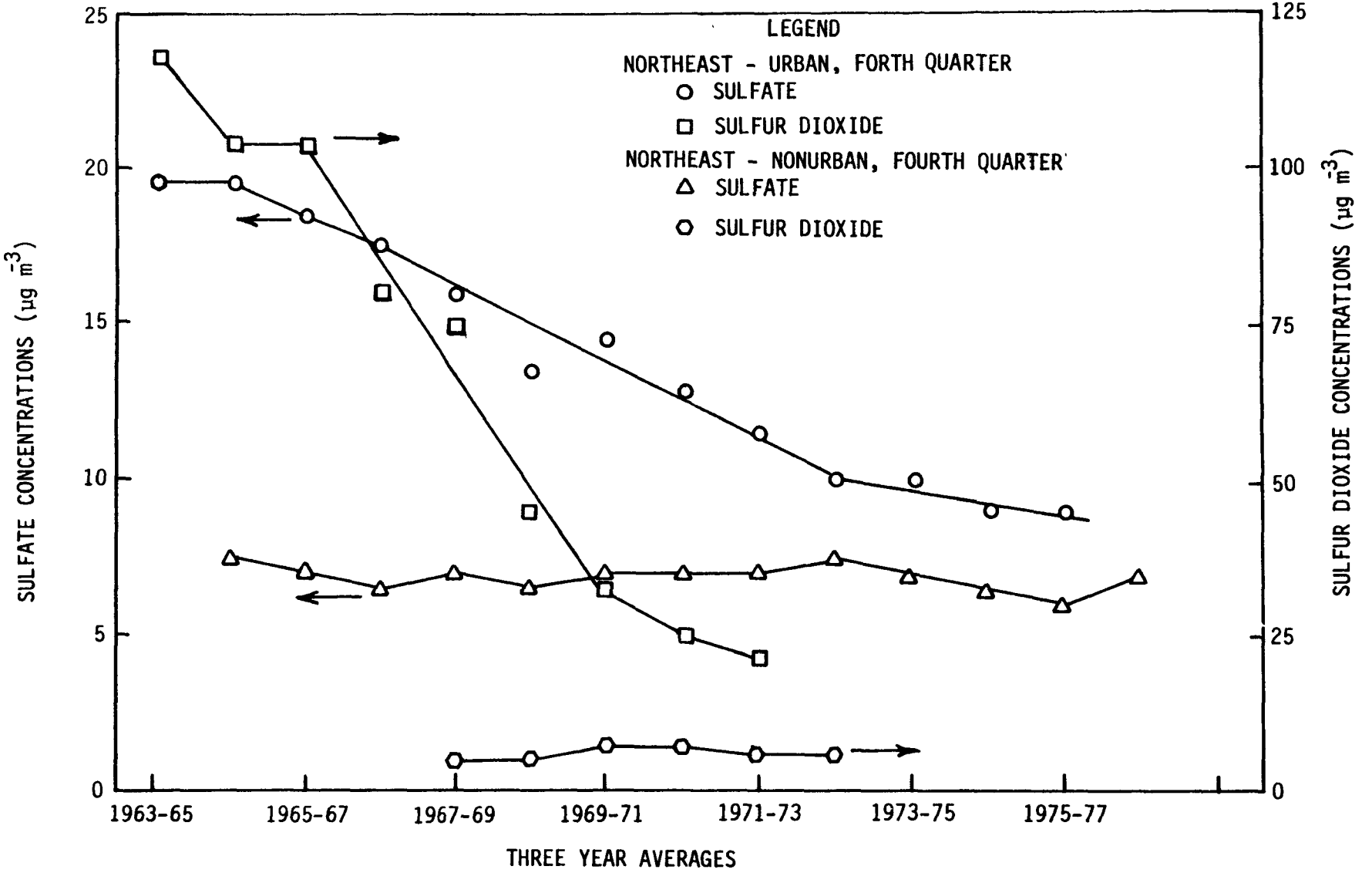

Figure 5-3. Three year running average sulfur dioxide and sulfate concentrations during fourth quarter of year for urban and nonurban sites in the northeastern United States. Adapted from Altshuller (1980).

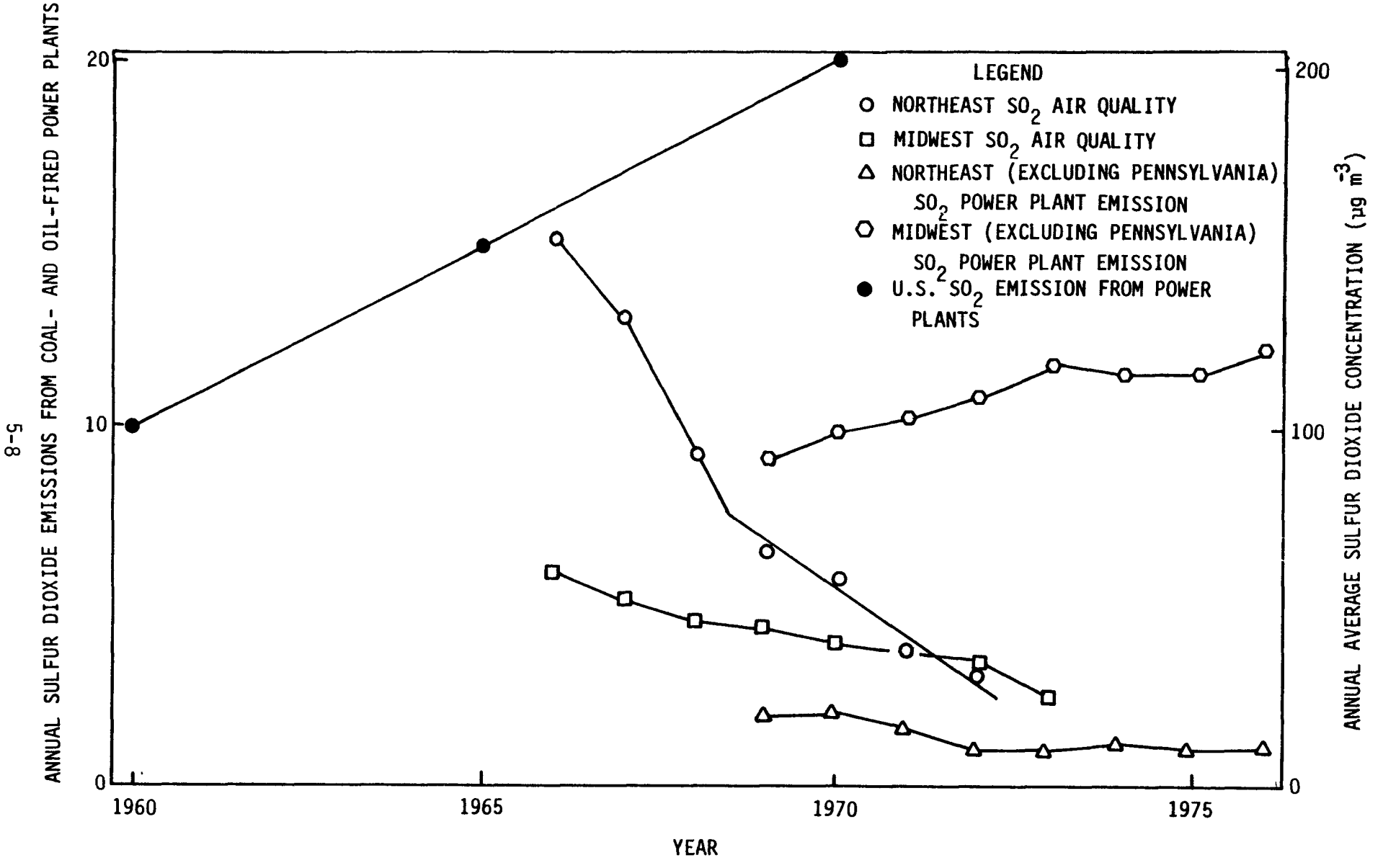

Figure 5-4. Annual average urban ambient air concentrations and emissions (million tons) of sulfur dioxide in northeastern and midwestern United States. Adapted from Altshuller (1980).

TABLE 5-1. SULFUR DIOXIDE CONCENTRATIONS AT NONURBAN SITES IN THE EASTERN UNITED STATES (in $\mu g\ m^{-3}$) (ADAPTED FROM NASN DATA BANK)

Site	First quarter	Second quarter	Third quarter	Fourth quarter	Annual average
Acadia National Park, ME					
1968	8	7	5	9	10
1969	12	9	8	8	9
1970	15	7	8	15	11
1971	19	11	7	9	13
1972	6	6	6	7	7
1973	9	ND[a]	ND	ND	-
Coos County, NH					
1970	ND	ND	12	8	-
1971	12	10	7	9	9
1972	7	6	4	9	9
1973	13	ND	ND	ND	-
Calvert County, MD					
1970	ND	ND	10	18	-
1971	20	15	8	9	13
1972	5	6	6	9	7
1973	12	9	ND	8	-
Shenandoah National Park, VA					
1968	20	5	6	11	10
1969	16	7	9	11	11
1970	16	6	11	8	11
1971	15	8	7	10	11
1972	10	5	5	19	9
1973	18	8	6	7	9

TABLE 5-1. (CONTINUED)

Site	First quarter	Second quarter	Third quarter	Fourth quarter	Annual average
Jefferson County, NY					
1970	ND	ND	16	ND	-
1971	8	5	6	7	7
1972	3	5	5	9	6
1973	8	19	ND	25	-
Monroe County, IN					
1967	19	5	6	33	11
1968	13	7	7	12	10
1969	19	10	8	18	14
1970	13	8	16	10	12
1971	11	8	7	14	11
1972	15	10	7	15	11
1973	30	11	10	10	15

[a]ND = not detectable.

between urban and nonurban SO_2 concentrations narrowed substantially in the 1970's.

Mueller et al. (1980) reported measurements from the Sulfate Regional Experiment (SURE) obtained from a 54-station nonurban network operated in August and October 1977 and mid-January, February, April, July, and October 1978. The SO_2 concentrations measured in New England and the Southeast were almost always below 26 $\mu g\ m^{-3}$, except during January-February 1978. Monthly average isopleths for SO_2 of between 26 and 52 $\mu g\ m^{-3}$ included varying portions of several midwestern and mid-Atlantic States from month to month during the study. Monthly average SO_2 concentrations of about 80 $\mu g\ m^{-3}$ were shown for small areas in August 1977 and January-February 1978. The highest SO_2 concentrations tended to be in portions of the Ohio River Valley and western Pennsylvania. These concentrations of SO_2 at SURE sites were substantial compared to those reported at urban sites in the late 1970's. However, other measurements in western Pennsylvania in July and August 1977 resulted in average SO_2 concentrations of 18 $\mu g\ m^{-3}$ (Pierson et al. 1980a), which are substantially lower than those reported by Mueller et al. (1980).

SO_2 measurements at rural sites in Union Co., KY, Franklin Co., IN, and Ashland Co., OH, were reported between May 1980 and August 1981. Monthly average SO_2 concentrations ranged from as low as 8 to 10 $\mu g\ m^{-3}$ during summer months to as high as 30 to 40 $\mu g\ m^{-3}$ during the winter months (Shaw and Paur 1983).

A number of Canadian monitoring networks were established during the 1970's (Whelpdale and Barrie 1982). While precipitation measurements have received the greater emphasis in these networks, air quality measurements for sulfur dioxide are available from the Air and Precipitation Monitoring Network (APN) (Barrie et al. 1980, 1983; Whelpdale and Barrie 1982). Six monitoring sites east of Manitoba are in operation at rural locations. Sulfur dioxide is collected on a 24-hour integrated basis on a chemically impregnated filter. A low-volume sampler operates at a flow rate of about 20 $\ell\ min^{-1}$ at an elevation of 10 meters. The geometric means of 24-hour average SO_2 concentrations on a $\mu g\ m^{-3}$ basis for the period November 1978 to December 1979 are: Long Point, Ontario, 11; Chalk River, Ontario, 5.5; ELA-Kenora, Ontario, 0.86; Kejimkujik, Nova Scotia, 0.86 (Barrie et al. 1983). Large concentration fluctuations are observed at these sites and are attributed to the alternating presence of clear background air and air polluted by large SO_2 sources in the Lower Great Lakes area (Barrie et al. 1980).

In Europe, annual mean SO_2 concentrations range from about 20 $\mu g\ m^{-3}$ in rural areas of the United Kingdom, the Netherlands, and the Federal Republic of Germany to concentrations of 2 $\mu g\ m^{-3}$ or lower in the remote areas of northern and western Europe (Ottar 1978). This range of SO_2 concentrations over rural areas in Europe is close to the range of concentrations discussed above for rural areas of North America.

Georgii (1978) has reviewed aircraft measurements of SO_2 over the European Continent. The average concentration of SO_2 decreased from about 5 $\mu g\ m^{-3}$ at 2 to 3 km altitude to 1 $\mu g\ m^{-3}$ at 5 km altitude. From other

aircraft flights, Georgii and Meixner (1980) obtained a mean concentration of 1.3 $\mu g\ m^{-3}$ above 6 km over Europe.

5.2.2.3 Concentration Measurements at Remote Locations--Meszaros (1978) reviewed remote measurements of SO_2 concentrations. Several investigations had been reported of SO_2 concentrations as a function of latitude over the Atlantic Ocean. Concentrations of SO_2 ranging from 0.1 to 0.2 $\mu g\ m^{-3}$ were observed at latitudes above 60°N and below 10°N in the northern hemisphere as well as in the southern hemisphere. Between latitudes of 10°N and 60°N over the Atlantic Ocean SO_2 concentrations increase to 1 $\mu g\ m^{-3}$ at 25°N and at 55°N latitude and peak at about 3 $\mu g\ m^{-3}$ at 40°N latitude. These large increases in SO_2 concentrations at midlatitude were attributed to continental emission sources. Other investigations resulted in measurements of SO_2 averaging 0.3 $\mu g\ m^{-3}$ over the Pacific Ocean and 0.2 $\mu g\ m^{-3}$ over the Indian Ocean (Meszaros 1978).

Measurements of SO_2 concentrations were obtained in aircraft flights over remote areas as part of the 1978 Global Atmospheric Measurements Experiment of Tropospheric Aerosols and Gases (GAMETAG) by Maroulis et al. (1980). The areas sampled were between 57°S and 70°N and included the central and southern Pacific Ocean and the western section of the United States and Canada. The average SO_2 concentrations reported in pptv were as follows: northern hemisphere, boundary layer, 89; free troposphere, 122; southern hemisphere, boundary layer, 57; free troposphere, 90. The SO_2 concentrations in pptv over marine and continental environments were as follows: marine boundary layer, 54; free troposphere, 85; continental boundary layer, 112; free troposphere, 160. The boundary layer SO_2 concentrations were in the 0.1 to 0.3 $\mu g\ m^{-3}$ range in reasonable agreement with other remote measurements (Meszaros 1978). Bonsang et al. (1980) reported SO_2 concentrations ranging from 0.03 $\mu g\ m^{-3}$ over the tropical Indian Ocean to 0.3 $\mu g\ m^{-3}$ over the Peruvian upwelling. A relationship was identified between the atmospheric SO_2 concentrations and the biological activity in sea surface waters (Bonsang et al. 1980).

The SO_2 concentrations measured at many remote sites are factors of 10 to 100 less than those measured at rural sites in eastern North America (Section 5.2.2.2). However, the SO_2 plume from eastern North America appears to cause large increases in the SO_2 concentrations measured at midlatitudes well into the Atlantic Ocean (Meszaros 1978). A similar impact of large plumes from strong source areas has been observed at several rural Canadian sites (Barrie et al. 1983).

5.2.2.4 Comparison of Sulfur Dioxide Emissions and Ambient Air Concentration --In Chaper A-2, Section 2.3.2, the historical trends in sulfur dioxide emissions are discussed. Total sulfur dioxide emissions increased rapidly during the 1950's, more slowly during the 1960's, peaked at or somewhat after 1970, and decreased somewhat by 1975. The sulfur dioxide emissions from electric utility fossil-fuel power plants continued to increase until 1975. The sulfur dioxide emissions from industrial sources started to decrease rapidly after about 1965 and continued to decrease into the 1970's. By state, the historical trends varied substantially. After 1970 the sulfur dioxide emissions in New England decreased substantially. In Kentucky and

West Virginia the sulfur dioxide emissions continued to increase from 1950 into the 1970's. In the area consisting of the states of Pennsylvania, New York, Ohio, Indiana, and Illinois, the sulfur dioxide emissions increased rapidly between 1950 and 1960, remained about constant from 1960 to 1970, and decreased after 1970.

As discussed in Section 5.2.2.1, sulfur dioxide concentrations within urban areas started decreasing during the 1960's and continued decreasing into the 1970's. These decreases in sulfur dioxide concentrations within urban areas are consistent with the decreases in sulfur dioxide emissions from industrial sources. Within some urban areas on the east coast of the United States emission regulations also resulted in either the use of low-sulfur coal or residual fuel oil in power plants (Altshuller 1980). As a result, sulfur dioxide emissions from power plants as well as industrial sources decreased in these urban areas from the late 1960's onward.

No clear trends are evident in the sulfur dioxide concentrations in nonurban areas on a regional average basis. This lack of trend in sulfur dioxide concentrations in nonurban areas does not appear consistent with the increases in sulfur dioxide emissions which did occur after 1965 from electric utility plants constructed in nonurban areas (Chapter A-2, Section 2.3.2). However, the varying patterns of trends of emissions from state to state do complicate the relationships between emissions and ambient air concentrations in nonurban areas. In general, there was a shift from emissions from industrial sources discharged near ground level to emissions from tall stacks of power plants. A substantial fraction of sulfur dioxide emissions from electric utility power plants with tall stacks in nonurban areas are emitted aloft and remain aloft over long distances. A portion of these emissions are eventually removed by wet scavenging while another portion can pass on aloft into Canada or over the Atlantic. These sulfur dioxide emissions would not contribute to sulfur dioxide concentrations measurable at ground-level monitoring sites in the United States. As a result, the increase in ground level sulfur dioxide concentrations should not be proportional to the incremental increase in the power plant emissions after 1965. Therefore the increment in terms of sulfur dioxide concentrations would be relatively small and difficult to measure at nonurban monitoring sites by the sulfur dioxide sampling and analysis procedure used.

5.2.3 Sulfate

5.2.3.1 Urban Concentration Measurements--In 1963 the National Air Sampling Network collected particulate matter on high-volume (HIVOL) samplers and began analyzing for sulfur as water-soluble sulfate at urban sites in the United States.

The potential for a positive sulfate artifact resulting from collection and conversion of SO_2 on glass-fiber filters was discussed by Lee and Wagman (1966). Subsequent laboratory studies have shown that the magnitude of such an artifact depends on temperature, SO_2 concentration, the air volume per unit area of filter surface, and other parameters (Coutant 1977, Meserole et al. 1976). The conversion of SO_2 to sulfate on clean glass-fiber filter

surfaces was sensitive to temperature but showed little dependency on humidity. A substantially smaller artifact was obtained on surfaces coated with ambient air particulates than on uncoated filter surfaces. Coutant (1977) estimated sulfate loading errors from the use of untreated glass-fiber filters under usual flow conditions in HIVOL samplers to be in the range of 0.3 to 3.0 $\mu g\ m^{-3}$.

The results reported from field observations have varied widely from small or negligible to large artifact effects (Appel et al. 1977, Pierson et al. 1976, Stevens et al. 1978). However, differences in sampling techniques and analytical procedures used complicated comparisons. It will be assumed that sulfate artifacts are not large enough to influence substantially the trends in sulfate concentrations observed. If the sulfate artifacts were substantial, part of the decreases in ambient air sulfate concentrations would have to be attributed to the concurrent reductions in sulfur dioxide. Conversely, increases also occurred in ambient air sulfate concentrations. These increases were even larger than indicated, if they occurred at the same time a positive sulfate artifact was decreasing.

At most urban sites in the western United States in the 1960's, sulfate concentrations were below 10 $\mu g\ m^{-3}$; at three-quarters of the urban sites in the eastern United States concentrations were above 10 $\mu g\ m^{-3}$ (Altshuller 1973). The general order of decreasing sulfate concentrations by geographic region in the 1960's and 1970's was: (1) East Coast, (2) Midwest (east of Mississippi), (3) Southeast, (4) West Coast, (5) Midwest (west of Mississippi), and (6) western states. Average sulfates for urban sites in the western United States ranged from 30 to 50 percent of the concentration of sulfate at urban sites on the East Coast.

The excess in urban sulfate concentrations over the regional background of sulfate is a measure of the contributions by local primary sources and atmospheric transformations within the urban area (Altshuller 1976, 1980). Although regional background levels of SO_2 were small compared to urban concentration levels, regional background levels of sulfate have been substantial in the eastern United States compared to urban concentration levels (Altshuller 1976, 1980). These regional background levels of sulfate are formed from atmospheric transformations of sulfur dioxide to sulfate (see Chapter A-4).

Control of local sulfur oxide emissions by reductions in fuel sulfur content resulted in a substantial reduction in ambient air sulfate concentrations, particularly in the first and fourth quarters of the year (Altshuller 1980). The largest decreases occurred in urban areas in the northeastern United States, but smaller decreases also occurred in urban areas in the Midwest and Southeast. In contrast, during the third quarter of the year, ambient air sulfate concentrations increased in the 1960's and 1970's, and then decreased somewhat at some sites. Increasing sulfate concentrations during the third quarter occurred well into the 1970's at some sites in the Ohio River Valley region and at sites in the South.

The urban excess, the difference between the average urban and the average regional (nonurban) sulfate concentration in a region, decreased substantially between 1965-67 and 1976-78 in the North, Midwest, and Southeast during the first and fourth quarters of the year (Altshuller 1980). Smaller decreases in the urban excess occurred in the second and third quarter in the Northeast and Midwest, but increases occurred in the southeastern urban areas.

The increase in third-quarter sulfate concentrations at urban sites in the late 1960's into the 1970's occurred on the average in the northeast, southeast, and midwestern regions, indicating geographic-scale processes at work. The increases occurred consistently at sites in the Ohio River Valley area and adjacent areas in the Southeast. Regional-scale sulfate episodes or potential episodes increased in frequency during the same period. Most of these episodes occurred in the June-through-August period of each year (Altshuller 1980). Therefore, the higher sulfate concentrations in the summer months at urban sites are likely to be associated with large regional-scale processes (Altshuller 1980, Hidy et al. 1978, Mueller et al. 1980).

In the late 1970's, the average urban sulfate concentrations by quarter of the year in the northeastern, southeastern, and midwestern United States had the order: third quarter > second quarter > first quarter > fourth quarter (Altshuller 1980). The first- and fourth-quarter average urban sulfate concentrations in the Northeast and Southeast were below 10 $\mu g\ m^{-3}$; the third-quarter average urban sulfate concentrations in the Southeast and Midwest were at 15 $\mu g\ m^{-3}$. The urban excess, the difference between the average urban and average nonurban sulfate concentrations, had decreased by the late 1970's compared to earlier years, except in the Southeast. Regional trends at urban sites in the United States also have been discussed by Frank and Possiel (1976). Plots of the regional distribution of sulfates were developed.

5.2.3.2 Urban Composition Measurements--The composition of the sulfate in urban areas has been the subject of a number of investigations. In several investigations of aerosol composition within urban areas, including Secaucus, NJ, Philadelphia, PA, Chicago, IL, and Charleston, WV, the sulfate appeared to be in the form of ammonium sulfate [$(NH_4)_2SO_4$] (Wagman et al. 1967, Lee and Patterson 1969, Patterson and Wagman 1977, Lewis and Macias 1980). However, no special precautions were taken to preserve sample acidity.

Tanner et al. (1979) using a coulometric modification of the Gran titration, reported aerosol samples in New York City to be slightly on the acidic side of $(NH_4)_2SO_4$ in winter (February 1977), but to have the more acidic average composition of letoricite, $(NH_4)_3H(SO_4)_2$, in the summer (August 1976). These investigators also found sulfate to be highly correlated with ammonium in both summer and winter aerosols. Lioy et al. (1980) during a high sulfate episode in the east on 3 to 9 August 1977, observed high acidities at nonurban sites, as did Pierson et al. (1980a). However, in New York City the aerosol appeared to be nearly neutral, suggesting higher ammonia fluxes in and near New York City.

Coburn et al. (1978) measured the acidity of sulfate aerosols in St. Louis, MO, by an in situ thermal analysis technique during a 16-day period in late April to early May 1977. Although the acidity reached a one-to-one ratio of $[NH_4^+]$ to $[H^+]$ on one morning, for the most part the sulfate aerosol tended to be in the form of $(NH_4)_2SO_4$.

In earlier measurements in the Los Angeles area during 1972 and 1973, sufficient ammonium ion appeared to be present to neutralize the sulfate to $(NH_4)_2SO_4$ except near strong local sources of sulfur oxides (Appel et al. 1978). However, the authors did point out that the techniques used could not distinguish between neutralization of acidic constituents before and after collection. In subsequent measurements in July 1979 at Lennox near strong sulfur sources, significant levels of H_2SO_4 and particulate acidity were obtained (Appel et al. 1982). Sulfuric acid constituted 10 to 20 percent of the total sulfate.

It would appear that the sulfate aerosol in urban areas tends toward the composition of $(NH_4)_2SO_4$, but that its composition is variable with more of a tendency toward acidic species in the summer.

5.2.3.3 Nonurban Concentration Measurements--Altshuller (1973) pointed out large differences in the range and average concentrations for sites in the eastern compared to the western United States based on measurements of sulfate concentrations at nonurban sites in 1965-68. Relatively little overlap occurred in frequency ranges, with the sulfate concentrations at eastern sites averaging 8.1 $\mu g\ m^{-3}$, and those at western sites averaging 2.6 $\mu g\ m^{-3}$. At 10 percent of the western sites, annual average concentrations were as low as 0.5 to 1.0 $\mu g\ m^{-3}$. The eastern and western sites appeared to represent separate and distinct populations as far as sulfate concentrations were concerned (Altshuller 1973). A continental background of less than 1 $\mu g\ m^{-3}$ was indicated by the minimum sulfate concentration levels at eastern and western nonurban sites. A more detailed stratification of results on sulfate concentrations at nonurban sites in the United States indicates the order of decreasing sulfate concentrations in the 1965-72 period to be: (1) East Coast and Midwest (east of Mississippi River), (2) Southeast, (3) Southwest, (4) Midwest (west of Mississippi River) and West Coast, and (5) Mountain States.

Between 1963-65 and 1976-78, sulfate concentrations at nonurban sites (Acadia National Park, ME; Coos County, NH; Orange County, VT; Washington County, RI; Calvert County, MD; and Shenandoah National Park, VA) varied only slightly in the first, second, and fourth quarters of the year (Figures 5-1 to 5-3) (Altshuller 1980). The first- and fourth-quarter trends showed both small increases and decreases in sulfate concentration at the nonurban sites in the Northeast, Southeast, and Midwest (Altshuller 1980). The second-quarter trends either were positive or showed no change in these three regions.

At the nonurban sites in the northeastern and midwestern United States, the third-quarter sulfate concentrations increased during the 1960's, peaked in the early 1970's, and subsequently decreased, just as at the urban sites in these regions (Altshuller 1980). This upward trend occurred most consistently for nonurban sites in the Ohio Valley area.

Although urban sites showed decreases in sulfate concentration during the winter quarters, presumably due to local-scale reductions of sulfur oxide emissions (Altshuller 1980), no substantial changes were experienced at nonurban sites distant from such local influences. Conversely, since third-quarter trends were presumably influenced strongly by larger regional processes, both urban and nonurban sites in the same region and even across regions should show similar behavior. The second quarter showed intermediate behavior. Despite the large upward trends in sulfur emissions from power plants during the 1960's and 1970's (Figure 5-4), very small increases were measured at nonurban sites in the Midwest or East. The only substantial upward trends were in the third quarter of the year at nonurban sites. The trend downward after the early 1970's at the midwestern nonurban sites during the third quarter of the year appears consistent with the downward trend of sulfur emissions in most midwestern states between 1970 and 1978 (Chapter A-2, Table 2-14).

A plot of the regional distributions of nonurban sulfate concentrations averaged from months in 1977 and 1978 are shown in Figure 5-5 (Hilst et al. 1981). Sulfate concentrations were the highest in the Ohio Valley area followed by other parts of the Midwest, mid-Atlantic states and Southeast. During summer months in 1977 and 1978, Mueller et al. (1980) observed a broader regional distribution of sulfates than observed during the entire study period, with high sulfate concentrations extending all the way from the Ohio River Valley to the Atlantic Seaboard.

In the late 1970's the average nonurban sulfate concentrations in the eastern and midwestern United States had the same ordering by quarter of the year as at urban sites: third quarter > second quarter > first quarter > fourth quarter (Altshuller 1980). Based on sulfate measurements made from May 1980 to August 1981 at three rural sites in the Midwest, Shaw and Paur (1983) reported monthly average concentrations ranging from as low as 3 $\mu g\ m^{-3}$ in some winter months to 12 to 15 $\mu g\ m^{-3}$ in the summer months. The seasonal variations in sulfate concentrations were just the opposite of those of sulfur dioxide. As a result, the percentage of particle sulfur of total sulfur measured ranged from 5 to 10 percent in the winter months to more than 40 percent in the summer months.

Diurnal sulfate concentrations were measured at two rural sites, one in Kentucky and the other in Virginia, during the summer of 1976 (Wolff et al. 1979). Two types of diurnal patterns for sulfate concentrations were observed. On one group of days, the sulfate concentrations peaked in mid-afternoon at about the same time the ozone concentrations peaked. Downward mixing of sulfate from the layer aloft, as the noctural inversion layer broke up, was suggested as being responsible for a substantial fraction of the sulfate in these afternoon peaks. The second diurnal pattern involved sulfate concentration peaking between 2000 and 0400 hours at night. This type of diurnal behavior appeared to be most pronounced on clear nights when ground fog developed. A few days fell into neither of these two patterns. These latter days were characterized by very low sulfate concentrations, < 5 $\mu g\ m^{-3}$, and occurred after passage of a cold front.

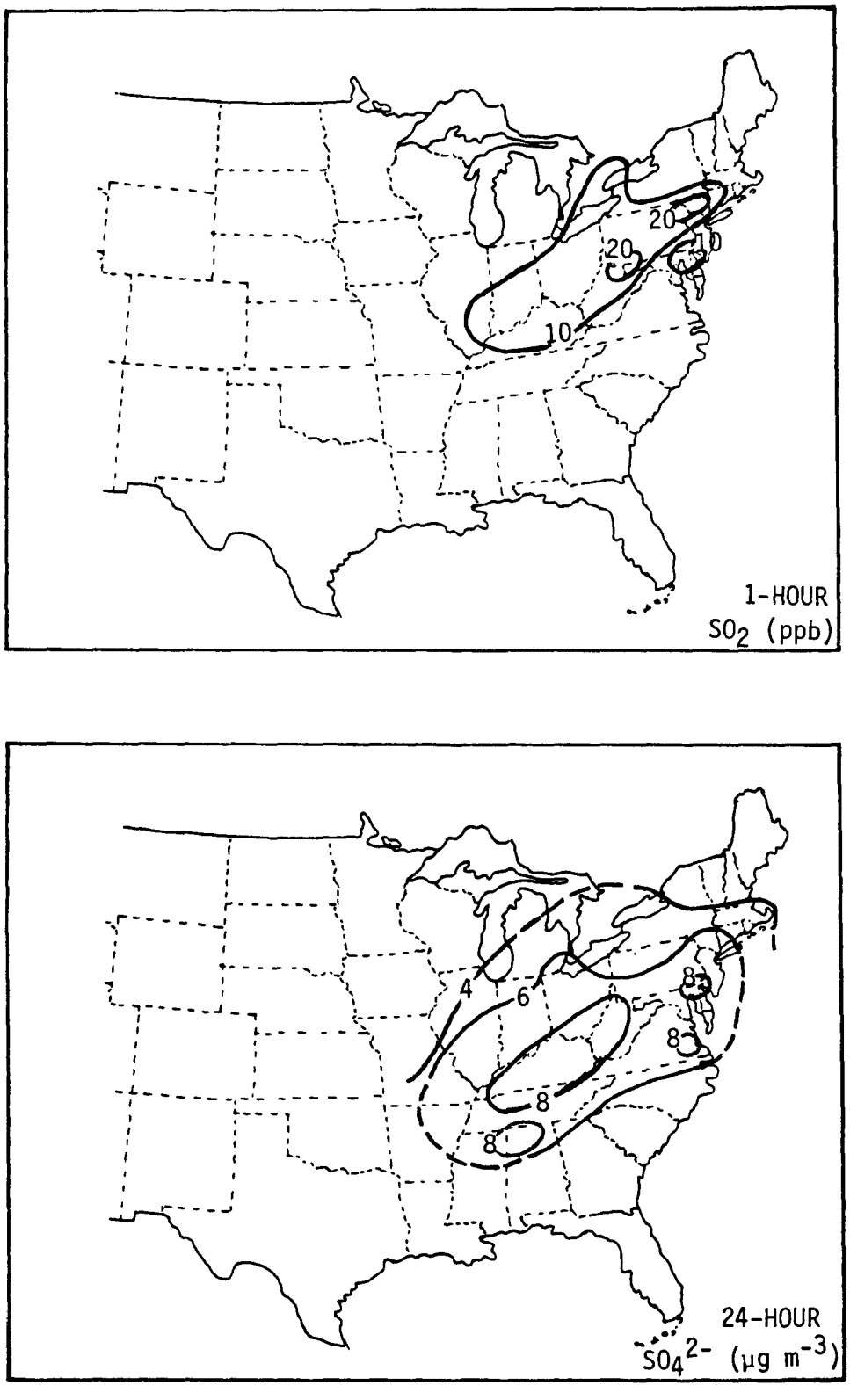

Figure 5-5. Sulfur dioxide (arithmetic mean) and sulfate (geometric mean) concentrations. Data obtained during 5 months between August 1977 and July 1978. Adapted from Hilst et al. (1981).

The sulfate concentrations measured at rural monitoring sites outside of St. Louis, MO, were 80 and 90 percent of the sulfate concentrations at urban sites within St. Louis during the years 1975 through 1977 (Altshuller 1982). These results also are consistent with a strong regional influence on sulfate concentration distributions.

Vertical profile measurements were obtained from aircraft flights over southeastern Ohio in early August 1977 and January 1978 (Mueller et al. 1980). Measurements were made in the layer between 0.3 and 1.5 km and at a higher layer between 1.5 and 3 km above mean sea level. On the average, the sulfate concentrations in the lower layer were similar to those obtained at ground sites. The sulfate concentrations in the upper layer were smaller than in the lower layer. In August 1977, the aircraft measurements indicated that the sulfate concentrations in the lower layer were about twice as high in the afternoon hours as in the morning hours. In a winter period, the sulfate concentrations varied little between the morning and afternoon hours in the lower layer aloft. The sulfate concentrations in the lower layer in the winter were about one-third of those in the afternoon in the summer.

Twenty-four-hour average sulfate concentrations were measured in the Canadian APN concurrently with SO_2 concentrations (Barrie et al. 1980, 1983; Whelpdale and Barrie 1982). Atmospheric particulate matter was collected on a Whatman 40 particulate filter, which preceded the chemically impregnated filter used to collect sulfur dioxide. Sulfate was determined by means of ion chromatography. The geometric means of the 24-hr average sulfate concentrations on a $\mu g\ m^{-3}$ basis for the period November 1978 to December 1979 are: Long Point, Ontario, 1.0; Chalk River, Ontario, 1.9; ELA-Kenora, Ontario, 1.0; Kejimkujik, Nova Scotia, 1.8 (Barrie et al. 1983). Sulfate concentrations do not decrease as rapidly as do SO_2 concentrations with distance from major source regions. Sulfate concentrations, just as SO_2 concentrations, show large fluctuations attributed to the alternate presence of clean air and polluted air from large source regions (Barrie et al. 1980).

Concentrations of sulfate as a function of percentage cumulative frequency are plotted in Figure 5-6 (Barrie et al. 1983). Results from Canadian sites for the period November 1978 to December 1979 are compared with those obtained in the eastern United States during 1974-75. Except for the highest sulfate concentrations experienced at Canadian sites in lower Ontario, the sulfate concentrations at Canadian sites fall well below those at sites in the United States. This is particularly so for the Canadian sites more remote from large source regions.

5.2.3.4 Nonurban Composition Measurements--Charlson et al. (1974) reported evidence obtained with a semiquantitative humidographic technique of acidic sulfate species frequently present at a rural site outside of St. Louis during September 1973. The acidic composition was variable (Charlson et al. 1974, 1978a). The sulfate aerosols were acidic more frequently at the rural site than at the urban site. There was no dependence on wind direction nor on synoptic conditions, consistent with regional sources of the sulfate aerosol (Charlson et al. 1974).

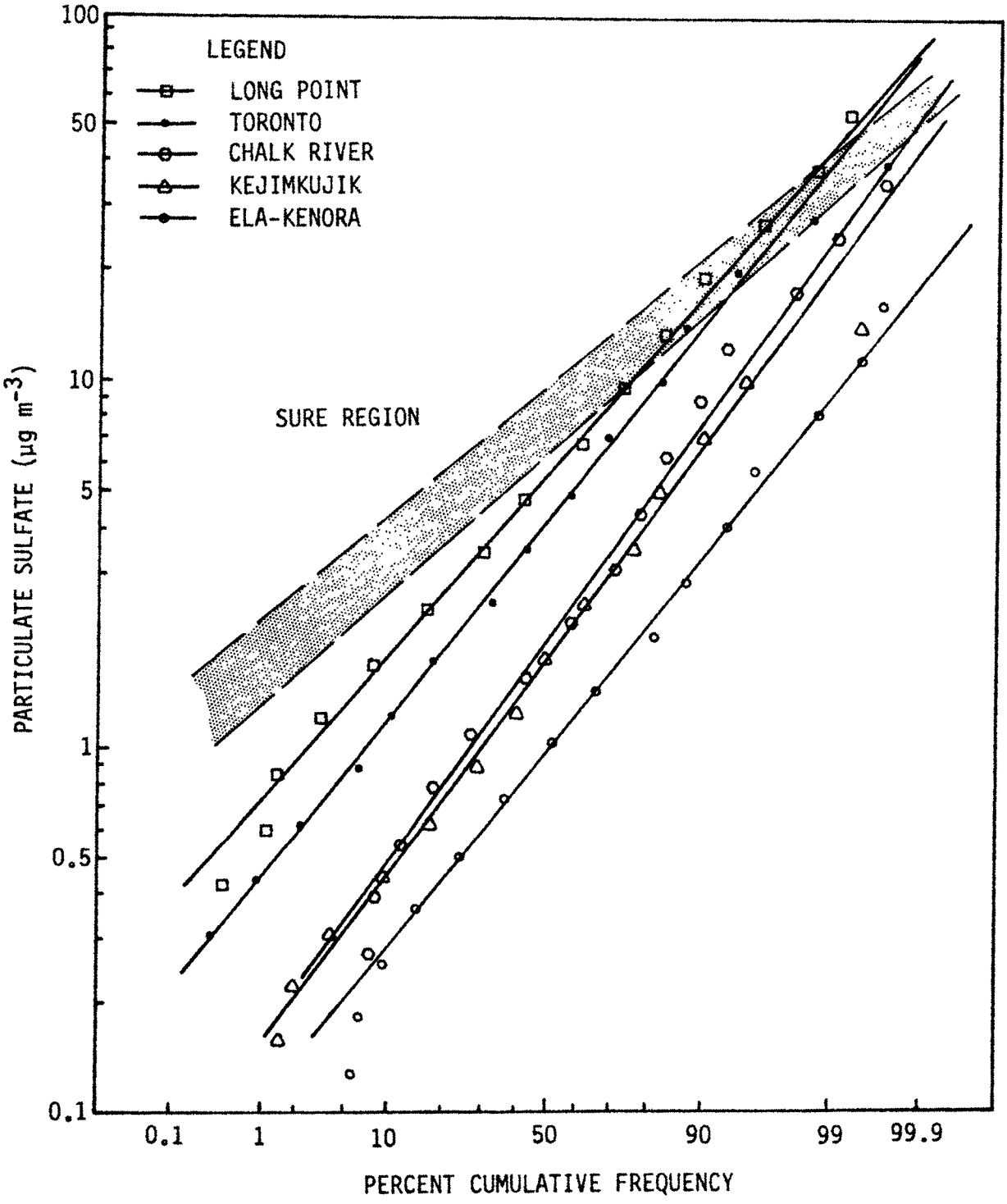

Figure 5-6. A comparison of the cumulative frequency distribution of daily sulfate concentration at several rural locations in eastern Canada for the period Nov. 1978 to Dec. 1979 with that for the 'SURE' region in the north eastern United States for 1974-75. Adapted from Barrie et al. (1983).

Samples were obtained at 125 m above ground level on a meteorological tower at Brookhaven National Laboratory from May through November 1975 (Tanner et al. 1977). The ratio of $[H^+]$ to $[NH_4^+]$ in ng m^{-3} varied from 0 to 1.6:1. In 9 of the 11 samples taken $[NH_4^+]$ was substantially in excess of $[H^+]$, particularly for the three samples collected in October and November, which were predominantly in the form of $(NH_4)_2SO_4$. Use of a diffusion battery sampling technique indicated that particles below the optical range were more acidic than the particles that effectively scatter light. It also was observed that air mass passage over water from source areas resulted in more acidic particles in the suboptical range than air mass passage over land.

Aerosol measurements were made at a rural site at Glasgow, IL, during a 9-day period late in July 1975 (Tanner and Marlow 1977). During the earlier portion of the sampling period with little or no strong acidity measurable, the air mass backward trajectories indicated reasonably direct transit from urban and/or power plant sources. Stagnation conditions occurred on 29-30 July with movement of the air mass from St. Louis past the vicinity of large power plant sources. Significant strong acidity was measurable in the aerosols reaching the Glasgow, IL, site during this period.

Measurements of sulfate aerosol composition were made in Research Triangle Park, NC, during 4 days in July 1977 (Stevens et al. 1978). Care was taken to preserve the acidity of the samples with use of a diffusion denuder to remove ammonia during collection and with preservation of the samples over nitrogen before analysis. The amount of strong acidity measured was highly variable among the 16 samples. In about half the samples, the strong acidity was zero or near zero. In three of the samples, the ratio of $[H^+]$ to $[NH_4^+]$ in neq m^{-3} was near 1:1. The highest ratio of $[H^+]$ to $[NH_4^+]$ occurred concurrently with the highest sulfate concentration.

Measurements of aerosol composition were carried out at a site in Tennessee at 646 m altitude in the Great Smoky Mountains National Park in the latter part of September 1978 (Stevens et al. 1980). Each of the 12 aerosol samples collected and analyzed for strong acidity were acidic. The average acidity was close to that of NH_4HSO_4. The higher ratios of $[H^+]$ to $[NH_4^+]$ occurred with the higher sulfate concentrations. Because no denuder was used to remove ammonia, some neutralization could have occurred. Therefore, it is possible that the samples were even more acidic than indicated by the measurements.

Weiss et al. (1982) at the Shenandoah Valley site obtained $(NH_4^+)/(SO_4^{2-})$ molar ratios ranging from 0.5 to 2.0 with strong diurnal variations. The particles were most acidic in midafternoon and least acidic between 0600 and 0900 hours.

Sulfate composition measurements were made on samples collected at 853 m on top of a tower on the summit of Allegheny Mountain in southeastern Pennsylvania between 24 July and 11 August 1977 (Pierson et al. 1980a). On the average, the $[H^+]$ was slightly in excess of $[NH_4^+]$, corresponding to a composition near that of NH_4HSO_4. The concentrations of the othercations were so low that $[H^+]$ and $[NH_4^+]$ were the predominant

cations associated with $[SO_4^{2-}]$, and the sum of $[H^+]$ and $[NH_4^+]$ was essentially stoichiometric with $[SO_4^{2-}]$. For sulfate concentrations above 15 $\mu g\ m^{-3}$ the $[H^+]$ to $[SO_4^{2-}]$ mole ratio was between 1:1 and 2:1 and approached 2:1 for several samples. Therefore, appreciable amounts of H_2SO_4 must have been present at the high sulfate concentration levels.

Lioy et al. (1980) reviewed in detail the high sulfate episode during August 3-9, 1977. The occurrence of a strong acid distribution on a regional scale was identified by these workers, based on measurements at High Point, NJ, Brookhaven, NY, and Allegheny Mountain (Pierson et al. 1980a).

Measurements of sulfate composition have been made by an infrared spectrophotometric technique (Kumar et al. 1982) at five nonurban sites in the eastern and midwestern United States near Rockport, IL; Racquette, NY; State College, PA; Charlottesville, VA; and Upton, NY. The average acidities by season of the year at these locations ranged from slightly more acidic than $(NH_4)_2SO_4$ to that equivalent to $(NH_4)_3H(SO_4)_2$, although acidities equivalent to that of NH_4HSO_4 were observed also. The acidities were reported to be higher in summer and winter than in spring and fall. Varying diural patterns were observed but acidities tended to be higher in the daylight hours than at night.

Acidity measurements were made on samples collected from aircraft and on the ground at a number of locations in the midwestern and eastern United States during the months of April, July, August, and November (Ferek et al. 1983). The higher acidities were obtained aloft and at Whiteface Mountain, NY during the spring and summer months. Acidities at these locations often corresponded to compositions between $(NH_4)_3H(SO_4)$ and NH_4HSO_4 and in some samples were more acid than NH_4HSO_4. Acidities were lower at ground level locations than aloft, in the midwest than in the east, and in November compared to the summer months.

In several investigations, the tendency was for the higher acidities to occur concurrently with the higher sulfate concentrations (Stevens et al. 1978, 1980; Pierson et al. 1980a).

In summary, there appears to be substantially more evidence for strong acidic species at rural than urban sites. The highest acidities in aerosols have been measured at mountain locations and in samples collected from aircraft aloft.

5.2.3.5 Concentration and Composition Measurements at Remote Locations--Meszaros (1978) reviewed available sulfate measurements at remote locations. He estimated an average sulfate concentration of 1.3 $\mu g\ m^{-3}$ over the Atlantic Ocean. The sulfate concentration as a function of latitude has two maxima. One of these occurs near 40°N latitude where SO_2 also has a maximum concentration and the other occurs south of the equator. Around 40°N the sulfate concentration is 2 $\mu g\ m^{-3}$, but decreases to below 1 $\mu g\ m^{-3}$ above 50°N. Meszaros estimated sulfate concentrations of about 0.3 $\mu g\ m^{-3}$ over clean areas in the Northern Hemisphere.

Gravenhorst (1978) obtained an average sulfate concentration of excess sulfate (excluding the contribution of sea salt) of 0.9 $\mu g\ m^{-3} \pm 0.5\ \mu g\ m^{-3}$. The excess sulfate tended to be acidic.

Measurements of sulfate were made at a remote sampling site in the Faroe Islands during February 1975 (Prahm et al. 1976). During a period when air masses were crossing the site after traveling only over the North Atlantic, excess sulfate averaged 0.14 $\mu g\ m^{-3}$. During another period when air masses had passed over the British Isles upwind, the excess sulfate averaged 1.07 $\mu g\ m^{-3}$.

An excess of submicron sulfur particles also was measured at a site in Bermuda (Meinert and Winchester 1977). The excess sulfur was attributed to long-range transport from the North American Continent.

Aerosol samples were collected from aircraft flying in the central and southern Pacific Ocean and remote areas of North America during GAMETAG by Huebert and Lazrus (1980a). The ranges of sulfate concentrations in different environments in $\mu g\ m^{-3}$ were: continental boundary layer, < 0.25 to 0.5; marine boundary layer, 0.36 to 3.6; free troposphere, < 0.06 to 0.35.

As indicated by the results of Meinert and Winchester (1977), Meszaros (1978), and by Prahm et al. (1976), remote sites can presumably be fumigated by continental sources well upwind.

5.2.3.6 Comparison of Sulfur Oxide Emissions and Ambient Air Concentrations of Sulfate--Ambient air concentrations of sulfate are the result of (1) primary sulfate emissions and (2) the secondary sulfate formed by conversion of a portion of the sulfur dioxide emissions to sulfate in the atmosphere. The relative contributions of primary and of secondary emissions to ambient air sulfates will vary with geographical location and time of year.

Altshuller (1980) concluded that reductions of fuel sulfur content within urban areas in the northeastern United States caused substantial reductions in primary sulfate emissions. This reduction in primary sulfate emissions in turn appeared to account for the decrease in ambient air sulfate concentrations during the first and fourth quarters of the year. In contrast, the ambient air sulfate concentrations increased during the third quarter of the year in urban areas. These increases in ambient air sulfate concentrations appear to relate to the increases in regional scale emissions of sulfur dioxide and sulfate.

In nonurban areas in the eastern United States during the late 1960's into the early 1970's small increases in ambient air sulfate concentrations occurred in the first and second quarters of the year. A substantial increase in ambient air sulfate concentrations occurred from the mid-1960's into the early 1970's during the third quarter of the year at nonurban sites in the northeastern and midwestern United States (Altshuller 1980).

Less than a proportional increase in ambient air sulfate concentrations should occur because part of the sulfate formed from the incremental

emissions of sulfur dioxide remains aloft (Chapter A-2, Section 2.3.2). The sulfate aerosol formed from the sulfur dioxide emissions in plumes from tall stacks remains aloft long distances, particularly during the cooler months of the year (Chapter A-3, Section 3.4.1). A portion of the sulfate emitted aloft will be removed by wet scavenging and a portion will pass into Canada or over the Atlantic. This portion of the sulfate will not contribute to sulfate concentrations measured at ground level monitoring sites in nonurban areas in the United States. During the third quarter of the year, deeper mixing within the boundary layer occurs more frequently and brings the plume down to the ground shorter distances downwind of the stack (Chapter A-3, Section 3.4.1). Therefore, a larger portion of the incremental sulfur oxide emissions as sulfate should be measurable during the third quarter of the year at ground-level monitoring sites in nonurban areas in the United States.

Increases in visibility and turbidity with increases in sulfur oxide emissions from the 1950's or 1960's into the 1970's have been observed, particularly during the third quarter of the year (Husar and Patterson 1980). The trends with time and the seasonal patterns of airport visibility measurements over horizontal ranges and turbidity measurements through the entire air mass closely resemble those of the sulfate concentrations. This is to be expected because sulfate accounts for a large part of the light extinction at rural sites in the eastern United States (Section 5.8).

5.2.4 Particle Size Characteristics of Particulate Sulfur Compounds

5.2.4.1 Urban Measurements--Particle size distributions have been reported in a number of urban locations for sulfur as sulfate in collected particulate matter. Similar results do not appear to be available for sulfur in any other valence state. Stevens et al. (1978) attempted to analyze for sulfite in samples from South Charleston, WV, Research Triangle Park, NC, New York, NY, and Philadelphia, PA. The sulfite content of the samples did not exceed the minimum detection limit of 8 ng m^{-3}. By comparison with the fine particle sulfur concentration, this results in less than 0.1 percent of the extractable sulfur as sulfite or 2 percent of the total fine particle (< 3.5 μm) sulfur as sulfite.

A five-stage impactor with stage mass median diameters (MMD's) of 1.9, 3.6, and 7.2 μm with a backup filter was used at two sites in Pittsburgh, PA, in 1963-64 to separate particulate matter into size fractions (Corn and Demaio 1965). Sulfate was measured by a turbidimetric method. A substantial amount of the sulfate was reported to be in larger particles with MMD's between 1.9 and 3.6 μm.

Size distribution of sulfate in particulate matter was determined by Roesler et al. (1965) at sites in Chicago, IL, and Cincinnati, OH. A six-stage Andersen cascade impactor was used for particle size distributions. Sulfate was measured by a turbidimetric method. The MMD's obtained at the sites in Cincinnati and Chicago were 0.4 μm and 0.3 μm, with nearly 90 percent of the sulfate less than 3.5 μm.

Wagman et al. (1967) obtained sulfate size distributions at sites in Chicago, IL, Cincinnati, OH, and Philadelphia, PA, during 1965. Lee and Patterson

(1969) reported ammonium size distributions during the same time periods at these sites. A six-stage Andersen cascade impactor was used for size separations. Sulfate was analyzed by the turbidimetric method, and ammonium was determined by the Nessler method with alkaline potassium mercuric iodide. The average MMD's for sulfate and ammonium were similar, with an overall range from 0.35 to 0.66 μm. The higher MMD in Philadelphia was attributed in part to dust generated from road construction near the site. Eighty percent of the sulfate was less than 2 μm at all of the sites.

Sulfate particle size increased with humidity at all sites (Wagman et al. 1967). Substantial scatter occurred with MMD ranging from less than 0.2 μm at lower humidities to 0.6 to 0.8 μm at higher humidities at three mid-western sites. At the site in Philadelphia, PA, the MMD exceeded 1 μm at higher humidities. Correlation of MMD's with absolute humidities was poor.

Ludwig and Robinson (1968) obtained particle size distribution of samples collected in the Los Angeles and San Francisco Bay areas of California in 1964-65. A Goetz aerosol spectrometer was used. The analytical procedure involved high-temperature reduction of the sulfur in the sample to hydrogen sulfide in a microcombustion furnace and iodimetric microcoulometric titration for the hydrogen sulfide. Average MMD's were computed from measurements at several sites in Los Angeles and the San Francisco Bay area. Except at the Lennox, CA, site, the MMD's ranged from 0.2 to 0.4 μm. The Lennox site is directly downwind of a number of emission sources, including an oil refinery and a sewage treatment plant, and is 2 miles from the ocean, which may account for the higher MMD at this site.

Ludwig and Robinson (1968) reported that at these West Coast sites, samples collected during periods of higher relative humidity (RH) had the higher MMD's for sulfur-containing particles. The weighted average MMD varied from 0.1 μm in the 12.5 to 27.5 percent RH class to 1.1 μm in the 72.5 to 87.5 percent RH class.

Ludwig and Robinson (1968) also observed diurnal decreases in the sulfate size distribution by time of day as follows: forenoon > afternoon > early morning > evening. Wagman et al. (1967) did not observe consistent diurnal changes in sulfate size distribution from site to site. In fact, only the Chicago, IL, site showed significant changes in sulfate size distribution with sulfate size decreasing by time of day as follows: morning > midday > evening. Therefore, in Chicago and at the West Coast sites, sulfate particles tended to be smaller during the evening hours. Both groups of investigators reported no relation between diurnal variations in sulfate size and humidity changes, but no explanation in terms of atmospheric processes was suggested.

Particle size distributions for sulfate and other species were obtained in Riverside, CA, during the first half of November 1968 (Lundgren 1970). Samples were collected on a four-stage Lundgren impactor. The average MMD for sulfate was about 0.3 μm with the range of MMD's for the 10 samples collected varying from 0.1 to 0.6 μm. On the average, about 90 percent of the sulfate in the collected particles was below 1.7 μm. Particle size

distributions of sulfate also were reported by Appel et al. (1978) for the Los Angeles, CA, Basin area as 0.3 to 0.4 μm for most samples.

Patterson and Wagman (1977) obtained particle size distribution of collected samples for a number of species including sulfate and ammonium in Secaucus, NJ, near New York, NY, between 29 September and 10 October 1970. Seven-stage Andersen cascade impactors were used at 28 ℓ min^{-1}, with either Gelman type A glass-fiber or Millipore® backup filters. Sulfate was analyzed by the methods used previously (Wagman et al. 1967, Lee and Patterson 1969). The air masses traveling across the site were classified into four visual range classes. For sulfate and ammonium, the MMD's, by visual range class, were:

Visual range (mi)	Sulfate (μm)	Ammonium (μm)
> 26	0.60	0.26
13 to 26	0.39	0.34
8 to 13	0.46	0.38
< 8	0.40	0.36

The MMD's for sulfate and ammonium were reasonably similar except for the background case of > 26 miles. For this condition, much more of the mass of the sulfate was in the range 0.54 to 0.95 μm than was the case for ammonium. Almost all of the sulfate and ammonium in the collected particles was below 1.5 μm.

Tanner et al. (1979) measured sulfate in August 1976 and February 1977 in New York, NY, using a diffusion battery along with HIVOL sampling. The diffusion battery was used to classify particles by size less than 0.25 μm before filter sampling and analysis. During the summer month, about 50 percent of the sulfur-containing aerosols were less than 0.25 μm; during the winter month only 25 percent were less than 0.25 μm.

Stevens et al. (1978) concluded from measurements for sulfur along with other metals in New York, NY, Philadelphia, PA, Charleston, WV, St. Louis, MO, Portland, OR, and Glendora, CA, that sulfate in the fraction less than 3.5 μm had to be associated predominantly with ammonium and hydrogen ions in urban areas. If all of the metals were assumed to be in the form of sulfates, only 10 to 32 percent of the sulfate would be accounted for as metal sulfates at these urban sites. Because it is likely that most of the metals would be in the form of oxides, halides, or carbonates rather than sulfates, these estimates would form upper limits.

Separation of particles into two fractions with a fine fraction consisting of particles less than 3.5 μm involves use of a virtual impactor or dichotomous sampler (Stevens et al. 1978). The percentages of sulfur found in the size range less than 3.5 μm at various sites were: New York, NY--93%; Philadelphia, PA--85%; Charleston, WV--92%; St. Louis, MO--79%; Portland, OR--83%; Glendora, CA--87%. Sampling was done in the winter months of 1975 and 1977. In additional measurements reported from a site in Charleston, WV, 91 percent of the sulfur measured during a period in the summer of 1976 was in the fine particle size range (Lewis and Macias 1980). Altshuller (1982) analyzed data on particulate sulfur measured with dichotomous samplers at

urban sites in St. Louis, MO. From 80 to 90 percent of sulfur measured was fine particle sulfur with no substantial seasonal pattern between the third quarter of 1975 and the fourth quarter of 1976.

5.2.4.2 Nonurban Size Measurements--Junge (1954, 1963) reported on the particle size of sulfate aerosols at Round Hill, MA, 50 miles south of Boston, and at a site south of Miami, FL. He found most of the particles containing sulfate to be in the 0.08 to 0.8 μm range rather than in the 0.8 to 8 μm range. Junge (1963) found the average composition of the particles between 0.08 and 0.8 μm to correspond to a mixture of $(NH_4)_2SO_4$ and $(NH_4)HSO_4$.

Charlson et al. (1974) found strong acidity in particles at Tyson Hollow, MO, 35 km WSW of the Arch in St. Louis, using an integrating nephelometer with humidity control (humidograph). Because the nephelometer would respond to particles predominantly in the optical range, 0.1 to 1 μm, the technique associates acidity with submicron-size acid sulfate particles. In subsequent work in the St. Louis area, well over 90 percent of sulfur in particles measured at rural sites near St. Louis were found to be in the fine particle size range with little, if any, seasonal variation (Altshuller 1982).

Measurements of particle size distribution of sulfates were made with a diffusion battery technique at Glasgow, IL, 104 km NNW of the Arch in St. Louis, from July 22-30, 1975 (Tanner and Marlow 1977). About 50 percent of the sulfate containing particles were less than 0.25 μm in size. The higher acidities were associated with the submicron particles.

In the previously mentioned sulfate measurements in the Great Smoky Mountains National Park, strong acidity was associated with the fine particle size fraction (Stevens et al. 1980). It was estimated that ammonium bisulfate constituted 61 percent of the fine particle mass.

Pierson et al. (1980a) used an Andersen eight-stage cascade impactor to obtain particle size distributions for sulfate and hydrogen ions at a tower on Allegheny Mountain in southwestern Pennsylvania. The particle size distribution curves for sulfate and hydrogen ion were almost identical, with an average MMD of 0.8 μm. About 90 percent of the sulfate and hydrogen ion content was less than 3 μm. The $[H^+]$-to-$[SO_4^{2-}]$ ratios were somewhat higher for particles between 0.7 and 1.1 μm than for those less than 0.7 μm, or between 1 and 2 μm. Acidity was measured in even larger particles but the $[H^+]$ to $[SO_4^{2-}]$ ratio was lower than for particles less than 2 μm (Pierson et al. 1980a).

Aircraft outfitted with particle sizing equipment were flown across portions of Arizona, Utah, Colorado, and New Mexico on 5 and 9 October 1977 (Macias et al. 1980). The MMD for sulfur in the collected particles was not reported, but can be approximated as less than 0.5 μm. Sulfur particles less than 1 μm constituted 92 percent of the sulfur content.

5.2.4.3 Measurements at Remote Locations--Gravenhorst (1978) found the excess sulfate in marine aerosols to be present in submicron-size particles. The sulfate associated with sea salt was present in supermicron particles.

Meinert and Winchester (1977) also found the excess sulfate to be present in submicron-size particles in samples collected in Bermuda. Similarly, the excess sulfate in samples collected off the West African coast was in submicron-size particles and the larger particles appeared to contain the sulfate associated with sea salt (Bonsang et al. 1980).

5.3 NITROGEN COMPOUNDS

5.3.1 Introduction

The nitrogen oxides and their atmospheric reaction products constitute a more complex group of chemical species than do sulfur dioxide and particulate sulfates. Unlike sulfates, nitrate composition frequently is dominated by volatile species, nitrous acid, nitric acid, and organic nitrates, particularly peroxyacetyl nitrates. Nitrous oxide, although present in significant trace concentrations in the atmosphere, does not react within the troposphere.

Nitric oxide, the predominant nitrogen oxide in emissions can be converted rapidly to nitrogen dioxide by reactions with oxy radicals and ozone in the atmosphere. Subsequent atmospheric reactions result in the formation of nitric acid. Nitric acid and ammonia are in equilibrium with ammonium nitrate. Ammonium nitrate formation is favored by lower temperatures and sufficiently high levels of ammonia. Mixed nitrate-sulfate aerosol systems also play a significant role in determining the nitric acid concentration, as does relative humidity. Nitrous acid can form at night but is rapidly photolyzed in daylight. A wide variety of volatile organic nitrates can be synthesized in the laboratory; however, many are short-lived in the atmosphere or, if present, occur at parts-per-trillion concentrations. The exceptions are the peroxyacetyl nitrates (PAN), which are present at significant concentration levels relative to the other nitrogen oxides and their acids. Because the peroxyacetyl nitrates and their precursors are in reversible equilibrium, nitrogen dioxide can be regenerated and nitric acid may be formed as these species undergo atmospheric transport.

As a consequence of the atmospheric reactions discussed above, several species containing nitrogen can contribute directly or indirectly to acidic deposition.

5.3.2 Nitrogen Oxides

5.3.2.1 Historical Distribution Patterns and Current Concentrations of Nitrogen Oxides--Nitric oxide is the most commonly emitted oxide of nitrogen. Less than 10 percent of nitrogen oxides are emitted as nitrogen dioxide (NO_2). Exceptions are found in emissions from some types of diesel and jet turbine engines and tail gas from nitric acid plants, which can contain from 30 to 50 percent nitrogen dioxide. Because nitric oxide (NO) converts rapidly to NO_2 in the atmosphere, NO_2 is the predominant form of nitrogen found outside cities.

Historical trends for NO and NO_2 are not available from nonurban sites but are available from a limited number of urban sites. Because of these

limitations, it is not useful to separate historical trends from current measurement results.

5.3.2.2 Measurements Techniques-Nitrogen Oxides--Most of the nitrogen oxide measurements made during the 1970's involved use of chemiluminescent analyzers. While the chemiluminescent technique can be used to analyze nitric oxide directly and specifically, analysis of nitrogen dioxide or nitrogen oxides (NO + NO_2) requires a converter to reduce nitrogen dioxide to nitric oxide. However, it has been found that such converters also will reduce other nitrogen compounds to nitric oxide. Winer et al. (1974) reported that commercial chemiluminescent analyzers equipped with either molybdenum or with carbon converters quantitatively reduced peroxyacetyl nitrate to nitric oxide. Nitric acid also was observed to cause a response in chemiluminescent analyzers, but the response to nitric acid was not determined quantitatively.

Spicer and coworkers discussed the use of various converters or scrubbers (Spicer 1977, Spicer et al. 1976b, Spicer and Miller 1976). Nearly quantitative, but somewhat variable chemiluminescent responses to nitric acid have been obtained (Spicer and Miller 1976, Spicer et al. 1976b). The reduction of nitric acid to nitric oxide by a stainless steel converter was shown to increase rapidly from below 10 percent to over 90 percent between 400 C and 550 C. However, the use of the lower temperature also reduces the efficiency of conversion of nitrogen dioxide to nitric oxide by stainless steel converters, so lowering the temperature would not be a satisfactory approach (Spicer et al. 1976b). Although carbon converters will reduce nitrogen dioxide to nitric oxide efficiently at lower temperatures than stainless steel, the nitric acid reduction also continues to occur efficiently down to 140 C. Nylon filters or scrubbers remove nitric acid but not peroxyacetyl nitrate and provide a basis for analyzing nitric acid differentially (Spicer et al. 1976b). Use of ferrous sulfate as a scrubber was found to remove nitric acid with high efficiency, but it also removed a variable fraction of peroxyacetyl nitrate (Spicer et al. 1976b). Use of such scrubbers with chemiluminescent instruments permits the analysis not only of nitrogen oxides but also of other nitrogen compounds (Kelly and Stedman 1979b, Spicer et al. 1976b, Spicer 1979).

5.3.2.3 Urban Concentration Measurements--The Air Quality Criteria for Oxides of Nitrogen (U.S. EPA 1982) contains detailed compilations of ambient air concentrations of nitrogen dioxide in U.S. urban areas. Pertinent data from the criteria document are summarized in the following discussion. Average NO and NO_2 concentrations at Continuous Air Monitoring Program (CAMP) sites were comparable, while peak concentrations of NO tended to exceed peak concentrations of NO_2.

Trends in NO_2 concentrations at the six CAMP sites in Philadelphia, PA, Chicago, IL, Cincinnati, OH, Denver, CO, St. Louis, MO, and Washington, DC, and at other sites in Los Angeles, CA, Azusa, CA, Newark, NJ, and Portland, OR, have been tabulated and statistically analyzed.

The annual mean concentrations of NO_2 at the sites ranged from 50 to 150 $\mu g\ m^{-3}$ with the higher concentrations occurring at the sites in downtown

Los Angeles and in Chicago. The maximum 1-hr NO_2 concentrations at these sites ranged from 200 to 1500 $\mu g\ m^{-3}$. Peak 1-hr concentrations above 750 $\mu g\ m^{-3}$ were frequently measured in downtown Los Angeles and Azusa, CA, but infrequently, if at all, at other sites. Both upward and downward trends with time were measured at these sites.

At 31 urban sites during 1976, the maximum 1-hr concentrations ranged from 216 to 815 $\mu g\ m^{-3}$. The annual mean concentrations at two-thirds of these sites ranged from 50 to 100 $\mu g\ m^{-3}$.

Seasonal behavior in NO_2 concentrations varied at urban sites, with a summer peak occurring at a site in Chicago, IL, winter peaks at sites in Denver, CO, and Lennox, CA, but no significant seasonal trends at other sites in California.

The diurnal patterns of NO_2 concentrations are available by quarter of the year at eight sites (Trijonis 1978). Except for the two sites in the western part of the Los Angeles Basin, the diurnal patterns show two peaks--one in the morning hours, the other late in the afternoon or during the evening hours. At the two sites in Los Angeles, only a single peak late in the morning hours was observed. These peaks varied in size from site to site and with the quarter of the year.

5.3.2.4 Nonurban Concentration Measurements--Measurements made of nitric oxide and nitrogen dioxide at suburban and at rural locations in the United States are tabulated in Table 5-2. Mean and maximum concentrations of nitrogen oxides are listed. At eastern nonurban locations the mean concentrations of nitric oxide ranges from 1 to 10 $\mu g\ m^{-3}$ while the mean concentrations of nitric oxide at western rural locations were at or below 1 $\mu g\ m^{-3}$. Maximum concentrations of nitric oxide at a number of sites exceeded mean concentrations by factors of 10 to 30. At eastern nonurban locations the mean concentrations of nitrogen dioxide ranges were from 2 to 27 $\mu g\ m^{-3}$, but most of the mean values ranged from 4 to 14 $\mu g\ m^{-3}$. At two western rural sites the mean concentrations of nitrogen dioxide were at or below 3 $\mu g\ m^{-3}$. Maximum concentrations of nitrogen dioxide at most sites listed in Table 5-2 exceed mean concentrations by factors of 5 to 10. Although mean concentrations of nitrogen dioxide at a site exceed mean concentrations of nitric oxide, maximum concentrations of nitric oxide at a number of sites equal or exceed maximum concentrations of nitrogen dioxide. This latter effect suggests that occasional fumigations by strong local sources of nitric oxide can occur at many rural locations.

The range of mean nitrogen dioxide concentrations of 4 to 14 $\mu g\ m^{-3}$ given above compares with the 50 to 100 $\mu g\ m^{-3}$ range obtained for many urban sites (Section 5.3.2.3). Additional measurements related to the gradient of nitrogen dioxide concentrations between urban and rural sites are available from the RAPS/RAMS monitoring results in the St. Louis area (U.S. EPA 1982). During an air pollution episode in St. Louis during 1 and 2 October 1976, nitrogen dioxide as well as other compounds including ozone were elevated in concentration. The diurnal patterns and concentrations of nitrogen dioxide at rural compared to urban sites were substantially different. The diurnal patterns at urban sites included two peaks in nitrogen dioxide, one in the

TABLE 5-2. MEASUREMENTS OF CONCENTRATIONS OF NITROGEN OXIDES AT SUBURBAN AND RURAL SITES

Site (Type)	Period of measurement (method)	Nitric oxide, $\mu g\ m^{-3}$ Mean	Max.	Nitrogen dioxide, $\mu g\ m^{-3}$ Mean	Max.	Reference
Montague, MA (R)	Aug.-Dec. 1977 (chemilumin.)	3	78	7	73	Martinez and Singh 1979
Ipswhich, MA (R)	Dec. 54-Jan. 55 (colorimetric)	ND	ND	2.6	3.8	Junge 1956
Scranton, PA (S)	Aug.-Dec. 1977 (chemilumin.)	3	70	11	64	Martinez and Singh 1979
DuBois, PA (R)	June-Aug. 1974 (chemilumin.)	ND	ND	19	70	Research Triangle Institute 1975
Bradford, PA (R)	July-Sept. 1975 (chemilumin.)	2.4	34	5.1	68	Decker et al. 1976
McHenry, MD (R)	June-Aug. 1974 (chemilumin.)	ND	ND	11	60	Research Triangle Institute 1975
Indian River DE (S)	Aug.-Dec. 1977 (chemilumin.)	3	114	5	48	Martinez and Singh 1979
Lewisburg, WV (R)	Aug.-Dec. 1977 (chemilumin.)	1	33	4	28	Martinez and Singh 1979
Shenandoah, VA (R)	July-Aug. 1980 (chemilumin.)	1	NA	4	NA	Ferman et al. 1981
Research Triangle Park, NC (S)	Nov. 65-Jan. 66 Sept. 66-Jan. 67 (colorimetric)	2.3 NA	NA NA	10.6 14.3	NA NA	Ripperton et al. 1970

TABLE 5-2. CONTINUED

Site (Type)	Period of measurement (method)	Nitric oxide, $\mu g\ m^{-3}$ Mean	Max.	Nitrogen dioxide, $\mu g\ m^{-3}$ Mean	Max.	Reference
Research Triangle Park, NC (S)	Aug.-Dec. 1977 (chemilumin.)	10	249	13	145	Martinez and Singh 1979
Green Knob, NC (R) Appalachian Mt.	Sept. 1965 (colorimetric)	2.7	NA	6.4	NA	Ripperton et al. 1970
Florida, southeast coast	July-Aug. 1954 (colorimeteric)	ND	ND	1.8	3.7	Junge 1956
DiRidder, LA (R)	June-Oct. 1975 (chemilumin.)	1.9	17	4.9	43	Decker et al. 1976
Wilmington, OH (S)	June-Aug. 1974 (chemilumin.)	ND	ND	13	90	Research Triangle Institute 1975
McConnelsville, OH (R)	June-Aug. 1974 (chemilumin.)	ND	ND	12	70	Research Triangle Institute 1975
Wooster, OH (S)	June-Aug. 1974 (chemilumin.)	ND	ND	13	90	Research Triangle Institute 1975
New Carlisle, OH (R)	July-Aug. 1974 (chemilumin.)	6.0	64	27	NA	Spicer et al. 1976a
Ashland, Co., OH (R)	May-Dec. 1980 (chemilumin.)	4.3	NA	15.6	NA	Shaw et al. 1981 Shaw et al. 1981

TABLE 5-2. CONTINUED

Site (Type)	Period of measurement (method)	Nitric Oxide, $\mu g\ m^{-3}$ Mean	Max	Nitrogen Dioxide, $\mu g\ m^{-3}$ Mean	Max	Reference
Franklin Co., IN (R)	May-Dec. 1980 (chemilumin.)	3.0	NA	14.3	NA	Shaw et al. 1981
Union Co., KY (R)	May-Dec. 1980 (chemilumin.)	2.5	NA	12.3	NA	Martinez and Singh 1979
Giles Co., TN (R)	Aug.-Dec. 1977 (chemilumin.)	5	96	11	55	Martinez and Singh 1979
Creston, IA (R)	June-Sept. 1975 (chemilumin.)	4.7	28	4.3	25	Decker et al. 1976
Wolf Point, MT (R)	June-Sept. 1975 (chemilumin.)	< 1.0	NA	1.5	NA	Decker et al. 1976
Pierre, SD (R), site 40 km WNW of Pierre	July-Sept. 1978 (chemilumin.)	< 0.25	NA	2.3	NA	Kelly et al. 1982
Jetmore, KA (R)	April-May 1978 (chemilumin.)	1.2	NA	7.5	NA	Martinez and Singh 1979

R = Rural.

S = Surburban.

ND = Not determined.

NA = Not available.

late morning hours and the other during the evening hours. At suburban sites only an evening peak in nitrogen dioxide occurred, while at rural sites no peak in nitrogen dioxide concentration was observed. The evening peaks in nitrogen dioxide concentration within the city ranged from 250 to 500 $\mu g\ m^{-3}$, while the concurrent concentrations of nitrogen dioxide at the outermost rural sites, 40 km from the center of the city, ranged from 20 to 40 $\mu g\ m^{-3}$. Similarly the 24-hr average concentrations of nitrogen dioxide ranged from 200 to 265 $\mu g\ m^{-3}$ at urban sites but averaged only 20 $\mu g\ m^{-3}$ at rural sites. These results demonstrate the rapid decrease in nitrogen dioxide concentrations that can occur from urban sites to adjacent rural sites.

The cumulative frequency distributions of hourly nitrogen dioxide concentrations reported in two studies (Decker et al. 1976, Research Triangle Institute 1975) are reproduced in part in Table 5-3. Except at the sites evaluated as suburban (Table 5-2), nitrogen dioxide concentrations exceeding 40 $\mu g\ m^{-3}$ occur very infrequently at nonurban sites. Even at those sites considered to be in suburban locations, nitrogen dioxide concentrations were infrequently above 60 $\mu g\ m^{-3}$. The highest nitrogen dioxide concentrations at nonurban locations infrequently fall within the range of mean nitrogen dioxide concentrations at urban sites.

The distinction between suburban and rural sites was made on the basis of three factors: (1) geographical location, (2) frequency of elevated concentrations of nitric oxide, and (3) the ratio of nitric oxide to nitrogen oxides ($NO + NO_2$). The third of these factors was discussed in some detail by Martinez and Singh (1979). They found this ratio tended to be lower at rural than at urban or suburban sites. At the four SURE sites they considered rural, the ratios of NO to NO_X ranged from 0.11 to 0.33 and averaged 0.23. At the five SURE sites they considered suburban, the ratios of NO to NO_X ranged from 0.21 to 0.43 and averaged 0.33.

Some of the relationships discussed above may be somewhat biased by the tendency in a number of the studies involving nonurban sites to limit the measurements to the warmer months of the year. Nitrogen dioxide concentrations during the winter months have been reported to exceed those during the summer months by 50 to 100 percent (Shaw et al. 1981). Nevertheless, the measurements available do indicate a rapid decrease in nitrogen oxide concentrations from urban to suburban to rural locations in the eastern United States.

5.3.2.5 Measurements of Concentrations at Remote Locations--The results of measurements for nitrogen oxides from a number of studies carried out at remote locations are tabulated in Table 5-4. The distinction between remote and rural locations is somewhat arbitary. In this discussion, locations at which concentrations of nitrogen dioxide of less than 1 $\mu g\ m^{-3}$ were frequently measured are considered to be remote. However, substantially higher concentrations of nitrogen oxides were observed at a number of these locations on those occasions that polluted air masses crossed over the measuring sites.

TABLE 5-3. CUMULATIVE FREQUENCY DISTRIBUTION OF HOURLY CONCENTRATIONS OF NITROGEN DIOXIDE AT RURAL AND SUBURBAN LOCATIONS

Site/reference	Measurement period	Percent of hourly average concentrations greater than stated concentrations			
		20 $\mu g\ m^{-3}$	40 $\mu g\ m^{-3}$	60 $\mu g\ m^{-3}$	80 $\mu g\ m^{-3}$
DuBois,PA Research Triangle Institute 1975	June-Aug. 1974	13.2	1.0	0.2	0.0
Bradford, PA Decker et al. 1976	July-Sept. 1975	2.1	0.1	0.0	0.0
McHenry, MD Research Triangle Institute 1975	June-Aug. 1974	6.9	0.2	0.1	0.0
Wooster, OH Research Triangle Institute 1975	June-Aug. 1974	23.8	6.9	1.9	0.3
McConnelsville, OH Research Triangle Institute 1975	June-Aug. 1974	5.6	0.5	0.1	0.0
Wilmington, OH Research Triangle Institute 1975	June-Aug. 1974	14.9	2.6	1.1	0.5
Creston, IA Decker et al. 1976	July-Sept. 1975	0.2	0.0	0.0	0.0
Wolf Point, MT Decker et al. 1976	July-Sept. 1975	0.4	0.0	0.0	0.0
De Ritter, LA Decker et al. 1976	July-Sept. 1975	4.8	0.3	0.0	0.0

TABLE 5-4. CONCENTRATIONS OF NITROGEN OXIDES MEASURED AT REMOTE LOCATIONS

Sites	Measurement period (method)	Concentrations in $\mu g\ m^{-3}$			Remarks	Reference
		NO	NO_2	NO_x[a]		
Colorado, USA Niwot Ridge	Jan. and April 1979 (chemilumin.)	0.02-0.06	NA	0.4-0.5		Kelly et al. 1980
Colorado, USA Niwot Ridge	Dec. 1980 to Jan. 1981 (chemilumin.)	NA	NA	< 0.1		Bollinger et al. 1982
Colorado, USA Fritz Peak	Fall 1974; Summer Spring 1975-76 (absorption spectroscopy)	NA	< 0.2	NA		Noxon 1978
	Dec. 1977 (chemilumin.)	NA	NA	0.2-0.5		Kley et al. 1981
Island of Hawaii Mauna Kea	Nov. 1954 (colorimetric)	ND	2	ND		Junge 1956
Laramie, WY	Summer 1975 (chemilumin.)	0.01-0.06	NA	0.2-0.8		Drummond 1976
Ireland, Adrigole Co. Cork	Aug.-Sept. 1974 (chemilumin.)	$\leq$ 0.2	0.8	NA	Maritime air	Cox 1977
Ireland, Loop Head	April 1979 (Diff. opt. abs. uv)	ND	0.3	ND	Maritime air	Platt and Perner 1980
Ireland, Loop Head	June 1979 (chemilumin.)	< 0.01	0.16	NA	Maritime air	Helas and Warneck 1981

TABLE 5-4. CONTINUED

Sites	Measurement period (method)	Concentrations in $\mu g\ m^{-3}$			Remarks	Reference
		NO	NO_2	NO_x[a]		
Tropical Areas	1965-1966 (colorimetric)	0.1-0.6	0.4-0.8		Under canopy of forest	Lodge and Pate 1966, Lodge et al 1976
		0.3-0.5	0.6-0.9		Above canopy of forest	
		0.3-0.8	0.6-0.1		Riverbank	
		0.3-0.8	0.6-0.9		Seashore and maritime	

At Niwot Ridge in the Rocky Mountains 20 miles west of Boulder, CO, Kelly et al. (1980) reported average concentrations of 0.4 to 0.5 μg m^{-3} in clean air, while Bollinger et al. (1982) reported nitrogen oxide concentrations below 0.1 μg m^{-3} in a number of clear air masses passing this site. In contrast, Kelly et al. (1980) observed nitrogen oxide concentrations up to 40 μg m^{-3} when polluted air arrived from the east. At Adrigole on the coast of Ireland, Cox (1977) measured nitrogen dioxide concentrations below 1 μg m^{-3} in maritime air but also reported measuring maximum hourly concentrations of nitrogen dioxide of 10 μg m^{-3} and a maximum daily average value of about 3 μg m^{-3}. Similarly at Loop Head, the concentrations of nitrogen dioxide measured in maritime air by Platt and Perner (1980) were below 0.3 μg m^{-3}, in other air masses they measured nitrogen dioxide concentrations from 4 to 5 μg m^{-3}. Therefore, although the sites listed in Table 5-4 are listed as remote, it was not uncommon for air masses containing nitrogen oxide concentrations overlapping those at rural locations to pass across these sites.

In aircraft flights up to 5 to 6 km over West Germany, Drummond and Volz (1982) measured nitrogen dioxide concentrations in the 0.1 to 1 μg m^{-3} range. Kley et al. (1981) measured nitrogen oxide concentrations as low as 0.1 μg m^{-3} at 7 km over the vicinity of Wheatland, WY. During the 1977 and 1978 GAMETAG flights, nitric oxide concentrations equal to or below 0.1 μg m^{-3} were measured in maritime and in continental air at 6 km.

The measurements at the surface and aloft at remote locations result in very low concentrations of nitrogen oxides in clean air masses. The background concentrations at the surface and aloft at remote locations can be 10 to 100 times lower than at rural locations in eastern North America (Tables 5-2 and 5-3). The higher concentrations measured at remote locations are attributed by the various investigators to polluted air masses from populated areas. Therefore, natural sources of nitrogen oxides do not appear likely to contribute significantly to the nitrogen oxide concentration levels in eastern North America.

5.3.3 Nitric Acid

5.3.3.1 Urban Concentration Measurements--Nitric acid (HNO_3) measurements have been limited to short studies within urban areas. Continuous coulometry (Spicer et al. 1976b, Spicer 1977) with a detection limit of about 2 ppb (5.16 μg m^{-3}) and Fourier transform infrared spectroscopy (FTIR) with a detection limit of 6 ppb (15.48 μg m^{-3}) (Tuazon et al. 1978, 1980, 1981a, b; Hanst et al. 1982) were used to obtain the ambient air measurements for HNO_3 listed in Table 5-5. An intercomparison study was conducted on the 10 different techniques for measuring nitric acid in Claremont, CA, during an 8-day period in August and September 1979 (Forrest et al. 1982, Spicer et al. 1982a). The methods compared included chemiluminescence, infrared, diffusion denuder, and filtration techniques. The nitric acid concentrations ranged from 1.8 to 37.0 μg m^{-3} or 0.7 to 14.4 ppb based on the median values of the 10 methods (Spicer et al. 1982a).

The average HNO_3 concentrations in the Los Angeles Basin area ranged from 7 to 40 μg m^{-3} (Table 5-5). The Riverside site where the highest ammonia

TABLE 5-5. CONCENTRATIONS OF NITRIC ACID, PEROXYACETYL NITRATE, AND AMMONIA AT URBAN SITES IN THE UNITED STATES

Site	Period of year	Concentrations, μg m^{-3}						References
		HNO_3		PAN		NH_3		
		Avg	Max	Avg	Max	Avg	Max	
West Los Angeles, CA (Cal. State Univ.)	June 1980	18.1	30.0	35	80	2.1	5.6	Hanst et al. 1982
West Covina, CA	Aug-Sept. 1973	7.7	103.2	10	95	2.1	9.1	Spicer 1977
Claremont, CA (Harvey Mudd College)	Oct. 1978	41.3	126.4	25	185	5.6	21.0	Tuazon et al. 1981b
Claremont, CA (Harvey Mudd College)	Aug-Sept. 1979	20.6	56.8	20	55	0.7-2.8[a]	8.4	Tuazon et al. 1981a
Riverside, CA (UC Riverside)	Oct. 1976	5.2-12.9[a]	20.6	45	90	14.0	42.0	Tuazon et al. 1978
Riverside, CA (UC Riverside)	July-Oct.	12.9-18.1[a]	51.6	30	90	14.7	92.4	Tuazon et al. 1980, 1981a
St. Louis, MO	July-Aug 1973	7.7	206.4[b]	10	95	2.8	11.2	Spicer 1977
Dayton, OH	July-Aug 1974	15.5	139.3[b]	ND	ND	ND	ND	Spicer et al. 1976a

ND = Not determined.

[a]Many individual values were below detectability limits (DL); lower concentrations listed based on assuming values below DL equaled zero; upper concentration values listed based on assuming values below DL equaled following concentrations: HNO_3, 12.9 μg m^{-3}; PAN, 10 μg m^{-3}; NH_3, 2.1 μg m^{-3}.

[b]These values appear unusally high when compared with NO_x, PAN and O_3 concentrations reported as present during same time periods.

concentrations were measured had the lower HNO_3 concentrations. This follows from the equilibrium between nitric acid and ammonia, with ammonium nitrate aerosol being shifted toward aerosol formation in the presence of high ammonia concentrations.

$$NH_4NO_3 \rightleftharpoons NH_3 + HNO_3.$$

The maximum HNO_3 concentrations reported at several midwestern sites are higher than those at Los Angeles area sites. These maximum concentrations also are unusually high in comparison with the NO_x, ozone, and peroxyacetyl nitrate concentrations measured concurrently. Therefore, these values are suspect.

The averages of 24-hr HNO_3 concentrations are small compared with the corresponding NO_x concentrations. The NO_x concentrations averaged over the study period were: St. Louis, MO, 111 $\mu g\ m^{-3}$; West Covina, CA, 343 $\mu g\ m^{-3}$ and Dayton, OH, 134 $\mu g\ m^{-3}$ (Spicer et al. 1976a, Spicer 1977).

The diurnal patterns at the Los Angeles area sites for HNO_3 concentration are similar to that of the ozone with peaking in the afternoon hours (Spicer 1977; Tuazon et al. 1981a,b; Hanst et al. 1982). Nitric acid decreases appreciably in concentration during the night. In Dayton, OH, and in St. Louis, MO, the diurnal profiles of nitric acid showed both morning and afternoon peaks, unlike ozone and PAN, which peaked only in the afternoon hours (Spicer et al. 1976b, Spicer 1977). However, the nitric acid concentrations frequently were near the limits of detectability.

5.3.3.2 Nonurban Concentration Measurements--Measurements of nitric acid at suburban and rural sites are listed in Table 5-6. Some of the earliest measurements of nitric acid in ambient air were made at two sites outside of Dayton, OH--Huber Heights, a surburban location, and New Carlisle, OH, a small town (Spicer et al. 1976a). Analyses were made by continuous coulometry. The average concentrations of nitric acid were in the 2.6 to 5.2 $\mu g\ m^{-3}$ range. The maximum concentration of 116.1 $\mu g\ m^{-3}$ reported at New Carlisle appears to be too high.

Nitric acid measurements were obtained at Pittsburg, a small town in northern California (Appel et al. 1980). Tandem filter technique was used with a Teflon prefilter for collection of particulate nitrate and either a nylon or NaCl-impregnated filter was used to collect HNO_3. Positive interference problems are known to occur because of nitrate loss from the particulate collected on the prefilter, due to volatilization onto the filter used to collect HNO_3. The range of nitric acid concentrations was 0.7 to 3.9 $\mu g\ m^{-3}$ (Table 5-6).

Nitric acid was measured by Spicer et al. (1982c) at Beverly Airport, MA (Table 5-6). The nitric acid concentrations usually were below the limit of detection of 2 ppb (5.16 $\mu g\ m^{-3}$) of the chemiluminescent technique used. An integrated filter technique also was used for nitric acid involving the use of a Teflon prefilter and a nylon backup filter.

TABLE 5-6. MEASUREMENTS OF CONCENTRATIONS OF NITRIC ACID, PEROXYACETYL NITRATE AND AMMONIA AT SUBURBAN AND RURAL LOCATIONS

Site	Period of measurement	Concentrations, $\mu g\ m^{-3}$						References
		HNO_3		PAN		NH_3		
		Avg	Max	Avg	Max	Avg	Max	
Beverly Airport, MA (S)	July-Aug. 1978	2.6	$\leq$ 5.2	9.0	110	ND	ND	Spicer et al. 1982c
Van Hiseville, NJ (R)	July-Aug. 1979	< 2.1	11.6	2.5	32.5	ND	ND	Spicer and Sverdrup 1981
Luray, VA (R)	July-Aug. 1979	1.0	2.1	ND	ND	1.3	2.9	Cadle et al. 1982
Research Triangle Park, NC (S)	June-July 1980	2.1	2.4	ND	ND	0.4	0.6	McClenny et al. 1982
Huber Hts., OH (S)	July-Aug. 1974	2.1	38.7	< 5	50	< 0.7	11.9	Spicer et al. 1976b
New Carlisle, OH (R)	July-Aug. 1974	5.2	116.1	ND	ND	ND	ND	Spicer et al. 1976b
Croton, OH (R)	August, 1980	1.8	9.8	ND	ND	0.4	0.6	McClenny et al. 1982
Warren, MI (S)	Sept.-Oct. 1979	0.8	< 2.6	ND	ND	0.8	2.8	Cadle et al. 1982
	Jan.-Feb. 1980	1.3	5.2	ND	ND	0.6	< 1.4	
	May-June 1980	2.4	15.5	ND	ND	0.9	5.6	

TABLE 5-6. CONTINUED

Site	Period of measurement	Concentrations, μg^{-3}						References
		HNO_3		PAN		NH_3		
		Avg	Max	Avg	Max	Avg	Max	
Abbeville, LA (R)	June-Aug. 1979	1.8	NA	ND	ND	2.1	NA	Cadle et al. 1982
Commerce City, CO (S)	Nov.-Dec. 1978	2.1	NA	ND	ND	1.3	2.9	Cadle et al. 1982
Thurber Ranch, AZ (35 mi. SE Tucson)	July-Aug. 1981	1.6	5.2	ND	ND	0.8	1.5	Farmer and Dawson 1982
Pittsburg, CA (S)	February 1979	2.1	4.1	ND	ND	0.4	0.8	Appel et al. 1980

ND = Not determined.

NA = Not available.

In this same study (Spicer et al. 1982c), aircraft flights were made following the urban plume of Boston, MA, over the Atlantic Ocean. On one flight it was possible to measure the nitric acid formed not only in the urban plume, 10.3 $\mu g\ m^{-3}$, but also in the Salem power plant plume, 15.5 $\mu g\ m^{-3}$. The plumes were over the Atlantic Ocean north of Cape Cod.

Measurements of nitric acid concentrations were made during July and August 1979 at Van Hiseville, NJ, in the New Jersey pine barrens (Spicer and Sverdrup 1981). Nitric acid was measured by the chemiluminescence technique, and inorganic nitrate (HNO_3 and NO_3^-) was determined by use of the Teflon prefilter and nylon backup filter collection method. These authors suggested that the potential for loss of nitrate off the Teflon prefilter onto the nylon filter, resulting in a positive interference problem, made it desirable to consider the filter method as acceptable only for measuring the concentrations of total inorganic nitrate. On the average, the total inorganic nitrate during the study was 5 $\mu g\ m^{-3}$ and the estimate of nitric acid concentration was less than 0.8 ppb or 2 $\mu g\ m^{-3}$ (Table 5-6). The average diurnal profile for nitric acid peaked at 1500 hours. The ozone and PAN concentrations peaked at about the same time in the afternoon.

McClenny et al. (1982) reported measurements of nitric acid in Research Triangle Park, NC, and a rural area near Croton, OH (Table 5-6). Analyses were made by the tungstic acid integrative sampling method, which has a sensitivity of 0.07 ppb (0.18 $\mu g\ m^{-3}$). Nitric acid is effectively adsorbed on a tungstic acid surface, subsequently desorbed into carrier gas, and passed on to a NO_x chemiluminescent analyzer. Maximum concentrations of nitric acid and of ozone occurred near midday at both sites, with lower nighttime concentrations for both but not as large a decrease for nitric acid.

Measurements of nitric acid by filter techniques at several suburban and rural sites (Table 5-6) were reported by Cadle et al. (1982). At the Abbeville, LA, and the Commerce City, CO, sites, nitric acid concentrations were obtained by difference between the inorganic nitrate collected on a microquartz filter and particulate nitrate collected on a Teflon filter. However, subsequent tests indicate that the nitric acid may have been overestimated. The second method involved removal of nitrate on a Teflon filter followed by removal of nitric acid on a nylon filter. The positive interference problem possible with this second technique has already been discussed.

The average diurnal profile for nitric acid from measurements at Abbeville, LA, shows a single late morning peak for nitric acid and an afternoon peak for ozone. Nitric acid concentrations were found to increase from fall to winter to spring in 1979-80 at the Warren, MI, site (Cadle et al. 1982).

Both Appel et al. (1980) and Cadle et al. (1982) concluded that the concentrations of nitric acid and ammonia at their measuring sites were too low to result in the formation of ammonium nitrate in particulate matter.

Kelly and Stedman (1979b) measured nitric acid by a chemiluminescent technique at a rural site about 15 miles east of Boulder, CO. The nitric acid

concentrations during February 1978 usually were in the 1.3 to 12.9 μg m^{-3} range with many of the concentrations of nitric acid in the 2.6 to 5.2 μg m^{-3} range.

A collection method involving condensation of water vapor onto a cooled surface was used by Farmer and Dawson (1982) to collect nitric acid (Table 5-6). During part of the sampling period in early August 1981, sulfur dioxide and nitric acid concentrations were well correlated. The authors associated this behavior with transport and chemical transformations occurring within smelter plumes fumigating the site.

The average nitric acid concentrations at most of the suburban and rural sites were at or below 2.6 μg m^{-3} with the concentrations frequently occurring in the 0.7 to 2.1 μg m^{-3} range (Table 5-6). These concentrations of nitric acid are about a factor of 10 lower than the nitric acid concentrations measured at urban sites (Table 5-5). The nitric acid concentrations at suburban and rural sites also are about a factor of 5 to 10 lower than the nitrogen dioxide concentrations at surburban and rural sites (Table 5-2).

5.3.3.3 Concentration Measurements at Remote Locations--Measurements of nitric acid also are available at a number of remote or relatively remote locations (Huebert and Lazrus 1978, 1980a,b; Huebert 1980; Kelly et al. 1980). Kelly and coworkers measured nitric acid concentrations at a relatively remote site, Niwot Ridge, in the Rocky Mountains 20 miles west of Boulder, CO, between December 1978 and August 1979. A high sensitivity chemiluminescent instrument was used with nitric acid measured by thermal decomposition to nitrogen dioxide followed by $FeSO_4$ reduction of the nitrogen dioxide. Some interference by PAN was observed in tests with this technique for measuring nitric acid. In clear air masses the nitric acid concentrations often were below the detection limit but, when measurable, were in the 0.13 to 0.26 μg m^{-3} range. When polluted air reached the site, the nitric acid concentrations frequently were 0.5 μg m^{-3} or more and values over 2.6 were measured occasionally.

Huebert (1980) and Huebert and Lazrus (1978, 1980a,b) measured nitric acid on samples collected from aircraft or shipboard over remote areas of the Pacific Ocean and western North America. Samples were collected using the same sort of tandem filter technique discussed earlier. Samples were collected from aircraft as part of project GAMETAG. Surface concentrations of nitric acid in the equatorial Pacific region averaged 0.1 μg m^{-3} (Huebert 1980). The concentrations of nitric acid measured in the boundary layer ranged from less than 0.03 to 2.22 μg m^{-3}, with a median range of 0.15 to 0.21 μg m^{-3} (Huebert and Lazrus 1980a). The free troposphere nitric acid concentrations ranged from less than 0.08 to 1.39 μg m^{-3} with a median of 0.31 μg m^{-3}. The nitric acid concentrations in the boundary layer in remote areas are a factor of 5 to 10 lower than at rural locations in eastern North America.

5.3.4 Peroxyacetyl Nitrates

Peroxyacetyl nitrates can be determined by electron capture gas chromatography down to the 0.1 ppb (0.5 $\mu g\ m^{-3}$) concentration level and below. This method can be used in urban, rural, or remote locations. Long path FTIR spectroscopy has been used to measure peroxyacetyl nitrate at locations within the Los Angeles Basin area.

5.3.4.1 Urban Concentration Measurements--Peroxyacetyl nitrate concentrations have been tabulated when obtained concurrently with nitric acid and ammonia concentrations in Table 5-5. Many other measurements of peroxyacetyl nitrate have been made in urban areas.

Additional average peroxyacetyl nitrate measurements made in the Los Angeles Basin area are shown in Table 5-7. The highest peroxyacetyl nitrate concentrations have been reported from the sites in the western part of the Los Angeles Basin area. In the eastern part of the Los Angeles Basin area, average peroxyacetyl nitrate concentrations usually have been measured in the 5 to 25 $\mu g\ m^{-3}$ range.

Maximum peroxyacetyl nitrate concentrations occur late in the morning or early afternoon in downtown Los Angeles (Mayrsohn and Brooks 1965) and progressively later in the afternoon passing from west to east across the Los Angeles Basin area from downtown Los Angeles to Pasadena (Hanst et al. 1975) to West Covina (Spicer 1977) to Claremont (Tuazon et al. 1981a,b) to Riverside (Pitts and Grosjeans 1979). Pitts and Grosjeans (1979) also reported seasonal variations in peroxyacetyl nitrate diurnal peak concentrations. Two peaks were observed at the site in Riverside, CA. The earlier peak was associated with formation of peroxyacetyl nitrate from local emissions while the later peak was associated with formation of peroxyacetyl nitrate from emissions in air masses traveling from west to east across the Los Angeles Basin. The peroxyacetyl nitrate concentrations were observed to decrease at night, but were still present at significant concentrations (Spicer 1977; Pitts and Grosjeans 1979; Tuazon et al. 1981a,b).

The average peroxyacetyl nitrate concentrations reported within some urban and suburban areas in the United States are shown in Table 5-8. The average peroxyacetyl nitrate concentrations at a few sites have been within the 5 to 50 $\mu g\ m^{-3}$ range (Lonneman et al. 1976). However, at other urban and surburban locations the average peroxyacetyl nitrate concentrations have ranged from 1.5 to 4.5 $\mu g\ m^{-3}$. The times of maximum peroxyacetyl nitrate concentration during the day usually were reported to occur during the afternoon hours in Houston, TX (Westberg et al. 1978a), St. Louis, MO (Spicer 1977), and New Brunswick, NJ (Brennen 1980). At sites in the Houston, TX, area peroxyacetyl nitrate concentrations usually were below detectability limits at night (Westberg et al. 1978a), but were present at measurable concentrations at other sites (Spicer 1977, Brennen 1980, Singh et al. 1982).

Only a limited number of measurements of the next higher member of the peroxyacetyl nitrate series, peroxypropionyl nitrate, have been obtained in urban areas (Darley et al. 1963; Lonneman et al. 1976; Singh et al. 1979,

TABLE 5-7. AVERAGE PEROXYACETYL NITRATE MEASUREMENTS FROM THE LOS ANGELES BASIN AREA

Site	Year	Concentration $\mu g\ m^{-3}$	Reference
Los Angeles	1961	100	Renzetti and Bryan 1961
	1965	155	Mayrsohn and Brooks 1965
	1976	40	Lonneman et al. 1976
	1979	25	Singh et al. 1981
Pasadena	1973	150	Hanst et al. 1975
Claremont	1980	65	Grosjean 1981
Riverside	1967-68	19	Taylor 1969
	1975-76	18	Pitts and Grosjean 1979
	1977	8	Singh et al. 1979
	1980	6	Singh et al. 1982
	1980	24.5	Temple and Taylor 1983

TABLE 5-8. PEROXYACETYL NITRATE MEASUREMENTS FROM SEVERAL URBAN AND SUBURBAN AREAS IN THE UNITED STATES

Site	Year	Concentration $\mu g\ m^{-3}$	Reference
Hoboken, NJ	1970	18.5	Lonneman et al. 1976
St. Louis, MO	1973	31.5	Lonneman et al. 1976
Houston, TX (Lange)	1976	2.0	Westberg et al. 1978a
Houston, TX			
(West Hollow)	1977	3.0	HAOS 1979
(Aldine)		4.5	
(Crawford)		3.0	
(Fuqua)		3.0	
(Jack Rabbit)	1978	4.0	Martinez et al. 1982
New Brunswick, NJ	1978-80	2.5	Brennen 1980
San Jose, CA	1978	4.5	Singh et al. 1979
Oakland, CA	1979	2.0	Singh et al. 1981
Phoenix, AZ	1979	4.0	Singh et al. 1981
Denver, CO	1980	2.0	Singh et al. 1982
Houston, TX	1980	2.0	Singh et al. 1982
Chicago, IL	1981	2.0	Singh et al. 1982
Pittsburgh, PA	1981	1.5	Singh et al. 1982
Staten Island, NY	1981	3.5	Singh et al. 1982

1981, 1982). The peroxypropionyl nitrate concentrations measured usually averaged 10 to 20 percent of peroxyacetyl nitrate concentrations.

The ratios of average peroxyacetyl nitrate to nitric acid concentrations at urban sites can vary widely. For example, the ratio of average PAN to HNO_3 concentrations was about 3:1 during the 1978 study in Claremont, CA (Tuazon et al. 1981a), but this ratio averaged only 1:3 during the 1973 study at West Covina, CA (Spicer 1977). The ratios of PAN to HNO_3 concentrations also can vary substantially from day to day at the same site.

Nitrogen dioxide and/or nitrogen oxide ($NO + NO_2$) have been measured concurrently with PAN and HNO_3 in several studies. The average ratios of the 23-hr average concentrations of ($PAN + HNO_3$) to ($PAN + HNO_3 + NO_x$) in West Covina, CA, and in St. Louis, MO, were 0.1 (Spicer 1977). The average ratio of ($PAN + HNO_3$) to ($PAN + HNO_3 + NO_2$) concentrations measured in Riverside, CA, was 0.2 (Tuazon et al. 1980). Grosjean (1983), using a commercial chemiluminescent analyzer, found PAN and HNO_3 to interfere quantitatively with the NO_2 measurements. The observed concentrations of NO_2 were corrected using the concurrent measurements of PAN and HNO_3. The ratios of ($PAN + HNO_3$) to ($PAN + HNO_3 + NO_x + NO_3^-$) in Grosjean's results ranged from 0.01 to 0.39 and averaged 0.18. On the average, the results of these several studies (Spicer 1977, Tuazon et al. 1980, Grosjean 1983) indicate that ($PAN + HNO_3$) accounts for from 10 to 20 percent of the measured nitrogen species in these urban areas.

5.3.4.2 Nonurban Concentration Measurements--Concentration measurements of peroxyacetyl nitrate and peroxypropionyl nitrate at rural and remote locations are given in Table 5-9. Additional measurements of peroxyacetyl nitrate concentrations are listed in Table 5-6. The average concentrations of peroxyacetyl nitrate are in the range of 0.5 to 5 $\mu g\ m^{-3}$ overlapping the range of average PAN concentrations at urban and suburban sites. The concentrations of PAN at the remote sites, Reese River, NV, Badger Pass, CA, and Point Arena, CA, are about 0.5 $\mu g\ m^{-3}$.

Lonneman et al. (1976) observed two diurnal patterns of PAN concentrations at the site near Wilmington, OH. One pattern involved afternoon and evening elevation in PAN and in ozone concentrations. The other pattern involved a flat diurnal profile for the PAN concentrations, but an elevation in ozone concentrations. An afternoon peaking of the PAN concentrations also was observed at the Sheldon Wildlife Preserve, TX (Westberg et al. 1978b). At night, measurable concentrations of PAN were obtained at both of these rural sites.

The concentrations of peroxyacetyl nitrate at rural sites were in about the same concentration range as measured for nitric acid at rural sites (Tables 5-6 and 5-9). The concentrations of PAN at remote locations of about 0.5 $\mu g\ m^{-3}$ were about the same as those reported for nitric acid by Huebert and Lazrus (1980a) at remote locations.

TABLE 5-9. PEROXACETYL NITRATE MEASUREMENTS AT RURAL AND REMOTE SITES IN THE UNITED STATES

Site	Nature of site	Period of measurement	Concentration, μg m^{-3} PAN Avg	PAN Max	PPN Avg	PPN Max	Reference
Wilmington, OH	Rural-continental	August 1974	NA	20.5	ND	ND	Lonneman et al. 1976
Huntington Lake, IN	Rural-continental	April 1981	2.5	NA	ND	ND	Spicer et al. 1983
East Central Missouri	Rural-continental	February 1981	3.5	NA	ND	ND	Spicer et al. 1983
Sheldon Wildlife Preserve, TX	Rural-continental	October 1978	4.0	15.0	ND	ND	Westberg et al. 1978a
Jetmore, KA	Rural-continental	June 1978	1.25	2.5	ND	ND	Singh et al. 1979
Reese River, NV	Remote-high altitude	May 1977	0.55	1.3	0.22	0.50	Singh et al. 1979
Badger Pass, CA	Remote-high altitude	May 1977	0.65	1.10	0.28	0.50	Singh et al. 1979
Mill Valley, CA	Rural-maritime	January 1977	1.50	4.15	0.22	0.60	Singh et al. 1979
Point Arena, CA	Remote-maritime	Aug. - Sept. 1973	0.40	1.40	ND	ND	Singh et al. 1979

ND = Not determined.

NA = Not available.

5.3.5 Ammonia

Unlike nitric acid and peroxyacetyl nitrate, which are formed through atmospheric reactions involving precursor hydrocarbons and nitrogen oxides, ammonia is emitted directly into the atmosphere from near-surface sources (Chapter A-2, Sections 2.2.2.7 to 2.2.2.10). Consistent with ammonia being emitted from ground-level sources, ammonia concentrations have been found to decrease with altitude (Georgii and Muller 1974, Hoell et al. 1983). Ammonia has a significant role in neutralization of acid sulfate and nitric acid in the atmosphere (Brosset 1978). In addition ammonia, when it undergoes deposition, can participate significantly in chemical reactions in soil.

Various techniques have been used to sample and analyze ammonia. Long path FTIR spectroscopy was used at several sites in the Los Angeles Basin area (Tuazon et al. 1978, 1980, 1981a,b; Hanst et al. 1982). Dual catalyst chemiluminescent instrumentation was used in Los Angeles, St. Louis, and the Dayton area (Spicer et al. 1976a, Spicer 1977). This procedure depended on the fact that ammonia is oxidized to nitric oxide by high temperature but not low temperature catalysts while nitrogen dioxide is reduced by both high and low temperature converters. A tandem filter technique involving a Teflon prefilter and two oxalic-acid-impregnated fiberglass filters has been used at several locations (Cadle et al. 1982). Both positive and negative interferences can occur. A similar tandem filter technique with a glass fiber prefilter was employed by Appel et al. (1980). Another method involved use of oxalic-acid-coated glass tube diffusion denuders. Another technique involved collection on Chromosorb T beads and desorption either into an opto-acoustic detector or a chemiluminescent analyzer (McClenny and Bennett 1980). Harward et al. (1982) also used the acoustic detector. The tungstic acid technique was used by McClenny et al. (1982) to measure ammonia. Gaseous ammonia and nitric acid are separated from particulate species as a result of their more rapid diffusion to the walls of a tungstic-acid-coated Vycor tube. The ammonia is desorbed into a carrier gas and readsorbed on a second tungsten-oxide-coated tube which passes nitric acid now in the form of nitrogen dioxide. The ammonia is desorbed into a chemiluminescent analyzer as nitrogen dioxide.

5.3.5.1 Urban Concentration Measurements--The concentrations of ammonia measured at a number of urban locations are given in Table 5-5. The highest concentrations of ammonia in ambient air have been measured at Riverside, CA (Tuazon et al. 1978, 1980, 1981a). These high concentrations were attributed to ammonia emissions from feed lots upwind of the site in Riverside. Nitric acid was observed to decrease in concentration with increases in ammonia concentration at Riverside (Tuazon et al. 1978, 1980) due to the ammonium nitrate equilibrium relationship. The ammonia concentrations at sites in Claremont, West Covina, and Los Angeles were substantially lower than in the Riverside area (Spicer 1977, Tuazon et al. 1981a,b). Such a gradient in concentrations of ammonia is consistent with strong localized sources of ammonia rather than more uniform basin-wide emissions of ammonia. The ammonia concentrations measured in St. Louis (Spicer 1977) were not substantially different from those measured at locations in the Los Angeles Basin area other than the Riverside area. Concentrations of ammonia remain

high at night in Los Angeles and St. Louis (Spicer 1977) consistent with surface emissions of ammonia into the shallower mixing layers occurring during the nighttime hours.

5.3.5.2 Nonurban Concentration Measurements--Earlier measurements of ammonia concentrations at nonurban locations were in the range from less than 0.07 $\mu g\ m^{-3}$ to several factors of ten times greater (Breeding et al. 1973, 1976; Lodge et al. 1974). Other measurements of ammonia that were obtained concurrently with nitric acid concentration measurements are given in Table 5-6. Average concentrations range from 0.35 to 2.1 $\mu g\ m^{-3}$ and maximum concentrations reported ranged up to 11.9 $\mu g\ m^{-3}$. However, this latter concentration value observed at Huber Heights, OH, is unusually high compared to the maximum concentration values at other suburban and rural locations.

Several additional studies have been reported at nonurban sites. Ammonia was measured at several sites on Cedar Island off the coast of North Carolina in August 1978 (McClenny and Bennett 1980). The ammonia concentrations ranged from 2.1 to 2.4 $\mu g\ m^{-3}$. The highest concentrations were measured immediately above marsh grass. A few measurements also were made at Research Triangle Park, NC, and these ammonia concentrations were in the 2.8 to 4.2 $\mu g\ m^{-3}$ range. Measurements of ammonia also were made nearby in southeastern Virginia at a site bordering the Great Dismal Swamp (Harward et al. 1982). The ammonia concentrations obtained in August and September 1979 ranged from 1.0 to 2.8 $\mu g\ m^{-3}$ and averaged 1.9 $\mu g\ m^{-3}$. Measurements were made for comparison at Hampton, VA. The average ammonia concentration was lower in air masses arriving over water than over land. The ammonia concentration also was lower during periods of rain.

At Hampton, VA, the ammonia concentrations decreased from the 1.4 to 2.1 $\mu g\ m^{-3}$ range in late summer to less than 0.14 $\mu g\ m^{-3}$ in the early winter (Harward et al. 1982). A decrease in ammonia concentrations also was observed at Warren, MI, from 0.9 $\mu g\ m^{-3}$ in the spring to 0.6 $\mu g\ m^{-3}$ in the winter (Cadle et al. 1982). Although such seasonal changes have been associated with changes in soil emissions and fertilizer volatilization, higher temperatures also could explain the shift in the ammonium nitrate equilibrium resulting in higher ambient air ammonia concentrations (Cadle et al. 1982).

5.3.6 Particulate Nitrate

Serious difficulties have been experienced in obtaining accurate ambient air measurements of particulate nitrates. During recent years substantial positive and negative artifacts have occurred during the sampling of nitrates from air. The artifacts arise as follows:

(1) Positive artifacts derived from
    (a) adsorption of nitric acid by filter medium,
    (b) adsorption of nitrogen dioxide by filter medium,
    (c) loss of nitric acid onto the collected particulate matter on a filter as a result of chemical reactions with, or adsorption by, the particulate matter.

(2) Negative artifacts derived from
   (a) reactions of particulate nitrate in the collected matter with strong acids in the particulate matter, resulting in release of nitric acid;
   (b) volatization of ammonium nitrate from the filter to form gaseous nitric acid and ammonia.

As a result of the artifact problems given above the earlier nitrate measurements reported in the literature are likely to be questionable, if not erroneous.

Most of the early measurements of particulate nitrate involved analysis for nitrates in samples collected on glass fiber filters in high-volume (HIVOL) samplers (NAS 1977, U.S. EPA 1982).

A number of investigators have observed in measuring particulate nitrate in source emissions (Pierson et al. 1974) and in ambient air studies (Witz and MacPhee 1977; Stevens et al. 1978; Spicer and Schumacher 1977, 1979; Appel et al. 1979, 1981a; Witz and Wendt 1981; Shaw et al. 1982; Witz et al. 1982) that much higher particulate nitrate concentrations were measured on glass fiber filters than on Teflon, quartz, and some other filter types. Nitric acid was demonstrated to be adsorbed on glass fiber filters in laboratory studies (Okita et al. 1976, Spicer and Schumacher 1977, 1978, 1979, Appel et al. 1979). Nitrogen dioxide also has been shown in laboratory studies to be adsorbed on glass fiber filters (Spicer and Schumacher 1977, 1978, 1979; Rohlach et al. 1979). Appel et al. (1979) reported a positive artifact from nitrogen dioxide at high ozone concentrations. However, adsorption of nitric acid rather than nitrogen dioxide appears to be the dominant source of the positive interference (Appel et al. 1979, 1981a).

Substantial positive nitrate artifacts have been measured on a number of other filter types including Teflon-impregnated fiber filters (Pierson et al. 1980b), silicone resin coated glass fiber filters (Appel et al. 1979), cellulose filters (Appel et al. 1979), cellulose acetate filters (Spicer and Schumacher 1978, 1979, Appel et al. 1979), and nylon filters (Okita et al. 1976, Spicer 1977, Spicer and Schumacher 1978, 1979). Smaller but measurable positive artifacts have been reported on some types of quartz filters including Gelman microquartz (Appel et al. 1978, Spicer and Schumacher 1977, 1979) and Pallflex Tissuquartz (Spicer and Schumacher 1977, Forrest et al. 1980).

Negligible positive artifacts have been obtained on Fluoropore (Teflon) filters (Stevens et al. 1978, Appel et al. 1979, 1980, 1981a,b; Pierson et al. 1980b) on polycarbonate filters (Spicer and Schumacher 1977), and on ADL quartz filters (Spicer and Schumacher 1978, 1979). However, atmospheric particulate matter on Teflon filters can retain nitric acid (Appel et al. 1980).

Harker et al. (1977) observed that an inverse relationship occurred between ambient air sulfate and nitrate concentrations in samples collected at West Covina, CA. A group of controlled photochemical experiments were designed to investigate this behavior. When sulfuric acid was generated and collected

concurrently with nitrates on Gelman Spectro Grade A glass fiber filters, the nitrate concentration was lower than in the absence of sulfuric acid. The researchers concluded that the sulfuric acid reacted with and caused the release of nitrate probably as nitric acid from the surface of the aerosol particles (Harker et al. 1977). The possibility of a negative artifact effect on Fluoropore filters as a result of reaction with sulfuric acid and as a result of volatization of ammonium nitrate was discussed by Appel et al. (1979).

Pierson et al. (1980a,b) observed losses of nitrate off of Fluoropore filters, an effect associated with the high sulfuric acid concentrations measured at the Allegheny Mountain site. Appel et al. (1981b) also found that particulate nitrate collected on Teflon filters at Lennox, CA decreased with increasing amounts of ambient air sulfuric acid. About half the nitrate was lost at ambient air sulfuric acid concentrations of 10 $\mu g\ m^{-3}$. About 50 percent of the nitrate collected could be lost from Teflon filters at higher ambient temperatures, 29 to 35 C, and about 30 percent RH (Appel et al. 1981a). No losses of nitrate appeared to occur from samples collected during the night and morning hours. In samples collected at Research Triangle Park, NC, large losses of particulate nitrate, up to 90 percent off Teflon filters, occurred particularly during the day (Shaw et al. 1982).

Laboratory experiments were carried out by Appel et al. (1981b) to investigate the losses of nitrate off Teflon filters loaded with submicron ($\leq$ 0.2 μm) ammonium nitrate particles. With equal loadings of ammonium nitrate and sulfuric acid on the Teflon filters, over 90 percent of the nitrate was lost off the filters after exposure to a clean air stream at 90 percent RH for six hours. Volatization of nitrate under the same conditions in the absence of sulfuric acid resulted in 30 to 50 percent losses of ammonium nitrate. Losses of about 90 percent of the nitrate occurred when the filters were exposed to 17 to 23 ppb of hydrochloric acid. Forrest et al. (1980) observed losses of preloaded nitrate from Pallflex Tissuquartz exposed to sulfuric acid. Particulate nitrates other than ammonium nitrate can be present in the atmosphere but they, unlike ammonium nitrate, do not volatize readily.

The artifact problems discussed above appear to have been dealt with satisfactorily by use of diffusion-denuder tubes. These tubes are used to remove gaseous species and to pass aerosols (Stevens et al. 1978). This technique was proposed for use with nitrate species by Shaw et al. (1979) and demonstrated by Appel et al. (1981a) and by Shaw et al. (1982). Ambient air measurements using this approach are of particular importance (Appel et al. 1981a, Forrest et al. 1982, Shaw et al. 1982, Spicer et al. 1982a, Tanner 1982).

5.3.6.1 Urban Concentration Measurements--As discussed above, much higher ambient air nitrate concentrations have been measured on glass fiber filters than on Teflon and other inert filters. The magnitude of the actual net positive artifact on ambient air samples cannot be estimated. Therefore, the substantial body of ambient air nitrate concentrations obtained on glass fiber filters will not be considered (NAS 1977, U.S. EPA 1982). The same problem probably applies to the measurements on cellulose filters used to

collect samples in the Los Angeles Basin during 1972 and 1973 (Appel et al. 1978). Appel et al. (1981a), using Gelman A glass fiber filters in low volume sampling over 2 to 8 hour periods, obtained reasonable agreement for many of the samples between the nitrate values on glass fiber filters and a total inorganic nitrate (nitrate particulate plus nitric acid) sampling system. However, Shaw et al. (1982) did not observe glass fiber filters to collect nitric acid with reproducible efficiency at the subambient pressure in their sampling assembly. While Appel et al. (1981a) concluded that glass fiber filters give an approximation of total inorganic nitrate, Shaw et al. (1982) did not consider glass fiber filters to be satisfactory collectors of total inorganic nitrate. Neither group used the 24-hr high volume sampling procedure. While it is clear that 24-hr average HIVOL samples are totally inadequate for measurement of particulate nitrate, it is not clear to what extent such sampling might have provided an adequate measurement of total inorganic nitrate.

Because of the large losses of nitrate off Teflon and quartz filters, the ambient air measurements made with these filters are also in question (Spicer 1977, Spicer and Schumacher 1977, Appel et al. 1979, Spicer et al. 1979). Although the measurements can be considered lower limit estimates, the losses of nitrate are so large as to make such estimates of little value.

Nitrate measurements also are available from particle-size distribution studies made using cascade impactors (Lee and Patterson 1969, Lundren 1970, Moskowitz 1977, Patterson and Wagman 1977, Appel et al. 1978). However, these cascade impactors and the backup filters used with them have the potential for similar types of artifact problems discussed above. Therefore, it is not possible to know whether such nitrate measurements are of value either.

The remaining nitrate measurements are those made recently using gas diffusion denuders to remove nitric acid. Appel et al. (1981a) collected inorganic nitrate on a Teflon prefilter followed by a nylon or NaCl/W41 backup filter. Particulate nitrate was collected with the same tandem filter system after removing the nitric acid with the diffusion denuder. This arrangement allows nitric acid to be determined by difference. Diurnal nitrate concentration profiles obtained with this system were plotted for the period between 23 July and 27 July 1979 at Claremont, CA (Harvey Mudd College). The particulate nitrate peaked in concentration during the late morning hours. Particle nitrate concentrations exceeded nitric acid concentrations between 2200 and 1200 hours. The average particle nitrate concentration during this period was 25 $\mu g\ m^{-3}$. The average particle nitrate concentration moderately exceeded the average nitric acid concentration.

Forrest et al. (1982), as part of an intercomparison study (Spicer et al. 1982a) at Harvey Mudd College in Claremont, CA, measured nitrates by using the gas diffusion denuder technique. Two assemblies, each with a Fluoropore prefilter followed by two pairs of NaCl impregnated filters, were used, with one assembly at the exit of a diffusion denuder. Measurements of nitrates were made with this system between 27 August and 3 September 1979. The particulate nitrate concentrations tended to peak in the morning hours. The

particulate nitrate concentrations exceeded the nitric acid concentrations in the evening and morning hours. This diurnal pattern was the same as observed at this site earlier in the summer by Appel et al. (1981a). The average particulate nitrate concentration was 13.4 μg m^{-3}. This concentration moderately exceeded the average nitric acid concentration. Lower nitrate concentrations were obtained in August and September than were measured in July (Appel et al. 1981a). The peak ozone concentrations also were somewhat lower during this period (Spicer et al. 1982b) than in the period in July (Appel et al. 1981a). The results indicate that the later period was one of lesser photochemical activity.

5.3.6.2 Nonurban Concentration Measurements--Discussion earlier in this section notes that the nitrate concentrations obtained at nonurban sites using glass fiber filter HIVOL sampling are considered too unreliable to use. The Teflon impregnated HIVOL filters employed by Mueller et al. (1980) have similar problems associated with them (Pierson et al. 1980b). Even with a positive artifact associated with their nitrate measurements, Mueller et al. (1980) usually measured less than 1 μg m^{-3} of nitrate at rural sites, and during the spring and summer months the nitrate concentrations reported were at or below 0.5 μg m^{-3}. Pierson et al. (1980b) sampled with Fluoropore Teflon and quartz filters at Allegheny Mountain; on Fluoropore filters an average nitrate concentration obtained was 0.5 μg m^{-3}, but the negative artifacts likely to occur with these filters also may make these measurements unreliable.

Shaw et al. (1982) made measurements of nitrates, using a diffusion denuder at a site in Research Triangle Park, NC during 16 days in June, July, and August 1980. The assembly used contained a cyclone to remove coarse particles. The cyclones were shown to pass nitric acid efficiently. The cyclone was followed by a manifold to which were connected tandem Teflon and Nylon filter holders, one of which had a diffusion denuder between it and the manifold. The particulate nitrate concentrations measured exceeded the nitric acid concentrations in the late evening and early morning hours, as was observed at Claremont, CA (Appel et al. 1981a, Forrest et al. 1982). During the late morning, afternoon, and early evening hours, the particulate nitrate concentrations were substantially lower than the nitric acid concentrations. Averaging the entire study period, the particulate nitrate concentration was 1.0 μg m^{-3} and the particulate nitrate was 37 percent of the total inorganic nitrate. The average particulate nitrate concentration at this nonurban site was 4 percent (Appel et al. 1981a) and 7 percent (Forrest et al. 1982) of the average particulate nitrate concentrations measured in Claremont, CA.

Tanner (1982) used the same diffusion denuder assembly arrangement as Forrest et al. (1982) at a site within Brookhaven National Laboratory on Long Island, NY. Measurements of nitrates were made several hours each day on 7, 8, and 9 November 1979. The average particulate nitrate concentration was 1.7 μg m^{-3} and constituted about one-third of the total inorganic nitrate measured. As at the Research Triangle Park, NC site, the particulate nitrate concentration at this site was only a small fraction of the particulate nitrate concentrations measured at Claremont, CA (Appel et al. 1981a, Forrest et al. 1982).

5.3.6.3 Concentration Measurements at Remote Locations--Huebert (1980) and Huebert and Lazrus (1978, 1980b) used a tamden filter assembly consisting of a Teflon prefilter followed by a base-impregnated cellulose filter to collect nitrates. As already discussed, these filters have positive and negative artifacts. In combination such types of filters are adequate for measuring total inorganic nitrate but are questionable for the accurate measurement of particulate nitrate and nitric acid individually (Appel et al. 1981a, Spicer and Sverdrup 1981, Forrest et al. 1982). Teflon filters alone were used to collect particulate nitrate at remote locations (Huebert and Lazrus 1980a), but these filters have the negative artifact problems already discussed. Based on such measurements at remote locations, the authors concluded that particulate nitrate concentrations exceed nitric acid concentrations in the marine boundary layer (Huebert 1980), but particulate nitrate concentrations are much lower than nitric acid concentrations in the free troposhere (Huebert and Lazrus 1978, 1980b).

5.3.7 Particle Size Characteristics of Particulate Nitrogen Compounds

The available literature on measurement of particle size characteristics of particulate nitrogen compounds is based on studies done between 1966 and 1976. Therefore, the investigators could not have been aware of the positive and particularly the negative artifact problems with particulate nitrate sampling discussed earlier in this section.

The last stage of the cascade impactors used consists of cellulose acetate or glass fiber filters. Because of losses of nitric acid on such filters substantial overestimates of the amount of nitrate on the last stage are likely. This would result in the mass median diameters computed being too small. However, losses of nitric acid and particulate may occur on the upper stages of the impactors. The Lundgren impactor has substantial wall losses (Lundgren 1967, 1970). The impactor stages usually were constructed of stainless steel. Shaw et al. (1982) found at least 88 percent of nitric acid in air passed through a stainless steel cyclone. This may be an indication that nitric acid is unlikely to be lost to other stainless steel surfaces, but no studies have been made.

The situation is complicated by the use of films and coatings over the original stainless steel surfaces. Appel et al. (1978) used polyethylene strips coated with a sticky hydrocarbon resin, while Moskowitz (1977) used a thin film of vaseline on stainless steel strips. No measurements have been made on losses of nitric acid or of nitrogen dioxide to such surfaces. If losses did occur on the upper stages of the impactors only, the mass median diameters computed would be too large. It is impossible to estimate the extent to which artifact problems may shift the apparent size distributions in these impactors. Nevertheless, some qualitative results of these impactor studies appear reasonable, and these will be discussed.

The larger mass median diameters given in Table 5-10 were computed from measurements at locations near the ocean likely to be influenced by air masses moving off the ocean. As can be seen from the mass median diameters of particulate nitrate from the work of Appel et al. (1978), the diameters tended to decrease from sites near the ocean, Dominguez Hills, CA, to those

TABLE 5-10. MASS MEDIAN DIAMETERS REPORTED FOR NITRATE FROM PARTICLE SIZING WITH CASCADE IMPACTORS

Site	Measurement period	Reference	Mass median diameter in μm for nitrate
Cincinnati, OH (CAMP Site)	3/14-23/66	Lee and Patterson (1969)	0.23 (est)
Fairfax, OH	3/25-4/21/66	Lee and Patterson (1969)	0.59
Riverside, CA U. Cal. Campus	11/1-15/68	Lundgren (1970)	0.8
Secaucus, NJ	9/29-10/10/66	Patterson and Wagman (1977)	
	Background		0.20
	Level A		2.6
	Level B		0.38
	Level C		0.37
Dominquez Hills, CA	10/4-5/73	Appel et al. (1978)	1.64
	0/10-11/73		0.72
West Covina, CA	7/23-24/73	Appel et al. (1978)	1.13
	7/26/73		0.62
Pomona, CA	8/16-17/73	Appel et al. (1978)	0.68
Rubidoux, CA	9/5-6/73	Appel et al. (1978)	0.33
	9/18-19/73		0.34

well inland, Rubidoux, CA. At Dominguez, CA and to a lesser extent at West Covina, CA farther inland, a substantial coarse mode fraction of particles greater than 2 μm were measured.

Moskowitz (1977) observed the same sort of pattern of particle size distributions of particulate nitrate in the South Coast Air Basin. The particle size distribution of nitrate indicated two modes. One mode was located between 0.05 and 1 μm, while the other mode was between 2 and 8 μm (8 μm was an arbitrary upper cutoff). At Hermosa Beach, CA, on the coast, the concentration of submicron nitrate was small with most of the nitrate in the 2 to 8 μm range. At Pasadena, CA, the size distribution of particulate nitrate was bimodal with significant amounts of nitrate in both size ranges. At Chino, CA, well inland, a large part of the particulate nitrate was in the submicron range. Coarse mode nitrate was still present. Chino is a cattle-feeding area with high ammonia concentrations available to react with nitric acid to form submicron ammonium nitrate.

Several studies provide results bearing on the chemical composition of the nitrates in the fine and coarse modes. Grosjean and Friedlander (1975) claimed that ammonium nitrate accounted for 95 percent of the measured nitrate, based on infrared spectra of extracts from samples collected on water-washed Gelman type A glass fiber filters in Pasadena, CA during 1973. O'Brien et al. (1975) usually observed the presence of ammonium nitrate based on infrared spectra and paper chromatograms of samples collected on prewashed Gelman type A glass fiber filters at several locations in California. At Santa Barbara, CA, a sample collected within a mile of the ocean contained 16 percent nitrate, but no ammonium ion was detected. The authors suggested that the nitrate was sodium nitrate formed from the reaction of nitrogen dioxide with sodium chloride. Lundgren (1970), in the samples collected at Riverside, CA, identified by x-ray diffraction very hygroscopic, crystalline-like particles making up a large part of the 0.5 to 1.5 μm size range as ammonium nitrate.

High-resolution mass spectrometric measurements were applied to samples collected during a smog episode at West Covina, CA (Cronn et al. 1977). Ammonium nitrate and sodium nitrate were identified as present in the size range below 3.5 μm. The ammonium nitrate concentration substantially exceeded the sodium nitrate concentrations measured.

Kadowaki (1977) size-classified particle nitrate using an Andersen sampler with a type A Gelman glass fiber backup filter in Nogoya, Japan. The size distribution of nitrate was bimodal. The submicron nitrate was shown to be ammonium nitrate and the coarse particles sodium nitrate based on analysis by paper chromatography. Increases in coarse mode nitrate were observed when sea salt aerosols were transported to the sampling location.

5.4 OZONE

Ambient air concentrations of ozone are of interest with regard to acidic deposition for several reasons. Ozone can contribute to adverse effects on field crops, forest trees, and other forms of vegetation (Chapter E-3, Section 3.3.1). Ozone in combination with sulfur dioxide can cause damage to

vegetation. Ozone also may interact with acidic deposition to cause damage to vegetation. However, the results of the several studies completed to date are preliminary and inconclusive. Transformations of sulfur dioxide to sulfate in aqueous droplets in clouds, fogs, and acid mists may be contributed to significantly by reactions with ozone. Therefore, ozone concentrations both at ground level and aloft, cloud heights, are of interest.

This presentation will not include a discussion of ozone concentration measurements within cities. The literature on ozone measurements within cities is too extensive to consider in detail here. A discussion of ambient air ozone concentration levels within cities can be found in the Air Quality Criteria for Ozone (U.S. EPA 1978a).

Most of the ozone measurements made from the early 1970's to the present at ground level and from aircraft have used chemiluminescent ozone analyzers. Investigators using these instruments at rural sites and in aircraft believe the method to be reliable, specific, and precise (Research Triangle Institute 1975, Decker et al. 1976).

Ozone is formed in the atmosphere from the reaction of oxygen molecules with atomic oxygen. The atomic oxygen is formed from the photolysis of nitrogen dioxide. Ozone reacts very rapidly with nitric oxide. Maintaining the production of ozone in the atmosphere requires the presence of radical species produced from the reactions of nitrogen oxides in sunlight with organic vapors (U.S. EPA 1978a). Peroxyacetyl nitrates and nitric acid also are formed in the atmosphere by the reaction of radical species formed in these reactions with nitrogen dioxide. Hydroxyl radicals, OH, are particularly important in their reactions with organic vapors to form other radicals, with nitrogen dioxide to form nitric acid, and with sulfur dioxide to form sulfates. Therefore, homogeneous photochemical reactions are important to the formation of a number of the chemical species discussed in this document.

Ozone is formed in the stratosphere and can be transported into the troposphere by tropospheric extrusion events. Aircraft measurements provide evidence for the transport of ozone from stratospheric extrusions to within a few kilometers of the surface (Viezee and Singh 1982). Direct evidence for transport from the stratosphere, free troposphere, and through the planetary boundary layer to rural locations near sea level is lacking (Viezee and Singh 1982). The air packets from the stratosphere have been observed to level out horizontally at a few kilometers above the surface. Ozone previously transported to these altitudes eventually will be transported to the surface by vertical movements, depending on the lifetime of ozone under these circumstances. A number of reports in the literature note stratospheric ozone contributing to ozone concentration levels at or near the surface (Viezee and Singh 1982). If stratospheric ozone extrusions are an important source of ozone at rural locations, a spring maximum and a fall minimum in ozone concentrations would be expected.

Another source of ozone at the surface could be the reactions of biogenic hydrocarbons. Because background nitrogen oxide concentrations are so low (Section 5.3.2.5), biogenic hydrocarbons, if present at significant ambient air concentrations, would have to mix with anthropogenic nitrogen oxides to

react. However, the ambient air concentrations of biogenic hydrocarbons in urban and rural locations outside of forest canopies are too low to generate significant concentrations of ozone (Altshuller 1983).

Ozone formed in homogeneous photochemical reactions in the atmosphere from anthropogenic precursors can be present at elevated concentration levels at rural locations as a result of one or more of the following processes: (1) local synthesis, (2) fumigation by a specific urban or industrial plume, (3) a high pressure system near the rural location. Ozone concentrations generated from these processes are higher in the warmer than in the cooler months of the year. If homogeneous photochemical reactions of anthropogenic precursors are the more significant source, the higher ozone concentrations would be expected to occur in the late spring, summer months, and early fall.

5.4.1 Concentration Measurements Within the Planetary Boundary Layer (PBL)

Average ozone concentrations in rural areas have been reported as low as 20 to 40 $\mu g\ m^{-3}$, at night and during the early morning hours (Martinez and Singh 1979, Research Triangle Institute 1975, Decker et al. 1976, Evans et al. 1982). Maximum ozone concentrations often are found downwind of the core areas of large cities. Maximum annual one-hour ozone concentrations in the ranges of 800 to 1300 $\mu g\ m^{-3}$ have been observed during most years between 1964 and 1978 at several locations in the South Coast Air Basin (Trijonis and Mortimer 1982, Hoggan et al. 1982). Well out into the eastern part of the South Coast Air Basin at San Bernardino and Redlands maximum annual one-hour ozone concentrations of 600 to 800 $\mu g\ m^{-3}$ have been measured (Trijonis and Mortimer 1982, Hoggan et al. 1982).

A number of studies on urban plumes of large cities in the United States have been reported. The effects of these plumes on elevated ozone concentrations have been shown to extend out to distances as far as several hundred kilometers downwind. Measurements have been made on the flow of the New York metropolitan area plume into southern New England (Cleveland et al. 1976, 1977, Siple et al. 1977, Spicer et al. 1979), the Boston plume into the Atlantic Ocean (Spicer et al. 1982c), the Philadelphia-Camden plume (Cleveland and Kleiner 1975), the Chicago metropolitan area plume (Swinford 1980, Sexton and Westberg 1980), the St. Louis plume (White et al. 1976, 1977; Hester et al. 1977, Spicer et al. 1982b), and the Houston plume (Westberg et al. 1978a,b).

The concentrations of ozone measured within these urban plumes typically ranged up to between 300 to 500 $\mu g\ m^{-3}$. In the case of a city the size of St. Louis, MO, an urban plume 30 to 50 km wide was observed downwind (White et al. 1977). The ozone concentrations within the St. Louis plume were about twice the concentrations in the background in adjacent rural areas. A definable plume containing excess ozone concentrations over rural background also has been demonstrated to occur shorter distances downwind of small cities such as Springfield, IL (Spicer et al. 1982b).

Impacts of urban plumes from large or medium-sized cities within several hundred kilometers on elevated ozone concentration levels at specific

nonurban sites have been reported. Examples of such observations include those made at Research Triangle Park, NC, Duncan Falls, OH, and Giles Co, TN (Martinez and Singh 1979); at Kisatchie National Park, LA and Mark Twain National Park, MO (Evans et al. 1982); and at a rural site outside of Glasgow, IL (Rasmussen et al. 1977). The peak ozone concentrations reported during such episodes at these nonurban sites ranged from 140 to 260 $\mu g\ m^{-3}$.

Davis et al. (1974) reported measurement of excess ozone concentrations within power plant plumes. Measurements of ozone in four power plant plumes in the States of Washington, New Mexico, and Texas by Hegg et al. (1977) did not show any excess of ozone in the plumes over that in surrounding air out to distance of 90 km. Other measurements of power plant plumes in the States of New Mexico and Texas by Tesche et al. (1977) revealed ozone depletion within the plumes in the vicinity of the stack and a gradual increase in ozone concentrations to background levels far downwind. Gillani et al. (1978) observed a significant ozone excess in the Labadie power plant plume 190 km and 9 hours downwind during 9 July 1976. The ozone concentration within the plume at this distance downwind was 220 $\mu g\ m^{-3}$, about 100 $\mu g\ m^{-3}$ above the rural background. Before 5 hours downwind an ozone deficit was observed. During another day in July 1976 a transition from an ozone deficit to an ozone excess was observed after only 2 hours. On both days the first indication of ozone production was observed around 1400 hours. There appears to be less likelihood of observing excess ozone in power plant plumes in the western than in the eastern United States. This result may be associated with the availability of more hydrocarbon in rural air in the eastern United States to diffuse in and react with excess nitrogen oxide in the plume. Observations of the direct effect of power plant plumes on ground level ozone concentrations at rural locations are lacking.

Several studies have been made of the effects of high pressure systems on ozone concentrations over the midwestern and eastern United States (Research Triangle Institute 1975, Decker et al. 1976, Husar et al. 1977, Vukovich et al. 1977, Wolff et al. 1977). The distribution of ozone concentrations relative to a moving high pressure system have been represented for several rural locations in Pennsylvania, at Creston in southwestern Iowa, and at Wolf Point in northeastern Montana (Decker et al. 1976, Vukovich et al. 1977). A relative minimum in the maximum diurnal ozone concentration occurs somewhere in the region between the initial frontal passage and the high pressure center. The highest ozone concentrations diurnally occur after the high pressure center passes the site or on the back side of the high pressure system. The exception was at Wolf Point, MT, where no substantial variation in the ozone concentrations was seen as the high pressure system passed through that location. Meteorological analysis indicated no reason why the average downward transport by general subsidence or by enhanced vertical mixing should increase the ozone concentration in the backside of the high pressure system. The aircraft measurements showed no indication on the average that the vertical gradient of ozone through the troposphere is greater in the eastern than in the western United States. Therefore, the elevated ozone concentrations measured from Iowa eastward could not be attributed to downward transport of ozone. It was concluded that the most

appropriate explanation was the availability of sufficient amounts of precursors reacting to form ozone within the high pressure systems. The backside of the high pressure systems is the region where air parcels have the highest residence times for precursors to react to form ozone.

The peak ozone concentrations during the movement of the high pressure system were between 200 and 500 $\mu g\ m^{-3}$ at the Pennsylvania sites, 150 $\mu g\ m^{-3}$ at Creston, IA and less than 100 $\mu g\ m^{-3}$ at Wolf Point, MT. Such high pressure systems were influencing the sites much of the time in the July to September period. For example, at one or another of the rural sites where measurements were being made in 1973, 1974, and 1975, a high pressure center or ridge was within 450 miles of the site between 80 and 90 percent of the time (Decker et al. 1976, Vukovich et al. 1977).

A study of factors responsible for higher ozone concentrations also was made over the Gulf Coast area (Decker et al. 1976). Elevated ozone concentrations of 160 $\mu g\ m^{-3}$ or more were frequently measured in plumes downwind of cities, major refineries, and petrochemical installations. Ozone concentrations over the Gulf of Mexico usually were lower than over land except when the air parcels had previously passed over continental sources of pollution.

Diurnal profiles of ozone concentrations averaged over study periods or quarter of year are available from several studies (Research Triangle Institute 1975, Decker et al. 1976, Vukovich et al. 1977, Martinez and Singh 1979, Evans et al 1982) at the rural sites discussed and additional sites. The average profiles are very similar, with ozone concentrations rising in the morning hours, peaking in the afternoon, and falling after establishment of the noctural inversion in the evening hours through the night to 0600 or 0700 hours. From a 1974 study made between June 14 and August 31 (Research Triangle Institute 1975), the average 0900 to 1600 ozone concentrations of interest in crop yield studies can be computed for the rural sites as follows: Wilmington, OH, 125 $\mu g\ m^{-3}$; McConnelsville, OH, 117 $\mu g\ m^{-3}$; Wooster, OH, 119 $\mu g\ m^{-3}$, McHenry, MD, 116 $\mu g\ m^{-3}$; DuBois, PA, 132 $\mu g\ m^{-3}$.

In some of the studies discussed above, either sulfate measurements or visibility measurements as a surrogate for fine particles are available (Decker et al. 1976, Husar et al 1977). The sulfate concentrations (in $\mu g\ m^{-3}$) and the sulfate as a percentage of total suspended particulate from west to east were as follows: Wolf Point, MT, 1.8, 6.2; Creston, IA, 7.2, 9.2; Bradford, PA, 9.9, 29.0. These measurements show the same directional characteristics from west to east as do the ozone concentrations. Husar et al. (1977) analyzed an episode during late June 1976, finding that the geographical location of high ozone concentrations roughly corresponded to areas of low visibility and high sulfate concentrations. The air quality measurements at St. Louis during June through August of 1975 showed that ozone concentrations above 160 $\mu g\ m^{-3}$ roughly coincided with light extinction coefficients above 5. Therefore, a similar behavior occurs for ozone and for light scattering aerosols such as sulfate.

5.4.2 Concentration Measurements at Higher Altitudes

Ozone measurements at several higher altitude mountainous sites have been compiled by Singh et al. (1978). Hourly ozone concentrations are as high as 140 to 160 μg m^{-3} during the spring months, and as low as 40 to 60 μg m^{-3} during the fall months. While the seasonal patterns tend to be consistent, the absolute concentrations differ from year to year. Relatively high summer ozone concentrations have been observed at some sites (Singh et al. 1978). Viezee and Singh (1982) have assembled results from recent aircraft observations. Observations between the altitudes of 1.5 and 4.5 km indicate ozone concentrations during May in the 110 to 150 μg m^{-3} range and during October in the 70 to 90 μg m^{-3} range. A summary of aircraft observations of ozone concentrations during stratospheric air extrusions results in a power curve from which the ozone concentration obtained is 140 μg m^{-3} at 3 km, 210 μg m^{-3} at 5 km and 330 μg m^{-3} at 7 km. Based on these aircraft measurements compared to the elevated ozone concentrations attributed to stratospheric ozone at sites between sea level and 3 km, Viezee and Singh (1982) believe that reports of ozone concentrations above 200 μg m^{-3} near the surface attributed to stratospheric air extrusions are unlikely and should be reexamined.

5.5 HYDROGEN PEROXIDE

The oxidation of sulfur dioxide in aqueous droplets by hydrogen peroxide may be the most important of the mechanisms for conversion of sulfur dioxide to sulfuric acid (Chapter A-4). Therefore, the measurements of hydrogen peroxide concentrations are of considerable interest.

Several chemical methods for measuring hydrogen peroxide in ambient air and in rainwater are in use. Both the reaction of titanium sulfate and 8-quinolinol with hydrogen peroxide (Cohen and Purcell 1967) and the reaction of titanium (IV) tetrachloride with hydrogen peroxide (Pilz and Johann 1974) have been used in colorimetric procedures for measuring hydrogen peroxide in air. The chemiluminescent oxidation of luminol by hydrogen peroxide in the presence of Cu(II) catalyst is the basis of a sensitive automated system for continuous monitoring of hydrogen peroxide in the atmosphere (Kok et al. 1978b). Addition of a known amount of scopoletin to a buffered sample containing hydrogen peroxide followed by addition of horseradish peroxidase to catalyze the oxidation by scopoletin results in fluorescence decay (Zika et al. 1982). The amount of hydrogen peroxide is determined by difference in the fluorescence before and after addition of the horseradish peroxidase.

The long-path Fourier transfer infrared technique has not proved applicable to measuring hydrogen peroxide because of its high detectability limit of about 56 μg m^{-3} (Tuazon et al. 1981a).

Recent studies (Heikes et al. 1982, Zika and Saltzman 1982) indicate that hydrogen peroxide can be produced from other species within aqueous solutions. These results suggest that methods involving collection in aqueous solutions may not provide useful measurements of ambient air hydrogen peroxide concentrations. Both groups found hydrogen peroxide to be generated within the aqueous collecting solutions when ozone in oxygen-nitrogen

mixtures is passed through aqueous solutions in bubblers or impingers. Heikes et al. (1982) also observed that sulfur dioxide vapor acts as a negative interferent by depleting hydrogen peroxide in its aqueous collection or formation.

5.5.1 Urban Concentration Measurements

Ambient concentrations of hydrogen peroxide up to 56 $\mu g\ m^{-3}$ in Hoboken, NJ and 251 $\mu g\ m^{-3}$ in Riverside, CA were measured in 1970 by Bufalini et al. (1972) using Cohen and Purcell's (1967) method. Subsequent measurements of hydrogen peroxide in 1977 at sites in Claremont, CA and Riverside, CA gave hydrogen peroxide concentrations typically ranging from 14 to 70 $\mu g\ m^{-3}$ with a maximum concentration near 140 $\mu g\ m^{-3}$ (Kok et al. 1978a). Three chemical methods (Cohen and Purcell 1967, Pilz and Johann 1974, Kok et al. 1978b) were used in intercomparisons. The hydrogen peroxide concentrations measured by the three methods differed by as much as a factor of two to three. Substantial ozone concentrations were present in the atmosphere during most of the time hydrogen peroxide was being measured.

Subsequent measurements of hydrogen peroxide were made in 1979 and 1980 in the Los Angeles Basin area at sites within Los Angeles, Claremont, and Palo Verde, CA (Kok 1982). In Los Angeles at California State University, the hydrogen peroxide concentrations on 18 and 19 June 1980 ranged between about 0.7 and 3.5 $\mu g\ m^{-3}$. The hydrogen peroxide concentrations were 1 to 2 percent of the maximum ozone concentrations. At Claremont, CA, hydrogen peroxide measurements were reported during a number of days in June to September 1979 and in September 1980. In June and July 1979 the hydrogen peroxide concentrations were much higher than reported in August 1979 and September 1979 and 1980. Peak concentrations exceeded 14 $\mu g\ m^{-3}$ in June and July, while in August and September the hydrogen peroxide concentrations were only a few ppb. At Point San Vincente, located in the Palo Verde peninsula, on 11 and 12 September 1980 the hydrogen peroxide concentrations peaked at 8 to 11 $\mu g\ m^{-3}$. The maximum hydrogen peroxide concentrations compared to the maximum ozone concentrations show no distinct relationship (Kok 1982).

Heikes et al. (1982) obtained about equal amounts of hydrogen peroxide in each of three impingers in series sampling ambient air over a series of days in February and March 1981 at Boulder, CO. If the ambient air hydrogen peroxide was collected efficiently in the first impinger, the ambient air hydrogen peroxide concentrations ranged from 0.4 to 3.1 $\mu g\ m^{-3}$. Approximately equivalent amounts of hydrogen peroxide measured in the second and third impingers indicate substantial amounts of hydrogen peroxide were generated in solution.

5.5.2 Nonurban Concentration Measurements

Measurements of hydrogen peroxide concentrations were obtained by the luminol chemiluminescence technique at a rural site east of Boulder, CO in February 1978 (Kelly and Stedman 1979a). The hydrogen peroxide concentrations ranged from 0.4 to 4 $\mu g\ m^{-3}$ during this period.

Hydrogen peroxide was measured in water condensate by the luminol chemiluminescence technique at rural sites near Tucson, AZ (Farmer and Dawson 1982). In more remote areas around Tucson the hydrogen peroxide concentrations were about 1.4 $\mu g\ m^{-3}$, while at a Thurber Ranch site the hydrogen peroxide ranged up to 6 $\mu g\ m^{-3}$. The hydrogen peroxide concentration was observed to drop off drastically when high sulfur dioxide concentrations were measured. With a correction for the interference by sulfur dioxide, the authors estimated that the hydrogen peroxide reached 10 $\mu g\ m^{-3}$.

5.5.3 Concentration Measurements in Rainwater

Because the key interest in hydrogen peroxide is with respect to its behavior in solution, available measurements of hydrogen peroxide in rainwater will be discussed.

Hydrogen peroxide in rainwater collected in Claremont, CA during 1978 and 1979 was analyzed by luminol chemiluminescence (Kok 1980). The hydrogen peroxide content of the rainwater over long sampling intervals dropped off substantially during precipitation events. The highest hydrogen peroxide concentration obtained was 1590 $\mu g\ \ell^{-1}$, but hydrogen peroxide concentrations also frequently were below 100 $\mu g\ \ell^{-1}$. The lower concentrations could be accounted for by the absorption of less than 0.14 $\mu g\ m^{-3}$ of hydrogen peroxide from ambient air into the cloud water.

Measurements of hydrogen peroxide in rainwater also were made in Claremont, CA during 1980 and 1981 (Kok 1982). Hydrogen peroxide concentrations were found to be extremely variable in rainwater samples during the course of a storm. The results were interpreted as suggesting that hydrogen peroxide is incorporated into the rain at cloud levels. Most of the hydrogen peroxide concentrations in the rainwater samples were at or below 500 $\mu g\ \ell^{-1}$.

Hydrogen peroxide was measured in rainwater samples collected in Miami, FL and the Bahama Islands (Zika et al. 1982). The concentration of hydrogen peroxide in rainwater, expressed as $\mu g\ \ell^{-1}$, ranged from 3.06 to 25.5 x 10^2 in Miami, FL samples and was 6.8 x 10^2 in a sample collected in the Bahama Islands. The variations of hydrogen peroxide concentrations during the precipitation events were different from the changes in sulfate and nitrate concentrations. The authors believed that the results for hydrogen peroxide were consistent with a substantial part of the hydrogen peroxide being present as a result of its being generated within the cloudwater rather than being present as a result of rainout and washout of gaseous hydrogen peroxide.

5.6 CHLORINE COMPOUNDS

5.6.1 Introduction

Chlorine can exist in a number of gaseous and particulate forms in the atmosphere. The gases can include hydrogen chloride, chlorine gas, and carbon-containing vapors such as phosgene and halocarbons. The particulate forms include sodium chloride, usually as sea salt particles from the bursting of

bubbles at the sea surface (Junge 1963). Ammonium chloride also has been reported (Cronn et al. 1977).

The most likely form for gaseous chloride is hydrogen chloride. Chlorine gas reacts rapidly with hydrogen-containing organic molecules to abstract hydrogen and form hydrogen chloride (Hanst 1981). Phosgene (Cl_2CO) has been measured in the ppt range in the ambient atmosphere (Singh et al. 1977b). Numerous chlorocarbons have been measured in the ppt to ppb range in urban atmospheres (Singh et al. 1982) and in the ppt range at rural and remote sites (Singh et al. 1977a,b). Most chlorocarbons have long residence times in the atmosphere (Singh et al. 1981). Their inert chemical structure tends to limit their rates of dry deposition and wet scavenging to very low values. The shorter-lived chlorinated olefins react in the laboratory to form chlorine-containing products such as hydrogen chloride, phosgene, chlorinated acetyl chlorides, and chlorinated peroxyacetyl nitrates (Gay et al. 1976). The chlorinated acetyl chlorides and chlorinated peroxyacetyl nitrates have not been detected in the ambient atmosphere.

A number of the same type of artifact problems may exist for particulate chlorine measurements as for particulate nitrate measurements because of the volatility of hydrogen chloride. However, such studies of sampling of chlorides on filters are not available.

5.6.2 Hydrogen Chloride

Junge (1963) reported early measurements of gaseous chlorine-containing compounds that probably were hydrogen chloride. His measurements at three sites gave the following average concentrations in $\mu g\ m^{-3}$: Florida--1.6, Ipswich, MA--4.4, and Hawaii--1.9. Gaseous chlorine compounds were measured by the same technique by Duce et al. (1965) on the island of Hawaii. The concentrations of gaseous chlorine compounds ranged from less than 0.3 $\mu g\ m^{-3}$ to 218 $\mu g\ m^{-3}$ although the gaseous chlorine concentrations were at or below 10 $\mu g\ m^{-3}$ in most samples. The halide ion analysis does not permit identification of the original chemical species collected.

Although hydrogen chloride has been measured by infrared techniques in a number of studies in the stratosphere, limited effort has gone into its measurement in the troposphere. Farmer et al. (1976) reported both tropospheric and stratospheric measurements at the ground and from aircraft. The tropospheric mixing ratio at ground level was 10^{-9} corresponding to 1.5 $\mu g\ m^{-3}$, with the mixing ratio decreasing to 10^{-10} in the upper troposphere. At ground level, the tropospheric levels were essentially the same inland in the Mohave Desert, CA, as near the coast (Farmer et al. 1976). Hydrogen cloride was not detected by the FTIR system with a 1 km pathlength in measurements at Riverside and Claremont, CA (Tuazon et al. 1981b). The established detection limit was about 12 $\mu g\ m^{-3}$.

5.6.3 Particulate Chloride

Junge (1963) measured comparable amounts of particulate chloride to gaseous chlorine-containing compounds. His measurements gave the following average concentrations in $\mu g\ m^{-3}$: Florida--1.5 and Hawaii--5. Duce et al.

(1965) measured particulate chloride on a four-stage cascade impactor. The total chloride concentrations ranged from 0.5 to 137 μg m^{-3}. Three of the nine samples had total chloride concentrations of 39, 95 and 137 μg m^{-3}; the remainder had concentrations below 10 μg m^{-3}.

Particulate chloride concentration distribution was measured at about 30 sites in the Houston-Galveston, TX area on 2 days in June and 2 days in September 1975 (Laird and Miksad 1978). The natural background of chloride varied from 0.2 to 6.6 μg m^{-3} with wind speed and direction. The higher background concentrations corresponded to the stronger inland penetration of fresh maritime air from the Gulf of Mexico. Significant incremental concentrations of 5 to 10 μg m^{-3} above background were observed, particularly in the industrialized Pasadena-Houston Ship Channel area.

At urban and nonurban locations somewhat inland, atmospheric chloride concentrations typically average 1 μg m^{-3} and less (Gartrell and Friedlander 1975, Flocchini et al. 1976, Paciga and Jervis 1976, Crecelius et al. 1980, Dzubay 1980).

5.6.4 Particle Size Characteristics of Particulate Chlorine Compounds

Junge (1963) discussed the particle size characteristics of chloride particles. The chloride particles associated with maritime air are found in the 1 to 10 μm range. Measurements at a rural coastal site 50 miles south of Boston, MA (Round Hill), support these conclusions. In contrast, chloride particles less than 1 μm were associated with processes occurring over land.

Gladney et al. (1974) reported measurements of chloride on cascade impactors at several sites in the Boston, MA area. The shapes of the site distribution curves for a number of samples indicated that the chloride present was predominantly marine aerosol and that there also was a strong correlation between sodium and chloride for these samples. The concentrations of both chloride and sodium were usually low, and the size distributions flatter, when the winds were from inland.

The size distribution of chloride particles at Secaucus, NJ, have been reported for varying visibility conditions (Patterson and Wagman 1977). The MMD increased from the background condition of best visibility of 0.17 μm to 1.1 μm under the poorest visibility conditions experienced. The size distributions for chloride appeared to be trimodal. Particles less than 0.5 μm were associated with lead aerosols from automobile exhaust, the particles near 1 μm with the contribution from sea salt, and the largest particles with dredging operations.

The particle size distributions of chloride particles were reported at several sites in Toronto, Canada, by Paciga and Jervis (1976). The chloride had a mass median diameter of 0.6 μm during the summer at this inland site. The sources of chlorides were associated with lead aerosols from automobiles and emissions from a power plant and an incinerator. Winter samples showed a 10-fold increase in chloride concentration, and an increase in the MMD of

chloride to about 9 μm. These increases were attributed to salting of roadways.

Hardy et al. (1976) reported chloride size distributions at three sites in the Miami, FL area. Two of the sites were 2 km from the seacoast and the third, 15 km inland. The cascade impactor stages collecting particles larger than 2 μm contained most of the mass. There was a low concentration of chloride on the stages collecting particles between 0.25 and 1 μm, but the concentration increased again on the filter used to collect particles less than 0.25 μm. The small-particle chloride was attributed to chlorine associated with lead aerosols emitted from gasoline-powered vehicles. The large particles were associated with particles emitted from the sea surface.

Particle size distributions of chloride were measured by Lee and Patterson (1969) at sites in Philadelphia, PA, Cincinnati, OH (Fairfax), and Chicago, IL, in the summer and fall. The MMD's obtained were all near 0.85 μm. Lee and Patterson concluded that the chlorides at these sites were primarily influenced by industrial and vehicular emissions rather than sea salt aerosols.

5.7 METALLIC ELEMENTS[1]

The various interests and possible concerns related to metallic elements have been discussed briefly in the introduction to this chapter. Alkaline earth elements such as calcium and magnesium can help neutralize acidic materials either during precipitation events or as a result of dry deposition. Manganese and iron are possibly of consequence in the chemical transformations of sulfur dioxide to sulfur (Chapter A-4, Section 4.3.5). Aluminum, manganese, nickel, zinc, lead and mercury are discussed elsewhere in this document (Effects Chapters) in relation to possible adverse effects in soil, lakes and streams, and indirect effects on health.

5.7.1 Concentration Measurements and Particle Sizes in Urban Areas

An extensive literature base on the air quality measurements of metallic elements in urban areas is available. It is not appropriate to discuss this literature in great detail. Concentrations of most of the elements of interest here have been reported by Stevens et al. (1978) for six urban areas. These measurements along with particulate sulfur concentrations are given in Table 5-11 as examples of reasonably representative urban concentration levels of these elements. This study is useful in also providing the percentages of these elements in particles below and above 3.5 μm at these urban sites. Sulfur is the most abundant element, followed by calcium, aluminum, iron and lead.

---

[1]Editor's note: Although several public reviewers objected to the inclusion of Section 5.7 on metallic elements and Section 5.8 on visibility, during the November 1982 Technical Review Meeting, the reviewers and author viewed these discussions as useful and their inclusion justified.

Lead concentration measurements have been extensively reviewed in the Air Quality Criteria for Lead (U.S. EPA 1977b). In urban communities the percentage of monitoring sites with measurements falling within selected annual average lead concentration intervals during 1966 to 1974 were as follows: less than 500 ng m^{-3}, 8; 500 to 999 ng m^{-3}, 38; 1000 to 1999 ng m^{-3}, 45; 2000 to 3999 ng m^{-3}, 8; 4000 to 53000 ng m^{-3}, 1. The lead concentrations at over 80 percent of these monitoring sites were in the 500 to 1999 ng m^{-3} range. The average concentrations of lead at the urban sites given in Table 5-11 also fall within this concentration range.

The National Academy of Sciences (1975) review on nickel contains a compilation of measurements of ambient air nickel concentrations from the National Air Surveillance Networks. The overall average ambient air concentrations of nickel at urban sites was 21 ng m^{-3}. Nickel, as vanadium, is associated with the type of fuel oils used in cities within the northeastern United States. In such areas the average nickel concentrations often are in the 100 to 300 ng m^{-3} range during the first and fourth quarters. The nickel concentration listed at a site in New York City in Table 5-11 is at the lower end of this range.

The percentages of fine (less than 3.5 μm) compared to coarse particles (greater than 3.5 μm) in Table 5-11 indicate that sulfur, nickel, zinc and lead are most often associated with fine particles. Calcium, aluminum, and iron are usually found in coarse particles. Sulfur and lead show the least variability in size distribution. As discussed earlier (Section 5.2.4), most of the particle sulfur is present in submicron particles. Lead also is associated mostly with submicron particles in urban areas (Robinson and Ludwig 1967, Lee et al. 1968, Lundgren 1970, Gillette and Winchester 1972, Martens et al. 1973, Patterson and Wagman 1977). Patterson and Wagman (1977) found 70 percent of the zinc measured in background air and 80 to 90 percent of the zinc measured in more polluted air on particles less than 1.5 μm with most of the zinc associated with particles between 9.5 and 1.5 μm.

Those elements present in coarse particles would be expected to be subject to rapid deposition near their areas of emission. Fine particles have small dry deposition velocities (Chapter A-7, Section 7.4.2). However, atmospheric dispersion should tend to rapidly decrease the ambient air concentrations of both coarse and fine particles associated with primary emissions from urban sources.

Mercury occurs as a vapor in the atmosphere but also can be associated with particles. Mercury concentrations have been measured in ambient air in several urban areas. In Washington, DC a mercury vapor concentration of 3.2 ng m^{-3} was measured during February 1972 (Foote 1972). Dams et al. (1970) reported mercury concentrations of 4.8 ng m^{-3} on particulate matter collected in East Chicago, IN. In Los Altos, CA in the San Francisco Bay area, mercury vapor concentrations varied from 1 to 25 ng m^{-3} in winter and from 1.5 to 2 ng m^{-3} up to 50 ng m^{-3} in summer (Williston 1968). This area has Franciscan sediments high in mercury, 100 to 200 ppb, and two mercury mines exist within 25 miles of Los Altos. The lowest concentrations were observed with strong westerlies bringing clear marine air ashore after rainy weather (Williston 1968).

TABLE 5-11. CONCENTRATIONS AND PERCENTAGES OF ELEMENTS PRESENT AS FINE PARTICLES IN PARTICULATE MATTER AT SITES IN THE UNITED STATES

Site Period of measurement	Parameter	Concentrations and percentages, ng m^{-3} S	Ca	Al	Mn	Fe	Ni	Zn	Pb
New York City, NY[a] February 1977	Conc. ng m^{-3}	5936	1509	969	99	1340	75	458	1227
	% Fine[b]	93	24	13	56	29	76	81	86
Philadelphia, PA[a] Feb.-March 1977	Conc. ng m^{-3}	3550	1104	690	31	904	37	186	1115
	% Fine	87	15	7	55	24	81	80	85
Charleston, W VA[a] April-Aug. 1976 and January 1977	Conc. ng m^{-3}	4119	924	1372	19	788	1	50	757
	% Fine	92	10	19	37	21	67	60	82
St. Louis, MO[a] December 1975	Conc. ng m^{-3}	3526	2130	--[c]	73	1338	25	221	1076
	% Fine	79	6	--[c]	55	25	60	67	77
Portland, OR[a] February 1977	Conc. ng m^{-3}	1679	832	1385	48	1123	52	91	1040
	% Fine	83	8	15	56	17	81	67	83
Glendora, CA[a] March 1977	Conc. ng m^{-3}	1852	541	>331	11	484	17	61	706
	% Fine	87	18	NA	45	26	82	74	87
Smoky Mt., PA[d] July-Aug. 1977	Conc. ng m^{-3}	3948	338	215	ND	146	2	<12	114
	% Fine	95	5	9	NA	19	50	>75	85

[a]Stevens et al. 1978.

[b]Percentage of mass of element present as particles less than 3.5 μm.

[c]Concentrations reported not consistent with other Al measurements at site.

[d]Stevens et al. 1980.

NA = not available.

ND = not determined.

5.7.2 Concentration Measurements and Particle Sizes in Nonurban Areas

The concentrations of the metallic elements of interest and sulfur in particles are given at a number of rural and remote sites within the United States and Canada in Table 5-12. Sulfur in particles collected at the two sites in the eastern United States is in large excess to the other elements. Calcium, aluminum, and iron usually are the next most abundant elements. The three elements at the Smoky Mountains, TN site, as at the urban sites, are found to a large extent in the coarse particles (Table 5-12). All of the elements listed except for sulfur and aluminum occur at substantially lower concentrations at the rural and remote sites than at the urban sites (Tables 5-11 and 5-12). Lead concentrations at the three rural continental sites are a factor of 10 to 20 below those at the urban sites. At the Quillayute, WA site, lead concentrations in Pacific maritime air are a factor of 300 to 600 lower than at the urban sites. Nickel concentrations at the rural and remote sites show similar behavior compared to nickel at urban sites. However, zinc does not show concentration reductions as large at rural compared to urban sites as do lead and nickel.

Additional measurements of sulfur, zinc, and lead have been reported for the period October 1979 to May 1980 and from the 40-site Western Fine Particle (WFP) Network, including the States of Arizona, New Mexico, Utah, Colorado, Wyoming, Montana, North Dakota, and South Dakota (Flocchini et al. 1981). Sulfur concentrations rarely exceeded 100 ng m^{-3} and frequently were below 500 ng m^{-3} on the average at these sites. Lead concentrations were in the 30 to 80 ng m^{-3} range, but on the average were below 50 ng m^{-3} at almost all of the sites. The overall mean concentration of coarse particles was 8000 ng m^{-3} with 60 percent associated with soil elements and their associated oxides. The percentage of iron in fine particles (less than 2.5 μm) for the sites in the study area ranged from 10 to 35 percent with the range at most sites between 15 and 25 percent. These percentages are in good agreement with those for fine particle iron at the urban sites and at the Smoky Mountains site (Table 5-11).

Dams and Dejonge (1976) measured aerosol composition from August 1973 to April 1975 at Jungfraujoch (3752 m above sea level) in Switzerland and also tabulated unpublished results by K. A. Rahn obtained at Lakely in marine air at North Cape, Norway during the winter of 1971-72. The concentrations in ng m^{-3} of the elements considered above were as follows: Jungfrau, Al, 51; Mn, 1.5; Fe, 36; Zn, 9.9; Pb, 4.4; Lakely, Al, 43; Mn, 2.5; Fe, 51; Zn, 8.9; Pb, 5.6. These concentrations are not much different than at Twin Georges in the Northwest Territory, Canada.

A number of the rural and remote sites discussed are in mountainous and marine locations. It is reasonable that the concentrations of most elements would be low. In particular, sources of soil-derived elements would be limited near such sites. In areas with significant numbers of unpaved roads, agricultural activities, and other sources of windblown soils, the concentrations of soil-derived elements should be substantially higher. The much higher concentrations of aluminum at Chadron, NB and Colstrip, MT (Table 5-12) than at mountainous and marine sites are consistent with this expectation.

TABLE 5-12. CONCENTRATIONS OF ELEMENTS IN PARTICULATE MATTER AT NONURBAN SITES IN THE UNITED STATES AND IN CANADA

Site Period of measurement	ng m^{-3} S	Ca	Al	Mn	Fe	Ni	Zn	Cd	Pb	References
Alleghany Mountain, PA July-August 1977	4690	330	70	9	320	ND	20	3	90	Pierson et al. 1980b
Smoky Mountains, TN September 1978	3948	338	215	ND	146	2	$\leq$12	ND	114	Stevens et al. 1980
Chadron, NB 1973	ND	ND	535	6	ND	ND	16	0.6	45	Struempler 1975
Colstrip, MT May-September 1975	550	390	930	9	410	0.6	6.5	ND	14	Crecelius et al. 1980
Quillayute, WA										Ludwick et al. 1977
April-November 1974[a]	ND	ND	ND	0.7	25.3	0.1	4.2	ND	1.9	
December-May 1975[a]	ND	ND	ND	0.8	13.1	0.1	11.3	ND	1.8	
Twin Georges, NW Terr., Canada	ND	ND	66	1.5	71	ND	3.8	ND	ND	Dams and Dejonge 1976

[a]only those days included with trajectories having marine histories for at least three days before arriving at the Quillayute, WA site.

ND = not determined.

Ambient air concentrations of mercury vapor at nonurban sites have been summarized as a function of soil conditions (U.S. Geological Survey 1970). Over areas without mercury containing minerals, ambient air concentrations of mercury vapor were in the 3 to 9 ng m^{-3}. Over areas containing mercury minerals, ambient air concentrations of mercury vapor were in the 7 to 53 ng m^{-3} range, while in the vicinity of known mercury mines the mercury vapor concentrations reached the 24 to 108 ng m^{-3} range. Mercury concentrations were found to peak at midday and to decrease rapidly with altitude (U.S. Geological Survey 1970).

At nonurban locations on the beach in the San Francisco Bay area mercury vapor concentrations of 3.1 ng m^{-3} have been reported (Foote 1972). Williston (1968) collected samples at 10,000 foot altitudes 20 miles offshore of the San Francisco Bay area and obtained concentrations of mercury vapor of 0.6 to 0.7 ng m^{-3}. At a rural site, Niles, MI, a mercury concentration of 1.9 ng m^{-3} was measured in particulate matter (Dams et al. 1970). Ambient air mercury vapor concentrations of 25 ng m^{-3} were reported in samples collected in Research Triangle Park, NC (Long et al. 1973).

5.8 RELATIONSHIP OF LIGHT EXTINCTION AND VISUAL RANGE MEASUREMENTS TO AEROSOL COMPOSITION

Visual range measurements can be influenced by a number of natural and man-made factors. Visual range can be reduced substantially on an episodic basis by rain, fog, snow, and by windblown dust and sand. Rayleigh scattering by air molecules contributes to light extinction and limited visual range, but the contribution is small except in remote areas. Nitrogen dioxide is the only other gas in the atmosphere with the potential to contribute significantly to light extinction, but its concentration in the atmosphere usually is too low for it to contribute substantially in practice. Particles in the size range between about 0.1 and 2 μm are effective light scattering components of the atmosphere while elemental carbon particles are effective absorbers of light (Charlson et al. 1978b). Most of the emphasis in this section will be on the relationships between aerosol composition and visual range and light extinction.

Sulfates and nitrates as suspended aerosol components of the atmosphere contribute to visibility reduction through light scattering. These aerosols also contribute to acidic deposition and its effects. To the substantial extent that visual range and light extinction are accounted for by sulfates and nitrate concentrations in the atmosphere, these visibility measurements can serve as surrogates for concentration measurements in geographical areas where concentration measurements are not available. Because aerosol concentrations are related to deposition rates, the visibility measurements also can be related to deposition or to the potential for deposition.

5.8.1 Fine Particle Concentration and Light Scattering Coefficients

A number of investigators have demonstrated a proportionality between fine particle concentration and light scattering coefficient. Sulfates and nitrates, in some locations, are major components of the fine particle concentration.

Waggoner and Weiss (1980) obtained a ratio of fine particle concentration to the light scattering coefficient, b_{sp}, of 0.36 g m^{-2} (corrected for temperature) from measurements at five urban and rural locations in the western United States. In Denver, CO, Groblicki et al. (1981) obtained a ratio of fine particle concentration to b_{sp} of 0.29 g m^{-2}. In Houston, TX, Dzubay et al. (1982) obtained a very high correlation coefficient of 0.987 between fine particle concentration and b_{sp} and a ratio of 0.28 g m^{-2}. The ratios obtained in Denver and in Houston are in reasonable agreement with the results obtained by Waggoner and Weiss (1980).

At a site in the Shenandoah Valley, VA, Weiss et al. (1982) obtained a correlation coefficient of 0.94 for the measurements of fine particle concentration as related to b_{sp} and a ratio of 0.24 g m^{-2}. A cyclone was used to eliminate particles above 1 μm from the measurement as fine particles. Ferman et al. (1981) made measurements at the same site during the same period. These workers obtained a correlation coefficient of 0.91 for the measurements of fine particle concentration as related to b_{sp} and a ratio of 0.14 g m^{-2}. However, a substantially higher particulate size cutoff was used by Ferman et al. than by Weiss et al.

Although there is variability in the ratio of fine particle concentration to b_{sp} from site to site, consistently high correlation coefficients are obtained at individual sites. The variability in ratio is related to the corresponding variability in the ambient air aerosol composition (White and Roberts 1977, Ferman et al. 1981).

5.8.2 Light Extinction or Light Scattering Budgets at Urban Locations

At several locations in the South Coast Air Basin concurrent measurements of light scattering and of aerosol composition were available from the 1973 Aerosol Characterization Experiment (ACHEX). White and Roberts (1977) analyzed these results to obtain relationships between light scattering and aerosol composition. Sulfate, nitrate and organic aerosols all made a substantial contribution to the overall aerosol concentrations at these locations. The average percentage contribution of aerosol classes to the light scattering (based on all emission sources) was as follows: sulfate, 47; nitrate, 39; organics, 14. Except at high humidities, the contribution, on a unit mass basis, of sulfate was higher than that of nitrate. A lack of dependence on humidity of the contribution of sulfate to light scattering was found. In contrast Cass (1976), from similar measurements in the South Coast Air Basin, did find a dependence on humidity of both the contributions of sulfates and nitrates to light scattering. The sum of species other than sulfates, nitrates, and organics was found to have about one-third the effectiveness of sulfate on a unit mass basis in contributing to light scattering (White and Roberts 1977).

In Riverside, CA the average percentage contributions of aerosol classes to the light scattering coefficient were found to be 70 to 75 percent for sulfate and 20 to 25 percent for nitrate on a unit mass basis (Pitts and Grosjean 1979). No statistical association could be found in this study between light scattering with organic carbon or any other aerosol species measured.

In November and December 1978 at a location in Denver, concurrent measurements were made of both light scattering and adsorption of nitrogen dioxide, and of ammonium, sulfate, nitrate, organic carbon, elemental carbon and other species in the fine particle fraction (Groblicki et al. 1981). Of the chemical species measured the percentage contributions to the light extinction were as follows: sulfate as ammonium sulfate, 20; nitrate as ammonium nitrate, 17; organic carbon, 12; elemental carbon, 38 (scattering, 6.5, adsorption, 31.2); remainder of fine particle mass, 6.6; nitrogen dioxide, 5.7. Elemental carbon was found to be the most effective species on a unit mass basis in contributing to light extinction. Both sulfate and nitrate were found to have their contributions to light scattering dependent on relative humidity. Sulfate was a more effective scatterer on a unit mass basis than nitrate or organic carbon. The sum of other fine particle species showed a much lower effectiveness on a unit mass than the other species specifically considered above.

During September 1980 in Houston, TX concurrent measurements were made of light scattering and light extinction, of nitrogen dioxide, and of sulfate, nitrate, carbon-containing compounds and many other species (Dzubay et al. 1982). The percentage contributions of the chemical species measured to light extinction were as follows: sulfate and associated cations, 32; nitrate, 0.5; carbon, 17 to 24 (scattering, 11, adsorption, 6 to 13); other aerosol components, 4; water, 16; nitrogen dioxide, 5; Rayleigh (air), 6. The crustal elements constituted 29 percent of the total mass concentration of particulates, but only 2.9 percent of the fine particle mass. As a consequence, the crustal elements only contributed 2.6 percent of the light extinction. No functional relationships of sulfate and nitrate including humidity were used. Instead, the contribution of water to light extinction was computed separately. If the contribution of water is associated predominately with sulfates, the sulfates and associated species would account for about one-half of the light extinction.

The contribution of light extinction associated with nitrates was much smaller in Houston than in Los Angeles and Denver (White and Roberts 1977, Groblicki et al. 1981, Dzubay et al. 1982). Nitrates were determined in both Houston and Denver studies on Teflon filters, so a negative nitrate artifact would be expected in both sets of measurements. Therefore, at least on a relative basis, the nitrate concentrations in Denver should have been much higher than in Houston. The difference in season during which sampling was done may in part explain the differences in nitrate concentration obtained. In the measurements used by White and Roberts (1977) glass fiber filters were used, so overestimates of nitrate concentration are to be expected. Pitts and Grosjean (1979) made measurements with tandem filters and concluded that there was only a moderate, 11 percent on average, nitrate artifact correction.

All of the studies at urban locations discussed above involved concurrent air quality and instrumental light scattering absorption or extinction measurements. Several other studies have used visibility measurements combined with HIVOL sampling results obtained at sites within the same urban area (Trijonis and Yuan 1978a,b; Leaderer et al. 1979). Aside from the usual limitations in regression models themselves, these studies are subject to a number of other

possible sources of error. These sources of error include some related to airport visibility measurements: (1) inadequate sets of markers, (2) changes in markers, and (3) changing environment in vicinity of airports. The differences in the locations where the visibility and the air quality measurements are taken can also result in differences in aerosol concentration and composition at these locations. The lack of compositional measurements on some significant species can result in overestimations of the contributions of measured species. Such overestimations can occur when there are good correlations between measured and unmeasured species. The use of glass fiber filters in the HIVOL samplers means that positive nitrate artifacts are likely, as discussed earlier in this chapter.

Despite the limitations discussed above, the airport studies do provide results at a number of urban locations at which more acceptable studies are not available. The estimated contributions of the chemical species measured to light extinction budgets has been tabulated and discussed elsewhere (U.S. EPA 1979) and will be only briefly discussed here. On the average, for the midwestern and northeastern locations used (Trijonis and Yuan 1978b, Leaderer et al. 1979) the average percentages and ranges of percentage contributions of chemical species measured to the light extinction were as follows: sulfates 56, 27 to 81; nitrates, 2, 0 to 14; remainder of TSP, 8, 0 to 44; unaccounted for, 34, 19 to 73. At southwestern sites (Trijonis and Yuan 1978a) the nitrates were reported to make a larger contribution to light extinction than at the midwestern and northeastern locations considered.

5.8.3 Light Extinction or Light Scattering Budgets at Nonurban Locations

At Allegheny Mountains, PA, concurrent light scattering and air quality measurements were made during the latter part of July and early August 1977 (Pierson et al. 1980a,b). The authors comment that the multiple regression analyses showed b_{sp} to be remarkably insensitive to any aerosol constituent but sulfate or its associated cations. Sulfate alone accounted for 94 $\pm$ 7 percent of the variability in b_{sp}. An even better correlation was found for b_{sp} with the product of sulfate and humidity than with sulfate alone. With respect to visual range the authors concluded that "sulfate may be a good index of visibility (and vice versa) if humidity is taken into account."

In the Shenandoah Valley/Blue Ridge Mountain area of Virginia several groups of investigators made measurements during July to August of 1980 (Ferman et al. 1981, Stevens et al. 1982, Weiss et al. 1982). Ferman et al. (1981) obtained light scattering and light absorption measurements, nitrogen dioxide concentrations, and aerosol composition measurements. The aerosol composition of the fine particle mass was reported. Based on these results, the observed light extinction on a percentage basis could be accounted for as follows: sulfate (including water), 78; carbon-containing compounds, 15.5 (scattering, 13, absorption, 2.5); nitrogen dioxide, 0.3; Rayleigh (air), 5. For the periods in the upper decile of b_{sp} values the sulfate (and water) accounted for 4 percent of the light extinction. Weiss et al. (1982), from their measurements at the same site, also concluded that all of the water at 70 percent RH was associated with sulfate and ammonium. The sulfate with associated cations and water accounted on average for 70 percent of the light

scattering. This result is in reasonable agreement with the 78 percent obtained by Ferman et al. (1981). Stevens et al. (1982) measured aerosol composition, but not light extinction. However, it is of interest to compare their composition results for the fine particle mass with those obtained by Ferman et al. (1981). The percentage of the fine particle mass contributed by the various chemical species (do not add up to 100 percent) from the Ferman et al. study and the Stevens et al. study, respectively were as follows: sulfate as ammonium bisulfate, 55.4, 60.8; elemental carbon, 5.4, 5.7; organic carbon (measured carbon x 1.2), 23.6, 4.1; nitrate as ammonium nitrate, 0.6, ND; Pb-Br-Cl, 0.2, 0.3; crustal (estimated from Si), 7.3, 1.1. The higher percentage for sulfates and the lower percentage for organic carbon in the Stevens et al. (1982) study would result in an even larger contribution of sulfates to light extinction than found by Ferman et al. (1981).

At another location in the eastern mountains of the United States, Great Smoky Mountains, TN, aerosol composition, but no light extinction measurements, were made (Stevens et al. 1980). The percentage of the fine particle mass contributed by the various chemical species (do not add up to 100 percent) were as follows: sulfate as ammonium bisulfate, 56; elemental carbon, 5; organic carbon (measured carbon x 1.2), 11; Pb-Br-Cl, 0.5; crustal, 0.5. The percentages of sulfates and elemental carbon at the Great Smoky Mountains site were nearly the same as at the Shenandoah Valley site. In contrast, the organic carbon and the crustal elements made up a substantially lower percentage of the fine particle mass at the Great Smoky Mountains site (Stevens et al. 1980) than reported by Ferman et al. (1981) at the Shenandoah Valley site.

In the midwestern United States at rural sites in Missouri and in the Ozark Mountains, Weiss et al. (1977) concluded that essentially all of the aerosol light scattering was due to sulfates. Measurements of sulfate as ammonium sulfate at rural sites in the vicinity of St. Louis indicate that 45 to 50 percent of the fine particle mass was ammonium sulfate in the first and fourth quarters of the year and over 70 percent of the fine particle mass was ammonium sulfate in the third quarter of the year (Altshuller 1982). As in nonurban sites in the eastern United States, the sulfates in the midwest are the major contributors to the fine particle mass.

In the southwestern United States at nonurban locations, concurrent measurements of light extinction and of aerosol composition have been made (Macias et al. 1980). From samples obtained in flights over the Southwest the average percentage contributions of chemical species to light scattering were as follows: sulfate as ammonium sulfate, 16; silicon dioxide, 16: other fine mode particles, 8; coarse mode particles, 4; Rayleigh (air), 44. In measurements at a nonurban site, Zilnez Mesa, AZ, measurements of light extinction and aerosol composition were made (Macias et al. 1981). The average percent contributions to light extinction were as follows: sulfate as ammonium sulfate, 18; organic carbon, 33; elemental carbon, 12; nitrate, 2; other fine particles, 20; coarse particles, 15. In individual measurements Rayleigh scattering contributed from 16 to 54 percent. The light extinction budgets at these western nonurban sites are clearly substantially different than at eastern nonurban sites. Sulfates at these western nonurban

sites make a much smaller contribution to the light extinction than at eastern sites. Carbon-containing particles, other fine mode species, coarse mode species, and Rayleigh scattering are relatively more important at western than eastern nonurban sites. However, the light extinction is smaller and the visual range much greater at the western nonurban sites because the absolute amounts of aerosol species are so much smaller.

The contributions of sulfates compared to other chemical species to light extinction at rural sites in the midwestern and eastern United States appear more important than in western urban areas (White and Roberts 1977, Pitts and Grosjean 1979, Groblicki et al. 1981) and western nonurban locations (Macias et al. 1980, 1981). At eastern rural sites visibility should be a good index or surrogate for sulfates (Pierson et al. 1980a, Ferman et al. 1981, Weiss et al. 1982). It is less evident that visibility in the western United States can be used as a surrogate for sulfates or for sulfates and nitrates.

5.8.4 Trends in Visibility as Related to Sulfate Concentrations

Several investigations have indicated that the patterns of historical visibility at airport sites and sulfate trends in the eastern United States are consistent with each other (Trijonis and Yuan 1978b; Husar et al. 1979; Altshuller 1980; Sloane 1982a,b). The improvements in visibility in the first and fourth quarters of the year appear consistent with the decreases in sulfate concentrations. Similarly, the deterioration of visibility during the 1960's into the 1970's was consistent with the increase in sulfate concentrations. Further deterioriation in visibility during the 3rd quarter of the year did not occur later in the 1970's, again consistent with the trends in sulfate concentrations (Altshuller 1980, Sloane 1982b).

5.9 CONCLUSIONS

The following statements summarize the discussion in this chapter on the atmospheric concentrations and distributions of chemical substances. Table 5-13 summarizes measurements of sulfur, nitrogen, and chlorine compounds in rural areas.

- Sulfur dioxide concentrations have been high in urban areas in the eastern United States, but decreased substantially during the 1960's and into the 1970's. The decreases in sulfur dioxide appear to be associated with local reductions in the sulfur content of fossil fuels (Section 5.2.2.1).

- In rural areas sulfur dioxide concentrations are appreciably lower than in urban areas. The differences in concentrations between urban and rural areas were not as great by the late 1970's as in earlier years. This change primarily is the result of the decreases in urban sulfur dioxide concentrations (Section 5.2.2.2).

- Measurements of sulfur dioxide concentrations at nonurban sites are limited and values are often near limits of detectability. No clear trends in nonurban sulfur dioxide concentrations with time are evident (Section 5.2.2.2).

TABLE 5-13. CONCENTRATIONS OF SULFUR, NITROGEN, AND CHLORINE COMPOUNDS AT RURAL SITES IN THE UNITED STATES IN THE 1970's

Compound	Range of Average concentrations, $\mu g\ m^{-3}$	
	East	West
Sulfur dioxide	10-20[a]	NA
Sulfur aerosols (as sulfate)	5-15[a]	1-3[a]
Nitrogen dioxide	10-20[b]	$\leq$ 2[c]
Nitrate aerosols	1[c]	NA
Nitric acid	0.3-1.3	$\leq$ 1[c]
Peroxyacyl nitrates	0.5-1[c]	0.1-0.3[c]
Ammonia	0.5-2[d]	0.5-2[c]
Hydrogen chloride		1-10[c]
Chloride aerosols		
Maritime	1-10[c]	1-10[c]
Inland	$\leq$ 1[c]	$\leq$ 1[c]

[a]Annual average.

[b]Summer months: August to December averages.

[c]Limited number of measurements.

NA=Not available.

- Sulfate concentrations decreased in eastern cities during the 1960's and into the 1970's except during the third quarter of the year (Section 5.2.3.1).

- In rural areas in the eastern United States sulfate concentrations have not increased substantially on an annual average basis, but increased significantly during the summer months (Section 5.2.3.3).

- Sulfate concentrations within rural areas in the eastern United States by the 1970's were almost as high as in adjacent urban areas (Section 5.2.3.3).

- Sulfate aerosols can contribute one-third to one-half the sulfur budget (sulfur dioxide plus sulfate) in rural areas within the eastern United States during the summer, but contribute relatively little to the sulfur budget in the winter months (Section 5.2.3.3).

- Sulfate aerosols are substantially higher in rural areas in the eastern United States than in remote areas of the western United States (Section 5.2.3.3).

- Sulfate aerosols occur predominately in the fine particle size range with much of the mass of sulfate aerosols concentrated between 0.1 and 1 μm. Particles in this size range deposit more slowly than does sulfur dioxide, so they can be transported substantial distances (Section 5.2.4).

- Sulfate aerosols tend to be more acidic in rural areas than in urban areas (Sections 5.2.3.2 and 5.2.3.4).

- Much of the sulfate aerosol has been reported to be in the form of strong acid species at locations in the eastern mountains of the United States during the summer months (Section 5.2.3.4).

- Sulfur dioxide and sulfate concentrations in remote areas are between a factor of 10 and 100 lower than the concentrations in rural areas in the eastern United States and adjacent areas of eastern Canada (Sections 5.2.2.2, 5.2.2.3 and 5.2.3).

- Nitrogen oxides reach about the same concentration range as sulfur dioxide in cities. Their concentrations have become more significant relative to sulfur dioxide with the decrease in sulfur dioxide emissions (Section 5.3.2.3).

- Nitrogen oxides are substantially lower in concentration in rural areas than in urban areas (Sections 5.3.2.3 and 5.3.2.4).

- Nitrogen dioxide concentrations are substantially lower in rural areas within the western United States than in the eastern United States (Section 5.3.2.4).

- At remote locations the concentrations of nitrogen oxides can be 10 to 100 times lower than in rural areas of the eastern United States (Section 5.3.2.5).

- The average concentrations of nitric acid or of peroxyacetyl nitrates are about a factor of ten lower than the average concentrations of nitrogen dioxide in both urban and rural areas (Sections 5.3.3.1 and 5.3.3.2).

- The average concentrations of nitric acid are in the same concentration range as the average concentrations of peroxyacetyl nitrates in rural areas (Section 5.3.3.2).

- The concentrations of nitric acid in the boundary layer in remote areas are a factor of 5 to 10 lower than in rural areas in the eastern United States (Section 5.3.3.3).

- The equilibrium between ammonia, nitric acid, and ammonium nitrate can be important in determining the ambient air concentrations of these chemical substances (Section 5.3.5).

- Several positive and negative nitrate artifacts on filters have been identified and investigated. Such artifacts make most of the measurements on single or tandem filter systems for particulate nitrate unreliable (Section 5.3.6).

- Measurements of particulate nitrate made using diffusion denuders appear to be reliable. At both urban sites in Los Angeles and rural sites in the eastern United States such measurements indicate that particulate nitrate concentrations can exceed nitric acid concentrations in the late evening and in the early morning hours. Conversely, nitric acid concentrations are higher than particulate nitrate concentrations in the late morning and afternoon hours (Sections 5.3.6.1 and 5.3.6.2).

- Particle size distributions of particulate nitrates are influenced by the same nitrate artifact problems. It does appear that the particle sizes of nitrates decrease in going from coastal locations inland in California. The reason is related to the greater abundance of submicron sodium nitrate aerosols in maritime air reacted with nitrogen dioxide, compared to the submicron ammonium nitrate aerosols found inland (Section 5.3.7).

- The concentrations of sulfate aerosols appear to be several times greater than the concentrations of nitric acid and particulate nitrate at rural sites in the eastern United States (Sections 5.2.3.3, 5.3.3.2 and 5.3.7).

- Ozone concentration levels in rural areas can result from one or more of the following processes: (1) local synthesis, (2) fumigation by urban or industrial plumes, (3) high pressure systems near rural sites, and (4) ozone formed in the stratosphere or free troposphere reaching ground level (Section 5.4).

- Rural locations within urban plumes may experience ozone concentrations in the range of 300 to 500 $\mu g\ m^{-3}$. Within high pressure systems, ozone concentrations at rural locations can range from 150 to 250 $\mu g\ m^{-3}$ (Section 5.4.1).

- At remote elevated sites, hourly ozone concentrations are as high as 140 to 160 $\mu g\ m^{-3}$ during the spring months and as low as 40 to 60 $\mu g\ m^{-3}$ in the fall months. Occasional observations of ozone concentrations in excess of 200 $\mu g\ m^{-3}$ attributed to stratospheric air extrusions at remote sites appear too high compared to aircraft measurements of ozone through the troposphere (Section 5.4.2).

- Ambient air measurements of hydrogen peroxide are in doubt because of recent demonstrations of in situ generation of hydrogen peroxide in aqueous solutions (Section 5.5).

- Hydrogen peroxide concentrations measured in rainwater usually correspond to those resulting from the absorption of less than 1 $\mu g\ m^{-3}$ of hydrogen peroxide from the ambient atmosphere (Section 5.5.3).

- The variations in hydrogen peroxide concentrations measured in rainwater during precipitation events are consistent with a substantial part of the hydrogen peroxide being generated within the cloudwater rather than being present as a result of rainout and washout of gaseous hydrogen peroxide (Section 5.5.3).

- The concentrations of particulate chloride compounds can be important near the ocean, but not inland. At inland sites particulate chlorides tend to be submicron in size and have been associated with automotive lead aerosol emissions and with emissions from combustion sources (Section 5.6.4).

- The concentrations of metallic elements in most urban areas occur at 1 to 2 $\mu g\ m^{-3}$ and below. The bulk of the calcium, aluminum, and iron occurs in coarse particles, while most of the lead and zinc occurs in fine particles. The substantial differences in size distribution should result in those elements found in coarse particles usually being of local origin, while the elements in fine particles are capable of being transported substantial distances (Section 5.7.1).

- Although lead aerosols are largely submicron in size, lead concentrations drop off rapidly from urban to rural to remote sites. At continental rural sites lead concentrations are a factor of 10 to 20 below concentrations at urban locations. At remote sites the lead concentrations are several hundred times lower than at urban sites (Section 5.7.2).

- High correlations exist between fine particle mass and light scattering coefficients (Section 5.8.1).

- At eastern rural sites sulfate accounts for a large part of the fine particle mass and the light extinction (Section 5.8.3).

- At western locations nitrate and carbon-containing particles make a substantial contribution to fine particle mass and to light extinction (Section 5.8.2).
- At rural sites in the eastern United States visibility measurements should be a good index or surrogate for particulate sulfate concentrations (Section 5.8.3).

5.10 REFERENCES

Altshuller, A. P. 1973. Atmospheric sulfur dioxide and sulfate distribution of concentration at urban and non-urban sites in the United States. Environ. Sci. Technol. 7:709-712.

Altshuller, A. P. 1976. Regional transport and transformation of sulfur dioxide and sulfates in the U.S. J. Air Pollut. Control Assoc. 26:318-324.

Altshuller, A. P. 1980. Seasonal and episodic trends in sulfate concentrations (1963-1978) in the eastern United States. Environ. Sci. Technol. 14:1337-1349.

Altshuller, A. P. 1982. Relationships involving particle mass and sulfur content at sites in and around St. Louis, MO. Atmos. Environ. 16:837-843.

Altshuller, A. P. 1983. Review: Natural volatile organic substances and their effect on air quality in the United States. Atmos. Environ. 17(11): 2131-2165.

Appel, B. R., E. M. Hoffer, U. Tokiwa, and E. L. Kothny. 1982. Measurement of sulfuric acid and particulate strong acidity in the Los Angeles Basin. Atmos. Environ. 16:589-593.

Appel, B. R., E. L. Kothney, E. M. Hoffer, and J. J. Wesolowski. 1977. Comparison of wet and instrumental methods for measuring airborne sulfate. EPA Report 600/7-77-128. Environmental Sciences Research Laboratory, Research Triangle Park, NC.

Appel, B. R., E. L. Kothney, E. M. Hoffer, G. M. Hidy, and J. J. Wesolowski. 1978. Sulfate and nitrate data from the California aerosol characterization experiment (ACHEX). Environ. Sci. Technol. 12:418-425.

Appel, B. R., S. M. Wall, Y. Tokiwa, and M. Haik. 1979. Interference effects in sampling particulate nitrate in ambient air. Atmos. Environ. 13:319-325.

Appel, B. R., S. M. Wall, Y. Tokiwa, and M. Haik. 1980. Simultaneous nitric acid, particulate nitrate and acidity measurements in ambient air. Atmos. Environ. 14:549-554.

Appel, B. R., S. M. Wall, Y. Tokiwa, and M. Haik. 1981a. Sampling of nitrates in ambient air. Atmos. Environ. 15:283-289.

Appel, B. R., S. M. Wall, Y. Tokiwa, and M. Haik. 1981b. Atmospheric particulate nitrate sampling errors due to reactions with particulate and gaseous strong acids. Atmos. Environ. 15:1087-1089.

Barrie, L. A., H. A. Wiebe, K. Aulsuf, and P. Felliu. 1980. The Canadian Air and Precipitation Monitoring Network APN. Atmos. Pollut. 8:355-360.

Barrie, L. A., K. G. Aulsuf, H. A. Wiebe, and P. Felliu. 1983. Acidic pollutants in air and precipitation at selected rural locations in Canada. In Proceedings of the American Chemist Society Symposium on Acid Rain. J. Teasley, ed. Ann Arbor Science, Ann Arbor, MI.

Bollinger, M. J., D. D. Parrish, C. Hahn, D. L. Albritton, and F. C. Fehsenfeld. 1982. NO_x measurements in clean continental air. 2nd Symposium Composition of the Nonurban Troposphere. Williamsburg, VA American Meterological Society, 45 Beacon St. Boston, MA.

Bonsang, B., B. C. Nzuyen, A. Gaudry and G. Lambert. 1980. Sulfate enrichment in marine aerosols owing to biogenic gaseous sulfur compounds. J. Geophys. Res. 85:7410-7416.

Breeding, R. J., J. P. Lodge, Jr., J. B. Pate, D. C. Sheesley, H. B. Klonis, B. Fogle, J. A. Anderson, T. R. Englert, P. L. Haagenson, R. B. McBeth, A. L. Morris, R. Pogue, and A. F. Wartburg. 1973. Background trace gas concentrations in the central United States. J. Geophys. Res. 78:7057-7064.

Breeding, R. J., J. B. Klonis, J. P. Lodge, J. B. Pate, D. C. Sheesley, T. R. Englert and D. R. Sears. 1976. Measurements of atmospheric pollutants in the St. Louis area. Atmos. Environ. 10:181-194.

Brennen, E. 1980. PAN concentrations in ambient air in New Brunswick, N. J. Final Report on EPA Grant 805827 to Environmental Sciences Research Laboratory, Research Triange Park, NC.

Brosset, C. 1978. Water-soluble sulfur compounds in aerosols. Atmos. Environ. 12:25-38.

Bufalini, J. J., B. W. Gay and K. L. Brubaker. 1972. Hydrogen peroxide formation from formaldehyde photooxidation and its presence in urban atmospheres. Environ. Sci. Technol. 6:816-821.

Cadle, S. H., R. J. Countess and N. A. Kelly. 1982. Nitric acid and ammonia in urban and rural locations. Atmos. Environ. 16:2501-2506.

Cass, G. R. 1976. The relationship between sulfate air quality and visibility at Los Angeles, CA. Inst. Technol. Environ. Quality Lab. Memo No. 18, Pasadena, CA.

Charlson, R. J., D. S. Covert, T. V. Larson, and A. P. Waggoner. 1978a. Chemical properties of tropospheric sulfur aerosols. Atmos. Environ. 12:39-53.

Charlson, R. J., A. P. Waggoner, and J. F. Thielke. 1978b. Visibility protection for Class I areas: the technical basis. Council on Environmental Quality, Washington, DC.

Charlson, R. J., A. H. Vanderpol, D. S. Covert, A. P. Waggoner, and N. C. Ahlquist. 1974. $H_2SO_4/(NH_4)_2SO_4$ background aerosol: optical detection in St. Louis region. Atmos. Environ. 8:1257-1267.

Cleveland, W. S. and B. Kleiner. 1975. The transport of photochemical air pollution from the Camden - Philadelphia urban complex. Environ. Sci. Technol. 9:869-872.

Cleveland, W. S., B. Kleiner, J. E. McRae and J. L. Warner. 1976. Photochemical air pollution: Transport from the New York City area into Connecticut and Massachusetts. Science 191:179-181.

Cleveland, W. S., B. Kleiner, J. E. McRae and R. E. Pasceri. 1977. The analysis of ground-level ozone data from New Jersey, New York, Connecticut and Massachusstts: Data quality assessment and temporal and geographical properties, pp. 185-196. In Vol 1, International Conference of Photochemical Oxidant Pollution and Its Control. B. Dimitriades, ed. EPA-600/3-77-0012. Environmental Sciences Research Laboratory, Research Triangle Park, NC.

Coburn, W. G., R. B. Husar, and J. D. Husar. 1978. Continuous in-situ monitoring of ambient particulate sulfur using flame photometry and thermal analysis. Atmos. Environ. 12:89-98.

Cohen, I. R. and T. C. Purcell. 1967. Spectrophotometric determination of hydrogen peroxide with 8-quinolinol. Anal. Chem. 39:131-132.

Corn, M. and L. Demaio. 1965. Particulate sulfates in Pittsburgh air. J. Air Pollut. Control Assoc. 15:26-30.

Coutant, R. W. 1977. Effect of environmental variables on collection of atmospheric sulfate. Environ. Sci. Technol. 11:873-878.

Cox, R. A. 1977. Some measurements of ground levels of NO, NO_2, and O_3. Concentration at an unpolluted maritime site. Tellus 29:356-362.

Crecelius, E. A., E. A. Lepel, J. C. Laul, L. A. Rancitelli, and R. L. McKeever. 1980. Background air particulate chemistry near Colstrip, Montana. Environ. Sci. Technol. 14:422-428.

Cronn, D. R., R. J. Charlson, R. L. Knights, A. L. Crittenden, and B. R. Appel. 1977. A survey of the molecular nature of primary and secondary components of particles in urban air by high-resolution mass spectrometry. Atmos. Environ. 11:929-937.

Dams, R. and J. De Jonge. 1976. Chemical Composition of Swiss aerosols from the Jungfraujoch. Atmos. Environ. 10:1079-1084.

Dams, R., J. A. Robbins, K. A. Rahn and J. W. Winchester. 1970. Nondestructive neutron activation analysis of air pollution particulates. Anal. Chem. 42:861-867.

Darley, E. F., K. A. Kettner, and E. R. Stephens. 1963. Analysis of peroxybeyl nitrates by gas chromatography with electron capture detection. Anal. Chem. 35:589-591.

Davis, D. D., G. Smith and G. Klauber. 1974. Trace gas analysis of power plant plumes via aircraft measurement: O_3, NO_x, and SO_2 chemistry. Science 186:733-736.

Decker, C. E., L. A. Ripperton, J. J. B. Worth, F. M. Vukovich, W. D. Bach, J. B. Tommerdahl, F. Smith and D. E. Wagoner. 1976. Formation and transport of oxidants along Gulf Coast and in northern U. S. EPA-45013-76-033 Office of Air Quality Planning and Standards, Research Park, NC.

Department of Health, Education, and Welfare. 1966. Air Quality Data from the National Air Quality Sampling Networks and Contributing State and Local Networks, 1964-1965. Robert A. Taft Sanitary Eng. Center, Cincinnati, OH.

Drummond, J. W. 1976. Atmospheric measurements of nitric oxide using a chemiluminescent detector. Ph.D. Dissertation, University of Wyoming, Laramie.

Drummond, J. W. and A. Volz. 1982. Simultaneous measurements of NO and NO_2 in the troposphere. 2nd Symposium Composition of the nonurban Troposphere. Williamsburg, VA American Meterological Society, 45 Beacon St. Boston, MA.

Duce, R. A., J. W. Winchester, and T. W. Van Nahl. 1965. Iodine, bromine and chlorine in the Hawaiian marine atmosphere. J. Geophys. Res. 70:1775-1799.

Dzubay, T. G. 1980. Chemical element balance method applied to dichotomous sampler data. Annal. New York Acad. Sci. 338:126-144.

Dzubay, T. G., R. K. Stevens, C. W. Lewis, D. H. Hern, W. J. Courtney, J. W. Tesch, and M. A. Mason. 1982. Visibility and aerosol composition in Houston, TX. Environ. Sci. Technol. 16:514-525.

Evans, G., P. Finkelstein, B. Martin, N. Possiel and M. Graves. 1982. The National Air Monitoring Background Network 1976-1980. Environmental Monitoring Systems Laboratory, U.S. Environmental Protection Agency, Research Triangle Park, NC.

Farmer, C. B., O. F. Raper, and R. H. Norton. 1976. Spectroscopic detection and vertical distribution of HCl in the troposphere and stratosphere. Geophys. Res. Let. 3:13-16.

Farmer, J. C. and G. A. Dawson. 1982. Condensation sampling of soluble atmospheric trace gases. J. Geophys. Res. 87:8931-8942.

Ferek R. J., A. L. Lazrus, P. L. Haagenson, and J. W. Winchester. 1983. Strong and weak acidity of aerosols collected over the northeastern United States. Environ. Sci. Technol. 17:315-324.

Ferman, M. A., G. T. Wolff and N. A. Kelly. 1981. The nature and source of haze in the Shenandoah Valley/Blue Ridge Mountains area. J. Air Pollution Control Assoc. 31:1074-1082.

Flocchini, R. G., T. A. Cahill, D. J. Shadoan, S. J. Lange, R. A. Eldred, P. J. Feeney, G. W. Wolfe, D. C. Simmeroth, and J. K. Suder. 1976. Monitoring California's aerosols by size and elemental composition. Environ. Sci. Technol. 10:76-82.

Flocchini, R. G., T. A. Cahill, M. L. Pitchford, R. A. Eldred, P. J. Feeney and L. L. Ashbaugh. 1981. Characterization of particles in the arid west. Atmos. Environ. 15:2017-2030.

Foote, R. S. 1972. Mercury vapor inside buildings. Science 177:513-514.

Forrest, J., R. L. Tanner, D. Spandau, T. D'Ottavio, and L. Newman. 1980. Determination of total inorganic nitrate utilizing collection of nitric acid on NaCl-impregnated filters. Atmos. Environ. 14:137-144.

Forrest, J., D. J. Spandau, R. L. Tanner, and L. Newman. 1982. Determination of atmospheric nitrate and nitric acid employing a diffusion denuder with a filter pack. Atmos. Environ. 16:1473-1485.

Frank, N. H. and N. C. Possiel, Jr. 1976. Seasonality and regional trends in atmospheric sulfates. 1976. Presented before Div. of Environmental Chemistry American Chemical Society San Francisco, CA.

Gartrell, G., Jr. and S. K. Friedlander. 1975. Relating particulate pollution to sources: The 1972 California aerosol characterization study. Atmos. Environ. 9:279-299.

Gay, B. W., Jr., P. L. Hanst, J. J. Bufalini, and R. C. Noonan. 1976. Atmosperic oxidation of chlorinated ethylenes. Environ. Sci. Technol. 10:58-67.

Georgii, H. W. 1978. Large scale spatial and temporal distribution of sulfur compounds. Atmos. Environ. 12:681-690.

Georgii, H. W. and F. X. Meixner. 1980. Measurement of the tropospheric and stratospheric SO_2 distribution. J. Geophys. Res. 85:7433-7438.

Georgii, H. W. and W. A. Muller. 1974. On the distribution of ammonia in the middle and lower troposphere. Tellus 26:180-184.

Gillani, N. V., R. B. Husar, J. D. Husar, and D. E. Patterson. 1978. Project MISTT: Kinetics of particulate sulfur formation in a power plant plume out to 300 km. Atmos. Environ. 12:589-598.

Gillette, D. A and J. W. Winchester. 1972. A study of aging of lead aerosols. Atmos. Environ. 6:443-450.

Gladney, E. S., W. H. Zoller, A. G. Jones, and G. E. Gordon. 1974. Composition and size distributions of atmospheric matter in Boston area. Environ. Sci. Technol. 8:551-557.

Gravenhorst, G. 1978. Maritime sulfur over the North Atlantic. Atmos. Environ. 12:707-713.

Groblicki, P. J., G. T. Wolff, and R. J. Countess. 1981. Visibility-reducing species in Denver "brown cloud" - I. Relationships between extinction and chemical composition. Atm. Environ. 15:2473-2484.

Grosjean, D. 1981. Critical evaluation and comparison of measurement methods for nitrogeneous compounds in the atmosphere. ERT Document no. P-A706-04. Prepared for CAPA-19 Project Group, Coordinating Research Council 219 Perimeter Center Parkway, Atlanta, GA. 30346.

Grosjean, D. 1983. Distribution of atmospheric nitrogenous pollutants at a Los Angeles area smog receptor site. Environ. Sci. Technol. 17:13-19.

Grosjean, D. and S. K. Friedlander. 1975. Gas-particle distribution factors for organic and other pollutants in the Los Angeles atmosphere. J. Air Pollut. Control Assoc. 25:1038-1044.

Hanst, P. 1981. Report of Research under Innovative Research program. U.S. Environmental Protection Agency, Environmental Sciences Research Laboratory, Research Triangle Park, NC.

Hanst, P. L., W. E. Wilson, R. K. Patterson, B. W. Gay, Jr., and L. W. Chaney. 1975. A spectroscopic study of California smog. EPA-65014-75-006. Research Triangle Park, NC.

Hanst, P. L., N. W. Wong and J. Bragin. 1982. A long-path infra-red study of Los Angeles smog. Atmos. Environ. 16:969-981.

Hardy, K. A., R. Akselsson, J. W. Nelson, and J. W. Winchester. 1976. Elemental constituents of Miami aerosol as function of particle size. Environ. Sci. Technol. 10:176-182.

Harker, A. B., L. W. Richards, and W. E. Clark. 1977. The effects of atmospheric SO_2 photooxidation upon observed nitrate concentrations in aerosols. Atmos. Environ. 11:87-91.

Harward, C. N., W. A. McClenny, J. M. Hoell, J. A. Williams, and B. S. Williams. 1982. Ambient ammonia measurements in coastal southeastern Virginia. Atmos. Environ. 16:2497-2500.

Hegg, D., P. V. Hobbs, L. F. Radke, and H. Harrison. 1977. Ozone and nitrogen oxides in power plant plumes, pp. 173-183. In Vol. 1, International Conference on Photochemical Oxidant Pollution and its Control. B. Dimitriades, ed. EPA-600/13-77-0012. Environmental Sciences Research Laboratory, Research Triangle Park, NC.

Heikes, B. G., A. L. Lazrus, G. L. Kok, S. M. Kunen, B. W. Gandrud, S. N. Gitlin and P. D. Sperry. 1982. Evidence of aqueous phase hudrogen peroxide synthesis in the troposphere. J. Geophys. Res. 87:3045-3051.

Helas, G. and P. Warneck. 1981. Background NO_x mixing ratios in air masses over the North Atlantic Ocean. J. Geophys. Res. 86:7283-7290.

Hester, N. E., R. B. Evans, F. G. Johnson and E. L. Martinez. 1977. Airborne measurements of primary and secondary pollutant concentrations in the St. Louis urban plume, pp.257-274. In Vol. 1, International Conference on Photochemical Oxidant Pollution and its Control. B. Dimitriades, ed. EPA-600/3-77-0012 Environmental Sciences Research Laboratory, Research Triangle Park, NC.

Hidy, G. M., P. K. Mueller, and E. Y. Tong. 1978. Spatial and temporal distributions of airborne sulfate in parts of the United States. Atmos. Environ. 12:735-752.

Hilst, G. R., P. K. Mueller, G. M. Hidy, T. F. Lavery, and J. G. Watson. 1981. EPRI Sulfate Regional Experiment: Results and Implications. Electric Power Research Institute, Palo Alto, California. Report No. EA-2165-SY-LD.

Hoell, J. M., J. S. Levine, T. R. Augustsson and C. N. Harward. 1983. Atmospheric ammonia: measurements and modeling. AIAAJ. In press.

Hoggan, M., A. Davidson, D. C. Shikiya and W. Lau. 1982. Air Quality Trends in California's South Coast Air. Basic South Coast Air Quality Management District, 9150 East Flair Drive, El Monte, CA.

Houston Area Oxidant Study (HAOS). 1979. Program Summary. Houston Chamber of Commerce, 1100 Milain St. Houston, TX.

Huebert, B. J. 1980. Nitric acid and aerosol nitrate measurements in the equatorial Pacific region. Geophys. Res. Lett. 7:325-328.

Huebert, B. J. and A. L. Lazrus. 1978. Global tropospheric measurements of nitric acid vapor and particulate nitrate. Geophys. Res. Lett. 5:577-580.

Huebert, B. J. and A. L. Lazrus. 1980a. Bulk composition of aerosols in the remote troposphere. J. Geophys. Res. 85:7337-7344.

Huebert, B. J. and A. L. Lazrus. 1980b. Tropospheric gas-phase and particulate nitrate measurements. J. Geophys. Res. 85:7322-7328.

Husar, R. B. and D. E. Patterson. 1980. Regional Scale Air Pollution: Sources and Effects. New York Academy of Sciences.

Husar, R. B., D. E. Patterson, J. M. Holloway, W. E. Wilson, and T. G. Ellestad. 1979. Trends of eastern U.S. haziness since 1948, pp. 249-256. In Proceedings of the Fourth Symposium on Atmospheric Turbulence, Diffusion and Air Pollution, American Meteorological Society, Reno, NV.

Husar, R. B., D. E. Patterson, C. C. Paley and N. V. Gillani. 1977. Ozone in hazy air masses. pp. 275-282. In Proceedings of the International Conference on Photochemical Oxidant Pollution and Its Control. Vol I. B. Dimitriades, ed. EPA-600/3-77-0012. Environmental Sciences Researh Laboratory. U. S. Environmental Protection Agency. Research Triangle Park, NC.

Jacobs, M. B. 1959a. Concentration of sulfur-containing pollutants in a major urban area, pp. 81-87. In Monograph No. 3. American Geophysical Union, Proceedings of a Symposium on Atmospheric Chemistry of Chlorine and Sulfur Compounds. J. P. Lodge, ed. Waverly Press, Inc., Baltimore, MD.

Jacobs, M. D. 1959b. Techniques for measurement of hydrogen sulfide and sulfur oxides, pp. 24-36. In Monograph No. 3. American Geophysical Union, Proceedings of a Symposium on Atmospheric Chemistry of Chlorine and Sulfur Compounds. J. P. Lodge, ed. Waverly Press, Inc., Baltimore, MD.

Junge, C. E. 1954. The chemical composition of atmospheric aerosols. I. Measurements at the Round Hill Field Station, June-July, 1973. J. Meteorol. 11:323-333.

Junge, C. E. 1956. Recent investigations in air chemistry. Tellus 8:127-139.

Junge, C. E. 1963. Air Chemistry and Radioactivity. Academic Press, New York.

Kadowaki, S. 1977. Size distribution and chemical composition of atmospheric particulate nitrate in the Nagoya area. Atmos. Environ. 11:671-675.

Kelly, T. J. and D. H. Stedman, 1979a. Measurements of H_2O_2 in rural air. Geophys. Res. Lett. 6:375-378.

Kelly, T. J. and D. H. Stedman. 1979b. Chemiluminescence measurements of HNO_3 in air. In current methods to measure atmospheric nitric acid and nitrate artifacts. (R. K. Stevens, ed.) EPH-600-12-79-051. Environmental Sciences Research Laboratory, US EPA Research Triangle Pk, NC 27711.

Kelly, T. G., D. H. Stedman, J. A. Ritter, and R. B. Harvey. 1980. Measurements of oxides of nitrogen and nitric acid in clean air. J. Geophys. Res. 85:7417-7425.

Kelly, N. A., G. T. Wolff, and M. A. Ferman. 1982. Background pollution measurements in air masses affecting the eastern half on the United States. I. Air masses arriving from the northwest. Atmos. Environ. 16:1077-1088.

Kley, D., J. W. Drummond, M. McFarland, and S. C. Liu. 1981. Tropospheric profiles of NO_x. J. Geophys. Res. 86:3153-3161.

Kok, G. L. 1980. Measurements of hydrogen peroxide in rainwater. Atmos. Environ. 14:653-656.

Kok, G. L. 1982. Measurements of formaldehyde in the California South Coast Air Basin. Report on EPA Grant no. CR-806629 to Environmental Sciences Research Laboratory. Research Triangle Park, NC 27711.

Kok, G. L., K. R. Darnall, A. M. Winer, J. N. Pitts, Jr., and B. W. Gay, Jr. 1978a. Ambient air measurements of hydrogen peroxide in the California South Coast Air Basin. Environ. Sci. Technol. 12:1077-1080.

Kok, G. L., T. Holler, M. Lopez, H. Nachtrieb, and M. Yuan. 1978b. Chemileminescent method for determination of hydrogen peroxide in the ambient atmosphere. Environ. Sci. Technol. 12:1072-1076.

Kumar, R., S. A. Johnson, and P. T. Cunningham. 1982. Seasonal and diurnal variations in the chemistry of ambient fine-particle aerosols in the northeastern United States. In 2nd Symposium Composition of Nonurban Troposphere. Amer. Meteorol. Soc., 45 Beacon St., Boston, MA, 02108.

Laird, A. R. and R. W. Miksad. 1978. Observations on the particulate chlorine distribution in the Houston-Galveston area. Atmos. Environ. 12:1537-1542.

Leaderer, B. R., T. R. Holford, and J. A. J. Stolwijk. 1979. Relationship between sulfate aerosol and visibility. J. Air Pollution Control Assoc. 29:154-157.

Lee, R. E., Jr. and P. K. Patterson. 1969. Size determination of atmospheric phosphate, nitrate, chloride, and ammonium particulate in several urban areas. Atmos. Environ. 3:249-255.

Lee, R. E., Jr., R. K. Patterson, and J. Wagman. 1968. Particle-size distribution of metal components in urban air. Environ. Sci. Technol. 2:288-290.

Lee, R. E., Jr. and J. Wagman. 1966. A sampling anomaly in the determination of atmospheric sulfate concentration. J. Am. Ind. Hyg. 27:266-271.

Lewis, C. W. and E. S. Macias. 1980. Composition of size-fractionated aerosol in Charleston, West Virginia. Atmos. Environ. 14:185-194.

Lioy, P. J., P. J. Samson, R. L. Tanner, B. P. Leaderer, T. Minnich, and W. Lyons. 1980. The distribution and transport of sulfate "species" in the New York Metropolitan area during the 1977 summer aerosol study. Atmos. Environ. 14:1391-1407.

Lodge, J. P. and J. B. Pate. 1966. Atmospheric gases and particulates in Panama. Science 153:408-410.

Lodge, J. P., P. A. Machado, J. B. Pate, D. C. Sheesley, and A. F. Wartburg. 1974. Atmospheric trace chemistry in the American humid tropics. Tellus 26:250-253.

Long, S. J., D. R. Scott, and R. J. Thompson. 1973. Atomic absorption determination of elemental mercury collected from ambient air on silver wool. Anal. Chem. 45:2227-2233.

Lonneman, W. A., J. J. Bufalini, and R. L. Scila. 1976. PAN and oxidant measurement in ambient atmosphere. Env. Sci. Technol. 10:374-380.

Ludwick, J. D., T. D. Fox, and S. R. Garcia. 1977. Elemental concentrations of northern hemispheric air at Quillayute, Washington. Atmos. Environ. 11:1083-1087.

Ludwig, F. L. and E. Robinson. 1968. Variations in the size distributions of sulfur-containing compounds in urban aerosols. Atmos. Environ. 2:13-23.

Lundgren, D. A. 1967. An aerosol sampler for determination of particle concentration as a function of size and time. J. Air Pollut. Control Assoc. 17:225-229.

Lundgren, D. A. 1970. Atmospheric aerosol composition and concentration as a function of particle size and time. J. Air. Pollution Control Assoc. 20:603-608.

Macias, E. S., D. L. Blumenthal, J. A. Anderson, and B. K. Cantrell. 1980. Size and composition of visibility-reducing aerosols in southwestern plumes. Ann. New York Acad. Sci. 338:233-257.

Macias, E. S., J. O. Zwicker, J. R. Ouimette, S. V. Hering, S. K. Friedlander, T. A. Cahill, G. A. Kuhlmey, and L. W. Richards. 1981. Regional haze case studies in the southwestern U.S. I. Aerosol chemical composition. Atm. Environ. 15:1971-1986.

Maroulis, P. J., A. L. Torres, A. B. Goldberg, and A. R. Bandy. 1980. Atmospheric SO_2 measurements on Project Gametag. J. Geophys. Res. 85:7345-7349.

Martens, C. S., J. J. Wesolowski, R Kaifer, and W. John. 1973. Lead and bromine size distributions in the San Francisco Bay area. Atmos. Environ. 7:905-914.

Martinez, J. R. and H. B. Singh. 1979. Survey of the Role of NO_x in Nonurban Ozone Formation. SRI Project 6780-8. U.S. Environmental Protection Agency, Research Triangle Park, NC.

Martinez, J. R., F. L. Ludwig, and C. Maxwell. 1982. 1978 Houston oxidant modeling study. Vol. 1: Data evaluation and analysis. SRI Project 7938. Environmental Sciences Laboratory. U. S. Environmental Protection Agency, Research Triangle Park, NC.

Mayrsohn, H. and C. Brooks. 1965. The analysis of PAN by electron capture gas chromatography. Presented at the Western Regional Meeting of the American Chemical Society, Nov. 18.

McClenny, W. A. and C. A. Bennett, Jr. 1980. Integrative technique for detection of atmospheric ammonia. Atmos. Environ. 14:641-645.

McClenny, W. A., P. C. Gailey, R. S. Braman, and T. J. Shelley. 1982. Tungstic acid technique for monitoring nitric acid and ammonia in ambient air. Anal. Chem. 54:365-369.

Meinert, D. L. and J. W. Winchester. 1977. Chemical relationships in the North Atlantic marine aerosol. J. Geophys. Res. 82:1778-1782.

Meserole, F. B., K. Schwitzgebel, B. F. Jones, C. M. Thompson, and F. G. Mesich. 1976. Sulfur dioxide interferences in the measurement of ambient particulate sulfates. Radian Corp. Report (Project 262) to Electric Power Research Inst., Palo Alto, CA.

Meszaros, E. 1978. Concentration of sulfur compounds in remote continental and oceanic areas. Atmos. Environ. 12:699-705.

Moskowitz, A. H. 1977. Particle size distribution of nitrate aerosols in the Los Angeles Air Basin. EPA-600/3-77-053. U.S. Environmental Protection Agency, Research Triangle Park, NC.

Mueller, P. K., G. M. Hidy, K. Warren, T. F. Lavery, and R. L. Baskett. 1980. The occurence of atmospheric aerosols in the north eastern United States. Ann. New York Acad. Sci. 338:463-482.

National Academy of Sciences. 1975. Nickel. Committee on Medical and Biologic Effects of Environmental Pollutants. Div. of Medical Sciences. National Research Council. ISBN 0-309-02314-9.

National Academy of Sciences. 1977. Nitrogen oxides. ISBNO-309- 02615-6. Printing and Publishing Office, National Academy of Sciences, 2101 Constitution Ave., NW Washington, D.C.

Noxon, J. F. 1978. Tropospheric NO_2. J. Geophys. Res. 83:3051-3057.

O'Brien, R. J., J. H. Crabtree, J. R. Holmes, M. C. Hoggan, and A. H. Bockian. 1975. Formation of photochemical aerosol from hydrocarbons. Atmospheric analysis. Environ. Sci. Technol. 9:577-582.

Okita, T., S. Morinoto, M. Izawa, and S. Konno. 1976. Measurement of gaseous and particulate nitrates in the atmosphere. Atmos. Environ. 10:1085-1089.

Ottar, B. 1978. An assessment of the OECD study on long range transport of air pollutants (LRTAP). Atmos. Environ. 12:445-454.

Paciga, J. J. and R. E. Jervis. 1976. Multielement size characterization of urban aerosols. Environ. Sci. Technol. 10:1124-1128.

Patterson, R. K. and J. Wagman. 1977. Mass and composition of an urban aerosol as a function of particulate size for several visibility levels. J. Aerosol Sci. 8:269-279.

Pierson, W. R., J. W. Butler, and D. A. Trayser. 1974. Nitrate and nitric acid emissions from catalyst-equipped automotive systems. Environ. Letts. 7:267-272.

Pierson, W. R., W. H. Mammerle, and W. W. Brachaczek. 1976. Sulfate formed by interaction of SO_2 with filters and aerosol deposits. Anal. Chem. 48:1808-1811.

Pierson, W. R., W. W. Brachaczek, T. J. Truex, J. W. Butler, and T. J. Korniski. 1980a. Ambient sulfate measurements on Allegheny Mountain and the question of atmospheric sulfate in the northeastern United States. Ann. New York Acad. Sci. 338:145-173.

Pierson, W. R., W. W. Brachaczek, T. J. Korniski, T. J. Truex, and J. W. Butler. 1980b. Artifact formation of sulfate, nitrate and hydrogen ion on backup filters: Allegheny mountain experiment. J. Air Pollut. Control Assoc. 30:30-34.

Pilz, W. and Johann, I. 1974. Die bestimmung kleinster mengen von wasser stoff peroxyd in luft. Int. J. Environ. Anal. Chem. 3:257-270.

Pitts, J. N., Jr. and D. Grosjean. 1979. Detailed characteristics of gaseous and size-resolved particulate pollutants at a south coast air basin smog receptor site. PB-302, 294 National Technical Information Service, Springfield, VA.

Platt, U. and D. Perner. 1980. Direct measurements of atmospheric CH_2O, HNO_2, O_3, NO_2, and SO_2 by differential optical absorption in the near UV. J. Geophys. Res. 85:7453-7458.

Prahm, L. P., U. Torp, and R. M. Stern. 1976. Deposition and transformation rates of sulfur oxides during atmospheric transport over the Atlantic. Tellus 28:355-372.

Rasmussen, R. A., R. Chatfield, and M. Holdren. 1977. Hydrocarbon and oxidant chemistry observed at a site near St. Louis. EPA-600/17-77-056. Environmental Sciences Research Laboratory. Research Triangle Park, NC.

Renzetti, N. A. and R. J. Bryan. 1961. Atmospheric sampling for aldehydes and eye irritation in Los Angeles Smog-1960. J. Air Pollut. Control Assoc. 11:421-424.

Research Triangle Institute. 1975. Investigation of rural oxidant levels as related to urban control strategies. EPA-450/3-75-036. U.S. Environmental Protection Agency, Research Triangle Park, NC.

Ripperton, L. A., L. Kornreich, and J. J. B. Worth. 1970. Nitrogen Dioxide and nitric oxide in non-urban air. J. Air Pollut. Control Assoc. 20:589-592.

Robinson, E. and F. L. Ludwig. 1967. Particle size distribution of urban lead aerosols. J. Air Pollut. Control Assoc. 17:664-669.

Roesler, J. F., H. J. R. Stevenson, and J. S. Nader. 1965. Size distribution of sulfate aerosols in the ambient air. J. Air Pollut. Control Assoc. 15:576-579.

Rohlach, L. A., W. C. Hawn, K. R. Williams, and T. P. Parsons. 1979. Nitrogen oxide interferences in the measurement of atmospheric particulate nitrate. EPRI EA-1031, Research Project 801-1. Electric Power Research Institute, 3412 Hillview Ave., Palo Alto, CA.

Schurr, S. H., B. C. Netschert, V. F. Eliasberg, J. Lerner, and H. H. Landsberg. 1960. Energy in the American economy 1850-1975. The John Hopkins Press, Baltimore, MD.

Sexton, K. and H. Westberg. 1980. Elevated ozone concentrations measured downwind of the Chicago-Gary Urban complex. J. Air Pollut. Control Assoc. 30:911-914.

Shaw, R. W. and R. J. Paur. 1983. Measurements of sulfur in gases and particles during sixteen months in the Ohio River Valley. Atmos. Environ. 17:1431-1438.

Shaw, R. W., T. G. Dzubay, and R. K. Stevens. 1979. The denuder difference experiment. Current methods to measure atmospheric nitric acid and nitrate artifacts, pp. 79-84. Report EPA-600/12-79-051. R. K. Stevens, ed. U.S. Environmental Protection Agency, Research Triangle Park, NC.

Shaw, R. W., R. J. Paur, and T. Royal. 1981. Ohio River Valley Study Sites, methods, data summary for 1980. Environmental Sciences Research Laboratory, Research Triangle Park, NC.

Shaw, R. W., Jr., R. K. Stevens, and J. Bowermaster. J. W. Tesch and E. Tew. 1982. Measurements of atmospheric nitrate and nitric acid: The denuder difference experiment. Atmos. Environ. 16:845-853.

Singh, H. B., F. L. Ludwig, and W. B. Johnson. 1978. Tropospheric ozone: Concentrations and variabilities in clean remote atmospheres. Atmos. Environ. 12:2185-2196.

Singh, H. B., L. J. Salas, and L. A. Cavanaugh. 1977a. Distribution, Sources and sinks of atmospheric halogenated compounds. J. Air Pollut. Control Assoc. 27:332-336.

Singh, H. B., L. J. Salas, H. Shigeishi, and A. Crawford. 1977b. Urban-nonurban relationships of halocarbons, SF_6, N_2O and other atmospheric trace constituents. Atmos. Environ. 11:819-828.

Singh, H. B., L. J. Salas, H. Shigeishi, A. J. Smith, E. Scribner, and L. J. Cavanaugh. 1979. Atmospheric distributions, sources, and sinks of selected holocarbons, hydrocarbons, SF, and NO_2. EPA-600/3-79-107, Research Triangle Park, NC.

Singh, H. B., L. J. Salas, A. J. Smith, and H. Shigeishi. 1981. Measurements of some potentially hazardous organic chemicals in urban environments. Atmos. Environ. 15:601-612.

Singh, H. B., L. J. Salas, R. Stiles, and H. Shipeishi. 1982. Measurements of hazardous organic chemicals in the ambient atmosphere. Report to EPA. Cooperatative Agreement 805990 to Environmental Sciences Research Laboratory. Research Triangle Park, NC.

Siple, G. W., C. K. Fitzsimmons, K. F. Zeller, and R. B. Evans. 1977. Long range airborne measurements of ozone off the coast of the northeastern United States, pp.249-258. In Vol. 1, International Conference on Photochemical Oxidant Pollution and its Control. B Dimitriades, ed. EPA-600/3-77-0012 Environmental Sciences Research Laboratory, Research Triangle Park, NC 27711.

Sloane, C. S. 1982a. Visibility trends - I. Methods of analysis. Atmos. Environ. 16:41-51.

Sloane, C. S. 1982b. Visibility trends - II. Mideastern United States 1948-1978. Atmos. Environ. 16:2309-2321.

Spicer, C. W. 1977. The fate of nitrogen oxides in the atmosphere, pp. 163-261. In Advances in Environmental Science and Technology. Vol 7. J. N. Pitts and R. L. Metcalf, eds. J. Wiley & Sons, New York.

Spicer, C. W. 1979. Measurement of gaseous HNO_3 by electrochemistry and chemiluminescence in current method to measure atmospheric nitric acid and nitrate artifacts. R. K. Stevens, ed. EPA 600/12-79-051.

Spicer, C. W. and D. F. Miller. 1976. Nitrogen balance in smog chamber studies. J. Air Poll. Control Assoc. 26:45-50.

Spicer, C. W. and P. M. Schumacher. 1977. Interferences in sampling atmospheric particulate nitrate. Atmos. Environ. 11:873-876.

Spicer, C. W. and P. M. Shumacher. 1978. Studies in effect of environmental variables on the collection of atmospheric nitrate and the development of a sampling and analytical nitrate method. EPA-600/2-78-009. U.S. Environmental Protection Agency, Research Triangle Park, NC.

Spicer, C. W. and P. M. Schumacher. 1979. Particulate nitrate; laboratory and field studies of major sampling interferences. Atmos. Environ. 13:543-552.

Spicer, C. W. and G. W. Sverdrup. 1981. Trace nitrogen chemistry during the Philadelphia oxidant data enhancement study. 1979. Report on contract no. 68-02-0338 to Office of Air Quality Planning and Standards. U.S. Environmental Protection Agency. Research Triangle Park, NC.

Spicer, C. W., J. L. Gemma, D. W. Joseph, P. R. Strickel, and G. F. Ward. 1976a. The Transport of Oxidant beyond Urban Areas. EPA-600/3-76-018. U.S. Environmental Protection Agency, Research Triangle Park, NC.

Spicer, C. W., J. L. Gemma, P. M. Schumacker and G. F. Ward. 1976b. The fate of nitrogen oxides in the atmosphere. Second year report by Battelle Columbus Lab. to Coordinating Research Council (CAPA-9-71).

Spicer, C. W., M. W. Holdren and G. W. Keigley. 1983. The ubiquity of peroxyacetyl nitrate in the lower atmosphere. Atmos. Environ. 17:1055-1058.

Spicer, C. W., J. E. Howes, Jr., T. A. Bishop, L. H. Arnold, and R. K. Stevens. 1982a. Nitric acid measurement methods: An intercomparison. Atmos. Environ. 16:1487-1500.

Spicer, C. W., D. W. Joseph, P. R. Sticksel, and G. F. Ward. 1979. Ozone sources and transport in the northeastern United States. Environ. Sci. Technol. 13:975-985.

Spicer, C. W., D. W. Joseph, and P. R. Sticksel. 1982b. An investigation of the ozone plume from a small city. J. Air pollut. Control Assoc. 32:278-281.

Spicer, C. W., J. R. Koetz, G. W. Keigley, G. M. Sverdrup, and G. F. Ward. 1982c. Nitrogen oxides reactions within urban plumes transported over the ocean. Report on contract no. 68-02-2957 to Environmental Sciences Research Laboratory, U.S. Environmental Protection Agency, Research Triangle Park, NC.

Stevens, R. K., T. G. Dzubay, D. T. Mage, R. Burton, G. Russwurm, and E. Tew. 1978. Comparison of Hi-Vol and dichotomous sampler results on nitrates and sulfates. Div. of Environ. Chem. Amer. Chem. Soc. 176th National Meeting, Miami, FL.

Stevens, R. K., T. G. Dzubay, R. W. Shaw, Jr., W. A. McClenny, C. W. Lewis, and W. E. Wilson. 1980. Characterization of the aerosol in the Great Smokey Mountains. Environ. Sci. Technol. 14:1491-1498.

Stevens, R. K., W. A. McClenny, T. G. Dzubay, M. A. Mason and W. J. Courtney. 1982. Analytical methods to measure the carbonaceous content of aerosols. In Particulate Carbon: Atmospheric Life Cycle. G. T. Wolff and R. L. KTimisoh, eds. Plenum Press, New York.

Struempler, A. W. 1975. Trace element composition in atmospheric particulates during 1973 and the summer of 1974 at Chadron, Neb. Environ. Sci. Technol. 9:1164-1168.

Swinford, R. 1980. Vertical ozone profile in the lower troposphere over Chicago. J. Air Pollut. Control Assoc. 30:794-796.

Tanner, R. L. 1982. An ambient experimental study of phase equilibrium in the atmospheric system: Aerosol H^+, NH_4^+, SO_4^{2-}, NO_3^- - $NH_3(g)$, $HNO_3(g)$. Atmos. Environ. 12:2935-2942.

Tanner R. L. and W. H. Marlow. 1977. Size discrimination and chemical composition of ambient airborne sulfate particles by diffusion sampling. Atmos. Environ. 11:1143-1150.

Tanner, R. L., R. Cederwall, R. Garber, D. Leahy, W. Marlow, R. Meyer, M. Phillips, and L. Newman. 1977. Separation and analysis of aerosol sulfate species at ambient concentrations. Atmos. Environ. 11:955-966.

Tanner, R. L., W. H. Marlow, and L. Newman. 1979. Chemical composition correlations of size-fractionated sulfate in New York City Aerosol. Environ. Sci. Technol. 13:75-78.

Taylor, O. C. 1969. Importance of peroxyacetyl nitrate (PAN) as a phytotoxic air pollutant. J. Air Pollut. Control Assoc. 19:347-351.

Temple, P. J. and O. C. Taylor. 1983. World-wide ambient measurements of peroxyacetyl nitrate (PAN) and implications for plant injury. Atmos. Environ. 17(8):1583-1587.

Tesche, T. W., J. A. Ogren and D. L. Blumenthal. 1977. Ozone concentrations in power plant plumes, pp. 157-171. In Comparison of Models and Sampling Data. Vol. II, International Conference on Photochemical Oxidant Pollution and Its Control. B. Dimitriades, ed. EPA-600/13-77-0012. Environmental Sciences Research Laboratory, Research Triangle Park, NC.

Trijonis, J. 1978. Empirical relationship between atmospheric nitrogen dioxide and its precursors. EPA-600/3-78-018. U.S. Environmental Protection Agency, Research Triangle Park, NC.

Trijonis, J. and S. Mortimer. 1982. Validation of the EKMA model using historical air quality data. EPA-600/3-82-015. Environmental Sciences Research Laboratory, Research Triangle Park, NC.

Trijonis, J. and K. Yuan. 1978a. Visibility in the southwest. An exploration of this historical data base. EPA Report 600/3-7-039 to Environmental Sciences Research Laboratory, Research Triangle Park, NC.

Trijonis, J. and K. Yuan. 1978b. Visibility in the northeast. Long-term visibility trends and visibility/pollutant relationships. EPA Report 600/3-78-075 to Environmental Sciences Research Laboratory, Research Triangle Park, NC.

Tuazon, E. C., R. A. Graham, A. M. Winer, R. R. Easton, and J. N. Pitts, Jr. 1978. A kilometer pathlength Fourier-transform infrared system for the study of trace pollutants in ambient and synthetic atmospheres. Atmos. Environ. 12:865-875.

Tuazon, E. C., A. M. Winer, R. A. Graham, and J. N. Pitts, Jr. 1980. Atmospheric measurements of trace pollutants by kilometer-pathlength FT-IR spectroscopy, pp. 254-300. In Advances in Environmental Sciences and Technology, Vol. 10. J. N. Pitts and R. L. Metcalf, eds. J. Wiley & Sons, New York.

Tuazon, E. C., A. M. Winer, R. A. Graham, and J. N. Pitts, Jr. 1981a. Atmospheric measurements of trace pollutants: Longpath Fourier transform infrared spectroscopy. EPA Grant No. R-804546. U.S. Environmental Protection Agency, Environmental Sciences Research Laboratory, Research Triangle Park, NC.

Tuazon, E. C., A. M. Winer, and J. N. Pitts, Jr. 1981b. Trace pollutant concentrations in a multiday smog episode in the California South Coast Air Basin by long path Fourier transform infrared spectroscopy. Environ. Sci. Technol. 15:1232-1237.

U.S. Environmental Protection Agency. 1977a. National air quality and emission trends report 1976. EPA-450/1-77-002. Office of Air Quality Planning and Standards, Research Triangle Park, NC.

U.S. Environmental Protection Agency. 1977b. Air quality criteria for lead. EPA-600/8-77-017. Office of Research and Development, Washington, D. C.

U.S. Environmental Protection Agency. 1978a. Air quality criteria for ozone and other photochemical oxidants. EPA-600/8-78-004. Superintendant of Documents, U.S. Printing Office, Washington, D. C.

U.S. Environmental Protection Agency. 1978b. National air quality and emission trends report 1977. EPA-450/2-78-052. Office of Air Quality Planning and Standards, Research Triangle Park, NC.

U.S. Environmental Protection Agency. 1979. Protecting visibility. An EPA report to Congress. EPA-450/5-79-008. Office of Air Quality Planning and Standards, Research Triangle Park, NC.

U.S. Environmental Protection Agency. 1982. Draft final air quality criteria for oxides of nitrogen. EPA-600/8-82-026. Environmental Criteria and Assessment Office, Research Triangle Park, NC.

U.S. Geological Survey. 1970. Mercury in the environment, a compilation of papers on the abundance, distribution and testing of mercury in vocks, soils, waters, plants and the atmosphere. Professional Paper No. 713. U.S. Government Printing Office. Washington, D. C.

Viezee, W. and H. B. Singh. 1982. Contribution of Stratospheric Ozone to Ground-Level Ozone Concentrations--A Scientific Review of Existing Evidence. Report on Grant CR809330010 to Environmental Sciences Laboratory, Research Triangle, NC.

Vukovich, F. M., W. D. Bach, Jr., B. W. Crissman, and W. J. King. 1977. On the relationship between high ozone in the rural surface layer and high pressure systems. Atmos. Environ. 11:967-983.

Waggoner, A. P. and R. E. Weiss. 1980. Comparison of fine particle concentration and light scattering extinction in ambient aerosol. Atmos. Environ. 14:623-626.

Wagman, J., R. E. Lee, Jr., and C. J. Axt. 1967. Influence of some atmospheric variables on the concentration and particle size distribution of sulfate in urban air. Atmos. Environ. 1:479-489.

Weiss, R. E., T. V. Larson, and A. P. Waggoner, 1982. In situ rapid-response measurement of $H_2SO_4/(NH_4)_2SO_4$ aerosols in rural Virginia. Environ. Sci. and Technol. 16:525-532.

Weiss, R. E., A. P. Waggoner, R. J. Charlson, and N. C. Ahlquist. 1977. Sulfate aerosol: Its geographical extent in the mideastern and southern United States. Science 195:979-981.

Westberg, H., K. Allwine, and E. Robinson. 1978a. Measurement of light hydrocarbons and oxidant transport-Houston Study 1976. EPA-600/3-78- 062. Environmental Sciences Research Laboratory, Triangle Research Triangle Park, NC.

Westberg, H., K. Sexton, and M. Holdren. 1978b. Measurements of ambient hydrocarbons and oxidant transport. Vol. I. Houston Study. Report on EPA Grant No. 805343 to Environmental Sciences, Research Laboratory, Research Triangle Park, NC.

Whelpdale, D. M. and L. A. Barrie. 1982. Atmospheric monitoring network operations and results in Canada. Water, Air, and Soil Pollut. 18:7-23.

White, W. H. and P. T. Roberts. 1977. On the nature and origins of visibility-reducing aerosols in the Los Angeles Basin. Atmos. Environ. 11:803-812.

White, W. H., J. A. Anderson, D. L. Blumenthal, R. B. Husar, N. V. Gillani, J. D. Husar, and W. E. Wilson, Jr. 1976. Formation and transport of secondary air pollutants: ozone and aerosols in the St. Louis urban plume. Science 194:187-189.

White, W. H., D. L. Blumenthal, J. A. Anderson, R. B. Husar, and W. E. Wilson, Jr. 1977. Ozone formation in the St. Louis urban plume, pp.237-247. In Vol 1, International Conference of Photochemical Oxidant Pollution and its Control. B. Dimitriades, ed. EPA-600/3-77-0012, Environmental Sciences Research Laboratory, Research Triangle Park, NC.

Williston, S. H. 1968. Mercury in the atmosphere. J. Geophys. Res. 73:7051-7055.

Winer, A. M., J. W. Peters, J. P. Smith, and J. N. Pitts, Jr. 1974. Response of commercial chemiluninescent NO-NO_2 analyzers to other nitrogen-containing compounds. Environ. Sci. Technol. 8:1188-1121.

Witz, S. and R. D. MacPhee. 1977. Effect of different types of glass filters on total suspended particulates and their chemical composition. J. Air Pollut. Control Assoc. 27:239-241.

Witz, S. and J. G. Wendt. 1981. Artifact sulfate and nitrate formation at two sites in the South Coast Air Basin. A collaborative study between the South Coast Air Quality Management District and the California Air Resources Board. Environ. Sci. Technol. 15:79-83.

Witz, S., M. Smith, M. Shu, and A. B. Moore. 1982. A comparison of mass, lead, sulfate, and nitrate concentrations in a field study using dichotomous, size-selective, and standard Hi-Vol samplers. J. Air Pollut. Control Assoc. 32:276-278.

Wolff, G. T., P. J. Lioy, G. D. Wight, R. E. Meyers, and R. T. Cederwall. 1977. An investigation of long-range transport of ozone across the midwestern and eastern United States. Atmos. Environ. 11:797-802.

Wolff, G. T., R. R. Monson, and M. A. Ferman. 1979. On the nature of the diurnal variation of sulfates at rural sites in the eastern United States. Environ. Sci. Technol. 13:1271-1276.

Zika, R. G. and E. S. Saltzman. 1982. Interaction of ozone and hydrogen peroxide in water: Implications for anlaysis of H_2O_2 in air. Geophys. Res. Letts. 9:231-234.

Zika, R., E. Saltzman, W. L. Chameides, and D. D. Davis. 1982. H_2O_2 levels in rainwater collected in South Florida and the Bahama Islands. J. Geophys. Res. 87:5015-5017.

THE ACIDIC DEPOSITION PHENOMENON AND ITS EFFECTS

A-6. PRECIPITATION SCAVENGING PROCESSES

(J. M. Hales)

6.1 INTRODUCTION

Precipitation scavenging is defined generally as the composite process by which airborne pollutant gases and particles attach to precipitation elements, and thus deposit to the Earth's surface.[1] This process constitutes a critically important pathway for atmospheric cleansing, and is a "natural-recovery" phenomenon which is absolutely essential for maintenance of a liveable global atmosphere. Conversely, however, the pollutant delivery resulting from precipitation scavenging often can be sufficiently large to impose severe impacts on a variety of surface receptors. Growing cognizance of this point has resulted in the "acid-precipitation issue" as it is generally perceived today.

The goal of this chapter is to provide the dedicated (but not necessarily expert) reader with an overview of precipitation scavenging, which discusses physical processes in a qualitative manner while at the same time establishing a solid basis of understanding. This is accomplished by first breaking down the scavenging process into a number of discrete steps, and then scrutinizing the associated physical mechanisms or individual and collective bases. This summary of physical processes emphasizes the importance of storm type and meteorological behavior on scavenging pathways. Relative to this, the subsequent section addresses storm climatology and storm classification, with emphasis on practical applications.

The next two sections deal respectively with past field studies of precipitation scavenging and precipitation-scavenging models. A qualitative emphasis continues throughout the modeling section, although sufficient equations are used to facilitate the general discussion. The chapter concludes with

---

[1] One should note that this definition pertains to removal from the gaseous medium of the atmosphere combined with deposition to the ground. An alternative definition, employed often throughout the open literature, pertains to the simple attachment of airborne pollutants to liquid water elements, without regard to whether the material is subsequently conveyed to the Earth's surface. Which of these definitions is used is unimportant so long as the precise definition is understood. The definition of "scavenging" adopted here will be utilized consistently throughout this text. When specific reference to the alternative situation is made, the terms "attachment" and "capture" will be employed essentially interchangeably.

an examination of predictive uncertainties, and the scientific advances which will be necessary to reduce these uncertainties to an acceptable level.

6.2 STEPS IN THE SCAVENGING SEQUENCE

6.2.1 Introduction

The precipitation scavenging process typically contains many parallel and consecutive steps, and as an introduction to this section it is appropriate to provide a brief overview of these intermeshing pathways. In a very general sense there are four major events in which a natural or pollutant molecule[2] may participate, prior to its wet removal from the atmosphere; depicted pictorially in Figure 6-1, these are:

1-2. The pollutant and the condensed atmospheric water (cloud, rain, snow, ...) must intermix within the same airspace.

2-3. The pollutant must attach to the condensed-water elements.

3-4. The pollutant may react physically and/or chemically within the aqueous phase.

3-5. The pollutant-laden water elements must be delivered to the
or(4-5.) Earth's surface via the precipitation process.

The interaction diagram of Figure 6-2 gives a somewhat more detailed portrayal of these four major events. Here the individual steps are represented as transitions of the pollutant between various states in the atmosphere, and one can note that a multitude of reverse processes are also possible; thus a particular pollutant molecule may experience numerous cycles through this complex of pathways prior to deposition. Indeed, Figure 6-2 indicates that this cycling process may continue even after "ultimate" deposition. By pollutant off-gassing and other resuspension processes, the deposited material can be re-emitted to the atmosphere, with the possibility of participating in yet another series of cycles throughout the scavenging sequence.

Another important feature of Figure 6-2 is that, while physicochemical reaction within the aqueous-phase is potentially an important step in the scavenging process, it is not essential. This contrasts to the remaining forward steps that must take place if scavenging is to occur. Despite its nonessential nature, this step is often of utmost importance in influencing scavenging rates, owing to its role in modifying reverse processes in the sequence. An example of this effect, already discussed in Chapter A-4, is

---

[2]Initial portions of this chapter will treat precipitation scavenging in a general sense, with limited reference to specific types of atmospheric material. The reader should continue to note, however, that the "natural or pollutant molecules" of primary concern in the present context are species associated with acid-base formation, such as SO_2, HNO_3, NH_3, sulfate, chloride, metallic cations, and so forth.

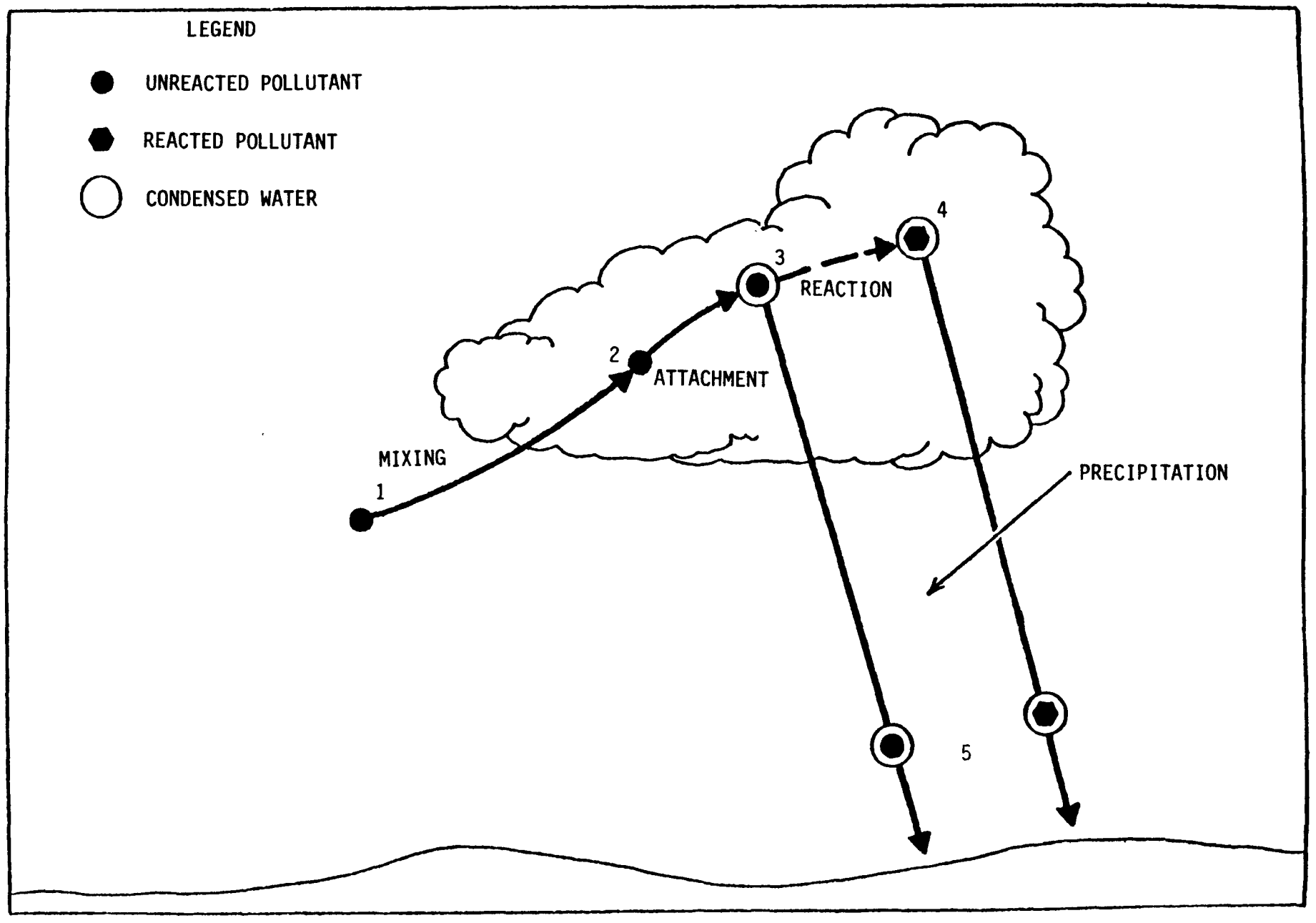

Figure 6-1. Steps in the scavenging sequence: Pictorial representation.

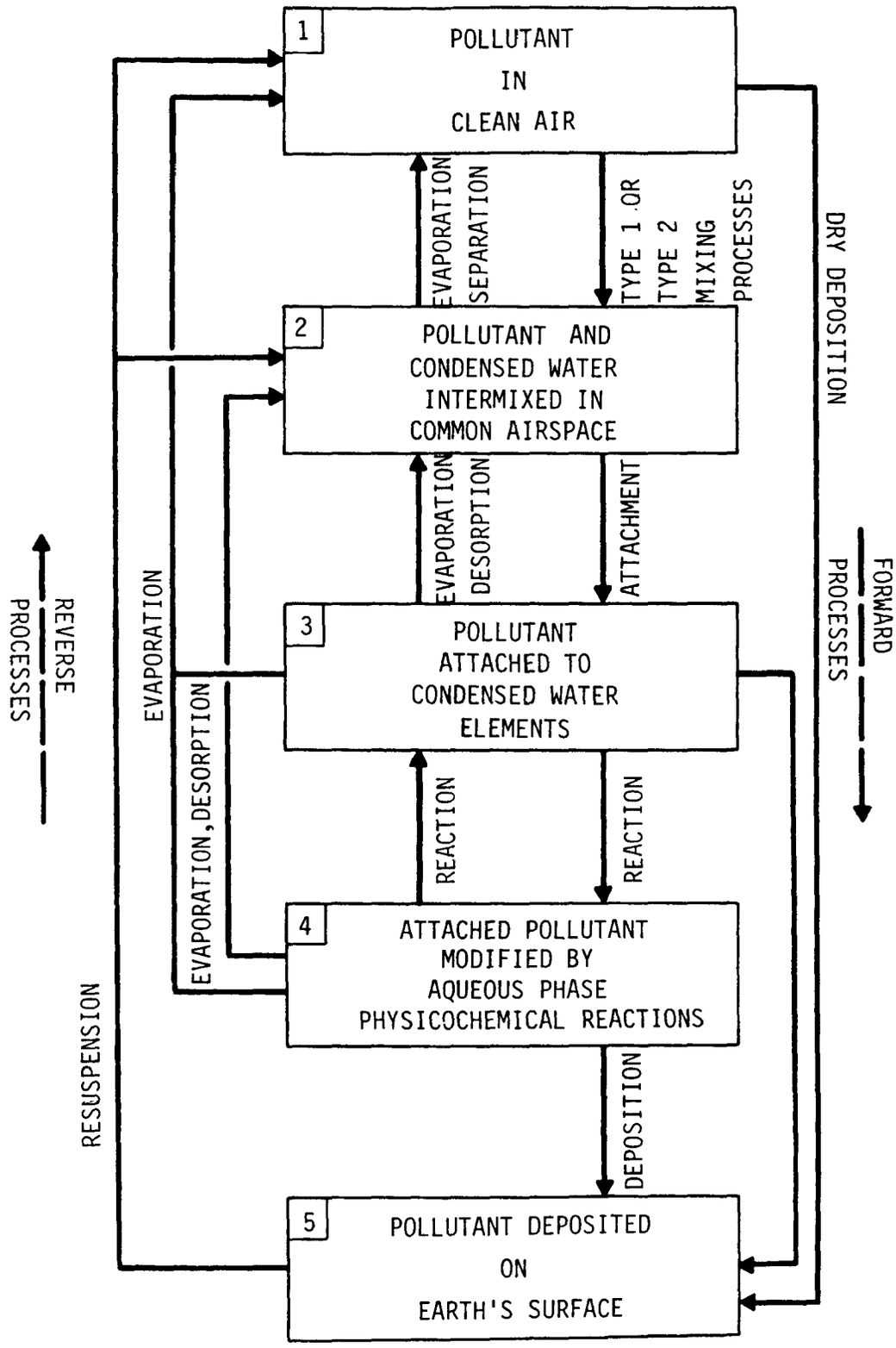

Figure 6-2. Scavenging sequence: Interaction diagram.

the devolatilization of dissolved sulfur dioxide via wet oxidation to sulfate. This effectively eliminates gaseous desorption from the condensed water and thus has a strong tendency to enhance the overall scavenging rate as a result.

From Figure 6-2 one can note also that precipitation scavenging of pollutant materials from the atmosphere is intimately linked with the precipitation scavenging of water. If one were to replace the word "pollutant" with "water vapor" in each of the steps, Figure 6-2 (with the exception of box 4) would provide a general description of the natural precipitation process. In view of this intimate relationship, it is not surprising that pollutant wet-removal behavior tends to mimic that of precipitation. Pollutant-scavenging efficiencies of storms, for example, are often similar to water-extraction efficiencies. This relationship is useful in practically estimating scavenging rates and will reappear continually in the ensuing discussion of wet-removal behavior.

Figure 6-2 is interesting also because of its indication that, if some particular step in the diagram occurs particularly slowly compared to the others, then this step will dominate behavior of the overall process. This is similar to the "rate-controlling step" concept in chemical kinetics, and has been applied rather extensively in practical scavenging calculations (Slinn 1974a). Finally, it is important to note that Figure 6-2 presents a framework for developing and evaluating mathematical models of scavenging behavior. Successful scavenging models must emulate these steps effectively and tend to reflect the structure of Figure 6-2 as a result. This point will be recalled later when scavenging models are examined specifically. The following subsections will address qualitative aspects of the scavenging sequence in the order of their forward progress to ultimate deposition.

6.2.2 Intermixing of Pollutant and Condensed Water (Step 1-2)

Upon first consideration, one often is inclined to dismiss pollutant-condensed-water intermixing as an unimportant or at least trivial step in the overall scavenging sequence. It is neither. In a statistical sense it usually is neither cloudy nor precipitating in the immediate locality of a freshly-released pollutant molecule; typically this molecule must exist in the clear atmosphere for several hours, or even days, before it encounters condensed water with which it may commingle. This in itself establishes step 1-2 as a potentially important rate-influencing event. Moreover, this extended dry period typically presents the pollutant with significant opportunities to react and/or deposit via dry processes; thus, the chemical makeup of precipitation is influenced profoundly by this preceding chain of events.

Significant insights to the behavior of step 1-2 can be gained via past analyses of storm formation (Godske et al. 1957) and the atmospheric water cycle (Newell et al. 1972). Several statistical analyses of precipitation occurrence (Rodhe and Grandell 1972, 1981; Gibbs and Slinn 1973; Junge 1974; Baker et al. 1979) have been applied as general interpretive descriptors of this step. These will not be examined in detail here; rather we shall

concentrate upon the mechanisms by which step 1-2 can occur, from a more pictorial viewpoint.

Two types of mixing processes exist whereby pollutant and condensed water can come to occupy common airspace; these are

1) Relative movement of the initially unmixed pollutant and condensed water, in a manner such that they merge into a common general volume; and

2) In situ phase change of water vapor, thus producing condensed water in the immediate vicinity of pollutant molecules.

The relative importance of Type-1 and Type-2 mixing processes will depend to some extent on the pollutant. If a particular pollutant is easily scavengable and if precipitation is occurring at the pollutant's release location, then Type-1 processes are likely to contribute significantly. If these two conditions are not met, the pollutant will usually mix intimately with makeup water vapor for some future cloud, and Type-2 processes will predominate. Based upon in-cloud vs below-cloud scavenging estimates (Slinn 1983) it is not unreasonable to estimate that, as a global average, roughly 90 percent of all precipitation scavenging occurs as the consequence of a Type-2 process.

As Figure 6-2 indicates, reverse processes can serve to reseparate pollutant and condensed water. Evaporation, for example, can reinject pollutant from cloudy to clear air, and relative motion such as precipitation "fall-through" can remove hydrometeors from contact with elevated plumes. Cloud formation-reevaporation cycles are particularly significant in this respect. Junge (1963), for example, estimates that a single cloud condensation nucleus is likely to experience on the order of ten or more evaporation-condensation cycles before it is ultimately delivered to the Earth's surface with precipitation. The rate-influencing effect of such cycling on precipitation scavenging is obvious. Additional types of cycles will be described below in conjunction with succeeding steps of the scavenging sequence.

6.2.3 Attachment of Pollutant to Condensed Water Elements (Step 2-3)

The microphysics of the pollutant-attachment process have been the subject of extensive research, and numerous reviews of this area have been prepared (Junge 1963, Davies 1966, Dingle and Lee 1973, Pruppacher and Klett 1978, Hales 1984, Slinn 1983, Slinn and Hales 1983). In the context of Figure 6-1, this process is complicated somewhat in the sense that, depending upon the particular attachment mechanism, Step 2-3 may occur either simultaneously or consecutively with Step 1-2.

Simultaneous commixing and attachment occur in the case of cloud-particle nucleation. This is a phase-transformation (Type-2) process wherein water molecules, thermodynamically inclined to condense from the vapor phase, migrate to some suitable surface for this purpose. Pollutant aerosol particles provide such surfaces within the air parcel, and the consequence is a

cloud of droplets (or ice crystals)[3] containing attached pollutant material.

Different types of aerosol particles possess different capabilities to nucleate cloud elements and grow by the condensation process. As a consequence, there is typically a competition for water molecules among the aerosol and associated cloud particles. Some will capture water with high efficiency and grow substantially in size. Others will acquire only small amounts of water, and still others remain essentially as "dry" elements. In addition, some particles may nucleate ice crystals, while others will be active only for the formation of liquid water. The nucleating capability of a particular aerosol particle is determined by its size, its morphological characteristics, and its chemical composition. Various aspects of this subject are discussed at length in standard cloud-physics textbooks (Mason 1971, Pruppacher and Klett 1978) and in the periodical literature (Fitzgerald 1974).

An additional important aspect of the cloud-droplet nucleation and growth process is the fact that once initiated, cloud-droplet growth does not proceed instantaneously to some sort of thermodynamic equilibrium. Because of diffusional constraints on delivering water molecules from the surrounding atmosphere, the growth in droplet diameter slows appreciably as droplet size increases (Slinn 1983). Superimposition of this lag on the continually fluctuating environment of a typical cloud results in a dynamic and complex physical system.

Finally, the competitive nature of the cloud-nucleation process results in significant impacts by the pollutant on the basic character of the cloud itself. If the local aerosol were populated solely by a relatively small number of large, hygroscopic particles, for example, one would expect any corresponding cloud to be composed chiefly of small populations of large droplets. If on the other hand the local aerosol were composed of large numbers of small, nonhygroscopic particles, the corresponding cloud should contain larger numbers of smaller droplets.

This is precisely what is observed in practice. Unpolluted marine atmospheres, for example, contain large sea-salt particles as a primary component of their aerosol burden. Warm marine clouds are noted for their wide droplet spectra containing large droplet sizes and their corresponding capability to form precipitation easily. Continental clouds, on the otherhand, are typically composed of larger populations of smaller droplets. Figure 6-3,

---

[3]At this point it is important to note that aerosols can participate in several types of phase transitions in cloud systems. These include vapor-liquid, vapor-solid, and liquid-solid transitions, in addition to a subset of interactions between numerous solid phases. Particles active as ice-formation nuclei are generally much less abundant than those active as droplet (or "cloud-condensation") nuclei. As will be demonstrated later, the relative abundance of ice nuclei can have a profound effect upon precipitation-formation processes and related scavenging phenomena.

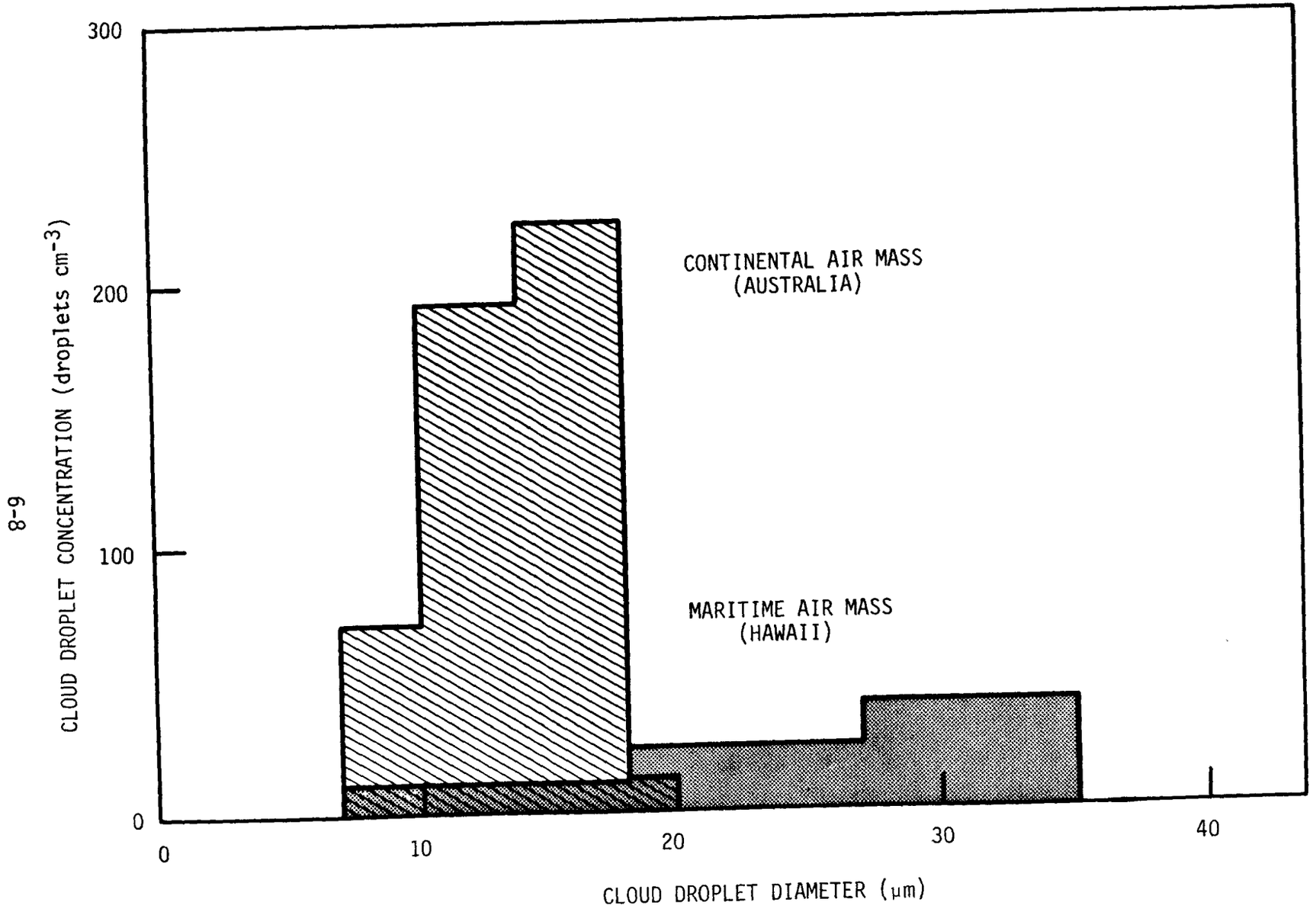

Figure 6-3. Cloud droplet spectra in convective clouds formed in maritime and continental air masses. Adapted from Squires and Twomey (1960).

prepared on the basis of results published by Squires and Twomey (1960), provides a good example of this point. Here, measured convective-cloud droplet spectra are compared for two different cloud systems. The continental air-mass cloud exhibits a distinct tendency toward smaller droplet sizes and larger populations, as compared to its maritime counterpart. It is interesting also in this context to note Junge's (1963) estimates with regard to relative amounts of aerosol participating in the nucleation process. Junge suggests that while 50 to 80 percent of the mass of continental aerosols can be expected to participate as cloud nuclei, as much as 90 to 100 percent of maritime aerosols can become actively involved.

As a concluding note in the context of nucleating capability and water competition, it should be pointed out that acid-forming particles, by their very nature, are chemically competitive for water vapor and thus tend to participate actively as cloud-condensation nuclei. This attribute tends to enhance their propensity to become scavenged early in storm systems and has a significant effect on the nature of the acid precipitation formation process.

There are numerous mechanisms by which pollutants can attach to cloud and precipitation elements after the elements already exist, and thus in a manner consecutive with Step 1-2. These mechanisms are itemized in the following paragraphs. They are typically active for both aerosols and gases, although the relative importances and magnitudes vary widely with the state of the scavenged substance.

Diffusional attachment, as its name implies, results from diffusional migration of the pollutant though the air to the water surface. This process may be effective both in the case of suspended cloud elements and falling hydrometeors. It depends chiefly upon the magnitude of the pollutant's molecular (or Brownian) diffusivity; because diffusivity is inversely related to particle size, this mechanism becomes less important as pollutant elements become large. Diffusional attachment is of utmost importance for scavenging of gases and very small aerosol particles. For all practical purposes, it can be ignored for aerosol particle sizes above a few tenths of a micron.

In concordance with Fick's law (Bird et al. 1960), diffusional transport to a water surface also depends upon the pollutant's concentration gradient in the vicinity of this surface. Thus if the cloud or precipitation element can accommodate the influx of pollutant readily, it will effectively depopulate the adjacent air, thus making a steep concentration gradient and encouraging further diffusion. If for some reason (e.g., particle "bounce off" or approach to solute saturation) the element cannot accommodate the pollutant supply, then further diffusion will be discouraged. If the cloud or precipitation element, through some sort of outgassing mechanism, supplies pollutant to the local air, then the concentration gradient will be reversed and diffusion will carry the pollutant away from the element.

Mixing processes inside cloud or precipitation elements play an important role in determining the accommodation of gaseous species. If mixing is slow, for example, it is likely that the element's outer layer will saturate with pollutant and thus inhibit further attachment processes. This is quite often a limiting factor in cases involving gas scavenging by ice crystals.

Internal mixing occurs as a consequence of diffusion and fluid circulation and has been analyzed by Pruppacher and his coworkers (Pruppacher and Klett 1978).

In general, diffusional attachment processes are sufficiently well understood to allow their mathematical description with reasonable accuracy, and numerous references are available as guides for this purpose (Pruppacher and Klett 1978, Hales 1984, Slinn 1983).

Inertial attachment processes depend directly upon the size of the scavenged particle, and thus are unimportant for gaseous pollutants. In a somewhat general sense this class of processes depends upon motions of pollution particles and scavenging elements relative to the surrounding air, which arise because both have finite volume and mass. The most important example of inertial attachment is the impaction of aerosols on falling hydrometeors. Here the hydrometeor (because of its mass and volume) falls by gravity, sweeping out a volume of space. Some of the aerosol particles (because of their mass) cannot move sufficiently rapidly with the flow field to avoid the hydrometeor and, thus, are impacted. In principle, impaction could occur even if the aerosol particles were point masses with zero volume. Assigning a volume to a particle further increases its chance of collision, simply on the basis of geometric effects. The inclusion of aerosol volume in this context has been generally referred to in the past literature as interception.

The effectiveness of impaction and interception depends upon both aerosol-particle and hydrometeor size; mathematical formulae exist which can be used conveniently to estimate the magnitudes of these processes (e.g., Hales 1984, Slinn 1983). These effects generally become unimportant for aerosols less than a few microns in size. In this context, it is interesting to note that a two-stage capture mechanism can exist, in which a small aerosol first grows via nucleation to form a larger droplet, which then can be captured by inertial attachment in a secondary process. This two-stage process has been postulated as an important mechanism in below-cloud scavenging (Radke et al. 1978, Slinn 1983). It is also an essential factor in the in-cloud generation of precipitation and is generally referred to as accretion.

A second example of inertial attachment is turbulent collision. In this case the particles and scavenging elements subjected to a turbulent field collide because of dissimilar dynamic responses to velocity fluctuations in the local air. This capture mechanism is thought to be of secondary importance and has received comparatively little attention in the literature although past theoretical treatments of turbulent coagulation processes (e.g., Saffman and Turner 1955, Levich 1962, Fuchs 1964) indicate that it may be significant for specific dropsize-particle size ranges.

While the mechanisms of diffusional and inertial attachment are efficient for capturing very fine and very coarse particles, respectively, a region of low efficiency should exist approximately in the 0.1 to 5.0 micron range where neither mechanism is effective. This effect is shown schematically for a given drop in Figure 6-4. Because its importance to scavenging was first recognized by Greenfield (1957), it has become known generally as the "Greenfield gap." Depending upon circumstances, several additional

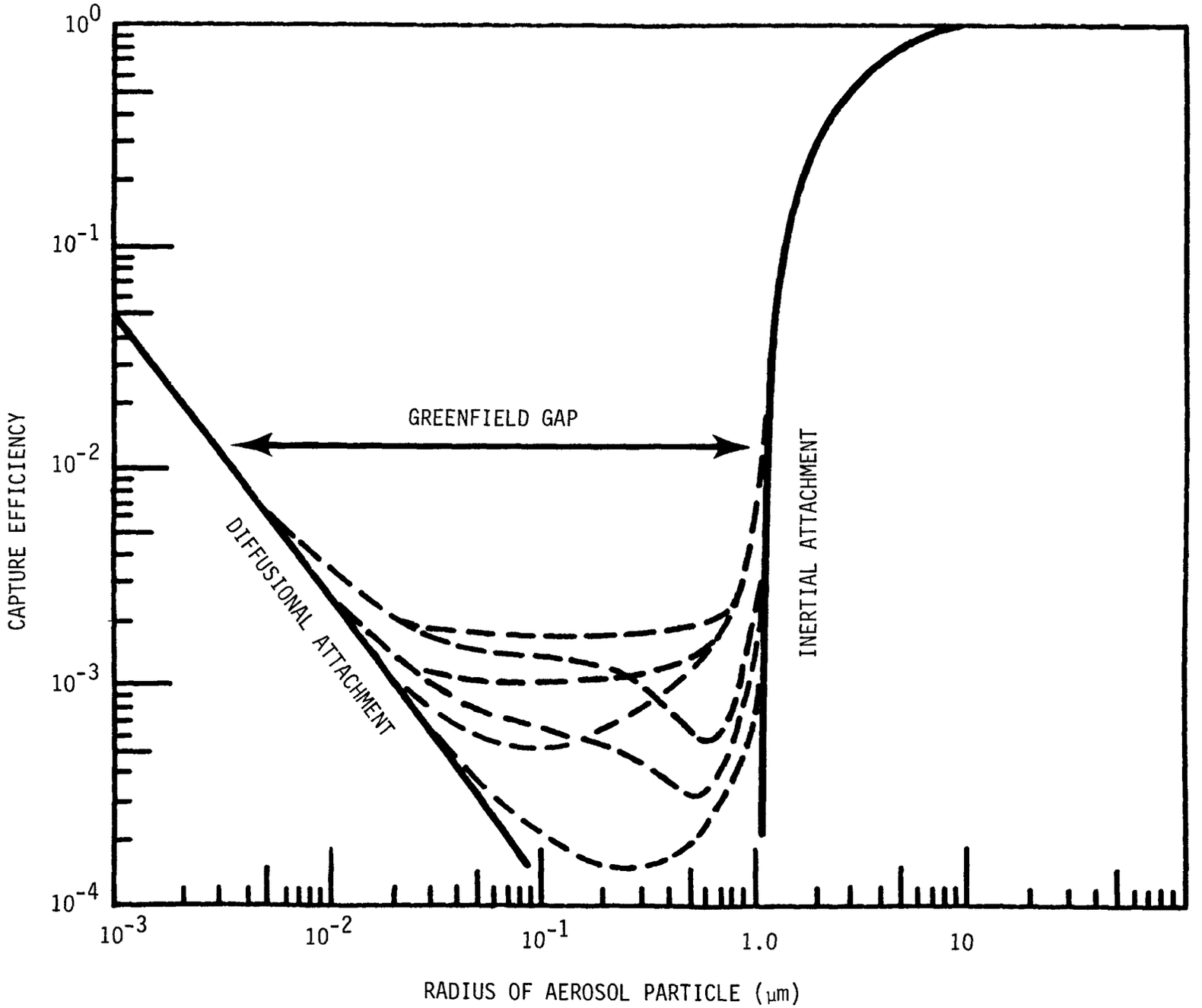

Figure 6-4. Theoretical scavenging efficiency of a falling raindrop as a function of aerosol particle size. Adapted from curves given by Pruppacher and Klett (1978). Dashed lines correspond to contributions by electrical and phoretic effects under chosen humidity and raindrop-charge conditions (see original reference for details).

attachment mechanisms (including the two-stage nucleation-impaction mechanism mentioned earlier) can serve to "fill" the Greenfield gap. Some of the more important of these are itemized in the following paragraphs.

Diffusiophoretic attachment to a scavenging element can occur whenever the element grows via the condensation of water vapor. In effect, the flux of condensing water vapor "sweeps" the surrounding aerosol particles to the element's surface. In a competitive cloud-element system where some droplets grow while others evaporate, diffusiophoresis can be a rather important secondary attachment mechanism. This is particularly true when the cloud contains mixtures of ice and liquid. Under such conditions, the ice crystals have a pronounced tendency, owing to their lower equilibrium vapor pressure, to gain water at the expense of the droplets. Known as the Bergeron-Findeisen effect, this process is important in precipitation formation as well as in diffusiophoretic enhancement.

Thermophoretic attachment results from a temperature gradient in the direction of the capturing element. Here the element acts essentially as a miniature thermal precipitator. Warmer gas molecules on the outward side of the aerosol particle impart a proportionately larger amount of momentum, resulting in a driving force toward the capturing element.[4]

Thermophoresis depends directly upon the temperature gradient in the vicinity of the capturing element. In cloud and precipitation systems local temperature gradients are caused most often by evaporation/condensation effects; thus, thermophoresis is usually strongly associated with diffusiophoresis,[5] and in fact these two processes often tend to counteract each other.

Phoretic processes are unimportant in the case of gaseous pollutants, owing to the overwhelming contributions of molecular diffusion. At present, the theory of diffusiophoretic/thermophoretic particle attachment is at a state where reasonably quantitative assessments can be made for simple systems such as isolated droplets (Slinn and Hales 1971, Pruppacher and Klett 1978, See Figure 6-4). Rough estimates are possible for more complex and interactive cloud/precipitation systems, but much remains to be done to make our knowledge of this area satisfactory.

Electrical attachment of aerosol particles to cloud and precipitation elements has been the subject of continuing study over the past three decades. Understanding of this process is currently at a state where relationships between aerosols and isolated droplets can be quantified with reasonable accuracy (Wang and Pruppacher 1977). In general, electrical charging of cloud and/or precipitation elements must be moderately high for electrical

---

[4]One should note that the precise mechanisms of thermal transport differ radically, depending upon particle size (cf., Cadle 1965).

[5]As noted by Slinn and Hales (1971), inappropriate treatment of this relationship has caused erroneous conclusions to be drawn in some of the past literature. The reader should be cognizant of this if more detailed pursuit is intended.

effects to become competitive with other capture phenomena, although such charging is certainly possible in the atmosphere, particularly in convective-storm situations. Understanding of electrical deposition in clouds of interacting drops is still relatively unsatisfactory.

While the mechanisms of attachment processes have been presented here on an individual basis, they tend in actuality to proceed in a simultaneous and competitive manner. Insofar as atmospheric cleansing is concerned, this is a fortunate circumstance, because some mechanisms tend to operate in physical situations where others are ineffective. Figure 6-4 gives an excellent illustration of this point. Theoretical attachment efficiencies appropriate to a 0.31 mm radius raindrop are presented for various electrical and relative-humidity conditions, demonstrating the capability of phoretic and electrical mechanisms to "bridge" the Greenfield gap. This simultaneous and competitive interaction of mechanisms serves to complicate profoundly the mathematics of the scavenging process, and lends an additional degree of difficulty to the problem of scavenging calculations. This aspect will continue to emerge throughout this chapter, especially during the discussion of scavenging models.

6.2.4 Aqueous-Phase Reactions (Step 3-4)

Aqueous-phase conversion phenomena have been discussed in some detail in Chapter A-4 and will not be examined further here except to note their general importance within the framework of the overall scavenging sequence. As noted previously in the context of Figure 6-2, aqueous-phase reactions are not essential to the scavenging process. Depending upon the pollutant material, however, these reactions often can have the effect of stabilizing the captured material within the condensed phase and, thus, enhancing the scavenging efficiency appreciably. Much needs to be learned before this important topic is satisfactorily understood.

6.2.5 Deposition of Pollutant with Precipitation (Steps 3-5 and 4-5)

Although a variety of mechanisms exist (e.g., impaction of fog on vegetation), the predominant means for depositing pollutant-laden condensed water to the Earth's surface is simply gravitational sedimentation. Sedimentation rates depend upon hydrometeor fall velocities, which depend in turn upon hydrometeor size. Thus, the processes by which the pollutant-laden cloud droplets grow to precipitation elements emerge as major determining factors in this final stage of the scavenging sequence.

Once attached to condensed water, a pollutant molecule has several alternative pathways for action (Figure 6-2). If the captured pollutant possesses some degree of volatility it may desorb back into the gas phase. Reverse chemical reactions may occur. Evaporation of the condensed water may, in effect, "free" the pollutant to the surrounding gaseous atmosphere. This multitude of pathways results in an active competition for pollutant. If the precipitation stage of the scavenging sequence is to be effective, it must interact successfully within this competitive framework.

Besides competing actively for pollutants, the above interactions produce a vigorous competition for water. This parallel relationship between pollutant scavenging and water scavenging, apparent in some of the preceding discussion regarding attachment processes, can be drawn even more emphatically when considering precipitation processes. The following paragraphs provide a brief overview of some of the more important mechanisms in this regard.

Once initial nucleation has occurred, cloud particles may grow further by condensation of additional water vapor. Net condensation will occur to the surface of a cloud element whenever water vapor molecules can find a more favorable thermodynamic state in association with it; and because clouds contain varieties of makeup elements having different thermodynamic characteristics, competition for water vapor usually exists. Such interactions are discussed at length in standard textbooks (Mason 1971, Pruppacher and Klett 1978). Slinn (1983) has developed a conceptual scavenging model in which condensational growth is an important rate-limiting step.

Thermodynamic affinity for water-vapor molecules depends upon the cloud-element's size, its pollutant burden, and its physical structure. These latter two factors often influence precipitation characteristics profoundly. In particular, the favored thermodynamic state of a water molecule in association with an ice crystal (as compared with a supercooled water droplet) results in rapid competitive growth of ice particles in mixed-phase clouds. This "Bergeron-Findeisen" process has been mentioned already in the context of diffusiophoretic and thermophoretic transport. Growth of large cloud elements via this process is the primary reason that ice-containing clouds tend to be so strongly effective as generators of precipitation water.

A further mechanism by which suspended cloud droplets can grow to form precipitation elements is coagulation. This process occurs via the collision of two or more cloud elements to form a new element containing the total mass (and pollutant burden)[6] of its predecessors. Coagulation occurs over size-distributed systems of cloud elements by a variety of physical mechanisms and, because of this, is a rather poorly understood and mathematically complex process. Comprehensive analyses of coagulation processes have been performed by Berry and Reinhardt (1974). Coagulation can be considered an important initiator of precipitation in single-phase clouds (water or ice). In mixed-phase clouds, the Bergeron-Findeisen process can be expected to enhance the coagulation process by widening the droplet size distribution, as well as contributing to precipitation growth in a direct sense.

Once a moderate number of precipitation-sized elements have been generated, the process of accretion rapidly begins to dominate as a means for generating precipitation water. As noted previously, this process occurs by the "sweeping" action of large hydrometeors falling through the field of smaller elements, attaching them on the way. As was the case with coagulation, the

---

[6]Coagulation is often referred to as autoconversion in the cloud-physics literature. It is interesting to notice in this context that, while coagulation tends to accumulate nucleated pollutants, the Bergeron-Findeisen process tends to re-liberate nucleated pollutants to the air.

accretion process tends to accumulate the pollutant burden of all collected elements.

Accretion can occur via drop-drop, drop-crystal, and crystal-crystal interactions. Drop-crystal interactions are particularly important in mixed-phase clouds; when supercooled droplets are accreted by falling ice crystals, the process is usually referred to as riming.

Although the above discussion has been confined primarily to deposition in conjunction with rain and snow, it should be emphasized that fog deposition often is an important secondary process for conveying pollutants to the Earth's surface. A "fog" is (rather pragmatically) defined here as any cloud adjacent to the Earth's surface. Classification of fog-bound pollutant deposition is problematic for two major reasons. The first of these is that no sharp demarcation exists between "fog droplets" and "water-containing aerosols;" thus, the choice of considering fog deposition as simply the dry-deposition of wet particles, or the wet-deposition of contaminated water depends primarily on personal preference. Secondly, no real distinction exists between fog droplets and precipitation. Cloud physicists often find it convenient to categorize condensed atmospheric water into "precipitation" and "cloud" classifications, with the presumption that cloud water has a negligible sedimentation velocity. Such a classification is of limited use when we consider fog deposition, however, because fog droplets do have significant gravitational fall speeds. A 50-micron diameter fog droplet, for example, will fall at a rate of about 10 cm s^{-1}. This, combined with the fact that typical fogs and clouds contain droplet-size distributions ranging between 0 to 100 microns (Pruppacher and Klett 1978), suggests that gravitational transport of fog droplets will indeed be a significant pollution-deposition pathway under appropriate circumstances.

In addition to purely gravitational transport, fog droplets have a strong tendency to impact on projected surfaces. The rates of fog impaction depend in a complex fashion upon drop size, wind velocity, and geometry of the projected object. The common observations of rime-ice accumulation on alpine forests and on power-transmission lines give direct testimony to the effectiveness of this process.

Chemical deposition by fogs is directly proportional to fog-bound pollutant concentration, and this fact often acts to enhance substantially the pathway's overall effectiveness. Owing to their proximity to the Earth's surface, fogs typically form in conjunction with high pollutant concentrations. Attaching particles and gases via the variety of mechanisms described in Section 6.2.3, the droplets typically accumulate extremely high burdens of material. It is not difficult to find evidence to support this point. Scott and Laulainen (1979), for example, reported sulfate and nitrate concentrations approaching 500 $\mu m\ \ell^{-1}$ in water obtained near the bases of clouds over Michigan, while the SUNY group has reported (Falconer and Falconer 1980) numerous similar concentrations (as well as extremely low pH measurements) in clouds sampled at the Whiteface Mountain, NY, observatory.

Recently, Waldman et al. (1982) have reported nitrate and sulfate concentrations in Los Angeles fogs ranging up to and beyond 5000 $\mu m\ \ell^{-1}$. This

compares with typical precipitation-borne concentrations of about 35 μm ℓ^{-1} for the northeastern United States.

Lovett et al. (1982) have applied a simple impaction model to estimate fog-bound pollutant deposition to subalpine balsam fir forests, and have concluded that chemical inputs via this mechanism exceed those by ordinary precipitation by 50 to 300 percent. This is undoubtedly an extreme case, and it would be more meaningful to possess a regional assessment indicating the general importance of fog deposition on an areal basis. This requires substantial effort, however, involving climatological fogging analysis (Court 1966) as well as numerous additional factors, and no really satisfactory evaluation of this type is presently available. Regardless, it is appropriated to conclude that fog-deposition processes probably play an important, if secondary role in pollutant delivery on a regional basis. In the future, more effort should address this important research area.

6.2.6 Combined Processes and the Problem of Scavenging Calculations

The preceding discussion of individual steps in the scavenging sequence has been intentionally presented on a highly visual and non-mathematical basis, with appropriate references given for the reader interested in more detailed pursuit. Despite the qualitative nature of this presentation, however, it should be obvious that the most direct and expedient approach to model development is first to formulate mathematical expressions corresponding to each of these steps, and then to combine them in some sort of a model framework that describes the composite process. This subject will be examined in greater detail in Section 6.5, which specifically addresses scavenging models.

6.3 STORM SYSTEMS AND STORM CLIMATOLOGY

In the present text the term "storm" is intended to denote any system in which precipitation occurs. This definition thus encompasses all occurrences, ranging from mild precipitation conditions up to and through the major and cataclysmic events.

6.3.1 Introduction

From the preceding discussion, it is easy to imagine that scavenging rates and pathways will be dictated to a large extent by the basic nature of the particular storm causing the wet removal to occur. Storms containing water that is predominantly in the ice phase, for example, will provide little opportunity for attachment mechanisms associated with droplet nucleation, accretion, or phoretic processes. The abundance of liquid water and the temperature distribution in a given storm will have a direct bearing on the degree to which aqueous-phase chemistry can occur. Storms containing no ice phase whatsoever will be generally ineffective as generators of precipitation, and thus will tend to inhibit the scavenging process. An interesting indication of the importance of storm type in this regard is presented in Figure 6-23 (see Section 6.5.4), which presents estimated scavenging efficiencies which vary extensively with storm classification. Different storm types differ profoundly with regard to inflow, internal mixing,

vertical development, water extraction efficiency, and cloud physics; consequently it is appropriate at this point to consider briefly the major classes and climatologies of storm systems occurring over the continental United States.

Two major points should be stressed at the outset of this discussion. The first of these is the essential fact that all storms are initiated by a cooling of air, which leads to a condensation process. Such cooling may occur by the transport of sensible heat, such as when a comparatively warm, moist air parcel flows over a cold land surface. The dominant cooling mode for most storm systems, however, is expansion, which occurs via vertical motion of the air parcel to elevations of lower pressure. The second noteworthy point in this context is that the overwhelming majority of storm systems is strongly associated with fronts between one or more air masses. The primary reason for this association is that thermodynamic perturbations and discontinuities associated with the frontal surfaces provide the opportunity for vertical motion (and thus expansion processes) to occur. This relationship is an essential component of storm classification systems, and will emerge repeatedly in the following discussion.

Overlaps in the characteristics of different storm types render a strict classification largely impossible. For practical purposes, however, it is convenient to segregate midlatitude continental storms into two classes, which are usually described as being "convective" and "frontal." These two major categories then can be subdivided further as deemed expedient for the purpose at hand, although it should be noted that significant overlap among storm types occurs even at this major level of classification. Frontal storms, for example, often possess significant convective character in their basic composition, and true convective storms often occur as the consequence of fronts. Because of this, the following discussion will use storm classification primarily as a descriptive aid and will not belabor taxonomic detail.

6.3.2 Frontal Storm Systems

Much of what is understood today regarding midlatitude frontal-storm systems stems from the pioneering work of the Norwegian meteorologist Bjerknes, who conducted a systematic survey of large numbers of storm systems and from this survey developed a conceptual model of frontal-storm development and behavior. Characterized schematically in Figure 6-5, the Bjerknes model can be understood most easily by considering a cool northern air mass, separated from a warm southern air mass by an east-west front, as indicated in Figure 6-5a. The progression of figures represents a typical result of the atmosphere's natural tendency to exchange heat from southern to northern latitudes across this front. This is often referred to as a "tongue" of warm air intruding into the cold air mass. In the northern hemisphere this wave will tend to propagate in an easterly direction; thus, the intrusion is bound by two moving fronts--a warm front followed by a cold front--as shown in Figure 6-5c.

Flows associated with the wave system occur in a manner such that a depression in atmospheric pressure occurs at the vertex of the warm-air intrusion;

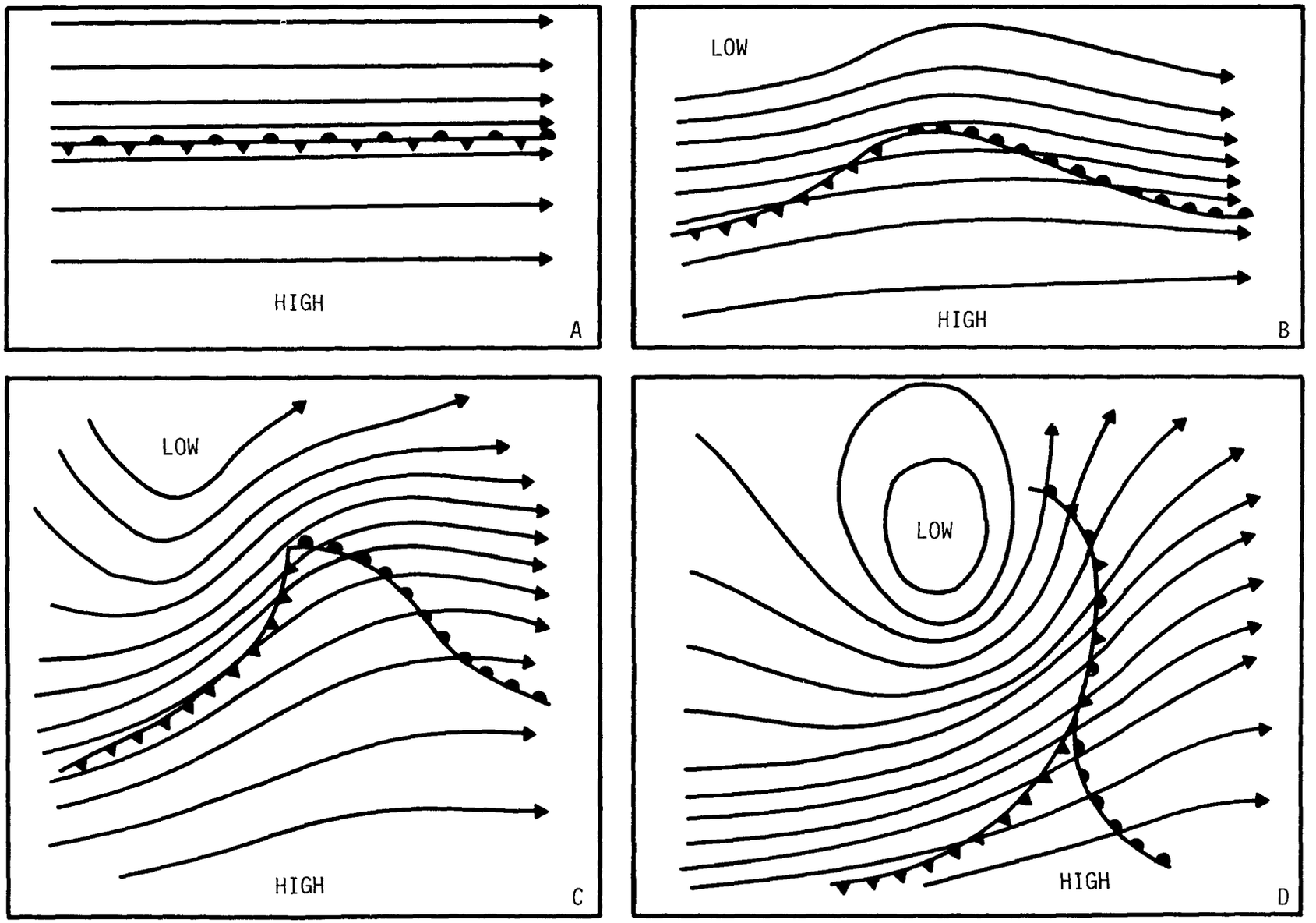

Figure 6-5. Cyclonic storm development according to Bjerknes's conceptual model.

as a consequence a general counterclockwise or "cyclonic" circulation pattern emerges. Because of this feature, Bjerknes's conceptual model is often referred to as the "Bjerknes cyclone theory," and frontal storms associated with this pattern are termed "cyclonic" storms. A typical feature of storms of this type is the tendency for the cold front to overtake the warm front and ultimately annihilate the wave. The "occluded" front created as a consequence of this behavior is shown schematically in Figure 6-5d. In view of this birth-death sequence of the Bjerknes cyclone model, the progression depicted in Figure 6-5 often has been termed the "life history" of a cyclone. Some idea of spatial scale and the general cyclonic flow pattern of a mature cyclone are given in Figure 6-6. In viewing these indicated flow patterns, however, the reader should note carefully that considerable vertical structure exists in such systems, and marked deviations of the wind field with elevation are typical. In particular, one should take care not to confuse the indicated general circulation patterns with corresponding surface winds.

Although created from the limited observational base available during the early twentieth century, the fundamental precepts of the Bjerknes theory have proven valid even as more sophisticated observational and analytical facilities have become available. Certainly non-idealities and deviations from this model occur; but its general concepts have proven to be immensely valuable as a conceptual basis and as an idealized standard for the assessment of actual storm systems. Comprehensive descriptive and theoretical material pertaining to such systems is available in the classic text by Godske et al. (1957), and more elaborate and modern extensions are given in the periodical literature (e.g., Browning et al. 1973, Hobbs 1978).

6.3.2.1 Warm-Front Storms--It is important to note that the plan views exhibited by Figure 6-6 are gross simplifications, since they do nothing to characterize the three-dimensional nature of the cyclonic system. If one were to construct a vertical cross section of the warm front (A-A' in Figure 6-6), then typically one would observe an inclined frontal surface as shown in Figure 6-7. (See Table 6-1 for definitions of cloud abbreviations.) In this situation the presence of warm air aloft creates a relatively stable environment, which inhibits vertical mixing of air between the two air masses. The warm, moist air moves up over the cold air wedge, expanding, cooling, and ultimately forming clouds and precipitation. Typically the warm air supplying moisture for this purpose has been advected from deep within the southern air mass, carrying water vapor and pollutant over extensive distances. This transport trajectory has been aptly compared to a "conveyor belt" for moisture by Browning et al. (1973). It is appropriate to note that this moisture conveyor belt is a conveyor belt for pollution as well.

Warm-front storms are often associated with long periods of continuous precipitation, although significant structure can exist within such systems. Important structurally in this regard are the prefrontal rain bands, which take the form of concentrated areas of precipitation embedded within the major storm system. At present, the factors contributing to rain-band formation are not totally understood, although mechanisms such as seeding from aloft by ice crystals and nonlinearities of the associated thermodynamic and flow processes undoubtedly contribute to a major extent.

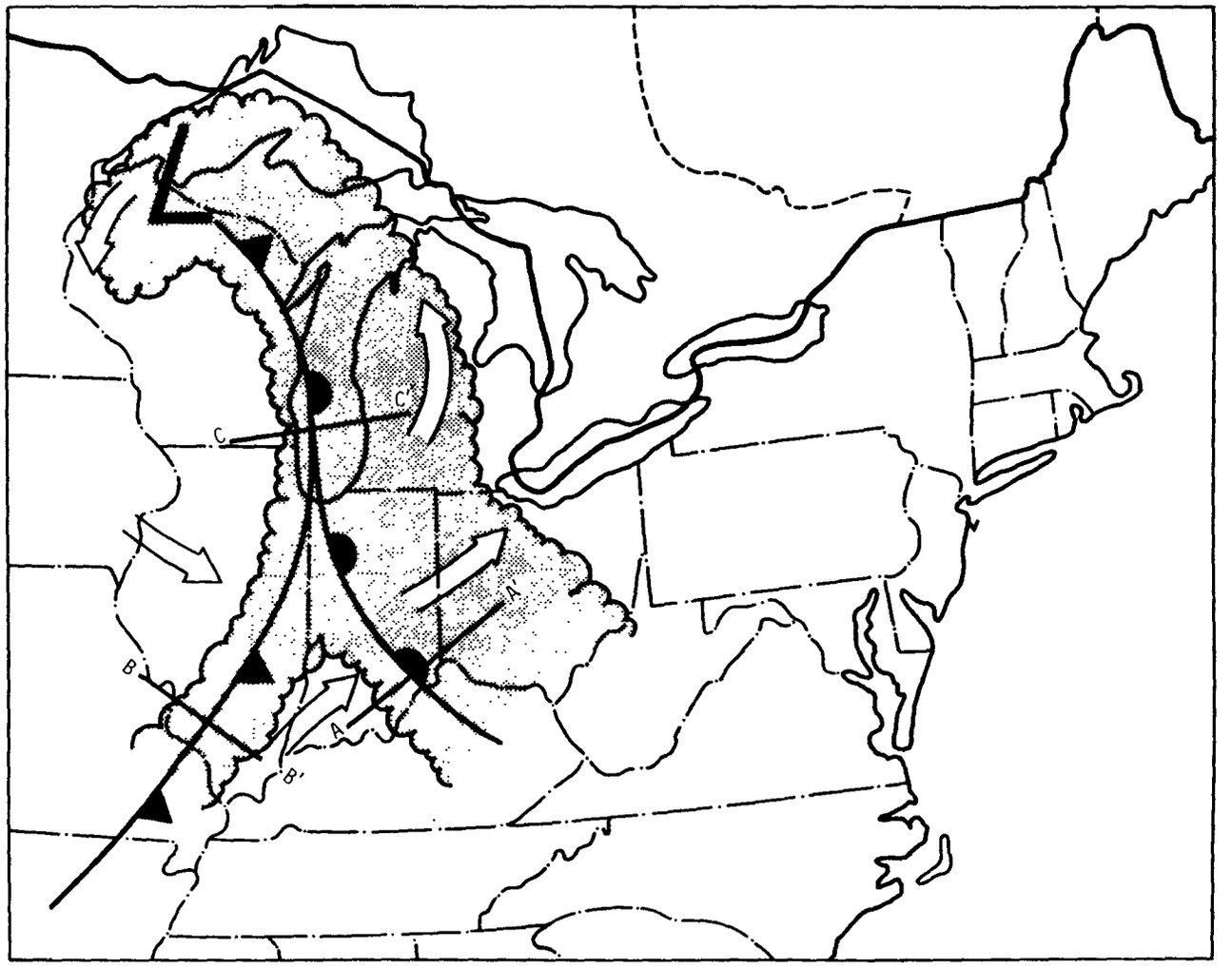

Figure 6-6. General flow patterns in the vicinity of an idealized cyclonic storm system. Arrows denote general circulation patterns and should not be interpreted as surface winds (cf. Figures 6-7, 6-8, and 6-9).

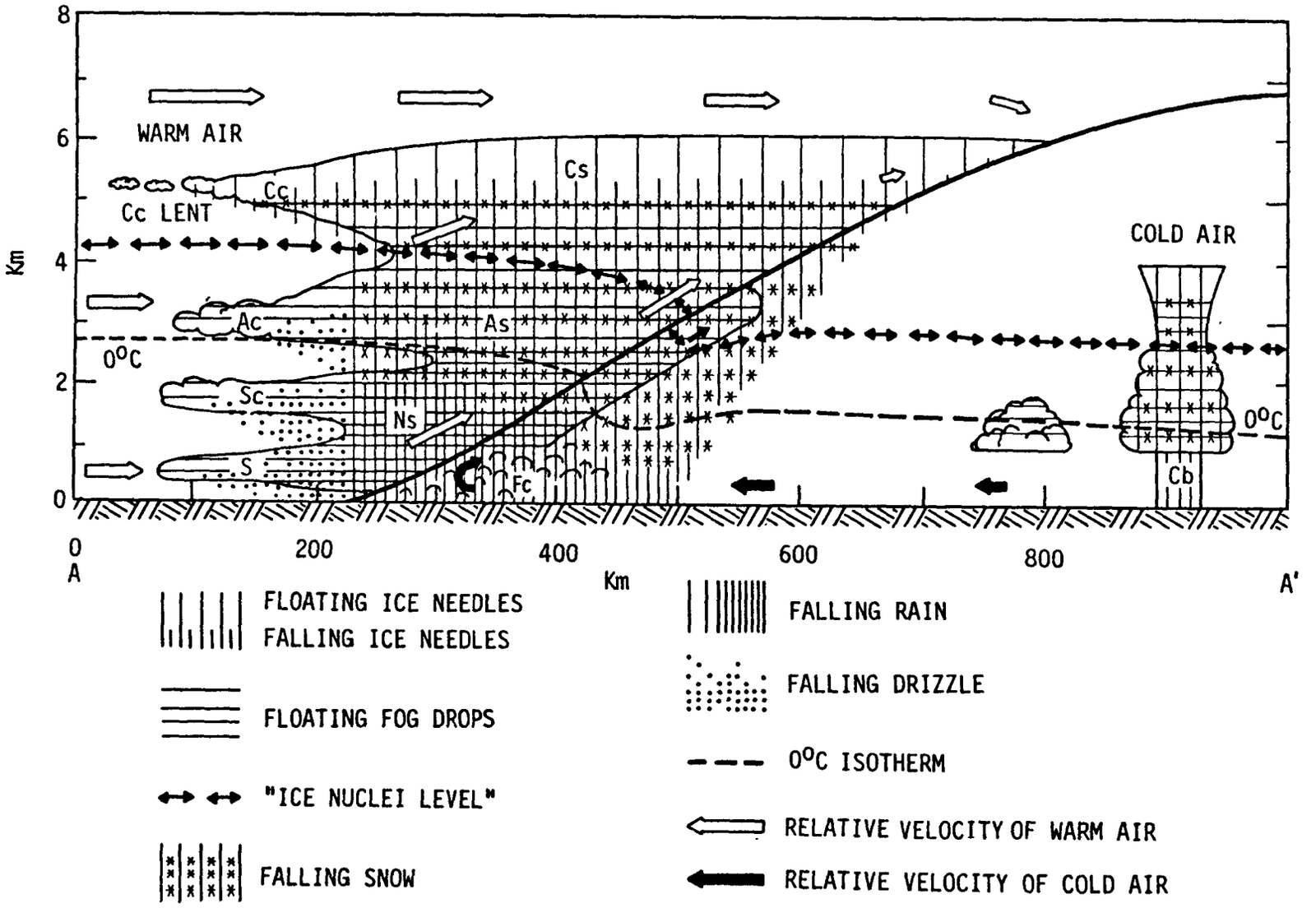

Figure 6-7. Vertical cross section of a typical warm front (Section A-A' on Figure 6-6). Adapted from Godske et al. (1957).

TABLE 6-1. SUMMARY OF CLOUD TYPES APPEARING IN FIGURES 6-7 THROUGH 6-9

Type	Abbreviation
Cirrus	Ci
Cirrostratus	Cs
Cirrocumulus	Cc
Altostratus	As
Atlocumulus	Ac
Stratus	St
Stratocumulus	Sc
Nimbostratus	Ns
Cumulus	Cu
Cumulonimbus	Cb

Warm-front storms usually can be expected to be rather effective as scavengers of pollution originating from within the warm air mass, especially if temperatures in the feeder region are sufficiently high to allow the presence of liquid water and the nucleation-accretion process. Scavenging of pollutants from the underlying cold air mass will usually be less effective, owing to the relative scarcity of clouds and generally less definitive flows in this sector. Scavenging in both regions will of course depend upon the physiochemical nature of the pollutant of interest and the microphysical attributes of the cloud system in general. Methods for estimating scavenging rates in such circumstances are discussed in Section 6.5.

6.3.2.2 Cold-Front Storms--A typical vertical cross section (B-B' in Figure 6-6) of a cold-front storm is shown in Figure 6-8. This differs substantially from the warm-front situation in the sense that, instead of flowing over the frontal surface, the warm air is forced ahead by the moving cold air mass. This action produces a more steeply inclined frontal surface that, combined with the presence of low-elevation warm air, creates a relatively unstable situation leading to convective uplifting and the formation of clouds and precipitation.

Although discussed here in a frontal-storm context, this precold-front situation composes an important class of convective storms, which will be discussed in some detail later. Scavenging rates and efficiencies associated with such storm systems will again depend upon the pollutant and the physical attributes of the particular cloud system involved.

6.3.2.3 Occluded-Front Storms--Because occluded fronts are formed via merger of warm and cold fronts, it seems reasonable to expect that storms associated with occlusions should share characteristics of the respective elementary systems. Figure 6-9, which shows a typical vertical cross section (Section C-C' on Figure 6-6) of an occluded system, demonstrates this point. Typically the easterly flow of warm air aloft maintains a relatively stable environment to the east of the occlusion, and clouds and precipitation occur in this region largely as a consequence of ascending flow from the south. Much more detailed accounts of occluded systems can be found in standard references such as the book by Godske et al. (1957).

6.3.3 Convective Storm Systems

An idealized cross section of a typical convective storm is shown in Figure 6-10. Such storms depend upon atmospheric instabilities to induce the necessary vertical motions and concurrent cooling and condensation processes; and as such they are most likely to occur under warm, moist conditions where the energetics are most conducive to this process. Often convective storm systems occur as "clusters" of cells, such as that shown in Figure 6-10, and exhibit a marked tendency to exchange moisture and pollutant between cells; thus, the flow dynamics and scavenging characteristics of such systems tend to be extremely complex.

Typically the moisture and pollutant input to a convective cell occurs primarily through the storm's updraft region (cf., Figure 6-10), although entrainment from upper regions is possible as well. Dynamics of this process

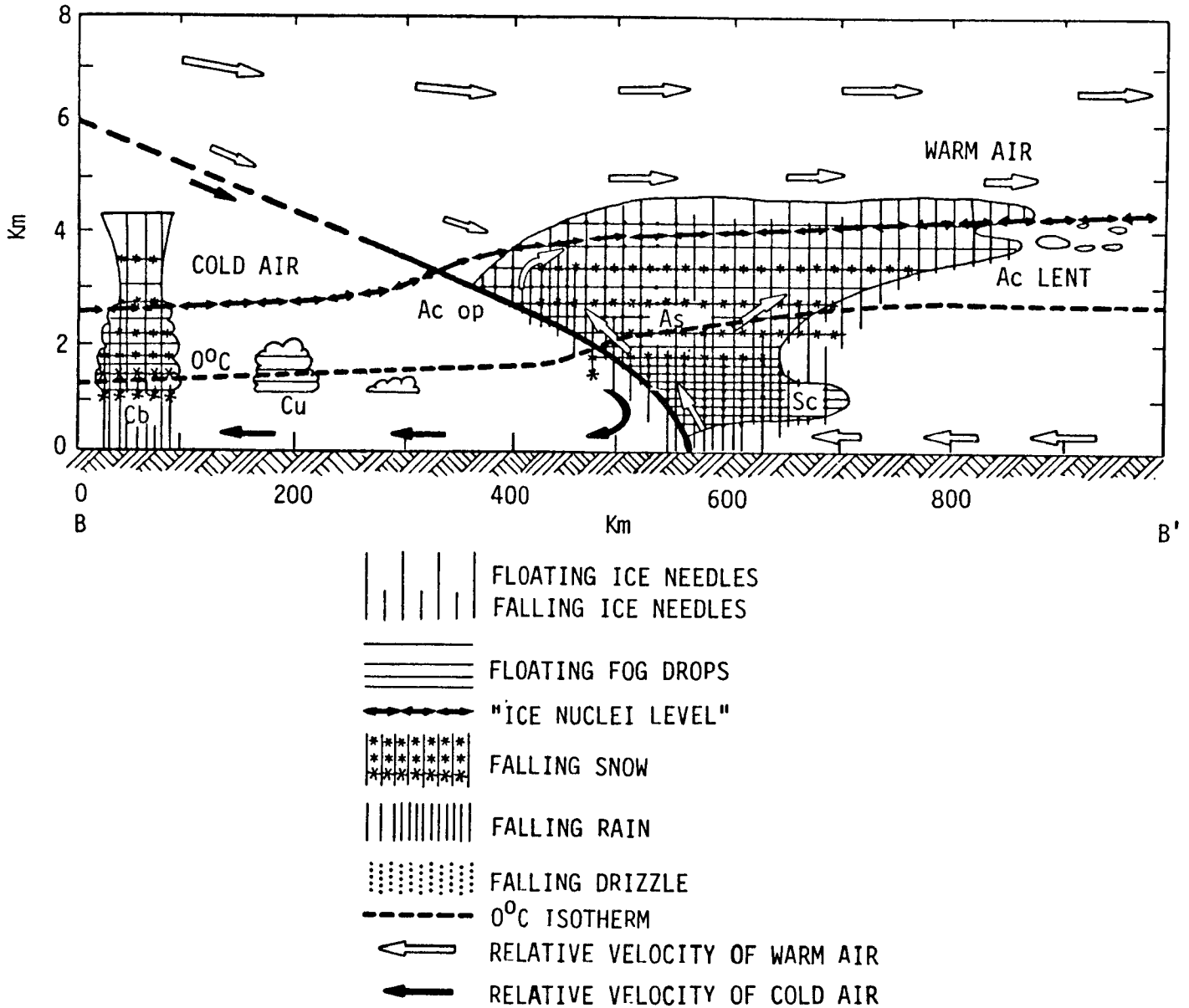

Figure 6-8. Schematic vertical cross section of a typical cold front (Section B-B' on Figure 6-6). Adapted from Godske et al. (1957).

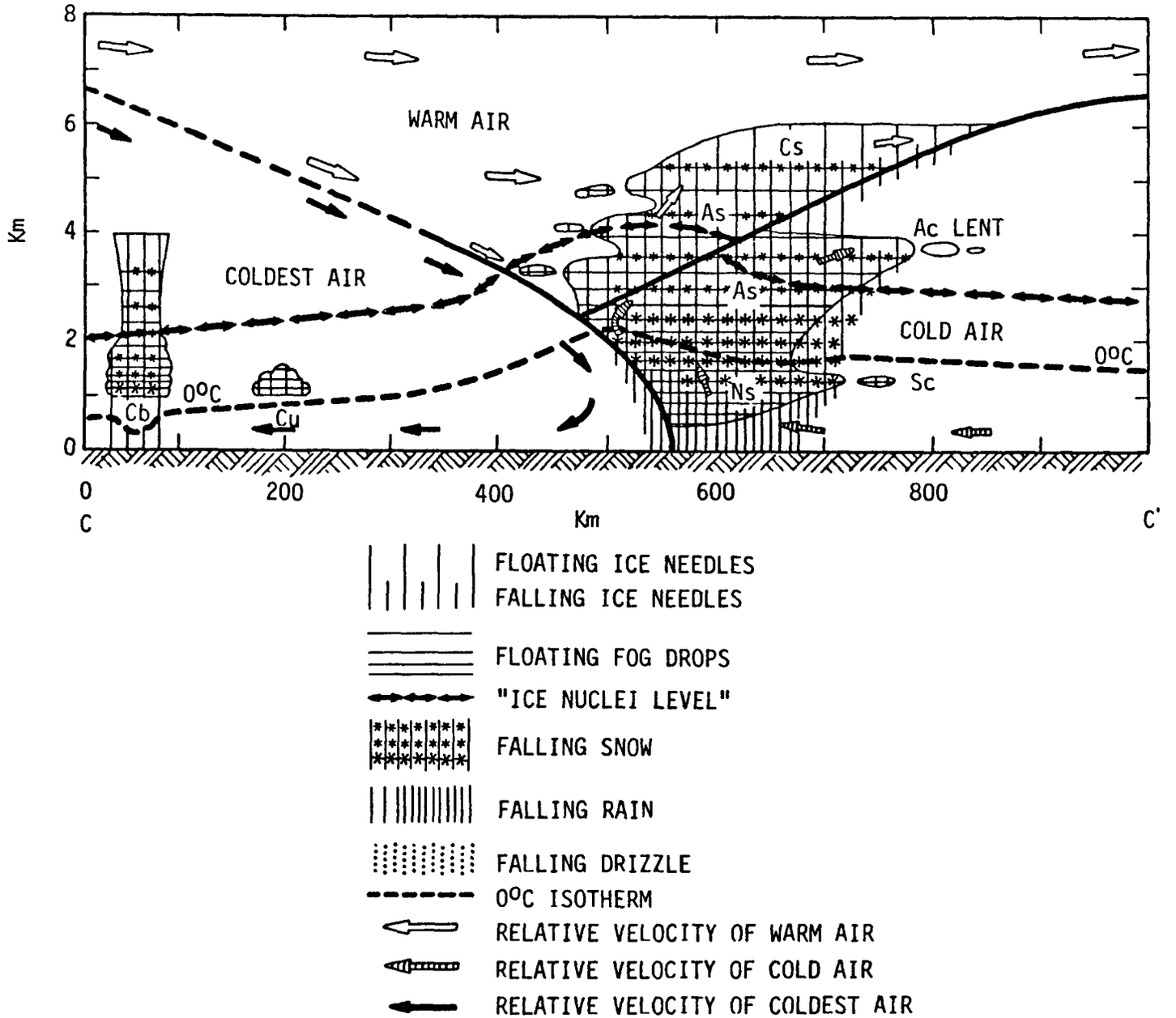

Figure 6-9. Schematic vertical cross section of a typical occluded front (Section C-C' on Figure 6-6). Adapted from Godske et al. (1957).

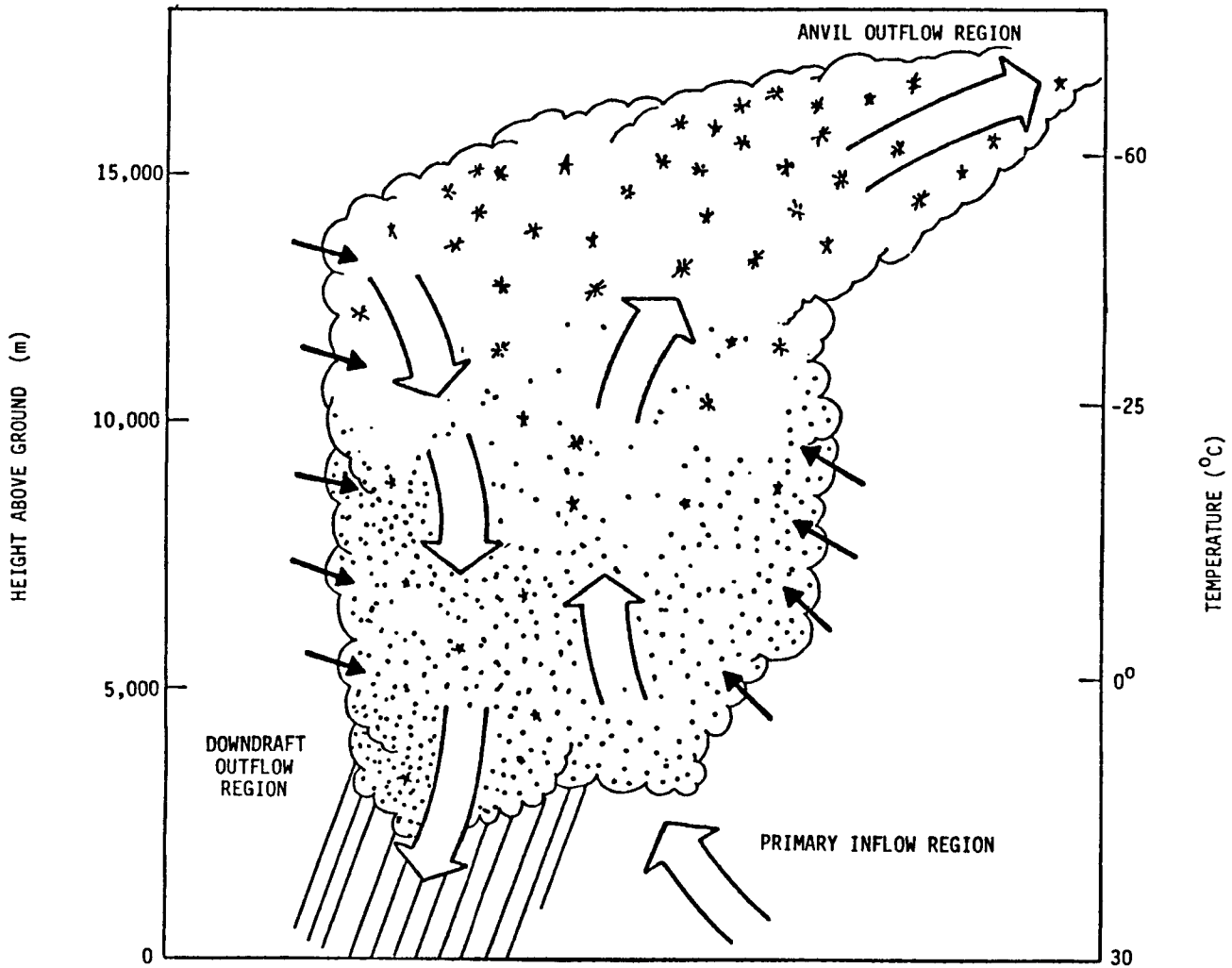

Figure 6-10. Idealized cross section of an isolated convective storm.

are such that violent updraft velocities often occur; these are capable of lifting entrained air, water vapor, and pollution to extremely high elevations (sometimes breaching the stratosphere). Along this course, entrained pollutant is subjected to a large variety of environments and scavenging mechanisms; as will be noted in Section 6.5, convective storms tend to be highly effective scavengers of air pollution.

As was stated earlier, convective storms often are associated with frontal systems, although frontal influence is not absolutely necessary for their presence. An isolated air mass, for example, is totally capable of acquiring sufficient energy and water vapor to induce a convective disturbance on its own accord. Perturbations arising from fronts, however, often contribute to the creation of convective activity--if for no other reason than supplying a "trigger" to initiate convection in a conditionally unstable atmosphere.

6.3.4 Additional Storm Types: Nonideal Frontal Storms, Orographic Storms and Lake-Effect Storms

As noted previously, the Bjerknes cyclone model represents something of an idealized concept, and numerous features can contribute to deviations from this "textbook" behavior. Orographic effects are highly important in this regard. Consider, for example, a cyclonic disturbance approaching the North American continent from across the Pacific Ocean; the frontal patterns typically lose much of their original identity after impacting with the western mountainous regions. In addition to the physical distortion of flow patterns, the lifting induced by the terrain encourages further precipitation, resulting in large spatial variability in rainfall patterns and pronounced local phenomena such as "rain shadows" and chinooks. Precipitation-formation and precipitation-scavenging processes associated with such systems tend to be highly complex.

Frontal systems often tend to reconstitute their structure after crossing the Rocky Mountains, but continental effects still impart a marked impact on their basic makeup. In the midwest-northeast region, for example, fronts tend to orient themselves in an east-west direction and become stationary for extended periods, often punctuated by several minor low-pressure areas. Even under relatively ideal conditions continental frontal storms tend to possess more convective flavor in their basic makeup than do their oceanic counterparts.

As indicated above, terrain-induced or "orographic" effects are usually most important in augmenting major storm systems, although relatively isolated orographic storms (such as oceanic "island-induced" storms) certainly do occur. Orographic effects obviously will tend to be most pronounced in regions where radical terrain changes occur; but even the small elevation changes typical of the Midwest can contribute significantly at times. Orographic effects also are suspected to influence storm behavior over substantial downwind distances. Lee waves from the Rocky Mountains, for example, have been suggested to trigger thunderstorm formation at extended distances.

Lake-effect storms are yet another example of a somewhat non-ideal phenomenon, which often is superimposed with more major meteorological patterns.

Typically such storms occur during fall and early winter, when land surfaces tend to be cooler than their adjoining water bodies. Considering an air parcel moving on an easterly course across Lake Michigan, for example, one can note that the warm lake surface should supply both heat and water vapor as it proceeds. As this parcel is advected across the downwind shore, however, two important things will occur. First, the cold land mass will extract heat from the air; second, the orographic lifting (on the order of a few tens of meters) will result in ascent, expansion, and further cooling. The net result is a lake-effect storm. Such storms can induce highly variable precipitation patterns in specific areas around the Great Lakes region. Although confined largely to this portion of the United States, these storms account for a majority of the snowfall that accumulates in specific cities such as Muskegon, MI, and Buffalo, NY. Some appreciation for the magnitude of this effect can be gained by viewing the climatological precipitation map given in Figure 6-11.

6.3.5 Storm and Precipitation Climatology

The exceedingly complex subject of storm climatology will be discussed here only to the point necessary to describe some key attributes and indicate references for more detailed pursuit. Factors especially important in the context of precipitation scavenging are temporal and spatial precipitation patterns, storm-trajectory behavior, and storm-duration statistics. These will be discussed in the following paragraphs.

6.3.5.1 Precipitation Climatology--Figure 6-12 provides climatological averages of monthly precipitation amounts at various stations throughout the United States. This figure, taken directly from the U.S. Climatological Atlas (1968), requires little elaboration at this point. It is interesting to note, however, that precipitation amounts do not vary radically throughout the year at most northeastern U.S. stations; this contrasts especially with the arid western stations, whose seasonal variabilities tend to be pronounced. It should be noted as well that actual precipitation amounts for a given single month can vary appreciably from the climatological averages presented here.

6.3.5.2 Storm Tracks--Because of the difficulties noted previously with regard to precise classification or definition of storms, a truly concise climatological summary of storm-pathway behavior is largely impossible. Some useful information can be generated, however, by observing the tracks of the cyclonic (low-pressure) centers associated with major storm systems. Klein (1958), for example, has conducted a systematic survey of cyclonic centers in the northern hemisphere and from this has constructed monthly climatological maps of low-pressure tracks. Figure 6-13, taken from the book by Haurwitz and Austin (1944), presents the combined results of the analyses by several previous authors. On the basis of the previous discussion it should be reemphasized that, owing to the complex flow processes associated with cyclonic systems, one should not interpret the motion of these low pressure centers as being identical with feeder trajectories for the storms themselves. Successful interpretation of such information in the context of source-receptor analyses requires careful and skilled meteorological guidance.

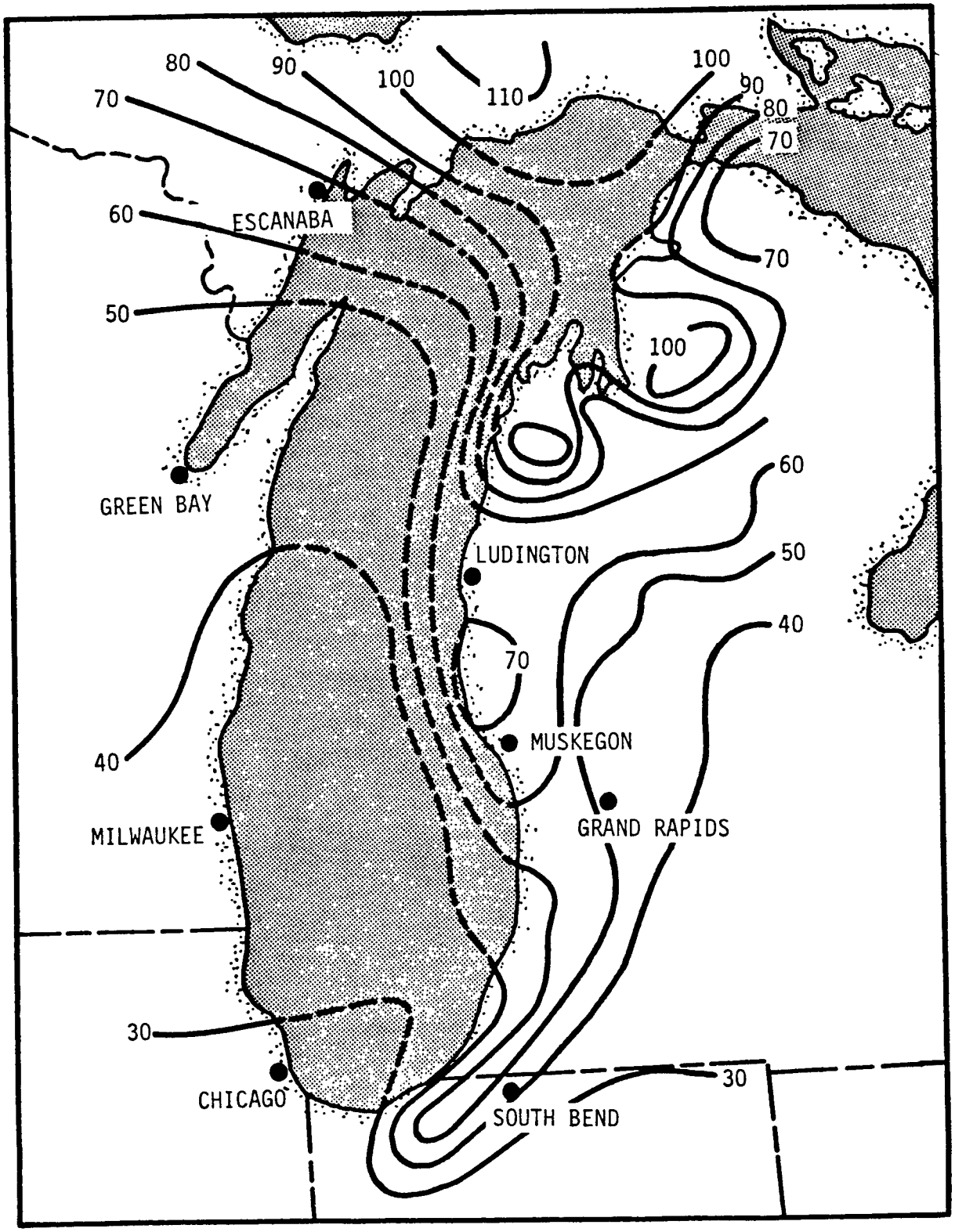

Figure 6-11. Average annual snowfall pattern (inches) over Lake Michigan and environs. Adapted from Changnon (1968).

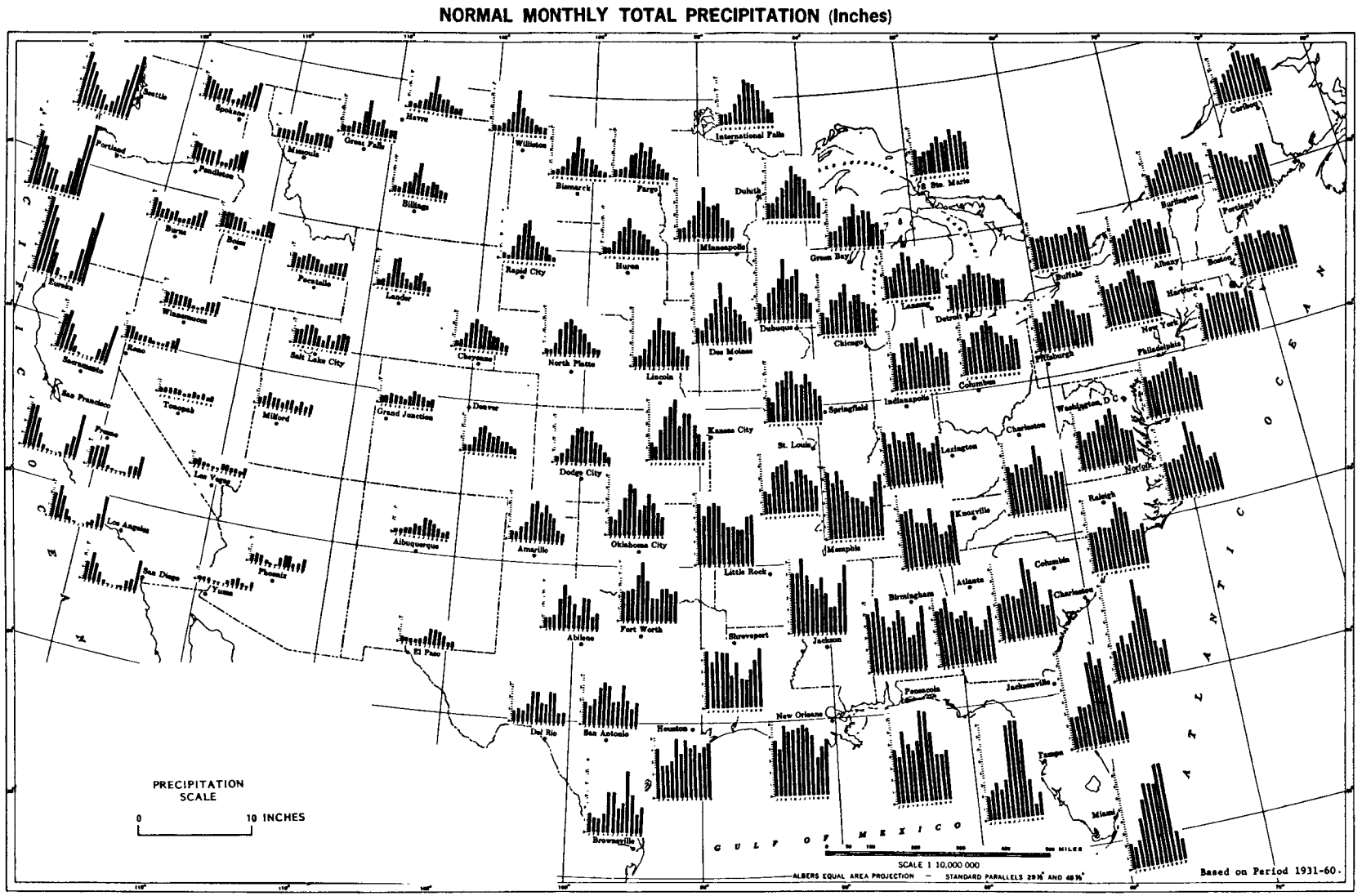

Figure 6-12. Climatological Summary of U.S. Precipitation. From U.S. Climatological Atlas (1968).

Several additional points should be emphasized in the context of Figure 6-13. Firstly, it should be noted that this presents a long-term composite average and that marked deviations from this pattern can be expected to occur with season. Secondly, the statistical variability of storm tracks is such that substantial departures from the long-term averages can be expected for any particular year. Finally, substantial evidence documents longer-term shifts in average storm-track distributions (Zishka and Smith 1980); thus, presentations (such as Figure 6-13) that are based upon historical data may vary considerably from storm patterns to be observed over the next twenty years. The implications of this with regard to long-term acidic deposition forecasting are obvious.

Additional features of cyclonic storm climatology can be found in standard climatological textbooks (e.g., Haurwitz and Austin 1944). Convective-storm climatology, which tends to be much more region-specific, can be evaluated from such references as well, although more recent weather modification programs such as METROMEX, NHRE, and HIPLEX have generated a considerable amount of new information in this area.

6.3.5.3 Storm Duration Statistics--In preparing regional scavenging models, it often is desirable to create some sort of statistical average of storm characteristics so that "average" wet-removal behavior can be defined. Although little activity has been devoted to this area until very recently, the usefulness of such an approach to regional model development suggests accelerated effort during future years.

The analysis by Thorp and Scott (1982) provides an example of one such effort. These authors compiled data from hourly precipitation records from northeastern U.S. stations to obtain seasonally-stratified duration statistics, which were expressed in terms of probability plots as shown in Figure 6-14. As can be noted from these plots, "average" storm durations during summertime are significantly less than durations of their wintertime counterparts, reflecting relative influences of short-term convective behavior. Some of the references given in Section 6.5 suggest potential modeling applications for these statistical summaries.

6.4 SUMMARY OF PRECIPITATION-SCAVENGING FIELD INVESTIGATIONS

For the purposes of this document "field investigations" of precipitation-scavenging mechanisms will be differentiated from routine precipitation-chemistry network measurements, which are intended primarily for characterization purposes. Of course a great deal of overlap occurs between these two classes of measurements, and significant reciprocal benefit is generated as a consequence of each. Some essential differences exist between the two, however, and it is convenient for present purposes to segregate them accordingly.

The primary distinguishing feature of a scavenging field investigation is that the study usually is designed around the basis of some sort of conceptual or interpretive model(s) of scavenging behavior, which is tested on the basis of the field data. If the model predictions and data disagree, then some basic precepts of the model must be invalid, and additional

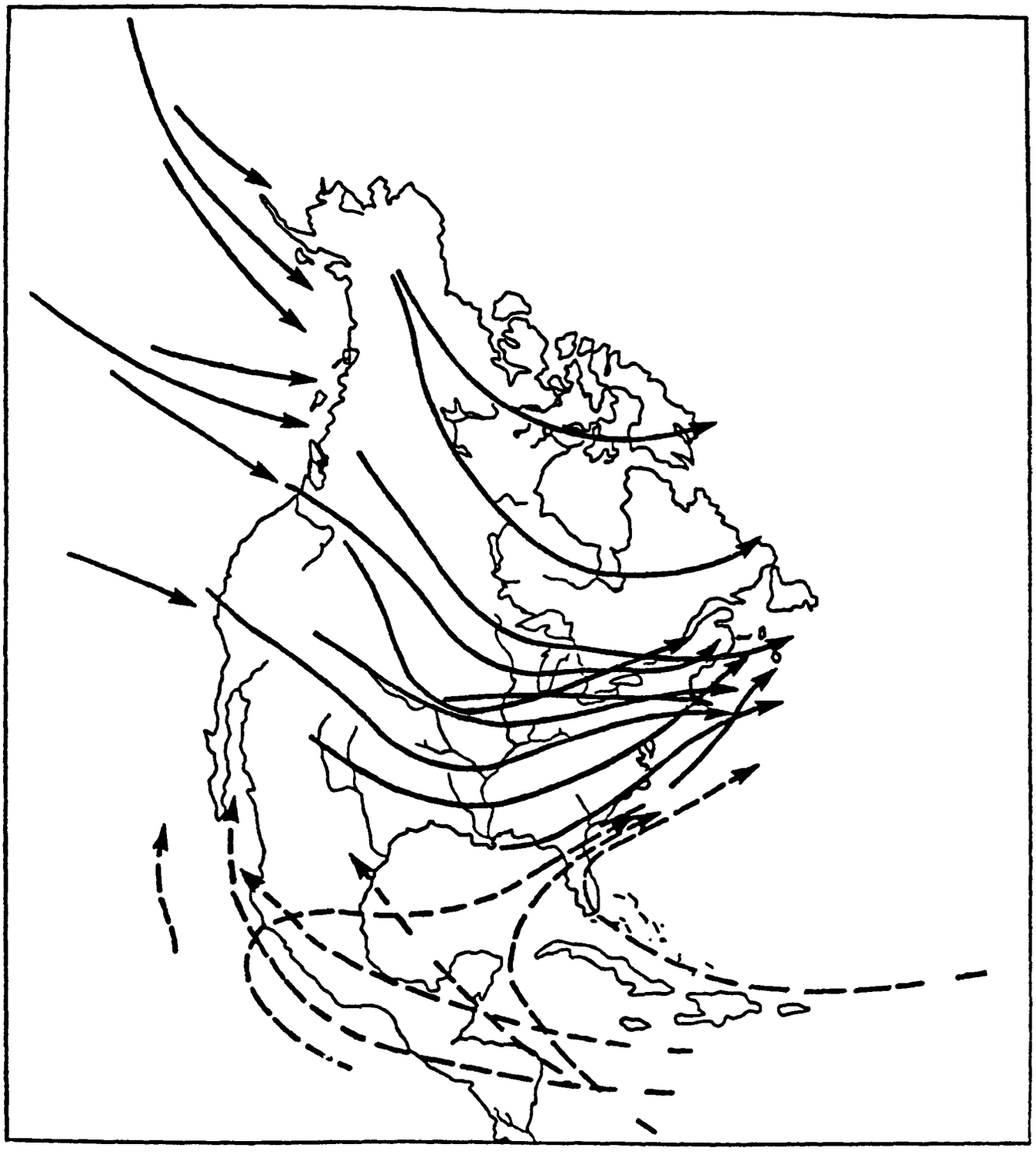

Figure 6-13. Major climatological storm tracks for the North American continent. Adapted from Haurwitz and Austin (1944). Dashed lines denote tropical cyclone centers, and solid lines denote those of extratropical cyclones.

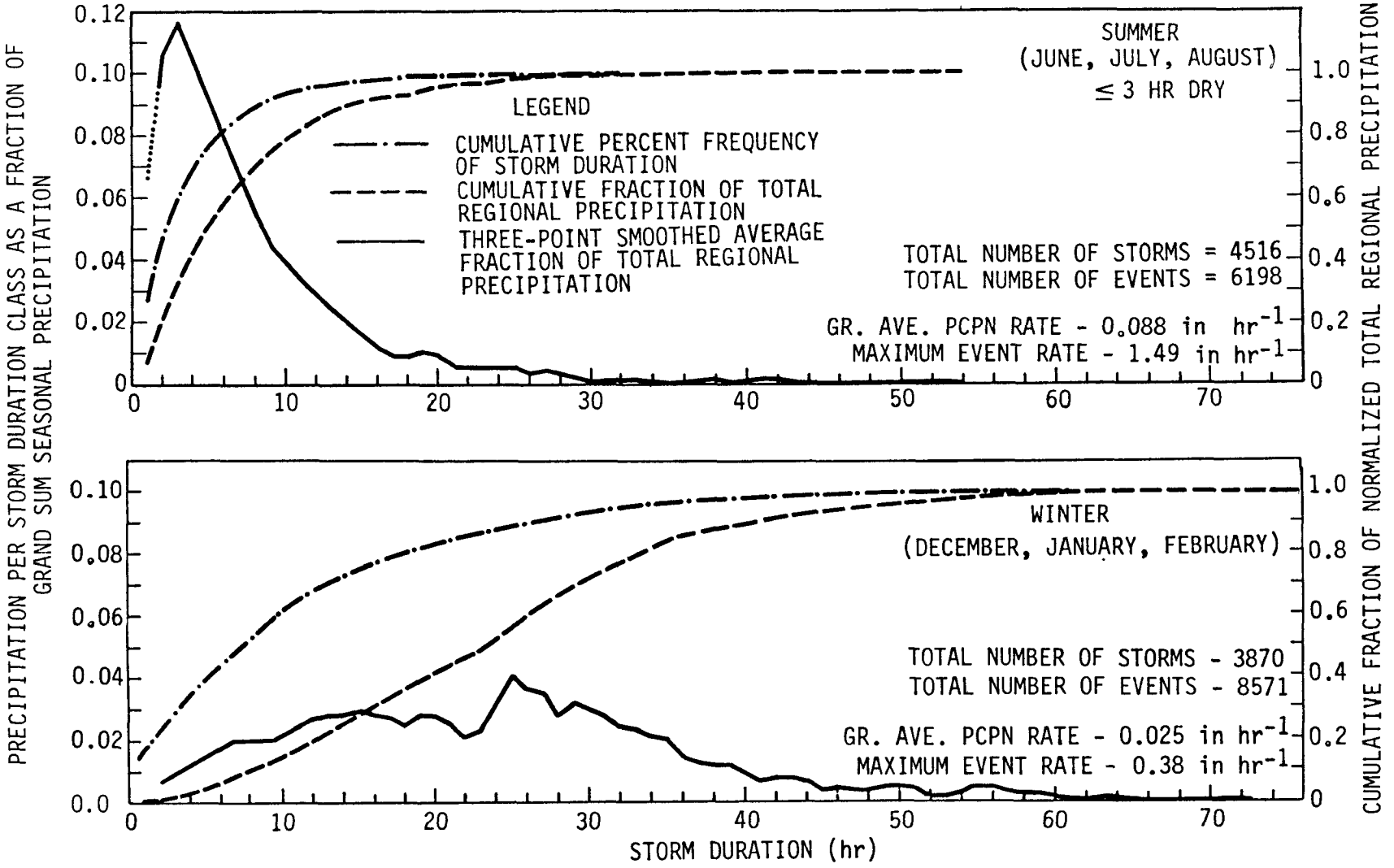

Figure 6-14. Frequency statistics for storm duration, cumulative fraction of total regional precipitation, and smoothed average fraction of total regional precipitation. Data from MAP3S region. Summer (top) frequency analysis allows up to 3 consecutive hours without precipitation to be counted as part of one storm. Winter (bottom) frequency analysis allows up to 6 consecutive hours without precipitation to be counted as part of one storm.

mechanistic insights must be generated to rectify the situation. In the event that predictions and data agree, then this may be taken as evidence that the precepts may be correct. Regardless of whether positive or negative results are obtained (and assuming that the field study has been well-designed and well-interpreted), an advance in understanding has been achieved. The importance of such input cannot be overemphasized. Examples exist wherein field investigations have demonstrated then-accepted models to be in error by several orders of magnitude (e.g., Hales et al. 1971). Field studies have been essential in keeping the models "honest."

Field studies of precipitation scavenging were begun in earnest during the early 1950's for the primary objective of radioactive-fallout assessment. Pioneering studies in this area that pertained to radioactive pollutant releases from point sources in anticipation of reactor accidents and related phenomena were performed in England by Chamberlain (1953). These constituted the basis for the washout-coefficient approach to scavenging modeling (see Section 6.5). Other studies focused primarily on nuclear-detonation fallout, thus approaching the scavenging problem from a more global point of view.

Following the English lead, nuclear-oriented studies were conducted by the United States, Canada, and the Soviet Union. These included studies of tracers as well as those of the radionuclides themselves; and although some of this material still remains in the classified literature, it may be stated with certainty that most of what we know today regarding scavenging processes has been generated as a consequence of the nuclear era. The review "Scavenging in Perspective" by Fuquay (1970) presents a comprehensive account of this early stage of scavenging field studies.

During the late 1960's field-experiment emphasis shifted to more conventional pollutants, with the general recognition of precipitation scavenging's importance in preserving atmospheric quality and its potential adverse impacts of deposition on the Earth's ecosystem. Since that time a variety of large and small field studies has been conducted. These are summarized in Table 6-2, which provides a logical classification in terms of source type, pollutant type, and geographical scale.

Although field studies have been focused strongly on quantitative aspects of precipitation scavenging, they have provided important qualitative information regarding acidic-precipitation processes as well. The ensemble of studies listed in Table 6-2 presents a rather cohesive base of evidence in this regard; and although some conflicting results and uncertainties do exist, a generally coherent picture can be constructed in several important areas. Although there is considerable overlap of source-receptor distance scales among these studies, they tend to group rather conveniently into three classes of areal extent: 0 to 20 km, 0 to 200 km, and 0 to 2000 km. These classes shall be termed loosely as "local," "intermediate," and "regional" scales in the following discussion, where key qualitative features are illustrated by considering the fate of specific acidic-precipitation precursors (SO_x, NO_x, and HCl) as they are transported over these increasing scales of time and distance.

TABLE 6-2. SUMMARIES OF SOME PRECIPITATION SCAVENGING FIELD INVESTIGATIONS

General source type	Specific source type	Selected references
Continuous Point Source	Tower releases of aerosols	Chamberlain (1953), Engelmann (1965), Dana (1970)
	Tower releases of radioactive gases and simulated tracers	Chamberlain (1953), Engelmann (1965)
	Tower releases of SO_2	Dana et al. (1972), Hales et al. (1973)
	Tower releases of tritiated water vapor	Dana et al. (1978)
	Tower releases of organic vapors	Lee and Hales (1974)
	Power-plant plumes	Dana et al. (1973, 1976, 1982), Granat and Rodhe (1973), Granat and Soderlund (1975), Hales et al. (1973), Barrie and Kovalick (1978), Hutcheson and Hall (1974), Enger and Hogstrom (1979), Radke et al. (1978)
	Smelter plumes	Kramer (1973), Larson et al. (1975) Millan et al. (1982), Chan et al. (1982)
"Instantaneous" and/ or Moving Sources	Aircraft releases of rare-earth tracers	Dingle et al. (1969), Slinn (1973), Young et al. (1976), Gatz[a] (1977), Changnon et al. (1981)
	Rocket releases of radioactive tracers	Shopauskas et al. (1969), Burtsev et al. (1976),

TABLE 6-2. CONTINUED

General Source Type	Specific Source Type	Selected References
Urban Sources	Uppsalla, Sweden	Hostrom (1974)
	St. Louis, MO Los Angeles, CA	Hales and Dana (1979a) Morgan and Liljestrand (1980)
General and Regional Sources	Regional pollution flowing into lake-effect storms	Scott (1981)
	General sources in western Canada	Summers and Hitchon (1973)
	Regional pollution in the eastern U.S. and Canada	MAP3S/RAINE (1981), Easter (1982), Mosaic (1979)
	Regional aerosol loadings at a specific receptor point	Graedel and Franey (1977), Davenport and Peters (1978)
Global and Stratospheric Sources	Cosmogenic radionuclides	Young et al. (1973)
	Nuclear fallout	Numerous studies; see Fuquay (1970)

[a]The reference by Gatz provides a comprehensive list of past tracer studies of precipitation scavenging.

On a local scale (0 to 20 km), field studies have generally demonstrated the precipitation scavenging of sulfur and nitrogen oxides from conventional utility and smelting sources to be minimal. The virtual absence of excess nitrate or nitrite ion in precipitation samples collected beneath such plumes (Dana et al. 1976) provides strong evidence that direct uptake of primary nitric oxide and nitrogen dioxide by precipitation and cloud elements is a negligibly slow process.

Nonreactive scavenging of plume-borne sulfur dioxide is solubility dependent and tends also to be a rather inefficient process, although it is definitely detectable in field studies conducted in relatively clean environments (Hales et al. 1973; Dana et al. 1973, 1976). This phenomenon, which is suppressed under conditions involving high rain acidity, is relatively well understood at present (Hales 1977, Drewes and Hales 1982).

Nonreactive scavenging of sulfate aerosol can be an efficient removal process. The preponderance of relevant field tests in Table 6-2, however, has demonstrated that wet deposition of sulfate from local power-plant and smelter plumes occurs rather slowly. This is undoubtedly a consequence of the small amounts of primary sulfate available for scavenging under such circumstances.

Field tests conducted under situations wherein sulfur trioxide was intentionally injected into the stack of a coal-fired power plant (Dana and Glover 1975) show correspondingly high sulfate scavenging rates, and it has been suggested that under certain operating conditions some types of power plants (especially oil-fired units) will produce sufficient primary sulfate to account for appreciable local deposition. To date, however, no really strong field evidence has supported this point. Hogstrom (1974) reported the observation of substantial sulfate scavenging from the local plume of an oil-fired power plant in Sweden, but these results are rather dependent upon the interpretation of background contributions. Granat and Soderlund (1975) performed a similar investigation in the vicinity of a second Swedish oil-fired plant and found a comparatively small scavenging rate.

Reactive scavenging of plume-borne sulfur dioxide to form rainborne sulfate is difficult to differentiate from primary sulfate removal. The previously noted findings of low excess sulfate in below-plume rain samples, however, suggest that neither process is particularly effective in near-source plume depletion.

The scavenging of hydrochloric acid to produce chloride and hydrogen ions in precipitation will most certainly be a highly effective process, depending upon the quantities of hydrochloric acid available. Considerable theoretical and laboratory work has been conducted in this area for space-shuttle impact assessment, and limited data suggest that hydrogen chloride is scavenged in measureable amounts from power-plant plumes (Dana et al. 1982).

With the exception of studies conducted under rather clean ambient conditions (e.g., Dana et al. 1973, 1976), the influence of background contributions has

made the interpretation of plume scavenging a difficult task. Typically the sulfate and nitrate concentrations in precipitation collected adjacent to the plume are quite variable, and subtracting this influence to determine source contributions involves substantial levels of uncertainty. This difficulty of "source attribution" at the local scale is compounded appreciably as greater scales of time and distance are considered.

On a more intermediate scale (0 to 200 km) an enhancement of sulfate and nitrate precipitation scavenging seems to occur, presumably because the precursors have had more opportunity to dilute and to react under these circumstances. Hogstrom (1974), using an extended network of samplers in the vicinity of Uppsala, Sweden, reported substantial scavenging rates of sulfur compounds. Hales and Dana (1979a) have observed summertime convective storms to remove appreciable fractions of urban NO_x and SO_x burdens in the vicinity of St. Louis, MO. Although both of these studies were subject to the usual uncertainties with regard to background contributions there is little doubt about their general conclusions of significant scavenging under such circumstances.

On a regional scale (0 to 2000 km) there are relatively few data from intensive field experiments. Precipitation-chemistry network data are of some use in this regard, however, and several analyses have applied these measurements to specific ends. One result of these analyses is the suggestion that, in the northeastern quadrant of the United States, roughly one third of the emitted NO_x and SO_x are removed by wet processes (Galloway and Whelpdale 1980). Network data for the Northeast (MAP3S/RAINE 1982) show also that the molar wet delivery rates of NO_x and SO_x are roughly equivalent. Combining this result with regional emission inventories suggests that nitrogen compounds begin to wet deposit with a significantly enhanced efficiency as distance scales become regional in extent.

The above changes in behavior with increasing scale seem to be a logical consequence of current understanding regarding the atmospheric chemistry of SO_x and NO_x. On local scales neither is scavenged very effectively owing to the chemical makeup of the primary emissions. On intermediate scales both groups have had some opportunity to react into more readily scavengable substances. Depending upon ambient conditions, nitrogen oxides will have participated to some extent in initial photolysis reactions and proceeded to form scavengable products such as nitric acid, peroxyacetyl nitrate, and nitrate aerosol. Sulfur dioxide also will have reacted homogeneously to a limited extent; more importantly, however, this compound will have been diluted to levels where limited reactants (and possibly catalysts) will facilitate its oxidation in the aqueous phase. On a regional scale this progression continues with the relative acceleration of NO_x scavenging.

Present field-study indications that NO_x scavenging may occur primarily through the attachment of gas-phase reaction products, while the scavenging of SO_x may depend much more heavily upon aqueous-phase oxidation processes, are also reflected in precipitation-chemistry data. A possible consequence of this difference in mechanisms is illustrated in Figure 6-15, which is a time-series of daily precipitation-chemistry measurements for a northeastern

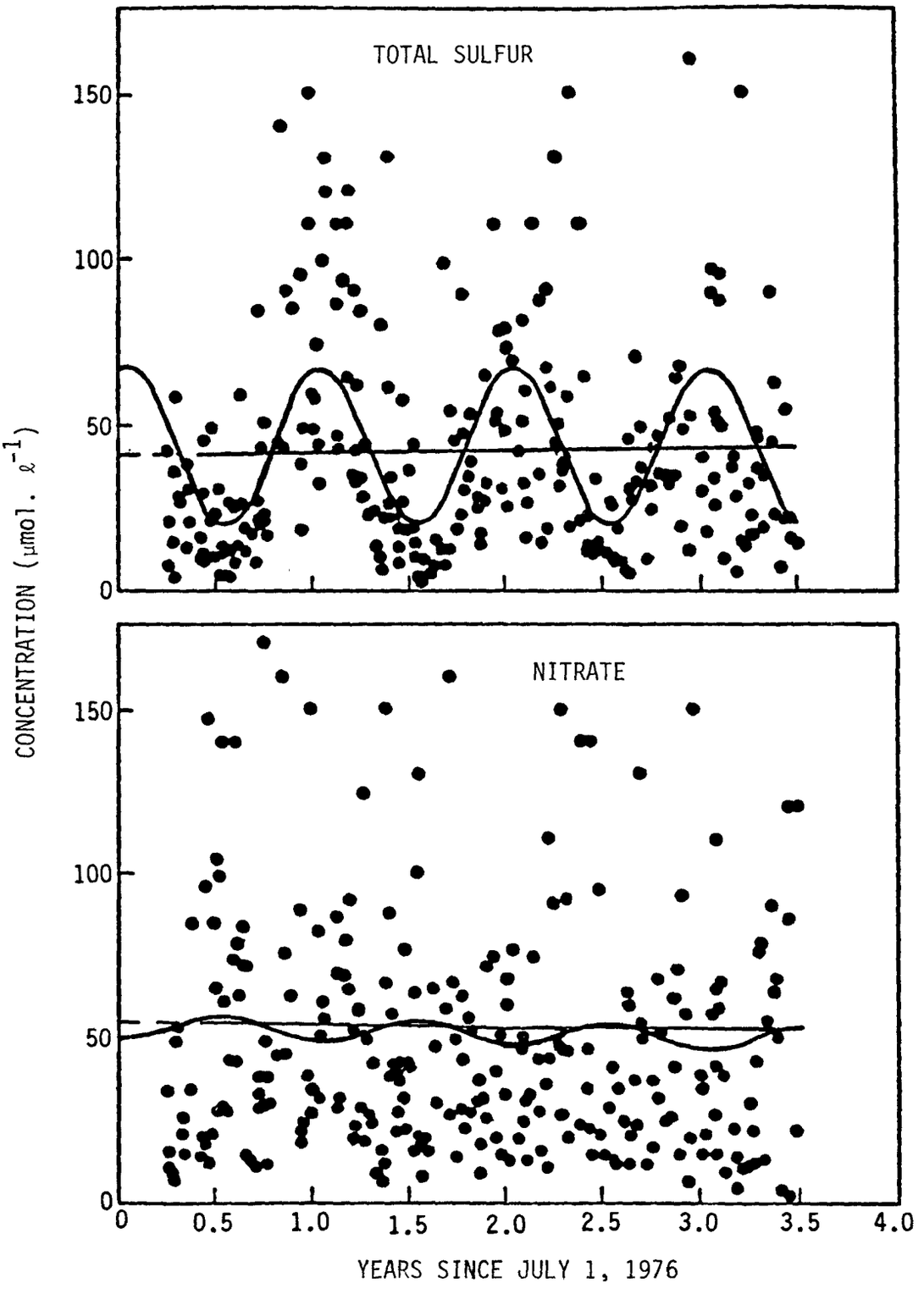

Figure 6-15. Sulfate and nitrate concentration data for event precipitation samples collected at Penn State University, PA. Lines are least-squares of linear and periodic functions (MAP3S/RAINE 1982).

U.S. site. The decidedly periodic[7] behavior of sulfate-ion concentrations in contrast to the largely disorganized behavior of nitrate-ion concentrations has been suggested to occur as a consequence of an aqueous-phase oxidation of sulfur dioxide, which proceeds more rapidly during summer months. Whatever the cause, it is readily apparent from this figure that scavenging mechanisms for these two species differ appreciably.

As noted above, most past field experiments have experienced difficulty in resolving precisely which source(s) of pollution has been responsible for material wet-deposited at sampled receptor sites, and this problem is typically amplified as time and distance scales increase. Source attribution is particularly uncertain on a regional scale, and the basic data obtainable from standard precipitation-chemistry networks are of little help in this regard. Combined with the lack of data from well-designed regional field studies, this problem of source attribution poses one of the most important and uncertain questions facing the acidic deposition issue at present.

As a consequence of this need, a major regional field experiment has recently been designed and conducted in the northeastern United States (MAP3S/RAINE 1981, Easter 1982). Known as the Oxidation and Scavenging Characteristics of April Rains (OSCAR) study, this field experiment was based upon the concept of characterizing, as completely as possible, the dynamic and chemical features of major cyclonic storm systems as they traverse the continent. Specific objectives were:

1. To assess spatial and temporal variability of precipitation chemistry in cyclonic storm systems, and to test the adequacy of existing networks to characterize this variability;

2. To provide a comprehensive, high-resolution data base for prognostic, regional deposition-model development; and

3. To develop increased understanding of the transport, dynamic, and physiochemical mechanisms that combine to make up the composite wet-removal process, and to identify source areas responsible for deposition at receptor sites.

---

[7]One should note in Figure 6-15 that the periodic functions are fit to the total data, whereas the linear regressions are fit only for the period January 1, 1977-December 31, 1979; thus the cyclic functions are not exactly symmetric about the linear regression curves. Some idea of statistical improvement in fit may be obtained using the expression

$$\hat{r}^2 = \frac{\sigma^2_{\text{linear regression}} - \sigma^2_{\text{periodic fit}}}{\sigma^2_{\text{linear regression}}}$$

where the σ^2's pertain to variances of the data points over the three and one-half period. For sulfate in Figure 6-15 $\hat{r}^2$ equals 0.22, indicating a significant reduction in variance; the corresponding $\hat{r}^2$ value for nitrate is 0.01, suggesting that no significant annual periodicity exists in this case.

The data collected and assembled by the OSCAR project are summarized in Table 6-3. These are being made available to the general user community in a computerized data base.

A general layout of the OSCAR precipitation-chemistry network is shown in Figure 6-16. The points and triangles on this map represent locations of sequential precipitation-chemistry stations on an "intermediate-density" network; the open square overlapping Indiana and Ohio depicts a concentrated network of 47 additional sites. Specific design criteria for this configuration are discussed in the supporting literature MAP3S/RAINE (1982).

The OSCAR data set is presently under intensive investigation, and only preliminary results are currently available. It is of interest to consider some of these results at this point, however, to evaluate the potential future utility of this material. One early result, presented by Raynor (1981), is primarily of qualitative interest and involves the first-sample - last-sample pH data obtained by the sequential rain samplers for individual storms, typified by the plots shown in Figures 6-17 and 6-18. It is interesting to note that Figure 6-17 is strongly reminiscent of annual- or multi-year-average plots for the northeastern United States in the sense that it shows the familiar acid "core" region centered upon Pennsylvania. The final-sample distribution in Figure 6-18 is quite different. Besides indicating a much cleaner sample set, very little structure exists in this final distribution. This relative cleanliness of late-storm precipitation is consistent with the general OSCAR finding that most of the pollutant is scavenged comparatively early in a storm's life cycle (Easter and Hales 1983a).

It should be noted in this context that field studies having higher spatial resolution (e.g., Semonin 1976, Hales and Dana 1979b) indicate that significant fine structure typically exists in spatial pH distributions. Much of this fine structure can be expected to be hidden within the relatively coarse sampling mesh shown in Figures 6-17 and 6-18.

Substantial source-receptor analysis is presently being conducted in conjunction with the Indiana-Ohio concentrated network. One early analysis, conducted for the 22-24 April 1981 storm is presented in Figure 6-19. Back trajectories of this type are currently being combined in diagnostic scavenging models with aircraft and surface data to evaluate source-receptor relationships in greater detail (Easter and Hales 1983a,b).

6.5 PREDICTIVE AND INTERPRETIVE MODELS OF SCAVENGING

6.5.1 Introduction

A precipitation-scavenging model can be defined as any conceptualization of the individual or composite processes of Figure 6-2, in a manner which allows their expression in mathematical form. Often such models take the form of submodels or "modules" within a larger calculational framework, such as a composite regional pollution code. When considered in a modular sense the lines connecting the boxes of Figure 6-2 can be considered as channels for information exchange within the overall framework, whereas the boxes (or

TABLE 6-3. SUMMARY OF DATA COLLECTED FOR THE OSCAR DATA BASE

METEOROLOGICAL DATA

- North American standard 12-hour upper air observations (rawinsondes)
- OSCAR special rawinsonde data
- North American 3-hour standard surface observations
- North American hourly precipitation amount data
- Trajectory forecast data (Limited Fine Mesh and Global Spectral Models)
- Gridded forecast data (Limited Fine Mesh Model)
- Satellite observations

PRECIPITATION-CHEMISTRY DATA

- OSCAR network: Sequential measurements of rainfall, field pH, lab pH, conductivity, NO_3^-, NO_2^-, SO_4^{2-}, SO_3^{2-}, Cl^-, NH_4^+, Ca^{2+}, Mg^{2+}, K^+, Na^+, Al^{3+}, PO_4^{3-}, total Pb
- Additional networks: Time-averaged data as available from sources such as NADP, CANSAP, CCIW, and APN
- Special rainborne H_2O_2 measurements

AIRCRAFT DATA

- Trace gases: O_3, NO/NO_x, SO_2, HNO_3, NH_3
- Aerosol parameters: Scattering coefficient (b_{scat}), Aitken nuclei, aerosol sulfur, sulfate size distribution, aerosol size distribution, aerosol acidity
- Cloud water chemistry: NO_3^-, NO_2^-, SO_4^{2-}, SO_3^{2-}, pH, NH_4^+, conductivity, Cl^-, Ca^{2+}, Mg^{2+}, K^+, Na^+, total Pb.
- Meteorological parameters: Temperature, humidity, liquid, water content, wind speed and direction, cloud droplet size distribution
- Position parameters: Latitude, longitude, altitude, time

TABLE 6-3. CONTINUED

SURFACE AIR CHEMISTRY DATA

- OSCAR SAC site (Fort Wayne 40°49.8'N, 85°27.6'W): H_2O_2, peroxyacetyl nitrate, sulfur aerosol size distribution, NH_3, SO_2, SO_4^{2-}, O_3, NO/NO_x, HNO_3, aerosol composition vs particle size, aerosol acidity
- Selected air quality data from specific surface monitoring sites throughout eastern North America

EMISSIONS

- MAP3S/RAINE standard inventory

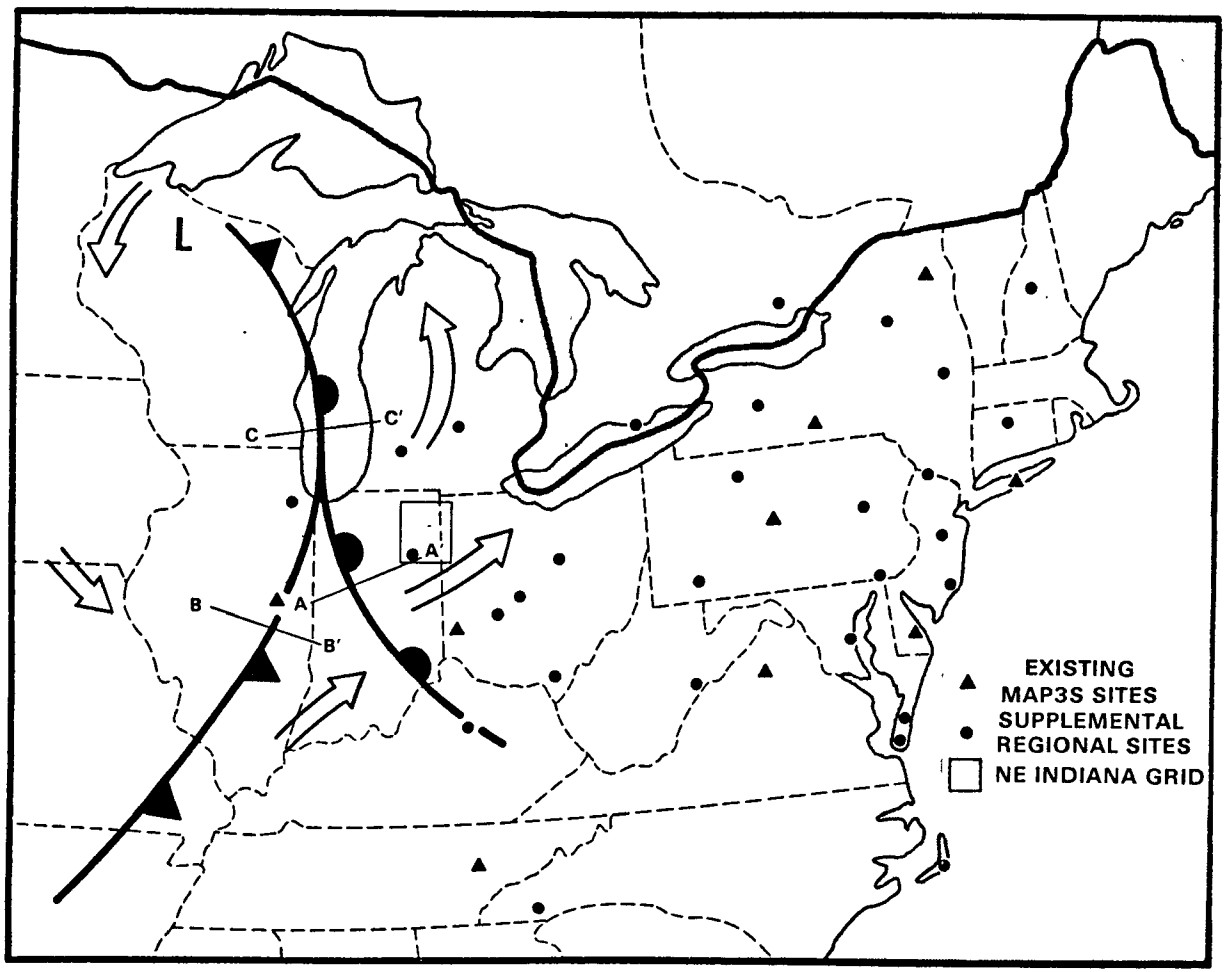

Figure 6-16. General layout of OSCAR sequential precipitation chemistry network, showing hypothetical "design-basis" cyclonic system.

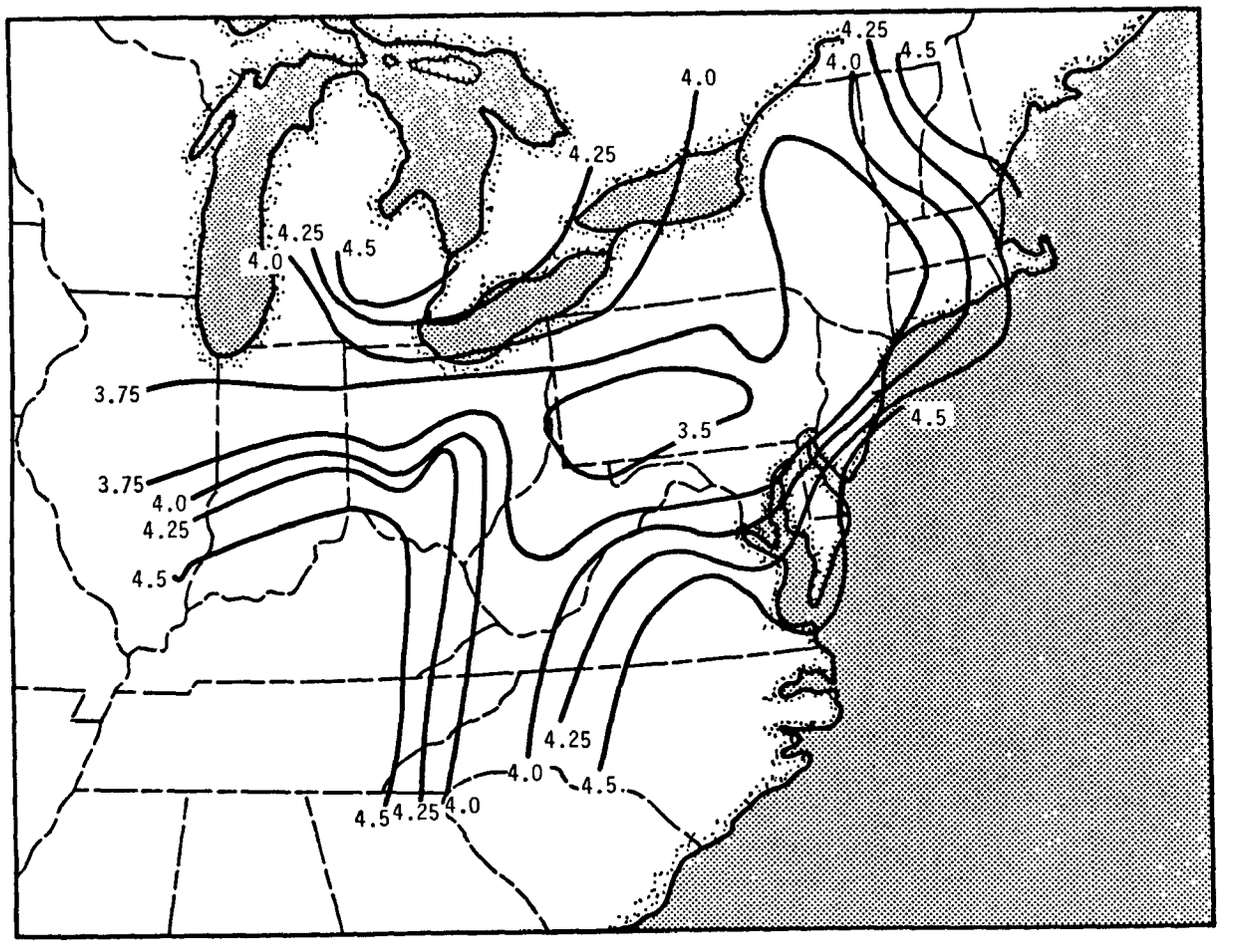

Figure 6-17. pH distribution for initial precipitation sampled during OSCAR storm of 22-24 April 1981.

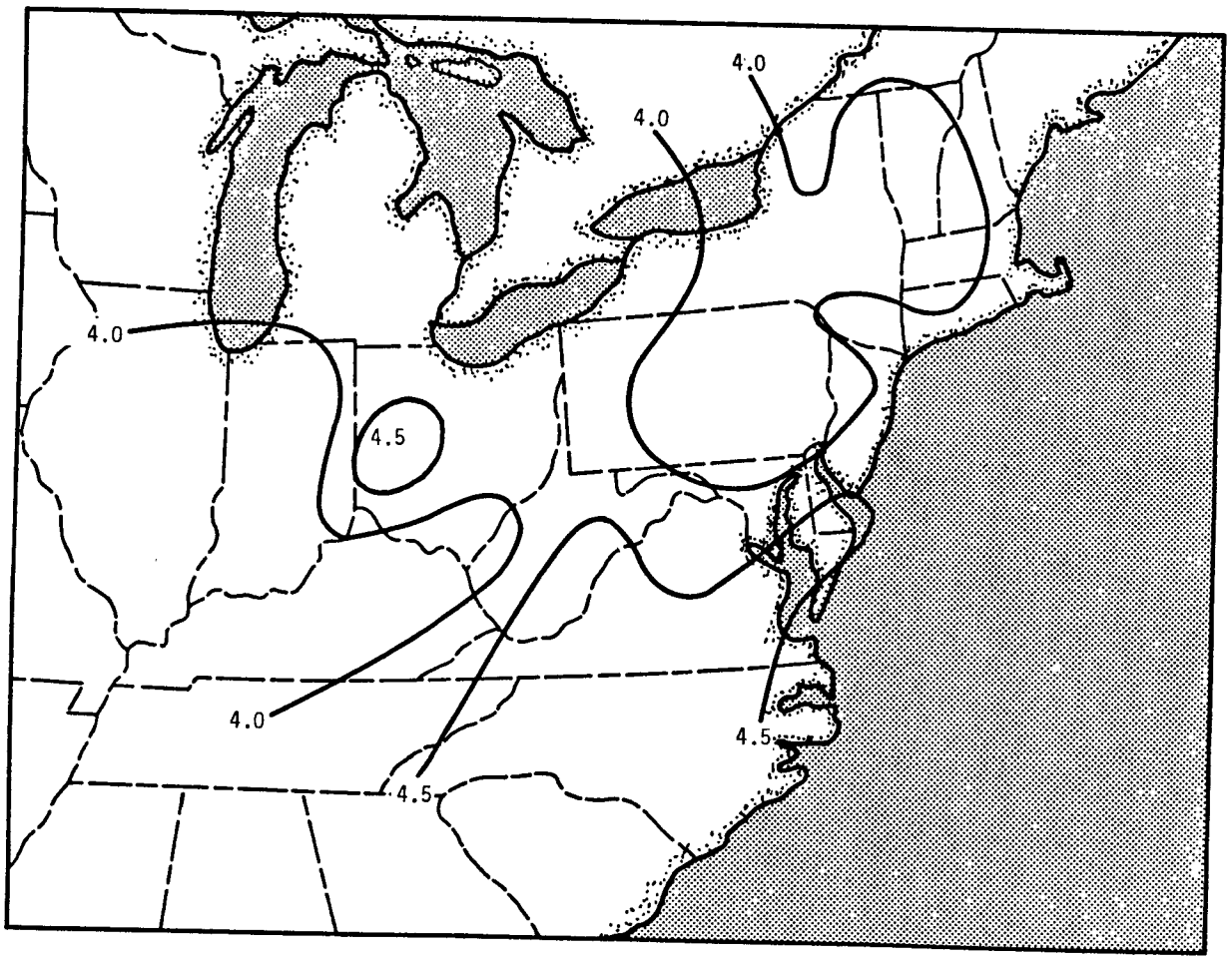

Figure 6-18. pH distribution for final precipitation sampled during OSCAR storm of 22-24 April 1981.

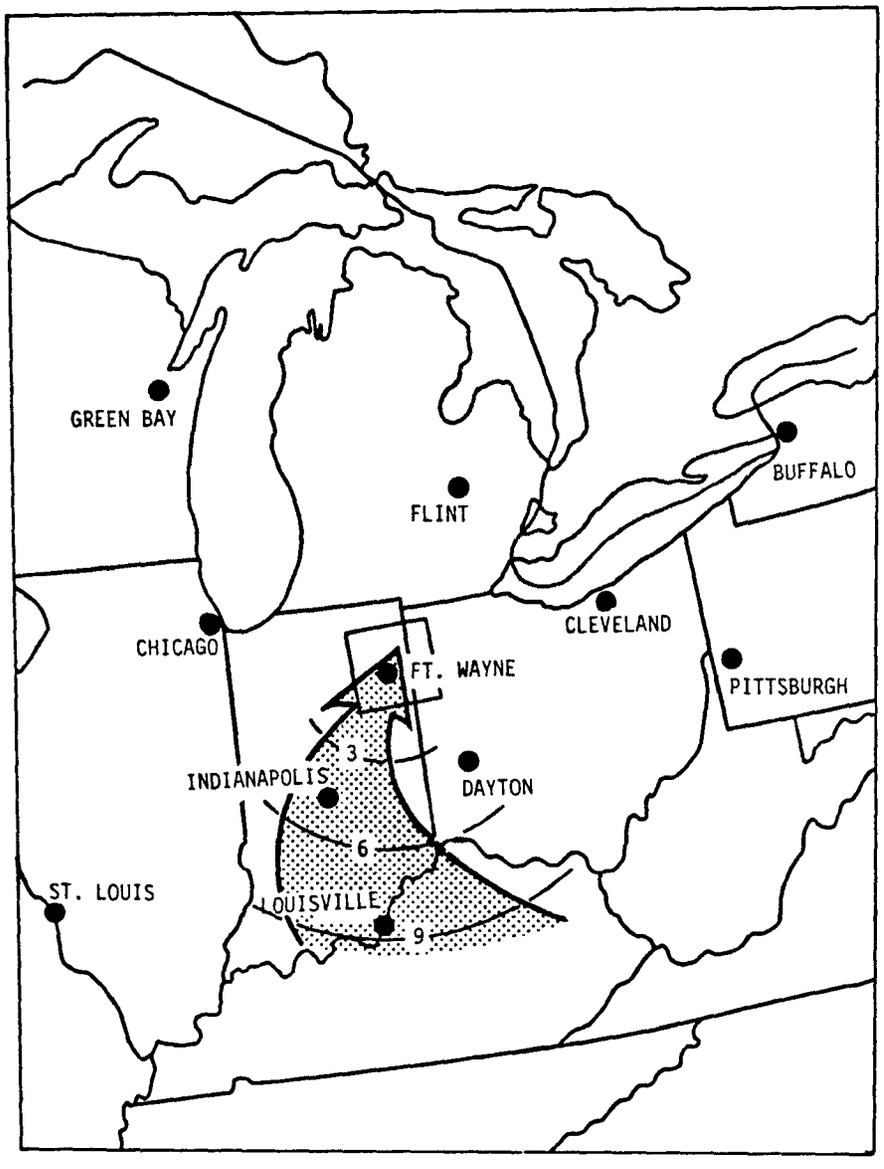

Figure 6-19. Loci of points contributing pollution to the high density network near 1400 EST on 22 April 1981. Contour intervals 3, 6, 9 represent travel times in hours from source regions. The large arrow represents the likely path of air originating from points 9 hours upwind of the receptors.

clusters of boxes) can be identified with the modules, themselves. This modular relationship is described in somewhat more detail in Chapter A-9, where composite regional models are discussed.

Scavenging models are currently in a rapidly-evolving state, and a profusion of associated computer codes and computational formulae is currently available. Indeed, one of the major problems in precipitation-scavenging assessment is determining precisely which model to select from the large number of available candidates. A major aim of the present subsection is to guide the reader in this pursuit.

There are a number of potential uses for precipitation-scavenging models, and the intended use will to a large extent determine just which model should be employed. Some of the more important potential uses are itemized as follows:

- Predicting the impact on precipitation chemistry of proposed new sources, source modifications, and alternate emission-control strategies;
- Predicting long-range precipitation chemistry trends;
- Estimating relative contributions of specific sources to precipitation chemistry at a chosen receptor point;
- Estimating transport of acidic-precipitation precursors across political borders;
- Estimating and predicting air-quality improvements occurring as a consequence of the scavenging process;
- Selecting sites for precipitation-chemistry network sampling stations;
- Designing field studies of precipitation scavenging; and
- Elucidating mechanistic behavior of the scavenging process on the basis of field measurements.

In selecting an appropriate model, the user should review his intended application carefully with regard to the pollutant materials of interest, time and distance scales, processes covered in Figure 6-2, source configuration, precipitation type, and mechanistic detail required. The question of pollutant materials is particularly important when precipitation acidity is of interest. Acidity in precipitation is determined by the presence of a multitude of chemical species, and in principle one must compute (via a model) the scavenging of each species and then estimate acidity on the basis of an ion balance:

$$[H^+] = \Sigma \text{ Anions} - (\Sigma \text{ Cations other than } H^+). \qquad [6\text{-}1]$$

Inorganic ions usually important in precipitation chemistry are itemized in Table 6-4. Organic species play a secondary role in the acidification

TABLE 6-4. SOME INORGANIC IONS IMPORTANT IN PRECIPITATION CHEMISTRY[a]

Cations	Anions
H^+	
NH_4^+	Cl^-
Na^+	NO_3^-
K^+	SO_3^{2-}
Ca^{2+}	SO_4^{2-}
Mg^{2+}	PO_4^{3-}
	CO_3^{2-}

[a]All ions are presented here in their completely-dissociated states. The reader should note, however, that various states of partial dissociation are possible as well (e.g., HSO_3^-, HCO_3^-).

process, which appears to vary widely by region. Modeling of all of these species simultaneously requires substantial effort, and all "acidic-precipitation" models to date have focused upon only one or just a few of the more important species, with contributions of the others estimated empirically. Currently, newer models tend to accommodate larger numbers of these species; but complete modeling coverage will not be achieved in the foreseeable future.

Mechanistic detail is another important feature determining the basic composition of a scavenging model. A comprehensive mathematical description of the scavenging process can become rapidly overwhelming, and there is usually a need to represent these relationships in a comparatively simple, albeit approximate, manner. The process of consolidating complex behavior in this fashion is often referred to as lumping the system's parameters. The resulting simplified expressions are termed parameterizations. Consolidating the effects of non-modeled species in empirical form, described in the preceding paragraph, is one example of lumping. Numerous other examples will arise throughout the remainder of this section.

This section will not attempt to provide the reader with a detailed treatise on how models should be formulated and applied.[8] The approach, rather, will be to develop a basic understanding of the fundamental elements of a scavenging model and then to provide a systematic procedure for choosing and locating appropriate models from the literature. The following subsection discusses the basic conservation equations, which constitute the conceptual bases for scavenging models in general. This discussion is followed in turn by two simple applications of these relationships, which are presented to illustrate usage and to define some terms commonly used in scavenging models. The final subsection attacks the problem of model selection, using a flowchart approach designed to guide the user to a valid choice in a systematic manner that avoids many of the pitfalls normally encountered in such endeavors.

6.5.2 Elements of a Scavenging Model

6.5.2.1 Material Balances--In Figure 6-2 the various arrows between boxes correspond physically to streams of pollutant and/or water. From this it is not difficult to realize that any characterization of this system must include material balances, which form the underlying structure for all scavenging models. To formulate a material balance, one simply visualizes some chosen volume of atmosphere, and sums over all inputs and outputs of the substance in question.

---

[8]For the reader interested in more detailed pursuit of this area, the works by Hales (1984) and Slinn (1983) are recommended. The Hales reference is something of a beginner's primer, while Slinn's treatment delves substantially deeper into mechanistic detail. Together they constitute a reasonable starting point for understanding and modeling basic scavenging phenomena.

Two basic types of material balance are possible:

1. "Microscopic" material balances, based upon summation over a limiting small volume element of atmosphere; and

2. "Macroscopic" material balances, based upon summation over a larger volume element of atmosphere (e.g., a complete storm system).

Microscopic material balances invariably lead to differential equations, which must be integrated over finite limits to obtain practical results. Macroscopic balances result in mixed, integral, or algebraic equations. Again the choice of material-balance type depends upon the specific modeling purpose at hand.

An important general form of the differential material balance for a chosen pollutant (denoted by subscript A) is given by the equations[9] (cf., Hales 1984)

$$\frac{\partial c_{Ay}}{\partial t} = -\tilde{\nabla}.c_{Ay}\tilde{v}_{Ay} - w_A + r_{Ay} \quad \text{(gas phase)} \qquad [6\text{-}2]$$

and

$$\frac{\partial c_{Ax}}{\partial t} - \tilde{\nabla}.c_{Ax}\tilde{v}_{Ax} + w_A + r_{Ax} \quad \text{(aqueous phase).} \qquad [6\text{-}3]$$

Here c_{Ay} and c_{Ax} denote concentrations of pollutant in the gaseous and condensed-water phases, respectively. The time rate of change of these concconcentrations within the differential volume element is related to the sum of inputs by 1) flow through the walls of the element, 2) interphase transport between the gaseous and condensed phases, and 3) chemical (and/or physical) reaction within the element. The $\tilde{v}$ terms in Equations 6-2 and 6-3 denote velocity vectors, while $\tilde{\nabla}.$ is the standard vector divergence operator. The interphase transport term w_A accounts for all "attachment" processes (impaction, phoresis, diffusion, ...) as well as any reverse phenomena such as pollutant-gas desorption, while the r terms denote chemical conversion rates in the usual sense. To formulate a usable model from these equations, one needs to specify values for the functions $\tilde{v}$, w, and r and then solve differential Equations 6-2 and 6-3 (subject to appropriate initial and boundary conditions) to obtain the desired concentration fields c_{Ay} and c_{Ax}. A simple example of this procedure is given in Section 6.5.4.

---

[9]Equations 6-2 and 6-3 are quite general in the sense that the velocity vectors denote velocity of pollutant (rather than that of the bulk medial and thus provide for all modes of transport (convective, diffusive, ...) without yet specifying how this transport is to occur. These equations are not yet time-smoothed; thus, no closure assumptions have been applied at this point.

6.5.2.2 Energy Balances--Many terms in Equations 6-2 and 6-3, especially $\tilde{v}_{Ax}$, w_A, and r_{Ax}, depend strongly upon the amount, state, and interconversion rates of condensed water; and it is important to note that atmospheric water itself obeys material-balance expressions of this form. In selecting a scavenging model, one often is confronted with the problem of deciding whether to estimate precipitation attributes and these related terms independently on the basis of assumptions or previous information, or to attempt to compute the desired entities directly by solving appropriate forms of Equations 6-2 and 6-3.

If the latter of these alternatives is chosen, then the inclusion of an energy-balance equation is mandatory. This need arises because the evaporation-condensation process influences, and is influenced by, a variety of energy-related considerations. These include temperature influences on vapor pressure and latent-heat effects, and can be incorporated in the model via an energy balance performed over the same element of atmosphere as that of the associated material balances. In microscopic form, a general expression of the energy balance (cf., Bird et al. 1960), is

$$\rho C_v \frac{\partial T}{\partial t} = - \nabla.\tilde{h} - p\nabla.\tilde{v} + \Gamma - D \; . \qquad [6\text{-}4]$$

Here the time rate of change of temperature relates to the sum of inputs by 1) flow through the walls of the element and 2) generation via a) compression work, b) latent heat effects, and c) frictional dissipation. The vector terms $\tilde{h}$ and $\tilde{v}$ denote sensible heat flux and fluid velocity, respectively, while Γ and D pertain to latent heat and dissipation; ρ and C_v denote fluid density and specific heat in the usual sense. A straightforward example of the incorporation of Equation 6-4 for scavenging modeling purposes is given by Hales (1982).

6.5.2.3 Momentum Balances--Solutions to Equations 6-2 to 6-4 depend upon the existence of some previous description of fluid velocity $\tilde{v}$ (or $\tilde{v}_{Ay}$ in the case of Equation 6-2). As was the case for the preceding parameters associated with the energy balance, velocity may be specified for the model on the basis of previous measurements or assumptions. Flow patterns in storm systems may be sufficiently complex to defy empirical specification, however, and the modeler may wish to compute the associated fields on the basis of a modeling approach. If this is to be done, a momentum-balance equation must be employed. In microscopic form the general momentum balance may be expressed (cf., Bird et al. 1960) as

$$\frac{\partial \rho \tilde{v}}{\partial t} = -\nabla.\rho\tilde{v}\tilde{v} - \nabla p - \tilde{F}_v + \rho g. \qquad [6\text{-}5]$$

Here the time rate of change of momentum ($\rho\tilde{v}$) is expressed as the sum of inputs by 1) flow through the walls of the element, 2) pressure forces, 3) viscous drag forces, and 4) gravitational forces. To apply Equation 6-5 for modeling purposes, one specifies frictional, pressure, and gravitational

terms and solves the differential equation subject to appropriate initial and boundary conditions to obtain fields of the velocity vector $\tilde{v}$. An example applying Equation 6-5 for scavenging modeling purposes is given by Hane (1978).

Incorporating energy and momentum balances, Equations 6-4 and 6-5, into a scavenging model is a rather challenging exercise, and a relatively small number of models that apply these equations for this purpose exists. The usual tack is simply to "pre-specify" the required parameters and proceed with material-balance calculations alone. Numerous examples of both types of models will be presented in Section 6.5.5.

6.5.3 Definitions of Scavenging Parameters

Four key parameters often arise in the context of scavenging models, and it is appropriate at this point to define these terms and indicate their general application. Reference to these entities as "parameters" is consistent with the usage applied in the previous section, in that they serve to "lump" the effects of a number of mechanistic processes in a simple formulation. These will be discussed sequentially in the following paragraphs.

The first parameter to be defined is the attachment efficiency. Also known as the capture efficiency, this term can be visualized most easily by considering a hydrometeor falling through a volume of polluted air space, as shown in Figure 6-20. This hydrometeor sweeps out a volume of air during its passage, and attachment efficiency is defined as the amount of collected pollutant divided by the amount initially in this volume. The efficiency can exceed 1.0 if pollutant from outside the swept volume becomes attached to the drop.

From the discussion in Section 6.2.3, it is apparent that attachment efficiency accounts for a multitude of processes. Usually the efficiency is less than 1; but mechanisms such as diffusion, electrical effects, and interception can give rise to larger values, especially when the collecting element's fall velocity is small. Efficiencies can be negative if the element is releasing pollutant to the surrounding atmosphere, such as in the case of pollutant-gas desorption. Typical efficiencies for aerosol particles collected by raindrops are shown in Figure 6-4.

Another important parameter is the scavenging coefficient. This entity is basically an expression of the law of mass action, defined by the form

$$\Lambda = \frac{w_A}{c_{Ay}} \qquad [6\text{-}6]$$

where (in a manner consistent with Equations 6-2 and 6-3) w_A is the rate of depletion of pollutant A from the gaseous phase by attachment to the aqueous phase in a differential volume element. This is similar to a rate of expression for a first-order, irreversible chemical reaction, and as such it applies strictly only to irreversible attachment processes (e.g., aerosols or highly-soluble gases). Λ can be related to the attachment efficiency E by the form (which assumes spherical hydrometeors)

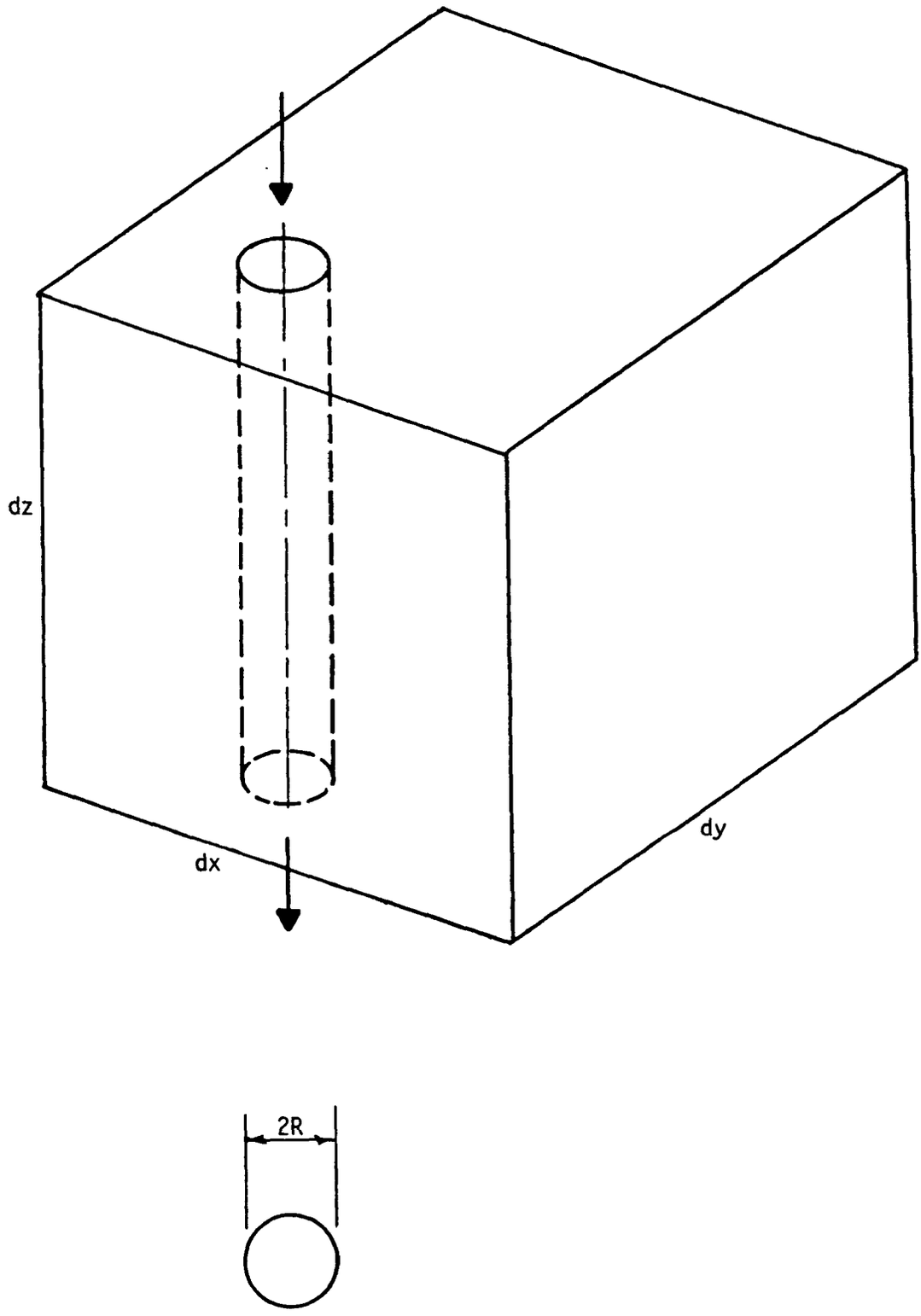

Figure 6-20. Schematic of a scavenging hydrometeor falling through a volume element.

$$\Lambda(a) = -\pi N_T \int_0^\infty R^2 v_z(R) E(R,a) f_R(R) dR \ , \qquad [6\text{-}7]$$

where a and R denote aerosol and hydrometeor radii, respectively; v_z is the hydrometeor fall velocity; and N_T and f_R are the total number and probability-density functions for the size-distributed hydrometeors residing in the volume element of Figure 6-20 at any instant in time. From this, one can note that Λ essentially extends the parameterization over the total spectrum of hydrometeor sizes.

Atmospheric aerosol particles are typically distributed over extensive size ranges. Because of this it is often desirable to possess some sort of an effective scavenging coefficient, which represents a weighted average over the aerosol size spectrum. Figure 6-21 presents a family of curves corresponding to such averages, which are based upon assumed log-normal particle-size spectra, with different geometric standard deviations. From these curves one can observe that for the same geometric mean particle size, changes in spread of the size distribution can result in dramatic changes in the effective scavenging coefficient.

Inclusion of reversible attachment processes in a scavenging model usually involves using the mass-transfer coefficient. This parameter can be defined in terms of the flux of pollutant moving from the scavenging element as

$$\text{Flux} = -\frac{K_y}{c}\left(c_{Ay} - h'\hat{c}_A\right) \ . \qquad [6\text{-}8]$$

Here K_y is the mass-transfer coefficient and $\hat{c}_A$ is the concentration, within the scavenging element, of collected pollutant; h' is essentially a solubility coefficient which, when multiplied by $\hat{c}_A$, produces a gas-phase equilibrium value. c is the molar concentration of air molecules, which appears in Equation 6-8 because of the manner in which K_y has been defined. Thus, the flux can be either to the drop or away from it, depending upon the relative magnitudes of the parenthetical terms. Equation 6-8 can be integrated over all drop sizes in a manner similar to that used in Equation 6-7 (cf., Hales 1972), to form the following expression for w_A:

$$w_A = \frac{4\pi N_T}{c} \int_0^\infty R^2 f_R(R) K_y(R) \left(c_{Ay} - h'\hat{c}_A\right) dR. \qquad [6\text{-}9]$$

The final scavenging parameter to be described here is the scavenging ratio. This entity is usually the result of a model calculation, rather than an input, and is defined by the form

$$\xi = \frac{\hat{c}_A}{c_{Ay}} \qquad [6\text{-}10]$$

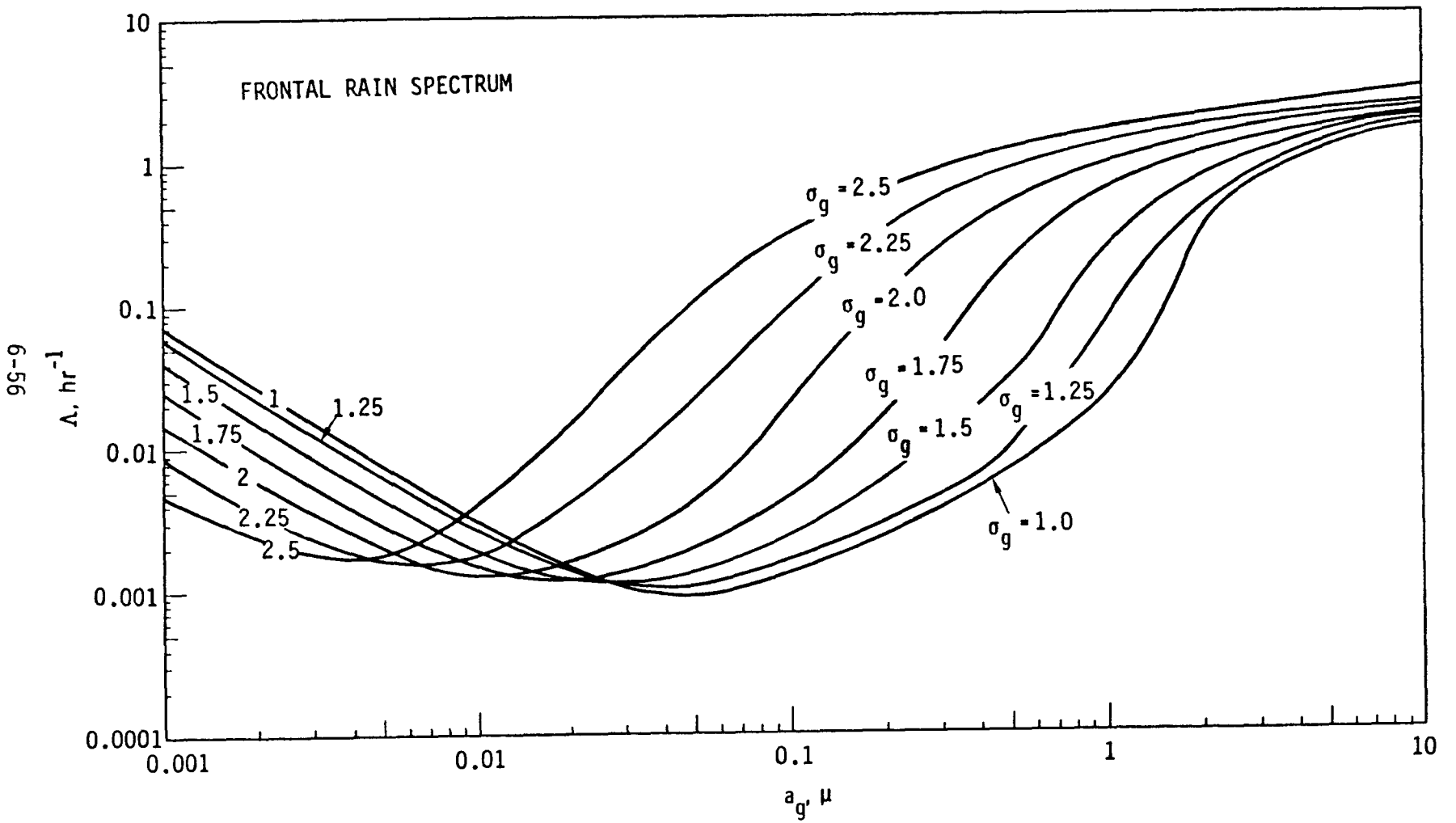

Figure 6-21. Computed effective scavenging coefficients for size-distributed aerosols. Based on a log-normal aerosol radius distribution with geometric means and standard deviations a_g and σ_g. A typical frontal-rain dropsize spectrum is assumed. Adapted from Dana and Hales[g](1976).

where $\hat{C}_A$ is the concentration of pollutant contained in a collected precipitation sample. ξ is a term immediately usable for a number of pragmatic purposes because once its numerical value is known, it can be applied directly to compute precipitation-chemistry concentrations on the basis of air-quality measurements. Tables of measured (Engelmann 1971) and model-predicted (Scott 1978) scavenging ratios have been published, although caution is advised in the application of these values. A simple example of scavenging-ratio application is given in the following section.

It is useful for the sake of visualization to discuss briefly the qualitative features of the scavenging parameters noted above. The parameter E is easy to visualize in the context of Figure 6-20; it is, simply, the collection efficiency of an individual cloud or precipitation element and as such should be expected to fall numerically in the approximate range between zero and one. The scavenging coefficient Λ can be visualized as a first-order removal rate, in much the same manner as that of a first-order reaction-rate coefficient. As such it may be used roughly as a characteristic time scale for wet removal. $\Lambda = 1\ hr^{-1}$, for example, would imply that the scavenging process will cleanse 100(1-1/e) percent of the pollutant in one hour if conditions remain constant and competitive processes do not occur. From this one can note that 1 hr^{-1} is a moderately large scavenging coefficient. Λ's ranging from zero to 1 hr^{-1} and beyond have been reported in the literature (cf., Figure 6-21).

The mass-transfer coefficient K_y is essentially a normalized interfacial flux of pollutant between the atmosphere and an individual droplet. Little needs to be said here regarding magnitudes of K_y, except to note that a variety of different definitions of K_y exist, and one must be cognizant of these definitions when employing values obtained from outside sources. The washout ratio, ξ, is essentially a measure of the concentrating power of precipitation in its extraction of pollutant from the atmosphere. As will be noted in the next section, precipitation often has the ability to concentrate airborne pollution by a factor of a million or more. ξ's ranging from below 100 up through 10^8 and higher have been reported in the literature.

The expected magnitudes and uncertainty levels associated with the scavenging parameters listed in this section depend strongly upon the substance being scavenged and the environment in which the scavenging takes place. Large aerosol particles in below-cloud environments, for example, are characterized by scavenging efficiencies in the range of 1.0 (Figure 6-4), which can be estimated with relatively high precision. Smaller particles, especially those in the "Greenfield-Gap" region, are much more difficult to simulate and associated errors in estimated efficiencies may approach an order of magnitude or more. Errors in these efficiency estimates will of course be compounded by uncertainties in raindrop size spectra, if extended to scavenging coefficients via Equation 6-7. In the case of gases, the mass-transfer coefficient usually can be estimated to within a factor of two or less; again this error can be expected to compound when integrated over assumed raindrop size-spectra.

In the case of in-cloud scavenging of aerosols our capability for estimating transport parameters is seriously impeded, owing to the profusion of

mechanisms and the complex environments involved. Typical uncertainties in both Λ and ξ can be expected to approach an order of magnitude in some cases. Some appreciation for the factors influencing in-cloud scavenging coefficients can be obtained from the work of Slinn (1977), who attempts to evaluate theoretical, "storm-averaged" values for Λ. An idea of the magnitudes and uncertainties of ξ is given in Figure 6-23.

In all cases involving reactive gases, the values of E, Λ, and ξ are heavily contingent upon the aqueous-phase chemical processes involved. Much remains to be accomplished in our understanding of aqueous-phase chemistry before a meaningful assessment of associated uncertainties is possible.

As a final note in this context it should be emphasized that uncertainties in scavenging parameters dictate uncertainties in scavenging calculations in a complex fashion, and that errors associated with the microscopic phenomena can be either amplified or attenuated by their applications in macroscopic models to produce practical results. Uncertainties associated with macroscopic modeling applications will be discussed at some length in a later section.

6.5.4 Formulation of Scavenging Models: Simple Examples of Microscopic and Macroscopic Approaches

As noted previously, the description given in this document will refrain in general from deriving and applying scavenging models explicitly. This is too broad and complex a subject to be discussed in detail here, and the reader is referred to the previously-cited literature for more detailed pursuit of this subject. For purposes of illustration, however, it is worthwhile to consider two very simple examples of scavenging-model formulation, which demonstrate the microscopic and macroscopic approaches to the problem. The present subsection is addressed to this task.

The microscopic material balance approach will be considered first. For this example, it is useful to visualize an idealized situation where rain of known characteristics is falling through a stagnant volume of atmosphere, which contains a well-mixed, nonreactive pollutant with concentration c_{Ay}. The air velocity is known ($\tilde{v}$=0), so solution of the momentum equation (Equation 6-5) is not required. The raindrop size distribution is presumed to remain constant; thus, evaporation-condensation and other energy-related effects are immaterial, and the energy equation (Equation 6-4) may be disregarded.

Because the pollutant is well-mixed, no concentration gradients occur; thus, the divergence term in Equation 6-2 is zero. Because of nonreactivity the reaction term is zero as well.

Now presume that the pollutant is an aerosol whose attachment can be characterized in terms of the known scavenging coefficient Λ, using Equation 6-6. The corresponding reduced form of Equation 6-2 is, then,

$$\frac{\partial c_{Ay}}{\partial t} = - \Lambda \, c_{Ay}. \qquad [6\text{-}2a]$$

Given some initial pollutant concentration c_{Ayo}, Equation 6-2a can be integrated to obtain the form

$$c_{Ay}(t) = c_{Ayo} \exp(-\Lambda t), \qquad [6\text{-}11]$$

which expresses the decrease of the gas-phase pollutant concentration with time. Counterpart expressions for rainborne concentrations may be derived by subjecting Equation 6-3 to a similar treatment.

The reader is cautioned to consider this treatment as an example only and to recognize that actual atmospheric conditions seldom conform to the idealizations invoked above. Gas-phase concentrations are usually not uniformly distributed in space, raindrop characteristics are usually not invariant with time, and wind fields are usually not well characterized by $\tilde{v} = 0$. Λ is usually not a time-independent constant, and many pollutants are usually not well characterized by the washout coefficient approximation. The pollutant often is not unreactive. Examples of existing models where these constraints are relaxed in various ways are presented in the following subsection.

Figure 6-22 illustrates the formulation of a macroscopic type of scavenging model. Here, in contrast to the differential-element approach, the material balances are formulated around a large volume element, in this case a total storm. If one denotes concentrations and flow rates of water and pollutant as follows:

c_{Ay} = airborne concentration of pollutant
H = airborne concentration of water vapor into cloud
$\hat{C}_A$ = concentration of scavenged pollutant in rainwater
ρ_w = density of condensed water
w_{in} = flow rate of water vapor into the storm
w_{out} = flow rate of water vapor out of the storm
f_{in} = flow rate of pollutant into the storm
f_{out} = flow rate of pollutant out of the storm
W = flow rate of precipitation out of the storm
F = flow rate of scavenged pollutant out of the storm,

then extraction efficiencies for water vapor and pollutant can be defined, respectively, as

$$\varepsilon_p = \frac{W}{w_{in}}, \qquad [6\text{-}12]$$

$$\varepsilon = \frac{F}{f_{in}}. \qquad [6\text{-}13]$$

If one further performs material balances over this storm system for pollutant and water vapor, and then combines the two, the following form is obtained:

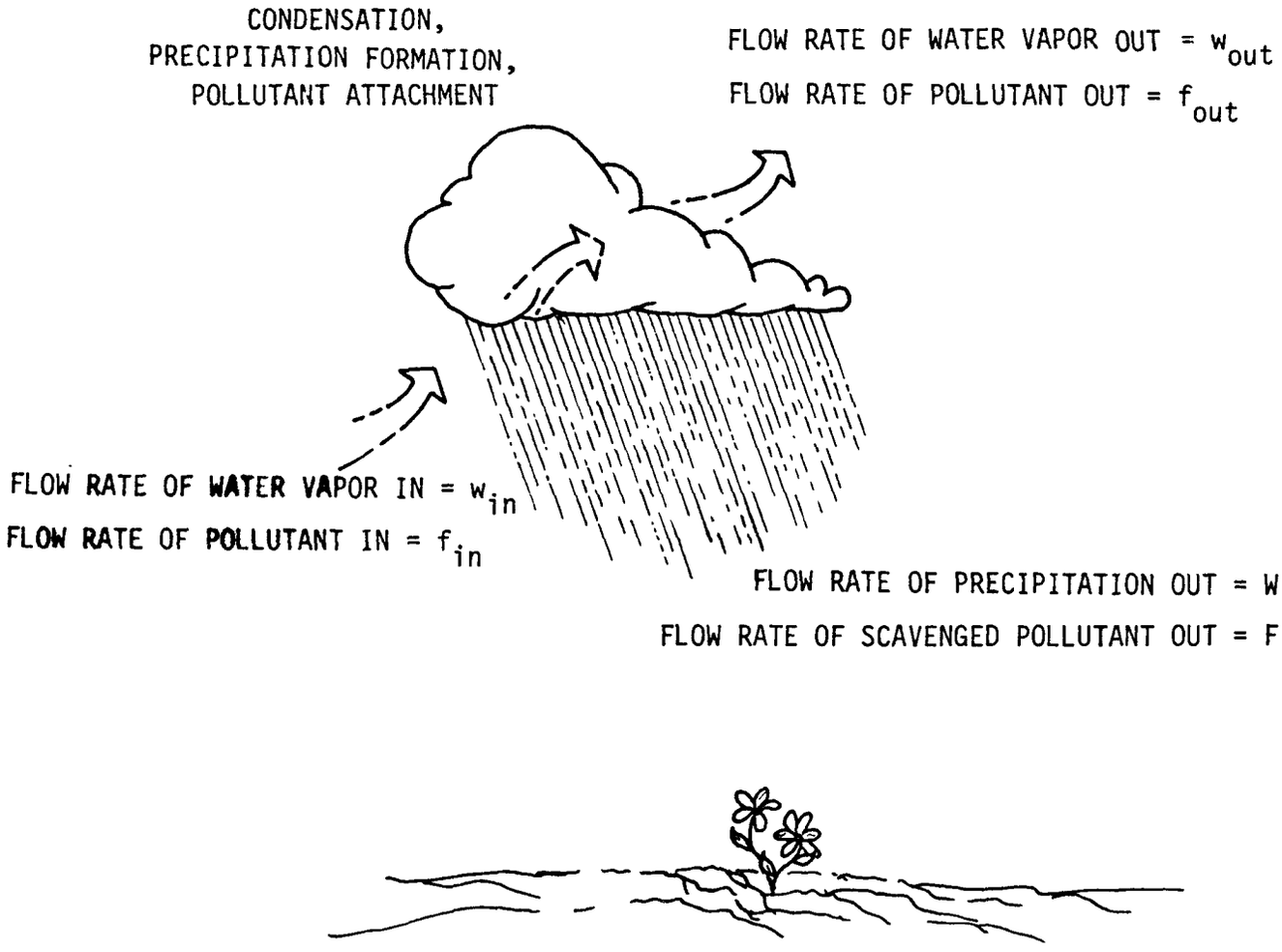

DEFINITIONS OF EFFICIENCIES:

WATER REMOVAL	POLLUTANT REMOVAL
$\varepsilon_p = \frac{W}{w_{in}}$	$\varepsilon = \frac{F}{f_{in}}$

Figure 6-22. Schematic of a typical macroscopic material balance.

$$\xi = \frac{\hat{C}_A}{C_{Ay}} = \frac{\varepsilon_p \rho_w}{\varepsilon H} \qquad [6\text{-}14]$$

where the scavenging ratio, ξ, is as defined earlier in Section 6.5.3.

Equation 6-14 is an important result in the sense that it demonstrates once again the strong linkage between water-extraction and pollutant-scavenging processes. If both occur with equal efficiency[10] ($\varepsilon_p = \varepsilon$) for example, then

$$\xi = \frac{\rho_w}{H} \approx 10\text{-}5 - 10\text{-}6. \qquad [6\text{-}15]$$

Experimentally-measured scavenging ratios often fall in this range, although wide variability is usually observed.

Using a rather involved series of arguments pertaining to cloud-physics processes and attachment mechanisms, Scott (1978) has created a family of curves expressing scavenging ratio as a function of precipitation rate. Shown in Figure 6-23, curves 1, 2, and 3 pertain respectively to convective storms, nonconvective warm-rain process storms, and cold storms where the Bergeron-Findeisen process is active.

A major assumption in Scott's analysis is that storms ingest pollutants in the form of aerosol particles which are active as cloud condensation nuclei. The analysis also assumes a steady-state storm system and complete vertical mixing of pollutant between the storm height and the surface. Under such conditions Scott's curves can be considered reasonably good estimators of actual scavenging behavior. More elaborate systems, involving reactive pollutants, gases, and nonhomogeneous systems, are discussed in references given in the following section.

6.5.5 Systematic Selection of Scavenging Models: A Flow-Chart Approach

Hales (1984) has suggested a flow-chart approach to aid in selecting a scavenging-model. Presented with a decision tree in Figure 6-24, the user proceeds by answering a series of questions that relate to the model's intended use, temporal and geographical scales, pollutant characteristics, choice between macroscopic and microscopic material balances, and type of

---

[10] There is no direct reason to expect that ε_p should be similar to ε in magnitude. In the absurd circumstance where all the pollutant is concentrated into one particle, for example, then scavenging of that pollutant by a very light rainfall would yield $\varepsilon = 1.0 >> \varepsilon_p$. Conversely a large storm processing an insoluble gaseous pollutant (SF_6, say) would provide $\varepsilon \approx 0 << \varepsilon_p$. For practical conditions involving acid-forming aerosols, however, the scavenging of water vapor and pollutant appears to be sufficiently related to allow $\varepsilon_p \approx \varepsilon$ to be employed as an approximate rule-of-thumb.

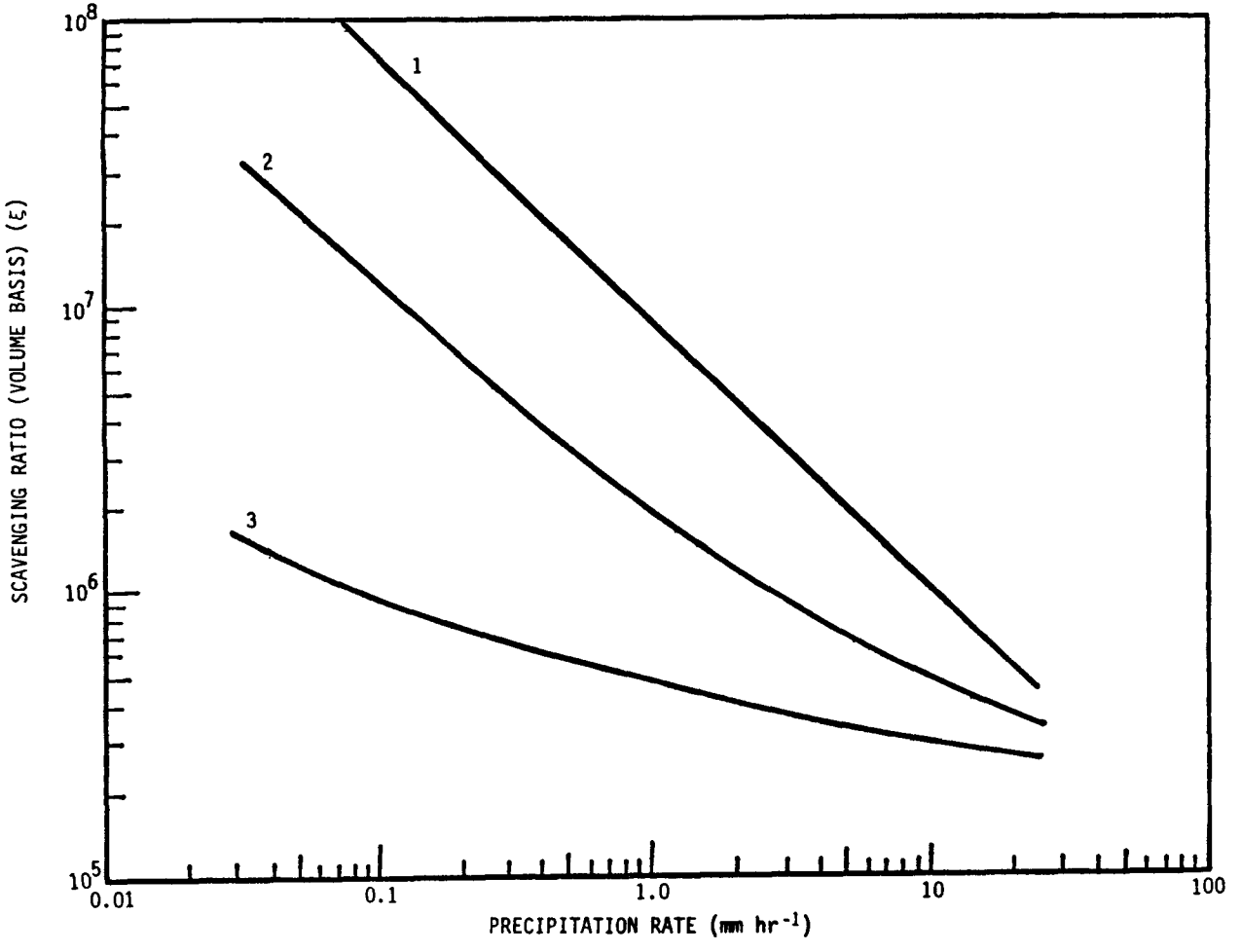

Figure 6-23. Scott's scavenging ratio curves: 1-convective storms; 2-warm, nonconvective storms; 3-cold storms, where Bergeron-Findeisen process is active (Scott 1978).

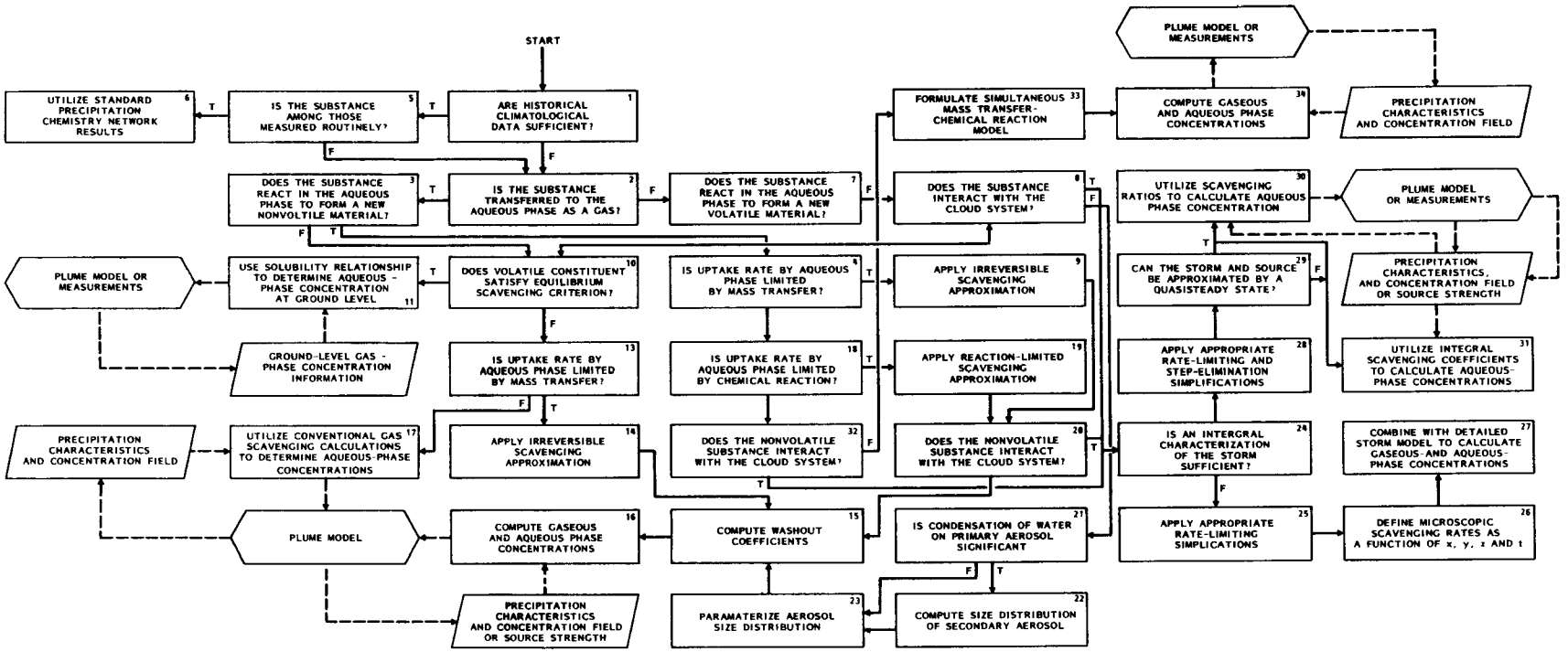

Figure 6-24. Flow chart for scavenging calculations.

conservation (i.e., material, energy, momentum) equations involved. Various pathways through this decision tree are discussed in the original reference.

Proceeding through Figure 6-24 in this manner, the user can arrive at simple or complex end points, depending upon the nature of his particular application. A trivial example is pathway 1-5-6, which instructs the user to disregard modeling and rely solely upon past measurements. The simple microscopic-balance example of Section 6.5.4 can be traced through pathway 1-2-7-8-21-23-15-16.

Table 6-5 itemizes some currently-available models, which can be related directly to the pathways of Figure 6-24. This provides the reader with a rapid and efficient means of access to current modeling literature, while minimizing the chance of pitfall encounters that can arise from the inadvertent use of inappropriate physical constraints. For a more definitive description of this model selection process, the reader is referred to the original reference (Hales 1984).

6.6 PRACTICAL ASPECTS OF SCAVENGING MODELS: UNCERTAINTY LEVELS AND SOURCES OF ERROR

Quantitatively assessing the predictive capability of present wet-removal models is a complex task, well beyond the scope of this document. There are, however, a number of general statements which are highly useful for focusing in on this question and for providing insights pertaining to model reliability. These are itemized sequentially below.

- The predictive capability of a scavenging model is strongly contingent upon its desired application.

  As noted in 6.5.1, a variety of different applications exist for scavenging models, and some are much more difficult to fulfill than others. One can, for example, employ existing regional models to reproduce distributions of annually-averaged, wet-deposited, sulfate ion in eastern North America with moderate success. If one is charged with the task of relating specific sources to deposition at a chosen receptor site, however, our predictive capability can be expected to be relatively imprecise. Similarly, if one is expected to forecast the change in deposition that would occur in response to some future change in emissions, then the associated uncertainty level would be very high indeed. The question of nonlinear response is of paramount importance in this last application.

  A large component of our uncertainty in predicting source attribution and transient response is based simply on the fact that we do not have adequate data bases for testing model performance for these applications. Our present models may in actuality be better predictors in this respect than anticipated, but because we have no immediate way of confirming this, our uncertainty level remains high (Section 6.4).

TABLE 6-5. PERTINENT LITERATURE REFERENCES FOR WET-REMOVAL MODELS

	Model	Type of Balance Equation(s)	Mechanism(s)	Typical Application	Pertinent References
1.	Classical Washout Coefficient	Material (Differential)	Irreversible Attachment	Below-cloud scavenging of aerosols and reactive gases	Chamberlain (1953), Engelmann (1968), Fisher (1975), Scriven and Fisher (1975), Wangen and Williams (1978)
2.	Distributed Washout Coefficient	Material (Differential)	Irreversible Attachment	Below-cloud scavenging of size-distributed aerosols	Dana and Hales (1976), Slinn (1983)
3.	"Two-Stage" Nucleation-Accretion	Material (Differential)	Irreversible Attachment	Condensation-enhanced below-cloud scavenging of aerosols	Radke et al. (1978), Slinn (1983)
4.	Nonreactive Gas Scavenging	Material (Differential)	Reversible Attachment	Below-cloud scavenging of nonreactive gases	Hales et al. (1973, 1979), Slinn (1974b), Barrie (1978)
5.	Reactive Gas Scavenging	Material (Differential)	Reversible Attachment with Aqueous-Phase Reaction	Below-cloud scavenging of reactive gases	Hill and Adamowicz (1977), Adamowicz (1979), Overton et al. (1979), Durham et al. (1981), Drewes and Hales (1982)
6.	In-Cloud Aerosol Scavenging	Material (Differential)	Irreversible Attachment	Scavenging in storm systems (nonreactive)	Junge (1963), Dingle and Lee (1973), Storebo and Dingle (1974), Klett (1977), Lange and Knox (1977), Slinn (1983)
7.	In-Cloud Aerosol Scavenging	Material (Integral)	Irreversible or Reversible Attachment	Scavenging in storm systems	Engelmann (1971), Gatz (1972), Scott (1978), Hales and Dana (1979a), Slinn (1983)
8.	In-Cloud Reactive Gas and Aerosol Scavenging	Material (Differential)	Transport, Reaction and Deposition	Scoping studies	Gravenhorst et al. (1978), Omstedt and Rodhe (1978)
9.	In-Cloud Reactive Gas and Aerosol Scavenging	Material (Integral)	Irreversible or Reversible Attachment with Chemical Reaction	Interpretation of field study data	Scott (1982)

TABLE 6-5. CONTINUED

Model	Type of Balance Equation(s)	Mechanism(s)	Typical Application	Pertinent References
10. Composite Analytical	Material (Differential)	Transport, Reaction and Deposition	Regional scale deposition	Astarita et al. (1979), Fay and Rosenzweig (1980)
11. Composite Trajectory	Material (Differential)	Transport, Reaction and Deposition	Regional scale deposition	Bolin and Persson (1975), Hales (1977), Eliassen (1978), Fisher (1975), Bass (1980), Heffter (1980), Henmi (1980), Sampson (1980), Bhumralkar et al. (1980), Kleinman et al. (1980), Shannon (1981), McNaughton et al. (1981), Patterson et al. (1981), Voldner (1981)
12. Composite Grid	Material (Differential)	Transport, Reaction and Deposition	Regional scale deposition	Liu and Durran (1977), Prahm and Christensen (1977), Wilkening and Ragland (1980), Lavery (1980), Lee (1981), Carmichael and Peters (1981), Lamb (1981)
13. Composite Statistical	Material	Transport, Reaction and Deposition	Scoping studies and life-time assessment	Rodhe and Grandell (1972, 1981)
14. Nonreactive	Material Energy and Momentum (Differential)	Irreversible Attachment, Nonreactive	In-cloud scavenging analysis	Molenkamp (1974), Hane (1978), Kreitzburg and Leach (1978)
15. Reactive	Material and Energy (Differential)	All modes of scavenging including chemical reaction	In-cloud scavenging analysis	Hales (1982)

Regardless of the above considerations it should be emphasized strongly that the first step in scavenging model evaluation must be the precise definition of the intended uses of the model. All subsequent efforts will be confounded in the absence of this focal point.

- The predictive capability of a scavenging model depends upon the choice of model.

At first sight this appears to be a self-evident and trivial statement. A profusion of scavenging models exists, however, and it is not at all difficult to choose an inappropriate candidate inadvertently. Such inappropriate selections have on occasion resulted in reported calculations which have been in error by several orders of magnitude (Section 6.5.1).

This component of error may of course be totally eliminated by selecting the most appropriate model for the intended application. The flow chart presented in Figure 6-24 is a useful guide for this purpose, especially for those only casually familiar with the field.

- The predictive capability of a scavenging model depends strongly upon the processes modeled.

As noted in the context of Figure 6-2 a scavenging model may encompass one, several, or all of the steps in the composite wet-removal sequence. If only a small portion of this sequence is being considered, the model depends heavily upon information supplied from the remaining components. This information may originate from assumptions, from empirical measurements, or from the output of other models. Assuming that all input information is error-free, then it may be stated generally that the more steps in Figure 6-2 encompassed by a given model, the greater will be its predictive uncertainty. This is simply a consequence of propagating errors and must be considered as a primary factor when one addresses the validation of wet-removal calculations.

- The predictive capability of a scavenging model depends upon its areal range.

This statement is largely a corollary of the one immediately above. As a scavenging model is extended to, say, a regional scale it is forced to include essentially all of the components of Figure 6-2. As noted previously, this is likely to increase uncertainty levels appreciably.

- The predictive capability of a scavenging model is contingent upon its temporal averaging time.

Owing to the propensity of stochastic phenomena to average out to mean values, the predictive capabilities of (especially regional) scavenging models can be expected to improve somewhat as averaging times increase (see Chapter A-9). This improvement is, of course, gained at the expense of sacrificing temporal resolution, and a value judgment is

necessary (again requiring a precise definition of intended model application) at this juncture.[11]

This observation should be tempered by the fact that, in addition to random errors, scavenging models can be expected to possess substantial systematic biases. In general these biases do not decrease with averaging time and in fact many lead to cumulative discrepancies on occasion. Examples of systematic errors are biases in trajectory calculations and artificial offsets induced by the superimposition of random events on nonlinear processes. Again the seriousness of such factors is heavily contingent on the intended model application (Section 6.5.1).

In general summary, it may be stated that several important factors lead to widely varying levels of uncertainty in scavenging-model predictions. One may predict, for example, the scavenging of SO_2 from a local power-plant plume by using existing models and expect to match measured results within a factor of two. On the other hand, similar predictions of, say, the fraction of sulfate at a given receptor which originated from some particular source can be expected to have orders-of-magnitude associated uncertainty. Both a comprehensive model-evaluation effort and a substantially-improved data base will be required before this situation can be remedied to any appreciable extent (Section 6.4).

6.7 CONCLUSIONS

This chapter has provided an overview of meteorological processes contributing to wet removal of pollutants and has summarized the current state of our capability to describe these complex phenomena in mathematical form. Because of the magnitude of this problem, it has been necessary to refrain from detailed descriptions of models and modeling techniques; rather, we have chosen to describe the general mathematical basis for wet-removal modeling, to give two simple examples of direct application, and then to supply the reader with a means for efficiently pursuing the available literature for specific applications of interest.

In conclusion to this discussion it is appropriate to summarize the state of these calculational techniques by asking the following questions:

- Just how accurate and valid are current wet-removal modeling techniques as predictions of precipitation chemistry and wet deposition; that is, how well do they fulfill the needs itemized in Section 6.5.1?

- What must be accomplished before the present capabilities can be improved?

---

[11]This issue is especially pertinent in view of the contention, often voiced by some scientists within the acid-precipitation effects community, that temporally-averaged results (averaging times of a few months or more) are totally adequate for assessment purposes.

The answers to these questions are somewhat mixed. Certainly the techniques discussed in this chapter, if used appropriately, are capable of order-of-magnitude determinations in many circumstances; and under restricted conditions they can even generate predictions having factor-of-two accuracy or better. Moreover, there is ample explanation in existing theories of wet removal to account easily for the spatial and temporal variabilities observed in nature.

These capabilities, however, cannot be considered to be very satisfactory in the context of current needs. The noted ability to explain spatial and temporal variability on a semiquantitative basis has not resulted in a large competence in predicting such variability in specific instances. Moreover, we possess very little competence in identifying specific sources responsible for wet deposition at a given receptor site. Finally, the order-of-magnitude predictive capability noted above hardly can be judged satisfactory for most assessment purposes.

In reviewing the discussions of this chapter against the backdrop of these deficits, several research needs become apparent. The most important of these are itemized in the following paragraphs:

- Much more definitive information is needed with regard to the scavenging efficiencies of submicron aerosols, for both rain and snow. Especially important in this regard is the effect of condensational growth of such aerosols in below-cloud environments (Section 6.5.3).

- We need to know much more about aqueous-phase conversion processes, which are potentially important as alternate mechanisms resulting in the presence of species such as sulfate and nitrate in precipitation. Because virtually nothing is known presently regarding the chemical formation of such species in clouds and precipitation, there is a tendency to lump these effects with physical removal processes in most modeling efforts, expressing them in terms of pseudo scavenging coefficients or collection efficiencies. Such phenomena must be resolved in finer mechanistic detail than this before a satisfactory treatment is possible, and this requires a knowledge of chemical transformation processes that is much more advanced than exists at present (Sections 6.2.4 and 6.5.3 and Chapter A-4).

- Much more extensive understanding of the competitive nucleation capability of aerosols in in-cloud environments is needed, especially for those substances that do not compete particularly well in the nucleation process. The influence of aerosol-particle composition--especially for "internally-mixed" aerosols (those containing individual particles composed of mixed chemical species)--is particularly important in this regard (Section 6.2).

- Identifying specific sources responsible for chemical deposition at a given receptor location requires that we possess a much more accomplished capability to describe long-range pollution transport. Progress in this area during recent years has been encouraging, but

much more remains to be achieved before we are sufficiently proficient for reliable source-receptor analysis (Section 6.4).

- We still need to enhance our understanding of the detailed microphysical and dynamic processes that occur in storm systems. Besides providing required knowledge of basic physical phenomena, such research is important in providing valid parameterizations of wet-removal for subsequent use in composite regional models (Section 6.4).

As a final note, it is useful to reflect once again on the fact that scavenging modeling research--as treated in this chapter--has been in a rather continuous state of development over the past 30 years. While progress has been indeed significant during this period, a number of important and unsolved problems still exist. Accordingly, one must use this perspective in assessing our rate of advancement during future years. Reasonable progress in resolving the above items can be expected over the next decade; but the complexity of these problems demands that a serious and sustained effort be applied for this purpose.

6.8 REFERENCES

Adamowicz, R. F. 1979. A model for the reversible washout of sulfur dioxide, ammonia, and carbon dioxide from a polluted atmosphere and the production of sulfate in raindrops. Atmos. Environ. 13:105-121.

Astarita, G., J. Wei, and G. Iorio. 1979. Theory of dispersion transformation and deposition of atmospheric pollution using modified Green's functions. Atmos. Environ. 13:239-246.

Baker, M. B., H. Harrison, J. Vinelli, and K. B. Erickson. 1979. Simple stochastic models for the sources and sinks of two aerosol types. Tellus 31:1-39.

Barrie, L. A. 1978. An improved model of reversible SO_2 washout by rain. Atmos. Environ. 12:407-412.

Barrie, L. A. and J. Kovalick. 1978. A wintertime investigation of the deposition of pollutants around an isolated power plant in northern Alberta. Atmospheric Environment Service, Environment Canada, REP ARQT-4-78.

Bass, A. 1980. Modeling long-range transport and diffusion. Proc. Second Conf. on App. Air Pol. Meteorol. AMS/APCA, New Orleans.

Berry, E. X. and R. L. Reinhardt. 1974. An analysis of cloud drop growth by collection. Part IV. A new parameterization. J. Atm. Sci. 31:2127-2135.

Bhumralkar, C. M., W. B. Johnson, R. H. Mancusco, R. H. Thuillier, and D. E. Wolf. 1980. Interregional exchanges of airborne sulfur pollution and deposition in eastern North America. Proc. Second Conf. on App. Air Pol. Meteorol. AMS/APCA, New Orleans.

Bird, R. B., W. E. Stewart, and E. N. Lightfoot. 1960. Transport Phenomena. John E. Wiley, New York, NY.

Bolin, B. and C. Persson. 1975. Regional dispersion and deposition of atmospheric pollutants with particular application to sulphur pollution over western Europe. Tellus 27:281-309.

Browning, K. A., M. E. Hardman, T. W. Harrold, and C. W. Pardoe. 1973. The structure of rainbands within a midlatitude cyclonic depression. Quart. J. Roy. Meteorol. Soc. 99:215-231.

Burtsev, I. E., L. V. Burtsevva, and S. G. Malakhov. 1976. Washout characteristics of a ^{32}P aerosol injected into a cloud. Atmospheric scavenging of radioisotopes. Symp. Proc. Palanga, USSR.

Cadle, R. D. 1965. Particle Size. Reinhold, New York, 390 pp.

Carmichael, G. R. and L. K. Peters. 1981. Application of the sulfur transport Eulerian Model (STEM) to a SURE data set. 12th Int. Tech. Meeting on Air Poll. Mod. and its App. NATO, Palo Alto.

Chamberlain, A. C. 1953. Aspects of travel and deposition of aerosols and vapor clouds. AERE Harwell, Report R1261, HMSO London.

Chan, W. H., M. A. Lusis, A. J. S. Tang, C. U. Ro, and R. J. Vet. 1982. Precipitation scavenging and dry deposition of pollutants from the INCO nickel smelter in Sudbury. Presented at Fourth International Conference on Precipitation Scavenging, Dry Deposition, and Resuspension. Santa Monica, CA.

Changnon, S. A. 1968. Precipitation scavenging of Lake Michigan Basin. Bull. 52. Illinois State Water Survey Report, Urbana, IL.

Changnon, S. A. A. Auer, R. Brahm, J. Hales, and R. Semonin. 1981. METROMEX: A Review and Summary. AMS Monograph, Vol. 18, Am. Meteorol. Soc., Boston, MA.

Court, A. 1966. Fog Frequency in the United States. Geog. Rev. N.Y., 56:543-550.

Dana, M. T. 1970. Scavenging of soluble dye particles by rain. In Precipitation Scavenging 1970. R. J. Engelmann and W. G. N. Slinn, eds. AEC Symposium Series.

Dana, M. T. and D. W. Glover. 1975. Precipitation scavenging of power plant effluents: Rainwater concentrations of sulfur and nitrogen compounds and evaluation of rain samples desorption of SO_2. PLN Annual Report to U.S. AEC, BNWL-1950.

Dana, M. T. and J. M. Hales. 1976. Statistical aspects of the washout of polydisperse aerosols. Atmos. Environ. 10:45-50.

Dana, M. T., D. R. Drewes, D. W. Glover, and J. M. Hales. 1976. Precipitation scavenging of fossil fuel effluents. Battelle-Northwest Report to EPA, EPA-600/4-76-031.

Dana, M. T., J. M. Hales, and M. A. Wolf. 1972. Natural precipitation washout of sulfur dioxide. Battelle-Northwest Report to EPA, BNW-389.

Dana, M. T., J. M. Hales, W. G. N. Slinn, and M. A. Wolf. 1973. Natural precipitation washout of sulfur compounds from plumes. Battelle-Northwest Report to EPA, EPA-R3-73-047.

Dana, M. T., A. A. N. Patrinos, E. G. Chapman, and J. M. Thorp. 1982. Wintertime precipitation chemistry in North Georgia. Proc. ACS Symposium on Acid Rain, Las Vegas, NV.

Dana, M. T., N. A. Wogman, and M. A. Wolf. 1978. Rain scavenging of tritiated water (HTO): A field experiment and theoretical considerations. Atmos. Environ. 12:1523-1529.

Davenport, H. M. and L. K. Peters. 1978. Field studies of atmospheric particulate concentration changes during precipitation. Atmos. Environ. 12:997-1008.

Davies, C. N. 1966. Aerosol Science. Academic Press, New York.

Dingle, A. N. and Y. Lee. 1973. An analysis of in-cloud scavenging. J. Appl. Meteorol. 12:1295-1302.

Dingle, A. N., D. F. Gatz, and J. W. Winchester. 1969. A pilot experiment using indium as tracer in a convective storm. J. Appl. Meteorol. 8:236-240.

Drewes, D. R. and J. M. Hales. 1982. SMICK: A scavenging model incorporating chemical kinetics. Atmos. Environ. 16:1717-1724.

Durham, J. L., J. H. Overton, and V. P. Aneja. 1981. Influence of gaseous nitric acid on sulfate production and acidity in rain. Atmos. Environ. 15:1059-1068.

Easter, R. C. 1982. The OSCAR Experiment. Proc. ACS Symposium on Acid Rain, Las Vegas, NV.

Easter, R C. and J. M. Hales. 1983a. Interpretations of the OSCAR data for reactive gas scavenging. Proc. Fourth International Conference on Precipitation Scavenging, Dry Deposition and Resuspension, Santa Monica, CA.

Easter, R. C. and J. M. Hales. 1983b. Mechanistic evaluation of precipitation-scavenging data using a one-dimensional reactive storm model. Battelle-Northwest report to EPRI, EPRI RP-2022-1.

Eliassen, A. 1978. The OECD study of long-range transport of air pollutants. Atmos. Environ. 12:479-487.

Engelmann, R. J. 1965. Rain scavenging of zinc sulphide particles. J. Atm. Sci. 22:719-724.

Engelmann, R. J. 1968. The calculation of precipitation scavenging. In Meteorology and Atomic Energy 1968. D. Slade, ed. U.S. AEC.

Engelmann, R. J. 1971. Scavenging prediction using ratios of air and precipitation. J. Appl. Meteorol. 10:493-497.

Enger, L. and U. Hogstrom. 1979. Dispersion and wet deposition of sulfur from a power-plant plume. Atmos. Environ. 13:797-810.

Falconer, R. E. and P. D. Falconer. 1980. Determination of Cloud Water Acidity at a Mountain Observatory in the Adirondack Mountains of New York State. J. Geophys. Res. 85:7465-7470.

Fay, J. A. and J. J. Rosenzweig. 1980. An analytical diffusion model for long-distance transport of air pollutants. Atmos. Environ. 14:355-365.

Fisher, B. E. A. 1975. The long range transport of sulfur dioxide. Atmos. Environ. 9:1063-1070.

Fitzgerald, J. W. 1974. Effect of aerosol composition of cloud-droplet size distribution: A numerical study. J. Atm. Sci. 31:1358-1367.

Fuchs, N. A. 1964. The Mechanics of Aerosols. Pergamon Press, Oxford, 407 pp.

Fuquay, J. J. 1970. Scavenging in perspective. In Precipitation Scavenging 1970. R. J. Engelmann and W. G. N. Slinn, eds. AEC Symposium Series 22.

Galloway, J. N. and D. M. Whelpdale. 1980. An atmospheric sulfur budget for eastern North America. Atmos. Environ. 14:409-417.

Gatz, D. F. 1972. Washout ratios in urban and non-urban areas. Proc. AMS Conf. on Urban Environment. Philadelphia, PA.

Gatz, D. F. 1977. A review of chemical tracer experiments on precipitation systems. Atmos. Environ. 11:945-953.

Gibbs, A. G. and W. G. N. Slinn. 1973. Fluctuations in trace gas concentrations in the troposphere. J. Geophys. Res. 78:574-576.

Godske, C. L., T. Bergeron, J. Bjerkness, and R. E. Bundgaard. 1957. Dynamic Meteorology and Weather Forecasting. Am. Meteorol. Soc., Boston, MA.

Graedel, T. E. and J. P. Franey. 1977. Field measurements of submicron aerosol washout by rain. In Precipitation Scavenging 1974. ERDA Symposium Series 41.

Granat, L. and H. Rodhe. 1973. A Study of fallout by precipitation around an oil-fired power plant. Atmos. Environ. 7:781-792.

Granat, L. and R. Soderlund. 1975. Atmospheric deposition due to long and short distance sources with special reference to wet and dry deposition of sulfphur compounds around an oil-fired power plant. MISU Report A-32, Stockholm University, Sweden.

Gravenhorst, G., T. Janssen-Schmidt, D. H. Ehhalt, and E. P. Roth. 1978. The influence of clouds and rain on the vertical distribution of sulfur dioxide in a one dimensional steady-state model. Atmos. Environ. 12:691.

Greenfield, S. M. 1957. Rain scavenging of radioactive particulate matter from the atmosphere. J. Meteorology 14:115-123.

Hales, J. M. 1972. Fundamentals of the theory of gas scavenging by rain. Atmos. Environ. 6:635-659.

Hales, J. M. 1977. An air pollution model incorporating nonlinear chemistry, variable trajectories, and plume-segment diffusion. Battelle-Northwest Report to EPA, EPA-450/3-77-012.

Hales, J. M. 1982. Mechanistic analysis of precipitation scavenging using a one-dimensional, time-variant model. Atmos. Environ. 16(7):1775-1783.

Hales, J. M. 1984. Precipitation chemistry: Its behavior and its calculation. In Air Pollutants and Their Effects on the Terrestrial Ecosystem. S. V. Krupa and A. H. Legge, eds. John M. Wiley, New York, NY.

Hales, J. M. and M. T. Dana. 1979a. Precipitation scavenging of urban pollutants by convective storm systems. J. Appl. Meteorol. 18:294-316.

Hales, J. M. and M. T. Dana. 1979b. Regional scale deposition of sulfur dioxide by precipitation scavenging. Atmos. Environ. 13:1121-1132.

Hales, J. M., J. M. Thorp, and M. A. Wolf. 1971. Field investigation of sulfur dioxide washout from the plume of a large coal-fired power plant by natural precipitation. Battelle-Northwest Final Report to Environmental Protection Agency, NTIS PB 203-129.

Hales, J. M., D. M. Miller, A. J. Alkezweeny, and R. N. Lee. 1979. Ozone formation related to power plant emissions. Science 202:1186-1188.

Hales, J. M., M. A. Wolf, and M. T. Dana. 1973. A linear model for predicting the washout of pollutant gases from industrial plumes. AICHE J. 19:292-297.

Hane, C. E. 1978. Scavenging of urban pollutants by thunderstorm rainfall: Numerical experimentation. J. Appl. Meteorol. 17:699-710.

Haurwitz, B. and J. M. Austin. 1944. Climatology. McGraw-Hill, New York, NY.

Heffter, J. L. 1980. Air resources laboratories atmospheric transport and dispersion model (ARL-ATAD). NOAA Tech. Memo, ERL-81.

Henmi, J. 1980. Long-range transport model of SO_2 and sulfate and its application to the eastern United States. J. Geophys. Res. 85:4436-4442.

Hill, F. B. and R. F. Adamowicz. 1977. A model for rain composition and the washout of sulfur dioxide. Atmos. Environ. 11:912-927.

Hobbs, P. V. 1978. Organization and structure of clouds and precipitation on the mesoscale and microscale in cyclonic storms. Rev. Geophys. and Space Sci. 16:741-755.

Hogstrom, U. 1974. Wet fallout of sulfurous pollutants emitted from a city during rain or snow. Atmos. Environ. 8:1291-1303.

Hutcheson, M. R. and F. P. Hall. 1974. Sulfate washout from a coal-fired power plant plume. Atmos. Environ. 8:23-28.

Junge, C. E. 1963. Air Chemistry and Radioactivity. Academic Press, New York.

Junge, C. E. 1974. Residence time and variability of tropospheric trace gases. Tellus 26:477-488.

Klein, W. H. 1958. The frequency of cyclones and anticyclones in relation to the mean circulation. J. Meteorol. 15:98-102.

Kleinman, L. J., J. G. Carney, and R. E. Meyers. 1980. Time dependence on average regional sulfur oxide concentrations. Proc. Second Conf. on App. Air Pol. Meteorol. AMS/APCA, New Orleans.

Klett, J. 1977. Precipitation scavenging in rainout assessment: The ACRA system and summaries of simulation results. LASL Report to ERDA, LA6763.

Kramer, J. R. 1973. Atmospheric composition and precipitation of the Sudbury Region. Alternatives 2:18-25.

Kreitzberg, C. W. and M. J. Leach. 1978. Diagnosis and prediction of tropospheric trajectories and cleansing. Proc. 85th National Meeting AICHE, Philadelphia, PA.

Lamb, R. G. 1981. A regional scale model of photochemical air pollution. Draft Report, Meteorology and Assessment Division, U.S. EPA/ESRL, Research Triangle Park, NC.

Lange, R. and J. B. Knox. 1977. Adaptation of a three-dimensional atmospheric transport-diffusion model to rainout assessments. Precipitation Scavenging 1974. R. S. Semonin and R. W. Beadle, eds. ERDA Symposium Series 41, CONF 741003.

Larson, T. V., R. J. Charlson, E. J. Knudson, G. D. Shristian, and H. Harrison. 1975. The influence of a sulfur dioxide point source on the rain chemistry of a single storm in the Puget Sound Region. Water, Air, Soil Pollut. 4:319-328.

Lavery, T. L. 1980. Development and validation of a regional model to simulate atmospheric concentrations of SO_2 and sulfate. Proc. Second Joint Conf. on App. Air Pol. Meteorol., New Orleans, LA.

Lee, H. N. 1981. An Alternate Pseudospectral Model for Pollutant Transport. Diffusion, and Deposition in the Atmosphere. Atmos. Environ. 15:1017-1024.

Lee, R. N. and J. M. Hales. 1974. Precipitation scavenging of organic contaminants. Battelle-Northwest Final Report to U.S. Army Research Office, Durham, NC.

Levich, V. G. 1962. Physicochemical Hydrodynamics. Prentice Hall, Englewood Cliffs, NJ, 700 pp.

Liu, M. K. and D. Durran. 1977. The development of a regional air pollution model and its application to the northern Great Plains. EPA Report, EPA-908/1-77-001.

Lovett, G. M., W. A. Reiners, and R. K. Olson. 1982. Cloud droplet deposition in subalpine Balsam Fir forests: Hydrological and chemical inputs. Science 218:1303-1304.

MAPS3S/RAINE. 1981. Biennial Progress Report. NTIS PNL-4096, U.S. EPA/DOE.

MAP3S/RAINE. 1982. The MAP3S/RAINE precipitation chemistry network: Statistical overview for the periods 1976-1980. Atmos. Environ. 16:1603-1631.

Mason, B. J. 1971. The Physics of Clouds. Clarendon Press, Oxford, UK. p. 579.

McNaughton, D., D. Powell, and C. Berkowitz. 1981. A User's Guide to RAPT. MAP3S/RAINE Report, PNL-3390.

Millan, M. M., S. C. Barton, N. D. Johnson, B. Weisman, M. Lusis, W. Chan, and R. Vet. 1982. Rain scavenging from tall stacks: A new experimental approach. Atmos. Environ. 16:2709-2714.

Molenkamp, C. R. 1974. A one-dimensional numerical model of precipitation scavenging with application to rainout of radioactive debris. Lawrence Livermore Laboratory, Report to U.S. AEC, UCRL-51627.

Morgan, J. J. and H. M. Liljestrand. 1980. Measurements and interpretation of acid rainfall in the Los Angeles Basin. Cal Tech Final Report AC-2-80, Pasadena, CA.

Mosiac. 1979. Acid From the Sky. Mosiac (National Science Foundation) 10:35-40.

Newell, R. E., J. W. Kidson, D. G. Vincent, and G. J. Baer. 1972. The General Circulation of the Tropical Atmosphere. Vols. 1 and 2. MIT Press, Cambridge, MA.

Omstedt, G. and H. Rodhe. 1978. Transformation and removal processes for sulfur compounds as described by a one-dimensional time-dependent diffusion model. Atmos. Environ. 12:503-509.

Overton, J. H., V. P. Aneja, and J. L. Durham. 1979. Production of sulfate in rain and raindrops in polluted atmospheres. Atmos. Environ. 13:355-367.

Patterson, D. E., R. B. Husar, W. E. Wilson, and L.F. Smith. 1981. Monte Carlo simulation of daily regional sulfur distribution. J. Appl. Meteorol. 20:404-420.

Prahm, L. P. and O. Christensen. 1977. Long-range transmission of pollutants simulated by a two-dimensional pseudospectral dispersion model. J. Appl. Meteorol. 16:896-910.

Pruppacher, H. R. and J. D. Klett. 1978. Microphysics of Clouds and Precipitation. D. Reidel Pub. Co., Boston, MA.

Radke, L. F., M. W. Eltgroth, and P. V. Hobbs. 1978. Precipitation scavenging of aerosol particles. Proc. Cloud Physics and Atmospheric Electricity. Am. Meteorol. Soc., Boston, MA.

Raynor, G. S. 1981. Design and preliminary results of the intermediate density precipitation-chemistry experiment. Report BNL 29992. For presentation at Third Joint AMS/APCA Conference on Applications of Air Pollution Meteorology, January. San Antonia, TX.

Rodhe, H. and J. Grandell. 1972. On the removal time of aerosol particles from the atmosphere by precipitation scavenging. Tellus 24:442-454.

Rodhe, H. and J. Grandell. 1981. Estimates of characteristic times for precipitation scavenging. J. Atm. Sci. 38:370-386.

Saffman, P. G. and J. S. Turner. 1955. On the collision of drops in turbulent clouds. J. Fluid Mech. 1:16-30.

Sampson, P. J. 1980. Trajectory analysis of summertime sulfate concentrations in the northeastern United States. J. Appl. Meteorol. 19:1382-1394.

Scott, B. C. 1978. Parameterization of sulfate removal by precipitation. J. Appl. Meteorol. 17:1375-1389.

Scott, B. C. 1981. Sulfate washout ratios in winter storms. J. Appl. Meteorol. 20:619-625.

Scott, B. C. 1982. Predictions of in-cloud conversion rates of SO_2 to SO_4 based upon a simple chemical and kinematic storm model. Atmos. Environ. 16:1735-1752.

Scott, B. C. and N. S. Laulainen. 1979. On the concentration of sulfate in precipitation. J. Appl. Meteorol. 18:138-147.

Scriven, R. A. and B. E. A. Fisher. 1975. The long range transport of airborne material and its removal by deposition and washout. Atmos. Environ. 9:49-68.

Semonin, R. G. 1976. The variability of pH in convective storms. Proc. First International Symposium on Acid Precipitation and the Forest Ecosystem. USDA Tech. Rept. NE-23, pp. 349-361.

Shannon, J. 1981. A regional model of long-term average sulfur atmospheric pollution, surface removal, and net horizontal flux. Atmos. Environ. 5:689-701.

Shopauskas, K., B. Styra, and E. Verba. 1969. Spreading and rainout of passive admixture injected into a cloud. 7th Int. Conf. on Condensation and Ice Nuclei, Vienna, Austria.

Slinn, W. G. N. 1973. In-cloud scavenging studies. Annual Report to U.S. AEC/DBER. Battelle-Northwest, BNWL-1751 pt. 1.

Slinn, W. G. N. 1974a. Rate limiting aspects of in-cloud scavenging. J. Atm. Sci. 31:1172-1173.

Slinn, W. G. N. 1974b. The redistribution of a gas plume caused by reversible washout. Atmos. Environ. 8:233-239.

Slinn, W. G. N. 1977. Some approximations for the wet and dry removal of particles and gases from the atmosphere. Water, Air, Soil Pollut. 7:513-543.

Slinn, W. G. N. 1983. Precipitation scavenging. In Atmospheric Sciences and Power Production. D. Randerson, ed. U.S. DOE.

Slinn, W. G. N. and J. M. Hales. 1971. A reevaluation of the role of thermophoresis as a mechanism of in- and below-cloud scavenging. J. Atm. Sci. 28:1465-1471.

Slinn, W. G. N. and J. M. Hales. 1983. Wet removal of atmospheric particles. EPA MONOGRAPH SERIES.

Squires, P. and S. Twomey. 1960. The relation between cloud droplet spectra and the spectrum of cloud nuclei. In Physics of Precipitation NAS/NRC Monograph No. 5. Am. Geophys. Union, Washington, D.C.

Storebo, P. B. and A. N. Dingle. 1974. Removal of pollution by rain in a shallow air flow. J. Atm. Sci. 31:533-542.

Summers, P. W. and B. Hitchon. 1973. Source and budget of sulfate in precipitation from Central Alberta, Canada. J. Air Pollut. Contr. Assoc. 23:194-199.

Thorp, J. M. and B. C. Scott. 1982. Preliminary calculations of average storm duration and seasonal precipitation rates for the northeast sector of the United States. Atmos. Environ. 16:1763-1774.

U.S. Climatological Atlas. 1968. U.S. Dept. of Commerce, Washington, D.C.

Voldner, E. C., K. Olson, K. Oikawa, and M. Loiselle. 1981. Comparison between measured and computed concentrations of sulfur compounds in eastern North America. J. Geophys. Res. 86(C6):5339-5346.

Waldman, J. M., J. W. Munger, D. J. Jacob, R. C. Flagan, J. J. Morgan, and M. R. Hoffman. 1982. Chemical composition of acid fog. Science 218:677-679.

Wang, P. K. and H. R. Pruppacher. 1977. An experimental determination of the efficiency which aerosol particles are collected by water drops in sub-saturated air. J. Atm. Sci. 34:1664-1669.

Wangen, L. E. and M. D. Williams. 1978. Elemental deposition downwind of a coal-fired power plant. Water, Air, and Soil Poll. 10:33-44.

Wilkening, K. E. and K. W. Ragland. 1980. Users Guide for the University of Wisconsin Atmopsheric Sulfur Computer Model (UWATM-SOX). Report to EPA/ Duluth Research Laboratory.

Young, J. A., C. W. Thomas, and N. A. Wogman. 1973. The use of natural and man-made radionuclides to study in-cloud scavenging processes. PNL Annual Report for 1972 to U.S. AEC/DBER, BNWL-1751 pt. 1.

Young, J. A., T. M. Tanner, C. W. Thomas, and N. A. Wogman. 1976. The entrainment of tracers near the sides of convective clouds. Annual Report to ERDA/DBER. Battelle-Northwest, BNWL-2000 pt. 3.

Zishka, K. M. and P. J. Smith. 1980. The climatology of cyclones and anticyclones over North America and surrounding ocean environs for January and July, 1950-77. Mon. Wea. Rev. 108:387-401.

THE ACIDIC DEPOSITION PHENOMENON AND ITS EFFECTS

A-7. DRY DEPOSITION PROCESSES

(B. B. Hicks)

7.1 INTRODUCTION (Eds.)

The presence of acidic and acidifying substances in the atmosphere is a result of natural and anthropogenic emissions, atmospheric transformations, and transport. Receptors are exposed to these substances through wet deposition, the processes of which were discussed in the previous chapter. These substances also impact on various receptors in the form of dry depositions. This chapter addresses many of the questions associated with the dry deposition phenomenon.

The acidic and acidifying substances associated with dry deposition include the gases, SO_2, NO_x, HCl, and NH_3 and the particulate aerosols of sulfate, nitrate, and ammonium salts. Some of the questions addressed are: How does dry deposition differ from wet deposition? How is dry deposition measured in the field, in the laboratory? What modeling techniques are available currently for predicting dry deposition for specified atmospheric concentrations and other controlling factors? The important issues addressed begin with the identification of the various chemical, physical, and biological factors that play an important role in the processes controlling the rate of dry deposition as a function of time and space. These processes take into account the aerodynamics near receptor surfaces, boundary layer effects, and other receptor surface phenomena.

The following chapter of the document discusses monitoring of dry and wet deposition. Wet deposition network data are analyzed and interpreted so as to provide maps of the U.S. and Canada with sampling site locations, median concentration data for specified sampling periods for sulfates, nitrates, ammonium ion, calcium, chloride, and pH.

7.2 FACTORS AFFECTING DRY DEPOSITION

7.2.1 Introduction

The rate of pollutant transfer between the air and exposed surfaces is controlled by a wide range of chemical, physical, and biological factors which vary in their relative importance according to the nature of the surface, the characteristics of the pollutant, and the state of the atmosphere. The complexity of the individual processes involved and the variety of possible interactions between them combine to prohibit easy generalization; nevertheless, a "deposition velocity", v_d, analogous to a gravitational falling speed, is of considerable use. In practice, knowledge of v_d enables

fluxes, F, to be estimated from airborne concentrations, C, as the simple product $v_d \cdot C$.

Particles larger than about 20 μm diameter will be deposited at a rate controlled by Stokes's law, although with some enhancement due to inertial impaction of particles transported near the surface in turbulent eddies. The settling of submicron particles in air is sufficiently slow that turbulent transfer tends to dominate, but the net flux is often limited by the presence of a quasi-laminar layer adjacent to the surface, which presents a considerable barrier to all mass fluxes and especially to gases with very low molecular diffusivity. The concept of a gravitational settling velocity is inappropriate in the case of gases. The case of particles between 1 and 20 μm diameter is especially complicated, because all of these various mechanisms are likely to be important.

Sehmel (1980a) presents a tabulation of factors known to influence the rate of pollutant deposition upon exposed surfaces. Figure 7-1 has been constructed on the basis of Sehmel's list and has been organized to emphasize the greatly dissimilar processes affecting the fluxes of gases and large particles. Small, sub-micron particles are affected by all of the factors indicated in the diagram; thus, simplification is especially difficult for deposition of such particles. In reality, Figure 7-1 already represents a considerable simplification, since it omits many potentially important factors. In particular, the diagram emphasizes properties of the medium containing the pollutants in question; a similarly complicated diagram could be constructed to illustrate the effects of pollutant characteristics. For particles, critical factors include size, shape, mass, and wettability; for gases, concern is with molecular weight and polarization, solubility, and chemical reactivity. In this context, the acidity of a pollutant that is being transferred to some receptor surface by dry processes is an especially important quality that may have a strong impact on the efficiency of the deposition process itself.

Figure 7-2 summarizes particle size distributions on a number, surface area, and volume basis. In this way, the three major modes are brought clearly to attention. The number distribution emphasizes the transient (or Aitken) nuclei range, 0.005 to 0.05 μm diameter, for which diffusion plays a role in controlling deposition. The area distribution draws attention to the so-called accumulation size range formed largely from gaseous precursors (0.05 to 2 μm diameter, affected by both diffusion and gravity). The remaining mode (2 to 50 μm diameter, most evident in the volume distribution) is the mechanically-generated particle range for which gravity causes most of the deposition. In most literature, the 2 μm diameter is used as a convenient boundary between "fine" and "coarse" particles.

As discussed in Chapter A-5, atmospheric sulfates, nitrates, and ammonium compounds are primarily associated with the accumulation size range. Figure 7-3 demonstrates that very little acidic or acidifying material is likely to be associated with the coarse particle fraction in background conditions. However, the larger particles include soil-derived minerals, some of which can react chemically with airborne and deposited acids. Moreover, it has been suggested that some of these larger particles may provide sites for the

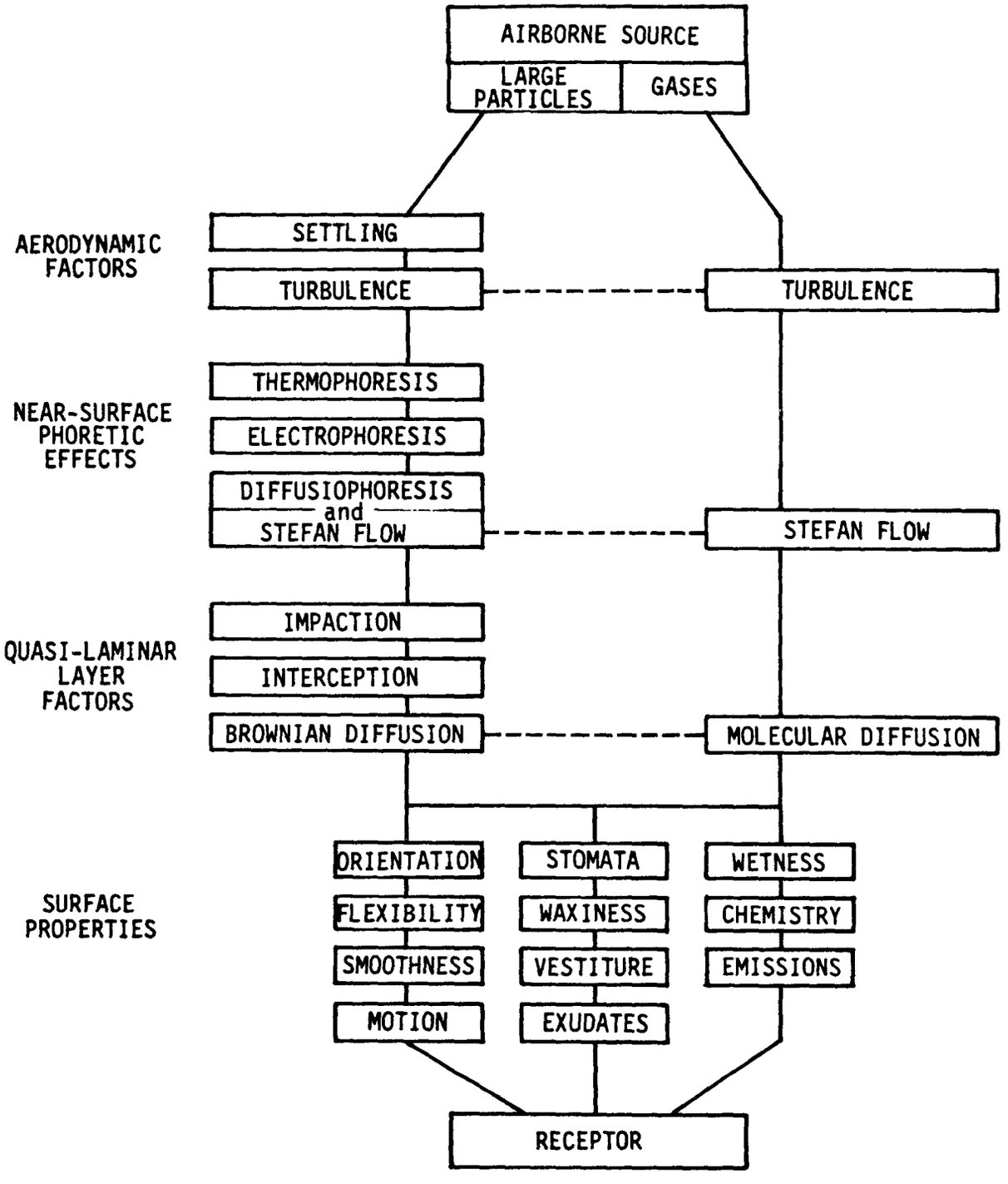

Figure 7-1. A schematic representation of processes likely to influence the rate of dry deposition of airborne gases and particles. Note that some factors affect both gaseous and particulate transfer, whereas others do not.

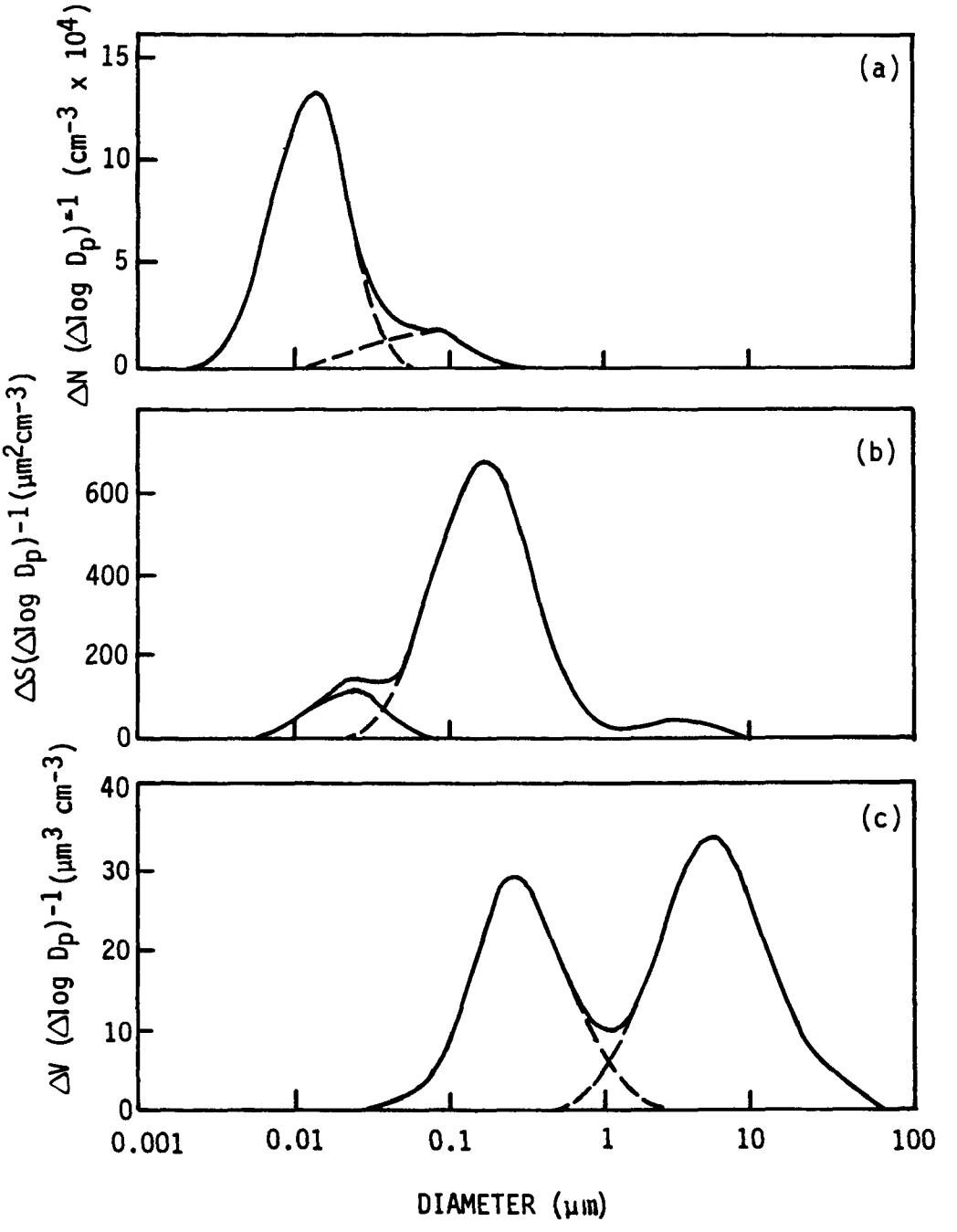

Figure 7-2. Diagrammatic representations of aerosol size distributions according to number concentration (a), surface area (b), and volume (c). Data are for typical urban area. Adapted from Whitby (1978).

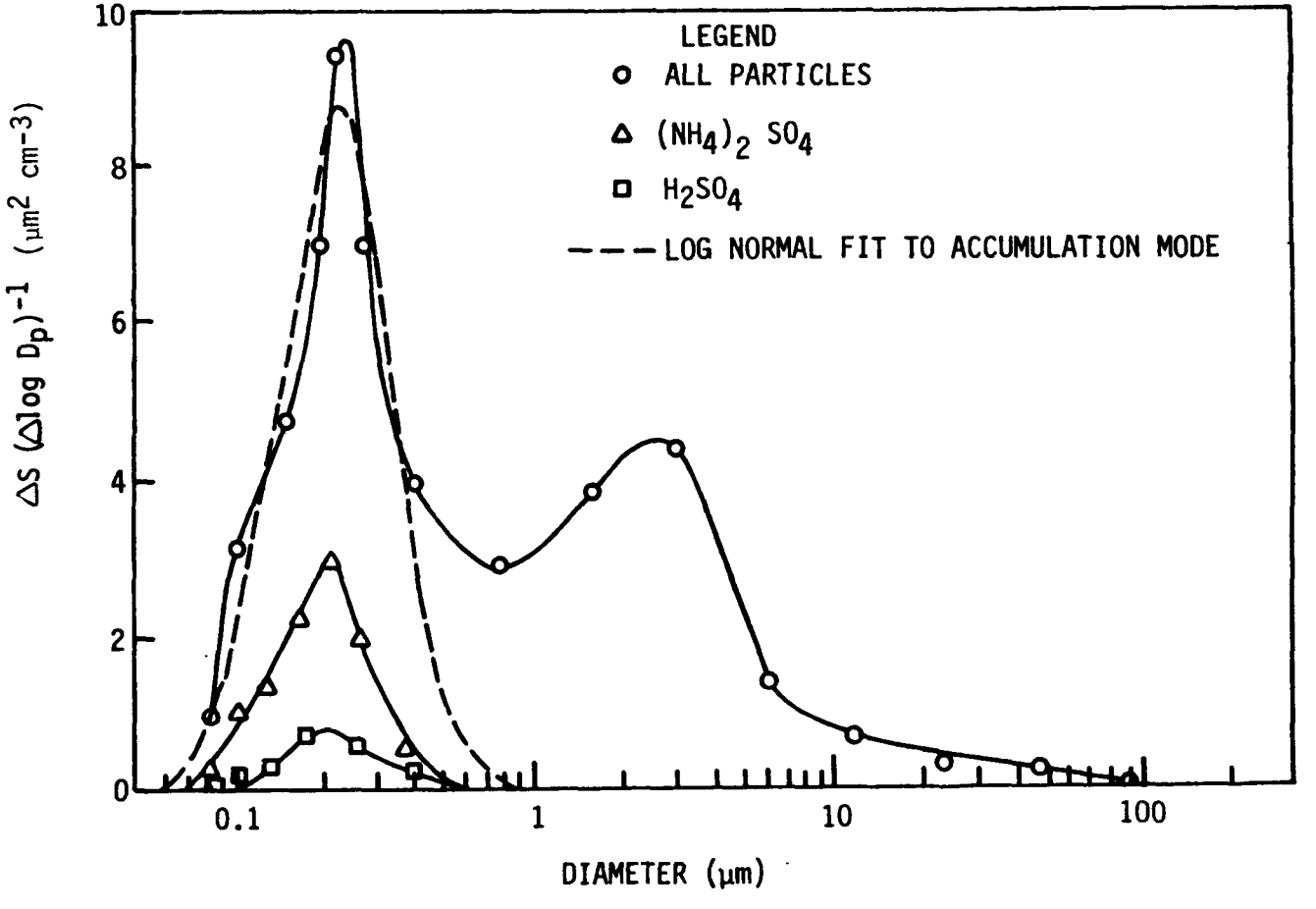

Figure 7-3. Surface area distributions of sulfate aerosol (and other) particles in background (oceanic) conditions, as determined by Whitby (1978) from the data of Meszaros and Vissy (1974).

catalytic oxidation of sulfur dioxide (e.g., when the particles are carbon; Cofer et al. 1981; Chang et al. 1981). Little is known about the detailed chemical composition of large particle agglomerates. However it is accepted that their residence time is quite short (i.e., they are deposited relatively rapidly), that there are substantial spatial and temporal variations in both their concentrations and their composition, and that their contribution to dry acidic deposition should not be ignored.

To evaluate deposition rates, several different approaches are possible. Average deposition rates can be deduced from field experiments that monitor changes over time in some system of receptors. More intensive experiments can measure the deposition of particular pollutants in some circumstances. Neither approach is capable of monitoring the long-term, spatial-average dry deposition of pollutants. To understand why, we must first consider in some detail the processes that influence pollutant fluxes and then relate these considerations to measurement and modeling techniques currently being advocated. The logical sequence illustrated in Figure 7-1 will be used to guide these discussions.

7.2.2 Aerodynamic Factors

Except for the obvious difference that particles will settle slowly under the influence of gravity, small particles and trace gases behave similarly in the air. Trace gases are an integral part of the gas mixture that constitutes air and, thus, will be moved with all of the turbulent motions that normally transport heat, momentum, and water vapor. However, particles have finite inertia and can fail to respond to rapid turbulent fluctuations. Table 7-1 lists some relevant characteristics of spherical particles in air (based on data tabulated by Fuchs 1964, Davies 1966, and Friedlander 1977). The time scales of most turbulent motions in the air are considerably greater than the inertial relaxation (or stopping) times listed in the table. These time scales vary with height, but even as close as 1 cm from a smooth, flat surface, most turbulence energy will be associated with time scales longer than 0.01 seconds, so that even 100 μm diameter particles would follow most turbulent fluctuations. However, natural surfaces are normally neither smooth nor flat, and it is clear that in many circumstances the flux of particles will be limited by their inability to respond to rapid air motions.

Naturally-occurring aerosol particles are not always spherical, although it seems reasonable to assume they are in the case of hygroscopic particles in the submicron size range. Chamberlain (1975) documents the ratio of the terminal velocity of non-spherical particles to that of spherical particles with the same volume. In all cases, the non-spherical particles have a lower terminal settling speed than do equivalent spheres. The settling speed ratio is indicated by a "dynamical shape factor," α, as listed in Table 7-2.

Thus, trace gases and small particles are carried by atmospheric turbulence as if they were integral components of the air itself, whereas large particles are also affected by gravitational settling which causes them to fall through the turbulent eddies. In general, however, the distribution of pollutants in the lower atmosphere is governed by the dynamic structure of the atmosphere as much as by pollutant properties.

TABLE 7-1. DYNAMIC CHARACTERISTICS OF UNIT DENSITY AEROSOL PARTICLES AT STANDARD TEMPERATURE AND PRESSURE, CORRECTED FOR STOKES-CUNNINGHAM EFFECTS (DATA ARE FROM FUCHS 1964, DAVIES 1966, FRIEDLANDER 1977)

Particle radius (μm)	Diffusivity ($cm^2\ s^{-1}$)	Stopping time (s)	Settling speed ($cm\ s^{-1}$)
0.001	1.28×10^{-2}	1.33×10^{-9}	1.30×10^{-6}
0.002	3.23×10^{-3}	2.67×10^{-9}	2.62×10^{-6}
0.005	5.24×10^{-4}	6.76×10^{-9}	6.62×10^{-6}
0.01	1.35×10^{-4}	1.40×10^{-8}	1.37×10^{-5}
0.02	3.59×10^{-5}	2.97×10^{-8}	2.91×10^{-5}
0.05	6.82×10^{-6}	8.81×10^{-8}	8.63×10^{-5}
0.1	2.21×10^{-6}	2.28×10^{-7}	2.23×10^{-4}
0.2	8.32×10^{-7}	6.87×10^{-7}	6.73×10^{-4}
0.5	2.74×10^{-7}	3.54×10^{-6}	3.47×10^{-3}
1.0	1.27×10^{-7}	1.31×10^{-5}	1.28×10^{-2}
2.0	6.10×10^{-8}	5.03×10^{-5}	4.93×10^{-2}
5.0	2.38×10^{-8}	3.08×10^{-4}	3.02×10^{-1}
10.0	1.38×10^{-8}	1.23×10^{-3}	1.20×10^{0}

TABLE 7-2. DYNAMIC SHAPE FACTORS, α, BY WHICH NON-SPHERICAL PARTICLES FALL MORE SLOWLY THAN SPHERICAL PARTICLES (CHAMBERLAIN 1975)

Shape	Ratio of axes	α
Ellipsoid	4	1.28
Cylinder	1	1.06
Cylinder	2	1.14
Cylinder	3	1.24
Cylinder	4	1.32
Two spheres touching, vertically	2	1.10
Two spheres touching, horizontally	2	1.17
Three spheres touching, as triangle	-	1.20
Three spheres touching, in line	3	1.34-1.40
Four spheres touching, in line	4	1.56-1.58

In daytime, the lower atmosphere is usually well mixed up to a height typically in the range 1 to 2 km, as a consequence of convection associated with surface heating by insolation. Pollutants residing anywhere within this mixed layer are effectively available for deposition through the many possible mechanisms. Atmospheric transfer does not usually limit the rate of delivery of pollutants to the surface boundary layer in which direct deposition processes are active. However, at night, the lower atmosphere may become stably stratified and vertical transfer of non-sedimenting material can be so slow that, at times, pollutants at heights as low as 50 to 100 m are isolated from surface deposition processes.

The fine details of turbulent transport of pollutants remain somewhat contentious. Notable among the areas of disagreement is the question of flux-gradient relationships in the surface boundary layer. It is now well accepted that the eddy diffusivity of sensible heat and water vapor exceeds that for momentum in unstable (i.e., daytime) but not in stable conditions over fairly smooth surfaces (see Dyer 1974, for example). However, it is not clear that the well-accepted relations governing heat or momentum transfer are fully applicable to particles or trace gases; some disagreement exists even in the case of water vapor. The situation is even more uncertain in circumstances other than over large expanses of horizontally uniform pasture. When vegetation is tall, pollutant sinks are distributed throughout the canopy so that close similarity with the transfer of any more familiar quantity such as heat or momentum is effectively lost. There is even considerable uncertainty about how to interpret profiles of temperature, humidity, and velocity above forests (Garratt 1978, Hicks et al. 1979, Raupach et al. 1979).

7.2.3 The Quasi-Laminar Layer

In the immediate vicinity of any receptor surface, a number of factors associated with molecular diffusivity and inertia of pollutants become important. Large particles carried by turbulence can be impacted on the surface as they fail to respond to rapid velocity changes. The physics of this process is similar to that of sampling by inertial collection.

Inertial impaction is a process that augments gravitational settling for particles in the size range typically between 2 and 20 μm (Slinn 1976b). Larger particles tend to bounce, and capture is therefore less efficient, while smaller particles experience difficulty in penetrating the quasi-laminar layer that envelops many receptor surfaces. Figures 7-2 and 7-3 show that many air-borne materials exist in the size range likely to be affected by inertial impaction. However, from the viewpoint of acidic particles, inertial impaction may not be important to dry deposition because most acidic species are associated with particles (see Figure 7-2) which are not strongly affected by this process. But, because many of the chemical constituents of soil-derived particles are capable of neutralizing deposited acids, inertial impaction may have important indirect effects upon acidic deposition.

To illustrate the role of molecular or Brownian diffusivity, it is informative to consider the simple ideal case of a knife-edged thin smooth plate, mounted horizontally and with edge normal to the wind vector. As air passes

over (and under) the plate, a laminar layer develops, of thickness $\delta = c(\nu x/u)^{1/2}$, where ν is kinematic viscosity, x is the downwind distance from the edge of the plate, and u is wind speed. According to Batchelor (1967), the value of the numerical constant c is 1.72. Thus, for a 5 cm plate in a wind speed of 1 m s^{-1}, we should imagine a boundary layer thickness reaching about 1.5 mm thick at the trailing edge.

Over non-ideal surfaces, the internal viscous boundary layer is frequently neither laminar nor constant with time. The layer generates slowly as a consequence of viscosity and surface drag as air moves across a surface. The Reynolds number, Re ($\equiv ux/\nu$, where u is the wind speed, x is the downwind dimension of the obstacle, and ν is kinematic viscosity), is an index of the likelihood that a truly laminar layer will occur. For large Re, air adjacent to the surface remains turbulent; viscosity is then incapable of exerting its influence. In many cases, it seems that the surface layer is intermittently turbulent. For these reasons, and because close similarity between ideal surfaces studied in wind tunnels and natural surfaces is rather difficult to swallow, the term "quasi-laminar layer" is preferred.

Wind-tunnel studies of the transfer of particles to the walls of pipes tend to support the concept of a limiting diffusive layer adjacent to smooth receptor surfaces. Transfer across such a laminar layer is conveniently formulated in terms of the Schmidt number, $Sc = \nu/D$, where ν is viscosity and D is the pollutant diffusivity. The conductance, or transfer velocity, v_1, across the quasi-laminar layer is proportional to the friction velocity u_*:

$$v_1 = Au_* \, Sc^{\alpha} \qquad [7\text{-}1]$$

where A and α are determined experimentally. Most studies agree that the exponent α is about -2/3, as is evident in the experimental data represented in Figure 7-4. However, a survey by Brutsaert (1975a) indicates exponents ranging from -0.4 to -0.8. The value of the constant A is also uncertain. The line drawn through the data of Figure 7-4 corresponds to $A \simeq 0.06$, yet the wind-water tunnel results of Moller and Schumann (1970) appear to require $A \simeq 0.6$. These values span the value of $A \simeq 0.2$ recommended for the case of sulfur dioxide flux to fibrous, vegetated surfaces (Shepherd 1974, Wesely and Hicks 1977).

Laminar boundary layer theory imposes the expectation that particle deposition to exposed surfaces will be strongly influenced by the size of the particle, with smaller particles being more readily deposited by diffusion than larger. It is clear that many artificial surfaces or structures made of mineral material will have characteristics for which the laminar-layer theories might be quite appropriate. However the relevance to vegetation can be questioned. Microscale surface roughness elements can penetrate the barrier presented by this quasi-laminar layer and should be suspected as sites for enhanced deposition of both particles and gases (Chamberlain 1967). Figure 7-5 is a photograph of the surface of a mature corn leaf (Zea mays), showing the dense blanket of leaf hairs, or trichomes, which covers the surface. These hairs are easily visible to the naked eye and provide an

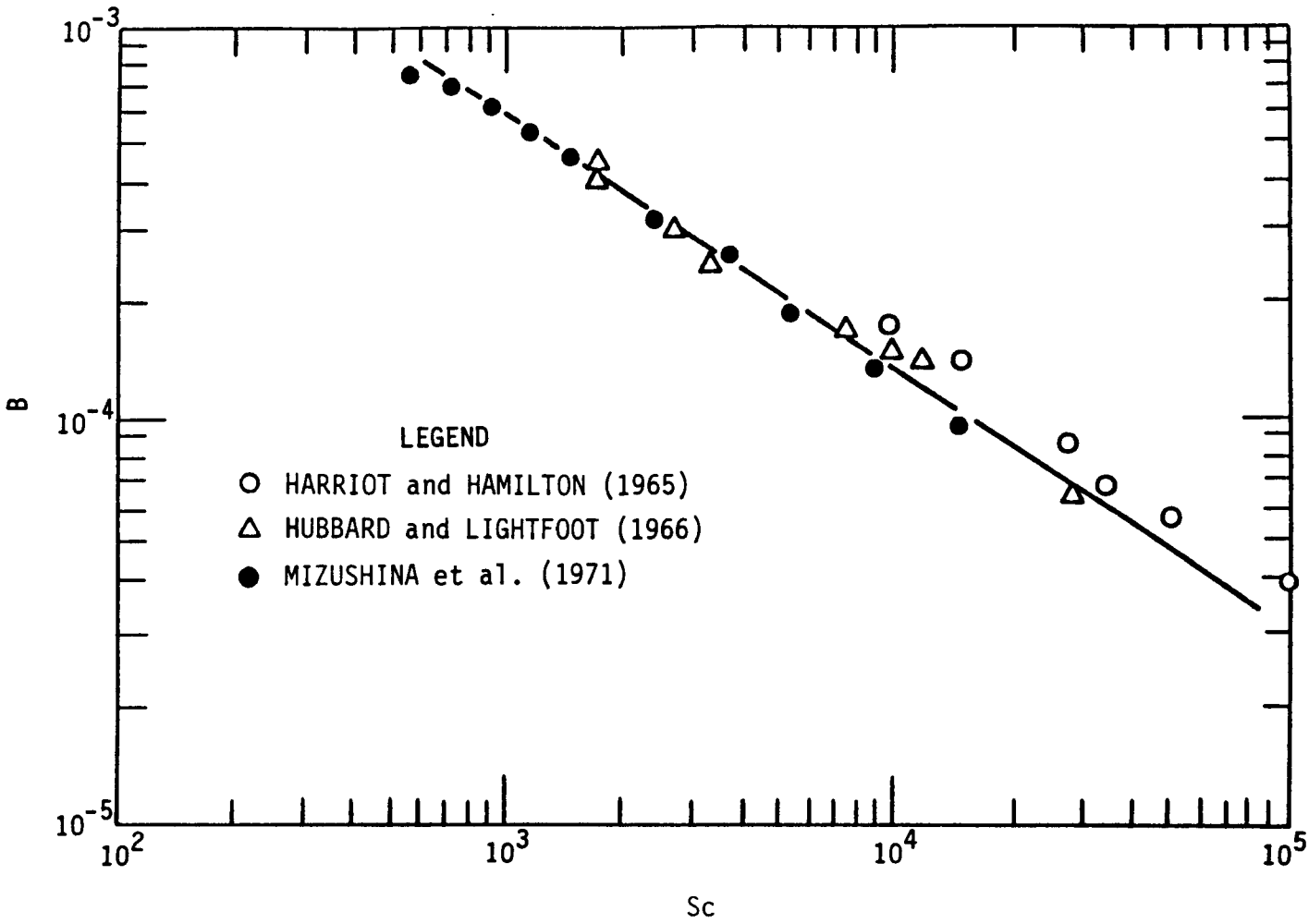

Figure 7-4. Laboratory verification of Schmidt-number scaling for particle transfer to a smooth surface. The quantity plotted is $B \equiv v_d/u_*$, evaluated for transfer across a quasi-laminar layer of molecular diffusion immediately adjacent to a smooth surface. Data are reported by Lewellen and Sheng (1980). The line drawn through the data is Equation 7-1, with exponent $\alpha = -2/3$ and constant of proportionality $A = 0.06$.

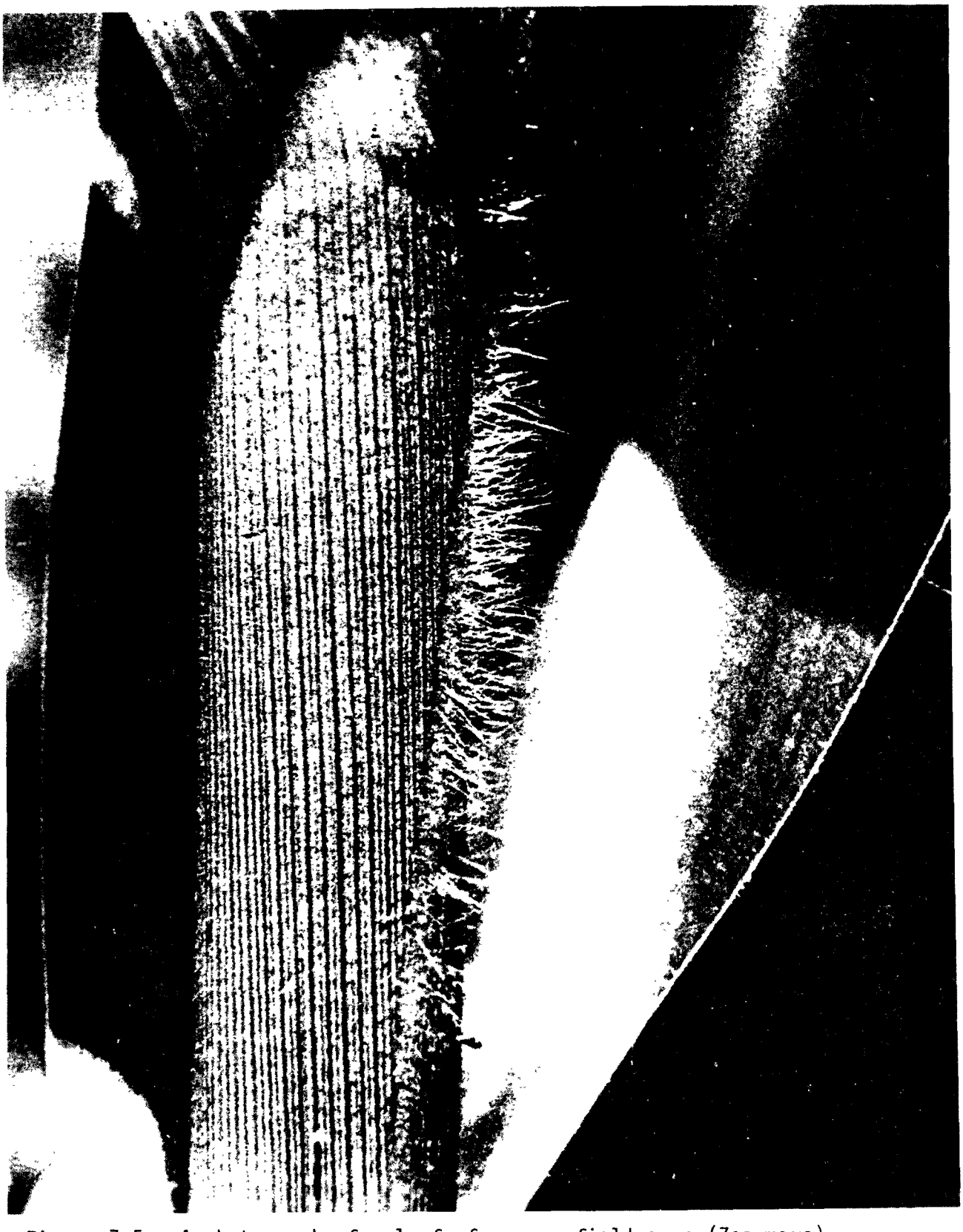

Figure 7-5. A photograph of a leaf of common field corn (Zea mays), highlighting the leaf hairs that potentially provide a mechanism for partially circumventing the otherwise limiting quasi-laminar layer in contact with the surface. (Photograph by R. L. Hart, Argonne National Laboratory)

obvious example of a case in which the limiting transfer characteristics of the quasi-laminar layer next to the surface might not be a critical issue.

7.2.4 Phoretic Effects and Stefan Flow

Particles near a hot surface encounter a force that tends to drive them away from the surface. Thermophoresis depends on the local temperature gradient in the air, on the thermal properties of the particle, on the Knudsen number, $Kn \equiv \lambda/r$ (where λ is the mean free path of air molecules, and r is the radius of the particle), and on the nature of the interaction between the particle and air molecules (see Derjaguin and Yalamov 1972). For very small particles (< 0.03 μm diameter, according to Davies 1967), this "thermophoresis" can be visualized as the consequence of hotter, more energetic air molecules impacting the side of the particle facing the hot surface. As a "rule of thumb", the thermophoretic velocity of very small particles (< 0.03 μm diameter) is likely to be about 0.03 cm s^{-1} (estimated from values quoted by Davies 1967). For larger particles, radiometric forces become important (Cadle 1966). In theory, thermal radiation can cause temperature gradients across particles that are not good thermal conductors, resulting in a mean motion of the particle away from a hot surface. For particles exceeding 1 μm diameter, the velocity will be about four times less.

Diffusiophoresis results when particles reside in a mixture of intermixing gases. In most natural circumstances, the principle concern is with water vapor. Close to an evaporating surface, a particle will be impacted by more water molecules on the nearer side. Because these water molecules are lighter than air molecules, there will be a net "diffusiophoresis" towards the evaporating surface.

Diffusiophoresis and thermophoresis both depend on the size and shape of the particle of interest and hence, neither can be predicted with precision, nor can safe generalizations be made. These subjects are sufficiently complicated that they constitute specialties in their own right. Excellent discussions have been given by Friedlander (1977) and Twomey (1977). These phoretic forces are generally small, and their influence on dry deposition can usually be disregarded.

Many workers include Stefan flow in general discussions of diffusiophoresis, but because of the conceptual difference between the mechanisms involved it is of current relevance to consider them separately. Stefan flow results from the injection into the gaseous medium of new gas molecules at an evaporating or subliming surface. Every gram-molecule of substrate material that becomes a gas displaces 22.41 liters of air, at STP. Thus, for example, a Stefan flow velocity of 22.41 mm s^{-1} will result when 18 g of water evaporates from a 1 m^2 area every second. Generalization to other temperatures and pressures is straightforward. Daytime evaporation rates from natural vegetation often exceed 0.2 g m^{-2} s^{-1} for considerable times during the midday period, resulting in Stefan flow of more than 0.2 mm s^{-1} away from the surface. Detailed calculation for specific circumstances is quite simple. For the present, it is sufficient to note that Stefan flow is capable of modifying surface deposition rates by an amount that is larger

than the deposition velocity appropriate for many small particles to aerodynamically smooth surfaces.

Electrical forces have often been mentioned as possible mechanisms for promoting deposition (as well as retention; see Section 7.1.5) of small particles, particularly through the "viscous" quasi-laminar layer immediately above receptor surfaces. Wason et al. (1973) report exceedingly high rates of deposition of particles in the size range 0.6 to 6 μm to the walls of pipes when a space charge is present. Chamberlain (1960) demonstrated the importance of electrostatic forces in modifying deposition velocities of small particles, when fields are sufficiently high. Plates charged to produce local field strengths of more than 2000 V cm^{-1}, experienced considerably more deposition of small particles than uncharged plates, by factors between 2 and 15. However, in fair-weather conditions, field strengths are typically less than 10 V cm^{-1}, so the net effect on particle transfer is likely to be small. Further studies of the ability of electrostatic forces to assist the transfer of particulate pollutants to vegetative surfaces were conducted by Langer (1965) and Rosinski and Nagamoto (1965). According to Hidy (1973), a series of experiments was conducted using single conifer needles and conifer trees. "For single needles or leaves, electrical charges on ~ 2 μm-diameter ZnS dust with up to eight units of charge had no detectable effect at wind speeds of 1.2 to 1.6 m s^{-1}. The average collection efficiency was found to be ~ 6 percent for edgewise cedar or fir needles, with broadside values an order of magnitude lower. Bounce-off after striking the collector was not detected, but re-entrainment could take place above ~ 2 m s^{-1} wind speed. Tests on branches of cedar and fir by Rosinski and Nagamoto (1965) suggested similar results as for single needles." It should be noted, however, that the electrical mobility of a particle is a strong negative function of particle size, ranging from 2 cm s^{-1} per V cm^{-1} of field strength for 0.001 μm-diameter particles, to 0.0003 cm s^{-1} per V cm^{-1} for 0.1 μm particles (Davies 1967).

7.2.5 Surface Adhesion

Most workers assume pollutants that contact a surface will be captured by it. For some gases, this assumption is clearly adequate. For example, nitric acid vapor is sufficiently reactive that most surfaces should act as nearly perfect sinks. Less reactive chemicals will be less efficiently captured. The case of particles is of special interest, however, because of the possibility of bounce and resuspension.

The role of electrostatic attraction in binding deposited particles to substrate surfaces remains something of a mystery. The process by which particles become charged and set up mirror-charges on the underlying surface is fairly well accepted. For smaller particles, the principle charging mechanism is thermal diffusion, leading to a Boltzman charge distribution. The resulting van der Waals forces are often mentioned as the major mechanism for binding particles once they are deposited. For large, non-spherical particles, dipole moments can be set up in natural electric fields and can help promote the adhesion at surfaces. These matters have been conveniently summarized by Billings and Gussman (1976), who provide mathematical relationships for evaluating the electrical energy of a particle on the basis of

its size, shape, dielectric constant, and the strength of the surrounding electrical field.

Condensation of water reduces the effectiveness of electrostatic adhesion forces, because leakage paths are then set up and charge differentials are diminished. However, the presence of liquid films at the interfaces between particles and surfaces causes a capillary adhesive force that compensates for the loss of electrostatic attraction. These "liquid-bridge" forces are most effective in high humidities, and for coarse particles (> 20 μm, according to Corn 1961).

Billings and Gussman (1976) draw attention to the effect of microscale surface roughness in promoting adhesion of particles to surfaces. Much of the experimental evidence is for particle diameters much greater than the height of surface irregularities (e.g., Bowden and Tabor 1950). It is the opposite case that is likely to be of greater interest in the present context, as will be discussed later.

7.2.6 Surface Biological Effects

The efficiency with which natural surfaces "capture" impacting particles or molecules will be influenced considerably by the chemical composition of the surface as well as its physical structure. The "lead candle" technique for detecting atmospheric sulfur dioxide is an historically interesting example of how chemical substrates can be selected to affect the deposition rates of particular pollutants.

Uptake rates of many trace gases by vegetation are controlled by biological factors such as stomatal resistance. In daytime, this is known to be the case for sulfur dioxide (Spedding 1969, Shepherd 1974, Wesely and Hicks 1977) and for ozone in most situations (Wesely et al. 1978). The similarity between sulfur and ozone is not complete, however, because the presence of liquid water on the foliage will tend to promote SO_2 deposition, and to impede uptake of ozone; the former gas is quite soluble until the solution becomes too acidic, whereas the latter is essentially insoluble (Brimblecombe 1978).

The role of leaf pubescence in the capture of particles has received considerable attention. Chamberlain (1967) tested the roles of leaf stickiness and hairiness in his wind-tunnel tests. He concluded that "with the large particles (32 and 19 μm) the velocity of deposition to the sticky artificial grass was greater than to the real grass, but with those of 5 μm and less, it was the other way round, thus confirming . . . that hairiness is more important than stickiness for the capture of the smaller particles." The importance of leaf hairs appears to be verified by studies of the uptake of ^{210}Pb and ^{210}Po particles by tobacco leaves (Martell 1974, Fleischer and Parungo 1974), and by the wind tunnel work of Wedding et al. (1975), who report increases by a factor of 10 in deposition rates for particles to pubescent leaves compared with smooth, waxy leaves. It remains to be seen how greatly biological factors of this kind influence the rates of deposition of airborne particles to other kinds of vegetation.

7.2.7 Deposition to Liquid Water Surfaces

Trace gas and aerosol deposition on open water surfaces is of considerable practical interest, especially considering concern with the acidification of poorly buffered inland waters. Air blowing from land across a coastline will slowly equilibrate with the new surface at a rate strongly dependent on the stability regime involved. If the water is much warmer than upwind land, dynamic instability over the water will cause relatively rapid adjustment of the air to its new lower boundary, but if the water is cooler, stratified flow will occur and adjustment will be very slow. In the former (unstable) case, dry deposition rates of all soluble or chemically reactive pollutants are likely to be much higher than in the latter. Clearly, air blowing over small lakes will be less likely to adjust to the water surface than will air blowing over larger water bodies. During much of the summer, inland water surfaces will tend to be cooler than the air, and hence may be protected from dry deposition because of the strongly stable stratification that will then prevail. This phenomenon will occur more frequently over small water bodies than larger ones (Hess and Hicks 1975).

Following the guidance of chemical engineering gas-transfer studies, workers such as Kanwisher (1963), Liss (1973), and Liss and Slater (1974), have considered the role of Henry's law constant and chemical reactivity in controlling the rate of trace gas exchange between the atmosphere and the ocean. In general, acidic and acidifying species like SO_2 are readily removed upon contact with a water surface. Thus, Hicks and Liss (1976) neglected liquid-phase resistance and derived net deposition velocities appropriate for the exchange of reactive gases across the air-sea interface. The work of Hicks and Liss is intended to apply to water bodies of sufficient size that the bulk exchange relationships of air-sea interaction research are applicable. Their considerations indicate that deposition velocities for highly soluble and chemically reactive gases such as NH_3, HCl, and SO_2 are likely to be between 0.10 percent and 0.15 percent of the wind speed measured at 10 m height. The analysis leading to this conclusion assumes that the molecular and eddy diffusivities can be combined by simple addition. This assumption has been shown to approximate the transfer of water vapor and sensible heat from water surfaces. However, for fluxes of trace gases, Deacon (1977) and Slinn et al. (1978) argue that it is better to introduce molecular diffusivity through a term analogous to the Schmidt (or Prandtl) number of Equation 7-1, with the exponent $\alpha \simeq -2/3$. (In contrast, the linear assumption used by Hicks and Liss implies $\alpha = -1.0$.) Hasse and Liss (1980) discuss the matter from the viewpoint of surface-film behavior, with emphasis on the role of capillary waves. In view of the uncertainties mentioned in discussion of Equation 7-1, further comment on the implications and ramifications of these alternative assumptions is not warranted.

In the limiting case of a trace gas of low solubility, the deposition velocity is determined by the large liquid-phase resistance, which is directly influenced by the Henry's law constant.

It is probable that breaking waves will modify the simple gas transfer formulation derived from chemical engineering pipe-flow and wind-tunnel work. It is not clear to what extent such features account for the apparent

discrepancy between the various Schmidt number dependencies of the kind expressed by Equation 7-1. However, the fractional power laws are basically extensions of laboratory work, whereas the unit-power, additive-diffusivities result is an approximation to field data. It is to be hoped that the two approaches produce results that will converge in due course.

Wind-tunnel results such as shown in Figure 7-6, indicate exceedingly low deposition velocities to water surfaces for particles in the size range of most acidic pollutants. As in the case of gas exchange, there are conceptual difficulties in extending these results to the open ocean. The role of waves in the transfer of small particles between the atmosphere and water surfaces remains essentially unknown. Not only does engulfment by breaking waves provide an alternative path across the quasi-laminar sublayer where molecular (or Brownian) diffusion normally controls the transfer, but also waves are a source of droplets which can scavenge particulate material from the air [see, however, the study of Alexander (1967) which indicates otherwise]. Hicks and Williams (1979) have proposed a simple model of air-sea particle exchange that extends smooth-surface, wind- and water-tunnel results (as in Figure 7-6) to natural circumstances, by permitting rapid transfer to occur whenever waves break. This results in very low deposition velocities in light winds, but rapidly increasing velocities when winds increase above about 5 m s^{-1}. Slinn and Slinn (1980) also suggest that particle transfer is more rapid than the wind-tunnel studies of Figure 7-6 might indicate, but they present an alternative hypothesis for this more rapid transfer: that hygroscopic particles grow rapidly when exposed to high humidities such as are found in air adjacent to a water surface, resulting in increased gravitational settling and impaction to the water surface.

7.2.8 Deposition to Mineral and Metal Surfaces

Acidic deposition is an obvious source of worry to architects, historians and others concerned with the potentially accelerated deterioration of structures (see Chapter E-7). Many popular building materials react chemically with acidic air pollutants, generating new chemical species that can contribute directly to the decay process even if they are rapidly and efficiently washed off by precipitation. Furthermore, in some cases the chemical product causes a visual degradation that cannot be easily rectified, such as the blackening of metal work exposed to hydrogen sulfide. Livingston and Baer (1983) summarize the various mechanisms involved, and relate them to the formulations that have been developed in laboratory studies.

The presence of water at the surface is known to be a key factor in promoting the fracturing and erosion of stone. Water penetrates pores and cracks and causes mechanical stresses both by freezing and by hydration and subsequent crystallization of salts (see Winkler and Wilhelm 1970, Fassina 1978, Gauri 1978). The earlier discussion of surface effects that influence dry deposition indicated that surface scratches and fractures will cause accelerated dry deposition rates in localized areas. Moreover, phoretic effects are likely to be more important than in the case of foliage (because dry surfaces exhibit wider temperature extremes than moist vegetation). Stefan flow associated with dewfall is also probably more important than for vegetation.

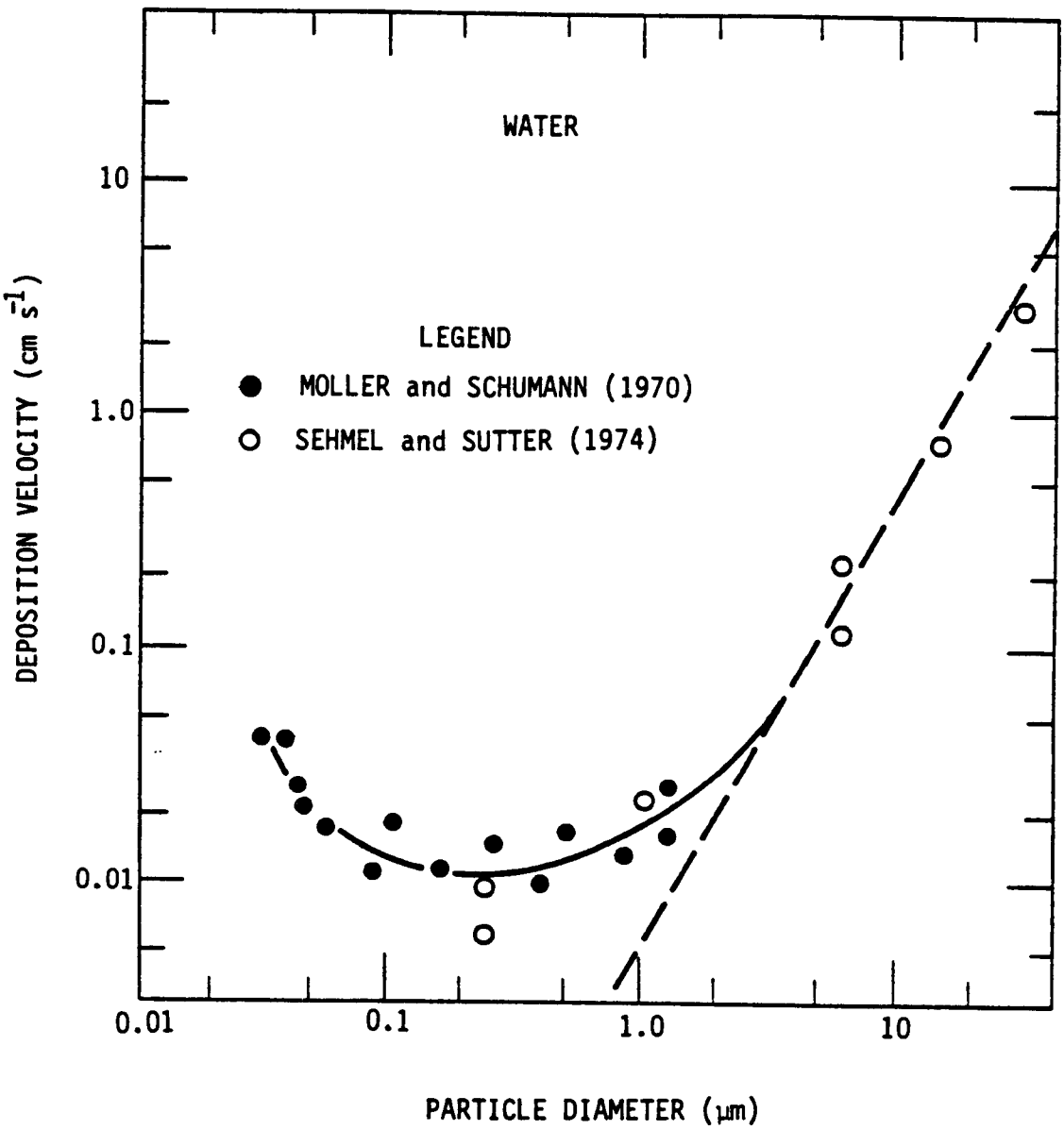

Figure 7-6. Results of wind tunnel studies of particle deposition to water surfaces. The dashed line at the right represents the terminal settling speed for 1.5 g cm^{-1} particles.

Some of the more important considerations can be summarized as follows (after Hicks 1982):

1. Particle fluxes will tend to be greatest to the coolest parts of exposed surfaces.

2. Both particle and gas fluxes will be increased when condensation is taking place at the surface, and decreased when evaporation occurs.

3. If the surface is wet, impinging particles will have a better chance of adhering, and soluble trace gases will be more readily "captured."

4. The chemical nature of the surface is important; if reaction rates with deposited pollutants are rapid, then surfaces can act as nearly perfect sinks.

5. Biological factors can influence uptake rates, by modifying the ability of the surface to capture and bind pollutants.

6. The texture of the surface is important. Rough surfaces will provide better deposition substrates than smoother surfaces, and will permit easier transport of pollutants across the near-surface quasi-laminar layer.

7. Microscale surface roughness features probably result in greater deposition velocities for aerosols, due to disruption of the quasi-laminar layer that normally limits transfer of particles to aerodynamically smooth surfaces.

The importance of these factors is emphasized by the results of corrosion tests conducted during the 1960's at 57 sites of the National Air Sampling Network (see Haynie and Upham 1974). The data indicate a nonlinear time dependence, such that the build-up of corrosion tends to reduce the rate of further deposition of the trace gases and aerosols causing the corrosion. Correlation analyses indicate significant effects of surface moisture, similar to what is outlined above, but no support is provided for the expectation that deposition rates will generally be greater to colder parts of exposed surfaces. Statistical analyses of the kind used by Haynie and Upham provide excellent information on the general features of corrosion of exposed metal surfaces, but generally fail to yield clear-cut evidence as to which processes are controlling the deposition that causes the corrosion. The subject of damage to materials surfaces is dealt with elsewhere in this document (Chapter E-7).

7.2.9 Fog and Dewfall

The processes that cause aerosol particles to nucleate, coalesce, and grow into cloud droplets are precisely the same as those which assist in the generation of fog. Whenever surface air supersaturates, fog droplets form on whatever hygroscopic nuclei are available. These small droplets slowly settle onto exposed surfaces, or are deposited by interception and impaction.

The characteristics of the liquid that is deposited are much the same as those of cloud liquid water (see Chapter A-6).

Low-altitude surface fogs form under conditions of strong stratification in which vertical turbulent transport is minimized. The frequency of fogs varies widely with location and with time of year. The depth is also highly variable. However, it must be assumed that fogs constitute a mechanism whereby the lower atmosphere (say the bottom hundred meters or so) can be cleansed of particulate and some gaseous pollutants.

At higher elevations, fog droplets are precisely the same as the cloud droplets that in other circumstances would grow and finally precipitate in substantially diluted form. The importance of cloud droplet interception has recently been demonstrated by Lovett et al. (1982), at an altitude of 1200 m in New Hampshire, where most of the net deposition of acidic species is by cloud droplet interception. The presence of liquid water on exposed surfaces helps promote the deposition of soluble gases and wettable particles. This surface water arises through the action of several mechanisms other than the direct effect of precipitation. Some plants exude fluid from foliage, usually at the tips of leaves, by a process known as guttation. Moisture can evaporate from the ground and recondense on other exposed surfaces, a mechanism known as distillation. However, these mechanisms are frequently confused with dewfall, which is properly the process by which water vapor condenses on surfaces directly from the air aloft. In practice, the origin of the surface moisture is immaterial to pollutants that come in contact with it. However, dewfall and distillation are processes that assist pollutant deposition through Stefan flow, whereas guttation does not. According to Monteith (1963), the maximum rate of dewfall is of the order of 0.07 mm hr^{-1}, so that the maximum Stefan flow enhancement of the nocturnal deposition velocity is about 8 cm hr^{-1} (see Section 7.2.4).

7.2.10 Resuspension and Surface Emission

Deposited particles can be resuspended into the air, and subsequently redeposited. The mechanisms involved are much the same as those that cause saltation of particles from the beds of streams and from eroding soils. These subjects are of great practical importance in their own right, and have been studied at length. Concern about resuspension of radioactive particles near sites of accidents or weapons tests injected a note of some urgency into related studies during the 1950's and 1960's, as evidenced in the large number of papers on the subject included in the volume "Atmosphere-Surface Exchange of Particulate and Gaseous Pollutants" (Engelmann and Sehmel 1976).

The momemtum transfer between the atmosphere and the surface is the driving force that causes surface particles to creep, bounce, and eventually saltate. There is a minimum frictional force that will cause particles of any particular size to rise from the surface. Bagnold (1954) identifies the momentum flux, u_*^2, as a controlling parameter, so that it is the few occurrences of strongest winds that are the most important. While most thinking seems to center on wide-spread phenomena like dust storms, Sinclair (1976) points out that dust devils provide a highly efficient light-wind mechanism for resuspending surface particles and carrying them to considerable altitudes.

Clearly, very large particles will not be moved frequently, or far. Very small particles are bound to the surface by adhesive forces that have already been discussed, and tend to be protected in crevices or between larger particles.

Chamberlain (1983) has provided a theoretical basis for linking saltation of sand particles and snowflakes, and for relating these phenomena to the generation of salt spray at sea.

It is not clear how saltation and related phenomena affect acidic deposition. Surface particles that are injected into the air by the action of the wind do not normally move far, nor do they offer much opportunity for interaction with other air pollutants (firstly, because they are confined in a fairly shallow layer near the surface, and secondly, because they have a very short residence time). Their effects are largely local.

Many smaller particles (in the submicron size range) are generated by reactions between atmospheric oxidants and organic trace gases emitted by some vegetation, especially conifers (Arnts et al. 1978). Once again, it is not obvious how these should best be considered in the present context of acidic deposition. This is but one of many natural surface-sources that provide a conceptual mechanism for injecting particles and trace gases into the lower atmosphere. The subject is dealt with in Chapter A-2.

7.2.11 The Resistance Analog

Discussing the relative importance of the various factors that contribute to the net flux of some particular atmospheric pollutant and determining which process might be limiting in specific circumstances are simplified by considering a resistance model analogous to Ohm's law. Figure 7-7 illustrates the way in which the concept is usually applied. An aerodynamic resistance, r_a, is identified with the transfer of material through the air to the vicinity of the final receptor surfaces. This resistance is defined as that associated with the transfer of momentum; it is dependent on the roughness of the surface, the wind speed, and the prevailing atmospheric stability. The aerodynamic resistance can be written as

$$r_a = (C_{fn} - \Psi_c/k)/u_* \qquad [7\text{-}2]$$

where C_{fn} is the appropriate friction coefficient (the square root of the familiar drag coefficient) in neutral stability, u_* is the friction velocity (a scaling quantity defined as the root mean covariance between vertical and longitudinal wind fluctuations), k is the von Karman constant, and Ψ_c is a stability correction function that is positive in unstable, negative in stable, and zero in neutral stratifications (see Wesely and Hicks 1977). Equation 7-2 is obtained by straightforward manipulation of standard micrometeorological relations, as given by Wesely and Hicks, for example. The value of k is usually taken to be about 0.4. Table 7-3 lists typical values of the friction coefficient for a range of surfaces.

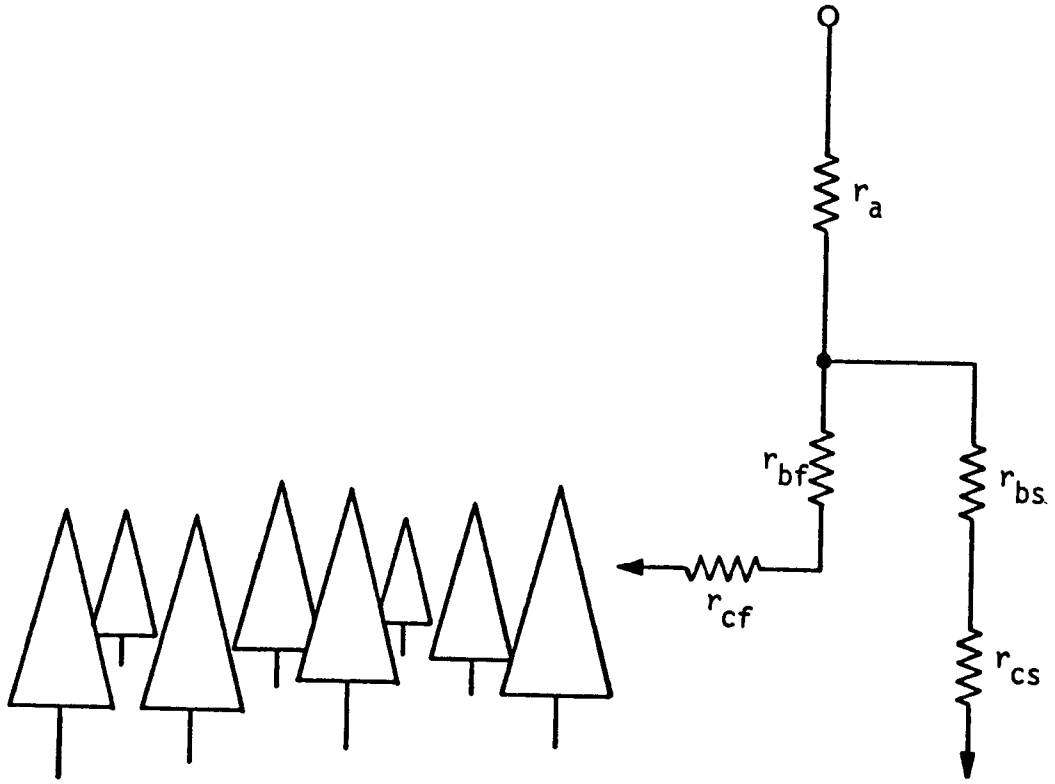

Figure 7-7. A diagrammatic illustration of the resistance model frequently used to help formulate the roles of processes like those given in Figure 7-1. Here, r_a is an aerodynamic resistance controlled by turbulence and strongly affected by atmospheric stability, r_{bf} and r_{bs} represent surface boundary layer resistances that are determined by molecular diffusivity and surface roughness, and r_{cf} and r_{cs} are the net residual resistances required to quantify the overall deposition process, to the eventual sink. The subscripts f and s are intended to indicate pathways to foliage and to soil respectively. There are many other pathways that might be important; the diagram is not intended to be more than a simple visualization of some of the important factors.

TABLE 7-3. ESTIMATES OF ROUGHNESS CHARACTERISTICS TYPICAL OF NATURAL SURFACES. VALUES OF THE FRICTION COEFFICIENT C_{fn} ($\equiv u_*/\bar{u}$) ARE EVALUATED FOR NEUTRAL CONDITIONS, AT A HEIGHT 50 CM ABOVE THE SURFACE OR TOP OF THE CANOPY

Surface	Approx. canopy height (m)	Roughness length (cm)	Neutral friction coefficient, C_{fn}
Smooth ice	0	0.003	0.042
Ocean	0	0.005	0.045
Sandy Desert	0	0.03	0.055
Tilled Soil	0	0.10	0.066
Thin Grass	0.1	0.70	0.095
Tall thin grass	0.5	5.	0.16
Tall thick grass	0.5	10.	0.21
Shrubs	1.5	20.	0.25
Corn	2.3	30.	0.29
Forest	10.	50.	0.23
Forest	20.	100.	0.24

The surface boundary resistance, r_b (separated further in Figure 7-7 between components r_{bf} and r_{bs}, associated with foliage and soil, respectively), is that which accounts for the difference between momentum transfer (i.e., frictional drag) at the surface and the passage of some particular pollutant through the near-surface quasi-laminar layer. In agricultural meteorology literature, a quantity B^{-1} is frequently employed for this purpose (Brutsaert 1975a). The relationship between these quantities can be clarified by relating both to the micrometeorological concept of a roughness length, z_0 (the height of apparent origin of the neutral logarithmic wind profile). Then the total atmospheric resistance, R, between the surface in question and the height of measurement z can be written as

$$\begin{aligned} R &= (ku_*)^{-1}(\ell n(z/z_{oc}) - \Psi_c) \\ &= (ku_*)^{-1}(\ell n(z/z_0) + \ell n(z_0/z_{oc}) - \Psi_c \\ &= r_a + (ku_*)^{-1} \cdot \ell n(z_0/z_{oc}) \end{aligned} \qquad [7\text{-}3]$$

where z_{oc} is a roughness length scale appropriate for the transfer of the pollutant. The residual boundary-layer resistance, $r_b = R - r_a$, is then

$$r_b = (ku_*)^{-1} \cdot \ell n(z_0/z_{oc}), \qquad [7\text{-}4]$$

which alternatively is written as

$$r_b = (u_* B)^{-1}. \qquad [7\text{-}5]$$

B is, therefore, a measure of the non-dimensionalized limiting deposition velocity for concentrations measured sufficiently close to a receptor surface such that the resistance to momentum transfer can be disregarded.

It should be noted that some workers refer to r_b as the aerodynamic resistance and use the symbol r_a for it, (e.g., O'Dell et al. 1977).

Shepherd (1974) recommends using a constant value $kB^{-1} = \ell n(z_0/z_{oc}) = 2.0$ for transfer to vegetation, on the basis of results obtained over rough, vegetated surfaces. However, the role of the Schmidt number in accounting for diffusion near a surface needs to be taken into account. Wesely and Hicks (1977) advocate using a Schmidt number relationship like that of Equation 7-1, so that surface boundary layer resistance would then be written as

$$r_b \simeq 5\ Sc^{2/3}/u_*. \qquad [7\text{-}6]$$

Equation 7-6 implies a value of 0.2 for A in the boundary layer relationship given by Equation 7-1, as was mentioned earlier.

The final resistances in the conceptual chain of processes represented diagramatically by Figure 7-7 are those which permit material to be transferred to the surface itself. For many pollutants, it is necessary only to consider the canopy foliage resistance, r_{cf}, but for some it is also necessary to consider uptake at the ground by invoking a resistance to transfer to soil

(or a forest floor), r_{cs}. In concept, it is also appropriate to differentiate between boundary layer resistances r_{bf} and r_{bs} for transfer to foliage and soil, respectively, as is shown in the diagram. Many other resistances can be identified and might often need to be considered, but further complication of Figure 7-7 is unnecessary. Its main purpose is illustrative.

Transfer of many trace gases to foliage occurs by way of stomatal uptake, which, because of stomatal physiology, imposes a strong diurnal cycle on the overall deposition behavior. Following initial work by Spedding (1969), studies of foliar uptake of sulfur dioxide have repeatedly confirmed the controlling role of stomatal resistance. Chamberlain (1980) summarizes results of experiments by Belot (1975) and Garland and Branson (1977), who compared surface conductances of sulfur dioxide with those for water vapor, over a broad range of stomatal openings (which largely govern stomatal resistance). The conclusion that stomatal resistance is the controlling factor when stomata are open appears to be well founded. However, once again, it is necessary to apply corrections to account for the diffusivity of the trace gas in question; the higher the molecular diffusivity of the gas, the lower the stomatal resistance.

Fowler and Unsworth (1979) point out that SO_2 deposition to wheat continues even when stomata are closed, at a rate suggesting significant deposition at the leaf cuticle. Thus, it is not always sufficient to compute the canopy-foliage resistance r_{cf} on the assumption that SO_2 uptake is via stomata alone (although this may indeed be a sufficient approximation in most circumstances). Instead, it is more realistic to estimate r_{cf} from its component parts via

$$r_{cf} \simeq (r_{st}^{-1} + r_{cut}^{-1})^{-1}/(LAI) \qquad [7\text{-}7]$$

(following Chamberlain 1980), where r_{st} is the stomatal resistance, and r_{cut} is the cuticular resistance. LAI is the leaf area index (total area of foliage per unit horizontal surface area). Note that in most literature the LAI is assumed to be the single-sided leaf area index. However, sometimes both sides of the leaves are counted.

The resistance analogy permits a closer look at the mechanisms that transfer gaseous material into leaves. Figure 7-8 illustrates the pathways involved: via stomatal openings and into the interior of the leaf (involving stomatal and mesophyllic resistances, r_{st} and r_m) or through the epidermis (involving a cuticular resistance, r_{cut}).

The resistance model is somewhat limited by the manner in which it structures the chain of relevant processes, each being represented by a resistance to transfer that occupies a prescribed location in a conceptual network. The structure of this network is sometimes not clear; furthermore, there are important processes that do not conveniently fit into the resistance model. Mean drift velocities (e.g., gravitational settling of particles) are not easily accommodated in the simple resistance picture, and it is doubtful whether some of the biological factors are relevant to the question of particle transfer. Studies of leaves show that stomata are typically slits

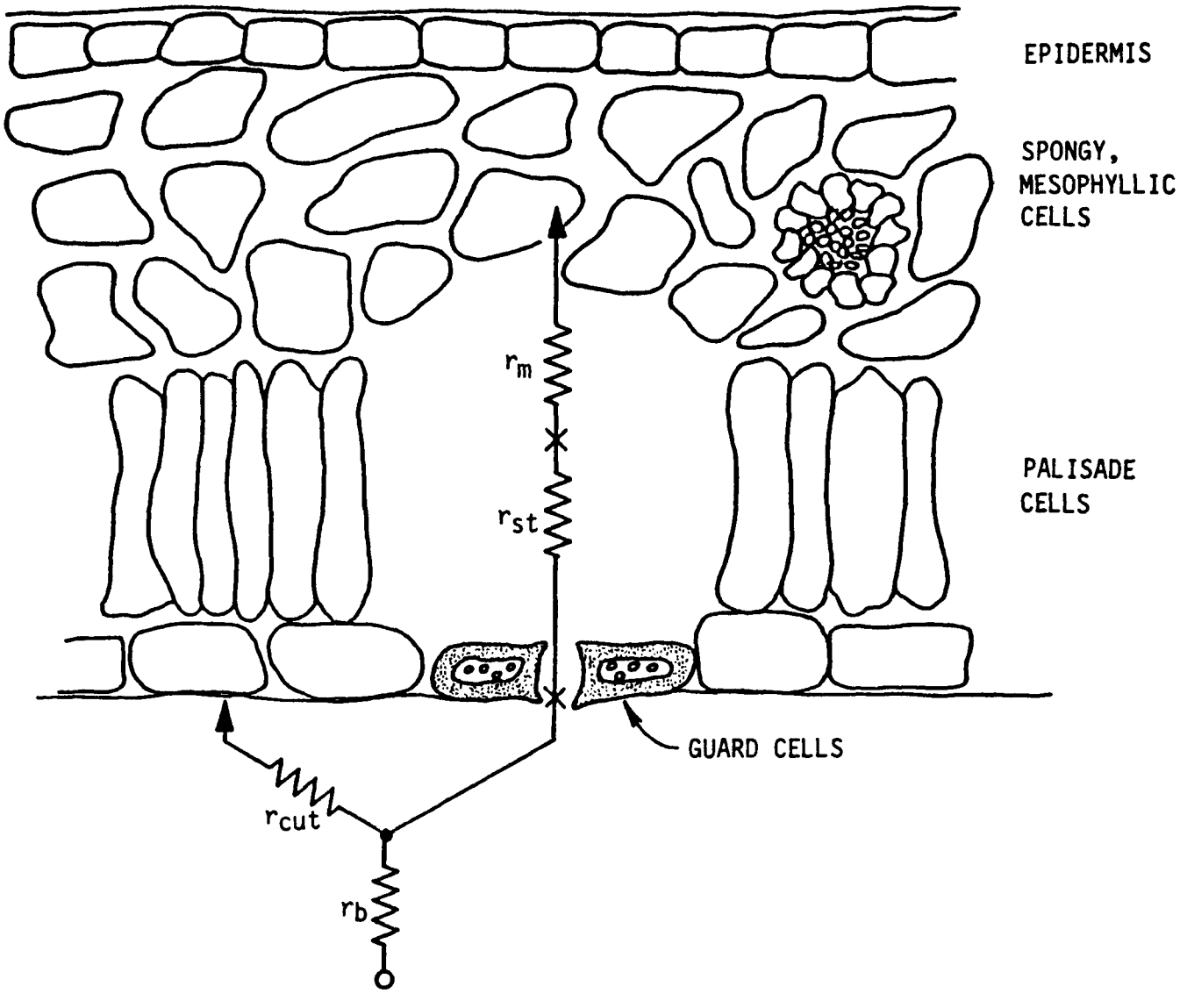

Figure 7-8. An illustration of the roles of different resistances associated with trace gas uptake by a leaf. Material is transferred along several possible pathways, of which two are shown. These involve cuticular uptake via a resistance r_{cut}, and transfer through stomatal pores (via r_{st}) into substomatal cavities, with subsequent transfer to mesophyllic tissue (via r_m). The way in which the various resistances are combined to provide the best visualization of the overall transfer process in not clear-cut.

of the order of 2 to 20 μm long. For stomatal uptake of particles to be a controlling factor of deposition, we would need to hypothesize spectacularly good aim by the particles.

7.3 METHODS FOR STUDYING DRY DEPOSITION

7.3.1 Direct Measurement

There is little question that the deposition of large particles is accurately measured by collection devices exposed carefully above a surface of interest. Deposit gauges and dust buckets have been important weapons in the geochemical armory for a long time. They are intended to measure the rate of deposition of particles which are sufficiently large that deposition is controlled by gravity. In studies of radioactive fallout conducted in the 1950's and 1960's, these same devices were used. In the case of debris from weapons tests, the major local fallout was of so-called hot radioactive particles, originating with the fragmentation of the weapon casing and its supporting structures, and the suspension of soil in the vicinity of the explosion. These large particles fall over an area of rather limited extent downwind of the explosion. This area of greatest fallout was the major focus of the work on fallout dry deposition. It was largely in this context that dustfall buckets were used to obtain an estimate of how much radioactive deposition occurred. It was recognized that collection vessels failed to reproduce the microscale roughness features of natural surfaces. However, this was not seen as a major problem, since the emphasis was on evaluating the maximum rate of deposition that was likely to occur so that upper limits could be placed on the extent of possible hazards. Nevertheless, efforts were made to "calibrate" collection vessels in terms of fluxes to specific types of vegetation, soils, etc. (Hardy and Harley 1958).

Much further downwind, most of the deposition was shown to be associated with precipitation, since the effective source of the radioactive fallout being deposited was typically in the upper troposphere or the lower stratosphere. The acknowledged inadequacies of collection buckets for dry deposition were then of only little concern, since dry fallout composed a small fraction of the total surface flux.

In the context of present concerns about acidic deposition, we must worry not only about large, gravitationally-settling particles, but also about small "accumulation-size-range" particles that are formed in the air from gaseous precursors, and about trace gases themselves. All of these materials contribute to the net flux of acidic and acidifying substances by dry processes. It is known that collection vessels do indeed provide a measure of the flux of large particles. However, accumulation-size-range particles, typically less than 1 μm diameter, do not deposit by gravitational settling at a significant rate. These small particles are transported by turbulence through the lower atmosphere and are deposited by diffusion to surface roughness elements, with the assistance of a wide range of surface-related effects (e.g., phoretic processes, Stefan flow, etc.), many of which will be influenced by the detailed structure of the surface involved.

Early work on the deposition of radioactive fallout made use of collection vessels and surrogate surface techniques that were frequently "calibrated" in terms of fluxes to specific types of vegetation, soils, etc. Studies of this kind were relatively easy, especially in the case of radioactive pollutants, because very small quantities of many important species could be measured accurately by straightforward techniques. Most of the radioactive materials that were of interest do not exist in nature, so experimental studies benefited from a zero background against which to compare observed data. Moreover, major emphasis was on the dose of radioactivity to specific receptors, a quantity strongly influenced by contributions of large, "hot" particles in situations of practical interest. Such circumstances included deposition of bomb debris, fission products, and soil particles from the radioactive cloud downwind of nuclear explosions. In such cases, highest doses were incurred near the source, and were due to these larger particles.

The applicability of collection vessels and surrogate surfaces in studies of the dry deposition of acidic pollutants is in dispute (see also Chapter A-8, Section 8.2). Principal among the conceptual difficulties concerning their use is their inability to reproduce the detailed physical, chemical, and biological characteristics of natural surfaces, which are known to control, or at least strongly influence, pollutant uptake in most instances. Furthermore, the continued exposure of already-deposited materials to airborne trace gases and aerosol particles undoubtedly causes some changes to occur, but of unpredictable magnitude and unknown significance. A recent intercomparison between different kinds of surrogate surfaces and collection vessels has indicated that fluxes derived from exposing dry buckets are greater than those obtained using small dishes, which in turn exceed values obtained using rimless flat plates (Dolske and Gatz 1982). This provides a tantalizing tidbit of evidence for an ordering of performance characteristics according to the total exposed surface area per unit horizontal projection. In this context, the similarity with arguments concerning leaf area index seems especially attractive. Micrometeorological data obtained during the same experiment fall between the extremes represented by the buckets and the flat plates.

Dasch (1982) reports on a comparison between many different configurations of flat-plate collection surfaces, pans, and buckets. The results indicate that glass surfaces provide the greatest flux estimates for almost all chemical species considered, and teflon the lowest. Plastic bucket data generally fall midway in the range.

Tracer techniques developed in the radioecology era for investigating fluxes to natural surfaces offer some promise. A β-emitting isotope of sulfur, S-35, lends itself to use in studies of SO_2 uptake by crops because measurements of low rates of sulfur accumulation are then possible. Garland et al. (1973), Owers and Powell (1974), Garland and Branson (1977), and Garland (1977) report the results of a number of studies of $^{35}SO_2$ uptake by various vegetated surfaces ranging from pasture to pine plantation, and by non-vegetated surfaces such as water.

In concept, it is feasible to extend studies of this kind to the deposition of sulfurous particles, but as yet no such experiment has been reported.

However, analogous studies of particle deposition using non-radioactive aerosol tracers have been carried out. In wind-tunnel experiments, Wedding et al. (1975) employed uranine dye particles in conjunction with lead chloride particles to study the influence of leaf microscale roughness on particle capture characteristics; uranine particles are relatively easy to measure by fluorimetry, whereas measurements of lead deposition require far more painstaking chemical analysis of the deposition surface. The particle sizes used by Wedding et al. were in the range 3 to 7 μm diameter.

Considerably larger particles have been used in many studies. In detailed wind-tunnel studies, Chamberlain (1967) used lycopodium spores (~30 μm aerodynamic diameter). Workers at Brookhaven National Laboratory extended these wind-tunnel techniques to real-world circumstances by conducting a series of experiments employing pollen in the same general size range (Raynor et al. 1970, 1972a,b, 1974).

In general, these methods of tracer measurement have not been applied to natural circumstances for the particle sizes of major interest in the present context of acidic deposition. An important exception concerns studies of deposition on snow surfaces. The retention of deposited material at the top of or within a snowpack has been studied in some detail and continues to be an intriguing area of research. Particulate materials such as sulfate were considered by Dovland and Eliassen (1976), who studied the accumulation upon snow surfaces during periods of no precipitation and found average deposition velocities in the range 0.1 to 0.7 cm s^{-1}, depending on the assumption made regarding the contribution by gaseous SO_2 deposition. Similar work by Barrie and Walmsley (1978) yielded average sulfur dioxide deposition velocities to snow in the range 0.3 to 0.4 cm s^{-1}, with a standard error equivalent to about a factor of two.

Eaton et al. (1978) and Dillon et al. (1982) present examples of the use of calibrated watersheds to estimate atmospheric deposition. Dry deposition fluxes are estimated as a residual between measured fluxes out of a conceptually-closed system, assumed to be in steady state, and measured wet deposition into it. Considerable effort is required to document annual chemical mass balances for specific watersheds. Once the effort is made, it appears possible to draw conclusions regarding dry deposition, although obviously such estimates will be the result of the difference between fairly large numbers. According to Eaton et al., the annual dry deposition flux estimate obtained at the Hubbard Brook Experimental Forest in New Hampshire is accurate to about ± 35 percent (one standard error). The data do not permit apportionment between gaseous and particulate sulfur inputs, but the total sulfur flux corresponded to a deposition velocity of about 0.6 cm s^{-1}.

7.3.2 Wind-Tunnel and Chamber Studies

Figure 7-1 illustrates the overall complexity of the problem of dry deposition. While it is indisputable that no indoor experiment can provide a comprehensive evaluation of pollutant deposition that would be applicable to the natural countryside, laboratory studies provide the unique attraction of controllable conditions. It is feasible to compare the relative importance

of various factors, as in Figure 7-1, and especially as in Figure 7-8, and to formulate these processes in a logical manner. In this general category, we must include the extensive wind-tunnel work referred to earlier, the pipe-flow and flat-plate studies conducted in experiments more aligned to problems of chemical engineering, and the chamber experiments favored by ecologists and plant physiologists. Distinction among these kinds of experiments is often difficult. Many exposure chambers and pipe-flow studies have features of wind tunnels.

The utility of chamber studies is well illustrated by the series of results reported by Hill (1971). By comparing the rates of deposition of various trace gases to oat and alfalfa canopies exposed in large chambers, Hill concluded that solubility was a critical parameter in determining uptake rates of trace gases by vegetation. The ordering of deposition velocities was: hydrogen fluoride > sulfur dioxide > chlorine > nitrogen dioxide > ozone > carbon dioxide > nitric oxide > carbon monoxide. Furthermore, the chamber studies indicated a wind speed dependence of the kind predicted by turbulent transfer theory, and demonstrated a physiological effect of chlorine and ozone uptake on stomatal opening: exposure to high concentrations of either quantity caused partial stomatal closure, thus limiting the fluxes of all trace gases that are stomatally controlled.

Experiments conducted by Judeikis and Wren (1977, 1978) yielded valuable information on the deposition of hydrogen sulfide, dimethyl sulfide, sulfur dioxide, nitric oxide, and nitrogen dioxide to non-vegetated surfaces (Table 7-4). The values listed were derived from initial deposition rates obtained before surface accumulation limited uptake rates. For comparison, surface resistances derived from Hill's (1971) studies of trace gas uptake by alfalfa are also listed. On the whole, the ordering of deposition velocities suggested by Hill's work appears to be supported, providing some justification for extending the ordering to CO, H_2S, and $(CH_3)_2S$ in the manner indicated in the table. Residual surface resistance to uptake of soluble gases by solid, dry surfaces appears to be substantially greater than for vegetation, which is as would be expected.

The values listed in Table 7-4 represent resistances to transport very near the surface, much like the surface boundary-layer resistance discussed earlier to which other resistances must be added to obtain values representative of natural, out-door conditions. The reciprocals of the tabulated numbers provide upper limits of the appropriate deposition velocities.

Similarly, informative data have been obtained about particle deposition on surfaces that can be contained in wind tunnels. Studies of this kind are an obvious extension of pipe-flow investigations by workers such as Friedlander and Johnstone (1957) and Liu and Agarwal (1974), which provide strong support for theories involving particle inertia and Schmidt number scaling. Wind tunnels provide a means to extend chamber and pipe-flow investigations to situations more closely approximating natural conditions.

Results obtained in studies of particle deposition to dry gravel (Sehmel et al. 1973a) are shown in Figure 7-9. Experiments on the deposition to wet gravel were also conducted. These indicated deposition velocities some 30

TABLE 7-4. RESISTANCES TO DEPOSITION (S CM^{-1}) OF SELECTED TRACE GASES, MEASURED FOR SOLID SURFACES IN A CYLINDRICAL FLOW REACTOR (JUDEIKIS AND STEWART 1976) AND FOR ALFALFA IN A GROWTH CHAMBER (HILL 1971)[a]

Pollutant	Substrate Surface		
	Adobe Clay	Sandy Loam	Alfalfa
CO	-	-	∞
H_2S	62.0	67.0	-
$(CH_3)_2S$	3.6	16.0	-
NO	7.7	5.3	10.0
CO_2	-	-	3.3
O_3	-	-	0.7
NO_2	1.3	1.7	0.5
Cl_2	-	-	0.5
SO_2	1.1	1.7	0.4
HF	-	-	0.3

[a]Solid-surface data are derived from Table 2 of Judeikis and Wren (1978). The alfalfa values are obtained from Table 1 of Hill (1971).

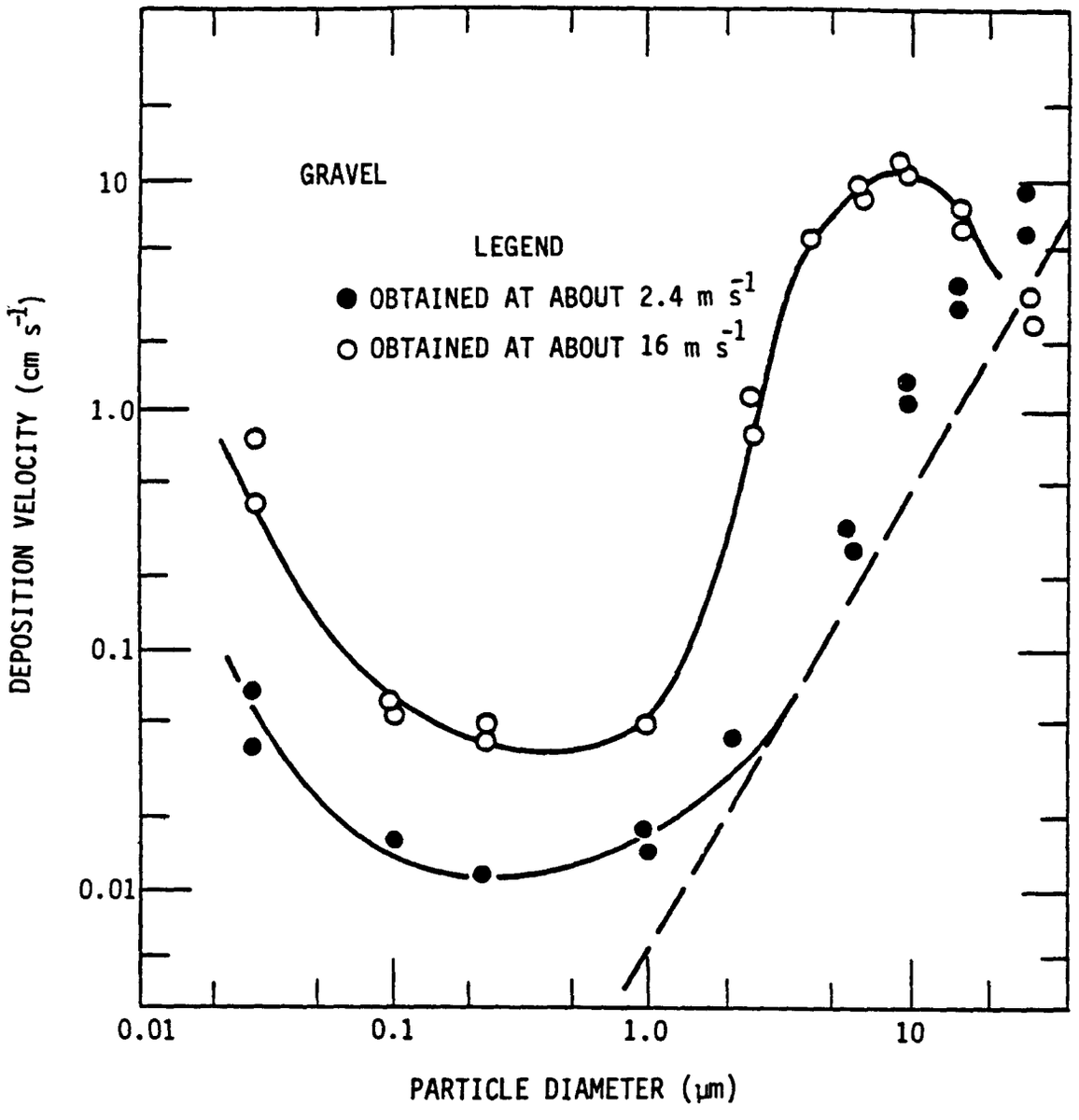

Figure 7-9. Results of wind-tunnel studies of particle deposition to 1.6 cm diameter dry gravel. Adapted from Sehmel et al. (1973a).

percent less than the values evident in Figure 7-9 (for particles in the 0.2 to 1.0 μm size range), as might be expected from considerations of Stefan flow and diffusiophoresis. When surface roughness was increased, deposition velocities also increased. The wind speed effect evident in these data is fairly typical and applies also in the case of vegetation (Figure 7-10).

Chamberlain (1967) extended his earlier (1966) wind tunnel studies of gas transfer to "grass and grass-like surfaces" by considering particle deposition to rough surfaces. Sehmel (1970) conducted similar wind-tunnel experiments, employing monodisperse particles ranging from about 0.5 to 20 μm diameter. Figure 7-10 combines results from Chamberlain (1967) and Sehmel et al. (1973b). The Chamberlain data refer to live grass, but the Sehmel et al. data were obtained using 0.7 cm high artificial grass. Moreover, the two sets of data were obtained at different wind speeds (Chamberlain, $u_* \simeq 70$ cm s^{-1}; Sehmel et al., $u_* \simeq 19$ cm s^{-1}). Further tests conducted by Chamberlain (1967) indicated that deposition velocities to natural grass exceeded those to artificial grass by a factor of about two for particles smaller than about 5 μm. This appears contrary to the indication of Figure 7-10, where v_d (natural) of Chamberlain is seen to be about half the v_d (artificial) of Sehmel et al. for sizes less than a few μm. The difference in u_* between their experiments amplifies this discrepancy, rather than resolving it. However, both data sets provide evidence for the deposition velocity particle-size dependence that is predicted by theory and supported by all such laboratory investigations.

7.3.3 Micrometeorological Measurement Methods

The factors that control pollutant fluxes are frequently surface properties such as stomatal resistance and soil moisture (for soluble gases), cuticular resistance and leaf area index (for strongly surface-reactive gases like HF and HNO_3), and microscale roughness (for sub-micron particles). Any measurement technique that interferes with a controlling property is likely to yield erroneous results; hence, considerable effort has been expended to develop and apply measurement methods that impose no surface or environmental modification. In concept, if an area is sufficiently homogeneous, flat, and contains no areas of strong sources or sinks, pollutant fluxes can be assumed to be constant with height. Therefore, questions regarding dry deposition can be addressed by measuring the flux of material through a horizontal layer of air at some more convenient level above the surface. The intent of any such study is to investigate dry deposition fluxes in carefully-documented natural situations to identify and quantify controlling properties. The results of these investigations are formulations of surface mechanisms, surface boundary layer resistances, stomatal resistances, etc. The demanding site criteria are required to enable these results to be obtained from the experiments; the surface parameterizations that are derived are far more widely applicable.

Several micrometeorological methods are suitable for measuring dry deposition fluxes in intensive case studies. The flux can be measured directly by eddy-correlation, a process that evaluates instantaneous products of the vertical wind speed, w, and pollutant concentration, C, to derive the time-average vertical flux F_c as

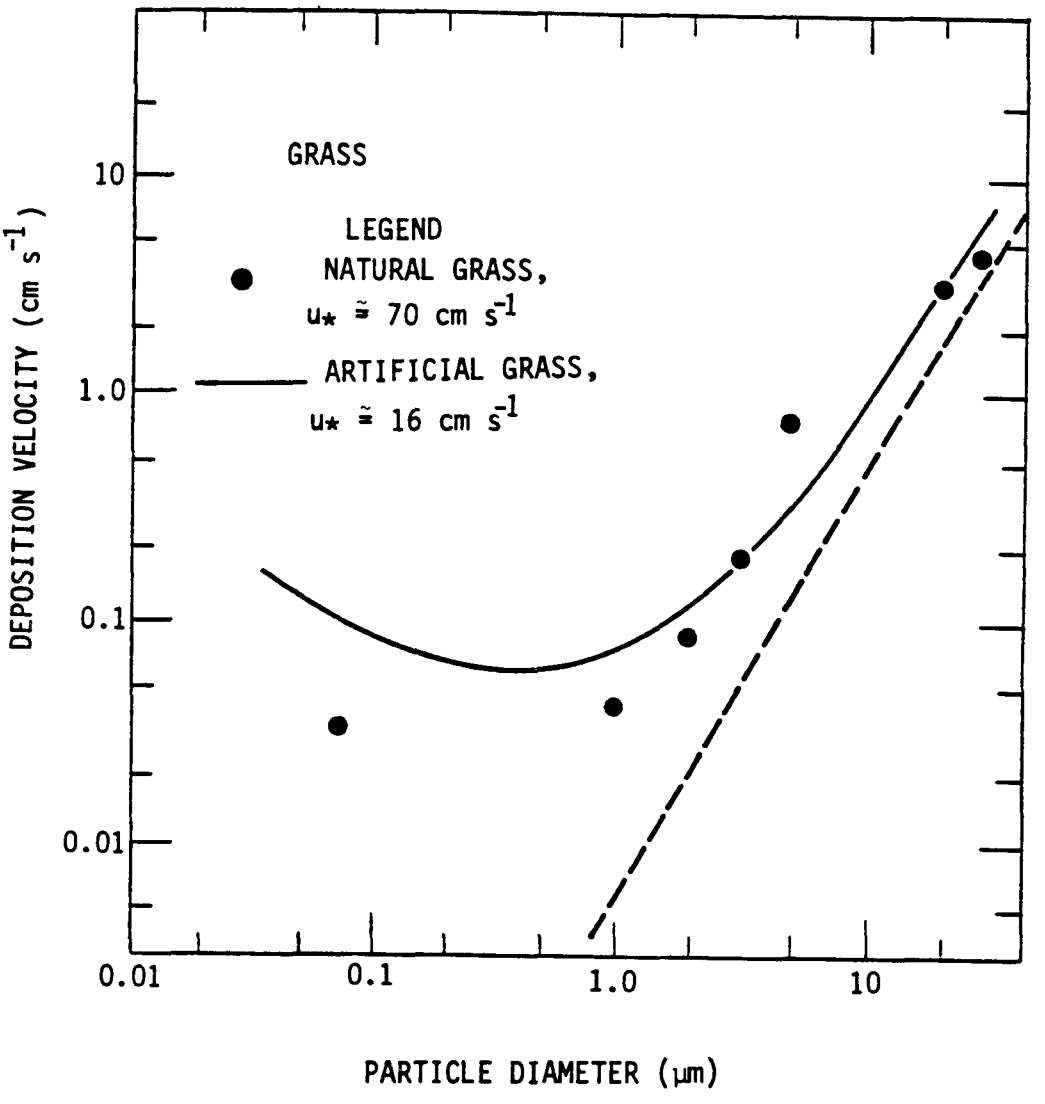

Figure 7-10. Results of wind-tunnel studies of particle deposition to grass, as reported by Chamberlain (1967) - dots; and by Sehmel et al. (1973b) - curve.

$$F_c = \rho\overline{w'C'} \qquad [7\text{-}8]$$

where ρ is the air density and the primes denote deviations from mean values. The over-bar indicates a time average. This is an extremely demanding task and constitutes a specialized field of micrometeorology. Details of experimental procedures are given, for example, by Dyer and Maher (1965), Kaimal (1975), and Kanemasu et al. (1979).

Figure 7-11 shows examples of sensor output signals fundamental to the eddy-correlation technique. Fast-response sensors of any pollutant concentration can be used; the trace shown for CO_2 in the diagram is an interesting example of considerable agricultural relevance. As a basic requirement, sensors suitable for eddy-correlation applications should have response times shorter than one second for operation at convenient heights on towers. For application aboard aircraft (Bean et al. 1972, Lenschow et al. 1980) considerably faster response is required.

Eddy-correlation methods have been used in field experiments addressing the fluxes of ozone (Eastman and Stedman 1977), sulfur (Galbally et al. 1979, Hicks and Wesely 1980), nitric oxides (Wesely et al. 1982b), carbon dioxide (Desjardins and Lemon 1974, Jones and Smith 1977), and small particles (Wesely et al. 1977).

Rates of transfer through the lower atmosphere are governed by turbulence generated by both mechanical mixing and convection. In this context, three atmospheric quantities cannot be separated: the vertical flux of material, the local concentration gradient ($\partial C/\partial z$), and its corresponding eddy diffusivity (K). Knowledge of any two of these quantities will permit the third to be evaluated. Often, when sensors suitable for direct measurement of pollutant fluxes are not available, assumptions regarding the eddy diffusivity are made to provide a method for estimating fluxes from measurements of vertical concentration gradients:

$$F_c = \rho K(\partial C/\partial z). \qquad [7\text{-}9]$$

Hicks and Wesely (1978) and Droppo (1980) have summarized a number of critical considerations. In particular, with a typical value of $u_* = 40$ cm s^{-1} and neutral stability, the concentration difference between adjacent levels differing in height by a factor of two is about 9 percent, for a 1 cm s^{-1} deposition velocity (v_d). In unstable (daytime) conditions, smaller gradients would be expected for the same v_d; in stable conditions, they would be greater.

The demands for high resolution by the concentration measurement technique are obvious. Nevertheless, a substantial quantity of excellent information has been obtained, especially concerning fluxes of SO_2 (Whelpdale and Shaw 1974, Garland 1977, Fowler 1978).

It should be emphasized that the stringent site uniformity requirements mentioned above for the case of eddy-correlation approaches are also relevant for gradient studies. Detecting a statistically significant difference

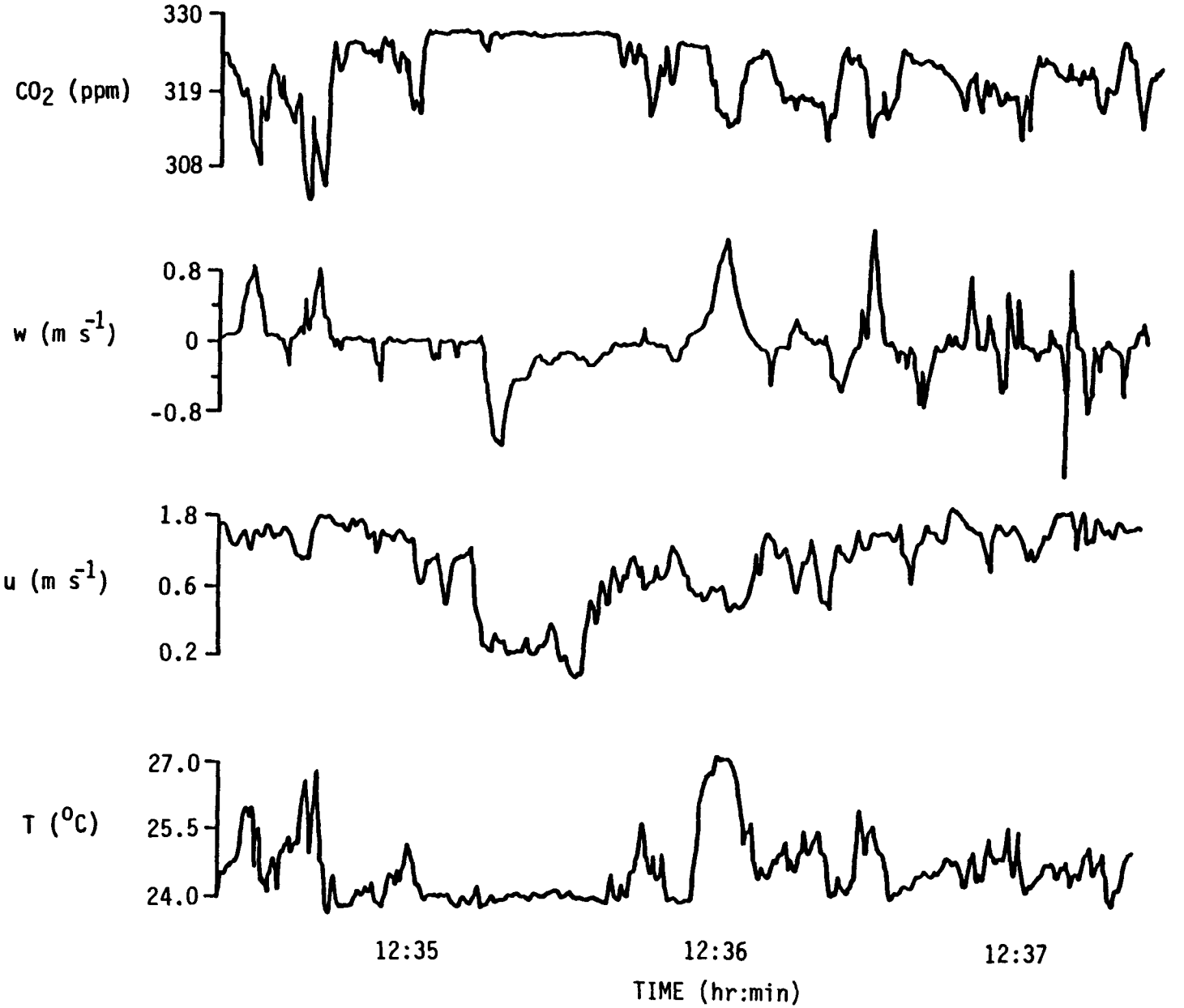

Figure 7-11. An example of atmospheric turbulence near the surface. These traces of CO_2 concentration, vertical velocity (w), wind speed (u), and temperature (T) were obtained over a corn canopy by workers at Cornell University at a few meters above the surface.

between concentrations at two heights is not necessarily evidence of a vertical flux and can only be interpreted as such after extremely demanding siting criteria have been satisfied.

Gradients of particle concentration present special problems because it is often not possible to derive internally-consistent results from alternative measurements. Droppo (1980) concludes that "(t)he particulate source and sink processes over natural surfaces cannot be considered as a simple unidirectional single-rate flux." Thus, the proper interpretation of gradient data in terms of fluxes might not be possible for airborne particles, even in the best of siting circumstances, because of the role of the surface in emitting and resuspending particles. In this case, eddy-correlation methods will still provide an accurate determination of the flux through a particular level, but this flux will be made up of a downward flux of airborne material and an upward flux of similar material of surface origin. Disentangling the two is likely to present a considerable problem.

None of the various micrometeorological methods has yet been developed to the extent necessary for routine application. Rather, they are research methods that can be used in specific circumstances, requiring considerable experimental care, the use of sensitive equipment, and fairly complicated data analysis. They are more suitable for investigating the processes that control dry deposition than for monitoring the flux itself.

Nevertheless, some new techniques for dry deposition measurement are presently under development. A "modified Bowen ratio" method is being developed in the hope that it might permit an accurate determination of vertical fluxes without the need for very rapid response or great resolution (Hicks et al. 1981). High-frequency variance methods are also being advocated but have yet to be fully investigated; for these, sensors having very rapid response are required. An eddy-accumulation method that bypasses the need for rapid response of the pollutant sensor is of long-standing interest (e.g., Desjardins 1977) but has yet to be applied to the pollutant flux problem with significant success.

7.4 FIELD INVESTIGATIONS OF DRY DEPOSITION

7.4.1 Gaseous Pollutants

Table 7-5 summarizes a number of recent field experiments on trace gas deposition to natural surfaces. The listing is drawn from a variety of sources (especially Sehmel 1979, 1980a; Garland 1979; and Chamberlain 1980); it is not meant to be exhaustive, but is intended to demonstrate that many of the available data on surface fluxes of trace gases are biased toward daytime conditions, when "canopy" resistances are usually the controlling factors. Extrapolation of these deposition velocities to nighttime conditions is dangerous on two grounds: first, because of the large changes that might accompany stomatal closure and, second, because of the much greater influence of aerodynamic resistance in nighttime, stable conditions.

Figure 7-12 illustrates the large diurnal cycle typical of the dry deposition rates of most pollutants. These observations were made over a pine

TABLE 7-5. RECENT EXPERIENCE ON TRACE GAS DEPOSITION TO NATURAL SURFACES

Worker	Method	Results and Comments
SO_2		
Hill (1971)	$^{35}SO_2$ with stable SO_2 carrier over alfalfa	$v_d \simeq 2.3$ cm s^{-1} (daytime) Implies $r_c \simeq 0.4$ s cm^{-1}
Garland et al. (1973)	$^{35}SO_2$ over pasture	$v_d \simeq 1.2$ cm s^{1} (daytime) $r_c \simeq 0.6$ s cm^{-1}
Owers and Powell (1974)	$^{35}SO_2$ over pasture	$v_d \simeq 1.3$ cm s^{-1} (daytime)
Shepherd (1974)	SO_2 gradients over grass	$v_d \simeq 1.3$ cm s^{-1} (daytime) $\simeq 0.3$ cm s^{-1} (autumn)
Whelpdale and Shaw (1974)	SO_2 gradients over snow, water, and grass	$v_d \simeq 1$ cm s^{-1} (daytime for grass, water, and snow)
Garland (1977)	SO_2 gradients, calcareous soils	$v_d \simeq 1.2$ cm s^{-1} $r_c \simeq 0.01$ s cm^{-1}
Fowler (1978)	SO_2 gradients, over - wheat - soybean	$v_d \simeq 0.4$ cm s^{-1} $v_d \simeq 1.3$ cm s^{-1}
Dannevik et al. (1976)	SO_2 gradients over wheat	$v_d \simeq 0.4$ cm s^{-1}
Garland and Branson (1977)	$^{35}SO_2$ over a pine plantation	$v_d \simeq 0.1 - 0.6$ cm s^{-1}

TABLE 7-5. CONTINUED

Worker	Method	Results and Comments
Belot (1975) (as summarized by Chamberlain 1980)	$^{34}SO_2$ over a pine plantation	$v_d < 1$ cm s^{-1}
Galbally et al. (1979)	Eddy correlation over pine forest	$v_d \simeq 0.2$ cm s^{-1}
Dovland and Eliassen (1976)	Accumulation to snow	$v_d \simeq 0.1$ cm s^{-1}
Barrie and Walmsley (1978)	Accumulation to snow	$v_d \simeq 0.2$ cm s^{-1}
NO_2		
Wesely et al. (1982b)	Eddy correlation	$v_d \simeq 0.6$ cm s^{-1} (daytime)
	-soybeans	$r_c \simeq 1.3$ s cm^{-1} (daytime)
		$\simeq 15$ s cm^{-1} (night)
O_3		
Galbally and Roy (1980)	Gradients over wheat	$v_d \simeq 0.7$ cm s^{-1}
		Implies $r_c \simeq 1.4$ s cm^{-1}
Wesely et al. (1978, 1982b)	Eddy correlation over a range of natural surfaces	$r_c \simeq 0.8$ s cm^{-1} (daytime)
		$\simeq 1.8$ s cm^{-1} (night)

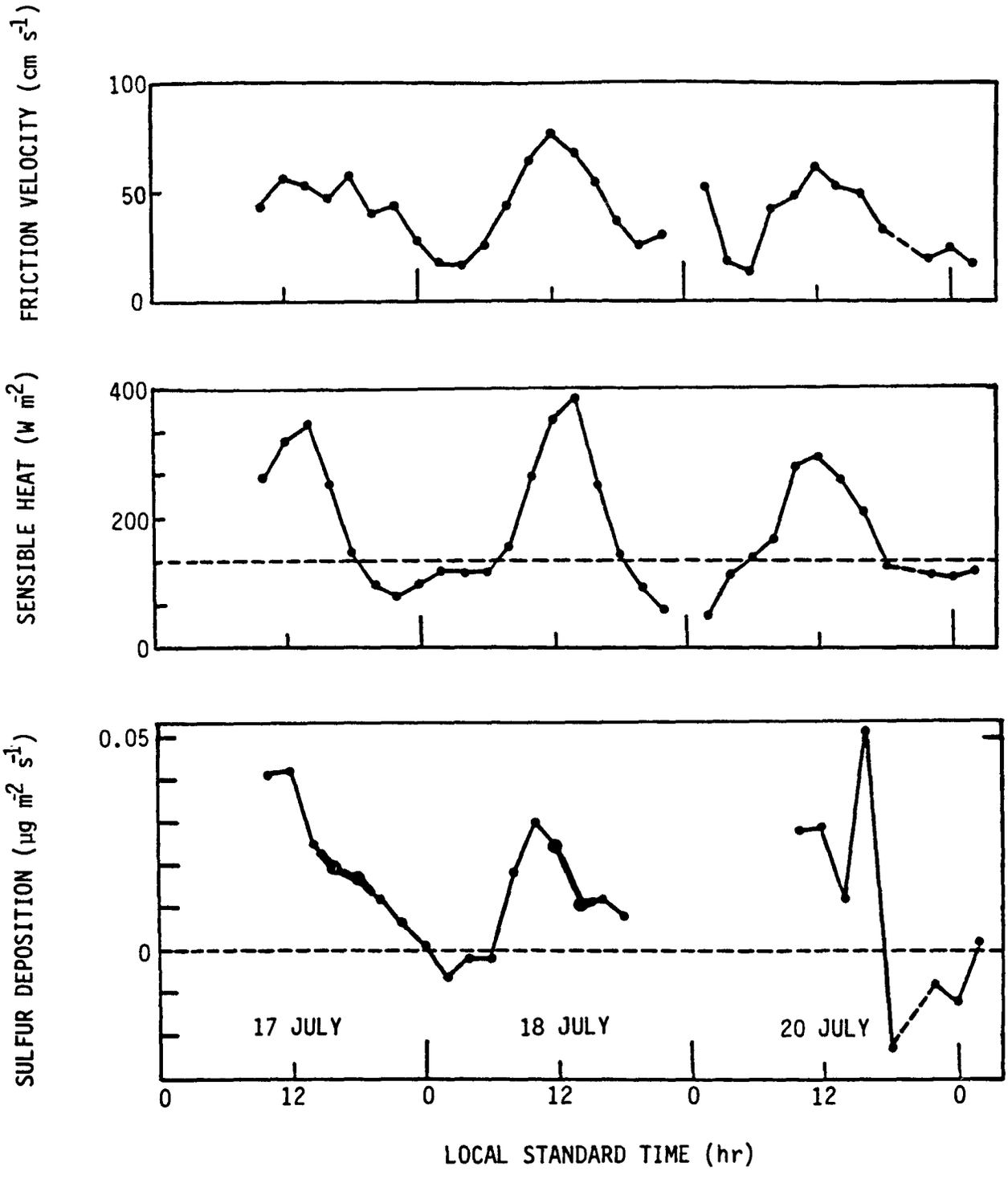

Figure 7-12. Records of sulfur flux, sensible heat flux, and friction velocity through 3 days of an intensive study of dry deposition to a pine plantation (Hicks and Wesely 1980). The darker portions of the sulfur data indicate periods when gaseous sulfur could not be detected. At all times, the data refer to total sulfur, usually made up of gaseous and particulate contributions.

plantation in North Carolina, using eddy correlation to measure each quantity (Hicks and Wesely 1980). The eddy fluxes of total sulfur demonstrate a diurnal cycle that appears to be as strong as for the meteorological properties, a result which is not surprising when it is remembered that many of the causative factors are common (e.g., vertical turbulent exchange). Some caution must be associated with interpreting the negative (upward) fluxes of sulfur evident on two periods as evidence of emission or resuspension from the canopy. Similarly large diurnal cycles of SO_2 deposition are reported by Fowler (1978), who introduces the further complexity of enhanced SO_2 deposition to wheat covered with dewfall. Using the notation of Figures 7-7 and 7-8, Fowler finds typical daytime values to be

$$r_a = 0.25 \text{ s cm}^{-1}$$
$$r_b = 0.25 \text{ s cm}^{-1}$$
$$r_{st} = 1.0 \text{ s cm}^{-1}$$
$$r_{cut} = 2.5 \text{ s cm}^{-1}.$$

For deposition to dry soil, Fowler suggests using $r_{cs} = 10.0$ s cm^{-1}, and $r_{cs} = 0$ when the soil is wet.

Aerodynamic resistance, r_a, influences the deposition of all non-sedimenting pollutants. It is not possible for any trace gas to have a deposition velocity greater than $1/r_a$, i.e., about 4 cm s^{-1} in the daytime conditions of Fowler's experiment. Because of stability effects, the maximum possible deposition velocity at night would be considerably lower. Many of the exceedingly large deposition velocities reported in the open literature appear to exceed the limits imposed by our knowledge of the aerodynamic resistance. Thus, several of the results included in the exhaustive tabulation presented by Sehmel (1980a) should be viewed more as indications of experimental error than as determinations of a physical quantity.

Figure 7-13 addresses the question of the time variation of the deposition velocity v_d. Values plotted are the maximum deposition velocity permitted by the prevailing aerodynamic resistance, evaluated directly from eddy fluxes of heat and momentum determined during the pine plantation experiment of Figure 7-12. In daytime, deposition velocities could be as much as 20 cm s^{-1} if the surface resistance is zero, implying $r_a \simeq 0.05$ s cm^{-1} during midday periods. At night, however, v_d can decrease to 0.1 cm s^{-1} on infrequent occasions but often is less than 2.0 cm s^{-1}. Fowler's recommendations are probably representative of the long-term average.

The importance of diurnal cycles in pollutant deposition and the close relationship with other meteorological quantities is further illustrated by Figure 7-14, which provides examples of the trend from nighttime, through dawn, and into the afternoon of the residual canopy resistance, r_c, for ozone and water vapor determined using eddy-correlation (Wesely et al. 1978). These data were obtained over corn (Zea mays) in July 1976. The upper sequence shows good matching between r_c for ozone and water vapor, with the former exceeding the latter by a small amount, on the average. As the day

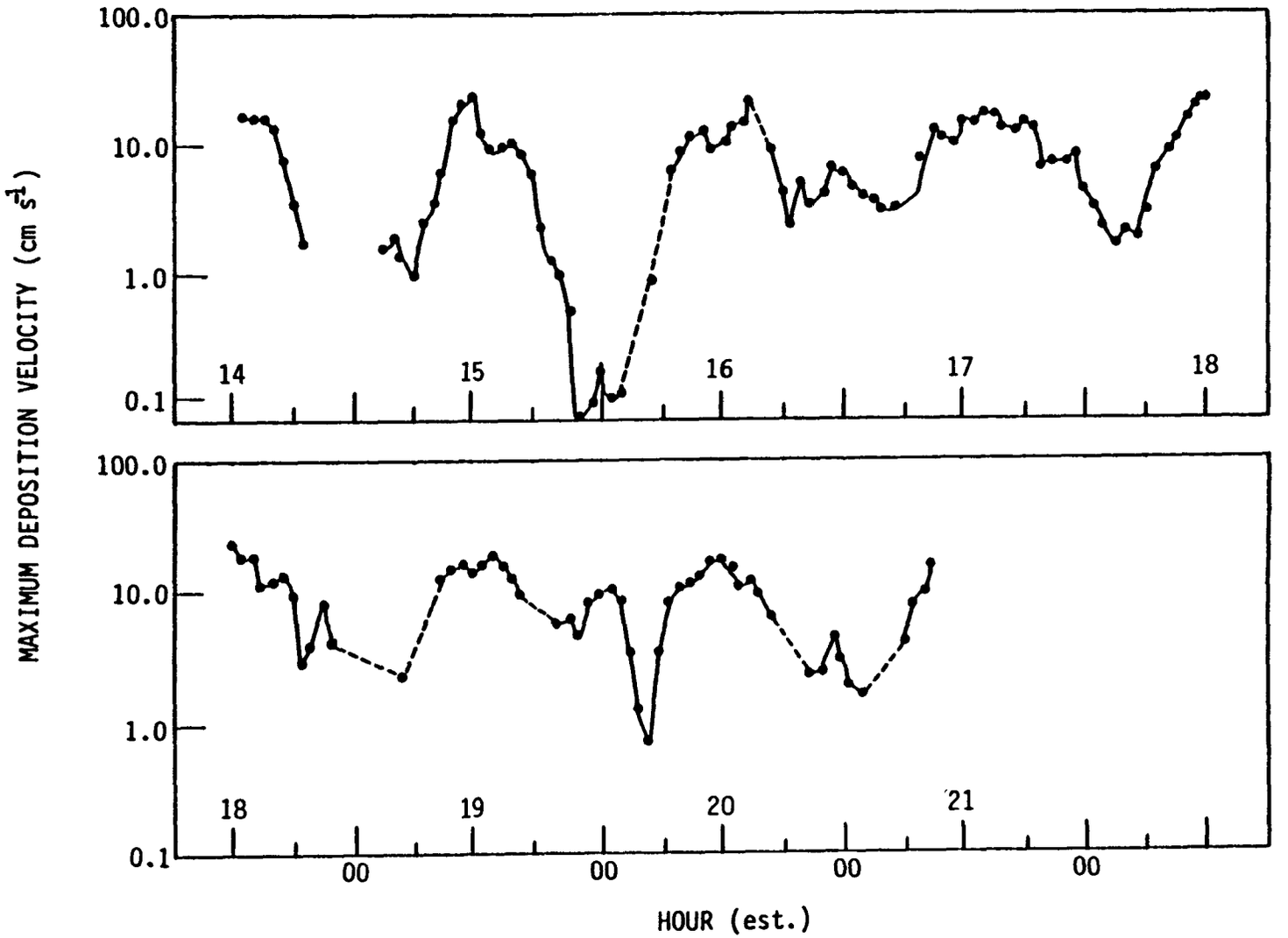

Figure 7-13. Values of the maximum possible deposition velocity of trace gases, determined as the inverse of the aerodynamic resistance, r_a, for the pine plantation experiment of Hicks and Wesely (1980).

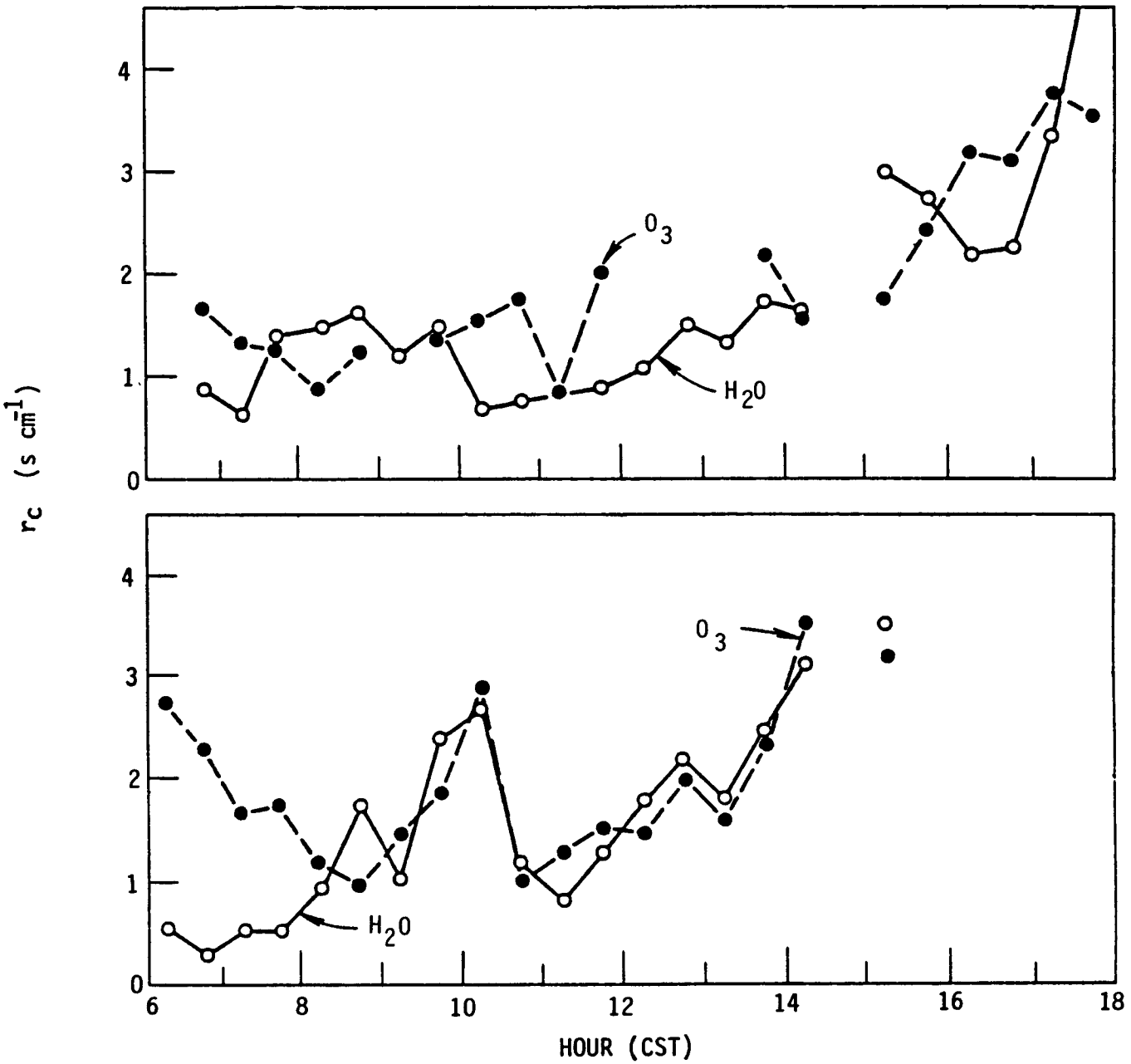

Figure 7-14. Evaluations of the residual "canopy resistance" r_c, to the transfer of ozone and water vapor, based on eddy fluxes measured above mature corn in central Illinois on 29 July 1976 (upper sequence) and 30 July 1976 (lower sequence). Data are from Wesely et al. (1978).

progresses, r_c increases gradually, presumably as a consequence of increasing water stress and eventual stomatal closure. The lower data sequence has two features of considerable interest. First, the gradual initial decrease of r_c for O_3 corresponded to a period of evaporation of dewfall (note the relatively low value of r_c for H_2O during the same period), suggesting that the presence of liquid water on the leaf surfaces might inhibit ozone deposition (much as might be expected on the basis of ozone insolubility in water). This would not be the case for SO_2 deposition (Fowler 1978). Second, the peak in both evaluations of r_c at about 1000 hr is associated with the passage of clouds, which caused a rapid and strong decrease in incoming radiation and lasted for about an hour. The peak is seen as further evidence for stomatal control, because some stomatal closure would be expected with reduced insolation.

The preceding discussion of both SO_2 and O_3 deposition confirms the generalization made by Chamberlain (1980) that the deposition of such quantities might be modeled after the case of water vapor transfer with considerable confidence.

Recently, Wesely et al. (1982b) have reported a field study in which both O_3 and NO_2 fluxes were measured. For a soybean canopy, bulk canopy resistances to ozone uptake exceeded water vapor values by about 0.5 s cm^{-1} during daytime, with r_c for NO_2 still greater by a similar amount.

7.4.2 Particulate Pollutants

No technique for measuring particle fluxes has been developed to the extent necessary to provide universally accepted data. Use of gradient methods, for example, is limited by the inability to resolve concentration differences of the order of 1 percent. Turbulence methods require rapid-response, yet sensitive chemical sensors which are not often available. In both cases, practical application is hindered by the need for a site meeting stringent micrometeorological criteria. Nevertheless, results from several applications of micrometeorological flux-measuring methods have been published. Table 7-6 provides a list that illustrates the narrow range of available information. The evidence points to a difference between the deposition characteristics of small particles and sulfate; the latter seems to be transferred with deposition velocities somewhat greater than the value of 0.1 cm s^{-1} that has been assumed in most assessment studies, and greater than the values appropriate for small particles, on the average. At this time, the possibility that sulfate fluxes are promoted by the strong effect of a few large particles cannot be dismissed.

As must be expected, taller canopies are associated with higher values of v_d, on the average. Figure 7-15 shows how small particle fluxes varied with time of day over a pine plantation in North Carolina during 1977 (Wesely and Hicks 1979). These eddy-correlation results display a run-to-run smoothness that engenders considerable confidence; moreover, they are supported by the finding that simultaneous eddy fluxes of momentum and heat closely satisfied the usual surface roughness and energy balance constraints. There is little doubt that the surface under scrutiny (or at least the air below the sensor) did indeed represent a source of particles rather than a sink for

TABLE 7-6. FIELD EXPERIMENTAL EVALUATIONS OF THE DEPOSITION VELOCITY OF SUBMICRON DIAMETER PARTICLES

Surface	Size and Method	Results and Comments
Snow		
Dovland and Eliassen (1976)	Lead aerosol, surface sampling	0.16 cm s^{-1} in stable stratification, greater values in neutral. All light-wind data.
Wesely and Hicks (1979)	0.05-0.1 μm particles eddy correlation	Net fluxes small but upwards; v_d too small to be determined.
Open Water		
Sievering et al. (1979)	0.2-1.0 μm particles, gradients	Gradients highly variable. Range of v_d typically 0.2 - 1.0 cm s^{-1} in magnitude. Including reversed gradients in long-term average reduces average v_d to near zero. (See Hicks and Williams 1979).
Williams et al. (1978)	0.05-0.1 μm particles, eddy correlation	Preliminary indications only: v_d very small, 95% certainty < 0.05 cm s^{-1}.
Bare Soil		
Wesely and Hicks (1979)	0.05-0.1 μm particles, eddy correlation	Surface frequently a source: v_d very low on the average, but often large for short periods.
Grass		
Sehmel et al. (1973b)	Polydispersed rhodamine-B particles with mass median diameter 0.7 μm, deposited to artificial grass exposed outdoors	Average $v_d \simeq 0.2$ cm s^{-1}
Chamberlain (1960)	Radon daughters deposited to natural grass. Work attributed to Megaw and Chadwick	$v_d \simeq 0.20$ cm s^{-1}

TABLE 7-6. CONTINUED

Surface	Size and Method	Results and Comments
Hudson and Squires (1978)	Cloud condensation nuclei fluxes measured by gradient methods over sagebrush and grass. Particle size probably 0.002-0.04 μm	$v_d \simeq 0.04$ cm s^{-1}
Davidson and Friedlander (1978)	~ 0.03 μm particles gradients over wild oats	Average $v_d \simeq 0.9$ cm s^{-1}
Wesely et al. (1977)	0.05-0.1 μm particles, eddy correlation	Direction of flux sometimes changes. During deposition periods, $v_d \simeq 0.8$ cm s^{-1}, but much lower on the average
Everett et al. (1979)	Particulate lead and sulfur, gradients	v_d greater for sulfur (~ 1 cm s^{-1}) than for lead from more local sources
Sievering (1982)	0.15-0.3 μm particle gradients over mature rye and wheat	v_d averaged 0.4 ± 0.3 cm s^{-1} in light winds, unstable stratification
Hicks et al. (1982)	Sulfate by eddy correlation	v_d as high as 0.7 cm s^{-1} in daytime, about 0.2 cm s^{-1} as a long-term average
Wesely et al. (1982a)	Sulfate by eddy correlation	v_d largest for daytime lush grass (~ 0.5 cm s^{-1}), much less for short dry grass (~ 0.2 cm s^{-1}), strongly stable conditions
Crops		
Droppo (1980)	Particulate trace metals, gradients: senescent maize	v_d varying widely with element, ranging up to about 1 cm s^{-1}
Wesely and Hicks (1979)	0.05-0.1 μm particles, eddy correlation: senescent maize	Strong diurnal variation in the direction of the flux. Long-term average $v_d \simeq 0.1$ cm s^{-1}

TABLE 7-6. CONTINUED

Surface	Size and Method	Results and Comments
Trees		
Hicks and Wesely (1978, 1980)	Sulfate particles, eddy correlation, Loblolly pine	Strong diurnal variability but less marked than for small particles; average $v_d \simeq 0.7$ cm s^{-1}
Wesely and Hicks (1979)	0.05-0.1 μm particles, eddy correlation	Very strong diurnal variation with the canopy a net source. During deposition periods, v_d probably greater than 0.6 cm s^{-1}
Lindberg et al. (1979)	Pb, Cd, S, etc. particles foliar washing	$v_d > 0.1$ cm s^{-1} for all quantities on the average
Wesely et al. (1982a)	Sulfate particles, eddy-correlation	v_d not significantly different from zero for a winter deciduous forest

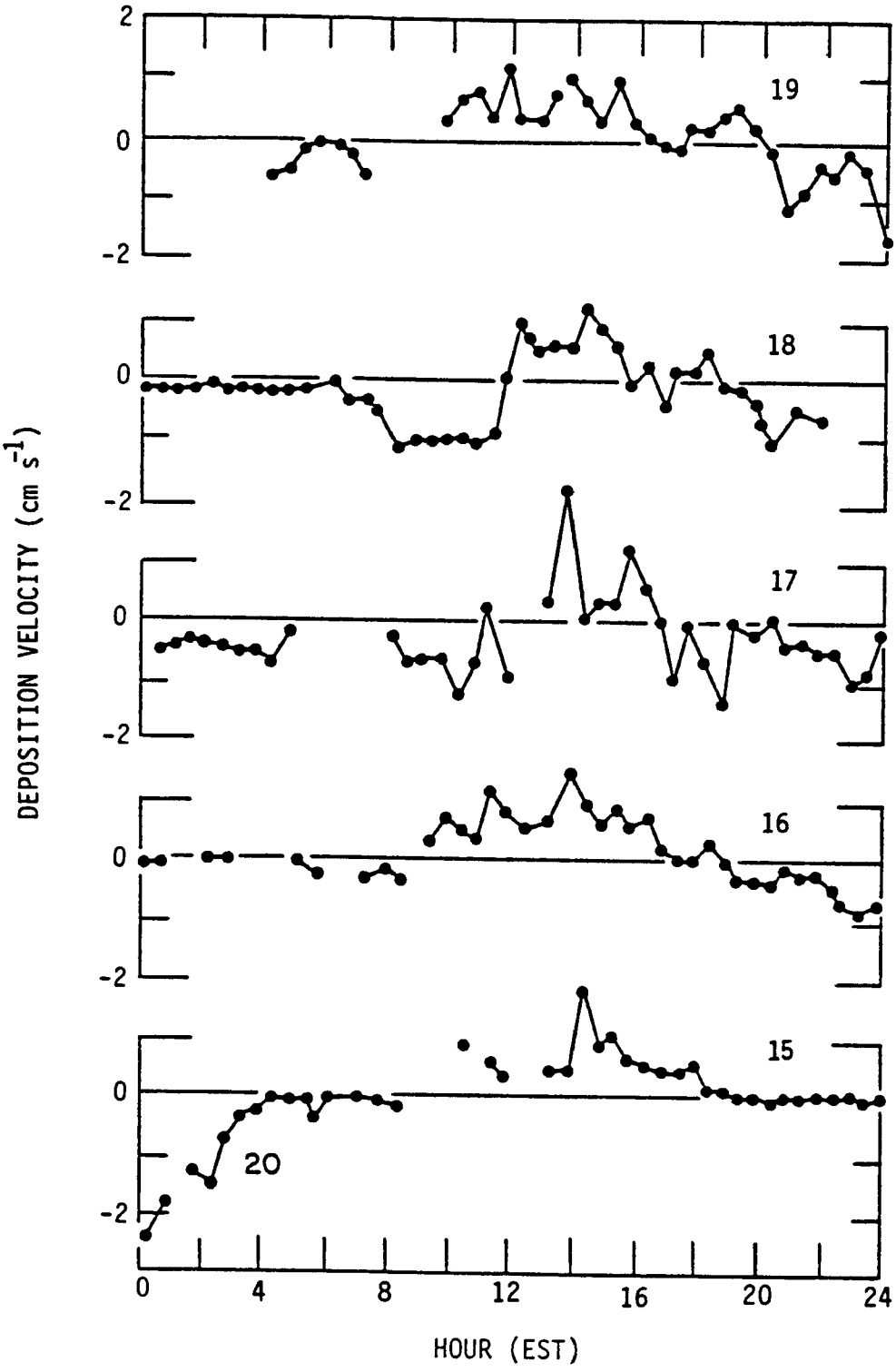

Figure 7-15. Deposition velocity of small particles (~0.1 μm) measured by eddy correlation above a pine plantation in North Carolina in 1977 (Hicks and Wesely 1978, Wesely and Hicks 1979). Note the strong diurnal cycle, with frequent extended periods of emission rather than deposition (as indicated by the negative "deposition velocities").

substantial periods (Arnts et al. 1978). A basic question then arises about the meaning of the measured deposition rates, since these probably represent a net result of continuing but varying surface emission and a deposition flux that is also varying with time. In particular, it is not obvious how to relate such results to the common situation in which we wish to evaluate the atmospheric deposition rate of some particulate pollutant that is not emitted or resuspended from the surface.

Figure 7-12 identifies periods of the 1977 pine plantation study during which no gaseous sulfur was detectable. These occasions were used by Hicks and Wesely (1978) to evaluate residual canopy resistances for particulate sulfur that averaged about 1.5 s cm^{-1} (with a standard error margin of about $\pm$ 15 percent) for 17 July, and about 1.1 s cm^{-1} ($\pm$ 25 percent) for 18 July.

Two tests of sulfate gradient equipment over arid grassland, reported by Droppo (1980), yielded values of 0.10 and 0.27 cm s^{-1} for v_d, in very light winds ($\sim$ 1 m s^{-1}). The residual surface resistances evaluated from his data are 7.7 and 3.3 s cm^{-1}, respectively. These values are considerably higher than the pine plantation results quoted above, but might not be wholly discordant when the nature of the surface present in the gradient studies is taken into account.

Results of an extensive series of eddy-correlation measurements of particulate sulfur fluxes to a variety of vegetated surfaces have been summarized by Wesely et al. (1982a). In daytime conditions, deposition velocities to grass range from about 0.2 to 0.5 cm s^{-1}. Values for a deciduous forest in winter (few leaves) are not significantly different from zero. In general, somewhat lower values are appropriate at night. In almost all of the cases summarized by Wesely et al., normalization of surface transfer conductances by u_* appears to reduce the residual variance. Hicks et al. (1982) present supporting data from another study of the same series, also over grassland.

Considerable controversy remains concerning the value of v_d appropriate for formulating the deposition of sulfate aerosol (and presumably all similar particles). Garland (1978) advocates the continued use of values of 0.1 cm s^{-1} or less, because experiments conducted over grass in England failed to detect a significant gradient. However, some of the experiments listed in Table 7-6 indicate quite high deposition velocities for sulfate particles. The possibility of a strong contribution by particles much larger than the usual accumulation-size mode has been discussed (Garland 1978), and different deposition velocities (0.025 and 0.56 cm s^{-1}) have been postulated for the submicron and larger particles, respectively.

There are great uncertainties about results obtained by deposition plates or other surrogate collection surfaces. Workers sometimes assume that the collection characteristics of some artificial surface are the same as those of the natural surface of interest. Clearly, this assumption will be valid when particles are sufficiently large that gravity is the controlling factor. However, small particles are transferred predominantly by turbulence, with subsequent impaction on the surface of microscale surface roughness elements;

these features of the collecting surface are not easily reproduced by commonly used artificial collecting devices. Monitoring the accumulation of particles in collection vessels continues to be a wide-spread practice (See Chapter A-8); however, relating the data obtained to natural circumstances is difficult (Hicks et al. 1981). In a special category of its own, however, is the method of foliar washing, as used by Lindberg et al. (1979). As applied in careful studies of particle dry deposition at the Walker Branch Watershed in Tennessee, this method of removing and analyzing material deposited on vegetation has succeeded in demonstrating long-term average values of v_d larger than the usually accepted values for several elements.

7.4.3 Routine Handling in Networks

The discussion given in this chapter is intended to focus on the processes that cause dry deposition, and on methods by which these processes can be investigated. Discussion of network monitoring of dry deposition is left for Chapter A-8. However, for the sake of completeness a brief summary of present capabilities to monitor dry deposition should be given here.

It is important to recognize dry deposition for what it is: a highly variable exchange of trace gases and aerosols between the atmosphere and exposed surfaces. In some special circumstances, natural surfaces are such that the accumulation of deposited material can be measured directly, such as in the case of some icefields, snowpacks, stone, and metals. However, in general there is no "monitor" that will give a clear-cut measurement of dry deposition rates to natural surfaces. Work on developing such a monitor must continue, but should be conducted with the realization that science has yet failed to develop such a device for monitoring the surface fluxes of meteorological quantities such as sensible heat, moisture, and momentum. Even in these cases, micrometeorological methods such as eddy correlation and gradient interpretation remain research tools that are applied with great care in intensive case studies. These field studies are intended to formulate the atmosphere/surface exchange in a manner that can then be extended to other situations. Laboratory and modeling studies provide the basic understanding necessary for developing the techniques for interpolating between infrequent direct measurements (by any available method) and for extending them to other situations.

It appears unlikely that collection-vessel or surrogate-surface methods will be capable of providing direct measurements of dry deposition fluxes of trace gases and aerosols to natural surfaces. Likewise, micrometeorological methods seem unable to address the case of particles that fall under the influence of gravity, and a micrometeorologically-based deposition "monitor" does not seem an immediate possibility. Thus, any network for evaluating dry deposition should concentrate on providing data from which surface fluxes can be evaluated, by applying the rapidly expanding understanding of dry deposition processes that is presently being developed. The minimum requirements would be for data on atmospheric concentrations of the relevant trace gas and aerosol species, and for sufficient meteorological data to enable appropriate deposition velocities to be calculated for specified surface characteristics and for the species of interest. Surrogate surface devices might be used to evaluate fluxes of particles falling under the influence of gravity.

These matters are discussed at greater length in Chapter A-8. A summary of methods for measuring dry deposition, with emphasis on the suitability of various techniques as deposition "monitors" has been presented by Hicks et al. (1981).

7.5 MICROMETEOROLOGICAL MODELS OF THE DRY DEPOSITION PROCESS

7.5.1 Gases

Almost all models of dry deposition of trace gases have as their foundation either the resistance analogy illustrated in Figures 7-7 and 7-8 or some equivalent to it. The convenience of this approach is obvious; it permits separate processes to be formulated and combined in a manner that mimics nature, while providing a clear-cut mechanism for determining which processes can be omitted from consideration in specific circumstances. The relevance of the resistance approach to the matter of particle deposition is not so obvious, especially when gravitational settling must be considered.

A useful start is to identify the properties of interest and possible processes that control the uptake of various gases:

SO_2: Uptake by plants is largely via stomata during daytime, with about 25 percent apparently via the epidermis of leaves (Fowler 1978). At night, stomatal resistance will increase substantially, but cuticular resistance should be unchanged. When moisture condenses on the depositing surface, associated resistances to transfer should be allowed to decrease to near zero (Murphy 1976, Fowler 1978). To a water surface, water vapor appears to provide an acceptable analogy to SO_2 flux.

O_3: Behavior is like SO_2 but with significant cuticular uptake at night (r_{cut} ~ 2 to 2.5 s cm^{-1} at night; see r_c quoted by Wesely et al. 1982b) and with surface moisture effectively minimizing uptake. Deposition to water surfaces, in general, is very slow.

NO_2: Similar to O_3 in overall deposition characteristics, but with a significant additional resistance (possibly mesophyllic; see Wesely et al. 1982a) of about 0.5 s cm^{-1}. Even though NO_2 is insoluble in water in low concentrations (see Chapter A-4), deposition to water surfaces might be quite efficient. Chamber studies (Table 7-4) indicate similar overall surface resistances for SO_2 and NO_2.

NO: Typical canopy resistances are in the range 5 to 20 s cm^{-1}, as indicated by chamber studies (Table 7-4) and field experiments (Wesely et al. 1982a). NO appears to be emitted by surfaces at times, possibly as a consequence of NO_2 deposition and of the intimate linkage with ozone concentrations (Galbally and Roy 1980).

HNO_3: Little direct information is available; however, on the basis of its high solubility and chemical reactivity, substantial similarity to

HF should be expected. Consequently, the use of $r_c = 0$ appears to be a reasonable first approximation.

NH_3: Again, no direct measurements are available but in this case similarity with SO_2 appears likely. Natural surfaces may be emitters of NH_3 because of a number of biological processes occurring in and on soil.

Variations in aerodynamic resistance must be expected to modulate all of the behavior patterns summarized above. In many circumstances, deposition rates at night will be nearly zero solely because atmospheric stability is so great that material cannot be transferred through the lower atmosphere. The evaluations given in Figure 7-12 are especially informative, because even over a pine forest whose surface roughness operates to maximize v_d, an occasion was encountered on one evening out of eight in which atmospheric stability was sufficient to constrain the deposition velocity of all airborne material to less than 0.1 cm s^{-1} (with the exception of gravitationally-settling particles).

Some models focus on micrometeorological aspects of the pollutant transfer question, others on the biological. Meteorological models tend to follow the lead of agricultural workers. Shreffler (1976) considers profiles of pollutant concentration above and through a canopy, making use of the familiar concepts of zero-plane displacement, leaf area density, and aerodynamic roughness. Interfacial transfer is formulated as recommended by Brutsaert (1975a). The results are shown to agree, in general form, with the experimental data of Chamberlain (1966; for Th-B).

Roth (1975) also uses micrometeorological relations to investigate gaseous dry deposition, adopting the general resistance format and emphasizing the time-dependency of the aerodynamic resistance and surface (i.e., canopy) resistance.

Brutsaert (1975b) applies theory to the cases of sensible heat and water vapor, and extends these to consider a general scalar quantity. He emphasizes that the common micrometeorological assumption that the roughness length is the same for all quantities can lead to considerable error.

O'Dell et al. (1977) consider details of leaf uptake mechanisms, with emphasis on stomatal and mesophyllic resistances. The model addresses questions of plant physiology in detail and is intended to permit comparison of uptake rates of different gaseous species, once air concentrations near leaves are known.

None of these above models considers all of the processes that have been discussed above, nor is it likely that any model will have sufficient generality to permit its use for all pollutants in all circumstances. To circumvent many of the difficulties involved, Sheih et al. (1979) prepared a land-use map of North America and coupled this with information regarding surface conditions to derive a spatial distribution of surface resistances appropriate for formulating the deposition of sulfur dioxide. By coupling these values with aerodynamic resistances characteristic of different

stability conditions and for different seasons, they produced a map of SO_2 deposition velocities suitable for use in numerical models and for interpreting concentration data (see Chapter A-8). This approach has not been extended to other pollutants.

7.5.2 Particles

Modeling of particle deposition is complicated by three major factors: (1) gravitational settling, which causes particles to fall through the atmospheric turbulence that provides the conceptual basis for conventional micrometeorological models (Yudine 1959); (2) particle inertia, which permits particles to be projected through the near-surface laminar layer by turbulence, but also prohibits particles from responding to the high-frequency turbulent motions that transport material near receptor surfaces; and (3) uncertainty regarding the processes that control particle capture. These three factors are interrelated in such a manner that clearcut differentiation of their separate consequences is not possible.

The problem has attracted the attention of many theoreticians, and many numerical models have been developed. Each model represents a selected combination of processes, chosen for consideration on the basis of the modeler's understanding of the problem. Without adequate consideration of all of the mechanisms involved, none of these models can be considered as a simulator of natural behavior. This is not to question the worth of such models, but rather to emphasize that each should be applied with caution, and only to those situations commensurate with its own assumptions.

The many numerical models can be classified in several different ways. Some extend chemical engineering results to surface geometries that are intended to represent plant communities. Others extend agrometeorological air-canopy interaction models by including critical aspects of aerosol physics. Both approaches have benefits, and the final solution will probably include aspects of each.

An excellent review of model assumptions has been given by Davidson and Friedlander (1978). They trace the evolution of models from the 1957 work of Friedlander and Johnstone (which concentrated on the mechanism of inertial impaction and assumed that particles shared the eddy diffusivity of momentum) to the canopy filtration models of Slinn (1974) and Hidy and Heisler (1978). Early work concerned deposition to flat surfaces and made various assumptions about the surface collection process. Friedlander and Johnstone (1957) permitted particles to be carried by turbulence to within one free-flight distance of the surface, upon which they were assumed to be impacted by inertial penetration of the quasi-laminar "viscous" sublayer. Beal (1970) introduced viscous effects to limit the transfer of small particles, while retaining inertial impaction of larger particles. Sehmel (1970) assumed that all particles that contact the surface will be captured and used empirical evidence obtained in his wind-tunnel studies to determine the overall resistance to transfer, assumed to apply at a distance of one particle radius from the surface. Sehmel's work has been updated recently to provide an estimate of deposition velocities to canopies of a range of geometries in different meteorological conditions (Sehmel 1980b).

The above models are based largely on observations and theory regarding the deposition of particles to smooth surfaces, usually of pipes. More micrometeorologically-oriented models have been presented by workers such as Chamberlain (1967), who extended the familiar meteorological concepts of roughness length and zero plane displacement to the case of particle fluxes. Much of this work was considered as an extension of models developed for the case of gaseous deposition to vegetation, which in turn were based on an extensive background of agricultural and forest meteorology, especially concerning evapotranspiration. A recent development of this genre is the canopy model of Lewellen and Sheng (1980), which uses recent techniques in turbulence modeling to reproduce the main features of subcanopy flow and combines these with particle deposition formulations like those represented in Figure 7-4. Lewellen and Sheng emphasize their model's omission of several potentially critical mechanisms, especially electrical migration, coagulation, evolution of particle size distributions, diffusiophoresis, and thermophoresis. To this list we can add a number of other factors about which little is known at this time, such as subcanopy chemical reactions, interactions with emissions, and the effect of microscale roughness elements.

Although outwardly simpler than the case of particle deposition to a canopy, deposition to a water surface has given rise to a similar variety of models. Once again, however, different models focus on different mechanisms. That of Sehmel and Sutter (1974) is based on their wind tunnel observations and lacks a component that can be identified with wave effects. Slinn and Slinn (1980) invoke the rapid growth of hygroscopic aerosol particles in very humid air to propose rather rapid deposition to open water; deposition velocities on the order of 0.5 cm s^{-1} appear possible in this case. On the other hand, Hicks and Williams (1979) propose negligible fluxes unless the surface quasi-laminar layer is interrupted by breaking waves. At present, none of these models has strong experimental evidence to support it. However, experimental and theoretical studies are proceeding, and a resolution of the matter can certainly be expected.

7.6 SUMMARY

All of the many processes that combine to permit airborne materials to be deposited at the surface have aspects that are strongly surface dependent. While broad generalities can be made about the velocities of deposition of specific chemical species in particular circumstances, wide temporal and spatial variabilities occur in most of the controlling properties. The detailed nature of the vegetation covering the surface is often a critical consideration. If depositional inputs to a special sensitive area need to be estimated, then this can only be accomplished if characteristics specific to the vegetation cover of the area in question are adequately taken into account.

Recent field studies investigating the fluxes of small particles have confirmed wind-tunnel results that point to a surface limitation. Studies of the rate of deposition of particles to the internal walls of pipes and investigations of fluxes to surfaces more characteristic of nature, exposed in wind tunnels, tend to confirm theoretical expectations that surface uptake is controlled by the ability of particles to penetrate a quasi-laminar layer

adjacent to the surface in question. The mechanisms that limit the rate of transfer of particles involve their finite mass. Particles fail to respond to the high frequency turbulent fluctuations that cause transfer to take place in the immediate vicinity of a surface. However, the momentum of particles also causes an inertial deposition phenomenon that serves to enhance the rate of deposition of particles in the 10 to 20 μm size range.

The general features of particle deposition to aerodynamically smooth surfaces are fairly well understood. Studies conducted so far support the theoretical expectation that particles smaller than about 0.1 μm in diameter will be deposited at a rate largely determined by Brownian diffusivity. In this instance, the limiting factor is the transfer by Brownian motion across the quasi-laminar layer referred to above. On the other hand, particticles larger than about 20 μm in diameter are effectively transferred via gravitational settling, at rates determined by the familiar Stokes-Cunningham formulation. Particles in the intermediate-size ranges are transferred very slowly. The minimum value of the "well" of the deposition velocity versus particle size curve is approximately 0.001 cm s^{-1}.

However, natural surfaces are rarely aerodynamically smooth. Wind-tunnel studies have shown that the "well" in the deposition velocity curve is filled in as the surface becomes rougher. Although studies have been conducted, in wind tunnels, of deposition fluxes to surfaces such as gravel, grass, and foliage, the situation involving natural vegetation such as corn, or even pasture, remains uncertain. It is well known that many plant species have foliage with exceedingly complicated microscale surface roughness features. In particular, leaf hairs increase the rate of particle deposition; studies of other factors, such as electrical charges associated with foliage and stickiness of the surface, indicate that a natural canopy might be considerably different from a simplified surface that is suitable for investigation in the laboratory and wind tunnel.

Caution should be exercised in extending laboratory studies using artificially-produced aerosol particles to the situation of the deposition of acidic quantities. Special concern is associated with the hygroscopic nature of many acidic species. Their growth as they enter into a region of high humidity and their liquid nature when they strike the surface are both potentially important factors that might work to increase otherwise small deposition velocities. Moreover, there is evidence that acidic species, especially sulfates, might be carried by larger particles; the rates of deposition of such complicated particle structures are essentially unknown. However, the shape of particles can have a considerable influence upon their gravitational settling speed and probably on their impaction characteristics as well.

It is not clear to what extent special considerations appropriate for acidic species, such as those mentioned above, contribute to the finding of unexpectedly high deposition velocities for atmospheric sulfate particles (sometimes exceeding 0.5 cm s^{-1}), as reported in some recent North American studies. European work has been fairly uniform in producing velocities closer to 0.1 cm s^{-1}, while North American experience has generated larger values.

It is informative to consider the flux of any airborne quantity to the surface underneath in terms of an electrical analog, the so-called resistance model developed initially in studies of agrometeorology. In this model, the flux of the atmospheric property in question is identified with the flow of current in an electrical circuit; individual resistances can then be associated with readily identifiable atmospheric and surface properties. While the electrical analogy has obvious shortcomings, it permits an easy visualization of many contributing processes and enables a comparison of their relative importance. Micrometeorological studies of the fluxes of atmospheric heat and momentum show that the aerodynamic resistance to transfer (i.e., the resistance to transfer between some convenient level in the air and a level immediately above the quasi-laminar layer) ranges from between 0.1 s cm^{-1} in strongly unstable, daytime conditions, to more than 10 s cm^{-1} in many nocturnal cases.

There are several resistance paths that permit gaseous pollutants to be transferred into the interior of leaves. An obvious pathway is directly through the epidermis of leaves, involving a cuticular resistance. An alternative route, known to be of significantly greater importance in many cases, is via the pores of leaves, involving a stomatal resistance that controls transfer to within stomatal cavities, and a subsequent mesophyllic resistance that parameterizes transfer from substomatal cavities to leaf tissue. Comparison among resistances to transfer for water vapor, ozone, sulfur dioxide, and gases that are similarly soluble and/or chemically reactive, shows that in general such quantities are transferred via the stomatal route, whenever stomata are open. Otherwise, cuticular resistance appears to play a significant role. Cuticular uptake of ozone and of quantities like NO and NO_2 appears to be quite significant, whereas for SO_2 this pathway appears to be less important. When leaves are wet, such as after heavy dewfall, uptake of sulfur dioxide is exceedingly efficient until the pH of the surface water becomes sufficiently acidic to impose a chemical limit on the rate of absorption of gaseous SO_2. However, the insolubility of ozone causes dewfall to inhibit ozone dry deposition.

The same conceptual model can be applied to the case of particle transfer with considerable utility. While the roles of factors such as stomatal opening become less clear when particles are being considered, the concept of a residual surface resistance to particle uptake appears to be rather useful. Studies of the transfer of sulfate particles to a pine forest have shown that this residual surface resistance is of the order of 1 to 2 s cm^{-1}. It appears probable that substantially larger values for residual surface resistance will be appropriate for non-vegetated surfaces, especially snow, for which the values are more likely to be approximately 15 s cm^{-1}. At this time, an exceedingly limited quantity of field information is available; however, it appears that in North American conditions the surface resistance to uptake of sulfate particles will be in the range 1.5 to 15 s cm^{-1}.

While sulfate particles have received most of the recent emphasis, the general question of acidic deposition requires that equal attention be paid to nitrate and ammonium particles. There is no information regarding the deposition velocities of these particles, but likewise there is no strong indication that they are different from the case of sulfate.

Regarding trace gas uptake, sulfur dioxide has received the majority of recent attention. Chamber studies and some recent field work indicate that highly reactive materials such as hydrogen fluoride (and presumably iodine vapor, nitric acid vapor, etc.) are readily taken up by a vegetative surface, whereas a second set of pollutants, including SO_2, NO_2, and O_3, seems to be easily transferred via stomata, and a third category of relatively unreactive trace gases is poorly taken up.

Transfer to water surfaces presents special problems, especially when the surface concerned is snow. As mentioned above, surface resistances to particle uptake by snow appear to be of the order 15 s cm^{-1}. Soluble gases will be readily absorbed by all water surfaces, so equivalence to transfer of water vapor might be expected. An important exception occurs in the case of SO_2, in which case absorbed SO_2 can increase the acidity of the surface moisture layer to the extent that further SO_2 transfer is cut off. Trace gas transfer to liquid water surfaces is influenced by the Henry's Law constant.

Wind-tunnel studies of particle transfer to water surfaces all show exceedingly small deposition velocities of particles in the 0.1 to 1 μm size range. Several workers have suggested mechanisms by which larger deposition velocities might exist in natural circumstances; for example, the growth of hygroscopic particles in highly-humid, near-surface air can cause accelerated deposition of such particles, and breaking waves might provide a route that bypasses the otherwise limiting quasi-laminar layer in contact with the surface. Once again field observations are lacking.

While large deposition velocities of soluble trace gases to open water surfaces might appear quite likely, water bodies are frequently sufficiently small that an air-surface thermal equilibrium cannot be achieved. Air blowing from warm land across a small, cool lake, for example, will not rapidly equilibrate with the smooth, cooler surface. Flow will then be stable and largely laminar, with the consequence that very small deposition velocities will apply for all atmospheric quantities. In many circumstances, especially in daytime summer occasions, deposition velocities are likely to be so small as to be disregarded for all practical purposes. On the other hand, during winter when the land surface is frequently cooler than the water, the resulting convective activity over small water bodies will induce the air to come into fairly rapid equilibrium with the water, and rather high deposition velocities (in agreement with the open water surface expectations) will probably be attained.

An associated special case concerns the effect of dewfall, which can accelerate the net transfer of trace gases and particles in some circumstances. The velocities of deposition involved are small; however, they permit an accumulation of material at the surface in conditions in which the atmospheric considerations are likely to predict minimal rates of exchange (i.e., limited by stability to an extreme extent). When surface fog exists, the highly humid conditions will permit airborne hygroscopic particles to nucleate and grow rapidly. This process provides a mechanism for cleansing the lower layers of the atmosphere of most airborne acidic particles. The small fog droplets that are formed around the hygroscopic acidic nuclei are transferred

by the classical process of fog interception, to foliage and other surface roughness elements.

Recent workshops (e.g., Hicks et al. 1981) have concluded that it is not possible to measure the dry deposition of acidic atmospheric materials by using exposed collection vessels because they fail to collect trace gases and small particles in a manner that can be related in a direct fashion to natural circumstances. However, surrogate surface methods appear to be useful in indicating space and time variations of deposition in some cases, and may provide reasonable estimates of fluxes to individual leaves under some conditions. It is possible to measure the flux of some airborne quantities by micrometeorological means, without interfering with the natural processes involved. These studies, and laboratory and wind-tunnel investigations, provide evidence that the controlling properties in the deposition of many trace gases and aerosols are associated with surface structure, rather than with atmospheric properties. The exception to this generalization is the nocturnal case, in which atmospheric stability may often be sufficient to impose a severe restriction on the rate of delivery of all airborne substances to the surface below.

7.7 CONCLUSIONS

The conclusions presented above can be summarized as follows:

- Dry deposition of small aerosol particles and trace gases is a consequence of many atmospheric, surface, and pollutant-related processes, any one of which may dominate under some set of conditions. The complexity of each individual process makes it unlikely that a comprehensive simulation will be developed in the near future (Section 7.2).

- The convenient simplicity afforded by the concept of a deposition velocity (or its inverse, the total resistance to transfer) makes it possible to incorporate dry deposition processes in models in a manner adequate for modeling and assessment purposes. The simplicity of the deposition velocity approach imposes limitations on its application. For example, using average deposition velocities is inappropriate when time-or space-resolved details of deposition fluxes are needed (Section 7.2.1).

- Sufficient information is known about the processes controlling the deposition of trace gases that in many instances deposition velocities can be considered to be known functions of properties such as wind speed, atmospheric stability, surface roughness, and biological factors such as stomatal aperture. Important exceptions concern the case of insoluble (or poorly soluble) gases, and deposition to non-simple surfaces such as forests in rough terrain (Section 7.2).

- The deposition of particles larger than about 20 μm diameter is controlled by gravity and can be evaluated using the straightforward Stokes-Cunningham relationship. Smaller particles are also

influenced by gravity, and many will contribute to the deposition of acidic and acidifying substances (Sections 7.2.2 and 7.2.3).

- The deposition of small particles remains an issue of considerable disagreement. On the whole, model predictions agree with the results of laboratory and wind-tunnel studies, at least for test surfaces that are usually smoother than pasture, but field experiments provide data that indicate greater deposition velocities. The reasons for the apparent disagreement are not yet clear (Sections 7.3, 7.4.2, and 7.5.2).

- Over water surfaces, there are almost no field data on the deposition of small particles. Different models have been put forward, predicting a wide range of deposition velocities. At this time, there is little evidence that would permit us to choose among them. The situation for trace gases like sulfur dioxide and ammonia is much better. On the whole, models agree with the available field data, although there is disagreement among the models on how factors such as molecular diffusivity should be handled (Sections 7.2.7 and 7.5.2).

- Dry deposition to the surfaces of materials used in the construction of buildings, monuments, etc., can be measured in many instances by taking sequential samples of the surface over extended periods. However, many of the drawbacks of surrogate-surface sampling are also of concern here (Section 7.2.8).

- Particulate material at the surface can creep, bounce, and eventually resuspend under the influence of wind gusts. The large particles entrained in this way can cause a local modification of the acidic deposition phenomenon that is associated with accumulation-size aerosol particles and trace gases of more distant origin (Section 7.2.10).

- For both case-study measurement purposes and for long-term monitoring, accurate measurements of pollutant air concentrations are necessary. For monitoring purposes, measurement of airborne pollutant concentrations in a manner carefully designed to permit evaluation of dry deposition rates by applying time-varying deposition velocities specific to the pollutant and site in question appears to be the most attractive option (Section 7.3).

- Micrometeorological methods for measuring dry deposition fluxes have been developed from the techniques conventionally used to determine fluxes of sensible heat, moisture, and momentum. These methods are technologically demanding, and their use in routine monitoring applications is not yet possible (Section 7.3.3).

7.8 REFERENCES

Alexander, L. T. 1967. Does salt water spray strontium-90 from the air? U.S.A.E.C. Health and Safety Laboratory Quarterly Summary Report HASL-181, I-21 - I-24.

Arnts, R. R., R. L. Seila, R. L. Kuntz, F. L. Mowry, K. R. Knoerr, and A. C. Dudgeon. 1978. Measurement of α-pinene fluxes from a loblolly pine forest. Proc. Fourth Joint Conference on Sensing of Environmental Pollutants. Am. Chem. Soc. 829-833.

Bagnold, R. A. 1954. The Physics of Blown Sand and Desert Dunes. Methuen and Company, London.

Barrie, L. A. and J. L. Walmsley. 1978. A study of sulphur dioxide deposition velocities to snow in northern Canada. Atmos. Environ. 12:2321-2332.

Batchelor, G. K. 1967. An Introduction to Fluid Mechanics. Cambridge University Press, Cambridge, MA. 615 pp.

Beal, S. K. 1970. Deposition of particles in turbulent flow on channel or pipe walls. Nucl. Sci. Eng. 40:1-11.

Bean, B. R., R. F. Gilmer, R. L. Grossman, and R. McGavin. 1972. An analysis of airborne measurements of vertical water vapor flux during BOMEX. J. Atmos. Sci. 29:860-869.

Belot, Y. 1975. Etude de la captation des pollutants atmospheriques par les vegetaux. C.E.A., Fontenay-aux-Roses, France.

Billings, C. E., and R. A. Gussman. 1976. Dynamic behavior of aerosols, pp. 40-65. In Handbook on Aerosols. R. E. Dennis, ed. U.S. ERDA TIC-26608, 142 pp.

Bowden, F. P., and D. Tabor. 1950. The Friction and Lubrication of Solids. Clarendon Press, Oxford.

Brimblecombe, P. 1978. Dew as a sink for sulphur dioxide. Tellus 30: 151-157.

Brutsaert, W. H. 1975a. The roughness length for water vapor, sensible heat, and other scalars. J. Atmos. Sci. 32:2028-2031.

Brutsaert, W. H. 1975b. A theory for local evaporation (or heat transfer) from rough and smooth surfaces at ground level. Water Resources Res. 11:543-550.

Cadle, R. D. 1966. Particles in the Atmosphere and Space. Reinhold Press, New York. 226 pp.

Chamberlain, A. C. 1960. Aspects of the deposition of radioactive and other gases and particles. Int. J. Air Pollut. 3:63-88.

Chamberlain, A. C. 1966. Transport of gases to and from grass and grasslike surfaces. Proc. Roy. Soc. London, A, 290:236-265.

Chamberlain, A. C. 1967. Transport of lycopodium spores and other small particles to rough surfaces. Proc. Roy. Soc. London, A, 296:45-70.

Chamberlain, A. C. 1975. The movement of particles in plant communities, pp. 155-203. In Vegetation and the Atmosphere, Volume 1, Principles. J. L. Monteith, ed. Academic Press, London.

Chamberlain, A. C. 1980. Dry deposition of sulfur dioxide, pp. 185-197. In Atmospheric Sulfur Deposition. D. S. Shriner, C. R. Richmond, and S. E. Lindberg, eds. Ann Arbor Science, Ann Arbor, MI.

Chamberlain, A. C. 1983. Roughness length of sea, sand and snow. Boundary-Layer Meteorol. 25:405-409.

Chang, S. G., R. Toossi, and T. Novakov. 1981. The importance of soot particles and nitrous acid in oxidizing SO_2 in atmospheric aqueous droplets. Atmos. Environ. 15:1287-1292.

Cofer, W. R., D. R. Schryer, and R. S. Rogowski. 1981. The oxidation of SO_2 on carbon particles in the presence of O_2, NO_2 and N_2O. Atmos. Environ. 15:1281-1286.

Corn, M. 1961. The adhesion of solid particles to solid surfaces, I. A review. J. Air Pollut. Contr. Assoc. 11:523-528.

Dannevik, W. P., S. Frisella, L. Granat, and R. B. Husar. 1976. SO_2 deposition measurements in the St. Louis regions, pp. 506-511. In Proceedings, Third Symposium on Atmospheric Turbulence, Diffusion, and Air Quality Raleigh, NC (American Meteorological Society).

Dasch, J. M. 1982. A comparison of surrogate surfaces for dry deposition collection. Proc. Fourth International Conference on Precipitation Scavenging, Dry Deposition, and Resuspension. Santa Monica, CA, 29 November - 3 December.

Davidson, C. I. and S. K. Friedlander. 1978. A filtration model for aerosol dry deposition: Application to trace metal deposition from the atmosphere. J. Geophy. Res. 83, C5:2343-2352.

Davies, C. N. 1966. Deposition from moving aerosols, pp. 393-446. In Aerosol Science. C. N. Davies, eds. Academic Press, New York. 468 pp.

Davies, C. N. 1967. Aerosol properties related to surface contamination, pp. 1-5. In Surface Contamination. B. R. Fish, ed. Pergamon Press, New York. 415 pp.

Deacon, E. L. 1977. Gas transfer to and across an air-water interface, Tellus 29:363-374.

Derjaguin, B. V., and Yu. I. Yalamov. 1972. The theory of thermophoresis and diffusiophoresis of aerosol particles and their experimental testing, pp. 1-200. In Topics in Current Aerosol Research, Part 2. G. M. Hidy and J. R. Brock, eds. Pergamon Press, New York. 384 pp.

Desjardins, R. L. 1977. Energy budget by an eddy correlation method. J. Appl. Meteorol. 16:248-250.

Desjardins, R. L. and E. R. Lemon. 1974. Limitations of an eddy-correlation technique for the determination of the carbon dioxide and sensible heat fluxes. Boundary-Layer Meteorol. 5:475-488.

Dillon, P. J., D. S. Jeffries, and W. A. Scheider. 1982. The use of calibrated lakes and watersheds for estimating atmospheric deposition near a large point source. Water, Air, and Soil Pollut. 18:241-258.

Dolske, D. A. and D. F. Gatz. 1982. A field intercomparison of sulfate dry deposition monitoring and measurement methods: Preliminary results. Proc. American Chemical Society Acid Rain Symposium, Las Vegas, NV, 30 March 1982.

Dovland, H. and A. Eliassen. 1976. Dry deposition on a snow surface. Atmos. Environ. 10:783-785.

Droppo, J. G. 1980. Experimental techniques for dry deposition measurements, pp. 209-221. In Atmospheric Sulfur Deposition, D. S. Shriner, C. R. Richmond and S. E. Lindberg, eds. Ann Arbor Press, Ann Arbor, MI. 568 pp.

Dyer, A. J. 1974. A review of flux-profile relationships. Boundary-Layer Meteorol. 7:363-372.

Dyer, A. J., and F. J. Maher. 1965. The "Evapotron". An Instrument for the Measurement of Eddy Fluxes in the Lower Atmosphere, CSIRO (Australia) Division of Meteorological Physics Technical Paper Number 15, 31 pp.

Eastman, J. A. and D. H. Stedman. 1977. A fast response sensor for ozone eddy-correlation flux measurements. Atmos. Environ. 11:1209-1211.

Eaton, J. S., G. E. Likens, and F. H. Bormann. 1978. The input of gaseous and particulate sulfur to a forest ecosystem. Tellus 30:546-551.

Engelmann, R. J., and G. A. Sehmel. 1976. Atmosphere-Surface Exchange of Particulate and Gaseous Pollutants. U.S. ERDA CONF-7409Z1, 988 pp.

Everett, R. G., B. B. Hicks, W. W. Berg, and J. W. Winchester. 1979. An analysis of particulate sulfur and lead gradient data collected at Argonne National Laboratory. Atmos. Environ. 13:931-9434

Fassina, V. 1978. A survey of air pollution and deterioration of stonework in Venice. Atmos. Environ. 12:2205-2211.

Fleischer, R. L. and F. P. Parungo. 1974. Aerosol particles on tobacco trichomes. Nature 250:158-159.

Fowler, D. 1978. Dry deposition of SO_2 on agricultural crops. Atmos. Environ. 12:369-373.

Fowler, D. and M. H. Unsworth. 1979. Turbulent transfer of sulphur dioxide to a wheat crop. Q. J. Roy. Meteorol. Soc. 105:767-783.

Friedlander, S. K. 1977. Smoke, Dust, and Haze. John Wiley and Sons, New York. 317 pp.

Friedlander, S. K. and H. F. Johnstone. 1957. Deposition of suspended particles from turbulent gas streams. Indust. Engr. Chem. 49:1151-1156.

Fuchs, N. A. 1964. The Mechanics of Aerosols. Pergamon Press, New York. 408 pp.

Galbally, I. E. and E. R. Roy. 1980. Ozone and nitrogen oxides in the southern hemisphere troposphere, pp 431-438. In Proceedings, Quadrennial International Ozone Symposium. August 4-9, 1980, Boulder, CO (available from IAMAP).

Galbally, I. E., J. A. Garland, and M. J. G. Wilson. 1979. Sulfur uptake from the atmosphere by forest and farmland. Nature 280:49-50.

Garland, J. A. 1977. The dry deposition of sulphur dioxide to land and water surfaces. Proc. Roy. Soc. London A 354:245-268.

Garland, J. A. 1978. Dry and wet removal of sulphur from the atmosphere. Atmos. Environ. 12:349-362.

Garland, J. A. 1979. Dry deposition of gaseous pollutants, pp 95-103 of WMO - No. 538: Papers presented at the WMO Symposium on the Long-Range Transport of Pollutants and its Relation to General Circulation Including Stratospheric/Tropospheric Exchange Processes, Sofia, 1-5 October.

Garland, J. A. and J. R. Branson. 1977. The deposition of sulphur dioxide to a pine forest assessed by a radioactive tracer method. Tellus 29:445-454.

Garland, J. A., W. S. Clough, and D. Fowler. 1973. Deposition of sulphur dioxide on grass. Nature 242:256-257.

Garratt, J. R. 1978. Flux-profile relationships above tall vegetation. Quart. J. Roy. Meteorol. Soc. 104:199-211.

Gauri, K. L. 1978. The preservation of stone. Scientific American 238:126-128, 131, 134-136.

Hardy, E. P., Jr., and J. H. Harley, Eds. 1958. Environmental contamination from weapons tests. U.S. AEC Health and Safety Laboratory Report, HASL-42A.

Harriott, P. and R. M. Hamilton. 1965. Solid-liquid mass transfer in turbulent pipe flow. Chem. Eng. Sci. 20:1073-1078.

Haynie, F. H. and J. B. Upham. 1974. Correlation between corrosion behavior of steel and atmospheric pollution data, pp. 33-51. In Corrosion in Natural Environments, ASTM STP 558, American Society for Testing and Materials.

Hasse, L., and P. S. Liss. 1980. Gas exchange across the air-sea interface. Tellus 32:470-481.

Hess, G. D. and B. B. Hicks. 1975. The influence of surface effects on pollutant deposition rates over the Great Lakes, pp. 238-247. In The Proceedings of the Second Federal Conference on the Great Lakes, ICMSE.

Hicks, B. B. 1982. Wet and dry surface deposition of air pollutants and their modeling, pp. 183-196. In Conservation of historic stone buildings and monuments. National Materials Advisory Board, National Academy Press, Washington, 365 pp.

Hicks, B. B. and P. S. Liss. 1976. Transfer of SO_2 and other reactive gases across the air-sea interface. Tellus 28:348-354.

Hicks, B. B. and M. L. Wesely. 1978. An examination of some micrometeorological methods for measuring dry deposition. U.S. EPA Report EPA-6000/7-78-116. 27 pp.

Hicks, B. B. and M. L. Wesely. 1980. Turbulent transfer processes to a surface and interaction with vegetation, pp. 199-207. In Atmospheric Sulfur Deposition. D. S. Shriner, C. R. Richmond, and S. E. Lindburg, eds. Ann Arbor Press, Ann Arbor, MI. 568 pp.

Hicks, B. B. and R. M. Williams. 1979. Transfer and Deposition of Particles to Water Surfaces, pp. 237-266. In Atmospheric Sulfur Deposition. D. S. Shriner, C. R. Richmond, and S. E. Lindberg, eds. Ann Arbor Science, Ann Arbor, MI. 568 pp.

Hicks, B. B., G. D. Hess, and M. L. Wesely. 1979. Analysis of flux-profile relationships above tall vegetation, an alternative view. Quart. J. Roy. Meteorol. Soc. 105:1074-1077.

Hicks, B. B., M. L. Wesely, and J. L. Durham. 1981. Critique of methods to measure dry deposition; concise summary of workshop. Presented at the 1981 National ACS Meeting, Atlanta, GA, Ann Arbor Science.

Hicks, B. B., M. L. Wesely, R. L. Coulter, R. L. Hart, J. L. Durham, R. E. Speer, and D. H. Stedman. 1982. An experimental study of sulfur deposition to grassland. Proc. Fourth International Conference on Precipitation Scavenging, Dry Deposition, and Resuspension. Santa Monica, CA, 29 November - 3 December.

Hidy, G. M. 1973. Removal processes of gaseous and particulate pollutants, pp. 121-176. In Chemistry of the Lower Atmosphere. S. I. Rasool, ed. Plenum Press, New York. 335 pp.

Hidy, G. M. and S. L. Heisler. 1978. Transport and deposition of flowing aerosols. In Recent Developments in Aerosol Science. D. Shaw, ed. John Wiley and Sons, New York.

Hill, A. C. 1971. Vegetation. A sink for atmospheric pollutants. J. Air Pollut. Contr. Assoc. 21:341-346.

Hubbard, D. W. and E. N. Lightfoot. 1966. Correlation of heat and mass transfer data for high Schmidt and Reynolds numbers. I/Ec Fundamentals 5:370-379.

Hudson, J. G. and P. Squires. 1978. Continental surface measurements on CCN flux. J. Atmos. Sci. 35:1289-1295.

Jones, E. P. and S. D. Smith. 1977. A first measurement of sea-air CO_2 flux by eddy correlation. J. Geophys. Res. 82:5990-5992.

Judeikis, H. S. and T. B. Stewart. 1976. Laboratory measurement of SO_2 deposition velocities on selected building materials and soils. Atmos. Environ. 10:769-776.

Judeikis, H. S. and A. G. Wren. 1977. Deposition of H_2S and dimethyl sulfide on selected soil materials. Atmos. Environ. 11:1221-1224.

Judeikis, H. S. and A. G. Wren. 1978. Laboratory measurements of SO_2 and NO_2 depositions onto solid and cement surfaces. Atmos. Environ. 12:2315-2319.

Kaimal, C. J. 1975. Sensors and techniques for the direct measurement of turbulent fluxes and profiles in the atmospheric surface layer. Atmospheric Technology 7:7-14.

Kanemasu, E. T., M. L. Wesely, B. B. Hicks, and J. L. Heilman. 1979. Techniques for calculating energy and mass fluxes, pp. 156-182. In Modification of the Aerial Environment of Plants. B. J. Barfield and J. F. Gerber eds. ASAE Monograph No. 2.

Kanwisher, J. 1963. On the exchange of gases between the atmosphere and the sea. Deep-Sea Res. 10:195-207.

Langer, G. 1965. Particle deposition on and re-entrainment from coniferous trees, Part II. Kolloid Z. 204 119-124.

Lenschow, D. H., A. C. Delany, B. B. Stankov, and D. H. Stedman. 1980. Airborne measurements of the vertical flux of ozone in the boundary layer. Boundary-Layer Meteorol. 19:249-265.

Lewellen, W. S. and Y. P. Sheng. 1980. Modeling and dry deposition of SO_2 and sulfate aerosols. Electric Power Research Institute Report EA-1452, 46 pp. (Available from EPRI, Research Reports Center, Box 50490, Palo Alto, CA 94303, USA).

Lindberg, S. E., R. C. Harris, R. R. Turner, D. S. Shriner, and D. D. Huff. 1979. Mechanisms and Rates of Atmospheric Deposition of Selected Trace Elements and Sulfate to a Deciduous Forest Watershed, Oak Ridge National Laboratory Report ORNL/TM-6674, 514 pp.

Liss, P. S. 1973. Processes of gas exchange across an air-sea interface. Deep-Sea Res. 20:221-238.

Liss, P. S. and P. G. Slater. 1974. Flux of gases across the air-sea interface. Nature 247:181-184.

Liu, B. Y. H. and J. K. Agarwal. 1974. Experimental observation of aerosol deposition in turbulent flow. Aerosol Science 5:145-155.

Livingston, R. A., and N. S. Baer. 1983. Mechanisms of air pollution-induced damage to stone. Proc. Sixth World Congress on Air Quality, IUAPPA, Paris, France, 16-20 May, 1983. In press.

Lovett, G. M., W. A. Reiners, and R. K. Olson. 1982. Cloud droplet deposition in subalpine balsam fir forests: Hydrological and chemical inputs. Science 218:1303-1304.

Martell, E. A. 1974. Radioactivity of tobacco trichomes and insoluble cigarette smoke particles. Nature 249:215-217.

Meszaros, A., and K. Vissy. 1974. Concentrations, size distributions and chemical nature of atmospheric aerosol particles in remote oceanic areas. J. Aerosol Sci. 5:101-109.

Mizushina T., F. Ogino, Y. Oka, and H. Fukuda. 1971. Turbulent heat and mass transfer between wall and fluid streams of large Prandtl and Schmidt numbers. Inter. J. Heat and Mass Transfer 14 1705-1716.

Moller, U. and G. Schumann. 1970. Mechanisms of transport from the atmosphere to the earth's surface. J. Geophys. Res. 75:3013-3019.

Monteith, J. L. 1963. Dew, facts and fallacies, pp. 37-56. In The Water Relations of Plants. A. J. Rutter and F. H. Whitehead, eds. John Wiley and Sons, New York.

Murphy, B. D. 1976. The influence of ground cover on the dry deposition rate of gaseous materials. Oak Ridge National Laboratory Report UCCCND/CSD-19, 33 pp.

O'Dell, R. A., M. Taheri, and R. L. Kabel. 1977. A model for uptake of pollutants by vegetation. J. Air Pollut. Contr. Assoc. 27:1104-1109.

Owers, M. J. and A. W. Powell. 1974. Deposition velocity of sulphur dioxide on land and water surfaces using a ^{35}S method. Atmos. Environ. 8:63-67.

Raupach, M. R., J. B. Stewart, and A. S. Thom. 1979. Comments on "Analysis of flux-profile relationships above tall vegetation, an alternative view" by Hicks et al. Q. J. Roy. Meteorol. Soc. 105:1077-1078.

Raynor, G. S., J. V. Hayes, and E. C. Ogden. 1974. Particulate dispersion into and within a forest. Boundary-Layer Meteorol. 7:429-456.

Raynor, G. S., E. C. Ogden, and J. V. Hayes. 1970. Dispersion and deposition of ragweed pollen from experimental sources. J. Appl. Meteorol. 9:885-895.

Raynor, G. S., E. C. Ogden, and J. V. Hayes. 1972a. Dispersion and deposition of Timothy pollen from experimental sources. Agric. Meteorol. 9:347-366.

Raynor, G. S., E. C. Ogden, and J. V. Hayes. 1972b. Dispersion and deposition of corn pollen from experimental sources. Agronomy J. 64:420-427.

Rosinski, J. and C. T. Nagamoto. 1965. Particle deposition on and reentrainment from coniferous trees, Part I. Kolloid Z. 204:111-119.

Roth, R. 1975. Der vertikale transport von Luftbeimengungen in der Prandtl-Schicht und die deposition-velocity. Meteorol. Resch. 28:65-71.

Sehmel, G. A. 1970. Particle deposition from turbulent airflow. J. Geophys. Res. 75 1766-1781.

Sehmel, G. A. 1979. Deposition and Resuspension Processes. Battelle, Pacific Northwest Laboratory Publication PNL-SA-6746.

Sehmel, G. A. 1980a. Particle and gas dry deposition: A review. Atmos. Environ. 14:983-1012.

Sehmel, G. A. 1980b. Model predictions and a summary of dry deposition velocity data, pp. 223-235. In Atmospheric Sulfur Deposition. D. S. Shriner, C. R. Richmond, and S. F. Lindberg, eds. Ann Arbor Press, Ann Arbor, MI. 568 pp.

Sehmel, G. A. and S. L. Sutter. 1974. Particle deposition rates on a water surface as a function of particle diameter and air velocity. J. de Recherches Atmospheriques 3:911-920.

Sehmel, G. A., W. H. Hodgson, and S. L. Sutter. 1973a. Dry deposition of particles. Battelle Pacific Northwest Laboratory Report BNWL-1850 3:157-162.

Sehmel, G. A., S. L. Sutter, and M. T. Dana. 1973b. Dry deposition processes. Battelle Pacific Northwest Laboratories Report BNWL-1751 1:43-49.

Sheih, C. M., M. L. Wesely, and B. B. Hicks. 1979. Estimated dry deposition velocities of sulfur over the Eastern United States and surrounding regions. Atmos. Environ. 13 1361 1368.

Shepherd, J. G. 1974. Measurements of the direct deposition of sulphur dioxide onto grass and water by the profile method. Atmos. Environ. 8:69-74.

Shreffler, J. H. 1976. A model for the transfer of gaseous pollutants to a vegetational surface. J. Appl. Meteorol. 15:744-746.

Sievering, H. 1982. Profile measurements of particle dry deposition velocity at an air-land interface. Atmos. Environ. 16:301-306.

Sievering, H., M. Dave, D. A. Dolske, R. L. Hughes, and P. McCoy. 1979. An experimental study of loading by aerosol transport and dry deposition in the southern Lake Michigan basin. U.S. Environmental Agency Report EPA-905/4-79-016.

Sinclair, P. C. 1976. Vertical transport of desert particulates by dust devils and clear thermals, pp. 497-527. In Atmosphere-Surface Exchange of Particulate and Gaseous Pollutants. R. J. Engelmann and G. A. Sehmel, eds. U.S. ERDA CONF-7409Z1. 989 pp.

Slinn, W. G. N. 1974. Analytical investigations of inertial deposition of small aerosol particles from laminar flows into large obstacles - Parts A and B, PNL Ann. Report to the USAEC, DBER, 1973; BNWL-1850, Pt. 3, Battelle-Northwest, Richland, WA; available from NTIS, Springfield, WA.

Slinn, W. G. N. 1976a. Formulation and a solution of the diffusion, deposition, resuspension problem. Atmos. Environ. 10:763-768.

Slinn, W. G. N. 1976b. Dry deposition and resuspension of aerosol particles - a new look at some old problems; pp. 1-40 of Atmospheric-Surface Exchange of Particulate and Gaseous Pollutants - 1974, R. J. Englemann and G. A. Sehmel, (Coord.), available as ERDA CONF-740921 from NTIS, Springfield, VA.

Slinn, S. A. and W. G. N. Slinn. 1980. Predictions for particle deposition on natural waters. Atmos. Environ. 14:1013-1016.

Slinn, W. G. N., L. Hasse, B. B. Hicks, A. W. Hogan, D. Lal, P. S. Liss, K. O. Munnich, G. A. Sehmel, and O. Vittori. 1978. Some aspects of the transfer of atmospheric trace constituents past the air-sea interface. Atmos. Environ. 12:2055-2087.

Spedding, D. J. 1969. Uptake of sulphur dioxide by barley leaves at low sulphur dioxide concentrations. Nature 224:1229-1231.

Twomey, S. 1977. Atmospheric Aerosols. Elsevier Scientific Publishing Company, Amsterdam. 302 pp.

Wason, D. T., S. K. Wood, R. Davies, and A. Lieberman. 1973. Aerosol transport. Particle charges and re-entrainment effects. J. Colloid Interface Sci. 43:144-149.

Wedding, J. B., R. W. Carlson, J. J. Stiekel, and F. A. Bazzaz. 1975. Aerosol deposition on plant leaves. Env. Sci. and Technol. 9:151-153.

Wesely, M. L. and B. B. Hicks. 1977. Some factors that affect the deposition rates of sulfur dioxide and similar gases on vegetation. J. Air Pollut. Contr. Assoc. 27:1110-1116.

Wesely, M. L. and B. B. Hicks. 1979. Dry deposition and emission of small particles at the surface of the earth. Proceedings Fourth Symposium on Turbulence, Diffusion and Air Quality (Reno NV, 15-18 January). Am. Meteorol. Soc., Boston, MA. pp. 510-513.

Wesely, M. L., D. R. Cook, R. L. Hart, B. B. Hicks, J. L. Durham, R. E. Speer, D. H. Stedman, and R. J. Trapp. 1982a. Eddy-correlation measurements of dry deposition of particulate sulfur and submicron particles. Proc. Fourth International Conference on Precipitation Scavenging, Dry Deposition, and Resuspension. Santa Monica, CA, 29 November - 3 December, in press.

Wesely, M. L., J. A. Eastman, D. R. Cook, and B. B. Hicks. 1978. Daytime variation of ozone eddy fluxes to maize. Boundary-Layer Meteorology 15: 361-373.

Wesely, M. L., J. A. Eastman, D. H. Stedman, and E. D. Yalvac. 1982b. An eddy correlation measurement of NO_2 flux to vegetation and comparison to O_3 flux. Atmos. Environ. 16:815-820.

Wesely, M. L., B. B. Hicks, W. P. Dannevik, S. Frisella, and R. B. Husar. 1977. An eddy correlation measurement of particulate deposition from the atmosphere. Atmos. Environ. 11:561-563.

Whelpdale, D. M. and R. W. Shaw. 1974. Sulphur dioxide removal by turbulent transfer over grass, snow, and other surfaces. Tellus 26:196-204.

Whitby, K. T. 1978. The physical characteristics of sulfur aerosols. Atmos. Environ. 12:135-139.

Williams, R. M., M. L. Wesely, and B. B. Hicks. 1978. Preliminary eddy correlation measurements of momentum, heat, and particle fluxes to Lake Michigan. Argonne National Laboratory Radiological and Environmental Research Division Annual Report. Jan. - Dec. 1978. ANAL-7865, Part III, pp. 82-87.

Winkler, E. M., and E. J. Wilhelm. 1970. Salt burst by hydration pressures in architectural stone in urban atmosphere. Geol. Soc. America Bull. 81: 567-572.

Yudine, M. I. 1959. Physical considerations on heavy-particle diffusion, pp. 185-191. In Advances in Geophysics, Volume 6. H. E. Landsberg and J. van Mieghem, eds. Academic Press, New York.

THE ACIDIC DEPOSITION PHENOMENON AND ITS EFFECTS

A-8. DEPOSITION MONITORING

8.1 INTRODUCTION (G. J. Stensland)

The previous two chapters have discussed the deposition processes by which acidic and acidifying substances in the atmosphere impact on various receptors. Wet deposition in the form of rain, fog, and snow and dry deposition of gases and particulate matter have been addressed.

This chapter considers both wet deposition monitoring during periods of precipitation and dry deposition monitoring during periods of no precipitation. Techniques are discussed for collecting deposition data on a routine basis to determine the broad spacial patterns of deposition and their changes over time. Most of the techniques are also applicable for measuring deposition over smaller space and time scales, such as in research projects to study transformation and scavenging processes (Chapters A-4, A-6, and A-7). The first section of this chapter will discuss techniques and data bases for wet deposition networks. The next section will emphasize dry deposition techniques.

The second major purpose of this chapter is to present and discuss data available from routine, long-term networks. Such data for dry deposition are limited and therefore are combined with the techniques discussion in Section 8.3. Section 8.4 will discuss wet deposition data. Section 8.5 will examine the data record from glacier studies. Glaciochemical investigations are given as a tool in historical delineation of acid precipitation problems such as a bench mark on the natural background void of anthropogenic pollution and contamination.

Wet deposition monitoring techniques vary with the chemical species being investigated. This wet deposition discussion will be limited to the major soluble species in precipitation which account for most of the measured conductance of the samples. This list would include the following ions: hydrogen, bicarbonate, calcium, magnesium, sodium, potassium, sulfate, nitrate, chloride, and ammonium. Experience has shown that measurements of the last eight ions in the list allow one to calculate a pH value which is usually in good agreement with the measured pH value. Samples from remote locations can be strongly affected by organic acids and are thus one group of exceptions (Galloway et al. 1982). The fact that we can often successfully calculate the pH of precipitation samples indicates that the rather small list of measured ions is probably sufficient for studies of wet deposition emphasizing the acid precipitation phenomena.

This chapter will present information relevant to the following questions: How good are the current network data? Are the networks adequately distributed and operated to provide a good evaluation of the temporal and spatial variations relative to pH and the acidic and acidifying substances of interest? Which measurements need improvement, what are the nature of the improvements, and the reasons for them? Are surrogate types of air and water quality measurements available for trend analysis?

The next chapter discusses the deposition models used to predict exposure of receptors to concentrations of specific pollutants. Such models are needed to predict deposition over prescribed periods and with required resolution.

8.2 WET DEPOSITION NETWORKS (G. J. Stensland)

8.2.1 Introduction and Historical Background

The measurement of chemicals in precipitation is not just a recent endeavor. In 1872, for example, Smith discussed the relationship between air pollution and rainwater chemistry in his remarkable book entitled Air and Rain: The Beginnings of Chemical Climatology. Gorham (1958a) reported that hydrochloric acid should be considered in assessing the causes of rain acidity in urban areas. Junge (1963) discussed the role of sea salt particles in producing rain from clouds. A valuable historical perspective on the subject of acid precipitation has recently been published by Cowling (1982).

There are several recent reports describing wet deposition networks and the data generated by them; the Acid Rain Information Book, prepared by GCA Corporation in 1980 for the U.S. Department of Energy (GCA 1980); the Battelle Northwest Laboratories (Dana 1980) report for the American Electric Power Service Corporation; and the Environmental Research and Technology Incorporated report for the Utilities Air Regulatory Group (Hansen et al. 1981) are but three examples.

Networks to monitor wet deposition can be physically characterized by:

1. Space scale--the total area covered by the sampling network.
2. Space density--the area represented by each site in the network, i.e., network area divided by the number of sites.
3. Time scale--the time span during which data were collected in the network.
4. Time density--the frequency of sample collection (the sampling interval).

Networks have been of all spatial and temporal scales and densities, ranging from 1 site operated for only a few days to more than 50 sites distributed over several European countries and operated for over 30 years, to the current rapidly growing NADP network with 115 sites as of mid-1983.

The time and space configurations of networks are dictated by scientific objectives and available financial resources. Networks are often classified either as research networks or as monitoring networks. Research networks usually have smaller space and time dimensions than do monitoring networks. However, the data generated by all types of monitoring networks are eventually used for research purposes, and the data from single site research networks are frequently used to monitor the changes in time of wet deposition. Therefore, characterizing networks according to monitoring or research purposes does not produce a unique distinction.

8.2.2 Definitions

Some widely used technical terms that relate to deposition monitoring are defined as follows:

pH - For typical rain and melted snow solutions the pH ranges from 3.0 to 8.0. The pH indicates the acidity, i.e., the free hydrogen-ion concentration, and mathematically $pH = -\log_{10}[H^+]$. Each unit of decrease on the pH scale represents a 10-fold increase of acidity. Chemically a pH of 7.0 is approximately neutral (for T = 20 C); a pH of less than 7.0 is acidic, and a pH of more than 7.0 is alkaline. Therefore, rainwater with a pH less than 7.0 is acidic. However, pure water in equilibrium with atmospheric carbon dioxide has a pH of about 5.6. Therefore, in practice many scientists adopt 5.6 as the reference value, with samples of rain and melted snow having pH less than 5.6 referred to as acidic precipitation. This pH = 5.6 reference point will be adopted for this chapter. (Values varying from 5.60 to 5.70 are quoted as the reference value by other authors.) Discussion to follow (Section 8.4.2) will indicate that natural rain in areas unaffected by man can have pH values of 5.0 or less and therefore the value of 5.6 is more arbitrary than natural. This point is also discussed in Chapter A-2, Section 2.2.5.

A more rigorous chemical discussion of pH is provided in Chapter E-4, Sections 4.2.2 and 4.4.3.1.

Weighted-mean concentration - The mean concentration of a precipitation constituent such as sulfate for five samples would be simply the sum of the five concentration values divided by five. The volume-weighted-mean concentration for five samples for sulfate is the sum of five products (each sample volume x the sulfate concentration in that sample volume) divided by the sum of the five volumes. The precipitation-weighted-mean concentration is calculated in the same way except the precipitation amount from a standard rain gauge is used instead of the volume from the precipitation chemistry sampling device. For the ions generally considered to be conservative when samples are mixed together (sulfate, nitrate, ammonium, chloride, calcium, magnesium, sodium, and potassium), the weighted-mean concentration for five samples is conceptually the same as the single value that would be measured if all five samples had been poured into one large container. This is not conceptually true for non-conservative ions (such as hydrogen and bicarbonate ions). However, if all the precipitation samples are in equilibrium with atmospheric carbon dioxide and have pH values less than about 5.0, then bicarbonate concentrations are relatively small and the hydrogen ion would be conserved

in the mixing process. The pH calculated for the volume- or precipitation-weighted-mean hydrogen concentration will be referred to in this chapter as the weighted pH.

Precipitation - The term wil be used to denote aqueous material in liquid or solid form, derived from the atmosphere. Dew, frost, and fog are technically included but in practice poorly measured, except by special instruments.

Acid rain - A popular term with many meanings, generally used to describe precipitation with a pH less than 5.6.

Acid precipitation - Water from the atmosphere in the form of rain, sleet, snow, and hail, with a pH less than 5.6.

Wet deposition - A term that refers to: (1) the amount of material removed from the atmosphere and delivered to the ground by rain, snow, or other precipitation forms; and (2) the process of transferring gases, liquids, and solids from the atmosphere to the ground during a precipitation event.

Dry deposition - A term for (1) the amount of material deposited from the atmosphere to the ground in the absence of precipitation; and (2) the process of such deposition.

Total atmospheric deposition - Transfer from the atmosphere to the ground of gases, aerosol particles, and precipitation, i.e., the sum of wet and dry deposition. Atmospheric deposition includes many different types of substances, non-acidic as well as acidic.

Acidic deposition - The transfer from the atmosphere to the ground of acidic substances, via wet or dry deposition.

Quality control and quality assurance - Each person involved in producing precipitation chemistry measurements, from site operators through central laboratory chemists, must carry out certain tests to continuously determine that his procedures and his equipment are "in control." Without such tests a technician might, for example, continue to measure pH with a malfunctioning electrode, an "out of control" electrode.

At the next higher level, the technician's supervisor must assure himself that his technician is producing high quality data, within the quoted limits of precision and bias. The supervisor gains this assurance, in part, by submitting check samples of specified chemical concentration. The technician is not told the "known" values and may not even recognize that a particular sample is designed to check his work; in this case the sample is a blind, unknown quality assurance sample.

The scientific data user will likely want to examine the same data set used by the supervisor to be assured that the data were of high quality.

The terms quality control and quality assurance are defined differently by various authors. The definitions for this chapter are the following:

Quality control - A system of activities that accomplishes two objectives:

1. To continuously control the quality of measurements within established tolerances; and

2. To provide data from tests to determine the precision and bias being achieved.

Quality assurance - A system of activities that verifies and maintains the quality of the measurements. The quality control activities of the analysts are one complement of the quality assurance system.

8.2.3 Methods, Procedures, and Equipment for Wet Deposition Networks

For ideal data comparability, all wet deposition networks should use the same equipment and procedures. In reality, this rarely happens. The following discussion outlines procedures and equipment which vary among networks, past and present, and indicates how the data used should be checked for data comparability.

Site selection - The selection of monitoring sites is based on criteria which should be described in the network documentation. The siting criteria depend on the objectives of the network.

Sample containers - The containers for collecting and storing precipitation vary, depending on the chemicals to be measured. Reuseable plastic collection containers are currently used in most acidic wet deposition networks. However, they are unacceptable for monitoring pesticides in precipitation. Glass collection containers are considered less desirable than plastic ones (Galloway and Likens 1979). Frequent quality control blank checks are necessary to monitor procedures for cleaning containers, and great care is necessary to maintain acceptably low blank levels. Acid washing procedures can potentially produce precipitation pH levels that are too low, while detergent washing may have the opposite effect. Several networks now avoid both of these washing procedures.

Sampling mode - There are three sampling modes. In bulk sampling the collection container is continuously exposed to the atmosphere for sampling and thus collects a mixture of both wet and dry deposition. Bulk sampling has been used frequently in the past and is still often used for economic reasons. For studies of total deposition, wet plus dry, bulk sampling may be suitable. A problem is that exactly what component of dry deposition is sampled by open containers is unknown. The continuously-exposed containers are subject to varying amounts of evaporation unless equipped with a vapor barrier. For studies to determine the acidity of rain and snow samples (the wet deposition component), bulk data pH must be used with great caution (only in conjunction with comprehensive system blank data which demonstrate that dry deposition did not significantly bias the results). For wet deposition sites that will be operated for a long time (more than one year), site operation and central laboratory expenses are large enough that wet-only or wet-dry samplers should be used instead of bulk samplers to maximize the scientific output from the project.

In wet-only sampling, dry deposition is excluded from the precipitation samples by automatic devices that uncover the sampling containers only during precipitation events. Three types of automatic wet-only samplers were evaluated for event collection in a Pennsylvania State University study, which found differences in both the reliability of the instruments and the chemical concentrations in the samples (dePena et al. 1980). In wet-dry sampling, the automatic collecting device includes one container to capture wet deposition and a second container to capture dry deposition where a precipitation sensor activates a motor which moves a cover from one container to the other. As with bulk sampling, the dry container of a wet-dry sampler collects a not-well-defined fraction of the total dry deposition.

For both wet-only and wet-dry sampling, the automatic device has been sometimes replaced by an observer making manual container changes, an undesirable alternative except in very special situations. Generally, projects have not collected and reported system blank data to prove that the manual procedure prevented bias due to dry deposition.

In sequential sampling, a series of containers are exposed to the atmosphere to collect wet deposition samples, with consecutive advances to new containers being triggered on a time basis, a collected volume basis, or a combination. Sequential samplers can be rather complicated and are usually operated only for short time periods during specific research projects. Again an observer sometimes replaces the automatic device to provide manual sequential sampling.

Field measurements - Conductivity, pH, sample weight or volume, and rainfall amount are frequently measured at field laboratories. Making these additional measurements requires that site operators have more training and work longer periods for each sample than operators at sites where samples are only collected and forwarded to a central analytical laboratory. Rainfall amount determined with a standard rain gauge is necessary as it provides an assessment of the fraction of the precipitation captured by the precipitation chemistry sampler, and thus, is useful to ascertain, after the fact, that an automatic sampler has not malfunctioned.

Sample handling - Chemical changes with time in the sample are decreased by refrigeration, aliquoting, filtering, and the addition of preservatives to prevent biological change. Peden and Skowron (1978) have reported that filtering is more effective than refrigeration for stabilizing Illinois samples. When the filtering procedure is used, it is important to obtain and evaluate frequent filter blank samples, because the chemistry of relatively clean rain samples can be easily altered.

The chemical changes with time seem to generally increase the measured pH. Central laboratory pH seems to be generally higher than the field pH measured at an earlier time but this has not been carefully documented and reported very often due, in part, to the problem in quality assuring the field data.

Analytical methods - Appropriate analytical methods are available to measure the major ions found in precipitation, but special precautions are necessary

because the concentrations are low; thus, the samples are easily contaminated. Although pH is deceptively easy to determine with modern equipment, achieving accurate results requires special care because of the low ionic strength of rain and snow samples. Frequent checks with low ionic strength reference solutions are required to avoid the frequent problem of malfunctioning pH electrodes.

Data screening - Network data are in effect screened out if technicians in the field or at the central laboratory discard samples because they look "unduly contaminated." After samples are analyzed the data can be flagged or removed because samples were not collected in the field according to standard protocol or because the data are statistical outliers. The data screening procedures should be documented and updated at regular intervals during the projects.

Quality control and quality assurance reports - For most wet deposition networks, too few quality control checks are performed routinely, too few procedures and results undergo continuous evaluation, and too few results are summarized into formal written quality assurance and quality control reports. This is even more true for past network operations. The reports that are available are often analytical laboratory reports that document the methods used to measure chemical parameters and the bias and precision of the analytical methods. However, for wet deposition monitoring networks, a much greater effort should be made to develop a quality program that addresses all of the steps leading to the data base. While quality assurance and quality control reports can be relatively easily produced for the analytical methods, some of the greatest uncertainties in comparing data from different networks involve estimating the bias and precision resulting from differences in sampling mode, sample handling, and possibly data handling.

Thorough quality assurance programs are costly. Therefore, a network must be quite large and be planned to run for a long time to warrant implementing an elaborate quality assurance program. A research project that operates five sites for one year, for example, generally cannot afford to produce an array of written documents to describe in detail all aspects of the quality assurance program.

Because different networks collect daily samples, weekly samples or monthly samples, the data user is often faced with deciding whether two different data sets are comparable. Thus, quality control reports for the separate networks should contain information to assess data bias and precision for the particular network and also for comparing results to other accepted networks. The use of colocated sites for various networks is one of the most direct ways to assess network design differences. Several colocated sites at locations having different meteorological and pollution environments are necessary to evaluate network data differences. The operation of colocated sites should be continuous rather than a one-time endeavor.

8.2.4 Wet Deposition Network Data Bases

The wet deposition data bases available for North America have been summarized by many authors (e.g., Eriksson 1952, Niemann et al. 1979, Miller

1981, Wisniewski and Kinsman 1982). Miller points out that the history of precipitation chemistry measurements in North America has been very erratic, with networks being established and disbanded without thought of long-term considerations. Miller suggested one possible time grouping of network data:

1. 1875-1955, the period when agricultural researchers measured nutrients in precipitation to determine the input to the soil system;

2. 1955-1975, the period when atmospheric chemists were measuring the major ions in precipitation to better understand chemical cycles in the atmosphere; and

3. 1975-present, the period when network measurements were often primarily to evaluate ecological effects.

Table 8-1 (Miller 1981) summarizes the "agricultural data bases" (taken largely from the review by Eriksson 1952).

Table 8-2 summarizes some regional- and national-scale wet deposition networks in Canada and the United States that have begun operation since 1955. These networks were generally not established to monitor acidic precipitation. The first two are no longer in operation. The PHS/NCAR and EML-DOE networks include sites influenced by large urban areas and thus are not as useful in addressing acidic precipitation issues on larger scales as are other networks. All the networks followed the pattern of the Junge network in measuring major inorganic ions that account for much of sample conductance. Sulfate was measured in all the networks; pH was not measured in the Junge network.

In addition to regional- and national-scale wet deposition networks, local networks also exist. These local networks:

1. may consist of only one site (e.g., Larson and Hettick 1956), or many sites concentrated in a rather small area (e.g., 85 sites in Gatz 1980);

2. may have operated for a year (e.g., the central Illinois study, Larson and Hettick 1956), or much longer (e.g., the Hubbard Brook data base, Likens 1976); and

3. may have studied a particular pollution source (e.g., the St. Louis area, Gatz 1980) or the plume from power plants (e.g., Li and Landsberg 1975, Dana et al. 1975).

Some of the local network data have been very useful in interpreting time trends of chemical concentrations in precipitation.

Wisniewski and Kinsman (1982) have prepared a detailed tabulation of national, regional, and state or province networks currently in operation in the United States, Canada, and Mexico. A total of 71 networks are described.

TABLE 8-1. AGRICULTURAL DATA BASES (1875-1955)

Period	Number of studies	Locations of sites
1875 -1895	3	Missouri, Kansas, Utah
1895 - 1915	7	Ottawa, Iowa, Tennessee, Wisconsin, Illinois, New York Kansas
1915 - 1935	8	Kentucky, Oklahoma, New York, Illinois, Texas, Virginia, Tennessee
1935 - 1955	6	Alabama, Georgia, Indiana, Minnesota, Mississippi, Tennessee, Massachusetts

TABLE 8-2. SOME NORTH AMERICAN WET DEPOSITION DATA BASES (1955-PRESENT)

NETWORK	PERIOD	APPROXIMATE NUMBER OF SITES	SAMPLING MODE[a]	SAMPLING INTERVAL
National				
Junge	1955-1956	60	W-M	Daily (with monthly compositing)
PHS/NCAR[b]	1959-1966	35	W	Monthly
WMO/EPA/NOAA[c]	1972-Present	17	W	Monthly (weekly after joining NADP in 1980)
CANSAP[d]	1977-Present	54	W	Daily (with monthly compositing) (monthly before 1980)
NADP[e]	1978-Present	115	W-D	Weekly
Regional				
US Geological Survey Eastern (USGS)	1964-Present	18	B	Monthly
Canadian Centre for Inland Waters (CCIW)	1969-Present	15	W	Monthly
Tennessee Valley Authority (TVA)	1971-Present	9	W-D	Biweekly
MAP3S[f]	1976-Present	9	W	Daily

TABLE 8-2. CONTINUED

NETWORK	PERIOD	NUMBER OF SITES	SAMPLING MODE[a]	SAMPLING INTERVAL
Canadian APN[g]	1978-Present	8	W	Daily
EML-DOE[h]	1977-Present	7	B, W-D	Monthly
EPRI-SURE[i]	1978-1981	9	W	Daily
UAPS[j]	1981-Present	20	W	Daily
U.S. EPA[k] Great Lakes	1977-Present	30	B, W	Monthly and Weekly

[a]B for bulk, W for wet-only with automatically opening device, W-M for wet-only via manual operation, W-D for wet-dry with automatic device.

[b]U.S. Public Health Service/National Center for Atmospheric Research.

[c]World Meteorological Organization/U.S. Environmental Protection Agency/National and Oceanic and Atmospheric Administration. These sites are now part of NADP.

[d]Canadian Network for Sampling Acid Precipitation.

[e]National Atmospheric Deposition Program. There were 115 operating sites on 1 July 1983 and the network was growing rapidly. In 1983, many of the NADP sites were also named as sites for inclusion in the National Trends Network (NTN).

[f]Multistate Atmospheric Power Production Pollution Study.

[g]Canadian Air and Precipitation Network.

[i]Electric Power Research Institute-Sulfate Regional Experiment.

[h]Environmental Measurements Laboratory of the U.S. Department of Energy.

[j]Utility Acid Precipitation Study. This was preceded at some of the same sites and with the same central laboratory by the 9 site, wet-only, daily sampling EPRI/SURE network.

[k]United States Environmental Protection Agency.

Whelpdale (1979) has prepared a tabulation of seven major wet deposition networks and programs in the world. These include CANSAP, MAP3S, and NADP (which have been included in Table 8-2); the Organization for Economic Cooperation and Development (OECD) network to study the long-range transport of air pollutants which operated from 1972 to 1975; and the three currently operating networks summarized in Tables 8-3 through 8-5. Most of the World Meteorological Organization (WMO) sites (see Table 8-3) in Canada, the United States, and Europe are sites operated as part of the CANSAP, NADP, or Economic Commission for Europe (ECE) networks. The ECE network (see Table 8-4) is noteworthy in that (1) only pH and sulfate are required to be measured in the precipitation samples (for many sites other major ions are also measured), (2) aerosol sulfate and gaseous sulfur dioxide must be measured, (3) each participating country has one or more laboratories to perform chemical analysis on samples collected in that country, and (4) the sample collection period is 24 hours. The European Atmospheric Chemistry Network (EACN) (see Table 8-5) is noteworthy in that its early data provided evidence that Scandanavian precipitation is acidic. Over the last 20 years, these data have been central to discussions of why Scandanavian precipitation is so acidic and what adverse effects are linked to this acidity. Whelpdale (1979) and Wallen (1981) discuss the European and world networks and provide maps of site locations.

8.3 MONITORING CAPABILITIES FOR DRY DEPOSITION (B. B. Hicks)

8.3.1 Introduction

Dry deposition delivers materials to the surface in both solid and gaseous phases, and sometimes in liquid (e.g., when the humidity is so great that "solid" hygroscopic particles are, in fact, wet), without the convenience of a natural process (precipitation) to organize and concentrate its delivery. Rainfall delivers pollutants in irregular but comparatively intense doses, in a manner that permits relatively simple sampling. Dry processes are far slower yet more continuous. Nevertheless, assessments such as by Galloway and Whelpdale (1980) and by Shannon (1981) suggest that wet and dry deposition processes are of roughly equal importance in the average deposition of specific chemical species.

As is explained at length in Chapter A-7, dry deposition rates are influenced strongly by the nature of the surface and by the configuration of appropriate sources. Surface emissions are held in close contact with the ground considerably more than are emissions released at greater altitudes, so that in the former case rates of dry deposition would be expected to be greater. As a direct consequence, dry deposition fluxes must be expected to be highest near sources, whereas the highest rates of wet deposition of the same pollutants may be found much farther downstream. Thus, a network designed specifically to study dry deposition will not be the same as one designed only to study wet. Nevertheless, the intent of most networks is to obtain the maximum amount of information on the deposition of pollutants by all processes; consequently, networks such as that of the U.S. National Atmospheric Deposition Program (NADP) have emphasized the importance of obtaining data on both wet and dry deposition rates and amounts.

TABLE 8-3. CHARACTERISTICS OF THE WORLD METEOROLOGICAL ORGANIZATION (WMO) AIR POLLUTION NETWORK (WHELPDALE 1979)

Program name: WMO BACKGROUND AIR POLLUTION NETWORK.

Organization/Country/Agency: World Meteorological Organization

Purpose: to obtain, on a global and regional basis, background concentration levels of atmospheric constituents, their variability and possible long-term changes, from which the influence of human activities on the composition of the atmosphere can be judged.

Number of stations: approximately 110.

Location: in 72 countries throughout the world.

Period of program: from 1970 continuing indefinitely.

Collector type: recommended procedure is to use either open buckets during periods of precipitation only, or automatic precipitation collectors with a tight seal. Some baseline stations and regional stations with extended programs also do air and particulate sampling (procedures are not yet standard).

Parameters: sample volume, SO_4^{2-}, Cl^-, NH_4^+, Ca^{2+}, Mg^{2+}, Na^{2+}, K^+, NO_3^-, alkalinity or acidity, electrical conductivity, pH.

Collection period: 1 month; some European stations have adopted the 24-hour sampling period of the Economic Commission for Europe (ECE) Cooperative Program for Monitoring and Evaluation of the Long-Range Transmission of Air Pollutants in Europe (EMEP).

Quality control: U.S. Environmental Protection Agency - sponsored reference precipitation sample exchanges.

Contact: Secretary General, World Meteorological Organization, Geneva, Switzerland. Directors, National Meteorological Services.

Data/Reports/References: WMO 1974, WMO Operations Manual for Sampling and Analysis Techniques for Chemical Constituents in Air and Precipitation, WMO No. 299, Geneva.

WMO/EPA/NOAA, 'Atmospheric Turbidity and Precipitation Chemistry Data for the World', Environmental Data Service, NCC, Asheville (annually).

TABLE 8-4. CHARACTERISTICS OF THE ECONOMIC COMMISSION FOR EUROPE (ECE) AIR POLLUTION NETWORK (WHELPDALE 1979)

Program name: COOPERATIVE PROGRAM FOR MONITORING AND EVALUATION OF THE LONG-RANGE TRANSMISSION OF AIR POLLUTANTS IN EUROPE.

Organization/Country/Agency: Economic Commission For Europe.

Purpose: to provide governments with information on the deposition and concentration of air pollutants, as well as on the quantity and significance of long-range transmission of pollutants and fluxes across boundaries.

Number of stations: operating or planned by 1979 - precipitation, 42; aerosol, 52; gas, 53 (~ 1 station/10^5 km^2).

Location: Europe and Scandinavia

Period of program: 1977 to 1980 (first phase).

Collector type: for precipitation: open polyethylene gauges and some automatic collectors; for air: pump and bubbler going to pump and filter pack; for particles: pump and bubbler going to pump and filter pack.

Parameters: precipitation: pH, SO_4^{2-}; optional - H^+, NO_3^-, NH_4^+, Mg^{2+}, Na^+, Cl^-, Ca^{2+}

aerosol: SO_4^{2-}; optional - TSP, H^+, NH_4^+

gas: SO_2; optional - NO_2

Collection period: 24 hours

Quality control: inter-laboratory sample exchange (NILU); laboratory quality assurance programs; statistical analysis of data; cation-anion balance, acidity-pH checks.

Special features: (1) network is part of a larger program which includes modeling, and comparison of field measurements and model calculations;

(2) some of these stations are stations in the EACN (see Table 8-5) and were stations in the Long Range Transport of Air Pollutants (LRTAP) network.

Contact: H. Dovland, Norwegian Institute for Air Research (NILU), Box 130, 2001 Lillestrøm, Norway.

TABLE 8-4. CONTINUED

Data/Reports/References: ECE 1977, Cooperative Program for Monitoring and Evaluation of the Long-Range Transmission of Air Pollutants in Europe - Recommendations of the ECE Task Force, ECE/ENV/15, Annexe 11, 10 pp.

Data listings will be published regularly by NILU.

TABLE 8-5. CHARACTERISTICS OF THE EUROPEAN ATMOSPHERIC CHEMISTRY NETWORK (EACN) (WHELPDALE 1979)

Program name: EUROPEAN ATMOSPHERIC CHEMISTRY NETWORK (EACN)

Organization/Country/Agency: International Meteorological Institute (IMI), Stockholm, Sweden.

Purpose: initially, to study the transport from the atmosphere to the ground of some nutrients, particularly nitrogen. It now has a more general atmospheric chemistry direction, including long-range transport and acidic rain.

Number of stations: a maximum of about 120 in 1959, currently about 50 ($\sim$ 1 station/10^5 km^2).

Location: Scandinavia and western Europe.

Period of program: started in 1946 in Sweden, expanded to western Europe in 1955; continuing.

Collector type: funnel and bottle thermostated to collect either rain or snow; automatic wet-only collectors (Granat type, AAPS type) coming into use.

Parameters: precipitation amount, pH, conductance, acidity, SO_4^{2-}, Cl^-, NO_3^-, NH_4^+, Na^+, K^+, Ca^{2+}, Mg^{2+}, HCO_3^-.

Collection period: 1 month

Quality control: inter-laboratory sample exchanges; laboratory quality assurance programs; cation-anion balance, measured-calculated conductivity, acidity-pH checks; much analysis of data.

Special features: (1) supplementary measurement programs in Swedish part of network examine network design aspects;

(2) several sites are equipped with air and particle sampling systems, primarily to investigate anthropogenic acidity-related phenomena.

Contact: L. Granat, Department of Meteorology, University of Stockholm, Arrhenius Laboratory, S-106 91 Stockholm, Sweden.

Data/Reports/References: Granat, L., 1972, Deposition of sulfate and acid with precipitation over northern Europe, Report AC 20, University of Stockholm, Department of Meteorology/International Meteorological Institute, Stockholm, 19 pp.

TABLE 8-5. CONTINUED

Granat, L., Soderlund, R. and Backlin, L., 1977, The IMI Network in Sweden. Present equipment and plans for improvement, Report AC40, University of Stockholm.

Granat, L., 1978, Sulfate in precipitation as observed by European Atmospheric Chemistry Network, Atmospheric Environment 12:413-424.

Data for period 1955-59 published in Tellus by Eriksson. Subsequent data available from Granat.

In Chapter A-7, Section 7.3, considerable attention has been given to methods by which dry deposition fluxes can be measured. The techniques discussed are those used for detailed case studies of deposition fluxes, intended to provide information on the processes that contribute to the net transfer of pollutants to the surface, and usually designed to help formulate the deposition process. The emphasis in Section 7.3 is on trace gases and submicron particles, which appear to be of major interest in the context of acidic and acidifying deposition. Few of the methods discussed are capable of long-term routine operation. The material that follows addresses similar questions, but the present emphasis will be on methods suitable for long-term monitoring of air pollution deposition fluxes either by direct measurement or by application of the deposition parameterizations resulting from the studies described in Chapter A-7. Many of the comments made earlier are equally applicable here. Repetition will be avoided as much as possible.

8.3.2 Methods for Monitoring Dry Deposition

Essentially two schools of thought on monitoring dry deposition exist. The first advocates the use of collecting surfaces and the subsequent careful chemical analysis of material deposited on them. For particles sufficiently large that deposition is controlled by gravity, surrogate surface and collection vessels have obvious applicability. Furthermore, they provide samples in a manner suitable for chemical analysis using fairly conventional techniques. Collecting vessels have been used for generations in studies of dustfall; standards governing the methods used have been in place for a considerable time (ASTM D 1739-70), and intercomparisons between measurement protocols have been conducted (Foster et al. 1974a). Collection vessels gained considerable popularity following their successful use in studies of radioactive fallout during the 1950's and 1960's. For some gaseous pollutants, species-specific surrogate surface techniques have been used to evaluate air concentrations rather than deposition fluxes. Standards exist concerning sulfation plates used to monitor sulfur dioxide concentrations (ASTM D 2010-65), and once again technique intercomparisons have been conducted (Foster et al. 1974b).

The second school of thought prefers to infer deposition rates from routine measurements of air concentration of the pollutants of concern and of relevant atmospheric and surface quantities. These inferential methods assume the eventual availability of accurate deposition velocities suitable for interpreting concentration measurements, and they assume that accurate concentration measurements can be made. They are applicable in cases in which deposition is not controlled by gravity, i.e., for trace gases or small particles. They do not provide samples as convenient for chemical analysis as do the various surrogate surface methods, but they do not impose any artificial modification to the detailed nature of the surface on which deposition is normally occurring.

Clearly, a comprehensive monitoring program would use both concentration monitoring and surrogate surface methods, since contributions of neither trace gases nor large particles can be rejected on the basis of present knowledge.

8.3.2.1 Direct Collection Procedures--There is no question that the deposition of large particles is adequately monitored by collection devices exposed carefully over the surface of interest. Deposit gauges and dust buckets have been in use in geochemistry for a considerable time, and their use is well accepted for measuring the rate of deposition of soil and other airborne particles sufficiently large that their deposition is controlled by gravity. In the era of concern about radioactive fallout, dustfall buckets were used to obtain estimates of radioactive deposition, especially of so-called local fallout immediately downwind of explosions. There was much concern about how well deposited particles were retained within collecting vessels. Some workers used water in the bottom of collectors to minimize resuspension of deposited material, and others used various sticky substances for the same purpose. It was recognized that the collection vessels failed to reproduce the microscale roughness features of natural surfaces. However, this was not viewed as a major problem because the need was to determine upper limits on deposition so possible hazards could be assessed.

Much farther downwind, so-called global fallout was shown to be associated with submicron particles similar to those of interest in the context of acid deposition. However, most of the distant radioactive fallout was transported in the upper troposphere and lower stratosphere, and deposition was mainly by rainfall. The acknowledged inadequacies of collection buckets for dry deposition collection of global fallout were of relatively little concern because dry fallout was a small fraction of the total surface flux.

Special wet and dry collecting vessels were developed and deployed worldwide. In their most highly-developed form, these devices employed covers that moved automatically to expose a wet collection bucket when precipitation was detected and to cover it and expose a dry collection bucket at all other times. The convenience and relative simplicity of these devices have contributed to their continued acceptance to this day. A major factor that led to their general acceptance was the finding that dry and wet collection buckets of the same geometry provided answers that satisfied the global budget of strontium-90 (Volchok et al. 1970). However, as mentioned above, worldwide radioactive fallout was primarily delivered to the surface via precipitation (as much as 95 percent in some locations). Consequently, an error of a factor of two or three in the measurement of the residual dry deposition component might not have been too obvious.

Concern regarding the meaning of collection-vessel data is not only recent. Hewson (1951) comments that the limitations of deposit gauges are like those of rain gauges. Deposit gauges are funnel-like collection devices that have been used for generations. They are familiar to most meteorologists, and the drawbacks involved are well known (Owens 1918, Ashworth 1941).

Bucket dry deposition data collected by the NADP have been examined for evidence of bird droppings and locally suspended soil particles (Hicks 1982). The results of chemical analyses of twice-monthly dryfall collections were examined for phosphate and calcium concentrations. High levels of phosphate were considered to be evidence of contamination by guano, and calcium was used as an indicator of soil-derived particles. The data indicate frequent

contamination of samples by bird droppings and by soil particles, presumably of local origin. It is obvious, however, that relatively simple remedial steps can be taken. Prongs arranged around collecting vessels can be used to minimize the effects of perching birds and the collectors can be placed sufficiently far above the surface that wind-blown soil particles will be collected only under extreme conditions.

A recent comparison of collection devices (Dolske and Gatz 1982) indicates that buckets of the kind normally used in wet/dry collectors yield sulfate dry deposition rates averaging about three times the values provided by flat surrogate surfaces. Hardy and Harley (1958) report large differences between radioactive fallout dry deposition rates to buckets and other artificial collection devices and to natural vegetation.

On all of the grounds mentioned above, there is reason to be concerned about the use of bucket collection devices for studies of acidic dry deposition. Surrogate surfaces such as flat, horizontal plates, share many of the conceptual problems normally associated with collection vessels, yet appear to have considerable utility in some special circumstances (see Chapter A-7, Section 7.3). For example, Lindberg and Harriss (1981) and Lindberg et al. (1982) show that the deposition of trace metals to surrogate surfaces mounted within a forest canopy is quite similar to the deposition to individual leaves, when expressed on a unit area basis. Later work (Lindberg and Lovett 1982) has extended these studies to particle-associated sulfate, nitrate, and ammonium. In general, it seems that the rates of deposition to surrogate surfaces are within a factor of about two of the rates measured to foliage elements. It is not yet clear how data concerning individual canopy elements can be combined to evaluate the net removal by a canopy as a whole.

8.3.2.2 Alternative Methods--The acknowledged limitations of surrogate-surface and collection-vessel methods for evaluating dry deposition have caused an active search for alternative monitoring methods. In general, these alternative methods have been applied in studies of specific pollutants for which specially accurate and/or rapid response sensors are available. The aim of these experiments has not been to measure the long-term deposition flux, but instead to develop formulations suitable for deriving average deposition rates from other, more easily obtained information such as air concentrations, wind speed, and vegetation characteristics.

Chapter A-7 discusses the processes involved and summarizes a number of recent experimental case studies. The results obtained in these detailed experiments are conveniently expressed in terms of the familiar deposition velocity, which enables deposition fluxes to be deduced directly from measurements of air concentration. The special case studies are providing a rapidly expanding body of information concerning the factors that determine deposition velocities. Once the important deposition processes are formulated and quantified, it will no longer be necessary to measure dry deposition fluxes directly because measurements of atmospheric concentration made in an appropriate manner could be used to infer them. This philosophy has formed the basis for monitoring networks in Scandinavia (Granat et al. 1977) and in Canada (Barrie et al. 1980). It should be noted that using the concentration-monitoring procedure does not remove completely the necessity

for conventional dustfall monitoring because the purpose of the concentration measurements is to permit evaluation of dry deposition rates only of those materials that do not fall under the control of gravity.

Several initiatives are underway to develop micrometeorological methods for monitoring the surface fluxes of particular pollutants. Hicks et al. (1980) have summarized a range of potential micrometerological methods and have evaluated their potential as routine monitors of dry deposition fluxes. They conclude that "at present, the most promising methods for monitoring are eddy accumulation, modified Bowen ratio, and variance." The first of these has been of special interest, because it offers the possibility of using slowly-responding chemical monitors to deduce deposition fluxes, bypassing the usual eddy-correlation requirement for a fast-response chemical sensor. The method compares air in updrafts with air in downdrafts (the former having slightly lower concentrations of depositing pollutants) by measuring each in separate sampling systems. Estimates of deposition velocity are readily obtained from such concentration differences, provided the samples are collected in an appropriate manner. The method has been demonstrated for meteorological variables (e.g., sensible heat; Desjardins 1977) for which updraft/downdraft differences are large but has yet to be successfully demonstrated for a slowly depositing quantity.

The techniques loosely classified as "modified Bowen ratio" all sidestep the need for direct measurement of the pollutant flux itself by relating some feature of pollutant concentration, such as the vertical gradient or the concentration variance in a selected frequency band, to the same characteristic of some better understood quantity for which the flux is known. Easy interpretation of this sort of information requires assumptions of similarity and of pollutant source and sink distributions that are often hard to verify, such as when researchers are working over forests. The method has been used in tests involving carbon dioxide (Allen et al. 1974) and ozone (Leuning et al. 1979), but has yet to be used to monitor pollutant fluxes.

Methods for deducing fluxes of atmospheric quantities from measurements of the variance of their concentration have been developed and applied primarily in studies of the transfer of sensible heat, moisture, and momentum. Techniques of this kind might be especially attractive for some pollutants, but once again a successful system has not been demonstrated. These three micrometeorological methods are identified by Hicks et al. (1980) as "possibly worthy for development for use in monitoring." However, each imposes special sensor requirements that appear difficult to satisfy. Methods based on measurement of concentration variance require rapidly responding sensors with low noise levels and linear response, and the eddy accumulation and modified Bowen ratio methods involve the acccurate measurement of concentration differences on the order of 1 percent.

Attempts to improve sampling by surrogate-surface methods are continuing. Recent comparisons between different kinds of surfaces and/or collection vessels have been reported by Dolske and Gatz (1982), Dasch (1982), and Sickles et al. (1982). Models of deposition processes are also being improved, and considerable emphasis is being given to the role of microscale

surface roughness features (e.g., in the model studies reported by Davidson et al. 1982). It must be expected that the lessons learned in such modeling exercises will be used to improve the similarity between artificial collection devices and natural surfaces.

In some circumstances, deposition fluxes can be measured directly using some special technique unique to the occasion. Efforts must be encouraged to compare fluxes determined by any micrometeorological, surrogate-surface, or collection vessel technique to the answers obtained in such special situations, which include suitably calibrated watersheds (Eaton et al. 1978, Dillon et al. 1982), snowpacks and icefields (Dovland and Eliassen 1976; Barrie and Walmsley 1978; Butler et al. 1980; Section 8.5), some lakes, and mineral surfaces.

8.3.3 Evaluations of Dry Deposition Rates

The paucity of accurate information on dry deposition rates to natural landscapes is a continuing problem to ecologists, geochemists, and meteorologists alike. Although relatively few data exist on which to base estimates of deposition rates using the techniques outlined above (and explained in detail in Chapter A-7), it is appropriate to consider in some detail a selected set of information to illustrate the techniques involved as well as to derive some initial estimates of deposition fluxes. The data set reported by Johnson et al. (1981) has been selected for this purpose. These data were obtained by using a limited network of particle samplers, modified to provide aerosol samples suitable for subsequent analysis by infrared spectroscopy.[1] The sites used were confined to the northeast quadrant of the United States: State College, PA; Charlottesville, VA; Rockport, IN; Upton, Long Island, NY; and Raquette Lake, NY. Between two and three years of data were obtained at each site, starting during 1977, except for the Raquette Lake site, where observations started late in 1978. Size-resolved measurements were made of sulfate, nitrate, ammonium, and total acidity of the aerosol. For the present, main attention will be given to the three chemical species.

A unique feature of the Johnson et al. data set is the fine time resolution of the data, designed specifically to enable detailed analysis of rapidly time-varying atmospheric phenomena. Figures 7-12, 7-13, and 7-14 demonstrate the inherent time dependence of the factors that control dry deposition, and the resulting strong diurnal cycle of the depositional flux. The data set of Johnson et al. permits the effects of this variability to be taken into account.

Figure 8-1 presents average diurnal cycles of sulfate, nitrate, and ammonium in aerosol measured in the surface boundary layer (at about 2 m elevation),

---

[1]It is appreciated that these data might be influenced by sampling difficulties, especially for ammonium and nitrate (see Chapter A-5). The intent here is to demonstrate the method by which deposition fluxes can be evaluated from suitably detailed concentration data. The purpose is not to attempt to quantify the various fluxes in an unequivocal manner.

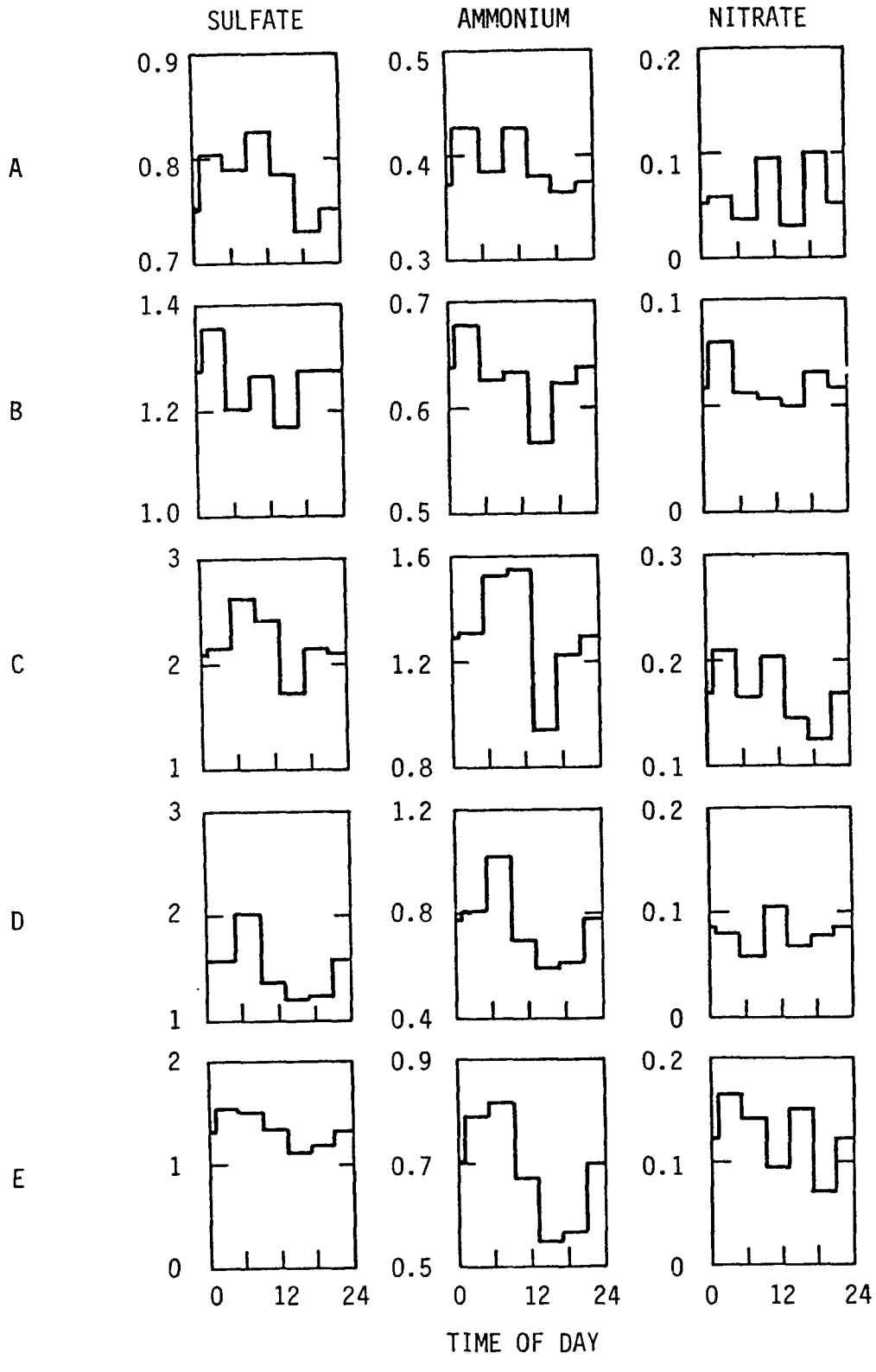

Figure 8-1. Average diurnal cycles of near-surface concentrations of sulfate, ammonium, and nitrate aerosol, as reported by Johnson et al. (1981) for rural sites located at Raquette Lake (NY; A), Upton, Long Island (NY; B), Rockport (IN; C), Charlottesville (VA; D), and State College (PA; E). Concentrations are all in $\mu g\ m^{-3}$

as given by Johnson et al. (1981). Figure 8-2 shows the average diurnal cycle of the aerodynamic resistance to transport between 2 m elevation and the surface, deduced from data presented by Hicks (1981) for arid grassland (actually the Wangara meteorological experiment; see Clarke et al. 1971) and by Hicks and Wesely (1980) for transfer to a pine plantation. These two examples are selected to demonstrate the large differences that occur in atmospheric transport above surfaces of different aerodynamic roughness. Averages are constructed over the same time intervals as were used in the aerosol sampling program.

For the aerosols under present consideration, surface and/or canopy resistances are not accurately known. However, scrutiny of Table 7-6 (Chapter A-7) and consideration of the related discussion leads to the conclusion that a value of about 1.5 s cm^{-1} is likely to be appropriate for the pine plantation case and about 5 s cm^{-1} for grassland. It should be emphasized, however, that considerable disagreement about these values remains, with many workers preferring to continue with the approximation 0.1 cm s^{-1} for the deposition velocity, regardless of the nature of the surface or the atmosphere. The various arguments that are involved will not be discussed here. Instead, we will apply the results of the experimental programs and overlook the fact that many of the detailed deposition models fail to agree.

To estimate deposition velocities suitable for interpreting the data of Figure 8-1, we must add these estimates of surface resistance to the time-varying aerodynamic resistances of Figure 8-2, yielding (as the inverse of the resulting sums) deposition velocities that have a small diurnal variation, averaging about 0.59 cm s^{-1} for the pine forest and about 0.17 cm s^{-1} for the grassland. It should be noted, in passing, that the lack of a strong diurnal cycle of the deposition velocity is a direct consequence of the assumption that the surface resistance is relatively large but constant with time, which is known to be erroneous for the case of trace gas transfer but is presently assumed for particles in the lack of sufficient understanding to permit a better assumption, notwithstanding the evidence of Figure 7-15 (Chapter A-7). Once again, it is clear that surfaces of different kinds will receive substantially different dry deposition fluxes.

Table 8-6 summarizes the deposition fluxes evaluated using the deposition velocities determined above and the diurnally-varying concentrations of Figure 8-1. It must be emphasized that the values quoted are indeed estimates; several potentially important factors are disregarded. For example, the special circumstances of snow cover have not been considered. The evaluations given in Table 8-6 are intended to provide realistic estimates of dry deposition rates to specific ecosystems rather than precise determinations appropriate for detailed analysis.

Sheih et al. (1979) have combined deposition data from many experimental sources with land-use and meteorological information to produce deposition velocity "maps" for sulfate aerosol. Figure 8-3 (from Masse and Voldner 1982) is a recent extension of this approach. If time-averaged concentrations of sulfate in air near the surface are known, then average deposition rates can be estimated by using the mean deposition velocities illustrated in the diagram.

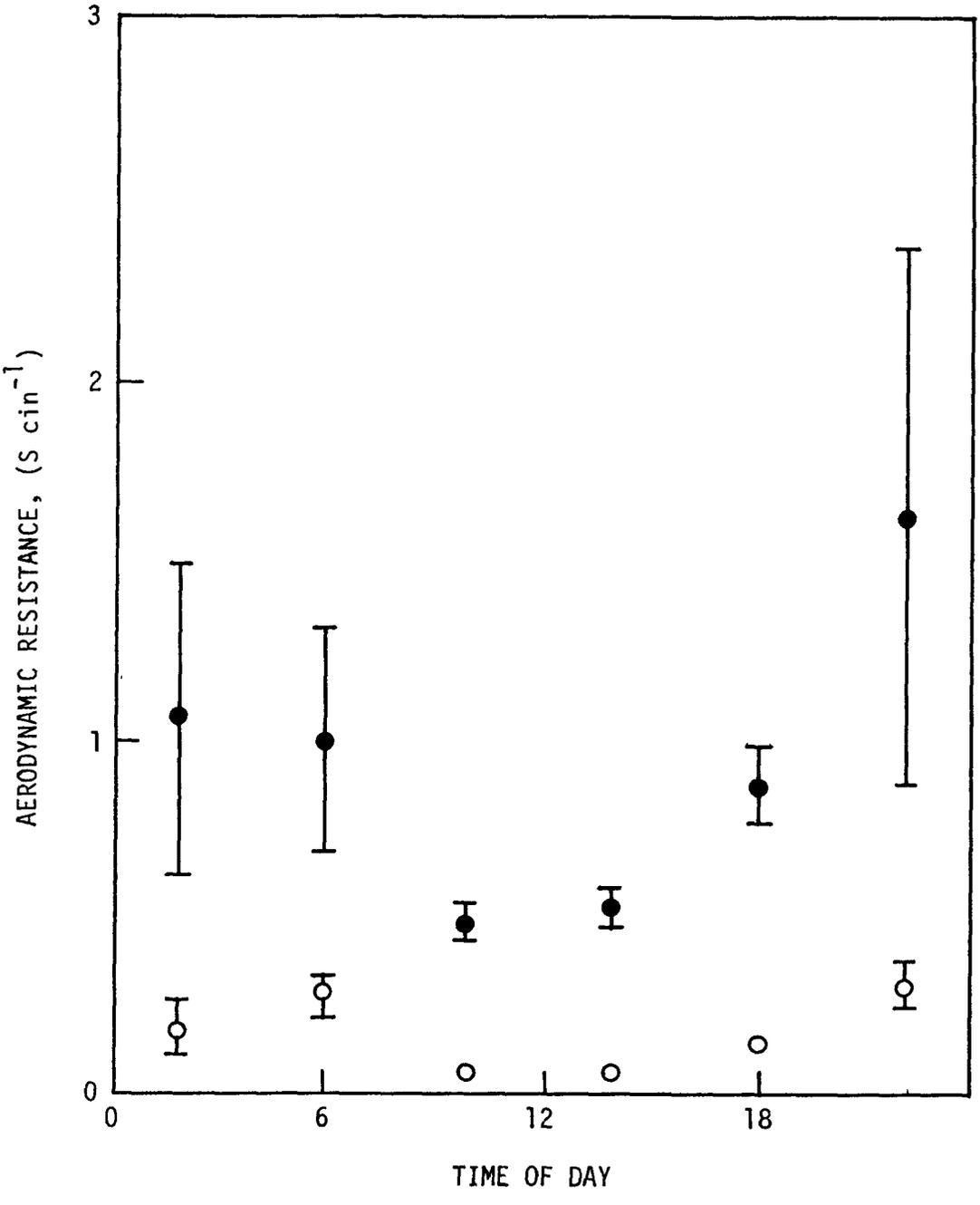

Figure 8-2. Average diurnal variability of atmospheric resistance to pollutant transfer to the surface from convenient measuring heights above the surface, for the cases of a pine plantation (open circles),and grassland (solid circles). Standard error bars are drawn wherever they are large enough to be visible.

TABLE 8-6. ESTIMATES OF AVERAGE DRY DEPOSITION LOADINGS TO AREAS OF FOREST AND GRASSLAND IN THE NORTHEAST UNITED STATES, BASED ON SULFATE, NITRATE, AND AMMONIUM PARTICLE CONCENTRATION DATA REPORTED BY JOHNSON ET AL. (1981).[a]

Location	Sulfur (SO_4 - S)	Nitrogen (NO_3 - N)	Nitrogen (NH_4 - N)
Raquette Lake (NY)	0.7 (0.5)	0.01 (0.03)	0.2 (0.6)
Upton, Long Island (NY)	0.2 (0.8)	0.01 (0.03)	0.3 (1.0)
Rockport (IN)	0.4 (1.3)	0.02 (0.07)	0.6 (2.0)
Charlottesville (VA)	0.3 (0.9)	0.01 (0.03)	0.3 (1.2)
State College (PA)	0.2 (0.8)	0.02 (0.05)	0.3 (1.0)

[a]The particle size range measured was 0.3 to 1.0 μm diameter. Fluxes to forests are given in brackets. Units are kg ha^{-1} yr^{-1} of elemental sulfur and nitrogen delivered by each chemical species. Note that these flux estimates are based on preliminary data, including rather crude evaluations of appropriate deposition velocities. Errors on the order of a factor of two must be expected.

As mentioned above, biological factors play an important role in determining deposition velocities appropriate for the deposition of trace gases. Stomatal resistance to sulfur dioxide transfer can vary by more than an order of magnitude between day and night (see Chamberlain 1980, for example). In consequence, exceedingly strong diurnal cycles of deposition must be expected and interpretation of trace gas concentration data obtained over long averaging times might be quite difficult. At this time, we lack rural trace gas concentration data that can be used to illustrate this point. However, the difficulties involved can be illustrated by the conceptual example of a situation in which the atmosphere aloft supplies some trace gas to surface air at a constant rate, with concentrations building at night when surface deposition is prohibited by biological factors. In daytime, the vegetated surface will act as an efficient sink and airborne concentrations near the surface will be reduced. In this situation, measurements of nighttime concentrations are essentially irrelevant to depositional flux calculations, yet they contribute most of the impact on average air quality that may be of considerable importance for other reasons.

Figure 8-4 (also from Masse and Voldner 1982) shows isopleths of estimated sulfur dioxide deposition velocity for eastern North America. The diagram is derived by combining land-use descriptions with meteorological and biological factors, as in the case of Figure 8-3 for sulfate aerosol. The analysis follows initial work reported by Sheih et al. (1979). Both of the deposition velocity maps reproduced here provide estimates typical of conditions in April. At other times, different distributions of deposition velocity apply.

At this time, no monitoring program in the United States reports air concentrations of pollutants in a manner such that dry deposition fluxes of acidic and acidifying pollutants can be readily evaluated, although several networks offering suitable information have operated for limited periods (see Hidy 1982, and see Figure 8-5). Such networks are in operation elsewhere, particularly in Scandinavia (Granat et al. 1977) and in Canada (Barrie et al. 1980). A wet-chemical device is used in the Scandinavian network, whereas filter-packs are used in the Canadian. No measurement method permits accurate measurement of all of the trace gases and small particles of importance in the context of acid precipitation. Sampling artifacts are discussed elsewhere in this document, as are problems associated with isokinetic sampling of particles. Furthermore, it is obvious that the quality of dry deposition data evaluation from any such concentration information is at the mercy of the deposition velocity assumptions made as the intermediate steps. If the need exists for accurate evaluations of average dry deposition rates of gases and small particles, then it seems necessary to place almost equal emphasis on the requirements for accurate concentration data and for reliable and appropriate deposition velocity evaluations. At the same time, it must be remembered that none of the various methods for interpreting concentration data is intended for use in the case of large particles that fall under the influence of gravity. In this particular case, use of collection devices remains an obvious preference.

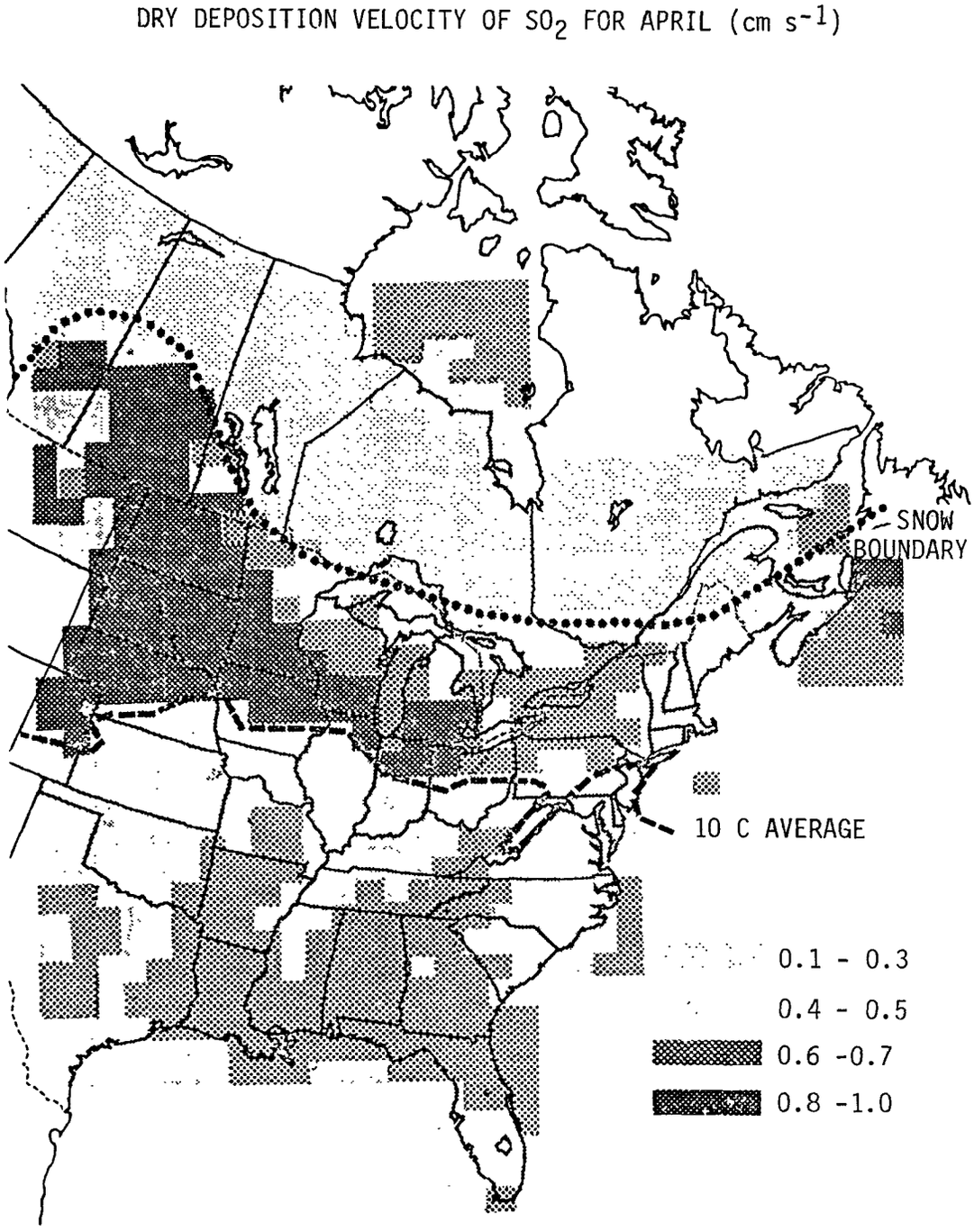

Figure 8-4. Calculated deposition velocities appropriate for sulfur dioxide over eastern North America. Adapted from Masse and Voldner (1982).

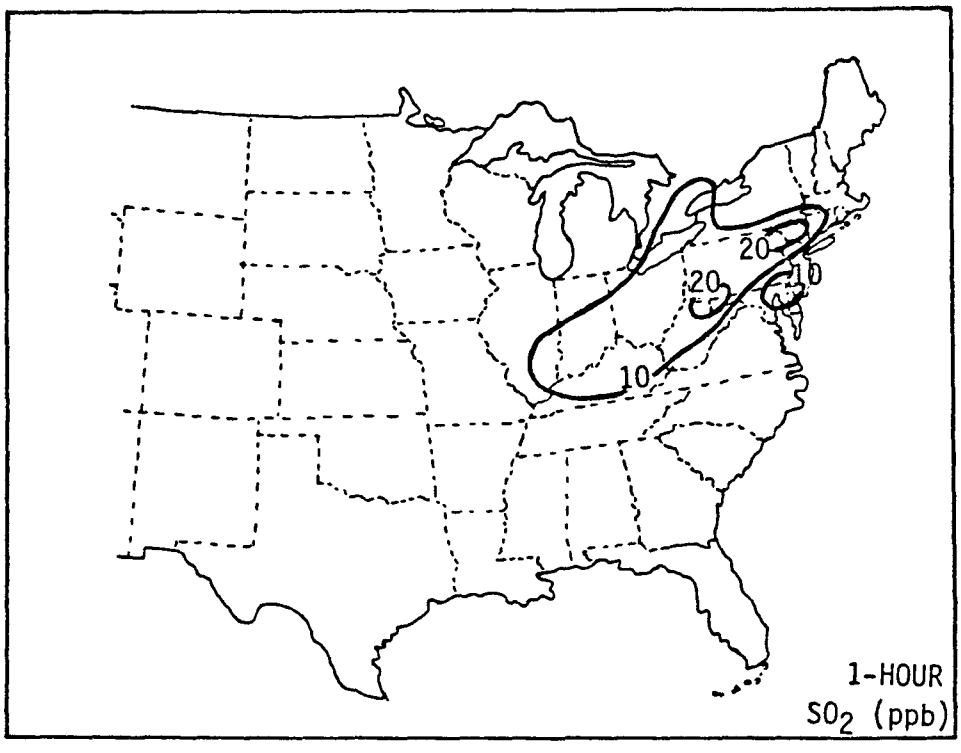

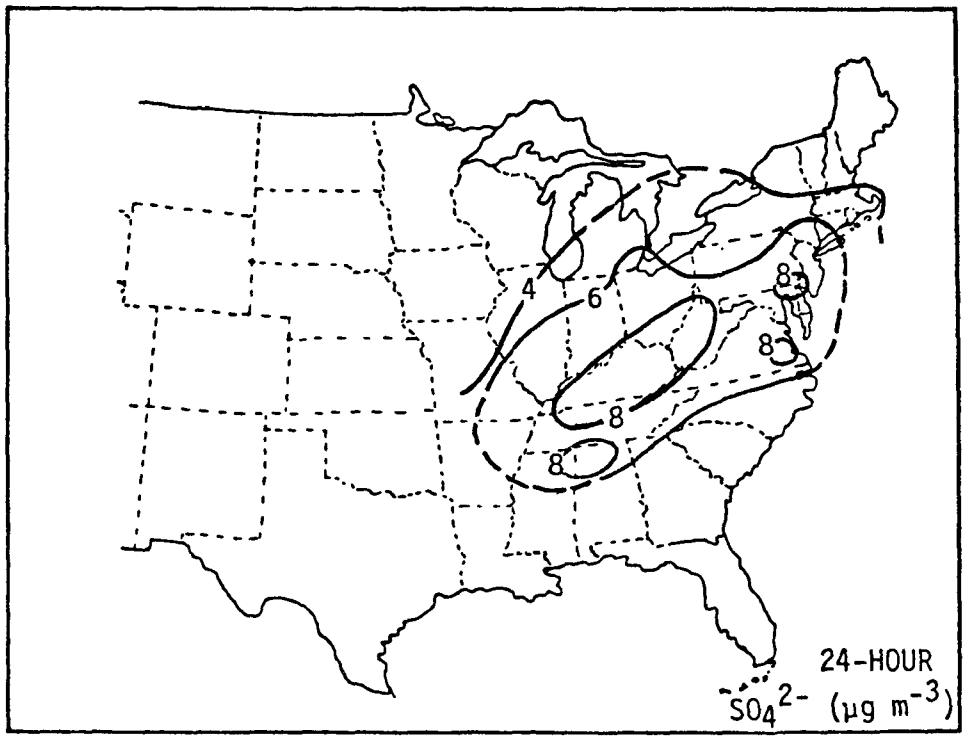

Figure 8-5. Examples of pollution concentration isopleth information of the kind suitable for applying deposition velocity maps such as in Figures 8-3 and 8-4. Shown are the arithmetic (for sulfur dioxide) and geometric (for sulfate) means of data obtained during 5 months between August 1977 and July 1978. Adapted from Hilst et al. (1981).

8.4 WET DEPOSITION NETWORK DATA WITH APPLICATIONS TO SELECTED PROBLEMS (G. J. Stensland)

8.4.1 Spatial Patterns

There is a vast amount of precipitation chemistry data available. This section will discuss the general spatial patterns for the United States and Canada. The first set of contour maps will be based on data from the National Atmospheric Deposition Program (NADP). Although data from other recent networks could have been included, this would not have altered the general patterns and could have added some additional uncertainties since, for example, sampling intervals other than weekly were used. At this time the NADP is the only network with sites throughout the United States and thus the NADP data will allow for comparisons between the West and the East, where the acidic precipitation problem is generally perceived to occur. New sites are currently being added, as part of the National Trends Network, that will increase site density in the West.

Concentration and deposition maps will be presented, with the contours drawn by hand instead of by computer. Different objective analysis and computer plotting packages do not produce identical contour maps. Likewise hand-drawn contour maps are somewhat subjective and thus, will not be identical when drawn by different analysts. Since data values will be shown on the contour maps in this section, the reader can determine if he agrees with the contour shapes. Sites with only a few samples can produce "bulls-eye" contour patterns; this effect has been minimized by using the hand-drawn contours instead of computer-produced contours. Because there are year-to-year variations in the average site concentrations of the ions it would be best in determining the general spatial patterns to include only sites with several years of data. However, at this time we do not have enough data to adopt this rule. Therefore for the hand-produced contours in this section, we did not try to precisely contour the site data values but instead did some subjective smoothing.

For some ions both the weighted-mean concentrations and the median concentrations will be included to allow for a comparison of these two measures of central tendency. For sites with a relatively small total sample number the median probably gives a better estimate of central tendency than the weighted means because in the latter, one or two samples with unusually large volumes can produce unreasonably large weighted means. No corrections for sea-salt influences have been made for the NADP data shown in this chapter.

For the combined picture of the United States and Canada, data maps adapted from the U.S./Canada Memorandum of Intent (MOI) report (U.S./Canada 1982) were used. In the MOI report only 1980 data were used, and therefore the reader has yet another type of contour map for purposes of comparison.

For many studies related to effects annual deposition values are needed. Other chapters in this document may have selected deposition values from monitoring networks which provided greater space densities in the area of concern as well as longer time records. These data can be compared to the 1980 deposition maps included in this chapter. Some maps have been included

in this chapter for specific use in effects studies, an example being the wet deposition nitrogen map which includes both nitrate and ammonium inputs of nitrogen.

The National Atmospheric Deposition Program (NADP) began in July 1978. By October 1978, 20 sites were operating, mostly in the Northeast. Figure 8-6 shows the number of weekly samples as of approximately the end of 1980 for weeks when at least 0.02 inches of liquid equivalent precipitation was collected (NADP 1978, 1979, 1980). The data were screened at the NADP Central Analytical Laboratory to remove data for samples that were obviously contaminated or collected by nonstandard procedures. The quantity of data varies from 6 weekly samples for a California site to 128 for the West Virginia site.

Figure 8-7 shows the median concentration contour pattern for sulfate. The low site density in some areas and the short data record for some sites suggest that the depicted patterns will be subject to change as more data become available. The medians displayed on the contour map are better indicators of central tendency for small data sets than are other statistical parameters. The site data values are shown on the maps to indicate the degree of subjective smoothing involved in drawing the contour lines. For example the 2.0 mg ℓ^{-1} contour line in Figure 8-7, cutting through northern Wisconsin, could have been placed further north to accommodate the 2.2 mg ℓ^{-1} value at the Isle Royale National Park site. However, from Figure 8-6 one notes that the 2.2 mg ℓ^{-1} value is the median of only eight values and thus can not be considered very reliable. The 2.0 mg ℓ^{-1} contour line passes through the north-central Wisconsin site having a median value of 1.3 mg ℓ^{-1} illustrating that a subjective decision was made to show rather smooth contour lines instead of lines bent to match each site value. On most of the maps in this section, contour lines to the left of an imaginary line from northwestern North Dakota to southeastern Texas have been dashed to indicate that in these areas the site density and length of data record are such that the contour lines probably do not well represent the true patterns.

Sulfate in precipitation has a strong seasonal pattern for sites in the Northeast (Bowersox and dePena 1980, Pack and Pack 1980, Pack 1982). Thus, several years of data will be required before a very stable annual average pattern can be expected. Figure 6-15 in Chapter A-6 shows the seasonal pattern for sulfate and also indicates the great variability among event samples for sulfate and nitrate at the Pennsyvania State MAP3S site.

Consistent with the known emission pattern for sulfur dioxide, the higher sulfate concentrations in Figure 8-7 are in the Northeast. The contour values decrease eastward across New York and New England. The limited data for Arizona show a sulfate maximum in the Southwest. Because a similar maximum is present in the calcium map (see Figure 8-11), soil dust is thought to be the major source for this maximum. Possible sample evaporation after collection or enhanced raindrop evaporation must also be considered as partial explanations for the high concentrations of all the ions in the precipitation of the Southwest. The arid site at Bishop, CA, also has an extremely large sulfate value, but only six samples are available. The

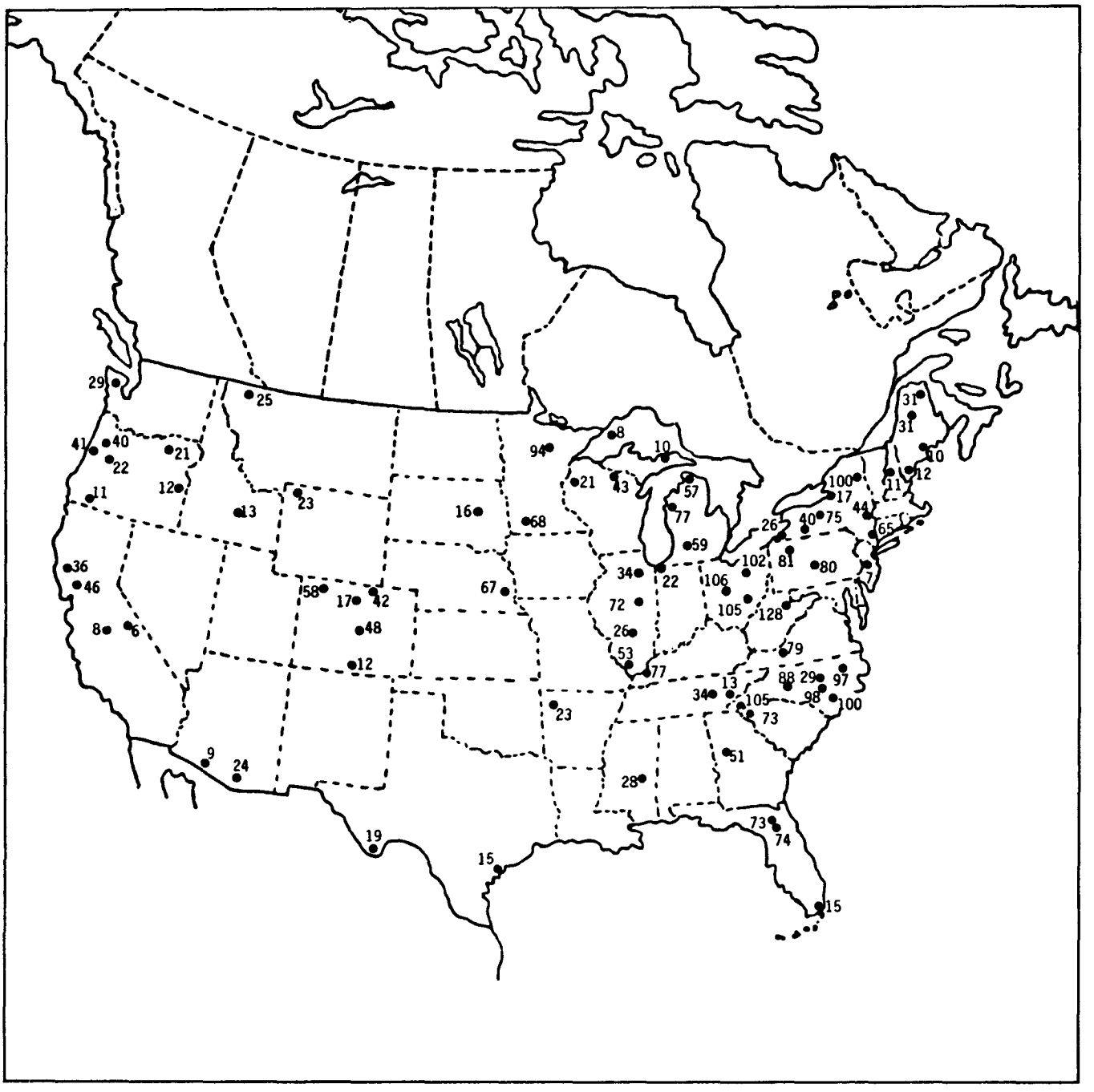

Figure 8-6. Map of National Atmospheric Deposition Program site locations and number of wet deposition samples for each site through approximately December 1980 (using data from NADP 1978, 1979, and 1980).

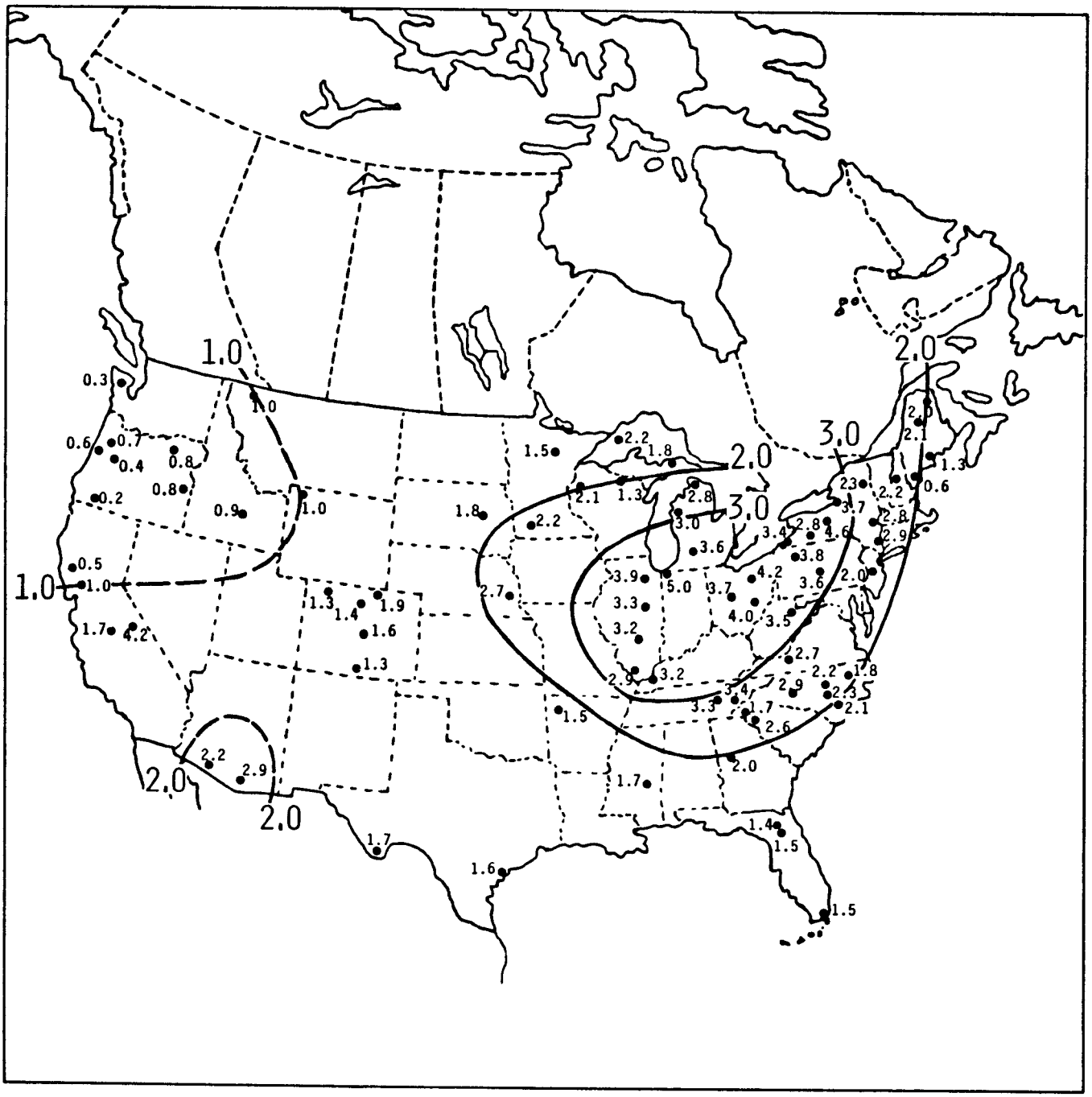

Figure 8-7. Map of median sulfate concentrations (mg ℓ^{-1} as SO_4^{2-}) for NADP wet deposition samples through approximately December 1980 (using data from NADP 1978, 1979, and 1980).

sample-volume-weighted-average sulfate values shown in Figure 8-8 are generally similar to those for the median values (but not true for Bishop, CA).

Pack (1980) found the MAP3S and EPRI-SURE precipitation chemistry data from August 1978 to June 1979 to be comparable. The precipitation-weighted-average sulfate values in an area from central Illinois to western Massachusetts were 2.9 mg ℓ^{-1} or greater. The maximum sulfate values were 3.3, 3.4, and 3.7 mg ℓ^{-1} for three sites in Ohio and Pennsylvania. The five NADP sites in Ohio and Pennsylvania have sample-volume-weighted-average concentrations of 3.3, 3.5, 3.6, 3.7, and 4.0 mg $^{-1}$ for the data record indicated in Figure 8-8. These values are very similar to those reported by Pack.

Figure 8-9 shows the nitrate pattern, which has general similarities to that for sulfate. Again the higher values in the northeastern quadrant of the United States are consistent with the known anthropogenic NO_x emission pattern. One difference is that in Figure 8-9 the values in South Dakota and Nebraska are about the same as those in Ohio but this is not true for sulfate in Figure 8-7. The rather high nitrate values at the upper plains sites do not seem to be consistent with known anthropogenic combustion NO_x sources. The nitrate maximum in east central California is questionable because of the small number of samples (see Figure 8-6). Recent research has indicated that most of the available air quality data for nitrate in the Northeast are of limited value because of sampling problems (Spicer and Schumacher 1977); therefore, the precipitation nitrate data patterns become increasingly important.

Figure 8-10 shows the contour pattern for the ammonium ion. The general pattern has some similarities to that for nitrate in Figure 8-9. As for nitrate, the values for the northwest Indiana site are elevated, probably indicating the effect of the upwind industrial areas. There is a definite maximum in the upper plains, probably due to ammonia emissions from livestock production. In particular, there are several large cattle feedlots in the vicinity of the Nebraska site. The site just east of Lake Ontario had elevated values for both ammonium and nitrate but only 17 samples were available (see Figure 8-6). The ammonium values are lowest in the Northwest; the median values of 0.02 are analytical detection limit values.

Figure 8-11 shows the calcium concentration pattern, the values for which are very high in the Southwest and relatively high in the upper Plains. Dust from soils and unpaved roads probably accounts for the generally elevated calcium levels in the central United States. Urban and industrial sources may account for the relatively high values at the site in Indiana. The central Illinois site with a median value of 0.28 mg ℓ^{-1} is an example of a site surrounded by an area of intensive cultivation, with corn and soybeans being the major crops in the area. The median calcium concentration there is surprisingly low, considering the surroundings, and indicates that the sampler is quite successful in preventing dust leakage into the collection vessel.

Figure 8-12 shows the chloride concentration pattern. Sites closer to the major chloride source, the sea, have higher levels.

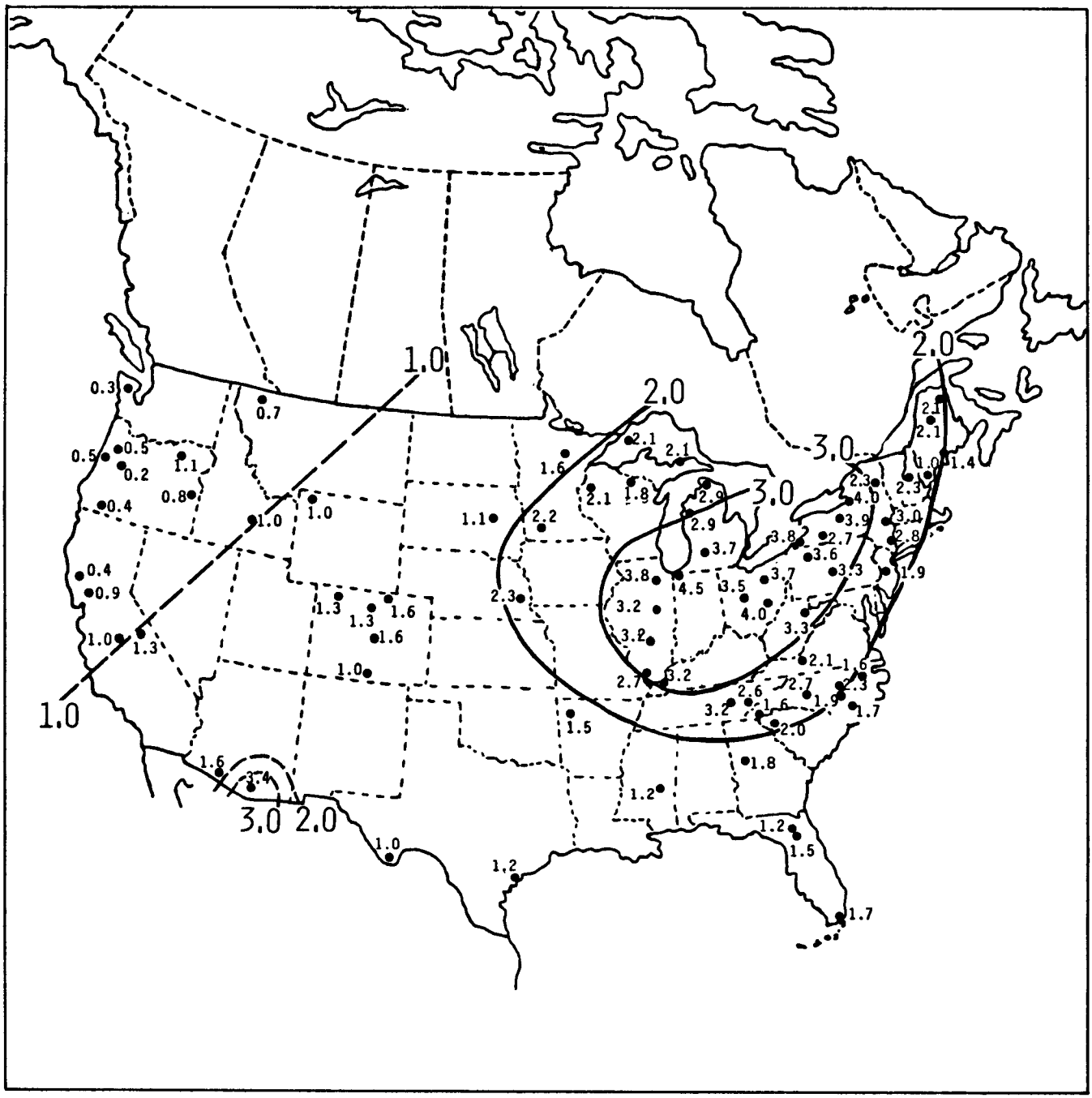

Figure 8-8. Map of volume-weighted-average-sulfate concentrations (mg ℓ^{-1} as SO_4^{2-}) for NADP wet deposition samples through approximately December 1980 (using data from NADP 1978, 1979, and 1980).

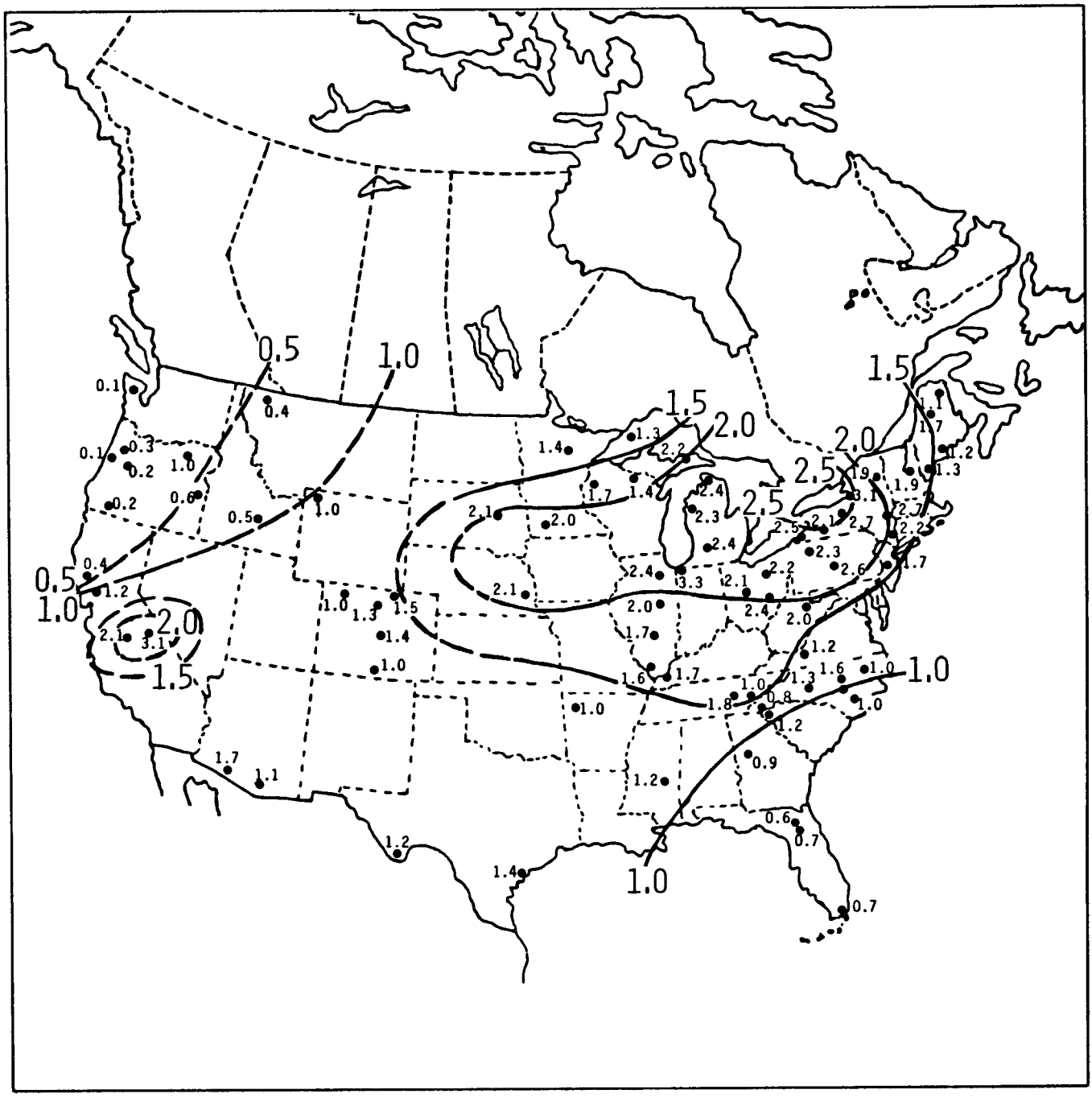

Figure 8-9. Map of median nitrate concentrations (mg ℓ^{-1} as NO_3^-) for NADP wet deposition samples through approximately December 1980 (using data from NADP 1978, 1979, and 1980).

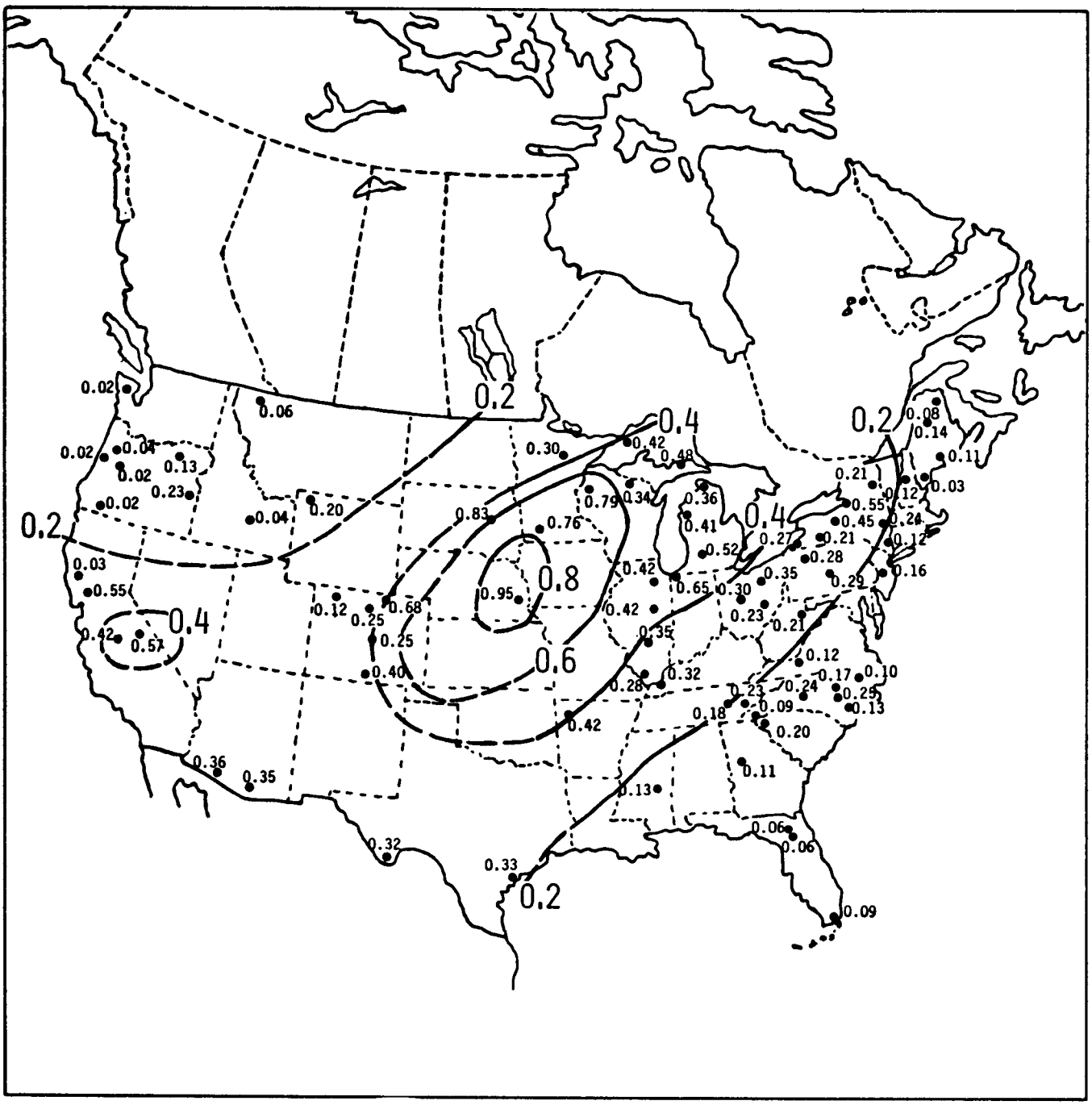

Figure 8-10. Map of median ammonium ion concentrations (mg ℓ^{-1} as NH_4^+) for NADP wet deposition samples through approximately December 1980 (using data from NADP 1978, 1979, and 1980).

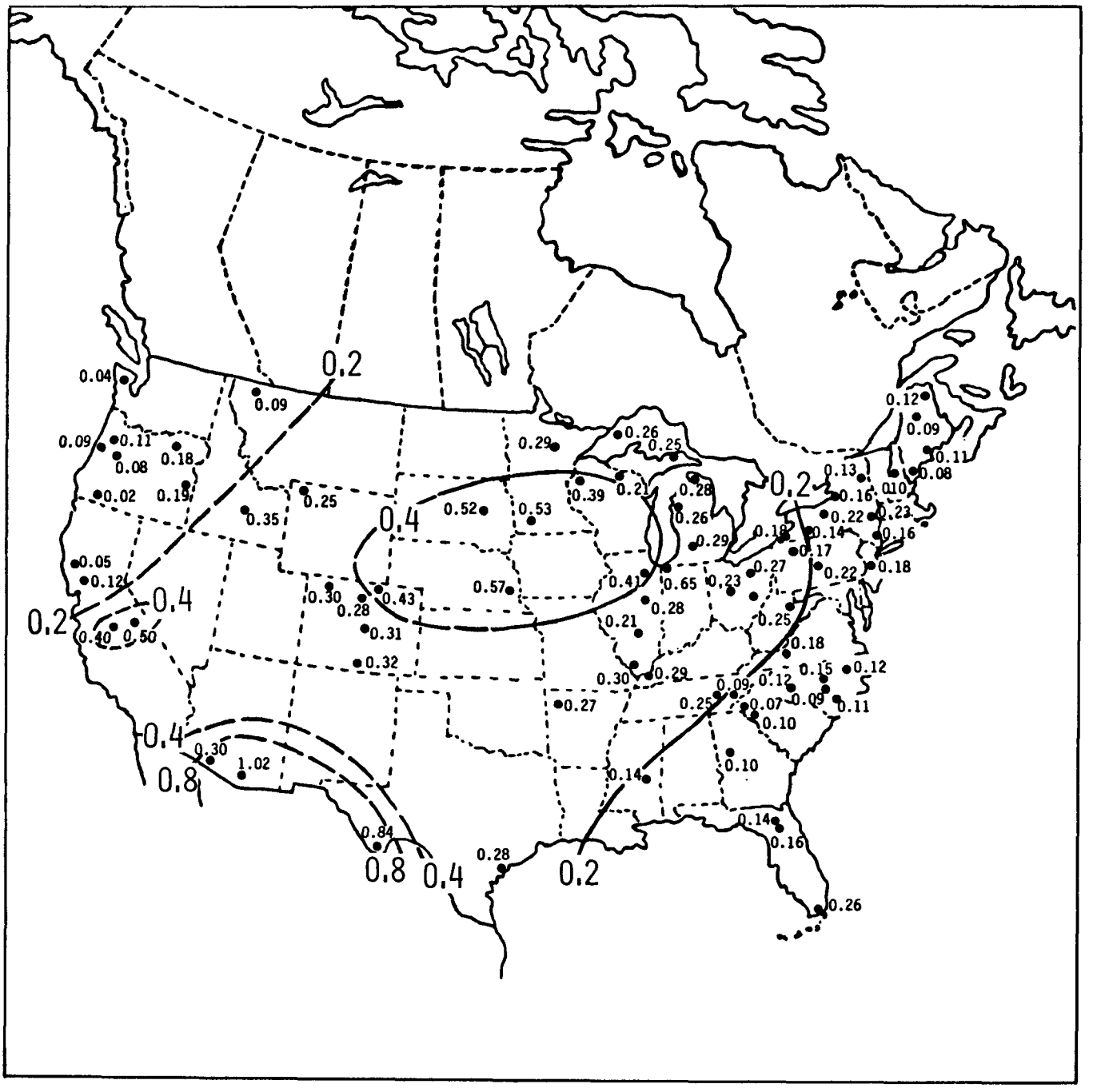

Figure 8-11. Map of median calcium concentrations (mg ℓ^{-1}) for NADP wet deposition samples through approximately December 1980 (using data from NADP 1978, 1979, and 1980).

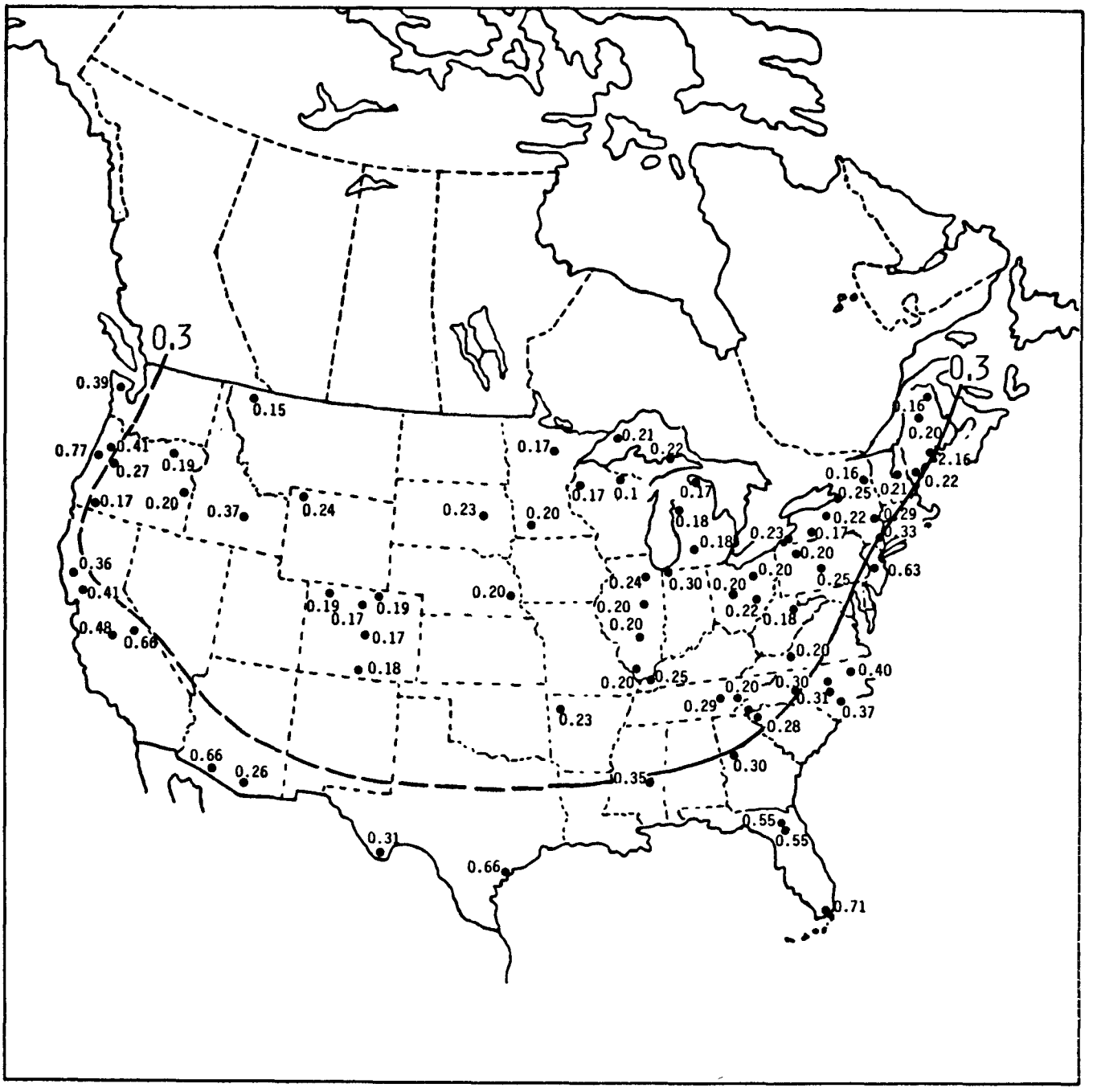

Figure 8-12. Map of median chloride concentrations (mg ℓ^{-1}) for NADP wet deposition samples through approximately December 1980 (using data from NADP 1978, 1979, and 1980).

In addition to the ions displayed in Figures 8-7 through 8-12, magnesium, potassium, and sodium are measured in NADP and most other networks. The data in Table 8-7 demonstrate the relative importance of all the ions at three NADP sites. The concentrations in Table 8-7 are expressed in microequivalents per liter in order to allow a direct evaluation of the contribution of each ion to the anion or cation sum. If all ions were being measured and if there were no analytical uncertainty, then the anion sum would equal the cation sum. In Table 8-7, the values for hydrogen ion concentration, H^+, were calculated from the measured median pH value, and the values for bicarbonate, HCO_3^-, were calculated by assuming that the sample was in equilibrium with atmospheric carbon dioxide. Although the sulfate and nitrate levels shown are similar at the MN and NY sites, the pH differs greatly due to the much higher levels of the ammonium, calcium, magnesium, sodium, and potassium ions at the Minnesota site. These ions are frequently associated with basic compounds. The data in Table 8-7 suggest that the concentrations of all the major ions must be considered if the time and space patterns of pH are to be fully understood. Currently sites in Ohio, New York, Pennsylvania, and West Virginia have the feature shown for the New York site in Table 8-7 where H^+, SO_4^{2-}, and NO_3^- are the dominant ions. For the New York site, the acidity (H^+) could be 98 percent accounted for if all the SO_4^{2-} had been sulfuric acid while nitrate, as nitric acid, could have accounted for about 55 percent of the acidity. By applying multiple linear regression analysis, Bowersox and dePena (1980) have concluded for a central Pennsylvania site that on the average the principal contributor to (H^+) is sulfuric acid, but the acidity in snow is determined principally by nitric acid.

Figure 8-13 shows the median pH from the NADP data. Except in Minnesota, western Wisconsin, and southern Florida, the region east of the Mississippi River has median pH values less than 5.0, while the Northeast has values less than 4.7. The pH data are frequently reported as the pH calculated from the sample-volume-weighted hydrogen ion concentration, which will be referred to as the weighted pH values in this chapter. When weighted pH values are considered, the Northeast still has average pH values less than 4.7. However, the weighted pH values at the Nebraska and southwestern Minnesota sites are 4.95 and 5.14, respectively, compared to median values of 5.95 and 6.19. Therefore, the averaging procedure needs to be specified in detailed analyses and comparisons of pH patterns.

Figures 8-14 through 8-23 show data consolidated for the single year 1980 from NADP, MAP3S, and CANSAP, as well as the APN and Ontario Ministry of the Environment (OME) networks (Barrie and Sirois 1982, Barrie et al. 1982). Site data were included in the analysis if the site had been in operation for at least two-thirds of the year. For the CANSAP and MAP3S sites, precipitation-weighted-average concentrations were calculated and used in the figures. For NADP sites, sample volume-weighted-average concentrations were used. Deposition values were calculated by multiplying the concentrations by the 1980 precipitation amounts. Contour lines of ion concentrations and depositions were drawn by hand. The structure in the concentration contours indicates that all site values were assumed to be equally valid or representative. The authors elected to not draw contour lines in the western United States due to the small number of sites. The contour lines for deposition

TABLE 8-7. MEDIAN ION CONCENTRATIONS FOR 1979 FOR THREE NADP SITES (μ eq ℓ^{-1})

	GA[a]	MN[b]	NY[c]
No. Samples	42	37	49
SO_4^{2-}	38.9	45.8	44.8
NO_3^-	.6	24.2	25.0
Cl^-	8.2	4.2	4.2
HCO_3^- (calculated)	0.3	10.3	0.1
Anions	59.0	84.5	74.1
NH_4^+	5.5	37.7	8.3
Ca^{2+}	5.0	28.9	6.5
Mg^{2+}	2.4	6.1	1.9
K^+	0.7	2.0	0.4
Na^+	17.6	13.7	4.9
H^+	17.8	0.5	45.7
Cations	49.3	88.9	67.7
Median pH	4.75	6.31	4.34

[a]The Georgia Station site in west central Georgia.

[b]The Lamberton site in southwest Minnesota.

[c]The Huntington Wildlife site in northeastern New York.

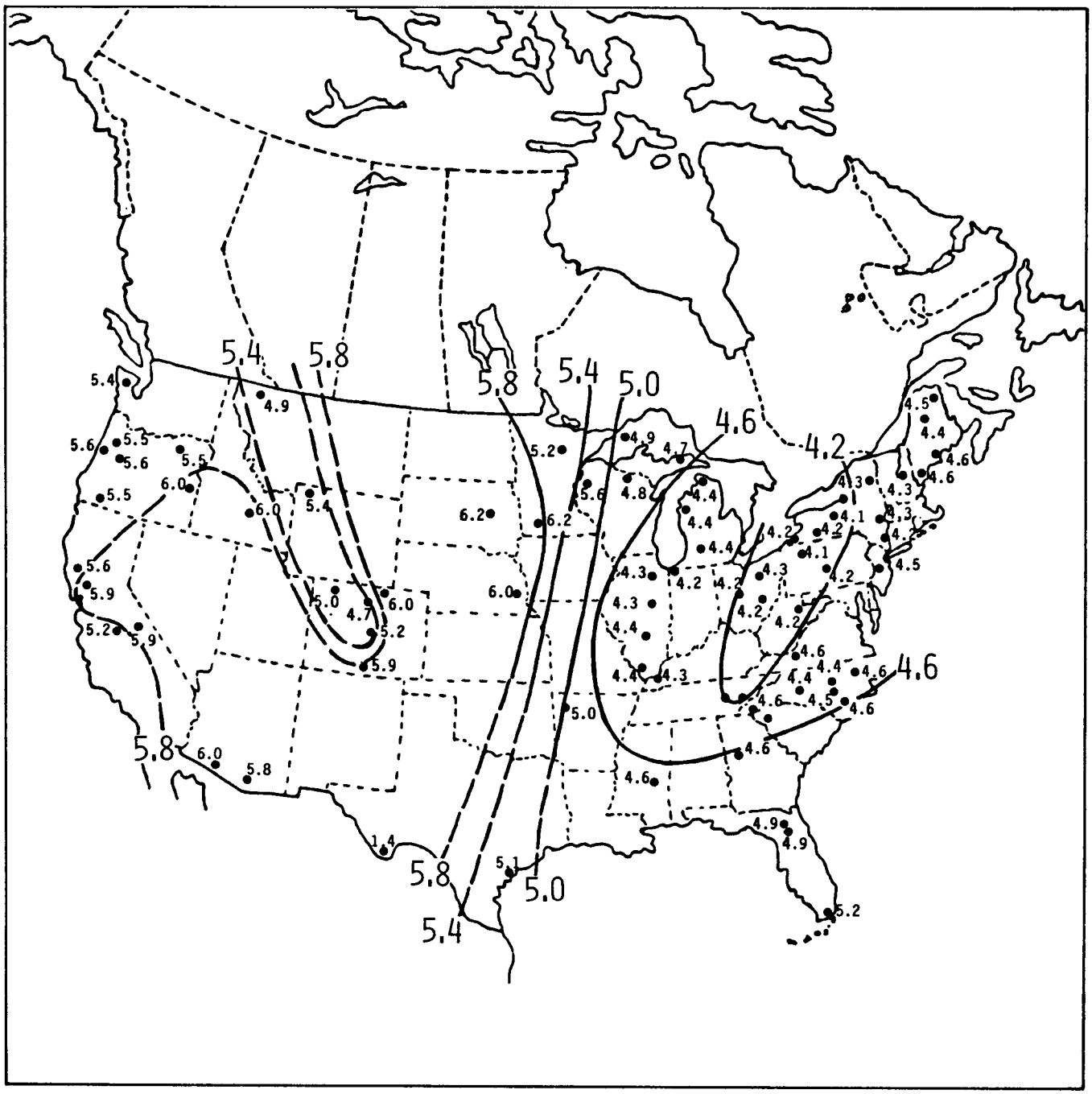

Figure 8-13. Map of median pH for NADP wet deposition samples through approximately December 1980 (using data from NADP 1978, 1979, and 1980).

have more structure than appears justified. This resulted from using the concentration field to calculate deposition values at the 250 Class I Canadian weather service sites and on a 100 km x 100 km grid in the United States. Thus, the greater density of weather sites that measure precipitation amounts resulted in more structure in the deposition contours than if the precipitation amounts at the smaller number of chemistry sites had been used. The maps by Barrie et al. (1982) were presented with the units of millimoles per liter and millimoles per square meter. For this chapter, sites values were converted to the units shown in Figures 8-14 through 8-23; the published contour lines are used, but they have been redrawn.

Figure 8-14 shows data for sulfate. The Canadian sulfate data were corrected for sea salt but the U.S. data were not. Corrections for sulfate are generally negligible (< 5 percent) except at locations within 5 km of open ocean areas (Barrie et al. 1982). The general pattern for sulfate in the Northeast is similar in Figures 8-8 and 8-14. However, by carefully comparing the location of the 1.9 and 2.9 mg ℓ^{-1} contours in Figure 8-14 with the 2.0 and 3.0 mg ℓ^{-1} contours in Figure 8-8, we note that spatial differences of more than 200 kilometers are sometimes evident. In central Illinois and western New York the NADP and MAP3S sulfate values differ by more than 25 percent. For western New York, the NADP and MAP3S sampling locations are about 25 miles apart. In the MAP3S program, very small precipitation samples, which generally have high ion concentrations, are not analyzed. The actual reasons for the rather large differences in 1980 sulfate ion concentrations at these two locations are not known and would require a detailed study.

Figure 8-15 shows the 1980 nitrate concentration pattern. The high nitrate values in the western plains of Canada are attributed to wind-blown dust. In the east the highest values are in southern Ontario. The notch in the 1.9 mg ℓ^{-1} contour in Pennsylvania and New York might be rather important if it is real. Such features should be useful in relating emission patterns to acid precipitation patterns. However, at this time, the fine structure in the sulfate and nitrate patterns is unreliable. The uncertainty in the location of the contour lines for different areas, averaging times, averaging procedures, site densities, and networks has not been determined. The correlative evidence for a general link between known emission sources and the composition of precipitation is, however, convincing. When quality data are available for a sufficiently long period of time and the uncertainties in the placement of the contour lines are established, it may then be possible to use such patterns to answer more specific questions such as transport distances and scavenging mechanisms.

Figure 8-16 displays the 1980 ammonium pattern. The very high concentrations observed in Figure 8-10 are not found in Canada.

Figures 8-17 and 8-18 show the weighted pH and hydrogen ion concentrations. The lowest pH values are found in Ohio, Pennsylvania, New York, West Virginia, and southern Ontario. The 5.0 contour line through the central United States is peculiar to the weighted-averaging procedure as was discussed in relation to Figure 8-13. The area in the United States enclosed by

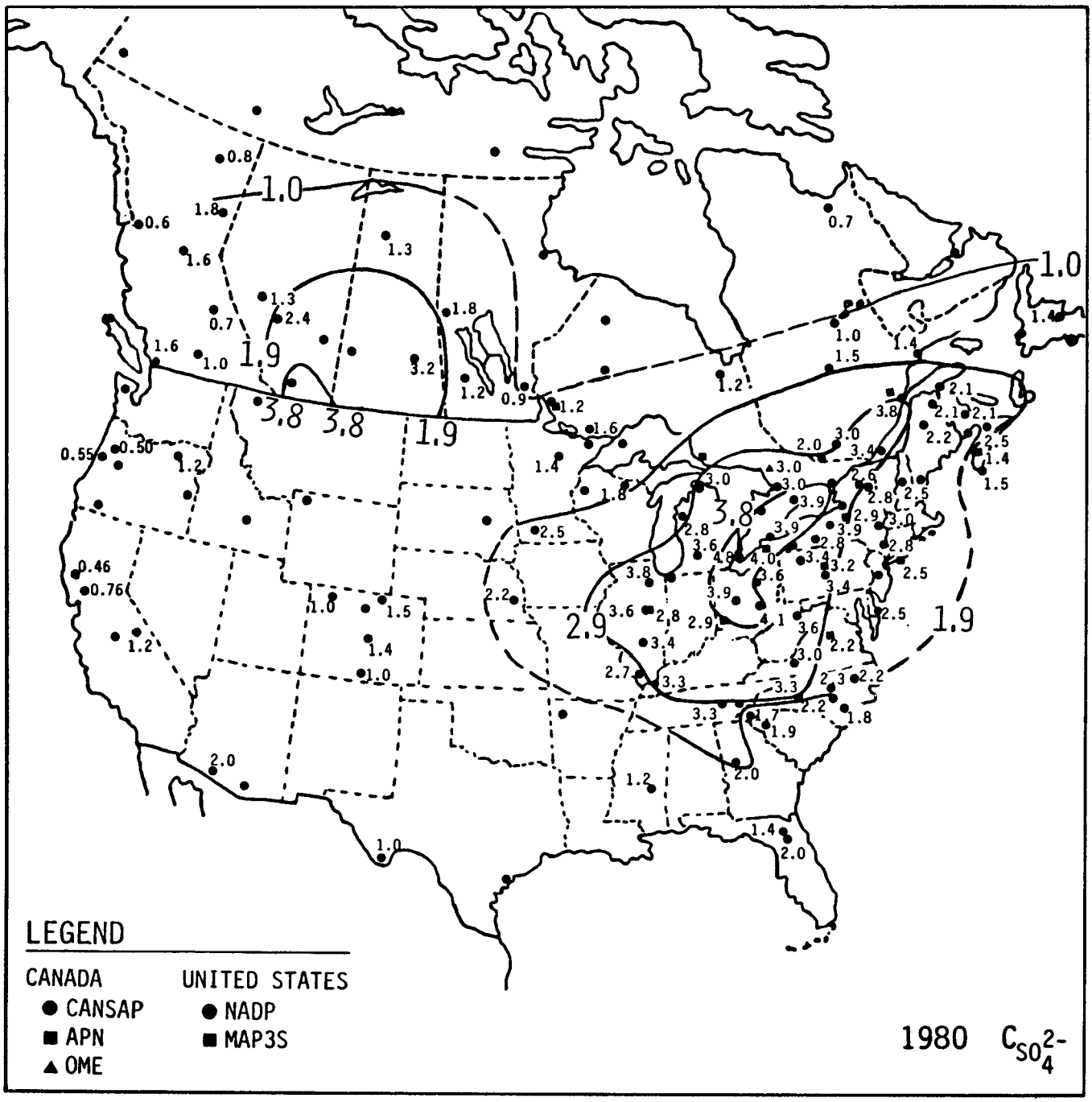

Figure 8-14. Weighted-average-sulfate ion concentrations for 1980, for wet deposition samples (mg ℓ^{-1}). Adapted from Barrie et al. (1982).

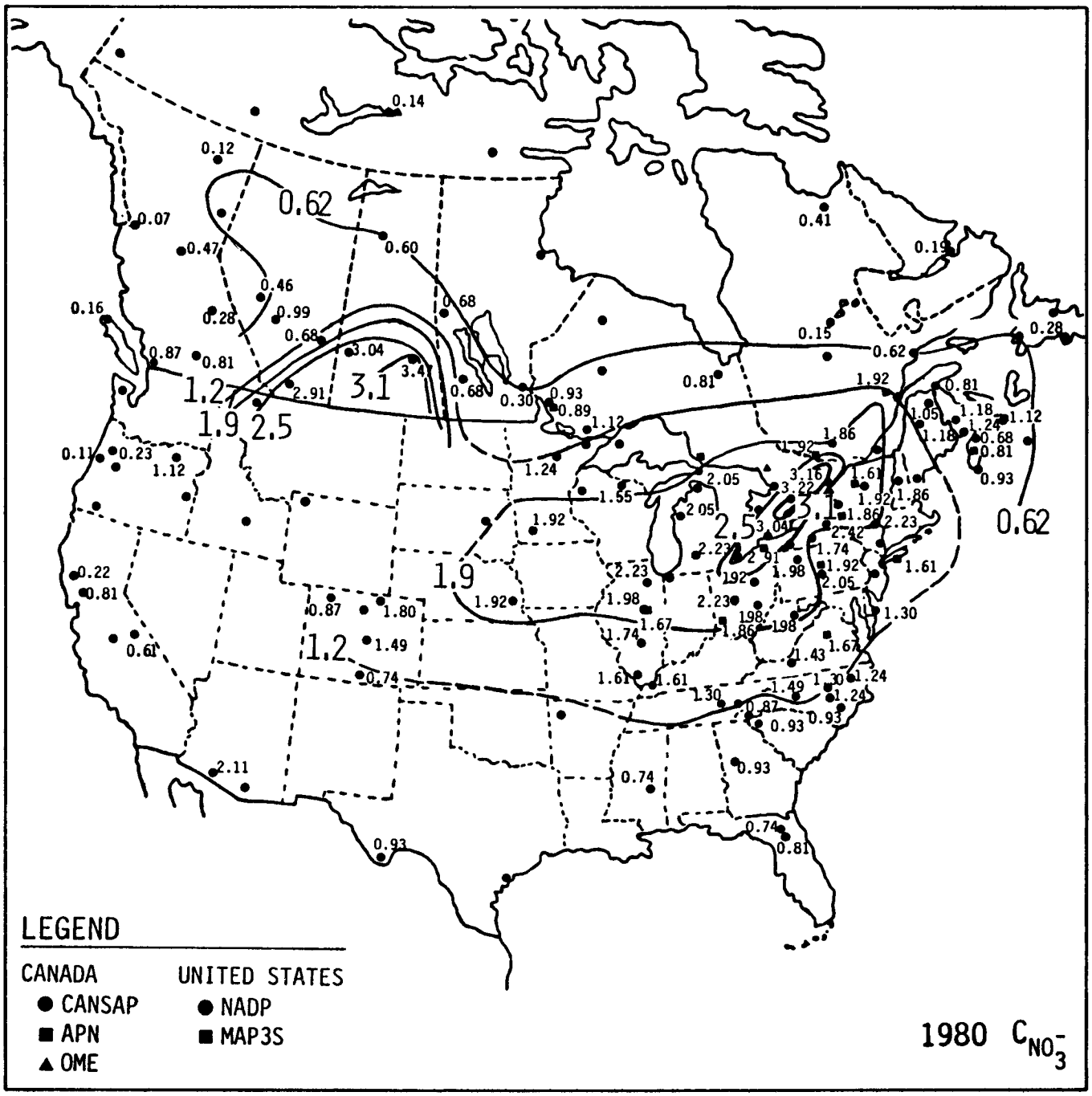

Figure 8-15. Weighted-average-nitrate ion concentrations for 1980, for wet deposition samples (mg ℓ^{-1}). Adapted from Barrie et al. (1982).

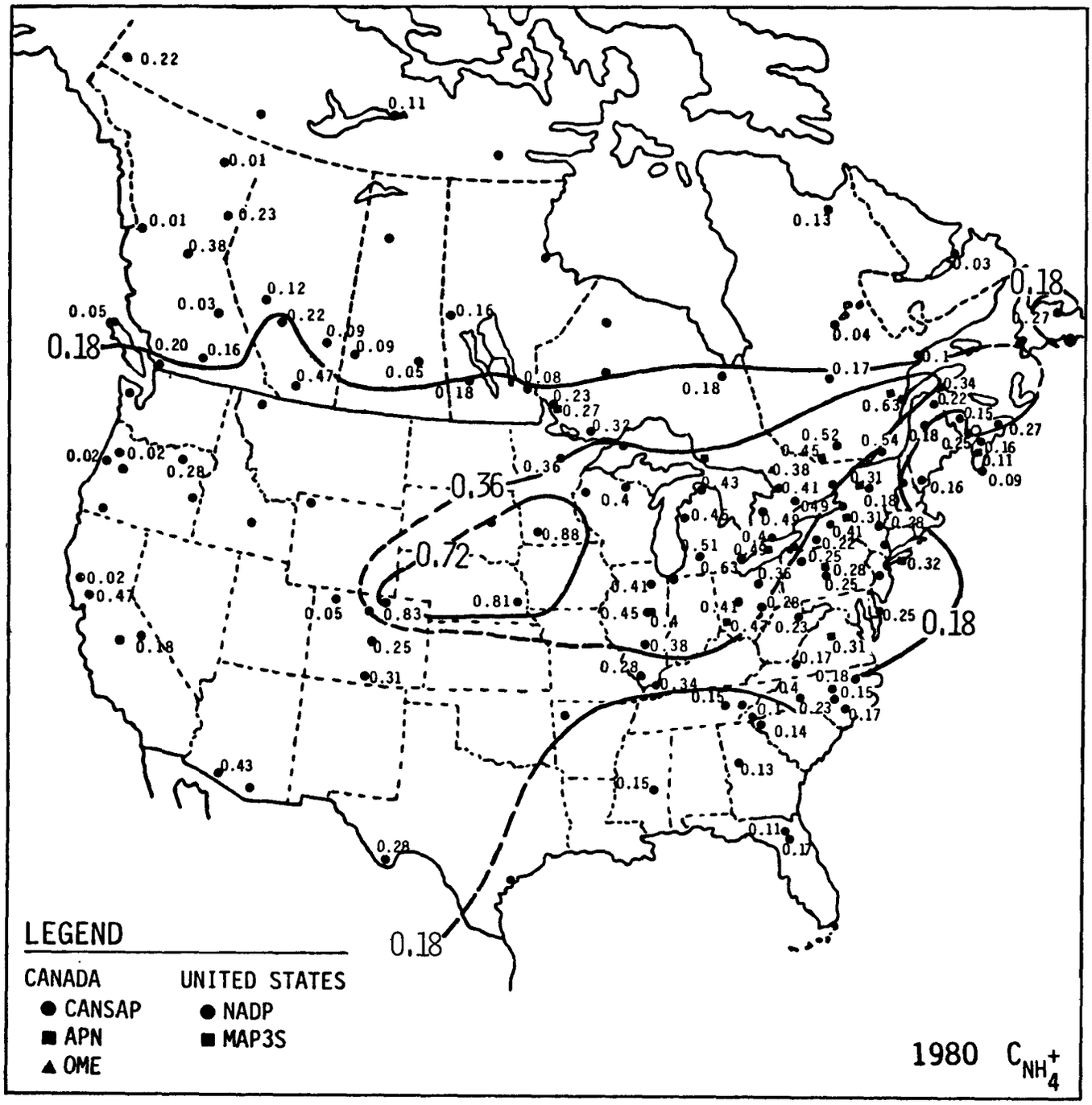

Figure 8-16. Weighted-average-ammonium ion concentrations for 1980, for wet deposition samples (mg ℓ^{-1}). Adapted from Barrie et al. (1982).

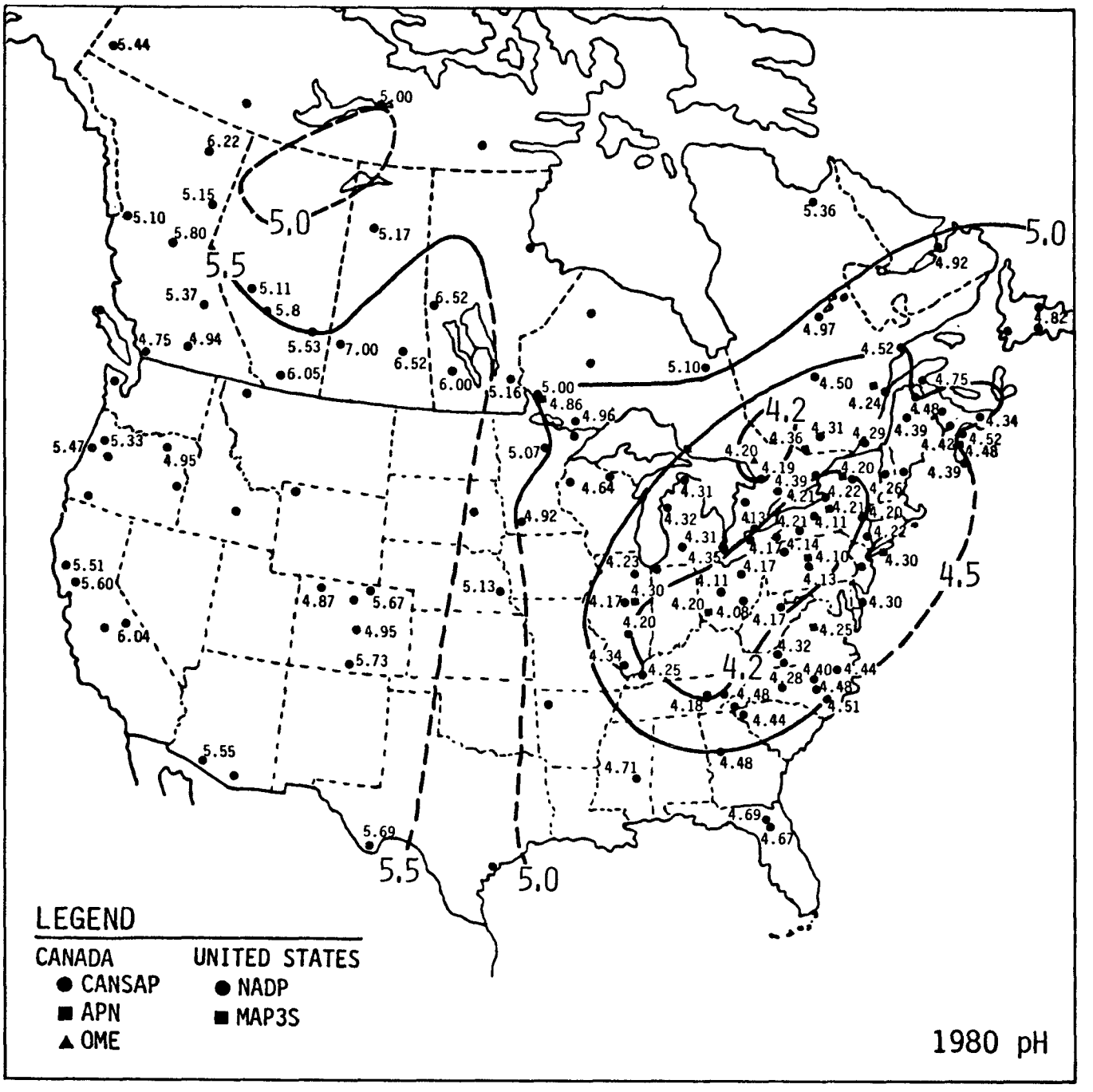

Figure 8-17. pH from weighted-average-hydrogen ion concentration for 1980, for wet deposition samples. Adapted from Barrie et al. (1982).

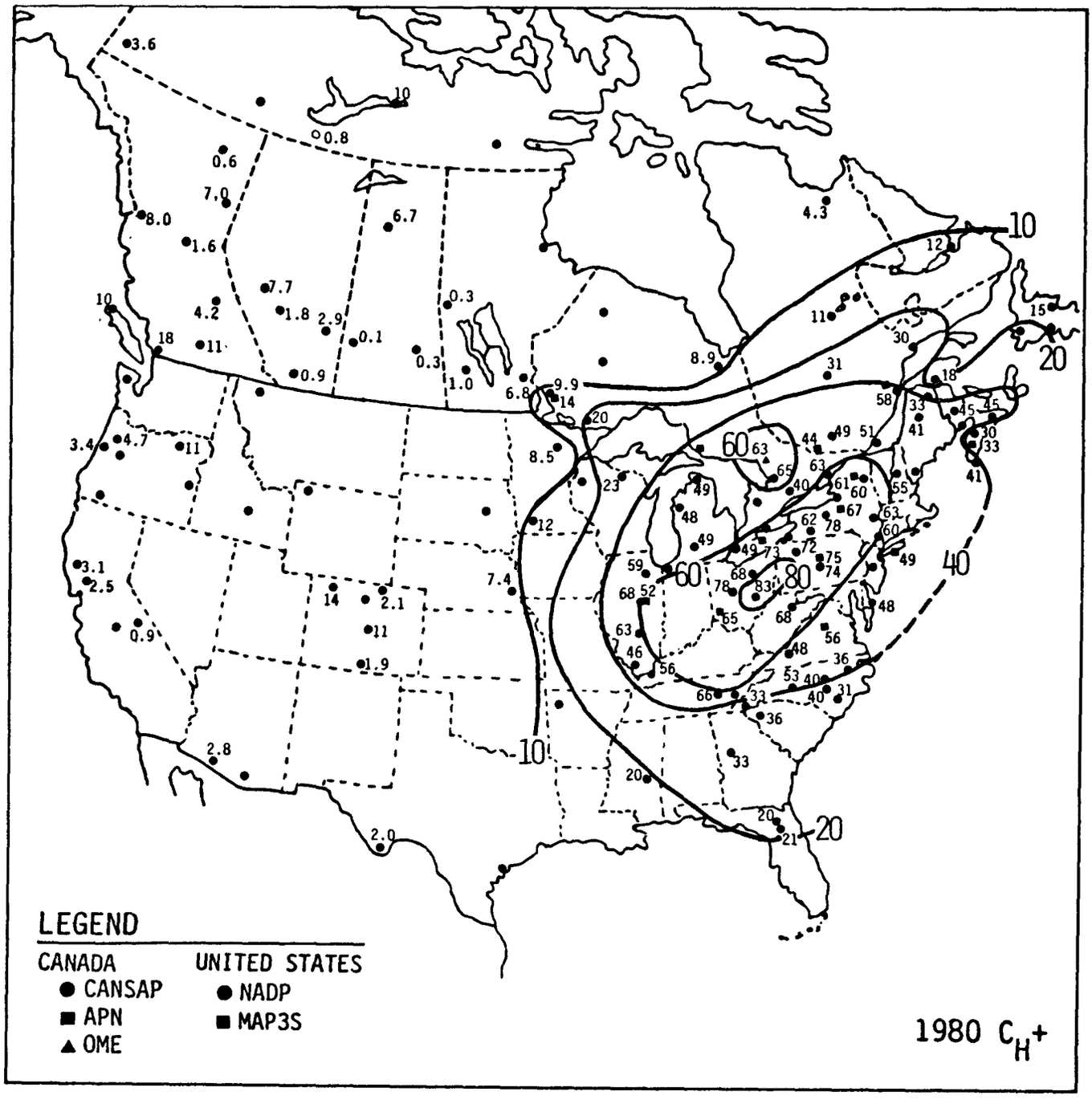

Figure 8-18. Weighted-average-hydrogen ion concentrations for 1980, for wet deposition samples ($\mu eq\ \ell^{-1}$). Adapted from Barrie et al. (1982).

the 4.2 contour line is substantially larger in Figure 8-17 as compared to Figure 8-13. The larger area of intense acidity in Figure 8-17 is due to the pH values of 4.17 and 4.20 in Illinois. The pH values in Ohio in Figure 8-17 are lower than those in Figure 8-13. The data in Table 8-8 provide a comparison between 1979 and 1980 and between median and weighted pH values. The weighted pH values for sites in Table 8-8 are on the average about 0.07 units lower than the median values. On the average, the 1980 median pH values are 0.07 unit lower than the 1979 values; the 1980 weighted pH values are 0.10 unit lower. So both the year-to-year variation and the choice of weighted pH instead of median pH contribute to the apparent larger and more intense area of acidity in the United States in 1980 compared to 1979. It is useful to remember that a decrease of 0.10 pH unit corresponds to a 26 percent increase in acidity (free hydrogen ion concentration).

Figures 8-19 to 8-23 depict wet deposition for 1980. The wet deposition patterns are probably more variable from year-to-year than concentration patterns because of the added variability of annual precipitation patterns.

The variability in concentration between weekly precipitation chemistry samples for eight sites distributed across the United States is shown in Table 8-9. The negative values in the table represent analytical detection limit concentrations. The 90 percentile values for each site divided by the corresponding 10 percentile values have the following mean and standard deviation values:

Na^+:	27.8 ± 8.5	Cl^-:	7.3 ± 3.0
NH_4^+:	24.8 ± 14.3	NO_3^-:	7.1 ± 1.9
K^+:	18.2 ± 12.3	SO_4^{2-}:	6.4 ± 2.0
Ca^{2+}:	11.9 ± 4.6	conductance:	4.6 ± 1.0
Mg^{2+}:	11.5 ± 3.4	pH:	$1.28 \pm .09$

For H^+, the inverse ratio values (i.e., 10 percentile divided by 90 percentile) are 24.6 ± 16.1. The detection limit values were used in the calculations so the resulting ratio values are lower limits (applies mainly to NH_4^+). In summary, then, the cations are more variable than the anions or conductance.

8.4.2 Remote Site pH Data

Galloway et al. (1982) have reported precipitation chemistry data for the five remote sites listed in Table 8-10. The average pH values listed in Table 8-10 vary from 4.78 to 4.96, far below the often used reference value of 5.6. The samples were collected within 24 hours after a storm had ended. At sites where bulk deposition was sampled, the collectors were installed for a maximum of 24 hours before an event began in order to minimize dry deposition amounts. Galloway et al. noted that previous research at the San Carlos location had indicated that the precipitation was acidic (Clark et al. 1980, Herrera 1979, Jordan et al. 1980). However, since samples analyzed for

TABLE 8-8. NUMBER OF WEEKLY SAMPLES (N) AND AVERAGE pH VALUES FOR 1979 AND 1980

	1979			1980		
	N	Median pH	Weighted pH	N	Median pH	Weighted pH
Bondville, IL	32	4.34	4.35	38	4.29	4.17
Salem, IL	-	-	-	23	4.33	4.20
Delaware, OH	49	4.34	4.25	45	4.15	4.11
Caldwell, OH	44	4.22	4.15	44	4.15	4.08
Wooster, OH	45	4.29	4.25	44	4.21	4.17

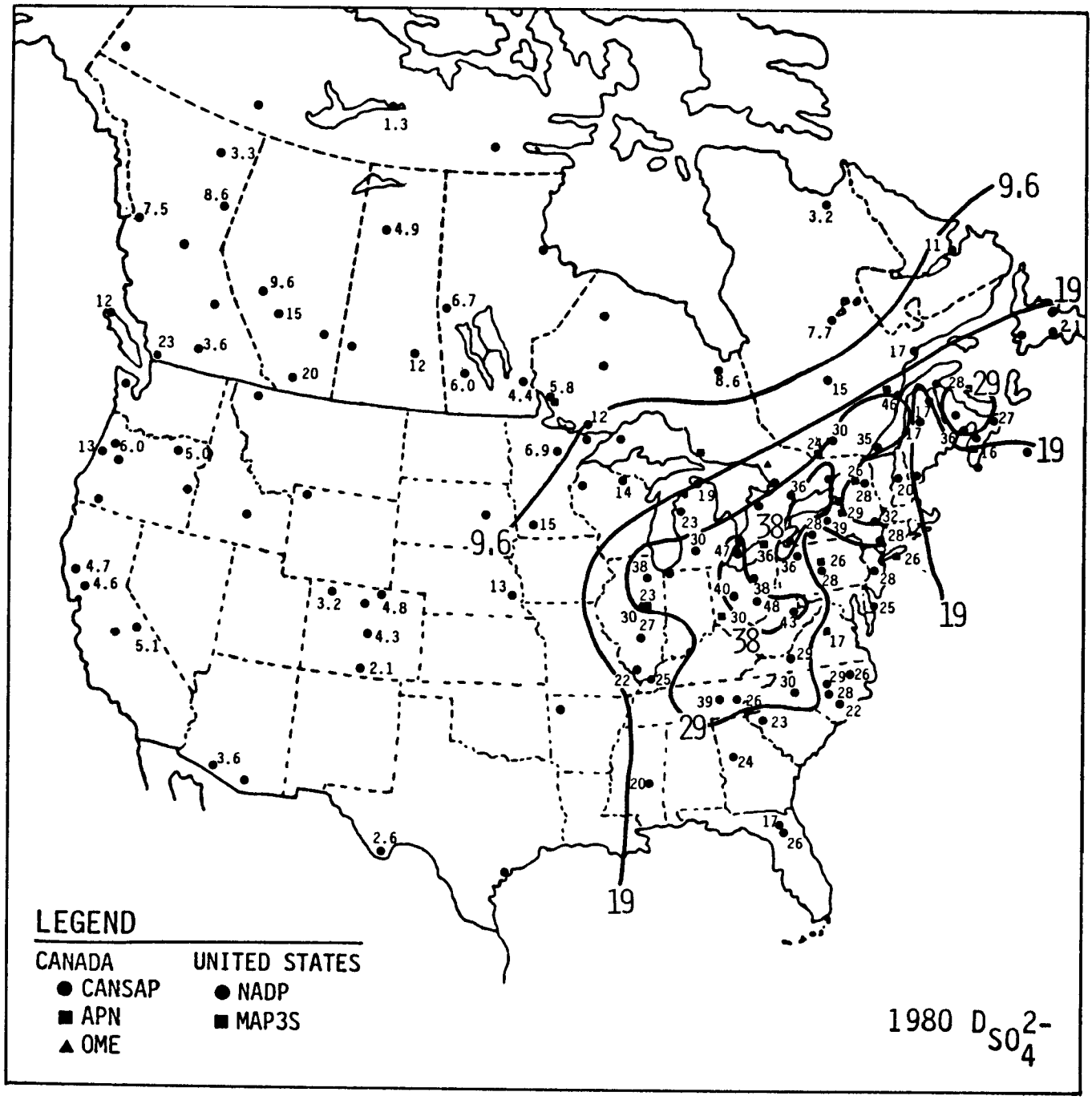

Figure 8-19. Sulfate ion deposition for 1980 for wet deposition samples (kg ha^{-1}). Adapted from Barrie et al. (1982).

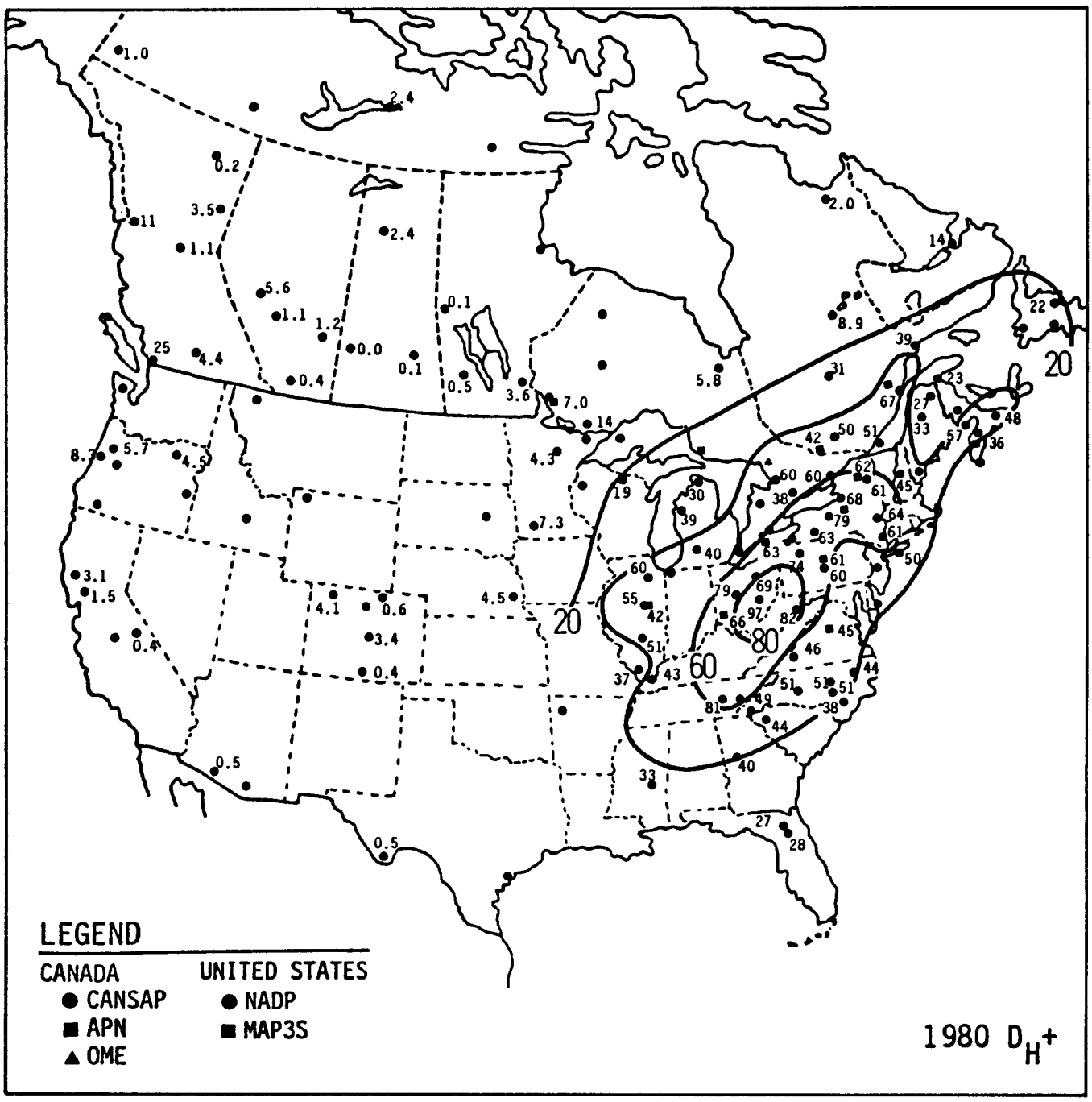

Figure 8-20. Hydrogen ion deposition for 1980 for wet deposition samples (meq m^{-2}). Adapted from Barrie et al. (1982).

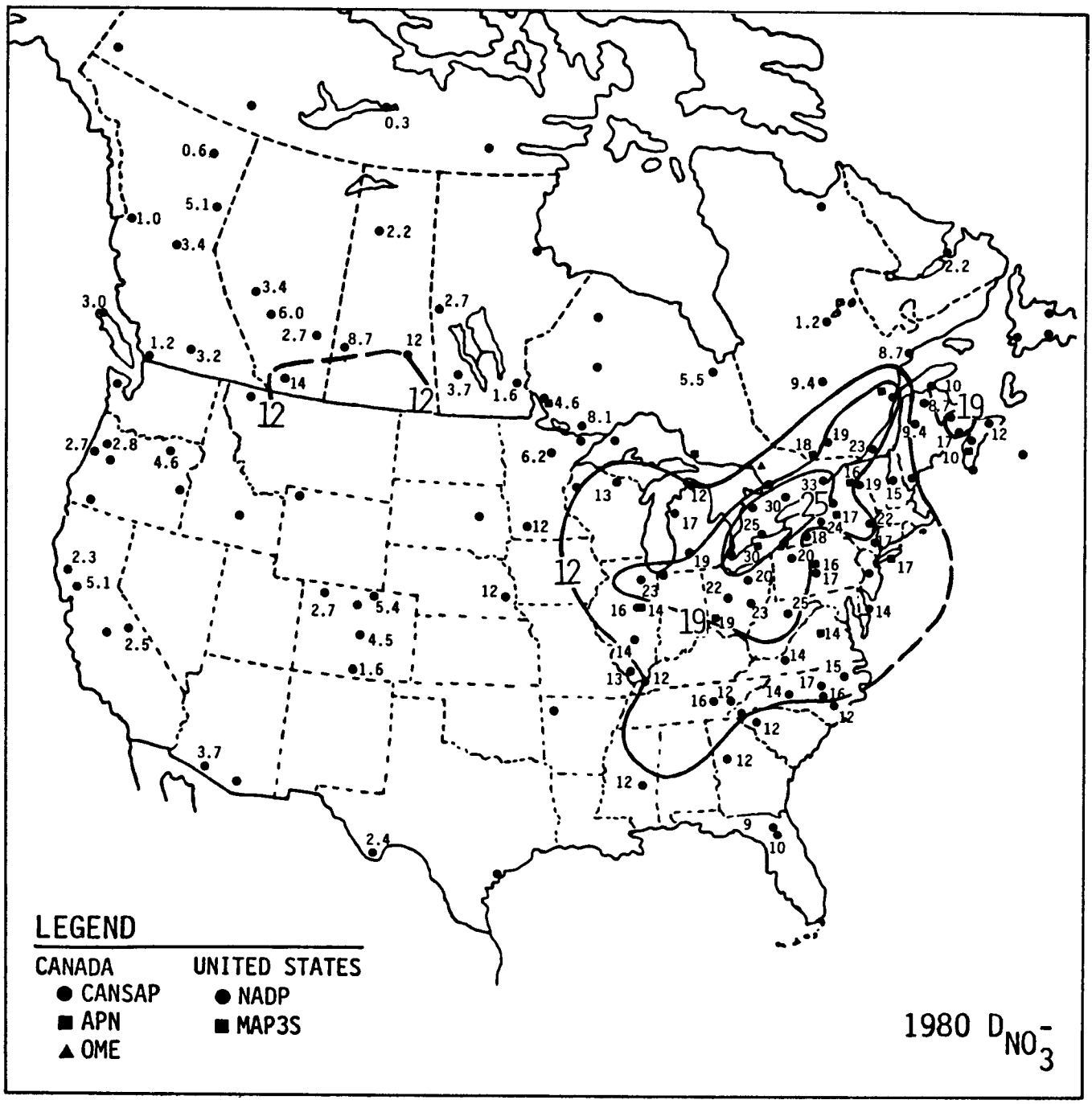

Figure 8-21. Nitrate ion deposition for 1980 for wet deposition samples (kg ha^{-1}). Adapted from Barrie et al. (1982).

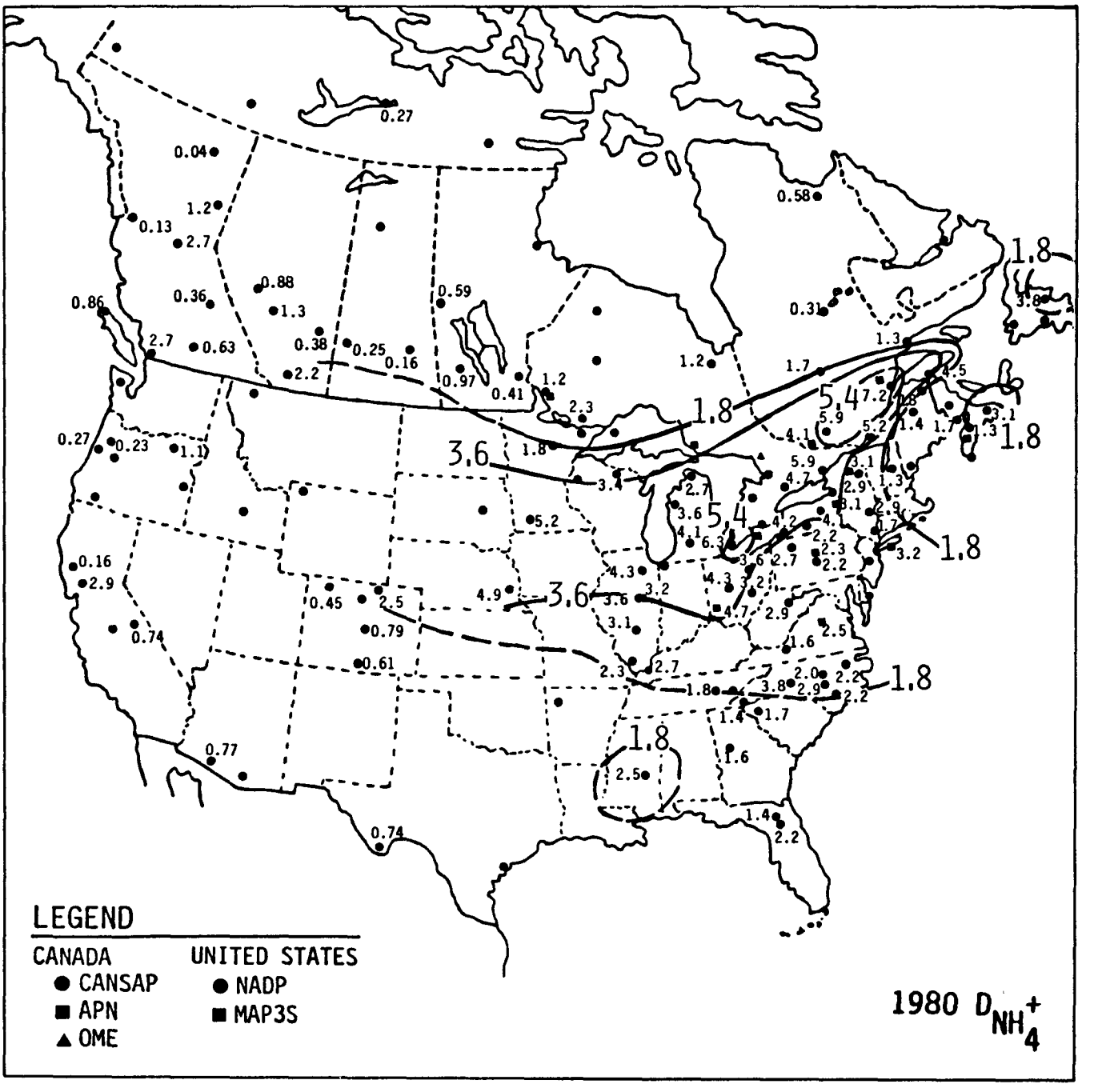

Figure 8-22. Ammonium ion deposition for 1980 for wet deposition samples (kg ha^{-1}). Adapted from Barrie et al. (1982).

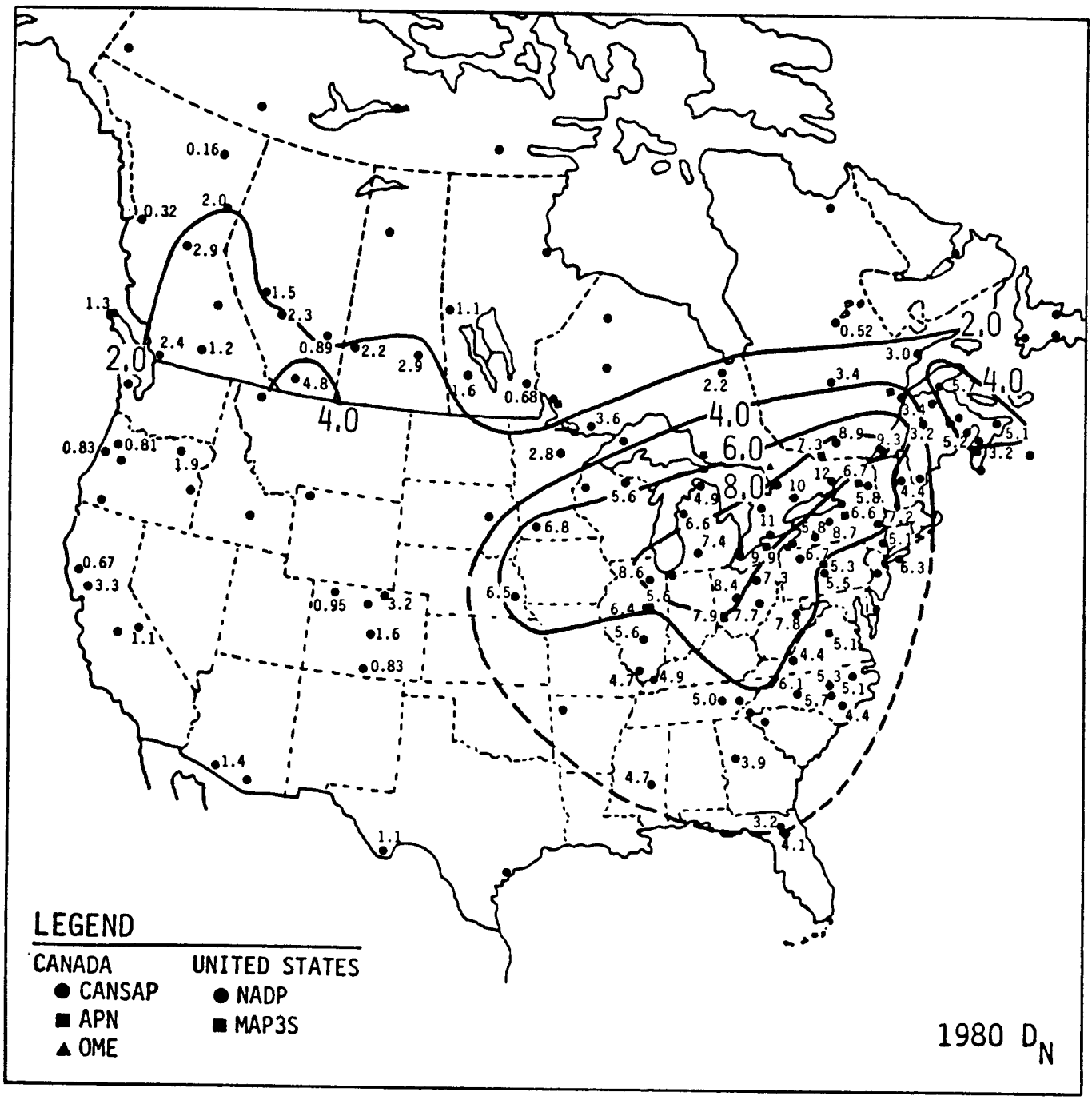

Figure 8-23. Total nitrogen deposition (calculated from nitrate and ammonium deposition) for wet deposition samples (kg ha^{-1}). Adapted from Barrie et al. (1982).

TABLE 8-9. TEN, FIFTY, AND NINETY PERCENTILE ION CONCENTRATIONS (mg ℓ^{-1}), pH, AND CONDUCTANCE FOR EIGHT NADP SITES[a]

Sites	Percentiles	(Ca^{2+})	(Mg^{2+})	(K^{+})	(Na^{+})	(NH_4^{+})	(NO_3^{-})	(Cl^{-})	(SO_4^{2-})	pH	λ[b]	No. of Samples
NE-ME[c]	10	.04	.006	-.002	.018	-.02	.31	.09	.64	4.20	7.0	31
	50	.12	.020	.015	.088	.08	1.08	.16	1.98	4.46	19.5	
	90	.36	.071	.049	.707	.38	2.52	.42	3.50	5.70	29.2	
NE-NY	10	.04	.009	.005	.017	-.02	.58	.06	.70	3.99	9.5	100
	50	.13	.022	.018	.081	.21	1.88	.16	2.31	4.30	27.0	
	90	.45	.090	.050	.623	.64	4.49	.35	5.90	4.83	53.4	
WV	10	.08	.010	.014	.025	-.02	.82	.08	1.54	3.92	15.1	128
	50	.25	.030	.035	.100	.21	2.00	.18	3.47	4.25	31.4	
	90	.78	.080	.084	.650	.65	4.64	.37	7.00	4.59	61.7	
GA	10	.04	.013	.005	.065	-.02	.30	.14	.91	4.11	8.3	91
	50	.10	.030	.027	.278	.11	.88	.30	2.00	4.62	16.6	
	90	.42	.134	.124	1.291	.55	2.10	1.35	5.91	5.65	40.3	
Central IL	10	.06	.011	.007	.015	.16	.92	-.03	1.91	3.98	16.0	72
	50	.28	.035	.027	.065	.42	1.96	.20	3.27	4.31	27.5	
	90	.98	.143	.094	.195	1.18	4.26	.40	5.60	4.65	51.2	
N-MN	10	.09	.016	.017	.032	-.02	.50	.07	.51	4.52	6.9	94
	50	.29	.043	.044	.139	.30	1.42	.17	1.50	5.17	12.0	
	90	1.04	.183	.154	1.014	1.01	3.41	.35	3.50	6.15	24.3	
NE-CO	10	.10	.013	.009	.043	.11	.90	.08	.67	5.30	6.2	42
	50	.43	.052	.076	.189	.68	1.48	.19	1.88	6.03	12.7	
	90	2.08	.245	.391	1.222	2.51	5.42	.57	5.44	6.86	33.4	
NW-OR	10	.05	.012	.010	.077	-.02	.10	.20	.21	4.95	3.7	99
	50	.17	.036	.033	.288	.04	.33	.41	.73	5.52	6.8	
	90	.31	.106	.144	2.150	.14	1.10	1.68	1.77	6.50	21.9	

[a]All measurements were made at the central laboratory and all samples were weekly collections when the equivalent collected rainfall was $\geq$ 0.05 cm (using data from NADP 1978,1979, and 1980).

[b]Conductance in μSiemens cm^{-1}.

[c]NE-Me indicates a site by identifying a region within a state and then the state. In this example, the site is the NADP site in the northeastern part of Maine (cf. Figure 8-6).

TABLE 8-10. pH AND CONTRIBUTIONS TO FREE ACIDITY (%) FOR FIVE REMOTE SITES (ADAPTED FROM GALLOWAY ET AL. 1982)

	St. Georges, Bermuda	Poker Flat, Alaska	Amsterdam Island	Katherine, Australia	San Carlos, Venezuela
Collector Type	W/D[a] and Bulk	W/D	Bulk (Funnel and Bottle)	W/D	Bulk
No. Samples[b]	67	16	26	40	14
Average pH[c]	4.79	4.96	4.92	4.78	4.81
pH Range[d]	3.8-6.2	4.7-5.2	4.3-5.4	4.2-5.4	4.4-5.3
H_2SO_4	$\lesssim$ 111[e]	$\lesssim$ 65	$\lesssim$ 73	$\lesssim$ 33	$\lesssim$ 18
HNO_3	$\lesssim$ 35	$\lesssim$ 17	$\lesssim$ 14	$\lesssim$ 26	$\lesssim$ 17
HX[f]	$\gtrsim$ 0	$\gtrsim$ 18	$\gtrsim$ 13	$\gtrsim$ 41	$\gtrsim$ 65

[a]W/D refers to an automatic sampler which collects a wet-only sample in one container and a dryfall sample in the second container.

[b]These samples were treated with chloroform at the field sites. Samples with volumes less than about 500 ml were not treated with chloroform at the field sites.

[c]Average pH here refers to the pH corresponding to the weighted-average hydrogen ion concentration.

[d]This range is for pH measurements made at the Virginia laboratory, on the samples treated with chloroform.

[e]Values greater than 100% simply indicate that the equivalence of sulfate exceeded the equivalence of free acidity.

[f]The authors indicate that HX could be HCl, organic acids, or H_3PO_4 but they believe it was organic acid.

constituents other than H^+ were collected monthly in these studies, Galloway et al. felt dry deposition effects would have been too large to allow for a valid comparison with their own samples.

In the study by Galloway et al. (1982) samples with adequate volume were split in the field into two 250 ml aliquots. One of the aliquots was treated with chloroform to prevent biological activity. They found that the untreated aliquots were subject to pH changes during storage and shipment, with the acidity decreasing. This evidence, combined with results from ion chromatograph measurements (Keene et al. 1983), indicated that the sample changes were associated with degradation of organic acids in the samples. Estimates of the importance of organic acids compared to sulfuric and nitric acids at the five remote sites are shown in the last line of Table 8-10. The importance of organic acids is clearly site dependent and varied from > 65 percent at the Venezuelan site to a negligible contribution at the Bermuda site. Although the percentages can be rather large, in absolute units the values are less than about 16 $\mu eq\ \ell^{-1}$ (the free acidity for pH equals 4.8). The presence of organic acids again illustrates that a simple comparison of pH data is insufficient to address time trends of acidity associated with anthropogenic emissions.

Measurements in June 1980 of the pH and the major inorganic ions for over 300 samples collected in Hilo, Hawaii showed that the acidity was due mainly to sulfuric acid instead of nitric or hyrochloric acid (Miller et al. 1984). Since about one to four weeks elapsed between collection and pH measurements, it is possible that any significant organic acid contribution would have been missed due to sample changes as reported by Galloway et al. (1982). In the same study, about 75 additional samples collected at different elevations on the island of Hawaii were measured for pH within 24 hours and again about 5 months later. The hydrogen ion concentrations were observed to typically decrease by 10 to 20 $\mu eq\ \ell^{-1}$. For some of the samples, pH changes related to the slow dissolution of dust particles could be definitely ruled out. Thus it seems likely that organic acids are making a significant contribution to some rain samples collected in Hawaii.

It has often been stated that the pH of natural precipitation is controlled by the equilibrium with atmospheric CO_2, producing pH values of 5.6. Charlson and Rodhe (1982) have examined various aspects of the atmospheric sulfur and nitrogen cycles for areas unaffected by anthropogenic perturbations. They conclude that, in maritime areas where basic constituents such as ammonia gas and $CaCO_3$ have low concentrations, substantial variations in precipitation pH should be expected, perhaps in the range of pH 4.5 to 5.6, due to the variability of the sulfur cycle alone. Charlson and Rodhe and several other authors have thus pointed out that it is not appropriate to use pH = 5.6 as a reference value against which human influences should be judged. Charlson and Rodhe emphasize that generally pH will be a poor indicator of manmade acidification, and instead the natural elemental cycles must be studied in order that manmade influences on these cycles can be recognized and quantified.

8.4.3 Precipitation Chemistry Variations Over Time

8.4.3.1 Nitrate Variation Since the 1950's--Likens (1976) reported significant increases in the annual volume-weighted concentrations of nitrate in data from New York and the Hubbard Brook Experimental Forest, New Hampshire. Additionally, various other authors conclude that NO_X emissions from fossil fuel combustion are the most important sources of precipitation nitrate increases in the eastern United States, but that the role of increased fertilizer use has not been rigorously assessed.

The Hubbard Brook precipitation chemistry data record is important because the record is relatively long, weekly bulk collections having been made continuously since 1964. A recent examination of the nitrate data at Hubbard Brook suggests an erratic trend of increasing nitrate from 1964 to about 1971, followed by a leveling off or a slight decrease from 1971 to 1981 (NAS 1983). The annual average values range from about 1.40 mg ℓ^{-1} in 1965-66 to 1.74 mg ℓ^{-1} in the early 1970's. The NAS report (1983) indicates that the NO_X emissions in the Northeast increased by 26 percent between 1960 and 1970 and then decreased 4 percent by 1978. Thus, the NAS report notes that wet nitrate concentrations at Hubbard Brook appeared to reflect emissions trends in the Northeast.

Comparing the 1955-56 Junge data (Figure 8-24) with the current NADP data in Figures 8-9 and 8-25, reveals a broad spatial picture of the increased nitrate levels. The average nitrate concentrations in Figure 8-24 were obtained by weighting the quarterly values of nitrate reported by Junge (1958) with the quarterly precipitation for the sites (Stensland 1979). Attention should be focused on the eastern United States, where the NADP data record is most complete. The nitrate concentrations are clearly greater in the recent NADP data than they are in the 1955-56 Junge data. The approximate magnitude of the increase is consistent with the reported increase in combustion-related NO_X emissions over the same time period (cf. Chapter A-2, Table 2-1 and Figure 2-7). However, it would be inappropriate to infer a quantitative relationship between NO_X emissions and increases in precipitation nitrate concentrations because error bars for the emission and precipitation data are not yet available and the transport, transformation, and wet and dry removal processes are not well understood.

Brezonik et al. (1980) indicated that nitrate had increased by a factor of 4.5 in Florida rainfall since the mid-1950's. They found, for a Gainesville site, that the average bulk nitrate value was 24 percent larger than the corresponding wet-only value, and thus concluded that differences in collector type explained only a small fraction of the overall large nitrate increase.

The volume-weighted-nitrate concentrations in Figure 8-25 are generally lower than the median values shown in Figure 8-9. The difference appears to be very substantial when the 2.0 contour is compared in the two figures. However, the extension of the 2.0 contour in Figure 8-9 into South Dakota and Nebraska results from data at only three sites, and illustrates why it is important to show the data values at the sites instead of only contour lines. The volume-weighted concentrations for the 75 sites in Figure 8-25 are, on

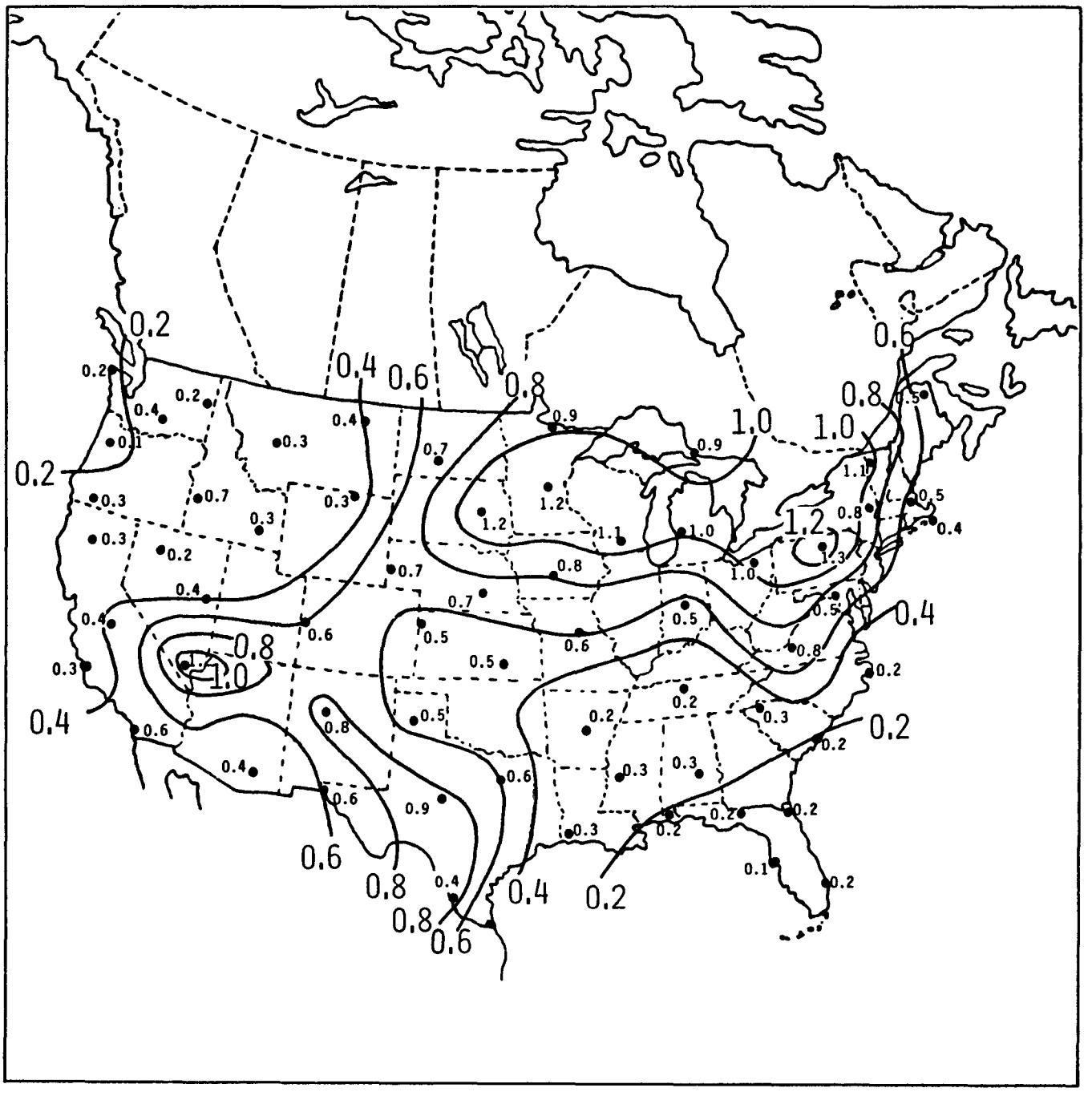

Figure 8-24. Map of precipitation-weighted-average-nitrate concentrations (mg ℓ^{-1} as NO_3^-) for the 1955-56 Junge data. Adapted from Stensland (1979).

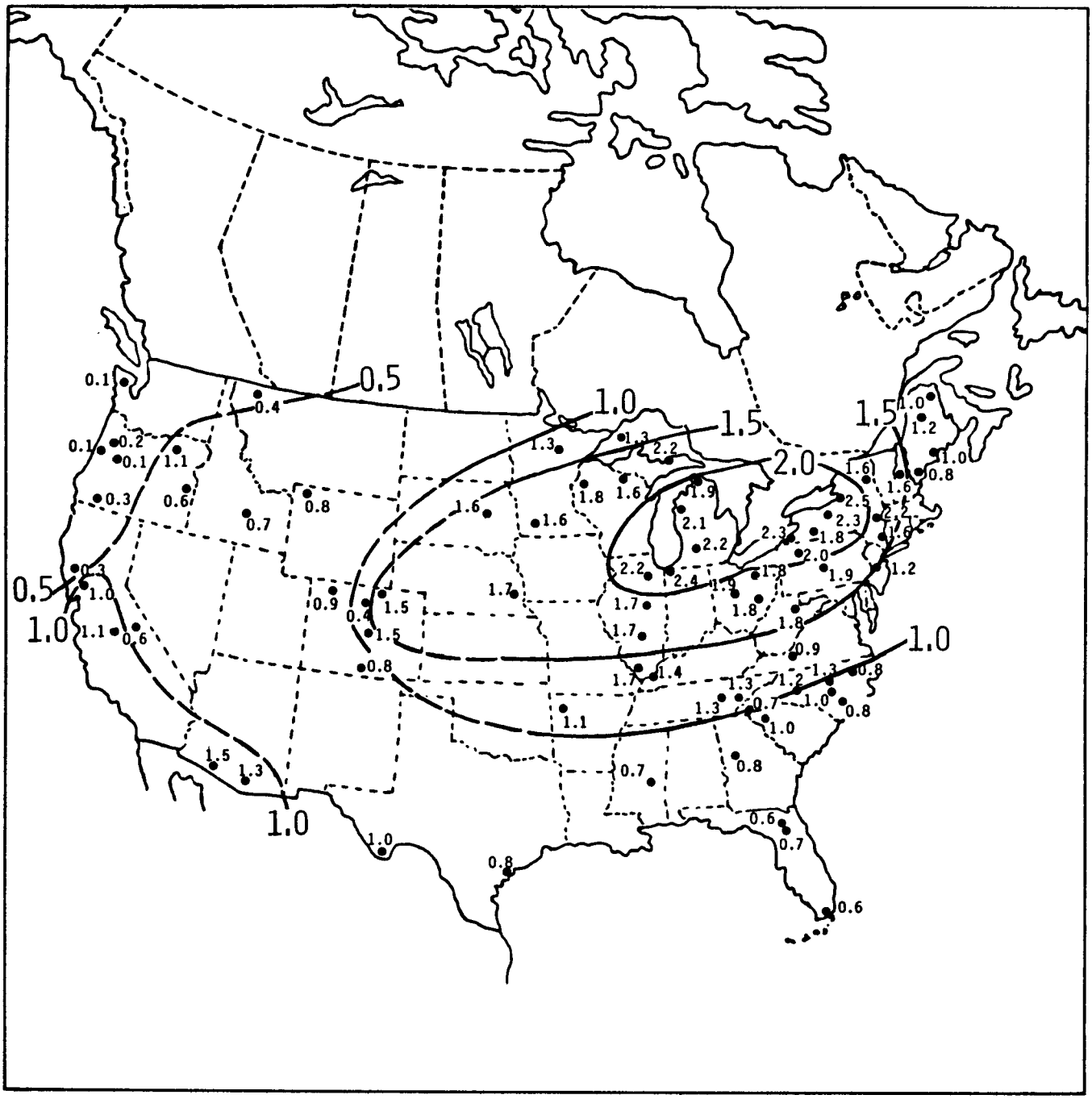

Figure 8-25. Map of volume-weighted-average-nitrate concentrations (mg ℓ^{-1}) for NADP wet deposition samples through approximately December 1980 (using data from NADP 1978, 1979, and 1980).

the average, 14 percent lower than the median values in Figure 8-9. By way of comparison, the volume-weighted-sulfate values in Figure 8-8 were only 5 percent lower than the median sulfate values in Figure 8-7.

8.4.3.2 Temporal pH Variation Since the 1950's--Cogbill and Likens (1974) and Likens and Butler (1981) have published eastern U.S. maps of precipitation pH for the mid-1950's, 1960's, and 1970's. Likens and Butler have concluded from this mixture of calculated and measured pH values that there has been a large spread and probable intensification of acid precipitation (pH < 5.6) in eastern North America during the past 25 years. These specific conclusions were based on trends shown on the pH maps, but trends in emissions and precipitation concentrations of sulfur and nitrogen compounds were qualitatively considered.

Stensland (1979) also calculated the pH distribution for 1955-56 from Junge's data. He found it necessary to apply a correction factor to the calculated pH values to bring the values into agreement with measured pH values, the largest correction being required for calculated pH > 6.0. The resulting pH map for 1955-56 by Stensland is very similar to the Likens and Butler map for 1955-56. Stensland (1979) also presents a series of pH maps to demonstrate that the calculated pH pattern is very sensitive to the concentrations of calcium and magnesium. Tables 8-11 and 8-12 demonstrate the significance of these sensitivity tests (Stensland and Semonin 1982). The 1977-78 data in Table 8-11 are for 1 year of sampling at two MAP3S sites with automatic, wet-only deposition collectors. The 1955-56 Junge data for a nearby site, at Williamsport, PA, were from a bulk collector. However, because the operators at the Junge sites were instructed to place the bulk collectors out only when precipitation was imminent, the procedure can be described as manual, wet-only collection. The magnesium concentration at Williamsport was estimated (Stensland 1979) because Junge did not measure this parameter. The data in the column labeled 'change' in Table 8-11 indicates that the difference in the calculated pH for the two time periods, 4.67 versus 4.18, is due more to the change in the cations instead of the change in the anions.

A similar analysis for Illinois is shown in Table 8-12. The 1953-54 data in Table 8-12 are a summary of the results of Larson and Hettick (1956). The Larson and Hettick samples were wet-only deposition samples for which the collection funnel was rinsed, just prior to sample collection, to reduce the possibility of contamination by dust between rain events. The 1977-78 data in Table 8-12 are also from an automatic, wet-only collector at the same site used for the Larson and Hettick study. The decrease in calcium plus magnesium is the major reason for the increased acidity of the 1977-78 Illinois samples. Comparison with the 1980 data for the NADP site located 10 kilometers from the Larson and Hettick site results in the same conclusion.

Both the 1953-54 Larson and Hettick samples and the 1955-56 Junge samples were collected during the severe drought of the 1950's. Stensland and Semonin (1982) have hypothesized that this drought produced unusually high dust levels in the atmosphere. In turn, the high dust levels produced unusually high pH values for the available precipitation chemistry data for the 1950's. When the calcium plus magnesium levels measured by Junge are reduced to levels currently being measured, the calculated pH for the entire

TABLE 8-11. WEIGHTED AVERAGE CONCENTRATIONS[a] ($\mu eq\ \ell^{-1}$) FOR MAP3S AND JUNGE DATA. ADAPTED FROM STENSLAND AND SEMONIN (1982)

	Cornell Univ. NY 9/21/77-9/29/78	Penn. State Univ. 9/24/77-9/15/78	Mean of the two sites		Williamsport, PA 7/1/55-6/30/56		Change ($\mu eq\ \ell^{-1}$)
Ca^{2+}	5.4	4.5	5.0		38.4		
				+=6.3		+=54.0	-47.7
Mg^{2+}	1.5	1.1	1.3		15.6		
Na^{+}	1.5	1.5	1.5		20.9		-19.4
K^{+}	.6	.7	.6		3.6		-3.0
NH_4^{+}	13.4	12.9	13.2		5.0		+8.2
Sum	22.4	20.7	21.6		83.5		
SO_4^{2-}	55.4	55.5	55.4		72.5		-17.1
NO_3^{-}	27.4	27.6	27.5		21.1		+6.4
Cl^{-}	4.4	4.5	4.4		11.3		-6.9
Sum	87.2	87.6	87.3		104.9		
Calculated pH	4.19	4.17	4.18		4.67		
Measured, Weighted pH	4.15	4.16					
Number of Samples	55	80					

[a]MAP3S data are sample volume-weighted averages and Junge data are precipitation-amount-weighted averages.

TABLE 8-12. MEDIAN PRECIPITATION CONCENTRATIONS ($\mu eq\ \ell^{-1}$) AT CHAMPAIGN, ILLINOIS. ADAPTED FROM STENSLAND AND SEMONIN (1982)

	5/21/77-1/16/78	10/26/53 8/12/54	Change ($\mu eq\ \ell^{-1}$)
Cations			
Ca^{2+}	10.5	84.5[a]	-71.6
	}+=12.9		
Mg^{2+}	2.4		
Na^{+}	1.9	7.1	-5.2
K^{+}	0.5	2.2	-1.7
NH_4^{+}	17.7	18.6	-0.9
Sum	33.0	112.4	
Anions			
SO_4^{2-}	78.9	64.5	+14.4
NO_3^{-}	29.8	20.2	+ 9.6
Cl^{-}	4.8	7.3	- 2.5
Sum	113.5	92.0	
Calculated pH	4.09	6.52	
Measured, Weighted pH	4.02	-	
Number of Samples	63	30	

[a]Measured hardness.

Northeast is less than 4.6. Stensland and Semonin suggest (1) that the drought-corrected pH pattern for the 1950's should be compared with current data and (2) that the error bars associated with the calculations make it difficult to discern a pH time trend over the last 25 years.

Hansen and Hidy (1982) have discussed other features of the historical data record that make establishing the magnitude of the pH time trend difficult, and Barrie et al. (1982) have reviewed information relative to acidity trends in North America and state:

> As a consequence of this continuing debate, one can conclude that it is presently unsafe to utilize existing network data to draw any reliable conclusions with regard to acidity trends in eastern North America.

The NAS report (1983) and the recent article by Hidy et al. (1984) discuss trends in acid precursor emissions and their precipitation products, including the effect on precipitation acidity. The precipitation chemistry discussion is focused on the Northeast, and especially on the Hubbard Brook and USGS bulk precipitation chemistry data sets. The NAS report points out that a linear regression analysis of the Hubbard Brook sulfate data shows that the concentrations at that site declined by about 33 percent from 1965-66 to 1979-80. The SO_2 emissions for the U.S. EPA-designated regions of the eastern United States were examined. It was concluded that the decline in wet sulfate at Hubbard Brook fairly closely reflected the reduction in SO_2 emissions within the Northeast itself, and did not reflect the trends in SO_2 emissions in the Midwest and other distant source regions. In the 1964-77 time period, there was no statistically significant trend in precipitation pH or hydrogen ion deposition at the Hubbard Brook site. The USGS bulk data for the three sites in northeastern and north- central New York showed significant declines in sulfate in the 1965-78 time period for two sites and no trend at the other site (Hidy et al. 1984). In general terms, these USGS data thus qualitatively support the Hubbard Brook data.

Hidy et al. (1984) also state that changes in precipitation sulfate between 1965 and 1980 at rural sites in central New York State and New Hampshire were more influenced by SO_2 emissions changes in nearby source regions than by those from more distant source regions. However, Hidy et al. found that no proportional relationship between nearby source region emissions and wet sulfate existed for other USGS bulk deposition sites in western New York and north-central Pennsylvania.

The concluding statement in the NAS report concerning the influence of local vs distant sources is the following:

> On the basis of currently available empirical data, we cannot in general determine the relative importance for the net deposition of acids in specific locations of long-range transport from distant sources or more direct influences of local sources.

Thus, although the NAS report (1983) mentions that sulfate and nitrate deposition data in the Northeast appeared to reflect emissions trends in the Northeast, a strong concluding statement concerning the importance of nearby sources versus distant sources was not made.

8.4.3.3 Calcium Variation Since the 1950's--Table 8-13 shows precipitation calcium concentrations for various networks, sites, and time periods. The calcium levels for the MAP3S and NADP networks are small relative to those for the other networks. Bulk samples were collected in the USGS network, probably accounting for the higher calcium levels for that network. However, urban areas such as the Albany, NY, USGS site, can also produce relatively high atmospheric dust levels, and thus, high calcium levels in air and precipitation samples. The NCAR and WMO networks used automatic, wet-only collectors, but, because of sampler design, the covers probably did not make firm contact with the sampling bucket (Stensland and Semonin 1984). Thus, dust probably leaked in during nonprecipitation periods, producing the relatively high calcium concentrations and shifting the precipitation pH to higher values.

If dust leaks into the sampling containers of wet-only collectors or is included in the precipitation sample via bulk sampling, the measured pH may be significantly different than that for rain and snow that falls into clean containers. This sampling deficiency will often be strongly influenced by the local environment, and will likely be quite variable on both short- and long-term time scales. For a given collector, the problem will be most severe in arid regions. The data in Table 8-13 suggest this problem can also occur in the eastern United States. The magnitude of this dust leakage effect should be continuously evaluated at all sampling sites through collection, analysis, and reporting of appropriate blank samples. These steps have been taken in very few networks in the past, and they are only rarely taken now.

For the Junge 1955-56 data, it has been shown that the precipitation calcium concentrations for the Plains States and eastward were on the average about a factor of 4 higher than current levels; for the western states, the calcium was about a factor of 6.0 higher (Stensland and Semonin 1984). As discussed in the previous section, the higher values in the east may have been due to drought; for the west, the higher levels were probably due to sampling problems, specifically bias due to dry deposition contamination and evaporation. But, regardless of the reason for the higher levels of the crustal elements, their effect on pH trends is significant and must be considered.

8.4.4 Seasonal Variations

Herman and Gorham (1957) reported that snow sampled in the early 1950's contained lower sulfur and nitrogen concentrations than did rain sampled during the same period. They speculated that this difference might have resulted from snow's having a lower collection efficiency than rain or from arctic air bearing snows being cleaner than tropical air. In the late 1960's, Fisher et al. (1968) observed lower precipitation sulfate in the cold season. Bowersox and dePena (1980), Pack and Pack (1980), and Pack (1982)

TABLE 8-13. CALCIUM CONCENTRATIONS (mg ℓ^{-1}) FOR VARIOUS NETWORKS, SITES, AND TIME PERIODS. ADAPTED FROM HANSEN ET AL. (1981)

Sites	Junge[a] 1955-56	NCAR[b] 1960-66	WMO[c] 1974-76	USGS[d] 1966-78	MAP3S[e] 1978-79	NADP[f] 1979
Rocky Mountain						
Alamosa, CO			2.65			
Grand Junction, CO	3.41	7.25				
Pawnee, CO						0.53
Midwest						
Grand Island, NE	3.12	0.96				
Huron, SD	2.40		2.74			
Lamberton, MN						0.58
Mead, NE						0.53
St. Cloud, MN	1.02	1.12				
Northeast						
Albany, NY		1.97		2.83		
Caribou, ME	0.63	0.39	0.36			
Hinkley, NY				0.70		
Huntington, NY						0.13
Mays Point, NY				1.48		
Ithaca, NY					0.14	
Williamsport, PA	0.77					
Southeast						
Charlottesville, VA					0.05	
Georgia Station, GA						0.10
Greenville, SC	0.31	0.30				
Raleigh, NC			0.20			
Roanoke, VA	0.32					
Sterling, VA		0.67				

[a]Weighted averages, manual wet-only sampling, July 1955-June 1956.
[b]Weighted averages, wet-only sampler, NCAR/Public Health Service.
[c]Medians, wet-only sampler.
[d]Medians, bulk sampler.
[e]Medians, wet-only sampler, July 1978-June 1979.
[f]Medians, wet-only sampler.

reported strong seasonal variations in sulfate in precipitation at MAP3S sites in New York, Pennsylvania, and Virginia.

Bowersox and Stensland (1981) analyzed NADP data for seasonal variations in sulfate and nitrate. Because the data base was small, two to seven sites were grouped in five regions in the eastern United States and the data for each region were averaged for the cold season (November to March) and the warm season (May to September). The resulting warm-to-cold-period ratios for sulfate varied from about 2.0 in the New England region to 1.25 in the Illinois region. The investigators noted that aerosol sulfate has a similar seasonal variation but that SO_x emissions for the Northeast have a relatively small seasonal variation.

For nitrate, Bowersox and Stensland (1981) found a maximum warm-to-cold-period ratio of 1.5 for the region in the Southeast, but three of the remaining regions had little or no seasonal variation. Determining whether different patterns of seasonality for nitrate and sulfate are predicted by numerical simulations would be valuable. The acidity of the precipitation was greater in the warm period for all the regions and reflected the mixture of the patterns for sulfate and nitrate.

Bowersox and dePena (1980) found only slightly higher nitrate in precipitation in the winter than they did in other seasons at the MAP3S site in Pennsylvania. Hydrogen had a strong maximum in the warm months and sulfate was the principal anion affecting acidity. Nitrate, at concentrations similar to those of sulfate, did not correlate well with hydrogen ion in liquid precipitation but did correlate with hydrogen ion in snow and frozen precipitation.

The seasonal pattern of precipitation sulfate concentration is different for western Europe than it is for the eastern United States. Granat (1978) averaged the data for many European sites and reported a maximum sulfate concentration in the spring, being 1.6 times greater than the minimum value observed in the fall. The sulfur emissions in the region are at maximum in the winter (Ottar 1978).

8.4.5 Very Short Time Scale Variations

The concentrations of the major ions in precipitation vary considerably during a rainshower (Robertson et al. 1980). Samples collected sequentially during rainshowers in Arizona had calcium variations up to 1000 percent over a sampling period of less than 15 minutes (Dawson 1978). Dawson found that the correlation between ions having a common source were not significantly different from those between components not having a common immediate source. Therefore, Dawson concluded that the observed concentration changes were primarily determined by precipitation processes.

8.4.6 Air Parcel Trajectory Analysis

Attempts have been made to link the precipitation chemistry patterns to the emission source regions through the use of air parcel trajectory analysis. There are many different approaches to calculate trajectories of air parcels.

Forland (1973) used surface geostrophic analysis to determine air parcel trajectories. This analysis involved using surface air pressure gradients to calculate the wind speed and direction, which dictate the movement of the air parcels. Recently, many investigators have calculated trajectories with the National Oceanic and Atmospheric Administration Air Resources Laboratory (ARL) model, which uses as input data surface layer wind observations (Miller et al. 1978, Wilson et al. 1980, Miller et al. 1981). With the ARL model, an average wind for the surface layer, such as the layer 300 to 1500 meters above the ground, is used to calculate the trajectories. Many scientists argue that air parcel trajectory techniques need to be further developed and verified with field experiments. Especially questionable are the trajectory calculations in areas of very low and variable wind speed and in areas near the separation of different air masses, i.e., near weather fronts.

Some conclusions from recent trajectory studies are as follows. Forland (1973) found that, for a site at the southwestern tip of Norway, the precipitation pH values were 4 to 5 for air parcels originating in central Europe or England and 5.1 to 6.6 for parcels originating in the North Sea. He concluded that acidic precipitation in southern Norway is mainly a result of SO_2 emissions from northern Europe. Ottar (1978) reported that aerosol sulfate at European sites examined by sector (air parcel) analysis showed that sectors associated with high concentrations are directed towards areas of major sulfur emissions. Similar analysis for precipitation illustrated that, to a large extent, acidity is strongly influenced by the availability of ammonia, with air masses passing over the sea showing the least degree of neutralization.

Jickells et al. (1982) used the ARL trajectory analysis to stratify the pH of precipitation samples collected at Bermuda. They found that pH was generally less than 5.0 for trajectories originating in the eastern United States and frequently greater than 5.0 for trajectories originating in areas southwest to southeast of Bermuda. Thus, they concluded that rainwater originating over continental North America was markedly more acidic than rainfall from the other sectors.

Wolff et al. (1979) used trajectory analysis to characterize precipitation pH for samples from eight sites in the New York City area. They found higher pH values for air parcels from the ocean or from the north and lower pH for air parcels from the south through northwest sectors. The lowest average pH was for air parcels from the southwest sector. They also classified the precipitation events according to synoptic meteorological conditions and found air mass thunderstorms and precipitation associated with cold fronts in the absence of closed lows to be the most acidic. Whether the low pH cases identified in this study were more strongly related to source direction or to characteristics of the scavenging processes taking place in these convective types of precipitation events seems open to question since showers and thunderstorms are usually associated with southwesterly flow.

Raynor and Hayes (1981) also classified pH data by synoptic type and found the lowest pH with cold fronts and squall lines, or with thunderstorms and rainshowers. Although these are predominately warm season rainfall types, Raynor and Hayes found that the low pH was not a function of season alone.

The question of the importance of atmospheric transformation and scavenging processes in explaining the observed association between southwest trajectories and low pH is discussed by Wilson et al. (1980), who maintain that:

> Normally, trajectory analysis of individual events will lead to some basic source-receptor relationships. Vital information is still missing on the overall transport/transformation processes that take place in the atmosphere relevant to the formation and deposition of "acid rain"....In summary, the known source regions for precursor gases to "acid rain" cannot yet be unequivocally linked to receptor with the meteorological, physical and chemical information available today.

Wilson et al. (1982) emphasize the importance of recognizing the relation between precipitation amount and ion concentration. When they normalized the MAP3S data for 1977-79 for precipitation amount they found that the sulfate deposition per centimeter of precipitation was about the same at the MAP3S Illinois site and the Pennsylvania site. Stated another way, much more sulfate was deposited annually at the Pennsylvania site than at the Illinois site, mainly because of the greater annual precipitation amount.

Wilson et al. (1982) used trajectory analysis to examine the directional variability of wet deposition at the Whiteface Mountain MAP3S site in northeastern New York and at the MAP3S site in east-central Illinois. For the New York site, the southwest sector was found to contribute 56 percent of the water deposited, and 62 to 65 percent of the H^+, SO_4^{2-}, and NO_3^-. The same sector contributed 71 percent of the water deposited and 64 to 76 percent of the H^+, SO_4^{2-}, and NO_3^- at the Illinois site. The authors state that:

> The fact that few major pollutant sources lie within the southwest sector traversed by trajectories arriving at Illinois indicates that a knowledge of air mass histories further back in time may be necessary to adequately identify all important source regions.

8.5 GLACIOCHEMICAL INVESTIGATIONS AS A TOOL IN THE HISTORICAL DELINEATION OF THE ACIDIC PRECIPITATION PROBLEM (W. B. Lyons and P. A. Mayewski)

Precipitation in the Northern Hemisphere has been recently recognized to have hydrogen ion concentrations 10 to 100 times higher than expected for natural precipitation (Likens and Bormann 1974, Cogbill and Likens 1974, Lewis and Grant 1980). However, controversy has arisen regarding the nature of the acidity of the precipitation sampled and whether, indeed, the pH of North American precipitation has increased over time (Miller and Everett 1979, Lerman 1979, Stensland 1980, Sequeria 1981, Charlson and Rodhe 1982). In most locations pH records have been constructed rather imperfectly due to differences in sampling, handling, and analytical procedures used (Galloway and Likens 1976, 1978; Galloway et al. 1979). The lower pH's measured in Northern Hemisphere precipitation are thought to be due to the input of sulfur and nitrogen oxides from fossil fuel-burning (Likens and Bormann 1974) and in some cases hydrogen chloride (Gorham 1958a). Few baseline data,

however, are available on the pH of precipitation in areas of the Northern Hemisphere remote from North American and European sources of anthropogenic sulfur emissions. In addition, monitoring records of pH and acidic chemical species are of rather short time duration (~ 15 to 20 years at most), limited geographic coverage, and provide little useful information prior to the early 1960's (Hornbeck 1981). Baseline studies of pH and related chemical species as well as historical time series data are warranted if we are to understand man's effect on the environment.

The National Academy of Sciences (1978) recommends that historical studies of glacier snow and ice should be conducted. Such studies are needed to better understand the atmospheric transport of anthropogenically-introduced chemical species to remote areas. In addition, a more recent NAS report (1980) states that a major scientific goal of the 1980's should be to "identify the significant natural and anthropogenic factors contributing to acid rain." Detailed glaciochemical studies should provide this type of needed information.

Snow and ice cores collected from appropriately chosen glaciers provide samples of entrapped chemical species that, unlike those derived from any other medium, are nearly to entirely unaltered since their deposition. This technique has barely been applied to the study of acid precipitation despite the fact that it provides a very sensitive record of precipitation chemistry.

8.5.1 Glaciochemical Data

Past glaciochemical studies (early studies are reviewed in Langway 1970) have provided information concerning 1) the documentation of individual storm events (Warburton and Linkletter 1978, Mayewski et al. 1983a), 2) the dating and seasonal accumulation of snow and ice (Langway et al. 1975, Herron and Langway 1979, Butler et al. 1980, Mayewski et al. 1983b), as well as 3) long-term climatic change (Delmas et al. 1980b, Thompson and Mosley-Thompson 1981, Johnson and Chamberlain 1981). Our discussion will deal primarily with the use of glaciochemical studies in delineating the acid precipitation phenomenon. The text that follows is divided into a section on primary measurements including sulfate, nitrate, pH, and total acidity, and a section concerning analog measurements or trace metals. For both primary and analog measurements the discussion is subdivided into results from polar glaciers and from alpine glaciers.

The glacier division adopted in this text is used primarily as a means to separate the results of glaciochemical studies for review purposes. Polar glaciers, including the Antarctic and Greenland ice sheets, are characteristically lower in temperature and accumulation rate and larger in size than alpine glaciers. Hence, polar glaciers classically are used to retrieve longer glaciochemical time-series, often with less subannual detail than time-series from alpine glaciers. Although there are many fewer glaciochemical studies available from alpine glaciers, they are included here because these glaciers are less remote from industrialized sites than are polar glaciers and, therefore, have considerable potential as proxy indicators of man's effect on the environment.

8.5.1.1 Sulfate - Polar Glaciers--The early work by Koide and Goldberg (1971), Weiss et al. (1975), and Cragin et al. (1975) and more recent work by Busenberg and Langway (1979) has suggested that the concentration of sulfate in recent Greenland snow and ice (past 20 yr) has increased by at least a factor of two. This increase has been attributed to fossil-fuel burning. However, other investigations have suggested that these enrichments may be also linked to natural processes and/or local contamination (Boutron 1980, Boutron and Delmas 1980).

Herron (1982) most recently indicates that SO_4^{2-} has been enriched by a factor of 1.6 to 3.7 in Greenland snow and ice in the past 200 years and that this enrichment is due to the burning of fossil fuel. No anthropogenic input of SO_4^{2-} has been observed in Antarctic ice cores (Delmas and Boutron 1978, 1980; Herron 1982). Recent work by Rahn (Kerr 1981) indicates that the northern polar regions receive pollutant SO_4^{2-} on a seasonal basis, and mass budget considerations indicate that approximately 2.5 times the natural atmospheric emission leaves eastern North America every year (Galloway and Whelpdale 1980). Shaw's (1982a) work confirms that of Rahn, indicating that the Arctic haze observed in Alaska has its source in Eurasia, with smelting operations in Siberia being a possible major contributor.

Natural processes may also have a profound effect on SO_4^{2-} profiles in glacier ice. For example, Bonsang et al. (1980) have shown that aerosols of marine origin have much higher SO_4/Na ratios than seawater, indicating that SO_4^{2-} enrichments in precipitation need not be all due to anthropogenic emissions. Recent work by Hammer et al. (1980) indicates that Greenland ice concentrations of SO_4^{2-} are greatly affected by world-wide volcanism. The active volcano Mt. Erebus may be a major sulfate source to the Antarctic continent (Radke 1982). Volcanically produced SO_4^{2-} has been observed in Antarctic and Greenland ice cores (Kyle et al. 1982, Herron 1982). As one proceeds away from the ocean in both Antarctica and Greenland, sea salt becomes less of a contributor to the SO_4^{2-} concentration in the ice and snow (Boutron and Delmas 1980), and in Antarctica gas-derived SO_4^{2-} as well as NO_3^- and Cl^- becomes very important (Delmas et al. 1982).

In addition to the possible volcanic input of SO_2 into the atmosphere, biogenic emission, particularly in lower latitude regions, may also be an important contributor of SO_2 (Lawson and Winchester 1979, Stallard and Edmond 1983, Haines 1983). Due to the very long residence time of sulfate in Antarctic aerosols (Shaw 1982b), the oxidation of marine-derived gases such as dimethyl-sulfide may be a major contributor of sulfate to Antarctic precipitation (Delmas 1982). Herron (1982) has also suggested a biogenic source for a portion of the sulfate observed in Greenland ice. Gas adsorption onto particles may also be an important source of SO_4^{2-} in some locations (Mamane et al. 1980). It is also thought that the sulfate present in Arctic aerosols is formed from the conversion of continentally-produced pollutant SO_2 during transport (Rahn and McCaffrey 1980).

8.5.1.2 Nitrate - Polar Glaciers--The work of Parker et al. (1977, 1982) shows downhole variations in the NO_3^- concentration of snow and ice. Parker et al. (1977) have suggested that this historic variation is due to changes in sunspot, auroral, and/or cosmic ray activities and not due to

variations in anthropogenic inputs. These workers have recently observed seasonal, 11- and 22-yr periodicities as well as long-term changes in Antarctic ice (Parker et al. 1982). The highest values were associated with winter darkness and heightened solar activity. They observed no anthropogenic NO_3^-. Kyle et al. (1982) have observed volcanically-introduced NO_3^- in Antarctic ice. However, Aristarain (1980) has observed on James Ross Island, Antarctica, no variation in NO_3^-, on at least the seasonal level. Risbo et al. (1981) and Herron (1982), on the other hand, observed no relationship of NO_3^- with solar activity in Greenland. Herron (1982) did note a seasonal variation of NO_3^- in Greenland ice; however, the highest values were associated with the summer season. He also observed an anthropogenic doubling of NO_3^- in surface samples, indicating for the first time the introduction of NO_3^- into this region, probably through fossil-fuel burning.

8.5.1.3 pH and Acidity - Polar Glaciers--Hammer (1977, 1980; Hammer et al. 1980) has measured the acidity of Greenland ice cores and found a "background" value of pH ~ 5.4 although much lower values appear during times of high volcanic input (e.g., Laki Eruption in 1783, pH of ice = 4.4). However, in most cases Hammer has not measured pH directly but rather has used conductivity techniques.

Berner et al. (1978) first measured the acidity of Antarctic ice by using strong acid titrations. They observed values ranging from 6.0 to 7.5. Delmas et al. (1980a) found an average pH in Antarctic ice of 5.3. These investigators, like Berner et al. (1978), used the strong acid titration technique rather than direct measurements of pH. More recent work (Legrand et al. 1982) has substantiated the fact that Antarctic precipitation is acidic with maximum reported values of 7 $\mu eq\ \ell^{-1}$.

Much of the earlier pH work on glacier snow and ice is unusable due to possible sampling and handling artifacts (e.g., filtration and hence degassing prior to analysis, and sample storage in glass rather than plastic; Gorham 1958b; Elgmork et al. 1973).

The polar data on acid anion concentrations suggest there has been a negligible contribution of fossil fuel by-products transported to Antarctica, as expected due to its great distance from Northern Hemispheric sources. The most recent data, those of Herron (1982), indicate however that Greenland has been affected by fossil-fuel burning with SO_4^{2-} and NO_3^- enrichments in surface snows of ~ 2 above preindustrial times. However, it should be noted that these enrichments are based on very few data points, and more detailed study may be warranted.

8.5.1.4 Sulfate - Alpine Glaciers--To our knowledge, no published data exist for SO_4^{2-} concentrations in glacier ice from alpine areas.

8.5.1.5 Nitrate - Alpine Glaciers--Butler et al. (1980) have observed values of from < 0.03 to 2.80 μM in a short core from Athabasca Glacier, Alberta. They observed higher values during the warmer months of the year. In addition, their mean NO_3^- value was approximately 15 times lower than that observed in central Alberta snows close to populated areas. High elevation

surface samples from Kashmir, India, demonstrate values as high as 1.3 μM in snow from pristine air masses (Mayewski et al. 1983a)). Nitrate values of between < 0.1 and 4.4 μM have been obtained from a ~ 17 m core on Sentik Glacier in Kashmir, India, close to the surface sampling site discussed in Mayewski et al. (1983a). The source of the NO_3^- is unknown, although variations in air mass source and/or accumulation rate may be important.

8.5.1.6 pH and Acidity - Alpine Glaciers--Although identifying the pH of snow and ice may be more complex than simply measuring strong mineral acid contributions, Delmas and Aristarain (1979) have observed in the Mt. Blanc area of the French Alps strong mineral acid values that increase from ~ 0 μeq ℓ^{-1} for 1963 to above 10 μeq ℓ^{-1} in 1976. It should be pointed out, however, that this increase from 1963 to 1976 is only represented by 4 data points. It does however provide insight into the possible usefulness of high-altitude alpine glaciers as historic tools. Delmas and Aristarain (1979) have argued that this strong acid increase is due to increased fossil-fuel burning.

Clement and Vandour (1967) have reported pH values of snow from the southern French Alps in the range 4.2 to 7.0, noting changes in pH with time, type of snow, and elevation. These authors have suggested that, in general, low pH's correspond to winter snow accumulation, freshly fallen snows, and higher elevation snow. Lyons et al. (1982) and Mayewski et al. (1983a) have also observed an elevation vs pH relationship for Himalayan surface snows. These authors have suggested that the majority of the pH vs elevation trend observed is a function of increased CO_2 saturation with decreasing temperature. A number of workers (Scholander et al. 1961, Berner et al. 1978, Stauffer and Berner, 1978, Oeschger et al. 1982) have shown that polar ice and snow are easily "contaminated" with CO_2. If these data and the interpretations are correct, detailed ionic balance studies must be undertaken to understand completely the nature of the acidity and/or pH of ultrapure snow and ice.

More recently Koerner and Fisher (1982) have discussed the adsorption of CO_2 as it related to snow pH measurements and snow density. They have argued that the pH contribution due to CO_2 "contamination" should increase with depth in glacial ice. If this is true, the pH of snow and ice, especially downhole, may have little relevance to the acid precipitation phenomenon. The measurement of acidity via titration eliminates this contribution of CO_2 to pH from the ice as well as any contribution from the ambient atmosphere upon melting. The newly developed acid titration technique of Legrand et al. (1982) appears to be the best suited for snow and ice pH work.

8.5.2 Trace Metals - General Statement

In studies aimed at determining the effects of fossil-fuel burning on the environment, various investigators have used trace metal concentrations in precipitation as well as lacustrine sediments and soils as analogs of acidic compounds (Andren and Lindberg 1977, Galloway and Likens 1979, Wiener 1979, Anderssen et al. 1980, Jeffries and Snyder 1981). Mass budget calculations indicate that by burning fossil fuel man has contributed both metals as well

as acid into the atmosphere (Bertine and Goldberg 1971, Lantzy and Mackenzie 1979). However, some controversy exists as to whether this anthropogenic metal introduction via burning is regional or global in scale (e.g., Nriagu 1979, 1980; Landy et al. 1980; Boutron 1980; Boutron and Delmas 1980). This is coupled with the fact that contamination problems and analytical uncertainties severely limit the interpretation of much of the data and complicate the use of trace metal concentrations as acid surrogates (Murozumi et al. 1969, Boutron and Delmas 1980, Ng and Patterson 1981).

8.5.2.1 Trace Metals - Polar Glaciers--The original glaciochemical analyses of Pb in Greenland and Antarctic ice by Murozumi et al. (1969) indicated: 1) a rise from 1 ng kg^{-1} in Greenland prior to 800 BC to values greater than 200 ng kg^{-1} in 1968 with the sharpest rise since 1940, and 2) a rise in Antarctica from less than 1 ng kg^{-1} to 20 ng kg^{-1} in 1968. These authors suggest that the sharp rise in Greenland concentrations post-1940 was due to the increased consumption of leaded gasoline. The lower values in Antarctica were because most of the fossil-fuel burning occurs in the Northern Hemisphere and little if any troposphere mixing occurs across the equator. The work of Murozumi et al. (1969) also demonstrated much more terrestrial material in Greenland ice compared to Antarctic ice (~ 15 to 20 times more) while the Antarctic ice contained about twice as much sea salt as the Greenland precipitation. Unpublished work by Boutron and Patterson now indicates little if any increase (possibly a factor of 2; from 1.5 ng kg^{-1} to 3 to 4 ng kg^{-1}) in Pb in the surface snows of Antarctica compared to older ice samples, and that all previous data were erroneously high.

The work of Weiss et al. (1975) showed that in Greenland ice (Camp Century and Dye 3), Hg, Cd, and Cu were enriched in the surface layers, and they suggested that this enrichment was due to increased fossil-fuel burning. Similar surface enrichments were measured for Ag in Antarctic ice and attributed to weather modification programs such as cloud seeding (Warburton et al. 1973).

The work of Herron et al. (1977) suggested for the first time that "natural" enrichments of several orders of magnitude for several trace metals occur in the atmosphere. This work was corroborated by additional investigations on Alaskan snow (Weiss et al. 1978). The process causing this "natural" enrichment for metals such as Zn, Pb, Cd, Cu, As, Se, Hg, and even Na was suggested to be volcanism. Although volcanism may have a pronounced effect on atmospheric aerosol chemistry great distances from its source (Meiner et al. 1981), volcanic emission studies are in conflict as to whether volcanism is a major source of volatile trace metals to the atmosphere (Unni et al. 1978, Lepel et al. 1978).

Due to its remoteness from North American emissions, it is now apparent that any enrichments of trace metals, with the possible exception of Pb in Antarctic ice may not be due to pollution but possibly to volcanism (Boutron and Lorius 1977, 1979; Boutron 1979a, Boutron 1983). Although metal enrichment factors show temporal changes, these changes do not vary systematically on a short-term or long-term basis (Boutron and Lorius 1979, Landy and Peel 1981). In addition, the present day metal fluxes of Cd, Cu, Zn, and Ag are similar to those 100 years ago, again suggesting little to no anthropogenic

input (Boutron 1979a). However, manmade radionuclides are measurable in Ross Ice Shelf samples in Antarctica as well as in Greenland (Koide et al. 1977, 1979). The detectable concentrations of these weapon test products in Antarctic ice do indicate that some high altitude interhemispheric transport of manmade products does occur (Koide et al. 1979). Obviously the mode of transport, the altitude of transport, and the size of the transporting particles all affect pollutant dispersion and distribution.

In Greenland, the recent findings of Ng and Patterson (1981) have confirmed the earlier work of Murozumi et al. (1969). Their data indicate that the concentration of "naturally" occuring Pb in ice during pre-industrial times was less than 1 ng kg^{-1} and that surface snows show a ~ 200-to-300 fold increase above this background level. These data, along with those collected by Patterson and his colleagues in the SEAREX group, confirm the hypothesis that Pb introduced by human activities is ubiquitous in the Northern Hemisphere. Furthermore, these data allow for a better understanding of pollutant dispersion from Northern Hemispheric sources and provide an inventory of current background levels of Pb in continental as well as oceanic areas (Shirahata et al. 1979, Schaule and Patterson 1981, Settle et al. 1982, Flegal and Patterson 1982). Whether the record of anthropogenically-introduced trace metals other than Pb can be discerned in Greenland snow and ice is still controversial (Herron et al. 1977; Boutron 1979a,b; Boutron and Delmas 1980; Nrigau 1980; Boutron 1980). Much more data gathering and detailed sampling should be accomplished in Arctic areas before this question can be adequately answered.

8.5.2.2 Trace Metals - Alpine Glaciers--Few data are available on time-series profiles of trace metals in alpine glacier ice and snow. Jaworoski et al. (1975) reported Cd and Pb values from Storbreen Glacier, Norway. The 1954-72 profiles of Pb show no trend with depth but a slight increase in Cd since 1965 appears. These authors have recently published metal data from a number of alpine glaciers including samples from Norway, the Austrian Alps, the Nepalese Himalayas, the Peruvian Andes, and the Ugandan Ruwenzori (Jaworoski et al. 1981). However, their Pb values from Antarctic snow and ice are orders of magnitude higher than accepted values (Murozumi et al. 1969, Boutron and Lorius 1979, Ng and Patterson 1981); hence, their entire data set must be considered suspect.

Briat (1978) has measured various trace metals in a profile (1948-74) on Mt. Blanc at 4280 m. Much temporal variation occurs in the data, but Briat argues that there has been a two-fold increase of Pb, Cd, and V since 1950 in the precipitation deposited at the Mt. Blanc site.

Based on the review of the literature, with the possible exception of Pb, Zn, and possibly V, one would be hard put to argue that the previous glaciochemical work has shown that fossil-fuel burning has affected the precipitation of glaciated areas. One of the problems with this interpretation, however, is the lack of data, especially from alpine glaciers in both areas close to and remote from man's activities. In addition, the previous alpine glaciochemical studies have produced time-series of only a few years.

In conclusion, the alpine glacier data available could be considered sparse at best, unreliable at worst, and the limited number of glaciers sampled does not provide an adequate picture as to the regional effect of fossil-fuel burning.

8.5.3 Discussion and Future Work

With the exception of Pb, SO_4^{2-}, and NO_3^- in the northern polar regions, little conclusive evidence is available from glacier ice and snow samples to interpret with any certainty the effect of fossil-fuel emissions through time. The large majority of stratigraphic information regarding trace metals and anionic acid species concentrations is from Antarctica and Greenland. Few if any data come from glacier ice and snow in lower latitude areas. Because a very large percentage of fossil-fuel burning takes place in the Northern Hemisphere, the Antarctic data provide little historic insight into past and present anthropogenic emissions. It is apparent, however, that Antarctic data do provide information concerning background concentrations of various chemical constituents in frozen precipitation. Until recently, the glacier data can be termed controversial in that different workers have interpreted the results in different ways (Herron et al. 1977, Murozumi et al. 1969, Boutron 1980, Nriagu 1980, Landy et al. 1980, Boutron and Delmas 1980). The most recent work of Ng and Patterson (1981) and Herron (1982) indicates more than a two-order-of-magnitude increase in Pb in the Greenland area and a factor of two increase in sulfate and nitrate.

Even less information is available from alpine glaciers. Although there is a suggestion that trace metal emissions have increased in alpine ice (Briat 1978) and that anthropogenic nitrate inputs occur in Canadian Rocky glaciers (Butler et al. 1980), it must be emphasized that little definitive information is available at this time to eludicate long-term historic trends in regions where they should be easily detected (i.e., midlatitude alpine regions both close to and remote from emission sites).

Owing to the potential post-depositional modifications inherent in many temperate ice sampling areas, the majority of time-series relationships sought through ice and snow analyses have been conducted on polar glaciers. Information concerning climatic events and hence records potentially pertinent to resolution of chemical time-series in polar regions have been retrieved for periods on the order of 10^0 to 10^4 years (i.e., Cragin et al. 1975, Hammer et al. 1980). Polar glaciers, however, owing to their low accumulation rates (mm to cm yr^{-1}) and unique geographic location provide only a portion of the potential snow and ice core record. Full realization of the potential climatic and, therefore, chemical sequences recoverable from snow and ice studies is currently in progress with the addition of temperate glacier snow and ice cores (i.e., Thompson 1980; Mayewski et al. 1983a,b). These glaciers, by virtue of their higher accumulation rates (cm to m yr^{-1}), provide short-term time series (10^0 to 10^2 yr) with considerable sub-annual detail. Proper selection of temperate glacier core sites, most particularly with respect to elevation and latitude is necessary if pristine snow and ice samples, unaffected by post-depositional effects such as melting and diffusion are to be recovered (Murphy 1970, Oeschger et al. 1977, Thompson 1980, Davies et al. 1982, Mayewski et al. 1983b). As Hastenrath

(1978) has demonstrated through direct measurement of net short- and long-wave radiation and albedo on Quelccaya ice cap, Peru, a condition of zero to negligible glacier surface melt can be maintained if the sampling site is at a high enough altitude, in this case 5400 m, even at 13° 56' latitude.

Although the recent work of Herron (1982) has contributed greatly to understanding the effect of fossil-fuel burning on precipitation in remote northern polar regions, more detailed ice sampling and analyses of the past 100 to 150 years record would provide a better comparison with records such as fossil-fuel burning through time in the Northern Hemisphere.

Sampling on glaciers requires great care in sample collection, handling, and analysis (Murozumi et al. 1969, Vosters et al. 1970, Boutron 1979c, Boutron and Martin 1979, Boutron and Delmas 1980). With the advent of "ultraclean" laboratories and procedures as well as more sophisticated coring and/or sampling devices (e.g., teflon coated augers and PICO's new all kevlar coring unit) this, we believe, can be accomplished for at least the anionic species of interest. If care in sample acquisition and handling is taken, modern analytical techniques such as isotope dilution mass spectrometry, flameless atomic absorption, auto-analyzer visible spectrophotometry, and ion chromatography can be used to determine the various chemical species of interest at extremely low levels.

To ascertain what is controlling the pH of the snow and ice sampled, ionic balances must also be undertaken (Granat 1972). This should at least involve determining NO_3^-, and SO_4^{2-} as well as Cl^- and NH_4^+. If possible Na^+, K^+, Ca^{2+}, Mg^{2+}, and PO_4^{3-} should also be determined in each sample. With this information the strong mineral acid contribution to the total H^+ concentration can be determined independently of pH or acid titration measurements. In addition to the glaciochemical studies, more information is needed on possible aerosol-snow fractionation and aerosol source location. Perhaps the most serious concern raised regarding the use of glaciochemistry as an historic time-series tool is the possibility that atmospheric compositions are not fully represented in resultant surface snow compositions. Although the correlation between the compositions at the South Pole were good (Zoller et al. 1974), similar studies in the Arctic yielded no correlation (Rahn and McCaffrey 1979).

Superimposed on these problems are the effects of seasonality of transport in the northern polar region (Rahn and McCaffrey 1980, Rahn et al. 1980), as well as the time lapsed between precipitation events (i.e., dry vs wet deposition) and snow-air fractionation (Rahn and McCaffrey 1979, Davidson et al. 1981). Rahn and McCaffrey (1980) have suggested that winter Arctic aerosols originate from polluted European sources and hence contribute fossil-fuel emission products to northern polar ice and snow. In addition, in the case of sulfate, the record in ice cores may be dampened with respect to what is observed in the atmosphere (Scott 1981). This demonstrates the need for complimentary air and snow/ice studies to evaluate properly the results of the latter. Little doubt exists that the aerosol-snow link requires extensive study and that aerosol studies are needed in conjunction with surface snow and ice sampling to enhance the resolution capabilities of such snow/ice studies (Davidson et al. 1981).

In addition, aerosol source and possible cyclicity in source(s) must be investigated in more detail. Source discrimination for certain chemical species has been undertaken in some glaciochemical studies (Gorham 1958a, Cragin et al. 1975, Busenberg and Langway 1979, Herron 1982). An effort should be made to better qualify the source of acids to the snow and ice. Samples could be analyzed for F^- using ion chromatography (Herron 1982). Samples with high F^- concentrations may have had a significant input of volcanic acid (Lazrus et al. 1979, Stoiber et al. 1980). Table 8-14 summarizes the potential sources of chemical species in the atmosphere and hence glacier snow and ice, with estimations of spatial and temporal controls on the input of these species to glacier sampling sites. As an example of the type of data needed to quantify the approach taken in Table 8-14, decreases in chemical concentration as a function of distance in Antarctica (Boutron et al. 1972, Johnson and Chamberlain 1981) have been investigated. This type of information is needed if a more quantitative assessment of anthropogenic vs natural sources is to be made. Determining metal or acid sources may also clarify the nature and cause of the high aerosol enrichment factors observed for most volatile elements, even in remote areas (Dams and DeJonge 1976, Davidson et al. 1981). Knowledge of the acid source in frozen precipitation is necessary if the problem of acid precipitation is to be completely understood.

8.6 CONCLUSIONS

The following conclusions may be drawn from the preceding discussion of deposition monitoring.

- Although precipitation sampling networks have been operated many times at many locations, assessments of national or regional patterns and trends must be cautiously used because of variability in the methods of collection and analytical techniques. Usually the networks have been of limited spatial or temporal extent (Section 8.1).

- Bulk sampling, used in many networks, does not generally provide data useful in determining quality of precipitation, although this approach has some potential to estimate total deposition (Section 8.2.3).

- Automatic devices designed to exclude dry deposition can produce wet deposition samples contaminated by dry deposition if the protective lid does not seal the collection bucket tightly. Wet deposition networks should be designed to estimate dry deposition contamination, by site and by chemical element (Section 8.2.3).

- Most precipitation chemistry networks have only measured the soluble fraction of the major inorganic ions. This procedure is reasonable for acidic wet deposition studies because these complements generally can be used to predict a pH that is close to the measured pH, especially for samples with pH less than 5.0 (Section 8.2.3).

- Understanding reasons for pH changes sometimes observed during handling and storage requires consideration of other chemical constituents and measurement of both the soluble and insoluble fractions (Section 8.2.3).

TABLE 8-14. POTENTIAL SOURCES FOR CHEMICAL SPECIES FOUND IN SAMPLES OF GLACIER ICE

Chemical Species	*1,4,5 Biogenic Emission	1,2,4,5,6 Crustal Weathering	1,2 Lightning Discharge	1,2,4,5 Seasalt	2,4,5 Volcanism	1,2,3,4,5 Anthropogenic Emission
Cl^-				▬	▬	
SO_4^{2-}	▬	▬ ? ▬		▬	▬	▬
NO_3^-	▬		▬		▬	▬
NH_4^+	▬		▬		▬ ? ▬	▬
PO_4^{3-}	▬	▬			▬ ? ▬	▬
Ca^{2+}		▬		▬		
Mg^2		▬		▬		
Na^+		▬		▬		
K^+	▬	▬		▬		▬
SiO_2		▬			▬ ? ▬	
Fe^{+2} & $+3$		▬				▬
Al^{+2} & $+3$		▬				▬
Mn^{+2} & $+4$		▬				▬
Volatile trace metals (Pb, Hg)	▬ ?	▬			▬	▬

* Source Characteristics

? - species production from this source uncertain.

Temporal Distribution
- 1 - cyclic (seasonal)
- 2 - non-cyclic (inter-annual &/or intra-annual)
- 3 - significant only as of post-AD 1850

Spatial Distribution and magnitude of species
- 4 - distance &/or elevation source to site
- 5 - atmospheric circulation pattern source to site
- 6 - aerial distribution of local ice-free terrain

(increasing importance of factors such as 5 (i.e., monsoonal flow) and 6 increase likelihood of 1 compared to 2)

- Sampling networks should be operated for periods of many years to determine variability in the general patterns of precipitation quality. Deposition patterns over time are highly variable because they include the variability of both the ion concentration and the precipitation amount patterns (Sections 8.2.3 and 8.2.4).

- Regional and national wet deposition networks with automatic collectors have been operated continuously in the United States and Canada since the late 1970's (Section 8.2.4).

- These networks provide reasonable resolution of major ion concentrations for eastern precipitation but, to date, only an indication of what western patterns might generally be. The difference in sampling site density accounts for the difference in our knowledge of precipitation chemistry in the two areas. Inadequate site density in the west will be corrected in the near future through the National Trends Network (Section 8.4.1).

- Maximum sulfate, nitrate, and hydrogen ion concentrations in precipitation are observed in the northeast quadrant of the United States. Levels decrease to the west, south, and northeast toward New England. Elevated levels extend into southeastern Ontario, Canada (Section 8.4.1).

- Highest calcium concentrations occur in the central regions of the United States (Section 8.4.1).

- Highest chloride concentrations occur along the coasts, consistent with a marine source (Section 8.4.1).

- Patterns for each of these ions are fairly consistent with the known source regions (Section 8.4.1).

- On the broad scale, nitrate in U.S. precipitation has likely increased since the 1950's, in conjunction with NO_x emissions increases (Section 8.4.3.1).

- Calcium measured in U.S. precipitation has decreased, perhaps due to lack of extreme drought recently as compared to the 1950's, but more certainly due to improved sampling procedures (Section 8.4.3.3).

- A combination of drought effects, the mixing of urban data with more regionally representative data, and the mixing of bulk data and lower quality wet-only data with higher quality wet-only data, has led to statements concerning increasing acidity of precipitation which are quantitatively difficult to support. In general, it appears difficult to use historical U.S. network data to discern the precipitation pH time trend as related to the acid precursor emissions (Section 8.4.3.2).

- The most reliable long-term trends for precipitation chemistry are available for the Hubbard Brook Forest site in New Hampshire (record continuous since 1964). The nitrate data record suggests an erratic

trend of increasing nitrate from 1964 to about 1971, followed by a leveling off or slight decrease from 1971 to 1981. Wet sulfate at the site declined by about 33 percent from 1965-66 to 1979-80. Emissions of NO_x and SO_x are generally consistent with these observations for wet sulfate and nitrate. Although the emissions for the Northeast track the wet deposition record especially well, it is not yet possible to reliably and quantitatively separate out the contribution from long-range vs short-range transport. From 1964-77 there was no statistically significant trend in precipitation pH at the Hubbard Brook site (Sections 8.4.3.1 and 8.4.3.2).

- Sulfate and hydrogen ion concentrations are much higher in warm season precipitation in the eastern United States than in cold season precipitation. The trend follows the aerosol sulfate trend but not the trend of SO_x emissions (Section 8.4.4).

- Although precipitation pH in the northeastern United States has been reported to have decreased in the past 20 to 30 years, several recent reevaluations have suggested that the data do not support the idea of a sharply decreasing pH trend (Section 8.4.3.2).

- Remote site pH data indicate that the common reference to the CO_2 atmospheric equilibrium value of pH 5.6 is of limited value. Recent measurements in Hawaii and other locations not strongly influenced by alkaline dust, have indicated that the average precipitation pH is less than 5.0. Samples at some remote sites have been found to be chemically unstable, with pH rising with time, due to organic acid loss. These relatively acid samples at remote sites need to be explained to better understand the acidic samples in areas with strong anthropogenic influences (Section 8.4.2).

- Air trajectory analysis, frequently applied to precipitation chemistry in attempts to identify important source regions for receptor sites, is qualitative at best. Degree of success probably varies with location. Applying this fairly simple approach to such a complex problem leads to doubts about the utility of the approach (Section 8.4.6).

- Wet and dry deposition processes are roughly of equal importance in the average deposition of specific chemical species (Section 8.3.1)

- Direct methods of monitoring dry deposition consist of collecting vessels, surrogate surfaces, and concentration monitoring from which deposition rates are inferred. The latter applies to trace gases and small particles (< 1 to 5 μm diameter), i.e., where deposition is not controlled by gravity. Surrogate surface methods apply to particles of a size controlled by gravity and gases for which species-specific surfaces are used to evaluate air concentrations (Section 8.3.2.1)

- Micrometeorological methods have been developed as alternative monitoring techniques for surface fluxes. These include eddy-accumulation, modified Bowen ratio, and variance (Section 8.3.2.2)

- Limited data are available on which to base estimates of dry deposition rates using concentration techniques. A study conducted for sulfate, nitrate, and ammonium in aerosol measured in the surface boundary layer had a resolution of four-hour intervals and gave average diurnal cycles of near-surface concentrations (Section 8.3.3)

- Snow and ice cores collected from appropriately chosen glaciers provide samples of entrapped chemical species. This technique has barely been applied to the study of acid precipitation despite the fact that it provides a very sensitive record of precipitation chemistry. Little definitive information is available at this time to elucidate long-term historic trends in regions where they should be easily detected (i.e., midlatitude alpine regions both close to and remote from emission sites) (Section 8.5.3).

8.7 REFERENCES

Allen, L. H., Jr., R. J. Hanks, J. K. Aase, and H. R. Gardner. 1974. Carbon dioxide uptake by wide-row grain sorghum computed by the profile Bowen-ratio. Agronomy J. 66:35-41.

Andren, A. W. and S. E. Lindberg. 1977. Atmospheric input and origin of selected elements in Walker Branch Watershed, Oak Ridge, Tennessee. Water, Air, Soil Pollut. 8:199-215.

Anderssen, A. M., A. H. Johnson, and T. G. Siccama. 1980. Levels of Pb, Cu and Zn in the forest floor of the northeastern U.S. J. Environ. Qual. 9:293-296.

Aristarain, A. J. 1980. Otude glaciologique de la callote polaire de L'ile James Ross (Peninsule Antarctique) CNRS Lab. de Glaciol. et Geophys. de L'Environ. 322. 130 p.

Ashworth, J. R. 1941. Atmospheric pollution and the deposit gauge. Weather 3:137-140.

Barrie, L. A. and A. Sirois. 1982. An analysis and assessment of precipitation chemistry measurements made by CANSAP (The Canadian Network for Sampling Precipitation): 1977-1980. Report AQRB-82-003-T. Atmospheric Environment Service, Downsview, Canada. 163 pp.

Barrie, L. A., J. L. Walmsley. 1978. A study of sulphur dioxide deposition velocities to snow in northern Canada. Atmos. Environ. 12: 2321-2332.

Barrie, L. A., J. M. Hales, K. G. Anlauf, J. Wilson, A. Wiebe, D. M. Whelpdale, G. J. Stensland, and P. W. Summers. 1982. Preliminary data interpretation. U.S. Canadian MOI, Monitoring and Interpretation Sub-Group, Report No. 2F-I.

Barrie, L. A., H. A. Wiebe, K. Anlauf, and P. Fellin. 1980. The Canadian air and precipitation monitoring network APN, pp. 355-365. In Atmospheric Pollution 1980. M. M. Benarie, ed. Studies in Environmental Science, Vol. 8. Elsevier Scientific Publishing Company, Amsterdam.

Berner, W., B. Stauffer, and H. Oeschger. 1978. Past atmospheric composition and climate, gas parameters measured on ice cores. Nature 276:53-55.

Bertine, K. K. and E. D. Goldberg. 1971. Fossil Fuel combustion and the major sedimentary cycle. Science 173:233-235.

Bonsang, B., B. C. Nguyen, A. Gaudry, and G. Lambert. 1980. Sulfate enrichment in marine aerosols owing to biogenic gaseous sulfur compounds. J. Geophys. Res. 85:7410-7416.

Boutron, C. 1979a. Past and present day troposheric fallout fluxes of Pb, Cd, Cu, Zn and Ag in Antarctica and Greenland. Geophys. Res. Lett. 6:159-162.

Boutron, C. 1979b. Trace element of snows of Greenland along an east-west transect. Geochim. Cosmochim. 43:1252-1258.

Boutron, C. 1979c. Reduction of contamination problems in sampling of Antarctic snows for trace element analysis. Analytica Chimica Acta 106:127-130.

Boutron, C. 1980. Trace metals in remote Antarctica snows: Natural or anthropogenic? Nature 284:575-576.

Boutron, C. 1983. Respective influence of global pollution and volcanic eruptions on the past variations of the trace metals content of Antarctica snows since 1880's. J. Geophys. Res. In press.

Boutron, C. and R. Delmas. 1980. Historical record of global atmospheric pollution revealed in polar ice sheets. Ambio 9:210-215.

Boutron, C. and C. Lorius. 1977. Trace element content in East Antarctic snow samples. I.A.H.S. Publ. 118:164-171.

Boutron, C. and C. Lorius. 1979. Trace metals in Antarctica snows since 1914. Nature 277:551-554.

Boutron, C. and S. Martin. 1979. Preconcentration of dilute solutions at the 10^{-12} g/g level by nonboiling evaporation with variable variance calibration curves. Analytical Chem. 51:140-145.

Boutron, C., M. Echevin, and C. Lorius. 1972. Chemistry of polar snows. Estimation of rates of deposition in Antartica. Geochim. Cosmochim. Acta 36:1029-1041.

Bowersox, V. C. and R. G. dePena. 1980. Analysis of precipitation chemistry at a central Pennsylvania site. J. Geophys. Res. 85:5614-5620.

Bowersox, V. C. and G. J. Stensland. 1981. Seasonal patterns of sulfate and nitrate in precipitation in the United States. In Proceedings of the 74th Annual Meeting, Air Pollution Control Association, Philadelphia, PA. June 21-26. Paper No. 81-6.1.

Brezonik, P. L., E. S. Edgerton, and C. D. Hendry. 1980. Acidic precipitation and sulfate deposition in Florida. Science 208:1027-1029.

Briat, M. 1978. Evaluation of level of Pb, V, Cd, Zn and Cu in the snow of Mt. Blanc during the last 25 years. Atmos. Pollut. 1:225-227.

Busenberg, E. and C. C. Langway, Jr. 1979. Levels of ammonium, sulfate, chloride, calcium and sodium in snow and ice from southern Greenland. J. Geophys. Res. 84:1705-1708.

Butler, D., B. Lyons, J. Hassinger, and P. A. Mayewski. 1980. Shallow core snow chemistry of Athabaska Glacier, Alberta. Canadian J. Earth Sciences 17:278-281.

Chamberlain, A. C. 1980. Dry deposition of sulfur dioxide, pp. 185-197. In Atmospheric Sulfur Deposition. D. S. Shriner, C. R. Richmond, and S. E. Lindberg, eds. Ann Arbor Science, Ann Arbor, MI. 568 pp.

Charlson, R. J. and H. Rodhe. 1982. Factors controlling the acidity of natural rainwater. Nature 295:683-685.

Clark, H. L., K. E. Clark, and B. L. Haines. 1980. Acid rain in Venezuelan Amazon. In Tropical Ecology and Development, p. 683, International Society of Tropical Ecology, Kuala Lumper, Malaysia.

Clarke, R. H., A. J. Dyer, R. R. Brook, D. G. Reid, and A. J. Troup. 1971. The Wangara experiment: Boundary-layer data. Tech. Paper No. 19, CSIRO, Division of Meteorological Physics, Aspendale, Victoria, Australia. 362 pp.

Clement, P. and J. Vandour. 1967. Observations on the pH of melting snow in the Southern French Alps. Arctic Alpine Environ. 205-213.

Cogbill, C. V. and G. E. Likens. 1974. Precipitation in the northeastern United States. Water Resour. Res. 10:1133-1137.

Cowling, E. B. 1982. Acid precipitation in historical perspective. Environm. Sci. Technol. 16(2):110A-123A.

Cragin, J. H., M. M. Herron, and C. C. Langway, Jr. 1975. The chemistry of 700 years of precipitation at Dye 3, Greenland. Cold Regions Research and Engineering Laboratory, Research Report 341.

Dams, R. and J. DeJonge. 1976. Chemical composition of Swiss aerosols from the Jungfraujoch. Atmos. Environ. 10:1079-1084.

Dana, M. T. 1980. Distribution of contaminants. Research Report To American Electric Power Corporation by Battelle Columbus Laboratories, Columbus, OH. 79 pp.

Dana, M. T., J. M. Hales, and M. A. Wolf. 1975. Rain scavenging of SO_2 and sulfate from power plant plumes. J. Geophys. Res. 80:4119-4129.

Dasch, J. M. 1982. A comparison of surrogate surfaces for dry deposition monitoring, Proceedings 4th International Conference on Precipitation Scavenging, Dry Deposition, and Resuspension, Santa Monica, California, 23 November to 3 December 1982.

Davidson, C. I., J. M. Miller, and M. A. Pleskow. 1982. The influence of surface structure on predicted particle dry deposition to natural grass canopies. Water, Air, and Soil Pollut. 18:25-43.

Davidson, C. I., C. Liyang, T. C. Grimm, M. Nasta, and M. P. Qumooss. 1981. Wet and dry deposition of trace elements into the Greenland ice sheet. Atmos. Environ. 15:1-9.

Davies, T. D., C. E. Vincent, and P. Brimblecombe. 1982. Preferential elution of strong acids from a Norwegian ice cap. Nature 300:161-163.

Dawson, G. A. 1978. Ionic composition of rain during sixteen convective showers. Atmos. Environ. 12:1991-1999.

Delmas, R. J. 1982. Antarctic sulphate budget. Nature 299:677-678.

Delmas, R. and A. Aristarain. 1979. Recent Evolution of Strong Acidity of Snow at Mt. Blanc. Proc. 13th Inter. Coll., Atm. Pollut., Volume 1, Elsevier, Amsterdam 233-237.

Delmas, R. and C. Boutron. 1978. Sulfate in Antarctic snow: Spatio-temporal distribution. Atmos. Environ. 12:723-728.

Delmas, R. and C. Boutron. 1980. Are the past variations of the stratospheric sulfate burden recorded in central Antarctic snow and ice layers? J. Geophys. Res. 85:5645-5649.

Delmas, R., A. Aristarain, and M. Legrand. 1980a. The acidity of polar precipitation: a natural reference level for acid rains. In Ecological Impact of Acid Precipitation. D. Drablos and A. Tollan, eds. Proc. of an International Conference, Sandefjord, Norway. SNSF Project, Oslo.

Delmas, R., J. M. Ascencio, and M. Legrand. 1980b. Polar ice evidence that atmospheric CO_2 20,000 year B. P. was 50% of present. Nature 284:155-157.

Delmas, R., M. Briat, and M. Legrand. 1982. Chemistry of south polar snow. J. Geophys. Res. 87:4314-4318.

dePena, R. G., J. A. Pena, and V. C. Bowersox. 1980. Precipitation collectors intercomparison study. Dept. of Meteorology, The Pennsylvania State University, State College. 57 pp.

Desjardins, R. L. 1977. Energy budget by an eddy correlation method. J. Appl. Meteorol. 16:248-250.

Dillon, P. J., D. S. Jeffries, and W. A. Scheider. 1982. The use of calibrated lakes and watersheds for estimating atmospheric deposition near a large point source, Water, Air, and Soil Pollut. 18:241-250.

Dolske, D. A. and F. D. Gatz. 1982. A field intercomparison of sulfate dry deposition monitoring and measurements methods: Preliminary results, presented at the American Chemical Society Acid Rain Symposium, Las Vegas, Nevada. 30 March, 1982.

Dovland, H., and A. Eliassen. 1976. Dry deposition on a snow surface, Atmos. Environ. 10:783-785.

Eaton, J. S., G. E. Likens, and F. H. Bormann. 1978. The input of gaseous and particulate sulfur to a forest ecosystem. Tellus 30:546- 551.

Elgmork, K., A. Hagen, and A. Langfland. 1973. Polluted snow in southern Norway during the winters, 1968-1971. Environ. Pollut. 4:41-52.

Eriksson, E. 1952. Composition of atmospheric precipitation. Tellus 4:280-303.

Fisher, D., A. Gambell, G. Likens, and F. Bormann. 1968. Atmospheric contributions to water quality of streams in the Hubbard Brook Experimental Forest, New Hampshire. Water Resour. Res. 4:1115-1126.

Flegal, A. R. and C. C. Patterson. 1982. Lead in the central Pacific (Abstract). Amer. Geophys. Union:L041A-15.

Forland, E. J. 1973. A study of the acidity in the precipitation in southwestern Norway. Tellus 25:291-298.

Foster, J. F., G. H. Beatty, and J. E. Howes, Jr. 1974a. Final report on interlaboratory cooperative study of the precision and accuracy of the measurement of dustfall using ASTM method D1739, ASTM Data Series Publication DS 55-S4. 45 pp.

Foster, J. F., G. H. Beatty, and J. E. Howes, Jr. 1974b. Final report on interlaboratory cooperative study of the precision and accuracy of the measurement of sulfation in the atmosphere using ASTM method D2010, ASTM Data Series Publication DS 55-S2. 45 pp.

Galloway, J. N. and G. E. Likens. 1976. Calibration of collection procedures for the determination of precipitation chemistry. Water, Air and Soil Pollut. 6:241-258.

Galloway, J. N. and G. E. Likens. 1978. The collection of precipitation for chemical analysis. Tellus 30:71-82.

Galloway, J. N. and G. E. Likens. 1979. Atmospheric enhancement of metal deposition in Adirondack lake sediments. Limnol. Oceanogr. 24:427-433.

Galloway, J. N. and D. M. Whelpdale. 1980. An atmospheric sulfur budget for eastern North America. Atmos. Environ. 14:409-417.

Galloway, J. N., B. J. Cosby, and G. E. Likens. 1979. Acid precipitation: Measurement of pH and acidity. Limnol. Oceanogr. 24:1161-1165.

Galloway, J. N., G. E. Likens, W. C. Keene, and J. M. Miller. 1982. The composition of precipitation in remote areas of the world. J. Geophys. Res. 87:8771-8786.

Gatz, D. F. 1980. Associations and mesoscale spatial relationships among rainwater constituents. J. Geophys. Res. 85:5588-5598.

GCA Corporation. 1980. Acid Rain Information Book - Draft Final Report. DOE Contract AC02-79EV10273-1, GCA Corp., Bedford, MA.

Gorham, E. 1958a. Atmospheric pollution by hydrochloric acid. Quart. J. Royal Meteorol. Soc. 84:274-276.

Gorham, E. 1958b. The salt content of some ice samples from Nordaustlandet (North East Land) Svalbard. J. Glaciol. 3:181-186.

Granat, L. 1972. On the relation between pH and the chemical composition in atmospheric precipitation. Tellus 24:550-560.

Granat, L. 1978. Sulfate in precipitation as observed by the European atmospheric chemistry network. Atmos. Environ. 12:413-424.

Granat, L., R. Soderlund, and L. Backlin. 1977. The IMI network in Sweden - present equipment, methods and plans for improvement. International meteorological Institute in Stockholm Report AC-40 (November 1977).

Haines, B. 1983. Forest ecosystem SO_4-S input-output discrepancies and acid rain: Are they related. Oikos 41:139-143.

Hammer, C. U. 1977. Past volcanism revealed by Greenland ice sheet impurities. Nature 270:482-486.

Hammer, C. U. 1980. Acidity of polar ice cores in relation to absolute dating, past volcanism and radio-echoes. J. Glaciology 25:359-372.

Hammer, C. U., H. B. Clausen, and W. Dansgaard. 1980. Greenland ice sheet evidence of past-glacial volcanism and its climatic impact. Nature 288:230-235.

Hansen, D. A. and G. M. Hidy. 1982. Review of questions regarding rain acidity data. Atmos. Environ. 16:2107-2126

Hansen, D. A., G. M. Hidy, and G. J. Stensland. 1981. Examination of the basis for trend interpretation of historical rain chemistry in the Eastern United States. ERT P-A097, Environmental Research and Technology, Inc., Westlake Village, CA.

Hardy, E. P., Jr. and J. H. Harley, eds. 1958. Environmental contamination from weapons tests. U.S. AEC Health and Safety Laboratory Report HASL-42A.

Hastenrath, S. 1978. Heat budget measurements on the Quelccaya ice cap, Peruvian Andes. J. Glaciology 20:85-97.

Herman, F. and F. Gorham. 1957. Total mineral material, acidity, sulfur and nitrogen in rain and snow at Kentville, Nova Scotia. Tellus 9:180-183.

Herrara, R. A. 1979. Nutrient distribution and cycling in an Amazonian caatinga forest on spodosols in Southern Venezuela. Ph.D. Thesis, Dept. of Soil Science, Univ. of Reading, England.

Herron, M. M. 1982. Impurities of F^-, Cl^-, NO_3^-, and SO_4^{2-} in Greenland and Antarctic precipitation. J. Geophys. Res. 87(C4):3052-3060.

Herron, M. M. and C. C. Langway, Jr. 1979. Dating of Ross Ice Shelf cores by chemical analysis. J. Glaciology 24:345-357.

Herron, M. M., C. C. Langway, H. V. Weiss, and J. H. Cragin. 1977. Atmospheric trace metals and sulfate in the Greenland ice sheet. Geochim. Cosmochim. Acta 41:915-920.

Hewson, E. W. 1951. Atmospheric pollution, pp. 1139-1157. In Compendium of Meteorology. American Meteorological Society, Boston, MA., 1334 pp.

Hicks, B. B. 1981. An analysis of Wangara micrometeorology: surface stress, sensible heat, evaporation, and dewfall. NOAA Technical Memorandum ERL ARL-104. June 1981. 34 pp.

Hicks, B. B. 1982. Measurement techniques: dry deposition. Presented at the National Research Council (Canada) Symposium on Monitoring and Assessment of Airborne Pollutants with Special Emphasis on Long Range Transport and Deposition of Acidic Materials. August 30- September 1, Ottawa, Canada (NOAA/ARATDL Cont. No. 82/7).

Hicks, B. B. and M. L. Wesely. 1980. Turbulent transfer processes in the canopy and at vegetation surfaces, pp. 199-207. In Atmospheric Sulfur Deposition. D. S. Shriner, C. R. Richmond, and S. E. Lindberg, eds.). Ann Arbor Science, Ann Arbor, MI. 568 pp.

Hicks, B. B., M. L. Wesely, and J. L. Durham. 1980. Critique of methods to measure dry deposition (workshop summary). U.S. EPA Report EPA-600/9-80-050, 69 pp. NTIS PB81-126443.

Hidy, G. M. 1982. Bridging the gap between air quality and precipitation chemistry. Water, Air, Soil Pollut. 18:191-198.

Hidy, G. M., D. A. Hansen, R. G. Hendry, K. Ganesan, and J. Collins. 1984. Trends in historical acid precursor emissions and their airborne and precipitation products. J. Air Pollut. Contr. Assoc. 31(4):333-353.

Hilst, G. R., P. K. Mueller, G. M. Kidy, T. F. Lavery, and J. G. Watson. 1981. EPRI Sulfate Regional Experient: Results and Implications. Electric Power Research Institute, Palo Alto, California. Report No. EA-2165-SY-LD.

Hornbeck, J. W. 1981. Acid rain: Facts and fallacies. J. Forestry 79:438-443

Jaworoski, Z., M. Bysiek, and L. Kownacka. 1981. Flow of metals into the global atmosphere. Geochim. Cosmochim. Acta 45:2185-2199.

Jaworowski, Z., J. Bilkiewicz, E. Dobosz, and L. Wodkiewicz. 1975. Stable and radioactive pollutants in a Scandinavian glacier. Environ. Pollut. 9:305-315.

Jeffries, D. S. and W. R. Snyder. 1981. Atmospheric deposition of heavy metals in central Ontario. Water, Air, Soil Pollut. 15:127-152.

Jickells, T., A. Knap, T. Church, J. Galloway, and J. Miller. 1982. Acid rain on Bermuda. Nature 297:55-57

Johnson, B. B. and J. M. Chamberlain. 1981. Sodium, magnesium, potassium and calcium concentrations in ice cores from the Law Dome, Antarctica. Geochim. Cosmochim. 45:771-776.

Johnson, S. A., R. Kumar, P. T. Cunningham, and T. A. Lang. 1981. The MAP3S aerosol sulfate acidity network: a progress report and data summary. Argonne National Laboratory Report ANL-81-63. 139 pp.

Jordan, C., F. Golley, J. Hall, and J. Hall. 1980. Nutrient scavenging of rainfall by the canopy of an Amazonian rain forest. Biotropica 12:61.

Junge, C. E. 1958. The distribution of ammonia and nitrate in rain water over the United States. Trans. Amer. Geophys. Union 39:241-248.

Junge, C. E. 1963. Air Chemistry and Radioactivity. Academic Press, New York. 382 pp.

Keene, W. C., J. N. Galloway, and J. D. Holden. 1983. Measurements of weak organic acidity in precipitation from remote areas of the world. J. Geophys. Res. 88:5122-5130.

Kerr, R. A. 1981. Pollution of the Arctic atmosphere confirmed. Science 212:1013-1014.

Koerner, R. M. and D. Fisher. 1982. Acid snow in the Canadian high arctic. Nature 295:137-140.

Koide, M. and E. D. Goldberg. 1971. Atmospheric sulfur and fossil fuel combustion. J. Geophys. Res. 76:6589-6595.

Koide, M., E. D. Goldberg, M. M. Herron, and C. C. Langway. 1977. Transuranic depositional history in South greenland firn layers. Nature 269:137-139.

Koide, M. K., R. Michel, E. D. Goldberg, M. M. Herron, and C. C. Langway, Jr. 1979. Depositional History of artificial radionuclides in the Ross Ice Shelf, Antarctica. Earth Planetary Sci. Lett. 44:205-223.

Kyle, P., J. Palais, and R. Delmas. 1982. The volcanic record of Antarctic ice cores: Preliminary results and potential for future investigations. Annals of Glaciology 3:172-177.

Landy, M. P. and D. A. Peel. 1981. Short term fluctuations in heavy metal concentrations in Antarctic snow. Nature 291:144-146.

Landy, M. P., D. A. Peel, and E. W. Wolff. 1980. Trace metals in remote Arctic snows: natural or anthropogenic? Nature 284:574-574.

Langway, C. C., Jr. 1970. Stratagraphic analysis of a deep ice core from Greenland. The Geological Society of America. Special Paper 125.

Langway, C. C., J. H. Cragin, G. A. Klouda, and M. M. Herron. 1975. Seasonal variations of chemical continuents in annual layers of Greenland deep ice deposits. CRREL Rpt. 347. 5pp.

Lantzy, R. J. and F. T. Mackenzie. 1979. Atmospheric trace metals: global cycles and assessment of man's impact. Geochim. Cosmochim. Acta 43:511-525.

Larson, T. E. and I. Hettick. 1956. Mineral composition of rainwater. Tellus 8:191-201.

Lawson, D. R. and J. W. Winchester. 1979. Sulfur, Potassium and Phosphorus Associations in Aerosols from South American Tropical Rain Forests. J. Geophys. Res. 84:3723-3727.

Lazrus, A. L., R. D. Cadle, B. W. Gandrud, J. P. Greenberg, B. J. Huebert, and W. I. Rose. 1979. Sulfur and halogen chemistry of the stratosphere and of volcanic eruption plumes. J. Geophys. Res. 84:7869-7875.

Legrand, M. R., A. J. Aristarain, and R. J. Delmas. 1982. Acid titration of polar snow. Anal. Chem. 54:1336-1339.

Lepel, E. A., K. M. Stefansson and W. H. Zoller. 1978. The enrichment of volatile elements in the atmosphere by volcanic activity: Augustine Volcano 1976. J. Geophys. Res. 83:6213-6220.

Lerman, A. 1979. Geochemical Processes: Water and Sediment Environment. John Wiley and Sons, New York. 481 pp.

Leuning, R., M. H. Unsworth, H. N. Newman, and K. M. King. 1979. Ozone fluxes to tobacco and soil under field conditions. Atmos. Environ. 13: 1155-1163.

Lewis, W. M., Jr. and M. C. Grant. 1980. Acid precipitation in the Western United States. Science 207:176-177.

Li, Ta-Yung and H. E. Landsberg. 1975. Rainwater pH close to a major power plant. Atmos. Environ. 9:81-88.

Likens, G. E. 1976. Acid precipitation. Chem. Eng. News 54:29-44.

Likens, G. E. and F. H. Bormann. 1974. Acid rain: a serious regional environmental problem. Science 184:1176-1179.

Likens, G. E. and T. J. Butler. 1981. Recent acidification of precipitation in North America. Atmos. Environ. 15:1103-1109.

Lindberg, S. E., and G. M. Lovett, 1982; Dry deposition of particles to inert and foliar surfaces in a foresting canopy, Proceedings 4th International Conference on Precipitation Scavening, Dry Deposition, and Resuspension, Santa Monica, California, 28 November to 3 December 1982.

Lindberg, S. E. and R. C. Harriss. 1981. The role of atmospheric deposition in an eastern U.S. deciduous forest. Water, Air, Soil Pollut. 16:13-31.

Lindberg, S. E., R. C. Harriss, and R. R. Turner. 1982. Atmospheric deposition of metals to forest vegetation. Science 215:1609-1611.

Lyons, W. B., P. A. Mayewski, and N. Ahmad. 1982. Acidity of Recent Himalayan Snow. 38th Eastern Snow Conf.

Mamane, Y., E. Ganor, and A. E. Donagi. 1980. Aerosol composition of urban and desert origin in the eastern Mediterranean I. Water, Air, Soil Pollut. 14:29-43.

Masse, C., and E. Voldner. 1982. Estimation of dry deposition velocities of sulfur over Canada and the United States east of the Rocky Mountains, Proceedings 4th International Conference on Precipitation Scavenging, Dry Deposition, and Resuspension, Santa Monica, California, 28 November to 3 December 1982.

Mayewski, P. A., W. B. Lyons, and N. Ahmad. 1983a. Chemical composition of a high altitude fresh snowfall in the Ladakh Mountains. Geophys. Res. Lett. 10:105-108.

Mayewski, P. A., W. B. Lyons, and N. Ahmad. 1983b. Reconnaissance Glacio-chemical studies in the Indian Himalayas, 38th Eastern Snow Conf. In press.

Meiner, F. X., H. W. Georgii, G. Ockelmann, H. Jager, and R. Reiter. 1981. The arrival of the Mt. St. Helens eruption cloud over Europe. Geophys. Res. Lett. 8:163-166.

Miller, J. M. 1981. Trends in precipitation composition and deposition. Work Group 2, Report 2-14, United States-Canada. Memorandum of Intent, July. Chapter II.

Miller, M. L. and G. E. Everett. 1979. A detailed analysis of the scientific evidence concerning acidic precipitation. Am. Chem. Soc. Meeting. Washington, D.C. 155-157.

Miller, J. M., J. N. Galloway, and G. E. Likens. 1978. Origin of air masses producing acid precipitation at Ithaca, New York. Geophys. Res. Letters 5:757-760.

Miller, J. M., G. J. Stensland, and R. G. Semonin. 1984. The chemistry of precipitation on the island of Hawaii. NOAA Technical Report, Air Resources Laboratory, Rockville, MA. In press.

Murphy, E. J. 1970. The generation of electromotive forces during the freezing of water. J. Colloid and Interface Sci. 32(1):1-11.

Murozumi, M., T. J. Chow, and C. Patteson. 1969. Chemical concentrations of pollutant lead aerosols, terrestrial dusts and sea salts in Greenland and Antarctic snow strata. Geochim. Cosmochim. Acta 33:1247-1294.

National Atmospheric Deposition Program. 1978. National Atmospheric Program Data Reports. Vol. I (1-2). Available from NADP Coordinator's Office, Natural Resource Ecology Laboratory, Colorado State University, Fort Collins, CO.

National Atmospheric Deposition Program. 1979. National Atmospheric Program Data Reports. Vol. II (1-4). Available from NADP Coordinator's Office, Natural Resource Ecology Laboratory, Colorado State University, Fort Collins, CO.

National Atmospheric Deposition Program. 1980. National Atmospheric Program Data Reports. Vol. III (1-4). Available from NADP Coordinator's Office, Natural Resource Ecology Laboratory, Colorado State University, Fort Collins, CO.

National Academy of Sciences. 1978. The Tropospheric Transport of Pollutants and other Substances to the Oceans. National Academy Press, Washington, D.C. 243 pp.

National Academy of Sciences. 1980. The Atmospheric Sciences: National Objectives for the 1980's. National Academy Press, Washington, D.C. 130 pp.

National Academy ofSciences. 1983. Acid Deposition: Atmospheric Processes in Eastern North America. National Academy Press, Washington, D.C. 375 pp.

Ng, A. and C. C. Patterson. 1981. Natural concentrations of lead in ancient Arctic and Antarctic ice. Geochim. Cosmochim. Acta 45:2109-2121.

Niemann, B. L., J. Root, N. Van Zwalenburg, and A. L. Mahan. 1979. An integrated monitoring network for acid deposition: A proposed strategy. Interim report R-023-EPA-79. 236 pp.

Nriagu, J. 1979. Global inventory of natural and anthropogenic emissions of trace metals to the atmosphere. Nature 279:409-411.

Nriagu, J. O. 1980. Trace metals in remote Arctic snows: natural or anthropogenic? Replies. Nature 284:575-577.

Oeschger, H., U. Schotterer, B. Stauffer, W. Haeberli, and H. Rothlisberger. 1977. First results from alpine core drilling projects. Ziet. fur. Gletsch. und Glazial 13:193-208.

Oeschger, H., B. Stauffer, A. Neftel, J. Schwander, and R. Zumbrunn. 1982. Atmospheric CO_2 content in the past deduced from ice-core analysis. Annals of Glaciology 3:227-232.

Ottar, B. 1978. An assessment of the OECD study on long range transport of air pollutants (LFAP). Atmos. Environ. 12:445-454.

Owens, J. S. 1918. The measurement of atmospheric pollution. Quart. J. Roy. Meteorol. Soc. 44:149-170.

Pack, D. H. 1980. Precipitation chemistry patterns: A two-network data set. Science 108:1143-1145.

Pack, D. H. 1982. Precipitation chemistry probability--the shape of things to come. Atmos. Environ. 16:1145-1157.

Pack, D. H. and D. W. Pack. 1980. Seasonal and annual behavior of different ions in acidic precipitation. World Meteorological Organization Special Environmental Report No. 14, 303-313.

Parker, B. C., E. J. Zellar, L. E. Heiskell, and W. J. Thompson. 1977. Nitrogen in South Polar ice and snow: Tool to measure past solar, auroral and cosmic ray activities. Antarctic J. 133-134.

Parker, B. C., E. J. Zellar, and A. J. Gow. 1982. Nitrate fluctuations in Antarctic snow and firn: Potential sources and mechanisms of formation. Annals of Glaciology 3:243-248.

Peden, M. E. and L. M. Skowron. 1978. Ionic stability of precipitation samples. Atmos. Environ. 12:2343-2349.

Radke, L. F. 1982. Sulphur and sulphate from Mt. Erebus. Nature 299:710-712.

Rahn, K. A. and R. J. McCaffrey. 1979. Compositional differences between Arctic aerosol and snow. Nature 280:479-480.

Rahn, K. A. and R. J. McCaffrey. 1980. On the origin and transport of the winter Arctic aerosol. In Aerosols: Anthropogenic and Natural, Sources and Transport. Annals N.Y. Acad. Sci. 338:486-503.

Rahn, K. A., E. Joranger, A. Semb, and T. J. Conway. 1980. High winter concentration of SO_2 in the Norwegian Arctic and transport from Eurasia. Nature 287:824-826.

Raynaud, D., R. Delmas, J. M. Ascencio, and M. Legrand. 1982. Gas extraction from polar ice cores: a critical issue for studying the evolution of atmospheric CO_2 and ice sheet surface elevation. Annals of Glaciology 3:265-272.

Raynor, G. S. and J. V. Hayes. 1981. Acidity and conductivity of precipitation on central Long Island, New York, in relation to meteorological variables. Water, Air, Soil Pollut. 15:229-245.

Risbo, T., H. B. Clausen, and K. L. Rasmussen. 1981. Supernovae and nitrate in the Greenland ice sheet. Nature 294:637-639.

Robertson, J. K., T. W. Dobzine, and R. C. Graham. 1980. Chemistry of precipitation from sequentially sampled storms. U.S. EPA Report 600/4-80-004. p. 116.

Schaule, B. K. and C. C. Patterson. 1981. Lead concentrations in the northeast Pacific: Evidence for global anthropogenic perturbations. Earth Planet. Sci. Lettr. 54:97-116.

Scholander, P. F., E. A. Hemmingsen, L. K. Coachman, and D. C. Nutt. 1961. Composition of Gas Bubbles in Greenland Ice Bergs. J. Glaciology 3:813-822.

Scott, B. C. 1981. Sulfate washout ratios in winter storms. S. Appl. Meteorol. 20:619-625.

Settle, D. M., C. C. Patterson, K. K. Turekian, and J. K. Cochran. 1982. Lead precipitation fluxes at tropical oceanic sites determined from Pb^{210} measurements. J. Geophys. Res. 87(C2):1239-1245.

Sequeria, R. 1981. Acid Rain: some preliminary results from global data analysis. Geophys. Res. Lett. 8:147-150.

Shannon, J. D. 1981. A model of regional long-term average sulfur atmospheric pollution, surface removal, and net horizontal flux. Atmos. Environ. 13:1155-1163.

Shaw, G. E. 1982a. Evidence for a central Eurasian source area of Arctic haze in Alaska. Nature 299:815-818.

Shaw, G. E. 1982b. On the residence time of the Antarctic ice sheet sulfate aerosol. J. Geophys. Res. 87(C6):4309-4313.

Sheih, C. M., M. L. Wesely, and B. B. Hicks. 1979. Estimated dry deposition velocities of sulfur over the eastern United States and surrounding regions, Atmos. Environ. 13:1361-1368.

Shirahata, H., R. W. Elias, C. C. Patterson, and M. Koide. 1979. Chronological variations in concentrations and isotopic compositions of anthropogenic lead in sediments of a remote subalpine pond. Contribution #3186: Division of Geological and Planetary Sciences. Cal. Inst. Tech.

Sickles, J. E. III, W. D. Bach, and L. L. Spiller. 1982. Comparison of several techniques for determining dry deposition flux, Proceedings 4th International Conference on Precipitation Scavenging, Dry Deposition and Resuspenion, Santa Monica, California, 28 November to 3 December 1982.

Smith, R. A. 1872. Air and Rain - The Beginnings of a Chemical Climatology. Longmans, Green, and Co., London, England.

Spicer, C. W. and P. M. Schumacher. 1977. Interferences in sampling atmospheric particulate nitrate. Atmos. Environ. 11:873-876.

Stallard, R. F. and J. M. Edmond. 1983. Geochemistry of the Amazon I: Precipitation chemistry and the marine contribution to the dissolved load at the time of peak discharge. J. Geophys. Res. 88:9671-9688.

Stauffer, B. and W. Berner. 1978. CO_2 in Natural Ice. J. Glaciology 21:291-300.

Stensland, G. J. 1979. Calculation of precipitation pH, with application to the Junge data, pp. 79-108. In Study of Atmospheric Pollution Scavenging. DOE Contract EY-76-S-02-1199. Illinois State Water Survey, Urbana, IL.

Stensland, G. J. 1980. Precipitation chemistry trends in the Northeastern United States, pp. 87-108. In Polluted Rain. Y. Taft, M. W. Miller, and P. E. Morrow, eds. Plenum Press, New York.

Stensland, G. J. and R. G. Semonin. 1982. Another interpretaion of the pH trend in the United States. Bull. Amer. Meteorol. Soc. 63:1277-1284.

Stensland, G. J. and R. G. Semonin. 1984. Response to comment on another interpretation of the pH trend in the United States. Bull. Amer. Meteorol. Soc. 6:in press.

Stoiber, R. E., S. N. Williams, and L. L. Malinconico. 1980. Mount St. Helens, Washington, 1980 volcanic eruption: Magmatic gas component during first 16 days. Science 208:1258-1259.

Thompson, L. G. 1980. Glaciological investigations of the tropical Quelccaya ice cap, Peru. J. Glaciology 25:69-84.

Thompson, L. G. and E. Mosley-Thompson. 1981. Microparticle concentration variation linked with climatic: Evidence from polar ice cores. Science 212:812-815.

U.S./Canada Memorandum of Intent on Transboundary Air Pollution. 1982. Atmospheric Sciences and Aanalysis, Work Group 2. Final Report, November, 1982.

Unni, C., W. Fitzgerald, D. Settle, G. Gill, B. Ray, C. Patterson, and R. Duce. 1978. The impact of volcanic emissions on the global atmospheric cycles of S, Hg and Pb. Trans. Am. Geophys. Un. 59:1223.

Volchok, H. L. and R. T. Graveson. 1975. Wet/dry fallout collection. Proc. of the Second Federal Conf. on the Great Lakes. Interagency Commission on Marine Science and Engineering, Argonne National Laboratory, Argonne, IL. pp. 259-264.

Volchok, H. L., M. Feiner, H. J. Simpson, W. S. Broecker, V. E. Noshkin, V. T. Bowen, and E. Willis. 1970. Ocean fallout - the Crater Lake experiment. J. Geophys. Res. 75:1084-1091.

Vosters, M., F. Hanappe, and P. Buat-Menard. 1970. Determination of Cl, Na, Mg, K, and Ca, in firn sample 66-A-2 from New Byrd Station, Antarctica-Comparison with work of Murozumi, Chow, and Patterson. Geochim. Cosmochim. Acta 34:399-401.

Wallen, C. C. 1981. Monitoring potential agents of climatic change. Ambio 9:222-228.

Warburton, J. A. and G. O. Linkletter. 1978. Atmospheric process and the chemistry of snow on the Ross Ice Shelf, Antarctica. J. Glaciology 20:149-162.

Warburton, J. A., G. O. Linkletter, M. S. Owens, and L. G. Young. 1973. Measurements of Silver content of Antarctic snow and firn. International Symposium on the chemistry of Sea/Air Particulate Exchange Processes, Oct.

Weiss, H. V., K. Bertine, M. Koide, and E. Goldberg. 1975. The chemical composition of a Greenland glacier. Geochim. Cosmochim. Acta 39:1-10.

Weiss, H. V., M. M. Herron, and C. C. Langway. 1978. Natural enrichment of elements in snow. Nature 274:352-353.

Whelpdale, D. M. 1979. Tabulations of features of major networks and programs. In Ecological Effects of Acid Precipitation, Workshop Proceedings, EPRI EA-79-6-LD, Electric Power Research Institute, Palo Alto, CA.

Wiener, J. G. 1979. Aerial inputs of cadmium, copper lead and manganese into a freshwater pond in the vicinity of a coal-fired power plant. Water, Air, Soil Pollut. 12:343-353.

Wilson, J. W., V. A. Mohnen, and J. A. Kadlecek. 1982. Wet deposition variability as observed by MAP3S. Atmos. Environ. 16(7):1667-1676.

Wisniewski, J. and J. D. Kinsman. 1982. An overview of acid rain monitoring activities in North America. Bull. Am. Meteorol. Soc. 63:598-618.

Wilson, J., V. Mohnen, and J. Kadlecek. 1980. Wet deposition in the northeastern United States. State University of New York, Albany, NY, ASRC Pub. 796, December 1980. pp. 139.

Wolff, G. T., P. L. Lioy, H. Golub, and J. S. Hawkins. 1979. Acid precipitation in the New York metropolitan area: its relationship to meteorological factors. Environ. Sci. and Tech. 13:209-212.

Zoller, W. H., E. S. Gladney, and R. A. Duce. 1974. Atmospheric concentrations and sources of trace metals at the South Pole. Science 183: 198-200.

THE ACIDIC DEPOSITION PHENOMENON AND ITS EFFECTS

A-9. LONG-RANGE TRANSPORT AND ACIDIC DEPOSITION MODELS

(C. M. Bhumralkar and R. E. Ruff)

9.1 INTRODUCTION

The previous chapters have described our state-of-knowledge of the fundamental physical and chemical processes that affect effluents as they are transported between sources and receptors. When transport covers distances of 500 kilometers and above, models that numerically simulate these physicochemical processes are called Long-Range Transport (LRT) models. Currently, justifiable concern about the adequacy of these models leads researchers to test LRT model performance quantitatively by comparing model calculations with field measurements. However, such comparisons have been severely hindered by data bases that are limited in spatial and temporal coverage and in the types of parameters that have been measured. As a result, how well model results compare with the real world is not known. Current research attempts to improve this situation.

Dozens of different LRT models have been used to establish quantitative relationships between acidic deposition and emission levels. Most of these have dealt strictly with sulfur dioxide and sulfate. There is large variation of the inherent detail from simple to complex models. The complex models attempt to incorporate the most detailed (but not necessarily established) treatments that the state-of-knowledge will permit. However, in practice, no conclusive evidence indicates that detailed models can outperform the simpler models. Both types have given unverified answers, but the simpler ones have done so at a much more attractive cost. Fortunately, researchers have recognized the need to continue work on simple and complex models while awaiting improved data bases that will help resolve existing questions about performance and applicability.

Several of the models discussed in this chapter have been studied by the modeling group (U.S./Canada 1982) established under auspices of the Memorandum of Intent (MOI) on Transboundary Air Pollution signed by the United States and Canada on 5 August 1980. However, some of the models studied by this group, hereafter referred to as the MOI group, are not specifically mentioned by name. Rather, this chapter focuses on generic model types representative of the various approaches employed to date.

9.1.1 General Principles for Formulating Pollution Transport and Diffusion Models

The problem of transport can be reduced to solving an equation representing the conservation of mass. Written in terms of the concentration of a

particular chemical species, say C_i, this equation is

$$\frac{\partial C_i}{\partial t} + \vec{V}\cdot\nabla C_i = S_i - R_i + k_i\nabla^2 C_i \qquad [9\text{-}1]$$

where:

$\vec{V}$ = velocity vector,
S_i = sources of species i,
R_i = sinks of species i, and
k_i = molecular diffusivity of species i.

The process of physical transport is complicated because the atmospheric velocity field is not constant in either time or space. To incorporate the effect of the fluctuation in velocity field on transport, an averaging assumption is introduced by which all the variables are redefined as mean values:

$$C_i = \bar{C}_i + C_i' . \qquad [9\text{-}2]$$

where $\bar{C}_i$ is the average concentration and C_i' is the instantaneous deviation from the average.

Equation 9-1 is then averaged using mean values to give:

$$\frac{\partial \bar{C}_i}{\partial t} + \vec{V} \cdot \bar{C}_i = \bar{S}_i - \bar{R}_i + \bar{k}_i\nabla^2\bar{C}_i - \nabla \cdot \overrightarrow{C'V'} \qquad [9\text{-}3]$$

where the last term is called the turbulent correlation term. Generally, the turbulent correlation term is interpreted as a flux of species i across some surface due to the turbulent velocity, V', i.e.,

$$\nabla \cdot \overrightarrow{C_i'V_i'} = -\nabla \cdot K_i\nabla\bar{C}_i \qquad [9\text{-}4]$$

which formally defines K_i, the eddy diffusivity of the i species. Because the eddy diffusivity K_i is much larger than the molecular diffusivity k_i, the latter term can be neglected in Equation 9-3. Thus the equation

$$\frac{\partial \bar{C}_i}{\partial t} + \vec{V} \cdot\nabla \bar{C}_i = \bar{S}_i - \bar{R}_i + \nabla \cdot K_i\nabla \bar{C}_i \qquad [9\text{-}5]$$

can be used as a representation of the conservation of mass.

Significance has been attached to the difference between the second term on the left side and the last term on the right side of Equation 9-5. The former represents advection or bulk movement of the average concentration by the average velocity; the latter represents the diffusion of material by theturbulent velocity field. Most considerations in atmospheric transport

and diffusion modeling are based on a simplification and idealization of either or both of these processes.

9.1.2 Model Characteristics

Air quality models have a variety of characteristics that can be defined in terms of:

- Frame of reference
- Average temporal and spatial scales
- Treatment of turbulence
- Transport
- Reaction mechanisms
- Removal mechanisms.

These models may be steady state or time dependent; may incorporate the effect of complex terrain on wind flow and deposition; and may treat emissions from point sources or area sources or both, perhaps distinguishing between elevated and ground emissions. Table 9-1 shows some of the significant characteristics of the three model types classified by frame of reference.

Most LRT models are related to a coordinate system or reference frame that may be fixed either at the Earth's surface, at the source of the pollutant (for either fixed or moving sources), or on a puff of pollutant as it moves downwind from the source. Models whose reference frames are fixed at the surface, or on the source, are called Eulerian models; those whose frames are fixed on the puff of pollutant are called Lagrangian. Lagrangian models are usually more practical than Eulerian models in accounting for emissions from individual source locations and describing diffusion as the pollutants are carried by the wind. Eulerian models are more capable of accounting for topography, atmospheric thermal structure, and nonlinear processes such as those governing reactive pollutants.

9.1.2.1 Spatial and Temporal Scales--Atmospheric motions span a range of spatial scales from the microscale (centimeters) to large synoptic scales (1000 km). LRT models employ input data representative of the synoptic scale because of the large transport distances (500 to 2500 km). This includes incorporation of data from the rather sparse upper air network in North America (approximately 50 stations for the eastern United States and southeastern part of Canada; these stations measure winds and temperatures aloft twice a day). When source-to-receptor distances of less than 500 km become important, a model capable of treating sub-synoptic scale motions should be employed. In general, LRT models do not have this capability.

For temporal scales, the assumption has been that the physical and biological effects are dominated by long term (e.g., annual) dosages of acidic precursors. However, it appears that insufficient interaction has occurred among the modelers and effects researchers on this subject.

9.1.2.2 Treatment of Turbulence--Atmospheric turbulence dilutes and mixes gaseous and particulate pollutants as they are transported by the mean wind.

TABLE 9-1. CHARACTERISTICS OF POLLUTION TRANSPORT MODELS BY FRAME OF REFERENCE[a]

Model class (frame of reference)	Types of models	Space	Time	Treatment of turbulence	Reaction mechanism	Removal mechanism	Ability to quantify source-receptor relationship
Eulerian	Rollback Statistical Gaussian plume and puff Box and multi-box Grid	Site-specific/ local Regional	Daily (Episodic)	Implicit Eddy diffusivities Complex formulation (higher moment theory)	Nonreactive Nonlinearly reactive	Implicit Dry and wet	Possible but difficult to implement
Lagrangian	Gaussian plume and puff Trajectory Box and multibox Statistical trajectory	Site-specific/ local Regional	Daily or long-term (monthly seasonal annual)	Well-mixed volume Eddy diffusivities	Nonreactive Heavily parameterized, linearly reactive	Dry and wet	Yes
Hybrid (mixed Eulerian-Langrangian	Trajectory Particle-in-cell Puff-on-cell Physical	Local and regional	Daily or long-term (monthly seasonal annual)	Implicit Eddy diffusivities Complex formulation (not applicable to physical models)	Nonreactive Nonlinearly reactive	Dry and wet	Yes

[a]Adapted from Drake et al. (1979) and Hosker (1980).

Turbulence, one of the most important atmospheric phenomena, is produced by the wind, temperature, and, to a lesser extent, humidity gradients that occur in the atmosphere.

In a given model, atmospheric turbulence may be represented by a well-mixed volume, semi-empirical diffusion coefficients, eddy diffusivities, Lagrangian statistics, or more complex (higher-moment) turbulence models. The well-mixed volume approach basically ignores turbulence except in a loosely implicit manner. The most common parameters in current pollution transport models are semi-empirical diffusion coefficients determined from field diffusion studies over flat terrain, usually under neutral stability conditions. Most working-grid and multibox models use the eddy diffusivity formulation, which is based on theoretical, physical, and numerical studies of the planetary boundary layer (PBL).

To account for some of the physical inconsistencies in the eddy diffusivity formulation, several investigators have developed more complex formulations of turbulence. These require specifying more parameters and thus introduce additional uncertainties and increase computational costs.

Some models have incorporated turbulence effects by applying Lagrangian sta-statistics generated from field data. This presents a problem because most field data are obtained in an Eulerian framework.

9.1.2.3 Reaction Mechanisms--LRT models describe the fates of airborne gases and particles. As these pollutants are transported, physical and chemical changes may occur. These may be nonreactive mechanisms, reactive (photochemical and nonphotochemical) mechanisms, gas-to-particle conversions, gas/particle processes, and particle/particle processes. However, not all of these processes are explicitly treated in LRT models.

Both the SO_2/sulfate and photochemical models have gas-to-particle components to account for the production of particles directly from gases via gaseous reactions or condensation. In LRT models this treatment most frequently is limited to the conversion of sulfur dioxide to sulfate. Other acidic precursors (e.g., NO_2) usually are ignored. The gas/particle components in the models take into account particle growth by condensation or gas absorption. Particle/particle processes in aerosol models treat coagulation, breakup, condensational growth, and diffusion of particles.

9.1.2.4 Removal Mechanisms--Removal is the reduction of mass of airborne pollutants by either wet or dry deposition. Wet deposition is the removal of pollutants by precipitation elements, by both below-cloud and in-cloud scavenging processes. Dry deposition is the removal of pollutants by transfer from the air to exposed surfaces.

Removal mechanisms used in pollution transport models can vary widely. Some models listed in Table 9-1 (such as rollback or statistical models) are not well suited to deposition modeling because they do not treat physical processes explicitly. Others (such as Gaussian or Langrangian trajectory models) treat these processes in a rather straightforward manner. Grid models are especially well suited to use complex precipitation scavenging and

cloud dynamics in treating wet deposition, although this capability has not been exercised very often.

9.1.3 Selecting Models for Application

9.1.3.1 General--LRT modeling specialists have made progress in developing new techniques to meet the challenges of simulating pollution transport and deposition. A number of excellent comprehensive reviews of transport models have been prepared, for example, Fisher (1978), Drake et al. (1979), MacCracken (1979), Smith and Hunt (1979), Bass (1980), Eliassen (1980), Hosker (1980), Niemann et al. (1980), and Johnson (1981). These and other review papers have indicated that most of the existing models have been used to:

- Estimate contributions of given sources to receptors of interest.
- Estimate consequences of projected emissions changes.
- Fill gaps between observations.
- Assist in field study planning, determining such factors as which variables to measure and where to site stations.
- Assist in interpreting data, e.g., by inferring transformation or deposition rates.

Most of these tasks can be accomplished only by using models in concert with field measurements where available.

9.1.3.2 Spatial Range of Application--Model calculations have been performed over spatial scales classified as short range (< 100 km), intermediate range (100 to 500 km), and long range (> 500 km). Table 9-2 lists some of the model types that are commonly used for each of these ranges. Terminology specific to spatial scales has changed over the years. Lately, the terms regional and long-range transport have both been used to describe models capable of treating distances of 100 km and greater.

Generally, the Gaussian plume model has been the choice for short-range calculations. For intermediate ranges, a Gaussian plume model is sound if uncertainty about dispersion coefficients at these distances is taken into account. Applying intermediate range Gaussian models in this range presents problems if wind and precipitation distributions vary significantly. In complex terrain, shorelines, or forested terrain, a trajectory model, with plume or puff dispersion, is more appropriate for intermediate ranges. For long-range transport, trajectory ensemble models, box models, or grid models can be used.

9.1.3.3 Temporal Range of Application--Table 9-3 lists general types of models on the basis of the averaging time used in their applications. A host of Lagrangian trajectory-type LRT models have been used for long-term applications. Some modelers (e.g., Bhumralkar et al. 1981) have also developed a

TABLE 9-2. MODEL TYPES USED WITH DIFFERENT SPATIAL RANGES

Spatial Range	Model Type
Short (< 100 km)	Gaussian plume Trajectory Particle-in-cell Puff-on-cell
Intermediate (100-500 km)	Gaussian plume Trajectory Grid Particle-in-cell Puff-on-cell
Long (> 500 km)	Trajectory Grid Box

TABLE 9-3. SHORT-TERM AND LONG-TERM MODELS

Temporal Range	Model Type
Short term (hourly, daily)	Gaussian puff Lagrangian trajectory Particle-in-cell Puff-on-cell Grid
Long term (monthly, seasonal, and annual)	Gaussian plume and puff Lagrangian trajectory Statistical trajectory

short-term model, modifying the long-term model by incorporating a more detailed treatment of boundary layer and diffusion processes. A few Eulerian models have been developed for long-range and short-term applications (e.g., Durran et al. 1979).

9.2 TYPES OF LRT MODELS

Table 9-4 lists some of the LRT models that have been developed to date. Their properties are discussed below.

9.2.1 Eulerian Grid Models

The Eulerian grid model divides the geographical area of the volume of interest into a two- or three-dimensional array of grid cells. Advection, diffusion, transformation, and removal (deposition) of pollutant emissions in each grid cell are simulated by a set of mathematical expressions, generally involving the K-theory assumption (that the flux of a scalar quantity is proportional to its gradient). Some finite-difference technique is usually employed in the numerical solution of these equations.

The major advantages of the Eulerian grid approach are:

- Eulerian grid models are capable of sophisticated three-dimensional physical treatments.
- The approach can handle nonlinear chemistry.
- Data input is simplified on the Eulerian grid.

The disadvantages of the Eulerian grid approach are:

- Such models usually require large amounts of computer time, computer storage, and input data.
- These models, when they incorporate nonlinear modules, are cumbersome to use to determine contributions from individual sources.
- Artificial (computational) dispersion can be significant.

9.2.2 Lagrangian Models

9.2.2.1 Lagrangian Trajectory Models--A characteristic feature of these models is that calculations of pollutant diffusion, transformation, and removal are performed in a moving frame of reference tied to each of a number of air "parcels" that are transported around the geographical region of interest in accordance with an observed or calculated wind field.

As indicated in Table 9-4, Lagrangian trajectory models can be either receptor oriented, in which trajectories are calculated backward in time from the arrival of an air parcel at a receptor of interest, or source oriented,

TABLE 9-4. LONG AND INTERMEDIATE RANGE TRANSPORT MODELS

Model Type and Method	Investigator
Eulerian	
Finite Differencing	Lavery et al. (1980); Durran et al. (1979); Carmichael and Peters (1979); Egan et al. (1976); Nordø (1974, 1976); Pedersen and Prahm (1974)
Pseudospectral method	Berkowicz and Prahm (1978); Prahm and Christensen (1977), Christensen and Prahm (1976); Fox and Orsag (1973)
Lagrangian	
Statistical trajectory	Fay and Rosenzweig (1980); Venkatram et al. (1980); Shannon (1979); Fisher (1975, 1978); Mills and Hirata (1978); Sheih (1977); McMahon et al. (1976); Bolin and Persson (1975); Scriven and Fisher (1975); Rodhe (1972, 1974)
Receptor oriented[a]	Samson (1980); Henmi (1980); Olson et al. (1979); Ottar (1978); Szepesi (1978); Eliassen and Saltbones (1975)
Source oriented	Bhumralkar et al. (1981); Bhumralkar et al. (1980); Heffter (1980); Powell et al. (1979); Johnson et al. (1978); Maul (1977); Wendell et al. (1976)
Hybrid: Mixed	
Lagrangian-Eulerian	
Particle-in-cell (PIC) Atmospheric diffusion	Sklarew et al. (1971)
Particle-in-cell (ADPIC)	Lange (1978)
Puff-on-Cell	Sheih (1978)

[a]Receptor oriented models usually have options to compute forward (source oriented) and backward trajectories.

in which trajectories are calculated forward in time from the release of a pollutant-containing air parcel from an emission source.

Most source-oriented Lagrangian trajectory models simulate continuous pollutant emissions by discrete increments or "puffs" of emission occurring at set time intervals, usually between 1 and 24 hr, depending upon the designed averaging time of the model outputs. Such models simulate movement and behavior of a pollutant plume from a continuous source, as shown by one of the four approaches illustrated in Figure 9-1 (Bass 1980).

Some of the advantages of Lagrangian trajectory models are:

- The models may be used to estimate contributions from individual sources.
- The models are relatively inexpensive to run on a computer.
- Pollutant mass balances are easily calculated.
- Individual sources or receptors can be treated separately.

The disadvantages of these models are:

- The extension to three dimensions is not straightforward.
- Nonlinear physical and chemical formulations are difficult to incorporate.
- Horizontal and vertical diffusion are highly parameterized.

The two most important features of the Lagrangian trajectory model are its capability for calculating detailed source-receptor contributions and its computational efficiency. To achieve the latter, most models of this type are more highly parameterized and thus are potentially less physically realistic than some Eulerian grid approaches.

9.2.2.2 Statistical Trajectory Models--As shown in Table 9-4, several Lagrangian models are characterized as statistical trajectory models. Although many different kinds of statistical trajectory models exist, each has one or more of the following characteristic features that distinguish the type:

- Large numbers of air trajectories are calculated either forward in time from source areas or backward in time from receptor areas, and the results are statistically analyzed to give average pollutant contributions.
- Meteorological variables are frequently averaged over long time periods before such parameters as concentrations and depositions are calculated.

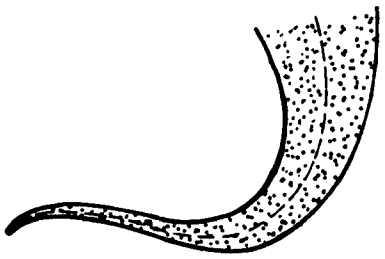

CONTINUOUS PLUME MODEL

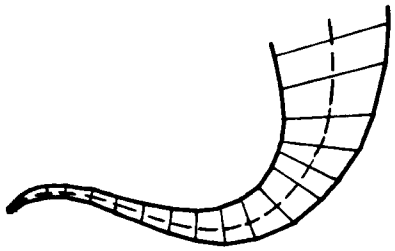

SEGMENTED PLUME MODEL

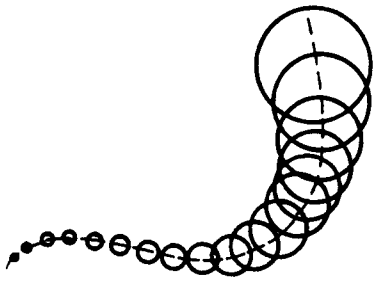

PUFF SUPERPOSITION MODEL

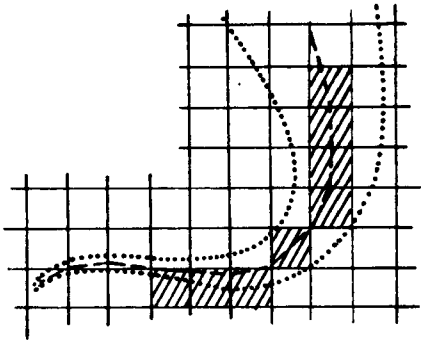

"SQUARE PUFF" MODEL

Figure 9-1. Trajectory modeling approaches. Adapted from Bass (1980).

Statistical trajectory models have the following advantages:

- Computational requirements are modest.
- The models are cost efficient for repeated runs using alternative emissions scenarios.
- The models do not suffer from computational dispersion.
- The models may be used to estimate contributions from individual sources.
- Pollutant mass balances can be estimated.

Disadvantages of statistical trajectory models are:

- Most types are not adaptable to short averaging times (i.e., episodes).
- Dispersion and other processes are usually highly parameterized.
- Some types ignore dependence between meteorological variables (e.g., wind and precipitation).

In summary, the low computational cost of statistical trajectory models is often obtained at the expense of physical realism.

9.2.3 Hybrid Models

In the hybrid (mixed Lagrangian/Eulerian) approach, pollutants, whose distribution is represented by Lagrangian particles or puffs, are transported through a fixed Eulerian grid that divides physical space into several cells. The particles or puffs are moving horizontally in a derived velocity field in the model domain. The hybrid approach offers advantages of both Eulerian and Lagrangian models. For example, hybrid models can provide treatment of nonlinear reactions between the compounds of interest (in the Eulerian framework) and the source-receptor relationship (in the Lagrangian framework). One of the main disadvantages of the hybrid approach (especially the particle-in-cell method) is that to simulate spatial distribution of pollution satisfactorily, a large number of particles must be used. This has been obviated considerably by the POC (puff-on-cell) method developed by Sheih (1978).

9.3 MODULES ASSOCIATED WITH CHEMICAL (TRANSFORMATION) PROCESSES

9.3.1 Overview

Primary air pollutants undergo reactions in the atmosphere, forming secondary pollutants such as ozone from NO_x-hydrocarbon reactions and sulfates from SO_2 oxidation reactions. The compounds that appear in rainwater are mainly

sulfate and nitrate anions and hydrogen and ammonium cations; they typically account for more than 90 percent of the ions in rainwater.

Theoretical, laboratory, and field experiments seem to indicate that both homogeneous and heterogeneous processes are important. However, the range of transformation rates, the conditions by which they vary, and the actual mechanisms still largely remain beyond simulation capabilities.

9.3.2 Chemical Transformation Modeling

As source emissions are changed from gases to aerosols, or (through a reaction with other materials in the atmosphere) to different compounds, their wet and dry removal rates will change, affecting their subsequent concentrations. Furthermore, the chemical transformations at any given time will depend on prior transformation, dilution, and removal.

Considerable research has been performed to understand the combined processes of atmospheric transport, diffusion, wet/dry removal, and chemical transformation. The LRT model normally incorporates a separate module that treats each of these processes. As is the case with most modules, chemical routines are most often gross simplifications of more detailed kinetic models that were developed independently of the overall modeling effort.

There are two approaches to modeling chemical transformations:

- By approximation with simplified first-order reactions. As described in Chapter A-4, the conversion of SO_2 to sulfate is usually treated this way.

- With more complex sets of reactions describing transformations among many compounds. However, only a few developmental models (e.g., Carmichael and Peters 1979) employ nonlinear mechanisms.

The simplified first-order approximations can be used with all approaches to the modeling of pollution transport: Eulerian, statistical or Lagrangian trajectory, and hybrid models. The multireaction schemes are most suitable for implementation in Eulerian or hybrid models. Lagrangian models, under some special circumstances, can use multireaction schemes. In general, this is possible only when the emissions from one source can be treated separately from those of other sources. Thus, such models can treat the chemical transformations taking place in a plume from an isolated source within the vicinity of that source, extending out to the point where it begins to overlap significantly with plumes from other major sources.

9.3.2.1 Simplified Modules--Currently, many models treat transformations either by assuming that they take place at a constant rate or by using simple first-order reactions. This type of treatment usually ignores secondary pollutants (e.g., ozone, HC) and their dependence on time of day, season, and latitude (Altshuller 1979). This simplified treatment usually ignores any heterogeneous reactions that may take place. Please refer to Chapter A-4 for a detailed discussion on linearity vs nonlinearity in transformation models.

The currently used simple modules of chemical transformation are chosen such that the model results are consistent with observations rather than on the basis of their consistency with theory. Because most models have been trajectory models and, therefore, superposition of plumes is assumed, linear chemistry is required to treat transformation. It is common for models to assume that about 1 percent of the SO_2 is converted to SO_4^{2-} each hour. Many models have yet to consider dependence on temperature, relative humidity, photochemical activity, time of day/year, particulate loading, or concentrations of other pollutants. To illustrate dependencies of model calculations to such parameters, a recent set of model calculations has made the transformation rate a function of zenith angle and of source type. This resulted in a variation of 5 to 10 percent in predicted SO_2 and SO_4^{2-} concentrations in comparison with results from the same model using a fixed transformation rate.

9.3.2.2 Multireaction Modules--Although more realistic treatment is possible with multireaction simulations (particularly with Eulerian models), their implementation is often difficult. For example, the model reaction schemes frequently emphasize photochemical processes because those processes are more easily defined. The reactions between the pollutants may be well known and characterized. The chemical models may simulate laboratory smog-chamber experiments, with their well-defined conditions and concentrations, quite reasonably. Nevertheless, the application of these multireaction sets to the real world is often difficult because of the wide variety of ambient conditions and pollutant concentrations that occur. The detailed knowledge required for simulating many of the reactions calls for air quality or meteorological data not available on a sufficiently dense spatial scale, horizontally and vertically. Data assumptions that must then be made to exercise the detailed chemical modules are often not very different, philosophically, from the cruder reaction assumptions in simpler models.

Another major weakness of most chemical transformation modules is the way heterogeneous reactions are handled. Under conditions of high humidity or weak sunlight, these reactions are important. In the context of acidic deposition, many of the more important heterogeneous reactions involve conversion from sulfur dioxide to sulfate. Among the catalysts and reactants are:

- Oxygen
- Iron
- Manganese
- Carbon (soot)
- Ozone
- Hydrogen peroxide.

Freiberg and Schwartz (1981) have pointed out some of the difficulties in handling heterogeneous reactions involving sulfur compounds. They note that heterogeneous formation of sulfate can take place over a number of different paths, including uncatalyzed oxidation, reactions with oxidizing agents (e.g., ozone or hydrogen peroxide), oxidation catalyzed by transition metal ions, or surface-catalyzed reactions. Furthermore, all the processes are complicated by finite mass transfer rates between phases. Although

heterogeneous transformations are undeniably important, their inclusion in chemical transformation modules has heretofore been cursory at best.

Chapter A-4 describes a variety of the chemical transformation mechanisms that have been proposed. However, incorporating such mechanisms into a long-range transport model with spatial resolutions of tens of kilometers (typically 80 km) is not always consistent with the sub-grid scale of the actual physical process. In general, the spatial scale is more consistent with urban modeling (typically less than 5 km). For this reason, some compromise must be struck between a comprehensive chemical scheme and practical application in LRT modeling. A number of factors must be considered in striking this compromise; these factors will relate to the intended applications of the model. For example, if only source/receptor relationships entailing total amounts of sulfur are required, chemical transformations involving sulfur compounds are important only to the degree that they affect removal processes. When pH is important, the number of important reactants and reactions increases dramatically to include a broad range of sulfur- and nitrogen-containing compounds, oxidants, potential catalysts, and precursors to all of these.

9.3.3 Modules for NO_x Transformation

Until quite recently, treatment of nitrogen pollutants in LRT models had been set aside in favor of work on sulfur pollutants. This is partially because of the emphasis on sulfur pollutants in the past few years and partially because nitrogen chemistry has been considered too complex for incorporation into a simple model. One problem has been how to incorporate NO_x chemistry into present models that require a linear parameterization; another problem is the difference in the time scales on which NO_x and SO_x chemistry occurs. For example, in LRT models, because of the relatively slow rate of conversion of SO_2 to SO_4^{2-}, it is possible to use coarse emission grids and a 3-hr integration time step, which enables these models to be used economically. However, with the more rapid NO_x chemistry, such coarse spatial and temporal resolution cannot be justified, thereby making model application impractical.

The problem of modeling NO_x conversion in the atmosphere can also be attributed to two other considerations. First, the primary end products of NO_x conversion in the atmosphere (mainly, HNO_3 and PAN) do not appear until after most of the NO has been converted to NO_2, which takes approximately 2 to 3 hours. This reaction delay for fresh emissions into an air column must be preserved in a transport model. The second point is that most of the end products in both the simulation and measurements in urban air masses are gaseous. These account for at least 90 percent of converted nitrogen in the atmosphere. Aerosol nitrates constitute only about 5 to 10 percent of the end product (Spicer et al. 1981).

Despite the difficulties discussed above, researchers have started to incorporate NO_x chemistry into LRT models. However, these NO_x modules have not yet been evaluated by comparison of results with reliable measurements. Most of the researchers have assumed that the NO_x conversion could be handled by simple first-order rate equations analogous to those for SO_2.

Recently, an intermediate product, PAN, was introduced into the calculations in a short-term version of the ENAMAP model (Bhumralkar et al. 1982). The research suggests application of the simplified set of reactions and constants given in Table 9-5. In this approach first-order rate equations are used to determine the concentrations of the reaction products. For example, the rate equation for NO_2 is:

$$\frac{d[NO_2]}{dt} = -a(k_n[NO_2])+b(k_p[PAN]). \qquad [9\text{-}6]$$

The other reaction products (PAN, HNO_3, and NO_3^-) are governed by similar equations. In this example, the partition constants, a and b, are unity. For the other products, these constants are different and are chosen to give the partition percentages given in Table 9-6. Table 9-6 shows that a large proportion of PAN is formed during the day but is removed at night. This removal is caused by thermal decomposition and is accompanied by a conversion of PAN to NO_2.

The above formulation neglects the explicit incorporation of hydrocarbons (HC), primarily the influence of the HC/NO_x ratio. As described in Chapter A-4, this ratio appears to have a strong influence on the NO_2 conversion rate and on the ratio of PAN to HNO_3.

9.4 MODULES ASSOCIATED WITH WET AND DRY DEPOSITION

9.4.1 Overview

Existing pollution transport models represent pollution deposition removal in several different ways. The simplest approach involves incorporating a nonspecific decay form intended to treat both wet and dry processes. As pointed out by a number of reviewers, such as MacCracken (1979), Eliassen (1980), and Hosker (1980), the values of deposition coefficients used in various pollution transport models vary widely, sometimes by more than a factor of ten. This is partly caused by the different model formulations, but it also reflects, in a major way, a basic lack of knowledge in the area. The problem of incorporating removal by deposition in LRT models is made more difficult because the measurements of deposition coefficients for many chemical species of interest are either nonexistent or exhibit a major degree of variability even when stratified, indicating that the values of coefficients are influenced by a number of factors. Some of the factors known to have significant effects on wet and dry depositions are:

Wet deposition:

- Atmospheric properties
  - Precipitation rate and type
  - Cloud type and size
  - Storm intensity
  - Temperature and humidity.

TABLE 9-5. AN EXAMPLE OF CHEMICAL REACTIONS AND RATES (HR^{-1}) FOR AN NO_x MODULE (BHUMRALKAR ET AL. 1982)

Reaction	Reaction Rate	
	Day	Night
$NO \rightleftarrows NO_2$[a]	---	---
$NO_2 \xrightarrow{k_n} PAN + HNO_3 + NO_3^-$	0.1	0.02
$PAN \xrightarrow{k_d} PAN + HNO_3 + NO_3^-$	0.1	0
$PAN \xrightarrow{k_p} NO_2$	0	0.02

[a]The ratio NO_2/NO is assumed to be at equilibrium with a value of 2 during the day and 50 at night.

TABLE 9-6. PARTITION OF CONVERSION PRODUCTS OF EXAMPLE NO_x REACTIONS (BHUMRALKAR ET AL. 1982)

Product	Day (%)	Night (%)
HNO_3 (gas)	40	85
PAN (gas)	50	0
NO_3^- (aerosol)	10	15

- Pollutant properties
  - Form (and size distribution if particulate)
  - Solubility and reactivity
  - Concentration vertical profile
  - Location relative to clouds.

Dry deposition:

- Atmospheric properties
  - Solar radiation
  - Wind speed
  - Atmospheric stability
  - Surface aerodynamic roughness
  - Humidity.
- Pollutant properties
  - Form (and size distribution if particulate)
  - Concentration vertical profile
  - Solubility and reactivity.
- Vegetation properties
  - Type, size, leaf area, density
  - Stomatal condition
  - Growth stage
  - Stress condition
  - Wetness.
- Other surface (non-vegetation) properties

The current models account for wet and dry deposition with highly parameterized treatments that do not explicitly include many of the factors in the above lists. Some of the effects of these variables can be considered to be "averaged out" over the long travel distances and large spatial averaging areas involved in interregional-scale modeling. Comparing model-calculated depositions to available measured values produces information useful to help select suitable values for such "integrated" values of deposition coefficients. In general, however, much additional fundamental knowledge about the deposition processes is needed to facilitate further progress in developing models for studying acidic deposition problems.

The discussion in this chapter is strictly confined to modules for treatment of wet and dry deposition in current pollution transport models. The basic theory and principles pertaining to these have been described in Chapters A-6 and A-7.

9.4.2 Modules for Wet Deposition

9.4.2.1 Formulation and Mechanism--Various parameterization techniques are used for modeling washout in terms of rainfall rate and characteristic

scavenging efficiency. These offer at least the capability to describe wet deposition formally. Precipitation rates can be highly variable, and spatially limited, especially during active convective situations. Therefore, it is difficult, if not impossible, to categorize rainfall rate on a scale adequate to describe the fate of a plume, especially in its early stages.

In existing models, removal by wet deposition has been parameterized in terms either of the scavenging coefficient, Λ, or washout ratio, W, (Dana 1979; refer to Chapter A-6 for a more comprehensive discussion of the scavenging coefficient). The former results from the assumption that wet deposition is an exponential decay process obeying the equation:

$$C_t = C_0 \exp(-\Lambda t) \qquad [9\text{-}7]$$

where:

C_t = atmospheric concentration at time t,
C_0 = atmospheric concentration at initial time, and
Λ = scavenging coefficient (in units of time^{-1}).

The concept of a washout ratio is used frequently in steady-state models. It is defined as the concentration of contaminant in precipitation divided by its concentration in air (usually at the surface level); i.e.,

$$W = \frac{X}{C} \qquad [9\text{-}8]$$

where:

X = concentration of contaminant in precipitation,
C = concentration of contaminant in unscavenged air, and
W = washout ratio (dimensionless).

The spatial and temporal distribution of the concentrations determine how Λ and W are related. For example, for the simple case of pollutant washout from a column of air having a uniform concentration over height, h, one obtains:

$$\Lambda = \frac{WR}{h} \qquad [9\text{-}9]$$

where:

R = the precipitation intensity.

The values of washout coefficients, at least for SO_2 and SO_4^{2-}, vary widely among various modelers, with disagreement even on which pollutant is scavenged most efficiently.

9.4.2.2 Modules Used in Existing Models--Wet deposition is usually calculated by using Equation 9-7 and allowing Λ to vary with position to account for precipitation changes over the region of interest. However, the basic problem in applying Equation 9-7 is the actual evaluation of Λ, which

depends on the characteristics of the rainfall and the scavenged effluent. Also, because the scavenging rate approach inherently assumes an irreversible collection process, it is suitable for gases only if they are extremely reactive. For gases that form simple solutions in water, it is essential to account for possible desorption of gas from droplets as they fall from regions of high concentrations toward the ground (Hosker 1980).

The wet deposition of soluble gases in Gaussian plume models has been calculated under simplifying assumptions of steady state, negligible chemical reactions, and vertical fall of raindrops. However, many gases of interest become acids when in solution, and their solubility then becomes a function of pH. Inability to calculate actual pH forces an empirical approach to estimating washout ratios, W, for gases, similar to those for particulates. However, some empirical approaches (e.g., Barrie 1981) have suggested ways of estimating improved SO_2 washout ratios.

Some models represent wet deposition in terms of wet deposition velocity, V_W, given by

$$V_W = \frac{\text{wet flux}}{\text{concentration in air at the surface}} . \qquad [9\text{-}10]$$

This has been estimated from empirically determined washout ratios W given by Equation 9-8 (Slinn 1978). Because wet flux to the surface is simply $X \cdot R$ (where R is the precipitation rate), V_W has been estimated by using

$$V_W = WR . \qquad [9\text{-}11]$$

The wet deposition velocity has been used in models for the wet removal process. In some cases, the washout ratio has been used directly to give an exponential decay term for a plume if the thickness of the wet layer of plume is known (Heffter et al. 1975, Draxler 1976).

In Lagrangian puff and trajectory models (e.g., Bhumralkar et al. 1981) wet deposition is generally treated via an exponential decay term (Equation 9-7) where the parameter depends on the characteristics of the effluent and the precipitation. This technique is applicable to irreversible scavenging of particles and highly reactive gases.

In Eulerian grid models, wet deposition is generally handled by an exponential decay term, $\exp(-\Lambda t)$, although some models simply assume that all the effluent is scavenged immediately when precipitation is encountered (e.g., Peterson and Crawford 1970, Sheih 1977). An interesting variation is contributed by Bolin and Persson (1975), who calculate the wet removal rate from

$$\beta \int_0^\infty \chi dz. \qquad [9\text{-}12]$$

The coefficient β is an "expected" overall scavenging rate that takes into account the probability of rainfall, its likely duration and intensity, and

the actual scavenging rate β expected for such precipitation (Rodhe and Grandell 1972). Evidently β can vary with locale and season; the method seems best suited to long-term-average investigations. Wet deposition velocities, washout ratios, or both, do not seem to have been used in grid models to any extent. However, work on such formulations is in progress.

Complex numerical models dealing with wet deposition, including cloud dynamics, have been described by Molenkamp (1974), Hane (1978), and others. These models deal with the equations of motion for cloud formation, precipitation formation, and the various scavenging phenomena that may apply. For example, an interactive cloud-chemistry model has been used to calculate effects of cloud droplet growth and SO_2 oxidation within the droplet on pH. With this approach, nucleation scavenging can be examined for different types of clouds (e.g., wave cloud and stratus cloud). This type of work is still in a research phase. It requires parameterizations of only partially understood processes and (like most deposition models) is still unvalidated. Such research, while potentially useful, is presently unsuitable for practical application.

In hybrid (Lagrangian plus Eulerian) transport models (e.g., particle-in-cell), treatment of wet deposition is more complicated. Whereas it is relatively easy to deal with aerosols/particulates, problems occur in dealing with gases. However, the wet deposition velocity concept can be used for gases in these types of models.

9.4.2.3 Wet Deposition Modules for Snow--It is sometimes necessary to differentiate between wet deposition by snow and rain. This is based on the following considerations:

- The scavenging coefficients vary with season and depend on the precipitation intensity.
- The scavenging coefficient is a function of raindrop and snowflake size distribution and effective scavenging area.
- The scavenging coefficient is strongly dependent on the type of snow (e.g., plane dendrites are much more effective as scavengers than grouped); no such differentiation is applicable to rain.

To date, very few LRT models have incorporated the above considerations explicitly in the modeling of wet deposition.

9.4.2.4 Wet Deposition Modules for NO_x--Very little information is available in the literature concerning treatment of wet deposition of nitrogen compounds in transport models. As a general rule, the information that has been given is expressed as a fraction of the rates estimated for sulfur compounds. The approach is obviously crude, and this is certainly an area where extensive use could be made of data bases that have been collected in recent years.

McNaughton (1981) has made some progress in developing relationships among sulfate, nitrate, and precipitation pH for use in modeling. He has used wet deposition observations available from a number of research and monitoring networks, including MAP3S (Multistate Atmospheric Power Production Pollution Study), EPRI (Electric Power Research Institute), NADP (National Atmospheric Deposition Program), CANSAP (Canadian Network for Sampling Precipitation), and Ontario Hydro, in model evaluation studies (e.g., McNaughton 1980). It may be noted that, whereas deposition networks are not as dense as modelers of pollution transport and deposition would prefer, considerable wet deposition data exist for model verification.

9.4.3 Modules for Dry Deposition

9.4.3.1 General Considerations--The dry deposition rate of gases and particles has usually been parameterized using a deposition velocity V_d, defined by the equation

$$V_d = F/C \qquad [9\text{-}13]$$

where

F = the flux of material,
C = the ambient concentration at a particular height, and
V_d (which is a function of height) refers to the same level as the concentration measurement.

This simplified treatment of a deposition velocity conveniently ignores the complexities of the governing processes as described in Chapter A-7. However, such simplifications are consistent with other treatments imbedded in LRT models. Sehmel (1980) has summarized many of the parameters that affect dry deposition rates; these concepts are examined in Chapter A-7.

A common approach used in many models has been to assume a constant dry deposition velocity for each pollutant over the entire model domain. Of course, this is unrealistic because pollutants are absorbed differently by different surfaces (e.g., vegetation, soil, or water), and because atmospheric stability can also be a factor, particularly during nighttime.

Recently, models have used dry deposition velocities that are functions of land-use types and atmospheric stability. Sheih et al. (1979) have prepared maps of surface deposition velocities for sulfur dioxide and sulfate particles over eastern North America that take into account land use, atmospheric stability, and seasonal differences. Variations in deposition rates for nitrogen compounds can also be mapped in a similar fashion, although the necessary field studies for characterizing different surfaces and stabilities are only beginning to be conducted.

Among the reasons for characterizing deposition rate according to season is that the character of the Earth's surface changes from season to season--deciduous vegetation changes with the growth and loss of leaves; in grasslands, the grass dies and is replaced by a snow cover. The reason for including atmospheric stability as part of the categorization scheme is

that dry deposition depends on the concentration of material in the lowest layers, just above the surface. These low-level concentrations in turn depend on the rate at which material is transported from higher layers to replace that which is lost to the surface; these transfer rates depend on atmospheric stability. The latter effect can be simulated more directly if the atmosphere is subdivided into layers for purposes of modeling. A compromise can be struck between detailed simulation of the vertical structure of the atmosphere and stability-based parameterization, using a surface layer formulation, which controls deposition based on observed vertical distribution of the material of concern.

Verifying dry deposition simulations is currently difficult because we lack monitoring instrumentation. A number of carefully controlled field measurements of dry deposition fluxes have been made, principally by the eddy correlation method. The results can be used in examining the scientific validity of the parameterization used in the models.

9.4.3.2 Modules Used in Existing Models--In Lagrangian puff/trajectory models, generally the vertically integrated concentration of puffs is depleted by an exponential factor

$$e^{-k_d t} \qquad [9\text{-}14]$$

where:

$$k_d = \frac{\text{dry deposition flux}}{\text{vertically integrated concentration}} \ .$$

Most of these models compute the dimensionless value for k_d from

$$k_d = \frac{V_d \cdot C}{h}$$

where h is the height of the surface layer. For simpler models there is only one uniformly mixed layer, so h is simply the mixing height. Some Lagrangian models (e.g., Shannon 1981) incorporate several layers in the vertical, and dry deposition processes are allowed to remove material from only the surface layer. Eddy diffusivity controls the redistribution between the vertical layers. These models sometimes also include treatments that allow the dry deposition velocities to vary with season, time of day, type of underlying surface, and atmospheric stability.

In Eulerian grid type models, dry deposition is treated in a way similar to that discussed above. These models are especially well suited to use the relation between mass flux, dry deposition velocity, and concentration at or just above the surface. Constant values for V_d are often used, probably for simplicity, although some grid models (Durran et al. 1979) include an algorithm that allows V_d to vary in time and space, reflecting changes in terrain, ground cover, and atmospheric conditions.

9.4.3.3 Dry Deposition Modules for NO_x--As stated previously, most models treat the sulfur oxide-sulfate cycle exclusively. The nitrogen oxides-nitrate cycle is being treated in only a few models (e.g., Bhumralkar et al. 1982). For these models, the mathematics of dry deposition treatment remains the same is it was for the sulfur version. However, the values for the dry deposition velocity are different. Chapter A-7 gives a comparison of experimentally determined dry deposition velocities.

9.4.4 Dry Versus Wet Deposition

The relative significance of dry and wet deposition in LRT models has not been examined in a systematic way, but is now being studied via field experiments. In early field experiments, the emphasis was on the wet removal process; consequently, few data on dry deposition were collected and hence large uncertainties exist on dry deposition velocities.

A reasonable comparison between dry and wet removal rates can be made when the deposition modules incorporate the roles of pollutant release height and precipitation frequency. For example, whereas dry deposition will play an important role in removing pollutants near ground level, wet deposition can be expected to be spotty and intermittent because of naturally-occurring spatial and temporal variation in precipitation events.

9.5 STATUS OF LRT MODELS AS OPERATIONAL TOOLS

9.5.1 Overview

The ability to simulate complex physical and chemical processes of the natural environment is essential for making regulatory and policy decisions. There is no economical way to gather enough observations to determine, from the data alone, all the possible combinations that can occur in the real world. In addition, the effect of altering the existing situation cannot be assessed by collecting observations before such alterations take place. Thus, modeling supported by monitoring data is the only practical means by which the efficacy and advisability of control strategies can be assessed.

The past decade has seen increasing concern about production and long-distance travel of pollutants such as sulfates and nitrates and deposition of these precursors of acid on sensitive areas at long distances from sources. Such concern has given impetus to developing and applying several LRT models, not only for studying acidic deposition processes but also for policy-making and regulatory purposes.

The understanding of the complex processes that act to transform and transport pollutants is incomplete, and the capacities of even the largest computers do not permit easy simulation of the almost infinite combination of physics, chemistry, and hydrodynamics of the real world. It is therefore necessary to simplify and parameterize the mathematical simulations. The effects of these simplifications are not fully understood and understanding will not be achieved until the models undergo rigorous evaluation. The evaluation is not limited to the model itself, but must extend to the data base that drives the model and the data base that is used to assess

performance. In the remainder of this section, model applicability and performance are discussed along with their attendant data requirements.

9.5.2 Model Application

9.5.2.1 Limitations in Applicability--Ideally, the choice of a particular model as an operational tool is based on the specifications of the particular application at hand; how well the model has performed in comparable applications; and the availability of suitable data to drive the model. In turn, the specifications of the application should be determined by certain air quality regulations (when applicable) and the ecological effects being addressed. Such criteria determine the spatial and temporal scales and the chemical compounds that the selected model must treat.

The spatial ranges of concern might require treatment of long-range transport (> 500 km), intermediate-range transport (100 to 500 km), short-range transport (< 100 km), or combinations of all three. The discussion here has focused on the long-range problem with the assumption that the resolution is sufficient for smaller (spatial) scale problems. When the receptor locations of interest are influenced by large sources within distances of 500 km, the resolution in these LRT models may be inadequate (unless they include smaller scale treatments). Obviously, for some applications, this is a serious limitation in almost all existing LRT models.

In most LRT models, temporal scales germane to acidic deposition have been assumed to be long-term (e.g., monthly, seasonal, and annual averages). The underlying assumption is that the effects of acidic deposition result from long-term build-ups, not short-term episodes. Only a limited number of models have been developed to address the short-term (e.g., 3-hr averages). Most of these applications have focused on ground level concentrations, not depositions, of certain acid precursors (primarily SO_2). Until recently, treatment of wet deposition was ignored in most short-term models. Now, a host of short-term models treat both wet and dry depositions of acid precursors. However, much less effort has been put into the evaluation of these long-range, short-term models in comparison with those designed for long-term calculations. As a result almost no knowledge exists on the performance of short-term models in calculating depositions of acidic compounds.

A major problem is that there are certain types of applications for which no single model may be appropriate. The majority of LRT models have been designed to calculate long-term concentrations and depositions of sulfur dioxide and sulfate. Some of these models also treat nitrogen oxides and nitrates, but much less is known about model performance for nitrogen oxides or any other reactive compounds (other than sulfur). For more complete chemical systems, LRT models are still in the research phase and, in general, are not ready as operational tools.

9.5.2.2 Regional Concentration and Deposition Patterns--A better understanding of LRT model design and application can be obtained by examining

one particular Lagrangian modeling approach--the EURMAP/ENAMAP--on the basis that it can be considered as a typical example of such models. There are two versions of EURMAP (European Regional Model of Air Pollution): EURMAP-1 (Johnson et al. 1978) is a long-term model that calculates monthly, seasonal, and annual values; EURMAP-2 (Bhumralkar et al. 1981) is a short- term model that calculates 24-hr values. ENAMAP-1, Eastern North American Model of Air Pollution (Bhumralkar et al. 1980) is a closely related version of EURMAP-1 that has been adapted for application to the geographical region covering the eastern United States and southeastern Canada, as illustrated in Figure 9-2.

The EURMAP and ENAMAP models are designed to have minimal computation requirements for making long-term calculations while simulating the most important processes involved in the transboundary air-pollution problem. These models can be used to calculate daily, monthly, seasonal, and annual SO_2 and SO_4^{2-} air concentrations; SO_2 and SO_4^{2-} dry and wet deposition patterns; and interregional exchanges resulting from the SO_2 and SO_4^{2-} emissions over a specified domain. The models use long sequences of historical meteorological data as input, retaining all the original temporal and spatial detail inherent in the data.

The short-term models, EURMAP-2 and ENAMAP-2, use the same general design as the long-term models but have a number of important differences, which are necessary to incorporate more details into the emissions and meteorological simulations to be consistent with the much shorter (24-hr) averaging time. In particular, atmospheric boundary-layer processes have been treated in a more detailed manner than in long-term versions.

The results from both EURMAP and ENAMAP models are obtained in the following forms:

- Graphical displays of the distribution of SO_2 and SO_4^{2-} concentrations
- Graphical displays of the distributions of SO_2 and SO_4^{2-} wet and dry depositions
- Tabulated results showing the interregional exchanges of sulfur pollution between individual source and receptor regions.

Examples are presented in Figures 9-3 and 9-4 and Table 9-7, respectively, of each of the above types of products resulting from the ENAMAP application.

9.5.2.3 Use of Matrix Methods to Quantify Source-Receptor Relationships--For long-range transport, environmental assessment must consider potential impacts of emissions on areas far removed from the source. Transport across the boundaries of air quality planning regions, states, and even nations can be important. At the present state-of-the-art of modeling, the models that have been used to quantify source-receptor relationships are based on the principle of tracking the trajectories of emitted pollutants. These models are used to compute "transport matrices" (e.g., Table 9-7) that permit

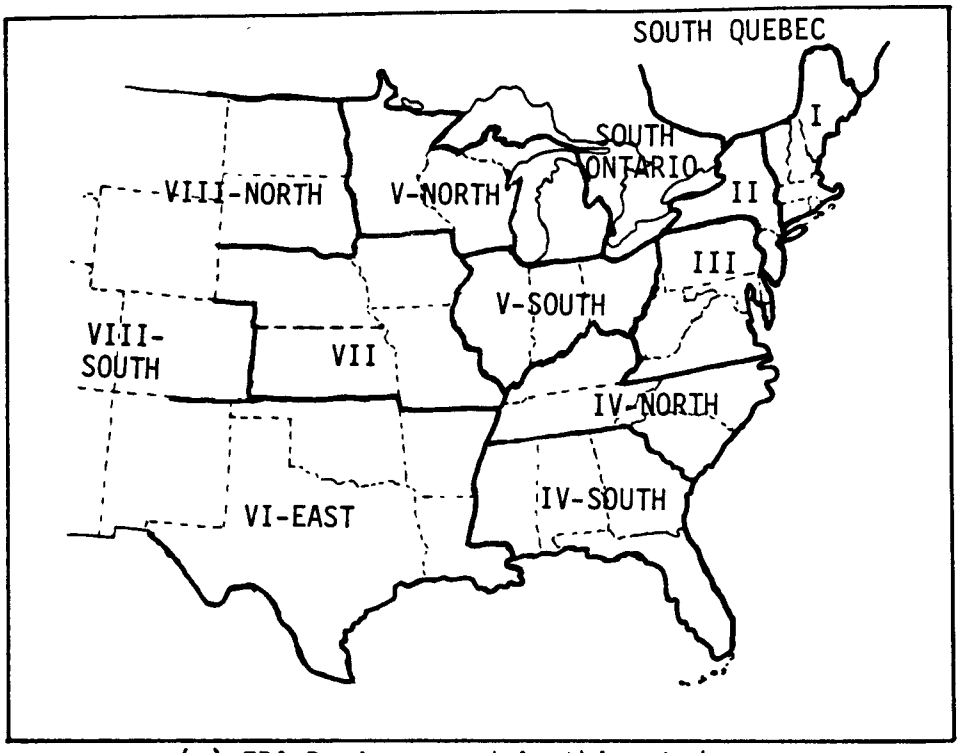

(a) EPA Regions used in this study

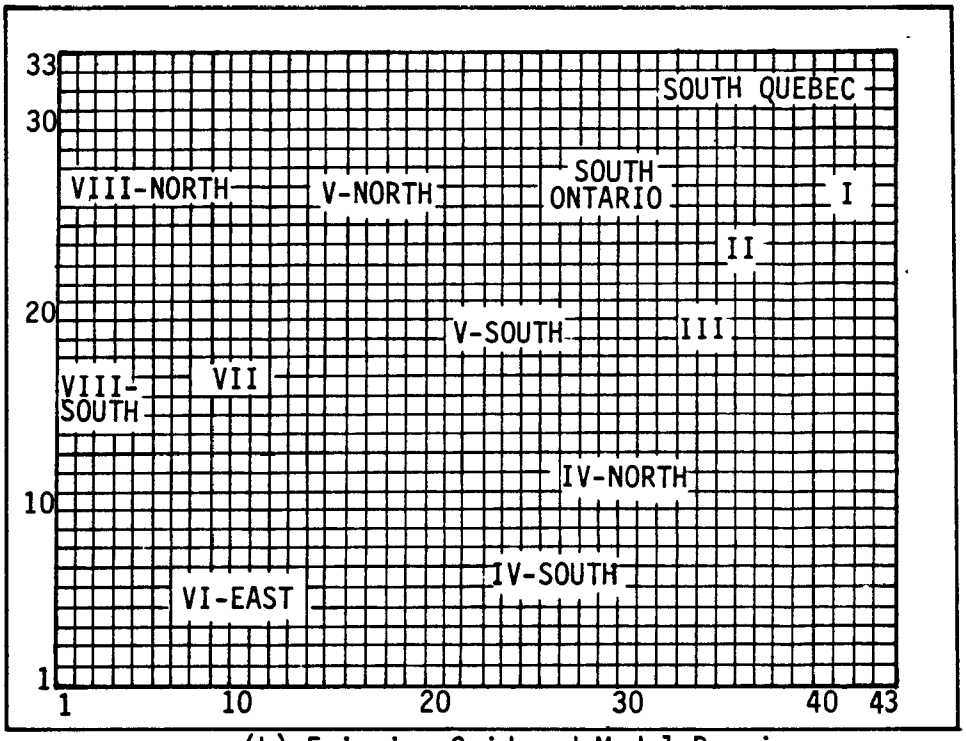

(b) Emission Grid and Model Domain

Figure 9-2. Eastern North American domain and EPA regions used in the ENAMAP modeling study. Adapted from Br[illegible] (1980).

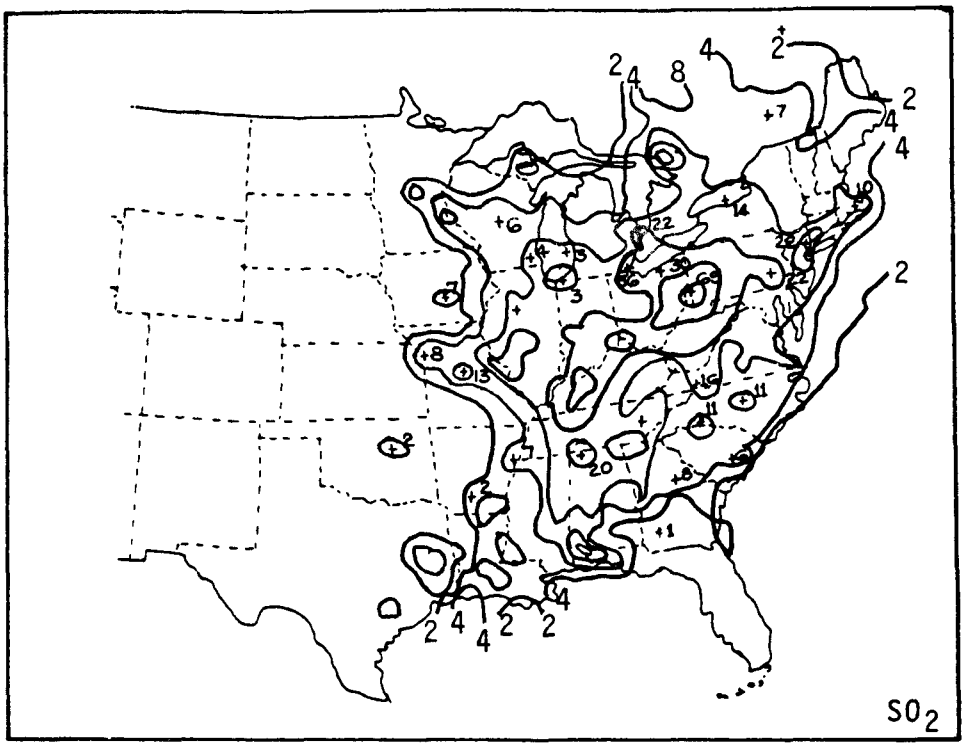

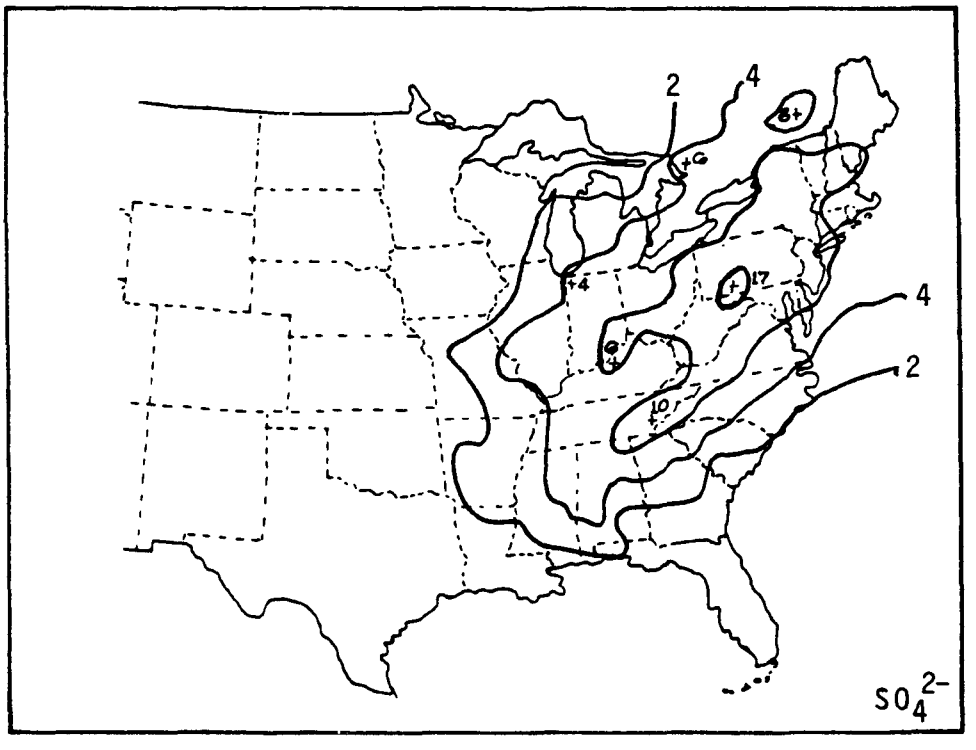

Local maximum values shown apply at points marked by plus signs.

Figure 9-3. Calculated SO_2 and SO_4^{2-} concentrations ($\mu g\ m^{-3}$) for August 1977. Adapted from Bhumralkar et al. (1980).

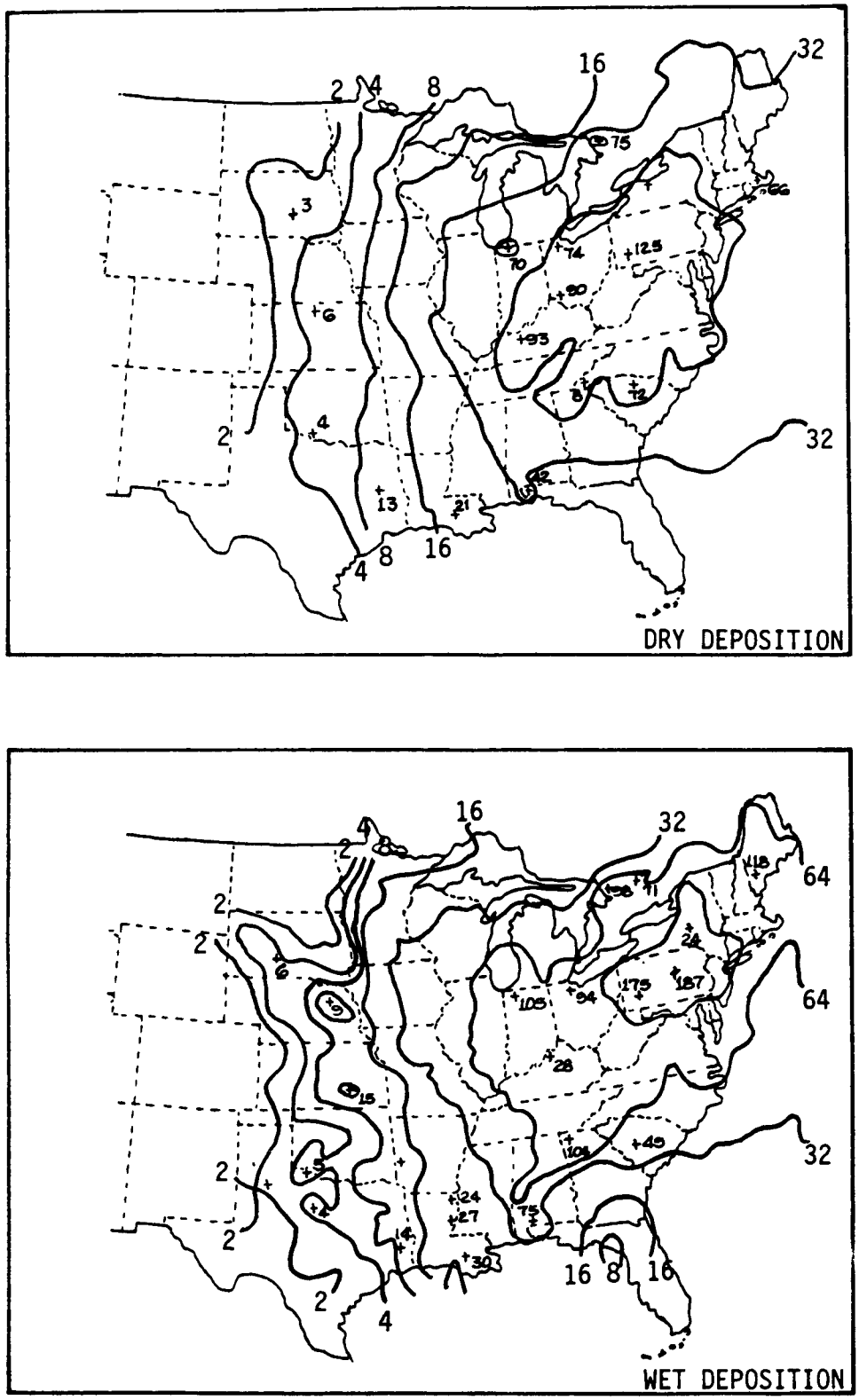

Local maximum values shown apply at points marked by plus signs

Figure 9-4. Calculated annual dry and wet depositions of SO_4^{2-} (10 mg m^{-3}). for 1977. Adapted from Bhumralkar et al. (1980).

TABLE 9-7. ANNUAL INTERREGIONAL EXCHANGES OF SULFUR DEPOSITION FOR 1977 AS CALCULATED BY THE ENAMAP - 1 MODEL (BHUMRALKAR ET AL. 1980)

TOTAL CONTRIBUTION TO S DEPOSITIONS WITHIN RECEPTOR REGIONS (kilotons)

EMITTER REGION	1	2	3	4	5	6	7	8	9	10	11	12	13
1 VIII - NORTH	10.	1.	0.	2.	0.	0.	0.	0.	0.	0.	0.	0.	0.
2 V - NORTH	3.	655.	290.	46.	0.	3.	229.	6.	24.	78.	50.	18.	23.
3 S. ONTARIO	0.	66.	820.	2.	0.	1.	49.	2.	7.	74.	87.	40.	87.
4 VII	1.	43.	10.	367.	0.	26.	137.	22.	41.	12.	3.	2.	2.
5 VIII - SOUTH	0.	0.	0.	0.	0.	0.	0.	0.	0.	0.	0.	0.	0.
6 VI - EAST	1.	4.	1.	40.	1.	401.	7.	35.	6.	1.	0.	0.	0.
7 V - SOUTH	2.	186.	145.	135.	0.	14.	1566.	59.	425.	520.	92.	30.	26.
8 IV - SOUTH	0.	8.	7.	16.	0.	44.	31.	949.	279.	25.	2.	1.	2.
9 IV - NORTH	0.	19.	24.	11.	0.	13.	221.	108.	929.	159.	15.	7.	6.
10 III	0.	11.	57.	3.	0.	1.	178.	14.	141.	1363.	179.	56.	21.
11 II	0.	1.	53.	0.	0.	0.	1.	1.	4.	37.	204.	65.	14.
12 I	0.	0.	1.	0.	0.	0.	1.	0.	2.	9.	91.	207.	22.
13 S. QUEBEC	0.	2.	105.	0.	0.	0.	1.	0.	0.	2.	8.	41.	204.
TOTAL (K TON S)	18.	997.	1514.	621.	1.	503.	2422.	1197.	1856.	2280.	732.	467.	407.

PERCENT CONTRIBUTIONS TO S DEPOSITIONS WITHIN RECEPTOR REGIONS

EMITTER REGION	1	2	3	4	5	6	7	8	9	10	11	12	13
1 VIII - NORTH	55.	0.	0.	0.	6.	0.	0.	0.	0.	0.	0.	0.	0.
2 V - NORTH	19.	66.	19.	7.	0.	1.	9.	0.	1.	3.	7.	4.	6.
3 S. ONTARIO	3.	7.	54.	0.	0.	0.	2.	0.	0.	3.	12.	9.	21.
4 VII	3.	4.	1.	59.	0.	5.	6.	2.	2.	1.	0.	0.	0.
5 VIII - SOUTH	0.	0.	0.	0.	0.	0.	0.	0.	0.	0.	0.	0.	0.
6 VI - EAST	7.	0.	0.	6.	92.	80.	0.	3.	0.	0.	0.	0.	0.
7 V - SOUTH	9.	19.	10.	22.	1.	3.	65.	5.	23.	23.	13.	6.	6.
8 IV - SOUTH	1.	1.	0.	3.	0.	9.	1.	79.	15.	1.	0.	0.	1.
9 IV - NORTH	0.	2.	2.	2.	0.	3.	9.	9.	50.	7.	2.	1.	1.
10 III	2.	1.	4.	1.	0.	0.	7.	1.	8.	60.	24.	12.	5.
11 II	1.	0.	4.	0.	0.	0.	0.	0.	0.	2.	28.	14.	3.
12 I	0.	0.	0.	0.	0.	0.	0.	0.	0.	0.	12.	44.	5.
13 S. QUEBEC	0.	0.	7.	0.	0.	0.	0.	0.	0.	0.	1.	9.	50.

assessment of air pollution impacts for multiple scenarios of emissions. (Please refer to Chapter A-2 for discussion on natural and anthropogenic emissions that contribute to acidic deposition.) The transport matrix concept is based on the assumption that the average concentration deposition of a pollutant in one geographic region (the "receptor") is the sum of contributions received from emissions in every other region (the "sources"). The matrix method has been used in several assessment studies and for analyses of policy issues (Ball 1981).

Table 9-8 (from Ball 1981) exemplifies some of the features of results presented in the matrix format. The Brookhaven National Laboratory (BNL) AIRSOX model (Meyers et al. 1979) was used to generate the results which quantify the transport of sulfates from one Federal (EPA) region to another. Terms along the diagonal of the matrix are the intraregional (locally produced) contributions. Summation of the off-diagonal contributions of the receptor regions gives the imported fraction of sulfate concentrations. Table 9-8 shows that the imported fraction varies from 6 percent (Region 9) to 92 percent (Region 1). Examining the individual contributions to the Region 1 totals in the first column, it is seen that slightly over one-half the total impact of 5.461 $\mu g\ m^{-3}$ is calculated to originate from Region 5, which has an incremental contribution of 2.817 $\mu g\ m^{-3}$.

While the matrix method is a reasonable way to present the source-receptor relationship results of the transport models in a convenient form, important questions remain about their validity in general and also about the accuracy of matrices derived with current models. Chemical and physical processes that transform and remove air pollutants such as sulfur oxides from the air often are not linear in terms of the amount of pollutant present. However, most large-scale, long-range transport models in current use are based on linear approximations. This is due to the difficulties in simulating nonlinear processes and lack of knowledge about the processes.

Finally, all the model results must be regarded as preliminary. The results presented previously (Figures 9-2, 9-3; Table 9-7) primarily indicate the type of information and the format that can be provided for use by others. The results (Tables 9-7 and 9-8) also give some useful indications, or trends, regarding the relative importance of various source regions on the sensitive receptor areas presently of interest. But at this time the absolute values of the numbers in the matrices should not be given too much importance, and certainly the results of any one model should not be taken in preference to the others.

9.5.3 Data Requirements

9.5.3.1 General--Figure 9-5 shows schematically how the components of a general transport model are interconnected and how they interact with basic data sources. The diagram represents a model that is meteorologically diagnostic in that it does not attempt to generate meteorological information from dynamic principles but instead makes maximum use of available meteorological observations. Two other categories of input information are required in addition to meteorological data: geographical information (e.g., surface characteristics and topography) and detailed emissions data from both point

TABLE 9-8. INTERREGIONAL CONTRIBUTIONS TO SULFATE CONCENTRATIONS AMONG FEDERAL REGIONS (BALL 1981)

	Receptor									
Emitter	1	2	3	4	5	6	7	8	9	10
1	0.453	0.059	0.009	0.002	0.000	0.000	0.000	0.000	0.000	0.000
2	0.540	1.199	0.328	0.037	0.009	0.000	0.000	0.000	0.000	0.000
3	1.232	2.212	4.728	0.518	0.171	0.012	0.001	0.000	0.000	0.000
4	0.646	0.934	2.559	3.832	1.042	0.256	0.209	0.007	0.000	0.000
5	2.817	4.120	5.640	1.730	4.420	0.121	0.617	0.026	0.000	0.000
6	0.035	0.058	0.098	0.228	0.293	1.032	0.755	0.278	0.068	0.003
7	0.174	0.295	0.322	0.283	0.966	0.169	1.113	0.050	0.000	0.000
8	0.008	0.014	0.007	0.006	0.114	0.059	0.243	0.530	0.026	0.061
9	0.008	0.019	0.014	0.011	0.041	0.484	0.287	0.791	1.848	0.250
10	0.000	0.000	0.000	0.000	0.007	0.004	0.012	0.080	0.026	0.316
Local	0.453 (8%)	1.199 (13%)	4.728 (34%)	3.832 (58%)	4.420 (63%)	1.032 (48%)	1.113 (34%)	0.530 (30%)	1.848 (94%)	0.316 (50%)
Import	0.461 (92%)	7.712 (87%)	8.976 (66%)	2.815 (42%)	2.642 (37%)	1.105 (52%)	2.124 (66%)	1.232 (70%)	0.121 (6%)	0.314 (50%)
Total	5.914	8.911	13.704	6.647	7.062	2.137	3.237	1.762	1.969	0.630

Note: Values are from BNL AIRSOX model for average of January and July 1974 meteorology; units are micrograms per cubic meter.

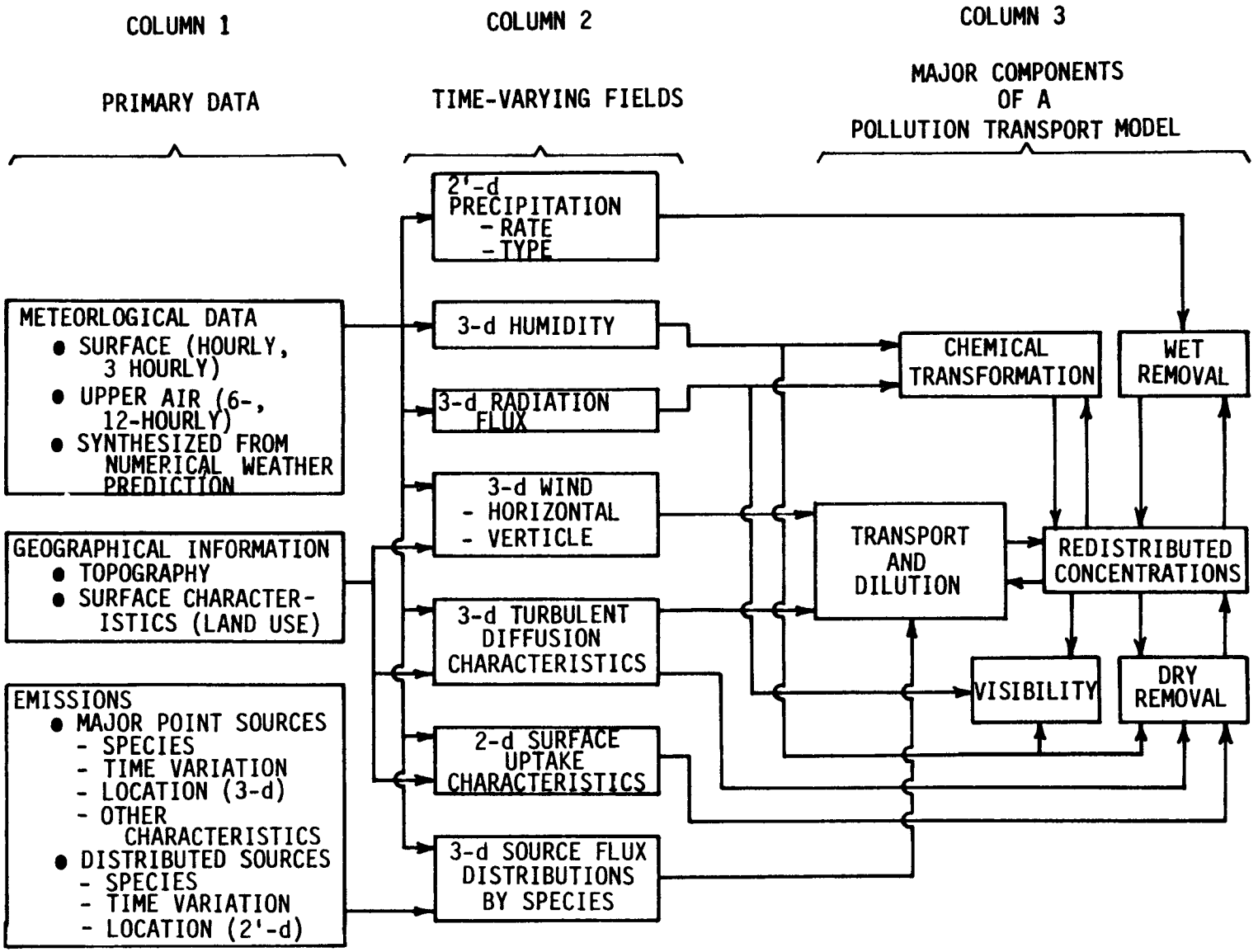

Figure 9-5. Interaction among the data sources and components of a pollution transport model.

and distributed sources. Input data requirements are shown in column 1 of the figure.

All LRT models are to a large extent driven by a set of time-varying scalar and vector fields like those shown in column 2 of Figure 9-5. Some of the input data required in transport model simulations, such as rainfall rate (used in calculating wet deposition) and humidity (used in chemical transformations), can be generated from data processing components external to the LRT model. The boxes in column 3 represent the major components of a model. Although some processes must be simulated in all types of models (Lagrangian/Eulerian), the choice of formulation influences the character of the model's other components.

9.5.3.2 Specific Characteristics of Data Used in Model Simulations--It is evident that to obtain accurate, meaningful, and useful information from models, the input data must be of a quality and quantity consistent with the structure and assumptions of the model in question. The following discussion examines these aspects in some detail.

9.5.3.2.1 Emissions. Characterization of emissions directly affects model results. Comprehensive sulfur emission inventories have been prepared for western Europe (Semb 1978) and North America (Mann 1980, Mueller et al. 1979). The SURE, Sulfate Regional Experiment, emissions (Mueller et al. 1979), and MAP3S (MacCracken 1979) emission inventories were specifically prepared to meet the needs of LRT models.

Two major sources of error in emission inventories can be identified. The first of these relates to the surrogates for emissions that are used (e.g., fuel consumption rates, population densities, employment figures, traffic, and industrial production rates). The second potential source of error lies in the factors or algorithms used to convert these surrogates into estimates of emissions at a particular time and place. These uncertainties must be quantified because they will directly affect any model's performance. For example, a major uncertainty is the importance of primary sulfates (e.g., SO_x emitted from the stacks already in the form of sulfate). This has become a controversial issue during the last year because of possible implications involving comparisons of local sources and distant sources and their relative contributions to sulfur concentrations and depositions.

The inventories are normalized to annual average emission rates with seasonal and diurnal adjustment factors (multipliers) incorporated. However, these factors are average values and are subject to large errors at any particular simulation time. Spatial resolution is typically 80 km because the inventories are gridded to that size. Emissions from large point sources are usually inventoried separately such that the modeler has the option to treat these sources separately or to combine their emissions into the 80 x 80 km grid cells.

Klemm and Brennan (1981) have estimated the uncertainties in annual emission rates in the SURE inventory. Their estimates were separated by broad source categories. For sulfur dioxide emissions, the error ranged from 12 percent for electric utility sources to 32 percent for commercial sources and had an

overall error value of 17 percent. In other words, the estimated emissions were said to be within 17 percent of the actual emissions from the sources inventoried. (Their analysis was restricted to anthropogenic sources.) Their error estimate for NO emissions was also 17 percent but was thought to be low because of the high uncertainty for transportation source emissions. Errors in sulfate, nitrogen dioxide, and hydrocarbon emission values were estimated to be several times higher than those for sulfur dioxide.

9.5.3.2.2 Meteorological Data. Existing LRT models operate in the diagnostic mode using available meteorological measurements, which are quite sparse. To date the wind fields for the LRT models are interpolated directly from these measurements and have not been coupled with the calculations of boundary layer models (BLMs). The BLMs use the meteorological measurements as initial conditions to solve the hydro-dynamic equations that govern the wind flow. The marriage of BLM and LRT models is a current research topic.

Most of the meteorological data for North America are obtained from the National Climatic Center (United States) and the Atmospheric Environment Service (Canada). Some special data (e.g., meteorological tower data) are also available. Most LRT models require upper air winds (e.g., 500 m) that must be derived from an estimated 50 upper air stations (for eastern North America) taking measurements every 12 hr. These measurements must be interpolated in time (e.g., 3-hr time steps) and space (e.g., 50-km resolution) prior to being operated on by the LRT model. It is recognized that the existing density of stations (less than one every 100,000 km^2) is insufficient to compute realistic trajectories on a short-term basis. It is assumed (with some supporting evidence) that, for long-term calculations, the distribution of calculated trajectories is a reasonable approximation of the distribution of actual trajectories. However, insufficient field data exist to quantify the accuracy of this assumption.

Detailed cloud and precipitation data are needed by the model for the estimation of wet removal. These precipitation data are obtained from standard reporting surface stations. Hourly data are available within the United States, but only daily values are reported in Canada. Cloud data are not currently used by any of the models and, hence, treatment of in-cloud processes is completely ignored. This is a major limitation in the data bases and models. Cloud data are not available in a readily useful form and as a result, it appears that most modelers have chosen not to pursue the rather massive effort to incorporate such data.

Other important data for model simulations pertain to atmospheric stability, mixing height, and surface characteristics. These are critical in calculating diffusion coefficients. Information about surface characteristics (land use type) is used in estimating dry deposition velocities. For estimating wet removal parameters, considerably detailed cloud and precipitation data are required.

9.5.4 Model Performance and Uncertainties

9.5.4.1 General--The evaluation of model performance must consider accuracies inherent in:

- the model itself--i.e., the package of algorithms containing the mathematics designed to represent the physical processees germane to acid deposition;

- the raw information (unprocessed input data) that must be transformed into a format compatible with the model;

- the preprocessors--i.e., the procedures that operate on the raw information generating the model compatible input; and

- the test data base containing the measurements that are compare with the model calculations.

A major limitation in most assessments of model performance is that the cause of disagreements between calculations and measurements cannot be isolated among the four items mentioned above. Normally, the four items are considered as a package with the assumption that, if agreement is "good," the model is a "valid" representation of the real world.

The primary objectives of model evaluation are to ensure that modeled physical and chemical processes are as representative as possible of real-world conditions and to quantify the uncertainties inherent in the model. Some progress has been made toward developing an accepted protocol for performance evaluation (Fox 1981). A widely accepted protocol proposed by Bowne (1980) lists three steps in the evaluation process:

- Technical evaluation: "Does the model perform as intended and is it scientifically sound?"

- Operational evaluation: "Does the model compute the correct values?"

- Dynamic evaluation: "Can the model be extended or adapted to other regions?"

To answer the questions posed in Bowne's protocol, four kinds of analysis should be performed:

- Accuracy analysis--use of accepted performance measures to quantify the model's performance relative to observed conditions

- Diagnostic analysis--identification of conditions associated with accuracies and inaccuracies in the model's performance

- Uncertainty analysis--quantification of the modeling uncertainties, both inherent in the model and in the response of the model to uncertainties in the input data

- Scientific Evaluation--a comprehensive technical evaluation of the model's conformity with the appropriate physical and computational principles.

With the exception of the last item in the above list, an appropriate data base is essential for the required analysis.

9.5.4.2 Data Bases Available for Evaluating Models--Extensive data bases that can be used to evaluate transport models are scarce; however, enough data exist to calculate performance measures over fairly broad confidence intervals. Niemann's (1981) examination of the available data bases indicated that, while they may be adequate for initial evaluation of sulfur pollution transport models and perhaps wet sulfur deposition, they are inadequate for substantially refining the current generation of models.

The data from the years 1978 and 1980 are most frequently used for LRT model evaluation. The former corresponds to the second year of SURE, during which the most comprehensive air quality data base was collected. However, the coverage and quality of precipitation chemistry data were not up to the standard that existed in the year 1980, when several Canadian and United States networks were operational (see Chapter A-8). Of the networks, the NADP offers the most coverage, having approximately 100 sites with the greatest density in the eastern United States. However, regional air quality data coverage was not comprehensive in 1980, and it appears that only the Canadian APN network collected daily (regional) sulfate concentration data. (The MOI group has assembled this data base for 1980.) Evaluation data bases are also available from other parts of the world, especially from western Europe, which has provided data bases that have been used to evaluate performance of several LRT models (e.g., Eliassen and Saltbones 1975; Johnson et al. 1978; Bhumralkar et al. 1980, 1981).

9.5.4.3 Performance Measures--Various groups have been developing procedures for evaluating models (e.g., Martinez et al. 1980, Ruff 1980, U.S./Canada 1982).

Many of the widely used performance measures require data bases from relatively dense networks of ground stations. Data bases for evaluating performance of pollution transport models often emphasize airborne sensors. Many of the performance measures are suitable for application to airborne observations, but some are not. This is a weakness in current evaluation methodologies. There seems to be a need for performance measures and evaluation methodology that can take full advantage of all the available airborne data.

Model evaluation statistics and displays generally try to answer the following questions:

- How closely does a model calculation match the corresponding observed value?
- How well do the fluctuations in the predictions follow the fluctuations of the measured parameter in time and space?

For the most part, paired values of observations, C_o, and predictions, C_p, are used to calculate quantitative measures that address the above questions. A difference, d, is defined such that:

$$d = C_o(x,t) - C_p(x,t) \quad . \qquad [9\text{-}15]$$

When answering the first question in the above list, we often define this difference in terms of measurements and predictions from the same place, x, and time, t.

If the difference, d, is always zero, the model would be considered perfect. Most often, the average and standard deviation of d are computed because they are measures of the model bias and precision, respectively. Correlation coefficients are also used as performance measures and accompanied by scatterplots with regression coefficients. These statistics and graphical displays of scatterplots (and sometimes frequency distribution comparisons) have been used by modelers since the time of the early model evaluation studies. One of the reasons they remain useful is that they are more or less the universally accepted language on the subject.

9.5.4.4 Representativeness of Measurements--The evaluation of model performance has been discussed in terms of how well the results from the model, or from one of its components, agree with some observed value. This assumes that the observed values are accurate and representative. To legitimize this assumption, extensive quality assurance measures should govern the acquisition and verification of the data base. Most data bases have been subjected to considerable screening to ensure that data are consistent and reliable, but it is not clear that the measurements (especially precipitation) are representative of conditions on the scale represented by the model. This must be taken into account when comparisons are made.

9.5.4.5 Uncertainties--Modeling uncertainty consists of two components. One part of the uncertainty can be thought of as "reducible" by means of improvements to the model and its prescribed input data; a second part is considered "irreducible" and is generally attributed to the uncertainty inherent in the small-scale and short-term fluctuations in atmospheric behavior, which never can be completely characterized by the finite amount of data used for input to existing LRT models. To date little progress has been made on this subject.

Some estimates of the reducible uncertainty could be made by conducting a sensitivity analysis. In such an analysis the model's sensitivity to input errors (or data parameterization errors) can be qualified and distinguished from errors in the basic formulation. Methods to estimate the irreducible uncertainty are currently being developed by the research community. For instance, a recently proposed model evaluation framework (Venkatram 1982) incorporates statistics that attempt to quantify these uncertainties.

9.5.4.6 Selected Results--Numerous examples of LRT model evaluation exercises exist in the open literature. However, most of these are presented in a qualitative manner or with very minimal statistical evidence. Despite the desirability to know the statistical significance of results, researchers have usually neglected to compute confidence intervals associated with their comparisons of model calculations with field observations. However, research programs underway will greatly enhance existing information on the

subject. The MOI, EPRI, EPA, and National Park Service are all sponsoring such studies, and results are appearing in the literature, e.g., Stewart et al. (1983).

In this presentation, example model evaluation studies are presented to be more or less illustrative of the state of knowledge. The first study (Voldner et al. 1981) examined seasonal averages of concentration and depositions calculated by a modified Long-Range Transport of Air Pollutants (LRTAP) program and compared them with atmospheric sulfate concentrations from the SURE network and precipitation sulfate concentrations from the CANSAP network. For the month of October 1977, the examination found that the monthly average computed sulfate concentrations and depositions agreed with the measurements within 60 percent. This agreement held for the four combinations of wet and dry removal parameteric values that were presented. The correlation coefficient between measurements and predictions varied from 0.55 to 0.59 for atmospheric sulfate concentrations and from 0.86 to 0.91 for precipitation sulfate concentrations.

In another study (Mayerhofer et al. 1981), monthly averaged sulfur dioxide and sulfate atmospheric concentrations calculated by the ENAMAP model, were compared with measurements from the SURE network for January and August, 1977. Scatterplots of the sulfate comparison are presented in Figure 9-6. The correlation coefficients are 0.51 and 0.23 for January and August, respectively, but substantial over-prediction occurred at most stations. The sulfur dioxide concentrations (Figure 9-7) compared more favorably with correlation coefficients of 0.71 (January) and 0.48 (August).

The preliminary Phase III results of the MOI group addressed the comparisons of observations and model calculations of sulfate concentrations and wet depositions. The eight models listed in Table 9-9 were exercised to calculate annual and monthly averages for the year 1978. The model calculations were compared with measurements from the SURE, MAP3S, and CANSAP programs using performance measures described earlier in this section. A very limited partial listing of the MOI results is given in Table 9-10. This listing allows one to visually compare the average model calculation ($\bar{C}$), the bias ($\bar{d}$), and the root-mean-square error (s_d). It was noted that the number of locations used in the evaluation did vary among models. The MOI group also noted that the models appeared to perform better for wet deposition than for the ambient concentration. They found this surprising because wet deposition is episodic in nature, whereas the model results were presented as non-episodic or longer term. No consideration was given to SO_2 concentrations because they were considered to be always affected by local sources. A major conclusion of the MOI is that it is not possible to recommend a "best" model (among the eight compared) because of the uncertainties in the emissions and precipitation data and in the measurement data used for evaluation. The major point here is that, in a limited number of studies, monthly concentration and deposition concentrations are often moderately correlated (in a statistical sense) to measured values and often agree within a factor of 2. Hence, LRT model results may provide a useful estimate. However, the accuracy and uncertainties of these estimates must be quantified more thoroughly. Also, the evaluation studies are limited strictly to comparisons of sulfur dioxide and sulfate concentrations.

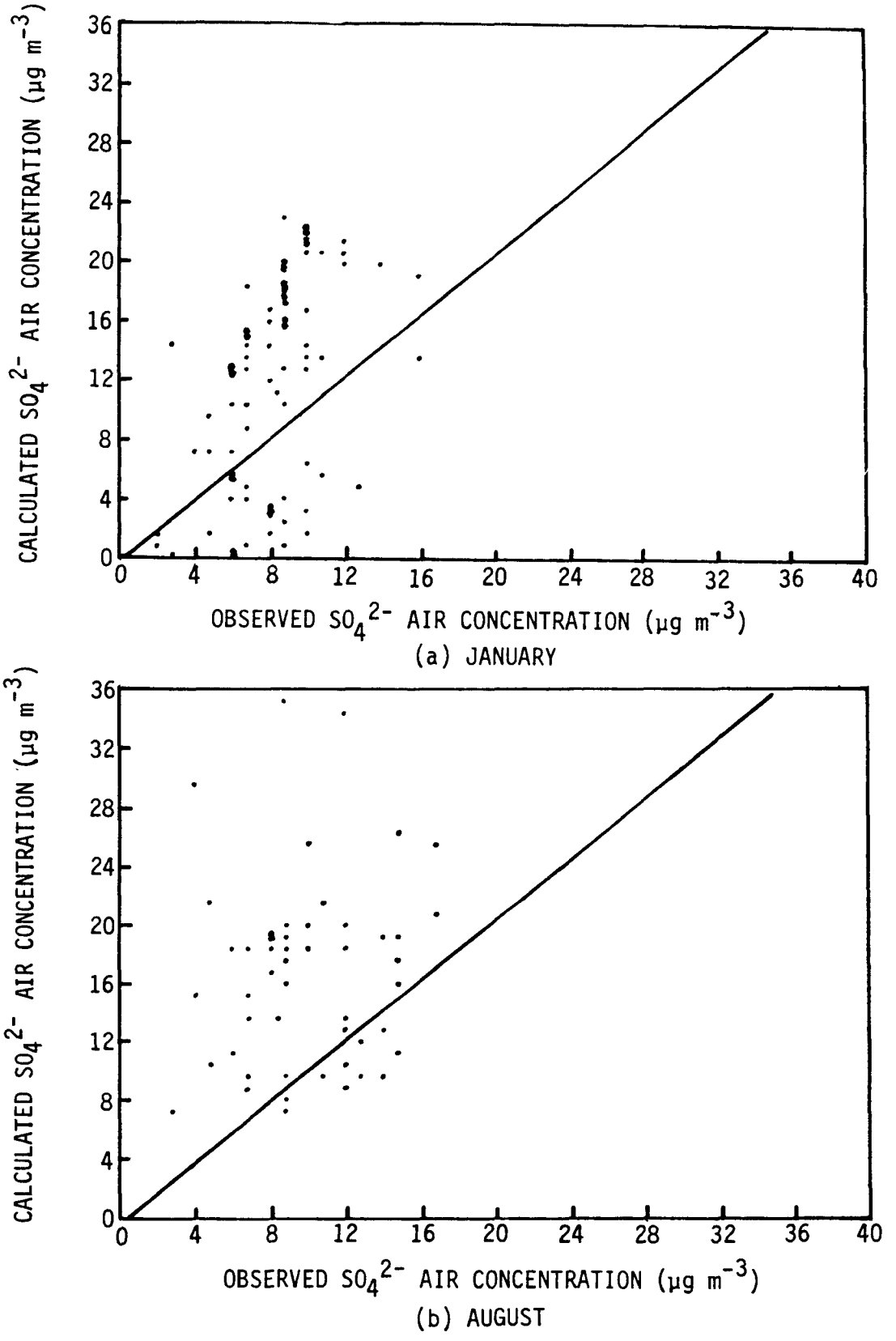

Figure 9-6. Scatter diagram of observed monthly values vs calculated monthly values of SO_4^{2-} concentrations for January and August 1977. Adapted from Mayerhofer et al. (1981).

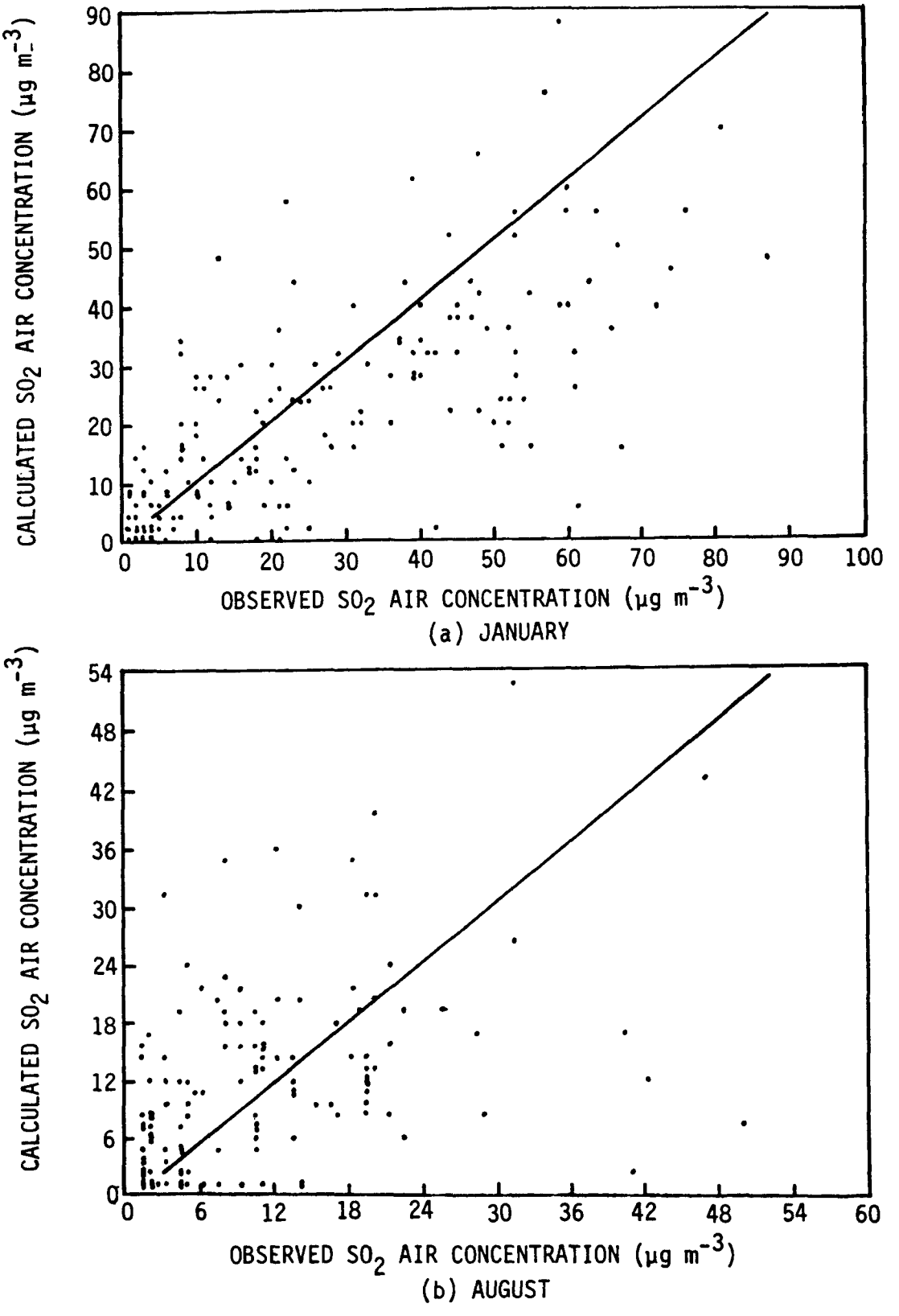

Figure 9-7. Scatter diagram of observed monthly values vs calculated monthly values of SO_2 concentrations for January and August 1977. Adapted from Mayerhofer et al. (1981).

TABLE 9-9. LONG-RANGE TRANSPORT MODELS ASSEMBLED BY THE MOI REGIONAL MODELING SUBGROUP

Model Name	Acronym	Reference[a]
Atmospheric Environment Service Long-Range Transport Model	AES	Olson et al. 1979
Advanced Statistical Trajectory Regional Air Pollution Model	ASTRAP	Shannon 1981
Center for Air Pollution Impact and Trends Analysis - Monte Carlo Model Planning, Ltd.	CAPITA	Patterson et al. 1981
Eastern North American Model of Air Pollution	ENAMAP-1	Bhumralkar et al. 1980
Transport of Regional Anthropogenic Nitrogen and Sulfur (TRANS) Model of Meteorological and Environmental Planning, Ltd.	MEP	Weisman 1980
Ontario Ministry of Environment Long-Range Transport Model	MOE	Venketram et al. 1980
University of Illinois Regional Climatological Dispersion Model	RCDM-3	Fay and Rosenzweig 1980
University of Michigan Atmospheric Contributions to Interregional Deposition Model	UMACID	Samson 1980

[a]Some of the model characteristics may have been revised since these references were printed.

TABLE 9-10. MOI PRELIMINARY COMPARISON BETWEEN MODELED AND MEASURED SULFATE CONCENTRATIONS AND DEPOSITIONS

Model	January			July			Annual		
	$\bar{\hat{C}}$	$\bar{d}$	s_d	$\bar{\hat{C}}$	$\bar{d}$	s_d	$\bar{\hat{C}}$	$\bar{d}$	s_d
	(a) Sulfate Concentrations ($\mu g\ m^{-3}$), 1978								
AES	7.5	-0.7	2.4	8.5	2.7	2.3	10.0	-0.9	1.7
MOE[a]	-	-	-	-	-	-	7.0	2.1	2.3
MEP	4.0	2.6	1.7	11.9	-0.4	2.1	8.3	0.8	0.9
ENAMAP	5.4	1.3	1.8	8.1	3.5	3.6	-	-	-
UMACID	6.2	-0.4	0.4	10.8	0.5	2.4	-	-	-
CAPITA	7.5	-0.7	1.8	11.9	-0.3	3.2	10.3	-1.2	1.6
RCDM	3.1	3.7	1.6	9.0	2.6	2.7	7.2	1.9	1.6
ASTRAP	6.0	0.8	3.0	8.9	2.6	3.2	7.2	1.9	2.8
	(b) Sulfate Depositions ($kg\ ha^{-1}\ period^{-1}$), 1978								
AES[b]	0.8	-0.1	0.6	0.9	0.2	0.4	9.7	1.2	4.0
MOE[b]	-	-	-	-	-	-	10.1	0.8	2.8
MEP[b]	0.8	0.0	1.0	0.2	0.7	0.4	6.5	4.4	2.5
ENAMAP	0.8	0.0	0.2	0.7	0.6	0.4	-	-	-
UMACID	0.1	0.3	0.3	0.1	0.9	0.3	-	-	-
CAPITA	0.5	0.2	0.7	0.8	0.3	0.2	6.4	4.5	3.5
RCDM	0.4	0.3	0.7	0.4	0.7	0.5	6.6	4.2	4.1
ASTRAP	0.7	0.0	0.8	0.9	0.2	0.3	8.1	2.7	4.3

[a]Background of 2 $\mu g\ m^{-3}$ added to the calculation.

[b]Background of 2 $kg\ ha^{-1}$ added to the annual calculations only.

9.6 CONCLUSIONS

A host of Eulerian and trajectory models have been developed to treat long-range transport (LRT) problems. The majority of these models have been of the trajectory type--statistical or Lagrangian--and primarily have been developed to calculate long-term (monthly and annual) averages for sulfur dioxide and sulfate concentration and depositions over transport distances of 500 km and above. The Eulerian grid model is capable of treating complex physical and chemical processes in a more realistic manner than the trajectory model, but this capability has not been employed frequently on the LRT scale. Hence, treatments in the most detailed Lagrangian trajectory models are similar in complexity to those in Eulerian models.

Current LRT models treat the processes of transport, diffusion, chemical transformation, and (wet and dry) deposition, but even the most detailed treatments represent gross simplifications of existing knowledge about these processes. The effect of these simplifications on model performance has yet to be determined. These limitations lead to somewhat more specific conclusions described below:

- At present, calculations from LRT models alone are not a sufficient basis for estimating levels of acidic deposition because the validity of the modeled source-to-receptor relationships has not been established (Sections 9.4.1 and 9.5.4).

- In a limited number of model evaluation studies comparing sulfur dioxide and sulfate concentrations, LRT model calculations are moderately correlated with field measurements. A more definitive statement on this subject should be possible within the next year when the results of current model evaluation studies are reported. Unfortunately, such a statement probably will address sulfur compounds only, ignoring other compounds germane to acidic deposition (e.g., nitrogen oxides) (Section 9.5.4).

- In general, LRT models are capable of treating only large synoptic scale processes. As a result, many important smaller (sub-grid) scale processes are ignored (Section 9.5.3). These include lack of treatment of:

  - processes in individual clouds and precipitation events (cloud data are not treated by existing models and precipitation data are not sufficiently resolved),

  - effects of nearby sources (e.g., within 100 km of a receptor) whose effluents may dominate acidic precursor concentrations in certain situations, and

  - gross differences in the transport winds that might occur within the small scale.

- Previous and existing measurement programs have not provided sufficient data to evaluate models or model components to the extent

needed. Additionally, the raw (input) data operated on by the models need improvement in spatial and temporal detail. The sparcity of the existing upper air meteorological network is a prime example of this problem (Sections 9.4.1 and 9.5.3).

Current research programs are addressing many of the topics mentioned above and progress is inevitable. Some of this effort is devoted to quantifying model accuracy and uncertainty using existing data bases. Better guidelines on how and when to use LRT results ultimately will emerge.

9.7 REFERENCES

Altshuller, A. P. 1979. Model predictions of the rates of homogeneous oxidation of sulfur dioxide to sulfate in the troposphere. Atmos. Environ. 13:1653-1661.

Ball, R. H. 1981. Matrix methods to analyze long-range transport of air pollutants. Department of Energy. DOE/EV-0127.

Barrie, L.A. 1981. The prediction of rain acidity and SO_2 scavenging in eastern North American. Atmos. Environ. 15:31-41.

Bass, A. 1980. Modelling long-range transport and diffusion, pp. 193-215. In Proceedings of the 2nd Joint Conference on Applications of Air Pollution Meteorology, New Orleans, LA, March 24-27, 1980. American Meteorological Society, Boston, MA.

Berkowicz, R. and L. P. Prahm. 1978. Pseudospectral simulation of dry deposition from a point source. Atmos. Environ. 12:379-387.

Bhumralkar, C. M., R. M. Endlich, K. C. Nitz, R. Brodzinsky, and P. Mayerhofer. 1982. Lagrangian long-range air pollution model for Eastern North America. 13th International Technical Meeting of Air Pollution Modeling and Its Application NATO/CCMS. Ile des Embiez, France.

Bhumralkar, C. M., R. L. Mancuso, D. E. Wolf, R. H. Thuillier, and W. B. Johnson. 1980. Adaptation and Application of the EURMAP-1 Model to Eastern North America. Final Report, Project 7760, EPA Contract 68-02-2959, SRI International, Menlo Park, CA.

Bhumralkar, C. M., R. L. Mancuso, D. E. Wolf, and W. B. Johnson. 1981. Regional air pollution model for calculating short-term (daily) patterns and transfrontier exchanges of airborne sulfur in Europe. Tellus 33:142-161.

Bolin, B. and C. Persson. 1975. Regional dispersion and deposition of atmospheric pollutants with particular application to sulfur pollution over western Europe. Tellus 27(3):281-310.

Bowne, N. E. 1980. Validation and performance criteria - air quality models. In Proceedings of the 2nd Joint Conference on Applications of Air Pollution Meteorology. American Meteorological Society, Boston, MA.

Carmichael, G. R. and L. K. Peters. 1979. Numerical simulation of the regional transport of SO_2 and sulfate in the eastern United States, pp. 337-344. In Proceedings of the 4th Symposium on Turbulence, Diffusion, and Air Pollution, Reno, NV, January 15-18, 1979. American Meteorological Society, Boston, MA.

Christensen, O. and L. P. Prahm. 1976. A pseudospectral model for dispersion of atmospheric pollutants. J. Appl. Meteor. 15:1284-1294.

Dana, M. T. 1979. Overview of wet deposition and scavenging, pp. 263-274. In Atmospheric Sulfur Deposition. D. S. Shriner, C. R. Richmond, and S. E. Lindberg, eds. Ann Arbor Science, Inc., Ann Arbor, MI.

Drake, R. L., D. J. McNaughton, and C. Huang. 1979. Available air quality models. Appendix D of Mathematical Models for Atmospheric Pollutants, EPRI EA-1131, Project 805. Electric Power Research Institute, Palo Alto, CA.

Draxler, R. R. 1976. A Diffusion-Deposition Scheme for Use Within the ARL Trajectory Model. Technical memo ERL-ARL-63. National Oceanic and Atmospheric Administration/Laboratories, Silver Spring, MD.

Durran, D., M. J. Meldgin, M. K. Liu, T. Thoem, and D. Henderson. 1979. A study of long range air pollution problems related to coal development in the northern Great Plains. Atmos. Environ. 13:1021-1037.

Egan, B. A., K. S. Rao, and A. Bass. 1976. A three-dimensional advective-diffusive model for long-range sulfate transport and transformation, pp. 697-714. In Proceedings of the 7th International Technical Meeting on Air Pollution Modeling and Its Application, Airlie, VA, September 1976. Report of the Air Pollution Pilot Study, NATO Committee on the Challenges to Modern Society.

Eliassen, A. 1980. A review of long-range transport modeling. J. Appl. Meteor. 19:231-240.

Eliassen, A. and J. Saltbones. 1975. Decay and transformation rates of SO_2 as estimated from emission data, trajectories and measured air concentrations. Atmos. Environ. 9:425-429.

Fay, J. A., and J. J. Rosenzweig. 1980. An analytical diffusion model for long-distance transport of air pollutants. Atmos. Environ. 14:355-365.

Fisher, B. E. A. 1975. The long range transport of sulfur dioxide. Atmos. Environ. 9:1063-1070.

Fisher, B. E. A. 1978. The calculation of long term sulphur deposition in Europe. Atmos. Environ. 12:489-501.

Fox, D. G. 1981. Judging air quality model performance-review of the Woods Hole workshop. Bull. Am. Meteorol. Soc. 62:599-609.

Fox, D. G., and S. A. Orszag. 1973. Pseudospectral approximation to two-dimensional turbulence. J. Comput. Phys. 11:612-619.

Freiberg, J. E., and S. E. Schwartz. 1981. Oxidation of SO_2 in aqueous droplets: Mass-transport limitation in laboratory studies and the ambient atmosphere. Atmos. Environ. 15:1145-1154.

Hane, C. E. 1978. Scavenging of urban pollutants by thunderstorm rainfall: numerical experimentation. J. Appl. Meteorol. 17(5):699-710.

Heffter, J. L. 1980. Air Resources Laboratories Atmospheric Transport and Dispersion Model (ARL-ATAD). Technical Memo ERL-ARL-81, National Oceanic and Atmospheric Administration, Air Resources Laboratories, Silver Spring, MD.

Heffter, J. L., A. D. Taylor, and G. J. Ferber. 1975. A Regional-Continental Scale Transport, Diffusion, and Deposition Model. Technical memo ERL-ARL-50. National Oceanic and Atmospheric Administration, Air Resources Laboratories, Silver Spring, MD.

Henmi, T. 1980. Long-range transport model of SO_2 and sulphate and its application to the eastern United States. J. of Geophys. Research. 85:4436-4442.

Hosker, R. P., Jr. 1980. Practical application of air pollutant deposition models--current status, data requirements, and research needs. In Proceedings of the International Conference on Air Pollutants and Their Effects on the Terrestrial Ecosystem, Banff, Alberta, Canada, May 10-17, 1980. S. V. Krupa and A. H. Legge, eds. John Wiley and Sons, New York.

Johnson, W. B. 1981. Interregional exchanges of air pollution: model types and applications. Proceedings of the 11th International Technical Meeting on Air Pollution Modeling and Its Applications, Plenum Press, New York.

Johnson, W. B., D. E. Wolf, and R. L. Mancuso. 1978. Long-term regional patterns and transfrontier exchanges of airborne sulfur pollution in Europe. Atmos. Environ. 12:511-527.

Klemm, H.A. and R.J. Brennan. 1981. Emissions inventory for the SURE region. EPRI Report EA-1913. Electric Power Research Institute, Palo Alto, CA.

Lange, R. 1978. ADPIC--A three-dimensional particle in cell model for the dispersal of atmospheric pollutants and its comparison to regional tracer studies. J. Appl. Meteor. 17:320-329.

Lavery, T. F., R. L. Baskett, J. W. Thrasher, N. J. Lordi, A. C. Lloyd, and G. M. Hidy. 1980. Development and validation of a regional model to simulate atmospheric concentrations of SO_2 and sulfate, pp. 236-247. In Proceedings of the AMS/APCA 2nd Joint Conference on Applications of Air Pollution Meteorology, New Orleans, LA, March 24-27, 1980. American Meteorological Society, Boston, MA.

MacCracken, M. C. 1979. Simulation of regional precipitation chemistry. In Proceedings: Advisory Workshop to Identify Research Needs on the Formation of Acid Precipitation, D. H. Pack, eds., 2-75 to 2-92, EPRI Report EA-1074, Electric Power Research Institute, Palo Alto, CA.

Mann, C. O. 1980. NEDS Information. EPA Report 450/4-80-013. U.S. Environmental Protection Agency, Washington, D.C.

Martinez, J. R., H. S. Javitz, W. F. Dabberdt, and R. E. Ruff. 1980. Development and application of methods for evaluating highway air pollution models, In 2nd Joint Conference on Applications of Air Pollution Meteorology. American Meteorological Society, Boston, MA.

Maul, P. R. 1977. The mathematical model of the mesoscale transport of gaseous pollutants. Atmos. Environ. 11:1191-1195.

Mayerhofer, P. M., R. M. Endlich, B. E. Cantrell, R. Brodzinsky, and C. M. Bhumralkar. 1981. ENAMAP-IA long-term SO_2 and sulfate air pollution model: Refinement of transformation and deposition mechanisms. Final Report, EPA Contract 68-02-3424, SRI International, Menlo Park, CA.

McMahon, T. A., P. J. Denison, and R. Fleming. 1976. A long-distance air pollution transportation model incorporating washout and dry deposition components. Atmos. Environ. 10:751-761.

McNaughton, D. J. 1980. Initial comparisons of SURE/MAP3S sulfur oxide observations with long-term regional model predictions. Atmos. Environ. 14:55-63.

McNaughton, D. J. 1981. Relationships between sulfate and nitrate ion concentrations and rainfall pH for use in modeling applications. Atmos. Environ. 15(6):1075-1079.

Meyers, R. E., T. Y. Li, R. T. Cederwall, and L. I. Kleinman. 1979. A long range transport model for calculating the atmospheric impacts of residual sulfur oxides. BNL 26185-RI. Brookhaven National Laboratory, Upton, New York.

Mills, M. F. and A. A. Hirata. 1978. A multi-scale transport and dispersion model for local and regional scale sulfur dioxide/sulfate concentrations--formulation and initial evaluation. In Proceedings of the 9th International Technical Meeting on Air Pollution Modeling and Its Application, Toronto, Ontario, Canada, August 28-31, 1978. A report of the Air Pollution Pilot Study, NATO Committee on the Challenges to Modern Society.

Molenkamp, C. R. 1974. Numerical modeling of precipitation scavenging by convective clouds, pp. 769-793. In Precipitation Scavenging (1974), Proceedings of Symposium, Champaign, IL, October 14-18. R. G. Semonin and R. W. Beadle, coordinators, U.S. ERDA Technical Information Center, Oak Ridge, TN, 1977. Available from NTIS, Springfield, VA, as CONF-741003.

Mueller, P. K., G. M. Hidy, E. Y. Tong, and M. C. MacCraken. 1979. Implementation and coordination of the sulfate regional experiment (SURE) and related research programs, EPRI Report EA-1066. EPRI, Palo Alto, CA.

Niemann, B. L. 1981. Initial data bases for the intercomparison of regional air quality/acid deposition simulation models--description and applications. Presented at the 74th Annual Meeting of the Air Pollution Control Association, Paper 81-46.4.

Niemann, B. L., A. A. Hirata, B. R. Hall, M. T. Mills, P. M. Mayerhofer, and L. F. Smith. 1980. Initial evaluation of regional transport and subregional dispersion models for sulfur dioxide and fine particulates, pp. 216-224. In Proceedings of the 2nd Joint Conference on Applications of Air Pollution Meteorology, New Orleans, LA, March 24-27, 1980. American Meteorological Society, Boston, MA.

Nordø, J. 1974. Quantitative estimates of long-range transport of sulphur pollutants in Europe. Ann Meteor. 9:71-77.

Nordø, J. 1976. Long-range transport of air pollutants in Europe and acid precipitation in Norway. Water, Air, and Soil Pollut. 6:199-217.

Organization for Economic Cooperation and Development (OECD). 1977. The OECD programme on long-range transport or air pollutants: Measurements and findings. Director of Information OECD, Paris, France.

Olson, M. P., E. C. Voldner, K. K. Oikawa, and A. W. MacAfee. 1979. A concentration/deposition model applied to the Canadian long-range transport of air pollutants project: a technical description. Report No. LRTAP79-5, Environment Canada, Downsview, Ontario, Canada.

Ottar, B. 1978. An assessment of the OECD study on long-range transport of air pollutants (LRTAP). Atmos. Environ. 12:445-454.

Patterson, D. E., R. B. Husar, W. E. Wilson, and L. F. Smith. 1981. Monte Carlo simulation of daily regional sulfur distribution: Comparison with SURE sulfate data and visual range observations during August 1977. J. Appl. Meteorol. 20:404-420.

Pedersen, L. B. and L. P. Prahm. 1974. A method for numerical solution of the advection equation. Tellus 26:594-602.

Peterson, K. R. and T. V. Crawford. 1970. Precipitation scavenging in a large-cloud diffusion code, pp. 425-431. In Precipitation Scavenging, Proceedings of Symposium, Richland, WA. R. J. Engelmann and W. G. N. Slinn, coordinators, U.S. AEC Division of Technical Information, Oak Ridge, TN. Available from NTIS, Springfield, VA as CONF-700601.

Powell, D. C., D. J. McNaughton, L. L. Wendell, and R. L. Drake. 1979. A variable trajectory model for regional assessments of air pollution from sulfur compounds. Report No. PNL-2734, Battelle Pacific Northwest Laboratory, Richland, WA.

Prahm, L. P. and O. Christensen. 1977. Long-range transmission of pollutants simulated by a two-dimensional pseudospectral dispersion model. J. Appl. Meteor. 16:896-910.

Rodhe, H. 1972. A study of the sulfur budget for the atmosphere over northern Europe. Tellus 24:128-138.

Rodhe, H. 1974. Some aspects of the use of air trajectories for the computation of large-scale dispersion and fallout patterns. Advances in Geophysics 18B:95-109.

Rodhe, H., and J. Grandell. 1972. On the removal time of aerosol particles from the atmosphere by precipitation scavenging. Tellus 24(5):442-454.

Ruff, R. E. 1980. Evaluation of the RAM using the RAPS data base--part 2. Results. Final Report, Contract EPA/68-02-2770, SRI International, Menlo Park, CA.

Samson, P. A. 1980. Trajectory Analysis of Summertime Sulfate Concentrations in the Northeastern United States. J. Appl. Meteor. 19:1382-1394.

Scriven, R. A., and B. E. A. Fisher. 1975. The long-range transport of airborne material and its removal by deposition and washout. I. General observations. II. The effect of turbulent diffusion. Atmos. Environ. 9:49-68.

Sehmel, G. A. 1980. Deposition and reinsertion processes. Chapter 12 in Atmospheric Sciences and Power Production, D. Randerson, ed., U. S. Department of Energy.

Semb, A. 1978. Sulfur emissions in Europe. Atmos. Environ. 12:455-460.

Shannon, J. D. 1979. The advanced statistical trajectory regional air pollution model, pp. 376-380. In Proceedings of the 4th Symposium on Turbulence, Diffusion, and Air Pollution, Reno, NV, January 15-18, 1979. American Meteorological Society, Boston, MA.

Shannon, J. D. 1981. A model of regional long-term average sulfur atmospheric pollution, surface removal, and net horizontal flux. Atmos. Environ. 15:689-701.

Sheih, C. M. 1977. Application of a statistical trajectory model to the simulation of sulfur pollution over the northeastern United States. Atmos. Environ. 11:173-178.

Sheih, C. M. 1978. A puff-on-cell method for computing pollutant transport and diffusion. J. Appl. Meteor. 17:140-147.

Sheih, C. M., M. L. Wesely, and B. B. Hicks. 1979. Estimated dry deposition velocities of sulfur over the eastern United States and surrounding regions. Atmos. Environ. 13:1361-1368.

Sklarew, R. C., A. J. Fabrik, and J. E. Prager. 1971. A particle-in-cell method for numerical solution of the atmospheric diffusion equation, and application to air pollution problems. Report No. 3SR-844, Systems, Science and Software, La Jolla, CA.

Slinn, W. G. N. 1978. Parameterizations for resuspension and for wet and dry deposition of particles and gases for use in radiation dose calculations. Nucl. Safety 19(2):205-219.

Smith, F. B. and R. D. Hunt. 1979. The dispersion of sulfur pollutants over western Europe. Phil. Trans. Roy. Soc. London A290:523-542.

Spicer, C. W., G. M. Sverdrop, and M. R. Kuhlman. 1981. Smog chamber studies of NO_x chemistry in power plant plumes. Battelle-Columbus Laboratories, Columbus, Ohio.

Stewart, D. A., R. E. Morris, A. B. Hudischewsky, and M. K. Liu. 1983. Evaluation of episodic regional transport models of interest to the National Park Service. Final Report, SYSAPP 831020, Contract No. PX-001-2-0739, Systems Applications, Inc., San Rafael, CA.

Szepesi, D. J. 1978. Transmission of sulfur dioxide on local, regional and continental scales. Atmos. Environ. 12:529-535.

United States/Canada. 1982. Phase II Interim Report of Working Group 2. Final Report submitted to the U.S. Environmental Protection Agency, Washington, D.C., and Environment Canada, Ottawa, Ontario.

Venkatram, A. 1982. A framework for evaluating air quality models. Boundary-layer Meterology 24:371-385.

Venkatram, A., B. E. Ley, and S. Y. Wong. 1980. A statistical model to estimate long-term concentrations of pollutants associated with long-range transport. Internal Report, Ontario Ministry of the Environment, Toronto, Ontario, Canada.

Voldner, E.C., M.P. Olson, K. Oikawa, and M. Loiselle. 1981. Comparison between measured and computed concentrations of sulphur compounds in eastern North America. J. Geophys Res. 86(C6):5339-5346.

Weisman, B. 1980. Long range transport model for sulphur. 73rd Annual Meeting of the Air Pollutin Control Association. Montreal, Canada.

Wendell, L. L., C. D. Powell, and R. L. Drake. 1976. A regional scale model for computing deposition and ground-level air concentrations of SO_2 and sulfates from elevated and ground sources, pp. 318-324. In Proceedings of the 3rd Symposium on Atmospheric Turbulence, Diffusion and Air Quality, October 19-22, 1976, Raleigh, NC. Published by the AMS, Boston, MA. Also in Proceedings of the 7th International Technical Meeting on Air Pollution Modeling and Its Application, September 7-10, 1976, Airlie House, VA. A report of the Air Pollution Pilot Study, NATO Committee on the Challenges to Modern Society.

TECHNICAL REPORT DATA
(Please read Instructions on the reverse before completing)

1. REPORT NO.	2.	3. RECIPIENT'S ACCESSION NO.
600/8-83-016AF		

4. TITLE AND SUBTITLE
The Acidic Deposition Phenomenon and Its Effects:
Critical Assessment Review Papers
Volume I - Atmospheric Sciences

5. REPORT DATE

6. PERFORMING ORGANIZATION CODE

7. AUTHOR(S)
Editors - Rick A. Linthurst and Aubrey P. Altshuller

8. PERFORMING ORGANIZATION REPORT NO.

9. PERFORMING ORGANIZATION NAME AND ADDRESS
NCSU Acid Precipitation Program
North Carolina State University
1509 Varsity Drive
Raleigh, North Carolina 27606

10. PROGRAM ELEMENT NO.

11. CONTRACT/GRANT NO.

12. SPONSORING AGENCY NAME AND ADDRESS
US EPA/ORD
401 M Street, S.W.
Washington, D.C. 20460

13. TYPE OF REPORT AND PERIOD COVERED

14. SPONSORING AGENCY CODE
EPA/ORD

15. SUPPLEMENTARY NOTES
This project is part of a cooperative agreement between EPA and North Carolina State University

16. ABSTRACT

This document is a review and assessment of the current scientific knowledge of the acidic deposition phenonemon and its effects. The areas discussed include both atmospheric (Volume I) and effects (Volume II) sciences. Specific topics covered are: natural and anthropogenic emissions sources; transport and transformation processes; atmospheric concentrations and distributions of chemical substances; precipitation scavenging and dry deposition processes; deposition monitoring and modeling; and effects of deposition on soils, vegetation, aquatic chemistry, aquatic biology, materials and human health, indirectly through ingested food or water. Each of the above topics is reviewed in detail using the available literature, with emphasis on U.S. data, and where possible, conclusions are drawn based on the available data.

17. KEY WORDS AND DOCUMENT ANALYSIS

a. DESCRIPTORS	b. IDENTIFIERS/OPEN ENDED TERMS	c. COSATI Field/Group

18. DISTRIBUTION STATEMENT	19. SECURITY CLASS *(This Report)*	21. NO. OF PAGES
Release to Public		750
	20. SECURITY CLASS *(This page)*	22. PRICE

EPA Form 2220-1 (Rev. 4-77) PREVIOUS EDITION IS OBSOLETE

*U.S. GOVERNMENT PRINTING OFFICE : 1984 0-421-082/529